Ghenadii Korotcenkov *Editor*

The Handbook of Paper-Based Sensors and Devices

Volume 1: Materials and Technologies

Springer

The Handbook of Paper-Based Sensors and Devices

Ghenadii Korotcenkov
Editor

The Handbook of Paper-Based Sensors and Devices

Volume 1: Materials and Technologies

Springer

Editor
Ghenadii Korotcenkov
Department of Physics and Engineering
Moldova State University
Chisinau, Moldova

ISBN 978-3-031-91079-1 ISBN 978-3-031-91080-7 (eBook)
https://doi.org/10.1007/978-3-031-91080-7

This Springer imprint is published by the registered company Springer Nature Switzerland AG
The registered company address is: Gewerbestrasse 11, 6330 Cham, Switzerland

Preface

Recently, there has been a growing interest in the use of cellulose and cellulose-based paper in organic, flexible, printed, and wearable electronics, not only as a paper substrate but also as active materials or components in composite materials, where cellulose provides mechanical strength and favorable three-dimensional microstructure. Paper is a form of 2D material that is chemically processed from cellulose fibers. One should note that cellulose is the most abundant and renewable natural polymer on earth. Cellulose is the major constituent in all plants. However, cellulose is known to be in higher concentration in a plant stem than in its leaves. Moreover, cellulose is found in various sources, not only limited to plants (wood, annual crops, and residual agricultural waste) but also in marine animals (tunicates), algae, fungi, bacteria, invertebrates, and even amoeba. Over the last three decades, scientists have explored different ways to incorporate the unique properties of paper into electronics and sensorics. Due to its remarkable physical properties, mechanical strength, special surface chemistry, large area-to-volume ratio, optical transparency, excellent biological properties of cellulose, low cost, and solution processability, nanocellulose is widely used as a support for electronically active materials in applications, such as chemical, physical, optical, and biosensors and electronic devices for biomedicine, environment monitoring, healthcare, and energy technologies.

By now, especially in recent years, a lot of books have been published on nanocellulose and its applications. Among them are the following: N. Lin, G. Zhu (eds.) *Surface Modifications of Nanocellulose*, Elsevier, 2024; L. Hu, F. Jiang, C. Chen (eds.) *Emerging Nanotechnologies in Nanocellulose*, Springer, 2023; A.Z. Yaser, M.S. Sarjadi, and J. Lamaming (eds.) *Cellulose*, Taylor and Francis, 2023; V. Kumar, S. Saran, A. Pandey, C. R. Soccol (eds.) *Bacterial Cellulose*, Taylor and Francis, 2023; M. Shabbir (ed.) *Regenerated Cellulose and Composites*, Springer Nature, 2023; R. Oraon, D. Rawtani, P. Singh, C.M. Hussain (eds.) *Nanocellulose Materials*, Elsevier, 2022; A. Barhoum (ed.) *Handbook of Nanocelluloses*, Springer, 2022; S.M. Sapuan, M.N.F. Norrrahim, R.A. Ilyas (eds.) *Industrial Applications of Nanocellulose and Its Nanocomposites*, Woodhead Publishing, 2022; J.H. Lee (ed.) *Paper-Based Medical Diagnostic Devices*, Springer Nature, 2021; W.R. de Araujo,

T.R.L.C. Paixão (eds.) *Paper-Based Analytical Devices for Chemical Analysis and Diagnostics*, Elsevier, 2021, and others. However, most of these books are focused on the synthesis of nanocellulose, its properties, and its use in specific areas, such as biomedical and environment applications. In addition, as a rule, these books are not systematic in the choice of topics for chapters and consistency in the presentation of the material included in the book. In addition, detailed analysis of the various sensors, such as gas and humidity sensors, electrochemical sensors, physical sensors, optical sensors, and biosensors that can be made from and on the paper, is practically absent from these books. The same situation is observed with paper-supported devices, such as transistors, light diodes, memory, supercapacitors, solar cells, batteries, and RFID tags, designed for applications in electronics and energy technology. In this regard, it is impossible to get a complete picture of the possibilities of paper for the development of various efficient paper-based and paper-supported flexible and wearable devices. Therefore, we decided to close this gap and publish the book *The Handbook of Paper-based Sensors and Devices* that provides complete information both about cellulose in its various states and about the manufacturing and application of paper-based and paper-supported various flexible sensors, wearable monitoring systems, and flexible electronic, optoelectronic, and photoelectronic devices. We hope that our attempt to prepare such book was successful.

For convenience of practical use, this *Handbook* is divided into three parts: Vol. 1: *Materials and Technologies*, Vol. 2: *Sensors*, and Vol. 3: *Biomedical and Environment Engineering, Electronics, and Energy Technologies*.

Chapters in *Handbook of Paper-based Sensors and Devices. Vol. 1: Materials and Technologies* describe the physical, chemical, and electronic properties of cellulose, which give rise to an increased interest in this material. The different aspects of nanocellulose research, such as the synthesis of different morphological forms by various methods, various surface modification methods (chemical and physical), composite synthesis by various methods, and development of its hydrogels and aerogels, are discussed. Cellulose can also be synthesized in pure and highly crystalline microfibrillar form by bacteria. This specific form of nanocellulose, called bacterial cellulose, is discussed in a special chapter of this volume. An analysis of new trends in development of nanocellulose-based papers such as conductive, transparent, magnetic, thermoconductive, hydrophobic, and fire-resistant papers is also given. It is shown that paper is a versatile, flexible, porous, and eco-friendly material that can be used as a substrate for the development of low-cost electronic devices and various sensors. The analysis performed suggests также that, based on the results obtained, a new type of paper can be developed, which, depending on the processing, allows using the same locally modified substrate as a substrate for electronic circuits, as a matrix for an electrolyte, a dielectric, or an element that provides the device required functionality. Various technologies that are used in the development and fabrication of paper and paper-based devices are also discussed in detail in this volume. Criteria for choosing paper in the manufacture of sensors and electronic devices are also discussed in this book. Thus, this volume combines a general introduction to cellulose and basic techniques and technologies developed for

fabrication of paper-based sensors and electronic devices. I am confident that this information will be cognitive and interesting for readers.

The second volume *Sensors* is entirely devoted to the consideration of different types of sensors that can be developed based on the paper. These sensors include electrical, physical, optical, electrochemical, and biosensors. The book describes these sensors, analyzes the functional materials used in their manufacture, and discusses their advantages and disadvantages. Great attention in this volume is also paid to the consideration of areas such as healthcare, medical diagnostic, environment monitoring, and agriculture, where these sensors can be used with increased efficiency. For example, it is shown that the development of microfluidic paper-based sensors provides the potential for portable medical tests that can be used anywhere in the world, especially in resource-restricted countries. The analysis carried out in this volume shows that such technological innovations, i.e., the creation of intelligent and self-powered paper-based analytical devices, can open the way for paper materials to become key players in the ongoing Internet of Things (IoT) revolution. Finally, the challenges encountered in developing paper-based sensors and approaches that can be used to overcome the problems are analyzed.

The title of the third volume of *Biomedical and Environment Engineering, Electronics and Energy Technologies* indicates that this volume is focused on considering the application of paper and nanocellulose in such fields as biotechnology, new biomaterials, water treatment, food industry, electronics, and energy technologies. Cellulose and cellulose-based membranes can be used to absorb organic and inorganic toxins, filter bacteria, viruses, and ionic contaminants, photocatalytic dye removal, and detect aqueous toxins. It is shown that a large number of different devices can be developed based on paper, such as supercapacitors, batteries, fuel cells, generators, actuators, RFID tags, light diodes, thin film transistors, and solar cells, which have such important functional properties as bendability and increased efficiency. As it is known, flexibility and stretchability of electronics are crucial for next-generation electronic devices that involve skin contact sensing and therapeutic actuation. The chapters in this volume provide also a comprehensive overview of the manufacture, parameters, functional materials used, and applications of these devices. The book presents also the latest achievements, highlights new perspectives, and describes approaches based on the use of cellulose and paper in the development of green technologies and green electronics. Finally, the book highlights a number of challenges associated with developing paper-based devices.

Thus, the present three-volume book *The Handbook of Paper-Based Sensors and Devices* is the first one, devoted to consideration of all aspects of paper-based devices from synthesis of nanocellulose and paper fabrication to discussion of features of manufacturing various flexible sensors and electronic devices on paper substrates and their application in various fields. Combining this information in three volumes dedicated to a specific topic "materials and technologies," "sensors," and "bio- and environment engineering, electronics and energy technologies" could help readers in searching required information on the interested subject. This makes these books, which present interdisciplinary discussions of nanocellulose and paper-based sensors and devices across a wide range of topics, very useful and easy to use.

We believe that these books will enable the reader to understand the present status of paper-based sensors and devices and the role of paper in the development of new generation of sensors and electronic devices for various applications with enhanced efficiency. Well-known experts with extensive experience in the development of nanocellulose-based technology and paper-based sensors and electronic devices are involved in writing chapters for these books. Based on the content, it can be argued that this handbook can become a valuable reference for material scientists, biologists, doctors, and biochemical engineers, as well as for engineers working in the field of chemistry, biomedicine, biotechnology, ecology, electronics, agriculture, and food industry. This book will also be of interest for university and college faculties, post-doctoral research fellows, and senior graduate students carrying out research in the field of chemical sensing, biosensing, biomedicine, biomaterials, environment protection, and remediation. I hope very much that in these books everyone might find a specific information which could be of interest and useful in his/her area of scientific and professional interests.

Finally, I thank all the authors who contributed to these books. I am grateful that they agreed to participate in this project and for their efforts to prepare these chapters. This project would not have been possible without their participation. I am also very grateful to Springer for the opportunity to publish this book with their help. I am also grateful to the Moldova State University (research program no. 011208) for supporting my research. I am also grateful to my family, primarily my wife Irina, who always supports me in all my endeavors.

Chisinau, Moldova Ghenadii Korotcenkov

Contents

Part IV Paper-Based Device Technology

Editor and Contributors

About the Editor

Ghenadii Korotcenkov received his PhD in physics and technology of semiconductor materials and devices in 1976 and his doctor of science degree (doctor habilitat) in physics of semiconductors and dielectrics in 1990. He has more than 50 years of experience as a teacher and scientific researcher. For a long time, he was a leader of the gas sensor group and manager of various national and international scientific and engineering projects carried out at the Laboratory of Micro- and Optoelectronics, Technical University of Moldova, Chisinau, Moldova. International foundations and programs such as the CRDF, MRDA, ICTP, INTAS, INCO-COPERNICUS, COST, and NATO have supported his research. From 2007 to 2008, he carried out his research as an invited scientist at the Korea Institute of Energy Research (Daejeon). Then, from 2008 to 2018, Dr. G. Korotcenkov was a research professor in the School of Materials Science and Engineering at Gwangju Institute of Science and Technology (GIST) in Korea. Currently, G. Korotcenkov is a chief scientific researcher at Moldova State University, Chisinau, Moldova.

Scientists from the former Soviet Union know the results of G. Korotcenkov's research in the study of Schottky barriers, MOS structures, native oxides, and photoreceivers based on III–Vs compounds, such as InP, GaP, AlGaAs, and InGaAs. Since 1995, his current research interests include material sciences, focusing on metal oxide film deposition and characterization

(In_2O_3, SnO_2, ZnO, and TiO_2), surface science, thermoelectric conversion, and design of physical and chemical sensors, including thin film gas sensors.

G. Korotcenkov is the author or editor of 48 books and special issues, including the 11-volume *Chemical Sensors* series, published by Momentum Press (2010–2013); two-volume *Handbook of Gas Sensor Materials*, published by Springer (2013–2014); 15-volume *Chemical Sensors* series, published by Harbin Institute of Technology Press, China (2013–2015); three-volume *Porous Silicon: From Formation to Application* issue, published by CRC Press (2015–2016); three-volume *Handbook of Humidity Measurements*, published by CRC Press (2018–2020); three-volume *Handbook of II–VI Semiconductor-Based Sensors and Radiation Detectors*, published by Springer (2023); three-volume *Handbook of Paper-Based Sensors and Devices*, published by Springer (2025); and 6 proceedings of the international conferences published by Trans Tech Publ., Elsevier and EDP Sciences. In addition, he currently serves as the series editor of *Metal Oxides* book series, published by Elsevier. Since 2017, more than 40 volumes have been published within this series.

G. Korotcenkov is the author and coauthor of more than 675 scientific publications, including 40 review papers, 70 book chapters, and more than 200 peer-reviewed articles published in scientific journals: h-factor = 45 (Web of Science), h = 47 (Scopus), and h = 72 (Google Scholar citation, 2024). He holds 17 patents. He has presented more than 250 reports at National and International conferences, including 20 invited talks. G. Korotcenkov, as a cochairman or member of program, scientific, and steering committees, has participated in the organization of more than 40 international scientific conferences. Dr. G. Korotcenkov serves as a member of editorial boards in six international scientific journals. His name and activities have been listed in many biographical publications, including “Who’s Who.” G. Korotcenkov has also been listed as one of the "World's Ranking Top 2% Scientists" in Applied Physics/Analytical Chemistry in the Physics and Astronomy Cluster. His research activities have been honored by the National Prize of the Republic of Moldova (2022), the Honorary Diploma of the Government of the Republic of Moldova (2020), an

Award of the Academy of Sciences of Moldova (2019), the Prize of the Presidents of the Ukrainian, Belarus, and Moldovan Academies of Sciences (2004), an Award of the Supreme Council of Science and Advanced Technology of the Republic of Moldova as the best scientist of the year (2003), Senior Research Excellence Awards of Technical University of Moldova (2001, 2003, and 2005), the National Youth Prize of the Republic of Moldova in the field of science and technology (1980), among others. Some of his research results and published books have won awards at international exhibitions. G. Korotcenkov also received fellowships from the International Research Exchange Board (IREX, United States, 1998), Brain Korea 21 Program (2008–2012), and BrainPool Program (Korea, 2007–2008 and 2015–2017).

https://www.scopus.com/authid/detail.uri?authorId=6701490962

https://publons.com/researcher/1490013/ghenadii-korotcenkov/

https://scholar.google.com/citations?user=XR3RNhAAAAAJ&hl

https://www.researchgate.net/profile/G_Korotcenkov

Contributors

Roberto J. Aguado LEPAMAP-PRODIS Research Group, University of Girona. Maria Aurèlia Capmany, Girona, Spain

Nurali Alaudini Institute of Chemistry of Renewable Resources, BOKU University, Vienna, Austria

Konrad-Lorenz-Strasse 24, Tulln, Austria

Ana Almeida NOVA School of Science and Technology, Caparica, Portugal

Mona T. Al-Shemy Cellulose and Paper Department, National Research Centre, Giza, Egypt

María Cristina Area PROCYP, IMAM (UNaM-CONICET), Posadas, Argentina

Aleksandra Balachenkova St. Petersburg State University of Industrial Technologies and Design, Higher School of Technology and Energy, St. Petersburg, Russia

Thomas M. Brown Department of Electronic Engineering, CHOSE - Centre for Hybrid and Organic Solar Energy, Rome, Italy

Tor Vergata University of Rome, Rome, Italy

Longyan Chen Department of Biomedical, Industrial and Systems Engineering, Gannon University, Erie, PA, USA

Yi Chen Materials, Engineering and Manufacturing Research Group, Scion Institute, Rotorua, New Zealand

Angelica Corpuz Cagayan State University, Tuguegarao, Cagayan, Philippines

Sawsan Dacrory Cellulose and Paper Department, National Research Centre, Giza, Egypt

Claudio José Galdino da Silva Junior Instituto Avançado de Tecnologia e Inovação (IATI), Recife – PE, Brasil

Hamid Dehghan-Manshadi Layer and Nanotechnology Laboratory, Department of Chemical Technologies, Iranian Research Organization for Science and Technology (IROST), Tehran, Iran

Marc Delgado-Aguilar LEPAMAP-PRODIS Research Group, University of Girona. Maria Aurèlia Capmany, Girona, Spain

Alexandre D'Lamare Maia de Medeiros Instituto Avançado de Tecnologia e Inovação (IATI), Recife – PE, Brasil

Andréa Fernanda de Santana Costa Instituto Avançado de Tecnologia e Inovação (IATI), Recife – PE, Brasil

Centro Acadêmico da Região Agreste, Universidade Federal de Pernambuco (UFPE), Caruaru, PE, Brasil

Thaís Cavalcante de Souza Universidade Federal de Pernambuco (UFPE), Recife – PE, Brasil

Instituto Avançado de Tecnologia e Inovação (IATI), Recife – PE, Brasil

Yingran Duan Zhuhai Topchain Pharma Co., Ltd., Zhuhai, China

Nanci Ehman PROCYP, IMAM (UNaM-CONICET), Posadas, Argentina

Leo Bey Fen Department of Molecular Medicine, Faculty of Medicine, Universiti Malaya, Kuala Lumpur, Malaysia

Nanotechnology & Catalysis Research Centre (NANOCAT), Institute for Advanced Studies, University of Malaya, Kuala Lumpur, Malaysia

Soraya Ghayempour Department of Textile Engineering, Faculty of Engineering, Yazd University, Yazd, Iran

Philipp Yu Gorobtsov Kurnakov Institute of General and Inorganic Chemistry, Russian Academy of Sciences, Moscow, Russia

Andrews Nirmala Grace Centre for Nanotechnology Research, Vellore Institute of Technology, Vellore, India

Bharath Gunaseelan Centre for Nanotechnology Research, Vellore Institute of Technology, Vellore, India

Yeoh Hao Ing Department of Molecular Medicine, Faculty of Medicine, Universiti Malaya, Kuala Lumpur, Malaysia

Tabkrich Khumsap Chiang Mai University, Maung, Chiangmai, Thailand

Ghenadii Korotcenkov Department of Physics and Engineering, Moldova State University, Chisinau, Moldova

Falk Liebner Institute of Chemistry of Renewable Resources, BOKU University, Vienna, Austria

Konrad-Lorenz-Strasse 24, Tulln, Austria

Xin Li Beijing Key Laboratory of Lignocellulosic Chemistry, Beijing Forestry University, Beijing, China

Engineering Research Center of Forestry Biomass Materials and Energy, Ministry of Education, Beijing Forestry University, Beijing, China

Yin Long State Key Laboratory of Electronic Thin Films and Integrated Devices, University of Electronic Science and Technology of China, Chengdu, China

Mohammad Mazloum-Ardakani Department of Chemistry, Faculty of Science, Yazd University, Yazd, Iran

Pere Mutjé LEPAMAP-PRODIS Research Group, University of Girona. Maria Aurèlia Capmany, Girona, Spain

Loc Thai Nguyen Asian Institute of Technology, Pathum Thani, Thailand

Ashutosh Pandey Panipat Institute of Engineering and Technology, Panipat, Haryana, India

Niranjan Patra Department of Chemistry, Koneru Lakshmaiah Education Foundation, Vaddeswaram, Andhra Pradesh, India

Davide Piovesan Department of Biomedical, Industrial and Systems Engineering, Gannon University, Erie, PA, USA

Sven Plappert Institute of Chemistry of Renewable Resources, BOKU University, Vienna, Austria

Konrad-Lorenz-Strasse 24, Tulln, Austria

Elisa Rasouli Department of Molecular Medicine, Faculty of Medicine, Universiti Malaya, Kuala Lumpur, Malaysia

Leonie Asfora Sarubbo Instituto Avançado de Tecnologia e Inovação (IATI), Recife – PE, Brasil

Escola UNICAP Icam Tech, Universidade Católica de Pernambuco (UNICAP), Recife – PE, Brasil

Marimuthu Sathish Vellore Institute of Technology, Vellore, Tamil Nadu, India

Sathyanarayanan Shriswaroop Vellore Institute of Technology, Vellore, Tamil Nadu, India

Giovana Signori-Iamin LEPAMAP-PRODIS Research Group, University of Girona. Maria Aurèlia Capmany, Girona, Spain

Elizaveta P. Simonenko Kurnakov Institute of General and Inorganic Chemistry, Russian Academy of Sciences, Moscow, Russia

Nikolay P. Simonenko Kurnakov Institute of General and Inorganic Chemistry, Russian Academy of Sciences, Moscow, Russia

Tatiana L. Simonenko Kurnakov Institute of General and Inorganic Chemistry, Russian Academy of Sciences, Moscow, Russia

Annika Singh School of Lifesciences and Biotechnology, CSJMU, Kanpur, India

Mukesh K. Singh Uttar Pradesh Textile Technology Institute, Kanpur, India

Zeynab Skafi Department of Electronic Engineering, CHOSE - Centre for Hybrid and Organic Solar Energy, Rome, Italy

Tor Vergata University of Rome, Rome, Italy

Gopal Tamilselvi Vellore Institute of Technology, Vellore, Tamil Nadu, India

Quim Tarrés LEPAMAP-PRODIS Research Group, University of Girona. Maria Aurèlia Capmany, Girona, Spain

María Evangelina Vallejos PROCYP, IMAM (UNaM-CONICET), Posadas, Argentina

Glória Maria Vinhas Universidade Federal de Pernambuco (UFPE), Recife – PE, Brasil

Jie Wang Beijing Key Laboratory of Lignocellulosic Chemistry, Beijing Forestry University, Beijing, China

Engineering Research Center of Forestry Biomass Materials and Energy, Ministry of Education, Beijing Forestry University, Beijing, China

Feng Xu Beijing Key Laboratory of Lignocellulosic Chemistry, Beijing Forestry University, Beijing, China

Engineering Research Center of Forestry Biomass Materials and Energy, Ministry of Education, Beijing Forestry University, Beijing, China

Xuezhu Xu Guangdong Provincial Key Laboratory of Optical Information Materials and Technology and Institute of Electronic Paper Displays, South China Academy of Advanced Optoelectronics, South China Normal University, Guangzhou, China

National Center for International Research on Green Optoelectronics, South China Normal University, Guangzhou, China

Chongzuo Key Laboratory of Comprehensive Utilization Technology of Manganese Resources; Guangxi Key Laboratory for High-Value Utilization of Manganese Resources, College of Chemistry and Biological Engineering, Guangxi Minzu Normal University, Chongzuo, Guangxi, China

Chongzuo Key Laboratory of High-Value Utilization of Sugarcane Resources, Chongzuo, Guangxi, China

COFCO Corporation Chongzuo Sugar Co., Ltd., Chongzuo, Guangxi, China

Han-Ping Yu State Key Laboratory of High Performance Ceramics and Superfine Microstructure, Shanghai Institute of Ceramics, Chinese Academy of Sciences, Shanghai, China

Zhiqiang Zhai State Key Laboratory of Electronic Thin Films and Integrated Devices, University of Electronic Science and Technology of China, Chengdu, China

Hui Zhao Beijing Key Laboratory of Lignocellulosic Chemistry, Beijing Forestry University, Beijing, China

Engineering Research Center of Forestry Biomass Materials and Energy, Ministry of Education, Beijing Forestry University, Beijing, China

Ying-Jie Zhu State Key Laboratory of High Performance Ceramics and Superfine Microstructure, Shanghai Institute of Ceramics, Chinese Academy of Sciences, Shanghai, China

Part I
Introduction in Flexible Electronics

Chapter 1
Flexible Devices: Introduction

Yin Long and Zhiqiang Zhai

1.1 Introduction to Flexible and Stretchable Electronics

Flexible electronics, an emerging technology compatible with movable parts and arbitrarily curved surfaces, is expected to be a new application paradigm for large-area electronics. The rapid development of ultrathin sensors and actuators, electronic and optoelectronic devices, and soft biocompatible packaging layer designs is expected to significantly expand the range of applications for flexible electronics from the curved panels and foldable displays described above to flexible systems with curved surfaces and interfaces with complex geometries.

Flexible electronic technology, with its unique advantages, is gaining attention to address resource scarcity and environmental pollution (Ismail & Hanafiah, 2019). This technology integrates with fields like the Internet of Things, aerospace, healthcare, intelligent robotics, and industrial automation, facilitating more convenient and comfortable human-object interactions (Hu et al., 2023). Flexible sensors, crucial components of flexible electronic devices, are vital for data acquisition (Zhang et al., 2023a). Especially with the rapid advancement of real-time physiological monitoring, noninvasive medical diagnostics, sports rehabilitation, and human-computer interaction necessitate high-performance flexible sensors for wearable devices. Despite significant technological breakthroughs, challenges such as inadequate sensitivity (Zhang et al., 2023a), poor flexibility (Chen et al., 2023), complex fabrication processes (Fayomi et al., 2017), high costs (Senawi & Sheau-Ting, 2016), and electronic contamination from widespread use persist (Pariatamby & Victor, 2013).

Y. Long (✉) · Z. Zhai
State Key Laboratory of Electronic Thin Films and Integrated Devices, University of Electronic Science and Technology of China, Chengdu, China
e-mail: yinlong56@uestc.edu.cn

G. Korotcenkov (ed.), *The Handbook of Paper-Based Sensors and Devices*,
https://doi.org/10.1007/978-3-031-91080-7_1

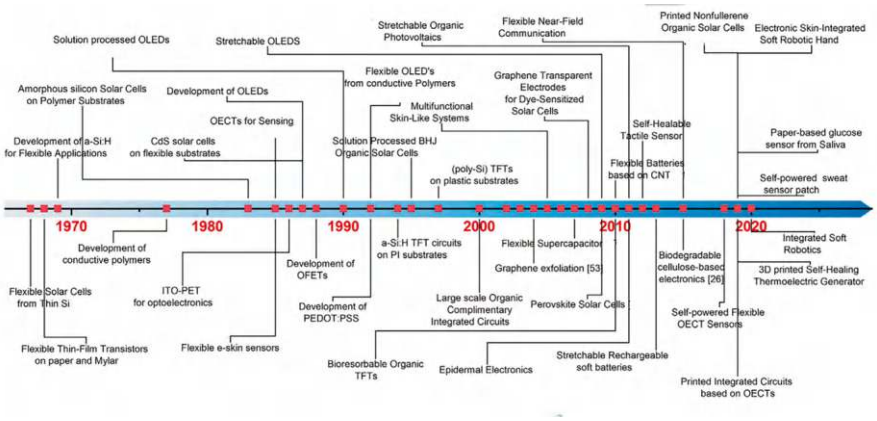

Fig. 1.1 Timeline of developments in materials, processing and applications for flexible electronics. Reprinted from Corzo et al. (2020). Published 2020 by Frontiers with open access

Wearable sensor systems with ultrathin, low-modulus, lightweight, highly flexible, and stretchable surfaces that form conformal contacts with organs or skin surfaces can provide new opportunities for human activity monitoring and personal healthcare. These wearable sensor systems can include various types of small physical sensors (temperature, pressure, and strain sensors), transmission modules, and self-contained power supplies, thereby facilitating low-cost wearable unobtrusive solutions for recording the electrophysiological activity that the human body generates on an ongoing basis.

In recent years, the rapid development of novel sensing materials, fabrication processes, and electrical sensing technologies has facilitated significant progress in the realization of flexible and stretchable sensor and electronic devices (see Fig. 1.1) with unique and advantageous properties such as transparency, high sensitivity, extreme thinness, ultra-lightweight, high flexibility and stretchability, super conformity, low cost, and large-area technology compatibility.

1.2 Construction Strategies for Flexible Electronic Materials and Devices

In the development of flexible wearable sensors, the selection of a suitable flexible substrate is fundamental to achieving optimal electromechanical and biological properties. Flexible substrates provide the necessary platform for integrating a variety of functional materials, while also ensuring comfort and adaptability to human skin or clothing. Commonly used flexible substrates include metal foils, polydimethylsiloxane (PDMS), polyimide (PI), polyethylene terephthalate (PET), and thermoplastic polyurethanes (TPU) and emerging flexible carbon-based, gel-based materials (see Chap. 2). These substrates have a range of properties such as

flexibility, stretchability, biocompatibility, and durability that are critical for practical applications in sports and health monitoring.

1.2.1 Materials

To construct effective flexible and stretchable electronics, functional materials must meet several critical requirements.

Bendability Materials should withstand repeated bending without significant changes in their physical or electrical properties. Stretchability: They need to be able to stretch and return to their original shape without losing functionality. Adhesion: Strong adhesion between different layers is crucial for maintaining structural integrity and performance over time. Biocompatibility and durability are especially important for wearable devices, as these properties ensure that the devices are safe and long-lasting when in contact with the skin. Processability refers to the ability to easily process the material into desired shapes and sizes without compromising its properties.

Materials that most fully satisfy these requirements include certain types of polymers, carbon-based materials, and metal nanomaterials. Polymers such as polydimethylsiloxane (PDMS) and thermoplastic polyurethane (TPU) offer excellent flexibility and biocompatibility. Carbon-based materials like graphene and carbon nanotubes provide high conductivity and mechanical strength while remaining lightweight and flexible. Metal nanomaterials, including silver nanowires and gold nanoparticles, can achieve both conductivity and flexibility, making them ideal for flexible electronics.

Several strategies can enhance the bendability of materials used in flexible electronics:

Transition from Bulk Materials to Nanomaterials: Using nanomaterials instead of bulk materials allows for greater flexibility due to their smaller size and higher surface area-to-volume ratio. Thickness Reduction: Thinner materials naturally have better flexibility and can bend more easily without breaking or degrading. Microstructuring and Perforation: Creating microstructures or perforations within the material can increase its flexibility by allowing parts of the material to move independently. Composite Materials: Combining different materials can result in composites that combine the best properties of each component, such as elasticity from polymers and conductivity from metals or carbon materials.

In constructing flexible wearable sensors, material and structure are critical for electromechanical and biological properties. Suitable materials, structures, and processing techniques must be chosen to meet performance requirements for practical applications, especially in human sports and health monitoring. Metal-based, carbon-based, polymer and composite materials perform well in wearable health monitoring fields, including strain, temperature, humidity, and gas detection, as well as electrophysiological monitoring.

Metals are widely used in flexible wearable sensors due to their high mechanical strength, electrical conductivity, and non-toxicity. Traditional metals like gold (Au), silver (Ag), and copper (Cu) are common in surface bioelectrodes, but their Young's modulus limits flexibility (Luo et al., 2017). Recently, metal nanomaterials and metal-based conductive fibers have overcome rigidity and become soft and stretchable for wearable health monitoring. Carbon and its derivatives are widely used in wearable devices due to their low cost, high conductivity, large specific surface area, chemical stability, and good mechanical properties. Common carbon materials include carbon nanotubes (CNTs), carbon black (CB), graphene, graphite, carbon fibers, and activated carbon (AC). For example, CB mixed with styrene-butylene-styrene (SEBS) triblock copolymers forms sensors for monitoring wrist activity, pulse wave, and heart rate. Polymer-based materials are widely used in wearable sensors due to their processability, stable mechanical properties, high ion mobility, elasticity, and strong corrosion resistance (Li et al., 2021). Several examples of polymers used in flexible electronics are shown in Fig. 1.2. Hydrogels are notable for their biocompatibility, Young's modulus similar to human skin, stimulus-responsive properties, and self-healing ability (Cherukhin and Xin, 2019). More detailed information on functional materials used in the development of flexible devices can be found in Qiao et al. (2023) and Chap. 22.

1.2.2 Structure

The peculiarity of producing bendable devices lies in the fact that flexible and wearable electronics typically do not require components at the nanometer scale. This characteristic allows for the use of simpler and more cost-effective manufacturing technologies, significantly reducing the overall cost of the developed devices. Such technologies include printing techniques, stamping and mossing, transfer printing, and textile manufacturing methods.

These production methods leverage existing industrial capabilities, making it possible to manufacture flexible and wearable devices on a larger scale while maintaining affordability and performance.

Clever structural design significantly enhances the performance and capabilities of wearable flexible devices. By utilizing innovative structures, traditionally non-ductile materials, such as metals, can become scalable and optimized for various applications including electromechanical and biological devices. The structural designs can be categorized into one-dimensional (1D), two-dimensional (2D), and three-dimensional (3D) structures (Fig. 1.3). These structures are often designed as twisted, helical, or entangled and are used to create fabric-type or fiber-type sensors. These sensors exhibit excellent electrical conductivity, tensile properties, and breathability and can be attached directly to clothing or skin to sense various physical changes like strain, pressure, bending, and twisting (Fig. 1.3a).

Two-dimensional structures refer to in-plane designs such as microstructures, serpentine sinuous structures, and fiber mesh structures. These structures enhance

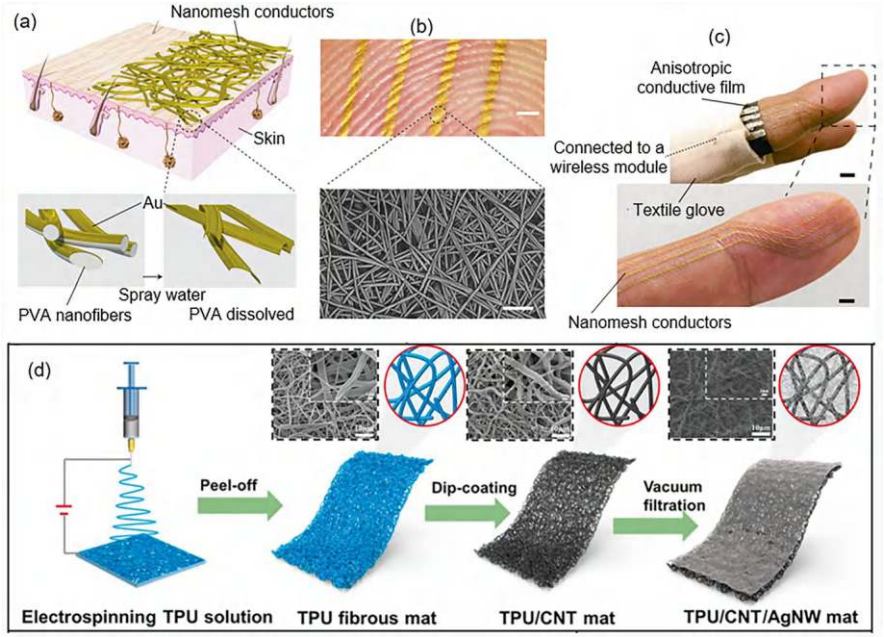

Fig. 1.2 Application of polymer nanomesh in flexible sensors. (**a–c**) Preparation process of the on-skin nanomesh electronics: (**a**) preparation of Au nanomesh conductors using PVA nanomesh as template. PVA meshes are dissolved by spraying water so that nanomesh conductors can adhere to the skin. (**b**) Picture of nanomesh conductor attached to the fingertip (scale bar represents 1 mm) and the SEM image of the nanomesh conductor after dissolving PVA nanomesh (scale bar represents 5 μm). This electrode can not only be used as a pressure sensor to realize touch sensing but also to monitor EMG, and the test results are almost the same as those of Ag–AgCl gel electrodes. The nanomesh can also be used to measure the skin impedance; (**c**) on-skin wireless sensor system based on the on-skin nanomesh electronics for touch sensing (scale bar represents 3 mm). (**d**) Preparation of the polyurethane (PU)/CNT/AgNWs strain sensor, and the SEM images of PU nanomesh, PU/CNT nanomesh, and PU/CNT/AgNWs nanomesh. (**a–c**) Reproduced with permission from Miyamoto et al. (2017). Copyright 2017: Springer Nature. (**d**) Reproduced from Wang et al. (2022). Published 2023 by Springer with open access

the performance of wearable health monitoring devices (Fig. 1.3b) (Miao et al., 2020; Seager et al., 2013). Microstructures include various microscale designs like hemispherical arrays, micro pyramids, and nano-springs, which improve sensitivity, elasticity, and electromechanical properties. Serpentine sinuous structures, often made from metals like gold or silver, increase the flexibility and extensibility of device interconnections, enhancing sensing performance (Fig. 1.3c) (Yue et al., 2012).

Three-dimensional structures extend beyond planar designs and include origami structures, paper-cutting structures, pre-stretching release-driven 3D structures, and cavity structures. These designs improve the sensor's ability to adapt to the human body, enhancing signal quality (Fig. 1.3e–g). Origami and paper-cutting techniques create complex, reversible shapes, improving material deformation and skin contact

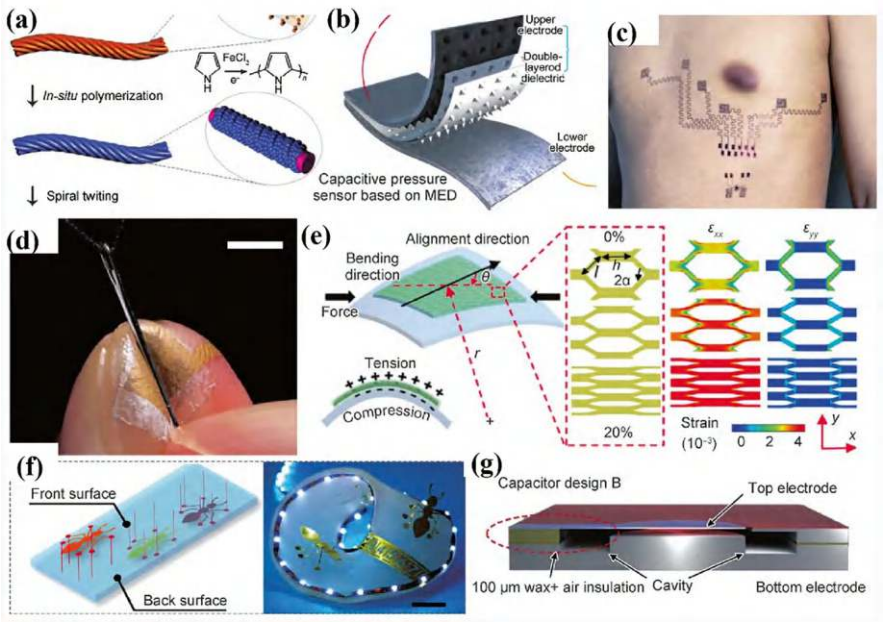

Fig. 1.3 Structural design of wearable flexible devices (**a**) 1D structure; (**b**) 2D microstructure; (**c**) 2D serpentine meander structure; (**d**) 2D fiber mesh structure; (**e**) three-dimensional origami paper-cut structure; (**f**) pre-stretch release driven three-dimensional structure. (**a**) Reprinted with permission from Nan et al. (2019). Copyright 2019: Wiley-VCH. (**b**) Reprinted with permission from Luo et al. (2021), Copyright 2021: Elsevier. (**c**) Reprinted with permission from Yin et al. (2022), Copyright 2022: Springer Nature. (**d**) Reprinted with permission from Lee et al. (2020), Copyright 2020: AAAS. (**e**) Reprinted with permission from Hong et al. (2021). Copyright 2021: AAAS

(Ghoneim et al., 2014; Ismail & Hanafiah, 2019; Pariatamby & Victor, 2013). These unique structural designs address challenges in sensor mechanical toughness, signal decoupling, accuracy, and sensitivity (Cataldi et al., 2017; Xiang et al., 2023).

1.2.3 Device Process

The preparation of functional components for wearable devices depends on their structural characteristics, with different processes suited to 1D, 2D, and 3D structures. One-dimensional linear structures are typically prepared using wet spinning and electrostatic spinning. Two-dimensional structures can be prepared using coating technology, deposition technology, and printing technology. Coating technology includes methods like spin coating, spraying, and dip-coating. Three-dimensional structures are usually prepared using micro-nanofabrication and printing techniques. These methods encompass photolithography, laser processing, anodic

Fig. 1.4 A fully flexible standalone integrated silicon electronic system with microprocessor, memory, BLE transceiver, antenna, an array of micro lithium-ion batteries, solar cells, and sensors with light actuator. Reprinted from Bonnassieux et al. (2021). Published 2021 by IOP Publishing with open access

aluminum oxide templating, folding methods, self-assembly technology, 3D printing technology, 4D printing technology, direct laser writing, and roll-to-roll technology. Each of these techniques offers unique advantages and is selected based on the specific requirements of the structure being fabricated. How far we have come in the development of flexible electronics can be judged by the image shown in Fig. 1.4.

1.3 Flexible and Stretchable Electronics Applications

Flexible and stretchable electronics, with their unique ability to bend, twist, and stretch without compromising functionality, are expected to revolutionize a wide range of fields. These advances are expected to have a significant impact on healthcare, consumer electronics, renewable energy, and automotive and industrial applications.

Flexible electronic skin can mimic the sensing ability of human skin, enabling real-time detection of environmental parameters such as humidity, pressure, and temperature. Applications include medical diagnostics, where e-skin can provide continuous health monitoring for patients, enhancing telemedicine and personalized medicine. In soft robotics, e-skin gives robots tactile sensitivity, improving interaction with delicate objects and environments. Wearable sensors integrated with machine learning algorithms provide precise physiological monitoring, tracking heart rate, breathing, sleep patterns, and physical activity. These devices can monitor patients remotely, enabling individuals to proactively manage their health. Additionally, wearable devices support human-computer interaction through advanced gesture and voice recognition technology, facilitating intuitive control of digital environments. Sports training also benefits from continuous performance tracking to help athletes optimize their training regimens.

Flexible displays are a leap forward in visual interfaces, offering lightweight, body-contour-adaptable screens. These displays can be seamlessly integrated into

smartwatches, foldable smartphones, and augmented reality (AR) glasses to enhance the user experience in consumer electronics. In healthcare, flexible displays can display biosignals directly on the skin, providing instant feedback for diagnosis. Flexible solar cells open up new possibilities for renewable energy solutions. Lightweight and moldable, flexible solar cells are ideal for portable electronics and can be integrated into clothing or accessories for on-the-go power generation. Flexible solar panels can be deployed in remote areas to power off-grid systems, contributing to sustainable development.

In summary, flexible and scalable electronics offer transformative potential across multiple industries, addressing challenges related to human-centered design, sustainability, and technology integration. As material science and manufacturing technologies continue to advance, these technologies will play an increasingly critical role in shaping the future of everyday life.

1.3.1 Wearable Intelligent Sensing Systems

Wearable sensing systems and machine learning are rapidly evolving fields with the potential to transform daily life. Wearable sensors are compact, lightweight devices worn on the body to monitor physiological and environmental parameters. These systems are used in health monitoring, sports training, and human-computer interaction, with their technology advancing rapidly and expanding across various commercial and medical applications (Han et al., 2023). Machine learning (ML), a key branch of artificial intelligence, enables computers to learn from experience and process complex, multivariate data, making it a powerful tool for interpreting and applying sensor data. ML plays a central role in fields such as autonomous navigation, financial analytics, and medical diagnostics (Sarker, 2021).

Integrating machine learning with wearable sensing systems offers several key advantages. First, it improves data processing accuracy by analyzing real-time sensor data for more precise predictions and decision-making. Second, ML enhances personalization by analyzing user habits and preferences to offer tailored recommendations.

1.3.1.1 Human-Computer Interaction

Gesture recognition is a key component of human-machine interaction (HMI), commonly used across various applications. Traditional gesture recognition often relies on visual technology, which can be affected by ambient lighting and environmental factors (Xiang et al., 2023; Yang et al., 2021a, 2021b). However, wearable sensors combined with machine learning offer a more reliable alternative. Liang et al. (2019) proposed a method for fusing multi-sensor datasets using a hierarchical support vector machine (HSVM) algorithm (Fig. 1.5). This approach was validated

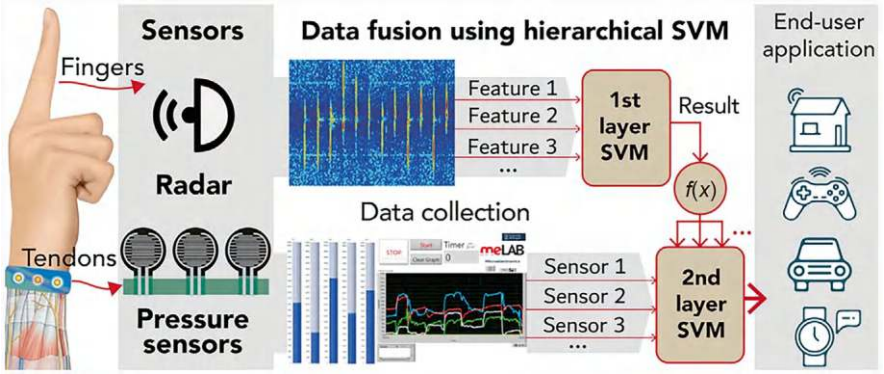

Fig. 1.5 Schematic of wearable pressure sensor-based machine learning algorithm for gesture recognition. Reprinted from Liang et al. (2019). Published 2019 by Wiley-VCH with open access

with a system that integrated radar and pressure sensor data, achieving classification accuracies of 76.7% and 69.0%, respectively (Feng et al., 2021).

Speech recognition technology enables computers to transcribe and understand human speech, but it faces challenges such as background noise and sound propagation issues. Machine learning algorithms can improve the performance of wearable systems for enhanced speech recognition accuracy (Fig. 1.6).

1.3.1.2 Physical Signs Monitoring

Wearable sensors are increasingly used to monitor key physiological signals, such as heart rate, respiration, sleep quality, and physical activity. These signals are essential for assessing an individual's health and are invaluable in medical and healthcare applications (Ahmad et al., 2002; Klosowski et al., 2014). When integrated with machine learning algorithms, wearable sensors can analyze physiological data, predict health outcomes, and extract meaningful insights. This combination enables remote patient monitoring and empowers individuals to manage their health more effectively (Kozierski et al., 2017). Respiratory monitoring, which measures parameters like respiratory rate, tidal volume, and expiratory flow rate, plays a critical role in diagnosing and managing respiratory diseases (Eren et al., 2019; Hara et al., 2015; Wang, 2024). Wearable respiratory sensors offer a noninvasive, convenient means of monitoring these parameters, facilitating early detection of conditions like restrictive and obstructive lung diseases. Researchers developed a computational fluid dynamics-assisted mask sensor network (Fig. 1.7a) that compensates for facial variability and environmental factors, ensuring accurate respiratory signal collection. This system achieved 100% accuracy in recognizing breathing patterns with machine learning assistance.

Electrocardiographic (ECG) monitoring is a standard technique for assessing heart function by measuring the electrical signals of the heart. Machine learning

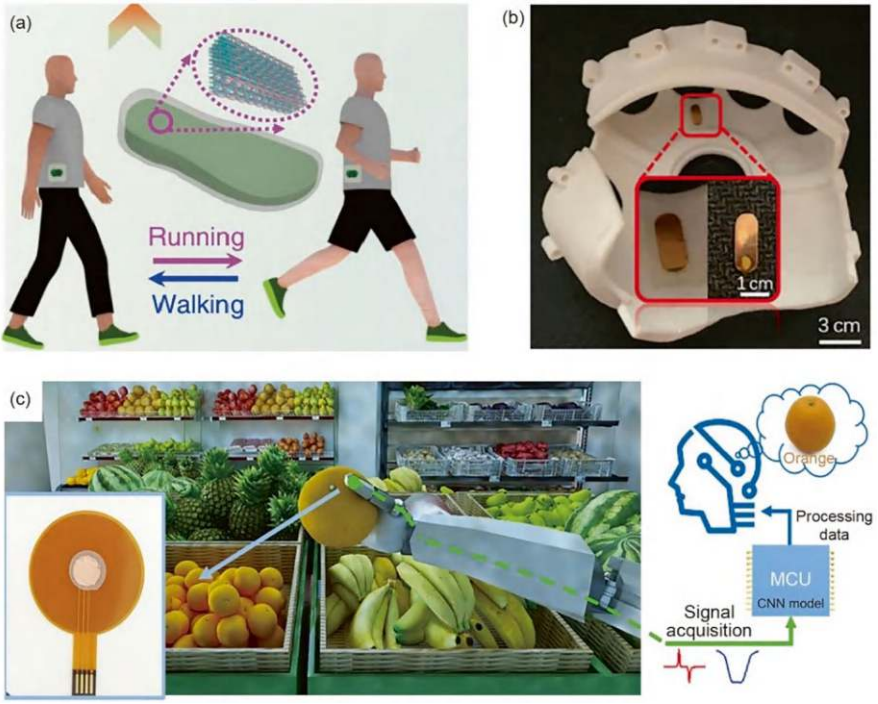

Fig. 1.6 User identification and object recognition. (**a**) Smart wearable systems for human motion monitoring and remote emergency rescue; (**b**) smart gloves with haptic feedback; (**c**) object recognition by a robotic gripper equipped with dual-mode tactile sensors. (**a**) Reprinted from (Dong K et al., 2020), Published 2020 by Springer Nature with open access. (**b**) Reprinted from (Zhu et al., 2020). Published 2020 by AAAS with open access. (**c**) Reprinted with permission from (Li et al., 2021), Copyright 2020: Elsevier

models can analyze ECG signals to assist in diagnosing heart diseases and detecting abnormalities (Buysman, 1978; Prinzmetal et al., 1956), while Shen et al. (2019) developed a 50-layer convolutional network algorithm that detected atrial fibrillation (AF) from photoplethysmogram (PPG) signals, even in the presence of motion artifacts, achieving a 95% detection accuracy.

This innovation enables enhanced analysis for a variety of applications in pharmaceuticals, life sciences, food screening, environmental monitoring, and biodefense (Chu et al., 2024; Liu et al., 2022; Niu et al., 2024).

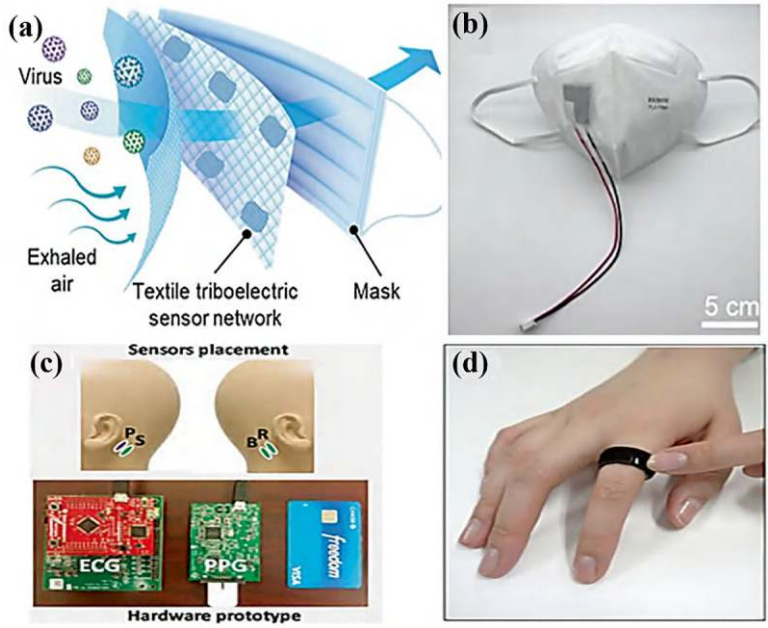

Fig. 1.7 Vital signs monitoring. (**a**) Mask sensor network; (**b**) smart mask with integrated self-powered respiratory sensor; (**c**) ECG sensor placed behind the ear; (**d**) circumferential wearable diagnostic device. (**a**) Reprinted with permission from Fang et al. (2022). Copyright 2022: Wiley-VCH. (**b**) Reprinted with permission from Zhang et al. (2022). Copyright 2022: ACS. (**c**) Reprinted from Li et al. (2023a). Published 2017 by IEEE with open access. (**d**) Reprinted from Kwon et al. (2020). Published 2020 by JMIR Publication with open access

1.3.2 E-Skin

Electronic skin (e-skin) refers to wearable sensors designed to mimic the sensory capabilities of human skin, enabling the detection of environmental parameters such as humidity, pressure, and temperature, and providing real-time feedback (Fig. 1.8a). Since the 1970s, researchers have been developing e-skin, and recent advancements have made it a promising technology for various applications, particularly in medical diagnostics, soft robotics, smart prosthetics, and human-computer interaction (Dong et al., 2018; Zhao et al., 2018).

E-skin typically consists of two key components: a flexible substrate and conductive fillers. The substrate provides mechanical flexibility, while the conductive fillers enable the sensor to detect changes in environmental conditions. Flexible film substrates, such as polydimethylsiloxane (PDMS), polyamide, and polyethylene terephthalate (PET), are commonly used due to their ease of manufacture and excellent flexibility. For instance, PDMS (Fig. 1.8b) is frequently utilized in the construction of high-sensitivity e-skin sensors, although its low compressibility and slow

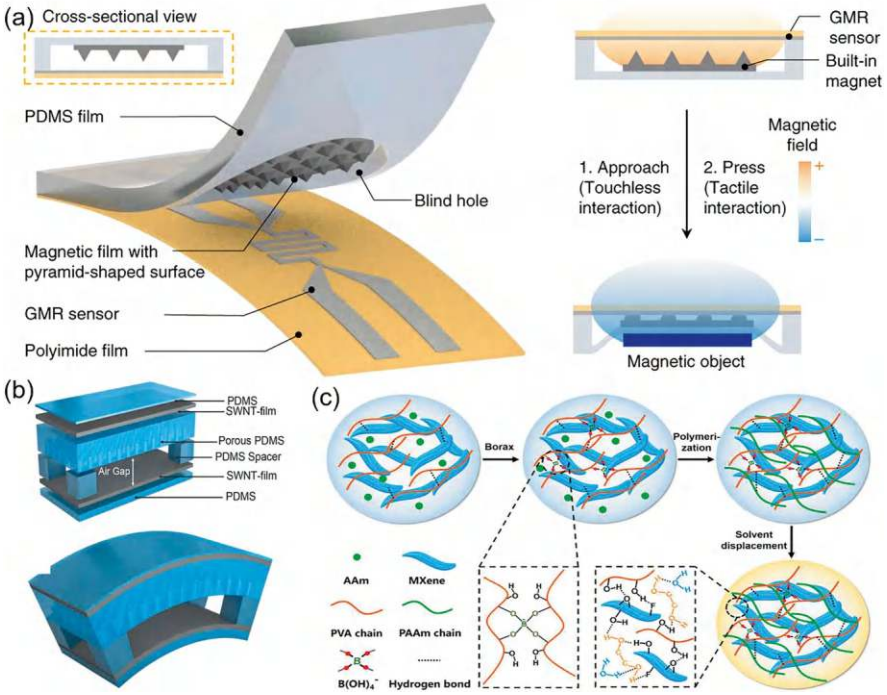

Fig. 1.8 (**a**) E-skin with different matrices; (**b**) PDMS matrix e-skin; (**c**) hydrogel based e-skin. (**a**) Reprinted from Ge et al. (2019). Published 2019 by Springer Nature with open access. (**b**) Reprinted with permission from Park et al. (2014). Copyright 2014: Wiley-VCH. (**c**) Reprinted with permission from Liao et al. (2019). Copyright 2019: Wiley-VCH

recovery time can limit its overall performance in some applications (Tan & Xu 2023; Zou et al., 2018). Hydrogels, which possess an elastic modulus similar to human skin, are another promising material for e-skin. Their high-water content and biocompatibility make them ideal for wearable sensors that require skin-like properties (Fig. 1.8c).

Despite their advancements, e-skin devices face several challenges. They must endure dynamic environments involving bending, twisting, and stretching without losing functionality. To address these challenges, e-skin needs to be highly adhesive, stretchable, and able to self-heal, while also maintaining biocompatibility and biodegradability, particularly in biomedical applications where the sensors may be in direct contact with human skin or implanted inside the body. Natural polymers, such as chitosan, are increasingly used as substrates because of their biodegradability and good cellular compatibility (Fig. 1.9b) (Chen et al., 2022b).

These advancements in material science and fabrication techniques have significantly improved the performance and applicability of E-skin, moving it closer to becoming a versatile tool for health monitoring and other advanced applications.

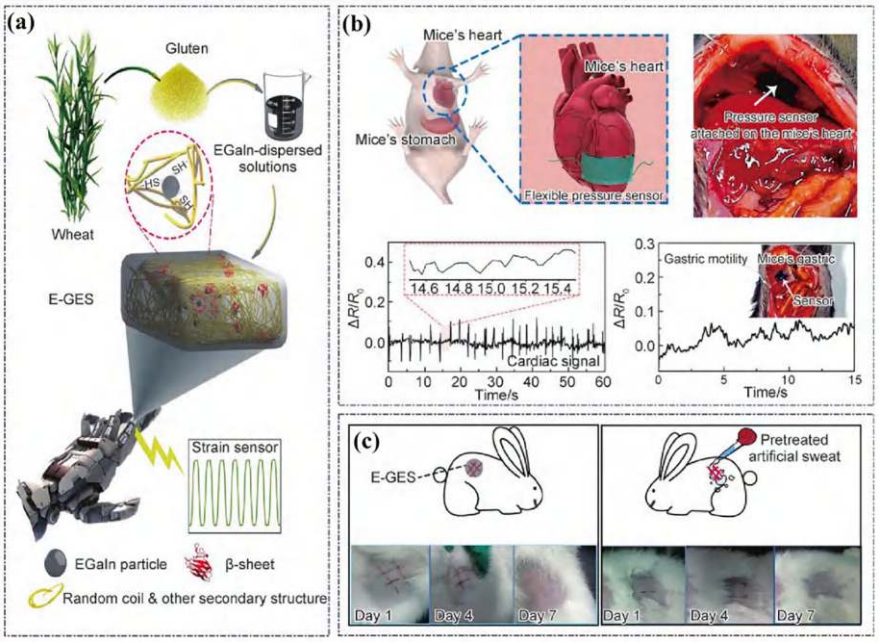

Fig. 1.9 E-skin biocompatibility: (**a**) Complex composite structures: EGaIn/gluten/silk protein hydrogel networks combining the benefits of metals, proteins, and hydrogels for creating biomedical applications with unique physical and chemical properties; (**b**) an advanced experimental device for detecting heartbeat signals directly from the epicardium (outer layer of the heart) of living mice was demonstrated. A small incision in the chest exposes the heart, allowing direct access to the epicardium without damaging the underlying myocardium, and a highly sensitive flexible electrode device that captures the subtle electrical activity associated with each heartbeat, providing precise measurements of heart rate, contractility, and other important physiological parameters; (**c**) EGaInA e-skin adhesion to rabbit skin wound. (**a**, **c**) Reprinted from Chen et al. (2022a). Published 2022 by Springer Nature with open access. (**b**) Reprinted with permission from Zhao et al. (2021). Copyright 2021: Elsevier

1.3.3 Display Technologies and Their Integration with Wearable Sensors

In modern electronic devices, displays are central to human-machine interaction, providing visual feedback and enabling user input (Bi et al., 2023; Brady et al., 2006). With advancements in technology, they have evolved from basic visualization tools to smart interfaces embedded in wireless sensor networks. This shift is evident in the Internet of Things (IoT), where smart displays serve as hubs, collecting data from connected devices and providing real-time feedback to users (Aggarwal et al., 2017; Bi et al., 2023). Recent trends focus on enhancing the integration of electronic devices with the human body for improved mobility, convenience, and interaction.

However, current smart displays remain rigid and heavy, limiting their compatibility with the soft, flexible nature of the human body. The next generation of displays is expected to be lightweight, flexible, and adaptable to body contours, resembling "skin-like" interfaces (Park et al., 2018; Zhang et al., 2023b). Progress in deformable sensor technology is paving way for light-emitting devices that can endure significant deformation and be worn directly on the body.

1.3.3.1 User Interactive Displays

Advancements in materials and device design have enabled displays to be more closely integrated with the human body, leading to the development of user-interactive displays that were previously impossible with traditional rigid systems (Aggarwal et al., 2017; Park et al., 2018; Zhao et al., 2020). For instance, Wang et al. developed an interactive active-matrix organic light-emitting diode (AMOLED) display (Fig. 1.10a, b), akin to an electronic skin, that instantly visualizes pressure applied to the display in multiple colors. Figure 1.10a, b show a fabricated multicolor AMOLED display and the same display in a curved form with all pixels activated (Molina-Lopez et al., 2019), respectively (Fig. 1.10c). The use of CNTs and

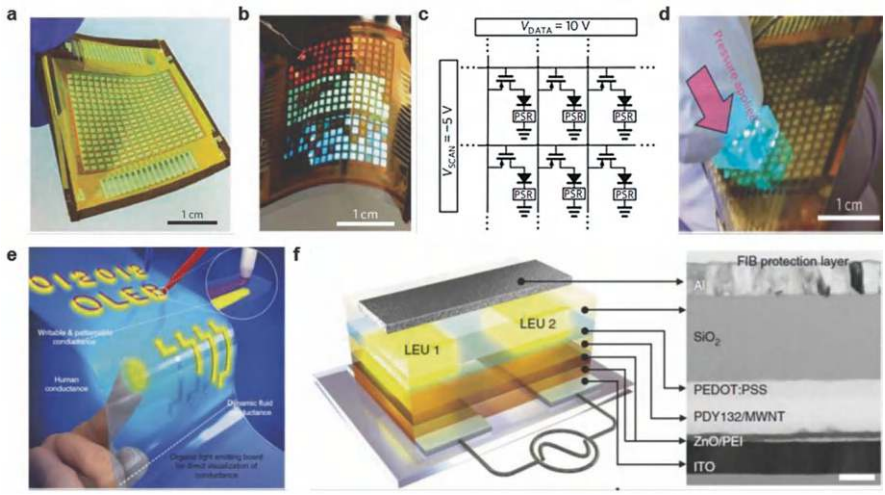

Fig. 1.10 User-interactive display. (**a**) Digital photograph of a user-interactive multicolor AMOLED display. (**b**) Photograph of activated and bent. (**c**) Schematic of the user-interactive AMOLED display circuitry. (**d**) Photographic image showing only localized luminescence of the pressed site. (**e**) Conceptual illustration of a user-interactive display for direct visualization of electrical conductance. (**f**) Construction of a user-interactive display showing a schematic (left) and corresponding high-resolution cross-sectional transmission electron microscope image showing layer information (right). (**a**–**d**) Reprinted with permission from Wang et al. (2013). Copyright 2013: Springer Nature. (**e**, **f**) Reprinted from Kim et al. (2017a). Published 2017 by Spanger Nature as open access

organic materials provided a high degree of flexibility, enabling individual pixels to withstand mechanical bending with a radius as small as approximately 4 mm (Sanguantrakul et al., 2024).

1.3.3.2 Sensor-Integrated Smart Displays for Health Monitoring

Smart display systems can visualize user biosignals for healthcare applications, integrating wearable sensors to display biological information on the user's skin in real time (Fig. 1.11a). Koo et al. (2017) recently demonstrated a health monitoring smart display capable of visualizing electrocardiogram (ECG) signals on the skin in real time (Fig. 1.11b) (Sanguantrakul et al., 2024). The developed system comprises a stretchable electrode that measures the ECG signals, which are then amplified using a CNT amplifier. The measured and amplified ECG signals are visualized through color-tunable OLEDs on the skin (Fig. 1.11c). Information is visualized by color changes depending on the shape of the retrieved signal (Fig. 1.11d). The rest of the system's electronic sensor and amplifier components are also micron-thin and provide a highly conformal fit to the skin. The ECG sensor is designed with a stretchable snake pattern, enabling a fully wearable system for real-time health monitoring of ECG signals (Bai et al., 2022).

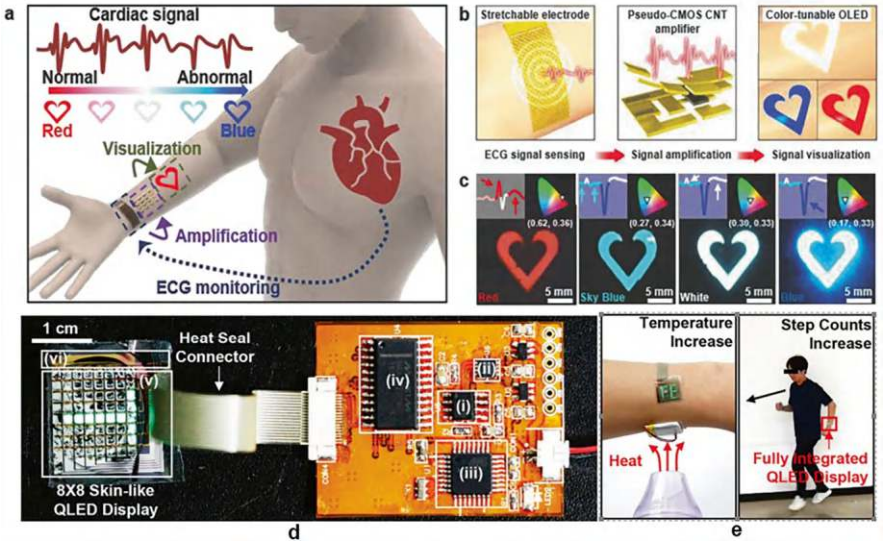

Fig. 1.11 Sensor-integrated smart display for health monitoring. (**a**) Schematic diagram showing the concept of a smart display for health monitoring. (**b**) Schematic diagram illustrating the ECG display procedure. (**c**) Digital photograph showing the color-tuned emission of a wearable OLED based on the shape of the ECG signal retrieved from the user. (**d**) Digital photograph of a QD-LED display integrated with a wearable electronic device. (**e**) Digital photograph of the capacitive touch sensor. (**a**–**c**) Reprinted with permission from Koo et al. (2017). Copyright 2017: ACS. (**d**, **e**) Reprinted with permission from Kim et al. (2017b). Copyright 2017: Wiley-VCH

1.3.3.3 Display for Assisted Pulse Oximetry

Wearable light-emitting devices are suitable for noninvasive biomedical sensing applications such as light sources and user-interactive displays (Fig. 1.11e). Specific examples include photoplethysmography (PPG) and pulse oximetry. PPG is based on the variation of light absorption with blood flow (Zhang et al., 2023b). After mounting a device consisting of a light source and photodetectors on a thin part of the body (e.g., fingertips), the system measures the change in absorbance of transmitted or reflected light as blood is pumped to the periphery with each cardiac cycle. Pulse oximetry is a PPG-based method for monitoring blood oxygen saturation, measuring the absorbance of two different wavelengths of light (Kim et al., 2022).

1.4 Challenges and Innovative Strategies

Wearable electronic devices necessitate a combination of thinness, lightweight construction, flexibility, and durability to align with human physiology and psychology while meeting personalized needs. However, these characteristics pose significant challenges in terms of mechanical robustness, managing hard and soft interfaces, and ensuring stretchability.

1.4.1 Mechanical Properties

Mechanical robustness is critical for flexible sensors to resist external and internal challenges. Strategies to address these challenges are as follows:

1. Use tough materials to absorb/disperse energy and reduce damage, thus enhancing the resistance to deformation. For example, a PDMS-MPU-IU with high tensile strength (1200%) and mechanical toughness (12,000 mJ/m^2) has been employed in electronic skin for monitoring daily human activities(Cui, 2019).
2. Structural optimization to better withstand external forces. For instance, a nanolattice with MEA, surface folds, and high toughness obtained by depositing CoCrNiTi exhibits high energy absorption (60 MJ/m^3) and can endure more than 50% strain (Fig. 1.9b) (Li et al., 2023b).

1.4.2 Multiple Signal Decoupling

As wearable sensors become thinner and more flexible, they face the challenge of multiple signal response crosstalk arising from coupling and external signal interference. Flexible materials produce responses to various stresses, leading to signal

interference. And the applied pressure also transmits to unstressed areas, triggering signal responses there. Moreover, changes in sweat and temperature can further interfere with signal detection, affecting the accuracy of pressure and strain signals.

To address these issues, one approach is to optimize material responses by using single-stimulus-responsive materials to reduce interference. For example, a MXene/Ag nanowire film integrated with microcontrollers was used to make precise pressure sensors for prosthetics, robotics, and artificial blood vessels (Cheng et al., 2015). Another strategy is to improve structural design to minimize inter-structural coupling.

1.4.3 Signal Stability and Accuracy

In flexible wearable sensors, signal stability and accuracy are of crucial importance due to the challenges of signal drift in long-term wear or complex environments. Several strategies can enhance stability. These are (i) selection of optimal technology and environmentally stable materials (Davoodi et al., 2020) and (ii) instrumental compensation of the observed drift in the characteristics of flexible sensors. For example, Wang et al., (2020) demonstrated this by incorporating a compensated thermistor with a similar shape and material as the sensing resistor into a Wheatstone-bridge feedback circuit, compensating for temperature and strain effects. These strategies, as illustrated in Fig. 1.12, offer the opportunity to significantly improve signal stability in flexible wearable sensors. Flexible film encapsulation also plays a crucial role by providing a biocompatible, inert, waterproof, and mechanically robust layer to protect sensitive components, reducing noise and signal drift (Adams et al., 2015).

1.4.4 Environmentally Friendly and Biosafety

Environmental protection, greenness, and degradability are key priorities in today's society, especially in the design and manufacturing of wearable sensors. Materials used in wearable sensors should be recyclable and biodegradable to minimize environmental impact. Paper-based sensor technology offers a promising solution, providing low-cost, biodegradable, and biocompatible substrates that are environmentally friendly. These sensors help reduce electronic waste, improve energy efficiency, and promote sustainable development.

Biosafety is another crucial aspect, directly affecting the safety, reliability, and user comfort of wearable devices. To ensure long-term wearability, wearable sensors must be biocompatible, avoiding toxicity, allergies, immune reactions, or discomfort when in contact with the skin. To enhance user experience, sensors should be thin, light, miniaturized, and highly integrated, as well as ergonomic, breathable, water-resistant, and strongly adhesive. Advanced processing techniques, such as

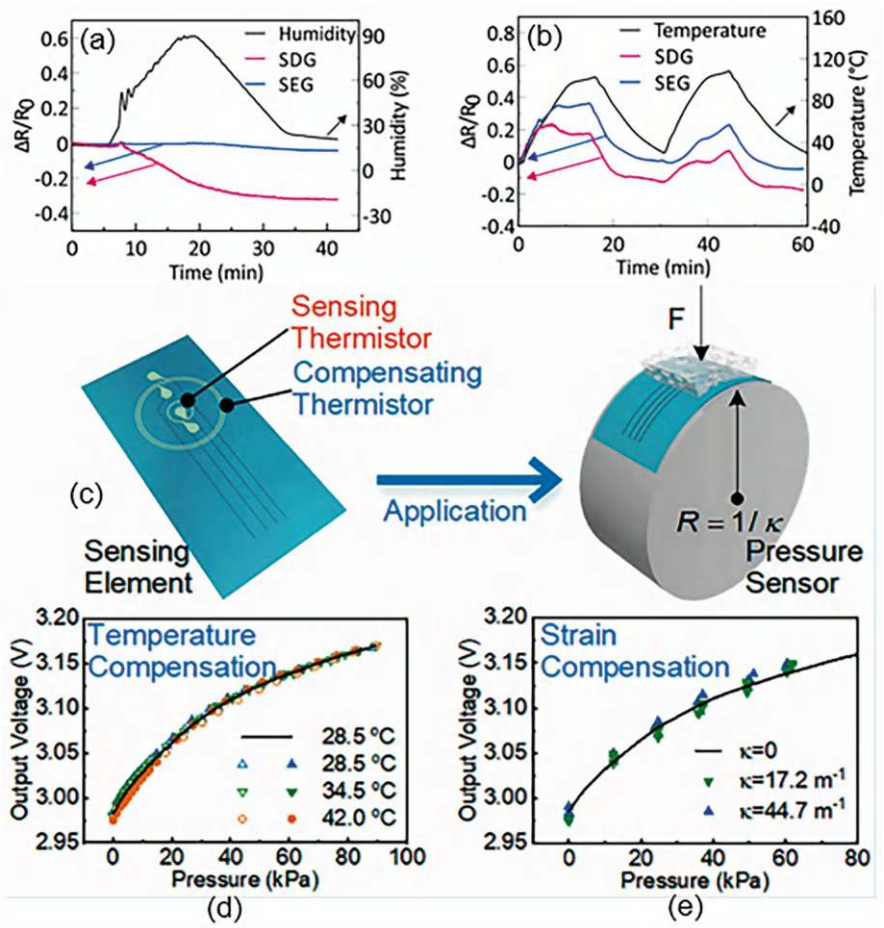

Fig. 1.12 Strategies to improve signal stability. (**a**, **b**) Use of environmentally stable materials. Sensor with surface-embedded graphene (SEG) coating as opposed to sensor with surface-deposited graphene (SDG) coating was found to be insensitive to humidity (**a**); the same order of sensitivity to temperature resulted in both types of sensors (**b**). (**c**, **d**) Circuit compensation. Results indicate that the temperature and strain effects can be tremendously eliminated using the proposed compensation method, which is fast, self-sustained, and expedient to realize. (**a**, **b**) Reprinted with permission from Davoodi et al. (2020). Copyright 2020: ACS; (**c**, **d**) Reprinted with permission from Wang et al. (2020). Copyright 2020: ACS

micro-nano processing and 3D printing, are essential to achieve these design goals (Chen et al., 2018; Cui, 2019).

1.5 Summary and Outlook

This chapter has introduced the fundamental construction strategies for flexible and stretchable electronics, covering key aspects such as materials, structure, and device processing. We have explored the selection of flexible electronic materials, including common substrates, conductive fillers, and their combinations, as well as their applications in sensors and wearable devices. Significant progress has been made in the use of flexible electronics for wearable intelligent systems, human monitoring, and e-skin technologies. The integration with display technologies has opened new avenues for user interaction and health monitoring. However, challenges remain in the areas of mechanical properties, signal stability, and environmental compatibility, which must be addressed for these technologies to reach their full potential.

As flexible electronics continue to advance, concerns regarding biosafety and environmental impact have become increasingly important. The use of synthetic polymers and metals in traditional flexible devices may raise potential environmental risks and biocompatibility issues. To address these concerns, the emerging concept of paper-based sensors offers a promising solution. Paper-based sensors are environmentally friendly, biodegradable, and can be engineered to retain the necessary flexibility and stretchability for diverse applications. These sensors, combined with innovative sensing technologies, present a sustainable alternative for health monitoring and environmental sensing, and hold great promise for future developments in flexible electronics. The shift toward paper-based materials could play a key role in reducing the ecological footprint of electronic devices while maintaining their performance and functionality.

References

Adams, J., Salvador, M., Lucera, L., Langner, S., Spyropoulos, G. D., Fecher, F. W., et al. (2015). Water ingress in encapsulated inverted organic solar cells: Correlating infrared imaging and photovoltaic performance. *Advanced Energy Materials, 20*, 1501065. https://doi.org/10.1002/aenm.201501065

Aggarwal, D., Zhang, W. Y., Hoang, T., Ploderer, B., Vetere, F., & Bradford, M. (2017). SoPhy: A wearable technology for lower limb assessment in video consultations of physiotherapy. In *Proceedings of ACM SIGCHI conference on human factors in computing systems (CHI), Denver, CO* (pp. 3916–3928). https://doi.org/10.1145/3025453.3025489

Ahmad, A. M., Siang, L. E., & Mohamad, F. (2002). Autopoietic modeling of speech recognition. In *Proceedings of 6th world multi-conference on systemics, cybernetics and informatics (SCI 2002)/8th international conference on information systems analysis and synthesis (ISAS 2002), Orlando, FL* (pp. 228–231).

Bai, L., Jin, Y., Shang, X., Shi, L. J., Jin, H. Y., Zhou, R., & Lai, S. Q. (2022). Bio-inspired visual multi-sensing interactive ionic skin with asymmetrical adhesive, antibacterial and self-powered functions. *Chemical Engineering Journal, 438*(135596), 438. https://doi.org/10.1016/j.cej.2022.135596

Bi, S., Jin, W., Han, X., Metts, J., Ostrosky, A. D., Lehotsky, J., et al. (2023). Flexible pressure visualization equipment for human-computer interaction. *Materials Today Sustainability, 21*, 35–36. https://doi.org/10.1016/j.mtsust.2023.100318

Bonnassieux, Y., Brabec, C. J., Cao, Y., Carmichae, T. B., Chabinyc, M. I., Cheng, K.-T., et al. (2021). The 2021 flexible and printed electronics roadmap. *Flexible and Printed Electronics, 6*, 023001. https://doi.org/10.1088/2058-8585/abf986

Brady, S., Carson, B., O'Gorman, D., Moyna, N., & Diamond, D. (2006). Combining wireless with wearable technology for the development of on-body networks. In *Proceedings of international workshop on wearable and implantable body sensor networks* (pp. 31–34). MIT. https://doi.org/10.1109/BSN.2006.16

Buysman, J. R. (1978). Delayed return of electrocardiographic tracing after defibrillatory electric shock caused by electrocardiographic monitor/electrode incompatibilities. *The American Journal of Cardiology, 42*(3), 523. https://doi.org/10.1016/0002-9149(78)90954-2

Cataldi, P., Ceseracciu, L., Athanassiou, A., & Bayer, I. S. (2017). Healable cotton-graphene nanocomposite conductor for wearable electronics. *ACS Applied Materials & Interfaces, 9*(16), 13825–13830. https://doi.org/10.1021/acsami.7b02326

Chen, D., Lou, Z., Jiang, K., & Shen, G. Z. (2018). Device configurations and future prospects of flexible/stretchable Lithium-ion batteries. *Advanced Functional Materials, 28*(51), 288–291. https://doi.org/10.1002/adfm.201805596

Chen, B., Cao, Y. D., Li, Q. Y., Yan, Z., Liu, R., Zhao, Y. J., et al. (2022a). Liquid metal-tailored gluten network for protein-based e-skin. *Nature Communications, 13*(1), 1206. https://doi.org/10.1038/s41467-022-28901-9

Chen, Y., Gao, Z., Zhang, F., Wen, Z., & Sun, X. (2022b). Recent progress in self-powered multifunctional e-skin for advanced applications. *Exploration (Beijing, China), 2*(1), 20210112. https://doi.org/10.1002/EXP.20210112

Chen, S., Cui, Z. L., Wang, H. Z., Wang, X. L., & Liu, J. (2023). Liquid metal flexible electronics: Past, present, and future. *Applied Physics Reviews, 10*(2), 021308. https://doi.org/10.1063/5.0140629

Cheng, T., Zhang, Y. Z., Lai, W. Y., & Huang, W. (2015). Stretchable thin-film electrodes for flexible electronics with high deformability and stretchability. *Advanced Materials, 27*(22), 3349–3376. https://doi.org/10.1002/adma.201405864

Cherukhin, I., & Xin, G. Y. (2019). Performance improvements in flexible polymer-based microwave devices. In *Proceedings of IEEE Asia-Pacific microwave conference (APMC), Singapore* (pp. 619–621). https://doi.org/10.1109/APMC46564.2019.9038351

Chu, Y., Lvzeng, Z., Lu, K. J., Chen, Y. Y., Shen, Y. C., Jing, K. J., et al. (2024). Magnetic porous hydrogel-enhanced wearable patch sensor for sweat Zinc ion monitoring. *Sensors, 24*(17), 778–799. https://doi.org/10.3390/s24175627

Corzo, D., Tostado-Blázquez, G., & Baran, D. (2020). Flexible electronics: Status, challenges and opportunities. *Frontiers in Electronics, 1*, 594003. https://doi.org/10.3389/felec.2020.594003

Cui, Z. (2019). Printing practice for the fabrication of flexible and stretchable electronics. *Science China Information Sciences, 62*(2), 224–232. https://doi.org/10.1007/s11431-018-9388-8

Davoodi, E., Montazerian, H., Haghniaz, R., Rashidi, A., Ahadian, S., Sheikhi, A., et al. (2020). 3D-printed ultra-robust surface-doped porous silicone sensors for wearable biomonitoring. *ACS Nano, 14*(2), 1520–1532. https://doi.org/10.1021/acsnano.9b06283

Dong, Z. M., Duan, B. X., Li, J. C., & Yang, Y. T. (2018). A stretchable flexible electronic platform for mechanical and electrical collaborative design. *Science China Information Sciences, 61*(6), 060418. https://doi.org/10.1007/s11432-017-9432-8

Dong, K., et al. (2020). Shape adaptable and highly resilient 3D braided triboelectric nanogenerators as e-textiles for power and sensing. *Nature Communications 11*, 2868. https://doi.org/10.1038/s41467-020-16642-6

Eren, C., Karamzadeh, S., & Kartal, M. (2019). The artifacts of human physical motions on vital signs monitoring. In *Proceedings of international scientific meeting on electrical-electronics and biomedical engineering and computer science (EBBT)*. Istanbul Arel University. https://doi.org/10.1109/EBBT.2019.8741668

Fang, Y., Xu, J., Xiao, X., Zou, Y., Zhao, X., Zhou, Y., & Chen, J. (2022). A deep-learning-assisted on-mask sensor network for adaptive respiratory monitoring. *Advanced Materials, 34*(24), 2200252. https://doi.org/10.1002/adma.202200252

Fayomi, C., Facpong, H. A., Mueller, J., & Roberts, G. W. (2017). Passive sensors for flexible hybrid-printed electronics systems: An IC designer view. In *Proceedings of 60th IEEE international Midwest symposium on circuits and systems (MWSCAS)* (pp. 807–810). Tufts University. https://doi.org/10.1109/MWSCAS.2017.8053046

Feng, Z., Wu, J. L., & Ni, T. L. (2021). RETRACTED: Research and application of multifeature gesture recognition in human-computer interaction dased on virtual reality technology. *Wireless Communications and Mobile Computing, 1*, 9842785. https://doi.org/10.1155/2023/9842785

Ge, J., Wang, X., Drack, M., Volkov, O., Liang, M., Bermúdez, G. S. C., et al. (2019). A bimodal soft electronic skin for tactile and touchless interaction in real time. *Nature Communications, 10*, 4405. https://doi.org/10.1038/s41467-019-12303-5

Ghoneim, M. T., Hanna, A. N., & Hussain, M. M. (2014). CMOS compatible fabrication of flexible and semi-transparent FeRAM on ultra-thin bulk monocrystalline silicon (100) fabric. In *Proceedings of 14th IEEE international conference on nanotechnology (IEEE-NANO), Toronto, Canada* (pp. 448–451). https://doi.org/10.1109/NANO.2014.6967961

Han, Y. T., Cui, Y. W., Liu, X. X., & Wang, Y. Q. (2023). A review of manufacturing methods for flexible devices and energy storage devices. *Biosensors (Basel), 13*(9), 896. https://doi.org/10.3390/bios13090896

Hara, S., Kawabata, T., & Nakamura, H. (2015). Real-time sensing, transmission and analysis for vital signs of persons during exercises. In *Proceedings of 37th annual international conference of the IEEE-Engineering-in-Medicine-and-Biology-Society (EMBC), Milan, Italy* (pp. 4017–4020). https://doi.org/10.1002/adma.201700375

Hong, Y., Wang, B., Lin, W. K., Jin, L. H., Liu, S. Y., Luo, X. W., et al. (2021). Highly anisotropic and flexible piezoceramic kirigami for preventing joint disorders. *Science Advances, 7*(11), eabf0795. https://doi.org/10.1126/sciadv.abf0795

Hu, L. X., Chee, P. L., Sugiarto, S., Yu, Y., Shi, C. Q., Yan, R., et al. (2023). Hydrogel-based flexible electronics. *Advanced Materials, 35*(14), 2205326. https://doi.org/10.1002/adma.202205326

Ismail, H., & Hanafiah, M. M. (2019). Discovering opportunities to meet the challenges of an effective waste electrical and electronic equipment recycling system in Malaysia. *Journal of Cleaner Production, 238*, 117927. https://doi.org/10.1016/j.jclepro.2019.117927

Kim, E. H., Cho, S. H., Lee, J. H., Jeong, B., Kim, R. H., Yu, S., Lee, T. W., Shim, W., & Park, C. (2017a). Organic light emitting board for dynamic interactive display. *Nature Communications, 8*, 14964. https://doi.org/10.1038/ncomms14964

Kim, J., Shim, H. J., Yang, J., Choi, M. K., Kim, D. C., Kim, J., Hyeon, T., & Kim, D. H. (2017b). Ultrathin quantum dot display integrated with wearable electronics. *Advanced Materials, 29*(38), 1700217. https://doi.org/10.1002/adma.201700217

Kim, D. S., Lee, Y. H., Kim, J. W., Lee, H., Jung, G., & Ha, J. S. (2022). A stretchable array of high-performance electrochromic devices for displaying skin-attached multi-sensor signals. *Chemical Engineering Journal, 429*, 132289. https://doi.org/10.1016/j.cej.2021.132289

Klosowski, P., Dustor, A., Izydorczyk, J., Kotas, J., & Slimok, J. (2014). Speech recognition based on open source speech processing software. In *Proceedings of 21st international science conference on computer networks (CN), Brunow, Poland* (pp. 308–317). https://doi.org/10.1007/978-3-319-07941-7_31

Koo, J. H., Jeong, S., Shim, H. J., Son, D., Kim, J., Kim, D. C., et al. (2017). Wearable electrocardiogram monitor using carbon nanotube electronics and color-tunable organic light-emitting diodes. *ACS Nano, 11*(10), 10032–10041. https://doi.org/10.1002/adfm.201801834

Kozierski, P., Sadalla, T., Drgas, S., Dabrowski, A., & Giernacki, W. (2017). Polish whispery speech recognition - minimum sampling frequency. In *Proceedings of 22nd international*

conference on methods and models in automation and robotics (MMAR), Miedzyzdroje, Poland (pp. 611–615). https://doi.org/10.1109/MMAR.2017.8046898

Kwon, S., Hong, J., Choi, E. K., Lee, B., Baik, C., Lee, E., et al. (2020). Detection of atrial fibrillation using a ring-type wearable device (CardioTracker) and deep learning analysis of photoplethysmography signals: Prospective observational proof-of-concept study. *Journal of Medical Internet Research, 22*(5), e16443. https://doi.org/10.2196/16443

Lee, S., Franklin, S., Hassani, F. A., Yokota, T., Nayeem, O. G., Wang, Y., et al. (2020). Nanomesh pressure sensor for monitoring finger manipulation without sensory interference. *Science, 370*(6519), 966–970. https://doi.org/10.1126/science.abc9735

Li, X. Y., Liu, J. Y., & Zhu, H. R. (2021). Functionalized and environment-friendly carbon materials for flexible and wearable electronic devices. In *Proceedings of international conference on optoelectronic materials and devices (ICOMD), Guangzhou, Peoples R China*. https://doi.org/10.1117/12.2628680

Li, J. C., Yin, J., Ramakrishna, S., & Ji, D. X. (2023a). Smart mask as wearable for post-pandemic personal healthcare. *Biosensors (Basel), 13*(2), 107063. https://doi.org/10.1016/j.nanoen.2022.107063

Li, X. C., Yao, L. Q., Song, W., Liu, F., Wang, Q., Chen, J., Xue, Q., & Lai, W. Y. (2023b). Intrinsically stretchable electroluminescent elastomers with self-confinement effect for highly efficient non-blended stretchable OLEDs. *Angewandte Chemie International Edition, 62*(2), e202213749. https://doi.org/10.1002/anie.202213749

Liang, X. P., Li, H. B., Wang, W. P., Liu, Y. C., Ghannam, R., Fioranelli, F., & Heidari, H. (2019). Fusion of wearable and contactless sensors for intelligent gesture recognition. *Advanced Intelligent Systems, 1*(7), 1900088. https://doi.org/10.1002/aisy.201900088

Liao, H., Guo, X. L., Wan, P. B., & Yu, G. H. (2019). Conductive MXene nanocomposite organohydrogel for flexible, healable, low-temperature tolerant strain sensors. *Advanced Functional Materials, 29*(39), 1904507. https://doi.org/10.1002/adfm.201904507

Liu, M. Y., Wang, S. Q., Zheng, H., Yang, X. Q., & Zhang, T. (2022). Research progress of flexible wearable sweat sensors based on microchannel design. *Chinese Journal of Analytical Chemistry, 50*(11), 1627–1638. https://doi.org/10.3390/mi8010012

Luo, M. H., Liu, Y. H., Huang, W. B., Qiao, W., Zhou, Y., Ye, Y., & Chen, L. S. (2017). Towards flexible transparent electrodes based on carbon and metallic materials. *Micromachines, 8*(1), 105580. https://doi.org/10.1016/j.nanoen.2020.105580

Luo, S., Zhou, X., Tang, X. Y., Li, J. L., Wei, D. C., Tai, G. J., et al. (2021). Microconformal electrode-dielectric integration for flexible ultrasensitive robotic tactile sensing. *Nano Energy, 80*, 105580. https://doi.org/10.1016/j.nanoen.2020.105580

Miao, Y., Wan, L. J., Ling, X. F., Chen, B., Pan, L. K., & Gao, Y. (2020). Mask-free preparation of patterned carbonized carboxymethyl cellulose on fabrics for flexible electronics. *ACS Applied Electronic Materials, 2*(3), 855–862. https://doi.org/10.1021/acsaelm.0c00084

Miyamoto, A., Lee, S., Cooray, N. F., Lee, S., Mori, M., Matsuhisa, N., et al. (2017). Infammation-free, gas-permeable, lightweight, stretchable on-skin electronics with nanomeshes. *Nature Nanotechnology, 12*(9), 907. https://doi.org/10.1038/nnano.2017.125

Molina-Lopez, F., Gao, T. Z., Kraft, U., Zhu, C., Öhlund, T., Pfattner, R., et al. (2019). Inkjet-printed stretchable and low voltage synaptic transistor array. *Nature Communications, 10*, 2676. https://doi.org/10.1038/s41467-019-10569-3

Nan, N., He, J. X., You, X. L., Sun, X. Q., Zhou, Y. M., Qi, K., et al. (2019). A stretchable, highly sensitive, and multimodal mechanical fabric sensor based on electrospun conductive nanofiber yarn for wearable electronics. *Advanced Materials Technologies, 4*(3), 1800338. https://doi.org/10.1002/admt.201800338

Niu, J. Q., Lin, S. J., Chen, D., Wang, Z. T., Cao, C., Gao, A., et al. (2024). A fully elastic wearable electrochemical sweat detection system of tree-bionic microfluidic structure for real-time monitoring. *Small, 20*(11), 2306769. https://doi.org/10.1002/smll.202306769

Pariatamby, A., & Victor, D. (2013). Policy trends of e-waste management in Asia. *Journal of Material Cycles and Waste Management, 15*(4), 411–419. https://doi.org/10.1007/s10163-013-0136-7

Park, S., Kim, H., Vosgueritchian, M., Cheon, S., Kim, H., Koo, J. H., et al. (2014). Stretchable energy-harvesting tactile electronic skin capable of differentiating multiple mechanical stimuli modes. *Advanced Materials, 26*(43), 7324–7332. https://doi.org/10.1002/adma.201402574

Park, J., Kim, J., Kim, S. Y., Cheong, W. H., Jang, J., Park, Y. G., et al. (2018). Soft, smart contact lenses with integrations of wireless circuits, glucose sensors, and displays. *Science Advances, 4*(1), eaap9841. https://doi.org/10.1126/sciadv.aap9841

Prinzmetal, M., Goldman, A., Massumi, R. A., Rakita, L., Schwartz, L., Kennamer, R., et al. (1956). Clinical implications of errors in electrocardiographic interpretation; heart disease of electrocardiographic origin. *Journal of the American Medical Association, 161*(2), 138–143. https://doi.org/10.1001/jama.1956.02970020018005

Qiao, Y., Luo, J., Cui, T., Liu, H., Hao Tang, H., et al. (2023). Soft electronics for health monitoring assisted by machine learning. *Nano-Micro Letters, 15*, 66. https://doi.org/10.1007/s40820-023-01029-1

Sanguantrakul, J., Hemakom, A., Soonrach, T., & Israsena, P. (2024). PDMS/CNT electrodes with bioamplifier for practical in-the-ear and conventional biosignal recordings. *Journal of Neural Engineering, 21*(5), 056017. https://doi.org/10.1088/1741-2552/ad7905

Sarker, I. H. (2021). Machine learning: Algorithms, real-world applications and research directions. *SN Computer Science, 2*, 160. https://doi.org/10.1007/s42979-021-00592-x

Seager, R. D., Chauraya, A., Zhang, S., Whittow, W., & Vardaxoglou, Y. (2013). Flexible radio frequency connectors for textile electronics. *Electronics Letters, 49*(22), 1371–1373. https://doi.org/10.1049/el.2013.2105

Senawi, N. H., & Sheau-Ting, L. (2016). Attributes to facilitate e-waste recycling behaviour. In *Proceedings of 4th international building control conference (IBCC), Kuala Lumpur, Malaysia*. https://doi.org/10.1051/matecconf/20166600058

Shen, Y., Voisin, M., Aliamiri, A., Avati, A., Hannun, A., & Andrew Ng, A. (2019). Ambulatory atrial fibrillation monitoring using wearable photoplethysmography with deep learning. In *Proceedings of the 25th ACM SIGKDD International Conference on Knowledge Discovery & Data Mining, KDD'19* (pp. 1909–1916). https://doi.org/10.1145/3292500.3330657

Tan, D., & Xu, B. A. (2023). Advanced interfacial design for electronic skins with customizable functionalities and wearability. *Advanced Functional Materials, 33*(49), 2306793. https://doi.org/10.1002/adfm.202306793

Wang, W., et al. (2022). Double-Layered Conductive Network Design of Flexible Strain Sensors for High Sensitivity and Wide Working Range. *ACS Applied Materials & Interfaces 14*, 36611–36621. https://doi.org/10.1021/acsami.2c08285

Wang, X. S. (2024). Application of IoT real-time monitoring based on optical sensors in residents' sports and health service system. *Optical and Quantum Electronics, 56*(4), 1602. https://doi.org/10.1007/s11082-023-06211-8

Wang, C., Hwang, D., Yu, Z., Takei, K., Park, J., Chen, T., Ma, B., & Javey, A. (2013). User-interactive electronic skin for instantaneous pressure visualization. *Nature Materials, 12*(10), 899–904. https://doi.org/10.1038/NMAT3711

Wang, L., Zhu, R., & Li, G. (2020). Temperature and strain compensation for flexible sensors based on thermosensation. *ACS Applied Materials & Interfaces, 12*(1), 1953–1961. https://doi.org/10.1021/acsami.9b21474

Xiang, S. W., Qin, L., Wei, X. F., Fan, X., & Li, C. M. (2023). Fabric-type flexible energy-storage devices for wearable electronics. *Energies, 16*(10), 4047. https://doi.org/10.3390/en16104047

Yang, X. Z., Chen, K. Q., & Wan, H. G. (2021a). An approach to dynamic gesture recognition based on instantaneous posture. In *Proceedings of 7th IEEE international conference on virtual reality (ICVR)* (pp. 90–95). Foshan University.

Yang, Z. T., Zhu, Z. T., Chen, Z. X., Liu, M. J., Zhao, B. B., Liu, Y. S., et al. (2021b). Recent advances in self-powered piezoelectric and triboelectric sensors: From material and structure design to frontier applications of artificial intelligence. *Sensors, 21*(24), 8422. https://doi.org/10.3390/s21248422

Yin, L., Wang, Y. H., Zhan, J., Bai, Y. Z., Hou, C., Wu, J. F., et al. (2022). Chest-scale self-compensated epidermal electronics for standard 6-precordial-lead ECG. *npj Flexible Electronics, 6*(1), 29. https://doi.org/10.1038/s41528-022-00159-7

Yue, B. B., Ding, X., & College of Textiles, D.U. (2012). Polypyrrole coated cotton fabric as flexible electrode for supercapacitor application. In *Proceedings of international forum on biomedical textile materials (IFBMTM)* (pp. 145–149). Donghua University.

Zhang, K., Li, Z., Zhang, J., Zhao, D., Pi, Y., Shi, Y., et al. (2022). Biodegradable smart face masks for machine learning-assisted chronic respiratory disease diagnosis. *ACS Sensors, 7*(10), 3135–3143. https://doi.org/10.1021/acssensors.2c01628

Zhang, Y. C., Tan, Y. R., Lao, J. Z., Gao, H. J., & Yu, J. (2023a). Hydrogels for flexible electronics. *ACS Nano, 17*(11), 9681–9693. https://doi.org/10.1021/acsnano.3c02897

Zhang, Y. H., Hu, Y. B., Jiang, N., & Yetisen, A. K. (2023b). Wearable artificial intelligence biosensor networks. *Biosensors & Bioelectronics, 219*, 125421. https://doi.org/10.1016/j.cej.2020.125421

Zhao, X. L., Wang, R., Xiao, X. H., Lu, C. Y., Wu, F. C., Cao, R. R., Jiang, C. Z., & Liu, Q. (2018). Flexible cation-based threshold selector for resistive switching memory integration. *Science China Information Sciences, 61*(6), 060413. https://doi.org/10.1007/s11432-017-9352-0

Zhao, H. H., Yan, S., Jin, X. H., Niu, P. Y., Zhang, G. Z., Wu, Y. K., & Li, H. J. (2020). Tough, self-healable and conductive elastomers based on freezing-thawing strategy. *Chemical Engineering Journal, 402*, 125421. https://doi.org/10.1016/j.cej.2020.125421

Zhao, L. J., Wang, L. L., Zheng, Y. Q., Zhao, S. F., Wei, W., Zhang, D. W., et al. (2021). Highly-stable polymer-crosslinked 2D MXene-based flexible biocompatible electronic skins for in vivo biomonitoring. *Nano Energy, 84*, 105921. https://doi.org/10.1016/j.nanoen.2021.105921

Zhu, M. L., Sun, Z. D., Zhang, Z. X., Shi, Q. F., He, T. Y. Y., Liu, H. C., Chen, T., & Lee, C. K. (2020). Haptic-feedback smart glove as a creative human-machine interface (HMI) for virtual/augmented reality applications. *Science Advances, 6*(19), eaaz8693. https://doi.org/10.1126/sciadv.aaz8693

Zou, Z. N., Zhu, C. P., Li, Y., Lei, X. F., Zhang, W., & Xiao, J. L. (2018). Rehealable, fully recyclable, and malleable electronic skin enabled by dynamic covalent thermoset nanocomposite. *Science Advances, 4*(2), eaaq0508. https://doi.org/10.1126/sciadv.aaq0508

Chapter 2
Conventional Substrates for Flexible Devices

Zeynab Skafi and Thomas M. Brown

2.1 Introduction

2.1.1 Flexible Electronic Devices

Traditional electronics is based on rigid substrates such as circuit boards, semiconductor wafers, and glass substrates, which lack flexibility and are unsuitable for wearable, conformal, and flexible electronic applications (Ling et al., 2018; Logothetidis, 2008; Zou et al., 2018). Thin-film devices can be bent, folded, twisted, compressed, stretched, and shaped into various forms while still delivering high electrical performance, reliability, and integration (Ling et al., 2018). Materials used in these technologies need to offer high flexibility as well as excellent physical and chemical characteristics (Zou et al., 2018). Examples of semiconductors include amorphous silicon (a-Si), organic semiconductors, perovskites, gallium nitride (GaN), and gallium arsenide (GaAs). Common materials used as electrodes include thin metal layers, graphene, carbon nanotubes (CNTs), conductive polymers (such as poly(3,4-ethylenedioxythiophene) polystyrene sulfonate (PEDOT:PSS), and polyaniline (PANI)), liquid metals, and metal nanowires (Liu et al., 2023b, 2024; Sun & Rogers, 2007). Apart from finding new materials for manufacturing, designing specialized flexible and stretchable structures is equally crucial (Zou et al., 2018). Flexible substrates, like polymer films (such as polyethylene terephthalate (PET) and polyethylene naphthalate (PEN)), graphene-based substrates, Ecoflex (a platinum-catalyzed silicone), liquid crystal polymer (LCP),

Z. Skafi · T. M. Brown (✉)
CHOSE—Centre for Hybrid and Organic Solar Energy, Department of Electronic Engineering, Tor Vergata University of Rome, Rome, Italy
e-mail: Thomas.brown@uniroma2.it

G. Korotcenkov (ed.), *The Handbook of Paper-Based Sensors and Devices*,
https://doi.org/10.1007/978-3-031-91080-7_2

paper, metal foils, and biodegradable materials, are promising to replace the rigid ones (such as Si and glass). When combined with printing-based manufacturing, these materials enable low-cost, roll-to-roll (R2R) processing for mass production (Logothetidis, 2008). In general, plastic foils and thin metal foils are considered the most common flexible alternatives to rigid glass substrates (Zardetto et al., 2011). Flexible electronic technology offers a wide variety of applications in cutting-edge technological areas, such as wearable and flexible sensors (such as fitness trackers and smartwatches and smart clothing) (Anwer et al., 2022; Jiang et al., 2021), healthcare and medical devices (such as implantable electronics, sensors for diagnostics, and electronic bandages) (Cusack et al., 2024), foldable and rollable displays (such as smartphones, flexible OLED, and e-paper displays) (Burns et al., 2005; Kim et al., 2023), e-skin and soft robotics (Hu et al., 2023), prosthetics and assistive technologies (Khoshmanesh et al., 2021), smart packaging (Biji et al., 2015), internet of things (IoTs) (Aouedi et al., 2024), electromagnetic interference (EMI) shielding (Wang et al., 2022), radio-frequency identification (RFID) tags (Zhang et al., 2022), flexible antennas (Kirtania et al., 2020), flexible batteries (Zhu et al., 2024), and flexible solar cells for outdoor and indoor applications (Aftab et al., 2024; Chakraborty et al., 2024); all of these have generated significant interest in the scientific and industrial world. Many advancements have been made in research, and some related products have already been designed and manufactured.

2.2 Parameters for Substrate Selection

Substrates play a critical role in achieving high-performance devices, as their properties directly impact the overall performance. The following are some key requirements for flexible substrates in electronic devices.

2.2.1 Optical Properties

Transparency is essential for applications where light must either pass through, such as in photovoltaics and photodetectors, or exit, such as in displays and lighting (Zardetto et al., 2011). For example, bottom-emitting displays typically require more than 85% total light transmission (TLT) in the 400–800 nm wavelength range, with haze levels below 0.7% (Cheng & Wagner, 2009; MacDonald, 2015). In photovoltaic applications, the substrate should allow maximum light transmission, ideally exceeding 90% in the visible and near-infrared range (Jung et al., 2019). Additionally, substrates for liquid-crystal displays (LCDs) must have low birefringence (Cheng & Wagner, 2009).

2.2.2 Electrical and Magnetic Properties

Most substrates for flexible electronics are insulating. This guarantees electrical isolation of the components. However, electrodes need to be deposited to enable conductivity. Metals are the preferred materials. If transparency is required, transparent conductive oxides (TCOs) are commonly used to create transparent conductive electrodes (TCEs). High conductivity is a crucial role in applications where efficient electrical flow is key, such as flexible circuit boards, sensors, displays, photovoltaics, EMI shielding, and energy storage systems. TCOs are typically deposited on the substrate to create TCEs. In some cases, metallic substrates, such as stainless steel or titanium, or polymers filled with graphitic particles are used to make the substrate conductive. In addition, for specific applications, certain magnetic properties might be required to support the formation of a magnetic field, as in magnetoresistive sensors and EMI shielding (Chen et al., 2023a; Pradhan et al., 2022).

2.2.3 Thermal Properties

For flexible substrates like polymers, the ability to withstand high temperatures is critical. The glass transition temperature (T_g) must match or exceed the maximum fabrication process temperature (T_{max}) (Dong et al., 2021a). Furthermore, the coefficient of thermal expansion (CTE) should be sufficiently low to match that of the deposited layers, typically inorganic materials with low CTEs, in order to prevent cracking or detachment during thermal cycling. High thermal conductivity is also crucial for efficiently cooling circuits that handle high electrical currents. Dimensional stability during processing is also important for plastic substrates (Cheng & Wagner, 2009; Dong et al., 2021a; MacDonald, 2015).

2.2.4 Mechanical Properties

A key requirement for substrates in flexible electronics is mechanical flexibility, which allows them to adapt to various conditions such as bending, stretching, and folding (Zardetto et al., 2011). This allows the substrates to withstand significant stress and strain without permanent deformation or loss of functionality, such as maintaining conductivity, which could be compromised if cracks form in brittle TCO films (Jung et al., 2019; Kim & Park, 2013). To achieve this, flexible substrates should have a low Young's modulus and high bending strength, enabling them to effectively release stress while maintaining their original performance (Subudhi & Punetha, 2023).

2.2.5 Chemical Properties

During the solution-based processing, the substrates are exposed to various chemicals, such as gases and solvents, and must therefore be chemically stable. For example, some polymers have poor resistance to organic solvents. This chemical weakness can be addressed by applying a solvent barrier (such as a layer of amorphous resin) to protect the underlying substrate (Castro-Hermosa et al., 2019; Jankowski et al., 2012). In addition, substrates must be a good barrier against oxygen ($<10^{-3}$ to 10^{-5} $cm^3/m^2/day$) and moisture ($<10^{-3}$ to 10^{-6} $g/m^2/day$) permeation depending on intrinsic stability of the device stack and applications (Cheng & Wagner, 2009).

2.2.6 Surface Roughness

In thin-film electronics, the surface roughness needs to be much lower than the thickness of the films being applied. For example, in photovoltaic devices, high surface roughness can increase the risk of electrical short circuits due to nonuniform surface coverage. However, some roughness over longer distances is acceptable for these devices (Cheng & Wagner, 2009). For the substrates with large roughness, the surface can be smoothed through planarization processes for polymer substrates or polishing for metal substrates (Skafi et al., 2024; Jung et al., 2019).

2.3 Flexible Substrates

2.3.1 Polymers as Substrate

Polymer-based materials are becoming increasingly important among the various flexible substrates used in emerging flexible electronics, particularly in displays and photovoltaics. In film substrate form, they enable the creation of lightweight, bendable, foldable, and potentially rollable optoelectronic devices, enabling new applications and installation possibilities that traditional rigid devices cannot achieve. As mentioned above, to replace glass, polymer substrates must offer similar properties, such as transparency, dimensional stability, oxygen and moisture barrier, solvent resistance, thermal stability, low CTE, and a smooth surface. Additionally, some applications may require a conductive layer. However, no plastic film provides all these properties, so polymer substrates that replace glass are typically multilayer composite structures. Despite their advantages, plastic substrates are less thermally and dimensionally stable than glass and are more prone to oxygen and moisture permeation. Listed below are some commonly used flexible polymer substrates for flexible electronics. Table 1 summarizes their key properties, while Fig. 2.1 illustrates examples of their applications in flexible electronics.

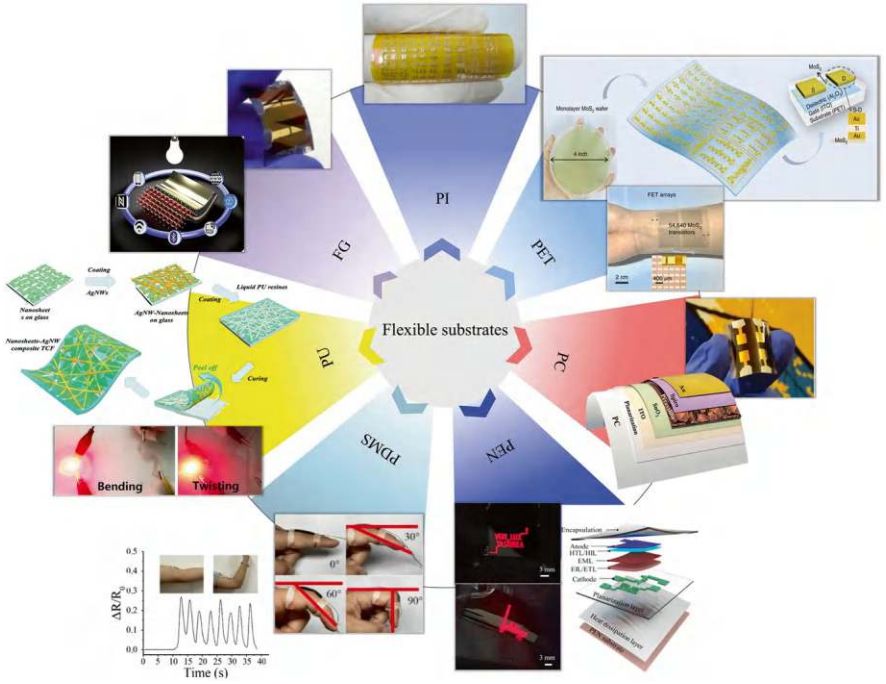

Fig. 2.1 Examples of applications of flexible polymer substrates in flexible electronics. PI: Semi-transparent and flexible surface acoustic wave (SAW) devices on polyimide (PI). Reproduced from ref. (Jin et al., 2013). Published 2013 by Springer Nature with the terms of the Creative Commons Attribution CC BY 4.0; PET: Flexible transistor arrays with integrated circuits on polyethylene terephthalate (PET). Reproduced with permission from ref. (Li et al., 2020). Copyright 2020: Springer Nature; PC: Flexible perovskite solar cells (PSCs) on polycarbonate (PC). Reproduced with permission from ref. (Skafi et al., 2024). Copyright 2024: John Wiley and Sons; PEN: Flexible top-emitting quantum-dot (QD) based light-emitting diodes (TQLED) fabricated on polyethylene naphthalate (PEN). Reproduced from ref. (Baek et al., 2023). Published 2023 by IOP with the terms of the Creative Commons Attribution CC BY-NC 4.0; PDMS: Flexible motion sensor on CNT/polydimethylsiloxane (PDMS) composite. Reproduced from ref. (Du et al., 2020). Published 2020 by MDPI with the terms of the Creative Commons Attribution CC BY 4.0; PU: MXene-silver nanowire (AgNW) composite transparent conductive film (TCF) with polyurethane (PU) as substrate for electromagnetic interference (EMI) shielding application. Reproduced with permission from ref. (Bai et al., 2021). Copyright 2021: Elsevier; FG: Flexible PSCs on flexible glass (FG). Reproduced from ref. (Castro-Hermosa et al., 2020). Published by CelPress with the terms of the Creative Commons Attribution CC BY-NC-ND 4.0

2.3.1.1 Polyethylene Terephthalate (PET)

PET is a commercially available thermoplastic polymer resin that belongs to the polyester family. Depending on its thickness, PET can range from stretchable and flexible to rigid, and it is notably lightweight. PET, particularly in the film form (~0.4–500 μm), has become the transparent substrate of choice due to its low cost (six times cheaper than PEN), good thermal stability, spin ability, UV stability, and moisture resistance (Faraj et al., 2011; Park et al., 2018b; Zardetto et al., 2011). PET

has a melting temperature (T_m) of 70–110 °C and a T_g of 115–258 °C depending also on the use of heat stabilizers (see Table 2.1) (Hassan et al., 2022). These properties make it suitable for various processing conditions without significant deformation. PET substrates are used in a wide range of flexible electronic applications, such as printed electronics (Batet et al., 2023), sensors (Na et al., 2016), and thin-film photovoltaics (Dagar et al., 2018). They are also highly desirable for display technologies, including organic light-emitting displays (OLEDs) (Gasonoo et al., 2023), resistive touch screens (Emamian et al., 2017), and electrowetting displays (Wang & Chen, 2020). This is largely due to their excellent optical properties, with over 85% optical transmission in the visible range, and their mechanical flexibility under bending or buckling conditions (Faraj et al., 2011). One of the challenges with PET is its natural shrinkage at temperatures above its T_g. However, this can be managed by blending it with highly heat-resistant bio-based polyesters (Park et al., 2020).

2.3.1.2 Polyethylene Naphthalate (PEN)

PEN is a type of polyester that is derived from naphthalene-2,6-dicarboxylic acid and ethylene glycol. It is emerging as a valuable substrate for flexible electronics, offering several advantages over traditional options like PET. With a higher T_g, shrinkage resistance, greater strength, higher modulus, improved crystallinity, and better oxygen and moisture barrier properties, PEN offers enhanced durability and the ability to withstand higher processing temperatures (see Table 2.1) (Hassan et al., 2022; Zardetto et al., 2011). These features make it an ideal substrate in

Table 2.1 Properties of different polymer flexible substrates materials

Substrate	PET	PEN	PC	PI	PDMS	PU
Glass transition temp. (T_g (°C))	70–110	120–155	145	155–360	−125	80
Melting temperature (T_m (°C))	115–258	269	115–160	250–452	–	180
Coefficient of thermal expansion (CTE) (ppm °C^{-1})	15–33	20	75	8–20	310	153
Density (g cm^{-3})	1.39	1.36	1.20–1.22	1.36–1.43	1.03	1.18
Working temp. (°C)	−50 to 150	–	−40 to 130	Up to 400	−45 to 200	130
Water adsorption (%)	0.4–0.6	0.3–0.4	0.16–0.35	1.3–3	>0.1	0.2
Solvent resistance	Good	Good	Poor	Good	Poor	Good
Transparency	Good	Good	Good	Poor	Good	Good
Dimensional stability	Good	Good	Fair	Fair	Good	Good
Ultimate elongation (%)	90	85	1–2	80	50–500	300–800
Surface roughness (nm)	30	15	74	30	–	–

Source: Reproduced with permission from ref. (Hassan et al., 2022). Copyright 2022: John Wiley and Sons

applications requiring robust mechanical and thermal properties, such as OLED displays (Li et al., 2021), printed electronics, and biosensors (Lamanna et al., 2020). Furthermore, its low surface roughness makes it suitable for high-performance thin-film devices, such as photovoltaics (Deng et al., 2023) and transistors (De Oliveira et al., 2016). However, its increased cost compared to PET may limit its widespread adoption and market potentioal (Serrano et al., 2020; Sierros et al., 2010). Despite this, PEN remains a highly attractive option for advanced flexible electronics due to its superior performance characteristics.

2.3.1.3 Polycarbonate (PC)

PC, a type of thermoplastic, has a relatively high glass transition temperature, low moisture absorption, and excellent transparency (∼90% in the visible spectrum). It is also flexible, lightweight, and cost-effective. It offers similar transparency to materials like PET (∼90%) and PEN (∼88.7%) (Patel & Wolden, 2013; Skafi et al., 2024). PC is used in electronic devices, including flexible transparent conductive films (TCFs) (Jeong et al., 2024), smart windows (SWs) (Alenazi, 2023), and EMI shielding (Astarlioglu et al., 2024), and solar cells (Skafi et al., 2024). Additionally, PC is gaining popularity in many countries for applications such as electronic IDs (e-IDs), e-passports, and e-resident permits, as it significantly improves the security of identification documents. This makes it a viable option for smart cards and ID cards. Despite these advantages, PC has some limitations, including poor chemical resistance (due to weak intermolecular forces and lack of crosslinks between the linear polymer chains), high moisture permeability, and potential surface roughness. To address these challenges, research has focused on improving PC's chemical resistance and surface smoothness using resin-based solvent resistance and planarization layers (Skafi et al., 2024). Furthermore, to reduce moisture permeability, researchers have suggested applying ultra-high permeation barriers (Castro-Hermosa et al., 2019; Erlat et al., 2005).

2.3.1.4 Polyimide (PI)

PI is known for its excellent thermal stability, mechanical robustness, chemical resistance, and electrical insulation properties. It is used in electronic devices, such as flexible circuit boards (Wang et al., 2020), antennas (Cang et al., 2021), solar cells (Koo et al., 2020), and sensors (Sahatiya et al., 2016). PI's ability to withstand high temperatures, with an operating range from −269 °C to 400 °C, makes it ideal for use in processes like sputtering and e-beam evaporation. Its strong adhesion to metal coatings and photoresists further enhances its suitability for microfabrication, allowing direct patterning on the material (Chen et al., 2021a, 2023b; Park et al., 2018a; Sahatiya et al., 2016). Despite these advantages, PI has certain limitations. For instance, traditional PI, like Kapton, absorbs visible light and has an amber hue, which restricts its use in transparent devices. This issue has been

addressed by synthesizing colorless polyimides using fluorinated dianiline, making them suitable for optoelectronic applications like displays (Park et al., 2018a; Spechler et al., 2015). Additionally, the high CTE of commercial PI films can cause internal stress when bonded to metals or inorganic materials, leading to warping and delamination. To solve this, research has focused on reducing the CTE of PI to better match that of metallic materials, improving device durability under thermal cycling. Another challenge is PI's hydrophobic and inert surface, which hinders the deposition of functional materials in processes involving water-based solutions. However, recent developments in mild, environmentally friendly surface modification techniques have made it possible to reduce PI's surface inertness without compromising its structural integrity (Fang & Tentzeris, 2018). By addressing these limitations through innovations in chemical composition and processing techniques, PI continues to play a critical role in the advancement of flexible electronics.

2.3.1.5 Polydimethylsiloxane (PDMS)

PDMS, a polymeric organo-silicon compound, has become a key material in flexible electronics due to its unique properties. PDMS offers several advantages over traditional plastic substrates, like PET (Chen et al., 2018; Sharma et al., 2021; Sharma & Chung, 2023; Qi et al., 2021). One of its main strengths is its high flexibility and stretchability, making it particularly suitable for stretchable and wearable electronics (Qi et al., 2021). PDMS also demonstrates high resilience to thermal stress, along with good chemical stability, biological compatibility, and transparency. These characteristics make it ideal for applications like flexible sensors (Cui et al., 2016), antennas (Salleh et al., 2023), electronic skins (Farman et al., 2023), and microfluidic systems (Li et al., 2013). However, a major limitation of PDMS is its poor adhesion to conductive materials like silver inks, which can result in cracking and delamination under strain. To overcome this, improving the adhesion of conductors is crucial. Surface modification methods, such as using silver-flake-based conductors, single-walled carbon nanotubes (SWCNTs), or stretchable conductors like liquid metallic alloys (e.g., Galinstan), can help expand the range of PDMS applications (Deng et al., 2024; Sondhi et al., 2018; Su et al., 2023).

2.3.1.6 Thermoplastic Polyurethane (TPU)

TPU has gained attention in flexible electronics due to its high elasticity, good flexibility, chemical stability, ease of processing, and cost-effectiveness (Chen et al., 2021b). Its low Young's modulus offers high stretchability and tensile strength (Pursula et al., 2018), making it ideal for applications, such as flexible strain sensors (Zhou et al., 2024), smart textiles (Griggs et al., 2024), EMI shielding (Wang et al., 2023), and on-skin healthcare electronics (Cho et al., 2024). TPU's good compatibility with conductive materials, such as silver nanowires (AgNWs) and

carbon nanomaterials, enhances conductivity. However, its low modulus and high thickness (often above 100 μm) can limit its conformability on curved surfaces like skin (Pursula et al., 2018). To address this, research has focused on optimizing the structure of TPU-based sensors through both macro- and microstructural design improvements, which enhance the flexibility and conductivity of the composite materials (Chen et al., 2021b). For example, modifying the surface of TPU with polyvinylpyrrolidone (PVP) enhances bonding with conductor (Zhao et al., 2024), preventing slippage during stretching and improving durability.

2.3.2 Ultra-Thin Glass as Substrate

Flexible glass is a promising material for flexible electronics due to properties like low surface roughness, dimensional stability, thermal stability (up to 700 °C), and good barrier properties against moisture and oxygen. With a water vapor transmission rate (WVTR) below 7×10^{-6} g/m^2/day, it offers a strong alternative to traditional polymer substrates like PET and PEN. It is also highly transparent, even at shorter wavelengths where PET and PEN typically absorb light (Castro-Hermosa et al., 2020; Wang et al., 2019). Its thin and flexible form, with thicknesses as low as 0.1 mm, makes it ideal for roll-to-roll (R2R) manufacturing, enabling large-scale, high-throughput production of devices (Garner et al., 2017a, b), including displays (Garner et al., 2013), sensors (Dadhich et al., 2023), and photovoltaics (Castro-Hermosa et al., 2020). However, flexible glass faces challenges in mechanical handling and processing, especially at larger sizes, which can reduce device conformality and increase the risk of breakage during production. To overcome these issues, polymer coatings have been developed to enhance mechanical stability, and ultra-thin glass options, such as Corning® Willow® Glass, have been introduced (Castro-Hermosa et al., 2020; Plichta et al., 2003). These advancements retain the benefits of traditional glass while adding the flexibility required for next-generation electronics. With its superior mechanical, thermal, and barrier properties, flexible glass is set to play a key role in advancing lighter, thinner, and more durable flexible electronics.

2.3.3 Metal Foils as Substrates

Metal foils offer an alternative to plastic films in flexible electronics, especially when high-temperature processing is needed, such as in the fabrication of inorganic thin-film solar cells (e.g., a-Si, CIS, CIGS) and silicon transistors. These foils, including materials like stainless steel (SS) and titanium, provide exceptional electrical conductivity, chemical resistance, and serve as superior barriers to moisture and oxygen compared to plastic substrates. However, SS foils, compared to glass,

Table 2.2 Properties of metal foil substrate materials

Substrate	T_{max} (°C)	CTE (ppm/K)	Optical transmission (visible)	Chemical sensitivity	Moisture uptake (%)	Surface roughness (as received)
Stainless steel (430)	900	10	Opaque	OK	~0	~1 μm
Stainless steel (304)	–	17	Opaque	OK	~0	~1 μm
Kovar (nickel-cobalt ferrous alloy)	800	5–6	Opaque	High	~0	~10 nm
Copper	–	17	Opaque	High	~0	
Aluminum	–	24	Opaque	High	~0	

Source: Reproduced with permission from ref. (D'Andrade et al., 2015). Copyright 2015: Elsevier

have a higher surface roughness due to the forging processing. Therefore, to use metallic foils with high surface roughness effectively, planarization or chemical mechanical polishing approaches can be employed to enhance the performance and reliability of flexible electronic devices made with these substrates (Hu et al., 2012). Thin metal foils, typically less than 125 μm thick, are flexible, making them ideal for applications like emissive or reflective displays, which do not require transparent substrates. In addition, metal foils show excellent dimensional stability with no shrinking or extension during processing. However, metal substrates need to be coated with insulating layers, such as SiN_x or SiO_2, to provide circuit isolation, with additional functions like serving as an adhesion layer and a barrier against chemicals used in the manufacturing process (Cheng & Wagner, 2009; Palavesam et al., 2018; Zardetto et al., 2011). Table 2.2 summarizes the key properties of various metal foil substrate materials.

2.4 Flexible Electronic Devices Based on Polymer Substrates

The most common flexible substrates for fabrication of flexible electronic devices are lightweight and thin polymer materials. Among various polymer substrates, PET and PEN are substrates of choice in flexible electronics, making lightweight, bendable, stretchable, and compatible devices with markets and applications that cannot be achieved with rigid devices. In recent years, flexible electronics have gained significant interest in applications like flexible solar cells, flexible displays, flexible transistors, flexible sensors, flexible integrated circuits, electronic skins, and many other fields. Figure 2.2 illustrates recent advancements in flexible electronics utilizing PET and PEN substrates.

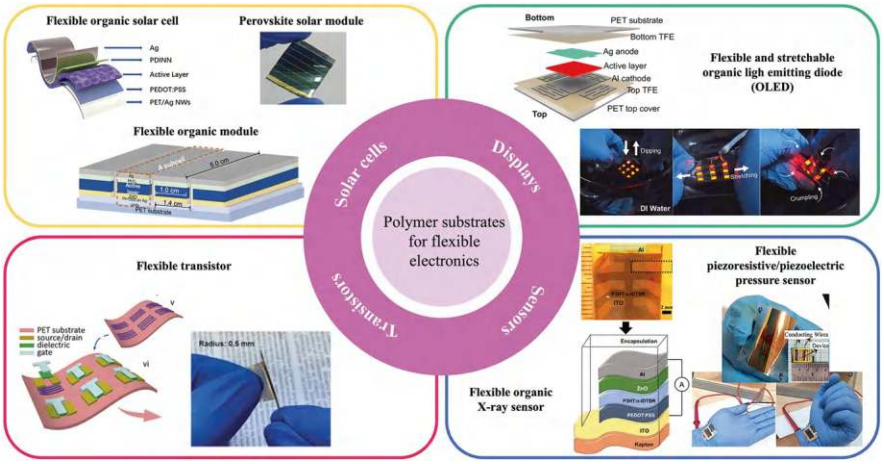

Fig. 2.2 Recent advancements in flexible electronics using conventional polymer substrates, i.e., polyethylene terephthalate (PET) and polyethylene naphthalate (PEN). Flexible organic solar cells: Reproduced with permission from ref. (Ye et al., 2023). Copyright 2023: John Wiley and Sons. Flexible organic module: Reproduced from ref. (Shen et al., 2023) with permission from John Wiley and Sons. Perovskite solar module: Reproduced with permission from ref. (Zhang et al., 2024a). Copyright 2024: John Wiley and Sons. Flexible and stretchable organic light-emitting diode (OLED): Reproduced from ref. (Nam et al., 2024). Published 2024 by Springer Nature with the terms of the Creative Commons Attribution CC BY 4.0. Flexible transistors: Reproduced from ref. (Zhang et al., 2024b). Published 2024 by Wiley with the terms of the Creative Commons Attribution CC BY 4.0. Flexible X-ray sensor: Reproduced with permission from ref. (Bashiri et al., 2024). Copyright 2024: John Wiley and Sons. Flexible piezoresistive/piezoelectric pressure sensor: Reproduced with permission from ref. (Kumari et al., 2024). Copyright 2024: American Chemical Society

2.4.1 Flexible Solar Cells

Flexible solar cells are supposed to be the foremost commercialization option of solar cells because the devices can be prepared by a roll-to-roll printing process and are suitable for mass production. More importantly, flexible solar cells prepared on ultrathin and lightweight polymer substrates can meet the demands from the emerging market of flexible electronics and find applications that cannot be achieved with conventional photovoltaic devices. As mentioned above, PET and PEN are the most prevalent plastic substrates used in flexible solar cells. Ye et al. (2023) reported the highly efficient and most flexible organic solar cells (OSCs) to date on PET by incorporating a ductile oligomeric acceptor (DOA) into the polymer donors (P_D) and small molecule acceptors (SMAs) photoactive film with a power conversion efficiency (PCE) of 17.91%. The best performing flexible cells demonstrated good mechanical stability by retaining 98% of the initial PCE after 2000 consecutive bending cycles (Ye et al., 2023). Additionally, large-area flexible OSCs on PET substrate, with 30 cm^2 modules utilizing PM6:Qx-1 as the photoactive layer, achieved a record PCE of 12.20% (Shen et al., 2023). The ability to be printed and

integrated on a variety of flexible substrates in different forms, combined with their lightweight, thin, and flexible nature, positions perovskite solar cells (PSCs) at the forefront of new-generation photovoltaic for a variety of different applications. By suppressing the crack formation and delamination using pentaerythritol triacrylate as a crosslinker in both the interface and bulk perovskite, the highest PCE of flexible PSCs is 24.9% (certified 24.48%) (Wu et al., 2024). For flexible perovskite modules, a certified record efficiency of 20.20% was achieved in January 2024 through the perovskite/hole transport layer (HTL) passivation strategy (Zhang et al., 2024a). Because of stability concerns and permeability of plastic substrates, a good market of entry is represented by indoor photovoltaic. Examples of flexible cells for indoor applications under artificial light include flexible PSCs on PET substrates, achieving a PCE of 32.5% under illumination of a cool white LED lamp (6500 K) at 1000 lx (Skafi et al., 2023). More recently, the highest efficiency for PET-based cells reached 41% under illumination from a warm white LED lamp (3000 K) at 1000 lx (Zhang et al., 2024a). The development of flexible photovoltaic technologies under both indoor and outdoor conditions is important as it brings flexible solar cells closer to commercialization, leading to lower manufacturing costs and easier integration into various applications, such as wearable technology or integrated buildings (Kim et al., 2021).

2.4.2 Flexible Displays

Displays have remarkably transitioned over the past decade from flat-panel liquid crystal displays (LCDs) to thin frameless displays, such as the self-luminous displays made of organic light-emitting diodes (OLEDs), quantum dot LEDs (QLEDs), and micro-LEDs (μLEDs). Given the critical trends in electronic devices, such as portability, user-friendliness, and multifunctionality, flexible displays have attracted significant interest (Kim et al., 2023). The most prevalent display technologies in the market currently are LED and OLED. These technologies are known for their lightweight nature, efficiency, thin device structures, and flexible components, making them suitable for commercial and human-comfortable applications, such as curved displays, foldable smartphones, rollable televisions, smart textiles, and wearable electronics (Nam et al., 2024). However, the future direction of the display industry relies on free-form displays capable of three-dimensional (3D) deformation and stretching, enabling functionalities such as multi-foldable, slidable, rollable, and stretchable screens. Stretchable displays, which can deform like human skin, can have potential applications such as artificial skin, electronic skin (e-skin), and feelable displays. To achieve these capabilities, these displays should be fabricated on elastic polymer substrates, like ultrathin PET films (Kim et al., 2023; Nam et al., 2024). Recently, Nam et al., reported a stretchable and water-resistant OLED on a thin PET film (12 μm) using vacuum evaporation, thin film encapsulation, and a nonselective laser patterning process. The fully encapsulated devices were fabricated by a 12-μm PET film, which was coated with a 6.5-μm-thick layer of acrylic

adhesive and laminated on top of the device. The mechanical stability and durability tests of these OLEDs displayed excellent stretchability, withstanding up to 95% strain and enduring 100,000 stretch-release cycles at 50% strain. Additionally, the effective protection of encapsulation layer was confirmed through operational lifetime and water-resistant storage lifetime measurements (Nam et al., 2024). Putting together flexibility of the display medium (electrophoretic) and the active-matrix backplane, Burns et al. demonstrated one of the first applications of flexible e-books, i.e., e-paper displays, via solution/printing-based manufacturing of polymer-based thin film transistors on low-cost PET flexible substrates. Using a novel multilayer pixel architecture, displays with an aperture ratio exceeding 85% was achieved and could be bent to a radius of curvature of 5 mm (Burns et al., 2005).

2.4.3 Flexible Transistors

Flexible transistors are electronic components that can switch or amplify electrical signals, but unlike traditional rigid transistors, they are fabricated on flexible substrates. Low temperature thin-film transistors (TFTs) can be made using materials such as carbon-based materials (such as graphene and CNTs), low-dimensional materials such as silver nanoparticles (Ag NPs) and Ag NWs, metal oxide materials (such as zinc oxide NWs (ZnO NWs) and zirconium oxide (ZrO_x)), and organic materials (such as pentacene, P3HT, and PEDOT:PSS) (Zhang et al., 2023). Many developments in the application of flexible transistors for the fabrication of flexible electronics have been reported, including uses in radio-frequency identification tags, bio-sensor interface circuits, microprocessors, and displays (Jakher & Yadav, 2024; Shi et al., 2023). Following that, Zhang et al. (2024b) fabricated a flexible field-effect transistor (FET) by directly integrating self-aligned crystalline, large-area in-plane silicon nanowire (SiNW) multi-channels onto large-area flexible PET substrates. They used a reliable transfer technique that preserved the original positioning and alignment of the NWs. The FETs displayed a high switching state current ratio $>10^5$, a low subthreshold swing of 175 mV dec^{-1}, and excellent durability at a small bending radius of 0.5 mm over 1000 bending cycles. The proposed strategy opens the way for the development of flexible displays, wearable electronics, and smart sensors by semiconductor NW channels, offering the advantage of low manufacturing costs (Zhang et al., 2024b).

2.4.4 Flexible Sensors

Over the past decade, flexible sensors have become the key elements in flexible wearable electronics and biomedical applications (Shen, 2021; Zazoum et al., 2022). Flexible sensors find applications in three areas, including human activity monitoring (such as motion monitoring and emotion recognition), artificial

intelligence (such as human-machine interfaces and electronic signatures), and healthcare (such as breath monitoring, wound healing monitoring, and joint motion monitoring). Conventional electronic sensors, typically made from metals or semiconductors, often lack the sensitivity and stretchability required for monitoring physiological signals, making them unsuitable for such applications. In contrast, flexible sensors offer high biocompatibility, enable real-time monitoring, and provide additional benefits. Depending on the application, high flexibility may be required, like for joint motion monitoring, or high sensitivity, as in pulse monitoring, while achieving both simultaneously remains a big challenge (Liu et al., 2023a; Zazoum et al., 2022). A recent study by Bashiri et al., published in November 2024, developed a highly sensitive and flexible sensor based on P3HT:o-IDTBR, deposited onto conductive Kapton substrates. The Kapton-based sensors demonstrated precise resolution of multiple 50-μm-wide X-rays, with a full-width half-maximum (FWHM) of (51.6 ± 1.9) μm, across energy ranges of 47–87.5 keV and dose rates of 0.21–0.45 kGy s^{-1}. While sensors fabricated on PET exhibited unreliable X-ray responses and significant FWHM broadening due to reverse polarity signals generated by the PET substrate. This study confirms the limitation of PET substrates for flexible radiation detectors, providing the first evidence of their quantitative and spatial challenges caused by radiation-induced charge generation (Bashiri et al., 2024).

Recently, a flexible piezo-resistive/piezoelectric sensor based on ZnO NWs has been developed on a PET substrate coated with indium tin oxide (ITO). This sensor showed a significant change in resistance, ranging from 100 Ω to 2400 Ω, under relaxation and bending conditions, respectively. The I-V curves of the ZnO NW-based flexible pressure sensor demonstrated a shift in current conduction from 24.40 mA to 0.30 μA when bent to 95.5° at +5 V, compared to when it was flat. Experiments showed improved sensitivity, attributed to the lower defect density in the CVD-grown NWs, in contrast to those made with hydrothermally grown nanowires. The fabrication method reported in this study is time-efficient and enables the creation of high-performance devices suitable for flexible and wearable technology (Kumari et al., 2024).

2.5 Unconventional Substrates for Flexible Electronics

As mentioned earlier, plastic substrates are the most common choice in flexible electronics. However, there is increasing interest in alternative materials that can improve foldability, stretchability, and compatibility, while also addressing the environmental risks associated with non-recyclable substrates. As a result, options such as biodegradable films, textiles (Wei et al., 2024), and paper (Castro-Hermosa et al., 2017; Dong et al., 2021b) are gaining more attention. Some biodegradable materials and plastics have been reported in the literature for fabricating flexible electronic devices such as regenerated cellulose or cellophane (Li et al., 2019), silk film (Wen et al., 2021), transparent wood film (Ma et al., 2024), starch-based

materials (Dong et al., 2024; Xiang et al., 2022), poly(lactic acid) film (Prontera et al., 2022), and chitosan film (Kumar et al., 2020). These advancements highlight the potential of sustainable materials as viable alternatives to traditional substrates, paving the way for greener and more eco-friendly flexible electronics.

2.6 Conclusion

In summary, flexible electronics has revolutionized modern technology, enabling high-performance devices with unique properties like bendability and conformability. This chapter reviewed the essential characteristics of flexible substrates, focusing on PET and PEN as leading materials, and highlighted advancements in key devices such as solar cells, displays, transistors, and sensors. Additionally, the potential of unconventional substrates emphasizing biodegradability and sustainability was discussed. These developments pave the way for broader adoption and future innovation in flexible electronics.

Acknowledgments The authors acknowledge the financial support from the Italian Ministry of University and Research (MUR) for the PRIN2022 REPLACE (Project no. 2022C4YNP8) and PRIN2022 PNRR INPOWER (project no. P2022PXS5S) grants. T.M.B. acknowledges also the Air Force Office of Scientific Research Biophysics Program (AFOSR Award Number FA9550-24-1-0320).

References

Aftab, S., Hussain, S., Kabir, F., Aslam, M., Rajpar, A. H., & Al-Sehemi, A. G. (2024). Advances in flexible perovskite solar cells: A comprehensive review. *Nano Energy, 120*, 109112. https://doi.org/10.1016/j.nanoen.2023.109112

Alenazi, D. A. K. (2023). Development of color-tunable photoluminescent polycarbonate smart window immobilized with silica-coated lanthanide-activated strontium aluminum oxide nanoparticles. *Inorganic Chemistry Communications, 150*, 110473. https://doi.org/10.1016/j.inoche.2023.110473

Anwer, A. H., Khan, N., Ansari, M. Z., Baek, S.-S., Yi, H., Kim, S., Noh, S. M., et al. (2022). Recent advances in touch sensors for flexible wearable devices. *Sensors, 22*, 4460. https://doi.org/10.3390/s22124460

Aouedi, O., Vu, T. H., Sacco, A., Nguyen, D. C., Piamrat, K., Marchetto, G., et al. (2024). A survey on intelligent internet of things: Applications, security, privacy, and future directions. *IEEE Communications Surveys and Tutorials*. https://doi.org/10.1109/COMST.2024.3430368

Astarlioglu, A. T., Oz, Y., Unal, E., Kilic, N. B., Celikli, C., Ozdemir, M., et al. (2024). Large-area (50 cm×50 cm) optically transparent electromagnetic interference (EMI) shielding of ZTO/Ag/ZTO: An analytical/numerical and experimental study of optoelectrical and EMI shielding properties. *Journal of Physics D: Applied Physics, 57*, 325301. https://doi.org/10.1088/1361-6463/ad44a7

Baek, G. W., Seo, H., Lee, T., Hahm, D., Bae, W. K., & Kwak, J. (2023). Highly bright and efficient flexible quantum dot light-emitting diodes on metal-coated PEN substrate. *Journal of Flexible and Printed Electronics, 2*, 243–251. https://doi.org/10.56767/jfpe.2023.2.2.243

Bai, S., Guo, X., Zhang, X., Zhao, X., & Yang, H. (2021). $Ti_3C_2T_x$ MXene -AgNW composite flexible transparent conductive films for EMI shielding. *Composites Part A: Applied Science and Manufacturing, 149*, 106545. https://doi.org/10.1016/j.compositesa.2021.106545

Bashiri, A., Large, M. J., Griffith, M. J., Papale, L., Philippa, B., Hall, C., et al. (2024). Flexible organic X-ray sensors: Solving the key constraints of PET substrates. *Advanced Functional Materials, 2415723*. https://doi.org/10.1002/adfm.202415723

Batet D., Vilaseca F., Ramon E., Esquivel JP. & Gabriel G. (2023) Experimental overview for green printed electronics: Inks, substrates, and printing techniques. Flexible and Printed Electronics 8: 024001. https://doi.org/10.1088/2058-8585/acd8cc.

Biji, K. B., Ravishankar, C. N., Mohan, C. O., Srinivasa, G. T., & K. (2015). Smart packaging systems for food applications: A review. *Journal of Food Science and Technology, 52*, 6125–6135. https://doi.org/10.1007/s13197-015-1766-7

Burns, S. E., Reynolds, K., Reeves, W., Banach, M., Brown, T., Chalmers, K., et al. (2005). A scalable manufacturing process for flexible active-matrix e-paper displays. *Journal of the Society for Information Display, 13*, 583–586. https://doi.org/10.1889/1.2012644

Cang, D., Wang, Z., & Qu, H. (2021). A polyimide-based flexible monopole antenna fed by a coplanar waveguide. *Electronics (Switzerland), 10*, 334. https://doi.org/10.3390/electronics10030334

Castro-Hermosa, S., Dagar, J., Marsella, A., & Brown, T. M. (2017). Perovskite solar cells on paper and the role of substrates and electrodes on performance. *IEEE Electron Device Letters, 38*, 1278–1281. https://doi.org/10.1109/LED.2017.2735178

Castro-Hermosa, S., Top, M., Dagar, J., Fahlteich, J., & Brown, T. M. (2019). Quantifying performance of permeation barrier—Encapsulation systems for flexible and glass-based electronics and their application to perovskite solar cells. *Advanced Electronic Materials, 5*, 1800978. https://doi.org/10.1002/aelm.201800978

Castro-Hermosa, S., Lucarelli, G., Top, M., Fahland, M., Fahlteich, J., & Brown, T. M. (2020). Perovskite photovoltaics on roll-to-roll coated ultra-thin glass as flexible high-efficiency indoor power generators. *Cell Reports Physical Science, 1*, 100045. https://doi.org/10.1016/j.xcrp.2020.100045

Chakraborty, A., Lucarelli, G., Xu, J., Skafi, Z., Castro-Hermosa, S., Kaveramma, A. B., et al. (2024). Photovoltaics for indoor energy harvesting. *Nano Energy, 128*, 109932. https://doi.org/10.1016/j.nanoen.2024.109932

Chen, J., Zheng, J., Gao, Q., Zhang, J., Zhang, J., Omisore, O. M., et al. (2018). Polydimethylsiloxane (PDMS)-based flexible resistive strain sensors for wearable applications. *Applied Sciences, 8*, 345. https://doi.org/10.3390/app8030345

Chen, C.-K., Lin, Y.-C., Hsu, L.-C., Ho, J.-C., Ueda, M., & Chen, W.-C. (2021a). High performance biomass-based polyimides for flexible electronic applications. *ACS Sustainable Chemistry & Engineering, 9*, 3278–3288. https://doi.org/10.1021/acssuschemeng.0c08959

Chen, T., Xie, Y., Wang, Z., Lou, J., Liu, D., Xu, R., et al. (2021b). Recent advances of flexible strain sensors based on conductive fillers and thermoplastic polyurethane matrixes. *ACS Applied Polymer Materials, 3*, 5317–5338. https://doi.org/10.1021/acsapm.1c00840

Chen, Q., Huang, L., Wang, X., & Yuan, Y. (2023a). Transparent and flexible composite films with excellent electromagnetic interference shielding and thermal insulating performance. *ACS Applied Materials & Interfaces, 15*, 24901–24912. https://doi.org/10.1021/acsami.3c03140

Chen, T., He, X., & Lu, Q. (2023b). Comprehensive performance of polyimide reinforced by multiple hydrogen bonds for flexible electronics application. *ACS Applied Polymer Materials, 5*, 5436–5444. https://doi.org/10.1021/acsapm.3c00767

Cheng, I.-C., & Wagner, S. (2009). Overview of flexible electronics technology. In W. S. Wong & A. Salleo (Eds.), *Flexible electronics: Materials and applications* (pp. 1–28). Springer US.

Cho, Y., Kim, K., Kim, D., Bissannagari, M., Lee, J., Hong, W., et al. (2024). Stretchable substrate surface-embedded inkjet-printed strain sensors for design customizable on-skin healthcare electronics. *ACS Applied Electronic Materials, 6*, 3147–3157. https://doi.org/10.1021/acsaelm.3c01682

Cui, J., Zhang, B., Duan, J., Guo, H., & Tang, J. (2016). Flexible pressure sensor with Ag wrinkled electrodes based on PDMS substrate. *Sensors (Switzerland), 16*, 2131. https://doi.org/10.3390/s16122131

Cusack, N. M., Venkatraman, P. D., Raza, U., & Faisal, A. (2024). Review—Smart wearable sensors for health and lifestyle monitoring: Commercial and emerging solutions. *ECS Sensors Plus, 3*(1), 017001. https://doi.org/10.1149/2754-2726/ad3561

D'Andrade, B. W., Kattamis, A. Z., & Murphy, P. F. (2015). Flexible organic electronic devices on metal foil substrates for lighting, photovoltaic, and other applications. In S. Logothetidis (Ed.), *Handbook of flexible organic electronics* (pp. 315–341). Woodhead Publishing.

Dadhich, B. K., Panda, B., Sidhu, M. S., & Singh, K. P. (2023). Nanodiamonds enable femtosecond-processed ultrathin glass as a hybrid quantum sensor. *Scientific Reports, 13*, 6286. https://doi.org/10.1038/s41598-023-30689-7

Dagar J., Castro-Hermosa S., Gasbarri M., Palma AL., Cina L., Matteocci F., et al. (2018) Efficient fully laser-patterned flexible perovskite modules and solar cells based on low-temperature solution-processed SnO_2/mesoporous-TiO_2 electron transport layers. Nano Research 11:2669–2681. https://doi.org/10.1007/s12274-017-1896-5.

De Oliveira, R. F., Casalini, S., Cramer, T., Leonardi, F., Ferreira, M., Vinciguerra, V., et al. (2016). Water-gated organic transistors on polyethylene naphthalate films. *Flexible and Printed Electronics, 1*, 025005. https://doi.org/10.1088/2058-8585/1/2/025005

Deng, F., Shen, Y., Li, Y., Han, X., Huang, M., & Tao, X. (2023). Highly efficient (>13%) and robust flexible perovskite solar cells using an ultrasimple all-carbon-electrode configuration. *ACS Applied Materials & Interfaces, 15*, 46054–46063. https://doi.org/10.1021/acsami.3c09761

Deng, Y., Bu, F., Wang, Y., Chee, P. S., Liu, X., & Guan, C. (2024). Stretchable liquid metal based biomedical devices. *npj Flexible Electronics, 8*, 12. https://doi.org/10.1038/s41528-024-00298-z

Dong, L., Zhang, B., Xin, Y., Liu, Y., Xing, R., Yang, Y., et al. (2021a). Fully integrated flexible long-term electrocardiogram recording patch with gel-less adhesive electrodes for arrhythmia detection. *Sensors and Actuators A: Physical, 332*, 113063. https://doi.org/10.1016/j.sna.2021.113063

Dong, Z., Liu, H., Yang, X., Fan, J., Bi, H., Wang, C., et al. (2021b). Facile fabrication of paper-based flexible thermoelectric generator. *npj Flexible Electronics, 5*, 6. https://doi.org/10.1038/s41528-021-00103-1

Dong, M., Soul, A., Li, Y., Bilotti, E., Zhang, H., Cataldi, P., et al. (2024). Transient starch-based nanocomposites for sustainable electronics and multifunctional sensing. *Advanced Functional Materials, 2412138*. https://doi.org/10.1002/adfm.202412138

Du, J., Wang, L., Shi, Y., Zhang, F., Hu, S., Liu, P., et al. (2020). Optimized CNT-PDMS flexible composite for attachable health-care device. *Sensors (Switzerland), 20*, 4523. https://doi.org/10.3390/s20164523

Emamian, S., Narakathu, B. B., Chlaihawi, A. A., Bazuin, B. J., & Zandi, A. M. (2017). Screen printing of flexible piezoelectric based device on polyethylene terephthalate (PET) and paper for touch and force sensing applications. *Sensors and Actuators A: Physical, 263*, 639–647. https://doi.org/10.1016/j.sna.2017.07.045

Erlat, A. G., Yan, M., Kim, T. W., Schaepkens, M., Liu, J., Heller, C. M., et al. (2005). Ultra-high barrier coatings for flexible organic electronics. In *48th annual technical conference proceedings (2005)* (pp. 116–120). Society of Vacuum Coaters.

Fang, Y., & Tentzeris, M. M. (2018). Surface modification of polyimide films for inkjet-printing of flexible electronic devices. In S. Rackauskas (Ed.), *Flexible electronics* (pp. 1–19). IntechOpen. https://doi.org/10.5772/intechopen.76450

Faraj, M. G., Ibrahim, K., & Ali, M. K. M. (2011). PET as a plastic substrate for the flexible opto-electronic applications. *The Optoelectronics and Advanced Materials – Rapid Communications, 5*, 879–882.

Farman, M., Surendra, P. R., Upadhyay, A. K., Kumar, P., & Thouti, E. (2023). All-polydimethylsiloxane-based highly flexible and stable capacitive pressure sensors with engi-

neered interfaces for conformable electronic skin. *ACS Applied Materials & Interfaces, 15*, 34195–34205. https://doi.org/10.1021/acsami.3c04227

Garner, S. M., Wu, K.-W., Liao, Y. C., Shiu, J. W., Tsai, Y. S., Chen, K. T., et al. (2013). Cholesteric liquid crystal display with flexible glass substrates. *Journal of Display Technology, 9*, 644–650. https://doi.org/10.1109/JDT.2013.2251860

Garner, S. M., Lewis, S. C., & Chowdhury, D. Q. (2017a). Flexible glass and its application for electronic devices. In *Proceedings of 24th international workshop on active-matrix flat panel displays and devices (AM-FPD). 14 August 2017, Kyoto, Japan* (pp. 28–33).

Garner, S. M., Li, X., & Huang, M.-H. (2017b). Introduction to flexible glass substrates. In S. M. Garner (Ed.), *Flexible glass: Enabling thin, lightweight, and flexible electronics* (pp. 1–33). Wiley.

Gasonoo, A., Beaumont, C., Hoff, A., Xu, C., Egberts, P., Pahlevani, M., et al. (2023). Water-processable self-doped hole-injection layer for large-area, air-processed, slot-die-coated flexible organic light-emitting diodes. *Chemistry of Materials, 35*, 9102–9110. https://doi.org/10.1021/acs.chemmater.3c01784

Griggs, T., Ahmed, J., Majd, H., Edirisinghe, M., & Chen, B. (2024). A bio-based thermoplastic polyurethane with triple self-healing action for wearable technology and smart textiles. *Materials Advances, 5*, 6210–6221. https://doi.org/10.1039/d4ma00289j

Hassan, M., Abbas, G., Li, N., Afzal, A., Haider, Z., Ahmed, S., et al. (2022). Significance of flexible substrates for wearable and implantable devices: Recent advances and perspectives. *Advanced Materials Technologies, 7*, 2100773. https://doi.org/10.1002/admt.202100773

Hu, X., Song, Z., Liu, W., Zhang, Z., & Wang, H. (2012). Chemical mechanical polishing of stainless steel foil as flexible substrate. *Applied Surface Science, 258*, 5798–5802. https://doi.org/10.1016/j.apsusc.2012.02.100

Hu, D., Giorgio-Serchi, F., Zhang, S., & Yang, Y. (2023). Stretchable e-skin and transformer enable high-resolution morphological reconstruction for soft robots. *Nature Machine Intelligence, 5*, 261–272. https://doi.org/10.1038/s42256-023-00622-8

Jakher, S., & Yadav, R. (2024). Organic thin film transistor review based on their structures, materials, performance parameters, operating principle, and applications. *Microelectronic Engineering, 290*, 112193. https://doi.org/10.1016/j.mee.2024.112193

Jankowski, P., Ogończyk, D., Lisowski, W., & Garstecki, P. (2012). Polyethyleneimine coating renders polycarbonate resistant to organic solvents. *Lab on a Chip, 12*, 2580–2584. https://doi.org/10.1039/C2LC21297H

Jeong, H.-J., Song, Y. H., Kim, H. W., & Park, Y. (2024). Highly conductive MXene/Ag nanowire/UV-resin/polycarbonate flexible transparent electrode for capacitive sensors. *Journal of Inclusion Phenomena and Macrocyclic Chemistry, 104*, 307–315. https://doi.org/10.1007/s10847-023-01203-3

Jiang, S., Stange, O., Bätcke, F. O., Sultanova, S., & Sabantina, L. (2021). Applications of smart clothing—A brief overview. *Communications in Development and Assembling of Textile Products, 2*, 123–140. https://doi.org/10.25367/cdatp.2021.2.p123-140

Jin, H., Zhou, J., He, X., Wang, W., Guo, H., Dong, S., et al. (2013). Flexible surface acoustic wave resonators built on disposable plastic film for electronics and lab-on-a-chip applications. *Scientific Reports, 3*, 2140. https://doi.org/10.1038/srep02140

Jung, H. S., Han, G. S., Park, N. G., & Ko, M. J. (2019). Flexible perovskite solar cells. *Joule, 3*, 1850–1880. https://doi.org/10.1016/j.joule.2019.07.023

Khoshmanesh, F., Thurgood, P., Pirogova, E., Nahavandi, S., & Baratchi, S. (2021). Wearable sensors: At the frontier of personalised health monitoring, smart prosthetics and assistive technologies. *Biosensors & Bioelectronics, 176*, 112946. https://doi.org/10.1016/j.bios.2020.112946

Kim, J.-H., & Park, J.-W. (2013). Improving the flexibility of large-area transparent conductive oxide electrodes on polymer substrates for flexible organic light emitting diodes by introducing surface roughness. *Organic Electronics, 14*, 3444–3452. https://doi.org/10.1016/j.orgel.2013.09.016

Kim, S., Quy, H. V., & Bark, C. W. (2021). Photovoltaic technologies for flexible solar cells: Beyond silicon. *Materials Today Energy, 19*, 100583. https://doi.org/10.1016/j.mtener.2020.100583

Kim, D. W., Kim, S. W., Lee, G., Yoon, J., Kim, S., Hong, J.-H., et al. (2023). Fabrication of practical deformable displays: Advances and challenges. *Light: Science & Applications, 12*, 6. https://doi.org/10.1038/s41377-023-01089-3

Kirtania, S. G., Elger, A. W., Hasan, M. R., Wisniewska, A., Sekhar, K., Karacolak, T., et al. (2020). Flexible antennas: A review. *Micromachines (Basel), 11*, 847. https://doi.org/10.3390/mi11090847

Koo, D., Jung, S., Seo, J., Jeong, G., Choi, Y., Lee, J., et al. (2020). Flexible organic solar cells over 15% efficiency with polyimide-integrated graphene electrodes. *Joule, 4*, 1021–1034. https://doi.org/10.1016/j.joule.2020.02.012

Kumar, R., Ranwa, S., & Kumar, G. (2020). Biodegradable flexible substrate based on chitosan/PVP blend polymer for disposable electronics device applications. *The Journal of Physical Chemistry. B, 124*, 149–155. https://doi.org/10.1021/acs.jpcb.9b08897

Kumari, M., Prasad, R. K., Singh, M. K., Iyer, P. K., & Singh, D. K. (2024). Piezoresistive/piezoelectric pressure sensor based on CVD-grown ZnO nanowires on polyethylene terephthalate substrate. *ACS Applied Electronic Materials, 6*, 6165–6173. https://doi.org/10.1021/acsaelm.4c00991

Lamanna, L., Rizzi, F., Bhethanabotla, V. R., & De Vittorio, M. (2020). Conformable surface acoustic wave biosensor for E-coli fabricated on PEN plastic film. *Biosensors & Bioelectronics, 163*, 112164. https://doi.org/10.1016/j.bios.2020.112164

Li, X., Wu, N., Rojanasakul, Y., & Liu, Y. (2013). Selective stamp bonding of PDMS microfluidic devices to polymer substrates for biological applications. *Sensors and Actuators A: Physical, 193*, 186–192. https://doi.org/10.1016/j.sna.2012.12.037

Li, H., Li, X., Wang, W., Huang, J., Li, J., Lu, Y., et al. (2019). Highly foldable and efficient paper-based perovskite solar cells. *Solar RRL, 3*, 1800317. https://doi.org/10.1002/solr.201800317

Li, N., Wang, Q., Shen, C., Wei, Z., Yu, H., Zhao, J., et al. (2020). Large-scale flexible and transparent electronics based on monolayer molybdenum disulfide field-effect transistors. *Nature Electronics, 3*, 711–717. https://doi.org/10.1038/s41928-020-00475-8

Li, Y., Wen, D., Zhang, Y., Lin, Y., Cao, K., Yang, F., et al. (2021). Highly-stable PEN as a gas-barrier substrate for flexible displays via atomic layer infiltration. *Dalton Transactions, 50*, 16166–16175. https://doi.org/10.1039/D1DT02764F

Ling, H., Liu, S., Zheng, Z., & Yan, F. (2018). Organic flexible electronics. Small. *Methods, 2*, 1800070. https://doi.org/10.1002/smtd.201800070

Liu, E., Cai, Z., Ye, Y., Zhou, M., Liao, H., & Yi, Y. (2023a). An overview of flexible sensors: Development, application, and challenges. *Sensors, 23*, 817. https://doi.org/10.3390/s23020817

Liu, H., Liu, D., Yang, J., Gao, H., & Wu, Y. (2023b). Flexible electronics based on organic semiconductors: From patterned assembly to integrated applications. *Small, 19*, 2206938. https://doi.org/10.1002/smll.202206938

Liu, K., Duan, T., Zhang, F., Tian, X., Li, H., Feng, M., et al. (2024). Flexible electrode materials for emerging electronics: Materials, fabrication and applications. *Journal of Materials Chemistry A, 12*, 20606–20637. https://doi.org/10.1039/D4TA01960A

Logothetidis, S. (2008). Flexible organic electronic devices: Materials, process and applications. *Materials Science and Engineering B, 152*, 96–104. https://doi.org/10.1016/j.mseb.2008.06.009

Ma, H., Liu, C., Yang, Z., Wu, S., Jiao, Y., Feng, X., et al. (2024). Programmable and flexible wood-based origami electronics. *Nature Communications, 15*, 9272. https://doi.org/10.1038/s41467-024-53708-1

MacDonald, W. A. (2015). Latest advances in substrates for flexible electronics. In M. Caironi & Y.-Y. Noh (Eds.), *Large area and flexible electronics* (pp. 291–314). Wiley.

Na, K., Ma, H., Park, J., Yeo, J., Park, J. U., & Bien, F. (2016). Graphene-based wireless environmental gas sensor on PET substrate. *IEEE Sensors Journal, 16*, 5003–5009. https://doi.org/10.1109/JSEN.2016.2531121

Nam, M., Chang, J., Kim, H., Son, Y. H., Jeon, Y., Kwon, J. H., et al. (2024). Highly reliable and stretchable OLEDs based on facile patterning method: Toward stretchable organic optoelectronic devices. *npj Flexible Electronics, 8*, 17. https://doi.org/10.1038/s41528-024-00303-5

Palavesam, N., Marin, S., Hemmetzberger, D., Landesberger, C., Bock, K., & Kutter, C. (2018). Roll-to-roll processing of film substrates for hybrid integrated flexible electronics. *Flexible and Printed Electronics, 3*, 014002. https://doi.org/10.1088/2058-8585/aaaa04

Park, S., Chang, H.-Y., Rahimi, S., Lee, A. L., Tao, L., & Akinwande, D. (2018a). Transparent nanoscale polyimide gate dielectric for highly flexible electronics. *Advanced Electronic Materials, 4*, 1700043. https://doi.org/10.1002/aelm.201700043

Park, S. J., Ko, T.-J., Yoon, J., Moon, M.-W., Oh, K. H., & Han, J. H. (2018b). Highly adhesive and high fatigue-resistant copper/PET flexible electronic substrates. *Applied Surface Science, 427*, 1–9. https://doi.org/10.1016/j.apsusc.2017.08.195

Park, S., Thanakkasaranee, S., Shin, H., Ahn, K., Sadeghi, K., Lee, Y., et al. (2020). Preparation and characterization of heat-resistant PET/bio-based polyester blends for hot-filled bottles. *Polymer Testing, 91*, 106823. https://doi.org/10.1016/j.polymertesting.2020.106823

Patel, R. P., & Wolden, C. A. (2013). Defect analysis and mechanical performance of plasma-deposited thin films on flexible polycarbonate substrates. *Applied Surface Science, 268*, 416–424. https://doi.org/10.1016/j.apsusc.2012.12.112

Plichta, A., Weber, A., & Habeck, A. (2003). Ultrathin flexible glass substrates. *MRS Online Proceedings Library, 769*, H9–H1. https://doi.org/10.1557/PROC-769-H9.1

Pradhan, G., Celegato, F., Barrera, G., Olivetti, E. S., Coisson, M., Hajduček, J., et al. (2022). Magnetic properties of FeGa/Kapton for flexible electronics. *Scientific Reports, 12*, 17503. https://doi.org/10.1038/s41598-022-21589-3

Prontera, C. T., Villani, F., Palamà, I. E., Maglione, M. G., Manini, P., Maiorano, V., et al. (2022). Fabrication and biocompatibility analysis of flexible organic light emitting diodes on poly(lactic acid) substrates: Toward the development of greener bio-electronic devices. *Polymers for Advanced Technologies, 33*, 1523–1532. https://doi.org/10.1002/pat.5618

Pursula, P., Kiri, K., Caffrey, C. M., Sandberg, H., Vartiainen, J., Flak, J., et al. (2018). Nanocellulose–polyurethane substrate material with tunable mechanical properties for wearable electronics. *Flexible and Printed Electronics, 3*, 045002. https://doi.org/10.1088/2058-8585/aae5d9

Qi, D., Zhang, K., Tian, G., Jiang, B., & Huang, Y. (2021). Stretchable electronics based on PDMS substrates. *Advanced Materials, 33*, 2003155. https://doi.org/10.1002/adma.202003155

Sahatiya, P., Puttapati, S. K., Srikanth, V. V. S. S., & Badhulika, S. (2016). Graphene-based wearable temperature sensor and infrared photodetector on a flexible polyimide substrate. *Flexible and Printed Electronics, 1*, 025006. https://doi.org/10.1088/2058-8585/1/2/025006

Salleh, S. M., Ain, M. F., Ahmad, Z., Abidin, I. S. Z., Seng, L. Y., & Osman, M. N. (2023). Stretchable and bendable polydimethylsiloxane- silver composite antenna on PDMS/air gap substrate for 5G wearable applications. *IEEE Access, 11*, 133623–133639. https://doi.org/10.1109/ACCESS.2023.3331590

Serrano, I. G., Panda, J., Edvinsson, T., & Kamalakar, M. V. (2020). Flexible transparent graphene laminates: Via direct lamination of graphene onto polyethylene naphthalate substrates. *Nanoscale Advances, 2*, 3156–3163. https://doi.org/10.1039/d0na00046a

Sharma, P. K., & Chung, J. Y. (2023). Evaluation of polydimethylsiloxane (PDMS) as a substrate for the realization of flexible/wearable antennas and sensors. *Micromachines (Basel), 14*, 735. https://doi.org/10.3390/mi14040735

Sharma, P. K., Gupta, N., & Dankov, P. I. (2021). Analysis of dielectric properties of polydimethylsiloxane (PDMS) as a flexible substrate for sensors and antenna applications. *IEEE Sensors Journal, 21*, 19492–19504. https://doi.org/10.1109/JSEN.2021.3089827

Shen, G. (2021). Recent advances of flexible sensors for biomedical applications. *Progress in Natural Science: Materials International, 31*, 872–882. https://doi.org/10.1016/j.pnsc.2021.10.005

Shen, Y.-F., Zhang, H., Zhang, J., Tian, C., Shi, Y., Qiu, D., et al. (2023). In situ absorption characterization guided slot-die-coated high-performance large-area flexible organic solar cells and modules. *Advanced Materials, 35*, 2209030. https://doi.org/10.1002/adma.202209030

Shi, R., Lei, T., Xia, Z., & Wong, M. (2023). Low-temperature metal-oxide thin-film transistor technologies for implementing flexible electronic circuits and systems. *Journal of Semiconductors, 44*, 091601. https://doi.org/10.1088/1674-4926/44/9/091601

Sierros, K. A., Cairns, D. R., Abell, J. S., & Kukureka, S. N. (2010). Pulsed laser deposition of indium tin oxide films on flexible polyethylene naphthalate display substrates at room temperature. *Thin Solid Films, 518*, 2623–2627. https://doi.org/10.1016/j.tsf.2009.08.002

Skafi, Z., Xu, J., Mottaghitalab, V., Mivehi, L., Taheri, B., Jafarzadeh, F., et al. (2023). Highly efficient flexible perovskite solar cells on polyethylene terephthalate films via dual halide and low-dimensional interface engineering for indoor photovoltaics. *Solar RRL, 7*, 2300324. https://doi.org/10.1002/solr.202300324

Skafi, Z., Castriotta, L. A., Taheri, B., Matteocci, F., Fahland, M., Jafarzadeh, F., et al. (2024). Flexible perovskite solar cells on polycarbonate film substrates. *Advanced Energy Materials, 14*, 2400912. https://doi.org/10.1002/aenm.202400912

Sondhi, K., Hwangbo, S., Yoon, Y. K., Nishida, T., & Fan, Z. H. (2018). Airbrushing and surface modification for fabricating flexible electronics on polydimethylsiloxane. *Journal of Micromechanics and Microengineering, 28*, 125014. https://doi.org/10.1088/1361-6439/aae9d6

Spechler, J. A., Koh, T.-W., Herb, J. T., Rand, B. P., & Arnold, C. B. (2015). A transparent, smooth, thermally robust, conductive polyimide for flexible electronics. *Advanced Functional Materials, 25*, 7428–7434. https://doi.org/10.1002/adfm.201503342

Su, L., Liang, M., Wang, J., Xin, X., Jiao, Y., Wang, C., et al. (2023). Robust orientation-3D conductive network enabled high-performance flexible sensor for traffic monitoring: Role of surface functionalization on self-assembled microspheres arrays. *Chemical Engineering Journal, 468*, 143564. https://doi.org/10.1016/j.cej.2023.143564

Subudhi, P., & Punetha, D. (2023). Progress, challenges, and perspectives on polymer substrates for emerging flexible solar cells: A holistic panoramic review. *Progress in Photovoltaics, 31*, 753–789. https://doi.org/10.1002/pip.3703

Sun, Y., & Rogers, J. A. (2007). Inorganic semiconductors for flexible electronics. *Advanced Materials, 19*, 1897–1916. https://doi.org/10.1002/adma.200602223

Wang, H., & Chen, L. (2020). Electrowetting-on-dielectric based economical digital microfluidic chip on flexible substrate by inkjet printing. *Micromachines (Basel), 11*, 1113. https://doi.org/10.3390/mi11121113

Wang X., Jin H., Nagiri RCR., Poliquit BZL., Subbiah J., Jones DJ., et al. (2019) Flexible ITO-free organic photovoltaics on ultra-thin flexible glass substrates with high efficiency and improved stability. Solar RRL 3:1800286. https://doi.org/10.1002/solr.201800286.

Wang, Y., Wang, H., Liu, F., Wu, X., Xu, J., Cui, H., et al. (2020). Flexible printed circuit board based on graphene/polyimide composites with excellent thermal conductivity and sandwich structure. *Composites: Part A, 138*, 106075. https://doi.org/10.1016/j.compositesa.2020.106075

Wang, X. Y., Liao, S. Y., Wan, Y. J., Zhu, P.-L., Hu, Y.-G., Zhao, T., et al. (2022). Electromagnetic interference shielding materials: Recent progress, structure design, and future perspective. *Journal of Materials Chemistry C, 10*, 44–72. https://doi.org/10.1039/D1TC04702G

Wang, C., Guo, Y., Chen, J., & Zhu, Y. (2023). Transparent and flexible electromagnetic interference shielding film based on Ag nanowires/ionic liquids/thermoplastic polyurethane ternary composites. *Composites Communications, 37*, 101444. https://doi.org/10.1016/j.coco.2022.101444

Wei, R., Liu, B., Wu, F., Zhou, X., & Liu, M. (2024). Chinese ink-coated elastic PU/PET fibers as multifunctional flexible wearable sensors. *Sensors and Actuators A: Physical, 380*, 116011. https://doi.org/10.1016/j.sna.2024.116011

Wen, D.-L., Sun, D.-H., Huang, P., Huang, W., Su, M., Wang, Y., et al. (2021). Recent progress in silk fibroin-based flexible electronics. *Microsystems & Nanoengineering, 7*, 35. https://doi.org/10.1038/s41378-021-00261-2

Wu, Y., Xu, G., Shen, Y., Wu, X., Tang, X., Han, C., et al. (2024). Stereoscopic polymer network for developing mechanically robust flexible perovskite solar cells with an efficiency approaching 25%. *Advanced Materials, 36*, 2403531. https://doi.org/10.1002/adma.202403531

Xiang, H., Li, Z., Liu, H., Chen, T., Zhou, H., & Huang, W. (2022). Green flexible electronics based on starch. *npj Flexible Electronics, 6*, 15. https://doi.org/10.1038/s41528-022-00147-x

Ye, Q., Chen, Z., Yang, D., Song, W., Zhu, W., Yang, S., et al. (2023). Ductile oligomeric acceptor-modified flexible organic solar cells show excellent mechanical robustness and near 18% efficiency. *Advanced Materials, 35*, 2305562. https://doi.org/10.1002/adma.202305562

Zardetto, V., Brown, T. M., Reale, A., & Di Carlo, A. (2011). Substrates for flexible electronics: A practical investigation on the electrical, film flexibility, optical, temperature, and solvent resistance properties. *Journal of Polymer Science Part B: Polymer Physics, 49*, 638–648. https://doi.org/10.1002/polb.22227

Zazoum, B., Batoo, K. M., & Khan, M. A. A. (2022). Recent advances in flexible sensors and their applications. *Sensors, 22*, 4653. https://doi.org/10.3390/s22124653

Zhang, M., Liu, Z., Shen, C., Wu, J., & Zhao, A. (2022). A review of radio frequency identification sensing systems for structural health monitoring. *Materials, 15*, 7851. https://doi.org/10.3390/ma15217851

Zhang, G., Xu, Y., Haider, M., Sun, J., Zhang, D., & Yang, J. (2023). Printing flexible thin-film transistors. *Applied Physics Reviews, 10*, 031313. https://doi.org/10.1063/5.0150361

Zhang, C., He, M., Wu, S., Gao, Y., Ma, M., Liu, C., et al. (2024a). Occlusal architecture of the buried interface enables record-efficiency flexible perovskite photovoltaic modules with enhanced in-plane bending mechanical endurance. *Advanced Functional Materials, 34*, 2313910. https://doi.org/10.1002/adfm.202313910

Zhang, T., Sun, Y., Hu, R., Qian, W., & Yu, L. (2024b). High-performance flexible silicon nanowire field effect transistors on plastic substrates. *Advanced Electronic Materials, 2400615*. https://doi.org/10.1002/aelm.202400615

Zhao, H., Xiao, X., Xing, H., Jia, X., & Jin, S. (2024). Synthesis of an ultrathin, self-adhesive, tough, and frigostable BP@PVP/TPU ionogel for strain sensors by electrospinning. *Materials Today Chemistry, 38*, 102102. https://doi.org/10.1016/j.mtchem.2024.102102

Zhou, Z., Tang, W., Xu, T., Zhao, W., Zhang, J., & Bai, C. (2024). Flexible strain sensors based on thermoplastic polyurethane fabricated by electrospinning: A review. *Sensors, 24*, 4793. https://doi.org/10.3390/s24154793

Zhu, X., Zhang, H., Huang, Y., He, E., Shen, Y., Huang, G., et al. (2024). Recent progress of flexible rechargeable batteries. *Science Bulletin (Beijing), 69*, 3730–3755. https://doi.org/10.1016/j.scib.2024.09.032

Zou, M., Ma, Y., Yuan, X., Hu, Y., Liu, J., & Jin, Z. (2018). Flexible devices: From materials, architectures to applications. *Journal of Semiconductors, 39*, 011010. https://doi.org/10.1088/1674-4926/39/1/011010

Part II
Paper as Multifunctional Material

Chapter 3
History of Paper and Traditional Papermaking Techniques

Aleksandra Balachenkova

3.1 Introduction

The search for a suitable career for written information has led mankind to a great variety of solutions: stone, metal, wood, and clay tablets were used in many ancient cultures. With time, these materials were consequently replaced by flexible ones, which were cheaper in preparation and more convenient to transport. Papyrus, made from a plant of the same name, was the predominant writing material in Egypt and then in the Greco-Roman world for almost four thousand years. It was used for religious, literary, and philosophical texts, as well as administrative and private documents. The word "paper" is derived from the Greek term "papyrus."

Parchment, made from the skins of sheep and other livestock, was developed at first by the Persians and then widely spread. It was more durable and flexible than papyrus, and its use led to the development of a book in the familiar form of a codex.

Palm leaves and birch bark were common types of writing material in South West Asia and in India. Palm leaves were usually bound together into books by a cord. Such form of book was also familiar to the Chinese, but instead of leaves they used bound bamboo tablets. Another popular writing material in China was silk fabric.

The question about the origin of the paper is debatable. Until the middle of the twentieth century, the hypothesis on the artificial invention of paper by the Chinese official Cai Lun in 105 AD prevailed, based, first of all, on the news of the Chinese chronicle of *Hou Han Shu* ("Chronicle of the Emperors of the Later Han Dynasty"). However, active archaeological and anthropological study of Central and East Asia, results of historical technologies research in the late nineteenth to the first half of the twentieth century, and, in general, the fact that paper is a relatively late material led

A. Balachenkova (✉)
Higher School of Technology and Energy, St. Petersburg State University of Industrial Technologies and Design, St. Petersburg, Russia

G. Korotcenkov (ed.), *The Handbook of Paper-Based Sensors and Devices*,
https://doi.org/10.1007/978-3-031-91080-7_3

to thinking of an earlier time of appearance of paper,[1] as well as the secondary nature of its technology and, accordingly, the opportunity of its technological precursors.

3.2 Technological Precursors of Papermaking

Technologically, the precursors of paper are ancient materials obtained from fibers of both plant and animal origin—felt, tapa, weaving products.

The technology of **felt making** (by the so-called "wet method") dates back to Neolithic times (5–2th thousand BC) and is a direct consequence of the domestication of sheep. The most ancient samples of felt (fifth century BC) were found in 1929 in the mounds of Pazyryk (Gorny Altai). The zone, where felt was spread, had a very wide coverage and extended from the subarctic to the subtropical zones in the Northern Hemisphere. Currently, live felt production by a wet method can be found in certain regions of Central Asia (in the territories of Mongolia, China, Kazakhstan, Kyrgyzstan, and Russia). This technology is based on the structure of wool fibers and is related to bends in the hair and presence of microscopic roughness on its surface. Felt elasticity is due to the sinuosity of the fibers, and strength is due to the roughness.

In preparation for felt making—felting—the pre-trimmed wool of domestic animals (mainly sheep) was combed and turned into a kind of cotton wool, thereafter it was evenly spread on a fabric with a rare weave and moistened with hot water. After the removal of water through the drainage holes in the fabric, it was rolled up and felting was started, i.e., squeezing and rolling on a smooth surface. The process lasted until a dense and closed felt sheet was obtained.

Other ancient technologies used plant fiber. In the Upper Paleolithic, based on the techniques of braiding and spinning fibers, primitive **weaving** arose, for the needs of which textile plants have been specially cultivated since the Neolithic period: hemp, flax, cotton, ramie, etc.

Appearance of a cover sheet material, called **"tapa"** by ethnologists (according to its name among the peoples of Oceania), also dates back to the Paleolithic period. Tapa was widely spread on all continents in the equatorial zone, where bast fiber is used for its manufacture, mainly from plants of the mulberry family (Moracea)—ficus (Central America) and mulberry trees (East and Southeast Asia). Tapa was widely used not only as a material for clothing and in primitive construction, but also for writing: among the Maya Indians, this material for writing was called *huun*, among the Aztecs—*amate*, in Indonesia—*dluwang*. The ancient Egyptian and Chinese varieties of tapa, papyrus, made from the bast of the plant of the same name (*Cyperus papyrus*), and the so-called "rice paper", from the bast of the *tung-tsaou*

[1] Until the last decades in China, there was a fierce political discussion between archaeologists who defended the fact of the earlier appearance of paper (second to first centuries BC) and employees of the All-China Research Institute of Paper Industry, who firmly adhered to the recorded date.

tree (*Tetrapanax papyriferum*), became the most famous worldwide (Hunter, 1987; Loeber, 1981).

It is convenient to consider the tapa-making technology using the example of papyrus production. A bast was extracted from the pre-harvested stem of the plant, which was then cut into thin strips and beaten off with a hammer, destroying the cell walls for appearance of a sticky juice. After that, the first layer of the material was formed by overlapping these strips, then the second layer was laid at a right angle to the first layer. At the end, the wet sheet was pressed for gluing and dried.

3.3 Paper Origin Hypotheses

The paper origin hypotheses that exist today can be divided into two large groups—"heroic" and "technological" (Pichol, 2000). Heroic concepts, as it was mentioned above, are associated with the name of Cai Lun and differ in evaluating the degree of his contribution to appearance of paper technology and distinguishing those aspects of his possible activities that led to appearance of "true" paper. The authors of technological concepts (which in turn can also be classified) discuss different ways and forms of influence of technological precursors of paper on its origin and further development. Let's dwell on two of these hypotheses that got scientific recognition and support most of all.

Thus, the American historian of Chinese origin Tsuen-Hsuin Tsien considered paper a derivative of weaving, suggesting that the idea of paper emerged from the experience of household washing of linen or silk fabrics. According to Tsien, at some moment there appeared a desire to collect wet fibers remaining with laundresses or inventory ones to produce a thin felt-like material (Tsien, 1985).

As one of the basic arguments in favor of association between paper and weaving, primarily silk spinning, the researcher cites an excerpt from the Chinese chronicle of Hou Han Shu, which tells about invention of paper by Cai Lun: "In ancient times writings and inscriptions were generally made on tablets of bamboo or on pieces of silk named 'chih'. But silk being costly and bamboo heavy, they were not convenient to use. Cai Lun then initiated an idea of making paper [chih] from the bark of trees, remnants of hemp, rags of cloth and fishing nets. He submitted the process to the Emperor in the first year of Yuan-Hsing period (105 year AD) and received praise for his ability. From this time paper has been in use everywhere and has universally called the 'paper [chih] of Marquise Cai'" (Tsien, 1985; Tchudin, 1994).

The hypothesis of the Swiss archaeologist and historian, former director of the Basel Paper Museum P. Tchudin, is associated with the definition of paper as a product of felting of plant fibers, which was very popular in the nineteenth and early twentieth centuries. This definition indicates the materials that served as the basis for the emergence of papermaking—felt and tapa. According to Tchudin, paper appeared as a product of a technological combination of these ancient technologies. Papermaking technology borrowed the raw material and the idea of its mechanical

processing from tapa manufacturing methods, and the principle of formation of sheets from a water-wet mass on a sieve from felting technology. Most probably, paper appeared when a very thin felt was needed (whether plant or animal one), which could not be obtained by traditional felting.

Based on this hypothesis, the origin of paper production in its modern form in China seems logical both from a geographical and historical, and technological points of view. The southern provinces of China were included in the tapa spreading area, and the northern regions of the country always bordered the areas where felt production was widespread. Similar conditions existed on the Hindustan peninsula, but archaeological data to date do not confirm the presence of any developed paper production in India before the eleventh to twelfth centuries (Teygeler, 1998; Rezavi, 2014), despite attempts of individual Indian researchers to prove the opposite (Gosavi, 1983, 1987).

Archaeological finds in Western and Northwestern China allowed to make a conclusion that the appearance of paper in its modern form, first of all, as a material for writing, was preceded by the period of existence of "paper felt" (or quasi-paper), not related to the needs of book craft or writing in general. The difference between quasi-paper and "true" paper[2] consists in the degree of fiber development and presence of sizing and fillers—they are absent in paper felt. The earliest surviving samples of paper felt, dating back to second to first centuries BC, were found during archaeological excavations in 1957 in the cave burial of Baqiao in the Chinese province of Shaanxi. Analysis of the burial showed that the fragments found served as a wrapper, and the "paper" pulp consisted of poorly developed hemp fibers.

As most paper historians now believe, Tsai Lun deserves credit not for the original invention, but for the rationalization of the already existing technology. His role was to select the most suitable composition for the paper pulp. Cai Lun changed the composition of the pulp (i.e., fibers and fillers), which led to a change in the properties of the material and made it more suitable for writing.

3.4 Ancient Far Eastern Paper

It was from the time of Cai Lun's activity that the rooting of paper production and its rapid spread in China began—from the north and northwest to the south and east. During the second century, the cost of paper production decreased significantly, which made it a very popular material for writing. Its market value, apparently, was already lower than the cost of silk: an excerpt of a private letter dating from 143 was preserved, which told about impossibility to make a copy of the liked literary work on silk due to its high cost compared to paper. At the same time, new types of paper appeared, intended, among other things, for artistic purposes. In the third to fourth centuries, paper as a text carrier almost completely replaced bamboo strips and,

[2] D. Hunter introduced this term in the context of the problem under consideration (Hunter 1987).

partially, silk (Tsien, 1985). Paper also found wide application in the manufacture of many ritual objects, including those accompanying funeral rites. In addition, China became the birthplace of paper architecture, and it was here that the use of paper for sanitary and hygienic purposes was first recorded (Bloom, 2001).

3.4.1 The Most Important Finds of Early Paper Samples

The main source of information about early Chinese paper is the numerous finds of its fragments in the so-called "dead" cities of northwestern China and in the oases of the Great Silk Road (Turpan, Khotan, and Kashgar) made by European and Chinese expeditions.

The largest number of manuscripts and paper fragments, including early ones, was found in Dunhuang, one of the outposts of the Great Silk Road. Dunhuang is now a chief city in Gansu Province, in Northwestern China. Here, on the outskirts of the Chinese Empire, from the fourth to the eleventh centuries, a large Buddhist complex was located in the Mogao Caves or Caves of the Thousand Buddhas. Monasteries, temples, schools, a library, and Buddhist universities are placed there. Local citizens continued to use these caves for housing after the Buddhist center ceased to exist; in 1900 one of them came across a walled-up library. After that, European expeditions flooded into Dunhuang, which took a huge number of manuscripts and other monuments of Chinese art to Europe. Currently, more than 20,000 paper scrolls from Dunhuang are stored in the manuscript collections of a number of European countries and in China. These are mainly manuscripts of works of the Buddhist canon, Confucian classics, literary and philosophical works, as well as a large number of business documents in Chinese, various Turkic languages, Sanskrit, Sogdian language, and Hebrew (Tsien, 1985; Menshikov, 1987; Rishel, 1998).

The value of the Dunhuang find for the history of early paper is that the manuscript paper was produced in different centers. It is also very important that almost all manuscripts can be dated, and thus one can judge the quality and composition of paper produced in each of the eight centuries—from the fourth to the eleventh.

The most ancient sample of "true" paper made of linen fiber was also discovered in Dunhuang, relatively recently (in 2006). The fragment preserved the remains of the text, based on which it was dated back to 8 BC (Xinhuanet, 2006).

3.4.2 Early Chinese Papermaking Technology

First of all, physical and chemical analyses of historical paper samples, as well as observations made by researchers in the regions of traditional papermaking, allow to reconstruct the early technology of manual paper production in China. The only complete and illustrated description of the technological process that came down to us—an article from the encyclopedia compiled by the Chinese scientist Song

Yingxing *Tiangong Kaiwu* (Exploitation of the Works of Nature)—is an indirect source, since it was published only in 1637 and describes mainly the production of paper from bamboo (see Fig. 3.1).

Raw Material As the centuries-long experience of hand papermaking showed, plant fiber with a high natural cellulose content is best suited as raw material for its manufacture. Fiber can be either primary (raw), i.e., extracted directly from the plant, or secondary, taken from recycled raw fiber, for example, from textile rags. The main types of fiber used in the historical production of paper are distinguished according to their location in the plant:

(a) Bast fiber (flax, hemp, paper mulberry, ramie, lokta, etc.)
(b) Fiber of seed balls (cotton).
(c) Fiber of leaves (sisal, esparto, Manila hemp, yucca).
(d) Fiber of stems (chee grass, wheat, rice).

The earliest attempts of paper composition by Cai Lun are reported by the "History of the Late Han [Dynasty]," which was already cited. Morphological analysis of the preserved samples of Chinese paper showed that secondary fiber of textile plants—hemp (*Canabis sativa*), flax (*Linum*), and ramie (*Boehmeria nivea*)—was main raw material for it up to third to fourth centuries. By the sixth century, bark paper of paper mulberry (*Brussonetia papyrifera*) became widespread. Bamboo (Bambusa) began to be used as feedstock for papermaking relatively late (at the beginning of the eighth century). Figure 3.1a, b just shows the stages of preparation of bamboo fiber, which consisted of harvesting stems, soaking them for a long time, and cooking in lye.

Beating[3] of fibrous raw materials was probably performed in mortars (see Fig. 3.1a). Morphological analysis of Dunhuang paper samples (fourth to eleventh centuries) shows that such a stage of the technological process as **filling**[4] already existed. The fillers were gypsum, chalk, and kaolin (white clay), widely used in China, known for the production of porcelain.

Sizing[5] was obviously made in a vat (so-called tub sizing): with this method of sizing, the glue was introduced into the paper pulp. The samples of the third to fourth centuries were sized with natural dextrin, which is a product of reserve accumulation in the grains of glutinous rice or millet varieties (Balachenkova & Tsypkin, 2017). From about fifth century, plant juice was added to paper, which not only reinforced the paper, but also protected it from insects. Due to its viscous consistency, this vegetable glue prevented the sheets from sticking together during

[3] Beating is the splitting of plant fibers in the presence of water to obtain paper pulp.

[4] Filling is a process in which mineral or plant fillers are introduced into the pulp. This helps to increase the whiteness of the paper, makes the paper opaque (if necessary), and increases the smoothness and plasticity of the paper.

[5] Sizing is a process in which substances are introduced into the paper that promote bonding of plant fibers and, due to this, increase the strength of the finished paper. In addition, a thin film of these substances forms on the surface of the finished sheets, giving the properties of ink and water resistance to paper.

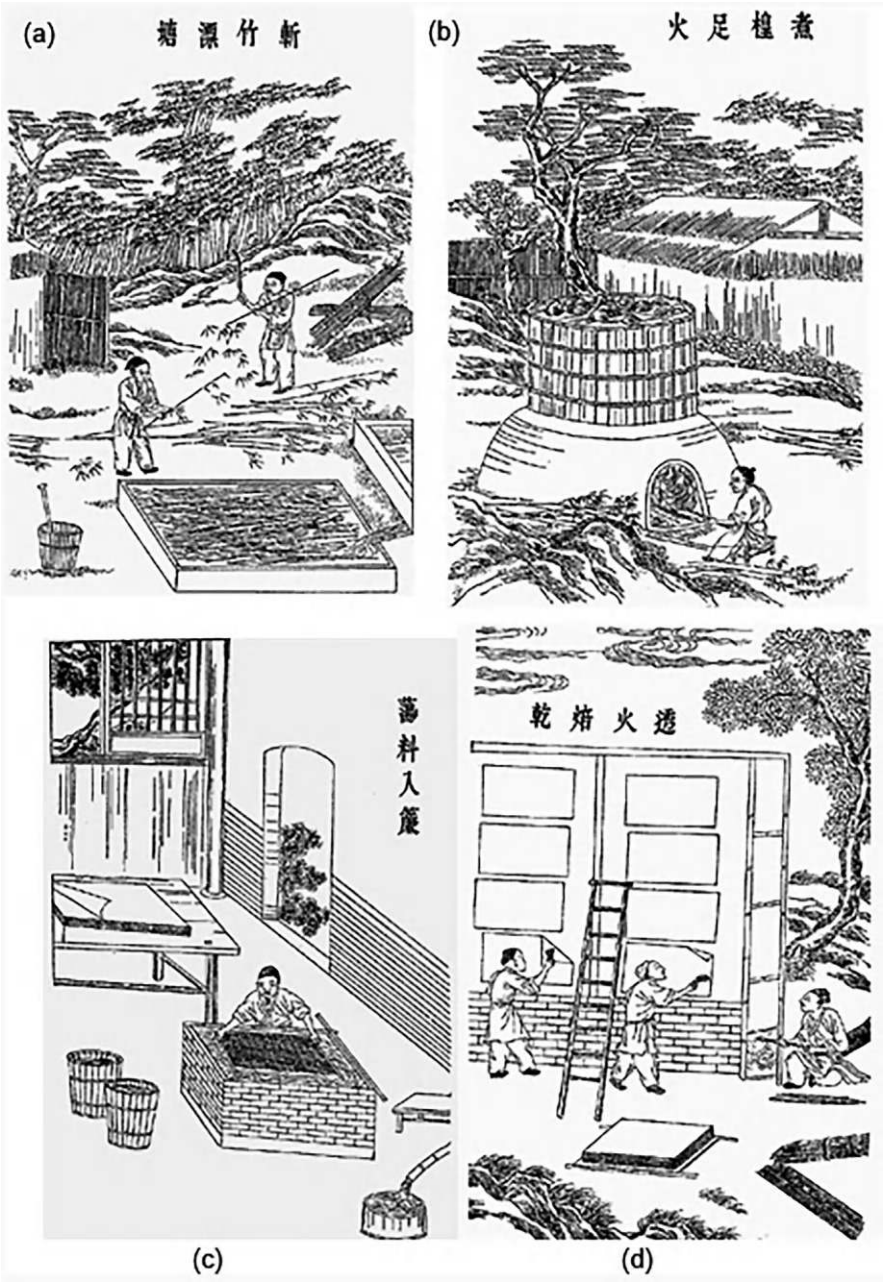

Fig. 3.1 Papermaking process in China. Woodcut from Tiangong Kaiwu, China, 1637. (**a**) Harvesting bamboo; (**b**) soaking bamboo stems and cooking in lye; (**c**) sheet forming by dipping method; (**d**) drying paper on a flat surface. https://www.worldhistory.org/image/1241/paper-making-process/

pressing and was called "paper medicine." In the manufacture of colored paper, mineral or vegetable dyes were also introduced into paper pulp before forming sheets (Tsien, 1985; Menshikov, 1987).

Sheet Forming[6] China became the birthplace of two main technologies of paper forming, which later spread worldwide. They were related to the use of two types of molds for forming sheets.

Some samples of early Chinese paper do not show visible to light screen imprints of a sheet-forming mold, which is indicative of using a sieve with a very small diameter of drainage holes for forming sheets. The paper mold used to make such paper had a rather primitive design, which was a rectangular bamboo frame with a piece of woven cloth stretched over it, and obviously had a household sieve as a prototype. This type of paper mold is called **wove mold**. The sheet-forming technology using such a wove mold was called the pouring method, and it is very close to ancient felt-making technology: fibrous pulp diluted with water was poured onto a linen sieve, which was then spread over the surface of the mold manually or using a primitive tool. During forming the mold, it could either lie on the surface of water ("floating mold") or, in the absence of reservoirs, be located above a hole for water runoff. This technique of sheet forming received the name of **pouring method**.

The wove mold had a significant drawback, which ultimately affected the production rate. The cloth, which formed the basis of the mold, as a material that had a fleecy surface, did not allow to remove the wet sheet immediately without damaging it. It was possible to remove the sheet only after drying, which significantly increased the production time of sheets from one mold and, accordingly, the number of molds required for production. Nevertheless, in China itself and in the countries of Central Asia, there are still areas where this technology is used in manual paper production.

In another group of samples of early Chinese paper, screen lines are visible to light. This paper was produced on a flexible screen made of thin bamboo ribs or reed stems, *laid* very close to each other and intertwined with a thread or horsehair. This type of paper mold is called **laid mold**. For ease of manipulation, the laid screen was placed on a wooden frame with stiffeners. Since the laid screen had a smooth surface and was flexible, it was possible to remove still-wet sheet from it quickly and easily. Use of a laid flexible mold made it possible to produce a significant number of sheets from one grid quickly, and eventually led to the emergence of a method of sheet forming by dipping the mold into a vat with pulp, so-called **dipping method**. Figure 3.1c shows the process of sheet forming by the dipping method.

For a long time, it was believed (Hunter, 1987; Tsien, 1985) that the pouring method was older, and it was superseded by the dipping method as more effective. P. Tchudin even designated them as "primary" and "secondary" technologies of sheet formation (Tchudin, 1994, 1999). However, recent studies of Chinese and Central Asian paper, undertaken by A. Helman-Ważny, proved that molds and

[6] Sheet forming is a process in which split fibers are combined into a paper sheet.

related methods of sheet forming arose almost simultaneously (Helman-Ważny, 2016a).

Pressing[7] of finished paper was present only when the sheets were formed on a laid mold. With the pouring technique, after the paper forming, they immediately began to dry finished sheets directly in the molds. Pressing was made using a primitive press, such as heavy boards or small stone slabs (Hunter, 1936, 1987).

Drying of pressed sheets formed by the dipping method took place on heated stones or smooth boards (Fig. 3.1d). After drying, the ready sheets were subjected to ***finishing***.[8] In the work *Shih Ming* ("Explanation of names"), dating back to the second to third centuries, it was already told about paper, which is "smooth and slippery like a whetstone" and "smooth and wide like a board," which indicates paper with a polished surface, possibly plastered or rubbed with starch (Menshikov, 1987).

3.4.3 Types of Ancient Chinese Paper

Dunhuang paper samples show an exceptional variety of Chinese paper types.[9] Fifth-century paper has various shades of brown and a smooth surface coated with a strengthening compound. The samples of the late fifth to early sixth centuries are yellow-colored paper, with a rough or smooth surface. The analysis of the papers of that time showed a stable uniformity of their composition—most of the samples are made of bast fibers of paper mulberry. This allowed to make a conclusion that by the sixth century, the papermaking process and the raw materials were standardized (Balachenkova & Tsypkin, 2017). In the eighth to tenth centuries, production of high-quality paper was greatly reduced as rebellions and wars disturbed the calmness of the Tang Empire (618–907). After the unification of the country under the auspices of the new Sung Dynasty (960–1279), production was resumed. Samples of Sung paper found in different collections demonstrate a steady uniformity of species and varieties. This suggests that national paper production standards reappeared in the Sung era (Menshikov, 1987).

According to written sources, special types of paper were used at the imperial court, which were distinguished for high quality and beauty. Chinese sources preserved information about the production of "honey fragrant paper," sparkling and waterproof; "red paper, thin and delicate" is mentioned (Menshikov, 1987). For a later time, we find the division of all numerous types of Chinese handmade paper

[7] Pressing is a process in which the finished sheet is dehydrated and compacted. The remaining moisture is removed during the drying process.

[8] Finishing is a set of operations that improve the consumer properties of paper.

[9] Currently, the concepts of "type" and "grade" of paper differ as follows: the term "type" refers to paper of a certain purpose, and the term "grade" usually defines the quality of the same type of paper. For classification of paper from remote historical eras, this division is not applicable, since researchers deal mainly with the only preserved type of paper—writing paper. Therefore, the introduction of grade and type classification seems very difficult.

into two types—*Xuan chih* and *Kao chih*. The first type is made of paper mulberry and bamboo bast and is intended for ordinary writing, calligraphy, and decorative purposes. The second one is used for packaging, sanitary and hygienic purposes, making wallpaper and folding screens, and for burning at funeral ceremonies. Kao chih is made primarily from hemp fiber, rice, and wheat straw (Koretsky, 1998; Tsien, 1985).

3.4.4 *Technological Modifications of Far Eastern Paper: Regions of Central Asia, Korea, Japan*

The paper from China was spread to the west across the routes of the Great Silk Road. Thus, in the culture of the peoples of Central Asia, first of all, among the Uighurs, paper began to be present as early as the third century. The distribution route of paper is shown in Fig. 3.2, and the history of paper production in the East is shown in Table 3.1.

It should be noted that early paper of Central Asian origin demonstrates a wide variety of fiber sources used for their production and vegetable glues. In addition, both the pouring and the dipping methods of sheet forming, which used both types of paper molds, were spread in this region almost everywhere. Central Asian paper includes a rather extensive system of technological types, despite the fact that its preserved functional types are limited, unlike in the Far East, mainly to writing and printing paper (Helman-Ważny, 2016b; Rishel, 1998; Trier, 1972).

Paper penetrated China's eastern neighbors as a carrier of Buddhist texts, which, in fact, made paper a sacred material in these countries. Korea got acquainted with paper in the fourth to fifth centuries, Japan in the early seventh century. In these countries, the technology using a laid bamboo mold and a dipping method of forming sheets was established immediately.

Fig. 3.2 The diffusion of papermaking across Eurasia. Reprinted from (Bloom, 2006). Published by Springer with open access

Table 3.1 History of paper production in the East

Country/ region	Production start date	Main raw materials	Method of formation	Mold type
China	First century BC to second century AD	Hemp, flax, ramie, bamboo, paper mulberry, straw	Pouring, dipping	Wove mold, laid (flexible) mold
Korea	Fifth century	Paper mulberry	Dipping	Laid (flexible) mold
Japan	Seventh century	Kozo, gampi, mitsumata, hemp, rice straw	Dipping	Laid (flexible) mold
Nepal	Seventh to ninth centuries	Lokta	Pouring	Wove mold
Tibet	Seventh to ninth centuries		Pouring	Wove mold
Bhutan	Seventh to ninth centuries	Sho	Pouring	Wove mold
			Dipping	Laid (flexible) mold
Sogdiana	Fifth century	Hemp, flax, ramie	Pouring	Wove mold
Arab caliphate	Eighth century	Hemp, flax, cotton, ramie	Pouring, dipping	Laid (flexible) mold
India	Twelfth century	Cotton, jute, ramie	Dipping	Laid (flexible) mold

Korea did not contribute principally new solutions to papermaking technology. The bast fibers of paper mulberry were the main raw material for paper production here. For many centuries, Korea has been increasing the production of handmade paper (hanji), creating large state-owned enterprises with division of labor, as well as introducing technological control of the state over numerous artisan industries. The large volumes of paper produced in Korea were due to the needs of the printing business, since appearance of paper in Korea almost coincided with the introduction of printing in the woodcut technique, also borrowed from China. The only specific feature of Korean handmade paper is the sheet-forming mold design, in which thin bamboo ribs were located in parallel to the narrow side of the frame, not the wide one (Hunter, 1936, 1987).

Japan did not just copy and adapt the technology borrowed from China to local conditions, but by introducing a number of innovations in the technique and technology of the craft raised them to a very high level, further expanding the possibilities of paper as a multifunctional material.

The main raw materials of Japanese handmade paper (washi) are the bast fibers of plants belonging to the mulberry family—kozo (*Brussonetia kazinoki*)—and mezereon family—gampi (*Wikstromia canescens*) and mitsumata (*Edgeworthia papyrifera*). Other types of plant fiber are also used, for example, hemp, rice straw, as well as waste paper is used very widely. In the eighth century, on the basis of the dipping method, the actual Japanese method of sheet forming, *nagashi-zuki* was

developed.[10] This is a method of so-called "dynamic" dipping, in which the papermaker manipulates the mold not only in the vertical, but also in the horizontal plane, making reciprocating movements. Thus, the number of inter-fiber bonds inside the formed sheet increases many times with this method of forming, making the paper especially strong. Another essential component of this method is (as in China) the introduction of a viscous agent, called *neri*, into the pulp. Commonly neri is obtained from the root stock of hibiscus (*Hibiscus manihot*). In the process of sheet forming, neri creates a surface film that retains long and thin fibrils on the surface of the mold and prevents the sheets from gluing during pressing (Barret, 2005; Hughes, 1982).

The evolution of the paper mold (*su-geta*) also takes place in Japan. The Japanese traditional mold consists of a bivalve wooden frame, inside which a flexible bamboo screen is inserted. Such mold design prevented the outflow of pulp beyond the edges of the mold during extraction of the mold from the vat, and also accelerated the forming process, since it gave the master the opportunity to replace the screen with a sheet with a clean one quickly (Barret, 2005; Hughes, 1982; Hunter, 1936; Loeber, 1982).

Since the scope of paper application in Japan is very large, there are dozens of types and hundreds of sorts of handmade paper (Hunter, 1936), which cannot be listed and described due to the volume of the chapter. Nevertheless, all of them can be brought into several large groups, distinguished by raw material: *cho-shi* (papers made of the bast fibers of mulberry trees, including *kozo-shi*), *gampi-shi* (papers made from gampi fibers), *mitsumata-gami* (papers made from mitsumata fibers), and *ma-shi* (papers made of hemp fiber, raw or generated from recycled rags) (Barret, 2005).

Technological traditions, local raw material, and aesthetic preferences that have developed in this region created a special Far Eastern type of handmade paper, which also includes paper of Central Asian origin. Its main characteristics include the following: very low average density (25–45 g/m^2); predominance of raw fiber in the average composition (secondary fiber is present in relatively small quantities); use of viscous vegetable glue, which retains long fibrils on the surface of the mold and prevents wet sheets from sticking together.

3.5 Ancient Handmade Paper of the Near East

The paper of Middle Eastern origin became an intermediate type, in other words, a "technological bridge" between the Eastern and Western types of handmade paper. The question of the date of acquaintance with paper and the beginning of local paper production in the territories of the Islamic world still remains insufficiently clarified. At the same time, it is obvious that the earliest center was Samarkand,

[10] Chinese and European sheet-forming methods in Japan are considered "static" and are designated by the term *tami-zuki.*

where its own paper could be produced from the fifth to sixth centuries (Tchudin, 1998). Historians also agree that the active and widespread use of paper in the Middle East should be associated with the name of Caliph Harun al-Rashid (776–809), who legalized the use of paper in the offices and administrative centers of the Arab Caliphate. Since the end of the eighth century, Baghdad was the largest center of paper production and trade in the Arab world. North African Arabs began to produce paper in the ninth century, and by the end of the tenth century, paper as a writing material completely replaced papyrus. In the early eleventh century, the first paper mill appeared in Muslim Iberia (Bloom, 2001).

Relatively numerous manuals on the book-making technology, as well as observations by anthropologists made in India, where manual production, introduced in the eleventh century by the Arabs, is still cultivated as one of the traditional folk crafts, allow to reconstruct the Arabic papermaking technology (Premchand, 1995; Teygeler, 1998). Figure 3.3 just shows the papermaking process practiced in Kashmir. The illustration depicts the processes of beating rags, washing the pulp on

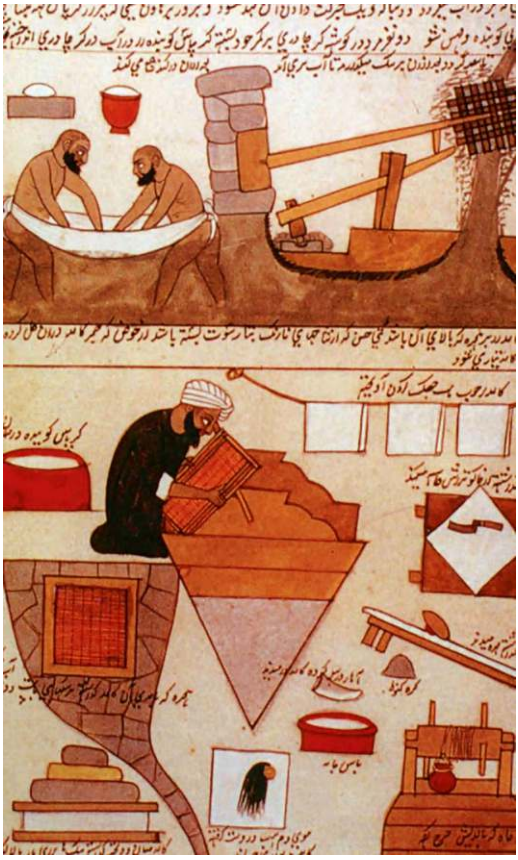

Fig. 3.3 Arab-type papermaking process in India. Guache miniature from a manuscript on various trades in Kashmir, 1850–1860. https://buzeon.ru/history/africa

a fabric, tied to the waists of two men, sheet forming by the dipping method, and paper being hung up on the rope.

As paper production reached the western regions of the Muslim world, the raw material had been changed radically. Raw hemp fibers (which were used to make paper in Samarkand) were everywhere replaced with rags. By the ninth century, recycled fibers (from rags) in the composition of Arabic paper already accounted for more than 80%. Being technologically oriented to both China and Central Asia, the Arab craftsmen began to use both dipping (Fig. 3.3) and pouring methods for forming sheets. It should be noted that they used a laid mold made, in the absence of bamboo, from the stems of herbaceous plants or from straw (Bloom, 2001; Tchudin, 1998).

Fermented or pre-boiled rags were beaten using millstones driven by water or manpower (Fig. 3.3). At the same time, the quality of fiber beating was low: there were usually unbroken threads in the pulp, and remains of unbeaten fabric were visible (Bloom, 2001).

Perhaps it was because of poor beating quality and low wear resistance of the molds that the Arabs introduced surface sizing in the form of a thick layer of starch paste, which hid the shortcomings of production. The process of cooking starch glue consisted of the following operations: a paste was prepared from starch and water and this mass was liquefied and boiled for a short time over high heat. The semi-liquid mass was filtered with a sponge or soft cloth and applied to paper. When the paper dried, it was subjected to polishing on a chestnut wood board with a polishing tool. The paper was sometimes polished by rubbing it with soap. Colored writing paper was widespread. The paper was dyed:

1. By direct impregnating the paper with an appropriate dying solution.
2. By introducing the dye into the starch paste, which allowed to produce sheets colored on both sides in different colors. The following dyes were mainly used: henna, saffron, safflower, mulberry, indigo, and verdigris (Kaziev, 1966).

Some craftsmen left zigzag marks on paper, which were probably placed on the still-wet sheets with a pointed tool. The role of these marks is not precisely defined; there are two points of view: either they served to count the sheets, or they were applied to mark the type or grade of paper, as later watermarks in Europe (Le Leannec-Bavaveas, 1999).

There were the following types of paper, named after their place of production, feedstock, format, and other distinctive features: Baghdadi, Samarkandi, Ispahani, Hatani (Chinese), Sultani, Kishmiri, Gauni, Mansouri, etc. (Kaziev, 1966; Tchudin, 1998).

3.6 Preindustrial Paper of the West

Paper, which was produced on the European continent, i.e., in Arab Spain and Italy, was initially produced using Arabic technology. However, over time, Italy made significant changes to it. The complex of these technical and technological innovations introduced in the middle of the thirteenth century is commonly called the "Italian paper revolution."

3.6.1 "Italian Paper Revolution" and Its Highlights

The main components of this technological transformation included the use of a stamper for beating rags, change of the material of paper molds, and use of screw presses and cloth for pressing wet sheets.

Stamper The main task of the Italian technologists was to solve the problem of poor beating quality, characteristic of the Arab production method. It was solved through the introduction and adaptation of a mechanism widely used in Italian cloth making to the conditions of paper production. In the practice of paper makers, it got the name of a stamper (see Fig. 3.4).

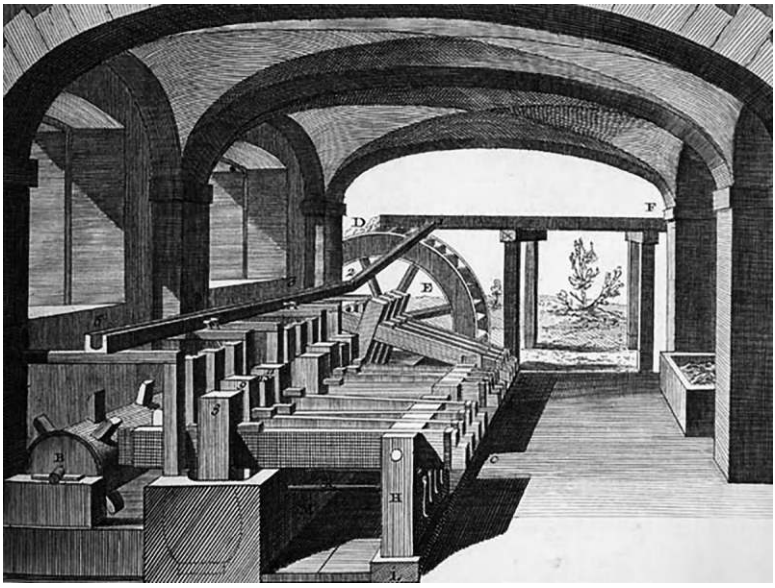

Fig. 3.4 Stamper. Engraved plate from Diderot Encyclopédie. https://paper.lib.uiowa.edu/european.php

A water wheel served as a usual engine of this device. There were cams or fingers on the wheel shaft, which were positioned in such a way that three cams pushing the levers were placed against each hammer along the periphery of the wheel shaft. Thus, each revolution of the water wheel shaft corresponded to three lifts of the hammer. The second important part of the stamper was a wooden deck, which had a length of up to 8 m or more. There were large hollows made in it—mortars. Each of them had a special purpose: usually the first three mortars (counting from the water wheel) served for half stuff beating, the next ones for stuff beating, and the last one for breaking lumps and diluting the pulp (Barret, 2011; Hills, 1988; Hunter, 1987; Tchudin, 1998, 1999).

Laid Mold with Wire Screen The prototype of the Italian laid metal mold is the Far Eastern laid mold. In order to make a laid wire screen, a row of thick wires—*laid lines*, located along the long side of the frame—were reinforced on a wooden frame. Before attaching these wires to the frame, they were intertwined with thinner wires at right angles to them—*chain lines*. The fact that the wire base of the mold makes it easy to label products by attaching a wire curved along a certain contour to it was quickly realized by Italian manufacturers. The imprint of the wire sign protruding above the surface of the screen became the most distinct element of the imprint of the mold; it was called a ***watermark*** (Fig. 3.5). Use of watermarks as trademarks has spread in Europe since the end of the thirteenth century extremely rapidly (Hunter, 1987; Hills, 1988; Tchudin, 1998, 1999).

Pressing Significant technical and technological innovations were introduced into the pressing process: to increase the production rate, output, and quality of paper, Italian craftsmen begin to use for pressing a screw press, obviously borrowed from

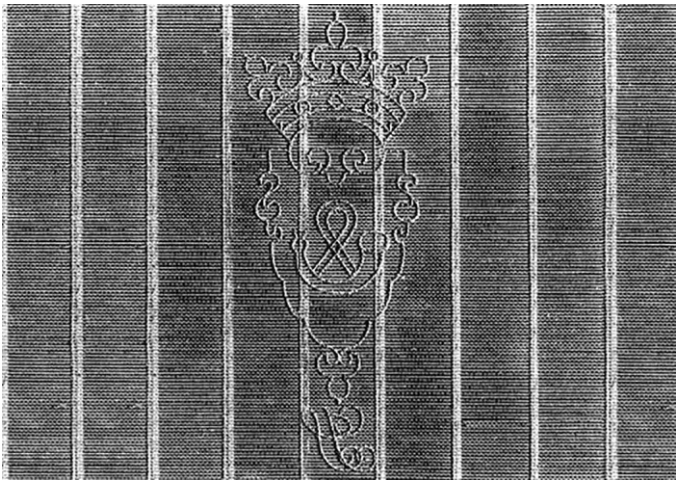

Fig. 3.5 Fragment of the European-type paper mold. https://www.vseobumage.ru/1310/istoriya-bumagi-epohi-razvitiya/

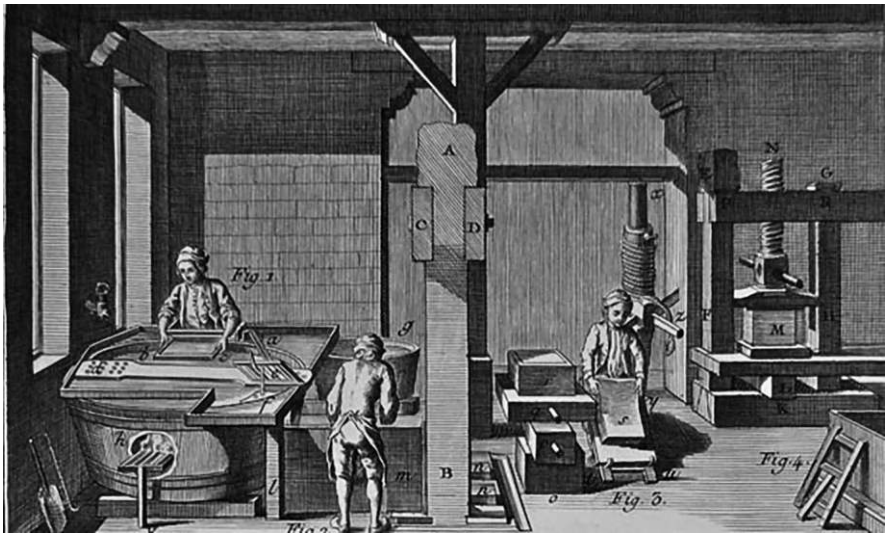

Fig. 3.6 Sheet forming, couching, and pressing. Engraved plate from Diderot Encyclopédie. https://paper.lib.uiowa.edu/european.php

the practice of winegrowers or cloth-makers (Fig. 3.6). In addition, cloth is used as a pressing means in Italy. Unlike the Far Eastern practice of papermaking, in which a viscous agent was introduced into paper pulp for preventing the sheets from sticking together during pressing, the Italian practice developed the idea of separation of wet sheets removed from the mold with cloth. Use of cloth simultaneously solved several problems: the fabric not only separated the sheets from each other and prevented them from sticking together, but absorbed moisture that was removed during pressing (Hills, 1988; Hunter, 1987; Tchudin, 1998, 1999).

3.6.2 Renaissance and Early Modern European Paper

The subsequent technical development of the craft in the fourteenth to sixteenth centuries was mainly expressed in the evolution of paper molds. Gradually, laid lines and chain lines became more and more thin, and the distance between chain lines decreased. The mold was completed with a deckle, an external frame into which the sheet mold itself was inserted. The deckle prevented the pulp from flowing out of the mold during dipping and determined the consumer format of the sheet (Hunter, 1987; Loeber, 1982; Tchudin, 1999).

Other technological modification concerns sizing. Starch paste, which in the practice of Arab production was applied with a brush to the surface of the finished sheet, is replaced with gelatin, and the sheets are sized by immersion in gelatin. This improved the quality of finished products significantly and accelerated the

production rate. Subsequently, alum was introduced into its composition for reduction of the cost of glue and its longer preservation (Hills, 1988; Hunter, 1987; Tchudin, 1998).

Technical innovations of this period were associated with the mechanization of the glazing process. They were expressed in the introduction of glazing hammers (1541), which had a water drive (Tchudin, 1999).

If the Italian paper revolution is considered to be the first period of mechanization of European hand papermaking, then in the seventeenth century its second stage began (Tchudin, 1999). At the end of the seventeenth century, there took place a radical change in the beating technique—a stamper was replaced with the Hollander beater or "engine" in papermaking terms (Fig. 3.7). The rags were beaten between the bars fixed on a solid wood roll or drum and another set of bars fixed on the bedplate on the bottom of the trough. The rags circulated in the engine round and round until they became pulped. The roll was attached using a jack. In terms of performance, the engine was twice as good as the stamper (Hunter, 1987; Hills, 1988).

If handmade paper of the European type is characterized in general, then its main features include the following: rags as the only type of raw material, and, consequently, shorter fibers; high average density (> 50 g/m^2); by its physical and mechanical characteristics, it is inferior to paper of the Far Eastern type.

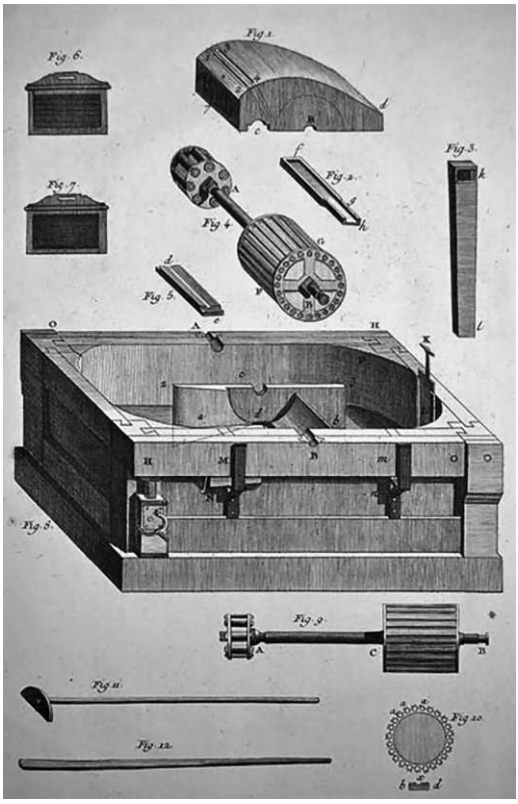

Fig. 3.7 Hollander beater. Engraved plate from Diderot Encyclopédie. https://paper.lib.uiowa.edu/european.php

In addition, in the eighteenth century, use of calenders with rollers for paper glazing was started; chemical bleaching of paper pulp was introduced. Since the second half of the eighteenth century, woven molds began to displace the laid ones gradually, and the paper acquired its modern texture (Balston, 1992; Hills, 1988). The end of the second stage of mechanization was marked by the invention of the papermaking machine by N.-L. Robert (1799) (see Fig. 3.8), which opened the way for industrial paper production (Clapperton, 1967). One of the first papermaking machines is shown in Fig. 3.9. For comparison, Fig. 3.10 shows a modern papermaking machine.

Fig. 3.8 First model of the papermaking machine invented by N.-L. Robert. https://www.worldhistory.org/image/17305/papermaking-machine/

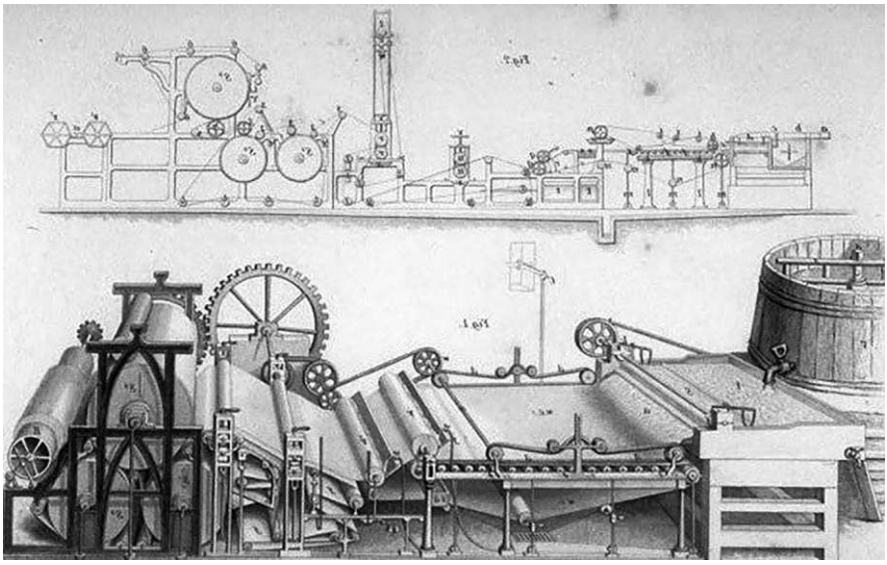

Fig. 3.9 One of the first papermaking machines. Reprinted with permission from (Clapperton, 1967). Copyright 1967: Elsevier

Fig. 3.10 Modern papermaking machine. https://www.gmpapermachinery.com/

References

Balachenkova, A., & Tsypkin, D. (2017). Lost research. Paper history. *Journal of the International Association of Paper Historians, 22*(2), 16–22.

Balston, J. N. (1992). *The elder James Whatman: England's greatest papermaker*, 3 vols. St. Edmundsbury Press.

Barret, T. (2005). *Japanese papermaking: Traditions, tools and techniques*. Floating World Editions.

Barret, T. (2011). *Paper throughout time: Non-destructive analysis of 14th through 19th century European style paper*. https://paper.lib.uiowa.edu/european.php (date of access 10.10.2024).

Bloom, J. (2001). *Paper before print. The history and impact of paper in the Islamic world*. Yale University Press.

Bloom, J. M. (2006). Papermaking: The historical diffusion of an ancient technique. In H. Jöns, P. Meusburger, & M. Heernan (Eds.), *Mobilities of knowledge* (Springer knowledge and space series) (Vol. 10, pp. 51–66). Springer.

Clapperton, R. H. (1967). *The paper-making machine*. Elsevier.

Gosavi, P. G. (1983). Did India invent paper? *IPH-Information, 17*, 7–11.

Gosavi, P. G. (1987). Quality of Ancient Indian paper. *IPH-Information, 21*, 103–111.

Helman-Ważny, A. (2016a). More than meets the eye: Fibre and paper analysis of the Chinese manuscripts from the silk roads. *STAR: Science & Technology of Archaeological Research, 2*(2), 1–14. https://doi.org/10.1080/20548923.2016.1207971

Helman-Ważny, A. (2016b). Overview of Tibetian paper and papermaking. In O. Almongi (Ed.), *Tibetian manuscript and xylograph traditions: The written word and its media within the Tibetian culture sphere* (pp. 171–197). Department of Indian and Tibetan Studies, Universität Hamburg.

Hills, R. (1988). *Papermaking in Britain. 1488–1988*. The Athlone Press.

Hughes, S. (1982). *Washi: The world of Japanese paper*. Kodansha International.

Hunter, D. (1936). *A papermaking pilgrimage to Japan, Korea and China*. Pinson Printers.

Hunter, D. (1987). *Papermaking: The history and technique of an ancient craft* (4th ed.). Dover Publications.

Kaziev, A. (1966). *Khudozhestvenno-tekhnicheskiie materialy i terminologiia srednevekovoi knizhnoi zhivopisi, kalligrafii i perepletnogo iskusstva* [Artistic and technical materials and terminology of medieval book painting, calligraphy and bookbinding]. Azerbaijan Academy of Sciences Publications.

Koretsky E. (1998) *Chinese handmade paper*. In: IPH congress book, vol. 12 (the 24th international congress of paper historians, Porto, Portugal, 11–20 September, 1998), pp. 162–163.
Le Leannec-Bavaveas, M.-T. (1999). Zigzag et filigranes sont-ils incompatibles? Enquete dans les manuscrits de la Bibliotheque nationale de France. *Bibliologia, 19*, 119–133.
Loeber, E. (1981). Prehistoric origins of paper. IPH. *Information, 13*, 87–94.
Loeber, E. (1982). *Paper mould and mouldmaker*. The Paper Publications Society.
Menshikov, L. N. (1987). Rukopisnaia kniga v Kitae 1 tysiacheletiia nashey ery [Handwritten book in China 1st Millenium AD]. In: *Rukopisnaya kniga v kulture narodov Vostoka* [Handwritten Book of the East], vol. 2, pp. 103–108 (in Russian).
Pichol, K. (2000). *Zur Erfindung des papiers—(re)construktion einer Entwicklung*. In: IPH-Congressbook, vol. 13 (The 25th international congress of paper historians, Dortmund, Germany, 8–14 September, 2000), pp. 147–159.
Premchand, N. (1995). *Off the deckle edge. A papermaking journey through India*. The Ancur Project.
Rezavi, S. A. (2014). Paper manufacture in medieval India. *Studies in People's History, 1*(1), 43–48.
Rishel, A.-G. (1998) *Looking at central Asian paper of Turkish, Tibetian and Chineese origin from the silk roads*. In: IPH congress book, vol. 11 (the 23d international congress of paper historians, Leipzig, Germany, 30 August–5 September, 1998), pp. 176–184.
Tchudin P. (1994) *The invention of paper*. In: IPH congress book, vol. 10 (The 22nd international congress of paper historians, Annonay, France, 2–8 September, 1994), pp. 17–21.
Tchudin, P. (1998). *Paper comes to Italy*. In: IPH congress book, vol. 12 (The 24th international congress of paper historians, Porto, Portugal, 11–20 September, 1998), pp. 61–66.
Tchudin, P. (1999). Le development technique de la papeterie, de ses debuts en Asie a l'Europe de la Renaissance. *Bibliologia, 19*, 1–16.
Teygeler R. (1998) *Handmade paper from India. Kagaj—Yesterday, today and tomorrow*. In: IPH congress book, vol. 12 (The 24th international congress of paper historians, Porto, Portugal, 11–20 September, 1998), pp. 185–194.
Trier, J. (1972). *Ancient paper of Nepal: Results of ethno-technological field work on its manufacture, uses and history*. Aarhuus.
Tsien, T.-H. (1985). Paper and printing in China. In J. Needham (Ed.), *Science and civilization in China* (Chemistry and chemical technology) (Vol. 5). Cambridge University Press.
Xinhuanet. (2006). New evidence suggests longer papermaking history in China. URL: http://news.xinhuanet.com/english/2006-08/08/content_4937457.htm

Chapter 4
Cellulose

Yingran Duan

4.1 Wood Fiber Structure

Cellulose, synthesized by plants, algae, and bacteria, is the most abundant natural polymer on the earth. Cellulose nanofibers derived from various species of plants are the longest and most widely studied cellulose nanofibers. Current industrially important cellulose nanofibers are primarily developed from woody biomass. Wood is typically composed of three major components: cellulose (~45%), hemicellulose (~25%), and lignin (~20%); the structure of wood can be considered as a fiber-reinforced composite—the fibrous cellulose bonded by surrounding hemicellulose and lignin adhesive.

The fibrous cellulose exhibits a hierarchical structure with the cellulose elementary fibrils as its nanoscale building blocks (Fig. 4.1). These elementary fibrils can be isolated from different plants through direct mechanical fibrillation (Wang et al., 2012), mechanical fibrillation after enzymatic hydrolysis (Marielle Henriksson et al., 2008), or mechanical fibrillation after chemicals such as 2,2,6,6-tetramethylp iperidine-1-oxyl radical (TEMPO)-mediated oxidation (Fukuzumi et al., 2009). While wood pulp is the most commonly used feedstock for nanofibril production, many different types of natural fibers have also been attempted.

The isolated fibrils often entangle/bundle with each other and form a network structure (Xu et al., 2013). Along the fibrils, there exist segments of amorphous and crystalline cellulose; the amorphous segments can be removed by acid hydrolysis so that only the needle-shaped cellulose nanocrystals are retained (Fig. 4.2). A recent paper has reviewed various available methods to produce the long, flexible fibrils and the short, rigid crystals (Khalil et al., 2014). Different terms have been used to describe these two types of nanoscale cellulosic materials in literature. Herein, the

Y. Duan (✉)
Zhuhai Topchain Pharma Co., Ltd., Guangdong, China
e-mail: yingran@youpuhui.com

G. Korotcenkov (ed.), *The Handbook of Paper-Based Sensors and Devices*,
https://doi.org/10.1007/978-3-031-91080-7_4

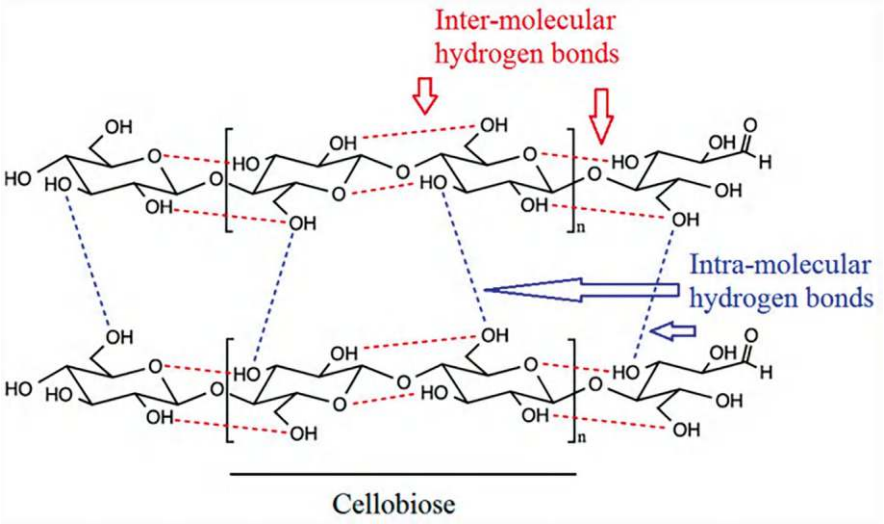

Fig. 4.1 Chemical structure of cellulose. Reprinted from (Baghaei & Skrifvars, 2020). Published 2020 by MDPI with open access

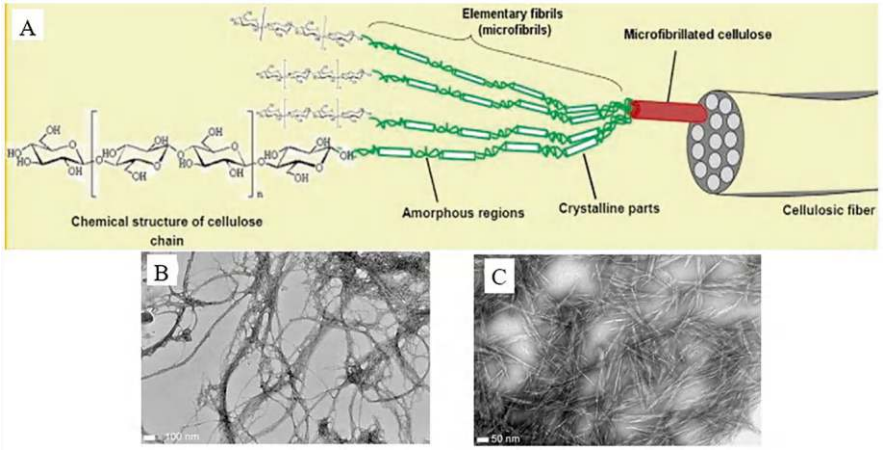

Fig. 4.2 (**a**) Hierarchical structure of fibrous cellulose and SEM images of (**b**) CNCs and (**c**) CNFs. A- adapted with permission from (Lavoine et al., 2012). Copyright 2012: Elsevier; B-C—reprinted with permission from (Xu et al., 2013). Copyright 2013: ACS

former is denoted by cellulose nanofibrils (CNFs) (Fig. 4.2c) and the latter by cellulose nanocrystals (CNCs) (Fig. 4.2b). CNFs and CNCs contain abundant hydroxyl groups (-OH) on their surfaces because of the structure of cellulose molecules. Other chemical groups such as carboxyl groups (from TEMPO oxidation) and sulfate groups (from sulfuric acid hydrolysis) are also present due to these chemical treatments. Diameters between 2 and 100 nm have been reported for CNCs and

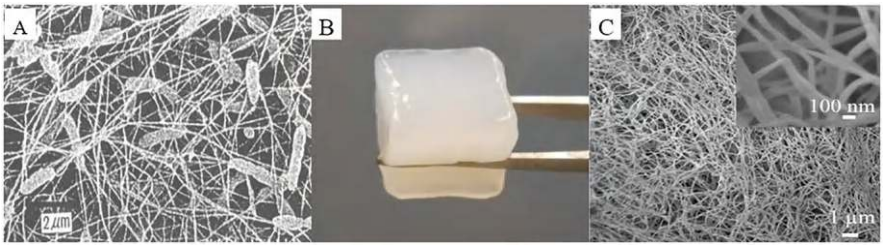

Fig. 4.3 (**a**) SEM of a bacterial cellulose network including the bacterial cells; (**b**) a bacterial cellulose pellicle; (**c**) SEM of supercritical carbon dioxide (CO_2)-dried bacterial cellulose aerogel. A- adapted with permission from (Klemm et al., 2001). Copyright 2001: Elsevier; B-C- reprinted with permission from (Xu et al., 2015). Copyright 2015: ACS

CNFs, and their length can vary between tens of nanometers to micrometers (Sacui et al., 2014). CNCs and CNFs show high tensile strength (> 1 GPa) and high modulus (about 40 GPa) (Sehaqui et al., 2012) (Tanpichai et al., 2012). Research on cellulose nanofibers has experienced explosive growth in recent years due to their high potential in a wide variety of advanced applications, which are derived from the nanofibers' high strength, high modulus, large aspect ratio/surface area, rich surface chemistry, optical properties, low density, and biobased nature (Xu et al., 2015).

Besides the plant-based cellulose nanofibers, bacterial cellulose (BC) represents another important category of cellulose nanofibers. BC is produced naturally by bacterium *Gluconacetobacter xylinum* through a fermentation process (Fig. 4.3). The product, bacterial cellulose pellicle, is formed at the air/liquid interface of the culture medium and is essentially a cellulose hydrogel containing networked BC nanofibers. High-purity/crystalline nanofibers can be readily obtained by removing the bacterial cells and other impurities by cleaning the gel with sodium hydroxide (NaOH) solution and water. Moduli of BC have been measured to be 78–114 GPa (Guhados et al., 2005; Hsieh et al., 2008).

4.2 Nanocellulose

4.2.1 Production of Cellulose Nanofibers

Nanocellulose is to name the big cellulosic family. Therefore, in this chapter, we need to classify each member. In fact, the nominature of "nanocellulose" comes later than the cellulose nanofibrils (abbreviated as CNFs since the year 2000), cellulose nanocrystals (CNCs), etc. Based on its size (Fig. 4.4), it is divided into nanoscale particles or cellulose nanofibers (or called nanofibrils), and microscale particles or cellulose nanostructured materials. The naming was confusing from the year 2000 till 2024. Since the nanocellulose may come from any source extracted from plants and agricultural residues including softwood, bamboo, jute fibers,

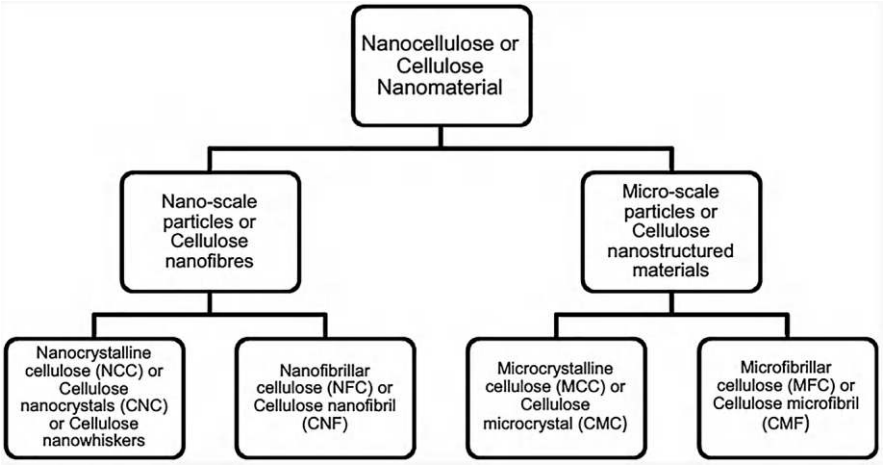

Fig. 4.4 Hierarchical levels of wood-based nanocellulose. Reprinted with permission from (Osong et al., 2016). Copyright 2016: Springer

coconut husk fibers, pineapple leaf, rice straw, and potato peel, or endure various chemical treatments such as TEMPO oxidation, it is generally classified into nanocrystalline cellulose (NCC) or cellulose nanocrystals (CNCs). Sometimes, it is also called cellulose nanowhiskers (CNW) when it is indeed very long with a high length to width aspect ratio. On the other hand, when it is in a microscale range, it is classified as microcrystalline cellulose (MCC) or cellulose microcrystal (CMC), which is exactly in stock for sale by a lot of pharmaceutical companies as an additive to drugs. Microfibrillar cellulose (MFC) or cellulose microfibril (CMF) is another product if the wood pulp endured only mechanical milling and retained its micro-sized cellulosic bundles.

In the natural sources such as plants and agricultural residues, some of the extraction is similar to that of paper pulping. As sketched in Fig. 4.5, it includes the following steps:

1. Lignin, hemicellulose, and other impurities are removed from the raw lignocellulosic materials through a typical pulping process, where chemicals such as NaOH and sodium chlorite ($NaClO_2$) (Chen et al., 2011) are often used.
2. The obtained pulp is destructured to produce CNFs through a nanofibrillation process such as multiple passes of mechanical grinding (Jiang et al., 2013; Wang et al., 2012), intensive ultrasonication (Chen et al., 2011), or microfluidization (Qing et al., 2013).

Either in laboratory or large-scale production, it has a strong different logic for MFC production and CNC production. First, the fiber suspension, which is usually the starting material, can be put into a machine such as blender/ball miller/fluidizer for mechanical production. Then, it undergoes pretreatment such as enzymatic pretreatment or TEMPO oxidation treatment. The CNC production is only with

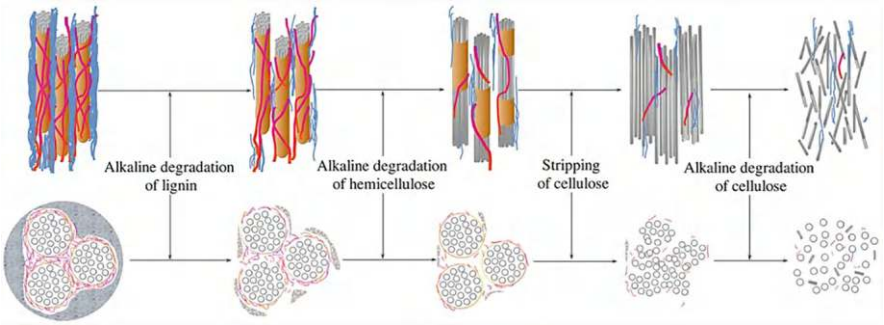

Fig. 4.5 Diagrammatic sketch of the degradation process of natural fibers in an alkaline environment. Reprinted with permission from (Wei & Meyer, 2015). Copyright 2015: Elsevier

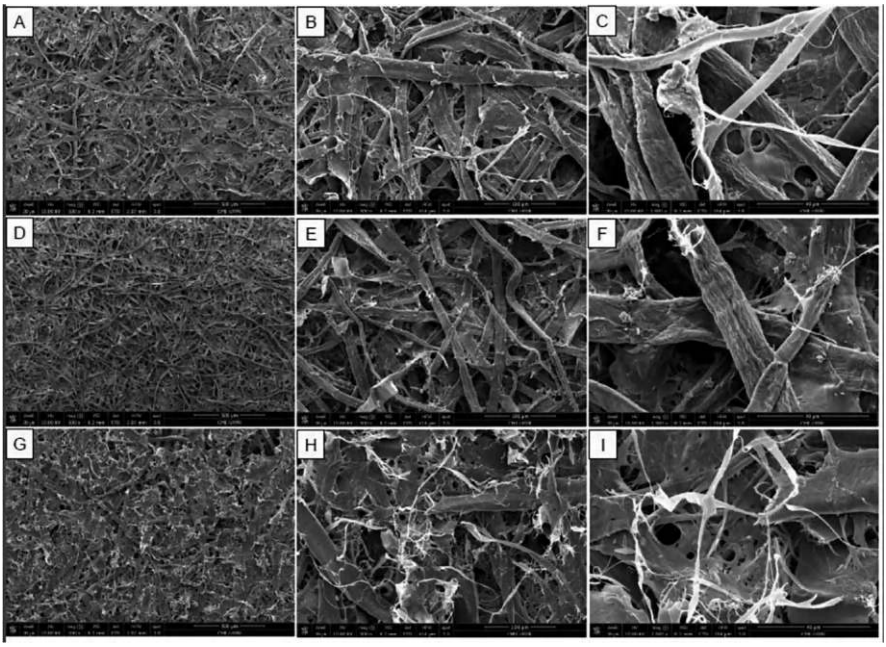

Fig. 4.6 SEM images of recycled fibers from cardboard (**a**, **b**, and **c**), printing and writing paper (**d**, **e**, and **f**), and newsprint (**g**, **h** and **i**) at magnification of 100, 500, and 2000 (left to right). Reprinted from (Viana et al., 2018). Published 2018 by UFLA—Universidade Federal de Lavras, as open access

chemical treatment by acids then dialysis to remove chemicals. Based on this understanding, researchers have extracted different nanocellulose from various resources, such as recycled fibers from cardboard (Fig. 4.6).

In general, CNFs with a wide range of diameter (10–1000 nm) and crystallinity (› 40% cellulose I) are typically obtained (Chen et al., 2011). Pretreatments before

the nanofibrillation by using various chemicals may change the crystalline structure in the obtained CNFs. The pretreatment (or further refinement) by TEMPO-mediated oxidation can result in highly uniform, extremely fine (2.09 nm) (Jiang et al., 2013) CNFs with a high aspect ratio. The TEMPO treatment leads to surface carboxylation of the CNFs, which causes ionic repulsion among the nanofibers and stabilizes CNF colloidal suspension. In general, the smaller the fiber diameter, the higher the degree of surface carboxylation.

CNCs are typically made from microsized cellulosic materials (e.g., wood pulp, microcrystalline cellulose, cotton, and other natural fibers) through an acid hydrolysis process that removes amorphous cellulose and other non-cellulose components. The hydrolysis conditions, including acid/fiber ratio, temperature, hydrolysis time, acid concentration, and sonication time, show strong effects on the yield, sulfur content (in the case sulfuric acid), anionic sites, zeta potential, width, length and aspect ratio of the produced CNCs (Table 4.1) (Brito et al., 2012). Depending on their origin and the hydrolysis conditions, CNCs with a diameter ranging from 2 to over 100 nanometer and a length up to hundreds of nanometer have been produced. For example, Santos et al. (2013) used pineapple leaves to produce CNCs. Acid hydrolysis using sulfuric acid (H_2SO_4) at 45 °C for 30 min generates needle-like (4 nm wide, 250 nm long), crystalline (73%) CNCs with a high thermal stability (225 °C). Hydrochloric acid (HCl) (Yu et al., 2013), phosphoric acid (H_2PO_4) (Espinosa et al., 2013), and hydrobromic acid (HBr) (Sadeghifar et al., 2011) have also been used for the hydrolysis reaction, which generates differently surface-functionalized CNCs with varying thermal stability (Lu et al., 2015). Recent studies have used new raw materials (Flauzino Neto et al., 2013) and facile manufacturing techniques (Leung et al., 2011), obtaining controlled aspect ratios (Kalashnikova et al., 2013), high CNC yield (94%) (Yu et al., 2013), and high maximum degradation temperature (364 °C) (Yu et al., 2013), desulfation (Jiang et al., 2010; Lin & Dufresne, 2014), as well as comparative studies on CNCs and CNFs.

CNC presents in the form of nanorod, nanowhiskers, and rod-like particles. They are characterized as sustainable and eco-friendly nanomaterials. CNCs possess unique properties of high aspect ratio, high surface area, high mechanical strength, and liquid crystalline nature. CNC possesses a relatively low aspect ratio; it has a typical diameter of 2–20 nm and wide length distribution from 100 to 600 nm (Islam & Rahman, 2018). The size, morphology, and crystallinity of the CNC are affected by the cellulose source and preparation method. The CNC can have a crystallinity level above 70%. The high degree of crystallinity is responsible for the higher rigidity. Most importantly, CNC materials can contain sulfate, hydroxyl, or carboxyl groups on their surface, which make them applicable for further functionalization by polymers, catalysts, or dye molecules, imparting to CNCs new characteristics and properties expanding the scope of their application (Habibi et al., 2010).

Since the preparation of cellulose fibers with a diameter of ~4 nanometers and a length of 500–1000 nanometers by the preparation and application of various nanocellulose have entered an era. It has now greatly grown and moved quickly toward nanotechnology and various applications (Saito et al., 2007). As a fact, nanocellulose is advantageous in many aspects; for example, it has a tunable fiber aspect

Table 4.1 Hydrolysis conditions and characteristics of CNC from different sources

	Source								
Hydrolysis conditions	Bamboo	Eucalyptus	Sisal	Curauá	Lemon seeds	Tomato peel	Doum tree	Sugar palm	Cotton fiber
Acid-fiber ratio (mL/g)	10/1	9/1	15/1	15/1	20/1	8.75/1		20/1	11/1
Temperature (°C)	60	50	50	50	45	45	50	45	50
Hydrolysis time (min)	12	50–65	30	45	90	30	30	45	45
H_2SO_4 concentration (wt%)	65	65	65	65	64	64	64	60	63.9
Sonication time (min)	4	1	7	7	30	5	5	30	–
Characteristics of CNCs									
Yield (%)	30	17	9	–	27.61	15.7		29	41.7
Sulfur content (% S)[a]	1.04	0.96	0.53	0.95	–	0.48			
Total anionic sites (mmol kg^{-1})[a]	324	275	166	297	–	–	–	–	–
Crystallinity index(%)	–	–	–	–	69.67	80.8	90	85.9	91.26
Zeta potential (mV)	−59 ± 2	−48 ± 7	−49 ± 2	−52 ± 1	−40.27	−52.4 ± 1		−61.5 ± 1	
Length (nm)[b]	100 ± 28	100 ± 33	119 ± 45	129 ± 32	145 ± 20.7	135 ± 50	450	130 ± 30	140.9
Width (nm)[b]	8 ± 3	7 ± 1	6 ± 1	5 ± 1	18.5 ± 6.5	7.2±1.8	5.3	9 ± 1.96	–
Height (nm)[c]	4.5 ± 0.9	4.5 ± 1.0	3.3 ± 1.0	4.7 ± 1.0	–	3.3 ± 1.2		–	–
Aspect ratio	22	22	36	27	8	21	85	15	–

[a]Sulfur content and total anionic sites values from conductometric measurements. [b] Length and width values from TEM observation. [c] Height values from AFM experiments.

Source:: Reprinted from (Peng et al., 2021). Published 2021 by MDPI as open access

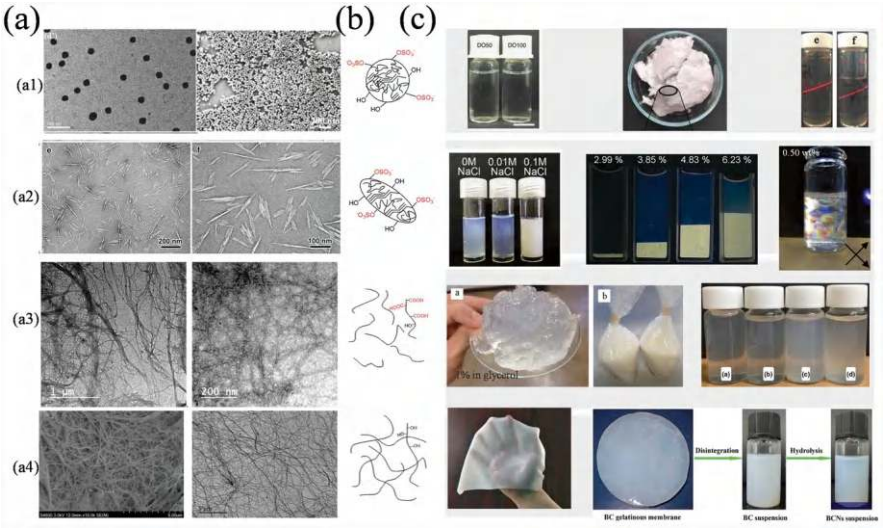

Fig. 4.7 TEM and SEM images of (**a**) nanocellulose, (**b**) sketch of particle shapes and functional groups, and (**c**) suspensions of nanocellulose. In these categories, the material in (a1) is cellulose nanosphere (CNS), (a2) is cellulose nanocrystals (CNC), (a3) is cellulose nanofibrils (CNF), and (a4) is bacterial cellulose (BC). Reprinted with permission from (Shen et al., 2023). Copyright 2023: Wiley-VCH GmbH

ratios of diameter to length (5–150 unitless), rich chemical activity, relatively large specific area (100–200 g/m^2), excellent mechanical properties (e.g., 7.5–7.7 GPa tensile strength and 110–220 GPa Young's modulus), tunable crystallinity, and easy surface functionality (Benítez & Walther, 2017; Tobjörk & Österbacka, 2011). What is more important is that, within these several decades, the nanocellulose has developed into a large family (Agarwal et al., 2017; Barbash et al., 2017; Jasmania & Thielemans, 2018), which at least includes cellulose nanofibrils (CNFs), nanocrystals (CNCs), and bacterial ones (BC), spheres (CSs), and a series of their derivatives (Fig. 4.7).

4.2.2 Industrialization

The industrial-scale production of nanocellulose materials was challenging in early 2010, though it has been speeding fast since 2020. For instance, currently, nanocellulose products are sold by Topchain Pharma Co., Ltd. Topchain Pharmaceutical Company is an enterprise specializing not only in the sales of nanocellulose but also in the research, production, and sales of microcrystalline cellulose, microcrystalline cellulose pellets, nanocrystalline cellulose, sulfonated nanocellulose, and oxidized nanocellulose.

The initial raw material comes from eucalyptus, which has a growth cycle of 6 years. The lignin, minerals, polysaccharides, and resins in the trunk are removed

Fig. 4.8 Hydrolysis reaction workshop, filtration, and purification system. The images included here are copyrighted by Topchain Pharma and used with their permission

through the sulfite method to obtain a dissolving pulp with a cellulose content of over 97%. The dissolving pulp is hydrolyzed again with dilute hydrochloric acid to obtain microcrystalline cellulose with a polymerization degree of less than 350. The microcrystalline cellulose is then hydrolyzed with sulfuric acid, cleaned, surface decorated, and spray-dried to obtain nanocrystalline cellulose with a particle size of 50 to 70 nm. At present, Topchain Pharmaceutical's production technology is advanced, unique, and mature, equipped with a hydrolysis reaction workshop (Fig. 4.8), a slurry storage system, and an automatic control system (Fig. 4.9). Its facilities and equipment are advanced and complete, and it has basically achieved localization of equipment, production automation, and informatization and is moving toward digital intelligence. The designed annual production capacity is 3000 tons of microcrystalline cellulose and 50 tons of nanocrystalline cellulose in its factory.

NCC100 (Fig. 4.10), a representative product developed by Topchain Pharma, is produced through the hydrolysis of microcrystalline cellulose into nanoscale

Fig. 4.9 Slurry storage system and Grade D clean workshop. The figures included here are copyrighted by Topchain Pharma and used with their permission

crystalline particles using sulfuric acid, followed by washing, purification, surface modification, concentration, and spray drying to obtain redispersible cellulose nanocrystalline particle powder. Its molecular formula is$(C_6H_{10}O_5)_n$, where n represents the number of repeating units in the cellulose chain. NCC100 possesses a unique crystal structure with an extraordinarily large specific surface area of 700 m^2/g and exceptional physicochemical properties.

4.2.3 Energy Consumption in Producing Cellulose Nanofibrils and Cellulose Nanocrystals

Production of CNFs is an energy-intensive process. Quiévy et al. (2010) found that energy consumption varied among three CNF production methods (i.e., homogenization, microfluidization, and microgrinding) using virgin wood pulp as feedstock. The energy consumption was found to be very high: 22 kWh/kg, 2.8 kWh/kg, and 3.4 kWh/kg for the three methods, respectively (Fig. 4.11a) (Spence et al., 2011). The energy was calculated based on electrical energy consumption ($E_e = V \bullet I \bullet t$, where V, I, t are the voltage, current, and time, respectively) based on the dry raw material mass (Tejado et al., 2012).

Figure 4.11b illustrates the effect of carboxylate concentration on the energy required to disintegrate cellulose fibers by plotting some of the limits reported in the literature and recalculating others from the experimental details provided there. The references to the disintegration energy in most of the works are often very vague and rarely contain a production yield associated with it, but similar limits appear

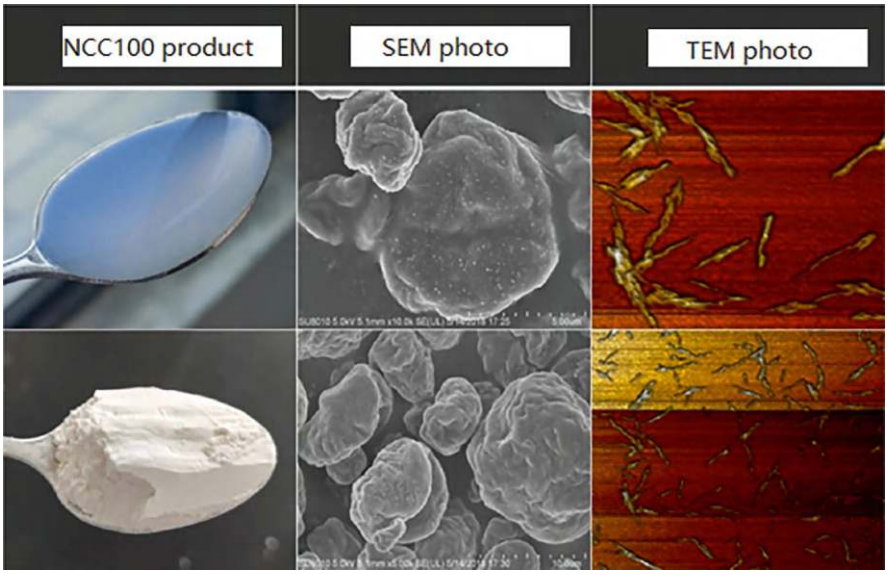

Fig. 4.10 NCC100 product's macro and micro diagram. The figures included here are copyrighted by Topchain Pharma and used with their permission. The cellulose nanocrystal suspension has a milky white and transparent appearance. Upon drying, it transforms into a fluffy white powder. This powder takes on irregular spherical shapes as a result of water removal during the drying process. When redispersed in a solvent, the cellulose nanocrystals return to their original needle-like form, as observed in the TEM images. The figures included here are copyrighted by Topchain Pharma and used with their permission

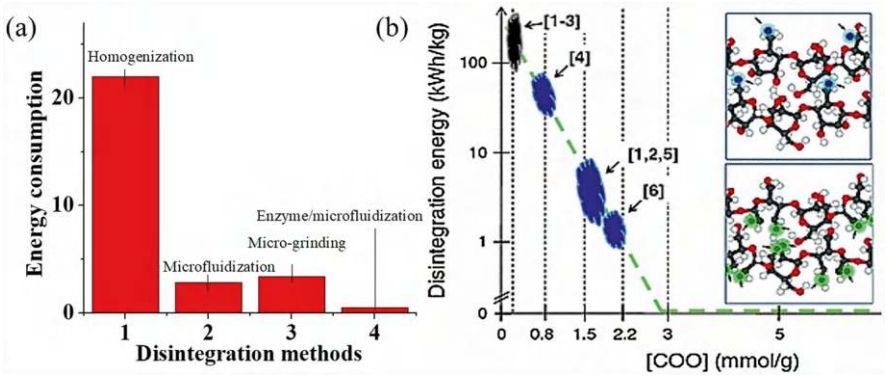

Fig. 4.11 (**a**) Energy consumption vs. disintegration methods; (**b**) energy consumption for mechanical disintegration with respect to functional groups (COO^-) introduced by TEMPO-oxidation. Dots in blue are sites present with hydroxyl –OH groups, in green are sites with COO^- groups. Reprinted with permission from (Tejado et al., 2012). Copyright 2012: Springer

repeatedly in one form or the other in patents and scientific papers. For instance, CNF was isolated from rice straw after TEMPO/NaClO/NaBr treatment ([COO] = 5 mmol/g) following a previous work (Saito et al., 2009); oxidized fibers were disintegrated in a domestic blender for 15 min and sediments centrifuged for ~10 min before imaging. Nanofibrils look long and slim (Xu et al., 2020a).

Reducing the energy consumption by pretreating the raw materials (e.g., environmentally friendly enzymatic treatment (M. Henriksson et al., 2007) and TEMPO-oxidation (Isogai et al., 2011) has been successfully attempted. Ankerfors (2012) found that the energy consumption could be reduced to 0.5–2.3 kWh/kg after pretreating the feedstock with chemicals or enzymes. It should be emphasized that the calculated energy consumptions for CNFs do not include the energy spent during the pulping process, which involves intensive heating and chemical reactions. As for the CNCs, the energy cost involved in their production is rarely studied. They may have a lower energy cost than CNFs because the hydrolysis reaction under mild conditions constitutes their main production process.

4.3 Nanofibrillated Cellulose

Nanofibrillated cellulose (NFC) refers to cellulose fibers that have been fibrillated to achieve agglomerates of cellulose microfibril units; NFCs have nanoscale (less than 100 nm) diameter and typical length of several micrometers. Several denominations exist for describing such material and most often nano/microfibrillated cellulose (NFC/MFC) is used. Nanofibrillated cellulose is described as a long and flexible cellulosic nanomaterial and is obtained from cellulose fiber by mechanical disintegration. Dilute suspensions of cut cellulose fibers from softwood pulp were treated by high shear forces to yield individualized cellulose microfibrils. The resulting suspensions showed a clear increase in viscosity after several passes through the homogenizer. Indeed, NFCs tend to form an aqueous gel at very low concentration (2% wt.) due to the strong increase of specific surface area and consequently the higher number of hydrogen bonds (arising from surface hydroxyl groups) for the same volume in comparison to native cellulosic fibers.

4.3.1 CNF Processing and Manufacturing

Nanofibrillated cellulose is currently manufactured from a number of different cellulosic sources. Wood is obviously the most important industrial source of cellulosic fibers, and is thus the main raw material used to produce NFC. Bleached Kraft pulp is most often used as a starting material for NFC production, followed by bleached sulfite pulp.

4.4 Property of Cellulose

4.4.1 Crystalline Properties

Typical X-ray diffraction patterns of CNCs and CNFs are compared in Fig. 4.12. The XRD results including peak angle (2θ), *d*-spacing, full width at half maximum (FWHM), average crystal size (thickness) in the direction normal to the reflecting plane (*L*), and crystallinity index (*CI*) are summarized in Table 4.2. The crystal size was determined by the Scherrer Equation (Scherrer, 1918):

$$FWHM\left(2\theta\right) = \frac{K\lambda}{L\cos\theta}, \tag{4.1}$$

where *K* is the Scherrer constant (0.89) and λ is the X-ray wavelength. *CI* of CNCs and CNFs can be determined based on XRD results using several different methods (Park et al., 2010). The Segal method allows rapid comparison of cellulose crystallinity and is commonly used in paper industry (Segal et al., 1959):

$$CI = \frac{I_{002} - I_{amorphous}}{I_{002}}, \tag{4.2}$$

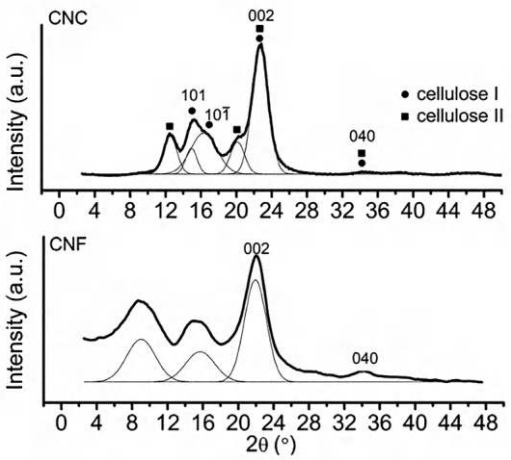

Fig. 4.12 Wide angle X-ray diffraction patterns of CNCs and CNFs. CNCs and CNFs derived from bleached dry lap eucalyptus pulp were kindly provided by the USDA Forest Service Lab. Their methods of production have been detailed in Wang et al. (2012). Briefly, CNCs were produced by sulfuric acid hydrolysis followed by repeated centrifugation, whereas CNFs were produced through a multi-pass high-pressure grinding process using a SuperMassColloider (MKZA6–2, Masuko Sangyo Co., Ltd., Japan). The as-received CNCs and CNFs were in the forms of 5.7 wt% suspension and 1.8 wt% gel (both in water), respectively. Figures were reprinted with permission from (Xu et al., 2013). Copyright 2013: ACS

Table 4.2 XRD results of pure CNCs and CNFs

	2θ	d (Å)	FWHM	L (Å)	CI (%) *(Segal)*	CI (%) *(calculated by area percentage)*
CNCs	12.5	7.1	0.996	35	81.0	95
	15.1	5.8	1.033	27		
	17.5	5.2	1.029	78		
	20.1	4.4	1.488	54		
	22.7	3.9	1.102	38		
	34.3	2.6	8.146	10		
CNFs	9.2	9.6	0.964	13	64.4	39
	14.9	6.0	1.370	15		
	22.4	4.0	1.135	29		
	33.9	2.6	1.984	42		

Source: Reprinted with permission from (Xu et al., 2013). Copyright 2013: American Chemical Society

Where I_{002} is the maximum intensity of the (002) diffraction and $I_{amorphous}$ is the intensity of amorphous diffraction, which is taken at 2θ angle between (002) and (101) peaks where the intensity is at a minimum. The second method separates amorphous and crystalline diffractions and calculates the ratio of the crystalline diffraction to the overall diffraction as *CI* using MDI Jade 6.5 software (Materials Data, Inc.) (Li et al., 2009).

As shown in Fig. 4.12, CNCs show diffraction peaks at 15.1°, 17.5°, 22.7°, and 34.3°, representing cellulose I crystal planes (101), $(10\bar{1})$, (002), and (040), respectively (Lee et al., 2012). Diffractions from cellulose II are also present in the CNC pattern at angles of 12.5°, 20.1°, 22.7°, and 34.3° (Oudiani et al., 2011). The coexistence of cellulose I and cellulose II in CNCs is attributed to the alkali pulping and acid hydrolysis processes that CNCs experience during production. Alkali and acid treatments to natural fibers transform cellulose I to cellulose II (Brown & Jurasek, 1979; Oudiani et al., 2011). XRD results of CNFs are surprisingly scarce in the literature. This study found that CNFs showed broadened and merged peaks, which also shifted to lower angles. In general, the diffraction peaks of ball-milled natural fibers also shift toward smaller angles with increasing milling time due to the superposition of broadened crystalline diffraction peaks on increasingly strong amorphous diffractions (Brown & Jurasek, 1979). This is also the case in this study. The high-pressure mechanical grinding used in CNF manufacturing could deform or even completely destruct cellulose crystals, leading to broadened and shifted diffraction peaks (Lee et al., 2012).

Crystallinity index (*CI*) values determined by both the Segal method and Jade software show that CNCs have higher crystallinity than CNFs, which is in agreement with the microstructures of the two nanofibers. However, the two methods show large differences in *CI* values, with the Jade software producing a larger value for CNCs and a lower value for CNFs. The differences are attributed to Segal method's over-simplicity and the resultant inaccurate results (Park et al., 2010).

4.4.2 Intrinsic Mechanical Properties

The properties of CNFs and CNCs isolated from different sources (bacteria, tunicate, plants, etc.) using different methods (e.g., acid, enzymatic, mechanical, and oxidative methods) vary significantly (Fig. 4.13) (Sacui et al., 2014). The variations are derived from the fact that different source materials, processing methods/conditions, and testing methods are used in the literature.

Cellulose nanofibers (i.e., CNFs, CNCs, and BC) in general compare favorably to other important nanoparticles/fibers such as nanoclay, carbon nanotubes/vapor growth carbon fibers (VGCF), boron (BN) nanotubes, and graphene (xGnP-Graphite NanoPlatelets) (Table 4.3). Young's modulus of the cellulose nanofibers is mostly measured by nano-indentation. In one report, the modulus of CNCs is measured to range between 18 and 50 GPa (Lahiji et al., 2010); in another, the modulus of BC was shown to be 78 GPa (Guhados et al., 2005). Other studies have reported the Young's modulus up to 130 GPa and the tensile strength of 10 GPa (Tanpichai et al., 2012). CNCs also show a very low coefficient of thermal expansion (CTE) and thermal conductivity (Diaz et al., 2014). These exceptional mechanical and thermal properties, combined with their large surface area/aspect ratio and low density, have made CNCs and CNFs ideally suited to the development of environmentally friendly polymer nanocomposites.

4.4.3 Chemical Properties

The mechanical properties of composites depend to a great extent on fiber/polymer interfacial bonding. Polymers such as PVA, PAM, PEG, and PEO have hydrogen-bond-forming groups that can interact with the hydroxyl (-OH), sulfate ($-OSO_3^-$),

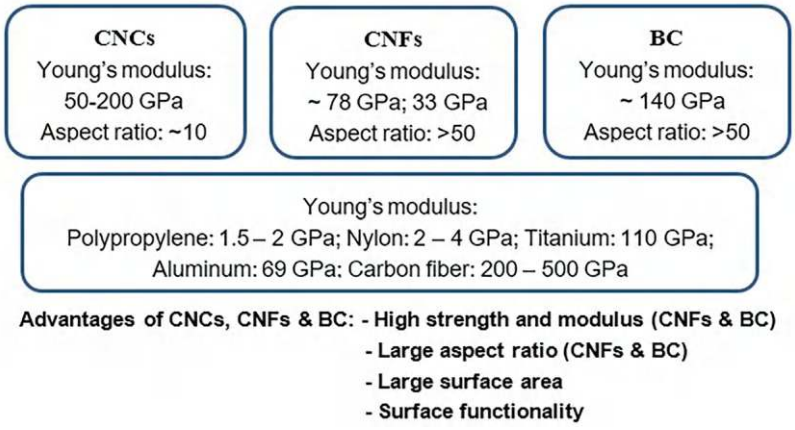

Fig. 4.13 Comparison of properties of CNC, CNF, BC, and some commonly used materials

Table 4.3 Properties of commonly used nanostructured materials

Parameters	Exfoliated nanoclay	Carbon nanotube, carbon fiber (VGCF)	BN nanotubes	Graphene (xGnP-Graphite)	Cellulose nanofibers
Physical structure	Platelet −1 nm x 100 nm	Cylinder NT—1 nm × 100 nm VGCF— 20 nm × 100 μm	Cylinder	Platelet −1 nm × 100 nm	Fiber-like
Chemical structure	Hydrous aluminum phyllosilicates	Hexagonal carbon	Boron nitride	Hexagonal carbon	Cellulose
Interactions	Hydrogen bond Dipole-dipole	π- π	Hydrogen bond	π- π	Hydrogen bond
Tensile modulus	0.17 TPa	NT—1.0-1.7 TPa VGCF—0.25-0.5 TPa	1 TPa	1.0 TPa	0.13 TPa
Tensile strength	1 GPa	NT—180 GPa VGCF—3-7 GPa	–	– (10–20 GPa)	10 GPa
Electrical resistivity	$>10^{10}$ Ωcm	NT—50×10^{-6} Ωcm VGCF— $5\text{-}100 \times 10^{-3}$ Ωcm	Insulator	50×10^{-6} Ωcm ‖ 1 Ωcm⊥	10^{10}–10^{16} Ωcm
Thermal conductivity	6.7×10^{-1} W/mK	NT—3000 W/mK VGCF—20-2000 W/mK	−3000 W/mK	3–6 W/mK⊥	Thermal insulator
Coefficient of thermal expansion	$8\text{–}16 \times 10^{-6}$	-1×10^{-6}	1×10^{-6}	-1×10^{-6} ‖ 29×10^{-6} ⊥	$8\text{–}16 \times 10^{-6}$
Density	2.8–3.0 g/cm^3	NT—1.2-1.4 g/cm^3 VGCF—1.8-2.1 g/cm^3	2.0 g/cm^3	2.0 g/cm^3	1.5 g/cm^3

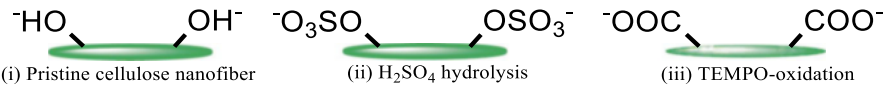

Fig. 4.14 Chemical groups on the cellulose nanofibers

and carboxyl (-COO^-) groups on the pristine or treated cellulose nanofibers (Fig. 4.14). For example, the hydroxyl groups on the side chains of PVA interact strongly with the polar sulfate or ionic (-COONa) groups introduced by sulfuric acid hydrolysis or TEMPO-oxidation during the synthesis of cellulose nanofibers (Zhang et al., 2015).

CNFs were acetylated because they could not be homogeneously dispersed in non-polar silicon oil due to their high surface polarity. The active hydroxyl groups (-OH) on the surfaces of CNFs react with acetic acid or acetic anhydrate to produce acetyl groups (-$COCH_3$) (Tingaut et al., 2010). The acetylation of CNFs lowers their hydrophilicity and thus improves their dispersion in non-polar solvents such as silicon oil. The stability of the acetylated CNF dispersion can be further improved by

adding chloroform into silicon oil due to the similarity between the polarity of the acetylated CNFs and chloroform (Tingaut et al., 2010). The suspension remained stable over 72 h. The acetylated CNFs is dispersed in a silicon oil/chloroform mixture (1:6), producing a stable translucent suspension. This suspension was used to spin the core part of the core-shell fibers in electrospinning.

Since the CNCs and CNFs have abundant –OH groups on their surfaces, they have been intensively explored to functionalize the nanofibers for different applications through esterification, silylation, polymer grafting, acetylation, etc. (Peng et al., 2011). These surface functionalization methods can improve their dispersibility in different solvents/polymer matrixes and expand their utilization in nanotechnology-related applications, including nanocomposites, drug delivery, protein immobilization, and inorganic reaction template.

4.4.4 Thermal Stability

Different cellulose-based materials have minor differences in thermal stability. Raw cellulose materials, such as cotton linter, typically exhibit a thermal decomposition temperature of around 360–370 °C. The cotton linter showed the highest thermal decomposition temperature. Other cellulose sources, such as cattail and hardwood, exhibited a similar thermal decomposition temperature of around 361 °C (Hai & Seo, 2018). Nanofibrillation via mechanical grinding treatment resulted in a significant decrease in the thermal decomposition temperature of the nanofibrillated cellulose (NFC) samples (Fig. 4.15). The NFC samples showed a 19–24 °C lower thermal decomposition temperature compared to their corresponding raw cellulose materials. Despite the reduced thermal stability due to the nanofibrillation process, the cotton-based NFC still demonstrated the highest thermal decomposition

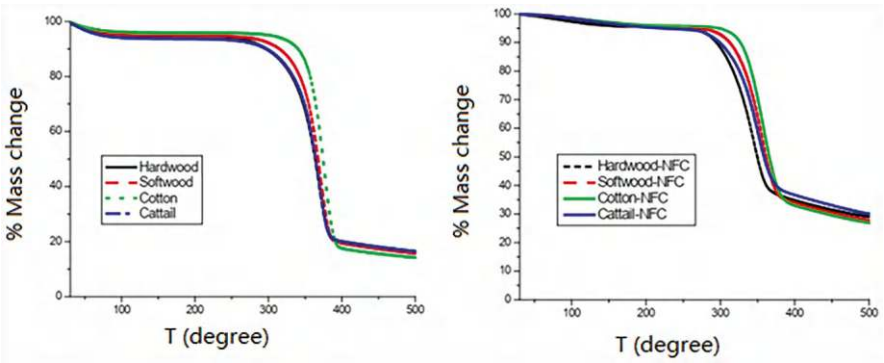

Fig. 4.15 Thermal stability of (**a**) raw cellulose materials and (**b**) NFCs with temperature change. Figures were reprinted with permission from (Hai & Seo, 2018). Copyright 2018: Cellulose Chemistry and Technology Journal

resistance among the nanocellulose materials tested. This suggests that the source of the cellulose, in addition to the processing methods, can play a crucial role in determining the thermal properties of the resulting nanocellulose-based materials. Understanding these factors is essential for the effective utilization and optimization of cellulose and nanocellulose materials in various applications where thermal stability is a critical concern.

4.4.5 Other Properties

Nanocellulose has its big family, respectively. Regarding the properties, for example, the surface modification of CNCs can not only retain the original properties of CNCs but also give new surface properties, such as hydrophobic (Wijaya et al., 2020), biocompatibility (Chu et al., 2020), antistatic properties (Liu et al., 2020), and dyeing properties (Cui et al., 2019). The surface of the CNCs contains numerous hydroxyl (-OH) groups which provide the main reaction site for modification. Esterification, etherification, oxidation, silylation, grafting of macromolecules are typical ways. Table 4.4 lists some representative methods of functional modification on both the surface and the terminal end of CNC that currently exist (Liu et al., 2019). We have listed the findings, advantages, and limitations of the approaches. All these surface modification methods are based on the following three aims: (1) to reduce the size of CNCs in dispersions with organic solvents by increasing the hydrophobicity of the surface of nanocrystallites; (2) to improve compatibility between CNCs and hydrophobic polymers matrix; and (3) to endow CNC additional attributes, such as biology, optics, mechanics, and electromagnetics by covalently bonding with functional macromolecules (Abushammala & Mao, 2019). In this article, we will detail the approaches mentioned earlier.

4.5 Conclusion

Table 4.5 provides comparative characteristics of cellulose in its various forms. A detailed analysis of cellulose nanofibers and nanocrystals highlights their unique properties, which can be tailored through manufacturing techniques and surface modification for a wide range of applications. However, as industrialization advances, addressing energy consumption and optimizing manufacturing processes will be critical to transforming nanocellulose from a promising material into one that can drive the development of green and waste-free technologies, flexible and wearable electronics, and low-cost analytical instruments. The ideas presented in this chapter highlight the importance of further research to improve our understanding of cellulose properties and explore new applications, ultimately paving way for the widespread adoption of nanocellulose in industry and technology.

Table 4.4 Functional modification of cellulose nanocrystals

Types of modification	Method	Findings	Advantages	Limitations	Ref.
Small molecule-functionalized CNCs	Grafted with lactic acid (CNC-g-LA)	High surface graft density, reduce the graft length to preserve the original size and morphology of CNCs	Green, simple, one-step; good dispersion in chloroform	Bad dispersion in water, ethanol, acetone, THF, toluene	Wu et al. (2018)
	Zinc phthalocyanine conjugate functionalization	Exhibited absorption and emission maxima at 690 and 715 nm	Photoluminescence-based technologies	Cost, activation of linker	Alam et al. (2020)
	Aldehyde functionalization	DOTA-NH_2 linked to the aldehyde	Makes the OH-groups on CNC surface accessible for other subsequent functionalization	Low reactivity	Imlimthan et al. (2019)
Macromolecule-functionalized CNCs	CNC-grafted biomacromolecule	Click reaction between azide-functionalized CNC and acetylene functionalized protein	Biocompatibility, low cytotoxicity, and nanometer size	Strict reagent selection due to protein's nature	Karaaslan et al. (2013)
	ATRP polymerization functionalization followed by mineralization of silica	Graft PDMAEMA brush with CNCs, form SiO_2 network in the polymer brush layer to achieve template	Forms microporous and mesoporous silica nanorods	Severe aggregates during solvent exchange for CNC	Morits et al. (2018)
	Polydopamine functionalization	Contact angle shift from 21 to 95.6°	Spontaneous clicking reaction	Low hydrophobicity	Shang et al. (2018)
	Azo-benzodiazepines functionalization	Hydrophobic	Massive potential in optical information storage, optical switching, and linear optics	Difficulties in purification and redispersion	Xu et al. (2020b)
	Aldehyde functionalization with polyetheramine	Forms arms of regular four-, five-, or six-branched stars	Create hierarchical structures	Few reactivity sites	Lin et al. (2019)

Source: Reprinted from (Peng et al., 2021). Published 2021 by MDPI as open access

Table 4.5 Comparative characteristics of nanocellulose fibers, cellulose nanocrystals, and bacterial nanocellulose

Properties/ applications	CNF (cellulose nanofibers)	CNC (cellulose nanocrystals)	BNC (bacterial nanocellulose)
Nature	Nanofibrillated cellulose	Elongated rod-like cellulose crystals, cellulose (nano) whiskers, or spherical	Microbial cellulose fibers
Source	Sugar beet, maize, banana, bagasse, wheat straw, jute, hemp, kenaf fibers, aquatic weeds, pineapple leaf, mulberry, cassava, alpha fiber, rice husk, cotton, coir, soy hull, etc.	Microcrystalline cellulose, BC, cotton, wood, sisal, pineapple leaves, coconut husk fibers, wheat straw, bagasse, bamboo, ramie, etc..	Synthesized in microbial culture using bacteria (such as *Acetobacter xylinum*, *agrobacterium*, *pseudomonas*, *rhizobium*, *Sarcin*)
Mode of preparation	Converting large lignocellulosic units (cm) to smaller units (nm)		Construction from tiny units (Å) to small units (nm)
Methodology	Mechanically induced destructuring strategy. Multiple mechanical shearing actions can effectively delaminate individual microfibrils from lignocellulosic fibers	Chemically induced destructuring strategy, such as acid hydrolysis, most significantly sulfuric acid	The microbial process requires no intensive chemical/physical steps to remove unwanted impurities or contaminants such as lignin, pectin, and hemicellulose
Energy and chemical requirements	High energy process with corrosive chemical reagents. Overall the method is not currently very sustainable		Noncorrosive chemicals and hence a completely green approach
Crystalline nature	CNF consists of both individual and aggregated nanofibrils made of alternating crystalline and amorphous cellulose domains	Through the removal of amorphous regions, a highly crystalline structure is produced	With the combination of glucose chains, microfibrils are formed and aggregated as ribbons
Cost	Low cost due to the use of renewable biomass as the source and inexpensive chemicals		High cost to support the growth of bacteria in a suitable culture medium
Yield	Low yield		Very low yield
Advantages	Lightweight, nanoscale dimensions, high surface area, unique morphology, low density and mechanical strength, easy to chemically modify, renewable, and biodegradable	Comparative low water-holding capacity, crystallinity, high axial stiffness, tensile strength, low coefficient of thermal expansion, renewable, and biodegradable	Excellent biocompatibility, high porosity, high flexibility, high water-holding capacity, high purity, high degree of polymerization and crystallinity, renewable, and biodegradable

(continued)

Table 4.5 (continued)

Properties/ applications	CNF (cellulose nanofibers)	CNC (cellulose nanocrystals)	BNC (bacterial nanocellulose)
Applications	Composites, membranes, various sensors, biomedical devices, drug delivery, paper production, packaging, paints, food, stimuli-responsive nanodevices, photonic crystals, barrier films, shape-memory polymers, energy storage, flexible and wearable electronics, light-emitting diodes and displays, separations, cosmetics, construction, etc.	Transparent barrier films, photonic, drug delivery, composites, optical and electronic flexible and wearable devices, energy storage, actuation and sensing, filtration, packaging, paints, coatings, adhesives, cosmetics, drugs, cements, nanodevices, construction, separation, food applications, etc.	Biomedical applications, including antimicrobial products, skin therapy, vascular grafts, tissue engineering, cartilage, bone and menisci materials, drug delivery, contact lenses, artificial organs, food and paper industry, flexible and wearable electronics, photocatalysis, biosensors, and optical devices

Source: Reprinted with permission from (Thomas et al., 2018). Copyright 2018:ACS

References

Abushammala, H., & Mao, J. (2019). A review of the surface modification of cellulose and nanocellulose using aliphatic and aromatic mono- and di-isocyanates. *Molecules, 24*, 2782. https://doi.org/10.3390/molecules24152782

Agarwal, U. P., Atalla, R. H., & Isogai, A. (2017). *Nanocelluloses: Their preparation, properties, and applications*. American Chemical Society. ISBN:9780841232181.

Alam, K. M., Kumar, P., Gusarov, S., Kobryn, A. E., Kalra, A. P., Zeng, S., et al. (2020). Synthesis and characterization of zinc phthalocyanine-cellulose nanocrystal (CNC) conjugates: Towards highly functional CNCs. *ACS Applied Materials & Interfaces, 12*(39), 43992–44006. https://doi.org/10.1021/acsami.0c07179

Ankerfors, M. (2012). *Microfibrillated cellulose: Energy-efficient preparation techniques and key properties*. Licentiate Thesis, KTH Royal Institute of Technology, Stockholm.

Baghaei, B., & Skrifvars, M. (2020). All-cellulose composites: A review of recent studies on structure, properties and applications. *Molecules, 25*, 2836. https://doi.org/10.3390/molecules25122836

Barbash, V. A., Yaschenko, O. V., & Shniruk, O. M. (2017). Preparation and properties of Nanocellulose from Organosolv straw pulp. *Nanoscale Research Letters, 12*, 241. https://doi.org/10.1186/s11671-017-2001-4

Benítez, A. J., & Walther, A. (2017). Cellulose nanofibril nanopapers and bioinspired nanocomposites: A review to understand the mechanical property space. *Journal of Materials Chemistry A, 5*, 16003–16024. https://doi.org/10.1039/C7TA02006F

Brito, B. S. L., Pereira, F. V., Putaux, J.-L., & Jean, B. (2012). Preparation, morphology and structure of cellulose nanocrystals from bamboo fibers. *Cellulose, 19*, 1527–1536. https://doi.org/10.1007/s10570-012-9738-9

Brown, R. D., & Jurasek, L. (1979). *Hydrolysis of cellulose: Mechanisms of enzymatic and acid catalysis*. The Maple Press.

Chen, W., Yu, H., & Liu, Y. (2011). Preparation of millimeter-long cellulose I nanofibers with diameters of 30–80 nm from bamboo fibers. *Carbohydrate Polymers, 86*, 453–461. https://doi.org/10.1016/j.carbpol.2011.04.061

Chu, Y., Song, R., Zhang, L., Dai, H., & Wu, W. (2020). Water-dispersible, biocompatible and fluorescent poly(ethylene glycol)-grafted cellulose nanocrystals. *International Journal of Biological Macromolecules, 153*, 46–54. https://doi.org/10.1016/j.ijbiomac.2020.02.286

Cui, Y., Huang, H., Liu, M., Chen, J., & Wei, Y. (2019). Facile preparation of luminescent cellulose nanocrystals with aggregation-induced emission feature through Ce(IV) redox polymerization. *Carbohydrate Polymers, 223*, 115102. https://doi.org/10.1016/j.carbpol.2019.115102

Diaz, J. A., Ye, Z., Wu, X., Moore, A. L., Moon, R. J., Martini, A., et al. (2014). Thermal conductivity in nanostructured films: From single cellulose nanocrystals to bulk films. *Biomacromolecules, 15*, 4096–4101. https://doi.org/10.1021/bm501131a

dos Santos, R. M., Flauzino Neto, W. P., Silvério, H. A., et al. (2013). Cellulose nanocrystals from pineapple leaf, a new approach for the reuse of this agro-waste. *Industrial Crops and Products, 50*, 707–714. https://doi.org/10.1016/j.indcrop.2013.08.049

Espinosa, S. C., Kuhnt, T., Foster, E. J., & Weder, C. (2013). Isolation of thermally stable cellulose nanocrystals by phosphoric acid hydrolysis. *Biomacromolecules, 14*, 1223–1230. https://doi.org/10.1021/bm400219u

Flauzino Neto, W. P., Silvério, H. A., Dantas, N. O., & Pasquini, D. (2013). Extraction and characterization of cellulose nanocrystals from agro-industrial residue—Soy hulls. *Industrial Crops and Products, 42*, 480–488. https://doi.org/10.1016/j.indcrop.2012.06.041

Fukuzumi, H., Saito, T., Iwata, T., Kumamoto, Y., & Isogai, A. (2009). Transparent and high gas barrier films of cellulose nanofibers prepared by TEMPO-mediated oxidation. *Biomacromolecules, 10*, 162–165. https://doi.org/10.1021/bm801065u

Guhados, G., Wan, W., & Hutter, J. L. (2005). Measurement of the elastic modulus of single bacterial cellulose fibers using atomic force microscopy. *Langmuir, 21*, 6642–6646. https://doi.org/10.1021/la0504311

Habibi, Y., Lucia, L. A., & Rojas, O. J. (2010). Cellulose nanocrystals: Chemistry, self-assembly, and applications. *Chemical Reviews, 110*, 3479–3500. https://doi.org/10.1021/cr900339w

Hai, L. V., & Seo, Y. B. (2018). Properties of nanofibrillated cellulose prepared by mechanical means. *Cellulose Chemistry and Technology, 52*, 741–747.

Henriksson, M., Henriksson, G., Berglund, L., & Lindström, T. (2007). An environmentally friendly method for enzyme-assisted preparation of microfibrillated cellulose (MFC) nanofibers. *European Polymer Journal, 43*, 3434–3441. https://doi.org/10.1016/j.eurpolymj.2007.05.038

Henriksson, M., Berglund, L. A., Isaksson, P., & Lindstro, T. (2008). Cellulose nanopaper structures of high toughness. *Biomacromolecules, 9*, 1579–1585. https://doi.org/10.1021/bm800038n

Hsieh, Y. C., Yano, H., Nogi, M., & Eichhorn, S. J. (2008). An estimation of the Young's modulus of bacterial cellulose filaments. *Cellulose, 15*, 507–513. https://doi.org/10.1007/s10570-008-9206-8

Imlimthan, S., Otaru, S., Keinänen, O., Correia, A., Lintinen, K., Santos, H. A., et al. (2019). Radiolabeled molecular imaging probes for the in vivo evaluation of cellulose nanocrystals for biomedical applications. *Biomacromolecules, 20*(2), 674–683. https://doi.org/10.1021/acs.biomac.8b01313

Islam, M. N., & Rahman, F. (2018). Production and modification of nanofibrillated cellulose composites and potential applications. In G. Koronis & A. Silva (Eds.), *Green composites for automotive applications* (pp. 115–141). Elsevier. https://doi.org/10.1016/B978-0-08-102177-4.00006-9

Isogai, A., Saito, T., & Fukuzumi, H. (2011). TEMPO-oxidized cellulose nanofibers. *Nanoscale, 3*, 71–85. https://doi.org/10.1039/c0nr00583e

Jasmania, L., & Thielemans, W. (2018). Preparation of nanocellulose and its potential application. *International Journal of Nanotechnology and Nanomedicine, 4*, 14–21. https://doi.org/10.17352/2455-3492.000026

Jiang, F., Esker, A. R., & Roman, M. (2010). Acid-catalyzed and solvolytic desulfation of H_2SO_4-hydrolyzed cellulose nanocrystals. *Langmuir, 26*, 17919–17925. https://doi.org/10.1021/la1028405

Jiang, F., Han, S., & Hsieh, Y.-L. (2013). Controlled defibrillation of rice straw cellulose and self-assembly of cellulose nanofibrils into highly crystalline fibrous materials. *RSC Advances, 3*, 12366. https://doi.org/10.1039/c3ra41646a

Kalashnikova, I., Bizot, H., Bertoncini, P., Cathala, B., & Capron, I. (2013). Cellulosic nanorods of various aspect ratios for oil in water Pickering emulsions. *Soft Matter, 9*, 952. https://doi.org/10.1039/c2sm26472b

Karaaslan, M. A., Gao, G., & Kadla, J. F. (2013). Nanocrystalline cellulose/β-casein conjugated nanoparticles prepared by click chemistry. *Cellulose, 20*, 2655–2665. https://doi.org/10.1007/s10570-013-0065-6

Khalil, H. P. S. A., Davoudpour, Y., Islam, M. N., Mustapha, A., Sudesh, K., Dungani, R., et al., et al. (2014). Production and modification of nanofibrillated cellulose using various mechanical processes: a review. *Carbohydrate Polymers, 99*, 649–665. https://doi.org/10.1016/j.carbpol.2013.08.069

Klemm, D., Schumann, D., Udhardt, U., & Marsch, S. (2001). Bacterial synthesized cellulose-artificial blood vessels for microsurgery. *Progress in Polymer Science, 26*, 1561–1603. https://doi.org/10.1016/S0079-6700(01)00021-1

Lahiji, R. R., Xu, X., Reifenberger, R., Raman, A., Rudie, A., & Moon, R. J. (2010). Atomic force microscopy characterization of cellulose nanocrystals. *Langmuir, 26*, 4480–4488. https://doi.org/10.1021/la903111j

Lavoine, N., Desloges, I., Dufresne, A., & Bras, J. (2012). Microfibrillated cellulose—Its barrier properties and applications in cellulosic materials: a review. *Carbohydrate Polymers, 90*, 735–764. https://doi.org/10.1016/j.carbpol.2012.05.026

Lee, K. Y., Tammelin, T., Schulfter, K., Kiiskinen, H., Samela, J., & Bismarck, A. (2012). High performance cellulose nanocomposites: Comparing the reinforcing ability of bacterial cellulose and nanofibrillated cellulose. *ACS Applied Materials & Interfaces, 4*, 4078–4086. https://doi.org/10.1021/am300852a

Leung, A. C. W., Hrapovic, S., Lam, E., Liu, Y., Male, K. B., Mahmoud, K. A., et al. (2011). Characteristics and properties of carboxylated cellulose nanocrystals prepared from a novel one-step procedure. *Small, 7*, 302–305. https://doi.org/10.1002/smll.201001715

Li, R., Fei, J., Cai, Y., et al. (2009). Cellulose whiskers extracted from mulberry: A novel biomass production. *Carbohydrate Polymers, 76*, 94–99. https://doi.org/10.1016/j.carbpol.2008.09.034

Lin, N., & Dufresne, A. (2014). Surface chemistry, morphological analysis and properties of cellulose nanocrystals with gradiented sulfation degrees. *Nanoscale, 6*, 5384–5393. https://doi.org/10.1039/c3nr06761k

Lin, F., Cousin, F., Putaux, J. L., & Jean, B. (2019). Temperature-controlled star-shaped cellulose nanocrystal assemblies resulting from asymmetric polymer grafting. *ACS Macro Letters, 8*(4), 345–351. https://doi.org/10.1021/acsmacrolett.8b01005

Liu, Y., Liu, Y. J., Meng, F. H., & Liu, J. L. (2019). Preparation, modification and functional application of cellulose nanocrystals. *Modern Chemical Industry, 39*(4), 58–62. https://doi.org/10.16606/j.cnki.issn0253-4320.2019.04.013

Liu, S. Y., Bin, G. Y., Ma, S., Wang, Y. H., & Huang, J. (2020). Antistatic structural color and photoluminescent membranes from co-assembling cellulose nanocrystals and carbon nanomaterials for anti-counterfeiting. *Chinese Journal of Polymer Science (English Edition), 38*, 1061–1071. https://doi.org/10.1007/s10118-020-2414-x

Lu, Q., Lin, W., Tang, L., Wang, S., Chen, X., & Huang, B. (2015). A mechanochemical approach to manufacturing bamboo cellulose nanocrystals. *Journal of Materials Science, 50*, 611–619. https://doi.org/10.1007/s10853-014-8620-6

Morits, M., Hynninen, V., Nonappa, N. A., Ikkala, O., Gröschel, A. H., et al. (2018). Polymer brush guided templating on well-defined rod-like cellulose nanocrystals. *Polymer Chemistry, 9*, 1650–1657. https://doi.org/10.1039/c7py01814b

Osong, S. H., Norgren, S., & Engstrand, P. (2016). Processing of wood-based microfibrillated cellulose and nanofibrillated cellulose, and applications relating to papermaking: a review. *Cellulose, 23*, 93–123. https://doi.org/10.1007/s10570-015-0798-5

Oudiani, A. E., Chaabouni, Y., Msahli, S., & Sakli, F. (2011). Crystal transition from cellulose I to cellulose II in NaOH treated Agave americana L. fibre. *Carbohydrate Polymers, 86*, 1221–1229. https://doi.org/10.1016/j.carbpol.2011.06.037

Park, S., Baker, J. O., Himmel, M. E., Parilla, P. A., & Johnson, D. K. (2010). Cellulose crystallinity index: Measurement techniques and their impact on interpreting cellulase performance. *Biotechnology for Biofuels, 3*, 10. https://doi.org/10.1186/1754-6834-3-10

Peng, B. L., Dhar, N., Liu, H. L., & Tam, K. C. (2011). Chemistry and applications of nanocrystalline cellulose and its derivatives: A nanotechnology perspective. *The Canadian Journal of Chemical Engineering, 89*, 1191–1206. https://doi.org/10.1002/cjce.20554

Peng, S., Luo, Q., Zhou, G., & Xu, X. (2021). Recent advances on cellulose nanocrystals and their derivatives. *Polymers (Basel), 13*, 1–34. https://doi.org/10.3390/polym13193247

Qing, Y., Sabo, R., Zhu, J. Y., Agarwal, U., & Cai, W. Y. (2013). A comparative study of cellulose nanofibrils disintegrated via multiple processing approaches. *Carbohydrate Polymers, 97*, 226–234. https://doi.org/10.1016/j.carbpol.2013.04.086

Quiévy, N., Jacquet, N., Sclavons, M., Deroanne, C., Paquot, M., & Devaux, J. (2010). Influence of homogenization and drying on the thermal stability of microfibrillated cellulose. *Polymer Degradation and Stability, 95*, 306–314. https://doi.org/10.1016/j.polymdegradstab.2009.11.020

Sacui, I. A., Nieuwendaal, R. C., Burnett, D. J., Stranick, S. J., Jorfi, M., Weder, C., et al. (2014). Comparison of the properties of cellulose nanocrystals and cellulose nanofibrils isolated from bacteria, tunicate, and wood processed using acid, enzymatic, mechanical, and oxidative methods. *ACS Applied Materials & Interfaces, 6*, 6127–6138. https://doi.org/10.1021/am500359f

Sadeghifar, H., Filpponen, I., Clarke, S. P., Brougham, D. F., & Argyropoulos, D. S. (2011). Production of cellulose nanocrystals using hydrobromic acid and click reactions on their surface. *Journal of Materials Science, 46*, 7344–7355. https://doi.org/10.1007/s10853-011-5696-0

Saito, T., Kimura, S., Nishiyama, Y., & Isogai, A. (2007). Cellulose nanofibers prepared by TEMPO-mediated oxidation of native cellulose. *Biomacromolecules, 8*, 2485. https://doi.org/10.1021/bm0703970

Saito, T., Hirota, M., Tamura, N., Kimura, S., Fukuzumi, H., Heux, L., et al. (2009). Individualization of nano-sized plant cellulose fibrils by direct surface carboxylation using TEMPO catalyst under neutral conditions. *Biomacromolecules, 10*(7), 1992–1996. https://doi.org/10.1021/bm900414t

Scherrer, P. (1918). Bestimmung der grösse und der inneren struktur von kolloidteilchen mittels röntgenstrahlen. *Göttinger Nachrichten Gesell, 26*, 98–100.

Segal, L., Creely, J. J., Martin, A. E., & Conrad, C. M. (1959). An empirical method for estimating the degree of crystallinity of native cellulose using the X-Ray diffractometer. *Textile Research Journal, 29*, 786–794. https://doi.org/10.1177/004051755902901003

Sehaqui, H., Mushi, N. E., Morimune, S., Salajkova, M., Nishino, T., & Berglund, L. A. (2012). Cellulose nanofiber orientation in nanopaper and nanocomposites by cold drawing. *ACS Applied Materials & Interfaces, 4*, 1043–1049. https://doi.org/10.1021/am2016766

Shang, Q., Liu, C., Hu, Y., Jia, P., Hu, L., & Zhou, Y. (2018). Bio-inspired hydrophobic modification of cellulose nanocrystals with castor oil. *Carbohydrate Polymers, 191*, 168–175. https://doi.org/10.1016/j.carbpol.2018.03.012

Shen, H., Peng, S., Luo, Q., Zhou, J., He, J. H., Zhou, G. F., et al. (2023). Nanopaper electronics. *Advanced Functional Materials, 33*(23), 2213820. https://doi.org/10.1002/adfm.202213820

Spence, K. L., Venditti, R., & a., Rojas OJ, Habibi Y, Pawlak JJ. (2011). A comparative study of energy consumption and physical properties of microfibrillated cellulose produced by different processing methods. *Cellulose, 18*, 1097–1111. https://doi.org/10.1007/s10570-011-9533-z

Tanpichai, S., Quero, F., Nogi, M., Yano, H., Young, R. J., Lindström, M., et al. (2012). Effective Young's modulus of bacterial and microfibrillated cellulose fibrils in fibrous networks. *Biomacromolecules, 13*, 1340–1349. https://doi.org/10.1021/bm300042t

Tejado, A., Alam, M. N., Antal, M., Han, Y., & Ven, T. (2012). Energy requirements for the disintegration of cellulose fibers into cellulose nanofibers. *Cellulose, 19*, 831–842. https://doi.org/10.1007/s10570-012-9694-4

Thomas, B., Raj, M. C., Athira, B. K., Rubiyah, M. H., Joy, J., Moores, A., et al. (2018). Nanocellulose, a versatile green platform: From biosources to materials and their applications. *Chemical Reviews, 118*(24), 11575–11625. https://doi.org/10.1021/acs.chemrev.7b00627

Tingaut, P., Zimmermann, T., & Lopez-Suevos, F. (2010). Synthesis and characterization of bionanocomposites with tunable properties from poly(lactic acid) and acetylated microfibrillated cellulose. *Biomacromolecules, 11*, 454–464. https://doi.org/10.1021/bm901186u

Tobjörk, D., & Österbacka, R. (2011). Paper electronics. *Advanced Materials, 23*, 1935–1961. https://doi.org/10.1002/adma.201004692

Viana, L. C., Potulski, D. C., de Muniz, G. I. B., Andrade, A. S. D., & Silva, E. L. D. (2018). Nanofibrillated cellulose as an additive for recycled paper. *Cerne, 24*, 140–148. https://doi.org/10.1590/01047760201824022518

Wang, Q. Q., Zhu, J. Y., Gleisner, R., Kuster, T. A., & Baxa, M. N. S. E. (2012). Morphological development of cellulose fibrils of a bleached eucalyptus pulp by mechanical fibrillation. *Cellulose, 19*, 1631–1643. https://doi.org/10.1007/s10570-012-9745-x

Wei, J., & Meyer, C. (2015). Degradation mechanisms of natural fiber in the matrix of cement composites. *Cement and Concrete Research, 73*, 1–16. https://doi.org/10.1016/j.cemconres.2015.02.019

Wijaya, C. J., Ismadji, S., Aparamarta, H. W., & Gunawan, S. (2020). Hydrophobic modification of cellulose nanocrystals from bamboo shoots using rarasaponins. *ACS Omega, 5*, 20967–20975. https://doi.org/10.1021/acsomega.0c02425

Wu, H., Selvaraj, N., Shu, J., Zhang, T., Zhou, L., Duan, Y., et al. (2018). Green and facile surface modification of cellulose nanocrystal as the route to produce poly(lactic acid) nanocomposites with improved properties. *Carbohydrate Polymers, 197*, 204–214. https://doi.org/10.1016/j.carbpol.2018.05.087

Xu, X., Liu, F., Jiang, L., Zhu, J. Y., Haagenson, D., & Wiesenborn. (2013). Cellulose nanocrystals vs. cellulose nanofibrils: a comparative study on their microstructures and effects as polymer reinforcing agents. *ACS Applied Materials & Interfaces, 5*, 2999–3009. https://doi.org/10.1021/am302624t

Xu, X., Zhou, J., Nagaraju, D. H., Nagaraju, D. H., Long, J., Marinov, V. R., et al. (2015). Flexible, highly graphitized carbon aerogels based on bacterial cellulose/lignin: Catalyst-free synthesis and its application in energy storage devices. *Advanced Functional Materials, 25*, 3193–3202. https://doi.org/10.1002/adfm.201500538

Xu, X., Zhou, H., Zhou, G., & Hsieh, Y.-L. (2020a). Photonic thin films assembled from amphiphilic cellulose nanofibrils displaying iridescent full-colors. *ACS Applied Bio Materials, 3*, 4522–4530. https://doi.org/10.1021/acsabm.0c00463

Xu, Z., Peng, S., Zhou, G., & Xu, X. (2020b). Highly hydrophobic, homogeneous suspension and resin by graft copolymerization modification of cellulose nanocrystal (CNC). *Journal Of Composites Science, 4*, 186. https://doi.org/10.3390/jcs4040186

Yu, H., Qin, Z., Liang, B., Na, L., & Long, C. (2013). Facile extraction of thermally stable cellulose nanocrystals with a high yield of 93% through hydrochloric acid hydrolysis under hydrothermal conditions. *Journal of Materials Chemistry A, 1*, 3938–3944. https://doi.org/10.1039/c3ta01150j

Zhang, Z., Wu, Q., Song, K., Ren, S., Lei, T., & Zhang, Q. (2015). Using cellulose nanocrystals as a sustainable additive to enhance hydrophilicity, mechanical and thermal properties of poly(vinylidene fluoride)/poly(methyl methacrylate) blend. *ACS Sustainable Chemistry & Engineering, 3*, 574–582. https://doi.org/10.1021/sc500792c

Chapter 5
Paper Engineering: General Considerations

Nanci Ehman, María Evangelina Vallejos, and María Cristina Area

5.1 Generalities in Paper and Paperboard Production

Paper and paperboard manufacturing plays an essential role in society, even today, in the current digital age. The papermaking industry has been adapted based on the diversification of products and processes since the early papermaking age. Paper-based products have been a commodity in continuous transition throughout history. The invention of the continuously operating papermaking machine in 1844, the introduction of chemical kraft pulping or fiber separation by mechanical actions, bleaching invention, and paper recycling are some example milestones of transitions (Bowden & Hamza, 2016).

The pulp and paper industry adaptation aspects remain the same as in the last years (e.g., market trends or consumer preferences). However, additional ones gained relevance (e.g., aspects like new laws related to the environment). Then, the versatility becomes more complex: the market is usually influenced by several factors, like technological evolution and the search for greater efficiency in the sector, environmental trends, changes in consumer preferences, market demand, new regulations, and changes in the industry (Fig. 5.1).

Let us consider energy efficiency to understand the complexity of the factors that influence the market. In recent years, some modifications to the process streams for pulp, paper, and paperboard production have partially allowed industries to reduce their carbon footprint. However, transitioning toward more efficient and ecological energy technologies is still challenging (Lipiäinen et al., 2022). During 2022, increases in energy prices in Europe reached records, which led to reduced operating cycles in paper machines. Therefore, a higher decrease in production was observed (even less than during the COVID-19 pandemic) (Confederation of European Paper Industries CEPI, 2023). The digital era has also shown some trends

N. Ehman (✉) · M. E. Vallejos · M. C. Area
PROCYP, IMAM (UNaM-CONICET), Posadas, Argentina

G. Korotcenkov (ed.), *The Handbook of Paper-Based Sensors and Devices*,
https://doi.org/10.1007/978-3-031-91080-7_5

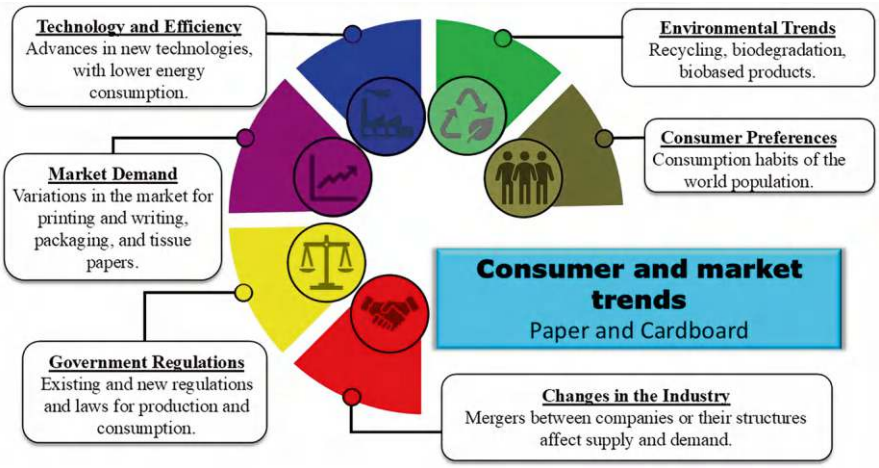

Fig. 5.1 Aspects influencing the versatility of the paper and paperboard industries

that do not seem cyclical but imply a structural change. However, the actual market demand factor can be more estimable; tools such as Big Data analytics allow the study of market behavior and decisions based on statistical values (Turulja et al., 2023). Finally, the term diversification of the pulp and paper industry goes beyond the traditional production of pulp, paper, and paperboard.

However, new opportunities arise through bioproducts, biomaterials, and energy generation, allowing for achieving greater circularity in the production process flow (Mongkhonsiri et al., 2018). These options would allow a successful transition toward more sustainability, higher rentability, recyclability increase, and diversified processes in the industry.

The conversion of raw materials into paper involves a series of operations. The stages vary according to the type of paper to be obtained, the raw material, the type of pulping, whether the process involves bleaching, the type of formation, and additives incorporation in the paper machine (Pathak & Sharma, 2023). To explain the traditional papermaking process, consider the bleached pine kraft paper production shown in Fig. 5.2.

The process begins with the reception of raw material at a wooden yard; then, the raw material is prepared by removing the bark and reducing the size of logs; finally, the chips are directed to pulping (in this case, chemical pulping). At the exit from the chemical pulping, the pulp is washed and sent to bleaching, where the lignin content is reduced. The bleached and cleaned pulp is then ready to form the filling in the stock preparation section. The pulp is refined, washed, filtered, and combined with other additives according to the final application required. Once the paste is ready, it goes to the paper machine, where the sheet is formed in the forming zone, where the highest amount of water is usually drained. The formed sheet then requires more water removal; therefore, it goes to the pressing and drying zone. Finally, the sheet has a moisture content of less than 10% and passes through calendering

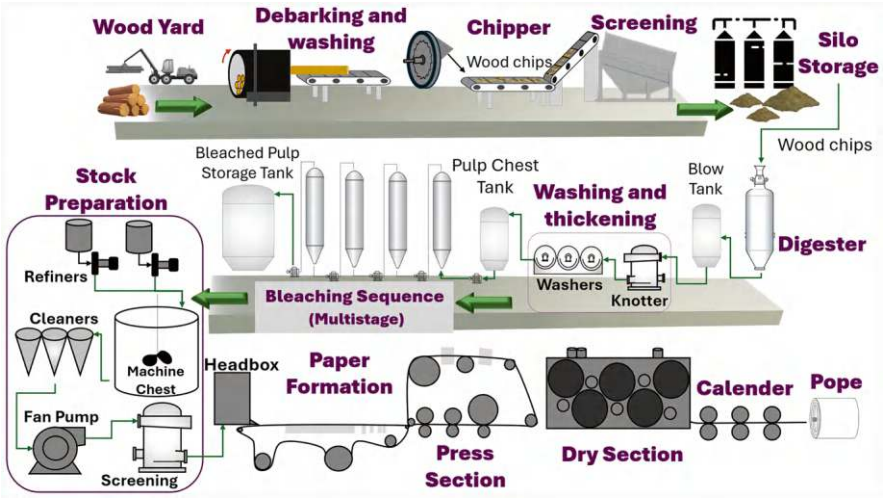

Fig. 5.2 Production process from raw material to paper

section, although sometimes also through a press size where better surface properties are given according to the type of paper to be obtained. If the paper is passed through a size-press, it must be dried again.

Secondary circuits that assist plant processes are added to the main paper manufacturing line (Fig. 5.2). In kraft pulping, some examples include pulping reagents line (white liquor, black liquor, caustic soda), white water in the papermaking machine, additives preparation, and auxiliary systems (energy, water, vapor, effluents) (Sixta, 2006).

5.2 Raw Material Conditioning

Pulp and paper can be manufactured from different plants, depending on the shape of their cells. Over time, cells die and become hollow structural units, typically consisting of a cell wall surrounding a cavity. This structure is known in paper technology as fiber. Maintaining similar operating conditions, the quality of the paper will depend on the fibers' length, diameter, flexibility, and strength, among others.

Coniferous species (softwoods, gymnosperms) have long fibers, producing a strong sheet because their length allows them to intertwine better. On the contrary, the so-called broadleaf woods (hardwoods, angiosperms) with short or rigid fibers generate fewer strength sheets. However, certain qualities of paper require the presence of short fibers to fill the interstitial spaces, achieving a more "closed" weave. The main component of the fiber walls is cellulose, followed by hemicelluloses and lignin. The latter is the "glue" material that holds the fibers together. Fibers also contain extractives and inorganics (Rowell et al., 2013).

The raw material conditioning for the pulping process will depend on the type of raw material. Usually, it is divided into three types: wood (softwoods and hardwoods), non-wood (grasses), and recycled paper (Liu et al., 2018). Although softwoods were the most used, hardwoods use is increasing markedly due to the constant demand for paper products. In countries with scarce wood resources, grasses (cereal straw, sugarcane bagasse, bamboo, etc.) or recycled papers are used (Liu et al., 2018). In wood derivatives, wood chips with similar sizes should enter the digester; therefore, the raw material must be debarked, chipped, and classified. In the case of a non-wood raw material, the material must be chopped and impurities removed. Finally, recycled paper requires classification and cleaning of the raw material.

5.2.1 Wood Handling

This stage conditions the wood to be used in pulping so that it is sufficiently uniform in size and free of bark or other impurities. Therefore, the wood logs must be debarked, chipped, and screened.

The wood bark contains many extractives (Sakai, 2010), which can interfere with the consumption of reagents in the digester and the bleaching sequence and lead to dirty and poor-quality cellulosic pulp. For this reason, if the raw material arrives at the factory as logs, it must be debarked. The logs are debarked, leaving the wood clean for the next stage, while the residue from the debarking is used as fuel (Ekbåge, 2020) to generate electricity or water vapor. In the paper industry, the technologies applied for debarking include drums, rings, rotation, flail, compression, or rosserhead systems (Chahal & Ciolkosz, 2019; Sixta, 2006). The drum debarking is the most popular system, and the bark is removed through the abrasion generated by the rotation of the drum and the collision between the logs due, in some cases with water addition (Latha et al., 2018).

Then, chipper equipment reduces the debarked logs to uniform sizes. The size is an essential parameter since it will influence the chemical impregnation during chemimechanical or chemical pulping (Sixta, 2006) and energy consumption or pulp quality in mechanical processes (Jones et al., 2004). For example, an accepted chip size in kraft pulping is an average of around 25 mm in length, 25 mm wide, and 4 mm thick (Quinde, 2020). Chips that are too far from this size are called rejected. The rejected wood chips involve oversized, pin chips, and fines and lead to problems in various stages of the process; for example, oversized or overthick chips produce uncooked generation and an increase in knotters, while fines lead to clogging in filtration and cleaning systems. Size reduction of wood logs using chippers involves drum, disc, and screw systems. The most applied technology is the disk chipper (a rotating disc provided with blades). The feeding of the logs can be done horizontally or vertically (Naimi et al., 2006).

A screening stage classifies the chips. The accepted chips continue toward the storage silos, and the oversized or overthick chips rejected are rechipped, while the pin chips and fines are sent to the boiler to be burned and generate energy or steam.

The wood chip screening can be carried out on equipment with mechanical operations, among which vibration systems (vibratory screening type) stand out or with methods based on air displacement (Sixta, 2006).

At the end of wood handling operations, the wood chips are stored in silos, ensuring that raw material can be constantly supplied to the pulping stage throughout the year and overcoming fluctuations in raw material receipt. In turn, some industries include silos where they receive outsourced chips, which must go through a classification process. Furthermore, the chips stored in silos are cheaper than logs, although it presents some advantages like loss of material and generation of dust in the environment (Bajpai, 2010).

5.2.2 Sugarcane Bagasse Handling

Sugarcane bagasse is a subproduct of the sugarcane industry used as a raw material to produce paper worldwide. The sugarcane bagasse handling in the paper industry involves cutting, depithing, cleaning, screening, and storage.

The depithing stage is necessary to eliminate the pith content, mostly parenchyma (around 30%). The sugarcane bagasse also contains fiber bundles and epidermal cells (Rainey & Covey, 2016). The fiber is sent to digesters (to produce 1 ton of paper, approximately 2 tons of sugarcane fiber without pith is required), and the pith separated in the depithing process is sent to the boiler to produce energy. The depithing methods could be divided into dry, wet, or moist depithing, and the industrial depithers include *Horkel* (Horton and Keller), *Peadco*, *SPW Pawert*, *Wesmaco*, and *KC-4* (Kimberly Clark) (Lois-Correa, 2012; Manohar Rao, 1986). The effect of depithing is positive for the subsequent storage stage. The greater the pith removal, the more fiber will be preserved since it will control the fermentation of sugars. Sugarcane bagasse deteriorates more than wood due to its initial moisture content, residual sugar and proteins, minerals, and the heterogeneity of its tissues (Aguilar-Rivera, 2011).

5.2.3 Recycled Paper as Raw Material

In paper and paperboard mills where recycled fiber is used, the raw material yard stores numerous recycled paper qualities. The relevance of this stage is the correct classification of the raw material, usually concerning the qualities of the type of recycled paper available in the raw material yard. The qualities are divided into five groups that correspond to different grades (CEPI, 2013; ERPA & CEPI, 2002):

- ***Ordinary grades***: Mixed paper and paperboard (unsorted, without unusable material, or with 40% maximum of magazines and newspapers), gray paperboard with and without print (no corrugated), supermarket corrugated paper and

paperboard (containing a minimum of 70% of corrugated board, the rest being other packaging papers and paperboard), corrugated paper and paperboard packaging, ordinary corrugated board (before old-corrugated container, OCC), unsold magazines (with or without glue, may contain non-paper components as attached product samples), newspaper and magazine mixtures with or without glue (containing a minimum of 50% of newspapers, variable classification), and sorted graphic paper (minimum of 80% newspapers and magazines. It must contain at least 30% newspapers and 40% magazines).

- ***Medium grades***: Newspapers (with a maximum of 5% of newspapers or advertisements colored), unsold newspapers (unsold daily newspapers, free from additional inserts or illustrated material), lightly printed white shavings (mainly mechanical pulp-based), heavily printed white shavings, sorted office paper, colored letters (correspondence, with or without print, writing paper, free from carbon paper and hardcovers), white wood-free books (books without hard covers, mainly of wood-free white paper, black printed only, maximum of 10% of coating), colored wood-free magazines (coated/uncoated magazines, non-flexible covers, bindings, non-dispersible inks and adhesives, poster papers, labels or label trim, maximum of 10% mechanical pulp-based), carbonless copy paper, bleached wood-free PE-coated board (from board manufacturers and converters), mechanical pulp-based computer print-out (mechanical pulp-based, sorted by colors, may include recycled fibers).
- ***High-quality grades***: Mixed lightly colored printer shavings (wood, wood-free), wood-free binders, tear white shavings, white wood-free letters, white business forms, white wood-free computer printout, printed bleached sulfate board, lightly printed bleached sulfate board, multi printing, white printed multiply board, white newsprint, white mechanical pulp-based coated and uncoated paper, white wood-free coated paper without glue, white shavings, unprinted bleached sulfate board.
- ***Kraft grades***: New shavings of corrugated board, used corrugated, clean used kraft sacks, unused kraft sacks, used kraft paper/board of a natural or white shade, new kraft/carrier kraft.
- ***Special grades***: Mixed recovered paper/board (unsorted paper and board, separated at source), mixed packaging, liquid board packaging (including used PE-coated liquid packaging board with or without aluminum content, a minimum of 50% by weight of fibers and the balance being aluminum or coatings), wrapper kraft, wet labels (1% glass content, maximum of 50% moisture), unprinted/printed white wet-strength wood-free papers.

In all cases, as the number of recycling increases, the fibers lose mechanical strength. Some companies use up to 10% of virgin fiber to reach the mechanical strength standards of the paper produced; therefore, in the raw material yard, it is also possible to find virgin pulp, bleached or unbleached, for reinforcement (Obradovic & Mishra, 2020). In addition to the quality of each type of paper, recycled paper may contain impurities such as adhesives, inks, stones, and metals, which will be eliminated during the following stages.

5.3 Pulp Types and Their Preparation

Wood and other fibrous plants are converted into fibers suitable for papermaking through different pulping processes. Depending on the method and machinery used, lignocellulosic raw materials are ground, cooked, digested, defibered, delignified, or reprocessed. These procedures are called pulping, and their purpose is the release of the fibers. Figure 5.3 summarizes different types of pulping that exist and their usual applications. The obtained pulp can be used for certain types of papers, although in most cases, subsequent treatments give the fibers better properties for their final use. Many pulping processes have been developed to achieve this goal most economically, each suitable for a different end-use.

Pulping processes are mainly divided into two general groups: chemical and mechanical. The main difference is due to the mechanism of action performed to release the fiber and remove the lignin. In chemical pulping, the substance that holds the fibers together (middle lamella lignin) is chemically dissolved to a point where defibration becomes possible without mechanical treatment. The disadvantage of these procedures is the large wood consumption with low yields. High-yield pulps are obtained with mechanical pulping, but shredding causes ruptures in the cell walls, and the pulps have very particular characteristics, which are only adequate for some kinds of paper. Since these pulps maintain appreciable amounts of lignin in their structure, they are called high-yield processes. Even if pulps are relatively weak, they provide pulps with better sheet formation, higher opacity, and other specific properties that make them virtually irreplaceable for some uses, such as newsprint. Disadvantages include lower resistance, high specific energy requirement, and limited capacity to reach a certain brightness.

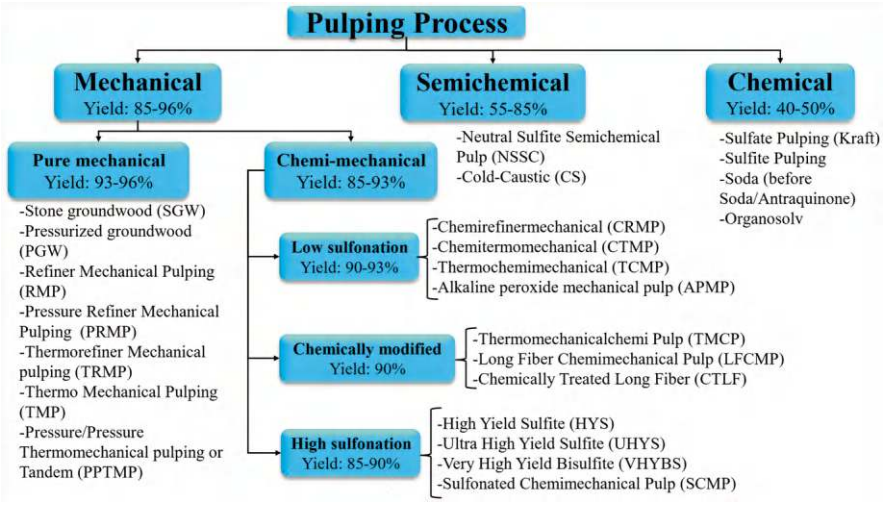

Fig. 5.3 Classification of pulping processes

The major groups of pulping processes and their main applications are indicated as follows:

- ***Pure mechanical processes***: Process with only mechanical action (can include temperature or pressure, but without any chemical addition). The treatments lead to yields between 93 and 96%. The main applications are printing and writing, paperboards, composite products, and molded pulp production. Examples include stone groundwood (SGW), pressurized groundwood (PGW), refiner mechanical pulping (RMP), pressure refiner mechanical pulping (PRMP), thermorefiner mechanical pulping (TRMP), thermomechanical pulping (TMP), and pressure or pressure/pressure thermomechanical pulping or tandem (PPTMP).
- ***Chemimechanical processes***: With yields between 85 and 93%. These processes can be further divided into three groups: low sulfonation process (yield: 90–93%, low impregnation chemical treatment before the mechanical process), chemically modified pulping (yield: 90%, chemical modification after a refining stage), and high sulfonation processes (yield: 85–90%, pretreatment with a high level of sodium sulfite before refining). Final uses include tissue, corrugated medium, thin papers, and paper food containers. High-sulfonated pulps are sometimes used as reinforcement fiber. Some examples are chemitermomechanical (CTMP), alkaline peroxide mechanical pulp (APMP), high yield sulfite (HYS), and sulfonated chemimechanical pulp (SCMP).
- ***Semichemical processes***: Chemical treatment, followed by refining with yields between 55 and 85%. Final applications are corrugated medium paperboard, printing and writing paper, and food containers. Example includes neutral sulfite semichemical pulp (NSSC).
- ***Chemical processes***: 100% chemical treatment with yields lower than 50%. The treatment is combined with pressure and temperature. End-uses include high-mechanical strength liner board, paper bags, printing and writing, fine paper and newsprint (sulfite). Examples include kraft or sulfate, sulfite, soda (before with the addition of anthraquinone, but subsequently banned), and organosolv pulping.

The application is not always specific to each pulp; in some cases, furnishings are used with several types of pulp to achieve a desired property. For example, the papers produced from mechanical pulps are often combined with chemical or semichemical pulps to provide mechanical strength. Another example is the pulps used in tissue paper production, which can combine CTMP fiber and bleached kraft fiber. Note that there are other stages in the paper machine (additives, finishing) that will optimize the properties of the paper produced.

5.3.1 Chemical Pulping

Chemical pulping involves wood chips cooking with suitable chemicals in an aqueous solution at elevated temperatures and pressures. Lignin, hemicelluloses, and short cellulose chains are progressively extracted (according to the quality of the

product to be obtained), so the pulp yield is low (between 40 and 50%). The remaining material can be bleached without much effort to high brightness. Because cellulose forms stronger bonds than lignin, the cellulose-rich fiber surfaces in a chemical pulp sheet produce strong papers. The two main methods are the kraft (alkaline) and the sulfite (acid) processes.

5.3.1.1 Kraft or Sulfate Process

The kraft pulping process globally prevails (80% of global production) due to its advantages in pulp strength (they have high resistance and can be applied to any raw material) and its efficient chemical reagent recovery system, with the production of simultaneous energy. The kraft pulping stage aims to dissolve the lignin and other non-cellulosic compounds by subjecting the chips to chemical reagents, temperature, and pressure for a given time.

The obtained kraft pulp (unbleached), characterized by a dark brown color, is used in paper bags (sugar, cement, etc.) and paperboard for packaging. Kraft pulp produces durable, permanent white papers, so bleached pulp is used for products that must remain unchanged over time, such as high-quality books or, in the case of long-fiber pulp, as reinforcing pulp.

In this process, the amount of lignin removed depends on the pulp's final use. The pulping process involves cooking wood chips in a sodium hydroxide (NaOH) and sodium sulfide (SNa_2) solution. The alkaline attack produces the lignin molecule breakdown into smaller fragments, whose sodium salts are soluble in the cooking liquor (Aravamuthan, 2004). The reaction time will depend mainly on the quality of the chip used. Still, it will also depend on other variables such as temperature, concentration, and quantity of the liquor's effective alkali and sulfide content. Figure 5.4 includes all the stages of kraft pulping and the reagents recovery cycle.

At the end of cooking in the digester, black liquor, which contains dissolved lignin and chemical by-products, is produced. Black liquor is highly polluting; however, the lignin can be burned to obtain energy, and the chemicals can be recovered. For this reason, there is a parallel cycle to the paper manufacturing one, called the chemical recovery cycle. The advantages of black liquor recovery include (Tran & Vakkilainen, 2016):

- Reduce the environmental impact of the process
- Cogeneration of electricity and steam
- Chemical recovery (white liquor)

The cycle begins with the concentration of the black liquor. The black liquor leaves the washing section with a concentration of around 15%. To optimize combustion, as much water as possible must be removed, which is done in multi-effect evaporators. When the liquor reaches 20–25% concentration, the overflow soap is separated in a tank. This is the precursor to producing tall oil. 40–80% of tall oil soap is separated from black liquor, with the remaining tall oil components soluble

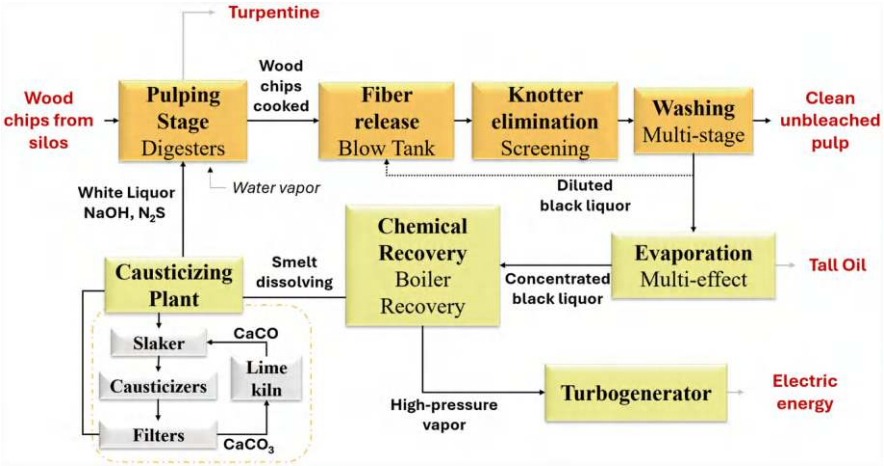

Fig. 5.4 Kraft pulping and chemical recovery system

in the black liquor (Churchill et al., 2024). Then, the liquor continues in the effects until it reaches a concentration of 50% solids.

The concentrated black liquor is sent to the recovery boiler to burn the organics (lignin, fiber, etc.) and recover the inorganic chemicals as smelt (sodium carbonate and sodium sulfide). The recovery boiler produces high-pressure steam, power, and green liquor (Bajpai, 2018a).

The green liquor contains sodium carbonate (Na_2CO_3) and sodium sulfide (Na_2S), resulting from the combustion of the black liquor. This green liquor undergoes a causticization process (mixing with CaO and producing NaOH), becoming white liquor again and returning to the cooking cycle (Sixta, 2006).

5.3.1.2 Sulfite Process

The sulfite process dominated the paper industry from the late nineteenth to the mid-twentieth century. However, it was limited by the types of wood available and contamination of the waste liquor, so it was replaced by the kraft process (Madhu et al., 2023). Later processes have overcome many of these problems, so sulfite pulp now represents only a small market segment. Although acid digestion is commonly used, some variations use a neutral or alkaline medium. Sulfite pulping is carried out using a mixture of sulfurous acid (H_2SO_3), sulfite ion ($SO_3^{=}$), or bisulfite (HSO_3^{-}) and a base at 120–150 °C to attack and solubilize the lignin. Sulfite pulping can involve different bases, such as Ca_2^{+} (pH = 2, "acidic sulfite"), Mg_2^{+} (pH = 5, "bisulfite" Magnefite), Na^{+} (any pH), and NH_3^{+} (pH <9, "alkaline sulfite").

Sulfite pulps are lighter than kraft pulps and bleach easily, but the papers are weaker than their kraft counterparts. It also produces fibers that are easier to refine but are not very flexible with resinous softwoods, tannin-containing hardwoods, and

any furniture containing bark (Bajpai, 2010). During the sulfite process, the lignin is sulfonated, leading to a technical lignin called lignosulfonates (Madhu et al., 2023). When hardwood is treated with sulfite, the preservation of cellulose and the attack on xylans are higher than in the kraft process (Sixta, 2006).

5.3.1.3 Soda Pulping

Soda pulping is preferred for cooking agricultural or agro-industrial waste such as straw or sugarcane bagasse (Pathak & Sharma, 2023). It consists of treating the fibers with a liquor of water and NaOH for a given time at temperatures around 140–170 °C (Andrade & Colodette, 2014). The black liquor containing lignin and sodium hydroxide (soda) is processed to recover the soda (Doherty & Rainey, 2006).

5.3.2 High-Yield Processes

Mechanical pulps contain almost all the lignin in the wood and require considerable mechanical treatment to separate and prepare the fibers. Since the discovery of mechanical pulps, pulps of varied yields and qualities have been manufactured by combining actions (mechanical, chemical, and thermal) and combining the arrangement of intermediate operations (purification, fractionation) (Blechschmidt & Heinemann, 2006).

The oldest method is the stone groundwood (SGW), in which the logs are forced under pressure against a rough rotating stone that rotates along the longitudinal axis of the logs in the presence of large volumes of water. The diluted suspension of fibers and fiber fragments is sieved to remove shives and other coarse particles. Then, it is thickened by water removal to form a pulp suitable for papermaking. Pressurized groundwood (PGW) works with high pressures (with compressed air), producing an increase in the boiling temperature of water, thereby partly avoiding evaporation at the wood-stone interface. Independently adjusting pressures and temperatures produces versatile pulp qualities.

Groundwood pulps have the lowest manufacturing cost but the lowest quality in terms of mechanical strength. Its use is almost limited to newsprint due to its excellent printing and optical characteristics and low energy consumption.

A later development of mechanical pulping uses chips instead of logs, producing pulps of comparatively better quality. The process consists of passing the chips through the discs of a refiner and managing the mechanical variables to obtain the desired quality. One of the advantages of this process over the previous one is its versatility, producing pulps with a wide range of physical properties. For example, in thermomechanical pulping (TMP), the chips are preheated with steam at a temperature close to 130 °C before defibration-refining. The process with pressurized primary and secondary stages is called pressure/pressure thermomechanical pulping or tandem (PPTMP). TMP pulp manufacture involves high energy consumption and

sophisticated equipment, obtaining, in return, pulps of superior quality, capable of replacing chemical pulps in many cases.

Chemithermomechanical pulping (CTMP) is a variant of mechanical pulping that includes a chemical impregnation stage before the thermal treatment in TMP pulping, resulting in pulps of superior quality.

Bleached chemithermomechanical pulps (BCTMP) encompass pulps produced from chips with a mild chemical pretreatment and bleached with hydrogen peroxide. The total yield for softwoods is higher than 90% and 87% for hardwoods. BCTMP pulp can partially substitute hardwood kraft pulps in coated and uncoated papers.

The development of chemimechanical pulping (CMP) allowed the production of hardwood high-yield pulps of acceptable qualities. The process consists of impregnating with chemicals (in low concentrations and for a short time) before refining, thus achieving some lignin degradation but without reaching the point of fiber separation. The cold soda process uses room-temperature caustic soda to soften the chips before refining. The pulp yield is between 85 and 90%.

Alkaline peroxide mechanical pulp (APMP) consists of the chemical treatment of the chips with sodium hydroxide, hydrogen peroxide, and stabilizers, with a simultaneous pulping and bleaching effect. This process was developed to improve the quality of hardwood chemimechanical pulps. With an adequate loading of reagents, it is similar (in tensile strength) to BCTMP but with lower specific energy consumption.

Semichemical processes combine chemical and mechanical methods. The wood chips are partially softened or cooked with chemicals, and the remaining pulping action is supplied mechanically, most often by disc refiners. These methods cover the entire range of pulps whose yields are between pure mechanical and pure chemical methods, that is, 55–85% yield referred to dry wood. The neutral sulfite pulping process (NSSC) applied to hardwoods is the most widely used semi-chemical process. It uses sodium sulfite as a cooking liquor, buffered with sodium carbonate to neutralize the organic acids released from the wood during cooking. In cold soda pulping (CS), the chips are impregnated with a sodium hydroxide solution in an open tank and defibered-refined in two stages.

5.3.3 Pretreatments and Alternative Pulping Processes

Pulping stage modifications are toward efficiency improvements, with lower environmental impacts and reduced process costs. Lignocellulosic pretreatment before pulping allows for improving the accessibility of the raw material or even separating some components before conventional pulping. Alkaline and acid treatment could be applied for hemicelluloses removal from previous kraft processes (Saukkonen et al., 2012). Steam explosion has also been used as a pretreatment, allowing the opening of wood structures and leading to a faster delignification in

chemical pulping (Jedvert et al., 2012). The screw extrusion has been applied as a physical pretreatment, sometimes assisted by alkaline or acid reagents (Guiao et al., 2022). In high-yield processes, such as in TMP pulping, for example, screw extrusion can be applied to remove extractives before the mechanical treatment (Tanase et al., 2010). In chemical pulping also was applied to reduce the consumption of chemicals, as in the case of kraft and soda-AQ pretreatment, where was applied screw extusion to reduce the alkali consmumption (Dong et al., 2012). Some alternative pulping processes are being investigated to achieve more efficient processes with less environmental impact. Organosolv pulping (Area et al., 2009; Imlauer Vedoya et al., 2022), for example, allows solvent recovery, while oxygen and alkali treatment allows improvements in delignification with low emissions (Esteves et al., 2022). The use of green solvents (deep eutectic solvents, ionic liquids, and ϒ-valerolactone) is another alternative (Ehman et al., 2023), as well as induced electric field-assisted systems (Zhang et al., 2024). Emerging pulping and pretreatment of conventional processes lead to integrated biorefinery systems. In recent years, some paper mills have migrated to biorefineries. In this way, in addition to paper production, other biomass component removal allows for obtaining high-value-added products.

One of the emerging technologies that could allow for less water, energy, and chemical consumption is the replacement of conventional digesters with extrusion systems. These systems merge high-shear mechanical actions with chemicals to benefit the delignification without high cellulose fiber damage. The twin-extrusion pulping process has been applied mainly to non-wood fibers, achieving pulp yields of up to 80% (Rodriguez Castellano, 2024).

Finally, biopulping for fiber separation utilizes specific microorganisms to depolymerize lignin. This process uses fungi on wood chips, facilitating lignin degradation by their enzymes. The process is slow compared to chemical processes and must be biologically controlled (Rullifank et al., 2020).

5.4 Bleaching Processes

The main objective of bleaching is to increase the pulp's brightness by eliminating or modifying some constituents of the brown pulps, such as lignin and its degradation products, resins, metal ions, non-cellulosic carbohydrates, and other impurities. The obtained brightness must be stable, i.e., that whiteness or resistance is not lost with aging. The light-absorbing substances in wood pulp are components derived from the lignin and resin of the original wood. Therefore, to make a white pulp, these substances must be chemically transformed in the solid state (to reduce their light absorption characteristics) or be oxidized, reduced, or hydrolyzed to make them soluble in aqueous solutions and be able to eliminate them from the pulp.

5.4.1 Chemical Bleaching

In chemical pulps bleaching, the total elimination of the substances that cause color (lignin and its degradation products, resins, and other impurities of different natures) is pursued. Bleaching requires several stages, both for technical and economic reasons, representing a continuation of cooking since it extracts the residual lignin with yield losses between 3 and 10% (Colodette & Borges Gomes, 2015). The pulp brightness at the end of a kraft process is around 25–30% and can achieve high (90–95%) and stable values (Dence & Reeve, 1996).

The bleaching of chemical pulps can involve ECF (elementary chlorine-free) and TCF (total chlorine-free) technologies. While ECF incorporates chlorine dioxide, TCF mainly uses oxygen (O), ozone (Z), enzymes (X), peracetic acid, and hydrogen peroxide (P).

Table 5.1 shows the competitive advantages and disadvantages of the different bleaching technologies. The main advantage of the ECF and TCF processes is the elimination of the release of high amounts of chlorinated dibenzofurans and dibenzo-p-dioxins effluents (Axegård, 2019). Bleaching should be performed without relevant fiber degradation. In ECF processes, the pulp reaches higher brightness without as much reduction in mechanical strength (Fleming & Sloan, 1994).

Traditional TCF sequences incorporate the O, Z, and P stages in several configurations. Oxygen as a delignifying agent is widely used with several fibrous resources, and the stage is generally applied after kraft pulping and before the bleaching sequence (Rodríguez et al., 2007). Ozone is highly reactive and, at the same time, not selective. Therefore, control of consistency, temperature, pH, and presence of metal ions in the process is required to avoid carbohydrate attack and subsequent loss of mechanical strength in the paper produced (Métais & Germer, 2018; Roncero & Vidal, 2007). Hydrogen peroxide has expanded considerably in recent times. Under severe conditions, peroxide can behave as a delignifying agent and is used in

Table 5.1 Advantages and disadvantages of chemical pulp bleaching technologies

	Advantages	Disadvantages
Chlorine	Low-cost process. Selective and effective bleaching. Dissolves metal ions in pulp and other impurities such as bark.	Environmental impact. AOXs (chlorine-containing molecules) like furans and dioxins. Highly corrosive process liquids.
ECF	Lower environmental impact compared to chlorine bleaching. Stable bleaching. Higher bleaching yield compared to TCF.	Some AOXs compounds, but not persistent. More expensive than the chlorine process.
TCF	Organochlorine compounds are not generated. Complies with the strict environmental regulations.	High investment cost in equipment and energy consumption. Lower bleaching yields than ECF. Greater loss of paper strength per unit of increase in brightness.

multi-stage bleaching sequences. In the bleaching peroxide stage, chelates can also be incorporated to maximize the selectivity of bleaching, achieving a more cost-effective process (Area & Felissia, 2005).

5.4.2 *High-Yield Pulps Bleaching*

High-yield pulps are bleached without removing lignin since its extraction would involve a loss in pulp yield, thus eliminating its main advantage over chemical pulps. Therefore, the bleaching of such pulps is carried out through treatments that destroy only the chromophore groups (causing color) without eliminating the pulp's constituents. The most used agents are peroxides (oxidants) and hydrosulfite (reducers).

Bleaching without lignin removal consumes large quantities of reagents without obtaining very high values, reaching 70–80% brightness. Besides, the brightness obtained is unstable, causing the so-called reversion, with the pulps turning yellowish over time.

5.5 Papermaking Machine

The papermaking machine is one of the fundamental sectors of the papermaking process. It transforms the fibrous suspension into sheets of paper or paperboard through several stages: stock preparation, sheet formation, pressing, drying, and finishing (Fig. 5.5).

The processes carried out on a paper machine greatly influence the properties of the paper produced, which is why optimizing the stages accordingly. An optimized papermaking machine process ensures continuous operation and fewer unscheduled

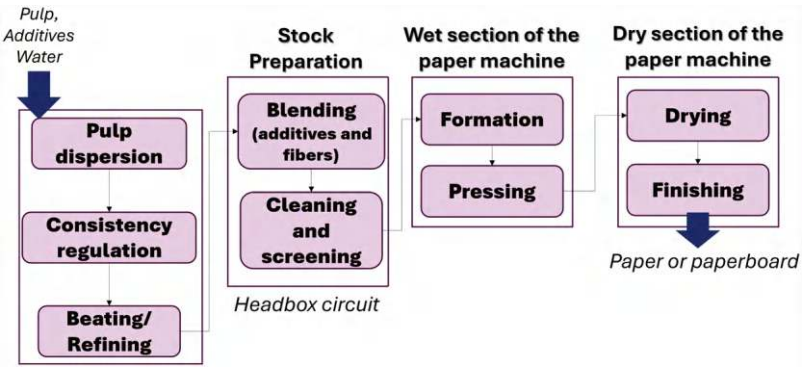

Fig. 5.5 Stages involved in the papermaking machine

stops that lead to large economic losses. The paper machine's "wet end" includes the machine head, forming section, and presses, whereas the "dry end" consists of the sections drying and winding (Hannu Paulapuro, 1999).

5.5.1 Stock Preparation

During the stock preparation stage, the fibrous (pulps) and non-fibrous (additives) raw materials are prepared and combined uniformly to prepare the composition from which the paper will be made.

5.5.1.1 Fiber Slurry Dispersion

The first operation on the paper machine is disintegration. It consists of transforming the fibrous material into a suspension, intending to individualize the fibers, and transporting them through the pipes to the next stage. During disintegration, dilution, agitation of the material, mixing, and dispersion of particles occur. In integrated mills, the fiber comes from the pulp tank (bleached or unbleached) at 3–6% consistency. The fiber is received as bales in a paper-only mill at 90–95% dryness. In the recycled fiber mill, the received recycled paper needs the separation of inks and other contaminants (Roux, 2001).

5.5.1.2 Beating/Refining

The refining (or beating in Hollander beater) purpose (Bajpai, 2010) is to subject chemical action on the cellulosic fibers to develop their papermaking properties, through two actions involving shear and compressive stresses. Examples of properties developed by the sheet due to the refining stage include density, specific volume, tensile strength, burst and tear strength, porosity, etc. During the refining stage, the cellulosic fiber undergoes transformations that can be divided into primary and secondary effects and can impact the final properties of the produced paper (Pathak & Sharma, 2023). Primary effects include external fibrillation and defoliation, internal fibrillation and swelling, fiber shortening, elimination of the primary wall, fines production, interfiber breaking bonds, and formation of new hydrogen bonds with water. Fiber elongation and compression, fractures in the cell wall, partial solubilization of hemicelluloses, fiber straightening (at low consistency), and undulation (at high consistency) are some of the secondary effects (Clarck, 1895; Page, 1989; Smook, 2019a). The industry has numerous geometries for refiners: disk, cylindrical, and conical are the most common. Manufacturers today face challenges in reducing the energy consumption of refiners in paper machines (Gharehkhani et al., 2015). The refining operation is commonly carried out in disc refiners. Some variants include single-disc or double-disc. Other designs available on the market are

the twin or the conical disc refiner (Sixta, 2006). In the wet-end section of the papermaking machine, several refiners are usually used, configured in series and parallel. In addition, the operating conditions will vary according to the type of raw material (Lumiainen, 2008).

5.5.1.3 Additives

Additives are reagents that combine with the cellulose fiber to impart a specific property to the paper or to aid in the production process (Scott, 1996). Two types of additives are usually employed: functional additives and auxiliary additives. Functional additives increase or improve an existing property or impart a new property to paper, and auxiliary additives are added to facilitate the performance of a functional additive or contribute to improving the conditions of the overall process (Scott, 1996). Table 5.2 summarizes the additives applied in the wet-end section of the papermaking machine. Mineral fillers are the second most used ingredient in some kinds of papers. The mineral fillers are natural or artificial insoluble mineral particles, generally white and finely divided (1–10 μm), incorporated into the paper or paperboard pulp for better quality and (or) low cost. Fillers are especially relevant in printing and writing papers. Some benefits of mineral fillers are fiber replacement (lower costs), higher light-scattering (higher opacity and brightness), lower air permeability (improved barrier), and smoother surface (better printability/lower grammage) (Costa & Cettolo, 2020).

Retention aids are reagents that allow the retention of small particles like fines or fillers in the formation section of the papermaking machine. The advantages of a good retention system are loss reduction in papermaking machines, improvement of drainage, and process efficiency (Cadotte et al., 2007). Some examples of retention aids include alum-based, natural polymers (like cationic starch), single-polymer systems (polyethylene imine, cationic polyacrylamide), with patching or bridging as the dominant mechanisms, and dual-polymer systems (poly-dimethyl diallyl ammonium chloride, a cationic polymer of low charge density and high molecular weight) (Wang et al., 2012). Cationic starch has been demonstrated to retain cellulose nanofibers in paper production furnishes (Tajik et al., 2018).

Wet and dry strength additives are applied to improve the paper's mechanical resistance, which is relevant in some final applications. Dry strength additives are usually water-soluble hydrophilic polymers and, in several cases, improve the retention and drainage rate (Marton, 1996). Wet strength additives can act as protective, reinforcing, and swelling prevention agents, protecting existing bonds and (or) forming new water-resistant bonds. Their ability to impart water-resistant properties is related to their polymeric nature, water solubility, cationic character, and reactivity (Francolini et al., 2023).

The brightening chemical reagents impart the brightness of paper using the same principle that the laundry detergent commercials. They convert invisible UV light to lower-energy visible light, generally blue, which masks the inherent yellowness (Bajpai, 2018b). Dyes and pigments are used to impart color to papers. A clear

Table 5.2 Additives in the wet-end section of the papermaking machine

Types	Additives	Functions	Examples	Ref.
Functional additives	Fillers	Improve optical and printing properties; reduces the furnishing cost	Titanium oxide, precipitated calcium carbonate (PCC), clay (hydrous kaolinite), precipitated aluminum silicate, ground limestone (GCC), talc, and gypsum	Costa and Cettolo (2020), Hubbe and Gill (2016)
	Internal sizing agents	Reduce the liquid penetration	Emulsions based on resins, waxes, stearates, alkyl ketene dimer (AKD), alkyl succinic anhydride (ASA), and microparticles	Scott (1996), Simino (2020)
	Wet strength agents	Improve the dry strength of papers (increase in mechanical properties like tensile, burst, tear strength, and elongation), e.g., Kraft liner, bags	Polyacrylamide, cationic polyacrylamide, cationic starch, natural vegetable gums, carboxymethyl cellulose, cellulose nanofibers, microfibrillated cellulose	Ehman et al. (2020), Jenkis (1995), Marton (1996), Vallejos et al. (2016)
	Dry strength agents	Improve the wet strength of papers, e.g., tissue for towels	Starch, cationic starch, chitosan, cellulose nanofibers, polyamide-epichlorohydrin (PAE), melamine formaldehyde, polyacrylamide (PAM), polyvinylamine (PVAm), polyethyleneimine (PEI)	Francolini et al. (2023), Linhart (1995)
	Optical brighteners, dyes, and pigments	Improve the appearance of brightness, add color to the paper	Azoles, coumarins, pyrazines, or naphthalimides, mineral pigments, optical brightener agents, and blue dye	Smook (2019b)
				Bajpai (2018b), Wallmon (2019)
Auxiliary additives	Retention aids	Improve the retention of fillers and fines	Inorganic salts, cationic starch, polyamines, polyvinyl amines, polyacrylamide	Au et al. (1995), Wang et al. (2012)
	Antifoams	Prevent the formation of foam	Alkyl polyether, silicone oils	Bajpai (2018b), Ginebreda et al. (2011), Smook (2019b)
	Biocides	Avoid the microorganism's growth	Peroxyacetic acid, hydrogen peroxide, halogenated, amides, aldehydes, carbamides thiazoles, nitro compounds	
	Acids and bases	pH control	Sulfuric acid, carbon dioxide	
	Pitch control	Prevent the formation of pitch	Talc, nonionic surfactants	
	Formation	Avoid the flocculation	Anionic PAM	
	Drainage	Increase the drainage rate in the wire	Cationic polymer, colloidal silica, bentonite	
	Specials	Impart specific property	Flame retardant, liquid resistance, etc.	

example is the use of dyes in the cardboard box industry from recycled paper, where the aim is to simulate the appearance of a cardboard box made of virgin fiber. Dyes can be acidic, basic, and direct. Acidic and direct dyes are sodium salts of colored acids, while alkaline dyes are salts of colored bases such as chlorides, sulfates, and oxalates (Smook, 2019b).

When necessary, so-called auxiliary additives are added, which help improve the performance of a functional additive or contribute to improving the conditions of the overall process. They include retention aids, antifoams, pitch control additives, biocides, etc. (Smook, 2019b).

Most additives are applied in the wet-end section of paper machines through various configurations to ensure efficient dosage and mixing, proper retention chemistry, and adequate application management (pH, loads, ionic demand, and consistency measurements). The main benefits of a correct additive incorporation system are enhanced paper machine efficiency, improved sheet formation, less deposit formation and paper breakage, and higher-quality paper (Simino, 2020). In some cases, even good management of additives in the wet section could address some problems associated with changes in the paper industry. An example could be the partial replacement of virgin fiber with recycled fiber or microfibrillated cellulose. Adequate management of fines retention agents and additives to remove contaminants from the recycled fiber is relevant. Also, sizing additives to reduce liquid absorption in papers is crucial in the paper market, as current trends are oriented toward paper-based food packaging. By optimizing additives use (like drainage agents, enzymes, fillers, and optical bleaching reagents, among others), operating costs through water circuit closure, refining energy consumption, and pulp bleaching can be reduced.

5.5.2 Wet-End Section

The wet-end section of the paper machine includes the head circuit, the forming zone, and the presses. Around 1% of the solid content suspended at the head circuit's exit begins to lose water through drainage in the formation zone until it reaches around 45% solids at the press's exit and before entering the dryers. Water removal at the dryer outlet by gravity, vacuum dewatering, pressing, and thermal drying totals about 90% (Li et al., 2003).

The paper must maintain a moisture content suitable for the applications and uniform throughout its structure to avoid problems in the following stages (Li et al., 2003). For example, in the cardboard corrugator equipment or during tissue paper creping, points where the moisture content of the sheet is a relevant factor.

5.5.2.1 The Head Circuit in the Papermaking Machine

The head circuit in the papermaking machine corresponds to the dilution pump circuit in which the pulp is mixed with additives, diluted, cleaned, and screened before its final discharge through headboxes in the formation zone. The head circuit

involves stages ranging from the machine storage container (named machine chest) to the headbox lip (Smook, 2019a). All components are relevant at this stage; however, an element that stands out is the dilution pump (fan pump).

The fan pump is a low-pulse, high-efficiency device that facilitates the mixing and dilution of the pulp sent to the papermaking machine. It is located after the point of dilution of the thick stock with white water. After dilution, the stock flows toward the headbox at a consistency of 0.5–1%, ready for papermaking. Reducing pump pulsations during layout is crucial to ensure consistent grammage (Sulzer, 2016).

Before the furnishing enters the paper-forming zone, it undergoes purification and cleaning. This stage aims to separate the desirable fibers or elements from the undesirable particles that may cause problems in the paper's manufacture, thus achieving a clean paper without stains and break/wear during paper manufacturing.

Screening and cleaning are carried out together on a papermaking machine. During cleaning, separation is carried out by density difference through hydrocyclons by dynamic separation. During the screening, separation is carried out by size difference through sieves by probabilistic separation. It should be noted that during cleaning, hydrocyclones with a small diameter develop greater centrifugal forces and greater efficiency in removing different types of small dirt particles. However, larger hydrocyclons diameters lead to greater efficiencies in removing impurities with large and less dense particles, such as long fibrous bundles (Julien Saint Amand, 2001).

5.5.2.2 Formation and Press Zones

The distributor and headbox function is to convert the flow from a pipe to the machine's cross direction, distributing the pipe flow uniformly along the full width of the machine. The jet is then deposited onto the forming section at uniform thickness and velocity, which considerably affects the quality of the paper formation (Bajpai, 2015; Poirier et al., 2001).

The forming zone consists of the machine fabric, which moves at a certain speed with the help of rollers. The upper part is the so-called table. At the bottom of the fabric are the drainage elements (which consist of foils, vacuum boxes, etc.) for collecting and recirculating the extracted water and elements for cleaning, returning, and tensioning the fabric. The main functions of this section are to form the sheet of paper through a filtration process and drain the water from the stock until it has sufficient strength to be transferred to the pressing sector (20% solids, Fig. 5.6). Therefore, it is relevant to maintain an efficient vacuum system (Uimonen, 2017). Drainage must be gradual, so the sheet should be drained as much as possible with static and low vacuum elements before passing through high vacuum elements to reduce drag on the fabric, decrease power requirements, and reduce the marking of the sheet by the fabric. A high vacuum will be applied at the end of the forming table, and as much water as possible should be removed without damaging the sheet. Energy savings can be achieved using non-woven and hybrid felts, which

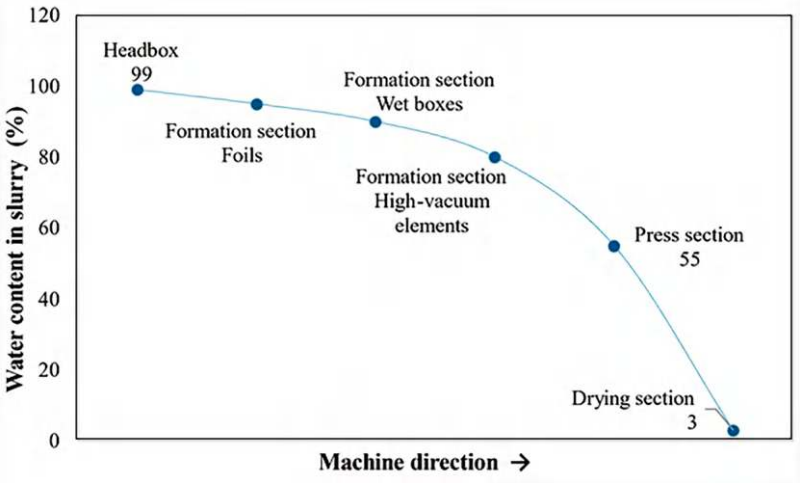

Fig. 5.6 Approximate water content profile in papermaking machine

maximize drainage in the suction box area or pressure areas with less vacuum (Silakoski & Korvenniemi, 2014).

Until the 1950s, almost all paper and board were formed on conventional Fourdrinier or Drum formers, respectively. Nowadays, the Twin-Wire Formers are widely used, where initial drainage happens in one or both directions. Yankee formers are of global use for tissue.

The presses consist of rolls between which the sheet passes over a porous felt that absorbs water. The functions of the press section are extracting water from the sheet of paper (from 20% to 35–45% solids), consolidating the fibrous weave, and reducing the surface roughness of the sheet. The approach area of the rolls is called the nip (Uimonen, 2017). It must be correctly adjusted to fulfill the press functions without damaging the sheet. The suction rollers in the press section collect and transfer the sheet of paper between the various felts for the correct dehydration of the sheet. These rollers have various vacuum zones, controlled precisely, necessary for their proper operation.

5.5.2.3 Approach Flow System

The approach flow system generally covers the stages from the machine chest to the headbox lip. The pulp(s), pumped from the pulp mill to the paper mill or purchased dry and then defibrated, is generally refined to develop the fiber papermaking properties by external and internal fibrillation. Once refined, the pulp(s) passes to the dosing system for the other added components. The paper properties will depend on the stock composition, that is, the type of fibrous raw material (softwoods and (or) hardwood pulps, mechanical, chemical, and (or) recycled pulps) and the other components added (additives, fillers). The stock is directed to the machine headbox after

undergoing rigorous screening and cleaning stages using screens and centrifugal cleaners.

5.5.3 *Dry Section of the Papermaking Machine*

The drying area is the largest section of the papermaking machine. It consists of multiple smooth-surfaced cylinders heated internally with steam, organized in two rows (upper and lower). The area is generally enclosed under a hood heated with hot air. This section's functions are to dry the sheet (from 35–45% to 94–97% solids), consolidate fiber bonding, and modify the sheet's surface characteristics.

Drying drums consist of steam-heated drying cylinders in direct contact with the wet paper as it exits the press section, ultimately producing a curl-free paper. The paper after the press section typically contains about 50% water. Heat energy in the form of steam is applied to remove the water, causing it to evaporate as it moves through the drying section. One of the most relevant indicators of efficiency in the drying section of a papermaking machine from the economic point of view is the production rate or the use of steam per unit of mass of paper manufactured, and it is usually an average of 2–2.5 t/t paper produced (Ghosh, 2011).

Once the sheet leaves the drying section, it is rolled into a wide pope at the end of the paper machine. The pope is then transported to the area of paper-finishing operations. Finishing treatments are generally carried out off-machine, although some may be carried out before winding:

- ***Smoothing****:* This operation consists of applying pressure through one or more pressing zones created by a series of steel rollers. This pressure reduces the thickness of the paper and minimizes thickness variation. Finally, it imparts desirable surface properties, primarily smoothness. Operation parameters involve pressure in the pressing zone, the retention time, and the number of presses.
- ***Surface sizing****:* It aims to hydrophobize the paper surface to avoid liquid penetration. The surface sizing is applied at the final of the drying section in the size press, generating a contact zone between the two rolls with the sizing solution on the side where the paper enters. The paper absorbs part of this solution, and the excess is removed in the contact zone, collected in a tray under the press, and recirculated to the contact zone (Bung, 2004). Configurations of size presses include vertical, horizontal, and inclined (45°) (Bajpai, 2018c).
- ***Coating***: It can be applied after drying and smoothing. It is generally used to fill empty spaces in the sheet and improve the printability of the paper.
- ***Calendering***: Increasing the brightness of the sheet by passing between smooth and fibrous surfaces, or supercalendering. Calendering can be carried out on or off a paper machine and, during the operation, the sheet is compressed and smoothed, creating separate sheets of uniform width and thickness. Sheet thickness is generally determined by the spacing between the pairs of rollers. Pressure

and speed are adjusted to achieve different thicknesses, surface finishes, and textures, resulting in products that can be glossy, matte, smooth, tacky, or embossed.

- ***Creeping:*** For tissue papers, creeping leads to a lower density, increased caliper, and numerous other desirable properties. Creping is performed after passing the sheet through the Yankee dryer (Qin et al., 2023).

5.6 Summary

This chapter provided an overview of pulp and paper operations and stages, from the reception of raw material to the finishing stage. During the preparation of the raw material, numerous alternatives have been mentioned, such as virgin fibers from wood or annual plants and secondary fibers that come from recycled paper and paperboard.

The processes involved in the separation of the individual fibers by chemical, semi-chemical, and mechanical pulping were explained indicating the optimization parameters toward the separation of the fiber, avoiding damage to the cell wall. An overview of bleaching sequences was also explained. The advantages and disadvantages of more recent sequences that avoid applying elemental or total chlorine were summarized and evaluated.

Washing, refining, and mixing with additives were mentioned as key steps (optimal furnish composition) to achieve an efficient formation and good quality in the performance of the final product. It also explained how the forming, pressing, and drying stages, as well as the finishing, influence the quality of the product. Therefore, the operating parameters must be controlled. Finally, secondary lines like black liquor recovery or the approach flow circuit were considered, highlighting their advantages.

References

Aguilar-Rivera, N. (2011). Efecto del almacenamiento de bagazo de caña en las propiedades físicas de celulosa grado papel. *Ingeniería, Investigación y Tecnología, 22*, 189–197.

Andrade, M. F., & Colodette, J. L. (2014). Dissolving pulp production from sugar cane bagasse. *Industrial Crops and Products, 52*, 58–64. https://doi.org/10.1016/j.indcrop.2013.09.041

Aravamuthan, R. G. (2004). Pulping/ chemical pulping. In J. Burley (Ed.), *Encyclopedia of Forest sciences* (pp. 904–910). Elsevier. https://doi.org/10.1016/B0-12-145160-7/00128-9

Area, M. C., & Felissia, F. E. (2005). Chelating agents management to obtain TCF bleached Eucalyptus grandis kraft pulps. *Appita Journal, 58*, 143–148.

Area, M. C., Felissia, F. E., & Vallejos, M. E. (2009). Ethanol-water fractionation of sugar cane bagasse catalyzed with acids. *Cellulose Chemistry and Technology, 43*, 271–279.

Au, C. O., Johansson, K., & Thorn, I. (1995). The use of retention and drainage aids in the wet-end. In C. O. Au & I. Thorn (Eds.), *Applications of wet-end paper chemistry*. Springer Science+ Business Media.

Axegård, P. (2019). The effect of the transition from elemental chlorine bleaching to chlorine dioxide bleaching in the pulp industry on the formation of PCDD/fs. *Chemosphere, 236*, 124386. https://doi.org/10.1016/j.chemosphere.2019.124386

Bajpai, P. (2010). Overview of pulp and papermaking processes. In *Environmentally friendly production of pulp and paper* (pp. 8–45). Wiley.

Bajpai, P. (2015). Basic overview of pulp and paper manufacturing process. In *Green chemistry and sustainability in pulp and paper industry* (pp. 11–39). Springer. https://doi.org/10.1007/978-3-319-18744-0_2

Bajpai, P. (2018a). Kraft spent liquor recovery. In P. Bajpai (Ed.), *Biermann's handbook of pulp and paper* (pp. 425–451). Elsevier. https://doi.org/10.1016/B978-0-12-814240-0.00017-3

Bajpai, P. (2018b). Additives for papermaking. In P. Bajpai (Ed.), *Biermann's handbook of pulp and paper* (pp. 77–94). Elsevier. https://doi.org/10.1016/B978-0-12-814238-7.00004-0

Bajpai, P. (2018c). Paper manufacture—Dry end operation. In P. Bajpai (Ed.), *Biermann's handbook of pulp and paper* (pp. 137–158). Elsevier. https://doi.org/10.1016/B978-0-12-814238-7.00006-4

Blechschmidt, J., & Heinemann, S. (2006). Mechanical pulping processes. In H. Sixta (Ed.), *Handbook of pulp* (pp. 1079–1111). Wiley. https://doi.org/10.1002/9783527619887.ch15

Bowden, C. W., & Hamza, M. F. (2016). Paper: History of development. In *Reference module in materials science and materials engineering*. Elsevier. https://doi.org/10.1016/B978-0-12-803581-8.02202-5

Bung, J. (2004). Surface sizing agents. *IPPTA, 16*, 29–43.

Cadotte, M., Tellier, M., Blanco, A., Fuente, E., van de Ven, T. G. M., & Paris, J. (2007). Flocculation, retention and drainage in papermaking: A comparative study of polymeric additives. *Canadian Journal of Chemical Engineering, 85*, 240–248. https://doi.org/10.1002/cjce.5450850213

CEPI. (2013). Guidance on the revised EN 643. https://www.pita.org.uk/images/PDF/CEPI_EN_643_Documentation.pdf

CEPI. (2023). Confederation of European Paper Industries. Key statistics 2023. *European Pulp & Paper Industry*. https://www.cepi.org/wp-content/uploads/2024/09/Key-Statistics-2023-FINAL-2.pdf

Chahal, A. S., & Ciolkosz, D. (2019). A review of wood-bark adhesion: Methods and mechanics of debarking for woody biomass. *Wood and Fiber Science, 51*, 288–299. https://doi.org/10.22382/wfs-2019-027

Churchill, J. G. B., Borugadda, V. B., & Dalai, A. K. (2024). A review on the production and application of tall oil with a focus on sustainable fuels. *Renewable and Sustainable Energy Reviews, 191*, 114098. https://doi.org/10.1016/j.rser.2023.114098

Clarck, J. (1895). *Pulp technology and treatment for paper*. M. Freeman Publications.

Colodette, J. L., & Borges Gomes, F. J. (Eds.). (2015). *Branqueamento de Polpa Celulósica. Da Produção da Polpa Marrom ao Produto Acabado*. Editora UFV.

Costa, E., & Cettolo, G. (2020). *Utilización de cargas minerales*. http://www.afcparg.org.ar/

Dence, C. W., & Reeve, D. W. (1996). *Pulp bleaching: Principles and practice* (1st ed.). TAPPI Press.

Doherty, B. & Rainey, T. (2006). Bagasse fractionation by the soda process. In Hogarth, D. (Ed.) *Proceedings of the Australian society of sugar cane technologists*, 2–5 May 2006, Australia, Queensland, Mackay. http://eprints.qut.edu.au/25678/

Dong, C., Pang, Z., Xue, J., Liu, Y., Chen, J., & Zhang, R. (2012). Effect of screw extrusion pretreatment on pulps from chemical pulping. *BioResources, 7*, 3862–3869.

Ehman, N., Felissia, F. E., Tarrés, Q., Vallejos, M. E., Delgado-Aguilar, M., Mutjé, P., & Area, M. C. (2020). Effect of nanofibers addition on the physical-mechanical properties of chemimechanical pulp handsheets for packaging. *Cellulose, 27*, 10811–10823. https://doi.org/10.1007/s10570-020-03207-5

Ehman, N., Vallejos, M. E., & Area, M. C. (2023). Top-down production of nanocellulose from environmentally friendly processes. In U. Shanker, C. M. Hussain, & M. Rani (Eds.), *Handbook of green and sustainable nanotechnology* (pp. 185–202). Springer. https://doi.org/10.1007/978-3-031-16101-8_46

Ekbåge, D. (2020). *Process modelling in pulp and paper manufacture. Application studies with aspects of energy efficiency and product quality*. PhD Thesis, Faculty of Health, Science and Technology. Karlstad University, Karlstad, Germane.

ERPA, & CEPI (2002). *European list of standard grades of recovered paper and board*. https://www.paperonweb.com/EN-643-154434A.pdf

Esteves, C. V. G., Brännvall, E., Östlund, S., & Sevastyanova, O. (2022). The effects of high alkali impregnation and oxygen delignification of softwood Kraft pulps on the yield and mechanical properties. *Nordic Pulp & Paper Research Journal, 37*, 223–231. https://doi.org/10.1515/npprj-2022-0022

Fleming, B., & Sloan, T. (1994) Low kappa cooking, TCF bleaching affect pulp yield, fiber strength. *Pulp & Paper*. http://www.risiinfo.com/db_area/archive/p_p_mag/1994/9412/94120111.htm

Francolini, I., Galantini, L., Rea, F., Di Cosimo, C., & Di Cosimo, P. (2023). Polymeric wet-strength agents in the paper industry: An overview of mechanisms and current challenges. *International Journal of Molecular Sciences, 24*, 9268. https://doi.org/10.3390/ijms24119268

Gharehkhani, S., Sadeghinezhad, E., Kazi, S. N., Yarmand, H., Badarudin, A., Safaei, M. R., & Zubir, M. N. M. (2015). Basic effects of pulp refining on fiber properties—A review. *Carbohydrate Polymers, 115*, 785–803. https://doi.org/10.1016/j.carbpol.2014.08.047

Ghosh, A. K. (2011). Fundamentals of paper drying—Theory and application from industrial perspective. In A. Ahsan (Ed.), *Evaporation, condensation and heat transfer*. https://doi.org/10.5772/21594

Ginebreda, A., Guillén, D., Barceló, D., & Darbra, R. M. (2011). Additives in the paper industry. In B. Bilitewski, R. M. Darbra, & D. Barceló (Eds.), *Global risk-based management of chemical additives* (pp. 11–34). Springer. https://doi.org/10.1007/698_2011_109

Guiao, K. S., Gupta, A., Tzoganakis, C., & Mekonnen, T. H. (2022). Reactive extrusion as a sustainable alternative for the processing and valorization of biomass components. *Journal of Cleaner Production, 355*, 131840. https://doi.org/10.1016/j.jclepro.2022.131840

Hannu Paulapuro, D. (Ed.). (1999). *Papermaking part 1, stock preparation and wet end* (2nd ed.). TAPPI Press.

Hubbe, M. A., & Gill, R. A. (2016). Fillers for papermaking: A review of their properties, usage practices, and their mechanistic role. *BioResources, 11*, 2886–2963.

Imlauer Vedoya, C. M., Area, M. C., Raffaeli, N., & Felissia, F. E. (2022). Study on soda–ethanol delignification of pine sawdust for a biorefinery. *Sustainability, 14*, 6660. https://doi.org/10.3390/su14116660

Jedvert, K., Saltberg, A., Theliander, H., Wang, Y., Henriksson, G., & Lindström, M. E. (2012). Mild steam explosion: A way to activate wood for enzymatic treatment, chemical pulping and biorefinery processes. *Nordic Pulp & Paper Research Journal, 27*, 828–835. https://doi.org/10.3183/npprj-2012-27-05-p828-835

Jenkis, S. (1995). The improvement of dry strength by synthetic polymers. In O. C. Au & I. Thorn (Eds.), *Applications of wet-end paper chemistry* (pp. 91–100). Springer-Sci.+Business Media.

Jones, T. G., Song, G. G., & Richardson, J. D. (2004). Effect of chipper setting on chip size distribution and mechanical pulp properties. *Appita Journal, 58*, 56–63.

Julien Saint Amand, F. (2001). Particle separation processes. In C. F. Baker (Ed.), *The Science of Papermaking, Trans. of the XIIth Fund. Res. Symp. Oxford* (pp. 81–191). FRC. https://doi.org/10.15376/frc.2001.1.81

Latha, A., Arivukarasi, M. C., Keerthana, C. M., Subashri, R., & Vishnu Priya, V. (2018). Paper and pulp industry manufacturing and treatment processes-a review. *International Journal of Engineering, 6*, 177–189.

Li, P. Y., Ramaswamy, S., & Bjegovic, P. (2003). Pre-emptive control of moisture content in paper manufacturing using surrogate measurements. *Transactions of the Institute of Measurement and Control, 25*, 36–56. https://doi.org/10.1191/0142331203tm070oa

Linhart, J. (1995). The practical application of wet strength resins. In C. O. Au & I. Thorn (Eds.), *Applications of wet-end paper chemistry* (pp. 102–118). Springer Science+ Business Media.

Lipiäinen, S., Kuparinen, K., Sermyagina, E., & Vakkilainen, E. (2022). Pulp and paper industry in energy transition: Towards energy-efficient and low carbon operation in Finland and Sweden. *Sustainable Production and Consumption, 29*, 421–431. https://doi.org/10.1016/j.spc.2021.10.029

Liu, Z., Wang, H., & Hui, L. (2018). Pulping and papermaking of non-wood fibers. In S. N. Kazi (Ed.), *Pulp and paper processing*. InTechOpen. https://doi.org/10.5772/intechopen.79017

Lois-Correa, J. A. (2012). Desmeduladores para una eficiente preparación de fibras de bagazo de caña en la industria de pulpa y papel. *Ingeniería. Investigación y Tecnología, 13*, 417–424.

Lumiainen, J. (2008). Refining of chemical pulp fibres. In H. Paulapuro (Ed.), *Papermaking part 1, stock preparation and wet end* (pp. 94–134). Finnish Paper Engineers' Association/Paperi ja Puu Oy, TAPPI Press.

Madhu, R., Periasamy, A. P., Schlee, P., Hérou, S., & Titirici, M.-M. (2023). Lignin: A sustainable precursor for nanostructured carbon materials for supercapacitors. *Carbon, 207*, 172–197. https://doi.org/10.1016/j.carbon.2023.03.001

Manohar Rao, P. J. (1986). Modern bagasse handling and storage practices. *Indian Pulp and Paper Technical Association Journal, 23*, 14–19.

Marton, J. (1996). Dry-strength additives. In J. C. Roberts (Ed.), *Paper chemistry* (pp. 83–97). Springer. https://doi.org/10.1007/978-94-011-0605-4_6

Métais, A., & Germer, E. (2018). Review of industrial ozone bleaching practices. *Paper360, 13*, 46–48.

Mongkhonsiri, G., Gani, R., Malakul, P., & Assabumrungrat, S. (2018). Integration of the biorefinery concept for the development of sustainable processes for pulp and paper industry. *Computers and Chemical Engineering, 119*, 70–84. https://doi.org/10.1016/j.compchemeng.2018.07.019

Naimi, L. J., Sokhansanj, S., Mani, S., Hoque, M., Bi, T., Womac, A. R., & Narayan, S. (2006). Cost and performance of woody biomass size reduction for energy production. In *Proceedings of 2006 CSBE/SCGAB, Edmonton, AB Canada, July 16–19, 2006*. American Society of Agricultural and Biological Engineers. https://doi.org/10.13031/2013.22065

Obradovic, D., & Mishra, L. N. (2020). Mechanical properties of recycled paper and cardboard. *The Journal of Engineering and Exact Sciences, 6*, 0429–0434. https://doi.org/10.18540/jcecvl6iss3pp0429-0434

Page, D. H. (1989). The beating of chemical pulps—The action and the effects. In C. F. Baker & V. Punton (Eds.), *Trans. of the IXth Fund. Res. Symp., Cambridge* (pp. 1–38). FRC. https://doi.org/10.15376/frc.1989.1.1

Pathak, P., & Sharma, C. (2023). Processes and problems of pulp and paper industry: An overview. *Physical Sciences Reviews, 8*, 299–325. https://doi.org/10.1515/psr-2019-0042

Poirier, N. A., Pikulik, I. I., & Gooding, R. (2001). Papermaking. In J. K. H. Buschow & R. W. Cahn (Eds.), *Encyclopedia of materials: Science and technology* (pp. 6739–6747). Elsevier. https://doi.org/10.1016/B0-08-043152-6/01193-1

Qin, T., Liu, L., Cao, H., Nie, S., Lu, B., Cheng, Z., Liu, H., & An, X. (2023). Creping technology and its factors for tissue paper production: A review. *European Journal of Wood and Wood Products, 81*, 1075–1091. https://doi.org/10.1007/s00107-023-01947-2

Quinde, A. (2020). Chip considerations. *Pulp & Paper Canada, 121*, 20–23.

Rainey, T. J., & Covey, G. (2016). Pulp and paper production from sugarcane bagasse. In S. G. Mundree (Ed.), *O'Hara, I.M* (pp. 259–280). Wiley. https://doi.org/10.1002/9781118719862.ch10

Rodriguez Castellano, W. (2024). *Extrusion pulping, a solution for non-wood fibers processing*. https://innofibre.ca/en/extrusion-pulping-a-solution-for-non-wood-fibers-processing/. Accessed 8 April, 2024.

Rodríguez, A., Jiménez, L., & Ferrer, J. L. (2007). Use of oxygen in the delignification and bleaching of pulps. *Appita Journal, 60*, 17–22.

Roncero, B., & Vidal, T. (2007). Optimization of ozone treatment in the TCF bleaching of paper pulps. *Afinidad, 64*, 420–428.

Roux, J.-C. (2001). Pulp treatment processes. In C. F. Baker (Ed.), *Trans. of the XIIth Fund. Res. Symp. Oxford* (pp. 19–80). FRC. https://doi.org/10.15376/frc.2001.1.19

Rowell, R. M., Pettersen, R., & Tshabalala, M. A. (2013). Chapter 3: Cell wall chemistry. In R. M. Rowell (Ed.), *Handbook of wood chemistry and wood composites* (pp. 33–72). CRC Press.

Rullifank, K.F., Roefinal, M.E., Kostanti, M., Sartika, L., Evelyn (2020) Pulp and paper industry: An overview on pulping technologies, factors, and challenges. IOP Conference Series: Materials Science and Engineering 845:012005. https://doi.org/10.1088/1757-899X/845/1/012005.

Sakai, K. (2010). Chapter 7: Chemistry of bark. In D. N. S. Hon & N. Shiraishi (Eds.), *Wood and cellulosic chemistry* (pp. 241–273). CRC Press Taylor & Francis Groups.

Saukkonen, E., Kautto, J., Rauvanto, I., & Backfolk, K. (2012). Characteristics of prehydrolysis-kraft pulp fibers from Scots pine. *Holzforschung, 66*, 801–808. https://doi.org/10.1515/hf-2011-0158

Scott, W. E. (1996). *Principles of wet end chemistry*. TAPPI Press.

Silakoski, L., & Korvenniemi, J. (2014). Fieltros TMO no tejidos e híbridos de Valmet: ahorro de energía y mejor vida útil total. *El Papel, 179*, 38–41.

Simino, H. D. (2020). Química del wet-end. NALCO water an ecolab company, in: Seminario AFCP La Química En La Industria Del Papel.

Sixta, H. (Ed.). (2006). *Handbook of pulp* (Vol. I). Wiley.

Smook, G. (2019a). Preparation of stock for papermaking. In *Handbook for pulp & paper technologists* (pp. 193–205). TAPPI Press.

Smook, G. (2019b). Non-fibrous additives to papermaking stock. In *Handbook for pulp & paper technologists* (pp. 223–232). TAPPI Press.

Sulzer. (2016). Minimizing pressure pulsations initiated by the Headbox feed pump. https://www.sulzer.com/en/-/media/files/products/pumps/axially-split-pumps/brochures/minimizingpressurepulsations_e00531.pdf

Tajik, M., Torshizi, H. J., Resalati, H., & Hamzeh, Y. (2018). Effects of cationic starch in the presence of cellulose nanofibrils on structural, optical and strength properties of paper from soda bagasse pulp. *Carbohydrate Polymers, 194*, 1–8. https://doi.org/10.1016/j.carbpol.2018.04.026

Tanase, M., Stenius, P., Johansson, L., Hill, J., & Sandberg, C. (2010). Mass balance of lipophilic extractives around impressafiner in mill and pilot scale. *Nordic Pulp & Paper Research Journal, 25*, 162–169. https://doi.org/10.3183/npprj-2010-25-02-p162-169

Tran, H., & Vakkilainen, E. (2016). *The kraft chemical recovery process*. TAPPI Press. https://www.tappi.org/content/events/08kros/manuscripts/1-1.pdf

Turulja, L., Vugec, D. S., & Bach, M. P. (2023). Big data and labour markets: A review of research topics. *Procedia Computer Science, 217*, 526–535. https://doi.org/10.1016/j.procs.2022.12.248

Uimonen, J. (2017). Energy savings in paper machine vacuum system—How to utilize modern vacuum and NIP dewatering technology. *Quarterly Journal of Indian Pulp and Paper Technical Association, 29*, 1–8.

Vallejos, M., Felissia, F., Area, M. C., Ehman, N., Tarrés, Q., & Mutjé, P. (2016). Nanofibrillated cellulose (CNF) from eucalyptus sawdust as a dry strength agent of unrefined eucalyptus handsheets. *Carbohydrate Polymers, 139*, 99–105. https://doi.org/10.1016/j.carbpol.2015.12.004

Wallmon, T. (2019). *The influences on the optical properties of paperboard due to dye additives*. Degree Project, KTH Royal Institute of Technology, Stockholm, Sweden.

Wang, S., Sun, X., You, F., Dai, H., Mao, S., & Wang, J. (2012). Application of cationic modified carboxymethyl starch as a retention and drainage aid in wet-end system. *BioResources, 7*, 3870–3882.

Zhang, L., Shao, G., Jin, Y., Yang, N., & Xu, X. (2024). Efficient delignification of wheat straw by induced electric field-assisted alkali pretreatment. *Industrial Crops and Products, 214*, 118564. https://doi.org/10.1016/j.indcrop.2024.118564

Chapter 6
Conventional Paper: Types and Properties

Nanci Ehman, María Evangelina Vallejos, and María Cristina Area

6.1 Paper Generalities

In the digital age, where technology dominates many interactions and processes, paper plays a key role. Even with the rise of technology, paper is a relevant medium in writing and printing and has become an essential material in the packaging industry.

Paper has historically been crucial for written communication and documentation. From the invention of the printing press to the digital age, paper has been used to record information, share knowledge, and preserve history. Textbooks, notebooks, and other printed materials are fundamental tools in teaching and learning. Although digital technologies have gained relevance, paper is still widely used in classrooms and libraries. Books, magazines, newspapers, and other printed materials are integral to culture, knowledge, and information dissemination. Paper is also versatile for artistic and creative expression, from painting and drawing to paper sculpture. For the packaging industry, the increase in online purchases and the search for more sustainable options by consumers has boosted the consumption of paper and cardboard, e.g., those intended for food packaging, with specific properties such as low liquids and grease proof.

Paper relevance is due to the intrinsic characteristics that make it an excellent material for numerous applications, such as high porosity, high surface area, good optical and mechanical properties, low or high liquid absorption as is or sizing, and biodegradability. These characteristics are developed during the production process, dependent on the application of paper or cardboard. For example, a long fiber will increase mechanical strength, while a short fiber will mainly influence the opacity and smoothness of the paper. As an example of a production process, parameters

N. Ehman (✉) · M. E. Vallejos · M. C. Area
PROCYP, IMAM (UNaM-CONICET), Posadas, Argentina

G. Korotcenkov (ed.), *The Handbook of Paper-Based Sensors and Devices*,
https://doi.org/10.1007/978-3-031-91080-7_6

such as the sizing stage will affect roughness, porosity, and water absorption. Zanuttini et al. (2008) previously defined some critical properties for paper and paperboards, such as high mechanical properties in kraft liners and bags, high softness in hygiene products, and good optical properties in printing and writing papers. These properties are based on their main parameters and require other specifications (Zanuttini et al., 2008).

It is essential to consider the type of paper produced to determine the desired parameters and, based on these parameters, identify which properties are relevant. For example, tissue paper needs softness, water absorption, and difficulty tearing during use. In this sense, volume, flexibility, and rigidity are three critical properties. Besides, paper porosity determines the absorption level (Morais & Curto, 2022).

6.2 Paper Properties

The functionality of paper is highly influenced by technical and physical properties that determine its characteristics. These properties impact not only the quality of the final product but also its durability, appearance, compatibility, and performance during application. Some of the key paper quality properties are shown in Fig. 6.1 and are classified into physical, mechanical, optical, and specific properties.

Most parameters can be modified during manufacturing to adapt the paper or paperboard to a specific application. For example, the grammage in paperboard can be increased through multi-ply systems; water absorption can be reduced with a coating; smoothness can be increased by calendering; and mechanical strength can be improved by adding dry strength additives.

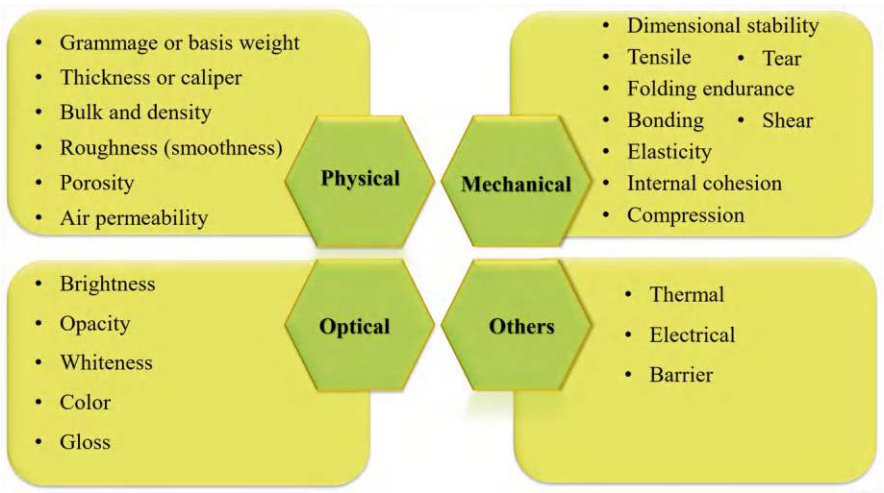

Fig. 6.1 Main properties in paper and paperboards

6.2.1 Physical Properties

6.2.1.1 Basis Weight or Grammage

The basis weight or grammage, generally expressed on an air-dry basis, determines the weight of a paper per unit area. The determination can be accomplished according to the TAPPI T410 standard (TAPPI, 2013). The standard also specifies the concept of ream as a specific area of paper or cardboard (usually expressed in numbers, such as 500 sheets) with a given dimension (Biermann, 1996).

Paper weights typically range from approximately 15 g/m^2 to over 200 g/m^2. Paper classification by basis weight is divided into four groups. The papers with the lowest weight are tissue. Values start at 14–18 g/m^2 for face tissue and handkerchiefs and reach 20–24 g/m^2 for kitchen towels (Tillmann, 2006). Most papers are included in the second group (grammage between 40 and 120 g/m^2): newsprints between 40 and 49 g/m^2, lightweight coated printing papers (LWC) between 35 and 80 g/m^2, and kraft sack paper (60–115 g/m^2) (Tillmann, 2006). Paperboard is the third group in the classification, and the grammage can reach around 200 g/m^2. Medium-to-high-weight products usually involve unbleached corrugated medium or bleached paperboards (Biermann, 1996). Finally, some boards, like liquid packaging boards, folding boards, or chipboards, can reach grammage values >200 g/m^2 (Paulapuro, 2000).

6.2.1.2 Caliper, Bulk, and Density

The caliper or thickness is the nominal distance between the two main surfaces of the paper/paperboard and is measured using a caliper or micrometer (Biermann, 1996). Both thickness and grammage are two primary physical properties of paper and are usually the most informed parameters during the paper/paperboard sale. In addition, they define the paper bulk.

The apparent density of paper or paperboard is defined as the mass per unit volume and is usually expressed in g/cm^3. The opposite is called bulk, determined by the ratio between grammage and thickness, expressed in cm^3/g. Bulk values are mainly influenced by fiber biometry, process fabrication, additives, refining, and actions in the drying section (Duarte Almeida Souza et al., 2011).

6.2.1.3 Roughness and Smoothness

At a microscopic level, paper is never perfectly smooth. A paper is considered smooth or rough based on its surface irregularities, being low or high, respectively. The roughness (smoothness) of papers and paperboards plays a crucial role in printing and determines the calendaring conditions and coating/ink consumption (Alam et al., 2012).

There are numerous methods to measure the paper or cardboard smoothness; the best known are the air base pass methods. The Bekk method is defined as the time required to draw atmospheric air between the surface of the test piece and a ring-shaped plane surface (Biermann, 1996). The Parker Print-Surf (PPS) method involves applying varying pressures and measuring the amount of air that passes between the paper and a measuring ring (Lagus, 2019) and is recommended for the low levels of roughness required (Zanuttini et al., 2008). Benstend method is also based on the air passage through a paper surface (Techlab Systems, 2023). A Benstend roughness value for LWC is around 20 mL/min, while a Kraft paper is around 700 mL/min (Tillmann, 2006). Some options to reduce paper roughness include sizing, coating, or calendering (Kasmani et al., 2013; Rautiainen, 2003; Stankovská et al., 2014; Vernhes et al., 2010). For example, during the printability of paperboards, the influence of surface roughness is higher when the paperboard is thinner (Rättö, 2005).

6.2.1.4 Air Permeability and Porosity

Porosity is the ratio between the void space and the total volume of the paper. The paper porosity influences compressibility and the ability of paper to absorb fluids like ink, oils, and water (Karlovits et al., 2018). Paper porosity can be indirectly evaluated by air permeability, but they are not the same. Porosity depends on the number of empty spaces, while air permeability depends on the interconnection of these pores. Therefore, air permeability refers to the ability of paper to be passed through by air.

One of the widely used techniques to measure air permeability in papers is the Gurley method, which measures the resistance of the structure of the paper to the passage of air (TAPPI, 2006a). It determines the time a given air volume takes to pass through a specific area under controlled pressure conditions. High time means high Gurley and, therefore, low permeability. On the contrary, low time implies high paper permeability. A standard volume of air is 100 ml. The factors that affect air permeability include paper composition, thickness, porosity, compression, and surface treatment (Hii et al., 2012; Mair, 2017; Park et al., 2016; Shallhorn & Gurnagul, 2009). Porosity has a high influence on the performance of some papers and paperboards. Papers with high porosity absorb water at a higher rate. This is useful in printing (ink absorption) and tissue applications. In printing papers, porosity significantly affects the absorption and distribution of inks (Dong et al., 2020).

In some cases, very high porosity leads to uneven prints. When seeking to maximize the barrier property of the paper, it is ideal to use a paper with very low porosity (Mazhari Mousavi et al., 2018). Less porous papers are usually denser and more resistant. In many cases, increased density is associated with better fiber bonds. Some papers, such as filter paper, require high porosity and permeability. However, if small solids are to be retained, the pore size must be small and in large quantities (Nong et al., 2019). One of the options to reduce the passage of fluids through a paper is through surface finishing, such as through the surface sizing process. Sizing

is used to enhance resistance properties and reduce the penetration of aqueous solutions to the finished product (Bung, 2004; Stankovská et al., 2014). This surface process is carried out in the size press section of the paper machine using a film size press, classic size press (horizontal, vertical, and angled), and spray size press (Hubbe, 2024). The surface wettability of the paper is determined by the contact angle method of a drop of fluid on the paper, Cobb, or Hercules tests (Biermann, 1996).

6.2.2 Optical Properties

A relevant aspect of the paper is how it is perceived visually. While paper can be produced using unbleached pulp, lignin is often removed from the fibers, or specific additives are included to create a brighter, more bleached paper, especially in those that will be printed. The interaction of paper with light has been extensively studied, leading to the establishment of standards for measuring various optical properties. These properties include opacity (R0), brightness (R∞), whiteness, color, and gloss. The optical characteristics of a paper refer to the pulp's ability to reflect, scatter, or absorb light. Once the light ray penetrates the first surface of the paper, it diffuses into the interior of the sheet until it is absorbed or emerges as diffuse reflectance or transmittance. ISO and TAPPI determinations involve standards to measure optical properties and Kubelka-Munk coefficients (Hubbe et al., 2008).

6.2.2.1 Brightness

Brightness measures the percentage reflectance of the pulp or paper about a standard when a beam of 457 nm wavelength is incident (blue region of the spectrum) (Dence & Reeve, 1996). The brightness values indicate a property related to the color of the pulp in a single number, which could be used to compare various types of pulps. Fully bleached sulfite pulps can have values as high as 94% ISO, whereas raw kraft pulps have as low as 15% ISO. Raw pulps have a wide range of brightness values, e.g., the sulfite pulps have up to 65% ISO, while kraft, soda, and semi-chemical pulps are darker. In mechanical pulps, the brightness is primarily a function of the species and condition of the wood (Bajpai, 2018).

6.2.2.2 Opacity

It is one of the fundamental properties of writing and printing papers. Opaque paper is difficult to see through and blocks visible light. It is measured as a contrast ratio at 557 nm. In paper manufacturing, mineral fillers with a high specific surface area and refractive index are often used to increase opacity (Alava & Niskanen, 2006). This also increases with the grammage and is strongly influenced by the paper reflectance since a paper can be opaque because it has a high specific surface area

or is dark and absorbs light (Farnood, 2009). Paper opacity is determined by paper weight and its absorption and diffusion coefficients. It increases with the increase of the three properties. As the absorption coefficient decreases with bleaching and the diffusion coefficient practically does not change, the bleached pulp will have a lower opacity than the raw pulp for the same grammage (Yu et al., 2006).

6.2.2.3 Color and Whiteness

Paper whiteness quantifies the reflected light in the full visible spectral range. Paper whiteness formulas are designed to closely parallel the experience of normal human vision and compare with paper brightness; this only quantifies a specific wavelength of reflected blue light (Sappi, 2017). The color of an object, including paper, is determined by the wavelengths of light it reflects. The CIELAB space is one of the mathematical models that quantify the color perceived by humans (SAPPI, 2013).

6.2.2.4 Specular Gloss

Specular paper gloss is defined as the perceived brightness associated with the luminous (specular) reflection of a surface. Specular gloss is related to the light reflection of objects that can be partly transparent or opaque (Weber, 2024). Gloss is related to shininess and depends on paper characteristics and illumination conditions (Farnood, 2009). Gloss finish paper has a highly smooth texture surface that provides a high degree of specular light reflectance (Biermann, 1996). Gloss is critical in magazines printing papers.

6.2.3 Mechanical Properties

The mechanical properties of paper and paperboard are critical during the conversion stages and its application.

6.2.3.1 Dimensional Stability and Curl

The ability of paper and paperboard to resist internal and external disturbance without changing their dimensions is called dimensional stability (Larsonn, 2008), for example, in the presence of water. Dimensional changes in paper originate from the swelling and contraction during the saturation of individual fibers. When uneven, they cause undesirable wrinkles and curvatures (Lindner, 2018). In some cases, methods have been chosen to improve the stability of the fibers by absorbing less water, thus avoiding fiber saturation: fiber esterification, mesh, coating, or sizing

(Caufield & Gunderson, 1988; Stankovská et al., 2014). One of the concepts related to dimensional stability is the coefficient of moisture expansion (CME), which indicates the change in the percentage of dimension per unit of percentage change in humidity (Nielsen & Priest, 1997). This term is related to the wet expansion of paper. More complete information can be obtained by moistening a manufactured paper, measuring its wet expansion, then freely drying it and measuring the total contraction. The difference between total contraction and wet expansion is called internal strains like curls or wrinkles. Paper curl is an out-of-plane deformation critical in paperboard converting or printing processes (Maass & Hirn, 2024; Muller, 2018).

6.2.3.2 Mechanical Properties of Papers

The correct performance of paper during its application must be guaranteed in all aspects. Some mechanical properties evaluated during paper manufacturing are tensile, tear, and burst strength, folding, rigidity, elasticity and compression, internal cohesion, and impact absorption.

Tensile strength is the ability of the paper to resist forces that try to stretch or tear it longitudinally (TAPPI, 2006b) and is critical in printing and packaging paper. Burst strength is the maximum pressure that cardboard or paper can withstand when a force perpendicular to its surface is applied through an inflated rubber diaphragm (TAPPI, 2015). It is important in some packaging solutions, e.g., paper bags for cement. Tear strength is the paper strength to the propagation of a tear. This property is critical in packaging papers where an accidental tear can compromise the contents. It has been previously shown that these properties are affected by several factors like humidity, grammage, furnish composition, fiber orientation, or refining (Levlin, 2013). For example, the refining depends on the fiber bonding capacity (Chen et al., 2016), and in some cases, additives such as microfibrillated cellulose have even been added to improve tensile, tear, and burst properties (Ehman et al., 2016, 2020; Tarrés et al., 2020; Vallejos et al., 2016). Folding resistance is the strength capacity of a paper to withstand folds without breaking on papers intended for notebooks or books. Stiffness is the ability of a paper to resist deformations and guarantees that the paper maintains its structure (Levlin, 2013). It assures content protection, while, in printing, it facilitates paper handling in machines. Elasticity is the capacity of a paper to deform and return to its original shape. It is relevant in printing and handling processes where the paper is continually tensioned. Internal bond is the force that holds the fibers together (TAPPI, 2000) and is critical in multilayer papers and printing and writing papers. There are two types of inner join tests. In both tests, the substrate is sandwiched between two metal plates. Double-sided tape is used to adhere each surface to its respective platen. First, the plates compress the medium to ensure a better adhesive bond. The plates are then separated perpendicular to the substrate surfaces to force the surfaces apart (Hutten, 2007).

6.2.3.3 Mechanical Properties of Paperboards

Tensile, elongation, burst, tear, and other properties are also evaluated, but some extra properties specifically characterize paperboard. Vertical compression resistance capacity is a critical property evaluated in paperboard or cardboard production (Kainulainen & Söderhjelm, 2013). In liner paper, the ring crush test (RCT) measures the ability to withstand a perpendicular force without crushing. Concora medium test (CMT), flat crush test (FCT), and column crush test (CCT) also measure the same properties but in the corrugating medium. A previous study on recycled fiber showed that a sheet formed with this type of fiber leads to lower compressive strengths than virgin fibers (Ghasemian et al., 2012). Eventually, the short-span compression test (SCT) replaces the RCT. However, it is necessary to understand that both have different failure modes. Besides, contaminants affect mainly RCT (Ju et al., 2005).

The stacking strength is critical in box storage stacking. It measures the ability of cardboard to support vertical weight over a long period without collapse (Malasri, 2022). Flexural strength is the ability of a cardboard to bend without breaking or deforming irreversibly (Carlsson & Fellers, 1980). Buckling strength measures lateral compression force resistance in packaging and transportation. Puncture strength measures the paperboard's strength to being punctured or pierced by sharp objects (Kainulainen & Söderhjelm, 2013).

6.2.4 Thermal Properties

When the paper needs to transport heat or reach certain temperatures, thermal properties are relevant. Generally, paper has a low conductivity due to its porous structure. Under standard temperature and pressure of 25 °C and 1 atm, paper and paperboard thermal conductivity is between 0.05 and 0.12 Wm/K (Čekon et al., 2017). Paperboard packaging represents a thermal barrier between the packaged product and the environment. A study showed that the thermal conductivity is much higher in the machine direction (Gray-Stuart et al., 2019). The thermal conductivity of a paper is also important to know the paper's behavior in the dry section and during calendering (Guérin et al., 2001).

6.2.5 Electrical Properties

The electrical properties of paper include its electrical resistivity, which determines its ability to resist the passage of current, and its dielectric constant, which measures its ability to store electrical charge (Sirviö et al., 2008). On the other hand, electrical stiffness measures its ability to withstand high voltages without breaking, while

dielectric losses indicate the amount of energy converted into heat. Electrical conductivity and capacitance are relative in printed electronics and capacitors (Jansson et al., 2022). Dielectric properties are affected by the moisture in the paper (Simula et al., 1998). Paper has been used as insulation in power transformers, evaluating the effect of humidity in the system and demonstrating that the increase in thermal conductivity caused by humidity became smaller as the temperature increased (Dombek et al., 2020).

6.3 Paper Classification

Papers and paperboards can be divided based on their application, basis weight (grammage), raw material, finishing, etc. Classification based on the volume production is divided into commodity and special papers (Tillmann, 2006). Commodity papers are intended for usual applications. Besides, as they have no added value, their prices fluctuate according to the market price. The large production volume of these commodities involves market risks (mainly a regulated market). The prices will be regulated by various factors such as supply, demand, prices of raw materials and services, and production capacity (CEPI, 2023).

On the contrary, specialty papers have a high added value but lower volume production. In specialty papers, the target consumer is more specific. Therefore, the industry is in a contractual risk market. Some examples of commodity papers and paperboards are tissue, newsprint, printing and writing paper, linerboard, or corrugated medium. Some examples of specialty papers or paperboards are wood pulp board, thermal paper, conductive paper, filter paper, and money paper. Papers and paperboards can also be grouped according to their grade (Smook, 1990), and they can differ in appearance, composition (fiber type, additives), papermaking production process, barrier or physical-mechanical properties, and end-use (Deshwal et al., 2019; Kirivanta, 2000; TAPPI, 2003).

6.3.1 Commodity Papers

Commodity papers and boards refer to types of paper and board used for general purposes without having specialized characteristics or properties (TAPPI, 2003; Zanuttini et al., 2008). They are standard products, widely available on the market, and used for everyday and generic applications that are often affordable and produced in large rolls or sheets for ease of use in large-scale printing processes (Table 6.1).

Table 6.1 Commodity papers classification

Grades			Critical properties	Applications
Writing and printing	Uncoated	Wood mechanical	Low roughness High dimensional stability High opacity High tensile strength, elongation, and TEA in machine direction High tear strength in machine and transverse directions	Newspapers
		Wood-free		Office papers, printing papers
	Coated	Wood mechanical	High tensile strength, elongation, and TEA in machine direction High tear strength Low roughness High dimensional stability High brightness, opacity, and whiteness	LWC, offset, magazine, letterpress
		Wood-free		Magazines, books
Tissue			Softness High water absorption High tensile strength in wet conditions Impurities-free Brightness	Sanitary products
Kraft paper	Bleached		Low water absorption High tensile strength, elongation, and TEA in machine direction High tear strength in the transverse direction High burst strength High porosity	Bags, sacks, wrapping paper
	Unbleached			

6.3.1.1 Printing and Writing Papers

The widespread availability of printing and writing paper makes it an essential component in everyday life, both professionally and personally, used in various applications. It has diverse applications in the business and administrative fields. Opacity is a fundamental characteristic of these papers, indicating their ability to prevent ink transfer from one side to the other. A higher level of opacity is particularly relevant for inhibiting the visibility of printed content on the reverse side of the sheet. Sometimes, it is combined with recycled fiber or reinforcement pulp (chemical fiber). Newsprint, employed in newspapers, is characterized by its lightweight and porous nature. It is lighter than other paper types, serving its primary purpose of cost-effective news dissemination. Since it is designed for swift ink absorption, it is ideal for large-scale printing, i.e., optimized for the economical and rapid production of extensive textual content.

In contrast to newsprint, magazine paper is typically a high-quality substrate featuring a smoother, glossier finish. Tailored to the specific demands of magazines, it prioritizes print quality, enhancing the visual appeal by highlighting images and graphics. While newsprint emphasizes printing efficiency, magazine paper prioritizes aesthetic quality.

Magazine paper (grammage, 45–130 g/m^2) undergoes a coating process with a mixture of materials to improve its quality. This coating enhances the paper's surface properties, such as smoothness, gloss, brightness, and printability. The coating also allows the inks to remain on the surface, resulting in sharper image prints. Coated paper is ideal for high-quality printing methods such as offset printing and digital printing. It is commonly used for producing high-quality printed materials where color fidelity and image reproduction are relevant.

Writing papers (grammage, 70–170 g/m^2) encompass a range of materials utilized for various written purposes, including books, notebooks, notepads, letterheads, and text document printing, besides copy paper. Their composition generally includes short fiber chemical pulp with a percentage of log fiber reinforcing pulp. These papers come in different grammages (weight of paper expressed as grams per square meter), available in standard formats and sizes, such as letter (8.5 × 11 inches in North America) or A4 (210 × 297 mm in the international system), as well as legal and others, facilitating compatibility with conventional printers and copiers. The surface texture can vary, offering smooth, textured, matte, and glossy finishes. While a whiter paper is preferred for high-quality printing, there is a growing preference for less bleached options due to ecological considerations.

6.3.1.2 Tissue Papers

Tissue is a light paper (grammage, 15–50 g/m^2) characterized by its softness and strength. It is generally produced from recycled pulp through a specialized process that includes drying through a large hot cylinder (Yankee dryer), generating thin, flexible sheets. Additional steps to produce tissue papers involve pleating, creping, or embossing (Vieira et al., 2022). Due to their soft and pleasant texture to the touch and high absorption capacity, tissue papers are ideal for products intended for direct contact with the skin, which is particularly important in personal hygiene applications. They come in different formats and sizes, from toilet paper rolls to paper towels and napkins. Also, they can be available in several varieties of layers (single, double, triple layer), which affects the strength and smoothness of the paper, which will depend on the final application. For example, more resistant and absorbent ones are sought for kitchen applications, while softness and absorbency in disposable tissues. However, a thicker and more resistant paper is required in tissue for public places.

Glossy tissue paper is exceptionally lightweight and has a delicate, elegant feel, making it ideal for various aesthetic applications. This paper is used in crafts, decoration, arts, and gift packaging. It is available in diverse colors, making it a popular choice for artistic, decorative, and packaging projects. It is sometimes used in

packaging as filler material in shipping to protect fragile items, for example, in products such as makeup and perfumes (see wrapping paper).

6.3.1.3 Kraft Papers

Kraft paper (grammage 50–134 g/m^2) (TAPPI, 2003) is the most used material in paper-based packaging and is produced by a sulfate treatment process. The material is available in unbleached, heavy-duty, or bleached white forms (Raheem, 2016) and is distinguished because of its strength and versatility. It is available in various weights, which allows applications ranging from light packaging (bags and sacks) to more robust materials (liner). In addition to its industrial uses, it is commonly used in handmade and artisanal items. Kraft paper is mainly employed in applications such wrapping, bags, and shipping sacks production, as well as in various converting processes including laminating, coating, etc., for containing flour and cement, or making gift bags or food packaging, among others. It is generally made from highly refined unbleached kraft and is handled in the paper machine to retain or reinforce the extensibility of the sheet.

Final actions could be performed in kraft papers to increase barrier or strength properties. Some examples are coating with resins to reduce the wetness of papers or mechanical creping actions during the drying process to improve the impact strength (Twede et al., 2015).

6.3.1.4 Wrapping Papers

Wrapping is a general classification of papers with sufficient strength and appropriate properties to wrap and protect almost any shape and size of contents. They are generally light, often decorated, and used for wrapping gifts, small packages, and light products. (Note that sometimes tissue paper is used for wrapping.).

6.3.1.5 Waxed Papers

Waxed papers undergo a conversion treatment with wax or waxy materials. The base papers are typically bleached kraft or sulfite, including tracing paper, greaseproof paper, and icing. Petroleum waxes, resins, and polymer additives are commonly used to improve the paper properties. Wax papers protect and preserve several foods and other products, like cosmetics, soap, and tobacco. Some types are sulfurized paper, barrier paper, and greaseproof paper.

6.3.1.6 Paperboards

Paperboard usually refers to a material with different characteristics compared to paper, like grammage, thickness and stiffness, structure, and end-use. Mostly, paperboard has a grammage higher than 150 g/m^2 and a thickness higher than 0.30 mm (Kirivanta, 2000). Its flexibility is lower compared to papers. Paperboard types include cartonboards and containerboards. Cartonboards are primarily used for food and pharmaceutical packaging, as well as cigarette boxes, while containerboards are mainly utilized for transporting product packaging.

Cartonboards are divided according to the type of raw material. These products require high thickness, stiffness, and Z-tensile strength, low roughness, and high brightness. The mentioned characteristics are achieved through a multilayer system, the composition of which will vary according to the final use. Figure 6.2 summarizes the cartonboard qualities. A solid unbleached or bleached board (SUS, SBS) is made of 100% chemical pulp, either bleached or unbleached. SB applications include high-quality gift boxes, labels, and luxury product containers.

Folding boxboard (FBB) combines layers of chemical, thermomechanical (TMP), or chemithermomechanical (CTMP) pulps. FBB is primarily used for food and pharmaceutical packaging, cigarette boxes, and graphics. Chemical fibers provide the strength standards that the market requires. FBBs are cheaper than SB and have a lower weight per unit area, allowing transport costs to decrease.

White-lined chipboard (WLC) involves layers of recycled pulps. Usually, the internal layer is composed of recycled fibers (around 80–100%) and an external top layer of chemical or semi-chemical bleached pulp with white pigment. An example is the pizza boxes, where a layer (back layer) could be recycled pulp and another layer of bleached chemical fiber (top layer). WLC is used, among others, in dry

Type	Description
SBS (SBB, GZ)	(1) White pigment, bleached chemical pulp (2) Bleached chemical pulp (3) Bleached chemical pulp (4) Top 2-3 coating layers, optional back ply
SUS	(1,2,3) Unbleached chemical pulp (4) Top 2-3 coating layers, optional back ply
FBB GC1	(1) Bleached chemical pulp (2) Mechanical pulp, TMP, or CTMP (3) Thicker chemical pulp and/or white pigment coated. The appearance of both sides is white (4) White pigment coated.
FBB GC2	(1) Bleached chemical pulp (2) Mechanical pulp, TMP (3) Mechanical pulp (4) White pigment coating
WLC GD	(1) Bleached chemical pulp (2,3) Recycled fiber (4) White pigment coating
WLC GT	1) Bleached chemical pulp (2) Recycled fiber (3, 4) White pigment

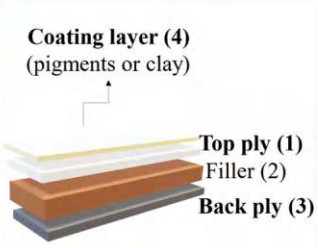

SBS: Solid bleached board
SUS: Solid unbleached board
FBB: Folding boxboard
FBB.GC1: White back folding boxboard
WLC: White-lined chipboard

Fig. 6.2 Cartonboards classification

foods, frozen and chilled foods, detergent powders, household goods, and engineering products.

A liquid packaging board (LP) is a multi-ply system that includes cellulose fiber, plastics, and aluminum. The addition of these materials leads to packaging properties suitable for its final application. Some examples include moisture strength, water, greaseproof, steam, oxygen, UV light barrier, and ability to retain acidic, alcohol, and alkaline substances (Ahuja et al., 2024). LP applications include milk, juices, and some carbonated drinks. Besides the ability to retain liquids, the requirements of LP to contain these foods are good runnability, cleanliness, and free of impurities (Kirivanta, 2000).

Corrugated container boards consist of two layers of liner (kraft liner of virgin fiber or test liner of secondary fiber) and the medium, or flute, used to strengthen or reinforce the cardboard. The linerboard layer is a lightweight paperboard used as liners or faces of corrugated boxes and for wrapping applications. Table 6.2 indicates some liner market varieties (CEPI, 2022). It is generally constructed of two layers, typically high-yield unbleached kraft pulp on a fourdrinier machine with a

Table 6.2 Linerboard varieties

Liners		Composition	Critical properties
Kraftliner	Brown	Unbleached kraft pulp	CD: Burst strength, SCT MD: SCT and tensile stiffness Sizing is required
	White uncoated	Bleached kraft pulp	Brightness ISO. Good optical properties are required in the white top CD and DM: Burst strength, SCT, and tensile stiffness Roughness Sizing is required
	White coated	Bleached kraft pulp with coating color pigments	CD and DM: Burst strength, SCT, and tensile stiffness Sizing is required Good brightness, roughness, and gloss
Testliner	Brown	Recycled unbleached fiber	CD: Burst strength, SCT MD: SCT and tensile stiffness Testliner grade (1–4), higher burst, and SCT values are considered superior-quality testliner
	Brown high-performance	Recycled unbleached fiber	CD: Burst strength, SCT MD: SCT and tensile stiffness Can be sized
	Top	Recycled with virgin fiber on top	Grades A, B, or C (brightness, roughness, burst, SCT-CD) Grades A and B must be sized
	Mottled	Recycled with bleached fiber on top	Brightness ISO. Good optical properties are required in the white top CD and DM: Burst strength, SCT, and tensile stiffness

CD Cross direction, *MD* machine direction

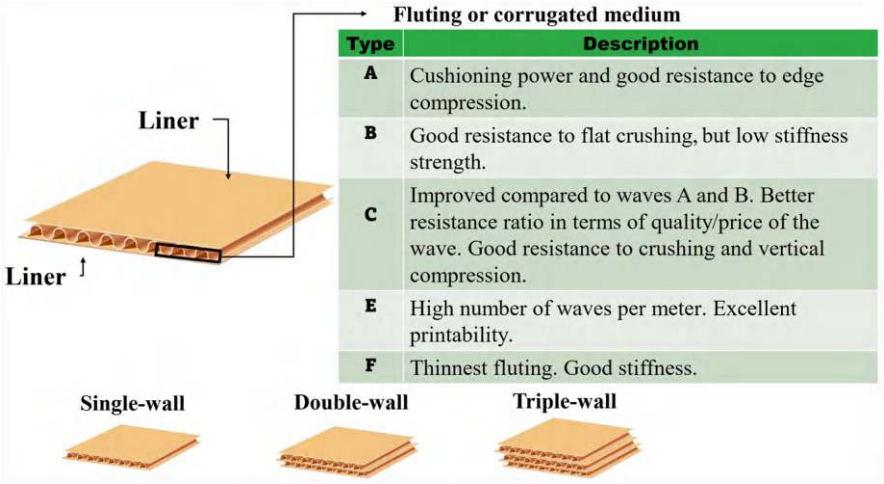

Type	Description
A	Cushioning power and good resistance to edge compression.
B	Good resistance to flat crushing, but low stiffness strength.
C	Improved compared to waves A and B. Better resistance ratio in terms of quality/price of the wave. Good resistance to crushing and vertical compression.
E	High number of waves per meter. Excellent printability.
F	Thinnest fluting. Good stiffness.

Fig. 6.3 Wave types and containerboard formation

secondary machine head. The thin topcoat is of relatively better quality for appearance and printability. Critical characteristics for liners include water absorption at a limited level, high tensile strength, elongation and TEA in the machine direction, high tensile strength in Z, and porosity in the acted interval (Zanuttini et al., 2008).

Corrugated medium or fluting is the internal layer in the containerboard. The fluting board is a pseudo-sinusoidal wave divided into different varieties (Fig. 6.3). Critical properties of this filler include high tensile strength, elongation, and TEA in the machine direction, high tensile strength in Z, porosity in a narrow range, high compression (CMT) in the machine direction, and high short-span compression (SCT) in the transverse direction (Zanuttini et al., 2008). Also, in both liner and medium corrugated boards, porosity plays a fundamental role during the formation of the containerboard. Adequate porosity, in combination with optimal application, will lead to good penetration of the borax-starch solution and good adhesion of the liner and medium corrugated layers (De la Mora García, 2019). Fluting paperboards can be produced using semi-chemical or recycled pulps (CEPI, 2022).

The containerboards can be made in a single wave, double wave (with three layers of paper and two layers of flute in the middle), or triple flute for progressively heavier contents (Astals, 1985).

6.3.2 Specialty Papers

Specialty papers are designed and manufactured for specific, often niche, applications beyond typical writing or printing purposes.

The characteristics of specialty papers vary widely based on the intended application, including weight, coatings, and other unique features necessary for their

designated use. They involve a variety of papers, among others, security papers (for printing secure documents), decorative papers (for producing decorative laminates and furniture surfacing), and release papers (which prevent the adhesive from sticking in adhesive tape manufacturing). Some more usual types are described below.

6.3.2.1 Filter Paper

Filter paper is a specialized type of paper designed for use in filtration techniques. Some of the types of filter papers are cellulose, bleached wood pulp, unbleached wood pulp, rag fiber, non-woven synthetics, alpha-cellulose, cellulose-rayon fiber, carbon impregnated, diatomaceous earth impregnated and are available in a variety of grammage, thicknesses, and micron retentions (Sentmanat, 2017). Filter papers are available in different grades and pore sizes, allowing the appropriate type to be selected based on the size of the particles that need to be retained (Table 6.3). Based on their determinations, filter papers can be classified as qualitative or quantitative (Hawach Scientific, 2019). Qualitative filters are divided into 13 different grades. The most used grades are grade 1 to grade 4: grade 1 (pore size 11 μm) and grade

Table 6.3 Whatman filter paper grades

Filter paper grade	Properties
Grade 1	Particle retention[a]: 11 μm; nominal thickness: 180 μm; nominal basis weight: 87 g/m^2; nominal ash content[2]: 0.06%
Grade 2	Particle retention: 8 μm; nominal thickness: 190 μm; nominal basis weight: 97 g/m^2; nominal ash content: 0.06%
Grade 3	Particle retention: 6 μm; nominal thickness: 390 μm; nominal basis weight: 185 g/m^2; nominal ash content: 0.06%
Grade 4	Particle retention: 25 μm; nominal thickness: 210 μm; nominal basis weight: 92 g/m^2; nominal ash content: 0.06%
Grade 5	Particle retention: 2.5 μm; nominal thickness: 200 μm; nominal basis weight: 100 g/m^2; nominal ash content: 0.06%
Grade 6	Particle retention: 3 μm; nominal thickness: 180 μm; nominal basis weight: 100 g/m^2; nominal ash content: 0.06%
Grade 591	Particle retention: 12 μm; typical thickness: 180 μm; basis weight: 161 g/m^2; nominal ash content: 0.06%
Grade 595	Particle retention: 7 μm; typical thickness: 180 μm; basis weight: 68 g/m^2; alpha cellulose: 98% minimum
Grade 597	Particle retention: 4–7 μm; typical thickness: 180 μm; basis weight: 85 g/m^2; alpha cellulose: 98% minimum
Grade 597L	Particle retention: 7 μm; typical thickness: 180 μm; basis weight: 82 g/m^2
Grade 598	Particle retention: 8–10 μm; typical thickness: 320 μm; basis weight: 140 g/m^2
Grade 602h	Particle retention: <2 μm; typical thickness: 160 μm; basis weight: 84 g/m^2

[a]At 98% efficiency; [2]determined by ignition at 900 °C
Source: Data extracted from https://www.cytivalifesciences.com/en

602 h (pore size of 2 μm). Quantitative filters (ash-free, high-purity papers) are applied to quantitative and gravimetric analyses.

Its uses include domestic (water, coffee) and industrial applications, such as the filtration of liquid samples in chemical analysis and air filtration in the air conditioning, involving the food, pharmaceutical, and automotive industries, among others. Studies on adding phenol-formaldehyde and carbon nanotubes to papers intended for filters have made it possible to obtain systems that allow nanoparticles to be eliminated. This leads to broader solutions to remove nanometer-sized particles and even polluting gases (Sun et al., 2021). Another study added nanoparticles (silica nanoparticles and polystyrene) to create superhydrophobic and superoleophilic filters. This would allow the removal of oil-based contaminants from the water (Wang et al., 2010). In medical applications, some examples of filter paper used are for diagnosing and (or) surveillance of infectious diseases for nucleic acid amplification tests and serological assays through dried blood spot assays (Smit et al., 2014).

6.3.2.2 Analytical Detection Paper

Analytical detection paper is designed for specific laboratory applications. Examples include pH indicators, humidity detection sensors, chromatography papers, qualitative and quantitative detectors, and specialized substance detection papers. Paper sensors for food packaging are one of the potential applications (Ehman et al., 2023). Food sensors based on carbon electrodes by aerosol jet printing have been used on chromatography papers for detecting the degradation of amino acids in protein-rich food like fish (Musaev et al., 2024). Paper sensors based on colorimetric changes have been also applied in the study of chicken meat monitoring to detect biogenic amines, demonstrating its potential applicability as smart packaging (Calabretta et al., 2023). Park et al. (2016) evaluated the behavior of porosity and permeability, two important factors in pressed sheets' fluid flow rate. This relates specifically to the applicability of the paper for microfluidic paper-based analytical devices (PAD) in biological sampling. The selection of paper substrate and the combination with different nanomaterials play a fundamental role in paper sensor development, significantly influencing their performance, sensitivity, and overall reliability. Among the options, you can identify those based on paper such as filter paper, nitrocellulose paper, chitosan-coated cellulose paper, graphene oxide-infused cellulose paper, and gold or silver nanoparticle deposited cellulose paper (Malik et al., 2024).

6.3.2.3 Electrical Paper

In the electronic industry and the manufacturing of electrical equipment, paper-based materials have been utilized for their electrical and dielectric insulating properties, and for their conductive capabilities in specialized applications. El Omari

et al. (2016) evaluated chemical retention methods and the effect of paper fines when fibers from annual and commercial plants were combined with two ferroelectric ceramics ($BaTiO_3$ and $SrTiO_3$). The addition of $SrTiO_3$ demonstrated an increase in the dielectric constant and better dispersion of particles (El Omari et al., 2016). Other studies involved the effect of the coating, finding that the dielectric constant of coated paper was higher than that of copy paper due to the higher filler content and greater density of the coated paper (Simula et al., 1998). Another application is image transfer in electrophotographic devices, where the dielectric constant and electrical conductivity are affected by the temperature, grammage of papers, and the addition of NaCl (Maldzius et al., 2010). An additional study also demonstrated the influence of carbohydrates derived from hemicelluloses on the dielectric constant, showing that it increases as the hemicelluloses content decreases (Saukkonen et al., 2015).

6.3.2.4 Photographic Paper

Photographic paper is a specialized type designed for printing photographs, allowing the reproduction of images with high quality and clarity. It has a layer of photosensitive emulsion on its surface that absorbs photosensitive inks or chemicals during printing. The photosensitive emulsion layer and other technologies allow the ink or chemicals to dry quickly, reducing the risk of smudging and ensuring a sharp print. It is often designed to resist fading and fading over time, ensuring that images maintain their quality for long periods. It can be available in various finishes, such as matte, glossy, satin, or luster, each with aesthetic and tactile characteristics. Photo paper weight can vary but tends to be heavier than standard printing and writing paper.

6.3.2.5 Vegetable Parchment Paper

Vegetable parchment paper is like parchment but made from vegetable cellulose instead of animal skin. It is manufactured with highly refined chemical pulp to develop its relevant properties: waterproof, fat-resistant, high strength, and transparency. Due to its transparency and resistance, vegetable parchment paper is also used in plans and artistic and craft activities. Unlike some conventional papers, vegetable parchment paper has higher heat resistance, so it is commonly used in baking applications, such as food wrapping or tray liners, as it can withstand high temperatures without burning or transferring flavors to the food. In some cases, its uses include packaging or wrapping.

6.3.2.6 Watercolor Paper

Watercolor paper is a specialized type of paper designed for artistic applications. It is usually white or cream and is manufactured to be durable and resistant to aging. It is available in different formats and weights. One of the most important characteristics of watercolor paper is its ability to absorb and retain water, allowing the watercolor paint to control mix and flow, providing greater control over the intensity of colors and creating wash effects. It is usually sized on one or both sides, which prevents the paint from absorbing too deeply into the fibers of the paper and makes it easier to correct or remove paint. Besides, it minimizes sagging when water is applied, helping to keep the surface flat during the painting process. Although watercolor paper absorbs water, it also allows paint to dry relatively quickly, allowing it to work in layers.

6.3.2.7 Thermal Paper

Thermal paper has a coating of heat-sensitive chemicals. Then, when a thermal printer applies heat in specific patterns, it produces a chemical reaction that generates the image or text on the paper. Uses involve devices such as receipt printers, credit card machines, cash registers, and other thermal printing equipment known for the quick printing speed of receipts and transaction vouchers, as they offer a fast and efficient way to produce documents in commercial environments. However, thermal paper has a limited lifespan of print retention, and the thermal image may fade over time due to exposure to light, heat, or time.

6.3.2.8 Carbonless Copy Paper

Carbonless copy paper is used to create copies of documents without the need for a copy machine or printer. It consists of several layers containing reactive chemicals, usually three or more, arranged in a set to allow the transfer of information from one sheet to another. The transfer occurs when pressing on to the top sheet. The pressure breaks the ink microcapsules in the bottom layer, releasing the ink and allowing it to transfer to the next sheet. This paper can transfer written or printed information from one sheet to another without using ink or traditional printing technology. It is available in diverse formats and sizes, making them easy to use in documents and applications. Carbonless paper applications are printing forms, invoices, and business documents. Although carbonless paper has been widely used, its popularity has declined due to the rise of digital technology and printers.

6.3.2.9 Paper Money

Paper money is printed paper designed to prevent counterfeiting and ensure authenticity. It is usually made from a blend of cotton and linen or other textile fibers, making them durable and resistant to wear and tear. Paper money often has built-in security issues making it difficult to replicate, like watermarks (images incorporated into the manufacturing process, visible only when holding the bill up to the light), threads with metalized or magnetic properties, special inks that change color or have specific optical properties when viewed from different angles; some embossed design elements, such as numbers and portraits, provide a palpable texture. Some paper money also are designed with holographic features to enhance to enhance the anti-counterfeiting: elements that change appareance when tilted, or fluorescent elements, which are visible only under ultraviolet light.

6.3.2.10 Self-Adhesive Paper

The self-adhesive paper has an adhesive layer on one side, typically covered by a release film or paper that must be removed before application. This type of paper allows for easy adhesion to surfaces without the need for additional glue. Common uses for self-adhesive paper include creating product labels, shipping addresses, file identification, and sealing packages.

6.4 Future Perspectives

The need to increase paper sustainability and the constant challenge of achieving better-performing papers and reducing plastic consumption, especially in the packaging industry, could lead to beneficial changes in paper products. The industry faces a challenge in trying to differentiate between breakthroughs and innovation. Process improvements, increases in paper quality, or increases in paper sustainability are often confused with short-term innovations, but they are just necessary breakthroughs. Despite this, it is possible to mention some paper and paperboard products with potential for short-term or long-term innovation (Fig. 6.4).

Papers and paperboards with coating systems (biobased, biodegradable, grease-proof based on biopolymers or natural resins, liquid barrier, antimicrobial) could replace current coatings based on synthetic polymers. In this sense, it would result in modifications of the existing equipment in the papermaking machine line, which could lead to short-term implementations. Size-press or laminating systems are potential candidates. However, other more advanced products, such as printed electronics, may require investment in the industry due to the need to install new equipment.

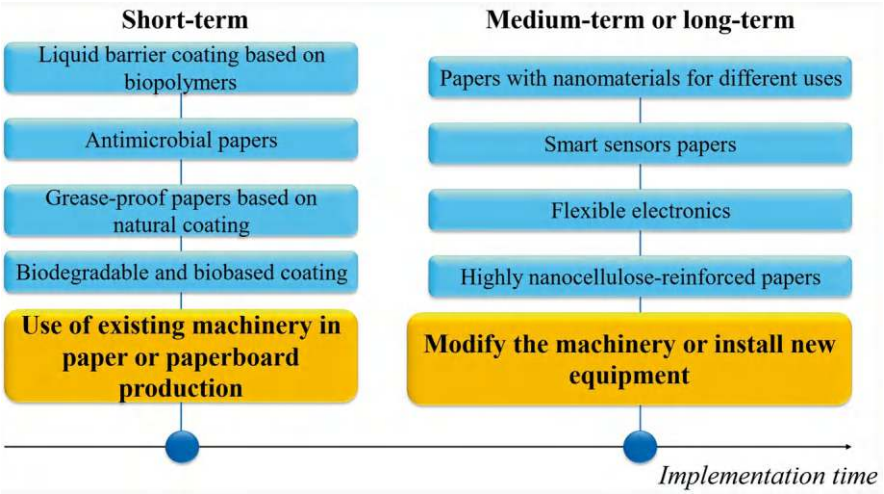

Fig. 6.4 Innovations in paper and paperboard production

6.5 Summary

Paper properties play a key role in its application. Paper properties play a key role in the final application, therefore it is necessary that they are optimized. Paper has numerous applications from those marketed as commodities such as printing and writing papers, tissue, and packaging, as well as special papers such as those used as filters, in sensors, etc.

The physical properties of papers and paperboards are an initial indicator of their applicability, while the mechanical properties demonstrate the strength to external forces. Also, the paper or paperboard perception is influenced by its optical characteristics, which will depend on raw material parameters, process, or incorporated additives. There are other more specific properties like barrier, thermal, or electrical properties, which are relevant for specific applications.

The properties mentioned are suitable for current applications, but they also give the paper the potential for the creation of sustainable products associated with a circular economy. However, to achieve more sustainable and functional products, development and innovation in the industry are still required.

References

Ahuja, A., Samyn, P., & Rastogi, V. K. (2024). Paper bottles: Potential to replace conventional packaging for liquid products. *Biomass Conversion and Biorefinery, 14*, 13779–13805. https://doi.org/10.1007/s13399-022-03642-3

Alam, A., Manuilskiy, A., Thim, J., O'Nils, M., Lindgren, J., & Lidén, J. (2012). Online surface roughness characterization of paper and paperboard using a line of light triangulation

technique. *Nordic Pulp & Paper Research Journal, 27*, 662–670. https://doi.org/10.3183/NPPRJ-2012-27-02-p662-670

Alava, M., & Niskanen, K. (2006). The physics of paper. *Reports on Progress in Physics, 69*, 669–723. https://doi.org/10.1088/0034-4885/69/3/R03

Astals, F., & Colom, J. F. (1985). Caracteristicas y propiedades del cartón ondulado. *Manutención y Almacenaje, 197*, 1–5.

Bajpai, P. (2018). Pulping fundamentals. In P. Bajpai (Ed.), *Biermann's handbook of pulp and paper* (pp. 295–351). Elsevier.

Biermann, C. J. (1996). Paper and its properties. In C. J. Biermann (Ed.), *Handbook of pulping and papermaking* (pp. 158–189). Academic Press.

Bung, J. (2004). Surface sizing agents. *IPPTA, 16*, 29–43.

Calabretta, M. M., Gregucci, D., Desiderio, R., & Michelini, E. (2023). Colorimetric paper sensor for food spoilage based on biogenic amine monitoring. *Biosensors (Basel), 13*, 126. https://doi.org/10.3390/bios13010126

Carlsson, L. A., & Fellers, C. N. (1980). Flexural stiffness of multi-ply paperboard. *Fibre Science and Technology, 13*, 213–223. https://doi.org/10.1016/0015-0568(80)90005-6

Caufield, D., & Gunderson, D. (1988). Paper testing and strength characteristics. In *TAPPI proceedings of the 1988 paper preservation symposium. October 19–21, Wahsington, DC* (pp. 31–40). TAPPI Press.

Čekon, M., Struhala, K., & Slávik, R. (2017). Cardboard-based packaging materials as renewable thermal insulation of buildings: Thermal and life-cycle performance. *Journal of Renewable Materials, 5*, 84–93. https://doi.org/10.7569/JRM.2017.634135

CEPI. (2022). *European list of corrugated base papers. CEPI Containerboard list of grades*. https://www.cepi-containerboard.org/

CEPI. (2023). Preliminary statistics 2023. *European Pulp & Paper Industry*. https://www.paperindustryworld.com/cepis-preliminary-statistics-2023/

Chen T, Xie Y, Wei Q, et al. (2016) Effect of refining on physical properties and paper strength of pinus massoniana and China fir cellulose fibers. BioResources 11:7839–7848. https://doi.org/10.15376/biores.11.3.7839-7848.

De la Mora García, D. Y. (2019). *Estudio del anclaje de los adhesivos en los papeles que componen el cartón corrugado*. PhD Thesis, Universidad de Guadalajara, Mexico.

Dence, C. W., & Reeve, D. W. (1996). *Pulp bleaching: Principles and practice* (1st ed.). TAPPI Press.

Deshwal, G. K., Panjagari, N. R., & Alam, T. (2019). An overview of paper and paper based food packaging materials: Health safety and environmental concerns. *Journal of Food Science and Technology, 56*, 4391–4403. https://doi.org/10.1007/s13197-019-03950-z

Dombek, G., Nadolny, Z., Przybylek, P., Lopatkiewicz, R., Marcinkowska, A., Druzynski, L., Boczar, T., & Tomczewski, A. (2020). Effect of moisture on the thermal conductivity of cellulose and aramid paper impregnated with various dielectric liquids. *Energies (Basel), 13*, 4433. https://doi.org/10.3390/en13174433

Dong, Y., Wang, B., Ji, H., Zhu, W., Long, Z., & Dong, C. (2020). Effect of papermaking conditions on the ink absorption and overprint accuracy of paper. *BioResources, 15*, 1397–1406. https://doi.org/10.15376/biores.15.1.1397-1406

Duarte Almeida Souza, G., Abreu, C., Amaral, J. L., & Brás, C. (2011). Office paper bulk optimization in a paper machine using multivariate techniques. *O Papel, 72*, 50–55.

Ehman, N., Imlauer, C., Felissia, F., & Area, M. C. (2016). Nanofibrillated cellulose from soda/ethanol-oxygen pulp of pine sawdust by oxidant treatments and mechanical fibrillation. In *Proceedings of workshop on insights and strategies towards a bio-based economy, November 22–25, Montevideo, Uruguay* (p. 1).

Ehman, N., Felissia, F. E., Tarrés, Q., Vallejos, M. E., Delgado-Aguilar, M., Mutjé, P., & Area, M. C. (2020). Effect of nanofibers addition on the physical-mechanical properties of chemimechanical pulp handsheets for packaging. *Cellulose, 27*, 10811–10823. https://doi.org/10.1007/s10570-020-03207-5

Ehman, N., Ponce de León, A., & Area, M. C. (2023). Fractionation stream components of wood-based biorefinery: New agents in active or intelligent primary food packaging? *BioResources, 18*, 6724–6726. https://doi.org/10.15376/biores.18.4.6724-6726

El Omari, H., Zyane, A., Belfkira, A., Taourirte, M., & Brouillette, F. (2016). Dielectric properties of paper made from pulps loaded with ferroelectric particles. *Journal of Nanomaterials, 2016*, 3982572. https://doi.org/10.1155/2016/3982572

Farnood, R. (2009). Optical properties of paper: Theory and practice. In S. J. I'Anson (Ed.), *Advances in pulp and paper research: Trans. of the XIVth Fund. Res. Symp. Oxford* (pp. 273–352). FRC. https://doi.org/10.15376/frc.2009.1.273

Ghasemian, A., Ghaffari, M., & Ashori, A. (2012). Strength-enhancing effect of cationic starch on mixed recycled and virgin pulps. *Carbohydrate Polymers, 87*, 1269–1274. https://doi.org/10.1016/j.carbpol.2011.09.010

Gray-Stuart, E. M., Bronlund, J. E., Navaranjan, N., & Redding, G. P. (2019). Measurement of thermal conductivity of paper and corrugated fibreboard with prediction of thermal performance for design applications. *Cellulose, 26*, 5695–5705. https://doi.org/10.1007/s10570-019-02462-5

Guérin, D., Morin, V., Chaussy, D., & Auriault, J.-L. (2001). Thermal conductivity of handsheets, papers and model coating layers. In C. F. Baker (Ed.), *The science of papermaking: Trans. of the XIIth Fund. Res. Symp. Oxford* (pp. 927–945). FRC. https://doi.org/10.15376/frc.2001.2.927

Hawach Scientific. (2019). *Comparison of quantitative and qualitative filter paper*. https://www.hawach.com/news/comparison-of-quantitative-filter-paper-and-qualitative-filter-paper.html

Hii, C., Gregersen, Ø. W., Chinga-Carrasco, G., & Eriksen, Ø. (2012). The effect of MFC on the pressability and paper properties of TMP and GCC based sheets. *Nordic Pulp & Paper Research Journal, 27*, 388–396. https://doi.org/10.3183/npprj-2012-27-02-p388-396

Hubbe, M. A. (2024). Size press practices and formulations affecting paper properties and process efficiency: A review. *BioResources, 19*, 1925–2002. https://doi.org/10.15376/biores.19.1.Hubbe

Hubbe, M. A., Pawlak, J. J. J., & Koukoulas, A. A. (2008). Paper's appearance: A review. *BioResources, 3*, 627–665. https://doi.org/10.15376/biores.3.2.627-665

Hutten, I. M. (2007). Testing of nonwoven filter media. In I. M. Hutten (Ed.), *Handbook of Nonwoven filter media* (pp. 245–290). Elsevier.

Jansson, E., Lyytikäinen, J., Tanninen, P., Eiroma, K., Leminen, V., Immonen, K., & Hakola, L. (2022). Suitability of paper-based substrates for printed electronics. *Materials, 15*, 957. https://doi.org/10.3390/ma15030957

Ju, S. M., Gurnagul, N., & Shallhorn, P. (2005). A comparison of the effects of papermaking variables on ring crush strength and short-span compressive strength of paperboard. In *Proceedings of PAPTAC 91st annual meeting* (pp. B153–B166).

Kainulainen, M., & Söderhjelm, L. (2013). End-use properties of packaging papers and boards. In J.-E. Levlin & L. Söderhjelm (Eds.), *Papermaking science and technology: pulp and paper testing*. Finnish Paper Engineers' Association and TAPPI.

Karlovits, I., Lavrič, G., & Nemeš, T. (2018). The influence of micro and macro porosity of paper on wet repellence mottling in offset printing. *Journal of Graphic Engineering and Design, 9*, 21–26. https://doi.org/10.24867/JGED-2018-2-021

Kasmani, J. E., Mahdavi, S., Alizadeh, A., Nemati, M., & Samariha, A. (2013). Physical properties and printability characteristics of mechanical printing paper with LWC. *BioResources, 8*, 3646–3656.

Kirivanta, A. (2000). Paperboard grades. In J. Gullichsen & H. Paulapuro (Eds.), *Papermaking science and technology* (Vol. 18, pp. 55–72). Fapet Oy.

Lagus, M. (2019). *Hydrophobic surface sizing of testliner*. MS Thesis, Faculty of Science and Engineering, Åbo Akademi University, Finland.

Larsonn, P. (2008). *Dimensional stability of paper: Influence of fibre-fibre joints and fibre wall oxidation*. Licenciate Thesis, Royal Institute of Technology, Sweden.

Levlin, J.-E. (2013). General physical properties of paper and board. In J.-E. Levlin & L. Söderhjelm (Eds.), *Papermaking science and technology. Pulp and paper testing* (pp. 138–160). Finnish Paper Engineers' Association and TAPPI.

Lindner, M. (2018). Factors affecting the hygroexpansion of paper. *Journal of Materials Science, 53*, 1–26. https://doi.org/10.1007/s10853-017-1358-1

Maass, A., & Hirn, U. (2024). Long term curl of printing paper due to ink solvent migration. *Materials and Design, 237*, 112593. https://doi.org/10.1016/j.matdes.2023.112593

Mair, C. (2017). Control of porous structure of paper in a continuous process. In W. Batchelor & D. Söderberg (Eds.), *Pulp and paper research: Trans. of the XVIth Fund. Res. Symp. Oxford* (pp. 367–381). FRC. https://doi.org/10.15376/frc.2017.1.367

Malasri, S. (2022). Stacking strength of corrugated boxes. In *Proceedings of engineering, science and technology (online conference)* (Vol. 20, pp. 299–307). Cloud Publications. https://doi.org/10.23953/cloud.iestoc.515

Maldzius, R., Sirviö, P., Sidaravicius, J., Lozovski, T., Backfolk, K., & Rosenholm, J. B. (2010). Temperature-dependence of electrical and dielectric properties of papers for electrophotography. *Journal of Applied Physics, 107*, 114904. https://doi.org/10.1063/1.3386466

Malik, S., Singh, J., Saini, K., Chaudhary, V., Umar, A., Ibrahim, A. A., Akbar, S., & Baskoutas, S. (2024). Paper-based sensors: Affordable, versatile, and emerging analyte detection platforms. *Analytical Methods, 16*, 2777–2809. https://doi.org/10.1039/D3AY02258G

Mazhari Mousavi, S. M., Afra, E., Tajvidi, M., Bousfield, D. W., & Dehghani-Firouzabadi, M. (2018). Application of cellulose nanofibril (CNF) as coating on paperboard at moderate solids content and high coating speed using blade coater. *Progress in Organic Coating, 122*, 207–218. https://doi.org/10.1016/j.porgcoat.2018.05.024

Morais, F. P., & Curto, J. M. R. (2022). Challenges in computational materials modelling and simulation: A case-study to predict tissue paper properties. *Heliyon, 8*, e09356. https://doi.org/10.1016/j.heliyon.2022.e09356

Muller, C. (2018). *Paper-based flexible laminates tendency to curl*. MS Thesis, Faculty of Engineering LTH, Lund University, Sweden.

Musaev, E., Cantù, E., Soprani, M., Serpelloni, M., Sardini, E., Ponzoni, A., De Angelis, C., & Baratto, C. (2024). Paper sensors for advanced smart packaging: Route to detection on the shelf and in real ambient. *IEEE Sensors Journal, 24*, 31598–31605. https://doi.org/10.1109/JSEN.2024.3401248

Nielsen, I., & Priest, D. (1997). Dimensional stability of paper in relation to lining and drying procedures. *Paper Conservator, 21*, 26–36. https://doi.org/10.1080/03094227.1997.9638596

Nong, G., Li, P., Li, Y., Xing, D., Zhu, T., Wu, J., Gan, W., Wang, S., & Yin, Y. (2019). Preparing tea filter papers with high air permeability from jute fibers for fast leaching. *Industrial Crops and Products, 140*, 111619. https://doi.org/10.1016/j.indcrop.2019.111619

Park, J., Shin, J., & Park, J.-K. (2016). Experimental analysis of porosity and permeability in pressed paper. *Micromachines (Basel), 7*, 48. https://doi.org/10.3390/mi7030048

Paulapuro, H. (2000). Paperboard grades. In H. Paulapuro (Ed.), *Paper and board grades* (pp. 55–74). Finnish Paper Engineers' Association and TAPPI.

Raheem, D. (2016). Use and production of paper packaging for food. In G. Smithers (Ed.), *Reference module in food science*. Elsevier. https://doi.org/10.1016/B978-0-08-100596-5.03202-9

Rättö, P. (2005). The influence of surface roughness on the compressive behaviour of paper. *Nordic Pulp & Paper Research Journal, 20*, 304–307. https://doi.org/10.3183/npprj-2005-20-03-p304-307

Rautiainen, P. (2003). Solutions for high quality LWC paper. *IPPTA Convention Issue* 2003:35–51.

SAPPI. (2013). Defining and communicating color: The CIELAB system. *SAPPI fine paper North America*, pp. 1–8.

SAPPI. (2017). Understanding paper whiteness. *SAPPI North America*, pp. 1–2.

Saukkonen, E., Lyytikäinen, K., Backfolk, K., Maldzius, R., Sidaravicius, J., Lozovski, T., & Poskus, A. (2015). Effect of the carbohydrate composition of bleached kraft pulp on the dielectric and electrical properties of paper. *Cellulose, 22*, 1003–1017. https://doi.org/10.1007/s10570-015-0556-8

Sentmanat, J. M. (2017). Filter paper for industrial filtration. *Filtnews*, April 2017, pp. 37–41. www.filterconsultant.com

Shallhorn, P., & Gurnagul, N. (2009). A simple model of the air permeability of paper. In S. J. I'Anson (Ed.), *Advances in pulp and paper research: Trans. of the XIVth Fund. Res. Symp. Oxford, 2009* (pp. 475–490). Fundamental Research Committee (FRC). https://doi.org/10.15376/frc.2009.1.475

Simula, S., Varpula, T., Ikäläinen, S., Seppä, H., Paukku, A., & Niskanen, K. (1998). Measurement of the dielectric properties of paper. In *Proceedings of NIP & digital fabrication conference* (Digital library 14: art00039_1) (pp. 157–160). https://doi.org/10.2352/ISSN.2169-4451.1998.14.1.art00039_1

Sirviö, P., Backfolk, K., Maldzius, R., Sidaravicius, J., & Montrimas, E. (2008). Dependence of paper surface and volume resistivity on electric field strength. *Journal of Imaging Science and Technology, 52*, 30501. https://doi.org/10.2352/J.ImagingSci.Technol.(2008)52:3(030501)

Smit, P. W., Elliott, I., Peeling, R. W., Mabey, D., & Newton, P. N. (2014). An overview of the clinical use of filter paper in the diagnosis of tropical diseases. *American Journal of Tropical Medicine and Hygiene, 90*, 195–210. https://doi.org/10.4269/ajtmh.13-0463

Smook, G. A. (1990). Paper and paperboard grades. In G. A. Smook (Ed.), *Handbook of pulp and paper terminology* (pp. 251–261). Angus Wilde Publications.

Stankovská, M., Gigac, J., Letko, M., & Opálená, E. (2014). The effect of surface sizing on paper wettability and on properties of inkjet prints. *Wood Research, 59*, 67–76.

Sun, W., Hui, L., Yang, Q., & Zhao, G. (2021). Nanofiltration filter paper based on multi-walled carbon nanotubes and cellulose filter papers. *RSC Advances, 11*, 1194–1199. https://doi.org/10.1039/D0RA08585E

TAPPI. (2000). *T569 Internal bond strength (Scott type)*. https://imisrise.tappi.org/TAPPI/Products/01/T/0104T569.aspx

TAPPI. (2003). *TIP 0404-36 Paper grade classifications*. https://www.complianceonline.com/images/supportpages/500792/sample_0404-36.pdf

TAPPI. (2006a). *T460 om-02 Air resistance of paper (Gurley method)*. https://www.tappi.org/content/sarg/t460.pdf

TAPPI. (2006b). *T494 om-01 Tensile properties of paper and paperboard (using constant rate of elongation apparatus)*. https://www.tappi.org/content/sarg/t494.pdf

TAPPI. (2013). *T410 om-08 Grammage of paper and paperboard (weight per unit area)*. https://www.tappi.org/content/tag/sarg/t410.pdf

TAPPI. (2015). *T403 om-15 Bursting strength of paper*. https://www.wewontech.com/testing-standards/200328002.pdf

Tarrés, Q., Area, M. C., Vallejos, M. E., Ehman, N. V., Delgado-Aguilar, M., & Mutjé, P. (2020). Lignocellulosic nanofibers for the reinforcement of brown line paper in industrial water systems. *Cellulose, 27*, 10799–10809. https://doi.org/10.1007/s10570-020-03133-6

Techlab Systems. (2023). *Roughness and porosity meter (Bendtsen method) BTA model*. https://techlabsystems.com/

Tillmann, O. (2006). Paper and board grades and their properties. In H. Holik (Ed.), *Handbook of paper and board* (pp. 446–466). Wiley.

Twede, D., Selke, S., Kamdem, D. P., & Shires, D. (2015). *Cartons, crates and corrugated board*. DEStech Publications, Inc..

Vallejos, M., Felissia, F., Area, M. C., Ehman, N., Tarrés, Q., & Mutjé, P. (2016). Nanofibrillated cellulose (CNF) from eucalyptus sawdust as a dry strength agent of unrefined eucalyptus handsheets. *Carbohydrate Polymers, 139*, 99–105. https://doi.org/10.1016/j.carbpol.2015.12.004

Vernhes, P., Dubé, M., & Bloch, J.-F. (2010). Effect of calendering on paper surface properties. *Applied Surface Science, 256*, 6923–6927. https://doi.org/10.1016/j.apsusc.2010.05.004

Vieira, J. C., Mendes, A. d. O., Ribeiro, M. L., Vieira, A. C., Carta, A. M., Fiadeiro, P. T., & Costa, A. P. (2022). Embossing pressure effect on mechanical and softness properties of industrial base tissue papers with finite element method validation. *Materials, 15*, 4324. https://doi.org/10.3390/ma15124324

Wang, S., Li, M., & Lu, Q. (2010). Filter paper with selective absorption and separation of liquids that differ in surface tension. *ACS Applied Materials & Interfaces, 2*, 677–683. https://doi.org/10.1021/am900704u

Weber, C. F. (2024). *Studies on gloss of printed surfaces*. PhD Thesis, Technische Universität Darmstadt, Germane. https://doi.org/10.26083/tuprints-00026741

Yu, D. M., Chen, K. F., Zhao, C. S., Yang, R. D., & Hong, Y. M. (2006). The influence of basis weight on opacity and light absorption coefficient of paper. *Transactions of China Pulp and Paper, 21*(1), 52–55.

Zanuttini, M., Antúnez, C., Clemente, A., Torres, A., Ferreira, P., & Mochiutti, P. (2008). Propiedades del Papel. In M. C. Area (Ed.), *Panorama de la industria de celulosa y papel en Iberoamérica* (pp. 235–275). Red Iberoamericana de Docencia e Investigación en Celulosa y Papel (RIADICYP).

Chapter 7
Chemical Modification of Cellulose

Giovana Signori-Iamin, Roberto J. Aguado, Quim Tarrés, Pere Mutjé, and Marc Delgado-Aguilar

Abbreviations

AGU	anhydroglucose unit
CA	cellulose acetate
CAB	cellulose acetate butyrate
CAP	cellulose acetate propionate
CN	cellulose nitrate
CNCs	cellulose nanocrystals
CNFs	cellulose nanofibers
CX	cellulose xanthate
CMC	carboxymethylcellulose
DAC	2,3-dialdehyde cellulose
EDC	N-(3-Dimethylaminopropyl)-N′-ethylcarbodiimide
EC	ethylcellulose
FAME	fatty acid methyl ester
HEC	hydroxyethylcellulose
MC	methylcellulose
PLA	poly (lactic acid)
ROP	ring-opening polymerization
TEMPO	2,2,6,6-tetramethylpiperidine 1-oxyl

G. Signori-Iamin · R. J. Aguado · Q. Tarrés · P. Mutjé · M. Delgado-Aguilar (✉)
LEPAMAP-PRODIS Research Group, University of Girona, Girona, Spain
e-mail: m.delgado@udg.edu

G. Korotcenkov (ed.), *The Handbook of Paper-Based Sensors and Devices*,
https://doi.org/10.1007/978-3-031-91080-7_7

7.1 Historical Perspective

The history of chemical modification of cellulose can be broadly divided into two main periods: the early chemical modifications, spanning from the 1840s to the 1920s, and the modern chemical modifications, beginning in the 1960s and continuing to the present day. Recently, with the advent of nanocellulosic materials, a potential third period is emerging, although many of the chemical modification strategies developed for nanocellulose are also being applied to traditional cellulose. Figure 7.1 provides a timeline with the main milestones of cellulose chemical modification.

7.1.1 Early Chemical Modifications (1840s–1920s)

The earliest reported chemical modification of cellulose corresponds to nitrocellulose (NC), attributed to Prof. Christian Friedrich Schönbein, a German-Swiss chemist affiliated to the University of Basel, in 1846 (Schönbein, 1847). However, other researchers had previously combined nitric acid with starch, wood, or paper and cardboard, leading to xyloidine and nitramidine, discovered in 1832 and 1838, respectively (Cheung, 2014). The success of the CN obtained by Schönbein lies in the practical formulation that he proposed, consisting of mixing one part of a fine cotton cloth in 15 parts of one-to-one sulfuric and nitric acid mixture. This process was corroborated with Prof. Rudolf Christian Böttger, a close collaborator of Schönbein working at the University of Frankfurt am Main. CN has found several uses in many industries, the explosives and military applications being the most well-known. Actually, CN is also known as guncotton due to its origin, as well as for its cotton-like appearance and high flammability and explosive character (Morris et al., 2023). However, NC also served as a platform to synthesize new cellulosic

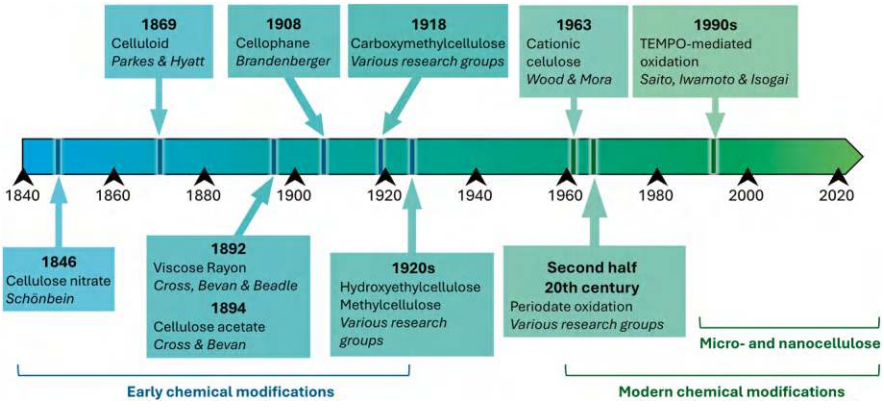

Fig. 7.1 Timeline of the main chemical modifications of cellulose

materials, such as the case of celluloid—a combination of NC and camphor—resulting in a moldable material that can be produced in the form of sheets and molded into various shapes. Celluloid, firstly reported under this name in 1869 by John Wesley Hyatt (Hyatt, 1870), was the result of an earlier work by Alexander Parkes in 1856 (Parkes, 1856). Hyatt patented a process for making a "horn-like material" with the combination of NC and camphor, aiming at substituting ivory from billiard balls. Twenty years later, in 1889, celluloid was used for photographic films, being patented by Hannibal Goodwin and the Eastman Kodak Company, and was used for most movie and photography films prior to the widespread use of acetate films around the 1950s.

Another relevant cellulose ester is cellulose acetate (CA), a thermoplastic cellulosic material broadly used in photographic films, textiles, and the plastic industry. While the French chemist Paul Schützenberger, in 1865 (Schützenberger, 1865), reported a process for acetylating cellulose with acetic anhydride. Cross and Bevan improved the method for producing CA and significantly contributed to practical and commercial aspects of the material, culminating in more efficient and practical techniques in 1894 (Cross & Bevan, 1894). CA is probably one of the most important cellulose derivatives, as it constitutes the precursor in the development of early plastics, and it is still relevant in various industries nowadays. While its use in the photography industry is residual with the irruption of digital photography, cellulose acetate is currently the raw material of cigarette filters, packaging films, and some biomedical devices (Marrez et al., 2019; Robertson et al., 2012; Voicu et al., 2016). In addition, more recently, CA has been extensively used for electrospinning applications, even in combination with nanostructured cellulose for the development of membranes with tunable permeability and surface characteristics (Bastida et al., 2024b; Khoshnevisan et al., 2018). As it will be later discussed, CA has led to significant advances in the field of cellulose esters, resulting in other esters by means of replacing hydroxy groups not only with acetate groups but also with propionate or butyrate groups, such as the case of cellulose acetate propionate (CAP) and cellulose acetate butyrate (CAB), respectively (Abdellah Ali et al., 2020; Xu et al., 2018). These mixed esters further enhance the versatility of cellulose derivatives, allowing for their use in a broader range of industrial applications. Specifically, the additional methylene groups in alkanoate moieties increase the solubility in organic solvents, help lower solution viscosity, and enhance the flexibility of the material (Tedeschi et al., 2018). In particular, CAB films have proven to be more ductile, more thermolabile, more moisture resistant, and opaquer than their CA and CAP counterparts (Kanis et al., 2014; Shanbhag et al., 2007).

Cellulose chemistry has also played a transformative role in the textile industry, providing a cellulose derivative alternative to silk and paving the way for the development of other man-made fibers. This is the case of viscose rayon, a regenerated cellulose xanthate that can form solid fibers. Viscose rayon was firstly reported in 1892 by Cross, Bevan, and Beadle, although Hilaire de Chardonnet, a French engineer, reported a CN-based artificial silk in the nineteenth century (Cross et al., 1892; Foster, 1924). The discovery of viscose rayon led to several innovations in the field of regenerated cellulose for textile applications, with some recent developments

such as Modal or Lyocell (Czaja et al., 2007). While both Modal and Lyocell are types of rayon, both appeared in the second half of the twentieth century, and they exhibit some differences in terms of production process and properties. On the one hand, Modal is a modified form of the viscose process, whereas Lyocell is made using a solvent spinning process that has been reported to be more environmentally friendly. This spinning process is performed after dissolution of cellulose in N-methylmorpholine N-oxide (NMMO), which is a non-toxic solvent. On the other hand, both Modal and Lyocell fibers are soft, but Lyocell has been reported to be generally stronger, particularly in terms of wet strength.

Still in the domain of regenerated cellulose, the Swiss chemist Jacques E. Brandenberger, in 1908, successfully created a transparent, flexible cellulose-based film. Dr. Brandenberger named this material cellophane, a combination of the terms "cellulose" and "*diaphane*," meaning transparent in French. Cellophane was first commercialized by the *La Cellophane Company*, founded by Bradenberger in 1912 (Brandenberger, 1915). This material gained popularity in the 1920s, when DuPont adopted the production and distribution in the United States, particularly for food packaging products (Gutjahr & Koch, 2003).

Another group of relevant cellulose derivatives is those produced by etherification. As will be discussed later, carboxymethylcellulose (CMC), hydroxyethylcellulose (HEC), methylcellulose (MC), and ethylcellulose (EC) constitute a group of cellulose ethers with a myriad of applications in many sectors. One of the earliest cellulose ethers was, in fact, EC. The ethylation of cellulose, replacing hydroxy groups with ethyl groups, was reported as early as the 1890s, but it was not commercialized until the 1920s for coatings, pharmaceuticals, and as a binder due to its film-forming ability. Followed by EC, MC was first developed around the 1920s, offering unique water solubility and gelation properties for a wide range of applications, including food products, but also building materials.

Between the 1910s and the 1920s, CMC appeared as a promising cellulose derivative as a thickener for food, pharmaceuticals, and detergents. The commercial scale production of CMC picked up momentum during the 1930s, with companies such as Hercules Inc. playing a key role in its industrial application (Klug & Tinsley, 1946). In parallel, HEC was found to be suitable for many water-based applications, such as thickener in paints, cosmetics, and personal care products. Each of these cellulose ethers represents a unique adaptation of cellulose chemistry, reflecting the interest in developing novel cellulosic materials and enhancing the scope of application of natural polymers.

Overall, the chemical modifications of cellulose during this first period represent a pivotal era in the history of material science and industrial chemistry. These innovations laid the foundation for the development of a wide range of synthetic and semi-synthetic materials with applications in many industries.

7.1.2 *Modern Chemical Modifications (1960s–Nowadays)*

From the 1960s onward, chemical modifications of cellulose have evolved significantly, although with less intensity than in the first period discussed in this chapter. Among the notable advancements in cellulose chemistry, cationization, periodate oxidation, TEMPO-mediated oxidation, and various modifications of nanocellulose deserve special mention.

Cationization emerged as a prominent modification technique in the 1960s, involving the introduction of cationic groups into the cellulose backbone usually induced by the reaction of reagents like 3-chloro-2-hydroxypropyltrimethylammonium chloride (CHPTAC) with cellulose, which introduced quaternary ammonium groups onto the cellulose chain (Moral et al., 2016; Prado & Matulewicz, 2014). Periodate oxidation of cellulose, though based on chemical knowledge dating to the early twentieth century, saw renewed interest and development in this second period (Maekawa et al., 1986; Siller et al., 2015). This interest, driven by the potential to create highly reactive intermediates suitable for further functionalization or cross-linking, resulted in the production of dialdehyde cellulose (DAC), opening opportunities for biomedical applications (e.g., wound dressings, drug delivery systems), but also as paper strengthening or hydrogels.

In the 1990s, promoted by the Japanese Professors Tsuguyuki Saito and Akira Isogai, TEMPO-mediated oxidation appeared as a selective, mild, and efficient way to introduce carboxyl groups into the cellulose fibers by means of oxidizing the primary hydroxy groups at the C6 position (Saito et al., 2007a). This process allowed the production of highly stable nanocellulose suspensions, which can result in transparent, strong, and biodegradable cellulose-based films and gels with potential applications as rheology modifiers, emulsifiers, paper strength agents, and biocomposites (Li et al., 2021; Tarrés et al., 2017). Indeed, most of the modifications in this second period have been oriented to the development of novel nanostructured cellulose materials, as will be discussed later.

7.2 Common Chemical Modifications of Cellulose

7.2.1 *Esterification*

At high enough temperature and with as little water as possible, the hydroxy groups of cellulose can react with carboxylic acids and/or organic acid anhydrides, resulting in a cellulose ester and water. The reaction also takes place with certain mineral acids, such as nitric acid, in the presence of sulfuric acid. One way or another, according to IUPAC's Gold Book, the product can be rightfully called a cellulose ester (Moss et al., 1995). Even cellulose xanthate (CX), generally synthesized by means of CS_2 (Xia et al., 2024), can be deemed an ester by extension. Besides CX,

other cellulose esters with high commercial relevance have already been introduced: CA, mixed esters such as CAP and cellulose acetate butyrate CAB, and CN.

CA, CAP, and CAB are employed for textiles, adsorbents, coatings, adhesives, membranes for dialysis and reverse osmosis, hollow fiber templates, cigarettes, and numerous drugs (Abdellah Ali et al., 2020; Maderuelo-Sanz, 2021; Wsoo et al., 2020). In general, CA and its mixed esters are appreciated for their processability, their solubility in common organic solvents such as acetone, their film-forming properties, their suitability for electrospinning, their toughness, and their tunable hydrophilic/hydrophobic character (Sharma et al., 2021). This character strongly depends on the degree of substitution (DS). Hence, cellulose monoacetate (DS ~ 1) can even be dissolved in water (Holtzapple, 2003), while cellulose triacetate (DS ~ 3) allows for the formation of superhydrophobic mats (Yoon et al., 2009). The conventional method for the acetylation of cellulose involves swelling air-dried cellulose fibers in glacial acetic acid and heating to *ca.* 40 °C, followed by an overstoichiometric addition of acetic anhydride and a catalytic addition of sulfuric acid (Chen et al., 2019). For CAP and CAB, the process also involves propionyl anhydride and butyryl anhydride, respectively (Xu et al., 2018).

CN, as aforementioned, is the supporting material of celluloid, extensively used for photographic film in the past. Until 2014, it was also the official material for table tennis balls (Inaba et al., 2017). Nowadays, CN is an important component in many ink formulations, paints for the automotive industry, nail varnishes, and lacquers for wood, leather, and aluminum foil (Muvhiiwa et al., 2021). Its solubility in common organic solvents, its flexibility, and its film-forming capabilities make CN irreplaceable for different industries. It is synthesized in a relatively simple way, by reacting cellulose in a mixture of nitric acid and sulfuric acid (homogeneous catalyst) at ordinary temperatures (20–40 °C) (Sun et al., 2010). For most current applications, the process aims at a DS close to 2, corresponding to cellulose dinitrate (Höfer et al., 2024). Total substitution leads to cellulose trinitrate, a mostly outdated explosive (Suter, 2013).

CX, the main constituent of cellophane, viscose rayon fabrics, and Modal fibers, is allegedly seeing a revamp in recent years (Morris, 2017; Singh & Murthy, 2017). Besides its traditional usefulness in packaging and clothing, it has also shown promising potential for the chelation of heavy metal ions in wastewater treatment (Reis et al., 2020). In a typical production process, cellulose is soaked in concentrated sodium hydroxide and subsequently treated with CS_2 (Butkova et al., 1979). The remarkable mechanical and barrier properties of CX films, their biodegradability, and their bio-sourced nature cannot be denied (Weißl et al., 2018), but neither can the safety issues and the environmental problems associated with the use and release of a hazardous chemical such as CS_2. These problems have motivated the surge of alternatives such as the lyocell process, which involves dissolution of cellulose in N-methylmorpholine N-oxide and ulterior regeneration, with no or little chemical derivatization (Singh & Murthy, 2017).

The mechanism for esterification implies the nucleophilic attack of cellulose's hydroxy groups on an electrophilic reagent. In acidic or neutral media, it is important for this reagent to be strongly electron deficient, so as to compensate for the

weak nucleophilicity of –OH groups. However, none of the main reagents used to produce common cellulose esters (nitric acid, carboxylic acids, and CS_2) are strong electrophiles. This is why sulfuric acid is used along with nitric acid in the production of CN, in such a way that nitronium ions (NO_2^+), more electrophilic, result from the interaction of both mineral acids (Marziano et al., 1998). This is also why acetylation is not performed in acetic acid alone, but in an acetic anhydride/acetic acid system, since anhydrides are more reactive than their carboxylic acid counterparts (Diop et al., 2011). Finally, this is why xanthation is performed in alkaline media: if the weak electrophile (CS_2) is not converted into a stronger electrophile, the weak nucleophile (–OH) will have to be converted into a stronger nucleophile ($–O^-$). These reactions are schematized in Figure 7.2, which shows only the most likely monosubstituted derivative for the sake of simplicity. The general reactivity order for esterification favors primary –OH groups: C-6 > C-2 > C-3 (Heinze et al., 2018a).

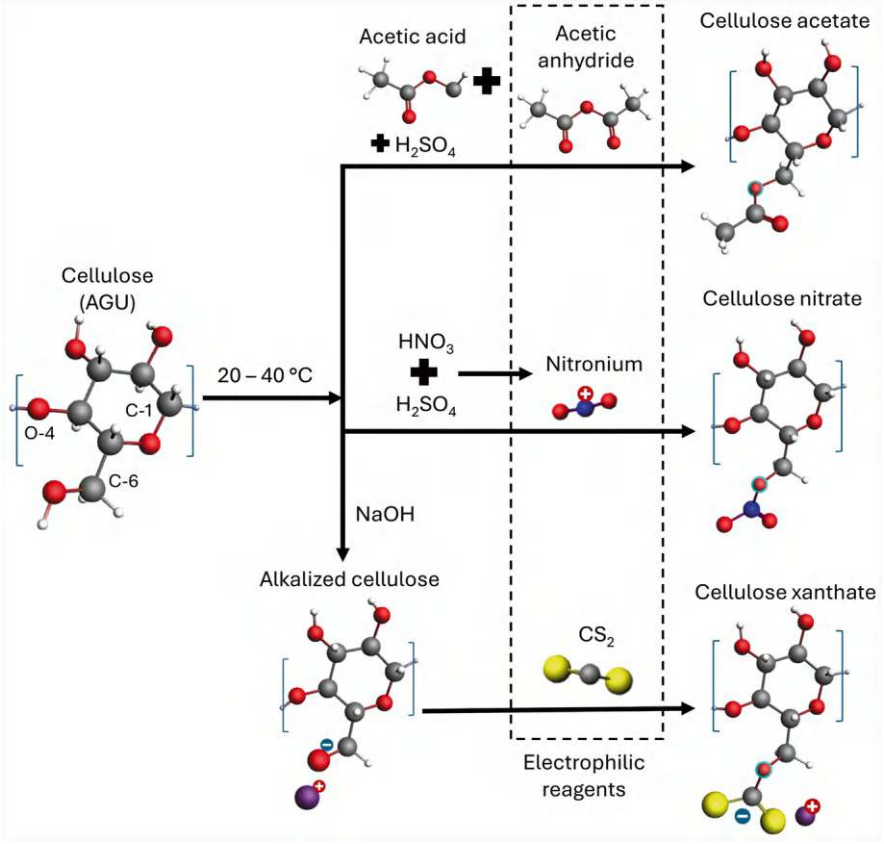

Fig. 7.2 Production of monosubstituted forms of representative cellulose esters, highlighting the linking oxygen atom in each case

Even if the main solvent for esterification is a carboxylic acid or a mixture of acids, the hydroxy groups of cellulose unavoidably compete with a more mobile nucleophile: water, an intrinsic component of cellulose fibers (Chen et al., 2022). Even if cellulose were completely dried, which could be counterproductive because the subsequent collapse of its fibrils would hamper the diffusion of reagents, the reaction itself produces water. In the particular case of xanthation, whose medium is alkaline, alkoxides compete with hydroxide ions for CS_2. All considered, anhydrides are non-reversibly hydrolyzed to the less reactive carboxylic acids, and CS_2 gives way to thiocarbonates (Rhodes et al., 2000). For nitration, this is less of a problem, since the hydration of nitronium ions simply regenerates nitric acid. In any case, the presence of water forces manufacturers to use overstoichiometric amounts of esterification reagents. Facing this challenge, many researchers have identified alternative solvent systems, such as 1,8-diazabicyclo[5.4.0]undec-7-ene/CO_2 or the ionic liquid 1-allyl-3-methylimidazolium chloride (Cao et al., 2010; Wolfs & Meier, 2021). Those systems can increase the selectivity of acetylation, at least when low DS values are desired.

Other cellulose esters such as cellulose sulfate, cellulose phosphate, and cellulose acetate phthalate enjoy certain niche markets. Specifically, the biological activity of cellulose sulfate justifies its use for drug delivery and microbe/cell immobilization (Zhang et al., 2015). Likewise, cellulose acetate phthalate is used in enteric-coated systems for biomedical applications (Harrison, 2007). Finally, cellulose phosphate can be employed for protein chromatography and for ion exchange (Li et al., 2002).

Moreover, some of the typical functionalities that are traditionally imparted to cellulose by etherification could be alternatively attained by esterification. For instance, the Fischer esterification of cellulose with concentrated oxalic acid offers an alternative to carboxymethylation (Bastida et al., 2024a), and the $SOCl_2$-mediated production of cellulose betainate could be compared with the synthesis of cationic cellulose ethers (Sievänen et al., 2015). An alleged advantage is the lower chemical and biological stability of the ester bond, leading to derivatives that are more biodegradable than their ether counterparts. However, the large excess of carboxylic acid required or the need to generate acyl chlorides (stronger electrophiles) are severe setbacks for the industrial implementation of such processes.

7.2.2 Etherification

Between 1850 and 1854, the great English chemist Alexander Williamson published four extremely influential studies on etherification (Williamson, 1903). Since then, it is known that compounds bearing hydroxy groups can give way to ethers by reacting with electrophiles, such as organohalides and epoxides, under alkaline conditions. Polysaccharides, including cellulose, are not exceptions. There are several ethers among the most marketed cellulose derivatives, namely carboxymethylcellulose (CMC), hydroxyethylcellulose (HEC), methylcellulose (MC), and

ethylcellulose (EC) (Sharma et al., 2015; Steger et al., 2022). All of them are typically synthesized from cellulosic feedstocks with low degrees of crystallinity, at 40–70 °C, in alkaline media, and following an S_N2 mechanism.

The synthesis of common ethers is schematized in Figure 7.3. It should be noted that substitution on C-6 is shown merely as an example, since substitution on C-2 or C-3 can also take place (Heinze et al., 2018b). In fact, depending on the alkali charge, the order of reactivity may vary from C-2 > C-6 > C-3, corresponding to moderately alkaline media, to C-6 > C-2 > C-3 for strongly alkaline media (Larsen et al., 2012). While primary alkoxides are generally more reactive nucleophiles than secondary alkoxides, the former tend to be more basic.

CMC is a common thickener, an anionic stabilizer for foams and emulsions, and even a strength agent in the food, pharmaceutical, textile, paper, and cosmetic industries. For instance, in the food industry, it is known as the additive E466. The electrophilic reagent par excellence to synthesize CMC is chloroacetic acid, or its sodium salt, with chloride as leaving group (Pinto et al., 2022). Undesired side reactions also generate sodium glycolate (Ünlü, 2013).

HEC, despite having a higher carbon-to-oxygen ratio, is more hydrophilic than native cellulose, due to the spacing effects exerted by the hydroxyalkyl moieties. Besides being a thickener and a non-ionic stabilizer, it can effectively work as a dispersing agent (Sharma et al., 2015). At industrial levels, HEC is produced by

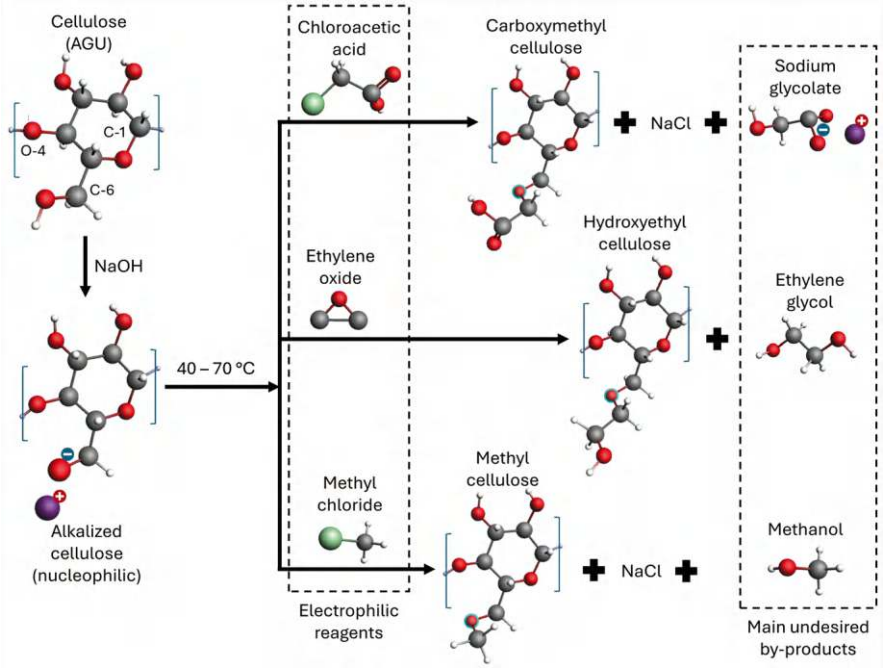

Fig. 7.3 Production of the most marketed cellulose ethers, highlighting the ether oxygen in each case and indicating the most abundant by-products

alkalizing cellulose with sodium hydroxide and subsequently making it react with the simplest epoxide: ethylene oxide (Basu et al., 2021).

MC is produced by heating cellulose with an alkali, generally NaOH, and then treating it with excess methyl chloride (or iodide). For EC, the electrophile is ethyl chloride (or iodide) instead. Their uses comprise that of emulsifier and thickener in different products such as lubricants or adhesives, as sizing agents in papermaking, and as encapsulating agents for nutrients or drugs (Rogers & Wallick, 2012).

Furthermore, common forms of cationic cellulose are also synthesized by etherification. For instance, the tensioactive agent going by the commercial name "Polyquaternium-10" typically results from the etherification of HEC ethoxylate with the epoxide of a quaternary ammonium salt (Siyawamwaya et al., 2016). The most frequent electrophilic reagent for this task, both in the cosmetics industry and in the literature, is 2,3-epoxypropyltrimethylammonium chloride (EPTAC) (Moral et al., 2017; Pedrosa et al., 2022).

The usefulness of alkalization is not limited to the ionization of cellulose, but also implies a loss in crystallinity. This is a lesson learnt from the mercerization of cotton, a process named after the so-called "father of textile chemistry": John Mercer (Holme & Blackburn, 2019). Concentrated sodium hydroxide is able to penetrate through cellulose crystallites, simultaneously causing a loss of crystallinity and a conversion of cellulose I to cellulose II (French, 2014). This enhances the overall reactivity of cellulose in two ways. First, it promotes fiber swelling, increasing the rate of diffusion of etherification reagents through the supramolecular structure of cellulose. Second, by disrupting this supramolecular structure, it allows the electrophilic reagents to reach cellulose chains that would be inaccessible otherwise.

Effective variants of the mercerization process include NaOH/urea, NaOH/thiourea, and iron(III)-tartrate-sodium complexes, resulting in the partial or total dissolution of fibers. Then, the apparently dissolved polymer is regenerated as mixtures of amorphous cellulose and cellulose II crystallites (Aguado et al., 2019; Yang et al., 2017). The disruption of the supramolecular structure of cellulose can also be attained by mechanical processes such as intensive grinding, beating, ball milling, and twin-screw extrusion (Elalami et al., 2022).

In aqueous media, the pK_a of the hydroxy groups of cellobiose has been estimated as roughly 13.5 (Bialik et al., 2016). In fact, the pH for the etherification of cellulose usually lies in the 12.7–13.8 range (Odabas et al., 2017; Pinto et al., 2022). Such strongly alkaline media imply undesired side reactions with subsequent loss of electrophilic reagent. Epoxides become unreactive diols, haloalkanes become alcohols, and (as aforementioned) chloroacetate becomes glycolate (Ünlü, 2013), as indicated in Figure 7.3. Moreover, within the common range of temperature for etherification (40–70 °C), cellulose suffers from depolymerization due to alkaline hydrolysis. In the literature, these problems are often avoided by resorting to aprotic solvents, such as the dimethyl acetamide/LiCl system, or deep eutectic solvents, such as aminoguanidine hydrochloride/glycerol (Heinze et al., 2018b; Li et al., 2018). Such systems allow for high degrees of substitution without the need for a large excess of electrophilic reagent. However, due to technical, economical, and

environmental reasons, marketed cellulose ethers are generally produced in alkaline aqueous slurries (Basu et al., 2021).

7.2.3 Oxidation

The oxidation of hydroxy groups to carbonyl groups and of the latter to carboxyl groups are basic reactions in organic chemistry (Tojo & Fernández, 2007). While etherification of cellulose toward CMC, the most commercially successful carboxylated derivative, generally implies disrupting the supramolecular structure of cellulose, oxidation requires neither deprotonation nor previous decrystallization. Oxidized cellulose derivatives, traditionally known as oxycellulose, are useful for various biomedical applications, including those of enterosorbent, mucoadhesive, and/or hemostatic agent (Gajdziok et al., 2010; Guo et al., 2013). Likewise, oxidative processes are also frequent pre-treatments leading to nanocellulose (Isogai et al., 2011).

Although many oxidizing agents can take electrons from hydroxy groups, a common problem is that glycosidic bonds are likewise prone to oxidative hydrolysis, even more so once nearby hydroxy groups have been oxidized (Cheng et al., 2016). Hence, the non-selective oxidation of cellulose with chromic acid, periodic acid, potassium dichromate in acidic medium, sodium hypochlorite in alkaline medium, sodium chlorite, or potassium permanganate traditionally results in oxycellulose with severe degradation (Hebeish et al., 1979; Shenai & Date, 1976). Furthermore, the strong topochemical character of the process usually implies heterogeneous products with large portions of unreacted material. Out of the traditional methods to oxidize a glucan toward a poly(glucuronic acid), oxidation with NO_2 probably stands as the most robust pathway to attain a high content of carboxyl groups with as little degradation as possible (Martina et al., 2009).

Some non-selective treatments for cellulose oxidation are still of interest in the recent literature. This is the case of persulfate salts, whose combined effects of hydrolysis (especially on non-crystalline domains) and oxidation are useful to produce cellulose nanocrystals (CNCs) (Chen et al., 2023). Furthermore, the existence of multiple pathways to activate the peroxydisulfate ion, including the use of novel homogeneous catalysts, makes room for innovation. For instance, in the presence of N,N,N′,N′-tetramethylethylenediamine, persulfate oxidation is faster and requires a lower concentration of oxidizer to attain a given degree of oxidation (Liu et al., 2020). As indicated in Figure 7.4, oxidation mainly takes place on the C-6 position of anhydroglucose units (AGUs) and on the glycosidic bonds within the least crystalline regions of cellulose. High levels of oxidation (above 1 mmol –COOH g^{-1}) often result in the solubilization of more than a third of the starting cellulosic material. This solubilized fraction, characterized by a low molecular weight and/or a high charge density, is known as the hydrolysate.

Despite the setbacks of oxycellulose production in what pertains to degradation, hydroxy groups can be oxidized with great selectivity in different ways. For instance,

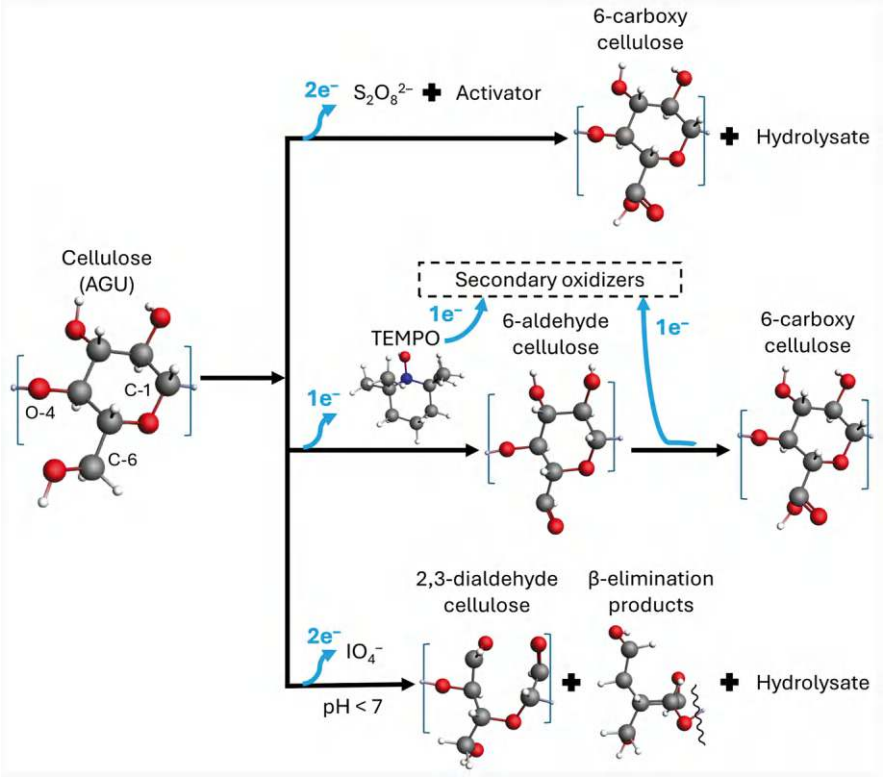

Fig. 7.4 Oxidation of cellulose with persulfate salts, TEMPO along with secondary oxidizers, and periodate salts

oxidation by NO_2 can be highly selective if the reaction is performed in a non-polar solvent such as CCl_4 (Wu et al., 2012). Nonetheless, as aforementioned, the use of water as solvent is generally more convenient due to the nature of cellulose fibers and to technical, economic, and environmental reasons.

One of the most popular methods for selective oxidation in aqueous media implies the use of 2,2,6,6-tetramethylpiperidine 1-oxyl (TEMPO) radical in catalytic proportions (Isogai et al., 2011; Spier et al., 2017). First, the stable nitroxyl radical is converted to its reactive N-oxoammonium salt by ClO^-, BrO^-, ClO_2, ClO_2^-, hydroperoxyl radicals, or other suitable secondary oxidizers (Hirota et al., 2009; Pääkkönen et al., 2017; Saito et al., 2007b). Then, the N-oxoammonium form of TEMPO selectively oxidizes primary alcohols, including the hydroxy groups at the C-6 position of AGU, to aldehydes. Finally, the role of the secondary oxidizers is double: they not only reactivate the reduced TEMPO, but also oxidize carbonyl groups to carboxyl groups (Fig. 7.4). Arguably, the most successful system to date involves a ternary system comprising TEMPO, NaBr, and NaClO at pH 9–11 (Mazega et al., 2024; Xu et al., 2014). NaClO, an inexpensive and highly available

reagent, works as the only spent oxidizer. It oxidizes Br^- ions to BrO^- ions, which in turn are stronger oxidizers to activate (and regenerate) TEMPO and to take electrons from carbonyl groups (Mazega et al., 2023). Although depolymerization of cellulose by ClO^- and BrO^- takes place to a certain extent, the high selectivity of the process, its reproducibility, and the possibility to carry out the reaction at room temperature justify the popularity of TEMPO-mediated oxidation.

For some applications, it is desired for cellulose derivatives to have carbonyl groups instead of carboxyl groups. In this sense, one of the most recurrent processes is periodate oxidation, leading to 2,3-dialdehyde cellulose (DAC) (Aouay et al., 2024; Li et al., 2019). Even though DAC remains, as Dalei et al. (2022) state, a niche material, it enjoys promising and actual applications for drug delivery, tissue engineering, packaging, and energy storage, besides being a common intermediate for other cellulose derivatives (Pedrosa et al., 2022). DAC is produced by oxidative cleavage of the bond between C-2 and C-3 in AGU, in such way that at least one of the secondary hydroxy groups is converted into a primary carbonyl group. β-Elimination and hydrolysis of glycosidic bonds are common side reactions (Fig. 7.4). In the simplest form of the synthesis, cellulose is soaked in an aqueous $NaIO_4$ solution at 23–50 °C and kept protected from ultraviolet radiation for 2–48 h. Often, researchers employ metal chlorides (NaCl, KCl, or LiCl), which have been found to improve oxidation kinetics, and acidic buffers (Sirviö et al., 2011; Dalei et al., 2022). The process can also lead to carboxyl groups if a secondary oxidant, such as $NaClO_2$, is present in the medium (Liimatainen et al., 2012).

7.3 Recent Advances in Chemical Modification of Cellulose

7.3.1 Nanocellulose Functionalization

Although the morphological characteristics and the presence of different functional groups may vary depending on the method of obtaining the nanocellulose, nanostructured cellulose is typically characterized by the presence of hydroxy groups on its surface. This gives nanocellulose a hydrophilic character but also a high reactivity. Recently, research in the field of nanocellulose has focused on the study of different surface modification treatments, including those displayed in Figure 7.5. These modifications aim to provide nanocellulose with properties that allow the use of this biomaterial in various applications.

7.3.1.1 Nanocellulose Carboxymethylation

Carboxymethylation of nanocellulose involves adding carboxymethyl groups to the surfaces of cellulose, giving them a negative charge. This process typically uses chloroacetic acid, which reacts with the primary hydroxy groups of the cellulose

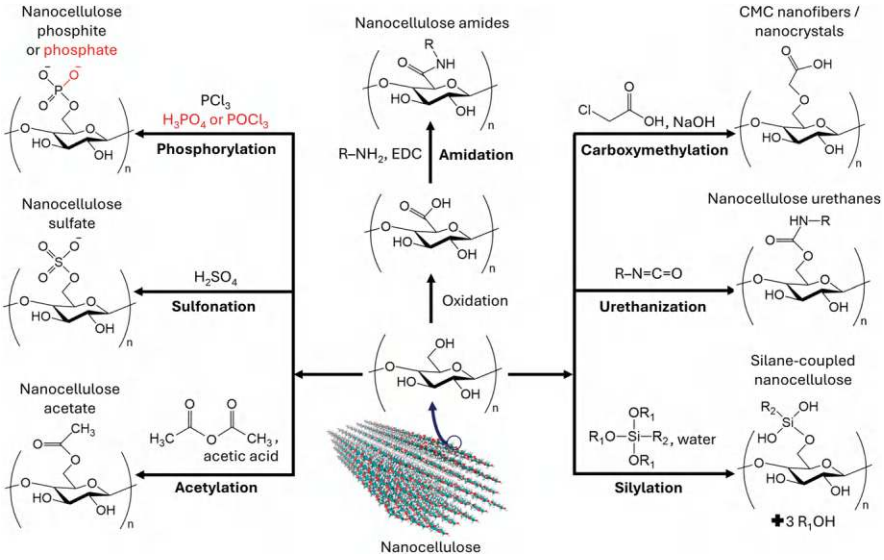

Fig. 7.5 Chemical modifications on nanocellulose, showing monosubstituted derivatives as examples. R, R_1, and R_2 mean arbitrary substituents, typically alkyl chains

monomers, creating a carboxymethylated derivative at position 6. Mechanical treatments are often used to enhance this modification (Siró et al., 2011). Surface ionization can be controlled through surface modification, aggregation, and dispersion, affecting the rheology and dehydration of cellulose nanofibrils, which in turn influences the final product properties. Cellulose surfaces contain hydroxy groups, allowing for the adjustment of surface ionization through electrostatic force adsorption methods and chemical treatments. The carboxymethylation reaction is commonly used to increase the anionic charge on cellulose fibers by introducing carboxymethyl (–CH_2COOH) groups into the hydroxy group sites. When these groups react with chloroacetic acid, they ionize in water, providing anionic charge to the cellulose fiber surface. The solubility and viscosity characteristics of water vary depending on the degree of substitution of the carboxymethyl groups. Furthermore, increasing the anionic loading can reduce the energy consumed during the fabrication of cellulose nanofibrils by mechanical treatments, if used as a pretreatment. The carboxymethylation reaction involves several steps: a suspension of nanofibrils in isopropanol is stirred for 30 min, followed by the addition of a 30% NaOH solution and further stirring for 30 min. Meanwhile, chloroacetic acid is dissolved in isopropanol and added to the nanocellulose and sodium hydroxide solution mixture. The reaction takes place for 1 h in a water bath at 65 °C and is neutralized with acetic acid to reach a pH of 7. The mixture is washed under vacuum conditions in the following order: isopropanol, methanol, ethanol, and methanol again. Finally, the pulp fibers are immersed in a 5% sodium bicarbonate solution to convert them into their sodium salt form (–COONa) (Siró et al., 2011).

7.3.1.2 Nanocellulose Phosphorylation

Phosphorylation of nanocellulose focuses on the incorporation of phosphate or phosphite groups into the cellulose chain. Several studies show how the presence of phosphate ester groups on the surface of nanocellulose could be interesting for its application in exterior wall insulation, the automotive sector, the manufacture of flame-retardant materials, etc.

Currently, there are different reaction routes for the phosphorylation of nanocellulose. Nanocellulose phosphate: The incorporation of H_3PO_4 ester groups into the cellulose chain is achieved by using pentavalent phosphate reagents such as $POCl_3$, P_2O_5, and H_3PO_4 (Illy et al., 2015). Although there are studies that show that the presence of urea allows achieving higher degrees of substitution, they result in laborious and costly procedures that do not make their production viable. These processes usually require two steps, a first stage of immersion of the fibers in the aqueous concentrated solution with H_3PO_4 and a subsequent curing stage of between 10 and 15 min at 100–150 °C (Patoary et al., 2023).

Nanocellulose phosphite: On the other hand, in the reaction of nanocellulose with trivalently phosphorus groups such as PCl_3, or by transesterification with $(CH_3O)_2PH$, it is possible to obtain cellulose phosphite esters with up to 8% phosphorus in the cellulose chain (Rol et al., 2020).

Phosphorylation of the cellulose takes place mostly in the amorphous zones, and there is a decrease in the degree of polymerization due to the hydrolyzation of the chain and the fibers swell (Rol et al., 2020).

In all cases, phosphorylated nanocellulose possesses cation exchange properties, due to the incorporation of anionic phosphate groups in its structure. This confers the nanocellulose with chelating properties, useful for the uptake of metals as well as cations in environmental applications (Qiao et al., 2021). On the other hand, phosphorylation also contributes to improving the thermal properties of nanocelluloses; however, it can lead to a decrease in tensile strength, depending on the degree of modification (Patoary et al., 2023).

7.3.1.3 Nanocellulose Sulfonation

Sulfonation is a crucial technique for giving anionic character to nanocellulosic materials' surfaces, in such a way that this negative charge is highly resistant to pH changes. This process involves using concentrated sulfuric acid, which not only catalyzes cellulose hydrolysis but also helps form half ester sulfate from the hydroxy groups existing on the nanocellulose. This treatment leads to highly stable colloidal suspensions.

During sulfonation, sulfuric acid causes sulfated groups to form on the nanocellulose surface. These groups create a negative charge, leading to a negative electrostatic layer that boosts water dispersibility. The negative charges also result in very stable nanocellulose suspensions and can lead to optically active films after controlled drying. However, a high degree of sulfate functionalization can affect the

nanoparticles' thermal stability. To counter this effect, neutralizing the nanoparticles with NaOH can improve their thermal stability. Additionally, using a combination of sulfuric acid, HCl, and sonication allows for obtaining nanocrystals (Mu & Gray, 2014).

Another approach to nanocellulose sulfonation involves using sodium periodate $NaIO_4$ and $NaHSO_3$ to treat nanofibrillar hardwood pulps. This method produces sulfonated fibrillar nanocellulose with diameters ranging from 10 to 60 nm. To achieve effective nanofibrillation, a minimum density of 0.18 mmol g^{-1} of sulfate groups is necessary (Ruiz-Palomero et al., 2016). This sulfonation method also produces a highly transparent and viscous gel, showcasing the versatility of sulfonated nanocellulose in various applications.

One of the primary uses of sulfonated nanocellulose is in dispersive phase micro solid extraction and determination of silver nanoparticles in food products. This sulfonation process is considered a more environmentally friendly alternative, as it avoids the use of halogenated waste, thus reducing the environmental impact of the process.

7.3.1.4 Nanocellulose Silylation

The addition of silanes to nanocellulose has attracted significant attention because they act as coupling agents due to their strong attraction to hydroxy groups. While this interaction occurs at room temperature, permanent grafting occurs through condensing Si–OH moieties with C–OH at higher temperatures during a curing process. However, achieving a high degree of substitution is challenging due to the drawbacks of the silylation process, which requires organic solvent exchange. The process for incorporating silane groups is well-known and involves two stages. First, hydrolysis occurs, leading to the formation of silanol groups from the hydrolysis of the alkoxy groups of the silane. The high presence of OH groups on the surface of nanocellulose promotes the adsorption of the silanol groups through hydrogen bonds. Subsequently, a condensation reaction enables the formation of Si–O–C bonds. Silane coupling imparts hydrophobicity when the Si atom is directly attached to an alkyl chain, but diverse functionalities (e.g., amino groups) are also possible (Guo et al., 2024).

Recently, several authors have reported the effect of different silylation agents on the structure, dispersion properties, hydrophobicity, and biodegradability of nanocellulose. Saini et al. (2016) conducted a study on the silylation of cellulose nanofibers using various aminosilanes. To achieve this, they first dissolved the aminosilanes in deionized water at room temperature and pH 10. The nanofibers were then immersed in these aminosilane solutions for 10 s and subsequently subjected to heat treatment at 110 °C for 2 h. The functionalized nanocelluloses demonstrated significant antibacterial activity (Saini et al., 2016).

Frank et al. (2018) modified cellulose nanofibers (CNFs) with hydrophobic alkoxysilanes containing methyl, propyl, or aminopropyl functional groups. In comparison to untreated CNFs, the stability of Si-CNFs in organic solutions was

enhanced, an effect that depended on the extent of silanization (Frank et al., 2018). Likewise, the incorporation of methyl trichlorosilane has been shown to be effective in making nanocellulose hydrophobic. It allows for the creation of a three-dimensional network structure on the nanocellulose, achieving superhydrophobicity without affecting its optical and mechanical properties (Wang & Huang, 2021).

7.3.1.5 Nanocellulose Acetylation

The acetylation of nanocellulose has been studied as a method to make nanocellulose hydrophobic. This process involves replacing the hydroxy groups on the surface of nanocellulose with acetyl groups. Acetylation is typically carried out using acetic anhydride and acetic acid in the presence of sulfuric acid or perchloric acid. Initially, the more accessible hydroxy groups from the amorphous regions of the nanocellulose are substituted, followed by the less accessible hydroxy groups in the crystalline parts as the reaction progresses. Under certain conditions, the maximum degree of substitution is 3.0, meaning that all hydroxy groups have been replaced. A degree of substitution close to 1 allows for better dispersion in polar solvents, while a higher degree of substitution promotes dispersion in hydrophobic non-polar solvents (Ghasemlou et al., 2021).

The literature discusses the importance of adjusting the degree of substitution by changing the proportions of acetic anhydride and acetic acid to broaden the potential applications of acetylated nanocellulose. However, acetylation rarely reaches a degree of substitution of 3.0 due to the presence of intact hydrogen bonds between the AGUs of the cellulose chains, which restricts the complete substitution of hydroxy groups. Research has also examined the impact of different acids and reaction conditions on acetylation efficiency. Boujemaoui et al. (2015) employed a combination of acid hydrolysis and Fischer esterification to chemically modify the nanocellulose surface with various organic acids, achieving substitution degree values that varied depending on the acid used. Other studies have focused on enhancing acetylation efficiency using specific reaction conditions, such as controlled temperatures and ultrasound, resulting in higher degrees of substitution values and improved dimensional stability of cellulose nanofibers (Manimaran et al., 2024).

7.3.1.6 Nanocellulose Urethanization

The modification of nanocellulose through urethanization involves a chemical reaction between isocyanates groups (R–N=C=O) and hydroxy groups (–OH) on the nanocellulose surface, resulting in the formation of urethane (–COONH) bonds. N-octadecyl isocyanate is one of the electrophilic reagents used in this type of modification. This reaction increases the hydrophobicity of nanocellulose and improves the dispersibility of CNCs and CNFs in organic solvents, which is crucial for applications requiring uniform dispersion in polymeric matrices (Shoseyov et al., 2019).

Biyani et al. (2013) developed an isocyanate-mediated coupling method to decorate CNCs with ureidopyrimidone, a compound that forms multiple hydrogen bonds. In this study, CNCs were reacted with 2-(6-isocyanatohexylaminocarbonylamino)-6-methyl-4[1H]-pyrimidinone in DMF at 100 °C using the catalyst dibutyl dilaurate. The ureidopyrimidone-functionalized CNCs were incorporated into polymer functionalized with the same compound, providing light self-repairing capabilities and improving the mechanical properties of the resulting material.

The urethanization reaction has also been used to improve the dispersibility of CNC in a poly(lactic acid) (PLA) matrix. Toluene diisocyanate (TDI) was employed in a dispersion of CNC in dimethylformamide (DMF) at 70 °C. The successful modification of CNC was confirmed by 13C NMR and FT-IR analysis, with a characteristic peak at 2272 cm^{-1} for –NCO. The modified CNC was used to prepare nanocomposites with PLA by solution casting with chloroform. The –OH terminal group of PLA was expected to react with the –NCO group of the modified CNC, producing urethane bonds between PLA and CNC, evidenced by the increased intensity of the FT-IR absorption band of the >C=O group of urethane. As a result, the PLA/CNC nanocomposite showed higher crystallinity and improved thermal and mechanical properties (Hassani et al., 2021).

7.3.1.7 Nanocellulose Amidation

The functionalization of nanocellulose through amidation is carried out to selectively react with specific components. This process is used in selective adsorption applications, colorimetric or fluorimetric determination, among others. Typically, the amidation of nanocellulose is performed on cellulose nanofibers with a high content of carboxylic groups (–COOH), such as those obtained through TEMPO-catalyzed oxidation pretreatment. This is because the amidation reaction is mediated by carbodiimides, which have low reactivity toward hydroxy groups. Among carbodiimides, N-ethyl-N-(3-(dimethylamino)propyl)carbodiimide (EDC) has been widely used in the literature for the amidation of nanocellulose (Wang et al., 2024).

As an example of application, Ruiz-Palomero et al. (2015) demonstrated the covalent binding of β-cyclodextrin to a nanocellulosic material that had undergone an amidation reaction, creating a specific sorbent for danofloxacin in milk. For this, a suspension containing nanocellulose, EDC·HCl, and N-hydroxysuccinimide in methanol, previously stirred for 20 min in an inert atmosphere, was mixed with a solution of ethylenediamine and triethylamine in methanol. The reaction was carried out at room temperature for 12 h.

7.3.2 *Bio-Based and Green Chemical Modifications*

7.3.2.1 Enzymatic Modifications

The use of endoglucanase enzymes for pretreating and obtaining nanocellulose has been extensively researched. However, these enzymes can also be employed to alter the surface and chemical composition of nanocellulose. Enzymatic methods offer numerous benefits, including high process efficiency, selectivity, and milder reaction conditions compared to the use of unspecific chemical agents.

Cellulosic and lignocellulosic materials have been successfully modified using various enzymes such as laccase, pectinase, lipase, and hexokinase. For example, the strength properties of fiberboards bonded with laccase have been proven superior to those bonded with urea-formaldehyde adhesive (Euring et al., 2013). Additionally, Jaušovec et al. (2015) reported the chemoenzymatic modification of CNFs using laccase as a biocatalyst and TEMPO or 4-amino-TEMPO as mediators under mild aqueous conditions (pH 5, 30 °C). This process allowed for the introduction and adjustment of aldehyde versus carboxyl groups on CNFs, along with the terminal aldehyde groups already present. Furthermore, the use of pectinase has been shown to introduce new functional groups on the nanocellulose surface. In a separate study, CNFs were modified using hexokinase and adenosine-5-triphosphate in the presence of Mg^{2+} ions, resulting in the creation of a phosphate group predominantly on the hydroxy groups positioned at C-6, confirming the formation of a tautomer structure (Karim et al., 2017).

7.3.2.2 Transesterification with Fatty Acid Esters

The use of vegetable oils to modify the surface of cellulose offers the potential to provide it with a hydrophobic character and to enhance its thermal stability. Vegetable oils, primarily triglycerides made up of glycerol molecules and long-chain fatty acids (linoleic, palmitic, stearic, oleic, linolenic, etc.), can be used to modify cellulose through processes such as esterification or transesterification. This provides fibers with a hydrophobic character and high thermal stability (Roman et al., 2024). Non-edible or inexpensive oils from industrial crops, such as castor oil or canola oil, are usually chosen for the task.

Typically, transesterification is conducted with diisocyanate or zinc acetate dihydrate as a binding agent. Transesterification leads to a slight increase in the crystalline index of nanocellulose, which has been associated with hydrolysis or crystallization of the amorphous portion under acidic conditions and high temperatures (Yoo & Youngblood, 2016). This kind of modification is typically carried out in two steps. First, the vegetable oil is transesterified with an alcohol, usually methanol, to produce fatty acid methyl ester (FAME). Upon conversion to FAME, the long hydrophobic hydrocarbon structure can be chemically bonded to cellulose

through a second transesterification reaction between the hydroxy groups of the polysaccharide and the ester bonds of the FAME (Wei et al., 2017).

7.3.3 Advanced Techniques

7.3.3.1 Mechanochemistry

Mechanochemistry is an environmentally friendly process that has become increasingly important in recent years. This method involves using mechanical actions to bring about chemical and physicochemical changes in substances. Depending on the treatment conditions, such as the reagent used, the time, and whether the state is solid or liquid, mechanochemistry can be used to extract nanocellulose from cellulosic fibers by combining mechanical and chemical actions. Research in mechanochemistry has explored various applications, such as grafting maleic anhydride onto nanocellulose surfaces in a single step, as well as modifying cellulose nanocrystals using milling treatments. While these processes have advantages such as simplicity and efficiency, they also have pending challenges, such as long reaction times. Furthermore, new combinations of mechanochemistry with deep eutectic solvents have been explored, showing promising results for the extraction and modification of nanocellulose. Mechanochemistry is generally considered to provide a sustainable and efficient approach for cellulose modification and nanocellulose production (Douard et al., 2022).

7.3.3.2 Click Chemistry

The recent use of click-type reactions to modify cellulose has caused a lot of excitement. Click chemistry offers the advantages of cleanliness, high atom economy, avoiding side reactions, high yields, and ease of separation (Gupta, 2024). Some of the specific modifications that have garnered interest include thiol-ene reactions, several kinds of nucleophilic addition, and azide-alkyne cycloadditions. However, since the hydroxy groups of cellulose will still compete with water for virtually any electrophile (even dichlorotriazine, highly reactive towards –OH), cellulose normally must undergo a previous modification that prepares it for click reactions.

Filpponen and Argyropoulos (2010) utilized copper(I)-catalyzed 1,3 Huisgen dipolar cycloaddition to connect functionalized nanocellulose with azide and alkyne groups, resulting in the formation of unique and regular arrays of nanorods. Such nanorods were then ready to mediate diverse azide-alkyne click reactions. In another context, paper, microcrystalline cellulose, CNF films, or CNCs can be functionalized toward carriers for drug delivery, pH-sensitive nanoparticles, anti-counterfeiting papers, immunosensors, and other advanced materials through photo-induced thiol-ene reactions (Liang et al., 2023).

7.3.3.3 Polymer Grafting

Grafting polymers onto cellulose fibers, nanofibers or nanocrystals involve modifying the glucan chains at the surface, offering diverse ways for the development of advanced materials. Many of the reactions described up to this point can be directly used for grafting. For example, a polymer or oligomer with terminal carboxyl groups can be attached to the primary hydroxy groups of cellulose chains by esterification. Likewise, the aldehyde groups of DAC can give way to Schiff bases with polymers containing primary amino groups. Finally, copper-catalyzed azide-alkyne cycloadditions can allow for the grafting of poly[methoxy(oligoethylene glycol methacrylate)] on CNCs (Roberts et al., 2020).

More specifically, there is probably more room for innovation in what pertains to in situ polymerization techniques over cellulosic materials. In ring-opening polymerization (ROP), polymer brushes are grown from the hydroxy groups on the surface of cellulose, which act as initiation sites. ROP can be used to graft and polymerize cyclic monomers, including lactones, onto the surface of CNCs. The ROP-mediated grafting of lactic acid oligomers or PLA onto nanocellulose has been extensively studied, often involving tin(II) octoate as a catalyst (Gomri et al., 2022). Alternatively, cellulose chains can be modified to introduce specific initiation sites for controlled polymerization techniques, such as atom transfer polymerization, which allows for a definite average molecular weight with low polydispersity (Habibi et al., 2013).

7.4 Conclusions and Prospects

The long tradition of cellulose derivatives has seen many changes since the first esterifications toward CN, CX, and CA, back in the nineteenth century. On one hand, formerly highly marketed cellulose esters have been progressively replaced with fossil-based plastics, which in some cases imply safer processes (e.g., the use of CS_2 for CX still raises issues). On the other hand, as understood from the literature reviewed herein, the growing interest in bio-sourced and biodegradable materials has caused a revamp of cellulose modification in the last two decades.

Common chemical modifications of cellulose include those that are customary for simple alcohols, namely esterification, etherification, and oxidation. The synthesis of both ethers and esters implies the nucleophilic attack of cellulose's hydroxy groups on electrophilic reagents. Nonetheless, the weak nucleophilicity of these groups usually forces manufacturers to employ high alkali charges in the production of CX, MC, HEC, and CMC, among other derivatives. Deprotonated hydroxy groups (alkoxy groups) are better nucleophiles, but in aqueous media they compete with OH^- ions. The resulting high pH of the system causes not only the hydrolysis of the electrophilic reagent (e.g., chloroacetate to glycolate), but also the depolymerization of cellulose. The use of aprotic organic liquids or certain deep eutectic

solvents allows for a higher reaction efficiency, but at the expense of lower techno-economic viability.

The weak nucleophilicity of hydroxy groups is also the reason why CA, CAP, and CAB are not synthesized by direct reaction of hydroxy groups with carboxylic acids, which are poor electrophiles. Instead, acids are used in combination with their more reactive counterparts, namely acetic anhydride, propionic anhydride, and butyric anhydride.

The most marketed cellulose derivatives are either ethers (CMC, HEC, MC) or esters (CA and its mixed esters, CN, CX). The ethers are often used as thickeners and/or stabilizers, while the esters are appreciated for their film-forming ability and their solubility in common organic solvents. In contrast, oxidized cellulose derivatives are currently regarded as niche markets, but they are of utmost importance in the literature. The oxidation of hydroxy groups to carboxyl groups is one of the most common chemical treatments leading to nanocellulose. This can be done in many non-selective ways, but the choice of TEMPO-mediated regioselective oxidation has become hugely popular in the last two decades. Furthermore, for some applications, it is desired for oxidation to stop at aldehydes. DAC, commonly produced by periodate oxidation, is a versatile platform toward many other cellulose derivatives.

Recent trends involve a focus on nanocellulose, be it CNFs or CNCs, and this is expected to be further developed in the near future. Some nanocellulose modifications include etherifications and esterifications that had previously been highly exploited for cellulosic fibers before research interests shifted to their nanoscale counterparts. In addition, the higher specific surface area of nanocellulose generates new possibilities for EDC-mediated amidation, silane coupling hydrophobization, silane coupling amination, phosphorylation, and other modifications that were used to display a more limited spectrum of applications when exerted on traditional cellulosic materials.

Despite the bio-sourced nature of cellulose, many of the common derivatizing agents, such as ethylene oxide and methyl chloride, are produced from fossil resources. It is reasonable to expect a shift toward naturally occurring agents, such as enzymes and fatty acids from vegetable oils. The latter, as discussed above for carboxylic acids in general, have low reactivity for the direct esterification of cellulose, but conversion into FAME and subsequent transesterification has been proposed as a successful workaround. Researchers will also tend to adapt cellulose to the overall advances in polymer chemistry, as it has been done in the case of click reactions (e.g., photoinduced thiol-ene reactions), and ROP-mediated grafting on the surface of cellulosic materials.

References

Abdellah Ali, S. F., William, L. A., & Fadl, E. A. (2020). Cellulose acetate, cellulose acetate propionate and cellulose acetate butyrate membranes for water desalination applications. *Cellulose, 27*, 9525–9543. https://doi.org/10.1007/s10570-020-03434-w

Aguado, R., Lourenço, A. F., Ferreira, P. J. T., Moral, A., & Tijero, A. (2019). The relevance of the pretreatment on the chemical modification of cellulosic fibers. *Cellulose, 26*, 5925–5936. https://doi.org/10.1007/s10570-019-02517-7

Aouay, M., Aguado, R. J., Bayés, G., Fiol, N., Putaux, J.-L., Boufi, S., & Delgado-Aguilar, M. (2024). In-situ synthesis and binding of silver nanoparticles to dialdehyde and carboxylated cellulose nanofibrils, and active packaging therewith. *Cellulose, 31*, 5687–5706. https://doi.org/10.1007/s10570-024-05918-5

Bastida, G. A., Aguado, R. J., Fiol, N., Delgado-Aguilar, M., Zanuttini, M. Á., Galván, M. V., & Tarrés, Q. (2024a). Emulsions, dipsticks and membranes based on oxalic acid-treated nanocellulose for the detection of aqueous and gaseous $HgCl_2$. *Cellulose, 31*, 5635–5651. https://doi.org/10.1007/s10570-024-05950-5

Bastida, G. A., Aguado, R. J., Galván, M. V., Zanuttini, M. Á., Delgado-Aguilar, M., & Tarrés, Q. (2024b). Impact of cellulose nanofibers on cellulose acetate membrane performance. *Cellulose, 31*, 2221–2238. https://doi.org/10.1007/s10570-024-05760-9

Basu, S., Malik, S., Joshi, G., Gupta, P. K., & Rana, V. (2021). Utilization of bio-polymeric additives for a sustainable production strategy in pulp and paper manufacturing: A comprehensive review. *Carbohydrate Polymer Technologies and Applications, 2*, 100050. https://doi.org/10.1016/j.carpta.2021.100050

Bialik, E., Stenqvist, B., Fang, Y., Östlund, Å., Furó, I., Lindman, B., Lund, M., & Bernin, D. (2016). Ionization of cellobiose in φqueous φlkali and the ьechanism of cellulose вissolution. *Journal of Physical Chemistry Letters, 7*, 5044–5048. https://doi.org/10.1021/acs.jpclett.6b02346

Biyani, M. V., Foster, E. J., & Weder, C. (2013). Light-pealable ыupramolecular тanocomposites иased on ьodified cellulose мanocrystals. *ACS Macro Letters, 2*, 236–240. https://doi.org/10.1021/mz400059w

Boujemaoui, A., Mongkhontreerat, S., Malmström, E., & Carlmark, A. (2015). Preparation and characterization of functionalized cellulose nanocrystals. *Carbohydrate Polymers, 115*, 457–464. https://doi.org/10.1016/j.carbpol.2014.08.110

Brandenberger, J. E. (1915). *Sensitive photographic film*. US Patent No. 1221825.

Butkova, N. T., Petrova, N. I., Tokareva, T. I., Malyugin, Y. Y., Pakshver, A. B., Finger, G. G., & Sofronova, I. S. (1979). Textile yarn from viscose with a lower NaOH/α-cellulose ratio due to a decrease in the carbon disulfide content. *Fibre Chemistry, 10*, 258–261. https://doi.org/10.1007/BF00545115

Cao, Y., Zhang, J., He, J., Li, H., & Zhang, Y. (2010). Homogeneous acetylation of cellulose at relatively high concentrations in an ionic liquid. *Chinese Journal of Chemical Engineering, 18*, 515–522. https://doi.org/10.1016/S1004-9541(10)60252-2

Chen, M., Li, R.-M., Runge, T., Feng, J., Feng, J., Hu, S., & Shi, Q.-S. (2019). Solvent-free acetylation of cellulose by 1-Ethyl-3-methylimidazolium acetate-catalyzed transesterification. *ACS Sustainable Chemistry & Engineering, 7*, 16971–16978. https://doi.org/10.1021/acssuschemeng.8b06333

Chen, P., Wohlert, J., Berglund, L., & Furó, I. (2022). Water as an intrinsic structural element in cellulose fibril aggregates. *Journal of Physical Chemistry Letters, 13*, 5424–5430. https://doi.org/10.1021/acs.jpclett.2c00781

Chen, Z., Xie, Z., & Jiang, H. (2023). Extraction of the cellulose nanocrystals via ammonium persulfate oxidation of beaten cellulose fibers. *Carbohydrate Polymers, 318*, 121129. https://doi.org/10.1016/j.carbpol.2023.121129

Cheng, X., Liang, H., Ding, A., Qu, F., Shao, S., Liu, B., Wang, H., Wu, D., & Li, G. (2016). Effects of pre-ozonation on the ultrafiltration of different natural organic matter (NOM) fractions: Membrane fouling mitigation, prediction and mechanism. *Journal of Membrane Science, 505*, 15–25. https://doi.org/10.1016/j.memsci.2016.01.022

Cheung, C. (2014). *Studies of the nitration of cellulose-application in new membrane materials*. Doctoral dissertation, University of British Columbia.

Cross, C. F., & Bevan, E. J. (1894). *Manufacture of cellulose acetate*. US Patent No. 513,466.

Cross, CF, et al. (1892) *Improvements in dissolving cellulose and allied compounds*. British Patent No. 8,700.

Czaja, W. K., Young, D. J., Kawecki, M., & Brown, R. M. (2007). The future prospects of microbial cellulose in biomedical applications. *Biomacromolecules, 8*, 1–12. https://doi.org/10.1021/bm060620d

Dalei, G., Das, S., & Pradhan, M. (2022). Dialdehyde cellulose as a niche material for versatile applications: An overview. *Cellulose, 29*, 5429–5461. https://doi.org/10.1007/s10570-022-04619-1

Diop, C. I. K., Li, H. L., Xie, B. J., & Shi, J. (2011). Effects of acetic acid/acetic anhydride ratios on the properties of corn starch acetates. *Food Chemistry, 126*, 1662–1669. https://doi.org/10.1016/j.foodchem.2010.12.050

Douard, L., Belgacem, M. N., & Bras, J. (2022). Extraction of carboxylated nanocellulose by combining mechanochemistry and NADES. *ACS Sustainable Chemistry & Engineering, 10*, 13017–13025. https://doi.org/10.1021/acssuschemeng.2c02783

Elalami, D., Aouine, M., Monlau, F., Guillon, F., Dumon, C., Hernandez Raquet, G., & Barakat, A. (2022). Enhanced enzymatic hydrolysis of corn stover using twin-screw extrusion under mild conditions. *Biofuels, Bioproducts Biorefining, 16*, 1642–1654. https://doi.org/10.1002/bbb.2400

Euring, M., Trojanowski, J., & Kharazipour, A. (2013). Laccase-mediator catalyzed modification of wood fibers: Studies on the reaction mechanism and making of medium-density fiberboard. *Forest Products Journal, 63*, 54–60. https://doi.org/10.13073/FPJ-D-12-00075

Filpponen, I., & Argyropoulos, D. S. (2010). Regular linking of cellulose nanocrystals via click chemistry: Synthesis and formation of cellulose nanoplatelet gels. *Biomacromolecules, 11*, 1060–1066. https://doi.org/10.1021/bm1000247

Foster, W. (1924). *Silk, its production and manufacture*. Sir Isaac Pitman & Sons, Ltd..

Frank, B. P., Durkin, D. P., Caudill, E. R., Zhu, L., White, D. H., Curry, M. L., Pedersen, J. A., & Fairbrother, D. H. (2018). Impact of silanization on the structure, dispersion properties, and biodegradability of nanocellulose as a nanocomposite filler. *ACS Applied Nano Materials, 1*, 7025–7038. https://doi.org/10.1021/acsanm.8b01819

French, A. D. (2014). Idealized powder diffraction patterns for cellulose polymorphs. *Cellulose, 21*, 885–896. https://doi.org/10.1007/s10570-013-0030-4

Gajdziok, J., Bajerová, M., Chalupová, Z., & Rabišková, M. (2010). Oxycellulose as mucoadhesive polymer in buccal tablets. *Drug Development and Industrial Pharmacy, 36*, 1115–1130. https://doi.org/10.3109/03639041003690031

Ghasemlou, M., Daver, F., Ivanova, E. P., Habibi, Y., & Adhikari, B. (2021). Surface modifications of nanocellulose: From synthesis to high-performance nanocomposites. *Progress in Polymer Science, 119*, 101418. https://doi.org/10.1016/j.progpolymsci.2021.101418

Gomri, C., Cretin, M., & Semsarilar, M. (2022). Recent progress on chemical modification of cellulose nanocrystal (CNC) and its application in nanocomposite films and membranes-a comprehensive review. *Carbohydrate Polymers, 294*, 119790. https://doi.org/10.1016/j.carbpol.2022.119790

Guo, B., Glavas, L., & Albertsson, A.-C. (2013). Biodegradable and electrically conducting polymers for biomedical applications. *Progress in Polymer Science, 38*, 1263–1286. https://doi.org/10.1016/J.PROGPOLYMSCI.2013.06.003

Guo, L., Huang, C., & Guo, J. (2024). Chapter 8: Hydrophobic modifications on nanocellulose. In N. Lin & G. Zhu (Eds.), *Surface modifications of Nanocellulose* (pp. 263–295). Elsevier.

Gupta, R. K. (2024). *Click chemistry*. CRC Press.

Gutjahr, H., & Koch, R. R. (2003). Direct print coloration. In L. W. C. Miles (Ed.), *Textile printing* (Revised 2 ed., pp. 153–178). Society of Dyers and Colourists.

Habibi, Y., Benali, S., & Dubois, P. (2013). In situ polymerization of bionanocomposites. In K. Oksman, A. P. Mathew, A. Bismarck, O. Rojas, & M. Sain (Eds.), *Handbook of green materials* (pp. 69–88). World Scientiific. https://doi.org/10.1142/9789814566469_0020

Harrison, K. (2007). Introduction to polymeric drug delivery systems. In M. Jenkins (Ed.), *Biomedical polymers* (pp. 33–56). Woodhead Publishing.

Hassani, F.-Z. S. A., Kassab, Z., El Achaby, M., Bouhfid, R., & el Kacem, Q. A. (2021). Mechanical modeling of hybrid nanocomposites based on cellulose nanocrystals/nanofibrils

and nanoparticles. In D. Rodrigue, A. Kacem Qaiss, & R. Bouhfid (Eds.), *Cellulose Nanocrystal/Nanoparticles Hybrid Nanocomposites* (pp. 247–270). Woodhead Publishing.

Hebeish, A., Moursi, A. Z., Waly, A., & El-Rafie, M. H. (1979). Dyeing of chemically modified cellulose. IV. Dyeing of oxidized celluloses with some reactive and direct dyes. *Journal of Applied Polymer Science, 24*, 385–394. https://doi.org/10.1002/app.1979.070240207

Heinze, T., El Seoud, O. A., & Koschella, A. (2018a). Cellulose esters. In T. Heinze, O. A. El Seoud, & A. Koschella (Eds.), *Cellulose derivatives: Synthesis, structure, and properties* (pp. 293–427). Springer International Publishing.

Heinze, T., El Seoud, O. A., & Koschella, A. (2018b). Etherification of cellulose. In T. Heinze, O. A. El Seoud, & A. Koschella (Eds.), *Cellulose derivatives: Synthesis, structure, and properties* (pp. 429–477). Springer.

Hirota, M., Tamura, N., Saito, T., & Isogai, A. (2009). Oxidation of regenerated cellulose with $NaClO_2$ catalyzed by TEMPO and NaClO under acid-neutral conditions. *Carbohydrate Polymers, 78*, 330–335. https://doi.org/10.1016/j.carbpol.2009.04.012

Höfer, T., Rössler, A., & Strube, O. I. (2024). Thermal debonding on demand for wood coatings via nitrocellulose-based primer. *Progress in Organic Coating, 188*, 108215. https://doi.org/10.1016/j.porgcoat.2024.108215

Holme, I., & Blackburn, R. S. (2019). John Mercer FRS, FCS, MPhS, JP: The father of textile chemistry. *Coloration Technology, 135*, 171–182. https://doi.org/10.1111/cote.12398

Holtzapple, M. T. (2003). Cellulose. In B. Caballero (Ed.), *Encyclopedia of food sciences and nutrition* (2nd ed., pp. 998–1007). Academic Press.

Hyatt, J. W. (1870). *Improvement in treating and molding Pyroxylin*. US Patent No. 105,338.

Illy, N., Fache, M., Ménard, R., Negrell, C., Caillol, S., & David, G. (2015). Phosphorylation of bio-based compounds: The state of the art. *Polymer Chemistry, 6*, 6257–6291. https://doi.org/10.1039/C5PY00812C

Inaba, Y., Tamaki, S., Ikebukuro, H., Yamada, K., Ozaki, H., & Yoshida, K. (2017). Effect of changing table tennis ball material from celluloid to plastic on the post-collision ball trajectory. *Journal of Human Kinetics, 55*, 29–38. https://doi.org/10.1515/hukin-2017-0004

Isogai, A., Saito, T., & Fukuzumi, H. (2011). TEMPO-oxidized cellulose nanofibers. *Nanoscale, 3*, 71–85. https://doi.org/10.1039/c0nr00583e

Jaušovec, D., Vogrinčič, R., & Kokol, V. (2015). Introduction of aldehyde vs. carboxylic groups to cellulose nanofibers using laccase/TEMPO mediated oxidation. *Carbohydrate Polymers, 116*, 74–85. https://doi.org/10.1016/j.carbpol.2014.03.014

Kanis, L. A., Marques, E. L., Zepon, K. M., Pereira, J. R., Pamato, S., de Oliveira, M. T., Danielski, L. G., & Petronilho, F. C. (2014). Cellulose acetate butyrate/poly(caprolactonetriol) blends: Miscibility, mechanical properties, and in vivo inflammatory response. *Journal of Biomaterials Applications, 29*, 654–661. https://doi.org/10.1177/0885328214542488

Karim, Z., Afrin, S., Husain, Q., & Danish, R. (2017). Necessity of enzymatic hydrolysis for production and functionalization of nanocelluloses. *Critical Reviews in Biotechnology, 37*, 355–370. https://doi.org/10.3109/07388551.2016.1163322

Khoshnevisan, K., Maleki, H., Samadian, H., Shahsavari, S., Sarrafzadeh, M. H., Larijani, B., Dorkoosh, F. A., Haghpanah, V., & Khorramizadeh, M. R. (2018). Cellulose acetate electrospun nanofibers for drug delivery systems: Applications and recent advances. *Carbohydrate Polymers, 198*, 131–141. https://doi.org/10.1016/j.carbpol.2018.06.072

Klug, E. D., & Tinsley, J. S. (1946). *Preparation of carboxyalkyl ethers of cellulose*. US Patent 2,517,577.

Larsen, F. H., Schöbitz, M., & Schaller, J. (2012). Hydration properties of regioselectively etherified celluloses monitored by 2H and 13C solid-state MAS NMR spectroscopy. *Carbohydrate Polymers, 89*, 640–647. https://doi.org/10.1016/j.carbpol.2012.03.067

Li, W., Zhao, H., Teasdale, P. R., John, R., & Zhang, S. (2002). Application of a cellulose phosphate ion exchange membrane as a binding phase in the diffusive gradients in thin films technique for measurement of trace metals. *Analytica Chimica Acta, 464*, 331–339. https://doi.org/10.1016/S0003-2670(02)00492-0

Li, P., Sirviö, J. A., Asante, B., & Liimatainen, H. (2018). Recyclable deep eutectic solvent for the production of cationic nanocelluloses. *Carbohydrate Polymers, 199*, 219–227. https://doi.org/10.1016/j.carbpol.2018.07.024

Li, J., Kang, L., Wang, B., Chen, K., Tian, X., Ge, Z., Zeng, J., Xu, J., & Gao, W. (2019). Controlled release and long-term antibacterial activity of dialdehyde nanofibrillated cellulose/Silver nanoparticle composites. *ACS Sustainable Chemistry & Engineering, 7*, 1146–1158. https://doi.org/10.1021/acssuschemeng.8b04799

Li, T., Chen, C., Brozena, A. H., Zhu, J. Y., Xu, L., Driemeier, C., Dai, J., Rojas, O. J., Isogai, A., Wågberg, L., & Hu, L. (2021). Developing fibrillated cellulose as a sustainable technological material. *Nature, 590*, 47–56. https://doi.org/10.1038/s41586-020-03167-7

Liang, H., Yin, D., Shi, L., Liu, Y., Hu, X., Zhu, N., & Guo, K. (2023). Surface modification of cellulose via photo-induced click reaction. *Carbohydrate Polymers, 301*, 120321. https://doi.org/10.1016/j.carbpol.2022.120321

Liimatainen, H., Visanko, M., Sirviö, J. A., Hormi, O. E. O., & Niinimaki, J. (2012). Enhancement of the nanofibrillation of wood cellulose through sequential periodate-chlorite oxidation. *Biomacromolecules, 13*, 1592–1597. https://doi.org/10.1021/bm300319m

Liu, Y., Liu, L., Wang, K., Zhang, H., Yuan, Y., Wei, H., Wang, X., Duan, Y., Zhou, L., & Zhang, J. (2020). Modified ammonium persulfate oxidations for efficient preparation of carboxylated cellulose nanocrystals. *Carbohydrate Polymers, 229*, 115572. https://doi.org/10.1016/j.carbpol.2019.115572

Maderuelo-Sanz, R. (2021). Characterizing and modelling the sound absorption of the cellulose acetate fibers coming from cigarette butts. *Journal of Environmental Health Science and Engineering, 19*, 1075–1086. https://doi.org/10.1007/s40201-021-00675-0

Maekawa, E., Kosaki, T., & Koshijima, T. (1986). Periodate oxidation of mercerized cellulose and regenerated cellulose. *Wood Research (Bulletin of the Wood Research Institute Kyoto University), 73*, 44–49.

Manimaran, M., Norizan, M. N., Kassim, M. H. M., Adam, M. R., Norrrahim, M. N. F., & Knight, V. F. (2024). Critical assessment of the thermal stability and degradation of chemically functionalized nanocellulose-based polymer nanocomposites. *Nanotechnology Reviews, 13*(1), 20240005. https://doi.org/10.1515/ntrev-2024-0005

Marrez, D. A., Abdelhamid, A. E., & Darwesh, O. M. (2019). Eco-friendly cellulose acetate green synthesized silver nano-composite as antibacterial packaging system for food safety. *Food Packaging and Shelf Life, 20*, 100302. https://doi.org/10.1016/j.fpsl.2019.100302

Martina, B., Kateřina, K., Miloslava, R., Jan, G., & Ruta, M. (2009). Oxycellulose: Significant characteristics in relation to its pharmaceutical and medical applications. *Advances in Polymer Technology, 28*, 199–208. https://doi.org/10.1002/adv.20161

Marziano, N. C., Tomasin, A., Tortato, C., & Zaldivar, J. (1998). Thermodynamic nitration rates of aromatic compounds. Part 4. Temperature dependence in sulfuric acid of $HNO_3 \rightarrow NO_2+$ equilibrium, nitration rates and acidic properties of the solvent. *Journal of the Chemical Society, Perkin Transactions, 2*, 1973–1982. https://doi.org/10.1039/A802521E

Mazega, A., Santos, A. F., Aguado, R., Tarrés, Q., Fiol, N., Pèlach, M. À., & Delgado-Aguilar, M. (2023). Kinetic study and real-time monitoring strategy for TEMPO-mediated oxidation of bleached eucalyptus fibers. *Cellulose, 30*, 1421–1436. https://doi.org/10.1007/s10570-022-05013-7

Mazega, A., Fortuny, M., Signori-Iamin, G., Aguado, R. J., Tarrés, Q., Santos, A. F., & Delgado-Aguilar, M. (2024). Near-infrared spectroscopy and multivariate analysis as real-time monitoring strategy of TEMPO-mediated oxidation of cellulose fibers from different feedstocks. *Cellulose, 31*, 3465–3482. https://doi.org/10.1007/s10570-024-05824-w

Moral, A., Aguado, R., & Tijero, A. (2016). Cationization of native and alkalized cellulose: Mechanismand kinetics. *Cellulose Chemistry and Technology, 50*, 109–115.

Moral, A., Aguado, R., Jarabo, R., & Tijero, A. (2017). Cationized fibers from pine kraft pulp: Advantages of refining before functionalization. *Holzforschung, 71*, 843–851. https://doi.org/10.1515/hf-2017-0023

Morris, B. A. (2017). Commonly used resins and substrates in flexible packaging. In B. A. Morris (Ed.), *The science and technology of flexible packaging* (pp. 69–119). William Andrew Publishing.

Morris, E., Pulham, C. R., & Morrison, C. A. (2023). Structure and properties of nitrocellulose: Approaching 200 years of research. *RSC Advances, 13*, 32321–32333. https://doi.org/10.1039/D3RA05457H

Moss, G. P., Smith, P. A. S., & Tavernier, D. (1995). Glossary of class names of organic compounds and reactivity intermediates based on structure (IUPAC recommendations 1995). *Pure and Applied Chemistry, 67*, 1307–1375. https://doi.org/10.1351/pac199567081307

Mu, X., & Gray, D. G. (2014). Formation of chiral nematic films from cellulose nanocrystal suspensions is a two-stage process. *Langmuir, 30*, 9256–9260. https://doi.org/10.1021/la501741r

Muvhiiwa, R., Mawere, E., Moyo, L. B., & Tshuma, L. (2021). Utilization of cellulose in tobacco (Nicotiana tobacum) stalks for nitrocellulose production. *Heliyon, 7*, e07598. https://doi.org/10.1016/j.heliyon.2021.e07598

Odabas, N., Amer, H., Henniges, U., Potthast, A., & Rosenau, T. (2017). A comparison of methods to quantify cationization of cellulosic pulps. *Journal of Wood Chemistry and Technology, 37*, 136–147. https://doi.org/10.1080/02773813.2016.1253100

Pääkkönen, T., Pönni, R., Dou, J., Nuopponen, M., & Vuorinen, T. (2017). Activation of TEMPO by ClO_2 for oxidation of cellulose by hypochlorite—Fundamental and practical aspects of the catalytic system. *Carbohydrate Polymers, 174*, 524–530. https://doi.org/10.1016/j.carbpol.2017.06.117

Parkes, A. (1856). *Patent for improvements in treating vegetable Fibres and other substances to render them waterproof and applicable to various useful purposes*. British Patent No. 2353.

Patoary, M. K., Islam, S. R., Farooq, A., Rashid, M. A., Sarker, S., Hossain, M. Y., Rakib, M. A. N., Al-Amin, M., & Liu, L. (2023). Phosphorylation of nanocellulose: State of the art and prospects. *Industrial Crops and Products, 201*, 116965. https://doi.org/10.1016/j.indcrop.2023.116965

Pedrosa, J. F. S., Rasteiro, M. G., Neto, C. P., & Ferreira, P. J. T. (2022). Effect of cationization pretreatment on the properties of cationic Eucalyptus micro/nanofibrillated cellulose. *International Journal of Biological Macromolecules, 201*, 468–479. https://doi.org/10.1016/j.ijbiomac.2022.01.068

Pinto, E., Aggrey, W. N., Boakye, P., Amenuvor, G., Sokama-Neuyam, Y. A., Fokuo, M. K., Karimaie, H., Sarkodie, K., Adenutsi, C. D., Erzuah, S., & Rockson, M. A. D. (2022). Cellulose processing from biomass and its derivatization into carboxymethylcellulose: A review. *Scientific African, 15*, e01078. https://doi.org/10.1016/j.sciaf.2021.e01078

Prado, H. J., & Matulewicz, M. C. (2014). Cationization of polysaccharides : A path to greener derivatives with many industrial applications. *European Polymer Journal, 52*, 53–75. https://doi.org/10.1016/j.eurpolymj.2013.12.011

Qiao, A., Cui, M., Huang, R., Ding, G., Qi, W., He, Z., Klemeš, J. J., & Su, R. (2021). Advances in nanocellulose-based materials as adsorbents of heavy metals and dyes. *Carbohydrate Polymers, 272*, 118471. https://doi.org/10.1016/j.carbpol.2021.118471

Reis, D. T., de Aguiar Filho, S. Q., Grotto, C. G. L., Bihain, M. F. R., & Pereira, D. H. (2020). Carboxymethylcellulose and cellulose xanthate matrices as potential adsorbent material for potentially toxic Cr^{3+}, Cu^{2+} and Cd^{2+} metal ions: A theoretical study. *Theoretical Chemistry Accounts, 139*, 96. https://doi.org/10.1007/s00214-020-02610-2

Rhodes, C., Riddel, S. A., West, J., Williams, B. P., & Hutchings, G. J. (2000). The low-temperature hydrolysis of carbonyl sulfide and carbon disulfide: A review. *Catalysis Today, 59*, 443–464. https://doi.org/10.1016/S0920-5861(00)00309-6

Roberts, M. G., Yu, Q., Keunen, R., Liu, J., Ngae Wong, E. C., Rastogi, C. K., Reilly, R. M., Allen, C., & Winnik, M. A. (2020). Functionalization of cellulose nanocrystals with POEGMA copolymers via copper-catalyzed azide–alkyne cycloaddition for potential drug-delivery applications. *Biomacromolecules, 21*, 2014–2023. https://doi.org/10.1021/acs.biomac.9b01713

Robertson, R. M., Thomas, W. C., Suthar, J. N., & Brown, D. M. (2012). Accelerated degradation of cellulose acetate cigarette filters using controlled-release acid catalysis. *Green Chemistry, 14*, 2266–2272. https://doi.org/10.1039/C2GC16635F

Rogers, T. L., & Wallick, D. (2012). Reviewing the use of ethylcellulose, methylcellulose and hypromellose in microencapsulation. Part 1: Materials used to formulate microcapsules. *Drug Development and Industrial Pharmacy, 38*, 129–157. https://doi.org/10.3109/03639045.2011.590990

Rol, F., Sillard, C., Bardet, M., Yarava, J. R., Emsley, L., Gablin, C., Léonard, D., Belgacem, N., & Bras, J. (2020). Cellulose phosphorylation comparison and analysis of phosphorate position on cellulose fibers. *Carbohydrate Polymers, 229*, 115294. https://doi.org/10.1016/j.carbpol.2019.115294

Roman, C., Delgado, M. A., Fernández-Silva, S. D., & García-Morales, M. (2024). Green oleogels based on elm pulp cellulose nanofibers: Effect of the nanofibrillation pre-treatment on their thermo-rheological behavior. *Cellulose, 31*, 321–333. https://doi.org/10.1007/s10570-023-05664-0

Ruiz-Palomero, C., Soriano, M. L., & Valcárcel, M. (2015). β-Cyclodextrin decorated nanocellulose: A smart approach towards the selective fluorimetric determination of danofloxacin in milk samples. *Analyst, 140*, 3431–3438. https://doi.org/10.1039/C4AN01967A

Ruiz-Palomero, C., Soriano, M. L., & Valcárcel, M. (2016). Sulfonated nanocellulose for the efficient dispersive micro solid-phase extraction and determination of silver nanoparticles in food products. *Journal of Chromatography. A, 1428*, 352–358. https://doi.org/10.1016/j.chroma.2015.06.023

Saini, S., Belgacem, M. N., Salon, M.-C. B., & Bras, J. (2016). Non leaching biomimetic antimicrobial surfaces via surface functionalisation of cellulose nanofibers with aminosilane. *Cellulose, 23*, 795–810. https://doi.org/10.1007/s10570-015-0854-1

Saito, T., Kimura, S., Nishiyama, Y., & Isogai, A. (2007a). Cellulose nanofibers prepared by TEMPO-mediated oxidation of native cellulose. *Biomacromolecules, 8*, 2485–2491. https://doi.org/10.1021/bm0703970

Saito, T., Kimura, S., Nishiyama, Y., & Isogai, A. (2007b). Cellulose nanofibers prepared by TEMPO-mediated oxidation. *Biomacromolecules, 8*, 2485–2491. https://doi.org/10.1021/bm0703970

Schönbein, C. F. (1847). II. On the discovery of gun-cotton. *Philosophical Magazine and Journal of Science, 31*, 7–12.

Schützenberger, P. (1865). *Process of acetylating cellulose*. French Patent No. 16313.

Shanbhag, A., Barclay, B., Koziara, J., & Shivanand, P. (2007). Application of cellulose acetate butyrate-based membrane for osmotic drug delivery. *Cellulose, 14*, 65–71. https://doi.org/10.1007/s10570-006-9091-y

Sharma, P., Modi, S. R., & Bansal, A. K. (2015). Co-processing as a tool to improve aqueous dispersibility of cellulose ethers. *Drug Development and Industrial Pharmacy, 41*, 1745–1758. https://doi.org/10.3109/03639045.2015.1058814

Sharma, A., Mandal, T., & Goswami, S. (2021). Fabrication of cellulose acetate nanocomposite films with lignocelluosic nanofiber filler for superior effect on thermal, mechanical and optical properties. *Nano-Structures Nano-Objects, 25*, 100642. https://doi.org/10.1016/j.nanoso.2020.100642

Shenai, V. A., & Date, A. G. (1976). Studies in chemically modified celluloses. IX. Oxidation of cellulose in the presence of chelating agents. *Journal of Applied Polymer Science, 20*, 385–391. https://doi.org/10.1002/app.1976.070200211

Shoseyov, O., Kam, D., Ben Shalom, T., Shtein, Z., Vinkler, S., & Posen, Y. (2019). Nanocellulose composite biomaterials in industry and medicine. In E. Cohen & H. Merzendorfer (Eds.), *Extracellular sugar-based biopolymers matrices* (pp. 693–784). Springer.

Sievänen, K., Kavakka, J., Hirsilä, P., Vainio, P., Karisalmi, K., Fiskari, J., & Kilpeläinen, I. (2015). Cationic cellulose betainate for wastewater treatment. *Cellulose, 22*, 1861–1872. https://doi.org/10.1007/s10570-015-0578-2

Siller, M., Amer, H., Bacher, M., Roggenstein, W., Rosenau, T., & Potthast, A. (2015). Effects of periodate oxidation on cellulose polymorphs. *Cellulose, 22*, 2245–2261. https://doi.org/10.1007/s10570-015-0648-5

Singh, S. C., & Murthy, Z. V. P. (2017). Study of cellulosic fibres morphological features and their modifications using hemicelluloses. *Cellulose, 24*, 3119–3130. https://doi.org/10.1007/s10570-017-1353-3

Siró, I., Plackett, D., Hedenqvist, M., Ankerfors, M., & Lindström, T. (2011). Highly transparent films from carboxymethylated microfibrillated cellulose: The effect of multiple homogenization steps on key properties. *Journal of Applied Polymer Science, 119*, 2652–2660. https://doi.org/10.1002/app.32831

Sirviö, J., Liimatainen, H., Niinimäki, J., & Hormi, O. (2011). Dialdehyde cellulose microfibers generated from wood pulp by milling-induced periodate oxidation. *Carbohydrate Polymers, 86*, 260–265. https://doi.org/10.1016/j.carbpol.2011.04.054

Siyawamwaya, M., Choonara, Y. E., Kumar, P., Kondiah, P. P. D., du Toit, L. C., & Pillay, V. (2016). A humic acid-polyquaternium-10 stoichiometric self-assembled fibrilla polyelectrolyte complex: Effect of pH on synthesis, characterization, and drug release. *International Journal of Polymeric Materials and Polymeric Biomaterials, 65*, 550–560. https://doi.org/10.1080/00914037.2016.1149843

Spier, V. C., Sierakowski, M. R., Reed, W. F., & de Freitas, R. A. (2017). Polysaccharide depolymerization from TEMPO-catalysis: Effect of TEMPO concentration. *Carbohydrate Polymers, 170*, 140–147. https://doi.org/10.1016/j.carbpol.2017.04.064

Steger, S., Eggert, G., Horn, W., & Krekel, C. (2022). Are cellulose ethers safe for the conservation of artwork? New insights in their VOC activity by means of Oddy testing. *Heritage Science, 10*, 53. https://doi.org/10.1186/s40494-022-00688-4

Sun, D.-P., Ma, B., Zhu, C.-L., Liu, C.-S., & Yang, J.-Z. (2010). Novel nitrocellulose made from bacterial cellulose. *Journal of Energetic Materials, 28*, 85–97. https://doi.org/10.1080/07370650903222551

Suter, U. W. (2013). Why was the macromolecular hypothesis such a big deal? In V. Percec (Ed.), *Hierarchical macromolecular structures: 60 years after the Staudinger Nobel prize I* (pp. 61–80). Springer.

Tarrés, Q., Boufi, S., Mutjé, P., & Delgado-Aguilar, M. (2017). Enzymatically hydrolyzed and TEMPO-oxidized cellulose nanofibers for the production of nanopapers: Morphological, optical, thermal and mechanical properties. *Cellulose, 24*, 3943–3954. https://doi.org/10.1007/s10570-017-1394-7

Tedeschi, G., Guzman-Puyol, S., Paul, U. C., Barthel, M. J., Goldoni, L., Caputo, G., Ceseracciu, L., Athanassiou, A., & Heredia-Guerrero, J. A. (2018). Thermoplastic cellulose acetate oleate films with high barrier properties and ductile behaviour. *Chemical Engineering Journal, 348*, 840–849. https://doi.org/10.1016/j.cej.2018.05.031

Tojo, G., & Fernández, M. (2007). Oxidation of alcohols to carboxylic acids via isolated aldehydes. In G. Tojo & M. Fernández (Eds.), *Oxidation of primary alcohols to carboxylic acids* (pp. 105–109). Springer.

Ünlü, C. H. (2013). Carboxymethylcellulose from recycled newspaper in aqueous medium. *Carbohydrate Polymers, 97*, 159–164. https://doi.org/10.1016/j.carbpol.2013.04.039

Voicu, S. I., Condruz, R. M., Mitran, V., Cimpean, A., Miculescu, F., Andronescu, C., Miculescu, M., & Thakur, V. K. (2016). Sericin covalent immobilization onto cellulose acetate membrane for biomedical applications. *ACS Sustainable Chemistry & Engineering, 4*, 1765–1774. https://doi.org/10.1021/acssuschemeng.5b01756

Wang, Y., & Huang, J.-T. (2021). Transparent, conductive and superhydrophobic cellulose films for flexible electrode application. *RSC Advances, 11*, 36607–36616. https://doi.org/10.1039/D1RA06865B

Wang, N., Zhu, G., & Lin, N. (2024). Fluorescent modifications on nanocellulose. In N. Lin & G. Zhu (Eds.), *Surface modifications of nanocellulose* (pp. 139–193). Elsevier.

Wei, L., Agarwal, U. P., Hirth, K. C., Matuana, L. M., Sabo, R. C., & Stark, N. M. (2017). Chemical modification of nanocellulose with canola oil fatty acid methyl ester. *Carbohydrate Polymers, 169*, 108–116. https://doi.org/10.1016/j.carbpol.2017.04.008

Weißl, M., Niegelhell, K., Reishofer, D., Zankel, A., Innerlohinger, J., & Spirk, S. (2018). Homogeneous cellulose thin films by regeneration of cellulose xanthate: Properties and characterization. *Cellulose, 25*, 711–721. https://doi.org/10.1007/s10570-017-1576-3

Williamson, A. W. (1903). Papers on etherification and on the constitution of salts. *Journal of the American Chemical Society, 25*(5), 548. https://doi.org/10.1021/ja02007a027

Wolfs, J., & Meier, M. A. R. (2021). A more sustainable synthesis approach for cellulose acetate using the DBU/CO_2 switchable solvent system. *Green Chemistry, 23*, 4410–4420. https://doi.org/10.1039/D1GC01508G

Wsoo, M. A., Shahir, S., Mohd Bohari, S. P., Nayan, N. H. M., & Razak, S. I. A. (2020). A review on the properties of electrospun cellulose acetate and its application in drug delivery systems: A new perspective. *Carbohydrate Research, 491*, 107978. https://doi.org/10.1016/j.carres.2020.107978

Wu, Y. D., He, J. M., Huang, Y. D., Wang, F. W., & Tang, F. (2012). Oxidation of regenerated cellulose with nitrogen dioxide/carbon tetrachloride. *Fibers and Polymers, 13*, 576–581. https://doi.org/10.1007/s12221-012-0576-z

Xia, L., Zhao, J., Lu, B., Liu, C., & Zhuang, X. (2024). Solar-responsive Bi_2S_3/ZnS heterojunction-loaded chitosan/cellulose sponges for adsorption-photocatalytic degradation of Congo red. *Fibers and Polymers, 25*, 1645–1654. https://doi.org/10.1007/s12221-024-00537-0

Xu, Q. H., Li, W. G., Cheng, Z. L., Yang, G., & Qin, M. H. (2014). TEMPO/NaBr/NaClO-mediated surface oxidation of nanocrystalline cellulose and its microparticulate retention system with cationic polyacrylamide. *BioResources, 9*, 994–1006.

Xu, Q., Song, L., Zhang, L., Hu, G., Chen, Q., Liu, E., Liu, Y., Zheng, Q., Xie, H., & Li, N. (2018). Synthesis of cellulose acetate propionate and cellulose acetate butyrate in a CO_2/DBU/DMSO system. *Cellulose, 25*, 205–216. https://doi.org/10.1007/s10570-017-1539-8

Yang, Y., Zhang, Y., Dawelbeit, A., Deng, Y., Lang, Y., & Yu, M. (2017). Structure and properties of regenerated cellulose fibers from aqueous NaOH/thiourea/urea solution. *Cellulose, 24*, 4123–4137. https://doi.org/10.1007/s10570-017-1418-3

Yoo, Y., & Youngblood, J. P. (2016). Green one-pot synthesis of surface hydrophobized cellulose nanocrystals in aqueous medium. *ACS Sustainable Chemistry & Engineering, 4*, 3927–3938. https://doi.org/10.1021/acssuschemeng.6b00781

Yoon, Y. I., Moon, H. S., Lyoo, W. S., Lee, T. S., & Park, W. H. (2009). Superhydrophobicity of cellulose triacetate fibrous mats produced by electrospinning and plasma treatment. *Carbohydrate Polymers, 75*, 246–250. https://doi.org/10.1016/j.carbpol.2008.07.015

Zhang, Q., Lin, D., & Yao, S. (2015). Review on biomedical and bioengineering applications of cellulose sulfate. *Carbohydrate Polymers, 132*, 311–322. https://doi.org/10.1016/j.carbpol.2015.06.041

Chapter 8
Surface Modification of the Paper Using Physical Methods

Hao Ing Yeoh, Niranjan Patra, Elisa Rasouli, and Bey Fen Leo

8.1 Introduction

Surface modification of cellulose is crucial given its extensive use in various applications where its natural properties may fall short. Although cellulose is a highly abundant, renewable, and biodegradable material (Heinze, 2015), its inherent characteristics, such as hydrophilicity and limited chemical reactivity (Coseri, 2017), can present challenges in processing and end-use applications. By altering the surface of cellulose, these limitations can be effectively overcome, leading to enhanced adhesion, wettability, and compatibility with other materials. This transformation enables cellulose to perform more effectively in a broader range of applications, making it a more versatile material overall.

The previous chapter discussed surface modification through chemical approaches, which offer a wide range of advantages, including enhanced functional properties, improved biocompatibility, and increased versatility of cellulose for various applications. Nevertheless, several limitations should be considered since altering the chemical compositions may cause challenge in preserving the bulk

H. I. Yeoh · E. Rasouli
Faculty of Medicine, Department of Molecular Medicine, Universiti Malaya, Kuala Lumpur, Malaysia

N. Patra
Department of Chemistry, Koneru Lakshmaiah Education Foundation, Vaddeswaram, Andhra Pradesh, India

B. F. Leo (✉)
Faculty of Medicine, Department of Molecular Medicine, Universiti Malaya, Kuala Lumpur, Malaysia

Nanotechnology and Catalysis Research Centre (NANOCAT), Institute for Advanced Studies, University of Malaya, Kuala Lumpur, Malaysia
e-mail: beyfenleo@um.edu.my

G. Korotcenkov (ed.), *The Handbook of Paper-Based Sensors and Devices*,
https://doi.org/10.1007/978-3-031-91080-7_8

properties of the paper. In addition, the environmental impact, particularly when scaling up, should also be considered given the increasing stringency of environmental regulations.

In this chapter, physical methods are introduced as a complementary approach to address certain limitations of chemical methods. Unlike chemical approaches, physical methods utilize physical forces and energy to modify surfaces while preserving the intrinsic bulk properties of the material. Common techniques such as corona discharge, plasma, ultraviolet (UV) radiation, and laser beams are widely used across industrial and research settings for various materials. This chapter aims to provide a comprehensive overview of physical surface modification techniques for different polymers, especially cellulose. The mechanisms, applications, and the advantages and limitations of these methods will be explored in detail in the following sections.

8.2 Surface Modification Using Physical Methods

8.2.1 Corona Surface Treatment

Corona surface treatment is a widely used method for enhancing the surface properties of polymeric materials, particularly to improve adhesion. It is a treatment in which the surface of the material is exposed to the corona discharge, an electrical discharge that causes ionization of the surrounding air, thus creating a reactive atmosphere. This treatment introduces polar functional groups and molecular changes to the surface of a material; therefore, the surface energy is increased and wettability for increased adhesion and printability is enhanced (Aydemir et al., 2021). Its efficiency and effectiveness make it a popular choice in various industries.

Mechanistically, the corona surface treatment involves generating a high-voltage corona discharge in an atmospheric environment. By producing a high potential difference between an electrode and the surface of the material, it ionizes air and produces different species like ozone, atomic oxygen, and other radicals in high concentration. These reactive species interact with the polymer surface, breaking C–H bonds to form new functional groups, such as carbonyl, C=O, hydroxyl, –OH, and carboxyl, –COOH, groups, among others. Popelka et al. (2018) observed that when linear low-density polyethylene (LLDPE) is corona-treated, high-energy species coming from the corona discharge induce the incorporation of polar functional group at the polymer surface. These reactions bear oxygen-containing functional groups and lead to a substantial increase in the surface energy of PE, which is otherwise non-polar and hydrophobic (Fig. 8.1). Such remarkable increase in surface roughness positively correlated with the time of exposure, leading to increased adhesive and wettability on substrate surface (Fig. 8.2).

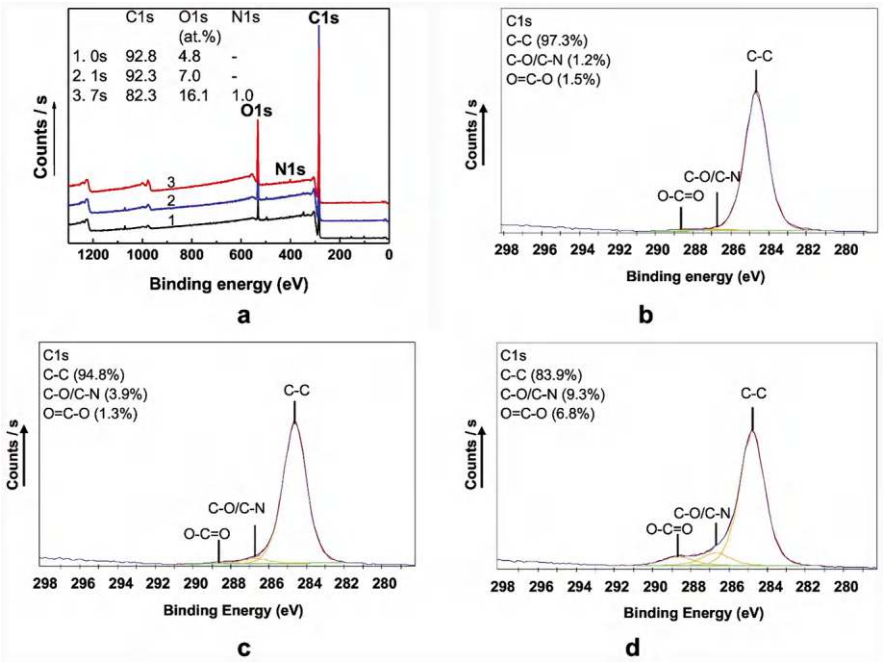

Fig. 8.1 XPS spectra of: (**a**) untreated and corona-treated LLDPE samples; and C1s spectra of LLDPE samples; (**b**) untreated, (**c**) 1 s corona-treated, and (**d**) 7 s corona-treated. Reproduced with permission from Popelka et al. (2018). Copyright 2018, Elsevier

8.2.1.1 Applications

Table 8.1 shows that corona surface treatment is widely used to improve the adhesion properties of inks, coatings, and adhesives on various flexible substrates made from materials, such as polyethylene, polypropylene, cellulose, and paper. These substrates, especially polymer substrates, are naturally non-polar, making it difficult for inks and coatings to adhere effectively. By enhancing the wettability of these films (Aydemir et al., 2021), corona treatment ensures optimized wetting, enabling strong and durable bonding for inks and coatings throughout their service life.

One of the outstanding field applications of corona surface treatment is the use in the manufacture of flexible packaging materials. Common items such as plastic bags, pouches, and wrappers, primarily made from polymers like polyethylene and polypropylene, mainly due to their excellent mechanical properties and cost-effectiveness. However, these materials possess poor adhesion properties, complicating the application of inks and coatings. This challenge is significant in food packaging since good-quality printing is needed for branding and product information.

A study by Nuntapichedkul et al. (2014) showed that corona treatment positively impacted the adhesion of inks to food packaging polypropylene films. The

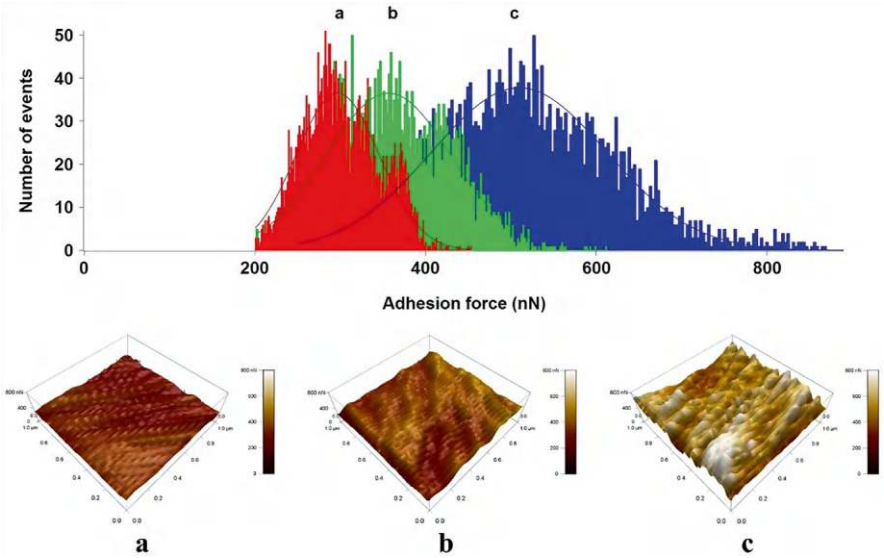

Fig. 8.2 Adhesion mapping of LLDPE: (**a**) untreated, (**b**) 1 s corona-treated, and (**c**) 7 s corona-treated. The adhesion force was positively associated with the exposure time of corona treatment. Reproduced with permission from Popelka et al. (2018) Copyright 2018, Elsevier

Table 8.1 Application of corona discharge for surface modification of flexible substrates

Object for treatment	Effect of treatment	Application	Reference
Polyethylene (PE) and polypropylene (PP)	Adhesion and wettability	Packaging materials	Aydemir et al. (2021), Nuntapichedkul et al. (2014)
Paper	Adhesion and wettability	Packaging materials	Mirmehdi et al. (2018)
Cellulose nanofibril films	Wettability	Printing and packaging	Andrade et al. (2018)
Polyamide fabric	Roughness and wettability	Textile	Gasi et al. (2020)
Octadecyltrichlorosilane (OTS)-coated paper cellulose	Wettability and micropatterning	Microfluidic paper-based analytical devices	Jiang et al. (2016)

treatment assured excellent adhesion of the ink and good quality of print due to the increment of the surface energy of the polypropylene film. The increased adhesion properties of the treated films were improving the gravure printability, meeting the hardest printing resolution of small grooves 10% and 5% dot.

Apart from synthetic materials, paper substrates have emerged as an ecofriendly alternative to address concerns associated with plastic waste and non-biodegradable materials. However, the intrinsic properties of biopolymer, such as poor mechanical properties, limited barrier properties, and high permeability to vapour and gases,

present challenges for packaging applications (Majeed et al., 2013). Composite materials offer a solution by combining biopolymers with other components to enhance performance. For instance, Mirmehdi et al. (2018) demonstrated that corona treatment improved the surface wettability of paper substrates, allowing optimal coating of cellulose nanofibrils and nanoclay composites. Additionally, Andrade et al. (2018) showed that corona treatment enhanced the contact angle and surface energy of nanofibril films, improving their tensile strength, wettability, and printing quality.

In the textile industry, corona treatment is widely used to improve dye uptake and coating adhesion on synthetic fibers. Utilizing a commercial hybrid corona-DBD plasma system, Gasi et al. (2020) modified polyamide fabric surfaces, inducing surface roughness and reducing contact angles. This enhanced dyeing efficiency and resulted in higher color strength in treated fabrics. In biomedical industry, corona surface treatment offers a straightforward approach for device fabrication, especially for biosensor. Electrochemical sensors, known for their high sensitivity and selectivity, rely heavily on the proper deposition of the recognition layer. By utilizing the low-energy cold plasma of helium gas, Wardak et al. (2020) had constructed a laccase-based sensor for dopamine detection. The modification was performed in such a manner that the laccase molecules were polymerized upon plasma treatment followed by deposition on the conductive materials, forming the biorecognition layer.

For the paper-based biosensor, Jiang et al. (2016) used a hand-held corona device, and a stencilled plastic mask to create hydrophilic channels on hydrophobized octadecyltrichlorosilane (OTS)-coated paper. By selectively exposing the open parts of the substrate to corona treatment, the team developed functional elements such as colorimetric assays and single-use wettability-switching valves. However, scalability for mass production remains a technical challenge.

8.2.1.2 Advantages and Limitations

Corona surface treatment offers several advantages, making it a preferred choice in many industrial applications. One of its primary advantages is cost-effectiveness. Compared to other chemical surface modification techniques, corona treatment equipment is relatively simple and inexpensive, making it accessible to a wide range of industries. The process also requires minimal disruption to continuous production lines, allowing for efficient treatment of large surface areas across various applications.

Another key advantage of corona treatment is its environmental friendliness. Unlike chemical surface treatments, which is based on the use of hazardous solvents and produce harmful waste, corona treatment uses air ionization and emits no toxic byproducts. This makes it an attractive option for industries aiming to reduce their environmental impact and comply with stringent environmental regulations.

However, corona treatment does have limitations. One significant drawback is surface aging—the treated surface will gradually lose its enhanced surface energy

over time (Lindner et al., 2018; Żołek-Tryznowska et al., 2020). For instance, PE films exposed to UV light or thermal conditions may lose their functional properties as free radicals attack the polymer, leading to the formation of alkyl radicals and oxygen-containing groups (El-Awady, 2003). This requires careful handling and storage of treated materials to maintain their enhanced properties.

Despite the fact that corona treatment is very effective, it may not be the best treatment for all materials, mainly the polymers that are taken to be very stable or have a high resistance towards oxidation. Polymers with good thermal stability may not respond well to corona treatment, as the reactive species generated from the discharge may not be strong enough to induce significant surface modifications. In cases where corona treatment does not provide the desired performance, alternative methods including plasma treatment could be considered (Nemani et al., 2018).

8.2.2 Plasma Surface Treatment

Plasma treatment is a versatile and efficient method for modifying surface properties of materials such as polymers, metals, and ceramics. Unlike corona treatment, which operates at atmospheric pressure, plasma treatment can be done under low pressure or vacuum conditions, using a variety of gases to achieve certain surface modifications. The process leverages the interaction between ionized gases and material surfaces, resulting in chemical and physical changes that enhance properties such as adhesion, wettability, and biocompatibility (Recek, 2019; Wolf & Sparavigna, 2010). Plasma treatment is applied in the aerospace, biomedical devices, electronics, and advanced materials, where precise surface engineering is critical.

Mechanistically, plasma surface treatment involves placing the material within a plasma field generated by supplying energy to a chosen gas. Commonly used gases include oxygen, nitrogen, argon, and fluorinated gases, selected based on the desired surface modification. Upon ionization, the gas forms a plasma that comprises electrons, ions, radicals, and neutral species. The reactive particles bombard the surface, leading to changes in the surface material such as etching processes, cross-linking, and hence the development of new chemical groups. For instance, plasma oxygen treatment is commonly used to increase the surface energy of polymers by introducing polar oxidative groups onto the surface, including hydroxyls and carbonyls.

Comparing the effect of cold oxygen plasma on three polymeric materials with varying degrees of crystallinity (i.e., crystalline high-density polyethylene (HDPE), crystalline-amorphous poly(chloro-paraxylylene) (parylene C), and amorphous aromatic polyether-based polyurethane (PU)) demonstrates the exposure of plasma greatly affects the surface of the materials irrespective of their crystallinity. Plasma etching generated the nanocorrugations on the surface of crystalline HDPE, while for the amorphous parylene C and PU, nano-sized pores were created on the surface as the result of etching. Meanwhile, the XPS analysis (Fig. 8.3) confirms surface

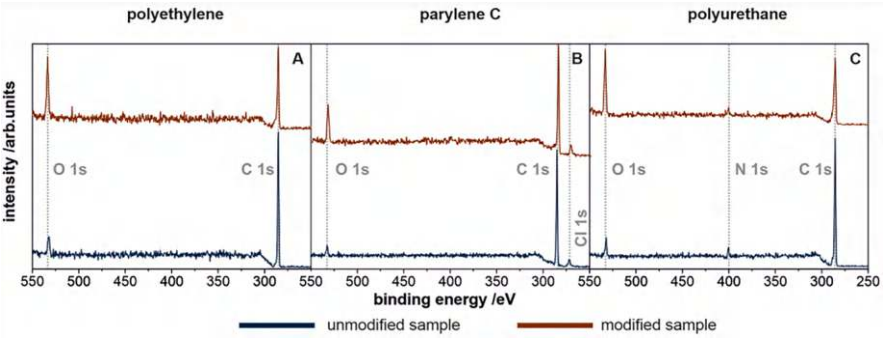

Fig. 8.3 The XPS survey scans (**a**–**c**) of the unmodified (blue lines) and oxygen plasma modified (1 min, 50 W, 0.14 mbar O_2) polymeric samples (orange lines): (**a**) high-density polyethylene, (**b**) parylene C, and (**c**) polyurethane. Reproduced with permission from Chytrosz-Wrobel et al. (2023). Copyright 2023, Elsevier

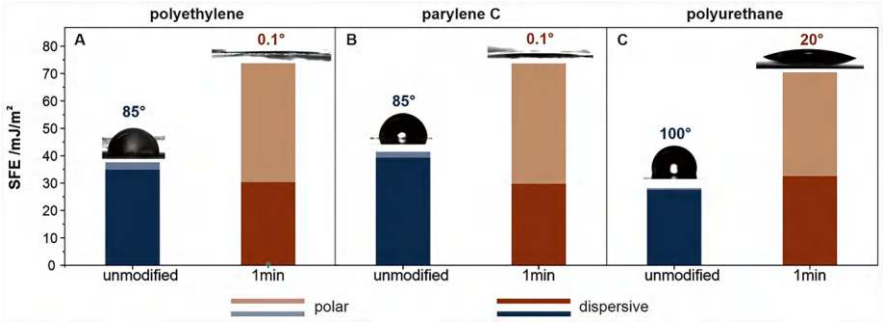

Fig. 8.4 SFE values for the unmodified (blue bars) and oxygen plasma-modified samples (orange bars) of (**a**) polyethylene, (**b**) parylene C, and (**c**) polyurethane, together with water contact angle values. Reproduced with permission from Chytrosz-Wrobel et al. (2023). Copyright 2023, Elsevier

oxidation in all materials, leading to improved wettability (Fig. 8.4), as demonstrated by reduced water contact angles (Chytrosz-Wrobel et al., 2023). These surface changes enhance adhesion to a range of coatings, adhesives, and biomedical implants, making oxygen plasma treatment highly effective for diverse applications (Liu et al., 2021; Primc & Mozetič, 2024).

In contrast, fluorine-containing plasma like that derived from tetrafluoromethane is highly effective for reducing surface energy, leading to hydrophobic surfaces that repel water and resist contaminants (Woodward et al., 2003). This process incorporates fluorine-containing groups and increases C=O bonds, significantly enhancing the hydrophobicity of polyimide (PI) films. This improvement is evidenced by the higher contact angles and reduced surface free energy, as shown in Fig. 8.5 (Aktas et al., 2024). This modification, in combination with laser ablation on the surface, imparts a biofouling-resistant property to the treated PI films, making them more effective in preventing bacterial contamination in biomedical device applications.

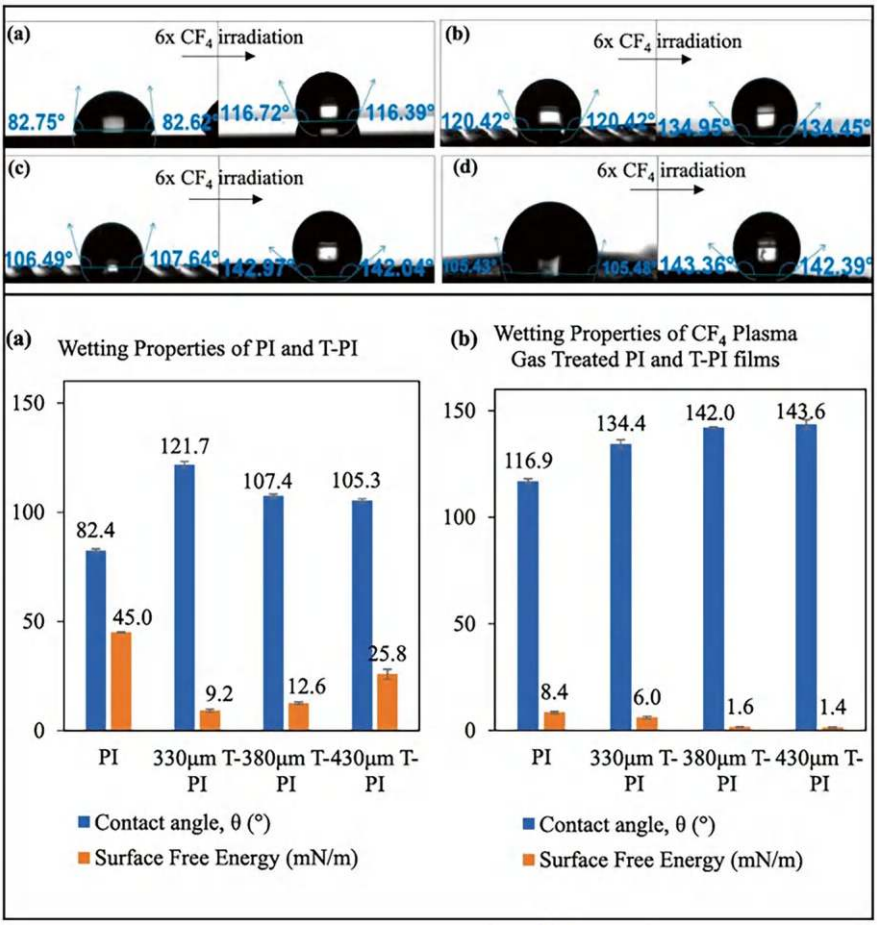

Fig. 8.5 (Up) Schematic diagram contact angle of PI surface after six times of CF_4 plasma treatment in combination of different diameter size after laser texturing, (a) PI, (b) 430 µm PI, (c) 380 µm PI, (d) 330 µm PI. (Down) Wettability of PI samples after texturing the with holes with different diameter sizes; (a) before CH_4 plasma treatment and (b) after CH_4 plasma treatment. Reproduced with permission from (Aktas et al., 2024). Copyright 2024, Elsevier

8.2.2.1 Applications

The versatility of plasma surface treatment makes it invaluable across various industries (Table 8.2). In electronics, plasma treatment is used to clean and activate the surfaces of semiconductor wafers before the lithographic and deposition processes. This ensures strong adhesion of subsequent layers, prevents delamination, and enhances the reliability of electronic devices. Similarly, in printed circuit board (PCB) fabrication, plasma is used for surface etching and cleaning, removing

Table 8.2 Application of plasma treatment for surface modification of various materials

Object for treatment	Effect of treatment	Application	References
Semiconductor wafer	Surface cleaning and adhesion	Electronics	Han et al. (2001)
Polylactic acid (PLA) or polyglycolic acid (PGA)	Biocompatibility and biodegradability	Tissue engineering scaffold	Zarei et al. (2023)
Polyethylene terephthalate (PET)	Biocompatibility, adhesion, and promoting cell growth	Cardiovascular stent	Recek (2019)
Cellulose paper	Microfluidics patterning	Microfluidic paper-based analytical devices	Akyazi et al. (2018)
Whatman filter paper			Li et al. (2008)
Whatman chromatography paper			Raj et al. (2020)
Cellulose paper	Antibodies immobilization	Electrochemical paper-based immunocapture assay	Scala-benuzzi et al. (2018)
		Paper-based chemiluminescence immunodevice	Zhao et al. (2016)
Whatman chromatography paper	Surface cleaning, improve hydrophilicity and roughness	Paper-based bioassay devices	Zhou et al. (2020)

photoresist residues, and improving the adhesive properties of copper layers to the respective substrate (Han et al., 2001).

In biomedical engineering, plasma treatment plays a critical role in modifying polymeric materials for tissue engineering scaffolds. Biocompatibility and biodegradability polymers such as polylactic acid (PLA) or polyglycolic acid (PGA), which nowadays are common materials for scaffold fabrication. However, most of these require further surface modification to improve cell attachment and proliferation. Zarei et al. (2023) demonstrated that argon plasma treatment, which introduces polar functional groups, significantly enhanced the hydrophilicity of PLA scaffolds. This resulted in enhanced cell attachment, growth, and a higher degradation rate, making these scaffolds ideal for applications like bone tissue engineering.

Nitrogen and oxygen plasma treatments have also been applied to polyethylene terephthalate (PET) films for cardiovascular stents (Recek, 2019). These treatments introduce functional groups and modify surface morphology, enhancing biocompatibility and alleviating the risk of thrombosis associated with the application of a stent. Improved adhesion and growth of endothelial cells on plasma-treated PET films are vital for the long-term success of cardiovascular implants.

In the paper-based device industry, plasma treatment facilitates the creation of hydrophilic microfluidic patterns on hydrophobized paper surfaces. For instance, Li et al. (2008) demonstrated a method that employs plasma treatment to produce

well-defined hydrophilic channels on hydrophobized paper. This further facilitate the development of flexible microfluidic systems with integrated functional elements, such as switches and filters. Likewise, Raj et al. (2020) had also utilize oxygen plasma as an etching agent, following the fluorocarbon plasma deposition to create the hydrophilic channels on paper surface. Additionally, plasma treatment effectively immobilize antibodies to the paper surface via the formation of aldehyde groups without requiring prior material pre-treatment (Scala-benuzzi et al., 2018; Zhao et al., 2016). By employing relatively inexpensive patterning agents for channel formation, plasma treatment significantly reduces material costs, offering a precise and cost-effective solution for the mass production of paper-based devices (Akyazi et al., 2018).

8.2.2.2 Advantages and Limitations

Plasma surface treatment offers numerous advantages that make it a preferred option in advanced manufacturing processes. One of its key advantages is the ability to control surface modifications at the nanoscale, allowing tailored customization to meet specific needs in industries, such as electronics, biomedical devices, or aerospace. This precision is complemented by the flexibility to select different gases, enabling customized surface modification for a wide range of materials. Another significant benefit of the plasma treatment is its environmentally friendly nature. The fact that plasma treatment is a dry process, and does not consume any solvents or chemicals, signifies a low danger to the environment and human health at large. This has made the plasma treatment more desirable for industries caring for sustainability and reduction in environmental impact.

However, plasma treatment has certain limitations. It can be more expensive compared to other surface modification methods because the process involves the use of special equipment, such as vacuum chambers and plasma generator apparatuses. Moreover, the effectiveness of the treatment can be influenced by factors such as the type of material, specific plasma parameters that are used as well as environmental conditions during and after the process. Surface modifications created through plasma treatment, like those from corona treatment, may degrade over time when exposed to environmental factors. This necessitates careful handling and storage of treated materials. Long-term stability can be a significant challenge, particularly for medical implants and high-performance coatings.

8.2.3 UV Surface Treatment

Ultraviolet (UV) surface treatment is a well-established technique used to modify the surface properties of materials (Dölle et al., 2020; Liu et al., 2023; Wang et al., 2022; Weber et al., 2023; Zea et al., 2022). The exposure of the substrate to ultraviolet light initiates photochemical reactions that actively promote surface

modification, ultimately altering both the chemical composition and structure of the surface (Borcia et al., 2011; Park et al., 2009). This method is particularly valuable in a variety of field such as biomaterials development (Sung & Rubner, 2002), electronics (Nemani et al., 2018), as well as paper-based sensors and devices due to its ability to enhance surface wettability, adhesion properties, and overall surface energy without altering the bulk properties of the material (Zea et al., 2022).

UV light can be categorized into three main types: UV-A (320–400 nm), UV-B (280–320 nm), and UV-C (200–280 nm). Among these, UV-C light is most commonly used for surface modification due to its high energy and ability to break chemical bonds on the surface of materials (Liu et al., 2023; NOVAGARD, 2020). The radiation, upon interacting with the surface molecules, leads to the formation of free radicals and other reactive species (Lohan et al., 2016). These reactive species can induce a variety of surface modifications. For instance, UV radiation can cause the oxidation of surface molecules, introducing oxygen-containing functional groups such as hydroxyl, carbonyl, and carboxyl groups. This increases the surface energy, thereby enhancing the wettability and adhesive properties of the substrate (Liu et al., 2023; Robotti et al., 2007).

López et al. (2020) demonstrated these effects on polytetrafluoroethylene (PTFE) surfaces. Exposure to UV light reduced the contact angle, while subsequent heat treatment restored the surface's hydrophobicity (Fig. 8.6). Additionally, when water was present during UV exposure, serving as a source of oxygen, polar groups were introduced, leading to a reduction in $–CF_3$ groups. XPS analysis further confirmed these changes, showing an increase in oxygen content and a decrease in fluorine content after UV treatment followed by a 30 min water submersion (Fig. 8.7).

On the other hand, the photo-degradation, inducing by UV light can break down organic contaminants or weakly bonded molecules on the surface, which effectively "clean" the substrate surface. This can improve the uniformity and consistency of subsequent coatings or functional layers (Clark et al., 2000; Retolaza et al., 2022). In some cases, UV treatment can also induce cross-linking of polymer chains on the surface, leading to changes in surface morphology and mechanical properties (Fu et al., 2020; Mhaske et al., 2022; Yin et al., 2020). This is particularly useful for improving the durability and mechanical stability of treated materials.

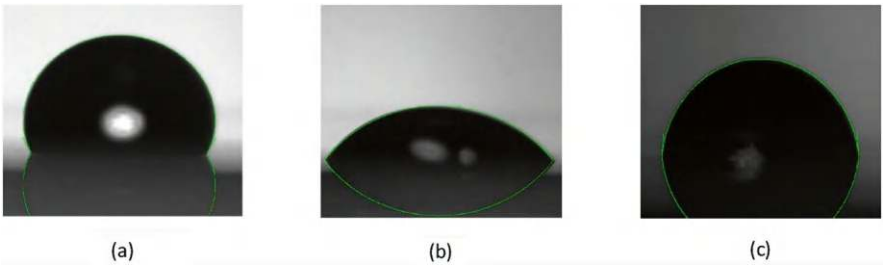

Fig. 8.6 Contact angle: (**a**) not treated PTFE, (**b**) treated PTFE (UV exposition time of 4 min), and (**c**) treated sample (heat treatment 3 h at 165 °C). Reproduced with permission from López et al. (2020). Copyright 2020, Elsevier

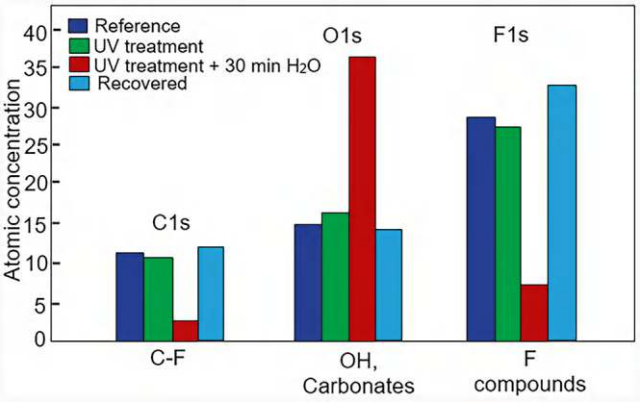

Fig. 8.7 Data analysis of XPS spectrum for carbon, oxygen and fluor. Adapted with permission from López et al. (2020). Copyright 2020, Elsevier

The effectiveness of UV surface treatment depends on several parameters, including the wavelength of UV light, exposure time, the intensity of the UV source, and the environment in which the treatment is conducted (Borcia et al., 2011). Among these, UV-C light (100–280 nm) is the most effective for surface modification due to its high energy, which can break chemical bonds on the surface of the paper (Borcia et al., 2011). The duration of exposure and the intensity of the UV light are critical factors that influence the extent of surface modification. Longer exposure times and higher intensities generally lead to more pronounced surface changes; however, excessive treatment can degrade the paper substrate, leading to loss of mechanical integrity (Belgacem & Gandini, 2005). Therefore, optimizing these parameters is essential to achieve the desired surface properties without compromising the structural integrity of the paper (Liyanage et al., 2021).

The environment in which UV treatment is conducted also plays a role in determining the outcomes of the treatment. For instance, the presence of oxygen during UV exposure can enhance the generation of ROS, leading to more effective oxidation and modification of the surface. Conversely, performing the treatment in an inert atmosphere may limit oxidation and lead to different surface characteristics (Belgacem & Gandini, 2005).

8.2.3.1 Applications

UV surface treatment has significant applications in electronic and biotechnology industries, offering tailored modifications that enhance functionality and reliability (Table 8.3). One primary benefits of UV treatment is the improvement of adhesion properties on paper surfaces crucial for depositing conductive materials such as graphene, silver nanoparticles, or conductive polymers. The increased surface energy post-treatment ensures uniform coating and strong adhesion, which is

Table 8.3 Application of UV treatment for paper surface modification

Object for treatment	Effect of treatment	Application	References
Whatman paper	Adhesion	Electrochemical paper-based devices	Zea et al. (2022)
Copper foil		Electronics	Bok et al. (2017)
Graphene		Electronics	Seo et al. (2015)
Paper	Biomolecules immobilization	Paper-based point-of-care test devices	Bordbar et al. (2021)
		Electrochemical paper-based devices	Seddaoui et al. (2023)
Paper	Microfluidic patterning	Paper-based microfluidic chips	Liang et al. (2023)
Paper board	Surface barrier to protect sensitive components	Food packaging	Andersson (2008), Nguyen et al. (2021)
Environmental surfaces	Cleaning and sterilization	Healthcare	Dai et al. (2012), Demeersseman et al. (2023), Li et al. (2024)

essential for the longevity and reliability of paper-based sensors and electronic devices (Bok et al., 2017; Seo et al., 2015).

In the fabrication of paper-based electronic circuits, UV treatment can be used to improve the adhesion of conductive inks to the paper substrate. By increasing the surface energy and introducing polar functional groups, UV treatment ensures better ink wetting and stronger adhesion, which is crucial for the performance and longevity of the device (Zea et al., 2022). For biosensor development, UV treatment can be used to functionalize the surface with specific chemical groups that enhance the immobilization of biomolecules, such as enzymes, antibodies, or DNA probes. This improves the sensitivity and specificity of the biosensor (Bordbar et al., 2021; Seddaoui et al., 2023).

The hydrophilicity of paper is critical in managing fluid dynamics within paper-based microfluidic devices. UV treatment can be used to control the hydrophilic or hydrophobic nature of specific regions, thereby directing fluid flow and improving the accuracy and efficiency of fluidic operations (Liang et al., 2023). In some paper-based electronic devices, it is necessary to create barrier layers to protect sensitive components from environmental factors, such as moisture and oxygen. The studies by Andersson (2008) and Nguyen et al. (2021) explored the use of UV treatment to enhance the protective properties of paperboard in food packaging, highlighting its significant potential for applications in paper-based devices. In addition, UV treatment also serves as an effective method for cleaning and sterilizing paper surfaces, decomposing organic contaminants and pathogens. This improves device performance while ensuring safety in applications like medical diagnostics and environmental monitoring (Dai et al., 2012; Demeersseman et al., 2023; Li et al., 2024).

8.2.3.2 Advantages and Limitations

UV surface modification stands out for its environmentally benefits as it emits no hazardous chemicals or excessive heat, making it a safer and greener alternative. This is particularly advantageous for companies prioritizing sustainability and environmental responsibility. Additionally, the process is highly cost-efficient, requiring minimal operational expenses and being conducted under atmospheric pressure. Hence, it is more accessible and attractive to companies across different scales. Its high scalability, coupled with the ability to rapidly treat large surface areas, further enhances its suitability for industries where speed and efficiency are important.

Despite its benefits, there are also challenges and limitations associated with this technique. One of the primary challenges is the depth of penetration of UV light, which is limited to the surface layers of the material. This makes it difficult to achieve uniform treatment on thicker or more complex substrates. In addition, the potential for degradation of the paper substrate due to prolonged or excessive UV exposure must be carefully managed to maintain the mechanical properties of the paper. Another challenge lies in the specificity of UV-induced reactions. While UV light can induce a wide range of chemical changes, it is often difficult to control these reactions with high precision. This can result in variability in the surface properties of treated materials, which may limit its suitability for applications requiring consistent outcomes. Careful optimization of process parameters and tailored approaches can help mitigate these limitations, ensuring UV surface modification continues to be a valuable tool across industries.

8.2.4 Laser Surface Treatment

Laser surface treatment is an advanced and precise technique used to modify material surfaces for various industrial and research applications (Dudek et al., 2023). Laser treatment operates on the principle of photothermal and photochemical interactions between the laser beam and the material surface. When the laser beam strikes the paper substrate, it can cause localized heating, ablation, melting, or photodecomposition, depending on the laser parameters, such as wavelength, pulse duration, energy density, and the material's optical properties (Siddiqui & Dubey, 2020). This level of control allows for targeted modifications that can improve material performance in applications ranging from electronics to biomedical devices.

Laser surface modification works in several mechanisms to alter the surface properties, such as thermal ablation, sintering, and fusion as well as photochemical reactions. Thermal ablation is a common mechanism used in surface modification where the laser energy is absorbed by the material, leading to its rapid heating and vaporization. This process can create microstructures on the material surface, which can enhance surface roughness, increase wettability, or create patterned features for device integration (Phipps, 2020). In certain cases, the laser can also induce

photochemical reactions on the paper surface, leading to changes in chemical composition or functionalization of the surface. For instance, laser irradiation can be used to graft functional groups onto the paper surface, enhancing its affinity for specific analytes in sensor applications (Harper et al., 2019; Hong et al., 2023; Manshina et al., 2024; Silva et al., 2024).

Figure 8.8 illustrates the SEM image of laser-ablated paper after the treatment of continuous-wave laser, nanosecond laser, and femtosecond laser, demonstrating a significant nanopore formation under different conditions. Further XPS analysis showed the breaking of C–C bonds after the continuous wave laser treatment, with increased formation of functional groups, such as hydroxyl and carbonyl groups (Zhao et al., 2024). On the other hand, laser treatment can also induce sintering or fusion of nanoparticles deposited on the material surface, thereby forming conductive pathways or coatings. This is particularly useful in fabricating flexible electronic circuits on paper (Laakso et al., 2009; Pajor-Świerzy et al., 2023; Sharif et al., 2023; Theodorakos et al., 2015).

The effectiveness of laser surface modification is influenced by a range of factors, primarily including laser parameters, material properties, and ambient conditions. Laser parameters such as wavelength, power density, and pulse duration play critical roles in determining the interaction between the laser and the material. For instance, the wavelength affects the material's absorption characteristics; shorter wavelengths are typically more effective for polymers, while longer wavelengths are suited for metals (Tan et al., 2024). Power density, or the energy delivered per unit area, dictates the extent of heating or material removal, with higher densities leading to more pronounced effects (Jeyaprakash et al., 2021). Additionally, pulse duration impacts the precision of the modification process, with shorter pulses enabling finer control over thermal effects and reducing collateral damage (Schmidt et al., 2023).

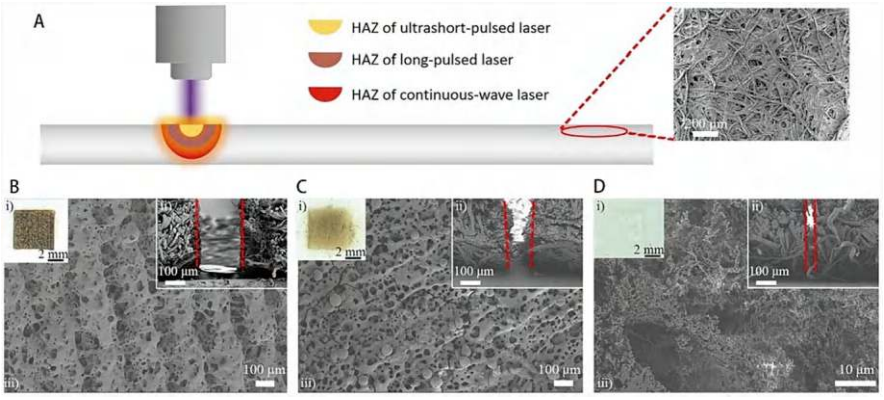

Fig. 8.8 Physical changes after laser ablation. (**a**) Schematic of heat-affected zone of continuous-wave, long-pulsed, and ultrashort-pulsed lasers. SEM image of ablated pristine paper with laser treatment: (**b**) continuous-wave laser, (**c**) nanosecond laser, and (**d**) femtosecond laser. Significant nanopores were observed in ablated paper, treated with different laser option. Reproduced with permission from Zhao et al. (2024). Copyright 2020, Elsevier

Material properties such as thermal conductivity, absorptivity, and melting point also significantly influence the outcome; materials with high thermal conductivity may require greater laser intensity to achieve the desired modifications (Guan et al., 2005; Pannitz et al., 2021). Ambient conditions, including the presence of gases or contaminants, further affect the quality of the laser treatment. Controlled environments are necessary to prevent unwanted reactions, such as oxidation, which can compromise the results (Reich et al., 2023). Understanding and optimizing these factors are crucial for achieving precise and effective surface modifications using lasers.

8.2.4.1 Applications

Precision is a defining characteristic of laser treatment, making it particularly well-suited for advanced manufacturing in a variety of industries (Table 8.4). In biomaterials engineering, Lu et al. (2022) fabricated hierarchical micro/nano-structures using femtosecond laser ablation on the surface of Ti alloys. These structures serve as a scaffold for the deposition of silver nanoparticles (AgNPs), forming a hydrophobic surface with a controlled release rate of Ag^{+}, balancing the antibacterial and osteointegration-promoting properties of material in orthopedic and dental implants. Similarly, Wang et al. (2024) combined picosecond laser treatment with friction stir machining to significantly improve the mechanical properties of β-titanium alloys. This treatment led to a reduction in friction coefficient and friction loss, mainly due to the formation of laser-induced periodic surface structures (LIPSS). This shed light to the novel surface modification strategy utilizing laser ablation to produce high-performance titanium implant.

In the soft manufacturing industry, Nd lasers (1064 nm wavelength) are widely used for cleaning various materials, including Whatman cellulose, rag paper, cotton,

Table 8.4 Application of laser surface modification across varies industries

Object for treatment	Effect of treatment	Application	References
Titanium alloy	Adhesion, cytocompatibility, and antibacterial properties	Orthopaedic and dental implants	Lu et al. (2022)
	Mechanical strength	Orthopedic implants	Wang et al. (2024)
Cellulosic materials	Cleaning	Soft manufacturing	Strlič et al. (2003)
Taffeta fabric	Surface functionalization	Soft manufacturing	Mizoguchi et al. (2001)
Paperboard	Nanostructure electrode patterning	Electrochemical paper-based devices	Araujo et al. (2017)
Fire-retardant treated cellulose	Conductivity	LIG-based electrochemical biosensors	Bhattacharya et al. (2022)

linen, silk, and wool. This process often induces chemical modifications in the materials, such as thermal degradation, which can be studied using visible and FTIR diffuse reflectance spectroscopy (Strlič et al., 2003). Excimer laser beams (ArF, KrF, and XeCl with wavelengths of 193, 248, and 308 nm, respectively) are also used for surface modifications of rayon taffeta fabric to increase the carbonyl groups along with the removal of both C–O and COO groups, which expend its use in regenerated cellulose fiber (Mizoguchi et al., 2001).

In the development of paper-based devices, laser treatment allows for precise patterning and micromachining of paper substrates, which is essential for creating microfluidic channels, electrode designs, and other functional components of paper-based devices. The non-contact nature of laser processing ensures minimal damage to the substrate while allowing for high-resolution features. Furthermore, the ability of laser treatment to modify the surface chemistry of paper, making it more suitable for specific sensor applications. For instance, through the pyrolysis process by using CO_2 laser on the superficial paperboard, Araujo et al. (2017) proposed a straightforward and cost-effective approach to create a conductive porous non-graphitizing carbon material, which greatly serves the electrochemical purpose due to its high conductivity and enhanced active/geometric area ratio. Similarly, the laser-induced graphene (LIG) can also be created on paper by using laser scribing, which provides a conductive and porous structure ideal for the construction of paper-based analytical devices. This array of applications highlights the transformative potential of laser surface treatment in material science, from improving mechanical properties to enabling novel designs for bioengineering and paper-based technologies.

8.2.4.2 Advantages and Limitations

Laser beam surface modification offers several advantages, making it a preferred technique in advanced manufacturing applications. One of the most notable benefits is the high precision and control it provides over the modification process. This precision allows for the creation of intricate precise structure that can be customized to meet the specific requirements of industries, such as nanotechnology, electronics, or biomedical devices. Furthermore, the minimal heat-affected zone (HAZ) associated with laser treatment is another crucial benefit. Since the heat generated by the laser is highly localized, the risk of thermal damage, distortion, or undesirable changes in material properties is greatly reduced. This helps preserve the integrity of the material while enhancing the overall quality of the modification.

Nevertheless, laser treatment comes with its own set of challenges. The major drawback is the high initial cost of equipment, which limits its use to high-end product manufacturing. Furthermore, the process requires a high level of technical expertise, as skilled operators are needed to manage the precise control and complex setup. Thus, future prospects would be more promising with the integration of artificial intelligence to enable data-driven decision-making and smart control over the operation. Despite the fact that laser treatment is efficient in precise modification processes, it may not be the best fit for all, especially for materials with

inherent characteristics, such as high reflectivity, low thermal conductivity, or sensitivity to thermal damage (Arulvel et al., 2023). These material characteristics can complicate the effectiveness of laser modification, limiting its applicability in certain cases.

8.3 Conclusions and Future Perspective

In conclusion, surface modification of cellulose is essential to address its inherent limitations and enhance its properties, including adhesion, wettability, and compatibility with other materials. This chapter has explored various physical methods, which serve as complementary approaches to chemical modifications, for improving cellulose's surface characteristics. Corona discharge increases surface energy through ionization, improving adhesion for coatings and inks, particularly in flexible packaging. Plasma treatment, utilizing various gases under vacuum conditions, offers precise control over surface modifications, enhancing properties like biocompatibility and adhesion for use in electronics and medical devices. UV treatment improves surface wettability and adhesion by introducing reactive species that modify surface chemistry, playing a key role in paper-based sensor and device development. Laser treatment provides high precision in creating surface patterns and functional coatings, making it a versatile tool for advanced manufacturing and paper-based electronics.

As the demand for sustainable and ecofriendly production methods grows, these advanced physical modification techniques present an opportunity to minimize waste and energy consumption while enhancing efficiency. Hence, developing advanced physical modification approaches that generate minimal waste will be essential in meeting these challenges. Furthermore, the versatility of cellulose, combined with innovative modification techniques, holds promise for expanding its applications in emerging fields such as green electronics (Li et al., 2020), and next-generation packaging solutions (Guillard et al., 2018), aligning with the increasing need for sustainable products.

Although each method offers distinct advantages, such as cost-effectiveness and environmental friendliness, they also come with limitations, including temporary effects, potential degradation, and the need for careful parameter control. Despite these challenges, physical modification techniques present viable solutions for enhancing the properties of cellulose, making it suitable for a broader range of applications and contributing to more sustainable manufacturing processes.

References

Aktas, C., Bhethanabotla, V., Ayyala, R. S., & Sahiner, N. (2024). Modifying wetting properties of PI film: The impact of surface texturing and CF_4 and O_2 plasma treatment. *Applied Surface Science, 656*, 159729. https://doi.org/10.1016/j.apsusc.2024.159729

Akyazi, T., Basabe-Desmonts, L., & Benito-Lopez, F. (2018). Review on microfluidic paper-based analytical devices towards commercialisation. *Analytica Chimica Acta: X, 1001*, 1–17. https://doi.org/10.1016/j.aca.2017.11.010

Andersson, C. (2008). New ways to enhance the functionality of paperboard by surface treatment - A review. *Packaging Technology and Science, 21*(6), 339–373. https://doi.org/10.1002/pts.823

Andrade, T., Lina, L., Pedro, B., Cunha, I., Alice, M., Gustavo, M., Denzin, H., Lourival, T., & Mendes, M. (2018). The effect of surface modifications with corona discharge in pinus and eucalyptus nanofibril films. *Cellulose, 25*(9), 5033–5049. https://doi.org/10.1007/s10570-018-1948-3

Araujo, W. R., Frasson, C. M. R., Ameku, W. A., Silva, J. R., Angnes, L., Thiago, R. L. C., & Paixão. (2017). Single-step reagentless laser scribing fabrication of electrochemical paper-based analytical devices. *Angewandte Chemie, 129*, 15309–15313. https://doi.org/10.1002/anie.201708527

Arulvel, S., Jain, A., Kandasamy, J., & Singhal, M. (2023). Laser processing techniques for surface property enhancement: Focus on material advancement. *Surfaces and Interfaces, 42*, 103293. https://doi.org/10.1016/j.surfin.2023.103293

Aydemir, C., Altay, B. N., & Akyol, M. (2021). Surface analysis of polymer films for wettability and ink adhesion. *Color Research & Application, 46*(2), 489–499. https://doi.org/10.1002/col.22579

Belgacem, M. N., & Gandini, A. (2005). The surface modification of cellulose fibres for use as reinforcing elements in composite materials. *Composite Interfaces, 12*(1–2), 41–75. https://doi.org/10.1163/1568554053542188

Bhattacharya, G., Fishlock, S. J., Hussain, S., Choudhury, S., Xiang, A., Kandola, B., et al. (2022). Disposable paper-based biosensors: Optimizing the electrochemical properties of laser-induced graphene. *ACS Applied Materials & Interfaces, 14*, 31109–31120. https://doi.org/10.1021/acsami.2c06350

Bok, S., Lim, G. H., & Lim, B. (2017). UV/ozone treatment for adhesion improvement of copper/epoxy interface. *JIEC, 46*, 199–202. https://doi.org/10.1016/j.jiec.2016.10.031

Borcia, C., Borcia, G., & Dumitrascu, N. (2011). Surface treatment of polymers by plasma and UV radiation. *Romanian Reports In Physics, 56*(1–2), 224–232.

Bordbar, M. M., Sheini, A., Hashemi, P., Hajian, A., & Bagheri, H. (2021). Disposable paper-based biosensors for the point-of-care detection of hazardous contaminations—A review. *Biosensors, 11*(9), 316. https://doi.org/10.3390/bios11090316

Chytrosz-Wrobel, P., Golda-Cepa, M., Stodolak-Zych, E., Rysz, J., & Kotarba, A. (2023). Effect of oxygen plasma-treatment on surface functional groups, wettability, and nanotopography features of medically relevant polymers with various crystallinities. *Applied Surface Science Advances, 18*, 100497. https://doi.org/10.1016/j.apsadv.2023.100497

Clark, T., Ruiz, J. D., Fan, H., Brinker, C. J., Swanson, B. I., & Parikh, A. N. (2000). A new application of UV-ozone treatment the preparation of substrate-supported, mesoporous thin films. *Chemistry of Materials, 12*(12), 3879–3884. https://doi.org/10.1021/cm000456f

Coseri, S. (2017). Cellulose: To depolymerize … or not to? *Biotechnology Advances, 35*(2), 251–266. https://doi.org/10.1016/j.biotechadv.2017.01.002

Dai, T., Vrahas, M. S., Murray, C. K., & Hamblin, M. R. (2012). Ultraviolet C irradiation: An alternative antimicrobial approach to localized infections? *Expert Review of Anti-Infective Therapy, 10*(2), 185–195. https://doi.org/10.1586/eri.11.166

Demeersseman, N., Saegeman, V., Cossey, V., Devriese, H., & Schuermans, A. (2023). Shedding a light on ultraviolet-C technologies in the hospital environment. *The Journal of Hospital Infection, 132*, 85–92. https://doi.org/10.1016/j.jhin.2022.12.009

Dölle, K., Goodman, N., & Lawrence, W. (2020). Application of ultraviolet treatment for paper production - An engineering study. *Journal of Engineering Research and Reports, 11*, 35–41. https://doi.org/10.9734/jerr/2020/v11i417068

Dudek, M., Sąsiadek-Andrzejczak, E., Jaszczak-Kuligowska, M., Rokita, B., & Kozicki, M. (2023). The surface modification of papers using laser processing towards applications. *Materials, 16*(20), 6691. https://doi.org/10.3390/ma16206691

El-Awady, M. M. (2003). Natural weathering, artificial photo-oxidation, and thermal aging of low density polyethylene: Grafting of acrylic acid onto aged polyethylene films. *Journal of Applied Polymer Science, 87*, 2365–2371. https://doi.org/10.1002/app.11990

Fu, Y. W., Sun, W. F., & Wang, X. (2020). UV-initiated crosslinking reaction mechanism and electrical breakdown performance of crosslinked polyethylene. *Polymers, 12*(2), 420. https://doi.org/10.3390/polym12020420

Gasi, F., Petraconi, G., Bittencourt, E., Lourenço, S. R., Castro, A. H. R., Miranda, D. S., et al. (2020). Plasma treatment of polyamide fabric surface by hybrid corona-dielectric barrier discharge: Material characterization and dyeing/washing processes. *Materials Research, 23*(1), e20190255. https://doi.org/10.1590/1980-5373-MR-2019-0255

Guan, Y., Sun, S., Zhao, G., & Luan, Y. (2005). Influence of material properties on the laser-forming process of sheet metals. *Journal of Materials Processing Technology, 167*(1), 124–131. https://doi.org/10.1016/j.jmatprotec.2004.10.003

Guillard, V., Gaucel, S., Fornaciari, C., & Angellier-coussy, H. (2018). The next generation of sustainable food packaging to preserve our environment in a circular economy context. *Frontiers in Nutrition, 5*, 121. https://doi.org/10.3389/fnut.2018.00121

Han, Q., Waldfried, C., Escorcia, O., Dahrooge, G., Berry, I., & City, E. (2001). *Plasma process for removing polymer and residues from substrates (Patent No. US 2002O185151A1)*. United States Patent and Trademark Office.

Harper, K. C., Moschetta, E. G., Bordawekar, S. V., & Wittenberger, S. J. (2019). A laser driven flow chemistry platform for scaling photochemical reactions with visible light. *ACS Central Science, 5*(1), 109–115. https://doi.org/10.1021/acscentsci.8b00728

Heinze, T. (2015). Cellulose: Structure and properties. In O. J. Rojas (Ed.), *Cellulose chemistry and properties: Fibers, nanocelluloses and advanced materials* (pp. 1–52). Springer. https://doi.org/10.1007/12_2015_319

Hong, S., Kim, J., Jung, S., Lee, J., & Shin, B. S. (2023). Surface morphological growth characteristics of laser-induced graphene with UV pulsed laser and sensor applications. *ACS Materials Letters, 5*(4), 1261–1270. https://doi.org/10.1021/acsmaterialslett.2c01222

Jeyaprakash, N., Yang, C.-H., & Raj Kumar, D. (2021). Laser surface modification of materials. In D. Yang (Ed.), *Practical applications of laser ablation*. IntechOpen. https://doi.org/10.5772/intechopen.94439

Jiang, Y., Hao, Z., He, Q., & Chen, H. (2016). A simple method for fabrication of microfluidic paper-based analytical devices and on-device fluid control with a portable corona generator. *RSC Advances, 6*(4), 2888–2894. https://doi.org/10.1039/c5ra23470k

Laakso, P., Ruotsalainen, S., Halonen, E., Mäntysalo, M., & Kemppainen, A. (2009). Sintering of printed nanoparticle structures using laser treatment. *Congress Proceedings, 102*, 1360–1366. https://doi.org/10.2351/1.5061499

Li, W., Liu, Q., Zhang, Y., Li, C., He, Z., Choy, W. C. H., et al. (2020). Biodegradable materials and green processing for green electronics. *Advanced Materials, 32*(33), 2001591. https://doi.org/10.1002/adma.202001591

Li, X., Tian, J., Nguyen, T., & Shen, W. (2008). Paper-based microfluidic devices by plasma treatment. *Analytical Chemistry, 80*(23), 9131–9134. https://doi.org/10.1021/ac801729t

Li, Y., Chen, X., Wang, Y., & Zhang, Y. (2024). Effects of environmental factors, measurement and modeling for germicidal efficiency of in-duct ultraviolet germicidal irradiation system. *Energy and Built Environment*. https://doi.org/10.1016/j.enbenv.2024.03.006

Liang, M., Zhang, G., Song, J., Tan, M., & Su, W. (2023). Paper-based microfluidic chips for food hazard factor detection: Fabrication, modification, and application. *Food, 12*(22), 4107. https://doi.org/10.3390/foods12224107

Lindner, M., Rodler, N., Jesdinszki, M., Schmid, M., & Sängerlaub, S. (2018). Surface energy of corona treated PP, PE and PET films, its alteration as function of storage time and the effect of various corona dosages on their bond strength after lamination. *Journal of Applied Polymer Science, 135*(11), 45842. https://doi.org/10.1002/app.45842

Liu, G., Song, Z., Gao, X., Wang, Y., & Li, Z. (2023). Surface modification of paper substrates by a printed UV curing varnish layer and a transferred transparent PEDOT: PSS electrode for paper-

based perovskite light-emitting devices in ambient air. *Surfaces and Interfaces, 43*, 103552. https://doi.org/10.1016/j.surfin.2023.103552

Liu, P., Wang, G., Ruan, Q., Tang, K., & Chu, P. K. (2021). Plasma-activated interfaces for biomedical engineering. *Bioactive Materials, 6*(7), 2134–2143. https://doi.org/10.1016/j.bioactmat.2021.01.001

Liyanage, S., Acharya, S., Parajuli, P., Shamshina, J. L., & Abidi, N. (2021). Production and surface modification of cellulose bioproducts. *Polymers, 13*(19), 3433. https://doi.org/10.3390/polym13193433

Lohan, S. B., Müller, R., Albrecht, S., Mink, K., Tscherch, K., Ismaeel, F., et al. (2016). Free radicals induced by sunlight in different spectral regions - In vivo versus ex vivo study. *Experimental Dermatology, 25*(5), 380–385. https://doi.org/10.1111/exd.12987

López, C. D., Cedeño-Mata, M., Dominguez-Pumar, M., & Bermejo, S. (2020). Surface modification of polytetrafluoroethylene thin films by non-coherent UV light and water treatment for electrowetting applications. *Progress in Organic Coating, 149*, 105593. https://doi.org/10.1016/j.porgcoat.2020.105593

Lu, L., Zhang, J., Guan, K., Zhou, J., Yuan, F., & Guan, Y. (2022). Artificial neural network for cytocompatibility and antibacterial enhancement induced by femtosecond laser micro/nano structures. *Journal of Nanbiotechnology, 20*(1), 365. https://doi.org/10.1186/s12951-022-01578-4

Majeed, K., Jawaid, M., Hassan, A., Bakar, A. A., Khalil, H. P. S. A., Salema, A. A., & Inuwa, I. (2013). Potential materials for food packaging from nanoclay/natural fibres filled hybrid composites. *Materials & Design, 46*, 391–410. https://doi.org/10.1016/j.matdes.2012.10.044

Manshina, A. A., Tumkin, I. I., Khairullina, E. M., Mizoshiri, M., Ostendorf, A., Kulinich, S. A., et al. (2024). The second laser revolution in chemistry: Emerging laser technologies for precise fabrication of multifunctional nanomaterials and nanostructures. *Advanced Functional Materials, 34*(40), 2405457. https://doi.org/10.1002/adfm.202405457

Mhaske, S. T., Mestry, S. U., & Patil, D. A. (2022). Cross-linking of polymers by various radiations: Mechanisms and parameters. In S. R. Chowdhury (Ed.), *Radiation technologies and applications in materials science* (1st ed., pp. 1–28). CRC Press. https://doi.org/10.1201/9781003321910-1

Mirmehdi, S., Ricardo, P., Hein, G., Isabel, C., De Luca, G., et al. (2018). Cellulose nano fibrils/nanoclay hybrid composite as a paper coating: Effects of spray time, nanoclay content and corona discharge on barrier and mechanical properties of the coated papers. *Food Packaging and Shelf Life, 15*, 87–94. https://doi.org/10.1016/j.fpsl.2017.11.007

Mizoguchi, K., Ishikawa, M., Ohkubo, S., Yamamoto, A., Ouchi, A., Sakuragi, M., et al. (2001). Laser surface treatment of regenerated cellulose fiber. *Composite Interfaces, 7*(5–6), 497–509. https://doi.org/10.1163/156855400750262978

Nemani, S. K., Annavarapu, R. K., Mohammadian, B., Raiyan, A., Heil, J., Haque, M. A., et al. (2018). Surface modification of polymers: Methods and applications. *Advanced Materials Interfaces, 5*(24), 1801247. https://doi.org/10.1002/admi.201801247

Nguyen, H. L., Tran, T. H., Hao, L. T., Jeon, H., Koo, J. M., Shin, G., et al. (2021). Biorenewable, transparent, and oxygen/moisture barrier nanocellulose/nanochitin-based coating on polypropylene for food packaging applications. *Carbohydrate Polymers, 271*, 118421. https://doi.org/10.1016/j.carbpol.2021.118421

NOVAGARD. (2020). *Understanding UV curing options for industry white paper*. Novagard, 1.0 (November), 1–9. Retrieved from https://www.eetdispensing.com/wp-content/uploads/2021/02/Novagard-White-Paper-UV-Curing.pdf

Nuntapichedkul, B., Tantayanon, S., & Laohhasurayotin, K. (2014). Practical approach in surface modification of biaxially oriented polypropylene films for gravure printability. *Applied Surface Science, 314*, 331–340. https://doi.org/10.1016/j.apsusc.2014.06.032

Pajor-Świerzy, A., Szyk-Warszyńska, L., Duraczyńska, D., & Szczepanowicz, K. (2023). UV-vis sintering process for fabrication of conductive coatings based on Ni-ag core–shell nanoparticles. *Materials, 16*, 7218. https://doi.org/10.3390/ma16227218

Pannitz, O., Lüddecke, A., Kwade, A., & Sehrt, J. T. (2021). Investigation of the in situ thermal conductivity and absorption behavior of nanocomposite powder materials in laser pow-

der bed fusion processes. *Materials and Design, 201*, 109530. https://doi.org/10.1016/j.matdes.2021.109530

Park, E. J., Carroll, G. T., Turro, N. J., & Koberstein, J. T. (2009). Shedding light on surfaces - Using photons to transform and pattern material surfaces. *Soft Matter, 5*(1), 36–50. https://doi.org/10.1039/b807472k

Phipps, C. R. (2020). *Laser ablation and its applications in space* (1st ed.). Springer. https://doi.org/10.1007/978-0-387-30453-3

Popelka, A., Novák, I., Al-Maadeed, M. A. S. A., Ouederni, M., & Krupa, I. (2018). Effect of corona treatment on adhesion enhancement of LLDPE. *Surface and Coating Technology, 335*, 118–125. https://doi.org/10.1016/j.surfcoat.2017.12.018

Primc, G., & Mozetič, M. (2024). Surface modification of polymers by plasma treatment for appropriate adhesion of coatings. *Materials, 17*(7), 1494. https://doi.org/10.3390/ma17071494

Raj, N., Breedveld, V., & Hess, D. W. (2020). Flow control in fully enclosed microfluidics paper based analytical devices using plasma processes. *Sensors and Actuators B: Chemical, 320*, 128606. https://doi.org/10.1016/j.snb.2020.128606

Recek, N. (2019). Biocompatibility of plasma-treated polymeric implants. *Materials, 12*(2), 240. https://doi.org/10.3390/ma12020240

Reich, S., Goesmann, M., Heunoske, D., Schäffer, S., Lueck, M., Wickert, M., & Osterholz, J. (2023). Change of dominant material properties in laser perforation process with high-energy lasers up to 120 kilowatt. *Scientific Reports, 13*(1), 21611. https://doi.org/10.1038/s41598-023-48511-9

Retolaza, A., Valentim, P. T., Bondarchuk, O., Freitas, M. A., Baptista, D., Amaral, M., & Sousa, P. C. (2022). A comparative study of the effect of different surface treatments on polymeric substrates. *Vacuum, 199*, 110918. https://doi.org/10.1016/j.vacuum.2022.110918

Robotti, E., Bobba, M., Panepinto, A., & Marengo, E. (2007). Monitoring of the surface of paper samples exposed to UV light by ATR-FT-IR spectroscopy and use of multivariate control charts. *Analytical and Bioanalytical Chemistry, 388*(5–6), 1249–1263. https://doi.org/10.1007/s00216-007-1370-4

Scala-benuzzi, M. L., Raba, J., Soler-illia, G. J. A. A., Schneider, R. J., & Messina, G. A. (2018). Novel electrochemical paper-based immunocapture assay for the quantitative determination of ethinylestradiol in water samples. *Analytical Chemistry, 90*(6), 4104–4111. https://doi.org/10.1021/acs.analchem.8b00028

Schmidt, M., Irsig, R., Duca, D., Peltz, C., Passig, J., & Zimmermann, R. (2023). Laser-pulse-length effects in ultrafast laser desorption. *Analytical Chemistry, 95*(51), 18776–18782. https://doi.org/10.1021/acs.analchem.3c03558

Seddaoui, N., Colozza, N., Gullo, L., & Arduini, F. (2023). Paper as smart support for bioreceptor immobilization in electrochemical paper-based devices. *International Journal of Biological Macromolecules, 253*, 127409. https://doi.org/10.1016/j.ijbiomac.2023.127409

Seo, J., Chang, W. S., & Kim, T. S. (2015). Adhesion improvement of graphene/copper interface using UV/ozone treatments. *Thin Solid Films, 584*, 170–175. https://doi.org/10.1016/j.tsf.2015.01.007

Sharif, A., Farid, N., McGlynn, P., Wang, M., Vijayaraghavan, R. K., Jilani, A., et al. (2023). Ultrashort laser sintering of printed silver nanoparticles on thin, flexible, and porous substrates. *Journal of Physics D: Applied Physics, 56*(7), 075102. https://doi.org/10.1088/1361-6463/acb367

Siddiqui, A. A., & Dubey, A. K. (2020). Laser surface treatment. In A. Sharma, S. Kumar, & Z. Duriagina (Eds.), *Engineering steels and high entropy-alloys*. IntechOpen. https://doi.org/10.5772/intechopen.91800

Silva, M., Santos, N. E., Pinto, M., Guieu, S., Oliveira, R., Figueira, F., et al. (2024). Photochemical modification of a diamond surface using a pulsed UV laser as the energy source. *Diamond and Related Materials, 147*, 111314. https://doi.org/10.1016/j.diamond.2024.111314

Strlič, M., Kolar, J., Šelih, V. S., & Marinček, M. (2003). Surface modification during Nd:YAG (1064 nm) pulsed laser cleaning of organic fibrous materials. *Applied Surface Science, 207*(1–4), 236–245. https://doi.org/10.1016/S0169-4332(02)01371-5

Sung, Y. Y., & Rubner, M. F. (2002). Micropatterning of polymer thin films with pH-sensitive and cross-linkable hydrogen-bonded polyelectrolyte multilayers. *Journal of the American Chemical Society, 124*(10), 2100–2101. https://doi.org/10.1021/ja017681y

Tan, C. Y., Wen, C., & Ang, H. Q. (2024). Influence of laser parameters on the microstructures and surface properties in laser surface modification of biomedical magnesium alloys. *Journal of Magnesium and Alloys, 12*(1), 72–97. https://doi.org/10.1016/j.jma.2023.12.008

Theodorakos, I., Zacharatos, F., Geremia, R., Karnakis, D., & Zergioti, I. (2015). Selective laser sintering of Ag nanoparticles ink for applications in flexible electronics. *Applied Surface Science, 336*, 157–162. https://doi.org/10.1016/j.apsusc.2014.10.120

Wang, D., Du, D., Dong, A., Li, J., Toursangsaraki, M., & Sun, H. (2024). Investigations on friction stir composite processing and picosecond laser-induced surface modification on mechanical properties of β-titanium alloy. *Materials Today Communications, 38*, 108041. https://doi.org/10.1016/j.mtcomm.2024.108041

Wang, L., Fei, Y., Gong, C., Shan, Y., Zhang, Z., Zhang, F., & Cheng, H. (2022). Comparative study of UV/H_2O_2 and UV/PMS processes for treating pulp and paper wastewater. *Water Science and Technology, 86*(8), 2032–2044. https://doi.org/10.2166/wst.2022.326

Wardak, C., Paczosa-bator, B., & Malinowski, S. (2020). Application of cold plasma corona discharge in preparation of laccase-based biosensors for dopamine determination. *Materials Science and Engineering: C, 116*, 111199. https://doi.org/10.1016/j.msec.2020.111199

Weber, D., Heimburger, R., Schondelmaier, G., Junghans, T., Zetzl, A., Zahn, D. R. T., & Schondelmaier, D. (2023). Cost-effective equipment for surface pre-treatment for cleaning and excitation of substrates in semiconductor technology. *Discover Applied Sciences, 5*(1), 21. https://doi.org/10.1007/s42452-022-05219-1

Wolf, R., & Sparavigna, A. C. (2010). Role of plasma surface treatments on wetting and adhesion. *Engineering, 2*(6), 397–402. https://doi.org/10.4236/eng.2010.26052

Woodward, I., Schofield, W. C. E., Roucoules, V., & Badyal, J. P. S. (2003). Super-hydrophobic surfaces produced by plasma fluorination of polybutadiene films. *Langmuir, 19*(8), 3432–3438. https://doi.org/10.1021/la020427e

Yin, P., Chen, C., Ma, H., Gan, H., Guo, B., & Li, P. (2020). Surface cross-linked thermoplastic starch with different UV wavelengths: Mechanical, wettability, hygroscopic and degradation properties. *RSC Advances, 10*(73), 44815–44823. https://doi.org/10.1039/d0ra07549c

Zarei, M., Sayedain, S. S., Askarinya, A., Sabbaghi, M., & Alizadeh, R. (2023). Improving physiomechanical and biological properties of 3D-printed PLA scaffolds via in-situ argon cold plasma treatment. *Scientific Reports, 13*(1), 14120. https://doi.org/10.1038/s41598-023-41226-x

Zea, M., Moya, A., Villa, R., & Gabriel, G. (2022). Reliable paper surface treatments for the development of inkjet-printed electrochemical sensors. *Advanced Materials Interfaces, 9*(21), 2200371. https://doi.org/10.1002/admi.202200371

Zhao, M., Li, H., Liu, W., Guo, Y., & Chu, W. (2016). Plasma treatment of paper for protein immobilization on paper-based chemiluminescence immunodevice. *Biosensors & Bioelectronics, 79*, 581–588. https://doi.org/10.1016/j.bios.2015.12.099

Zhao, X., Cui, C., Ma, L., Ding, Z., Hou, J., Xiao, Y., et al. (2024). Laser-ablated acoustofluidics-driven paper devices for controllable chemical engineering in color display applications. *Chemical Engineering Journal, 480*, 148245. https://doi.org/10.1016/j.cej.2023.148245

Zhou, W., Feng, M., Valadez, A., & Li, X. (2020). One-step surface modification to graft DNA codes on paper: The method, mechanism, and its application. *Analytical Chemistry, 92*, 7045–7053. https://doi.org/10.1021/acs.analchem.0c00317

Żołek-Tryznowska, Z., Prica, M., Pavlović, Ž., Cveticanin, L., & Annusik, T. (2020). The influence of aging on surface free energy of corona treated packaging films. *Polymer Testing, 89*, 106629. https://doi.org/10.1016/j.polymertesting.2020.106629

Chapter 9
Optimization of Paper Properties Via Surface Coating

Xin Li, Jie Wang, Hui Zhao, Ghenadii Korotcenkov, and Feng Xu

9.1 Introduction

Paper, owing to its low cost, environmental friendliness, superior mechanical properties, and ease of processing, stands as one of the oldest and most extensively utilized forms of cellulose substrates. The rapid evolution of papermaking technology has significantly enhanced human production and daily lives by producing a diverse array of paper products (Choi et al., 2024). However, traditional paper-based materials possess inherent limitations, such as their rich hydroxyl groups and porous structures, which result in inadequate barrier performance (Cheng et al., 2020). This necessitates surface treatment or composite processing to meet the stringent barrier requirements of various applications. To overcome these limitations and provide additional functionalities, various paper coatings are used. It is important to note that any material that can impart the desired properties to the paper when coated can be used as a coating material. In particular, these coatings can provide air, water, oil protection, antibacterial properties, improvement of mechanical properties (reinforced paper), and modification of physical properties such as weight, absorbency, gloss, opacity, water and gas permeability, smoothness, absorbency, brightness and color, etc. (Ye et al., 2023).

These coatings not only address the inherent limitations of traditional paper but also enable the development of advanced paper-based materials for emerging

X. Li · J. Wang · H. Zhao · F. Xu (✉)
State Key Laboratory of Efficient Production of Forest Resources, Beijing Forestry University, Beijing, China

Beijing Key Laboratory of Lignocellulosic Chemistry, Beijing Forestry University, Beijing, China
e-mail: xfx315@bjfu.edu.cn

G. Korotcenkov
Department of Physics and Engineering, Moldova State University, Chisinau, Moldova

G. Korotcenkov (ed.), *The Handbook of Paper-Based Sensors and Devices*,
https://doi.org/10.1007/978-3-031-91080-7_9

domains such as energy, sensing, optoelectronics, and flexible electronics (Yang et al., 2023). By imparting properties like hydrophobicity, conductivity, and flame retardancy, these coatings expand the versatility and applicability of paper in various fields, such as food packaging, paper conservation, shielding materials, and enhanced paper functionality for specialized applications (Zhao et al., 2024).

By employing diverse coating techniques, including bar coating, spray coating, spin coating, dip coating, laminating, evaporation, and sputtering, cellulose paper substrates are effectively integrated with functional coatings to yield high-performance paper-based materials. This chapter classifies these coated papers according to the coated materials, including polymer coating, nanocellulose coating, metallic coating, metal oxide coating, composite coating, recyclable coating, and other coatings. Its application and development trends in green packaging, electronic equipment, testing and analysis, and intelligent buildings and other fields are summarized and analyzed.

9.2 Coating Methods

To impart the desired properties to paper, a diverse range of coatings can be employed, formed from materials such as polymers, nanocellulose, starch, carbon-based materials, metals, and metal oxides. These materials have fundamentally different properties and therefore a wide variety of methods must be used to deposit them on the paper surface. These include bar coating, spray coating, spin coating, dip coating, laminating, evaporation, sputtering, etc. Each of the aforementioned coating technologies has its own advantages and disadvantages, rendering them suitable for diverse application scenarios.

9.2.1 Bar Coating

Bar coating, rod coating, or Mayer rod coating is widely used for paper coating due to its ease of operation and low cost compared to other coating methods. It involves a bar (such as a Mayer rod) being placed above a substrate and dragged over a solution or paste, resulting in the fluid or paste being spread into a thin film or coating (see Fig. 9.1). Bar coating can be performed manually or automated for greater precision and efficiency. Wires of different diameters wound on the rod will allow control over the coating thickness on the substrate. Stainless steel is the most commonly used material for both the rod and the wires due to its chemical resistance and high strength, making it less susceptible to damage. Rod speed and wire diameter are the two main parameters that can be varied to obtain a proper and specific coating thickness. The normal range of rod coating thickness is from 3 to 160 μm (Kunam et al., 2024).

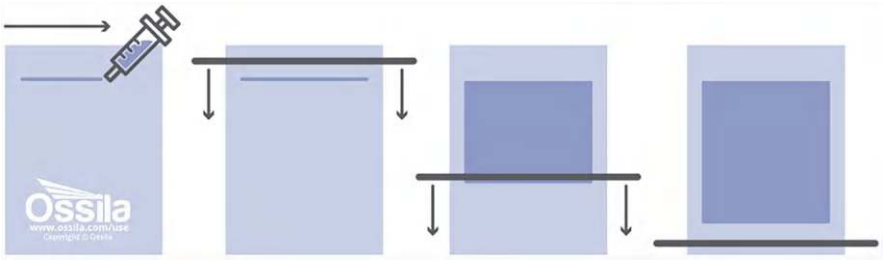

Fig. 9.1 Bar coating using a bar coater. https://www.ossila.com/pages/bar-coating

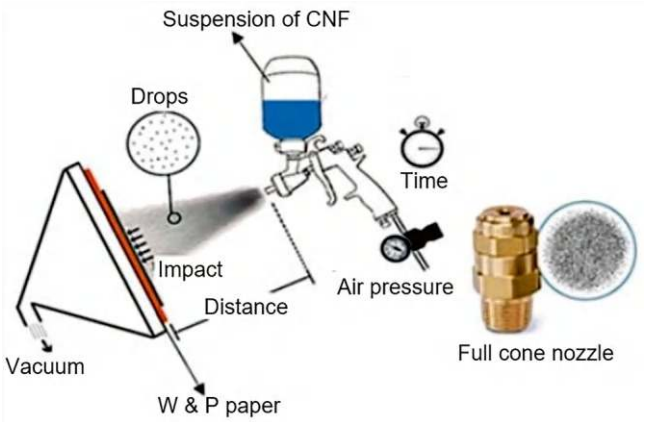

Fig. 9.2 Scheme of the experimental procedure used for spray coating on paper with cellulose nanofibrils (CNFs) suspension. Reproduced with permission from Mirmehdi et al. (2018). Copyright 2018: Taylor & Francis Group

9.2.2 Spray Coating

Spray coating primarily employs equipment like spray guns or spray bottles to atomize the solution into uniform and minute droplets, thereby achieving surface coating of the substrate (see Fig. 9.2). This method boasts advantages such as straightforward equipment, cost-effectiveness, and ease of operation (Nadeem et al., 2022). For instance, Ventrapragada et al. (2019) fabricated composite conductive paper by simply spraying carbon nanotubes (CNTs) onto commercial cellulose-based paper. The resulting material exhibited exceptional performance as a current collector for Li-ion batteries, displaying high energy density and remarkable cycle stability. Lan and Duan (2023) used spray pyrolysis of epoxy-based poly(vinyl silsesquioxane) (POSS)/polyvinylidene fluoride (PVDF) composite coating to protect archaistic paper. Electrospray can also be used to coat paper. Tarrés et al. (2022) used this method for deposition of cellulose nanofibers on paper.

9.2.3 Spin Coating

Spin coating represents a suitable technology for the fabrication of paper-based composite functional materials. This technique harnesses the centrifugal force generated by the high-speed rotation of the substrate to deposit the functional slurry, resulting in well-organized films with smooth surface and controllable thickness ranging from tens of nanometers to several micrometers. Spin coating has garnered extensive research attention in recent decades due to its time-efficiency, cost-effectiveness, slurry conservation, uniform coating, and controllable thickness compared to alternative technologies (Guan et al., 2023). Ke et al. (2024) explored the utilization of spin coating for electrode slurries, introducing a novel thin-film electrode architecture that facilitates the annealing step during the fabrication of traditional all-solid-state thin-film microbatteries. This approach enables low-temperature manufacturing, excellent cycling performance, and remarkable flexibility for integration.

9.2.4 Dip Coating

Dip coating, primarily utilized in laboratory research, offers simplicity and cost-effectiveness without sophisticated equipment, enabling easy adjustment of coating layer thickness. Although inconsistent coatings limit its industrial applications, it suits low-standard products, allowing large-scale use at a low price (Kakaei et al., 2019). This method involves depositing an aqueous-based liquid phase on the substrate surface by dipping it in a coating solution, followed by evaporation to remove excess liquid, leaving a unique dry coating layer. Various parameters, including immersion time, withdrawing speed, surface tension, density, viscosity of the coating solution, and substrate surface, determine the coating's thickness and morphology (Tang & Yan, 2017). Zeng et al. (2020) developed palm kernel oil (PKO)-coated paper, enhancing its liquid water barrier property with a water contact angle (WCA) of 120°. Wechakorn et al. (2020) created a simple colorimetric paper-based chemosensor for formaldehyde (FA) detection, where the filter paper's color changed from yellow to deep purple upon FA addition. The primary advantage of dip coating is its ability to deposit monolayers, while the main drawback is its time-consuming nature (Tosi et al., 2022).

9.2.5 Laminating

Optimization of paper properties via laminating is a crucial technique in the paper industry, significantly enhancing the quality and functionality of paper products. This process involves bonding one or more layers of material to the paper surface,

thereby improving its durability, appearance, and resistance to various environmental factors (Deshwal et al., 2019). For instance, the application of a polymeric film laminate can vastly improve the water resistance of paper. By laminating a thin layer of polyethylene or polypropylene to paper, manufacturers can create products that are resistant to moisture and humidity, making them suitable for outdoor use or in damp environments. Examples of paper laminating using size press coating and blade coating methods are shown in Fig. 9.3. Another example is the use of decorative laminates to enhance the aesthetic appeal of paper. These laminates, often featuring patterns, textures, or colors, can transform plain paper into visually striking materials suitable for high-end packaging, books, and other publications (Zhu et al., 2018). Therefore, laminating offers a versatile and effective means of enhancing paper quality. Whether it is improving durability, water resistance, or aesthetic appeal, laminating provides a wide range of benefits that cater to various industries and applications. However, it can also be time-consuming and require precise control to ensure optimal bonding and layer adherence (Jahangiri et al., 2024).

9.2.6 Evaporation and Sputtering

Beyond the aforementioned coating techniques, methods such as ion sputtering, magnetron sputtering, and vacuum evaporation are routinely utilized in the preparation of conductive composite paper. This paper is achieved through the integration of metals with paper substrates. Li et al. (2016) employed ion sputtering technology to deposit gold nanoparticles onto commercial art paper, followed by the modification of the metal layer with multi-walled carbon nanotubes. Thus, a disposable paper-based electrochemical sensor was fabricated. Liao et al. (2017) utilized direct current sputtering to deposit a thin film of gold nanoparticles onto sandpaper,

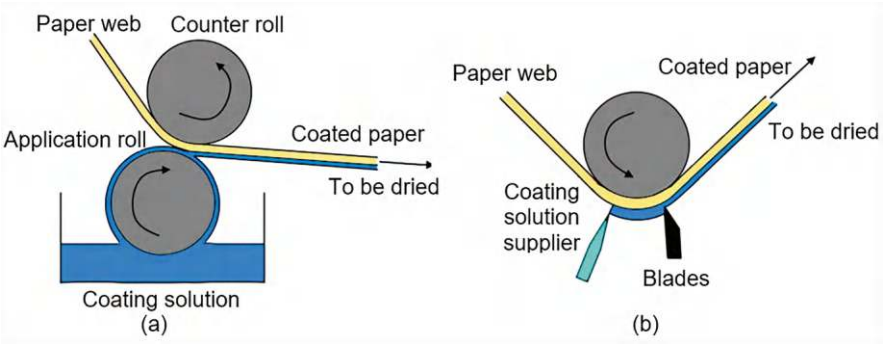

Fig. 9.3 Production of one-sided coated papers: (**a**) size press coating; (**b**) blade coating. The gap between the doctor blade and the roll on which the substrate is placed determines the coating thickness. Reprinted with permission from Sharma et al. (2020). Copyright 2020: Elsevier

ensuring a uniform distribution of the gold nanoparticles on the sandpaper surface. This composite film exhibited remarkable electrical conductivity.

9.2.7 Other Methods of Paper Coating

Of course, there are other methods of applying coatings to paper. For example, Putkisto et al. (2003) proposed using the dry method to apply polymer coatings to paper. The dry surface treatment employs the electrostatic deposition of dry, fine-sized particles and a thermomechanical surface treatment to fix the coating layer onto the substrate and to smoothen the coating surface (see Fig. 9.4). Ma, Zhu, et al. (2022) used chemical vapor deposition to coat calcium carbonate on the surface of ancient paper documents. By imparting superhydrophobic properties to the surface, the treated book paper exhibited excellent self-cleaning properties, long-term protection, reliable mechanical strength, and effective acidity neutralization effects. A more detailed description of the methods discussed above can be found in Chap. 28.

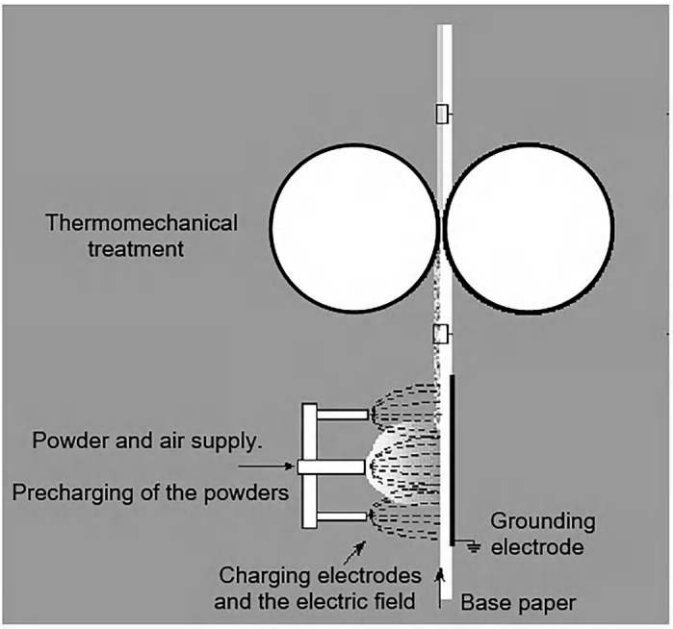

Fig. 9.4 The principle of the dry surface treatment in a one-sided process; the application and fixation steps. Reprinted from Putkisto et al. (2003). Published 2003 by TAPPI with open access

9.3 Paper Coating and Its Purpose

As stated earlier, paper coating serves a multitude of purposes, tailored to the specific needs of various applications. Let us consider the most popular ones in more detail based on the coating material used, including polymer coatings, nanocellulose coating, metallic coating, metal oxide coating, composite coatings, recyclable coating of the paper, and other coatings.

9.3.1 Polymer Coatings

Studies have shown that low surface energy polymer coatings can significantly improve the barrier properties of paper substrates (Jiang et al., 2022). At that, a wide variety of polymers can be used for coatings. Polysiloxanes, or silicones, are one such polymer. Polysiloxanes are an organic silicon polymer characterized by a unique molecular structure, featuring alternating silicon and oxygen atoms. Polysiloxane, being inherently safe, non-toxic, and environmentally benign, also exhibits favorable hydrophobicity. Its versatility allows for chemical grafting, physical blending, or compounding with diverse materials, thereby offering promising avenues for further development and application. Polydimethylsiloxane (PDMS) belongs to this group of polymers. Polydimethylsiloxane (PDMS) is an elastomer with excellent optical, electrical, and mechanical properties, which makes it well-suited for several engineering applications. In addition, the abundance of hydrophobic methyl groups within its structure imparts low surface energy properties to PDMS. This material exhibits remarkable attributes such as high-temperature resilience, exceptional waterproofness, and robust aging resistance, making it a cornerstone in the field of barrier materials for food packaging applications (Ye et al., 2024). For instance, Khan et al. (2019) utilized PDMS to formulate a hydrophobic epoxy resin, demonstrating significant self-cleaning efficiency. In a parallel study, Dai et al. (2022) devised an acrylate-terminated PDMS compound with enhanced hydrophobic properties.

In addition to silicones, conventional petroleum-based materials such as PVC (polyvinyl chloride), low-density polyethylene (LDPE), high-density polyethylene (HDPE), polystyrene, polypropylene, polyethylene terephthalate (PET), polymethylpentane (PMP), polyesters, fluorine-based derivatives, and waxes can be used to control the barrier properties of paper. Unconventional coating materials such as lignin-based coatings, polyvinyl alcohol (PVA), alkene-ketene dimer (AKD), and the combined use of PVA and AKD can also be used for these purposes (Kunam et al., 2024).

To give the coatings even more pronounced hydrophobic properties, additives can be added to the polymers. For example, fluorinated water and oil repellents, such as perfluorododecyl trichlorosilane (PDTS), which have significantly lower surface energy levels than water and oil, can be incorporated into polymer coatings.

These agents play a critical role in improving the barrier properties of polymer coatings on paper (Khanjani et al., 2018). In particular, Guo et al. (2017) synthesized superhydrophobic poly(ethylene terephthalate) (PET) and used a minimal amount of PDTS to modify it. The resulting coating significantly improved the water and oil resistance of fabric and paper (Park et al., 2015; Yuan et al., 2022). This modified product also demonstrated excellent chemical stability and mechanical properties.

Although fluorinated water and oil repellents such as traditional C8 fluorocarbon (FC) dendrimer have demonstrated commendable barrier properties, their molecular bonds are susceptible to breakdown at elevated temperatures. This leads to the formation of harmful perfluorinated compounds such as perfluorooctanoic acid (PFOA) and perfluorooctane sulfonate (PFOS) (Ma, Zhong, et al., 2022). These compounds have adverse effects on human health and pose potential risks to both ecosystems and living organisms (Cao et al., 2023; O'Rourke et al., 2022).

In recent years, the gradual replacement of C8 dendrimer with C6-FC dendrimer in polymer coatings has led to a significant reduction in the toxic properties of the coatings. However, such a replacement only reduces the content of PFOA and PFOS, but does not guarantee their complete absence (Cao et al., 2023). Therefore, research is being conducted to develop safer and more environmentally friendly polymer coatings that can provide effective barrier properties without posing a risk to health or the environment. In particular, in recent years, much interest has been shown in the use of various biopolymers to form various barriers on the surface of paper. The use of biopolymers also solves the problem of abandoning polymers made from fossil fuels, which have many environmental limitations. In particular, they are less suitable for recycling and can require even 500 years for very slow biodegradation. Some examples of the use of biopolymers as paper coatings are given in Table 9.1.

9.3.2 Nanocellulose Coating

Nanocellulose can be deposited onto the paper surface by a variety of methods. For example, Tarrés et al. (2022) used electrospray method for deposition of cellulose nanofibers on paper. They showed that the application of nanocellulose to the surface of paper reduces porosity and permeability, and thus improves its barrier properties to air, fat, water vapor, and even liquid water. Tarrés et al. (2022) are confident that nanocellulose-reinforced paper has the potential not only to partially replace conventional packaging paper, at least for special deliveries, but also to contribute to the replacement of non-biodegradable single-use plastics. It is important to note that the advantages of nanocellulose as a coating material for paper have been noted in many studies (Lengowski et al., 2023; Spagnuolo et al., 2022). Nanocellulose coating improves both the strength and durability of paper. In addition, nanocellulose is lightweight, highly absorbent, and improves barrier properties against fat, oil, and oxygen. Water permeability and gas permeability are reduced when

Table 9.1 Biopolymers for paper coating

Biopolymers	Substrates	Functions
Starch-citric acid	Printing paper	Water barrier
HPMC	Printing paper	Water barrier
Chitosan	Greaseproof paper; Kraft paper	Air, O_2, CO_2, N_2 and grease barrier
Chitosan-palmitic acid; chitosan-beeswax bilayer	Kraft paper	Water barrier, air barrier, grease barrier
Chitosan-sodium alginate; sodium alginate	Kraft paper; printing paper	Fat barrier
Sodium caseinate (NaCAS); NaCAS-chitosan	Printing paper	Water vapor barrier
Wheat gluten	Kraft paper	Oxygen barrier
Zein	Kraft paper	Water barrier, grease barrier
PLA; PLA-NFC; PHB; PHB/V-wax	Paperboard	Water barrier
Carboxymethylated NFC	Printing paper	Air barrier, oil barrier

HPMC hydroxypropyl methylcellulose, *NFC* nanofibrillated cellulose, *PHB* polyhydroxybutyrate, *PHB/V* polyhydroxybutyrate/valerate, *PLA* polylactic acid, *Zein* a class of prolamine protein
Source: Data extracted from Rastogi and Samyn (2015)

cellulose is nanosized because of the dense crystalline structure of the nanoparticles. Paper coated with nanocellulose becomes more compact, with fewer pores in the longitudinal section. In addition, the surface of the paper tends to be smooth after coating. Cellulose nanocrystal coatings on paper also reduce friction in paper devices and packaging while maintaining the optical properties of the coating. Nogi and Yano (2009) showed that a densely packed nanocellulose film is optically transparent because the dense packing of fibers with small spaces between them scatters light poorly. A nanocellulose film shows very good stability to light, temperature, and humidity aging (Dreyfuss-Deseigne, 2017). Its unique properties of transparency do not change after aging. Cellulose coatings are also compatible with food packaging and are biodegradable. Cellulose can also be used as one component of a composite used to form coatings for a variety of applications, including antibacterial coatings and intelligent food packaging (Wang et al., 2022).

9.3.3 Metallic Coatings

Metallized paper is the most common and used product of metallic coatings of the paper with a layer of aluminum (see Fig. 9.5). Silver and other metals can also be used. But it is much more expensive. Metallized paper is used to enhance both the product's protective properties during storage and for visual purposes. It is an incredibly durable material, demonstrating high resistance to tearing, punctures, and abrasion, and maintains its structural integrity in wet conditions. Additionally, the silvery sheen of this material has led to it becoming a key tool for designers,

Fig. 9.5 One of the stages of production of metallized paper. https://www.synponh.com/products/aluminized-transfer-tipping-base-paper-for-cigarette/

maximizing shelf appeal for packaging and labels. The high strength and creative offerings of this product make it a popular choice for the following applications.

There are two different methods that can be used to create metallized paper: (1) lamination, which involves bonding the paper to a sheet of aluminum that is 9–12 microns thick. This system is becoming less and less common due to the high consumption of aluminum. Therefore, the most widely used method nowadays is (2) vacuum metallization. This method consists of deposition of a thin layer of aluminum or other material in a vacuum chamber onto the surface of the paper substrate. In this case, 300 times less aluminum is used than in the previous case. The process of producing metallized paper by the direct high vacuum method consists of three independent processes, namely: (1) varnishing, (2) metallization, and (3) lacquering. A thin layer of varnish is applied to the coated substrate to prepare the surface for subsequent metallization. The paper is pre-coated with varnishes, which are applied to level the surface of the paper, to act as a barrier between the paper and the metallized layer, and to improve the adhesion of the evaporated metal. The varnish is applied in the varnisher by a process similar to gravure printing. After varnishing, the paper is passed through a hot air dryer to remove the varnish solvents and hence dry the paper until its moisture level is between 2 and 3%. Lacquering is used to protect the aluminum layer and make the surface suitable for printing.

Nowadays, metallized paper finds versatile applications in a variety of industries:

Packaging: Metallized paper acts as an excellent barrier against light, oxygen, moisture, and odors, which is critical to protecting packaged contents and extending shelf life, especially for sensitive products. It is commonly seen in food, cigarettes, cosmetics, and luxury goods packaging.

Labels: Labels for a variety of products are made from metallized paper to stand out on the shelves and enhance the product's appeal.

Publishing: Magazine and catalog covers, advertising inserts, brochures, and annual reports often use metallized paper to create greater visual impact.

Decorative: Metallized paper's ability to be embossed or display holographic effects makes it a popular choice for decorative applications, including greeting cards and luxury goods.

In addition, metallic coatings can be used to produce conductive paper with exceptional electrical conductivity properties, making it suitable for a wide range of electronic applications (Scheffler et al., 2005). Among the commonly utilized metal conductive materials, silver, copper, gold, and their corresponding nanowires have garnered significant attention due to their inherent conductivity properties (Naghdi et al., 2018). For example, Dogome et al. (2013) formulated silver nanoparticles into a conductive ink that was subsequently sprayed onto paper substrates, yielding cellulose-based conductive substrates with a resistivity of 2 Ω·cm. Preston et al. (2014) utilized coating techniques to integrate silver nanowires onto cellulose paper surfaces, creating flexible and transparent conductive substrates with a low sheet resistance of 13 $\Omega \cdot sq^{-1}$ and high transmittance of 91%. While the incorporation of metal materials enables the fabrication of highly conductive substrates, the inherent metallic sheen of these materials often compromises their transparency.

Metallic coatings also solve another important problem. With the widespread use of electronic devices, the harmful effects of electromagnetic wave pollution and electromagnetic interference (EMI) have become increasingly evident. To address this issue, Zhan et al. (2021) developed an innovative strategy involving the initial immersion of silver nanowires (AgNWs) on the surface of filter paper, followed by sputter deposition of nickel nanoparticles (NiNPs). Notably, this new material demonstrated an impressive electromagnetic shielding efficiency of 88.4 dB, effectively mitigating the damaging effects of electromagnetic waves. Moreover, the material demonstrated remarkable durability, maintaining its highly effective EMI shielding efficiency even after undergoing 1500 bending cycles or immersion in water, salt, or strong alkaline solutions for 2 h.

9.3.4 Metal Oxide Coating

Metal oxide and doped metal oxide materials, such as ZnO, Fe_3O_4, Al_2O_3, indium tin oxide (ITO), and aluminum-doped zinc oxide (AZO), can also be used for paper coating (Liu et al., 2020). In particular, Hu et al. (2013) deposited ITO onto carboxymethylated nanofibrillated cellulose film surfaces, resulting in conductive substrates with a sheet resistance of 12 $\Omega \cdot sq^{-1}$ and a transmittance of 65% at 550 nm. Khondoker et al. (2012) employed spin coating to apply ITO nanoparticles onto cellulose substrates, achieving a resistivity of 2.5×10^3 Ω·cm with an ITO particle loading of 15 wt%. Even though metal oxide materials exhibit both electrical conductivity and transparency, their brittleness renders them impractical for flexible electronic applications (Guan et al., 2024). Furthermore, achieving robust bonding between inorganic metals/oxides and organic paper substrates poses a significant challenge. Additionally, certain metal oxides employed as conductive materials necessitate high-temperature sintering, thereby limiting their applicability in paper-based conductive substrate systems (Leung et al., 2023).

However, it should be noted that developers cannot abandon metal oxides, the specific properties of which allow improving the properties of many paper coatings

designed for various applications. For example, ZnO, CuO, and TiO_2 have been found to have good antioxidant and antimicrobial properties, which makes them attractive in the development of new coatings for paper intended for use in many biomedical fields, agriculture, and food packaging industries (Nagajyothi et al., 2014; Zhang & Rhim, 2022). As a rule, these are composite coatings based on polymers (read Sect. 9.3.5). For example, the most common material matrix used with ZnO is chitosan (Yadav et al., 2021).

9.3.5 Composite Coatings

Composite coatings, which integrate multiple materials, offer a synergistic combination of properties such as enhanced durability, flexibility, and barrier performance, making them ideal for a wide range of applications in the paper industry.

For example, to prepare superhydrophobic paper, Wang et al. (2017) proposed using a surface coating containing stearic acid (SA), precipitated calcium carbonate (PCC) particles, and acrylated epoxidized soybean oil (AESO) as a binder. PCC is widely used as a filler for many paper products to reduce the production cost and improve the optical properties of paper. It is considered as a safe and environmentally friendly material. AESO is a macromonomer derived from soybean oil. As shown in Table 9.2, the surface of the original filter paper was superhydrophilic with the WCA close to 0°. When the coating formula consisted of AESO binder only, the WCA of the filter paper increased to 106°, indicating the strong hydrophobicity of AESO binder. When PCC particles were introduced into the coating formula, the increase in WCA of the filter paper was much more pronounced. Wang et al. (2017) suggested that the produced superhydrophobic paper should have good biodegradability due to the nature of the raw material.

SiO_2-based coating is another example of composite coatings. Silicon barrier coatings primarily harness the inherent low surface energy of organosilicon compounds to impart water and oil repellency. Within the realm of paper-based

Table 9.2 Effect of stearic acid concentration in PCC modification on the hydrophobicity of the coated paper

Sample	WCA (°)
Filter paper	0
Filter paper + binder[a]	106 ± 7
Filter paper + binder + PCC	125 ± 3
Filter paper + binder +3%SA-PCC	136 ± 5
Filter paper + binder +6%SA-PCC	139 ± 6
Filter paper + binder +9%SA-PCC	141 ± 4
Filter paper + binder +12%SA-PCC	146 ± 3
Filter paper + binder +15%SA-PCC	146 ± 2

Source: Reprinted from Wang et al. (2017). Published 2017 by Nanjing Forestry University with open access

[a] The solid percentage of the AESO-binder in all coating formulas was 20 wt%

packaging materials research, nano-SiO_2 materials stand as the most prevalently employed variety (Zhu et al., 2023). Nano-SiO_2 constitutes ultrafine particulate matter, which can be incorporated as fillers either through physical blending with polymers or chemical modification. The distinctive chain-like structure, arising from the aggregation of Si–O bonds and a molecular size spanning 1–100 nm, confers upon nano-SiO_2 both chemical stability and a substantial specific surface area (Shankar et al., 2024). Current investigations into the barrier properties of nano-SiO_2 primarily concentrate on its superhydrophobic modification within paper-based packaging materials. Notably, Zhao et al. (2023) employed post-treatment immersion techniques to integrate hydrophobic vapor-phase SiO_2 particles with nanocellulose films, yielding nanostructured rough surfaces that exhibited a remarkable WCA of 161.7°. The composite material exhibited superior self-cleaning and anti-fouling properties. Additionally, Li, Wang, et al. (2019) developed a robust superhydrophobic surface coating by spraying a blend of epoxy resin, polydimethylsiloxane (PDMS), and modified SiO_2 particles, achieving an ultrahigh WCA of 159.5°, exceptional durability, and enhanced barrier properties. Nevertheless, akin to many nanomaterials, nano-SiO_2 is susceptible to interparticle aggregation, posing difficulties in achieving uniform dispersion. Furthermore, the absence of adhesion between nano-SiO_2 particles and paper substrates hinders nano-SiO_2 standalone utilization as an effective barrier coating (Nabiyan et al., 2023).

Composite coatings can also solve other problems. For example, Chen et al. (2017) developed a new flexible conductive paper featuring superhydrophobic surface, electrothermal effects, and flame retardancy. For this, they used a composite coating. Hydroxyapatite nanowires and Ketjen Black were used as stable flame retardant and conductive materials, respectively. PDMS was included to impart superhydrophobic characteristics and enhance the mechanical strength of the paper. Experimental results showed that even after immersion in water for 120 s, the superhydrophobic flexible conductive paper maintained remarkable conductivity stability (change of only 3.65%). Its exceptional electrothermal properties enabled rapid heating to 224.25 °C within 10 s and maintained stable performance under direct flame heating for 7 min. It is noteworthy that the conductivity of the conductive paper retained 90.6% of its original value after flame treatment.

Li et al. (2021) also used the composite coating to fabricate multifunctional superhydrophobic functional materials based on cellulose paper. They used sputtering of MXene/Polypyrrole (PPy) composite on one side of filter paper and PDMS on the other side, followed by deposition of candle black. The resulting material exhibited exceptional EMI shielding performance and conductivity, demonstrating its ability to convert hydrokinetic energy into continuous electrical energy with a peak current reaching 0.8 nA. Li et al. (2021) believe that this multifunctional paper-based functional material has great potential for various applications including electronics and energy technology.

Another group of composite coatings is polymer coatings with antimicrobial and antibacterial properties. As a rule, such properties are associated with the presence of metal (Ag, Cu, Zn) and metal oxide (ZnO, TiO_2, CuO) nanoparticles (NPs)

in the coating. Nanoparticles (NPs) of these materials have a broad antibacterial and antimicrobial spectrum with short contact time, are readily available, easy to prepare, and highly stable in their intended applications and storage (Maruthapandi et al., 2022; Nigussie et al., 2018). In addition, these antibacterial compounds act against fungi, viruses, and protozoa in addition to bacteria. Such coatings with antimicrobial properties on packaging materials such as paper are of increasing interest for controlling or limiting the growth of microorganisms and preventing foodborne and hospital-acquired infections, as they can inhibit the colonization and transmission of pathogens. Intensive research is currently being conducted in this direction. For example, Sanmugam et al. (2017) proposed composite coatings based on chitosan, ZnO, and graphene oxide (GO). Dejen et al. (2020) successfully prepared ZnO/PVA nanocomposite, the antibacterial activity of which was evaluated against *E. coli* and *S. aureus*. Some examples of the use of nanocomposites containing Ag and ZnO NPs in food packaging materials are presented in Table 9.3.

Table 9.3 Some examples of food packaging materials containing Ag and ZnO nanoparticles

Composite polymer matrix	Notable properties
Liposomes/laurel essential oil/AgNPs	Good antioxidant and antimicrobial properties
Polylactic acid/AgNPs	Improved preservative properties
Polyvinyl alcohol/clay/AgNPs	Enhanced mechanical, light barrier, and water-resistant properties. High antimicrobial action against S. *typhimurium* and *S. aureus*
Polyethylene/Ag/TiO_2	Strong antibacterial activity
AgNPs/gelatin-ontmorillonite/cellulose acetate/and/or thymol	High strength properties, UV blocking, and oxygen barrier properties. Good antioxidant activity. High antimicrobial and antifungal activity
Carboxymethyl cellulose/curcumin/ZnO	Improved UV barrier and mechanical properties. Optimal functional films with antibacterial and antioxidant properties
Bacterial cellulose/*Gluconacetobacter xylinum*/ZnO	High antimicrobial activity against *Escherichia coli*, *Bacillus subtilis*, and *Candida albicans*
Gelatin/starch/ZnO	High antibacterial activity against *Staphylococcus aureus* and *Escherichia coli*
Starch/polyvinyl alcohol/ZnO	Enhanced water barrier, UV barrier, mechanical and antimicrobial properties against *Salmonella typhimurium*
Grape seed extract/carboxymethyl cellulose/ZnO	High activity against ABTS and DPPH oxidative free radicals. The film exhibited 100% UV protection. Enhanced mechanical and water vapor barrier properties. Potent antibacterial properties against foodborne pathogens of *E. coli* and *L. monocytogenes*
Pectin/ZnO	Enhanced UV-light barrier property

Source: Data extracted from Adeyemi and Fawole (2023)

9.3.6 Recyclable Coatings of the Paper

The application of polymer, metal, metal oxide coatings, and silicon-containing barrier coatings can significantly enhance the barrier and functional properties of paper. However, a major drawback of these coatings is their adverse impact on paper recyclability. Consequently, extensive research is currently focused on developing recyclable coatings for paper, often utilizing biomass-based polymers such as nanocellulose, starch, and their composites. These biomass-based polymers form a dense coating on paper substrates, akin to fluoropolymer copolymers, effectively blocking the penetration of water and oil droplets due to the hydrophobic/oleophobic groups on their polymer chains (Yuan et al., 2024). Notably, biomass-based polymers offer advantages such as abundant raw material sources, environmental friendliness, and reduced biological hazards, making them attractive alternatives for the development of barrier coatings on paper (Li et al., 2024).

9.3.6.1 Biomass-Based Barrier Coatings

For paper-based coating materials, polysaccharides such as starch, chitosan, carboxymethyl chitosan, sodium alginate, nanocellulose, and modified cellulose are commonly employed. Their chemical structures are illustrated in Fig. 9.6. These polysaccharide solutions inherently possess a certain viscosity, enabling good adhesion with paper and films (Jahangiri et al., 2024). Notably, biomass-based polysaccharides like chitosan and sodium alginate exhibit exceptional film-forming capabilities, allowing for the creation of efficient barrier films on paper substrates (Li & Rabnawaz, 2019). Several examples of such applications are given in Table 9.4.

Starch and modified starch represent the earliest employed additives in papermaking, offering advantages such as cost-effectiveness and straightforward processing procedures (Adewale et al., 2022). Zhong et al. (2019) modified oxidized cassava starch with different concentrations of octenyl succinic anhydride. It was found that when the starch concentration was maintained at 20% and the octenyl succinic anhydride concentration was 3%, the optimal water and oil resistance of the coating film was achieved. Ovaska et al. (2015) prepared barrier coatings composed of hydroxypropyl starch and talc, demonstrating remarkable oil resistance below 60 °C but experiencing a decline in oil resistance at 100 °C. Long et al. (2015) compared the barrier properties of chitosan and chitosan/cationic starch composites. The results showed that chitosan/cationic starch composite materials exhibited superior thermal stability and barrier properties due to their film-forming capabilities. Notably, chitosan was identified as the primary contributor to the enhanced oil resistance observed in these paper-based materials.

Current researches have focused on the utilization of hydroxy-rich biodegradable polysaccharides including chitosan, sodium alginate, and nanocellulose for enhancing the oil resistance of paper-based materials. These polymers effectively mitigate the migration of volatile organic compounds by sealing the interstices between

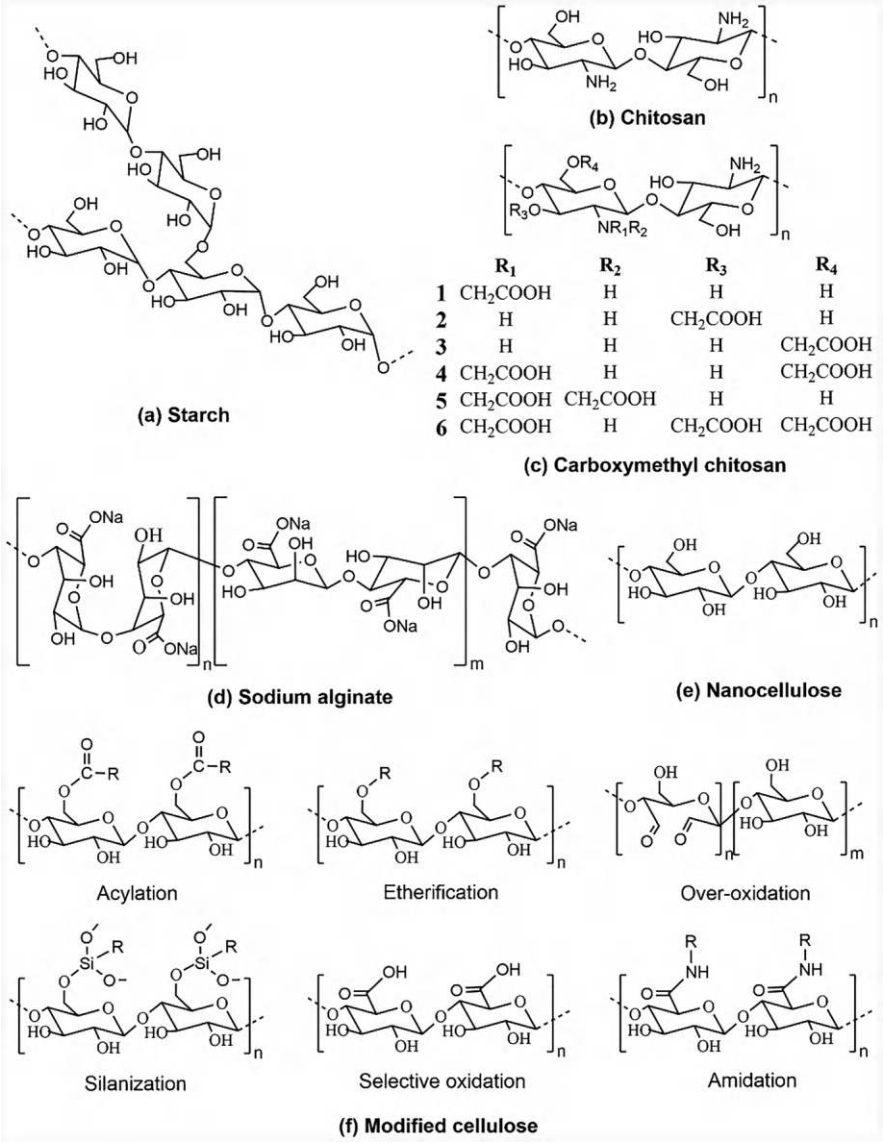

	R_1	R_2	R_3	R_4
1	CH_2COOH	H	H	H
2	H	H	CH_2COOH	H
3	H	H	H	CH_2COOH
4	CH_2COOH	H	H	CH_2COOH
5	CH_2COOH	CH_2COOH	H	H
6	CH_2COOH	H	CH_2COOH	CH_2COOH

Fig. 9.6 Chemical structures of different polysaccharides

paper fibers (Ruberto et al., 2024; Zhang et al., 2024). Moreover, their inherent properties such as good biocompatibility and biodegradability broaden the application potential, positioning them as vital components in the development of eco-friendly packaging barrier materials. Wang et al. (2021) coated paper substrates with a mixture of chitosan and montmorillonite, in which montmorillonite was strategically employed to augment the oil resistance of chitosan and reduce costs. The

Table 9.4 Mechanical testing on control paper before and after coating with chitosan

Mechanical testing	Control paper (uncoated paper)	Paper coated with chitosan	Paper treated with acetic acid
Tensile strength (kN/m)	6.03 ± 0.18	6.42 ± 0.38	5.63 ± 0.32
Burst strength (kPa)	310 ± 5	348 ± 18	298 ± 15
Tearing resistant (mN)	522 ± 26	538 ± 15	545 ± 29
Folding endurance (no.)	267 ± 29	318 ± 34	254 ± 32

Source: Reprinted from Zakaria et al. (2015). Published 2015 by Universiti Kebangsaan Malaysia with open access

study demonstrated that filling the paper fiber interstices with montmorillonite concurrently elevated the thermal stability and mechanical properties of the paper. For example, Table 9.1 shows that the tensile strength increased for coated paper with chitosan compared to uncoated paper and paper treated with acetic acid (Zakaria et al., 2015). This improvement after paper coating with chitosan was due to an improvement in the bond strength between the fibers in the paper. At the same time, acetic acid caused a decrease in paper strength due to fiber degradation. This was due to the hydrolysis of acid in the cellulose chain.

Sheng et al. (2019) successfully developed fluorine-free barrier coatings utilizing sodium alginate/hydroxypropyl cellulose and sodium alginate/propylene glycol alginate, fulfilling food packaging's oil resistance requirements with a single-layer application. Additionally, the low surface energy of the coatings improved the water barrier properties and the mechanical properties of the paper. Kansal and Rabnawaz (2021) grafted chitosan onto epoxidized sunflower oil to prepare biobased coatings with excellent waterproof and oil-resistant properties. Thermogravimetric analysis results confirmed that the coated paper substrate exhibited outstanding thermal stability at 250 °C. Xia et al. (2024) developed a bio-based coating for paper from carbamate starch (Sc), calcium lignosulfonate (CL), and cellulose nanofibrils (CNF). When the degree of substitution (Ds) of Sc was 0.10, the amount of CL was 1.00 g, and the amount of CNF was 0.65% of the weight of Sc, the paper coated with the resulting coating exhibited increased hydrophobicity and excellent mechanical, air-barrier, and UV-light-barrier properties. This coated paper has the potential for applications in the food packaging sector.

In addition to polysaccharide-based polymers, protein membranes also exhibit excellent barrier properties. Corn alcohol-soluble protein, a biodegradable polymer derived from corn waste, possesses inherent water resistance. By incorporating oil-resistant additives, this protein can be transformed into functional coatings suitable for food packaging applications (Brodnjak & Tihole, 2020). Hamdani, Li, Sirinakbumrung, and Rabnawaz (2020) utilized double-layer coating to prepare paper-based materials with excellent barrier properties. The foundational layer composed of polyvinyl alcohol imparted oil repellency, while the upper layer constructed from corn alcohol-soluble protein served as the hydrophobic barrier. This dual-layer design significantly enhanced the coated paper's resistance to water, oil, and heat, broadening its potential applications. Kansal et al. (2020) further employed 100% biodegradable food-safe materials composed of chitosan and corn

alcohol-soluble protein solution for double-layer coating. The coated paper demonstrated robust barrier and thermal stability, all while maintaining the mechanical properties of the paper. Subsequent recyclability tests verified that the coating could be efficiently separated from the paper, facilitating pulp utilization and coating material recycling.

Overall, biomass-based polymers typically enhance the barrier properties of paper-based materials through double or multiple coating methods. However, their processing is relatively complex, and occasional performance limitations pose challenges. The utilization of biomass-based polymers as paper coating materials generally faces the issue of high costs of raw materials (Yi et al., 2020). Therefore, to bolster their economic viability and research applicability, the pursuit of low-cost biomass-based polymer composite coatings has emerged as a promising new research frontier.

9.3.6.2 Biomass-Based Composite Barrier Coatings

Biomass-based composite barrier coatings are frequently incorporated to compensate for the barrier shortcomings of biomass-based polymer. By using chemical modification or physical double-layer coating, the barrier properties of paper-based materials are improved (Lin et al., 2019). Due to the advantages of biocompatibility and biodegradability, biomass-based composite barrier coatings have garnered considerable attention in the field of food packaging, where their eco-friendly nature aligns well with consumer preferences and industry trends. Song et al. (2020) employed tetramethoxysilane (TMOS) as a crosslinking agent, fostering the formation of a robust network structure by interlinking oleophobic sodium alginate with hydrophobic polydimethylsiloxane (PDMS). This innovative approach yielded a mixed coating that exhibited remarkable waterproof and oil-resistant properties. The results indicated that the coated paper possessed superior water and oil repellency. Li and Rabnawaz (2018) further validated the effectiveness of PDMS in paper coating, highlighting its simple production process, high safety standards, and pronounced waterproofing capabilities. Subsequently, Li, Rabnawaz, et al. (2019) grafted PDMS onto chitosan, utilizing this composite as a coating for unbleached kraft paper. The high film-forming ability of chitosan effectively minimized the fiber gaps on the paper's surface, thereby enhancing its oil resistance. Meanwhile, the incorporation of PDMS imparted excellent waterproof performance to the coated paper. Additionally, this group chemically grafted castor oil-encapsulated isocyanate onto chitosan, yielding a coating that not only demonstrated superior water and oil resistance but also had minimal impact on the mechanical properties of the paper (Li et al., 2020). Furthermore, to reduce the production cost of paper-based barrier materials, corn alcohol-soluble protein was mixed as a filler to decrease the amount of chitosan and PDMS (Hamdani, Li, Rabnawaz, et al., 2020).

Despite the biomass-based polymer barrier coatings have met performance standards, the current scope of practical utilization remains limited. To ensure the widespread adoption of high-performance paper-based barrier materials, it is imperative

to broaden the diversity and comprehensiveness of their application systems. Additionally, a deeper understanding of their underlying mechanisms of action, as well as the exploration of effective recycling strategies, is crucial (Asgher et al., 2020). By addressing these aspects, we can pave the way for the ubiquitous utilization of biomass-based barrier coatings in various industries.

9.3.7 Other Coatings

Other coatings for paper encompass a broad spectrum of materials and technologies, often tailored to impart specific functional properties beyond those achievable with traditional coatings. These include coatings formulated with advanced nanomaterials, such as nanoclays or quantum dots, to enhance optical properties or add functionalities like UV resistance (Tandey et al., 2024). Additionally, specialty coatings like those incorporating biocides can be used to impart antimicrobial properties to paper, making it suitable for hygiene-sensitive applications (Yuan et al., 2024). Furthermore, coatings designed to release active ingredients, such as fragrances or antioxidants, can be applied to paper to provide added value and functionality (Tan et al., 2020). The versatility of "Other Coatings" allows for the customization of paper properties to meet the unique needs of diverse industries and applications.

For example, carbon-based conductive materials, including CNTs, graphene (GE), and graphite, exhibit diverse properties suitable for high-performance electronic devices (Bulmer et al., 2021). CNTs feature exceptional mechanical, chemical, and electrical characteristics due to their hexagonal honeycomb-like structure (Hu et al., 2023). GE, a two-dimensional material, boasts large π bonds enabling high electrical conductivity (Ran et al., 2024). Graphite, a three-dimensional carbon form, demonstrates impressive thermal conductivity, high temperature resistance, and stable chemical properties (Liu et al., 2023). Research has shown that depositing multi-walled carbon nanotubes (MWCNTs)/graphene oxide (GO) nanocomposites onto fiber paper with nanocrystalline cellulose as a binder enhances conductivity and mechanical properties (Tang et al., 2014). GE-coated paper achieves notable sheet resistance, while CNC-dispersed carbon fibers/expanded graphite (CF/EG) improves dispersion stability and coating performance on cellulose paper (Lee et al., 2013; Liu et al., 2018). Despite their advantages of abundant resources and low costs, aggregation and uneven dispersion of carbon-based materials challenge their integration in flexible electronic devices (Zhang et al., 2018). Surface modification and ultrasonic treatments are effective strategies to enhance their dispersibility and optimize functionality within paper-based substrates (Li et al., 2022). The use of carbon-based materials to form conductive paper is discussed in more detail in the Chap. 13.

Turning to novel building materials, Cordt et al. (2021) have designed a thermal-induced self-healing superhydrophobic coating composed of wax and polysaccharide derivatives. This coating demonstrates high potential for engineering applications, offering a unique combination of durability and self-repair

capabilities. It is known that in nature, waxes provide excellent repellency and barrier properties. For example, both mineral waxes such as Paraflex paraffin grades as well as Paraflex Nowax organic waxes, based on hardened vegetable oils, yield equivalent barriers to polyethylene and provide moisture vapor transmission rate (MVTR) under tropical conditions (38 °C/90%RH) between 150 and 200 g/m^2/day/μm of coating (Krings, 2019). In contrast to plastic-coated paper, waxed paper is inherently biodegradable, degrading at about the same rate as leaf mulch. More recent studies have shown that contrary to common wisdom, wax-coated paper is repulpable for use in standard recycled paper production. In this way, wax-coated paper can offer a comprehensive solution of many problems, be that energy recovery, littering, recycling or composting. In other words, wax-based solutions, which are comparable in cost to plastic films and extrusion-coated paper, offer numerous environmental benefits. The layer or film thickness is often selected depending on the barrier requirements and typically ranges 10–100 μ.

9.4 Conclusions and Outlooks

In recent years, paper-based functional materials have undergone rapid advancements, fueled by the implementation of diverse processing methods. Among these, the coating method stands out for its simplicity, versatility, eco-friendliness, and integration capabilities. This chapter delved into the various modern coating materials and coating methods employed in this field, highlighting their unique characteristics and potential. Furthermore, it classified the paper-based functional materials by coating materials and reviewed the application research of paper-based functional materials that incorporate polymer coatings, nanocellulose coating, metallic coatings, metal oxide coating, composite coatings, recyclable coatings, and other special coatings. Moreover, the application performance, characteristics, and conditions of paper-based functional materials in these research fields are also analyzed and discussed, providing a reference for the further development of new coated paper-based materials with high performance.

Indeed, despite the significant progress made in the field of coated paper-based functional materials, there remain critical areas that necessitate further investigation. Specifically, the structural regulation, performance optimization, and the intricate response relationship within coated paper systems require deeper understanding. Additionally, the path toward large-scale production and widespread commercial application of these materials is fraught with challenges. In the next research work of coated paper-based functional materials, the following attempts can be made:

In the realm of barrier modification, there is a pressing need to redirect our efforts toward the development of environmentally benign alternatives to fluoride-based compounds. To this end, a heightened focus should be placed on the exploration and refinement of natural waxy materials, fatty acids, and other green reagents that offer comparable or enhanced barrier properties while minimizing ecological impact. By delving deeper into the properties and performance of these sustainable alternatives,

we can pave the way for the creation of eco-friendly coatings that not only safeguard against undesired permeation but also align with the principles of green chemistry and environmental protection.

The functional coatings employed in various applications are susceptible to degradation or malfunction under the cumulative effect of numerous external factors. To mitigate these vulnerabilities and bolster their industrial applicability, the incorporation of stimulus-responsive mechanisms, such as thermal and magnetic responsiveness, into the design of self-healing paper-based coatings is highly recommended. These smart coatings possess the capability to autonomously repair damage in response to specific stimuli, thereby extending their lifespan and maintaining optimal performance. The above reasons are enough to justify that the ongoing quest for interdisciplinary collaborative innovation and basic theoretical research of surface chemistry in order to fulfill the coated paper-based functional materials with high performance is not surprising.

Acknowledgments The present work was supported by the National Natural Science Foundation of China (No. 22308027) and the 5·5 Engineering Research & Innovation Team Project of Beijing Forestry University (No. BLRC2023B01). G.K. is also grateful to the Moldova State University for supporting his research (research program No. 011208).

References

Adewale, P., Yancheshmeh, M. S., & Lam, E. (2022). Starch modification for non-food, industrial applications: Market intelligence and critical review. *Carbohydrate Polymers, 291*, 119590. https://doi.org/10.1016/j.carbpol.2022.119590

Adeyemi, J. O., & Fawole, O. A. (2023). Metal-based nanoparticles in food packaging and coating technologies: A review. *Biomolecules, 13*, 1092. https://doi.org/10.3390/biom13071092

Asgher, M., Qamar, S. A., Bilal, M., & Iqbal, H. M. N. (2020). Bio-based active food packaging materials: Sustainable alternative to conventional petrochemical-based packaging materials. *Food Research International, 137*, 109625. https://doi.org/10.1016/j.foodres.2020.109625

Brodnjak, U. V., & Tihole, K. (2020). Chitosan solution containing zein and essential oil as bio based coating on packaging paper. *Coatings, 10*(5), 497. https://doi.org/10.3390/coatings10050497

Bulmer, J. S., Kaniyoor, A., & Elliott, J. A. (2021). A meta-analysis of conductive and strong carbon nanotube materials. *Advanced Materials, 33*(36), 2008432. https://doi.org/10.1002/adma.202008432

Cao, X. Z., Xin, S. H., Liu, X. X., & Wang, S. L. (2023). Occurrence and behavior of per- and polyfluoroalkyl substances and conversion of oxidizable precursors in the waters of coastal tourist resorts in China. *Environmental Pollution, 316*(1), 120460. https://doi.org/10.1016/j.envpol.2022.120460

Chen, F. F., Zhu, Y. J., Xiong, Z. C., Dong, L. Y., Chen, F., Lu, B. Q., & Yang, R. L. (2017). Hydroxyapatite nanowire-based all-weather flexible electrically conductive paper with superhydrophobic and flame-retardant properties. *ACS Applied Materials & Interfaces, 9*(45), 39534–39548. https://doi.org/10.1021/acsami.7b09484

Cheng, H., Li, L. J., Wang, B. J., Feng, X. L., Mao, Z. P., Vancso, G. J., & Sui, X. F. (2020). Multifaceted applications of cellulosic porous materials in environment, energy, and health. *Progress in Polymer Science, 106*, 101253. https://doi.org/10.1016/j.progpolymsci.2020.101253

Choi, W., Shin, J., Kim, Y. J., Hur, J., Jang, B. C., & Yoo, H. (2024). Versatile papertronics: Photo-induced synapse and security applications on papers. *Advanced Materials, 36*, 2312831. https://doi.org/10.1002/adma.202312831

Cordt, C., Geissler, A., & Biesalski, M. (2021). Regenerative superhydrophobic paper coatings by in situ formation of waxy nanostructures. *Advanced Materials Interfaces, 8*(2), 2001265. https://doi.org/10.1002/admi.202001265

Dai, X. H., Xu, X. M., Yu, X., Sun, X., Pan, J. J., Zhang, X. T., & Min, J. (2022). Cationic core/shell polysiloxane acrylate emulsion: Synthesis, film morphology, and performance on cotton pigment coloration. *Cellulose, 29*(3), 2093–2106. https://doi.org/10.1007/s10570-021-04396-3

Dejen, K. D., Zereffa, E. A., Murthy, H. C. A., & Merga, A. (2020). Synthesis of ZnO and ZnO/PVA nanocomposite using aqueous Moringa oleifera leaf extract template: Antibacterial and electrochemical activities. *Reviews on Advanced Materials Science, 59*(1), 464–476. https://doi.org/10.1515/rams-2020-0021

Deshwal, G. K., Panjagari, N. R., & Alam, T. (2019). An overview of paper and paper based food packaging materials: Health safety and environmental concerns. *Journal of Food Science and Technology, 56*(10), 4391–4403. https://doi.org/10.1007/s13197-019-03950-z

Dogome, K., Enomae, T., & Isogai, A. (2013). Method for controlling surface energies of paper substrates to create paper-based printed electronics. *Chemical Engineering and Processing, 68*, 21–25. https://doi.org/10.1016/j.cep.2013.01.003

Dreyfuss-Deseigne, R. (2017). Nanocellulose films in art conservation. *Journal of Paper Conservation, 18*(1), 18–29. https://doi.org/10.1080/18680860.2017.1334422

Guan, F. R., He, H., Li, Q. Y., Shen, Y., Kang, F., Zhang, C., & Zhai, H. Y. (2024). Transparent conductive films based on silver nanowires and SiO_2 nanoparticles for flexible electronics. *ACS Applied Nano Materials, 7*(7), 7845–7855. https://doi.org/10.1021/acsanm.4c00463

Guan, H. Y., Zhao, B., Zhao, W. W., & Ni, Z. H. (2023). Liquid-precursor-intermediated synthesis of atomically thin transition metal dichalcogenides. *Materials Horizons, 10*(4), 1105–1120. https://doi.org/10.1039/d2mh01207c

Guo, X. J., Xue, C. H., Jia, S. T., & Ma, J. Z. (2017). Mechanically durable superamphiphobic surfaces via synergistic hydrophobization and fluorination. *Chemical Engineering Journal, 320*, 330–341. https://doi.org/10.1016/j.cej.2017.03.058

Hamdani, S. S., Li, Z., Rabnawaz, M., Kamdem, D. P., & Khan, B. A. (2020). Chitosan-graft-poly(dimethylsiloxane)/zein coatings for the fabrication of environmentally friendly oil- and water-resistant paper. *ACS Sustainable Chemistry & Engineering, 8*(13), 5147–5155. https://doi.org/10.1021/acssuschemeng.9b07397

Hamdani, S. S., Li, Z., Sirinakbumrung, N., & Rabnawaz, M. (2020). Zein and PVOH-based bilayer approach for plastic-free, repulpable and biodegradable oil- and water-resistant paper as a replacement for single-use plastics. *Industrial and Engineering Chemistry Research, 59*(40), 17856–17866. https://doi.org/10.1021/acs.iecr.0c02967

Hu, L. B., Zheng, G. Y., Yao, J., Liu, N. A., Weil, B., Eskilsson, M., Karabulut, E., Ruan, Z. C., Fan, S. H., Bloking, J. T., McGehee, M. D., Wågberg, L., & Cui, Y. (2013). Transparent and conductive paper from nanocellulose fibers. *Energy & Environmental Science, 6*(2), 513–518. https://doi.org/10.1039/c2ee23635d

Hu, X. G., Lin, Z. H., Ding, L. M., & Chang, J. J. (2023). Recent advances of carbon nanotubes in perovskite solar cells. *SusMat, 3*(5), 639–670. https://doi.org/10.1002/sus2.158

Jahangiri, F., Mohanty, A. K., & Misra, M. (2024). Sustainable biodegradable coatings for food packaging: Challenges and opportunities. *Green Chemistry, 26*(9), 4934–4974. https://doi.org/10.1039/d3gc02647g

Jiang, X. F., Li, Q., Li, X. T., Meng, Y., Ling, Z., Ji, Z., & Chen, F. S. (2022). Preparation and characterization of degradable cellulose-based paper with superhydrophobic, antibacterial, and barrier properties for food packaging. *International Journal of Molecular Sciences, 23*(19), 11158. https://doi.org/10.3390/ijms231911158

Kakaei, K., Esrafili, M. D., & Ehsani, A. (2019). Graphene and anticorrosive properties. *Interface Science and Technology, 27*, 303–337. https://doi.org/10.1016/B978-0-12-814523-4.00008-3

Kansal, D., Hamdani, S. S., Ping, R. Q., Sirinakbumrung, N., & Rabnawaz, M. (2020). Food-safe chitosan-zein dual-layer coating for water- and oil-repellent paper substrates. *ACS Sustainable Chemistry & Engineering, 8*(17), 6887–6897. https://doi.org/10.1021/acssuschemeng.0c02216

Kansal, D., & Rabnawaz, M. (2021). Fabrication of oil- and water-resistant paper without creating microplastics on disposal. *Journal of Applied Polymer Science, 138*(3), e49692. https://doi.org/10.1002/app.49692

Ke, B. Y., Cheng, S. L., Zhang, C. C., Li, W. Y., Zhang, J., Deng, R. M., Lin, J., Xie, Q. S., Qu, B. H., Qiao, L., Peng, D. L., & Wang, X. H. (2024). Low-temperature flexible integration of all-solid-state thin-film lithium batteries enabled by spin-coating electrode architecture. *Advanced Energy Materials, 14*(12), 2303757. https://doi.org/10.1002/aenm.202303757

Khan, F., Rabnawaz, M., Li, Z., Khan, A., Naveed, M., Tuhin, M. O., & Rahimb, F. (2019). Simple design for durable and clear self-cleaning coatings. *ACS Applied Polymer Materials, 1*(10), 2659–2667. https://doi.org/10.1021/acsapm.9b00596

Khanjani, P., King, A. W. T., Part, G. J., Johansson, L. S., Kostiainen, M. A., & Ras, R. H. A. (2018). Superhydrophobic paper from nanostructured fluorinated cellulose esters. *ACS Applied Materials & Interfaces, 10*(13), 11280–11288. https://doi.org/10.1021/acsami.7b19310

Khondoker, M. A., Yang, S. Y., Mun, S. C., & Kim, J. (2012). Flexible and conductive ITO electrode made on cellulose film by spin-coating. *Synthetic Metals, 162*(21–22), 1972–1976. https://doi.org/10.1016/j.synthmet.2012.09.005

Krings, L. (2019). *Recyclable paper coatings* (pp. 36–37). Paramelt. https://www.paramelt.com/wp-content/uploads/2019/12/Recyclable-Paper-Coatings-2019_12-Packaging-Today.pdf

Kunam, P. K., Ramakanth, D., Akhila, K., & Gaikwad, K. K. (2024). Bio-based materials for barrier coatings on paper packaging. *Biomass Conversion and Biorefinery, 14*, 12637–12652. https://doi.org/10.1007/s13399-022-03241-2

Lan, Z., & Duan, W. (2023). Achieving surface hydrophobic and moisture-proof properties of ancient-book paper by in-situ protection of epoxy-based POSS/PVDF composite coating. *Bulletin of Materials Science, 46*, 73. https://doi.org/10.1007/s12034-023-02910-w

Lee, C. K., Lee, S. B., Hwang, S. W., Park, K. W., & Shim, J. K. (2013). Cellulosic binder-assisted formation of graphene-paper electrode with flat surface and porous internal structure. *Journal of Nanoscience and Nanotechnology, 13*(11), 7391–7395. https://doi.org/10.1166/jnn.2013.7860

Lengowski, E. C., Bonfatti, E. A., Jr., Simon, L. C., de Muniz, G. I. B., de Andrade, A. S., Leite, A. N., & de Miranda Leite, E. L. S. (2023). Nanocellulose coating on kraft paper. *Coatings, 13*, 1705. https://doi.org/10.3390/coatings13101705

Leung, T. S. W., Ramon, E., & Martínez-Domingo, C. (2023). Low-temperature plasma sintering of inkjet-printed metal salt decomposition inks on flexible substrates. *Advanced Engineering Materials, 25*(2), 2200834. https://doi.org/10.1002/adem.202200834

Li, C. J., Li, X., Wang, L., Xia, Z. A., Yang, J. X., Wang, N., Li, Y., & Zhang, H. (2024). Preparation of high-barrier performance paper-based materials from biomass-based silicone-modified acrylic polymer emulsion. *Polymer Engineering and Science, 64*(7), 3348–3362. https://doi.org/10.1002/pen.26774

Li, D. W., Wang, H. Y., Liu, Y., Wei, D. S., & Zhao, Z. X. (2019). Large-scale fabrication of durable and robust super-hydrophobic spray coatings with excellent repairable and anti-corrosion performance. *Chemical Engineering Journal, 367*, 69–179. https://doi.org/10.1016/j.cej.2019.02.093

Li, E., Pan, Y. M., Wang, C. F., Liu, C. T., Shen, C. Y., Pan, C. F., & Liu, X. H. (2021). Multifunctional and superhydrophobic cellulose composite paper for electromagnetic shielding, hydraulic triboelectric nanogenerator and Joule heating applications. *Chemical Engineering Journal, 420*, 129864. https://doi.org/10.1016/j.cej.2021.129864

Li, H. Y., Wang, W., Lv, Q., Xi, G. C., Bai, H., & Zhang, Q. (2016). Disposable paper-based electrochemical sensor based on stacked gold nanoparticles supported carbon nanotubes for the determination of bisphenol A. *Electrochemistry Communications, 68*, 104–107. https://doi.org/10.1016/j.elecom.2016.05.010

Li, W. G., Dong, W. K., Guo, Y. P., Wang, K. J., & Shah, S. P. (2022). Advances in multifunctional cementitious composites with conductive carbon nanomaterials for smart infrastructure. *Cement and Concrete Composites, 128*, 104454. https://doi.org/10.1016/j.cemconcomp.2022.104454

Li, Z., & Rabnawaz, M. (2018). Fabrication of food-safe water-resistant paper coatings using a melamine primer and polysiloxane outer layer. *ACS Omega, 3*(9), 11909–11916. https://doi.org/10.1021/acsomega.8b01423

Li, Z., & Rabnawaz, M. (2019). Oil- and water-resistant coatings for porous cellulosic substrates. *ACS Applied Polymer Materials, 1*(1), 103–111. https://doi.org/10.1021/acsapm.8b00106

Li, Z., Rabnawaz, M., & Khan, B. (2020). Response surface methodology design for biobased and sustainable coatings for water- and oil-resistant paper. *ACS Applied Polymer Materials, 2*(3), 1378–1387. https://doi.org/10.1021/acsapm.9b01238

Li, Z., Rabnawaz, M., Sarwar, M. G., Khan, B., Nair, A. K., Sirinakbumrung, N., & Kamdem, D. P. (2019). A closed-loop and sustainable approach for the fabrication of plastic-free oil- and water-resistant paper products. *Green Chemistry, 21*(20), 5691–5700. https://doi.org/10.1039/c9gc01865d

Liao, X. Q., Zhang, Z., Liang, Q. J., Liao, Q. L., & Zheng, Y. (2017). Flexible, cuttable, and self-waterproof bending strain sensors using microcracked gold nanofilms@paper substrate. *ACS Applied Materials & Interfaces, 9*(4), 4151–4158. https://doi.org/10.1021/acsami.6b12991

Lin, Z. Y., Xia, Y. Y., Yang, G. H., Chen, J. C., & Ji, D. X. (2019). Improved film formability of oxidized starch-based blends through controlled modification with cellulose nanocrystals. *Industrial Crops and Products, 140*, 111665. https://doi.org/10.1016/j.indcrop.2019.111665

Liu, X., Huang, K. X., Lin, X. X., Li, H. X., Tao, T., Wu, Q. H., et al. (2020). Transparent and conductive cellulose film by controllably growing aluminum doped zinc oxide on regenerated cellulose film. *Cellulose, 27*(9), 4847–4855. https://doi.org/10.1007/s10570-020-03147-0

Liu, Y. H., Ma, Z. K., He, Y., Wang, Y., Zhang, X. W., Song, H. H., & Li, C. X. (2023). A review of fibrous graphite materials: Graphite whiskers, columnar carbons with a cone-shaped top, and needle- and rods-like polyhedral crystals. *New Carbon Materials, 38*(1), 18–39. https://doi.org/10.1016/S1872-5805(23)60719-X

Liu, Y. X., Sun, B., Li, J. G., Cheng, D., An, X. Y., Yang, B., et al. (2018). Aqueous dispersion of carbon fibers and expanded graphite stabilized from the addition of cellulose nanocrystals to produce highly conductive cellulose composites. *ACS Sustainable Chemistry & Engineering, 6*(3), 3291–3298. https://doi.org/10.1021/acssuschemeng.7b03456

Long, Z., Wu, M. Y., Peng, H., Dai, L., Zhang, D., & Wang, J. H. (2015). Preparation and oil-resistant mechanism of chitosan/cationic starch oil-proof paper. *BioResources, 10*(4), 7907–7920. https://doi.org/10.15376/biores.10.4.7907-7920

Ma, D. H., Zhong, H. F., Lv, J. T., Wang, Y. W., & Jiang, G. B. (2022). Levels, distributions, and sources of legacy and novel per- and perfluoroalkyl substances (PFAS) in the topsoil of Tianjin, China. *Journal of Environmental Sciences, 112*, 71–81. https://doi.org/10.1016/j.jes.2021.04.029

Ma, X. C., Zhu, Z. D., Zhang, H. C., Tian, S. L., Li, X. H., Fan, H. M., & Fu, S. Y. (2022). Superhydrophobic and deacidified cellulose/$CaCO_3$-derived granular coating toward historic paper preservation. *International Journal of Biological Macromolecules, 207*, 232–241. https://doi.org/10.1016/j.ijbiomac.2022.02.179

Maruthapandi, M., Saravanan, A., Gupta, A., Luong, J. H. T., & Gedanken, A. (2022). Antimicrobial activities of conducting polymers and their composites. *Macromolecules, 2*(1), 78–99. https://doi.org/10.3390/macromol2010005

Mirmehdi, S., de Oliveira, M. L., Hein, P. R., Dias, M. V., Sarantópoulos, C. I., & Tonoli, G. H. D. (2018). Spraying cellulose nanofibrils for improvement of tensile and barrier properties of writing & printing (W&P) paper. *Journal of Wood Chemistry and Technology, 38*, 233–245. https://doi.org/10.1080/02773813.2018.1432656

Nabiyan, A., Muttathukattil, A., Tomazic, F., Pretzel, D., Schubert, U. S., Engel, M., & Schacher, F. H. (2023). Self-assembly of core-shell hybrid nanoparticles by directional crystallization of grafted polymers. *ACS Nano, 17*(21), 21216–21226. https://doi.org/10.1021/acsnano.3c05461

Nadeem, H., Athar, M., Dehghani, M., Garnier, G., & Batchelor, W. (2022). Recent advancements, trends, fundamental challenges and opportunities in spray deposited cellulose nanofibril films for packaging applications. *Science of the Total Environment, 836*, 155654. https://doi.org/10.1016/j.scitotenv.2022.155654

Nagajyothi, P. C., Sreekanth, T. V. M., Tettey, C. O., Jun, Y. I., & Mook, S. H. (2014). Characterization, antibacterial, antioxidant, and cytotoxic activities of ZnO nanoparticles using Coptidis Rhizoma. *Bioorganic & Medicinal Chemistry Letters, 24*, 4298–4303. https://doi.org/10.1016/j.bmcl.2014.07.023

Naghdi, S., Rhee, K. Y., Hui, D., & Park, S. J. (2018). A review of conductive metal nanomaterials as conductive, transparent, and flexible coatings, thin films, and conductive fillers: Different deposition methods and applications. *Coatings, 8*(8), 278. https://doi.org/10.3390/coatings8080278

Nigussie, G. Y., Tesfamariam, G. M., Tegegne, B. M., Weldemichel, Y. A., Gebreab, T. W., Gebrehiwot, D. G., & Gebremichel, G. E. (2018). Antibacterial activity of Ag-doped TiO_2 and Ag-doped ZnO nanoparticles. *International Journal of Photoenergy, 2018*, 5927485. https://doi.org/10.1155/2018/5927485

Nogi, M., & Yano, H. (2009). Optically transparent nanofiber sheets by deposition of transparent materials: A concept for a roll-to-roll processing. *Applied Physics Letters, 94*, 233117. https://doi.org/10.1063/1.3154547

O'Rourke, E., Hynes, J., Losada, S., Barber, J. L., Pereira, M. G., Kean, E. F., Hailer, F., & Chadwick, E. A. (2022). Anthropogenic drivers of variation in concentrations of perfluoroalkyl substances in otters (Lutra lutra) from England and Wales. *Environmental Science & Technology, 56*(3), 1675–1687. https://doi.org/10.1021/acs.est.1c05410

Ovaska, S. S., Geydt, P., Österberg, M., Johansson, L. S., & Backfolk, K. (2015). Heat-induced changes in oil and grease resistant hydroxypropylated-starch-based barrier coatings. *Nordic Pulp & Paper Research Journal, 30*(3), 488–496. https://doi.org/10.3183/npprj-2015-30-03-p488-496

Park, Y. G., Lee, Y. H., Rahman, M. M., Park, C. C., & Kim, H. D. (2015). Preparation and properties of waterborne polyurethane/self-cross-linkable fluorinated acrylic copolymer hybrid emulsions using a solvent/emulsifier-free method. *Colloid & Polymer Science, 293*(5), 1369–1382. https://doi.org/10.1007/s00396-015-3504-0

Preston, C., Fang, Z. Q., Murray, J., Zhu, H. L., Dai, J. Q., Munday, J. N., & Hu, L. B. (2014). Silver nanowire transparent conducting paper-based electrode with high optical haze. *Journal of Materials Chemistry C, 2*(7), 1248–1254. https://doi.org/10.1039/c3tc31726a

Putkisto, K., Maijala, J., Grön, J., & Rigdahl, M. (2003). Polymer coating of paper using dry surface treatment - Coating structure and performance. *Tappi Journal, 2*, 11.

Ran, J., Liu, Y. F., Feng, H. X., Shi, H. X., & Ma, Q. (2024). A review on graphene-based electrode materials for supercapacitor. *Journal of Industrial and Engineering Chemistry, 137*, 106–121. https://doi.org/10.1016/j.jiec.2024.03.043

Rastogi, V. K., & Samyn, P. (2015). Bio-based coatings for paper applications. *Coatings, 5*, 887–930. https://doi.org/10.3390/coatings5040887

Ruberto, Y., Vivod, V., Grkman, J. J., Lavric, G., Graiff, C., & Kokol, V. (2024). Slot-die coating of cellulose nanocrystals and chitosan for improved barrier properties of paper. *Cellulose, 31*(6), 3589–3606. https://doi.org/10.1007/s10570-024-05847-3

Sanmugam, A., Vikraman, D., Park, H. J., & Kim, H.-S. (2017). One-pot facile methodology to synthesize chitosan-ZnO graphene oxide hybrid composites for better dye adsorption and antibacterial activity. *Nanomaterials, 7*(11), 363. https://doi.org/10.3390/nano7110363

Scheffler, M., Dressel, M., Jourdan, M., & Adrian, H. (2005). Extremely slow Drude relaxation of correlated electrons. *Nature, 438*(7071), 1135–1137. https://doi.org/10.1038/nature04232

Shankar, V. S., Velmurugan, G., Raja, D. E., Manikandan, T., Kumar, S. S., Singh, J., Nagaraj, M., & Kumar, A. J. (2024). A review on the development of silicon and silica based nano materials in the food industry. *SILICON, 16*(3), 979–988. https://doi.org/10.1007/s12633-023-02748-1

Sharma, M., Murtinho, R. A. D., Valente, A. J. M., De Sousa, A. P., & Ferreira, P. J. T. (2020). A review on cationic starch and nanocellulose as paper coating components. *International Journal of Biological Macromolecules, 162*, 578–598. https://doi.org/10.1016/j.ijbiomac.2020.06.131

Sheng, J. J., Li, J. R., & Zhao, L. H. (2019). Fabrication of grease resistant paper with non-fluorinated chemicals for food packaging. *Cellulose, 26*(10), 6291–6302. https://doi.org/10.1007/s10570-019-02504-y

Song, Z. P., Tang, J. B., Wang, H. L., Guan, F. X., Wu, Y. T., & Liu, W. X. (2020). Water and oil resistance improvement of paper coated with aqueous mixture of hydrophilic and hydrophobic cross-linked copolymers. *BioResources, 15*(2), 3147–3160. https://doi.org/10.15376/biores.15.2.3147-3160

Spagnuolo, L., D'Orsi, R., & Operamolla, A. (2022). Nanocellulose for paper and textile coating: The importance of surface chemistry. *ChemPlusChem, 87*, e202200204. https://doi.org/10.1002/cplu.202200204

Tan, W. R., Aruna, X. Z. H., Zhang, L. Y., & Shen, W. (2020). Trace analysis on chromium (VI) in water by pre-concentration using a superhydrophobic surface and rapid sensing using a chemical-responsive adhesive tape. *Talanta, 218*, 121116. https://doi.org/10.1016/j.talanta.2020.121116

Tandey, K., Shrivas, K., Sharma, A., Kant, T., Tejwani, A., Tikeshwari, D. M. K., Pervez, S., & Ghosh, K. K. (2024). Nanomaterial-enabled portable paper-based colorimetric and fluorometric devices: Progress in point-of-care diagnosis. *Coordination Chemistry Reviews, 514*, 215919. https://doi.org/10.1016/j.ccr.2024.215919

Tang, X., & Yan, X. (2017). Dip-coating for fibrous materials: Mechanism, methods and applications. *Journal of Sol-Gel Science and Technology, 81*(2), 378–404. https://doi.org/10.1007/s10971-016-4197-7

Tang, Y. J., He, Z. B., Mosseler, J. A., & Ni, Y. H. (2014). Production of highly electro-conductive cellulosic paper via surface coating of carbon nanotube/graphene oxide nanocomposites using nanocrystalline cellulose as a binder. *Cellulose, 21*(6), 4569–4581. https://doi.org/10.1007/s10570-014-0418-9

Tarrés, Q., Aguado, R., Pèlach, M. A., Mutjé, P., & Delgado-Aguilar, M. (2022). Electrospray deposition of cellulose nanofibers on paper: Overcoming the limitations of conventional coating. *Nanomaterials, 12*, 79. https://doi.org/10.3390/nano12010079

Tosi, D., Sypabekova, M., Bekmurzayeva, A., Molardi, C., & Dukenbayev, K. (2022). Fiber surface modifications for biosensing. *Fiber Optic Biosensor, 2022*, 253–282. https://doi.org/10.1016/B978-0-12-819467-6.00010-X

Ventrapragada, L. K., Creager, S. E., Rao, A. M., & Podila, R. (2019). Carbon nanotubes coated paper as current collectors for secondary Li-ion batteries. *Nanotechnology Reviews, 8*(1), 18–23. https://doi.org/10.1515/ntrev-2019-0002

Wang, J., Han, X., Zhang, C., Liu, K., & Duan, G. (2022). Source of nanocellulose and its application in nanocomposite packaging material: A review. *Nanomaterials, 12*, 3158. https://doi.org/10.3390/nano12183158

Wang, K. P., Zhao, L. H., & He, B. H. (2021). Chitosan/montmorillonite coatings for the fabrication of food-safe greaseproof paper. *Polymers, 13*(10), 1607. https://doi.org/10.3390/polym13101607

Wang, Z., Yi, M., Zhang, Z., Guo, M., Lu, P., Chen, Z., & Wang, S. (2017). Fabrication of highly water-repelling paper by surface coating with stearic acid modified calcium carbonate particles and reactive biopolymers. *Journal of Bioresources and Bioproducts, 2*(2), 89–92. https://doi.org/10.21967/jbb.v2i2.91

Wechakorn, K., Supalang, S., & Suanpai, S. (2020). A Schiff base-based ratiometric chemosensor conjugated NBD derivative with the large stokes shift for formaldehyde detection. *Tetrahedron, 76*, 131411. https://doi.org/10.1016/j.tet.2020.131411

Xia, Y. Y., Wang, S. J., Meng, F. R., Xu, Z., Fang, Q., Gu, Z. G., Zhang, C. H., Li, P., & Kong, F. G. (2024). Eco-friendly food packaging based on paper coated with a bio-based antibacterial coating composed of carbamate starch, calcium lignosulfonate, cellulose nanofibrils, and silver

nanoparticles. *International Journal of Biological Macromolecules, 254*, 127659. https://doi.org/10.1016/j.ijbiomac.2023.127659

Yadav, S., Mehrotra, G. K., & Dutta, P. K. (2021). Chitosan based ZnO nanoparticles loaded gallic-acid films for active food packaging. *Food Chemistry, 334*, 127605. https://doi.org/10.1016/j.foodchem.2020.127605

Yang, L., Xu, W., Shi, X. L., Wu, M. L., Yan, Z. Y., Zheng, Q., Feng, G. N., Zhang, L., & Shao, R. (2023). Investigating the thermal conductivity and flame-retardant properties of BN/MoS_2/PCNF composite film containing low BN and MoS_2 nanosheets loading. *Carbohydrate Polymers, 311*, 120621. https://doi.org/10.1016/j.carbpol.2023.120621

Ye, M. T., Wang, S. D., Ji, X. X., Tian, Z. J., Dai, L., & Si, C. L. (2023). Nanofibrillated cellulose-based superhydrophobic coating with antimicrobial performance. *Advanced Composites and Hybrid Materials, 6*(1), 30. https://doi.org/10.1007/s42114-022-00602-3

Ye, Y. Y., Zhang, L., Zhu, Z., Xie, F. W., Meng, L. H., Yang, T., Qian, J. Y., & Chen, Y. (2024). Facile superhydrophobic modification on HPMC film using polydimethylsiloxane and starch granule coatings. *International Journal of Biological Macromolecules, 266*, 131191. https://doi.org/10.1016/j.ijbiomac.2024.131191

Yi, T., Zhao, H. Y., Mo, Q., Pan, D. L., Liu, Y., Huang, L. J., Xu, H., Hu, B., & Song, H. N. (2020). From cellulose to cellulose nanofibrils-a comprehensive review of the preparation and modification of cellulose nanofibrils. *Materials, 13*(22), 5062. https://doi.org/10.3390/ma13225062

Yuan, J. J., Yin, X., Qiu, Z. L., Shen, Y. J., Fang, L. F., Liang, Z. Y., Kong, Q. R., & Zhu, B. K. (2022). Fabricating superhydrophobic surfaces via coating amine-containing fluorinated emulsion and Michael addition reaction. *Journal of Coating Technology and Research, 19*(4), 1187–1198. https://doi.org/10.1007/s11998-021-00600-y

Yuan, L. B., Liu, R. Q., Zhou, Y. F., Zhang, R. Y., Chen, S., Yang, Q., Gu, Y. C., Han, L. B., & Yan, B. (2024). Janus biopolymer nanocomposite coating with excellent antibacterial and water/oxygen barrier performance for fruit preservation. *Food Hydrocolloid, 149*, 109528. https://doi.org/10.1016/j.foodhyd.2023.109528

Zakaria, S., Chia, C. H., Haslinda, W., Ahmad, W. H. W., Kaco, H., Chook, S. W., & Chan, C. H. (2015). Mechanical and antibacterial properties of paper coated with chitosan. *Sains Malaysiana, 44*(6), 905–911.

Zeng, K., Gu, J., & Cao, C. (2020). Facile approach for ecofriendly, low-cost, and water-resistant paper coatings via palm kernel oil. *ACS Applied Materials & Interfaces, 12*, 18987–18996. https://doi.org/10.1021/acsami.0c00067

Zhan, Y. H., Hao, X. H., Wang, L. C., Jiang, X. C., Cheng, Y., Wang, C. Z., Meng, Y. Y., Xia, H. S., & Chen, Z. M. (2021). Superhydrophobic and flexible silver nanowire-coated cellulose filter papers with sputter-deposited nickel nanoparticles for ultrahigh electromagnetic interference shielding. *ACS Applied Materials & Interfaces, 13*(12), 14623–14633. https://doi.org/10.1021/acsami.1c03692

Zhang, Q., Liu, L. B., Pan, C. G., Li, D., & Gai, G. J. (2018). Thermally sensitive, adhesive, injectable, multiwalled carbon nanotube covalently reinforced polymer conductors with self-healing capabilities. *Journal of Materials Chemistry C, 6*(7), 1746–1752. https://doi.org/10.1039/c7tc05432g

Zhang, W., & Rhim, J.-W. (2022). Titanium dioxide (TiO_2) for the manufacture of multifunctional active food packaging films. *Food Packaging and Shelf Life, 31*, 100806. https://doi.org/10.1016/j.fpsl.2021.100806

Zhang, Y. W., Guo, D. S., Shen, X., Tang, Z. F., & Lin, B. F. (2024). Recoverable and degradable carboxymethyl chitosan polyelectrolyte hydrogel film for ultra stable encapsulation of curcumin. *International Journal of Biological Macromolecules, 268*, 131616. https://doi.org/10.1016/j.ijbiomac.2024.131616

Zhao, J. C., Zhang, T., Li, Y. M., Huang, L. P., & Tang, Y. H. (2023). Fluorine-free, highly durable waterproof and breathable fibrous membrane with self-clean performance. *Nanomaterials, 13*(3), 516. https://doi.org/10.3390/nano13030516

Zhao, Y., Miao, B. J., Nawaz, M. A., Zhu, Q. S., Chen, Q. L., Reina, T. R., Bai, J. B., He, D. L., Al-Tahan, M. A., & Arsalan, M. (2024). Construction of cellulose nanofiber-$Ti_3C_2T_x$ MXene/silver nanowire nanocomposite papers with gradient structure for efficient electromagnetic interference shielding. *Advanced Composites and Hybrid Materials, 7*(2), 34. https://doi.org/10.1007/s42114-024-00839-0

Zhong, L., Ding, Y. J., Zhang, B., Wang, Z. G., Li, C., Fu, X., & Huang, Q. (2019). Effect of octenylsuccinylation of oxidized cassava starch on grease resistance and waterproofing of food wrapping paper. *Starch-Starke, 71*(7–8), 1800284. https://doi.org/10.1002/star.201800284

Zhu, P. H., Kuang, Y. D., Chen, G., Liu, Y., Peng, C. X., Hu, W., Zhou, P., & Fang, Z. Q. (2018). Starch/polyvinyl alcohol (PVA)-coated painting paper with exceptional organic solvent barrier properties for art preservation purposes. *Journal of Materials Science, 53*, 5450–5457. https://doi.org/10.1007/s10853-017-1924-6

Zhu, R. F., Fu, X. T., Jin, S. N., Ma, R., He, Z. B., Zhang, D., & Long, Z. (2023). Water and oil-resistant paper materials based on sodium alginate/hydroxypropyl methylcellulose/polyvinyl butyral/nano-silica with biodegradable and high barrier properties. *International Journal of Biological Macromolecules, 225*, 162–171. https://doi.org/10.1016/j.ijbiomac.2022.10.104

Part III
New Trends in Paper Fabrication

Chapter 10
Biocellulose

Ashutosh Pandey, Annika Singh, and Mukesh Kumar Singh

10.1 Introduction

Cellulose, the most abundant natural polymer on Earth, exists in several polymorphic forms (I, II, III, and IV) depending on its source and processing methods. Cellulose I, the native form found in plants and bacterial cellulose (BC), has a highly crystalline structure with two allomorphs, I_α (triclinic) and I_β (monoclinic). Chemical or physical treatments can convert Cellulose I into other polymorphs, such as Cellulose II, which is obtained through sodium hydroxide treatment and is known for its thermodynamic stability and enhanced chemical accessibility. Similarly, liquid ammonia treatment produces Cellulose III, characterized by disrupted hydrogen bonding and reduced crystallinity, while heating Cellulose III in glycerol yields Cellulose IV with a unique crystalline structure (Pandey et al., 2024b). Although plant-derived cellulose is abundant, its extraction involves extensive chemical and mechanical processing to remove impurities, such as lignin and hemicellulose, resulting in significant environmental impact. This has driven interest in bacterial cellulose (BC), a sustainable alternative that offers high purity and structural versatility (Balistreri et al., 2024; Rodrigues et al., 2024).

Bacterial cellulose (BC), also known as biocellulose, is a biopolymer synthesized by specific bacterial strains like *Acetobacter xylinum* at the air-water interface in sugar-rich nutrient media. First described by Brown in 1886, BC production typically occurs within 5–14 days. Although historically hindered by high production

A. Pandey (✉)
Panipat Institute of Engineering and Technology, Panipat, Haryana, India

A. Singh
School of Lifesciences and Biotechnology, CSJMU, Kanpur, India

M. K. Singh
Uttar Pradesh Textile Technology Institute, Kanpur, India

G. Korotcenkov (ed.), *The Handbook of Paper-Based Sensors and Devices*,
https://doi.org/10.1007/978-3-031-91080-7_10

costs and low yields, BC's unique properties have made it an attractive alternative to plant-derived cellulose. Unlike plant cellulose, BC consists solely of glucose monomers arranged in a highly crystalline, nanofibrillar three-dimensional network, resulting in superior tensile strength, water-holding capacity, and purity (Pandey et al., 2024c). Advances in bioreactor technologies have significantly improved BC production efficiency, enabling the fabrication of complex shapes and structures tailored for applications in smart materials, medical devices, and other high-value fields. BC's nanoscale fibril dimensions (20–100 nm) further enhance its suitability for advanced applications by allowing the incorporation of functional fillers like silver, graphene, and silica nanoparticles to improve durability and functionality (Kusuma et al., 2024; Lima et al., 2024).

The versatility of BC lies in its ability to be structurally and functionally modified through in situ or ex situ techniques. In situ modifications incorporate functional materials, such as chitosan or silver nanoparticles, directly into the culture medium, allowing these substances to integrate into the BC matrix. However, this approach can affect bacterial metabolism, reducing BC yield. In contrast, ex situ modifications involve post-synthesis treatments, where BC is impregnated with polymers or additives without compromising its structural integrity. These modifications enhance BC's mechanical, thermal, and functional properties, broadening its applicability in areas like biomedical engineering, filtration, packaging, and smart textiles. Moreover, BC's biocompatibility, biodegradability, and the potential to utilize waste-derived resources align with sustainability goals, positioning it as a promising material for a wide range of industrial and environmental applications. This chapter delves into the synthesis, properties, modifications, and applications of BC, highlighting its transformative potential across various sectors (Kusuma et al., 2024; Pandey et al., 2024a).

10.2 BC Fabrication

The fabrication of bacterial cellulose (BC) fundamentally differs from plant cellulose synthesis, despite their identical chemical composition. Plant cellulose synthesis begins with enzymatic processes that convert sucrose into glucose via sucrose synthase (SuSy) or through starch degradation by amylase. Glucose is phosphorylated into glucose-6-phosphate and subsequently metabolized into uridine diphosphate glucose (UDP-glucose), the precursor for cellulose synthesis. Cellulose synthase (CesA), organized in membrane-bound rosette complexes, polymerizes UDP-glucose into β-1 → 4 glucan chains. These chains integrate with lignin, hemicellulose, and pectin to form plant cell walls, which provide mechanical strength. In contrast, BC synthesis involves a simpler structure without lignin or hemicellulose components, focusing on the production of highly crystalline cellulose through unique microbial enzymatic pathways (Mishra et al., 2022; Pandey et al., 2024a).

In bacterial cellulose synthesis, carbon sources such as glucose, fructose, or industrial waste sugars are metabolized into UDP-glucose via glycolysis and the

pentose phosphate pathway. Among these, glucose is the most efficient carbon source for robust UDP-glucose synthesis and higher BC yields. The key genes bcsA (catalytic unit), bcsB (regulatory unit), and bcsD (responsible for fibrillar cellulose formation) govern the polymerization of long, unbranched β-1 → 4 glucan chains (Pandey et al., 2024a; Serra & Hengge, 2019). These chains are extruded extracellularly and crystallized into cellulose microfibrils through Van der Waals forces and hydrogen bonding, providing high mechanical strength and structural stability. Alternative carbon sources, like fructose, require additional metabolic steps that may reduce yields and modify BC properties. Industrial waste-derived reducing sugars, a sustainable alternative, often require detoxification to remove inhibitors, such as lignin residues or acidic by-products (Quijano et al., 2024; Rodrigues et al., 2024).

BC fabrication involves optimizing production conditions to achieve superior purity, crystallinity, and mechanical properties. Factors such as pH, oxygen availability, and bacterial strain selection (e.g., *Komagataeibacter* species) are crucial to maximizing yield and quality. The synthesis begins with the bacterial uptake of glucose or fructose as carbon sources, which are metabolized to UDP-glucose. The cellulose synthase complex polymerizes UDP-glucose into β-1 → 4 glucan chains, which aggregate into microfibrils and form BC ribbons extruded outside the cell. This process requires ATP for energy and cofactors like NAD+ and FAD for redox balance. BC's exceptional purity and crystallinity compared to plant cellulose make it a prime candidate for applications in medical devices, smart textiles, and sustainable products. Figure 10.1 (hypothetical) illustrates the enzymatic pathways for glucose and fructose metabolism, emphasizing the influence of carbon sources on BC yield, structure, and industrial scalability (Pandey et al., 2024a; Rodrigues et al., 2024).

10.3 Raw Materials for BC Fabrication

The selection of carbon and nitrogen sources is crucial in bacterial cellulose (BC) fabrication, as these raw materials significantly influence its yield, structure, and mechanical properties. The widely used Hestrin-Schramm (HS) medium includes 2% glucose as the primary carbon source, along with yeast extract and peptone as nitrogen sources. This composition supports effective microbial metabolism and BC synthesis. Alternative formulations, such as Yamamura medium (5% glucose), Kraft's medium (5% sucrose), and Bansal medium (2% glucose), have also been utilized to enhance production under various conditions. However, excessively high carbon concentrations in these media can result in the formation of inhibitory by-products, such as organic acids, which can adversely affect BC quality and yield (Mishra et al., 2022; Pandey et al., 2024c).

Carbon sources serve as the primary energy providers and precursors for BC biosynthesis, playing a key role in bacterial metabolic pathways. These pathways produce intermediary molecules like UDP-glucose and cellobiose phosphate, which

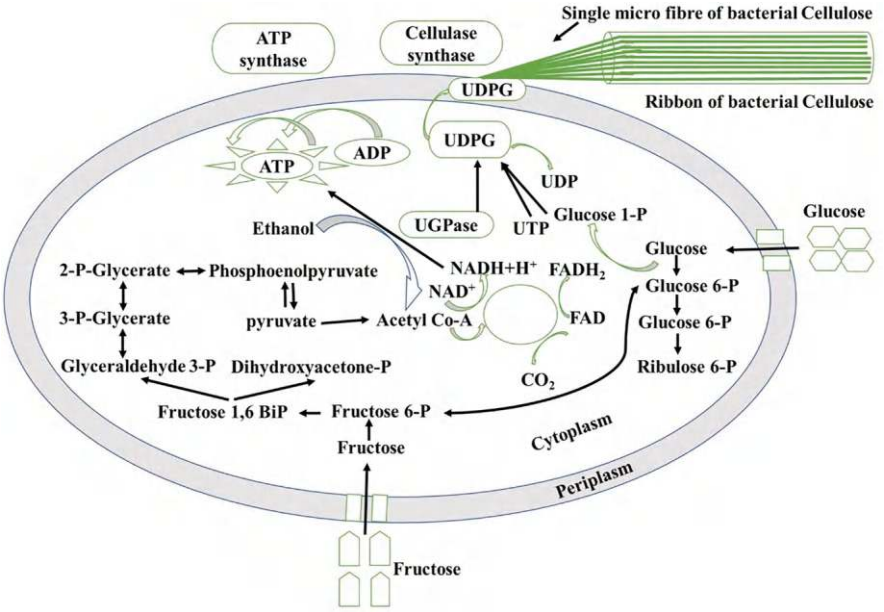

Fig. 10.1 Biosynthesis pathway of BC from glucose and fructose

are subsequently polymerized into cellulose by bacterial enzymes such as cellulose synthase. The choice of carbon source significantly affects the structure and properties of BC. Glucose, being directly metabolized through glycolysis and related pathways, is the most commonly used carbon source due to its efficiency and ability to produce high-quality BC. Fructose, metabolized through alternative routes, results in BC with enhanced porosity and flexibility, making it suitable for specific applications. Glycerol, on the other hand, increases the water-holding capacity of BC, making it ideal for moisture-retentive applications like wound dressings. Sucrose, a disaccharide, hydrolyzes into glucose and fructose, contributing to BC synthesis, although it may lead to by-product accumulation if present in excess (Pandey et al., 2024a; Serra & Hengge, 2019).

Nitrogen sources are equally essential for bacterial growth, protein synthesis, and enzyme activity. Organic nitrogen sources, such as yeast extract and peptone, are preferred due to their rich content of amino acids, vitamins, and growth factors. Yeast extract, in particular, enhances bacterial growth and BC yield by providing nucleotides, vitamins, and amino acids. Peptone, derived from protein hydrolysis, supplies peptides and amino acids that support robust microbial metabolism. While inorganic nitrogen sources like ammonium salts can be used, they are generally less effective due to their limited contribution to growth-enhancing factors (Pandey et al., 2024c; Quijano et al., 2024; Wang et al., 2019).

To make BC synthesis more sustainable, alternative raw materials derived from agricultural and industrial waste have been explored. Carbon sources such as fruit

peels (rich in glucose, fructose, and sucrose), molasses (a by-product of sugar processing), whey (containing lactose), and hydrolyzed cotton waste offer ecofriendly and cost-effective options (Pandey et al., 2024b, 2024c, 2024d). Nitrogen sources like corn steep liquor, soybean waste, and animal manure extracts provide essential nutrients and growth factors for microbial metabolism. These waste-derived raw materials not only reduce production costs but also align with sustainable and circular economy principles. The careful selection and optimization of carbon and nitrogen sources ensure efficient BC production with tunable properties suitable for diverse applications, including medical, textile, and environmental sectors (Pandey et al., 2024b; Quijano et al., 2024; Rodrigues et al., 2024).

10.4 BC Fabrication Methods

BC fabrication methods can be categorized into several approaches, including static cultivation, agitated cultivation, and bioreactor-based cultivation. Each method has distinct advantages and limitations. A key advantage of bacterial cellulose (BC) over other sources of cellulose is its ability to be fabricated into various shapes, such as fleeces, fibrous aggregates, foils, spheres, tubes, and films, according to specific application requirements, often within just a few days (Pandey et al., 2024a). Various bacterial species can synthesize BC, including *Salmonella*, *Escherichia coli*, *Agrobacterium*, *Achromobacter*, *Rhizobium*, *Aerobacter*, *Azotobacter*, *Sarcina*, and *Gluconacetobacter*. However, the most efficient producers are strains of *Acetobacter*, particularly *Acetobacter xylinum*, *Acetobacter hensenii*, and *Acetobacter pasteurianus*. These bacteria can rapidly synthesize BC, an ecofriendly, xeno-free, biodegradable, and biocompatible biomaterial, within a few days under optimal conditions. BC production methods, including static, agitated, and bioreactor cultures, significantly influence its morphology and properties, tailoring it for specific applications. Static cultures yield a gelatinous cellulose membrane on the surface of the nutrient medium, while agitated cultures produce diverse structures, such as spheres, pellets, or irregular masses. The physical crystal morphology and production process of BC depend on raw materials (carbon, oxygen, and nitrogen sources), synthesis conditions (static, dynamic, or reactor incubation), and the type of BC-synthesizing bacterium (e.g., *Komagataeibacter xylinus*), all of which impact BC's quality (Pandey et al., 2024c; Rodrigues et al., 2024). This strain, known for its high efficiency, can convert millions of glucose molecules into cellulose per hour. Recent research emphasizes using agricultural and industrial wastes as cost-effective nutrient sources, producing BC with comparable properties to those made from traditional HS media. These advancements highlight ecofriendly and economical approaches to BC fabrication for diverse applications (Pandey et al., 2024c; Serra & Hengge, 2019; Wang et al., 2019).

10.4.1 Static Culture Method

The static culture method is a widely used and traditional approach for bacterial cellulose (BC) production, where fresh nutrient solutions are incubated in containers under controlled conditions. According to Pandey et al. (2024a), the optimal conditions for BC biosynthesis are an incubation temperature of 28–30 °C and a culture medium pH of 5–6 for consistency over 1–7 days. In this method, BC forms as a hydrogel membrane at the air-liquid interface, supported by bacterial metabolism that generates carbon dioxide and enhances the acidity (pH ~3.5) of the BC synthesis medium, which becomes unfavorable for BC-synthesizing bacteria to grow. Additionally, gluconic acid accumulation, a byproduct of glucose metabolism, can lower the pH over time, creating suboptimal conditions for bacterial growth and cellulose synthesis. This requires frequent pH monitoring and adjustments. However, BC synthesis in static conditions has other drawbacks, such as the entrapment of bacteria within the pellicle, the requirement for more space for synthesis, and uneven oxygen supply. Uneven oxygen distribution across the air-liquid interface limits BC production efficiency, as oxygen is critical for the aerobic metabolism of *K. xylinus* (Pandey et al., 2024b). Regions of the culture lacking sufficient oxygen may lead to reduced bacterial activity and thinner or less uniform BC membranes as shown in Fig. 10.2. Over time, the BC film's thickness increases, and its production depends directly on the surface area of the air-liquid interface, where oxygen is available for aerobic bacterial metabolism. BC produced by this method features a 3D network of highly porous, overlapping, and intertwined cellulose ribbons, forming parallel but somewhat disorganized planes. This phenomenon occurs

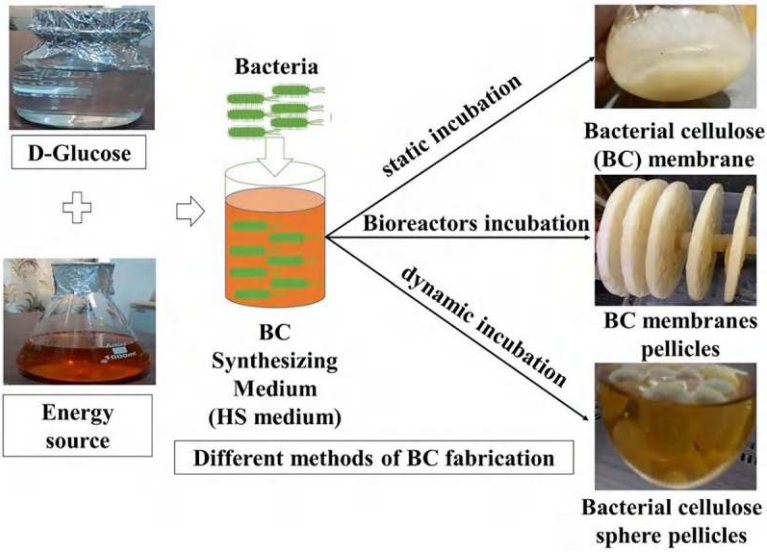

Fig. 10.2 Different methods of BC fabrication

as cellulose ribbons crystallize and form dense layers, which can also trap waste products, further affecting the bacterial microenvironment. Addressing these issues requires optimization of culture conditions or the development of alternative production methods, such as agitated or bioreactor cultures, which provide better oxygen distribution and process control (Pandey et al., 2024c; Quijano et al., 2024; Ullah et al., 2019; Wang et al., 2019).

10.4.2 The Agitated/Shaking Culture Method

The agitated/shaking culture method offers an alternative approach to static culture for bacterial cellulose (BC) production, aiming to address issues such as high costs and low production rates. This method enhances oxygen delivery, a critical factor in BC synthesis. Unlike static culture, which forms a flat BC membrane at the air-liquid interface, the agitated culture produces BC in diverse forms, including spheres, ellipsoids, and irregular masses, depending on factors such as rotational speed, culture duration, and bacterial concentration (as shown in Fig. 10.2). Agitated cultures facilitate continuous shear forces, influencing BC microstructure and enabling scalability. However, this method also has significant drawbacks. Excessive shear force and agitation can cause genetic instability in bacterial strains, reducing BC productivity (Quijano et al., 2024; Rodrigues et al., 2024; Wang et al., 2019). Additionally, the BC produced by this method often exhibits lower crystallinity, degree of polymerization, and mechanical properties compared to static culture. Another concern is the formation of gluconic acid, which can lower pH and inhibit bacterial growth. The non-Newtonian behavior of the medium during mixing also complicates production. Despite these challenges, agitated cultures allow for economical large-scale production, offering potential for industrial applications. The method's ability to produce BC in various shapes and sizes, including hollow and layered structures, provides versatility for specific applications. According to Pandey et al. (2024a) and Ullah et al. (2019), the optimum shaking frequency recorded was 120–125 rpm, which improved the production yield of BC.

10.4.3 The Bioreactor Culture Method

Bacterial cellulose (BC) production has been studied extensively to overcome the limitations of static and agitated cultures, such as low productivity, high costs, and long cultivation times. Various bioreactors have been developed to enhance BC yield and quality while reducing energy consumption and production costs, as shown in Fig. 10.2. Enriched oxygen bioreactors, such as stirred-tank and airlift bioreactors, were among the earliest innovations. Stirred-tank bioreactors provide enhanced oxygen transfer but require high energy input, whereas airlift bioreactors, first reported by Chao in 1997, offer a more energy-efficient alternative with reduced

shear stress. Modifications like internal-loop designs and oxygen-enriched air improved BC productivity, with yields reaching up to 10.4 g/L (Pandey et al., 2024c; Wang et al., 2019). However, the BC produced often had pellet morphology and limited mechanical properties. Rotating disc bioreactors, introduced in 2002, incorporated circular discs that alternated between air and liquid media to produce homogeneous BC with improved mechanical strength. Advances in this design, such as the inclusion of plastic composites (PCs), allowed semi-continuous production without re-inoculation, increasing yield and reducing costs. Modified static bioreactors, including trickling bed reactors, provide high oxygen transfer with minimal shear stress, producing BC with excellent properties like high purity, water-holding capacity, and thermal stability (Ullah et al., 2019). Another innovation, biofilm bioreactors, utilizes biofilm immobilization to enhance biomass density, achieving yields up to 7.05 g/L with superior crystallinity and thermal properties. Additionally, modified airlift bubble column bioreactors introduced rectangular net plates to manipulate BC properties like water-holding capacity and Young's modulus. These reactors achieved high productivity, with yields of up to 6.8 g/L using pure oxygen, although the BC produced exhibited lower crystallinity and mechanical strength. Each bioreactor type demonstrates unique advantages, and ongoing research continues to optimize their designs for cost-effective, large-scale BC production with tailored properties for diverse applications (Pandey et al., 2024c; Quijano et al., 2024; Wang et al., 2019).

10.5 Key Factors Influencing Bacterial Cellulose (BC) Fabrication

The synthesis of bacterial cellulose (BC) is a biotechnological process that requires the careful control of various parameters to optimize yield, quality, and properties. The cost and production yield of BC are largely dependent on factors, such as incubation conditions (static, dynamic, and aerodynamic), incubation temperature, pH of the nitrogen source, type of biosynthesizing bacterium, and the content of oxygen, carbon, and nitrogen sources in the medium. Among these, the carbon source plays a critical role in the extraction of cellulose. Understanding and manipulating these parameters allow researchers to tailor BC production for specific applications, such as biomedical devices, food packaging, and environmental remediation (Pandey et al., 2024c).

In 1954, Hestrin-Schramm medium was used to fabricate BC, and a reported yield of bacterial cellulose was 2.2 g/L after 67 h of incubation, showing that carbon utilization in cellulose conversion was only 1.7%. This was further optimized using different raw materials and incubation conditions (Pandey et al., 2024b). The following sections describe the key factors that influence BC fabrication:

10.5.1 Carbon and Oxygen Source

The cost and production yield of BC are influenced by the choice and efficiency of carbon sources. Traditional sources like sucrose, glucose, and glycerol are commonly used because they are readily metabolized by *Acetobacter xylinus* into UDP-glucose, the precursor for cellulose synthesis. Sucrose provides the highest BC yield (3.83 g/L) due to its hydrolysis into glucose and fructose, providing dual carbon sources. Glycerol (3.75 g/L) contributes high metabolic energy, while glucose (3 g/L) is directly utilized as a precursor. The concentration of the carbon source, when increased up to 60 g/L, also impacts production. However, carbon utilization efficiency remains low, around 5%, as significant glucose is oxidized to gluconic acid instead of being converted into cellulose (Pandey et al., 2024c).

To improve cost efficiency and yields, industrial waste materials have been explored as alternative carbon sources. Food and fruit by-products such as apple pomace, rotten bananas, sugar beet molasses, kitchen waste, and cheese whey produce higher BC yields because they contain not only simple sugars like glucose and fructose but also additional nutrients such as organic acids, vitamins, and minerals. These nutrients enhance bacterial growth and metabolic activity, leading to improved cellulose synthesis. For instance, sugar beet molasses yielded 4.56 g/L, and combined juices of rotten banana and mango achieved 4.81 g/L under static conditions, as shown in Table 10.1. These substrates provide a cost-effective and nutrient-rich alternative to conventional sources, making them valuable for sustainable and economical BC production (Pandey et al., 2024c; Quijano et al., 2024; Rodrigues et al., 2024).

10.5.2 Nitrogen Sources

Nitrogen is essential for bacterial growth and metabolism, as it plays a critical role in protein synthesis, enzyme activity, and the overall metabolic functions of *Acetobacter xylinus*. Traditional organic nitrogen sources, such as peptone and yeast extract, are commonly used in BC synthesis due to their high bioavailability and ability to enhance metabolic activity. These sources promote higher BC yields by providing amino acids, vitamins, and cofactors required for bacterial growth. The carbon-to-nitrogen (C:N) ratio is crucial, with a higher ratio favoring BC production over biomass accumulation, as it limits excessive cell growth while directing energy toward cellulose biosynthesis (Pandey et al., 2024c).

Industrial and agricultural waste-derived nitrogen sources, including cheese whey, soybean meal, potato peels, and kitchen waste, have also been successfully utilized to reduce costs and increase yields, as shown in Table 10.1. These waste materials contain not only nitrogenous compounds but also other nutrients like organic acids and trace elements that enhance bacterial metabolism. The mechanism involves the bacterial uptake of amino acids and peptides from these sources,

Table 10.1 Factors affecting the BC fabrications

S. No.	Waste material	Bacterium used	pH	Incubation condition		Yield (g/L)
				T (°C)	Time	
1.	Baggases waste	*Gluconacetobacter xylinus CH001*	6.7	28	Statical for 20 days	1.09
2.	Apple pomace and sugarcane	*Gluconacetobacter medellinensis*	4	28	Statical for 14 days	2.5
3.	Sugercane molasses	*Komagataeibacter rhaeticus*	6	30	Statical for 14 h	3.46–4.01
4.	Rotten banana and rotten mango juice	*Komagataeibacter medellinensis*	3.5	30	Static for 3 days	4.81
5.	Potato peel waste	*Gluconacetobacter xylinum ATCC 10245*	9	35	Static for 6 days	4.70
6.	Tobacco waste	*Acetobacter xylinum ATCC 23767*	6.5	30	Static for 7 days	2.27
7.	Oats hull and black tea	*Medusomyces gisevii Sa-12*	4.5	30	Static for 12 days	2.20
8.	Cashew apple juice with soybean molasses	*Gluconacetobacter xylinus*	5.5	30	Static for 7 days	4.50
9.	Kitchen waste	*Komagataeibacter rhaeticus*	6	30	Static for 10 days	4.76
10.	Oil palm frond juice	*Acetobacter Xylinum 0416*	4.5	30	Static for 14 days	2.88
11.	Corn stover	*Komagataeibacter xylinus*	6	30	Static for 120 h	4.44
12.	Bamboo dust	*Acetobacter xylinus*	5	30	2 days dynamic and 5 days static	5.8
13.	Sweet lime pulp	*Acetobacter xylinus*	5.65	29	7 days dynamic at 125.90 rpm	7.0
14.	Molasses	*Acetobacter xylinus*	5.68	29	7 days dynamic at 126.98 rpm	11.7
15.	Beehive	*Acetobacter xylinus*	5.68	29	7 days dynamic at 126.98 rpm	9.5

Source: Reprinted with permission from Pandey et al. (2024c). Copyright 2024: Springer Nature

which are then utilized in protein synthesis and enzymatic pathways critical for cellulose production. For instance, nitrogen extracted from sugar beet molasses and cheese whey has demonstrated high BC yields due to the presence of readily available nitrogen and other growth-promoting factors. This nutrient-rich composition accelerates metabolic processes, improving the efficiency of cellulose synthesis and contributing to sustainable and cost-effective BC production (Pandey et al., 2024c; Quijano et al., 2024; Rodrigues et al., 2024).

10.5.3 pH

The pH of the culture medium plays a critical role in BC synthesis by influencing the metabolic activity of *Acetobacter xylinus* and the stability of key enzymes involved in cellulose production. The optimal pH range for BC synthesis is typically between 4.0 and 7.0. Within this range, enzymes like cellulose synthase function efficiently, ensuring a steady conversion of UDP-glucose into β-1,4-glucan chains, which form the cellulose structure. Deviations from this range can denature enzymes, disrupt bacterial metabolism, and reduce cellulose yield and quality (Pandey et al., 2024b).

In acidic conditions (below pH 4.0), bacterial growth may be inhibited due to increased proton concentration, which interferes with cellular processes such as ATP generation and nutrient transport. Conversely, alkaline conditions (above pH 7.0) can destabilize membrane proteins and enzymes, reducing metabolic efficiency. The mechanism involves protonation or deprotonation of active enzyme sites, which directly affects their catalytic activity. Maintaining pH within the optimal range ensures a balanced environment for bacterial growth and efficient cellulose synthesis. Thus, real-time monitoring and periodic adjustment of pH during fermentation are essential for maximizing BC yield and maintaining consistent quality (Pandey et al., 2024c; Quijano et al., 2024; Rodrigues et al., 2024).

10.5.4 Incubation Temperature

Temperature is a critical factor influencing the metabolic activity and cellulose production efficiency of BC-producing bacteria like *Acetobacter xylinus*. These bacteria typically thrive at an optimal temperature range of 28–30 °C, where enzymatic processes such as cellulose synthase activity are maximized. This temperature range supports efficient conversion of UDP-glucose into β-1,4-glucan chains, the primary building blocks of bacterial cellulose (Pandey et al., 2024b, 2024c).

At higher temperatures, enzyme structures may denature, reducing their catalytic efficiency and leading to BC with lower crystallinity and weakened mechanical properties. Conversely, at lower temperatures, the metabolic rate of the bacteria slows down, resulting in reduced cellulose synthesis due to insufficient energy and precursor production. The mechanism involves temperature-dependent enzymatic kinetics and protein stability, which directly impact the biosynthetic pathway of cellulose. Maintaining the optimal incubation temperature is therefore essential for balancing bacterial growth, metabolic efficiency, and the quality of the produced cellulose (Pandey et al., 2024c; Quijano et al., 2024; Rodrigues et al., 2024).

10.5.5 Incubation Condition

The incubation conditions for BC production significantly influence its yield, properties, and structural characteristics. Static incubation promotes bacterial growth at the air-liquid interface, resulting in highly crystalline and mechanically robust BC, as the unidirectional assembly of fibers occurs without external disturbances. In contrast, dynamic conditions, such as agitation, can disrupt the orderly arrangement of cellulose fibers, leading to variations in morphology and reduced crystallinity. However, dynamic conditions often enhance oxygen availability, a critical factor for the aerobic metabolism of *Acetobacter xylinus*, thereby improving BC yield (Pandey et al., 2024b, 2024c).

For instance, under optimized dynamic conditions, BC production increased from 3 g/L in a static glucose medium to 3.8 g/L. Advanced reactor designs, such as rotating disk reactors, rotary biofilm contactors, and bioreactors with spin filters or silicone membranes, further enhance oxygen supply and microbial activity. These systems have achieved BC yields of up to 5.6 g/L by improving oxygen diffusion and bacterial growth. The mechanism underlying these effects is the oxygen-dependent activation of enzymes like cellulose synthase, which catalyzes the polymerization of UDP-glucose into cellulose. In recent studies, cost-effective BC was achieved with yields of 11.7 g/L from molasses, 9.5 g/L from beehive waste, and 7 g/L from sweet lime pulp waste after 7 days in simple dynamic incubators, as shown in Table 10.1. Thus, selecting appropriate incubation conditions and reactor designs is critical for optimizing BC properties and production efficiency for specific applications (Pandey et al., 2024c; Quijano et al., 2024; Rodrigues et al., 2024).

10.5.6 BC-Synthesizing Bacterium

Bacterial cellulose (BC) is produced by various species of Gram-negative bacteria, including *Acetobacter*, *Gluconobacter*, *Sarcina ventriculi*, *Agrobacterium*, and particularly *Komagataeibacter* and *Gluconacetobacter*. These bacteria have a unique ability to synthesize cellulose by converting simple sugars like glucose into long β-1,4-glucan chains through the enzyme cellulose synthase. The process occurs when glucose is metabolized into UDP-glucose, which is then polymerized to form cellulose at the bacterial cell membrane, often at the air-liquid interface. Among these strains, *Komagataeibacter xylinus* is particularly noted for producing BC with high crystallinity and mechanical strength, making it ideal for applications such as wound dressings, electronics, and biocomposites (Mishra et al., 2022; Pandey et al., 2024c). The choice of bacterial strain significantly influences the morphology, crystallinity, and yield of BC, as each strain has unique metabolic characteristics, growth rates, and cellulose-synthesizing capabilities. Strain selection should therefore be based on the desired properties of the final product and the specific requirements of the intended application (Pandey et al., 2024b; Rodrigues et al., 2024).

10.6 Features of Bacterial Cellulose

The features of bacterial cellulose (BC) can be engineered by manipulating various carbon and energy sources through different cultivation methods. These features can be controlled by adjusting the factors that influence BC production.

10.6.1 High Purity and Transparency

Bacterial cellulose (BC) is highly valued for its exceptional purity and transparency, attributes that stem from its unique biosynthetic origin. Unlike plant-derived cellulose, BC is naturally free from lignin and hemicellulose, ensuring a cleaner and more refined material. Its transparency, often exceeding 90% in thin films, makes it particularly suitable for applications requiring both functional efficiency and aesthetic appeal, such as wound dressings and cosmetics. Achieving high purity and transparency in BC relies on precise scientific methods. Controlled fermentation processes, including the use of pure glucose as a carbon source, play a crucial role in eliminating impurities. Maintaining optimal pH and temperature conditions minimizes microbial contamination and unwanted by-products. Furthermore, the nanoscale fibrillar structure of BC ensures minimal light scattering, contributing to its remarkable clarity. These properties are critical in practical applications. The high purity of BC reduces the risk of irritation or inflammatory responses in wound care products, while its transparency allows for real-time monitoring of wound healing progress. In cosmetics, the combination of purity and visual appeal enhances the product's effectiveness and marketability, making BC a preferred choice for innovative and high-performance applications (de Amorim et al., 2020; Girard et al., 2024).

10.6.2 Nanoporous Structure

The nanoporous structure of bacterial cellulose (BC) is a defining feature, with pore sizes typically ranging from 20 to 200 nm, closely resembling the extracellular matrix (ECM). This structural similarity facilitates critical cellular functions, including adhesion, proliferation, and differentiation, making BC an excellent biomaterial for regenerative applications. The porosity of BC can be finely tuned by modifying fermentation conditions. For instance, static cultures generally yield denser structures with smaller pores, while agitated cultures promote the formation of more porous networks. This adaptability allows for the customization of BC properties to suit specific applications. In tissue engineering, the controlled porosity of BC is particularly significant, as it ensures efficient nutrient transport, cell migration, and waste removal, all of which are essential for tissue regeneration and repair.

These characteristics make BC scaffolds highly effective in mimicking natural tissue environments and promoting healing (de Amorim et al., 2020; Mishra et al., 2022; Ullah et al., 2019).

10.6.3 Flexibility and Moldability

Bacterial cellulose (BC) exhibits exceptional flexibility and moldability, with a flexibility index (FI) of approximately 3.4. This property allows BC to conform to various shapes without cracking, making it ideal for applications that require pliability. The flexibility of BC arises from its unique nanofibrillar structure, which provides high mechanical strength while maintaining a certain degree of elasticity. The flexibility can be further enhanced by adjusting the water content during the drying process, which helps retain moisture and prevent brittleness. Additionally, incorporating plasticizers, such as glycerol, during fabrication reduces intermolecular forces between cellulose fibers, thereby increasing flexibility and making the material more pliable (Manan et al., 2022; Ullah et al., 2019; Wang et al., 2019). This flexibility is particularly advantageous in the design of wound dressings, as it enables the material to adapt to body contours and movements. The conformability of BC helps maintain consistent contact with the wound site, promoting better adherence and reducing the risk of displacement. As a result, BC-based dressings provide improved patient comfort, better coverage, and enhanced wound healing by reducing irritation and allowing for a more natural healing process (Pandey et al., 2024a; Ullah et al., 2019).

10.6.4 High Degree of Polymerization

The degree of polymerization (DP) of bacterial cellulose (BC) can reach up to 10,000, significantly contributing to its mechanical strength and resistance to enzymatic degradation. The DP refers to the length of the cellulose chains, with higher values indicating longer chains. Longer chains provide greater molecular weight, resulting in enhanced material stability, durability, and improved mechanical properties, such as tensile strength and resistance to breaking under stress. The DP of BC can be influenced by fermentation conditions, such as fermentation time and the specific strain of *Acetobacter* used. Extended fermentation periods allow for the synthesis of longer cellulose chains, thus increasing the DP (Manan et al., 2022; Ullah et al., 2019; Wang et al., 2019). In contrast, shorter fermentation times may lead to lower DP values, producing a more brittle material. This high DP is particularly advantageous for applications that require durability and strength, such as biomedical implants, wound dressings, and structural scaffolds. The enhanced mechanical strength ensures that BC-based materials can endure physiological stresses and maintain their integrity in harsh environments, such as within the

human body. Additionally, the resistance to enzymatic degradation means that BC remains stable over longer periods, making it suitable for long-term applications in medical and industrial fields (de Amorim et al., 2020; Girard et al., 2024; Ullah et al., 2019).

10.6.5 High Crystallinity

Bacterial cellulose (BC) exhibits high crystallinity, ranging from 60% to 90%, a critical property that enhances its mechanical and thermal performance. Crystallinity refers to the orderly arrangement of cellulose molecules in a crystalline structure, which provides BC with increased stability and strength. The high crystallinity improves BC's resistance to biodegradation, making it more durable and less prone to breakdown by microorganisms, a key factor for long-term applications. It also contributes to BC's mechanical strength, increasing its resistance to deformation and enhancing its ability to withstand external stresses without failure. Crystallinity in BC can be influenced by various fermentation conditions, such as temperature, the type of carbon source used, and fermentation time. Higher fermentation temperatures typically promote the formation of more crystalline cellulose, leading to enhanced structural integrity (Manan et al., 2022; Ullah et al., 2019; Wang et al., 2019). Additionally, specific carbon sources like glucose or other sugar derivatives can affect the polymerization and crystallization process, further influencing the final crystallinity of the BC. The high crystallinity of BC is particularly advantageous for applications requiring structural integrity and resistance to deformation, such as in medical devices, wound dressings, and tissue scaffolds. It ensures that BC-based materials maintain their shape and strength under stress, even in physiological environments. Moreover, its improved resistance to thermal degradation makes it suitable for high-temperature applications, broadening its use in various fields, including biomedicine and materials science (Mishra et al., 2022; Ullah et al., 2019).

10.6.6 Mechanical Properties

Bacterial cellulose (BC) exhibits impressive mechanical properties, with tensile strength reaching up to 954 MPa and Young's modulus ranging from 130 to 140 GPa, surpassing many natural fibers. These exceptional properties can be attributed to the high crystallinity and degree of polymerization (DP) inherent in BC. Crystallinity contributes to the material's structural integrity and resistance to deformation, while a high DP indicates longer cellulose chains that enhance the material's overall strength and stability. The higher the crystallinity and DP, the more tightly packed the cellulose fibers are, resulting in a stronger and more rigid material. The mechanical properties of BC can be fine-tuned by adjusting various fermentation

conditions. For instance, nutrient availability (such as the type and concentration of carbon sources) and fermentation temperature significantly influence the degree of polymerization and crystallinity (Manan et al., 2022; Ullah et al., 2019; Wang et al., 2019). Higher nutrient concentrations or optimized temperature conditions can increase DP and crystallinity, leading to enhanced mechanical properties. Conversely, modifying these parameters can allow for the production of BC with specific mechanical characteristics suitable for different applications. The high tensile strength and Young's modulus of BC make it an ideal material for demanding applications, particularly in biomedicine. In scaffolds and implants, BC must bear loads and resist deformation while maintaining structural integrity in physiological environments. The ability to tailor BC's mechanical properties through fermentation control allows for the development of customized materials for tissue engineering, medical implants, and other biomedical devices, offering durability and reliability under stress (de Amorim et al., 2020; Ullah et al., 2019).

10.6.7 Moisture Holding and Releasing Ability

Bacterial cellulose (BC) is capable of retaining up to 98% of its weight in water, a property facilitated by its highly porous structure and large surface area. The high-water retention is primarily due to the network of nano-sized pores within the BC structure, which creates numerous capillary forces that trap water molecules. Additionally, the hydroxyl groups present on the cellulose chains contribute to strong hydrogen bonding with water molecules, further enhancing moisture retention. The porous nature of BC also increases the surface area available for water absorption, enabling it to hold a substantial amount of moisture without compromising its structural integrity. This water retention ability can be fine-tuned by adjusting the porosity of BC through fermentation parameters such as agitation speed and nutrient composition. Increasing the agitation speed during fermentation, for example, results in a more porous structure, allowing for greater water uptake (Manan et al., 2022; Ullah et al., 2019; Wang et al., 2019). The inclusion of hydrophilic additives, such as glycerol or other plasticizers, during fabrication can further enhance BC's moisture-holding capacity by creating additional hydrophilic interactions within the material. This remarkable moisture retention is particularly advantageous for wound care applications, where maintaining a moist environment is critical for promoting faster healing and preventing scab formation. A moist environment aids in cellular activities like migration, proliferation, and collagen synthesis, which are essential for tissue repair. Furthermore, the high-water content in BC helps reduce the risk of infection by creating a barrier that inhibits bacterial penetration. Thus, BC's ability to retain moisture supports its use in wound dressings, offering an optimal environment for healing and improved patient outcomes (Pandey et al., 2024a).

10.6.8 Permeability to Liquids and Gases

Bacterial cellulose (BC) exhibits a unique permeability profile, allowing for efficient exchange of gases, such as oxygen (O_2) and carbon dioxide (CO_2), as well as liquids. This permeability is primarily attributed to the nano-porous structure of BC, which consists of interconnected pores of controlled size. The presence of these pores facilitates the diffusion of gases and liquids, ensuring an optimal environment for cellular activities, such as respiration and nutrient transport, which are essential in tissue engineering applications. The high surface area and fine porosity of BC enable it to support the passage of essential gases while restricting the entry of harmful pathogens or contaminants. The permeability of BC can be fine-tuned by adjusting the fermentation conditions, particularly the agitation speed. For instance, increasing the agitation during fermentation leads to the formation of a more porous structure, which enhances the material's ability to exchange gases and liquids. Additionally, the degree of porosity can be controlled by modifying the nutrient composition, temperature, and fermentation duration, allowing for a customized permeability profile suited to specific applications (Manan et al., 2022; Ullah et al., 2019; Wang et al., 2019). This property is particularly advantageous in applications like wound dressings, where both moisture retention and gas exchange are critical for optimal healing conditions. The ability to allow oxygen to reach the wound site while preventing moisture loss creates an ideal environment for cellular proliferation and tissue regeneration. Furthermore, efficient gas exchange prevents the buildup of carbon dioxide, which could hinder cell metabolism. Thus, BC's permeability profile ensures that it maintains a balanced environment, promoting faster healing and reducing the risk of infection, making it an excellent choice for advanced biomedical applications, particularly in tissue engineering and wound care (Girard et al., 2024).

10.6.9 Thermal Stability

Bacterial cellulose (BC) exhibits impressive thermal stability, maintaining its structural integrity up to temperatures of 250 °C. This exceptional stability is primarily due to BC's high crystallinity and degree of polymerization (DP), which contribute to its resistance to thermal degradation. The crystalline regions in BC, composed of tightly packed cellulose chains, help prevent the breakdown of the material when exposed to heat. Furthermore, the degree of polymerization (DP), which refers to the length of the cellulose chains, also plays a significant role in enhancing thermal stability, as longer chains are more resistant to thermal degradation. The thermal properties of BC can be optimized by adjusting fermentation parameters, such as nutrient composition, temperature, and fermentation time. For example, increasing the fermentation time or controlling the carbon source can lead to higher DP and crystallinity, further enhancing BC's thermal stability (Manan et al., 2022; Ullah

et al., 2019; Wang et al., 2019). The ability to manipulate these factors allows for the customization of BC's thermal properties to suit specific applications. This thermal stability is particularly advantageous in medical applications where sterilization is required. BC's ability to withstand autoclaving or other heat-based sterilization processes ensures that it retains its mechanical properties and functionality post-sterilization. This makes BC an ideal material for use in medical devices, wound dressings, and implants, where maintaining material integrity and performance during and after sterilization is crucial (Mishra et al., 2022). Therefore, BC's excellent thermal stability not only contributes to its longevity but also enhances its suitability for advanced biomedical applications.

10.6.10 Cell Adhesion and Proliferation

Bacterial cellulose (BC) significantly enhances cell adhesion and proliferation, with studies indicating up to 90% cell attachment rates. This high level of cell attachment is attributed to BC's biocompatible surface and its unique nanofibrous structure, which closely resembles the extracellular matrix (ECM) that supports cellular functions in tissues. The nanofiber arrangement provides a large surface area and topographical cues that facilitate cellular interactions, mimicking natural tissue environments (Manan et al., 2022; Ullah et al., 2019; Wang et al., 2019). The surface properties of BC can be further modified through chemical treatments, such as the incorporation of bioactive molecules, growth factors, or extracellular matrix proteins. These modifications promote specific cellular interactions, enhancing cell adhesion, migration, and proliferation. By controlling these surface characteristics, BC can be tailored to encourage the growth of various cell types, including fibroblasts, keratinocytes, and endothelial cells, which are crucial for tissue regeneration and repair. This property is particularly advantageous in the field of tissue engineering, where successful cell attachment and proliferation are essential for the functionality and integration of scaffolds with host tissues. BC scaffolds with enhanced cell adhesion promote faster tissue formation and improve the likelihood of integration with surrounding tissues, making them ideal for applications such as wound healing, skin regeneration, and organ scaffolding (de Amorim et al., 2020; Pandey et al., 2024a). Therefore, BC's ability to support and enhance cellular functions ensures its effectiveness in regenerative medicine and biomedical applications.

10.6.11 Biocompatibility

Bacterial cellulose (BC) is widely recognized for its outstanding biocompatibility, which is a crucial property for its use in medical applications. BC integrates seamlessly with human tissues without inducing significant immune responses, which is vital for ensuring the safety and effectiveness of implants and scaffolds. Scientific

studies have shown that BC promotes fibroblast proliferation and exhibits minimal inflammatory responses when implanted in vivo. This biocompatibility arises from its natural, non-toxic, and non-immunogenic properties, which prevent rejection and adverse immune reactions (Wang et al., 2019). The mechanism behind BC's biocompatibility is closely linked to its structure and composition. BC is composed of pure cellulose, lacking the lignin and hemicellulose present in plant-derived cellulose, which can sometimes trigger immune responses. Additionally, BC's nanofibrous structure closely mimics the extracellular matrix (ECM), promoting cell adhesion and facilitating tissue regeneration without causing irritation or toxicity. In vitro studies have shown that BC scaffolds support the attachment and proliferation of various cell types, including fibroblasts and endothelial cells, further validating its compatibility with human tissues (Ullah et al., 2019). This biocompatibility is especially advantageous for medical applications, such as implants and tissue engineering scaffolds, where favorable interaction with host tissues is essential for successful integration and functionality. BC's ability to foster tissue regeneration, without inducing rejection or inflammation, makes it an ideal material for applications like wound healing, artificial skin, and other regenerative medical treatments (Girard et al., 2024; Manan et al., 2022). Therefore, BC's excellent biocompatibility ensures its reliability and effectiveness in enhancing tissue regeneration while maintaining safety in clinical settings.

10.6.12 Biodegradability

The biodegradability of bacterial cellulose (BC) is primarily influenced by its structural characteristics, particularly its high crystallinity and dense fibrillar network. These features contribute to BC's resilience, as the tightly packed cellulose chains and crystalline regions make it less accessible to biodegrading enzymes. While BC is largely non-biodegradable in vivo due to the human body's lack of cellulase enzymes, it can be broken down by specific microorganisms in the environment (Manan et al., 2022). These microorganisms, such as *Cellulomonas* and *Trichoderma*, secrete cellulases that degrade cellulose into simpler sugars, initiating the biodegradation process. The biodegradation of BC occurs through enzymatic activity, where celluloses hydrolyze the cellulose polymer into glucose or oligosaccharides, making it accessible to microbial metabolism. However, the high crystallinity of BC presents a challenge for these enzymes, as it limits their access to the amorphous regions of the cellulose structure. This slow degradation rate can be advantageous in certain applications, particularly in medical implants or scaffolds, where controlled degradation is desired. The gradual breakdown of BC allows it to maintain its mechanical integrity over time, providing sustained support for tissue regeneration before it is eventually degraded by environmental microorganisms (Ullah et al., 2019; Wang et al., 2019). This slow biodegradability is beneficial for long-term applications like implants, where it is important for the material to provide continuous support during the healing process while gradually breaking down without

causing an inflammatory response. BC's ability to maintain structural integrity for extended periods before complete degradation enhances its suitability for use in medical devices and tissue engineering applications, offering a balance between durability and eventual bio-absorption (Mishra et al., 2022; Pandey et al., 2024a).

10.7 Applications of Bacterial Cellulose

10.7.1 Medicine

10.7.1.1 Wound Dressings

The three-dimensional nanoporous structure of bacterial cellulose (BC) has made it a highly effective material for wound dressings due to its intrinsic properties such as high-water retention and release ability, biocompatibility, biodegradability, oxygen permeability, and high crystallinity (~88%). These features promote a moist wound healing environment by preserving hydration, facilitating cell migration, and supporting tissue granulation (Picheth et al., 2017; Stumpf et al., 2018). BC's adaptability enables the incorporation of antimicrobial agents, such as silver nanoparticles and zinc nanoparticles, which enhance protection against pathogens like *E. coli* and *S. aureus*. Additives like collagen, aloe vera, and chitosan further support infection control and tissue regeneration. BC can also serve as a matrix for sustained drug delivery systems by incorporating agents like tetracycline and ibuprofen, improving advanced wound care (Pandey et al., 2024a; Zeng et al., 2023). Modified BC, such as hydrogels with quaternized chitosan or cryogels for hemorrhage control, demonstrates enhanced antimicrobial efficacy and rapid hemostasis, making BC an outstanding choice for future wound care applications (Deng et al., 2024; Li, Chu, et al., 2024).

10.7.1.2 Drug Delivery Systems

BC's hydrophilicity, biocompatibility, and modifiable surface chemistry make it an excellent candidate for drug delivery applications. Its porous structure can be enhanced using techniques like ethanol dehydration for better drug encapsulation or acetylation for hydrophobic drugs. Combinations with sodium alginate or gelatin create hydrogels that improve encapsulation efficiency and controlled release for various drugs (Balistreri et al., 2024). Drug delivery methods such as physical adsorption, covalent bonding, and nanoparticle embedding enable precise control over drug release profiles. For instance, BC/graphene oxide nanocomposites loaded with ibuprofen showed sustained release through a non-Fickian diffusion mechanism (Luo et al., 2017). Recent innovations, like BC nanoparticles derived from kombucha, exhibit scalable drug delivery platforms with excellent biodegradability (Balistreri et al., 2024). Functionalization with agents like sodium alginate or

cefoperazone demonstrates BC's ability to sustain drug release and enhance antibacterial activity, making it a versatile material for pharmaceuticals (Ji et al., 2021; Ye et al., 2024).

10.7.1.3 Tissue Engineering

BC's biocompatibility, mechanical strength, flexibility, and porosity make it highly suitable for tissue engineering applications. In skin tissue engineering, BC-based dressings create a moist environment, absorb excess fluids, and promote mechanical protection and healing (Hospodiuk-Karwowski et al., 2022). Incorporating antimicrobial agents like chitosan enhances these properties (Narayanan et al., 2023). For bone tissue engineering, BC scaffolds modified with hydroxyapatite (HAp) enhance mechanical properties and osteogenic potential, while combining BC with 3D printing improves scaffold customization and cell viability (Cakmak et al., 2020; Fooladi et al., 2023). In cartilage engineering, BC scaffolds functionalized with hyaluronic acid or glycosaminoglycans address limitations like pore size, improving cell infiltration and cartilage defect repair (Pang et al., 2020). Advanced designs, such as decellularized cartilage extracellular matrix composites, mimic native cartilage properties, promoting tissue regeneration (Li et al., 2022). Emerging methods like 3D printing with sacrificial molds further expand BC's potential for creating complex structures for tissue constructs and prosthetics (Abol-Fotouh et al., 2024).

10.7.2 Biotechnology Application of Bacterial Cellulose

This section underscores the significance of renewable biomaterials and enzyme immobilization as sustainable alternatives to oil-based resources. Enzymes, renowned for their efficiency as biocatalysts, are pivotal in biotechnology due to their selectivity and environmental benefits. However, their direct application is often hindered by high costs and low stability. Immobilizing enzymes onto biopolymer supports can significantly enhance their stability, activity, and recyclability, making them more suitable for various applications in biomedicine, food processing, bioenergy, and environmental protection. Biopolymers like alginate, chitosan, and cellulose are particularly effective carriers due to their abundance, biocompatibility, and biodegradability, positioning them as ideal solutions in green biotechnology (Bilal & Iqbal, 2019).

10.7.2.1 Application in Bioreactors

Bacterial cellulose (BC) has emerged as an excellent material for bioreactors due to its unique properties, including high mechanical strength, chemical stability, large surface area, and biocompatibility. BC acts as an efficient immobilization matrix for

enzymes, enhancing their stability, activity, and reusability. These properties make BC particularly useful for facilitating biocatalysis in various industrial and biomedical applications.

For instance, Chen et al. (2015) developed a BC hydrogel membrane, freeze-dried to preserve its nanostructure, which effectively immobilized fungal laccase. The enzyme retained 69% of its activity after seven cycles, demonstrating BC's potential for long-term use in bioreactors. Similarly, Estevinho et al. (2018) immobilized a hybrid enzyme composed of *Thermotoga maritima* β-galactosidase (TmLac) fused with a carbohydrate-binding module (CBM2) on BC. This approach showcased efficient enzyme binding and enhanced thermostability, although enzyme reuse was limited due to TmLac's inherent instability. Vasconcelos et al. (2020) further enhanced BC membranes' porosity through K_2CO_3 treatment, improving their enzymatic interactions and making them promising candidates for biomedical applications like bioactive wound dressings. Additionally, Buruaga-Ramiro et al. (2020) demonstrated that BC could immobilize lipase, resulting in nanocomposites with improved thermal stability, reusability, and activity, making them suitable for detergent and food processing industries. Li, Lv, et al. (2020) expanded BC's application by creating an enzymatic biofuel cell (EBFC) that immobilized laccase on amidoxime-modified BC, enabling efficient electricity generation and wastewater treatment. These studies underscore BC's versatility and reliability as a support material for bioreactors across various sectors.

10.7.2.2 Application in Biosensors

BC's biocompatibility, biodegradability, and nontoxicity, coupled with its excellent mechanical properties, make it an ideal substrate for biosensors. Modified BC membranes, integrated with conductive and functional materials, have enabled the development of highly sensitive and stable biosensors for medical diagnostics, environmental monitoring, and wearable applications.

For example, Jasim et al. (2017) developed electrically conductive BC membranes by incorporating polyaniline and single-walled carbon nanotubes. This modification enhanced electrical conductivity and thermal stability, making the material suitable for bioelectronic devices. Lv et al. (2018) created a self-powered biosensor by modifying BC with carbon nanotubes and gold nanoparticles, enabling efficient glucose detection with high stability and sensitivity. Rebelo et al. (2019) introduced an electrochemical biosensor using BC with a polyvinylaniline/polyaniline bilayer, facilitating neural stem cell differentiation and highlighting BC's potential in neural tissue engineering. Moreover, Gomes et al. (2020) developed a lactate biosensor using BC as a support for a screen-printed electrode modified with Prussian blue nanocubes and lactate oxidase. This sensor offered a wide detection range and low detection limits, ideal for wearable health-monitoring devices. In environmental applications, Xi et al. (2023) and Akki et al. (2024) demonstrated BC's potential in wastewater treatment by creating ultrafiltration membranes combined with nano silica and polyhexamethylene guanidine

hydrochloride, enhancing antibacterial properties and nanoparticle separation efficiency.

10.7.3 Bacterial Cellulose in Cosmetology: Facial Masks and Skincare

Bacterial cellulose (BC) has gained considerable attention in cosmetology, particularly in the formulation of facial masks, owing to its unique properties such as high moisture retention, excellent biocompatibility, and strong adherence to the skin. These characteristics make BC-based masks ideal for addressing various skincare concerns, from hydration and anti-aging to soothing and whitening effects. For instance, the Royal Skin Brightening Bio-cellulose Mask from Korea enhances skin elasticity and softness, while Tech Nature's Anti-aging Bio-cellulose Mask from France reduces wrinkles, promoting a smoother appearance. Similarly, the Aloe Bio-cellulose Mask from the USA is designed for post-treatment skin soothing, reducing irritation and aiding in recovery, and the DHC Bio-cellulose Mask from Japan targets pigmentation issues for a brighter complexion. Advanced formulations, like the Laboratoires l'Esthetic Face Mask from France, offer antioxidant and anti-pollution benefits, protecting against environmental damage, while Guangzhou Microcell's lightening masks focus on reducing dark spots and enhancing skin tone (Lima et al., 2024; Pang et al., 2020).

BC's utility in facial skincare extends beyond standard formulations to innovative material modifications for enhanced performance. For instance, BC integrated with bamboo plant extract improves adhesion and elasticity, while *Moringa oleifera* leaf powder enhances hydration. Other additives like milk by-products and tea polyphenols endow BC masks with antioxidant and whitening properties, while combinations like sericin-hyaluronic acid (HA) provide anti-aging effects. Similarly, BC membranes blended with cerium oxide nanoparticles impart antimicrobial and anti-inflammatory properties, making them suitable for sensitive or damaged skin. BC-based hydrogels infused with taurine or rutin deliver additional benefits, such as moisturization, antioxidant activity, and targeted drug delivery. These applications illustrate BC's adaptability in addressing diverse cosmetic needs while ensuring skin safety and efficacy (Amorim et al., 2020; Feng et al., 2024; Ho et al., 2015).

10.7.4 Applications of Bacterial Cellulose (BC) in the Food Industry

10.7.4.1 Novel Food Products

Bacterial cellulose (BC) has a long-standing history in the food industry, particularly in Asia, where it is used to produce traditional desserts like "Nata de coco" and "Nata de piña" in the Philippines (Mishra et al., 2022). Its wet membranes exhibit

a smooth, gelatinous texture, making BC suitable for edible applications. When processed with sugar alcohols or combined with alginate and calcium chloride, BC attains a palatable texture similar to that of fruit or mollusks. The US Food and Drug Administration (FDA) classified BC as a safe dietary fiber in 1992, recognizing its applications as a food additive and functional ingredient (de Amorim et al., 2020).

In the food industry, BC functions as a thickener, gelling agent, and stabilizer, improving the texture and rheology of mixtures. For example, BC has been used to stabilize Pickering emulsions, where its three-dimensional network at oil-water interfaces prevents coalescence and droplet aggregation. Additionally, its dietary benefits include fat substitution and cholesterol reduction, further extending its value in low-fat and health-oriented food products (Cacicedo et al., 2016). Research has demonstrated BC's potential in creating novel food textures and enhancing sensory attributes. Girard et al. (2024) utilized BC to develop reduced-fat ice cream with improved emulsification and melting resistance, while Urbina et al. (2021) found that BC improved rheological behavior and sensory characteristics in mayonnaise. BC-based gels for dairy desserts have also been developed, enhancing mouthfeel and functionality in such products (Hou et al., 2024; Hu et al., 2019; Singh et al., 2024).

10.7.4.2 Food Packaging

BC has gained prominence in food packaging as a sustainable alternative to petroleum-based materials due to its biodegradability, high mechanical strength, and excellent barrier properties. BC films provide protection against moisture and microbial contamination, extending food shelf life. When reinforced with other materials like starch and polylactic acid (PLA), BC films exhibit improved thermoresistance, transparency, and reduced gas permeability, making them suitable for high-performance food packaging applications (Cacicedo et al., 2016; Kuswandi et al., 2020).

For instance, BC-chitosan-polyvinyl alcohol films display superior UV-barrier properties while maintaining structural integrity under varying water activity levels (Cazón et al., 2019). Additionally, edible pH sensors have been developed using BC membranes with anthocyanins from red cabbage, providing a visual indicator of spoilage with stable responses for up to 22 days (Kuswandi et al., 2020). Innovations like oleofilms made from beeswax-in-water emulsions stabilized by BC nanofibers and carboxymethyl chitosan enhance mechanical strength and reduce water vapor permeability, making them ideal for food-grade coatings (Li, Ma, et al., 2020).

Further, BC-based films with antimicrobial properties have been developed by blending BC with chitosan, carboxymethyl cellulose (CMC), and glycerol, resulting in films with increased tensile strength and reduced microbial growth (Indriyati et al., 2021). Paper sheets coated with BC nanofibers, chitosan, and zinc oxide

(ZnO) show improved antibacterial and mechanical properties, with optimal results obtained using ZnO synthesized at 80 °C (Jabłońska et al., 2021). Advanced formulations such as nano-hydrogels combining wood cellulose, BC, and chitin have also been explored for packaging applications. These hydrogels demonstrate pseudoplastic behavior, enhancing mechanical properties and barrier performance (Jannatamani et al., 2022). BC-based antioxidant active packaging films incorporating silica nanoparticles show improved mechanical strength, UV protection, and water vapor barrier properties, with smaller nanoparticles providing superior antioxidant activity (Dong et al., 2022). Lastly, functional films integrating BC and gelatin with anthocyanins and fluorescein isothiocyanate have been developed for real-time monitoring of food freshness. These films change color in response to ammonia levels, making them ideal for active packaging of perishable foods like shrimp (Yang et al., 2024). The multifaceted applications of BC in novel food products and sustainable packaging materials demonstrate its potential to address functional, sensory, and environmental needs in the food industry, paving the way for further innovation (Haghighi et al., 2021; Koreshkov et al., 2024; Kusuma et al., 2024).

10.7.5 Environmental Applications of Bacterial Cellulose

Bacterial cellulose (BC) has garnered significant attention in environmental applications due to its renewable nature, exceptional structural properties, and potential for customization. Its biocompatibility, high mechanical strength, and tunable porosity make it an ideal material for addressing challenges in water purification, pollutant adsorption, and air filtration systems.

10.7.5.1 Membranes for Water Purification

BC membranes have demonstrated remarkable efficacy in water purification, particularly after functionalization with chemical groups or incorporation of nanoparticles. Functionalized BC membranes, for instance, have shown enhanced adsorption capacities for heavy metals like lead and cadmium (Bethke et al., 2018; Sharma et al., 2023). Hybrid BC membranes, such as BC/polyvinyl alcohol (PVA) composites, are effective in adsorbing dyes like methylene blue and toxic anions, including arsenates (Hu et al., 2019). Furthermore, BC-based nanohybrids with embedded copper oxide or silver nanoparticles provide antibacterial properties and photocatalytic capabilities, making them suitable for multifunctional water treatment (Almasi et al., 2020; Kumar et al., 2023). Recent studies have introduced solar-driven Janus-structured BC aerogels for desalination and bacterial decontamination, paving the way for sustainable and portable water purification systems (Chen et al., 2023; Zhang, Zhang, et al., 2024).

10.7.5.2 Adsorbent Materials for Pollutant Removal

BC has been widely studied as a base material for adsorbents, offering excellent pollutant removal efficiency due to its high surface area and modifiable surface chemistry. Functionalized BC membranes have achieved over 90% removal rates for heavy metals like cadmium and chromium, which are crucial for industrial wastewater treatment (Mir et al., 2024; Nguyen et al., 2024). Additionally, BC composites integrated with graphene oxide enhance structural strength and adsorption performance (Wang et al., 2024). Imprinted BC membranes have demonstrated selective removal of radioactive cesium from nuclear wastewater, showcasing their potential in environmental remediation (Zhang, Zheng, et al., 2024). Moreover, BC biochar composites have shown promising results in adsorbing dyes such as Rhodamine B and methylene blue, while BC/locust bean gum materials exhibit high reusability and cost-efficiency (Li, Li, & Li, 2024; Liu et al., 2024).

10.7.5.3 Air Filtration and Pollutant Capture

BC has emerged as a high-performing material for air filtration applications. BC membranes modified with silver nanowires exhibit excellent particulate matter (PM) removal capabilities, alongside antibacterial properties and breathability, making them suitable for personal protective equipment (Sharma et al., 2023; Wu et al., 2022). Furthermore, BC-based filters incorporated with manganese dioxide or graphitic carbon nitride enable catalytic degradation of airborne pollutants like formaldehyde and volatile organic compounds (Li, Zhang, et al., 2024; Wang et al., 2022). Directional BC aerogels have shown superior fine PM removal efficiency and reusability, making them ideal for indoor and industrial air filtration systems (Sun et al., 2023). Recent innovations, such as triboelectric nanogenerator-enhanced BC membranes, demonstrate their potential for wearable air filtration devices with advanced filtration of ultrafine particles (Chen et al., 2023; Zhu et al., 2024).

10.8 Commercialization of Bacterial Cellulose

The commercialization of bacterial cellulose (BC) has expanded across various industries due to its unique properties such as high purity, mechanical strength, biocompatibility, and water retention capacity. In the medical field, BC-based products like Nanoskin® (Innovatec, Brazil), which integrates silver ions for antimicrobial effects, and Epiprotect® (S2Medical AB, Sweden), used for burn and ulcer treatment, demonstrate its ability to enhance wound healing and tissue regeneration through moisture retention and porosity (Choi et al., 2022; Rodrigues et al., 2024). Similarly, in cosmetics, BC-based facial masks such as DHC Bio Cellulose Mask and Lancôme Blanc Expert Mask leverage BC's nano-fibrillar structure for superior skin adhesion and hydration, enabling effective delivery of active ingredients like

vitamin C and algae extracts (Girard et al., 2024; Quijano et al., 2024). Beyond these sectors, BC's application in smart textiles, advanced drug delivery systems, and biodegradable packaging showcases its potential as a sustainable alternative to traditional materials. Innovations like integrating nanomaterials and modifying BC's structure through genetic engineering are unlocking new possibilities, including tailored properties for medical implants and high-performance fabrics (Pang et al., 2020; Rodrigues et al., 2024).

Despite these advancements, commercialization faces challenges, including regulatory barriers and lack of standardization in BC production. Products, particularly in healthcare, must comply with strict safety and efficacy standards, which can delay market entry and increase costs. Moreover, the variability in BC quality due to unstandardized production protocols limits its broader adoption. Addressing these challenges requires collaborative efforts among researchers, industries, and regulatory bodies to establish standardized production methods and quality benchmarks. Advances in genetic engineering and recombinant DNA technology may also enable the consistent production of BC with desired properties, ensuring its scalability and reliability for diverse applications (Quijano et al., 2024; Rodrigues et al., 2024).

Looking ahead, BC's future lies in developing innovative composites, incorporating nanoparticles, and leveraging biotechnological advances for customized applications. Its biodegradable nature and compatibility with other biomaterials position it as a key player in sustainable development, particularly in ecofriendly packaging and textiles. As technological barriers are overcome, BC's role in addressing global challenges in healthcare, sustainability, and advanced materials science is expected to grow exponentially, reinforcing its status as a next-generation biomaterial (Girard et al., 2024; Pang et al., 2020; Quijano et al., 2024).

10.9 Conclusion

Bacterial cellulose (BC) has firmly established itself as a highly versatile and sustainable material, offering unique advantages across a wide range of industries due to its exceptional properties, such as high water retention, excellent biocompatibility, mechanical strength, and biodegradability. The fabrication process plays a crucial role in enhancing BC's properties for specific applications. Techniques like chemical modification, composite formation, and nanomaterial integration significantly improve its functionality, enabling customization for diverse applications in medical, cosmetic, food, and environmental sectors. In the medical field, BC is successfully used in wound care and drug delivery, while in cosmetics, it enhances the efficacy of skincare products. Its potential extends to food packaging, environmental remediation, and other ecofriendly applications, positioning BC as a promising alternative to synthetic materials. Despite challenges such as regulatory barriers and high production costs, ongoing advancements in BC fabrication technologies are expected to drive growth and expand its commercial adoption. With continued

innovation in fabrication methods, BC's properties can be further optimized, ensuring its effective integration into a wide range of applications.

10.10 Future Prospects

The future of BC holds immense potential, fueled by innovations in genetic engineering, fermentation processes, and advanced fabrication techniques that will enhance both its production efficiency and material properties. Standardizing production methods and establishing regulatory frameworks will streamline BC's market entry and ensure consistent quality across industries. As the global demand for sustainable materials continues to rise, BC's biodegradable nature aligns perfectly with environmental sustainability goals, reinforcing its potential as a cornerstone material in eco-friendly applications. Exploring new markets and expanding its applications in industries such as textiles, food packaging, and medical products will solidify BC's role as a key player in advancing sustainability and innovation across sectors.

References

Abol-Fotouh, D., Al-Hagar, O. E., & Roig, A. (2024). In situ shaping of intricated 3D bacterial cellulose constructs using sacrificial agarose and diverted oxygen inflow. *Carbohydrate Polymers, 343*, 122495. https://doi.org/10.1016/j.carbpol.2024.122495

Akki, A. J., Jain, P., Kulkarni, R., Kulkarni, R. V., Zameer, F., Anjanapura, V. R., & Aminabhavi, T. M. (2024). Microbial biotechnology alchemy: Transforming bacterial cellulose into sensing disease–A review. *Sensors International, 5*, 100277. https://doi.org/10.1016/j.sintl.2023.100277

Almasi, H., Mehryar, L., & Ghadertaj, A. (2020). Photocatalytic activity and water purification performance of in situ and ex situ synthesized bacterial cellulose–CuO nanohybrids. *Water Environment Research, 92*(9), 1334–1349. https://doi.org/10.1002/wer.1331

Amorim, J. D. P., Junior, C. J. G. S., Costa, A. F. S., Nascimento, H. A., Vinhas, G. M., & Sarrubo, L. A. (2020). Biomask, a polymer blend for treatment and healing of skin prone to acne. *Chemical Engineering Transactions, 79*, 205–210. https://doi.org/10.3303/CET2079035

Balistreri, G. N., Campbell, I. R., Li, X., Amorim, J., Zhang, S., Nance, E., & Roumeli, E. (2024). Bacterial cellulose nanoparticles as a sustainable drug delivery platform for protein-based therapeutics. *RSC Applied Polymers, 2*(2), 172–183. https://doi.org/10.1039/D3LP00184A

Bethke, K., Palantöken, S., Andrei, V., Roß, M., Raghuwanshi, V. S., Kettemann, F., & Rademann, K. (2018). Functionalized cellulose for water purification, antimicrobial applications, and sensors. *Advanced Functional Materials, 28*(23), 1800409. https://doi.org/10.1002/adfm.201800409

Bilal, M., & Iqbal, H. M. (2019). Naturally-derived biopolymers: Potential platforms for enzyme immobilization. *International Journal of Biological Macromolecules, 130*, 462–482. https://doi.org/10.1016/j.ijbiomac.2019.02.152

Buruaga-Ramiro, C., Valenzuela, S. V., Valls, C., Roncero, M. B., Pastor, F. J., Díaz, P., & Martínez, J. (2020). Bacterial cellulose matrices to develop enzymatically active paper. *Cellulose, 27*(6), 3413–3426. https://doi.org/10.1007/s10570-020-03025-9

Cacicedo, M. L., Castro, M. C., Servetas, I., Bosnea, L., Boura, K., Tsafrakidou, P., & Castro, G. R. (2016). Progress in bacterial cellulose matrices for biotechnological applications. *Bioresource Technology, 213*, 172–180. https://doi.org/10.1016/j.biortech.2016.02.071

Cakmak, A. M., Unal, S., Sahin, A., Oktar, F. N., Sengor, M., Ekren, N., & Kalaskar, D. M. (2020). 3D printed polycaprolactone/gelatin/bacterial cellulose/hydroxyapatite composite scaffold for bone tissue engineering. *Polymers, 12*(9), 1962. https://doi.org/10.3390/polym12091962

Cazón, P., Vazquez, M., & Velazquez, G. (2019). Environmentally friendly films combining bacterial cellulose, chitosan, and polyvinyl alcohol: Effect of water activity on barrier, mechanical, and optical properties. *Biomacromolecules, 21*(2), 753–760. https://doi.org/10.1021/acs.biomac.9b01457

Chen, L., Lou, J., Rong, X., Liu, Z., Ding, Q., Li, X., & Han, W. (2023). Super-stretching and high-performance ionic thermoelectric hydrogels based on carboxylated bacterial cellulose coordination for self-powered sensors. *Carbohydrate Polymers, 321*, 121310. https://doi.org/10.1016/j.carbpol.2023.121310

Chen, L., Zou, M., & Hong, F. F. (2015). Evaluation of fungal laccase immobilized on natural nanostructured bacterial cellulose. *Frontiers in Microbiology, 6*, 1245. https://doi.org/10.3389/fmicb.2015.01245

Choi, S. M., Rao, K. M., Zo, S. M., Shin, E. J., & Han, S. S. (2022). Bacterial cellulose and its applications. *Polymers, 14*(6), 1080. https://doi.org/10.3390/polym14061080

de Amorim, J. D. P., de Souza, K. C., Duarte, C. R., da Silva Duarte, I., de Assis Sales Ribeiro, F., Silva, G. S., & Sarubbo, L. A. (2020). Plant and bacterial nanocellulose: Production, properties and applications in medicine, food, cosmetics, electronics and engineering. A review. *Environmental Chemistry Letters, 18*, 851–869. https://doi.org/10.1007/s10311-020-00989-9

Deng, L., Li, F., Han, Z., Qu, X., Li, J., Zhou, Z., & Lv, X. (2024). Bacterial cellulose-based hydrogel with regulated rehydration and enhanced antibacterial activity for wound healing. *International Journal of Biological Macromolecules, 267*, 131291. https://doi.org/10.1016/j.ijbiomac.2024.131291

Dong, W., Su, J., Chen, Y., Xu, D., Cheng, L., Mao, L., & Yuan, F. (2022). Characterization and antioxidant properties of chitosan film incorporated with modified silica nanoparticles as an active food packaging. *Food Chemistry, 373*, 131414. https://doi.org/10.1016/j.foodchem.2021.131414

Estevinho, B. N., Samaniego, N., Talens-Perales, D., Fabra, M. J., López-Rubio, A., Polaina, J., & Marín-Navarro, J. (2018). Development of enzymatically-active bacterial cellulose membranes through stable immobilization of an engineered β-galactosidase. *International Journal of Biological Macromolecules, 115*, 476–482. https://doi.org/10.1016/j.ijbiomac.2018.04.081

Feng, Z., Wang, S., Huang, W., & Bai, W. (2024). A potential bilayer skin substitute based on electrospun silk-elastin-like protein nanofiber membrane covered with bacterial cellulose. *Colloids and Surfaces. B, Biointerfaces, 234*, 113677. https://doi.org/10.1016/j.colsurfb.2023.113677

Fooladi, S., Nematollahi, M. H., Rabiee, N., & Iravani, S. (2023). Bacterial cellulose-based materials: A perspective on cardiovascular tissue engineering applications. *ACS Biomaterials Science & Engineering, 9*(6), 2949–2969. https://doi.org/10.1021/acsbiomaterials.3c00300

Girard, V. D., Chaussé, J., & Vermette, P. (2024). Bacterial cellulose: A comprehensive review. *Journal of Applied Polymer Science, 141*(15), e55163. https://doi.org/10.1002/app.55163

Gomes, N. O., Carrilho, E., Machado, S. A. S., & Sgobbi, L. F. (2020). Bacterial cellulose-based electrochemical sensing platform: A smart material for miniaturized biosensors. *Electrochimica Acta, 349*, 136341. https://doi.org/10.1016/j.electacta.2020.136341

Haghighi, H., Gullo, M., La China, S., Pfeifer, F., Siesler, H. W., Licciardello, F., & Pulvirenti, A. (2021). Characterization of bio-nanocomposite films based on gelatin/polyvinyl alcohol blend reinforced with bacterial cellulose nanowhiskers for food packaging applications. *Food Hydrocolloids, 113*, 106454. https://doi.org/10.1016/j.foodhyd.2020.106454

Ho, B. K., Hyuna, A. C., Seok, P. H., & Khan, W. J. (2015). Biocellulose mask pack sheet containing scrub and preparing method thereof. Korean Patent No: KR20150124643A, 6 November 2015.

Hospodiuk-Karwowski, M., Bokhari, S. M., Chi, K., Moncal, K. K., Ozbolat, V., Ozbolat, I. T., & Catchmark, J. M. (2022). Dual-charge bacterial cellulose as a potential 3D printable mate-

rial for soft tissue engineering. *Composites Part B: Engineering, 231*, 109598. https://doi.org/10.1016/j.compositesb.2021.109598

Hou S., Xia Z., Pan J., Wang N., Gao H., Ren J., and Xia X. (2024) Bacterial cellulose applied in wound dressing materials: Production and functional modification–A review. *Macromol. Biosci. 24*(2): 2300333. https://doi.org/10.1002/mabi.202300333

Hu, Y., Liu, F., Sun, Y., Xu X., Chen, X., Pan, B., Sun, D.,& Qian, J., (2019). Bacterial cellulose derived paperlike purifier with multifunctionality for water decontamination. *Chemical Engineering Journal. 371*, 730–737. https://doi.org/10.1016/j.cej.2019.04.091

Indriyati, D. F., Primadona, I., Srikandace, Y., & Karina, M. (2021). Development of bacterial cellulose/chitosan films: Structural, physicochemical and antimicrobial properties. *Journal of Polymer Research, 28*, 1–8. https://doi.org/10.1007/s10965-020-02328-6

Jabłońska, J., Onyszko, M., Konopacki, M., Augustyniak, A., Rakoczy, R., & Mijowska, E. (2021). Fabrication of paper sheets coatings based on chitosan/bacterial nanocellulose/ZnO with enhanced antibacterial and mechanical properties. *International Journal of Molecular Sciences, 22*(14), 7383. https://doi.org/10.3390/ijms22147383

Jannatamani, H., Motamedzadegan, A., Farsi, M., & Yousefi, H. (2022). Rheological properties of wood/bacterial cellulose and chitin nano-hydrogels as a function of concentration and their nano-films properties. *IET Nanobiotechnology, 16*(4), 158–169. https://doi.org/10.1049/nbt2.12083

Jasim, A., Ullah, M. W., Shi, Z., Lin, X., & Yang, G. (2017). Fabrication of bacterial cellulose/polyaniline/single-walled carbon nanotubes membrane for potential application as biosensor. *Carbohydrate Polymers, 163*, 62–69. https://doi.org/10.1016/j.carbpol.2017.01.056

Ji, L., Zhang, F., Zhu, L., & Jiang, J. (2021). An in-situ fabrication of bamboo bacterial cellulose/sodium alginate nanocomposite hydrogels as carrier materials for controlled protein drug delivery. *International Journal of Biological Macromolecules, 170*, 459–468. https://doi.org/10.1016/j.ijbiomac.2020.12.139

Koreshkov, M., Takatsuna, Y., Bismarck, A., Fritz, I., Reimhult, E., & Zirbs, R. (2024). Sustainable food packaging using modified kombucha-derived bacterial cellulose nanofillers in biodegradable polymers. *RSC Sustainability, 2*(8), 2367–2376. https://doi.org/10.1039/D4SU00168K

Kusuma, A. C., Chou, Y. C., Hsieh, C. C., Santoso, S. P., Go, A. W., Lin, H. T. V., & Lin, S. P. (2024). Agar-altered foaming bacterial cellulose with carvacrol for active food packaging applications. *Food Packaging and Shelf Life, 42*, 101269. https://doi.org/10.1016/j.fpsl.2024.101269

Kumar, M., Pandey, A., Kumar, V., & Saran, S. (2023). Applications of bacterial cellulose in biomedical sector. In V. Kumar, S. Saran, A. Pandey, & C. R. Soccol (Eds.), Bacterial cellulose: Production, scale-up, and applications (pp. 154–168). CRC Press. https://doi.org/10.1201/9781003355434.ch12

Kuswandi, B., Asih, N. P., Pratoko, D. K., Kristiningrum, N., & Moradi, M. (2020). Edible pH sensor based on immobilized red cabbage anthocyanins into bacterial cellulose membrane for intelligent food packaging. *Packaging Technology and Science, 33*(8), 321–332. https://doi.org/10.1002/pts.2507

Li, B., Li, K., & Li, X. (2024). Fabrication of abundantly functionalized dendritic biochar composites as adsorbents for the high-efficiency removal of heavy metal ions and dyes. *Separation and Purification Technology, 337*, 126368. https://doi.org/10.1016/j.seppur.2024.126368

Li, M., Zhang, X. F., Qiu, J., & Yao, J. (2024). Flexible g-C_3N_4@ bacterial cellulose aerogels for integrated indoor air purification. *Colloids and Surfaces A: Physicochemical and Engineering Aspects, 698*, 134567. https://doi.org/10.1016/j.colsurfa.2024.134567

Li, Q., Ma, Q., Wu, Y., Li, Y., Li, B., Luo, X., & Liu, S. (2020). Oleogel films through the Pickering effect of bacterial cellulose nanofibrils featuring interfacial network stabilization. *Journal of Agricultural and Food Chemistry, 68*(34), 9150–9157. https://doi.org/10.1021/acs.jafc.0c03214

Li, X., Lv, P., Yao, Y., Feng, Q., Mensah, A., Li, D., & Wei, Q. (2020). A novel single-enzymatic biofuel cell based on highly flexible conductive bacterial cellulose electrode utilizing pollutants as fuel. *Chemical Engineering Journal, 379*, 122316. https://doi.org/10.1016/j.cej.2019.122316

Li, Y., Chu, C., Chen, C., Sun, B., Wu, J., Wang, S., & Sun, D. (2024). Quaternized chitosan/oxidized bacterial cellulose cryogels with shape recovery for noncompressible hemorrhage and wound healing. *Carbohydrate Polymers, 327*, 121679. https://doi.org/10.1016/j.carbpol.2023.121679

Li, Y., Xun, X., Xu, Y., Zhan, A., Gao, E., Yu, F., & Yang, C. (2022). Hierarchical porous bacterial cellulose scaffolds with natural biomimetic nanofibrous structure and a cartilage tissue-specific microenvironment for cartilage regeneration and repair. *Carbohydrate Polymers, 276*, 118790. https://doi.org/10.1016/j.carbpol.2021.118790

Lima, N. F., Maciel, G. M., Lima, N. P., Fernandes, I. D. A. A., & Haminiuk, C. W. I. (2024). Bacterial cellulose in cosmetic innovation: A review. *International Journal of Biological Macromolecules, 133*, 396. https://doi.org/10.1016/j.ijbiomac.2024.133396

Liu, Z. W., Wang, X. L., Xian, H. J., Zhong, J. H., Ye, X. G., Yang, Y. X., & Huang, C. (2024). Highly efficient malachite green adsorption by bacterial cellulose and bacterial cellulose/locust bean gum composite. *International Journal of Biological Macromolecules, 279*, 134991. https://doi.org/10.1016/j.ijbiomac.2024.134991

Luo, H., Ao, H., Li, G., Li, W., Xiong, G., Zhu, Y., & Wan, Y. (2017). Bacterial cellulose/graphene oxide nanocomposite as a novel drug delivery system. *Current Applied Physics, 17*(2), 249–254. https://doi.org/10.1016/j.cap.2016.12.001

Lv, P., Zhou, H., Mensah, A., Feng, Q., Wang, D., Hu, X., & Wei, Q. (2018). A highly flexible self-powered biosensor for glucose detection by epitaxial deposition of gold nanoparticles on conductive bacterial cellulose. *Chemical Engineering Journal, 351*, 177–188. https://doi.org/10.1016/j.cej.2018.06.098

Manan, S., Ullah, M. W., Ul-Islam, M., Shi, Z., Gauthier, M., & Yang, G. (2022). Bacterial cellulose: Molecular regulation of biosynthesis, supramolecular assembly, and tailored structural and functional properties. *Progress in Materials Science, 129*, 100972. https://doi.org/10.1016/j.pmatsci.2022.100972

Mir, I. S., Riaz, A., Roy, J. S., Fréchette, J., Morency, S., Gomes, O. P., & Messaddeq, Y. (2024). Removal of cadmium and chromium heavy metals from aqueous medium using composite bacterial cellulose membrane. *Chemical Engineering Journal, 490*, 151665. https://doi.org/10.1016/j.cej.2024.151665

Mishra, S., Singh, P. K., Pattnaik, R., Kumar, S., Ojha, S. K., Srichandan, H., & Sarangi, P. K. (2022). Biochemistry, synthesis, and applications of bacterial cellulose: A review. *Frontiers in Bioengineering and Biotechnology, 10*, 780409. https://doi.org/10.3389/fbioe.2022.780409

Narayanan, K. B., Bhaskar, R., Sudhakar, K., Nam, D. H., & Han, S. S. (2023). Polydopamine-functionalized bacterial cellulose as hydrogel scaffolds for skin tissue engineering. *Gels, 9*(8), 656. https://doi.org/10.3390/gels9080656

Nguyen, T. A., Oanh, D. T. Y., Nguyen, M. H., Nguyen, T. H., Nguyen, T. T. P., Le, T. H. N., & Nguyen, Q. T. (2024). Research to develop the ability to remove as (III) ions in water of an environmentally friendly hybrid material based on bacterial cellulose and graphene oxide. *Vietnam Journal of Chemistry, 62*, 600–614. https://doi.org/10.1002/vjch.202300419

Pandey, A., Singh, A., & Singh, M. K. (2024b). Novel low-cost green method for production of bacterial cellulose. *Polymer Bulletin, 81*, 6721–6741. https://doi.org/10.1007/s00289-023-05023-w

Pandey, A., Singh, A., & Singh, M. K. (2024c). Green synthesis and optimization of bacterial cellulose production from food industry by-products by response surface methodology. *Polymer Bulletin, 81*, 16965–16998. https://doi.org/10.1007/s00289-024-05492-7

Pandey, A., Singh, M. K., & Singh, A. (2024a). Bacterial cellulose: A smart biomaterial for biomedical applications. *Journal of Materials Research, 39*(1), 2–18. https://doi.org/10.1557/s43578-023-01116-4

Pandey, A., Singh, M. K., & Singh, A. (2024d). Low-cost bacterial cellulose production from agricultural waste for antibacterial applications. *Journal of Bioactive and Compatible Polymers, 40*(1), 08839115241293464. https://doi.org/10.1177/08839115241293464

Pang, M., Huang, Y., Meng, F., Zhuang, Y., Liu, H., Du, M., & Cai, Y. (2020). Application of bacterial cellulose in skin and bone tissue engineering. *European Polymer Journal, 122*, 109365. https://doi.org/10.1016/j.eurpolymj.2019.109365

Picheth, G. F., Pirich, C. L., Sierakowski, M. R., Woehl, M. A., Sakakibara, C. N., de Souza, C. F., & de Freitas, R. A. (2017). Bacterial cellulose in biomedical applications: A review. *International Journal of Biological Macromolecules, 104*, 97–106. https://doi.org/10.1016/j.ijbiomac.2017.05.171

Quijano, L., Rodrigues, R., Fischer, D., Tovar-Castro, J. D., Payne, A., Navone, L., & Barro, E. (2024). Bacterial cellulose cookbook: A systematic review on sustainable and cost-effective substrates. *Journal of Bioresources and Bioproducts, 9*, 379–409. https://doi.org/10.1016/j.jobab.2024.05.003

Rebelo, A. R., Liu, C., Schäfer, K. H., Saumer, M., Yang, G., & Liu, Y. (2019). Poly (4-vinylaniline)/polyaniline bilayer-functionalized bacterial cellulose for flexible electrochemical biosensors. *Langmuir, 35*(32), 10354–10366. https://doi.org/10.1021/acs.langmuir.9b01425

Rodrigues, D. M., da Silva, M. F., Almeida, F. L. C., de Mélo, A. H. F., Forte, M. B. S., Martín, C., & Goldbeck, R. (2024). A green approach to biomass residue valorization: Bacterial nanocellulose production from agro-industrial waste. *Biocatalysis and Agricultural Biotechnology, 56*, 103036. https://doi.org/10.1016/j.bcab.2024.103036

Serra, D. O., & Hengge, R. (2019). Cellulose in bacterial biofilms. In E. Cohen & H. Merzendorfer (Eds.), *Extracellular sugar-based biopolymers matrices* (Biologically-inspired systems) (Vol. 12, pp. 355–392). Springer. https://doi.org/10.1007/978-3-030-12919-4_8

Sharma, P., Mittal, M., Yadav, A., & Aggarwal, N. K. (2023). Bacterial cellulose: Nano-biomaterial for biodegradable face masks–a greener approach towards environment. *Environmental Nanotechnology, Monitoring & Management, 19*, 100759. https://doi.org/10.1016/j.enmm.2022.100759

Singh, A., Pandey, A., & Singh, M. K., (2024) , Bacterial cellulose: *A smart biomaterial for biomedical applications, 39*, 2–18. https://doi.org/10.1557/s43578-023-01116-4

Stumpf, T. R., Yang, X., Zhang, J., et al. (2018). In situ and ex situ modifications of bacterial cellulose for applications in tissue engineering. *Materials Science and Engineering: C, 82*, 372–383. https://doi.org/10.1016/j.msec.2016.11.121

Sun, B., Zhao, J., Wang, T., Li, Y., Yang, X., Tan, F., & Sun, D. (2023). Highly efficient construction of sustainable bacterial cellulose aerogels with boosting PM filter efficiency by tuning functional groups. *Carbohydrate Polymers, 309*, 120664. https://doi.org/10.1016/j.carbpol.2023.120664

Ullah, M. W., Manan, S., Kiprono, S. J., Ul-Islam, M., & Yang, G. (2019). Synthesis, structure, and properties of bacterial cellulose. In J. Huang, A. Dufresne, & N. Lin (Eds.), *Nanocellulose: From fundamentals to advanced materials* (pp. 81–113). Wiley. https://doi.org/10.1002/9783527807437.ch4

Urbina, L., Corcuera, M.A., Gabilondo, N., Eceiza, A., Retegi, A., (2021) A review of bacterial cellulose: sustainable production from agricultural waste and applications in various fields *Cellulose, 28* 8229–8253. https://doi.org/10.1007/s10570-021-04020-4

Vasconcelos, N. F., Andrade, F. K., Vieira, L. A. P., et al. (2020). Oxidized bacterial cellulose membrane as support for enzyme immobilization: Properties and morphological features. *Cellulose, 27*, 3055–3083. https://doi.org/10.1007/s10570-020-02966-5

Wang, J., Li, C., & Tang, Y. (2024). Constructing bacterial cellulose and its composites: Regulating treatments towards applications. *Cellulose, 31*, 7793–7817. https://doi.org/10.1007/s10570-024-06037-x

Wang, J., Tavakoli, J., & Tang, Y. (2019). Bacterial cellulose production, properties, and applications with different culture methods—A review. *Carbohydrate Polymers, 219*, 63–76. https://doi.org/10.1016/j.carbpol.2019.05.008

Wang, Z., Yang, Y., Zhang, X. F., & Yao, J. (2022). Immobilization of manganese dioxide into bacterial cellulose for efficient air cleaning. *Materials Today Communications, 33*, 104729. https://doi.org/10.1016/j.mtcomm.2022.104729

Wu, A., Hu, X., Ao, H., Chen, Z., Chu, Z., Jiang, T., & Wan, Y. (2022). Rational design of bacterial cellulose-based air filter with antibacterial activity for highly efficient particulate matter removal. *Nano Select, 3*(1), 201–211. https://doi.org/10.1002/nano.202100086

Xi, J., Lou, Y., Chu, Y., Meng, L., Wei, H., Dai, H., & Wu, W. (2023). High-flux bacterial cellulose ultrafiltration membrane with controllable pore structure. *Colloids and Surfaces A: Physicochemical and Engineering Aspects, 656*, 130428. https://doi.org/10.1016/j.colsurfa.2022.130428

Yang, S., Ding, Q., Li, Y., & Han, W. (2024). Bacterial cellulose/gelatin-based pH-responsive functional film for food freshness monitoring. *International Journal of Biological Macromolecules, 259*, 129203. https://doi.org/10.1016/j.ijbiomac.2024.129203

Ye, J., Li, J., Wang, X., Wang, Q., Wang, S., Wang, H., & Xu, J. (2024). Preparation of bacterial cellulose-based antibacterial membranes with prolonged release of drugs: Emphasis on the chemical structure of drugs. *Carbohydrate Polymers, 323*, 121379. https://doi.org/10.1016/j.carbpol.2023.121379

Zeng, A., Yang, R., Tong, Y., & Zhao, W. (2023). Functional bacterial cellulose nanofibrils with silver nanoparticles and its antibacterial application. *International Journal of Biological Macromolecules, 235*, 123739. https://doi.org/10.1016/j.ijbiomac.2023.123739

Zhang, D., Zhang, S., Liang, Q., Guan, M., Zhang, T., Chen, S., & Wang, H. (2024). A tent-inspired portable solar-driven water purification device for wilderness explorers. *Small, 20*, 2311731. https://doi.org/10.1002/smll.202311731

Zhang, X., Zheng, X., Xu, T., Li, G., Mei, J., Li, Z., & Ge, X. (2024). Construction of imprinted bacterial cellulose composite membranes for selective adsorption of cesium from low-concentration radioactive wastewater. *ACS Applied Nano Materials, 7*(16), 19233–19243. https://doi.org/10.1021/acsanm.4c03118

Zhu, M., Deng, Y., Zheng, Y., Hu, X., Xu, W., Xiong, R., & Huang, C. (2024). Tribo-charge enhanced and cellulose-based biodegradable nanofibrous membranes with highly fluffy structure for air filtration and self-powered respiration monitoring systems. *Journal of Hazardous Materials, 468*, 133770. https://doi.org/10.1016/j.jhazmat.2024.133770

Chapter 11
Nanopaper

Xuezhu Xu

11.1 Introduction

Nanopaper is a thin sheet mainly made of tightly packed nanostructures (such as nanocellulose, nanochitin, nanochitosan, nanographene, etc.) and possesses superior physicochemical properties compared to conventional paper. Nanopapers made out of the aforementioned nanomaterials are structured nanomaterial assemblies that can bridge the gap between the nanoscale properties of such nanomaterials and their macroscopic engineering applications. Figure 11.1 shows the fabrication timeline of the different types of nanopapers. Conventional paper production goes back more than 2000 years, while nanopapers are almost new products made in the last three decades that are increasingly being developed and used in various engineering applications. This chapter focuses on a brief introduction of different types of nanopapers, their fabrication/manufacturing methods, and properties.

X. Xu (✉)
Guangdong Provincial Key Laboratory of Optical Information Materials and Technology and Institute of Electronic Paper Displays, South China Academy of Advanced Optoelectronics, South China Normal University, Guangzhou, China

National Center for International Research on Green Optoelectronics, South China Normal University, Guangzhou, China

Chongzuo Key Laboratory of Comprehensive Utilization Technology of Manganese Resources, Guangxi Key Laboratory for High-value Utilization of Manganese Resources, College of Chemistry and Biological Engineering, Guangxi Minzu Normal University, Chongzuo, Guangxi, China

Chongzuo Key Laboratory of High-value Utilization of Sugarcane Resources, Chongzuo, China

COFCO Corporation Chongzuo Sugar Co., Ltd., Chongzuo, China
e-mail: xxzxu@m.scnu.edu.cn

G. Korotcenkov (ed.), *The Handbook of Paper-Based Sensors and Devices*,
https://doi.org/10.1007/978-3-031-91080-7_11

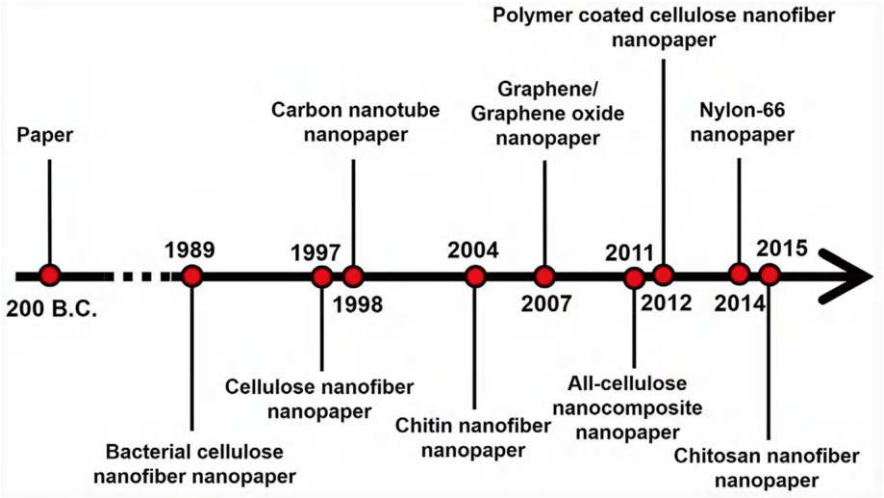

Fig. 11.1 The fabrication timeline of different types of nanopapers. Reprinted with permission from Naghdi et al. (2020). Copyright 2020: Elsevier

Figure 11.2a demonstrates different types of nanopapers based on their origin and raw materials. We classified nanopapers to three types including fully bio-nanopapers, bio/non-bionanocomposite nanopapers, and fully non-bio-nanopapers. It is important to mention that although hearing the name of "nanopaper," nanocellulose-based nanopaper will probably come to mind, and also a short literature review indicates that the majority of reports with "nanopaper" title refer to their (nano)cellulose-based type; however, there are other types of nanopapers with high potential applications especially in (bio)sensing technology. Therefore, this chapter refers to nanopapers made of different raw materials including nanocellulose, nanochitin, nanographene, etc., and their uses with extraordinary properties.

11.2 Fully Bio-Nanopaper

The term "comprehensive bio-nanopapers" refers to papers predominantly composed of cellulose nanofibers (CNF), chitin nanofibers (ChNF), and chitosan nanofibers (ChitoNF). These materials may also be known by other designations, such as cellulose whiskers, which can be referred to as cellulose crystals depending on their length. "Cellulose nanocrystals" is an alternative term for nano-crystalline cellulose particles (Xu et al., 2014). The term "nanofibrils" is used to describe fibers of greater length (Saito et al., 2007). Figure 11.2b illustrates the various production techniques for these bio-derived nanostructures. These nanomaterials are broadly categorized into three morphological types: nanospherical, nanocrystals, and nanofibers, differentiated primarily by their crystallinity and aspect ratio. Nanospherical and

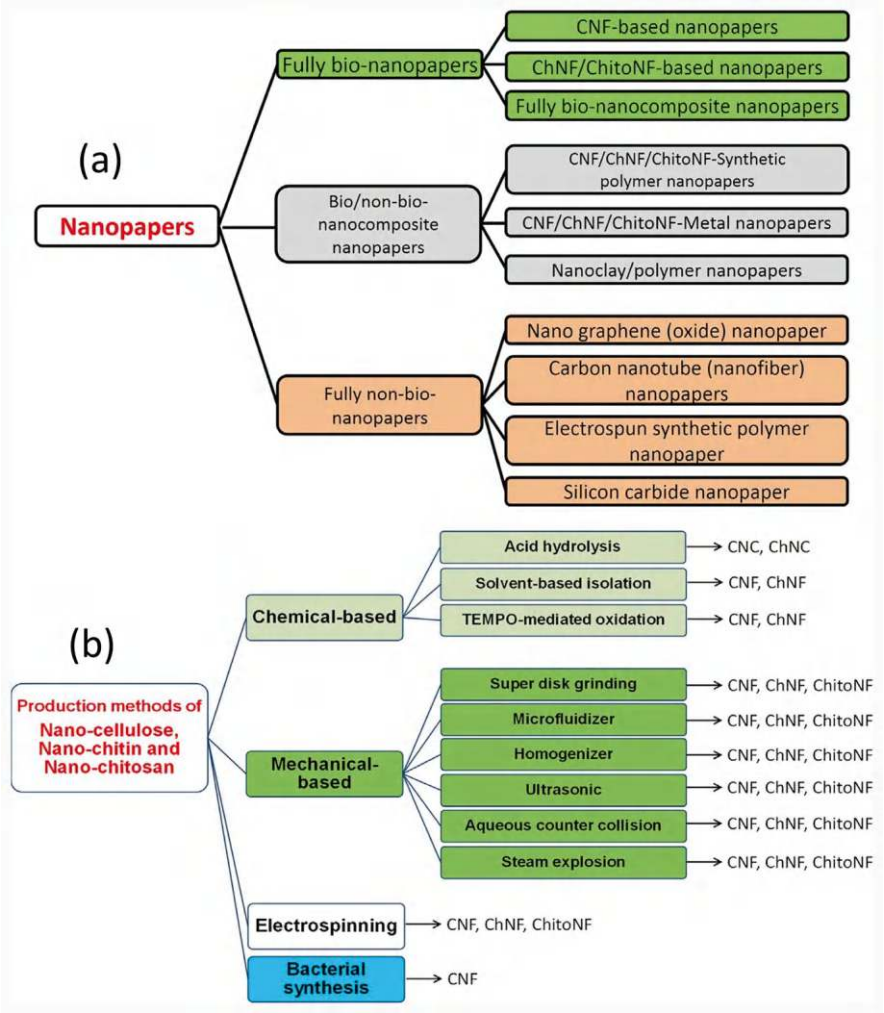

Fig. 11.2 (**a**) Different types of nanopapers (CNF, cellulose nanofiber; ChNF, chitin nanofiber; ChitoNF, chitosan nanofiber). (**b**) Different production methods of cellulose nanofiber (CNF), chitin nanofiber (ChNF), and chitosan nanofiber (ChitoNF) as raw materials to make nanopapers. Reprinted with permission from Naghdi et al. (2020). Copyright 2020: Elsevier

nanocrystals exhibit higher crystallinity compared to nanofibers (NFs), while NFs possess a more substantial aspect ratio than the other two forms. The creation of papers solely from nanospherical and nanocrystals is challenging due to their minimal aspect ratio; hence, the focus here is on papers made from bio-based NFs. Figure 11.3 outlines the key desirable attributes of comprehensive bio-nanopapers, which position them as strong contenders for future high-tech applications, such as in the field of sensors.

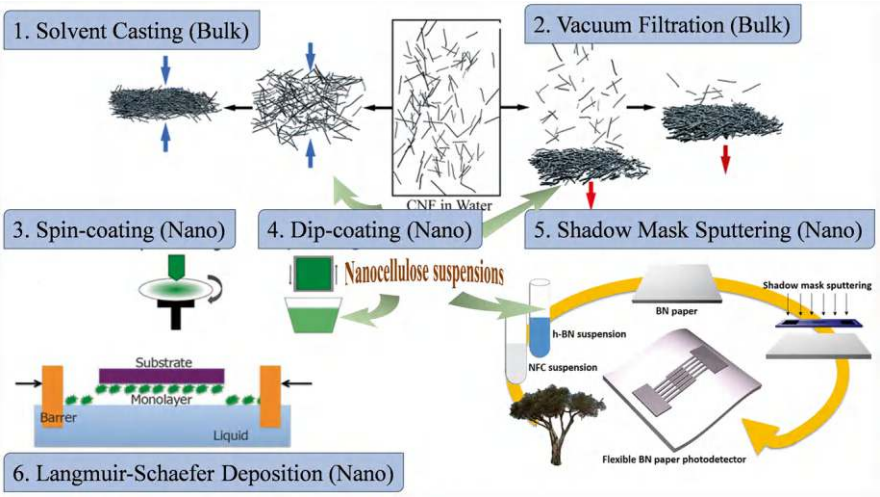

Fig. 11.3 Making nanopapers from materials by different techniques. Reprinted with permission from Shen et al. (2023). Copyright 2023: Wiley

Over the past 20 years, environmental concerns have gained prominence. Data indicates that the annual release of over 100 million tons of non-biodegradable synthetic plastics into the environment has had significant detrimental effects. In response, researchers are developing products designed to reintegrate into the natural ecosystem post-consumption, leveraging their technical characteristics. The incorporation of sustainable nano-biomaterials like CNF, ChNF, and ChitoNF into products such as nanopapers can mitigate environmental pollution due to their biodegradable properties. The exceptional properties of bio-nanopapers, including high mechanical strength, minimal porosity, smooth surfaces, excellent integrity, robust barrier capabilities, low thermal expansion coefficients, high transparency, reactive surfaces, and the abundance of raw materials, have piqued the interest of the research community. These bio-based nanomaterials encapsulate the beneficial traits of their raw materials, offering advantages from a technical, economic, and environmental perspective. The convergence of these remarkable features in bio-based nanomaterials has significantly spurred researchers across various domains to explore their wide-ranging applicability.

11.2.1 Cellulose-Based Nanopaper

Cellulose stands as the most plentiful biopolymer on Earth, derived from a variety of sources including wood, agricultural byproducts, bacteria, and animals. This versatile biopolymer can be processed into nanocellulose through various chemical and mechanical techniques. The resulting nanocellulose serves as a fundamental

material for the creation of nanopapers. Some types of nanocelluloses have impressively high intrinsic tensile strength of 1.6–6.4 GPa (Saito et al., 2013) and modulus up to 78–114 GPa (Guhados et al., 2005; Hsieh et al., 2008; Sehaqui et al., 2012; Tanpichai et al., 2012); their tensile properties are among the closest to carbon nanotubes, whose respective tensile strength and Young's modulus are estimated to be ~300 GPa and ~270–950 TPa (Wong et al., 1997; Yu et al., 2000).

11.2.1.1 Lignocellulose Nanofiber Nanopaper

The cellulose fibers within lignocellulose materials can be reduced to nanoscale structures, manifesting in three distinct morphologies: nanospherical, nanocrystals, and nanofibers, with nanofibers being particularly suitable for nanopaper formation. There are at least three types of wood-derived nanofibers suitable for nanopaper production. Wood is a composite of several primary components, such as cellulose, hemicellulose, lignin, extractives, and minerals. Wood nanofibers are isolated from raw wood through pure mechanical processes, devoid of chemical intervention, thus retaining a chemical composition akin to that of the original wood, justifying the term "wood cellulose nanofibrils (wood CNFs)" for these materials.

Lignocellulose nanofibers (LCNFs) are derived from unbleached wood pulps. The production of these nanostructures involves the use of chemicals like sodium hydroxide in the pulping process, which removes wood minerals, extractives, and portions of hemicellulose and lignin, leaving behind cellulose fibers interspersed with lignin/hemicellulose, resulting in the characteristic brown unbleached pulp (Naghdi et al., 2020). This pulp is then transformed into LCNFs primarily through mechanical methods, including super disk grinding, homogenization, and microfluidization.

CNFs by chemical oxidation to improve dispersibility also exists, such as TEMPO-oxidized cellulose nanofibers (TEMPO-CNFs) are a specialized type of cellulose nanofibers that have been chemically modified using a process known as TEMPO (2,2,6,6-tetramethylpiperidine-1-oxyl) oxidation. This process introduces a high density of carboxyl groups onto the surface of the cellulose nanofibers, which significantly alters their properties and makes them suitable for a variety of applications. Wood CNFs, LCNFs, and TEMPO-CNFs are subsequently fashioned into nanopapers using microparticle techniques such as vacuum filtration, casting, spraying, spin coating, and layer-by-layer assembly, resulting in films entirely composed of nanofibers without the need for chemical additives or adhesives. Figure 11.4 displays digital photos and SEM micrographs of LCNF and CNF nanopapers, both of which are translucent. The LCNF nanopaper exhibits a brown hue due to the presence of lignin, in contrast to the somewhat white appearance of the CNF nanopaper. The LCNF nanopaper comprises cellulose nanofibers intermingled with lignin and hemicellulose, whereas the CNF nanopaper consists of highly pure NFs, as evident in their corresponding SEM micrographs.

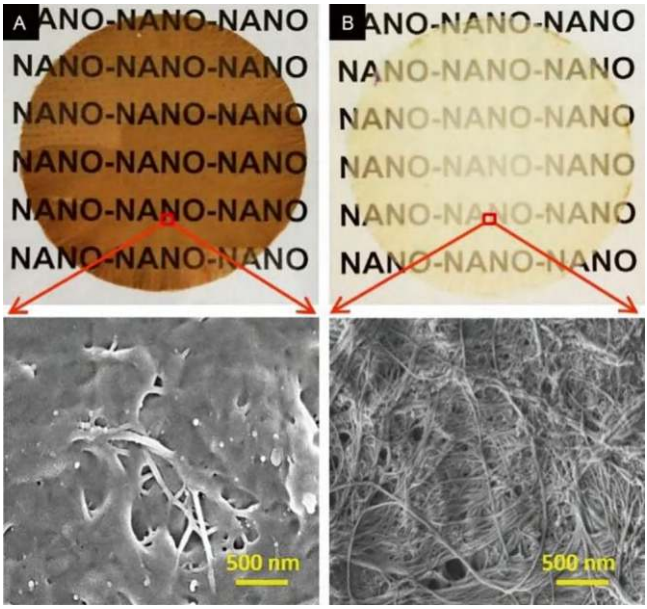

Fig. 11.4 The digital pictures (top) and SEM micrographs (bottom) of (**a**) LCNF (lignocellulose nanofibers) and (**b**) CNF (cellulose nanofibrils) nanopapers. Reprinted with permission from Naghdi et al. (2020). Copyright 2020: Elsevier

11.2.1.2 Bacterial Cellulose Nanofiber Nanopaper

Besides wood, nanocellulose also exists in other sources, where bacterial cellulose nanofibers (BCNF) are synthesized by certain bacterial species, notably *Acetobacter xylinum*, as they construct glucose and cellulose chains in an aqueous culture medium over approximately 2 weeks. The bacterial production of BCNF is considered an ecofriendly method due to its minimal environmental impact. Figures 11.5a–c show digital photos of the wet BCNF pellicle, its nanopaper, and the FE-SEM micrograph, respectively. Bacteria naturally produce BCNF in the form of a wet sheet with nanofibers of 30–60 nm in diameter and impurities from the cultivation media. After purification, a semi-transparent wet sheet is obtained, capable of absorbing water up to 99 times its dry weight, classifying it as a superabsorbent material. To fabricate BCNF nanopaper, the wet BCNF sheet is dried (Fig. 11.5b). Compared to wood CNF (WCNF), BCNF boasts superior mechanical strength, water absorption capacity, transparency, purity, thermal stability, and a higher degree of crystallinity (exceeding 80%). It also lacks lignin and hemicellulose in its primary material, resulting in the absence of carbonyl and carboxyl groups in its structure. Additionally, BCNF features a higher length-to-diameter ratio, a network structure, and a degree of polymerization ranging from 3000 to 9000. The enhanced properties of BCNF significantly influence the functional attributes of their nanopaper. For instance, its tensile properties and thermal stability are up to 114 MPa and

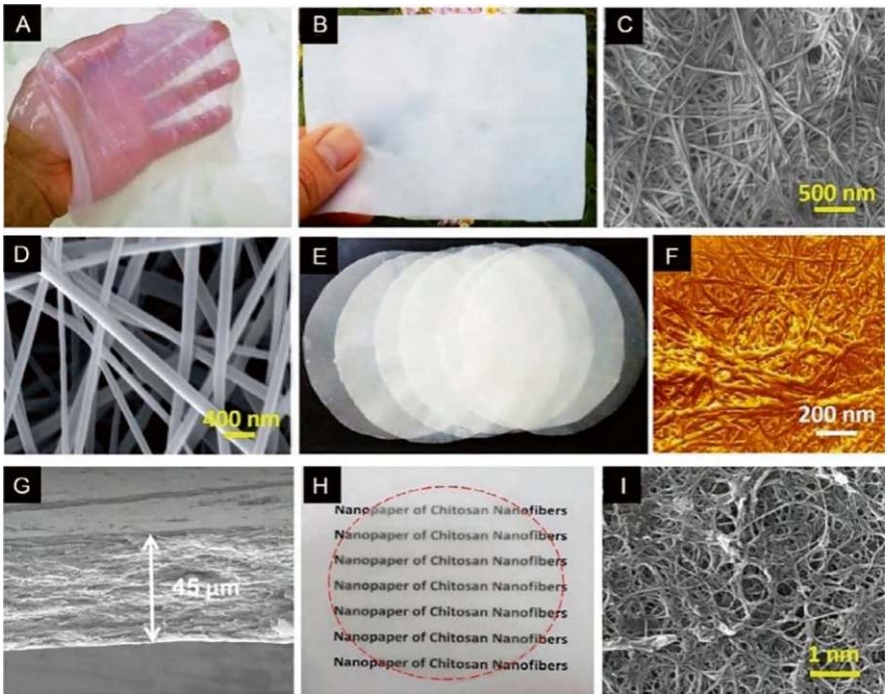

Fig. 11.5 The digital pictures of (**a**) wet BCNF (bacterial cellulose nanofibers) pellicle and (**b**) dried BCNF nanopaper. (**c**) FE-SEM images of BCNF nanopaper. (**d**) SEM image of electrospun cellulose acetate-based nanopaper. (**e**) The digital picture, (**f**) AFM micrograph, and (**g**) FE-SEM image (cross section view) of ChNF paper. (**h**) The digital picture of ChitoNF nanopapers and (**i**) the corresponding FE-SEM. (**a–c**, and **e–i**) reprinted with permission from public domain. Copyright 2024: Products page: https://nanonovin.com/new/n1/scr/products.php, Nano Novin Polymer Co. Sari, Iran. (**d**) reprinted with permission from Ahne et al. (2019). Copyright 2019: SAGE journals

270 °C for WCNF nanopaper, and 185 MPa and 320 °C for BCNF nanopaper, respectively.

11.2.1.3 Electrospun Cellulose Nanofiber Nanopaper

Electrospinning is a technique that transforms a polymer solution into fibers with diameters ranging from the nanoscale to the microscale. Electrospinning method produces a nonwoven nanopaper made from ESCNF. Unlike cellulose nanofibers derived from wood or bacteria, which are typically cellulose type I, ESCNFs are primarily composed of cellulose type II and amorphous cellulose. This is because the production of ESCNF involves dissolving cellulose in a suitable solvent and then electrospinning it into nanofibers, a process that alters the cellulose structure. Generally, converting cellulose derivatives like cellulose acetate into electrospun

fibers is more straightforward than pure cellulose due to the latter's poor solubility. Post-electrospinning, a porous non-woven cellulose (or cellulose derivatives) nanofiber nanopaper, is created (as shown in Fig. 11.5d), which can be compacted to achieve a high-density nanopaper.

11.2.2 Chitin/Chitosan Nanopaper

Chitin is a white, rigid, inelastic, nitrogenous polysaccharide, ranking as the second most abundant biopolymer on Earth after cellulose. It is found in the exoskeletons of crustaceans such as crabs and prawns, insects, and even in the cell walls of fungi. Chitosan is obtained by deacetylating chitin. Both chitin and chitosan can be disintergrated into nanofibers through various methods, as illustrated in Fig. 11.6. Nanofibers derived from chitin (ChNF) and chitosan (ChitoNF) can be further transformed into ChNF and ChitoNF nanopapers, as depicted in Fig. 11.5e–i. It presents all-chitin nanocomposite nanopaper (AChNC-nanopaper). Similar to ACNC-nanopaper, AChNC-nanopaper shares a comparable structure and

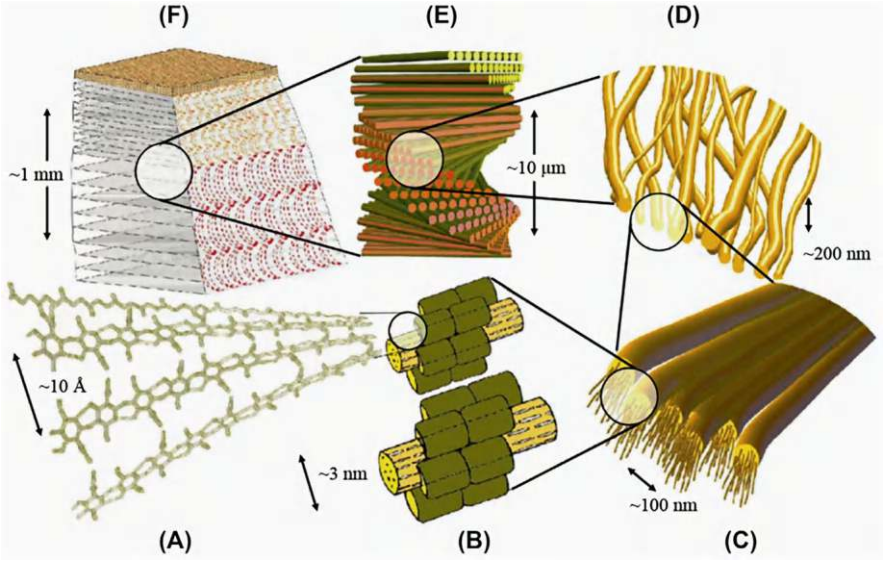

Fig. 11.6 Structural elements of the exoskeleton material (exocuticle, endocuticle) of the lobster *Homarus americanus*. The assembled polysaccharide chains of chitin hierarchy organization comprise six structural levels of chitin in crustaceans: (**a**) assembly of the chitin chains to form a-crystals; (**b**) nanofibers (clear cylinders) surrounded by proteins (dark); (**c**) settlement of nanofibrils in microfibers of chitin and protein; (**d**) lamina of a net fibers of chitin and proteins, a calcite crystallizes in the openings; (**e**) arrangement of laminas with a rotating orientation visible under the optical microscope; (**f**) structure of the cuticle (exo and endo) whose plane section shows the typical arched pattern as a consequence of the grades of rotation of the laminate biological nanocomposite tissue. Reprinted with permission from Raabe et al. (2005). Copyright 2005: Elsevier

properties. Both ACNC- and AChNC-nanopapers are highly tough and transparent, offering a broad spectrum of applications. Similar to CNF nanopaper, these nanopapers are translucent sheets. However, the mechanical properties of ChitoNF nanopaper are generally inferior to those of CNF and ChNF nanopapers, mainly due to the lower degree of polymerization and aspect ratio of ChitoNF.

In nature, crustaceans like crabs and lobsters have a very strong exoskeleton that is a hard, strong, and tough nanostructured composite based on chitin nanofibers as the major load-bearing component. During biosynthesis, chitin nanofibers are bound together by protein to form a network template for mineral deposition. Chitin is a white, hard, inelastic, nitrogenous polysaccharide found in the exoskeleton, as well as in the internal structure of invertebrates. Chitin is the second most abundant biopolymer after cellulose. Although chitin is produced in nature at a rate of 10^{10}–10^{11} tons/year, most chitin is thrown away as commercial waste. This is obviously due to the low workability of this biopolymer, since commercially available chitin powder is not soluble in any solvent but precipitates immediately. Because of its linear structure, chitin has high crystallinity and is arranged as nanofibers. Chitin is a biological component characterized by high affinity to metal ions, proteins, and polysaccharides, and possesses biological activities and high stiffness. The potential of chitin materials is in various applications, such as wound healing, antimicrobial, tissue engineering, cosmetics, food, fertilizer, anti-tumor and drug delivery, pulp, and paper.

The nanofibers are basically embedded in a protein matrix in exoskeleton of arthropods, as well as in the cell wall of mushrooms, fungi, and molds. Chitin nanofibers are present in layers twisted in a helicoid manner. The nanofibers have fine nanofiber networks with a uniform width of approximately 10 nm. Chitin nanofibers are also longer, more flexible and less degraded than the highly crystalline chitin whiskers. The method used for isolating chitin nanofibers is also successfully applied to the cell walls of mushrooms. Commercial chitin powders are also easily converted into nanofibers by mechanical treatment, since these powders consist of nanofiber aggregates. Grinders and high-pressure water-jet systems are effective for disintegrating chitin into nanofibers. Acidic conditions are the key factors to facilitate mechanical fibrillation. Surface modification is an effective way to change the surface property and to endow nanofiber surface with other properties. Several modifications to the chitin nanofiber surface are achieved, including acetylation, deacetylation, phthaloylation, naphthaloylation, maleylation, chlorination, TEMPO (2,2,6,6-tetramethylpiperidine-1-oxyl)-mediated oxidation, and grafting polymerization.

Chitin nanofibers possess high mechanical potential and are comparable to many non-renewable fossil-based materials, such as Kevlar, glass, aramid, or asbestos fibers because of the favorable crystal structure in terms of extended polymer chain conformation. Young's modulus of α-chitin crystals has been reported to be 150 GPa, similar to the value for cellulose crystals (134 GPa). With reference to cellulose materials, chitin in the form of nanowhiskers or dissolved chitin will often have lower mechanical potential as compared to long chitin nanofibers, especially in network-structured materials and polymer matrix composites. These chitin nanofibers are versatile building blocks for preparing nanopapers (Huang, 2017a).

Like cellulose, chitin naturally occurs as supramolecular crystalline nanofibers (3–5 nm) (Fig. 11.7), which are further held by strong hydrogen bonds to form fiber bundles of larger scales; this underlies the insolubility and recalcitrance of chitin. Accordingly, the production of transparent chitin nanopapers basically adopts fabrication techniques and solvent systems similar to those used for cellulose nanofibrils. For example, Nawawi et al. (2019) reported an chitin nanofibers with large shares of retained glucans (50–65%) with mild mechanical agitation and no acidic extraction step from mushrooms. The subsequent chitin nanopapers exhibited exceptionally high tensile strengths of >200 MPa and moduli of 7 GPa, which were

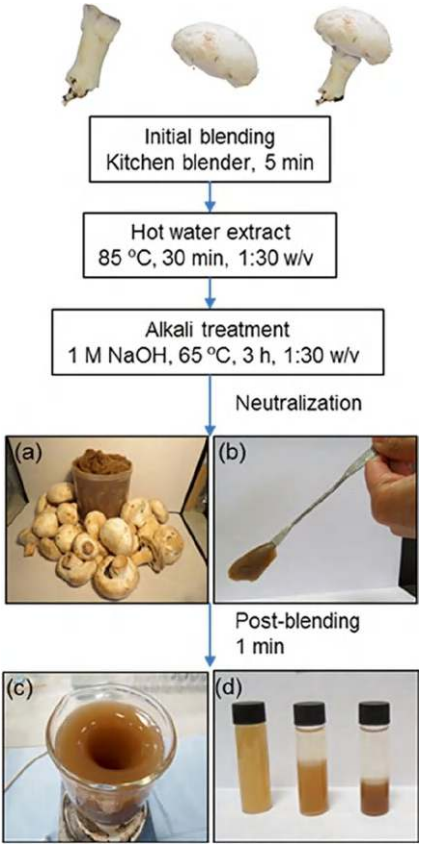

Fig. 11.7 (**a**) Schematic diagram and (**b**) visual representation of nanofiber extraction from common cultivated *Agaricus bisporus*: (a) extract from 3 kg whole mushroom containing approximately 42 g nanofibers, (b) consistency of 3% w/v extract obtained after chemical extraction, (c) 0.8% w/v whole mushroom suspension dispersed by 1 min post blending; this never dried suspension was used for nanopapers. (d) Stability test of 0.8% w/v whole mushroom chitin suspension after 7 d: left = never dried suspension; middle = resuspension of freeze-dried sample (fast freezing using liquid nitrogen); right = resuspension of freeze-dried sample (slow freezing using common freezer). Reprinted with permission from Nawawi et al. (2019). Copyright 2019: ACS

largely attributed to the preserved glucans in the mixture, imparting a composite nature to the nanopapers. Such a chitin source is notably different from the conventional crab process with crustacean chitin sources that do not incorporate glucans and where an acidic extraction step for the removal of minerals must always be included.

11.2.3 Fully Bionanocomposite Nanopaper

These nanopapers are predominantly composed of bio-based nanofibers as the primary component, embedded within a bio-based polymer matrix as a secondary component. A variety of fully bionanocomposite nanopapers can be crafted by combining different types of bio-based nanofibers with a diverse range of biopolymer matrices.

11.2.3.1 All-Cellulose/Chitin Nanocomposite Nanopaper

All-cellulose nanocomposite (ACNC) is a self-reinforced nanopaper composed of amorphous cellulose as the matrix and undissolved nanofibril cores as reinforcements. This structure was built as it benefits from the high Young's moduli of additive and high strain of matrix. Its fabrication involves two main solvent processes: solvent cementing and solvent nanowelding. In solvent cementing, cellulose is dissolved in a solvent to create a solution that impregnates cellulose nanofibers (CNFs). After rinsing, the CNFs are cemented with amorphous cellulose and hot-pressed to form ACNC-nanopaper. The solvent nanowelding process bonds two cellulose parts using a solvent without additives, creating a cohesive joint through partial dissolution and resolidification of cellulose surfaces.

11.2.3.2 CNF/ChNF/ChitoNF-Biopolymer Nanocomposite Nanopaper

The primary constituent of these nanocomposite nanopapers is bio-nanomaterials such as cellulose nanofibers (CNF), chitin nanofibers (ChNF), and chitosan nanofibers (ChitoNF), which serve as the reinforcement phase. These are complemented by a secondary phase consisting of various biopolymers, including gelatin, collagen, carboxymethyl cellulose, and diverse protein types, which act as the matrix. Figure 11.8b, c shows the SEM micrographs of such nanocomposites, showing nanopapers fabricated from chitin nanofibers at 85% weight concentration combined with 15% each of thermoplastic starch and gelatin. These nanocomposites are entirely derived from biological sources and are fully biodegradable, highlighting improved properties over traditional pure nanopapers.

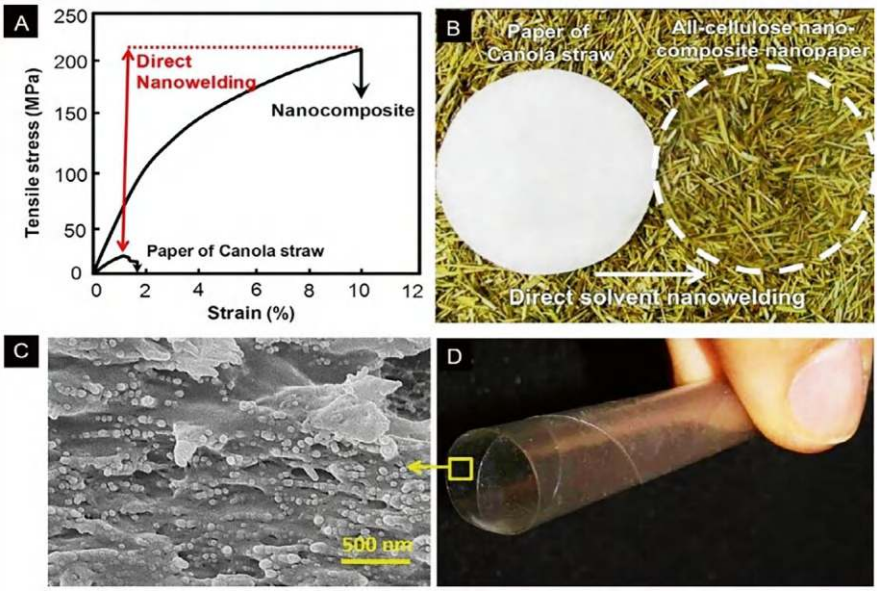

Fig. 11.8 (**a**) The tensile stress-strain curve of ACNC nanopaper made through solvent nanowelding process. (**b**) ACNC nanopaper compared to paper. (**c**) FE-SEM micrograph of welded cellulose nanofibrils in ACNC at nanoscale. (**d**) Pictures of the ACNC nanopaper demonstrating its nature highly-flexible and tough. Reprinted with permission from Yousefi et al. (2011). Copyright 2011: ACS publications

11.3 Bio/Non-bionanocomposite Nanopaper

Similar to fully bio-based nanocomposites, bio/non-bionanocomposite nanopapers are predominantly composed of nanomaterials, addressing challenges related to the dispersion and distribution of these nanomaterials within the composite. Many nanocomposite materials struggle to fully utilize the potential of nanomaterials due to inadequate dispersion, leading to suboptimal stress transfer and product quality. In contrast, nanocomposite nanopapers feature a highly integrated network of nanomaterials, eliminating issues related to distribution and stress transfer.The combination of CNF, ChNF, and ChitoNF as the main components with various synthetic polymers as the minor components results in the creation of nanocomposite nanopapers. For instance, a nanocomposite nanopaper encapsulated with epoxy polymer and composed of wood cellulose nanofibers (WCNF), bacterial cellulose (BC), and chitin nanofibers (ChNF) can be produced through analogous methods. The mechanical properties and transparency of these nanocomposite nanopapers have seen significant enhancements compared to those of unadulterated nanopapers.

11.3.1 CNF/ChNF/ChitoNF-Metal Nanopaper

CNF, ChNF, and ChitoNF combined with different micro- or nano-minerals/metals like nanoclay and nanosilver make a special type of nanocomposite nanopapers. These possess specialized properties that make them suitable for various applications, including use in sensors.

11.3.2 Nanoclay-Polymer Nanopaper

Nanoclays are two-dimensional, layered silicate minerals with layers that are 1-nanometer thick and possess exceptionally high mechanical properties. Nanoclay-based nanocomposite nanopapers can be fabricated using layer-by-layer assembly techniques, which allow for more precise control over thickness at the nanoscale and provide researchers with the ability to fine-tune their properties.

11.4 Fully Non-bio-Nanopaper

The realm of nanomaterials for fabricating nanopapers extends beyond natural nanofibers like cellulose. Various one-dimensional (1D) and two-dimensional (2D) nanomaterials, including carbon nanotubes, carbon nanofibers, graphene (oxide), and nanoclays, can be utilized to create nanopapers. These materials, characterized by their electrical properties, high aspect ratios, form robust entanglement networks, leading to the formation of functional structures.

11.4.1 Clay Nanopaper

Clay nanopapers are composed of nanoscale clay platelets that form a highly ordered, multilayered structure, resulting in thin, flexible, and lightweight materials. Besides, clay features high electrical insulation, thermal stability, and barrier capabilities; therefore, it plays a critical role in electronics when we need stable insulator. Researchers can adjust the arrangement and orientation of these platelets to customize the properties of clay nanopapers for specific uses. The production of clay nanopapers involves the careful assembly of nanoscale clay platelets. Techniques such as exfoliation and reassembly, which disperse clay platelets in a solvent before forming a thin film through controlled evaporation or filtration, are commonly employed. Layer-by-layer assembly leverages electrostatic interactions to create multilayered structures by depositing alternating layers of clay platelets

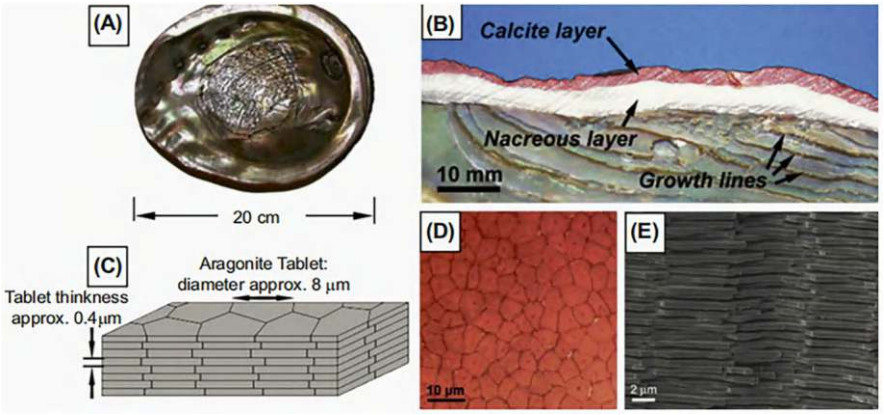

Fig. 11.9 The multi-scale structure of a seashell: (**a**) inside view of the shell; (**b**) cross-section of a red abalone shell; (**c**) schematic of the brick wall-like microstructure; (**d**) optical micrograph showing the tiling of the tablets; (**e**) scanning electron microscope of a fracture surface. Reprinted with permission from Espinosa et al. (2009). Copyright 2009: Elsevier

and functional materials. Direct deposition involves applying a thin layer of clay suspension onto a substrate, followed by drying and further processing.

Clay has an in-plane modulus of elasticity of about 270 GPa. Layered silicates are natural clays that are 2D inorganic building blocks with a thickness of about 1 nm, and they are cheap, easily exfoliated, and manipulated. Polymer/clay nanocomposites have received great interest. It still remains a great challenge to realize nanocomposites that allow the transfer of the exceptional mechanical properties of nanoclays to the macroscale properties of bulk materials. Figure 11.9 depicts the hierarchical structure of nacre found in seashells, such as the abalone shell, which can reach several centimeters in size (Espinosa et al., 2009). Young's modulus and stress at break can reach 40–70 GPa and 80–135 MPa, respectively. Its longitudinal cross-section reveals two distinct layers: a hard prismatic calcite layer that prevents penetration but is prone to brittleness, and a softer nacreous aragonite layer that can absorb mechanical energy and withstand larger deformations. At the mesoscale, the nacreous layer resembles a three-dimensional brick-and-mortar wall, consisting of densely packed microscopic aragonite tablets (5–8 mm in diameter and 0.5 mm thick) bonded by 20–30 nm thick protein adhesive layers. In nature, there exist many nanostructured inorganic-organic hybrid composites that form tissues of high mechanical functionality such as bone, antler, enamel, dentin, nacre, sea shells, and egg shells. These nanopaper-like structures combine high inorganic content with a unique combination of modulus, strength, and toughness. In nacre, nanopaper-like structure is evident not only in the predominant inorganic minerals—over 95 wt%—such as calcium carbonate, calcium phosphate, and amorphous silica, but also in a smaller fraction (1.5 wt%) of organic biopolymers like keratin, collagen, and chitin. This fascinating hierarchical structure is yet to be studied for a useful composite.

11.4.2 Nano-Graphene (Oxide) Nanopaper

Graphene, one single layer of sp^2 bonded carbon atoms arranged in a hexagonal lattice, has many outstanding attributes, such as extremely high electron carrier mobility (up to 200,000 $cm^2 \cdot V^{-1}\ s^{-1}$) (Allen et al., 2010), superior tensile modulus (1 TPa) (Lee et al., 2008), high-specific surface (2630 $m^2 \cdot g^{-1}$) (Kim et al., 2013), good thermal conductivity (~5000 $W \cdot m^{-1} \cdot K^{-1}$), and high optical transmittance (~97.7%) if we make a very thin nanopaper out of it (Nair et al., 2008). To make nanopaper, the first step is to disperse it. Many important applications, i.e., electrodes, require large quantity graphene to be ready in a form of liquid suspensions, inks, or dispersions (Xu & Hsieh, 2019). Nanopapers fabricated from graphene have unique properties; comparatively, the high electrical and thermal conductivities, minimal gas diffusivity, and robust corrosion resistance of this material are unique and are not found in other materials.

Graphene and graphene oxide nanopapers are thin sheets composed of nanoplatelets that enable the packing of highly concentrated nanoparticles into a film, resulting in exceptional properties such as high electrical and thermal conductivity, low gas diffusivity, and strong corrosion resistance; these advantages are not found in conventional nanopapers (Fig. 11.10a). Huang et al. developed a method for large-scale production of stable graphene colloids, achieving graphene nanopapers with electrical conductivity up to 4.45×10^4 S/m, tensile strength of 360 MPa, and Young's modulus of 102 GPa (Huang, 2017b). However, the performance of graphene nanopapers is often lower than that of individual graphene sheets due to weak van der Waals interactions, which limit their macroscopic properties. While techniques like chemical vapor deposition (CVD) can help retain graphene's superior qualities, they also introduce mechanical weaknesses. Adding organic or inorganic binders can enhance structural integrity but may compromise the unique features of graphene.

11.4.3 Carbon Nanotube (Nanofiber) Nanopaper

In comparison, carbon nanotubes (CNTs)—known as carbon nanofibers (CNFs) when they take on a solid, tube-like structure—demonstrate an exceptional combination of mechanical, electrical, and thermal properties. This makes them promising components for developing novel multifunctional materials across various applications. Young's modulus of individual CNTs can reach 1 TPa, which is five times higher than that of steel (200 GPa) while their density is only 1.2–1.4 g cm^{-3}. The tensile strength of CNTs falls in the range of 50–200 GPa. These values are over tenfold greater than any industrial fibers. CNTs also show ballistic conduction behavior for electricity and heat. The ballistic transport and mechanical stability allow them to carry high current densities up to 10^{10} A cm^{-2}, 3–4 orders of magnitude higher than those of most metals. The theoretical thermal conductivity of an

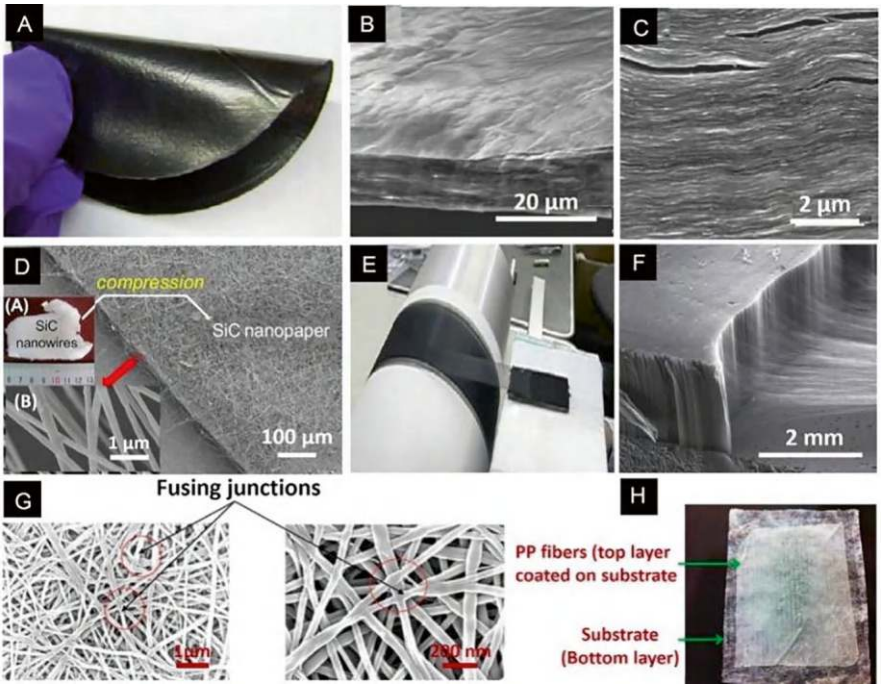

Fig. 11.10 (**a**) The digital picture of nano-graphene nanopaper. (**b**, **c**) SEM micro-graphs of nano-graphene oxide nanopaper. (**d**) SEM images and photographs (**a**) of SiC nanopaper (inset **b** is the enlarged image of rectangular area). (**e**) Optical images and (**f**) SEM of an MWCNT (multi-walled carbon nanotubes) nanopaper was drawn at 10 ms^{-1} and wound layer-by-layer on a polytetrafluoroethylene spool. (**g**, **h**) Synthetic polymer nanopapers: (**g**) Nylon-66 nanopaper and (**h**) polypropylene nanopaper. Panels (**a**–**f**) reprinted with permission from Huang (2017a). Copyright 2017: Elsevier. Panel (**g**) reprinted with permission from Lingaiah and Shivakumar (2013). Copyright 2013, Elsevier. Panel (**h**) reprinted with permission from Raghavan et al. (2013). Copyright 2013: SAGE journals

isolated single-walled carbon nanotube (SWCNT) could be as high as approximately 6600 W m^{-1} K^{-1} at room temperature. CNFs are similar to multi-walled CNTs but possess a larger diameter (50–200 nm) and longer length. Individual CNFs exhibited tensile strengths of 1.25–3 GPa and Young's modulus approaching 300 GPa. The thermal conductivity of CNFs can be inferred to be 2000 W m^{-1} K^{-1}. Carbon nanotube (nanofiber) nanopapers, as showed in Fig. 11.10e, f, are composed entirely of networks of carbon nanotubes or carbon nanofibers forming thin films. These nanopapers are characterized by their flexibility, lightweight nature, and impressive mechanical, electrical, thermal, and corrosion-resistant properties (Zhao et al., 2017).

11.4.4 Silicon Carbide Nanopaper

One-dimensional silicon carbide (SiC) nanowires serve as the optimal building blocks for SiC nanopapers. The fabrication of SiC nanopaper, as shown in Fig. 11.10d, involves a process utilizing acetone-assisted compression of SiC nanowires. The resulting nanopaper demonstrates excellent humidity sensing capabilities and heightened photo-electrocatalytic activity under ultraviolet (UV) irradiation. These features position SiC nanopaper for applications in high-performance sensors and innovative energy transfer devices.

11.4.5 Synthetic Polymer Nanopapers

Certain synthetic polymers, including polyurethane, polypropylene, polyvinyl fluoride, polyvinyl alcohol, and others, can be transformed into nanofibers and nanopapers. Techniques such as electrospinning, fiber fusing, melt blowing, and force spinning are employed to create these materials, resulting in the formation of nonwoven network thin sheets or nanopapers, as illustrated in Fig. 11.10g, h. The as-spun polymer nanofiber nanopapers naturally have a porous structure, which can be compacted to produce nanopapers with increased density and reduced porosity. This process enhances their utility in various applications by improving their mechanical and barrier properties.

11.5 Nanopaper Manufacturing Process

11.5.1 Raw Material Selection

Nanopaper is composed of tightly packed nanostructures, such as nanocellulose, nanochitin, nanochitosan, and nanographene, and the selection of these raw materials is crucial for determining the final product's properties and performance. Nanocellulose, sourced from wood pulp or agricultural residues, is valued for its excellent mechanical strength, lightweight nature, and biodegradability, with its high aspect ratio and surface area enhancing bonding and flexibility in nanopaper. Nanochitin and its deacetylated form, nanochitosan, derived from crustacean shells or fungal sources, provide unique biocompatibility and antibacterial properties, making them suitable for biomedical applications. Meanwhile, nanographene contributes exceptional electrical and thermal conductivity, significantly improving the mechanical properties of nanopaper while adding electrical functionality. Sustainability is also a key consideration in raw material selection; using renewable resources like agricultural byproducts or sustainably sourced cellulose helps minimize environmental impact and boosts nanopaper's appeal. Additionally, selecting high-purity materials is essential, as impurities can adversely affect the mechanical

and optical properties of the final product. By carefully combining these nanostructures, manufacturers can tailor nanopaper properties to meet specific application needs, ranging from packaging and electronics to biomedical uses.

11.5.2 Nanofibrillation

The process of nanofibrillation breaks down extracted raw materials, such as cellulose fibers and clay, into their nanoscale components. This is achieved through methods like mechanical shearing, chemical dissolution, enzymatic hydrolysis, or a combination of these techniques, which effectively disintegrate the fibers into nanoparticles, e.g., cellulose nanocrystals (Xu et al., 2014) and nanofibrils (Jiang & Hsieh, 2014a, 2014b; Lu & Hsieh, 2012). If needed, these materials can be processed into powders using spraying techniques, facilitating product transportation and compatibility with various solvents. Nowadays, nanoparticles are readily available for purchase on numerous websites, alleviating concerns for most researchers.

11.5.3 Dispersion

For cellulose, chitosan, and other biopolymer-based nanopapers, the nanofibrils or particles are typically dispersed in water to form a stable suspension (1–6 wt.%). For other inorganic nanoparticles, various organic solvents were adopted for a good dispersion.

11.5.4 Dewatering and Sheet Formation

The creation of nanopaper involves transforming a concentrated nanocellulose suspension into a thin, robust sheet. This transformation typically involves filtration followed by drying (Fig. 11.11), casting (Fig. 11.12), Mayer rod coating (Fig. 11.13),

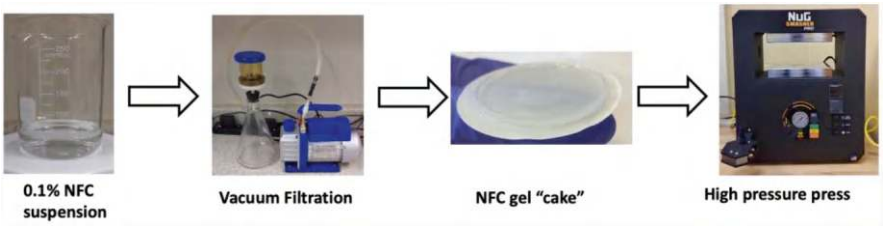

Fig. 11.11 A typical vacuum filtration funnel setup for nanopaper. Reprinted with permission from Espinosa et al. (2009). Copyright 2020: Elsevier

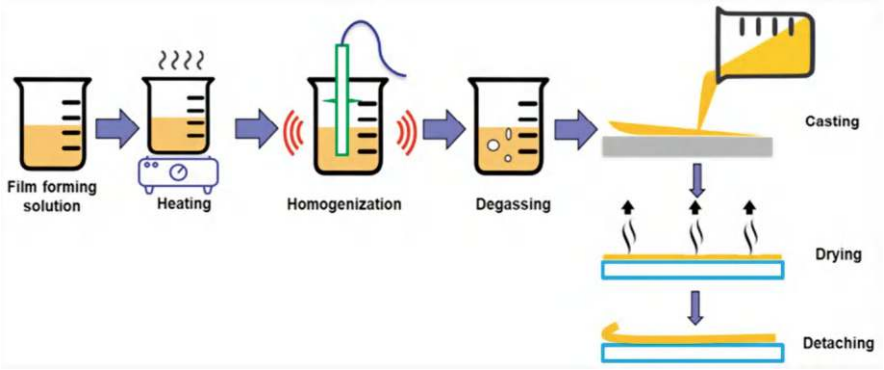

Fig. 11.12 Common wet casting techniques used for film formation. Reprinted from Prakoso et al. (2023). Published 2023 by MDPI with open access

Fig. 11.13 Schematic illustration showing the fabrication of OEC-CDs-NFC composite pastes and nanopaper. Reprinted with permission from Abulikemu et al. (2023). Copyright 2023: IOP publications

or spraying (Fig. 11.14). Then, air drying, vacuum drying (Fig. 11.11), or freeze-drying or hot pressing are employed to remove solvent in the host suspension.

11.5.5 Specialized Processes for Different Nanopapers

For graphene nanopapers, the dispersion of graphene oxide or other graphene derivatives is typically obtained in water or organic solvents. After casting, the sheet may undergo a reduction process to restore its conductivity. For clay platelets, it has to be dispersed and exfoliated to ensure a uniform distribution. Then, layer-by-layer

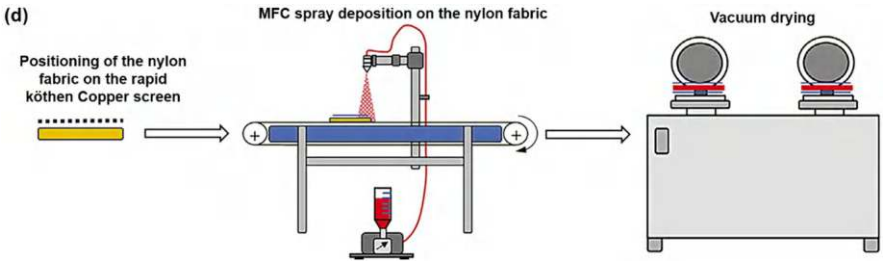

Fig. 11.14 Schematic illustration of the fabrication of CNP by spraying deposition. Reprinted with permission from Liu et al. (2022). Copyright 2022: Springer publications

assembly or other assembly techniques are used to create multilayered structures with enhanced barrier properties. Comparatively, the chitosan, being a cationic polymer, requires specific conditions to disperse in an aqueous solution. Cross-linking agents may be used after sheet formation to improve the mechanical properties.

11.5.6 Post-processing

After the drying process, nanopapers may undergo post-processing steps such as lamination, surface treatment, or additional cross-linking to enhance their performance characteristics.

11.6 Scaling Up and Industrialization

11.6.1 Pilot-Scale and Semi-Commercial Production

Pilot-scale production serves as a bridge between experimental and commercial manufacturing. It allows for the testing of processes and equipment at a larger scale while still being manageable in terms of cost and resources. Entities engaged in pilot-scale production, of NCC (nano-cellulose crystals), NFC (nano-fibril cellulose) such as research and development labs and small manufacturers—including notable examples like the US Forest Service—typically produce batches ranging from a few grams to several kilograms (as detailed in Table 11.1).

Table 11.1 Main centers possessing pilot or demonstration plants of different capacity

Center	Country	Unit	Type	Capacity
FP innovation	Canada	Pilot plant	NCC	10 kg/week
US Forest Service's Forest Products Laboratory	USA	Pilot plant	NCC	35–50 kg/day
Alberta innovates technology futures	Canada	Pilot plant	NCC	100 kg/week
Celluforce Inc.	Canada	Demonstration plant	NCC	1 ton/day
Biovision technologies Inc.	USA	Pilot plant	NCC	4 tons/year
Inventia	Sweden	Demonstration plant	NFC	100 kg/day
The US Forest Service	USA	Demonstration plant	NFC	500 kg/day

Source: Reprinted from Rebouillat and Pla (2013). Published 2013 by Scientific Research Publishing Inc. as open access

Fig. 11.15 Carbon-coated copper and aluminum foils to be used as an electrical collector in batteries. http://leary.com.cn/product.html?proTypeID=4648908854515008

11.6.2 Large-Scale Production

For nanopapers, it is still very early to find it in stock in the market, not matter which type. For graphene and carbon nanotubes, it is usually sold as conductive inks and pastes, which is easy to be used for the next step. CARBON NANOTUBE OR CARBON BLACK coated copper and aluminum foils are at large-scale produced (Fig. 11.15), produced by Leary company, Foshan city, China), which is to be used as an electrical collector in batteries. For nanocellulose, as investigated by the author, a handful of manufacturing plants are now operational with the capacity to produce hundreds to thousands of metric tons of nanopaper annually. However, due to high prices of up to 200–500 € m^{-2} without critical uses, most companies are selling powders (e.g., Topchain company, Zhuhai city, China) rather than nanopapers, and the number of such large-scale facilities remains limited, reflecting the current scale of demand (as indicated in the price column in Table 11.2).

Table 11.2 Properties and cost of classical printed electronics substrates (plastic and conventional paper) and cellulose nanopaper

Material	Surface roughness (nm)	Young modulus (GPa)	Thermal expansion coefficient (ppm K^{-1})	Transparency	Price (€ m^{-2})	Scale up
PET	≈0.5–2	≈2–2.5	50–200	Yes	4–6	Yes
Paper	≈10	≈2	–	No	6–7	Yes
Nanocellulose paper (NFCs)	≈2–40	≈10	≈8–13	Yes	15–200	No
Nanocellulose paper (TEMPO CNFs)	≈0.2–0.5	≈10–13	≈7.2–7.9	Yes	200–500	No

Source: Reprinted with permission from Rebouillat and Pla (2013). Copyright 2016: RSC

11.7 Properties

Nanopaper, characterized by its varied composition and fabrication methods, boasts a diverse array of properties that enhance its versatility for numerous applications. This section highlights some key properties of different types of nanopaper, while applications will be explored in further chapters.

11.7.1 Graphene Nanopaper

The unique sp^2 structure of graphite endows graphene nanopaper with remarkable properties, including exceptional electrical conductivity ranging from ~10^{-2} to 10^3 S/cm (associated with surface and internal functional groups, atom types, pore structure, or film thickness, as graphene consists of particles) (Fig. 11.16a), high mechanical strength with a tensile strength of approximately 100–150 GPa, and impressive thermal conductivity of ~2000–5000 W/m·K. Although insulating nanocellulose (or clay, chitin/chitosan) can also be used to create nanopapers, achieving electrical conductivity typically requires the incorporation of conductive materials like graphene. For instance, the addition of TEMPO-oxidized cellulose nanofibers (CNF) to graphene nanopaper can significantly reduce its electrical conductivity by several orders of magnitude (Fig. 11.16b). These properties make graphene nanopaper ideal for applications, such as transparent electrodes, flexible electronics, energy storage devices, lightweight composites, and thermal management systems.

11.7.2 Carbon Nanotube Nanopaper

Carbon nanopaper also exhibits high electrical conductivity and excellent thermal conductivity, making it suitable for electrodes in batteries, fuel cells, and supercapacitors (Fig. 11.17). This chapter highlights the properties of carbon nanotube

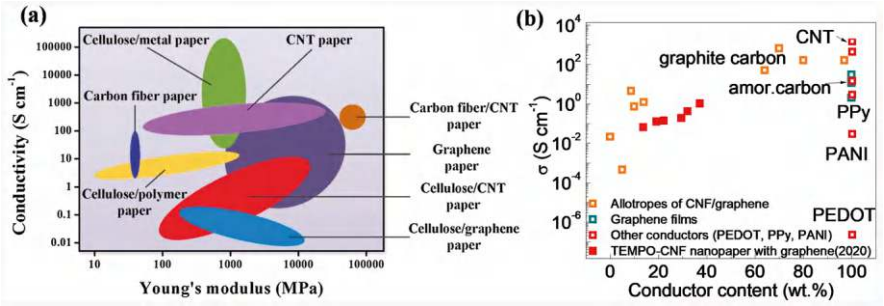

Fig. 11.16 Electrical properties of composite nanopapers: (**a**) Material selection diagram: electrical conductivity plotted against Young's modulus. Young's modulus, as a symbol of the mechanical strength, and electrical conductivity, representing the electrically conductive property, are compared among a variety of nanopapers. (**b**) Electrical properties of conductive CNFs by adding graphene. The diagram is helpful to provide design guidelines in materials selection of substrate for fabrication of paper electronics. (**a**) Reprinted with permission from Liu et al. (2017). Copyright 2017: Elsevier. (**b**) reprinted with permission from Xu and Hsieh (2019). Copyright 2019: RSC. Data extracted from Hudson et al. (2004), Lotya et al. (2009, 2010), Khan et al. (2010), Smith et al. (2011), Notley (2012), Carrasco et al. (2014), Paton et al. (2014)

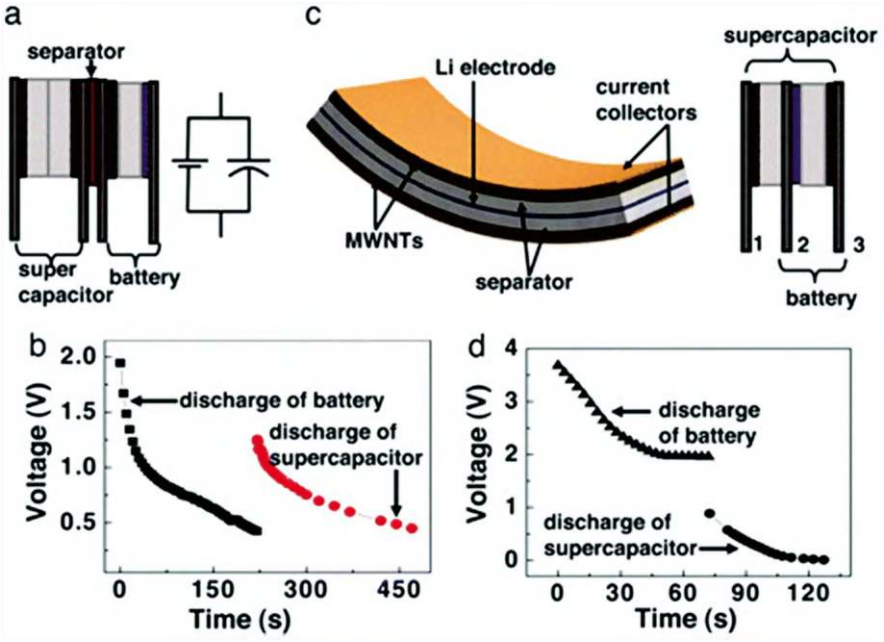

Fig. 11.17 Supercapacitor–battery hybrid energy devices based on a MWCNTs/polyaniline nanopaper. (**a**) Arrangement of a supercapacitor and a battery in a parallel configuration. (**b**) A discharge curve of a battery and a supercapacitor is plotted as a function of time. (**c**) Schematic diagram of a three-terminal hybrid energy device that can act as both a supercapacitor and a battery. (**d**) The discharge behavior of the battery and subsequent discharge of the supercapacitor. Reprinted with permission from Liu et al. (2022). Copyright 2007: Springer Nature

nanopaper, particularly its excellent electrical and mechanical strength, which makes it suitable for lightweight electronic components and related applications. Supercapacitors or these ones paired with batteries are ones of the kind. Carbon nanotube papers can be integrated in parallel, allowing the battery to charge the adjacent supercapacitor (see Fig. 11.17a–c, side and 3D view) (Liu et al., 2022). The battery comprises a lithium metal layer (anode) and a nanocomposite film (cathode) with an aqueous electrolyte (1 M $LiPF_6$). The supercapacitor, formed by a nanocomposite unit by using both multi-walled carbon nanotubes and cellulose, is positioned next to the lithium layer. The flexible CNT–cellulose–cathode nanocomposite sheets show great potential for energy storage applications, with performance comparable to other flexible solutions. Their robust thin-film structure ensures excellent electrochemical performance while accommodating mechanical deformations and extreme temperatures. In general, carbon nanotube nanopaper outperforms graphene nanopaper in terms of electrical conductivity. However, its cost can be up to 200 times higher than that of graphene. This significant price difference arises because carbon nanotubes do not occur naturally, while graphene is found in nature as graphite. The availability of these resources greatly influences their pricing.

11.7.3 Nanocellulose Nanopaper

Derived from renewable sources, nanocellulose is biodegradable and biocompatible, making it environmentally friendly and suitable for biomedical applications. Its high surface area enhances its ability to adsorb and filter various substances, making it ideal for filtration membranes and water purification. Nanocellulose nanopaper also acts as a barrier against gases and liquids, making it useful for packaging materials, food preservation, and controlled drug delivery, see a spray coating fabrication of pure CNF and quantum dots embedded nanopaper on rigid and flexible substrates (Fig. 11.18) (Abulikemu et al., 2023). It demonstrates the versatility and simplicity. This approach will enable us to fabricate biocompatible luminescent nanopaper and the other paper electronics (Fig. 11.18) via printing techniques and the others (Abulikemu et al., 2023).

11.7.3.1 Flexibility and Adaptability

Single nanocellulose has impressively high intrinsic tensile strength of 1.6–6.4 GPa (Saito et al., 2013) and modulus up to 78–114 GPa (Guhados et al., 2005; Hsieh et al., 2008; Sehaqui et al., 2012; Tanpichai et al., 2012); their tensile properties are among the closest to carbon nanotubes, whose respective tensile strength and Young's modulus are estimated to be ~300 GPa and ~270–950 TPa (Wong et al., 1997; Yu et al., 2000). These CNFs exhibited high flexibility by functioning as film material (Fig. 11.18) as well as adaptability when assembled into electronics (Fig. 11.19). The impressive surface-active characteristics and amphiphilicity of

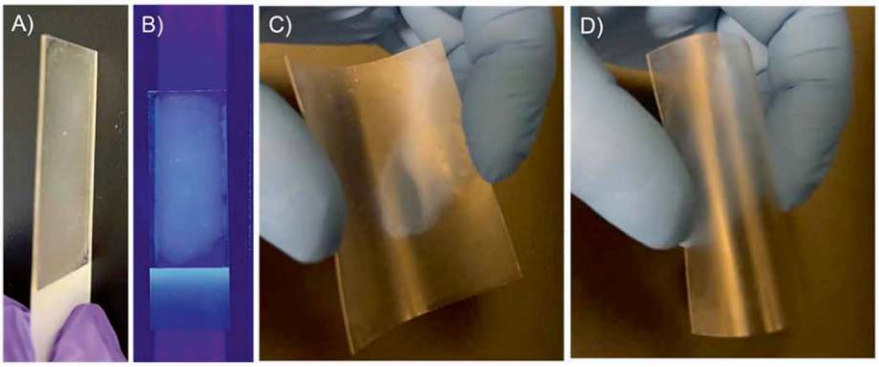

Fig. 11.18 Digital images of spray-coated nanopaper/film, (**a**) NFC-CDs on glass, (**b**) NFC-CDs on glass under UV light, (**c**, **d**) NFC-CDs on PET. Reprinted with permission from Abulikemu et al. (2023). Copyright 2023: IOP publications

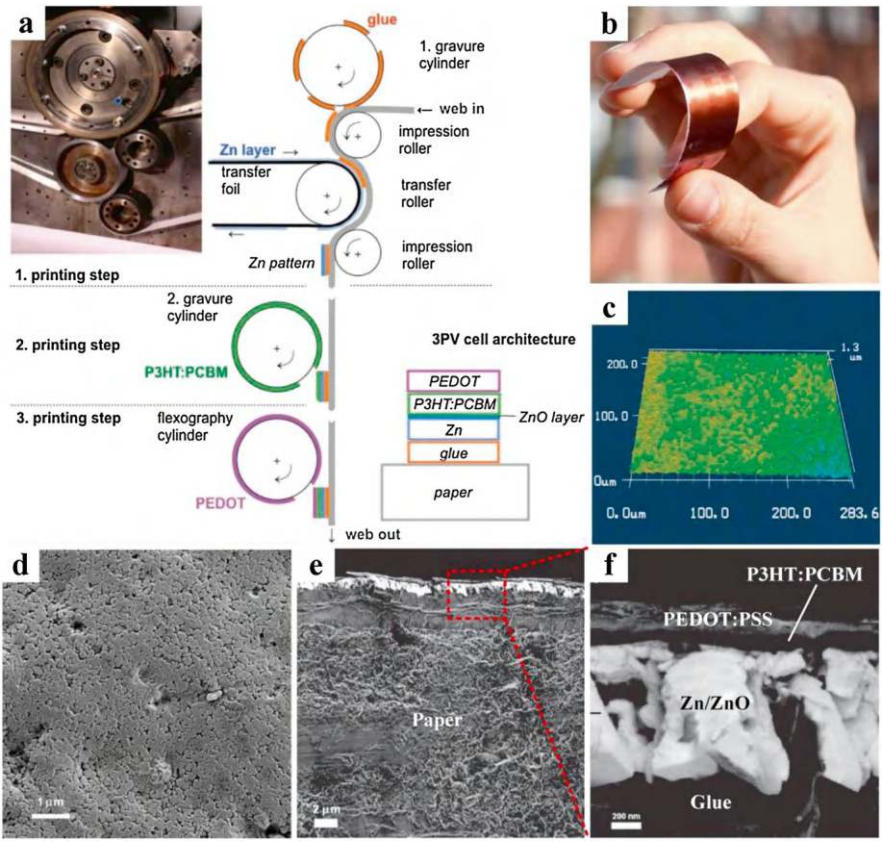

Fig. 11.19 Paper electronics fabricated by printing techniques. (**a**) Optical image and schematic diagram of the printing process. (**b**) Digital photograph of the printed photovoltaic cell. (**c**, **d**) Laser scanning image (**c**) and SEM image (**d**) of the surface morphology of the fabricated cell. (**e**, **f**) Cross-sectional SEM images of paper-based cell at lower (**e**) and higher (**f**) magnifications. Reprinted with permission from Abulikemu et al. (2023). Copyright 2011: IOP Publishing

CNFs couple with their potentially high strength, matching carbon nanomaterials have inspired us to exploit these CNFs as ideal aqueous exfoliating and functioning agent for graphene, a potential new frontier in liquid-phase exfoliation and application fields. Despite its impressive strength, nanopaper maintains a high degree of flexibility, allowing it to be bent, folded, or even rolled without compromising its structural integrity. This versatility opens up a wide range of design possibilities.

11.7.3.2 Strength and Durability

Nanopaper exhibits exceptional mechanical properties, with a tensile strength that can surpass that of steel. This remarkable strength-to-weight ratio makes it an ideal material for applications where lightweight and robust solutions are required, cellulose nanofibril (CNF) by (2,2,6,6-tetramethylpiperidin-1-yl)oxyl (TEMPO)-mediated nanofibrilation, as known for their nanoscale lateral dimensions (1–20 nm), 10^2–10^3 aspect ratios, excellent tensile strength σ ranging from 1.6 to 6.4 GPa (Saito et al., 2013) at moduli E of 78–114 GPa is nearly one-tenth of carbon nanotubes whose tensile strength is measured to be as high as ∼300 GPa at E of ∼270–950 GPa (Wong et al., 1997; Yu et al., 2000). Most often, CNFs are believed as a type of homogenous nanoparticles to make nanopaper and bulk films with functional properties (Bi et al., 2013; Park et al., 2010). When it dries from droplets, it dries into a homogenous film because abundant hydroxyl (–OH) and carboxylic ($–COO^-$) charges on surface keep them suspended quiet well in water (Jiang & Hsieh, 2013, 2014a, 2014b, 2016). For applications, CNF with lateral width and length of 2.7 nm, 0.1–1 μm was used as an excellent binder by binding an active material carbon-coated lithium iron phosphate ($LiFePO_4$) to graphite (as electrode) to prepare Li-ion batteries (Lu et al., 2016) Similarly, other types of inorganic, hydrophobic nanosheets were such as boron nitride (BN) (Li et al., 2015) and molybdenum disulfide (MoS_2) (Li et al., 2015) were reported successfully dispersed in solvent water by using CNFs. Excellent properties of graphene sheets makes it an important building block for actuators (Bi et al., 2013; Park et al., 2010). TEMPO-oxidized cellulose nanofibril (TOCN) film has a CTE of 3.8 ppm K^{-1} (Shimizu et al., 2013).

11.7.3.3 Nanocellulose Dielectric Layers

Nanocellulose and the other electrically insulating ones, while being an intrinsic insulator, are characterized by a dielectric feature. This is due to its abundant hydrogen bonds (–OH) that can easily align with an electric field (Luo et al., 2023), resulting in high dipole moments. Its unique chemical structure and spatial asymmetry contribute to strong polarity and impressive mechanical properties, alongside notable dielectric characteristics that are often overlooked. In capacitors, the dielectrics play an important role for energy storage, where energy density is defined as: energy density $= \frac{1}{2}\varepsilon_0\varepsilon_r E_b^2$, ε_r, ε_0 is the dielectric permittivity of the material and

vacuum (8.85×10^{-12} F/m), respectively, E_b is the breakdown strength energy storage density, Obviously, a high dielectric constant and breakdown field strength are essential for maximizing energy density. For example, nanocellulose exhibits a dielectric constant that surpasses many organic polymer dielectrics with dielectric constant of ~2. Actually, the dielectric constant of dry cellulose is approximately 6–8, while traditional paper-based materials have a dielectric constant of only 1.3–4. Recent studies indicate that cellulose nanopaper can achieve a relative dielectric constant as high as 5.3 at 1.1 GHz, significantly higher than conventional paper (Inui et al., 2014).

Theoretically, if the dipole moment (μ) of C–H bonds cancels out and shows the least dielectric constant (Mirabedini et al., 2007), see the calculation of its analog: $\mu(CH_4) = 0$. The more symmetric the polymer appears, the lower the dipole moment is. Comparatively, polyvinylidene fluoride (PVDF − $(C_2H_2F_2)_n$–) with –H and –F atoms have a higher μ, then has a constant up to ~8.5 or more when made into α-phase (Kalimuldina et al., 2020). All dipoles in the β phase of the PVDF polymer are aligned in the same direction to give a higher dipole moment (~8×10^{-30} Cm) per unit cell. Polarizability is a measure of how easily an electric field distorts an electron cloud. It is also related to the dipole moment; see the definition: $\alpha = \mu/E$ (unit: $\times 10^{-16}$ C·m²/V) (Prateek et al., 2016). Researchers have concluded that both applied electric fields and intrinsic molecular structures change polarizability. The larger the molecule (atom) is, the greater the distortion (hence α).

In thin-film transistors (TFTs), nanocellulose serves as a key dielectric layer, while the graphene, nanotubes, and clay are difficult to be used for this role. For the relationship between the capacitance of dielectric interlayer and TFT device performances, some equations need to be clarified. High saturation mobility (μ_{sat}) in a thin-film transistor is crucial for future high-resolution and fast response downstream products. High μ_{sat} leads to a high source-to-drain current (I_D) and a lower subthreshold swing (SS), see the below equation (Park et al., 2018):

$$I_D = \frac{W}{2L} \mu_{sat} C_i \left(V_G - V_T\right)^2 \tag{11.1}$$

$$SS = \frac{dV_G}{d\left(\log I_D\right)}, \tag{11.2}$$

where I_D is the source-to-drain current; W and L are the width and length of the channel, respectively; μ_{sat} is the saturation mobility; C_i is the capacitance per unit area of the gate insulator; V_G is the gate voltage; and V_G is the drain voltage. V_T was evaluated from the x-axis intercept of the plot versus V_G; a low SS is usually desired and means we need a lower gate-to-source voltage to tune the I_D (source-to-drain current). The nanocellulose supporting TFT exhibited good transistor electrical characteristics: the carrier mobility ~4.3×10^{-3} cm²/(Vs) and an electric current on/off ratio of 200. What is worth noting is that, bent and folded OFET has merely a 10% reduction in mobility. A bottom-contact organic TFT arrays, with a higher on-current of 10^{-5}A, a high on/off ratio of 10^6–10^8, and mobility of 1 cm²/V/s under

ambient air was reported (Fujisaki et al., 2014). Recent studies have leveraged the ionic conductivity of TEMPO-oxidized CNF to create electric double layers, which can lower the operational voltage of field-effect transistors (FETs). Other innovations include the use of cotton-based nanocrystalline cellulose membranes as substrates and gate dielectrics in metal oxide FETs, achieving high channel saturation mobility and significant on/off modulation ratios. As shown in Fig. 11.20, Gaspar et al. (2014) also reported the use of cotton-based nanocrystalline cellulose membranes simultaneously as the substrate and the gate dielectric in metal oxide field-effect transistors for the first time, fully processed at room temperature (Gaspar et al., 2014). Such hybrid FETs presented a high-channel saturation mobility (>7 $cm^2/V/s$), drain-source current on/off modulation ratio higher than 10^5, n-type enhancement operation, and subthreshold gate voltage swing of 2.11 V/decade. Nanocellulose can be ionized into a dielectric with an even higher dielectric constant, lowering the working voltage as well. For example, Grey et al. (2020) permeated solid CNC droplets with three different base ions (Li^+, Na^+, and K^+) to produce a membrane with improved electrochemical response compared with the original membrane while retaining its photonic properties. Electrochemical characterization showed capacitance of up to 2.5 $\mu F/cm^2$, which allows integrating them into a solid-gate electrolyte in an indium gallium zinc oxide transistor, enabling low-operating voltage (<2 V), on/off ratio of up to six orders of magnitude, and high saturation

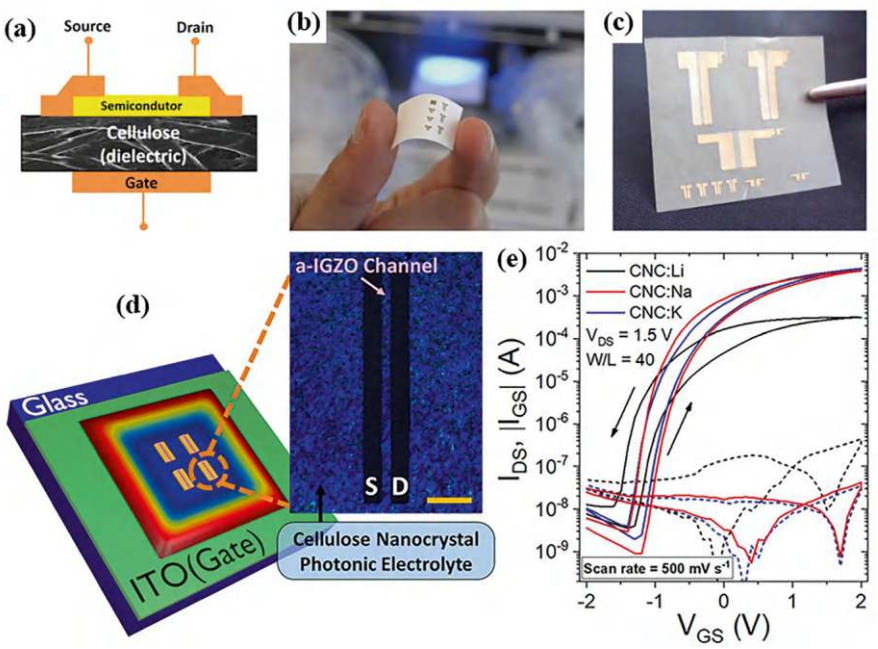

Fig. 11.20 Electronic devices developed at FCT-UNL where the cellulose paper is simultaneously the gate dielectric material and the substrate. Reprinted with permission from Gaspar et al. (2014). Copyright 2023: IOP Publishing

mobility >10 $cm^2/V/s$. Devices manufactured on Na^+ and K^+ permeated CNC films show the best properties, indicating pure capacitance charging of semiconductors.

The dielectric properties of nanocellulose nanopaper offer promising opportunities for future electronic applications. For a more in-depth exploration of its dielectric role, including additional functions and enhancements to electronic performance, refer to other publications such as Shen et al. (2023), which particularly emphasizes its extra functions and enhanced electronic performances.

11.7.3.4 Transparency and Optical Properties

Nanopaper can be engineered to achieve high transparency, with optical properties as transparent as glass, or iridescent as peakcooks (Xu & Hsieh, 2019). This combination of transparency and unique optical properties positions nanopaper as a promising material for various advanced applications in the nano- and microelectromechanical fields.

11.7.4 Chitin Nanopaper

The properties of chitin nanopaper are obvious especially for biomedical applications, wound dressings, and tissue engineering. Its antimicrobial properties make it useful for antibacterial and antifungal applications in food packaging, wound care, and medical devices. Chitin nanopaper offers good strength and flexibility, making it suitable for various applications. However, the develop is in its early laboratory study status; people still have not tried to utilize this in hospitals.

11.7.5 Clay Nanopaper

Clay nanopaper showed barrier properties against gases and liquids, making it suitable for packaging applications, especially for food and pharmaceuticals. It exhibits flame-retardant properties as well, enhancing the safety of various materials and products. The ready availability of clay and its inexpensive nature make clay nanopaper a cost-effective option for various applications. We believe the clay nanopaper will have a bigger picture in the future.

11.8 Conclusion

Nanopaper represents a significant advancement in material science, greatly shaped by the rapid progress in nanotechnology. Its wide variety of forms and properties, which include bio-based materials like cellulose and chitin, as well as non-bio alternatives such as graphene and silicon carbide, make it a highly versatile material for numerous applications. This chapter has detailed the key manufacturing processes, including the selection of raw materials, nanofibrillation, and sheet formation, to enhance the understanding of their unique characteristics.

Despite the challenges in achieving efficient, scalable, and high-quality production, alongside specific issues related to different nanopaper types, such as effective fibrillation, yield optimization, dispersion stability, large-scale exfoliation, and health risk management, the beneficial properties of nanopaper position it as a promising material for diverse applications. Ongoing research and technological developments are anticipated to further optimize manufacturing processes and broaden the potential uses of nanopaper.

References

Abulikemu, M., Tabrizi, B. E. A., Mofarah, H. M., Shad, K. R., & Jabbour, G. E. (2023). Recyclable luminescent carbon dots nanopaper for flexible electronics. *Flexible and Printed Electronics, 8*, 024004. https://doi.org/10.1088/2058-8585/acd200

Ahne, J., Li, Q., Croiset, E., & Tan, Z. (2019). Electrospun cellulose acetate nanofibers for airborne nanoparticle filtration. *Textile Research Journal, 89*(15), 3137–3149. https://doi.org/10.1177/0040517518807440

Allen, M. J., Tung, V. C., & Kaner, R. B. (2010). Honeycomb carbon: A review of graphene. *Chemical Reviews, 110*, 132–145. https://doi.org/10.1021/cr900070d

Bi, H., Yin, K., Xie, X., Ji, J., Wan, S., Sun, L., et al. (2013). Ultrahigh humidity sensitivity of graphene oxide. *Scientific Reports, 3*, 2714. https://doi.org/10.1038/srep02714

Carrasco, P. M., Montes, S., García, I., Borghei, M., Jiang, H., Odriozola, I., et al. (2014). High-concentration aqueous dispersions of graphene produced by exfoliation of graphite using cellulose nanocrystals. *Carbon, 70*, 157–163. https://doi.org/10.1016/j.carbon.2013.12.086

Espinosa, H. D., Rim, J. E., Barthelat, F., & Buehler, M. J. (2009). Merger of structure and material in nacre and bone - Perspectives on de novo biomimetic materials. *Progress in Materials Science, 54*, 1059–1100. https://doi.org/10.1016/j.pmatsci.2009.05.001

Fujisaki, Y., Koga, H., Nakajima, Y., Nakata, M., Tsuji, H., Yamamoto, T., et al. (2014). Transparent nanopaper-based flexible organic thin-film transistor array. *Advanced Functional Materials, 24*(12), 1657–1663. https://doi.org/10.1002/adfm.201303024

Gaspar, D., Fernandes, S. N., De Oliveira, A. G., Fernandes, J. G., Grey, P., Pontes, R. V., et al. (2014). Nanocrystalline cellulose applied simultaneously as the gate dielectric and the substrate in flexible field effect transistors. *Nanotechnology, 25*, 094008. https://doi.org/10.1088/0957-4484/25/9/094008

Grey, P., Fernandes, S. N., Gaspar, D., Deuermeier, J., Martins, R., Fortunato, E., et al. (2020). Ionically modified cellulose nanocrystal self-assembled films with a mesoporous twisted superstructure: Polarizability and application in ion-gated transistors. *ACS Applied Electronic Materials, 2*(2), 426–436. https://doi.org/10.1021/acsaelm.9b00652

Guhados, G., Wan, W., & Hutter, J. L. (2005). Measurement of the elastic modulus of single bacterial cellulose fibers using atomic force microscopy. *Langmuir, 21*, 6642–6646. https://doi.org/10.1021/la0504311

Hsieh, Y. C., Yano, H., Nogi, M., & Eichhorn, S. J. (2008). An estimation of the Young's modulus of bacterial cellulose filaments. *Cellulose, 15*, 507–513. https://doi.org/10.1007/s10570-008-9206-8

Huang, W. (2017a). Chitin nanopapers. In W. Huang (Ed.), *Nanopaper* (pp. 175–200). Elsevier. https://doi.org/10.1016/B978-0-323-48019-2.00006-2

Huang, W. (2017b). Graphene oxide nanopapers. In W. Huang (Ed.), *Nanopaper* (pp. 1–26). Elsevier. https://doi.org/10.1016/B978-0-323-48019-2.00001-3

Hudson, J. L., Casavant, M. J., & Tour, J. M. (2004). Water-soluble, exfoliated, nonroping single-wall carbon nanotubes. *Journal of the American Chemical Society, 126*, 11158–11159. https://doi.org/10.1021/ja0467061

Inui, T., Koga, H., Nogi, M., Komoda, N., & Suganuma, K. (2014). High-dielectric paper composite consisting of cellulose nanofiber and silver nanowire. In *IEEE 14th international conference on nanotechnology (IEEE-NANO)* (pp. 470–473). IEEE. https://doi.org/10.1109/NANO.2014.6967965

Jiang, F., & Hsieh, Y.-L. (2014a). Super water absorbing and shape memory nanocellulose aerogels from TEMPO-oxidized cellulose nanofibrils via cyclic freezing–thawing. *Journal of Materials Chemistry A, 2*, 350–359. https://doi.org/10.1039/C3TA13629A

Jiang, F., & Hsieh, Y.-L. (2014b). Amphiphilic superabsorbent cellulose nanofibril aerogels. *Journal of Materials Chemistry A, 2*, 6337–6342. https://doi.org/10.1039/C4TA00743C

Jiang, F., & Hsieh, Y.-L. (2013). Chemically and mechanically isolated nanocellulose and their self-assembled structures. *Carbohydrate Polymers, 95*, 32–40. https://doi.org/10.1016/j.carbpol.2013.02.022

Jiang, F., & Hsieh, Y.-L. (2016). Self-assembling of TEMPO oxidized cellulose nanofibrils as affected by protonation of surface carboxyls and drying methods. *ACS Sustainable Chemistry & Engineering, 4*, 1041–1049. https://doi.org/10.1021/acssuschemeng.5b01123

Kalimuldina, G., Turdakyn, N., Abay, I., Medeubayev, A., & Bakenov, Z. (2020). A review of piezoelectric PVDF film by electrospinning and its applications. *Sensors, 20*(18), 5214. https://doi.org/10.3390/s20185214

Khan, U., O'Neill, A., Lotya, M., De, S., & Coleman, J. N. (2010). High-concentration solvent exfoliation of graphene. *Small, 6*, 864–871. https://doi.org/10.1002/smll.200902066

Kim, T. Y., Jung, G., Yoo, S., Suh, K. S., & Ruoff, R. S. (2013). Activated graphene-based carbons as supercapacitor electrodes with macro- and mesopores. *ACS Nano, 7*(8), 6899–6905. https://doi.org/10.1021/nn402077v

Lee, C., Wei, X., Kysar, J. W., & Hone, J. (2008). Measurement of the elastic properties and intrinsic strength of monolayer graphene. *Science, 321*, 385–388. https://doi.org/10.1126/science.1157996

Li, Y., Zhu, H., Shen, F., Wan, J., Lacey, S., Fang, Z., et al. (2015). Nanocellulose as green dispersant for two-dimensional energy materials. *Nano Energy, 13*, 346–354. https://doi.org/10.1016/j.nanoen.2015.02.015

Lingaiah, S., & Shivakumar, K. (2013). Electrospun high temperature polyimide nanopaper. *European Polymer Journal, 49*, 2101–2108. https://doi.org/10.1016/j.eurpolymj.2013.04.030

Liu, H., Qing, H., Li, Z., Han, Y. L., Lin, M., Yang, H., et al. (2017). Paper: A promising material for human-friendly functional wearable electronics. *Materials Science and Engineering R: Reports, 112*, 1–22. https://doi.org/10.1016/j.mser.2017.01.001

Liu, W., Liu, K., Du, H., Zheng, T., Zhang, N., Xu, T., et al. (2022). Cellulose nanopaper: Fabrication, functionalization, and applications. *Nano-Micro Letters, 14*, 1–27. https://doi.org/10.1007/s40820-022-00849-x

Lotya, M., Hernandez, Y., King, P. J., Smith, R. J., Nicolosi, V., Karlsson, L. S., et al. (2009). Liquid phase production of graphene by exfoliation of graphite in surfactant/water solutions. *Journal of the American Chemical Society, 131*(10), 3611–3620. https://doi.org/10.1021/ja807449u

Lotya, M., King, P. J., Khan, U., De, S., & Coleman, J. N. (2010). High-concentration, surfactant-stabilized graphene dispersions. *ACS Nano, 4*, 3155–3162. https://doi.org/10.1021/nn1005304

Lu, H., Behm, M., Leijonmarck, S., Lindbergh, G., & Cornell, A. (2016). Flexible paper electrodes for Li-ion batteries using low amount of TEMPO-oxidized cellulose nanofibrils as binder. *ACS Applied Materials & Interfaces, 8*, 18097–18106. https://doi.org/10.1021/acsami.6b05016

Lu, P., & Hsieh, Y.-L. (2012). Preparation and characterization of cellulose nanocrystals from rice straw. *Carbohydrate Polymers, 87*, 564–573. https://doi.org/10.1016/j.carbpol.2011.08.022

Luo, Q., Shen, H., Zhou, G., & Xu, X. (2023). A mini-review on the dielectric properties of cellulose and nanocellulose-based materials as electronic components. *Carbohydrate Polymers, 303*, 120449. https://doi.org/10.1016/j.carbpol.2022.120449

Mirabedini, S. M., Arabi, H., Salem, A., & Asiaban, S. (2007). Effect of low-pressure O_2 and Ar plasma treatments on the wettability and morphology of biaxial-oriented polypropylene (BOPP) film. *Progress in Organic Coatings, 60*, 105–111. https://doi.org/10.1016/j.porgcoat.2007.07.007

Naghdi, T., Yousefi, H., Sharifi, A. R., Golmohammadi, H., & Golmohammadi, H. (2020). Nanopaper-based sensors. *Comprehensive Analytical Chemistry, 89*, 257–312. https://doi.org/10.1016/bs.coac.2020.02.003

Nair, R. R., Blake, P., Grigorenko, A. N., Novoselov, K. S., Booth, T. J., Stauber, T., et al. (2008). Fine structure constant defines visual transparency of graphene. *Science, 320*(5881), 1308. https://doi.org/10.1126/science.1156965

Nawawi, F. W., Lee, K. Y., Kontturi, E., Koon, Y. K., Eero, M., & Bismarck, R. J. (2019). Chitin nanopaper from mushroom extract: Natural composite of nanofibers and glucan from a single biobased source. *ACS Sustainable Chemistry & Engineering, 7*, 6492–6496. https://doi.org/10.1021/acssuschemeng.9b00721

Notley, S. M. (2012). Highly concentrated aqueous suspensions of graphene through ultrasonic exfoliation with continuous surfactant addition. *Langmuir, 28*, 14110–14113. https://doi.org/10.1021/la302750e

Park, J., Seo, J. H., Yeom, S. W., Yao, C., Yang, V. W., Cai, Z., et al. (2018). Flexible and transparent organic phototransistors on biodegradable cellulose nanofibrillated fiber substrates. *Advanced Optical Materials, 6*(9), 1701140. https://doi.org/10.1002/adom.201701140

Park, S., An, J., Suk, J. W., & Ruoff, R. S. (2010). Graphene-based actuators. *Small, 6*, 210–212. https://doi.org/10.1002/smll.200901877

Paton, K. R., Varrla, E., Backes, C., & Smith, R. J. (2014). Scalable production of large quantities of defect-free few-layer graphene by shear exfoliation in liquids. *Nature Materials, 13*, 624–630. https://doi.org/10.1038/nmat3944

Prakoso, F. A. H., Indiarto, R., & Utama, G. L. (2023). Edible film casting techniques and materials and their utilization for meat-based product packaging. *Polymers, 15*, 2800. https://doi.org/10.3390/polym15132800

Prateek, Thakur, V. K., & Gupta, R. K. (2016). Recent progress on ferroelectric polymer-based nanocomposites for high energy density capacitors: Synthesis, dielectric properties, and future aspects. *Chemical Reviews, 116*, 4260–4317. https://doi.org/10.1021/acs.chemrev.5b00495

Raabe, D., Romano, P., Sachs, C., Sawalmih, A. A., Brokmeier, H. G., Yi, S. B., et al. (2005). Discovery of a honeycomb structure in the twisted plywood patterns of fibrous biological nanocomposite tissue. *Journal of Crystal Growth, 283*, 1–7. https://doi.org/10.1016/j.jcrysgro.2005.05.077

Raghavan, B., Soto, H., & Lozano, K. (2013). Fabrication of melt spun polypropylene nanofibers by force spinning. *Journal of Engineered Fibers and Fabrics, 8*, 52–60.

Rebouillat, S., & Pla, F. (2013). State of the art manufacturing and engineering of nanocellulose: A review of available data and industrial applications. *Journal of Biomaterials and Nanobiotechnology, 4*, 165–188. https://doi.org/10.4236/jbnb.2013.42022

Saito, T., Kimura, S., Nishiyama, Y., & Isogai, A. (2007). Cellulose nanofibers prepared by TEMPO-mediated oxidation of native cellulose. *Biomacromolecules, 8*, 2485. https://doi.org/10.1021/bm0703970

Saito, T., Kuramae, R., Wohlert, J., Berglund, L. A., & Isogai, A. (2013). An ultrastrong nanofibrillar biomaterial: The strength of single cellulose nanofibrils revealed via sonication-induced fragmentation. *Biomacromolecules, 14*, 248–253. https://doi.org/10.1021/bm301674e

Sehaqui, H., Mushi, N. E., Morimune, S., Salajkova, M., Nishino, T., & Berglund, L. A. (2012). Cellulose nanofiber orientation in nanopaper and nanocomposites by cold drawing. *ACS Applied Materials & Interfaces, 4*, 1043–1049. https://doi.org/10.1021/am2016766

Shen, H., Peng, S., Luo, Q., Zhou, J., He, J. H., Zhou, G. F., et al. (2023). Nanopaper electronics. *Advanced Functional Materials, 33*(23), 2213820. https://doi.org/10.1002/adfm.202213820

Shimizu, M., Fukuzumi, H., Saito, T., & Isogai, A. (2013). Preparation and characterization of TEMPO-oxidized cellulose nanofibrils with ammonium carboxylate groups. *International Journal of Biological Macromolecules, 59*, 99–104. https://doi.org/10.1016/j.ijbiomac.2013.04.021

Smith, R. J., King, P. J., Lotya, M., Wirtz, C., Khan, U., De, S., et al. (2011). Large-scale exfoliation of inorganic layered compounds in aqueous surfactant solutions. *Advanced Materials, 23*, 3944–3948. https://doi.org/10.1002/adma.201102584

Tanpichai, S., Quero, F., Nogi, M., Yano, H., Young, R. J., Lindström, T., et al. (2012). Effective Young's modulus of bacterial and microfibrillated cellulose fibrils in fibrous networks. *Biomacromolecules, 13*, 1340–1349. https://doi.org/10.1021/bm300042t

Wong, E. W., Sheehan, P. E., & Lieber, C. M. (1997). Nanobeam mechanics: Elasticity, strength, and toughness of nanorods and nanotubes. *Science, 277*, 1971–1975. https://doi.org/10.1126/science.277.5334.1971

Xu, X., & Hsieh, Y. (2019). Aqueous exfoliated graphene by amphiphilic nanocellulose and its application in moisture- Responsive foldable actuators. *Nanoscale, 11*, 11719–11729. https://doi.org/10.1039/c9nr01602c

Xu, X., Wang, H., Jiang, L., Wang, X., Payne, S. A., Zhu, J. Y., et al. (2014). Comparison between cellulose nanocrystal and cellulose nanofibril reinforced poly(ethylene oxide) nanofibers and their novel shish-kebab-like crystalline structures. *Macromolecules, 47*, 3409–3416. https://doi.org/10.1021/ma402627j

Yousefi, H., Nishino, T., Faezipour, M., Ebrahimi, G., & Shakeri, A. (2011). Direct fabrication of all-cellulose nanocomposite from cellulose microfibers using ionic liquid-based nanowelding. *Biomacromolecules, 12*(11), 4080–4085. https://doi.org/10.1021/bm201147a

Yu, M., Lourie, O., Dyer, M. J., Moloni, K., Kelly, T. F., & Ruoff, R. S. (2000). Strength and breaking mechanism of multiwall carbon nanotubes under tensile load. *Science, 287*, 637–640. https://doi.org/10.1126/science.287.5453.637

Zhao, Y., Cabrera, E. D., Castro, J. M., & Lee, L. J. (2017). Carbon nanopaper: A platform to high-performance multifunctional composites. In W. Huang (Ed.), *Nanopaper* (pp. 87–120). Elsevier. https://doi.org/10.1016/B978-0-323-48019-2.00004-9

Chapter 12
Transparent Paper

Ana Almeida

12.1 Historical Point of View

Transparent materials have a fascinating history. Their production and use date to the Middle Ages and have evolved significantly up to the present day. Historically, there are documents written in the nineteenth century that refer recipes that can be used to produce translucent papers. The materials selected to produce translucent supports, used for example to trace drawings, included parchment, paper, oils, resins and drying agents. Transparent paper appears later than transparent parchment, and unfortunately, they are not well described in the catalogues. In the second half of the nineteenth century, recipes for impregnated or coated papers with linseed oil, copal resin and varnish made from sandarac and Venice turpentine dissolved in alcohol were mentioned (Laroque, 2004). Small-scale production of these transparent materials and industrial production coexisted during the nineteenth century before disappearing (Laroque, 2004). Cellulose was isolated by Anselme Payen in 1838, and he determined its empirical formula, $C_6H_{10}O_5$, by elemental analysis (Fisher, 1989; Payen, 1838). John Mercer, in 1844, discovered a technique to strengthen the fibres and increase their dyeing potential, now known as mercerization, that consisted of treating cellulose with strong alkalis (Wurtz & Friedel, 1876). This discovery combined with the increased consumption of newspapers led to a revolution in the papermaking industry and started a race for new raw materials, namely all types of wood-like materials (Laroque, 2004). The ever-growing concern for the environment has fuelled a rising fascination with cellulose and cellulose-based materials. Several researchers have embarked on the journey of isolating, characterizing and discovering novel uses for cellulose, one of the most abundant

A. Almeida (✉)
NOVA School of Science and Technology, Caparica, Portugal
e-mail: ana.almeida@fct.unl.pt

G. Korotcenkov (ed.), *The Handbook of Paper-Based Sensors and Devices*,
https://doi.org/10.1007/978-3-031-91080-7_12

low-cost and renewable materials on the planet (Magalhães & Almeida, 2023; Qiu & Hu, 2013).

12.2 Optical Properties of Paper

Paper is a material composed mainly of cellulosic fibres interconnected by hydrogen bonds consequence of water evaporation during production. The fibres, depending on the source, can be divided into softwood and hardwood pulps and consist of cellulose, lignin and hemicellulose. Paper can also be composed of mineral fillers and chemical additives (Jurič et al., 2013). The use of fillers enhances the optical properties of paper by increasing its light scattering capacity thought the augmentation of the specific surface area. These additives, such as calcium carbonate and kaolin, are added during the papermaking process to fill the gaps between fibres (Koivunen et al., 2009; Vahur et al., 2019). The appearance of paper is governed by its interaction with visible light. This interaction is influenced not only by the intrinsic properties of the paper but also by the conditions of illumination and the observer's perceptual response. The paper's surface characteristics, such as texture and coating, play a crucial role in how light is absorbed, reflected and scattered (Farnood, 2009). The conventional paper has a porous structure, high surface roughness and its optically opaque. Fibres in regular paper are arranged into a random fibrous network with several micro-sized air cavities, as represented in Fig. 12.1a. The typical fibre size is much larger than the optical wavelength in the regular paper so when

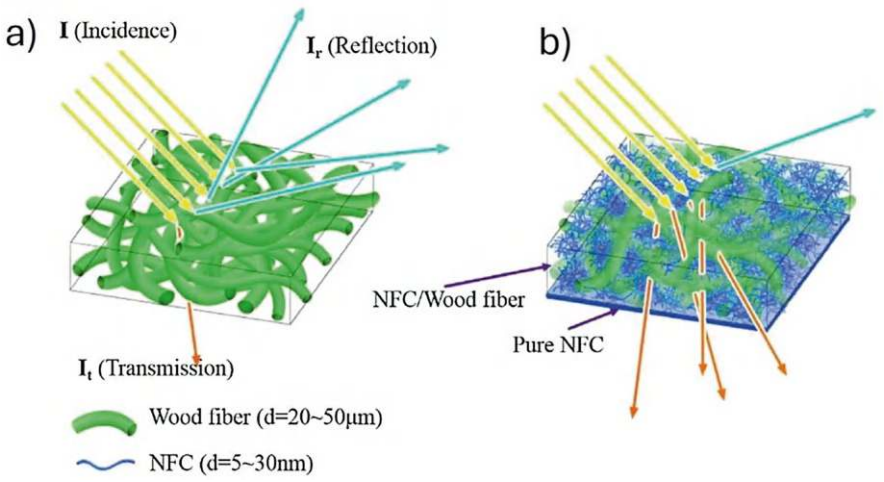

Fig. 12.1 Scheme representing (**a**) regular paper composed of micro-sized wood fibres and (**b**) regular paper infiltrated with nanofibrillated cellulose to decrease light scattering. The widths of the wood fibre and cellulose nanofibrils (CNF) are 10–50 μm and 5–30 nm, respectively. Reprinted with permission from Fang et al. (2013). Copywrite 2013: The Royal Society of Chemistry

a beam of incident light strikes the surface, the incident light is heavily reflected by the porous structure due to the intensive light scattering effect caused by the mismatch of the refractive index between cellulose and air. Therefore, conventional paper is opaque because only a small percentage of incident light propagates through the regular paper. If the voids present in the conventional paper are filled with cellulose nanofibrils (CNF), diameters of 5–30 nm as represented in Fig. 12.1b, the light scattering reduction occurs due to a decrease in the number of open spaces. There is also matching of refractive index of the hybrid paper (wood fibres and NFC) and air, which allows more light to pass through the paper instead of getting scattered.

Transparent paper made primarily from cellulose is biodegradable and derived from renewable resources. It offers optical transparency and can be engineered to be used in several applications. Transparent paper is gaining traction in flexible electronics, sensors and packing due to its lightweight and ecofriendly nature. The fact that is biodegradable makes it a more sustainable alternative to plastics that are typically synthetic and derived from petroleum-based resources.

12.3 Source, Production and Structure of Transparent Paper

The two main building blocks to produce transparent paper are cellulose and chitin, the two most abundant polymers in nature. Cellulose is the main molecule in the cell walls of higher plants but also can be produced by some species of bacteria and tunicates, a group of marine animals (Magalhães & Almeida, 2023). Cellulose has a large number of hydroxy groups, three per anhydroglucose unit (AGU), and every second AGU ring is rotated 180° in the plane to accommodate the preferred bond angles of the acetal oxygen bridges. Cellulose, a linear-chain polymer, has a repetitive unit called cellobiose. Nanoparticles can be obtained from cellulose using a top-down methodology that uses mechanical or chemical methods to deconstruct the material. Due to their highly reactive surface, the resulting nanomaterials can be easily chemically modified to obtain the desired properties. According to the American Paper and Pulp Association (TAPPI WI3021, Peachtree Corners, GA), we can define cellulose nanomaterials according to the diagram in Fig. 12.2 (Magalhães & Almeida, 2023; Mariano et al., 2014).

Cellulose microfibrils (CMF), with widths between 10 and 100 μm and lengths from 0.5 to 10 μm, are prepared from suspensions of wood-based materials through mechanical processing, such as high-pressure homogenizers. Cellulose nanofibrils (CNFs) are commonly prepared through mechanical delamination of softwood pulp using high-pressure homogenizers when no pretreatment is used or after chemical or enzymatic pretreatment to facilitate the mechanical disintegration of the material. Cellulose nanocrystals (CNCs), with widths between 3 and 10 nm and aspect ratios in the range of 5–50, can be produced by the removal of the amorphous regions from pure cellulose sources by acid hydrolysis. Cellulose stiff, short and rod-like

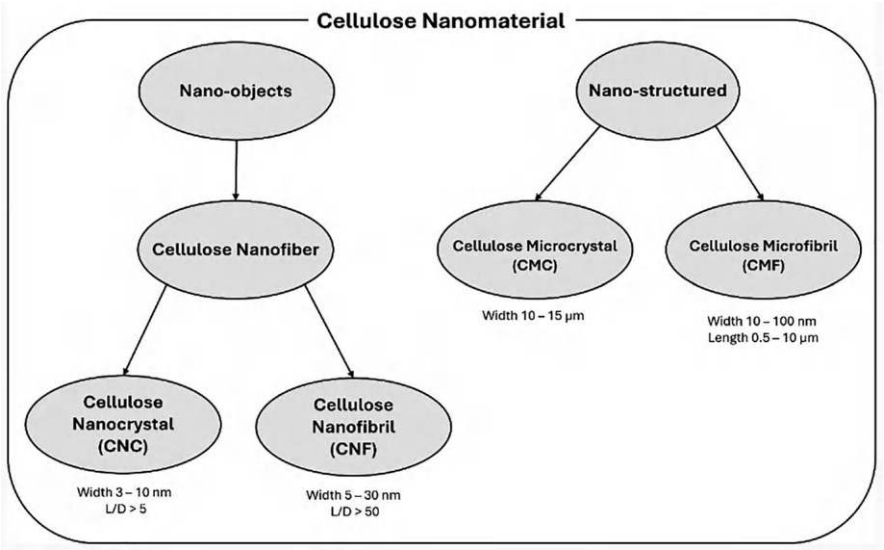

Fig. 12.2 The American Paper and Pulp Association (TAPPI WI3021) classification of cellulose nanomaterials. Adapted with permission from Mariano et al. (2014). Copyright 2014: Wiley

nanocrystals, obtained under thoroughly controlled temperature, agitation and time, can also be described as nanowhiskers (Magalhães & Almeida, 2023).

Chitin $(C_8H_{13}O_5N)_n$, the second most abundant polymer after cellulose, is a linear chain polymer whose repeating unit is $\beta(1 \rightarrow 4)$-2-acetamido-2-deoxy-β-D-glucose, with the characteristic acetamide group on the C2 position. Like cellulose, chitin is a mechanically robust polymer, nontoxic, biocompatible and biodegradable. It can be found in the cell wall of fungi and yeast, in the endoskeleton of cephalopods and in the exoskeleton of arthropods, such as crustaceans, molluscs and insects (Kumari & Kishor, 2020). Chitin, like cellulose, is insoluble in water and common organic solvents. To obtain chitin nanofibers, a series of chemical treatments followed by mechanical processing must be performed to remove unwanted compounds, such as proteins and minerals present in the biological source. After mechanical grinding, chitin gel of highly uniform nanofibers with widths of 10–20 nm is formed. To obtain chitin nanofibers, it is vital to use a method without drying at any point since after drying strong interfibrillar hydrogen bonds are formed, making it very difficult to disintegrate the film (Ifuku & Saimoto, 2012).

12.4 Cellulose and Chitin Nanofiber Transparent Paper

In 2009, Nogi et al. (2009) reported optically transparent "cellulose nanofiber paper" obtained from wood flour. The optical transparency was obtained by smoothing the nanofibre surface by polishing the sheet. Light scattering is partly suppressed

by deforming the fibres under temperature and pressure load prior to the polishing step. The surface-smoothing strategy allowed not only to obtain an optically transparent paper sheet but also contributed to a barrier to moisture, making suitable to be used without further chemical modification (Nogi et al., 2009). Biodegradable regenerated cellulose transparent films prepared from cotton linter pulps using a mixture of NaOH and urea in distilled water pre-cooled to −12.6 °C were reported in 2008. The prepared films exhibited structural homogeneity, good tensile strength and excellent optical transmittance (Qi et al., 2009).

Yousefi et al. (2011) reported the fabrication of all-cellulose nanocomposite transparent paper using solvent-based nanowelding. As solvent the authors used the ionic liquid 1-butyl-3-methylimidazolium chloride (BMIMCl), considered to be a green solvent due to its recyclability, thermal stability and low vapor pressure. The nanopaper produced from canola straw was transparent (76% at 800 nm) and presented good mechanical properties (Young's modulus of 20 GPa and tensile strength of 208 MPa) and complete barrier to air (Yousefi et al., 2011). High optical transparent and bendable cellulose films prepared from regenerated cellulose aqueous alkali solutions, with high mechanical strength and high oxygen barrier capabilities, were mentioned by Yang et al. (2011). The authors used as cellulose source filter paper pulp, microcrystalline cellulose powder and softwood kraft pulp and obtained a sheet-like hydrogel, that after washing and air drying presented a range of thickness from 30 to 60 μm (Yang et al., 2011).

Later in 2013, Nogi et al. (2013) reported an optically transparent nanopaper, assembled by a simple process that involved casting of nanofiber suspension, that maintains its transparency even when it's heated at 150 °C. This transparent paper is foldable, making it suitable for future applications that require a continuous roll-to-roll processing (Nogi et al., 2013). Transparent and flexible regenerated cellulose film can be obtained after dissolving cellulose fibres with 1-ethyl-3-methylimidazolium phosphorous methyl ester ionic liquid and regenerating the cellulose chains, due to establishment of new hydrogen bonds, in water (Zhu, Xiao, et al., 2013). In 2014, Fang, Zhu, Yuan, et al. (2014) reported the development of a transparent paper with optical transparency ~96% and haze of ~60%, making it an ideal candidate to be used in solar cell devices. Nanofibrillated cellulose obtained from TEMPO-oxidized wood pulp was diluted with water to 0.2 wt% and filtered using a PVDF 0.65 μm membrane filter. The obtained film was dried at room temperature under pressure between two regular filter papers. The TEMPO-oxidized process allowed for obtaining a wood pulp with high fragment content, which led to a high packing density in the transparent paper when compared to regular paper. The high packing density contributed not only to increasing the mechanical strength but also the optical transmittance observed for the transparent paper (Fang, Zhu, Yuan, et al., 2014). The previous works took advantage of reduction of cellulose fibre to nanofibrils to a diameter much smaller than the light wavelength, paper pore size as well as fibre packing to attenuate back scattering and increase of transparency of the material (Zhu, Parvinian, et al., 2013). In Fig. 12.3a, the influence of fibre diameter on optical transparency of the paper produced is evident for papers of the same thickness, transparency increases as fibre diameter decreases.

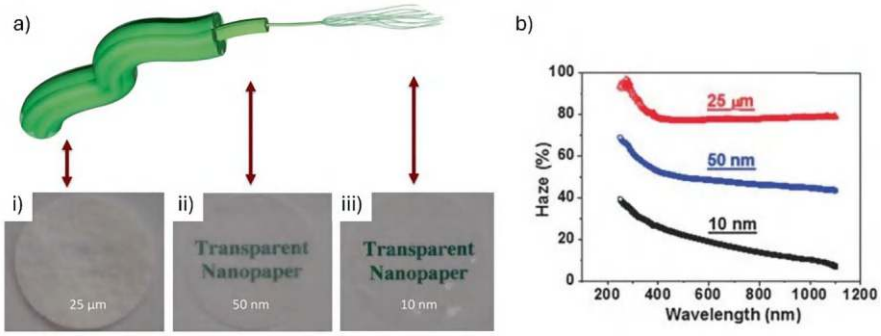

Fig. 12.3 (**a**) Schematic of the hierarchical structure for cellulose fibres and cellulose paper, with thickness of 40 mm, produced from fibres with different diameters: (i) 25 µm, (ii) 50 nm and (iii) 10 nm. As the fibre diameter decreases, the optical transparency increases. (**b**) Optical haze for paper with different fibre diameters, where it is possible to observe that larger cellulose fibres lead to larger haze values. Reprinted with permission from Zhu, Parvinian, et al. (2013). Copyright 2013: The Royal Society of Chemistry

The mechanical properties, transparency and haze of the substrates can be tuned by adjusting the fibre diameters and packing densities, making them suitable building blocks for engineering the next generation of transparent substrates with tailored optical and mechanical properties. Mesoporous transparent substrates built from cellulose nanofibres with tuneable optical properties, directly related to the fibre size, were reported in 2016 by Zhu, Song, et al. (2016) (Fig. 12.3b). The authors produced two different transparent papers with transmittance higher than 90%, where one presented haze <1.0% and other with haze >90%. The difference in haze was achieved by simply changing the packing and size of the cellulose fibres. The super-clear paper was produced with nanofibres obtained by TEMPO-oxidized wood pulp with uniform size (diameter ~10–20 nm and length ~500 nm) by casting method. The super hazy paper is produced via nanowelding of the same microfibres in ionic liquid. After saturation with the ionic liquid, the opaque microfiber paper was in situ hot-pressed to promote the dissolution of the surface of the fibre while maintaining the microfibre backbone. This nanowelding between the nanofibres leads to a high transparent paper because the dissolved cellulose under pressure fills the micro-sized cavities initially occupied with air in the paper, leading to denser packing when compared with regular paper (Zhu, Fang, et al., 2016). Light scattering inside the nanopaper is caused by the difference of the refractive index between the cellulose nanofibres and the air cavities. Hazy transparent nanopapers are mainly composed of cellulose nanofibres (solid cylinders) and some microsized cellulose fibres (hollow cylinders) that cause light scattering inside the nanopaper when flattened (Hsieh et al., 2017).

A clearly transparent nanopaper produced from alkaline-treated holocellulose pulp and TEMPO-oxidized nanofibres was reported in 2018 by Kasuga et al. (2018). The nanopaper haze depended on dispersion concentration obtained by combining dilution in water and sonication treatment followed by drying at 55 °C under

relative humidity of 25% overnight (Kasuga et al., 2018). Isobe et al. (2018) reported a new strategy to produce transparent cellulose nanopaper from concentrated nanofiber dispersions. The clear transparent nanopaper was obtained after drying at 80% relative humidity a highly concentrated (0.24–1.81 wt%) nanocellulose gel-like casted dispersion. This methodology allowed the authors to obtain a low-haze transparent nanopaper without the characteristic long drying time (Isobe et al., 2018). Regenerated transparent cellulose film prepared by dissolution of commercial coniferous pulp in the ionic liquid 1-allyl-3-methyl imidazolium chloride followed by regeneration in water was later reported in 2019 (Ma et al., 2019). To reduce the production time to obtain a transparent cellulose nanopaper, the temperature and humidity must be carefully controlled. TEMPO-oxidized cellulose nanofiber (3–5 nm wide) dispersion was casted into a petri dish and dried at temperatures ranging from 45 °C to 85 °C and relative humidities ranging from 35% to 75%. An airflow system removed the water vapor at the water/air interface and reduced the drying time. This multi-stage drying method using a humidity controlled chamber with an air flow system to obtain a transparent nanopaper with low haze was reported by (Li et al., 2020).

Septevani et al. (2022) reported a systematic study where the cellulose nanopaper was produced using oil palm empty fruit bunches. Properties such as transparency and tensile strength depended on the crystallinity and aspect ratio of the nanocellulose obtained using acid hydrolysis (sulphuric acid and phosphoric acid) (Septevani et al., 2022). Recently, a one-step method to produce transparent paper from modified bamboo nanocellulose using ball-milling and 3,4-dichlorophenyl isocyanate was reported by Liu et al. (2023). The authors mentioned that the nanopaper produced with modified nanocellulose was more transparent than unmodified nanocellulose and exhibited high ultraviolet light blocking capability (Liu et al., 2023). Huang et al. (2023) reported an air-permeable transparent cellulose nanopaper produced using softwood bleached kraft pulp. The clear transparent air-permeable nanopaper was prepared through a filtration-based solvent exchange process, where the water dispersion of TEMPO-oxidized cellulose nanofibres is transitioned to ethanol and hexane, followed by drying under continuous vacuum filtration. The obtained nanopaper had a porous structure (53.4%) with an individual dispersed nanofiber network, high transparency (92.9%), low haze value (7.22%) and air permeability of 7.8×10^6 mL μm m^{-2} day^{-1} kPa^{-1}. The possibility to obtain transparent permeable paper presented in this work is pointed out as an auguring way to develop clearly transparent, air-permeable sustainable materials (Huang et al., 2023). Mayer et al. (2024) proposed an alkaline treatment process to increase the optical transparency of the cellulose nanopaper. The mercerisation caused the partial conversion of cellulose I into II, contributing to increased strain to failure and toughness of the treated nanopaper. Additionally, the mercerisation contributed to reducing the porosity of the nanopaper and thus increasing the transparency (Mayer et al., 2024).

In 1992, Fink demonstrated the possibility of transforming wood into a transparent material (Fink, 1992), but it was abandoned until 2016, when the application of this material was rediscovered (Li et al., 2016; Zhu, Song, et al., 2016). The

production of transparent wood requires firstly the removal or modification of lignin using acidic/alkali treatments or redox agents. To ensure the production of a transparent material during these procedures, it is very important to accurately control the process conditions, such as concentration, treatment duration, pH and temperature range. Besides this, it is pivotal to prevent dehydration of the material to avoid the formation of undesirable chemical groups that impact the quality and mechanical behaviour of the final material. After lignin removal, there are two possible options to obtain transparent wood: direct cell wall densification or infiltration with a resin and its subsequent polymerization. These methodologies, depending on the type of wood used, are suitable to obtain transparent and flexible films (Mariani & Malucelli, 2024). In order to avoid structural failure after lignin removal, such as delamination, fragility and instability, and obtain a highly stable, rigid and well-preserved substrate, a lignin-retaining approach is adopted to bleach the wood and remove the chromophores (Li et al., 2017). Natural wood selectively delignified with its original growth ring patterns preserved after epoxy infiltration was reported in 2020. The aesthetic transparent wood obtained combined excellent optical transparency (transmittance of ~80% and haze of ~93%), UV-blocking ability, low thermal conductivity (0.24 W m^{-1} K^{-1}), high longitudinal tensile strength (91.95 MPa) and good scalability (Mi et al., 2020). In 2021, transparent wood composite sheets were obtained after dehydrated bleached samples of poplar wood were impregnated with epoxy resin and allowed to dry and cure at room temperature, as represented by the scheme in Fig. 12.4a. The bleaching process changes natural wood veneers to bright white, but 89.3% of lignin was preserved after bleaching, which is vital to maintain structural stability of the wood framework. After polymer infiltration the macro-pores, voids and lumens of the bleached wood were completely occupied with the epoxy resin, as observed in Fig. 12.4b. The optical transmittance obtained for the transparent wood (76.92% at 460 nm and ~83.53% at 550 nm) is comparable to that of transparent epoxy (88.80% and 90.21% at 460 nm and 550 nm, respectively) samples (Bisht et al., 2021). Considering the properties of transparent wood, this material can be the sustainable and scalable solution for applications such as optoelectronics, solar cells, smart windows and energy-saving building materials. But there is a need for the scientific community to invest in more practical solutions considering scalable manufacturing to allow the widespread use of transparent wood-based materials (Li et al., 2018; Mariani & Malucelli, 2024; Mi et al., 2020).

The production of chitin nanofiber transparent papers involves the same techniques and solvent systems as cellulose nanofiber transparent paper. Optically transparent nanofiber chitin sheets were developed by Hu, Zheng, et al. (2013) from commercially dried chitin powders. Combining high-pressure homogenization with grinding, the authors obtained transparent chitin nanopaper with high transparency in the range of visible light (400–800 nm) and transmittance ranging from 72.5% to 88.5% at 600 nm. The nanofibres with widths in the range of 10–50 nm formed a network, with antiparallel extended crystal structure, that contributed to the mechanical properties (tensile strengths >56.30 MPa and Young's moduli >4.59 GPa) (Hu, Li, et al., 2013). Later in 2016, Jin et al. (2016) reported the production of chitin transparent nanofibre paper using the centrifugal casting method combined with

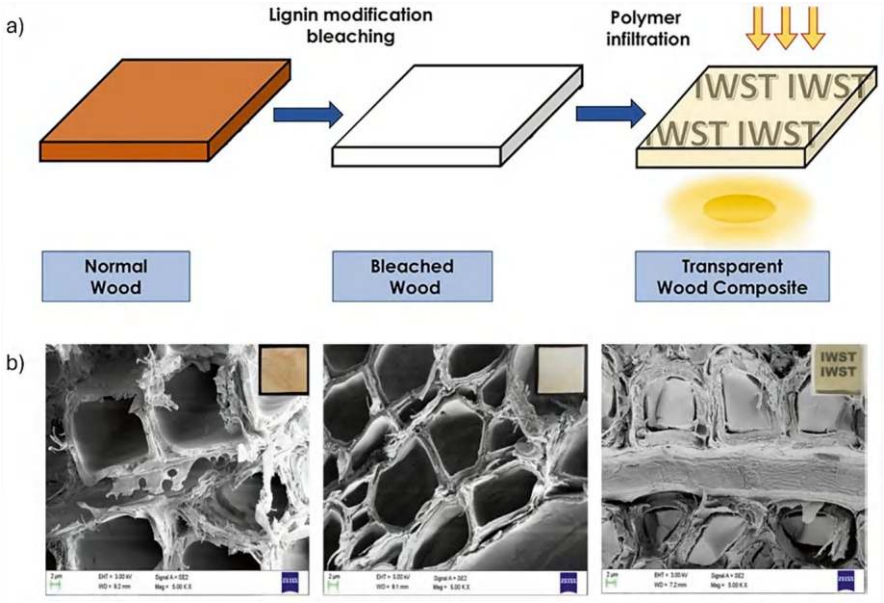

Fig. 12.4 Transparent wood composite: (**a**) schematic diagram of process of preparation of transparent wood composite, and (**b**) scanning electron microscopy images of normal wood, bleached wood and transparent wood composite (from left to right). Reprinted with permission from Bisht et al. (2021). Copyright 2021: Elsevier

vacuum hot pressing at 100 °C to increase flatness and eliminate residual solvent. The solvent evaporation induced self-assembly of the chitin nanofibers in a horizontally in-plane and a non-porous dense film. This chitin nanofibre paper was foldable and printable as common copy paper. Besides the optical transmittance of ≈92%, also presented an elastic modulus of 4.3 GPa (Jin et al., 2016). Recently, Khan et al. (2024) reported the manufacture of transparent thin nanopaper (234.5 μm) from chitin isolated from oyster mushrooms using an alkaline treatment. The nanopaper obtained from the mushroom chitin nanofiber extracts presented a brownish colouration and was opaque with a transmittance of 6–12% (Khan et al., 2024).

12.5 Composite Cellulose Nanopaper

A photoluminescent foldable nanopaper reported in 2015 by Xue et al. (2015) was built using a suction filtration method. Biocompatible zinc selenide (ZnSe) quantum dots (QD), semiconductor nanocrystals with light-emitting properties were synthetized and dispersed in the nanopaper matrix without aggregation. To improve transparency, an acrylic resin was used to coat the QD composite nanopaper. No cracks were observed when the QD nanopaper was rolled. The emission spectra of the QD

nanopaper, emission of cyan fluorescence, presents a red shift of 8 nm when compared to pristine QD; this is a good indicator of the preservation of their crystalline structure during the preparation of the composite paper. The addition of the QD did not compromise the good mechanical properties (tensile strength and Young's modulus) characteristic of the nanopaper. Even though the QD composite nanopaper presents a CTE higher than the nanopaper and can be used in the range from at least 0 to 150 °C, there is still a need to improve the resistance of the paper to water/organic solvents. The QD nanopaper suffered from a decrease in fluorescence intensity after being immersed in water or ethanol due to diffusion of the QD out of the nanopaper matrix (Xue et al., 2015). Park et al. (2017), in 2017, reported a flexible and transparent light-emitting cellulose nanopaper to be used as an active component in optoelectronics (Fig. 12.5). The electroluminescent nanopaper was built, as represented in Fig. 12.5a, where a transparent cellulose nanopaper embedded with luminescent phosphors is uniformly coated, on both sides, with silver nanowires. The green phosphors were positioned at the centre of the transparent nanocellulose paper, as shown in Fig. 12.5b, by sequential filtration of pure nanofibrillated cellulose suspension, nanofibrillated cellulose suspension with phosphors and pure nanofibrillated cellulose suspension. The light-emitting cellulose nanopaper was optically transparent with light emission on both sides (Fig. 12.5c) and colour control by adjusting AC frequency (Park et al., 2017).

Ryu et al. (2021) reported a flexible composite transparent paper with transmittance of ~70% that can withstand over 800% tensile strain. The composite stretchable transparent paper was produced by combining polydimethylsiloxane (PDMS) fibres with cellulose nanocrystals (CNCs). The electrospun PDMS fibres, after cured (diameters of ~1–2 μm), were embedded on a PDMS matrix, and the top surface was coated with a CNC solution to provide a rough and hydrophilic surface texture. To promote the connection between the CNC and the PDMS film, the authors used 2-hydroxyethyl cellulose, a surfactant with both hydrophilic and hydrophobic properties (Ryu et al., 2021). Xu et al. (2016) reported a simple methodology to produce a hybrid cellulose nanopaper, by combining cellulose nanofibrils (CNFs) and cellulose nanocrystals (CNCs), to be used in flexible electrodes. The hybrid cellulose nanopaper, with a layered structure, was produced by vacuum-assisted filtration of a stable suspension of predetermined weight ratio of CNFs and CNCs (first layer) and a suspension of Ag nanowires (second layer), followed by drying in a vacuum oven at 130 °C for 30 min. The CNFs contribute for the nanopaper strength and flexibility, while the CNCs act as rigid nanofiller responsible for low surface roughness and porosity. The optical properties of the cellulose nanopaper, such as transparency and haze, can be tailored by varying the CNC/CNF ratio. By tunning the ratio of CNC and CNF, the transparency and haze can be tuned. The transparency of the suspension CNC/CNF increases with the amount of CNF used (see Fig. 12.6a). The size of the cellulose fibres also influences the transparency, and it is possible to observe that the addition of CNC contributes to significantly increase the direct transparency across the entire wavelength, see Fig. 12.6b, where the direct transmittance of two cellulose nanopapers, one with 0% CNCs and other with 83.3%, and micropaper (Xu et al., 2016).

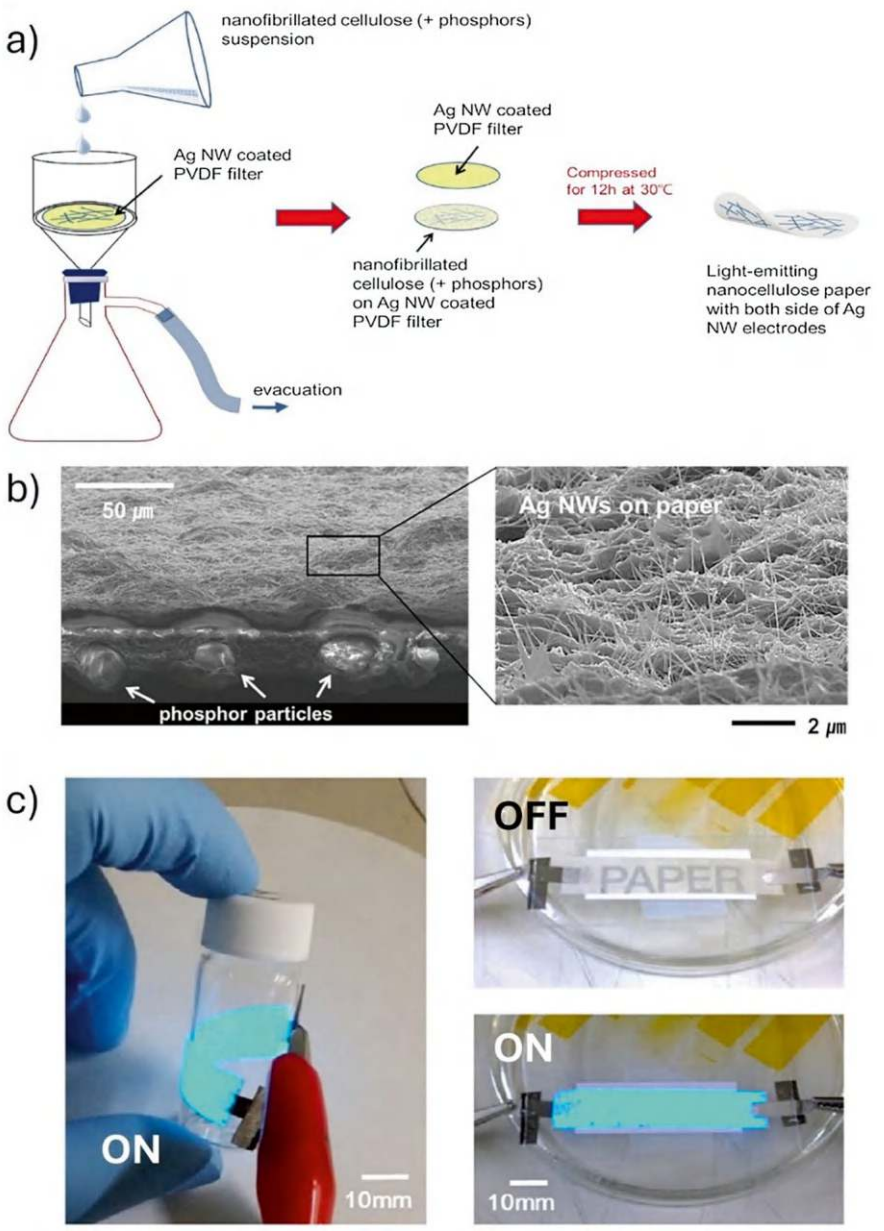

Fig. 12.5 Flexible and transparent light-emitting cellulose nanopaper: (**a**) schematic illustration of the procedure used to prepare, (**b**) scanning electron microscopy images of the cross-section and surface, and (**c**) image of the light-emitting transparent nanopaper exhibiting a blue light in both sides. Note that when the light-emitting nanocellulose paper is close to the background and the light emission is turned ON, it is impossible to observe the background. Adapted with permission from Park et al. (2017). Copyright 2017: Elsevier

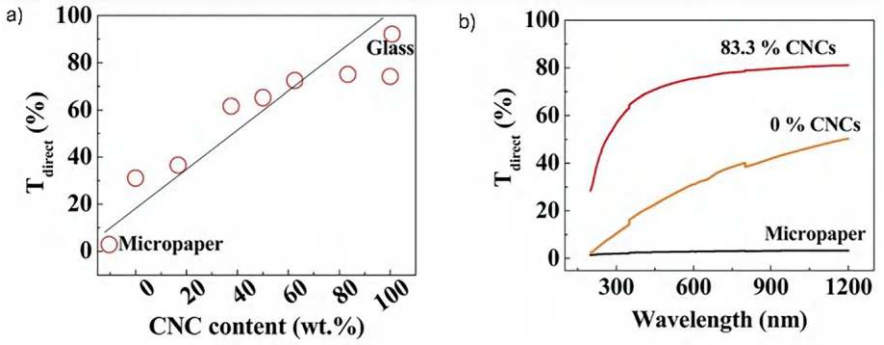

Fig. 12.6 Direct transmittance of the (**a**) micropaper as a function of the cellulose nanocrystals (CNCs) content at 600 nm wavelength and (**b**) micropaper, cellulose nanopaper (0% CNCs), and the hybrid cellulose nanopaper (83.3% CNCs). Reprinted with permission from Xu et al. (2016). Copyright 2016: The Royal Society of Chemistry

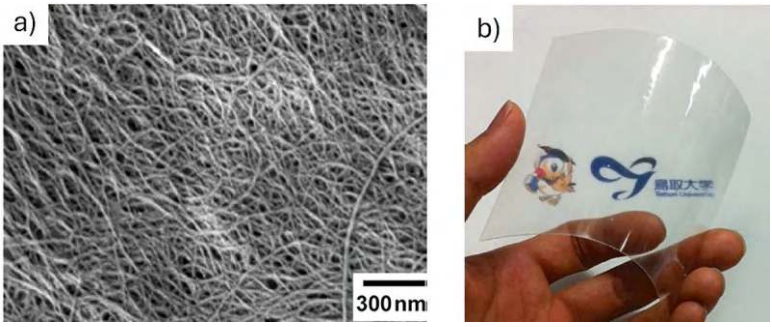

Fig. 12.7 Transparent chitin nanofiber composites: (**a**) scanning electron microscopy images of chitin nanofibers prepared from chitin powder from crab shells and (**b**) composite transparent chitin nanopaper. Reprinted with permission from Ifuku et al. (2011). Copyright 2011: Royal Society of Chemistry

12.6 Composite Chitin Nanopaper

In contrast to the temperature where 5 wt% of the initial mass degraded (T_{d5}) of bulk chitin, which is 285 °C, the thermal stability of chitin diminishes when converted in chitosan nanocrystals (T_{d5} = 277 °C), whereas it experiences a slight increase when transformed into chitosan nanofibers (T_{d5} = 301 °C). When compared to the T_{d5} of cellulose nanocrystals (250 °C), nanochitin materials demonstrate greater thermal stability, highlighting their higher potential to be used as nanofillers for composite transparent materials (Jin et al., 2021; Lam et al., 2012). Chitin nanofibers with a highly uniform structure (width 10–20 nm) and high aspect ratio, as can be seen in Fig. 12.7a, were used to prepare the composite nanopaper. The optically transparent chitin nanocomposite film (Fig. 12.7b), prepared using (meth)acrylic resin,

exhibited not only high transparency but also good tensile strength, flexibility and low thermal expansion (Ifuku et al., 2011).

Vacuum-filtered chitin nanopaper used as reinforcement within a transparent acrylic resin produced from a water suspension of chitin nanofibers, with widths of 20–30 nm obtained from crab shells, was reported in 2011. The dried sheets of chitin nanopaper were impregnated with acrylic resin under reduced pressure for 12 h. The incorporation of the chitin nanofibers contributed to improve the thermal expansion and the mechanical properties while maintaining the transparency of the neat resin. The manufactured composite is presented as a good candidate to be used as substrate in continuous roll-to-roll process to manufacture optoelectronic devices (Shams et al., 2011). Later, Shams and Yano (2015) reported the use of chitin nanofibers in a Pickering emulsion to produce a curved optically transparent composite by hot-pressing vacuum-filtering. The composites prepared using this process exhibited low thermal expansion when compared with the acrylic resin impregnation process. The high level of transparency obtained attributed to the lamellar structure attained when the resin softens, and the droplets are flattened (Shams & Yano, 2015).

12.7 Conductive Transparent Nanopaper

In many applications, paper is required to be conductive in addition to being transparent. Conductive nanopaper can be classified in two groups: electrically conductive ink on nanopaper and electrically conductive nanopaper. The first group is obtained using a two-step methodology were (1) the cellulose nanopaper is prepared by casting, precipitation in a non-solvent or vacuum filtration and drying of nanofibrillated cellulose (NFC) and cellulose nanocrystals (CNCs) and (2) impregnation with conductive polymers and particles (Brooke et al., 2023). Koga et al. (2014) reported a method to produce conductive transparent nanopaper using a simple filtration process. Uniformly connected conductive networks on cellulose nanopaper were assembled by filtration coating of aqueous dispersion of silver nanowires (AgNWs) and carbon nanotubes (CNTs). The conductive network presented a strong adhesion to nanopaper without affecting the transparency (Koga et al., 2014). Silver nanowires can be deposited on regenerated cellulose film, obtained using ionic liquids, to act as a high conductivity electron path. To bypass the loss of transparency, when Ag nanowires are added, the regenerated cellulose conductive film must be treated with nitric acid (HNO_3). The HNO_3 treatment promotes merging between the nanowires as well as between the cellulose nanofibers and Ag nanowires, thereby reducing film roughness and improving transmittance (Ma et al., 2019). In the second group, the conductive polymer or particles are incorporated prior to or during nanopaper production (Brooke et al., 2023). The encapsulation of AgNWs in a fibrous network of bamboo/hemp nanofibrillated cellulose was reported in 2015 (Song et al., 2015). The authors used hybrid hydrogels (bamboo NFC/hemp NFC/AgNWs), HPMC as crosslinker and pressured-extrusion

method under 0.6 MPa of N_2 gas to obtain an ultrathin, conductive nanopaper. The AgNWs were well-dispersed within the hybrid NFC network structure of the composite hybrid transparent nanopaper contributing for the low sheet resistance (1.9 Ohm $sq.^{-1}$) maintaining the high optical transmittance (86.41% at 550 nm). Besides the excellent mechanical performance, namely high flexibility and strong adhesion, the composite nanopaper maintains a stable electric conductivity after several cycles of peeling and bending at 135 °C (Song et al., 2015).

12.8 Applications

For over 15 years, researchers have explored the use of paper to assemble optoelectronic devices such as transistors, batteries, and solar cells (Eder et al., 2004; Fortunato et al., 2008; Poulin et al., 2022), as an "green" and low-lost alternative to plastic substrates. Transparent nanopaper is a promising substrate to replace plastic for electronic and optic applications due to its higher flexibility, printability and stability at high temperatures. Transparent nanopaper has additional useful properties, such being biocompatibile, non-toxicity and biodegradable, making it suitable for applications in biomedical electronics, packaging and sensing. In this section, some examples of recent progresses in these different areas where transparent paper has been used will be addressed.

12.8.1 Transistors

Transistors are fundamental components in electronics, consisting of a three-layer semiconductor material, typically silicon, and have three terminals: the emitter, base and collector. They are crucial components in audio devices, radios, computers and smartphones. Nanopaper with low surface roughness and small pore size produced by filtratering a nanofibrillated cellulose suspension followed by hot pressing was used to assemble a highly transparent and flexible organic field-effect transistor (OFET). The transparent paper made from nanocellulose fibres, average diameter ~10 nm, with a low surface roughness was used as a substrate in a transparent field-effect transistor (Fig. 12.8a). The low surface roughness is pointed as vital to prevent leakage between bottom gate electrodes and the semiconductor layer of the transistor. The transparent nanopaper presented a good ink adsorption due to the 3D fibre structure, making it a good candidate to be used in roll-to-roll printing. The nanopaper OFET produced (Fig. 12.8b), demonstrated good optical transmittance (83.5%) along with strong mechanical and electrical properties, making it a cost-effective candidate for a wide range of electronic applications (Huang et al., 2013).

A high-performance molybdenum disulphide (MoS_2) field-effect transistor (FET) built on transparent paper produced using nanofibrillated cellulose was

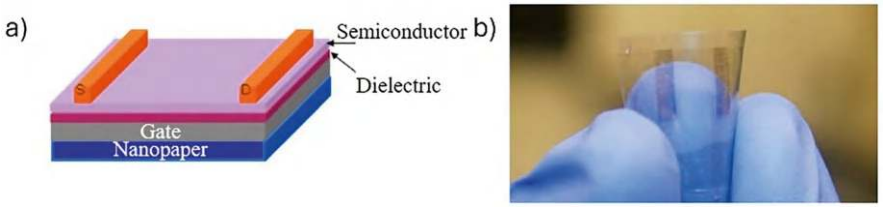

Fig. 12.8 Transparent transistor: (**a**) schematic of the nanopaper flexible organic field-effect transistor with a top contact geometry, and (**b**) picture of a fabricated transparent and flexible nanopaper transistor with transmittance of 89% and 84% at 55 nm, respectively. Adapted with permission from Huang et al. (2013). Copyright 2013 American Chemical Society

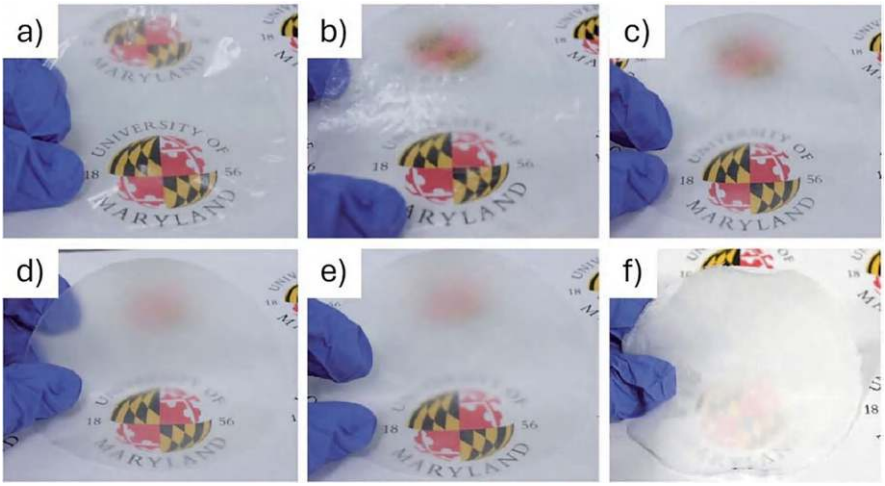

Fig. 12.9 Optical photos of highly transparent papers with tunable optical properties made of TEMPO-oxidized micro-sized wood fibres and/or nanofibrillated cellulose (NFC), with and NFC content of (**a**) 100%, (**b**) 80%, (**c**) 50%, (**d**) 20%, and (**e**) 0%, and of (**f**) regular paper. Reprinted with permission from Fang, Zhu, Bao, et al. (2014). Copyright 2014: The Royal Society of Chemistry

reported in 2014. The authors tuned the transmission haze of the transparent paper by regulating the weight ratio of the TEMPO-oxidized pulp to CNC. In Fig. 12.9, the pattern behind the various papers prepared can be clearly seen independently of the CNC content, and this indicates that the transmission haze of the papers does not influence the optical transparency. In this study, the FET was built by mechanically exfoliating a layer of MoS_2 (20 nm) onto the transparent nanopaper surface, patterning an Au contact electrode (50 nm) on top, depositing an Al_2O_3 layer (200 nm) with an electron-beam evaporator and finally patterning a top gate Au electrode (30 nm). The authors mention that the produced FET showed a large current on/off ratio, $I_{on}/I_{off} \sim 1 \times 10^5$, and indicate that this transparent nanopaper is an ideal candidate to replace plastic substrates in electronics (Fang, Zhu, Bao, et al., 2014).

12.8.2 Solar Cell Devices

Solar cell devices convert sunlight into electricity, are made primarily from semiconductor materials, such as silicon, which absorb photons from sunlight and release electrons to generate electric current. Solar cells are key components for a sustainable energy production helping to reduce the dependence on fossil fuels and greenhouse gas. The use of transparent nanopaper as substrate for the production of optoelectronic devices contributes to increase the light absorption in the active layer of the device (Zhu, Parvinian, et al., 2013). Hu, Li, et al. (2013) reported the use of a flexible transparent nanopaper, made from cellulose nanofibrils, to build a low-cost solar cell with a power conversion of 0.4% with a strong binding between the conductive coating and the nanopaper. The highly transparent nanopaper, with thickness of ~40 μm, was prepared using carboxymethylated nanofibrillated cellulose (NFC), diameter 10 nm and length ~2 μm, by disintegrating softwood cellulose fibres. Tin-doped indium oxide (ITO), carbon nanotubes (CNTs) or silver nanowires (AgNWs) were deposited onto the flexible and transparent nanopaper to make it conductive. In Fig. 12.10a it is possible to observe the transparent conductive nanopaper where the ITO film was deposited using radiofrequency magnetron sputtering. The diffusive transmittance for ITO, CNT and AgNW, at 550 nm is higher than 60% (Fig. 12.10b). The conductive paper performance is comparable with that on the plastic substrate, but the optoelectronic device would have a better performance if the nanopaper maintained the original surface smoothness after device assembly (Hu, Zheng, et al., 2013).

Nogi et al. (2015) reported a foldable nanofiber paper solar cell (Fig. 12.11a) with power conversion efficiency of 3.2%, as high as that of ITO-based solar cells and a short current density of 9.58 mA/cm^2. The nanofiber paper solar cell even maintained the power conversion under and after folding. The optically transparent

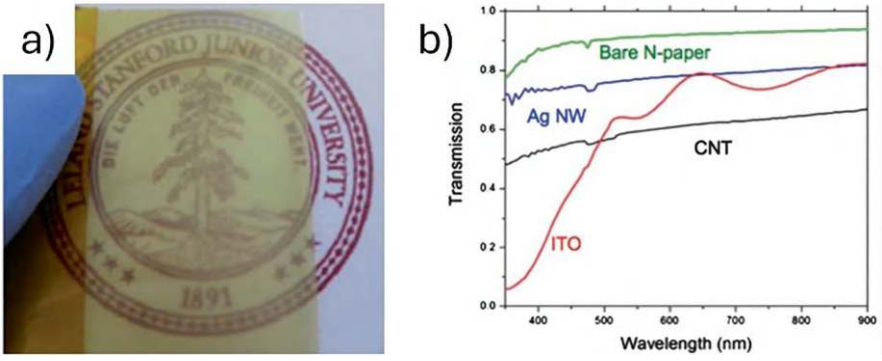

Fig. 12.10 Transparent and conductive nanopaper: (**a**) conductive nanopaper with a 300 nm film of tin-doped indium oxide (ITO) deposition with a performance of 12 Ω sq.$^{-1}$ and 65% total transmittance at 550 nm, and (**b**) diffusive transmittance as function of the wavelength for conductive nanopaper coated with carbon nanotubes (CNTs), ITO, and silver nanowires (AgNWs). Reprinted with permission from Hu, Zheng, et al. (2013). Copyright 2013: The Royal Society of Chemistry

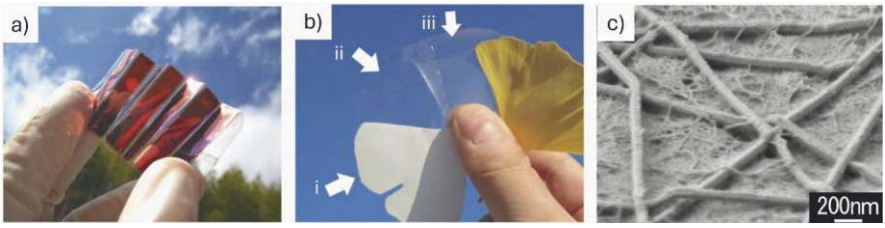

Fig. 12.11 Solar cell devices: (**a**) Photograph of the foldable and lightweight paper solar cell produced using the transparent conductive nanopaper; (**b**) photograph of cellulose (i) traditional write paper, (ii) transparent nanofiber paper, and (iii) transparent conductive nanofiber paper; and (**c**) scanning electron microscopy image of the transparent conductive nanofiber paper, where it is possible to observe the silver nanowires entangled with the cellulose nanofibers. Adapted from Nogi et al. (2015). Published 2015 by Nature Portfolio under the terms of the Creative Commons CC BY4.0

and electrically conductive nanofiber paper (Fig. 12.11b) used as substrate in the solar cell was produced by depositing silver nanowires on a silicon wafer drying plate. After drying, a cellulose nanofiber suspension was deposited on top of the Ag layer. Due to anisotropic shrinkage during drying of the cellulose nanofiber layer, that had a mechanical press effect, the number of electrical contacts between the Ag nanowires increased contributing for the low sheet resistance of 148 Ω/square achieved. The high affinity and high degree of entanglement between the cellulose nanofibers and the Ag nanowires, as can be seen in Fig. 12.11c, contributed for the high conductivity and generation of electrical power, under and after folding (Nogi et al., 2015).

Gao et al. (2019) developed a perovskite solar cell using transparent cellulose nanopaper made from a viscous solution of nanocellulose natural cotton coated with acrylic resin as flexible substrate. The coating with the acrylic resin protected the surface of the cellulose nanopaper from water and improved the transmittance, tensile strength and thermal stability, which facilitated the manufacturing of the flexible solar cell (Gao et al., 2019).

12.8.3 Flexible Optoelectronic Devices

The flexibility of the transparent nanopaper and regenerated cellulose films was pointed out as attractive to fabricate highly flexible organic light-emitting diodes (OLED) devices with stable performance in both flat and bent state. The prepared substrates, with roughness less than 20 nm, proved to be suitable to be used for printed electronics devices and roll-to-roll processing (Zhu, Xiao, et al., 2013). Wang et al. (2014) reported in 2014 the use of transparent cellulose nanofibers to build multilayer thin electrodes using the layer-by-layer assembly method. The produced electrodes proved to be suitable to prepare transparent flexible thin-film supercapacitors with excellent electrochemical performance but instabilities at

long-term cycling (Wang et al., 2014). Zhang et al. (2015) reported flexible conducting electrodes build by embedding a randomly distributed Ag nanowires network onto a translucent paper using the filtration coating process. The Ag nanowires adhesion to the translucent paper and transparency was improved by the encapsulation in a layer of acrylic resin. The electrode obtained using this strategy was transparent with light transmittance of more than 80%, good tensile properties consistent with bending and folding and excellent electrical conductivity. The authors mention that this method could be a boost for large-scale production of flexible optoelectronic devices using cellulose nanofibers (Zhang et al., 2015). In 2016 as a proof-of-concept, Jin et al. (2016) produced an OLED device using a 40 μm-thick chitin nanofiber transparent paper as substrate. The fabricated device exhibited a turn-on voltage of 2.5 V and a maximum luminance of 3890 cd m^{-2}, values nearly equivalent of the reference device built using a high-performance commercial polyethylene naphthalate substrate film (Jin et al., 2016). In 2016, Xu et al. reported a flexible electrode made from a hybrid CNC/CNF transparent paper that was damage-tolerant under folding deformation. The electrical resistance of the electrode developed presents a linear relationship with the tensile strain, making it a great candidate to be used as strain sensor (Xu et al., 2016).

12.8.4 Touch Screens

Fang et al. (2013) claim the production of the first transparent touchscreen, using transparent conductive hybrid cellulose paper, with excellent anti-glare effect. The nanofibrillated cellulose was obtained from wood fibres after TEMPO oxidization and homogenization and the NFC suspension was combined with bleached sulfate softwood pulp to fabricate the hybrid paper. The conductive paper electrode was obtained by dispersing carbon nanotubes onto the transparent paper. The strong interlaced network of micro-sized fibres reinforced by the nanofibrillated cellulose is responsible for the higher resistance to deformations of the transparent hybrid paper when compared to nanopaper. Silver patterns were formed by screen printing method on the conductive hybrid transparent paper to produce the touchscreen. The paper touchscreen was evaluated with the eGalaxTouch software and connected to a computer via USB. Besides being transparent, the produced material was writable and flexible, which are characteristics desirable for printed electronics (Fang et al., 2013).

12.8.5 Intelligent Food Packaging

In 2023, Al Tamimi et al. (2023) reported the use of cellulose nanopaper to build a simple food spoilage detector. The transparent nanopaper (thickness 80–90 μm) was produced using TEMPO-cellulose nanofibrils suspension and vacuum filtration method. To monitor the food freshness, nanopaper disks (6 mm in diameter)

previously immersed in a pH-sensitive dye bromocresol green were placed inside a sealed package containing chicken breast. As the meat spoiled, volatile amines were released, reacting with the dyed nanopaper and causing the disk color to change from yellow to blue. The authors suggest that, given the optical and mechanical properties of the produced nanopaper, along with the ability to display a distinct colour changes based on food freshness, it would be an ideal component for use in intelligent food packaging (Al Tamimi et al., 2023).

12.9 Summary and Outlook

Transparent nanopaper is an exciting option for the production of the next generation of green electronics and the key to alleviating the e-waste crisis. The growing market for biodegradable materials positions nanopaper as a key player in many areas, such as solar cells and flexible displays. Importantly, the use of transparent paper will have a major impact on the environment as it will reduce plastic waste and contribute to the development of a circular economy as it is derived from renewable sources and is biodegradable. However, the use of nanocellulose-based transparent nanopaper on a large scale still presents challenges, namely the high energy and cost of its production. Chitin can be considered as an alternative source for the production of transparent nanopaper, but additional investment from industry and academia is vital for its wider use. It must also be recognized that there are still hurdles to overcome in the production of transparent paper, such as surface roughness, water absorption and low decomposition temperature. Although the material shows promise for various applications, further research is needed to improve scalability, cost-effectiveness and optical and mechanical properties for its successful integration into various industries.

Acknowledgements This work was supported by the Associate Laboratory for Green Chemistry—LAQV, which is financed by national funds from FCT/MCTES (UIDB/50006/2020 and UIDP/50006/2020) and financed by national funds from FCT—Fundação para a Ciência e a Tecnologia, I.P., in the scope of the projects LA/P/0037/2020, UIDP/50025/2020 and UIDB/50025/2020 of the Associate Laboratory Institute of Nanostructures, Nanomodelling and Nanofabrication—i3N. Ana Almeida is grateful for the financial support from Fundação para a Ciência e a Tecnologia (FCT), Portugal, through project 2022.01619.PTDC DOI: 10.54499/2022.01619.PTDC.

References

Al Tamimi, Z., Chen, L., Ji, X., Vanderlaan, G., Gacura, M. D., & Piovesan, D. (2023). Preparation of nanopaper for colorimetric food spoilage indication. *Polymers, 15*, 3098. https://doi.org/10.3390/polym15143098

Bisht, P., Pandey, K. K., & Barshilia, H. C. (2021). Photostable transparent wood composite functionalized with an UV-absorber. *Polymer Degradation and Stability, 189*, 109600. https://doi.org/10.1016/j.polymdegradstab.2021.109600

Brooke, R., Lay, M., Jain, K., Francon, H., Say, M. G., Belaineh, D., et al. (2023). Nanocellulose and PEDOT: PSS composites and their applications. *Polymer Reviews, 63*, 437–477. https://doi.org/10.1080/15583724.2022.2106491

Eder, F., Klauk, H., Halik, M., Zschieschang, U., Schmid, G., & Dehm, C. (2004). Organic electronics on paper. *Applied Physics Letters, 84*, 2673–2675. https://doi.org/10.1063/1.1690870

Fang, Z., Zhu, H., Bao, W., Preston, C., Liu, Z., Dai, J., et al. (2014). Highly transparent paper with tunable haze for green electronics. *Energy & Environmental Science, 7*, 3313–3319. https://doi.org/10.1039/C4EE02236J

Fang, Z., Zhu, H., Preston, C., Han, X., Li, Y., Lee, S., et al. (2013). Highly transparent and writable wood all-cellulose hybrid nanostructured paper. *Journal of Materials Chemistry C, 1*, 6191–6197. https://doi.org/10.1039/C3TC31331J

Fang, Z., Zhu, H., Yuan, Y., Ha, D., Zhu, S., Preston, C., et al. (2014). Novel nanostructured paper with ultrahigh transparency and ultrahigh haze for solar cells. *Nano Letters, 14*, 765–773. https://doi.org/10.1021/nl404101p

Farnood, R. (2009). Optical properties of paper: Theory and practice. *Nordic Pulp & Paper Research Journal, 3*, 273–352. https://doi.org/10.15376/frc.2009.1.273

Fink, S. (1992). Transparent wood—A new approach in the functional study of wood structure. *Holzforschung, 46*, 403–408. https://doi.org/10.1515/hfsg.1992.46.5.403

Fisher, C. H. (1989). Anselm Payen pioneer in natural polymers and industrial chemistry. In R. B. Seymour (Ed.), *Pioneers in polymer science. Chemists and chemistry* (Vol. 10, pp. 47–61). Springer. https://doi.org/10.1007/978-94-009-2407-9_5

Fortunato, E., Correia, N., Barquinha, P., Pereira, L., Goncalves, G., & Martins, R. (2008). High-performance flexible hybrid field-effect transistors based on cellulose fiber paper. *IEEE Electron Device Letters, 29*, 988–990. https://doi.org/10.1109/LED.2008.2001549

Gao, L., Chao, L., Hou, M., Liang, J., Chen, Y., Yu, H.-D., & Huang, W. (2019). Flexible, transparent nanocellulose paper-based perovskite solar cells. *npj Flexible Electronics, 3*, 4. https://doi.org/10.1038/s41528-019-0048-2

Hsieh, M.-C., Koga, H., Suganuma, K., & Nogi, M. (2017). Hazy transparent cellulose nanopaper. *Scientific Reports, 7*, 41590. https://doi.org/10.1038/srep41590

Hu, L., Zheng, G., Yao, J., Liu, N., Weil, B., Eskilsson, M., et al. (2013). Transparent and conductive paper from nanocellulose fibers. *Energy & Environmental Science, 6*, 513–518. https://doi.org/10.1039/C2EE23635D

Hu, Q. Q., Li, D. G., Li, A. J., & Gu, W. B. (2013). Preparation and properties of optically transparent chitin nanofibers sheet by different simple mechanical methods. *Advances in Materials Research, 634-638*, 2232–2237. https://doi.org/10.4028/www.scientific.net/AMR.634-638.2232

Huang, J., Zhu, H., Chen, Y., Preston, C., Rohrbach, K., Cumings, J., & Hu, L. (2013). Highly transparent and flexible nanopaper transistors. *ACS Nano, 7*, 2106–2113. https://doi.org/10.1021/nn304407r

Huang, Y., Kasuga, T., Nogi, M., & Koga, H. (2023). Clearly transparent and air-permeable nanopaper with porous structures consisting of TEMPO-oxidized cellulose nanofibers. *RSC Advances, 13*, 21494–21501. https://doi.org/10.1039/D3RA03840H

Ifuku, S., Morooka, S., Norio Nakagaito, A., Morimoto, M., & Saimoto, H. (2011). Preparation and characterization of optically transparent chitin nanofiber/(meth)acrylic resin composites. *Green Chemistry, 13*, 1708–1711. https://doi.org/10.1039/C1GC15321H

Ifuku, S., & Saimoto, H. (2012). Chitin nanofibers: Preparations, modifications, and applications. *Nanoscale, 4*, 3308–3318. https://doi.org/10.1039/C2NR30383C

Isobe, N., Kasuga, T., & Nogi, M. (2018). Clear transparent cellulose nanopaper prepared from a concentrated dispersion by high-humidity drying. *RSC Advances, 8*, 1833–1837. https://doi.org/10.1039/C7RA12672G

Jin, J., Lee, D., Im, H.-G., Han, Y. C., Jeong, E. G., Rolandi, M., et al. (2016). Chitin nanofiber transparent paper for flexible green electronics. *Advanced Materials, 28*, 5169–5175. https://doi.org/10.1002/adma.201600336

Jin, T., Liu, T., Lam, E., & Moores, A. (2021). Chitin and chitosan on the nanoscale. *Nanoscale Horizons, 6*, 505–542. https://doi.org/10.1039/D0NH00696C

Jurič, I., Karlović, I., Tomić, I., & Novaković, D. (2013). Printing: Optical paper properties and their influence on colour reproduction and perceived print quality. *NPPRJ, 28*, 264–273. https://doi.org/10.3183/npprj-2013-28-02-p264-273

Kasuga, T., Isobe, N., Yagyu, H., Koga, H., & Nogi, M. (2018). Clearly transparent nanopaper from highly concentrated cellulose nanofiber dispersion using dilution and sonication. *Nanomaterials, 8*, 104. https://doi.org/10.3390/nano8020104

Khan, S. A., Rehman, M. M., Ameen, S., Saqib, M., Khan, M., & Kim, W. Y. (2024). High performance triboelectric nanogenerator based on purified chitin nanopaper for the applications of self-powered humidity sensing, gait monitoring, and hyperhidrosis sensor. *Sustainable Materials and Technologies, 40*, e00867. https://doi.org/10.1016/j.susmat.2024.e00867

Koga, H., Nogi, M., Komoda, N., Nge, T. T., Sugahara, T., & Suganuma, K. (2014). Uniformly connected conductive networks on cellulose nanofiber paper for transparent paper electronics. *NPG Asia Materials, 6*, e93–e93. https://doi.org/10.1038/am.2014.9

Koivunen, K., Niskanen, I., Peiponen, K.-E., & Paulapuro, H. (2009). Novel nanostructured PCC fillers. *Journal of Materials Science, 44*, 477–482. https://doi.org/10.1007/s10853-008-3095-y

Kumari, S., & Kishor, R. (2020). Chapter 1 - chitin and chitosan: Origin, properties, and applications. In S. Gopi, S. Thomas, & A. Pius (Eds.), *Handbook of chitin and chitosan*. Elsevier.

Lam, E., Hrapovic, S., Majid, E., Chong, J. H., & Luong, J. H. T. (2012). Catalysis using gold nanoparticles decorated on nanocrystalline cellulose. *Nanoscale, 4*, 997–1002. https://doi.org/10.1039/C2NR11558A

Laroque, C. (2004). History and analysis of transparent papers. *Paper Conservation, 28*, 17–32. https://doi.org/10.1080/03094227.2004.9638639

Li, C., Kasuga, T., Uetani, K., Koga, H., & Nogi, M. (2020). High-speed fabrication of clear transparent cellulose nanopaper by applying humidity-controlled multi-stage drying method. *Nanomaterials, 10*, 2194. https://doi.org/10.3390/nano10112194

Li, Y., Fu, Q., Rojas, R., Yan, M., Lawoko, M., & Berglund, L. (2017). Lignin-retaining transparent wood. *ChemSusChem, 10*, 3445–3451. https://doi.org/10.1002/cssc.201701089

Li, Y., Fu, Q., Yu, S., Yan, M., & Berglund, L. (2016). Optically transparent wood from a nanoporous cellulosic template: Combining functional and structural performance. *Biomacromolecules, 17*, 1358–1364. https://doi.org/10.1021/acs.biomac.6b00145

Li, Y., Yang, X., Fu, Q., Rojas, R., Yan, M., & Berglund, L. (2018). Towards centimeter thick transparent wood through interface manipulation. *Journal of Materials Chemistry A, 6*, 1094–1101. https://doi.org/10.1039/C7TA09973H

Liu, X., Wang, H., Wu, M., & Huang, Y. (2023). Transparent nanopaper from nanofibrillated bamboo pulp. *BioResources, 18*, 3995–4005. https://doi.org/10.15376/biores.18.2.3995-4005

Ma, X., Deng, Q., Wang, L., Zheng, X., Wang, S., Wang, Q., et al. (2019). Cellulose transparent conductive film and its feasible use in perovskite solar cells. *RSC Advances, 9*, 9348–9353. https://doi.org/10.1039/C9RA01301F

Magalhães, M. I., & Almeida, A. P. C. (2023). Nature-inspired cellulose-based active materials: From 2D to 4D. *Applied Biosciences, 2*, 94–114. https://doi.org/10.3390/applbiosci2010009

Mariani, A., & Malucelli, G. (2024). Transparent wood-based materials: A new step toward sustainability and circularity. *Next Materials, 5*, 100255. https://doi.org/10.1016/j.nxmate.2024.100255

Mariano, M., El Kissi, N., & Dufresne, A. (2014). Cellulose nanocrystals and related nanocomposites: Review of some properties and challenges. *Journal of Polymer Science Part B: Polymer Physics, 52*, 791–806. https://doi.org/10.1002/polb.23490

Mayer, F., Prado-Roller, A., Mautner, A., & Bismarck, A. (2024). Retain strength, gain ductility: Tough and transparent nanopapers by mercerisation. *Cellulose, 31*, 1533–1544. https://doi.org/10.1007/s10570-023-05714-7

Mi, R., Chen, C., Keplinger, T., Pei, Y., He, S., Liu, D., et al. (2020). Scalable aesthetic transparent wood for energy efficient buildings. *Nature Communications, 11*, 3836. https://doi.org/10.1038/s41467-020-17513-w

Nogi, M., Iwamoto, S., Nakagaito, A. N., & Yano, H. (2009). Optically transparent nanofiber paper. *Advanced Materials, 21*, 1595–1598. https://doi.org/10.1002/adma.200803174

Nogi, M., Karakawa, M., Komoda, N., Yagyu, H., & Nge, T. T. (2015). Transparent conductive nanofiber paper for foldable solar cells. *Scientific Reports, 5*, 17254. https://doi.org/10.1038/srep17254

Nogi, M., Kim, C., Sugahara, T., Inui, T., Takahashi, T., & Suganuma, K. (2013). High thermal stability of optical transparency in cellulose nanofiber paper. *Applied Physics Letters, 102*(18), 181911. https://doi.org/10.1063/1.4804361

Park, N.-M., Koo, J. B., Oh, J.-Y., Kim, H. J., Park, C. W., Ahn, S.-D., & Jung, S. W. (2017). Electroluminescent nanocellulose paper. *Materials Letters, 196*, 12–15. https://doi.org/10.1016/j.matlet.2017.03.003

Payen, A. (1838). Mémoire sur la composition du tissu propre des plantes et du ligneux. *J Comptes Rendus, 7*, 1052–1056.

Poulin, A., Aeby, X., & Nyström, G. (2022). Water activated disposable paper battery. *Scientific Reports, 12*, 11919. https://doi.org/10.1038/s41598-022-15900-5

Qi, H., Chang, C., & Zhang, L. (2009). Properties and applications of biodegradable transparent and photoluminescent cellulose films prepared via a green process. *Green Chemistry, 11*, 177–184. https://doi.org/10.1039/B814721C

Qiu, X., & Hu, S. (2013). Smart materials based on cellulose: A review of the preparations, properties, and applications. *Materials, 6*, 738–781. https://doi.org/10.3390/ma6030738

Ryu, M., Kim, J., Lee, S., Kim, J., & Song, T. (2021). Stretchable and transparent paper based on PDMS–CNC composite for direct printing. *Advanced Materials Technologies, 6*, 2100156. https://doi.org/10.1002/admt.202100156

Septevani, A. A., Burhani, D., Sampora, Y., Indriyati, S., Rosa, E. S., et al. (2022). A systematic study on the fabrication of transparent nanopaper based on controlled cellulose nanostructure from oil palm empty fruit bunch. *Journal of Polymers and the Environment, 30*, 3901–3913. https://doi.org/10.1007/s10924-022-02484-4

Shams, M. I., Ifuku, S., Nogi, M., Oku, T., & Yano, H. (2011). Fabrication of optically transparent chitin nanocomposites. *Applied Physics A: Materials Science & Processing, 102*, 325–331. https://doi.org/10.1007/s00339-010-5969-5

Shams, M. I., & Yano, H. (2015). Doubly curved nanofiber-reinforced optically transparent composites. *Scientific Reports, 5*, 16421. https://doi.org/10.1038/srep16421

Song, Y., Jiang, Y., Shi, L., Cao, S., Feng, X., Miao, M., & Fang, J. (2015). Solution-processed assembly of ultrathin transparent conductive cellulose nanopaper embedding AgNWs. *Nanoscale, 7*, 13694–13701. https://doi.org/10.1039/C5NR03218K

Vahur, S., Eero, L., Lehtaru, J., Virro, K., & Leito, I. (2019). Quantitative non-destructive analysis of paper fillers using ATR-FT-IR spectroscopy with PLS method. *Analytical and Bioanalytical Chemistry, 411*, 5127–5138. https://doi.org/10.1007/s00216-019-01888-x

Wang, X., Gao, K., Shao, Z., Peng, X., Wu, X., & Wang, F. (2014). Layer-by-layer assembled hybrid multilayer thin film electrodes based on transparent cellulose nanofibers paper for flexible supercapacitors applications. *Journal of Power Sources, 249*, 148–155. https://doi.org/10.1016/j.jpowsour.2013.09.130

Wurtz, A. & Friedel, C. (1876). Dictionnaire de chimie pure et appliquée: comprenant: la chimie organique et inorganique, la chimie appliquée à l'industrie, à l'agriculture et aux arts, la chimie analytique, la chimie physique et la minéralogie, Hachette, Paris.

Xu, X., Zhou, J., Jiang, L., Lubineau, G., Ng, T., Ooi, B. S., et al. (2016). Highly transparent, low-haze, hybrid cellulose nanopaper as electrodes for flexible electronics. *Nanoscale, 8*, 12294–12306. https://doi.org/10.1039/C6NR02245F

Xue, J., Song, F., Yin, X.-W., Wang, X.-L., & Wang, Y.-Z. (2015). Let it shine: A transparent and photoluminescent foldable nanocellulose/quantum dot paper. *ACS Applied Materials & Interfaces, 7*, 10076–10079. https://doi.org/10.1021/acsami.5b02011

Yang, Q., Fukuzumi, H., Saito, T., Isogai, A., & Zhang, L. (2011). Transparent cellulose films with high gas barrier properties fabricated from aqueous alkali/urea solutions. *Biomacromolecules, 12*, 2766–2771. https://doi.org/10.1021/bm200766v

Yousefi, H., Nishino, T., Faezipour, M., Ebrahimi, G., & Shakeri, A. (2011). Direct fabrication of all-cellulose nanocomposite from cellulose microfibers using ionic liquid-based nanowelding. *Biomacromolecules, 12*, 4080–4085. https://doi.org/10.1021/bm201147a

Zhang, Z., Wang, H., Li, S., Li, L., & Li, D. (2015). Transparent and flexible cellulose nanofibers/silver nanowires/acrylic resin composite electrode. *Composites Part A: Applied Science and Manufacturing, 76*, 309–315. https://doi.org/10.1016/j.compositesa.2015.06.010

Zhu, H., Fang, Z., Wang, Z., Dai, J., Yao, Y., Shen, F., et al. (2016). Extreme light management in mesoporous wood cellulose paper for optoelectronics. *ACS Nano, 10*, 1369–1377. https://doi.org/10.1021/acsnano.5b06781

Zhu, H., Parvinian, S., Preston, C., Vaaland, O., Ruan, Z., & Hu, L. (2013). Transparent nanopaper with tailored optical properties. *Nanoscale, 5*, 3787–3792. https://doi.org/10.1039/C3NR00520H

Zhu, H., Xiao, Z., Liu, D., Li, Y., Weadock, N. J., Fang, Z., Huang, J., & Hu, L. (2013). Biodegradable transparent substrates for flexible organic-light-emitting diodes. *Energy & Environmental Science, 6*, 2105–2111. https://doi.org/10.1039/C3EE40492G

Zhu, M., Song, J., Li, T., Gong, A., Wang, Y., Dai, J., et al. (2016). Highly anisotropic, highly transparent wood composites. *Advanced Materials, 28*, 5181–5187. https://doi.org/10.1002/adma.201600427

Chapter 13
Conductive Paper and Its Applications

Longyan Chen, Yi Chen, and Davide Piovesan

13.1 Introductions

The rapid advancement of electronic technology has fundamentally transformed a wide array of sectors, from consumer electronics and telecommunications to healthcare and renewable energy. As devices evolve, there is an increasing demand for components that are not only high-performing but also lightweight, flexible, and portable. In this chapter, we discuss the technology development, applications, and current challenges of conductive paper-based electronic devices.

13.1.1 The Need of Conductive Paper

Over the past few decades, electronics development has rapidly advanced, leading to increasingly sophisticated and efficient products and devices, such as mobile phones, computers, TVs, and displays. The technology innovation often results in shorter product lifecycles. Consumers are encouraged to replace older models with newer ones quickly. Consequently, the so-called electronic waste (E-waste) has become a growing concern, with discarded gadgets contributing to environmental pollution and limiting resource depletion. This becomes a pressing concern,

L. Chen (✉) · D. Piovesan
Department of Biomedical, Industrial and Systems Engineering, Gannon University, Erie, PA, USA
e-mail: chen084@gannon.edu

Y. Chen
Materials, Engineering and Manufacturing Research Group, Scion Institute, Rotorua, New Zealand

G. Korotcenkov (ed.), *The Handbook of Paper-Based Sensors and Devices*,
https://doi.org/10.1007/978-3-031-91080-7_13

prompting the search for sustainable alternatives that can support the growing need for eco-friendly solutions in the electronics industry.

On the other hand, conductive substrates, particularly printed circuit boards (PCB), provide basic supports and connect electronic components like resistors, capacitors, transistors, and chips. These conductive substrates are based on glass, ceramics, and/or semiconducting materials that are typically rigid and not recyclable. With the increasing requirement of the human-electronics interaction, there is a growing demand for the flexible conductive substrates that can allow electronics can be directly worn and/or integrated with human body without causing any harmful effect. For years, much research has aimed at developing alternative conductive substrates that are made of renewable resources, easy to dispose, flexible, and biocompatible to address these problems. Examples of these flexible substrate materials are paper (Kumar et al., 2019), thin metal foil (D'Andrade et al., 2014; Kumar et al., 2019), or plastic polymer (Li et al., 2023).

Since its invention more than 2000 years ago, paper has been used for writing, drawing, printing, packaging, information displaying, and storing. It is a highly sophisticated renewable material as it can be made thin, lightweight, and flexible depending on its pulp processing. The main constituents of paper are cellulose fibers, hemicellulose, and lignin. The cellulose fibers have a diameter of 10–50 μm and a length up to 2–5 mm. Inside the cellulose fibers, cellulose microfibrils interact with each other under hydrogen bond, providing excellent mechanical properties. The chemical nature of cellulose is highly attractive for certain applications as it allows liquid to penetrate within its hydrophilic fiber matrix without the need for an external pump (Liana et al., 2012). Furthermore, in conventional paper, these fibers typically form a highly porous structure, providing strong adsorption and faster transport of electrolytes, ions, and other conductive substances. Moreover, the cellulose microfibrils can be functionalized, with tunable properties such as hydrophilicity, as well as permeability and reactivity (Liana et al., 2012). Paper substrates are also adapted to printing technology, which makes the feasibility of making paper-based devices in an extremely low-cost way. Owing to these features, paper-based conductive substrates have become an excellent candidate for a various of applications, including flexible electronics, optoelectronics, energy storage, sensors, and biochemical sensors. Before introducing the fabrication of conductive paper substrates, it will be introductory to understand the demanding electrical properties and some considerations for the preparation of conductive paper, as discussed in the following.

13.1.2 Electrical Conductivity of Paper

Paper by itself is an intrinsically insulating fibrous matrix. Some of the most intriguing electrical properties of paper include volume and surface resistivity. The volume and surface resistivity of paper substrates at a relative humidity (RH) of 20–40% are typically 10^{10}–10^{14} Ω cm and 10^{11}–10^{15} Ω sq.$^{-1}$, respectively (Simula & Niskanen,

2000). Thus, for a long time, paper has been used as an insulating material in cables and capacitors, until it has been replaced by thinner plastic films or wraps. Different from plastic films, all these electrical properties in paper highly depend on RH. The absorption of water leaves a pathway for ions (mainly protons) to move. For instance, the volume resistivity of cellulose can decrease by a factor of 10^{12}, dropping to about 10^4 Ω·cm as the RH rises from 1% to 99% (Murphy, 1960). The resistivity is also affected by other factors, such as temperature (Chang et al., 2000), electrical field (Sirviö et al., 2008), measurement frequency and morphology (Cimbala et al., 2018), and compositions of the paper substrate (Hollertz et al., 2015). Because of the structure and composition difference in different paper, it is a challenge to compare the results in literature studies. A few standards, including IEC 60641, IEC 60554, IEC 61620, and IEC 60247, have been proposed for the electrical properties measurement under controlled environment (Gasser et al., 1999; Zhang et al., 2024).

13.1.3 Dielectric Properties of Paper

A dielectric is an insulating material that does not conduct electricity but can support an electric field. The dielectric properties of paper are essential for its performance as an insulating material in electrical applications. These key dielectric properties include: the dielectric constant, which measures the material's ability to store electrical energy; dielectric strength, indicating the maximum electric field it can withstand without breakdown; and the dielectric loss factor, which quantifies energy lost as heat in an alternating electric field (Simula et al., 1998). Understanding these characteristics is crucial for selecting appropriate paper for various applications, such as electrical insulation in transformers, capacitors, and printed circuit boards, ensuring reliability and safety. Simula et al. (1998) determined the dielectric constant (k) based on the ratio of the permittivity of the material (ε) and the permittivity of vacuum (ε_0),

$$\kappa = \varepsilon / \varepsilon_0 \tag{13.1}$$

The dielectric constant of dry paper was measured in 2.1 at 40% RH under measurement frequency range from 20 Hz^{-1} MHz, which is among the other typical measurement of values between 2 and 4. However, it should be noted that moisture and temperature also affect the dielectric properties. Maldzius et al. (2010) demonstrated that paper substrates exhibit exponential temperature dependence (up to 50 °C) at a constant RH of 50%, in conductivity, dielectric constant, charging decay time, and charging potential. Similarly, moisture has a significant effect on the conductivity and dielectric properties of three coated papers and copy paper. Another important factor to be considered is the migration of ions at low measurement frequencies, particularly at high moisture content and ionic content. Christie et al. (2004) reported exceptionally high values of the dielectric constant for cellophane,

reaching up to 10^9 at very low measurement frequencies (under mHz level) and a RH of 33%. This could be attributed to the accumulation of ions with opposite charges closed to contacts, resulting in a large, calculated dielectric constant and a high capacitance.

13.2 Conductive Paper and Fabrication Methods

Conventional conductive materials are essential in a wide range of electronic and electrical applications due to their ability to efficiently conduct electricity. These materials are characterized by their high electrical conductivity and are used in various forms, from bulk metals to thin films. Many conductive materials, including metal, organic polymers, carbon-based materials, and inorganic materials, have been used to prepare conductive paper substrates via various fabrication methods. These methods can be grouped into two categories: physical methods and chemical methods. In physical methods, conductive materials are introduced to the paper substrates via handwriting, printing, physical coating, vacuum filtration, and lithography processes. These processes usually do not change the chemical properties of the paper substrates. Some physical methods, such as writing and printing, have been used in our daily life, and they often are fast, easily accessible, inexpensive, and adapted to product scaling-up. In chemical methods, the paper substrates are treated and reacted with chemical reagents to synthesize conductive substances (such as in situ conductive seeds growth) or polymerize the absorbed conductive monomer to for conductive polymers. Since chemical reactions can be experimentally monitored and controlled, this would allow one to manipulate the conductive properties of paper substrate in a tunable and precise way, and it is particularly suitable for high-resolution and light weight electronic devices. However, it is worth noting that the selection of fabrication methods largely depends on the available conductive materials, the type of paper substrate, the applications, resources, and cost considerations. It is very difficult to discuss the pros and cons of these methods without further introducing the conductive materials and the need to produce the conductive paper. Hence, we summarize the common conductive materials that have been used for creating conductive paper substrates, and briefly discuss the pros and cons of the methods in the following.

13.2.1 Using Metals in Making Conductive Paper

Metal and metal-based materials are favored in various electronic applications due to their high electrical conductivity and excellent durability that provides mechanical strength and resistance to environmental factors. Different formats of metal materials in paper are discussed here.

13.2.1.1 Conductive Paper Based on Bulky Metal Materials

Bulky metals like silver, copper, and gold exhibit excellent conductivity, making them essential for electronics, electrical wiring, and conductive components. In one of their pioneer work, Whiteside research group extensively studied the deposition of a variety of metal materials (including Al, Zn, Cu, Pb, Ni, Sb, Sn, Ti, Ag, Bi, IN, Au, and Pt) onto the different paper substrates to make inexpensive, disposable, and foldable PCB. They examined the electrical conductivity, mechanical properties, melting point, and cost associated with the fabrication and materials (Siegel et al., 2010). These metal-based conductive materials offer excellent electrical signal. However, these bulk metal circuits are easy to fatigue by repeated folding. Additionally, the traditional high-temperature metal fabrication techniques were not feasible to deposit bulk metal on temperature sensitive paper substrate.

13.2.1.2 Conductive Paper-Based Micro-/Nano-Metal Materials

In recent years, metallic particles have been introduced to provide electrical conductivity to paper substrates. Despite the discreteness of the individual particle, the interconnect between these particles can be used as a pathway for electrical current to pass through (Chu et al., 2009; Smeacetto et al., 2008). Often, these metallic particles have size from micron to nanoscale. The unique 3D porous architecture of cellulose substrate can trap the micro-/nano-metallic particles inside the fiber network, and chemical bond can form between particles and cellulose hydroxyl groups, avoiding loss of electrical conductivity due to the fatigue of bulk metal.

These metallic micro−/nano particles were typically prepared from two ways, i.e., top-down physical approach and bottom-up chemical approach. In top-down approach, bulky metal materials were broken down into small parts of particles via milling (Yadav et al., 2012), laser ablation (Spizzichino & Fantoni, 2014), and spark ablation (Domaschke et al., 2018). While the bottom-up approaches, termed as "wet chemistry" methods, involve the growth of materials from both homogeneous and heterogeneous nucleation processes (Kim et al., 2014; Turkevich et al., 1951). It is worthy to note that the bottom-up approach offers many advantages: (1) the size and morphology of the particle are tunable by adjusting surfactants and reaction conditions; (2) the synthesis reactions are under the mild condition; and (3) the reaction can be easily scaled up which can further reduce the material cost. The as-made particles from bottom-up approach are further dispersed in aqueous or organic solvents and then transferred to paper substrates via various coating or deposition techniques, including spraying, dip coating, roll-to-roll bar coating, pen writing, and printing. The principle of these coating approaches has been well summarized in other review papers (Kumar et al., 2019; Zhang et al., 2018). In the following, we briefly discuss the printing techniques and the in situ synthesis method as they have been well studied and adapted to large-scale manufacture.

The most widely used printing methods are screen printing, flexography gravure, and inkjet (Tobjörk & Österbacka, 2011; Torvinen et al., 2012; Valdec et al., 2021;

Xu et al., 2021). The first two are suitable for higher viscosity inks or paste, where concentrated conductive particles were mixed with binders, solvents, and additives (Tobjörk & Österbacka, 2011) and a thick printing layer was generated. After printing, the solvent is removed via evaporation at elevated temperature (100–150 °C), resulting in adjacent particle coalescence. The layer conductivity depends on various parameters, including particle size, thickness, paper substrate, and sintering conditions. Typically, small particle size offers advantages in penetrating the cellulose porous network and provides a low resistivity under 5 μΩ·cm resistivity (higher than 200,000 S cm^{-1}) (Magdassi et al., 2010; Mo et al., 2019). Jansson et al. (2022) studied the screen printing and flexography using silver micro- and nanoparticle ink wetting phenomena on paper. They found that a paper moisture of 5–7% provided the best multilayer printing accuracy. In flexography, small particles, regularities of paper network, and rough surface that increase the ink penetration degree could improve the conductivity. In screen printing, microparticles are properly printable. The high solid content and viscosity increased the layer thickness to 12.6 μm, as compared to 302–632 nm in flexography, which resulted a rough surface. In general, the layer gets better conductivity with the increase in thickness. The screen-printing layer has a lower sheet resistance (<40 mΩ $sq.^{-1}$) due to this high layer thickness. Despite of good layer conductivity, the ink in screen printing tends to spread more along the surface irregularly, resulting in ragged edges. Some improvement in edge smoothness was reported by using roll-to-roll rotary screen printing. The resolution for screen- printed conductive line reflected by line width is from 150 to 200 μm.

Inkjet printing is one of the widely used approaches to transfer conductive materials to paper substrates, due to its cost-effectiveness, flexibility, and ease of use (Öhlund et al., 2012). Cu- or Ag-nanoparticle-based inks were commonly used. Inkjet inks have low viscosity, making the substrate properties very important for controlling ink spreading and reaching sufficient levels of print definition and performance. Resolution is typically limited to 20–40 μm (Raut & Al-Shamery, 2018), two to three times higher than that of the screen printing. Öhlund et al. (2012) studied the effect of paper surface properties, showing that to guarantee a good conductivity, the porous size is crucial, and it should be smaller than conductive film thickness, while the ink absorption and surface roughness contribute minor influence. An elevated curling temperature to 110 °C that could vanish molecular interaction between coating polymer and substrate surface increased the conductivity of paper substrates.

However, a common issue for ink-jet printing is the clogging problem due to the accumulation of the nanoparticles in the small nozzle. To overcome the clogging issue, Zhang et al. (2014) printed palladium salt ink solution particle ink on a photopaper, followed by electroless deposition of conductive copper line. The printed copper lines showed excellent conductivity of up to 3.9×10^7 S m^{-1} (>65% of bulk copper). A radio frequency identification (RFID) antenna, a micro inductive coil, and a complex circuit board had been successfully demonstrated, respectively. Similar strategies have been adapted to print conductive line by using silver precursor ink that can do in situ synthesis of Ag NPs on paper substrate (Wang, Du, et al.,

2019a) and combined with soft lithography to improve the line resolution down to 2.8 μm (Sung et al., 2013).

The resolution of conductive line is crucial to improve the functionality and reliability of circuits, especially in compact designs. The in situ chemical synthesis of nanoparticles offers a great advantage to reduce conductive line resolution and prevent nozzle clogging in inkjet printing. One of our previous works reported the use of nanopaper for in situ synthesis of Ag NPs (Chen et al., 2019). Instead of relying on cellulose porous network to trap the Ag precursor solution which may cause discrete particle agglomerates, the nanopaper can adsorb the Ag^{+} with abundant of carboxylic groups and produce a high densely packed silver nanoparticles layer with tunable thickness (up to several microns) via a facile successive ionic layer absorption and reaction (SILAR) process (Chen et al., 2019). Our recent work showed that using a similar process, a conductive line with 2 μm width can be achieved via soft lithograph with comparable conductivity to that of bulky silver (Chen et al., unpublished results).

13.2.1.3 Conductive Paper-Based One-Dimensional Metal Materials

The conductivity of the paper substrates can also benefit from one-dimensional (1D) metal materials, such as metallic nanowires or nanotubes. The high aspect ratio of 1D metal materials (e.g., silver nanowire, AgNWs) can secure the connection of the conductive line to improve conductivity significantly with only small amounts, reducing material costs and waste. In an earlier study, Komoda et al. (2012) printed a silver nanowire line-based antenna in the high-frequency radio on both paper substrates. Lee et al. (2016) loaded AgNWs on the cellulose paper by a repeated dip-coating process up to 50 cycles. The conductivity increased from 0.34 to 67.51 S cm^{-1} with the increase of dip-coating cycles. Due to their absorption in the near-UV region and limited scattering across the full wavelength spectrum (Tomiyama et al., 2020), Ag nanowire-based networks exhibit high transparency in the visible range on a large scale. A few studies fabricated the transparent conductive nanopaper substrate by incorporating AgNWs in the transparent nanopaper (Kim et al., 2018; Preston et al., 2014). As discussed in the sect. 13.3.1.3, these transparent and conductive paper substrates could be used as circuits, optoelectronic devices, thin-film solar cells, etc.

13.2.1.4 Conductive Paper Based on Liquid Metal Materials

Liquid metal (LM) materials can be alternative materials to imparting conductivity to paper-based substrates. Yuan et al. (2023) recently proposed directly depositing LM Gallium and BiINSn on common paper substrates. The LM materials own both excellent fluidity and electric conductivities as metals, though with poor wettability on paper. To improve the adhesion of the liquid metals to paper substrate, the group first absorbed the LM onto a silicon polymer sheet that has high adhesion to the

liquid metals and then smeared the LM-immersed polymer sheet to the paper substrate. The LM paper substrates showed similar electrical conductivity to that of pure liquid metal without obvious loss even under mechanical bending and rolling. Sun et al. (2017) also synthesized PIL $[Pyrmim]^{+}[Br]^{-}$ that could interact with graphite substrate due to pi-pi conjugated force. The pencil lead that contained the PIL-graphite composite was used to prepare a portable paper-based NIR sensor that could detect warm subjects.

13.2.2 Using Conductive Polymers (CPs) in Conductive Paper

The use of conductive polymers in organic electronics emerged following the 1977 discovery of highly conductive polyacetylene by Hideki Shirakawa, Alan MacDiarmid, and physicist Alan Heeger (Shirakawa et al., 1977). These as-made organic electronics offer significant advantages over inorganic materials, including exceptional flexibility and lightweight properties, making them ideal for wearable sensors. Conducting polymers (CPs) such as polypyrrole (PPy), polythiophene (PTh), poly(3,4-ethylenedioxy-thiophene) (PEDOT), and polyaniline (PANi) have become increasingly popular due to their long-term electrical and chemical stability (Kaur et al., 2015). In these polymers, the pi-electrons are delocalized due to continuous overlaps of the pi-orbitals. These electrons thus exhibit high mobility along the polymer backbone to form a conduction bank, giving these polymers electrical conductivity that lies between semiconductors (10^{-8} s cm^{-1}) and metals (10^{5} s cm^{-1}) (Fig. 13.1). "Doping" counterions near the extended pi-bonds can significantly improve the CPs electrical conductivity from over 1 s cm^{-1} to more than 1000 s cm^{-1}, bringing their electrical performance comparable to conductors such as graphite (Fielding et al., 2015).

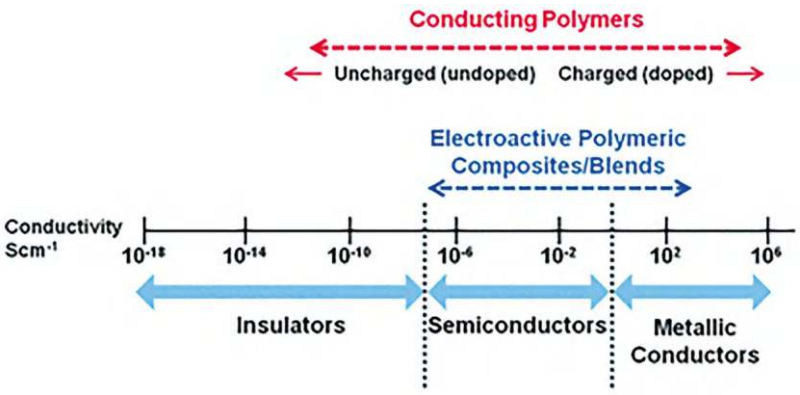

Fig. 13.1 Conductivity range of conducting polymers and conductive polymeric composites. Reprinted with permission from Kaur et al. (2015). Copyright 2015, RSC Publishing

A variety of techniques have been introduced to coat CPs on a paper substrate, including bar coating (roll-to-roll), physical deposition, and in situ polymerization. In an earlier study, Denneulin et al. (2008) investigated different substrate surface factors, including substrate surface roughness, chemical interaction, dopant, and coating thickness, that contribute to the conductivity of PEDOT:PSS-coated paper substrates via a roll-to-roll bar coating process. Overall, smooth paper substrates, such as vegetable parchment paper with lower surface energy, provide better conductivity compared to photo paper and tracing paper, owing to the formation of homogeneous coating layer and low chemical interaction between CPs and paper substrates. The addition of a second dopant ethylene glycol further decreased the electrical resistance on the paper. The gains in coating thickness and uniformity proved a significantly positive effect on the reduction of sheet resistance.

Different from direct coating, CPs can also be introduced on paper via in situ polymerization. In this case, uncoated cellulose paper with rough surface takes advantage. The porous structure allows the monomer of the CPs to penetrate the unique 3D cellulose network. CPs conductive tracks can then be built via in situ polymerization. Yuan et al. (2013) reported the soaking of cellulose printing paper in the Py monomer solution. The CP conductive layer was then synthesized by dipping monomer-soaked paper in an oxidizing agent $FeCl_3$ solution that contains HCl as a doping agent. A black and uniform conductive PPy film on the paper was prepared. The authors further reported using of this coated fiber to fabricate a solid-state supercapacitor (SC) with an aerial capacitance of 0.42 F cm^{-2}. While soaking paper in liquid, the cellulose fibers can act like a power-free pump to transport fluid via capillary action. Zhang et al. (2017) utilized this unique feature to create a paper microfluidic channel to guide the polymerization of P-toluenesulfonic acid-doped PPy (p-TSA-PPy) in cellulose network. A paper-based self-powered system was constructed. The structure of p-TSA-PPy/cellulose network dramatically increased the horizontal electrical conductivity, but also overcame the vertical electroconductivity issue, allowing for the top-channel-bottom conductive interconnections. The generated electrical output by this power paper was able to power up commercial light-emitting diodes (LEDs) or trigger a $Ru(bpy)_3^{2+}$ ECL sensing platform. The polymerization method was demonstrated to be a versatile tool to fabricate CPs/paper conductive substrate that have been used in SCs (Yao et al., 2013; Yuan et al., 2013), power devices (Wu et al., 2015), and transistor (Hyun et al., 2015; Irimia-Vladu, 2014).

Alternatively to in situ synthesis of CPs in porous cellulose network, Li et al. (2014) conducted the chemical polymerization PPy with free-standing bacterial cellulose nanofibrils (BC) to minimize the materials quantity. A vacuum filtration method was then used to prepare highly conductive BC-PPy/multiwall carbon nanotubes (MWCNT) electrodes. The as-made paper electrodes exhibited a high capacitance of 2.43 F cm^{-2} at a mass of 11.23 mg cm^{-2} under room temperature. In sum, owing to their high energy density, electrical stability, and great flexibility, CPs provide ideal conductive materials to bring paper as a conductive substrate, particularly in the flexible electronics applications.

13.2.3 Using Carbon-Based Nanomaterials in Conductive Paper

Carbon-based materials have become the most prevalent electrically conductive materials today. Different forms of carbon, such as graphene, fullerenes (C_{60}), carbon nanotubes (CNTs), and amorphous carbon, have garnered significant attention for energy storage applications. This interest stems from their low energy density, excellent electrical conductivity, high electrochemical stability, impressive mechanical strength, and outstanding corrosion resistance (Li et al., 2014; Ando et al., 1999). For example, graphene is lightweight and offers excellent electrical and thermal conductivity. It boasts a high specific surface area that can reach up to 2675 $m^2 g^{-1}$, exceptional mechanical properties with a Young's modulus approaching 1 TPa, and remarkable chemical stability (Lee et al., 2013; Mittal et al., 2017). The electron transport and high thermal and electrical conductance of CNTs can be up to 3000 $Wm\ K^{-1}$ and 1800 $S\ cm^{-1}$, respectively, which make CNTs as exceptional electrode materials (Kim et al., 2001). In the following, we discuss the fabrication of carbon-based conductive paper using different approaches.

13.2.3.1 Preparation of Carbon Paper Via Vacuum Filtration

Vacuum filtration (VF) is among the most widely used and relatively simple method for preparing paper active materials from cellulose. In this process, carbon-based electrode materials mixed with cellulose binder in a solvent and passed through a filter membrane under vacuum to prepare a 2D cellulose paper-based electrode materials. In an earlier study, Weng et al. (2011) fabricate graphene cellulose paper via VF for flexible supercapacitor application. The electrical resistivity was found 6 Ω cm (0.1667 $S\ cm^{-1}$), which is comparable to that of activated carbons (ca. 0.5–3 Ω cm). The membrane shows high stability with a decrease of only 6% after being bent 1000 times. Other works also have reported using similar strategies for incorporating CNTs (Hu, Ding, et al., 2010a; Meng & Manas-Zloczower, 2015), graphite sheet (Ren et al., 2012), graphene oxide (Li et al., 2020; Yang et al., 2017; Zhu et al., 2017), and active carbon with cellulose or nanocellulose as the electrodes mainly for electrochemical sensors (Caratelli et al., 2022; Hu, Ding, et al., 2010a) and energy storage applications (Santhiago et al., 2017). In these systems, active carbon materials provide the electrical conductance, while the binder mainly maintains the mechanical strength.

The performance of the paper substrates is often balanced between electrical properties and mechanical properties, which relies on carbon materials, the ratio of the two active components and binder, dispersion, and the molecular interaction. For example, Pang et al. (2015) studied the ratio of CNTs to the conductive paper substrate. Increasing the CNTs ratio from 10% to 70% could increase the thickness of the paper and hence bring up the conductivity from 0.0992 $S{\cdot}cm^{-1}$ to 2.613 $S{\cdot}cm^{-1}$.

However, the mechanical strength is inevitably dropped. On the other hand, the carbon materials are required to disperse in a solvent (often water) prior to VF. Due to their hydrophobic nature, higher contents of CNTs tends to form agglomerates, causing inhomogeneous conductance distribution. Surfactants are usually added to improve the dispersion of CNTs. For instance, Salajkova et al. (2013) added a surfactant nonylphenol POE-10 phosphate ester to disperse CNTs in cellulose nanofibrils solution. They were able to increase MWCNT content to 9.1 wt.% without obvious agglomerates and achieve the highest conductivity. However, with a further increase in MWCNT content to 16.7 wt.%, the agglomerates were observed again, resulting in an increase in the porous structure of the nanopaper structure. This indicates the weak interaction of MWCNT with nanocellulose fiber. To improve the synergy effect between the active carbon materials and binder materials, Meng and Manas-Zloczower (2015) reported a conductive paper film with tunable electrical conductivity by using cellulose nanocrystals (CNCs). A continuous network was able to form at CNT concentrations ranging from 10.2 to 11.6 wt.%. The CNT-enhanced CNC films display increased ductility and toughness compared to pure CNC films, which are attributed to the synergistic effects of CNCs and CNTs, as the densely packed CNC matrix protects junctions and entanglements within the continuous CNT network. The electrical conductivity could reach a conductivity of ~ 1 S cm^{-1} (converted from the surface resistivity of 100 Ω $sq.^{-1}$). Hamedi et al. (2014) reported that carboxylated cellulose nanofibril (CNF) could successfully exfoliate single-walled carbon nanotubes (SWCNTs) into individual nanotubes or small bundles and stabilize them in water. The electrical conductivity increased with SWCNTs content, peaking at 174 S cm^{-1} at a dispersion limit of 43 wt.%. However, adding 10 wt.% SWCNTs reduced modulus, strength, and strain-to-failure due to poor CNF-SWCNT interactions.

13.2.3.2 Preparation of Carbon Paper Via Printing Technology

Printing is a simple, cost-effective method for large-area, scalable fabrication. There is increasing demand for versatile paper-based electronics that require simple printing techniques for low-resistance pathways, high-performance carbon electrodes, and tunable electrical properties for wearable devices (Xu et al., 2021). However, the challenge is that the printed carbon electrodes based on commercial inks often exhibit poor electrochemical performance due to degradation (Kava et al., 2021). Hyun et al. (2015) demonstrated all-printed, foldable organic think film field-effect transistor (OTFTs) on untreated glassine paper using various printing techniques. High-quality, aligned graphene electrodes were created through screen printing and photonic annealing. Poly(3-hexylthiophene) and ion-gel dielectric layers were deposited via aerosol-jet and inkjet printing to form low-voltage OTFTs without extra treatments. The methods are compatible with roll-to-roll manufacturing, allowing for low-cost, high-throughput production. The devices demonstrated 23.5 (± 7) S cm^{-1} conductivity and excellent folding stability, thanks to the resilient

graphene electrodes and flexible ion-gel dielectric. However, the challenge is that it requires a very low surface roughness (~350 nm). Additionally, most fully printed methods currently in use rely on a water-based binder for the carbon particles, which is not suitable for wet surfaces and greatly limits their applications in areas such as electrochemical sensors (Liao et al., 2016). Santhiago et al. (2017) combined carbon ink with cellulose acetate as the binder and used sacrificial adhesive layers to pattern high loadings of conductive carbon ink on a paper substrate, allowing a resolution in width of ~500 μm. The conductive tracks are flexible and can be fully bent 20,000 times without losing the electrical performance. The inks could be modified with redox-active substances to detect hydrogen peroxide at low potentials. However, the sheet resistance is still high, about ~250 Ω sq.$^{-1}$ (i.e., ~4×10^{-5} S m^{-1} in conductivity).

One way to improve the conductivity of carbon materials is to incorporate a conductive polymer. Ma et al. (2008) demonstrated that the conductivity of SWCNT networks could be significantly enhanced by two orders of magnitude through the in situ polymerization of a highly conductive self-doped polymer, polyaniline boronic acid, around and along the CNTs. Kyrylyuk et al. (2011) developed a latex-based method that mixes fibrous SWCNTs with spherical PEDOT/PSS latex particles, enabling control over the percolation threshold in the nanocomposite. The π–π interactions enhance conductivity by forming conductive phases between the polymer matrix and carbon nanofillers, improving the electrical properties of the bulk polymer nanocomposites.

In recent years, 3D printing has gained popularity in conductive structures. Aeby et al. (2021) developed a cellulose-based ink for one-time 3D printing of paper-based SC. The electrode ink includes CNF, water, CNC, glycerin, activated carbon, and graphite, while the electrolyte ink contains CNC, glycerin, and NaCl. The printed devices can be folded to create an SC, and six supercapacitors were successfully printed in series on curved substrates to power a 3 V alarm clock. The electrical conductivities of 260.8 ± 20.1, 219.8 ± 21.3, and 228.1 ± 22.6 S m^{-1} were measured parallel, perpendicular, and at 45° to the printed lines, respectively.

Apart from the aforementioned approaches, other processes have been used to fabricate carbon-based conductive paper with good electrical conductivity and electrochemical performance, including writing (Xiong et al., 2024), pouring molding (Garino et al., 2019), hydrothermal method (Wu et al., 2021), and laser-induced graphene (Xiong et al., 2024). Particularly, the pencil-based writing provides a convenient way to draw electrical patterns on the paper. Guan et al. (2019) developed an energy storage ink made of CNT and Ag that can be directly applied using a ballpoint pen. The device allows for controlled writing and pressure application. After writing, the electrode is dried at 60 °C, resulting in a CNT/Ag paper-based electrode with a resistivity of $5.1 \times 10^{-4}\,\Omega\,\mathrm{cm}^{-1}$ (conductivity of 1961.18 S cm^{-1}).

13.2.4 Paper with Ionic Conductivity

Ionic liquids (ILs) are salts comprising a substituted heterocyclic organic cation and an organic/inorganic anion with a melting point at or below 100 °C. ILs are known for their unique physicochemical properties, including high thermal stability, tunable viscosity, and solvation capabilities. Montibon (2011) deposited ionic liquid [bmim]BF_4 on the microcrystalline cellulose (MCC) paper surface to create an ionic paper. Interestingly, the conductivity of the ionic paper did not change with different voltage applied. The conductivity of the ionic paper presented minimum changes under relatively low humidity conditions. The measurement of conductivity over different temperatures fitted well to a simple Arrhenius equation, followed with the hopping model of carrier ions, indicating the ionic paper held a behavior similar to a typical inorganic ion conductor. The research showed the ionic paper could be a good ionic conductor for fabricating compact electronic components. The coating can be reversible. However, conductivity could be affected by applying different forces during the rubbering coating process. Besides using IL as the conductive substance, Grau et al. (2016) used BMI-BF_4 to stabilize the paper actuator and electrodes before printing of the final electrode layer. The low vapor pressure of the ionic liquid provided no drying-related degradation effects, which is a common problem for ionic polymer–metal composite (IPMC) actuators hydrated with water-based solvents.

Polymer ionic liquids (PILs) are a subtype of polyelectrolytes consisting of ionic liquid monomer units incorporated into a macromolecular architecture through a polymer backbone. Compared to ILs, PILs possess interesting properties, such as film-forming ability and better electrochemical properties. Due to their higher viscosity, PIL-based coatings often do not need to be recoated. Direct immersion or dipping process is possible for certain classes of hydrophobic PILs (Ho et al., 2011). For example, Wang's group reported the infiltration of a PIL ionic gel in the filter paper that were used as flexible electrodes (Liu et al., 2019). The conductive ion gel paper has a good conductivity of 1.78×10^{-1} S m^{-1} and was adapted to an arbitrary shape by infiltration of blocking agents. An active-mode flexible all-paper-based piezoresistive sensor was fabricated. The sensor was self-powered by a triboelectric nanogenerator (TENG) that was also prepared under the ion-gel paper electrode.

13.2.5 Using Conductive Inorganic Materials in Conductive Paper

Recent research also exposed other inorganic materials as the conductive compounds for flexible devices fabrication. Particularly, a class of graphene-like 2D transition metal carbides and nitrides materials, termed as Mxenes, has shown great promise as potential electrode materials for energy storage devices. Ti_3C_2 is one of the most studied members of the MXene family due to its well-known etching

conditions and detailed theoretical and experimental studies, and its metallic conductivity (up to 6500 S cm^{-1}) (Dillon et al., 2016). Kurra et al. (2016) have employed Meyer rod coating of MXene slurry on commercially available printing. A four-point probe conductivity measurement showed that a 125-μm-thick HF-etched MXene film has a conductivity of 51 S cm^{-1}. However, the 2D MXene layer can stack easily between layers. Therefore, exfoliation of stacking layers into single layer with a spacer is necessary. Cellulose nanofibrils is among the first choice to separate the Mxene layers. Jiao et al. (2019) prepared bacterial cellulose/MXene composite paper electrode via a vacuum filtration method, obtaining a conductive paper with a conductivity of 190.2 S cm^{-1} for a mixing ratio MXene/BC-0.75:1 composite paper. Similarly, Tian et al. (2019) presented the robust MXene (Ti_3C_2Tx) nanocomposites created by incorporating wood CNFs, which enhance strength without sacrificing performance. A paper supercapacitor was prepared by vacuum filtration of the composites. With 20% CNF loading, the composites achieve 341 MPa strength (compared to 29 MPa for pristine MXene) while maintaining 298 F g^{-1} capacitance and 295 S cm^{-1} conductivity. The hybrid dispersions can be used as inks for printing flexible micro-supercapacitors, enabling the development of multifunctional lightweight devices. These robust and flexible MXene paper substrates showed promising potential in next-generation electric devices for various applications, including electromagnetic interference shielding (Zhu et al., 2021), and micro-SCs (Huang et al., 2019).

13.3 Applications of Conductive Paper

The idea to make paper as the conductive substrates could date back to the late 1960s, when Brody and Page at Westinghouse reported producing inorganic thin film field-effect transistors (TFTs) (Bacon, 1968; Brody, 1984). The process required evaporating conductor under vacuum and then deposited on an ultrasmooth surface, including paper. Body et al. also proposed a stenciling method to print transistors in a large scale on paper. The resultant transistor functionalized for 1000 h without measurable loss. It survived under bending, twisting, and coiling. Despite no practical application, partially due to high cost for using vacuum process, this concept highlighted the advantages of using paper as substrates for electronic applications, including flexibility, low cost, disposability, and lightweight characteristics. The concept was then revived during the last decades when CPs have been used in manufacturing electronics on low-cost flexible substrates (Forrest, 2004). A few earlier trials had successfully made cellulose paper conductive by using CPs (Shah & Malcolm Brown, 2005) or CNTs (Jung et al., 2008). Hu et al. (2009) later developed a paper-based electrode for energy storage devices using CNT-coated paper. Since then, numerous studies have reported the development of paper-based electronics in electrical circuits, (opto)electronics, energy harvesting and storage, and sensor and biosensing applications that are summarized briefly in the following.

Readers are also referred to Volume 2 of this handbook series for a detailed discussion.

13.3.1 Electronic Circuits and Optoelectronic Applications

Paper has long been explored as a substrate for electronic and optoelectronic applications due to its excellent flexibility, renewability, low cost, and lightweight nature (Fortunato et al., 2008; Polat et al., 2016). As the demand for flexible, lightweight, and transparent electronic devices continues to rise, researchers are increasingly drawn to the fabrication of transistors on flexible and soft substrates. For electronic applications, conductivepaper has been extensively studied as a circuit substrate, a component in transistors, and for multifunctional roles.

13.3.1.1 Electronic Circuits on Paper Substrates

As aforementioned, paper substrates offer advantages as a substrate for printed circuits applications. Compared to conventional rigid PCB substrates, paper is flexible and biodegradable. Whiteside group pioneered the work using paper as a foldable PCB by patterning metal wires on the cellulose paper. They demonstrated the applications of this paper-based flexible PCB in powering an LED light (Siegel et al., 2010). Paper is also adapted to modern printing technology. Zheng et al. (2013) showed a desktop printing of flexible circuits on paper via developing liquid metal ink. The circuit was further packed in a room temperature vulcanizing silicone rubber to stabilize the circuit function, achieving very limit electrical resistance change during bending. Andersson et al. (2014) printed a fully functional Arduino demonstration circuit board on paper using silver ink. They tested different adhesive materials to mount the standard surface mount components on conductive track and achieved the lowest added resistance by using anisotropic silver epoxy tapes. A number of electronic circuit building blocks have been printed on paper, including antennas (Rida et al., 2009; Yuan et al., 2016), accelerometers (Andò et al., 2016; Wang, Song, et al., 2018b), RIFD tags (Wang, Yan, et al., 2019c; Yang et al., 2017), and devices like organic semiconductor MOS transistors (Conti et al., 2020; Jiang et al., 2020). Similar to printing, electronic circuits and units can also draw on paper via handwriting low-resolution applications (Cunha et al., 2021; Han et al., 2014; Russo et al., 2011).These applications position paper as a versatile and sustainable solution for printing electronics. Sudheshwar et al. (2023) compared the concepts for both manufacturing PCBs and printing paper-based circuit boards as shown in Fig. 13.2. The printing technology on paper is considered as an additive manufacturing. Life cycle assessment comparisons have shown that printing electronics on paper offers a consistent sustainability advantage over traditional printed circuit boards, particularly in addressing global warming challenges.

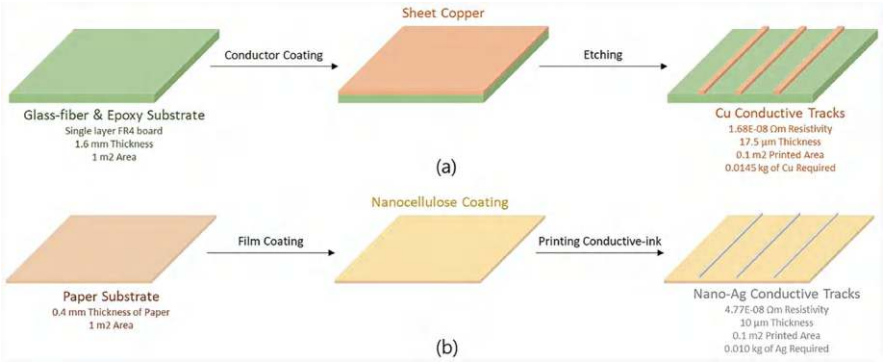

Fig. 13.2 Conceptual depiction of (**a**) subtractive manufacturing of PCBs and (**b**) additive manufacturing of printed electronics. Reprinted from Sudheshwar et al. (2023). Published 2023 by Elsevier with open access

13.3.1.2 Paper-Based Gate Dielectric

A gate dielectric layer serves as an insulating layer between the gate electrode and the semiconductor channel, allowing the gate to control the flow of current through the channel without direct electrical contact. The dielectric layer must have a high dielectric constant to effectively control the electric field and ensure efficient switching and minimal leakage current. Owing to its high dielectric constant and flexibility, cellulose paper has become an attractive option for use as a gate dielectric layer in next-generation electronics, such as flexible field effect transistors (FETs). Fortunato et al. (2008) first proposed a sheet of cellulose-fiber-based paper as the dielectric layer used in oxide-based semiconductor thin-film FETs. Figure 13.3 shows a scheme for the configuration of cellulose-based devices. This performance surpasses that of traditional amorphous Si TFTs or oxide-based TFTs on glass or silicon substrates, which require high-temperature annealing (200–300 °C). Additionally, the performance remained stable for 2 months after device fabrication, highlighting the environmental stability of the device. They further used CNC nanopaper as the dielectric layer, achieving a high channel saturation mobility of over 7 $cm^2\ V^{-1}\ s^{-1}$, with improvement in a drain-source current on/off modulation ratio up to 10^5 and a subthreshold gate voltage swing of 2.11 V/decade. The characteristics of the CNC nanopaper FETs have been measured under ambient air conditions, demonstrating good stability even 2 weeks after processing, without any encapsulation or passivation layer.

The cellulose paper dielectric layers have also been used in complementary metal oxide semiconductor (CMOS) circuits (Martins et al., 2013) and paper electrolyte-gated transistors (Cunha et al., 2017). Martins et al. (2013) demonstrated the use of a paper dielectric layer in CMOS digital, which harnesses the complementary operation of oxide FETs with electron and hole mobilities greater than 23 $cm^2\ V^{-1}\ s^{-1}$ and 1.3 $cm^2\ V^{-1}\ s^{-1}$, respectively. Lim et al. (2010) synthesized indium–gallium–zinc-oxide TTFs on glass and paper at low temperature, utilizing

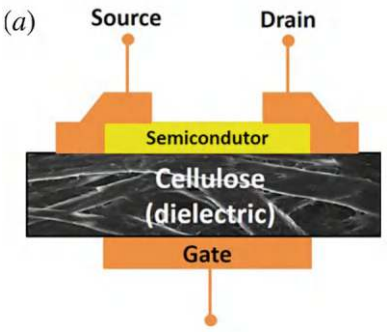

Fig. 13.3 Schema of the FET structure using the cellulose paper as the gate dielectric layer. Reprinted with permission from Gaspar et al. (2014). Copyright 2014, IOP Publishing

cyclotene-laminated cellulose paper as the gate dielectric layer. The paper-based TTFs showed similar performance to that of the glass-based TTFs. The study showed the possibility of a broad area of research toward fully cellulose-based electronics.

However, it should be well noted that the dielectric constant of paper can be affected by temperature, paper compositions, and moisture. Challenges remain for use of these paper-based dielectric substrates, in terms of stability and reliability in different conditions.

13.3.1.3 Paper-Based Optoelectronics

Optoelectronic devices depend on the interactions between light and matter, as well as the electronic properties of materials, to transform light into electrical signals or vice versa. Transparent conductive electrodes (TCEs) are necessary components in optoelectronics, such as touch screens, interactive devices, and top electrodes for solar cells. To this point, the use of regular cellulose paper in optoelectronics is not suitable as paper is opaque and it scatters incident light very well (Fortunato et al., 2008; Pan et al., 2022). Fortunately, nanopaper made from CNF shows a remarkable transmittance of up to 90% (Fukuzumi et al., 2009). The nanopaper also exhibits a high mechanical strength (223 MPa), very small thermal expansion (8.5 ppm K^{-1}), and superior smooth surface (<5 nm) (Huang, Zhu, et al., 2013a). These unique properties, combined with light weight, flexibility and renewability, make nanopaper a promising substrate for optoelectronics. Here we mainly discuss nanopaper-based optoelectronics.

In 2013, Hu's group first reported the fabrication of flexible OTFTs on highly transparent nanopaper (Huang, Zhu, et al., 2013a). OTFTs are the basic building blocks for flexible integrated circuits and displays. Owing to low surface roughness and high optical transmittance, the nanopaper could accommodate the transistor layers, with an effective carrier mobility of 4.3×10^{-3} cm^2 V^{-1} s^{-1} and on/off ratio up to 200, comparable to other n-type OFETs. Remarkably, a less than 10% decrease in mobility was found after bending and folding. Fujisaki et al. (2014) successfully fabricated a short-channel bottom-contact OTFT on nanopaper using a combination

of lithographic and solution-based methods. The nanopaper-based OTFTs demonstrated impressive carrier mobility, reaching up to 1 $cm^2\ V^{-1}\ s^{-1}$ (among the highest ones in paper-based OTFTs so far), along with a low hysteresis of less than 0.1 V in ambient conditions. Other types of organic transistors have also been developed on nanopaper for a variety of applications. For instance, Park et al. (2018) developed transparent organic phototransistors (OPTs) capable of detecting visible light using nontoxic organic active materials on nanopaper substrates. These OPTs operate in two modes and achieve a maximum responsivity of 54.8 A W^{-1}, along with a photosensitivity of 24.4 under white light at an intensity of 0.12 mW cm^{-2}.

The optical haze, which is a measurement of the degree of light scattering, is also crucial for optoelectronics (Yao et al., 2016). Zhu's group demonstrated the transmittance and optical haze on various substrates, revealing that nanopaper exhibits the highest diffusive transmittance, reaching up to 50%, while its specular transmittance is the lowest compared to regenerated cellulose film, which shows much lower values across most wavelengths (Zhu et al., 2013). Ha (2016) reported a transparent nanopaper-based anti-reflection coating for the photovoltaics application. The application of a paper coating significantly reduces light reflectivity and enhances the cell's power conversion efficiency. To gain both high optical transmittance and high transmittance haze in a broad range of wavelength, Yao et al. (2016) produced a plastic-paper that has an ultra-flat flexible surface to accommodate an organic light-emitting diode (OLED). The plastic-paper enhances light coupling in optoelectronic devices, leading to improved efficiency for both OLEDs and standard GaAs solar cells. This newly developed low-cost, high-performance transparent and hazy substrate paves the way for the next generation of display applications.

Nanopaper has also been used as a substrate for solar cells, where high transparency and high optical haze are required to gain enhanced light scattering and improve the absorption in the active materials. Hu's group introduced a solar cell by laminating active materials with TEMPO nanopaper, achieving an impressive transparency of 96% along with a high haze of around 60% (Fang et al., 2014). The solar cell exhibited an increase in power conversion efficiency (PCE) from 5.34 to 5.88%, about 10% enhancement than that without nanopaper lamination. Zhou et al. (2013) fabricated a polymer solar cell on CNC substrates, showing a PCE of 2.7% and exhibiting good rectification in the dark. They also created a solar cell via a film-transfer lamination method, further improving the PCE to 4.0%, which is a remarkable level of performance created on a renewable substrate. Nogueira's group successfully compared both CNF and CNC substrates and demonstrated their application in organic solar cells (Costa et al., 2016). For the first time, they explored how the different properties of these cellulose substrates affect the performance of organic solar cells. The PCEs of inverted organic solar cells using CNF, CNC, and glass substrates were 0.5%, 1.4%, and 3%, respectively. Yu and Sun (2018) also developed a flexible organic-inorganic hybrid perovskite solar cell (PSC) using transparent nanopaper, achieving a PCE of 4.25% and a power density of 0.56 W g^{-1}. These flexible PSCs also demonstrated excellent stability, retaining over 80% of their original efficiency after 50 bending cycles. Meanwhile, Wu et al. (2020) fabricated a water-resistant nanopaper-based organic solar cell. The nanopaper was

made from hydrophobic tobacco stalk of agroforestry residues. Owing to the synergy between light scattering and the intrinsic different refractive index of cellulose itself, the solar cell achieved the PCE up to 16.17%, which is one of the best results for natural materials for organic solar cell use, along with an effective wide-angle harvesting in the range from −45° to 45°.

13.3.2 Conductive Paper in Energy Technology

Energy storage devices, including batteries and supercapacitors, consist of two electrodes separated by an electrolyte. In batteries, electric charge is stored as chemical energy in a high density, through electrochemical redox reactions in the electrode materials (Faradaic processes). While supercapacitors store electrostatic charge by forming an electric double layer at the interface between the electrolyte and the electrodes (non-Faradaic processes). Conductive paper can be used as electrodes for battery and capacitor. Its hierarchically porous fibrous networks and hygroscopic properties particularly promote the storage of liquid conductive electrolytes. The thin paper layer serves as an effective separating membrane between electrodes in supercapacitor. In the following, we briefly discuss the application of conductive paper substrates in energy technology. Readers are highly encouraged to refer to the Part 4 of Volume 3 in this handbook series for more details.

13.3.2.1 Conductive Paper-Based Electrodes for Lithium-Ion Batteries (LIB)

Cellulose paper-based LIB has been the subject of extensive research (Juqu et al., 2022). The primary advantage of integrating lithium-ion batteries onto a paper substrate is that paper facilitates the control of electron and ion transfer throughout the entire battery structure, especially within the electrodes. This property contributes to achieving high-power performance (Juqu et al., 2022). In an early study, Wang et al . demonstrated the dipping of SWCNT on the surface of polycellulose paper immediately transformed the paper into a highly conductive channel for electron transport (Wang et al., 2012). A full cell, consisting of $LiFePO_4$/SWCNT/PPs and $Li_4Ti_5O_{12}$/SWCNT/PPs as cathode and anode electrodes, respectively, showed a first discharge capacity of 153.5 mA h g^{-1} with Coulombic efficiencies of 90.6% at 0.1 °C and discharge capacity of 102.6 mA h g^{-1} at high rate (10 °C), which is comparable to the metallic current collector.

However, the capacity of CNT membranes typically falls below 400 mA h g^{-1}, which does not meet the increasing demand for higher-capacity materials (Wang et al., 2010). To improve this, Wang, Guo, et al. (2018a) incorporated spherical carbon-coated molybdenum disulfide (MoS_2@C) in linear nitrogen-doped carbon nanotubes electrodes that are embedded in recycled paper. This N-CNT/MoS_2@C/RP film (N-M-RP film) serves as the anode material for paper-based LIBs,

achieving a discharge capacity of 989.6 mA h g^{-1} after 50 cycles, with a high initial Coulombic efficiency of 70.5% at a current density of 100 mA g^{-1}.

Conductive paper-based substrates have also reported as the electrodes for other high-performance batteries. For example, Huang, Sun, et al. (2013b) reported mesoporous graphene-sulfur paper used as electrodes in rechargeable lithium-sulfur batteries, which yielded a high specific discharge capacity of 1393 mA h g^{-1} and retained 689 mA h g^{-1} after 50 cycles. Liu et al. (2015) prepared paper-based Li-oxygen batteries with super-large theoretical capacity. The Li-O_2 battery exhibited an exceptionally high capacity of about 6500 mA h g^{-1} at a current density of 200 mA g^{-1} and reached about 50 cycles with the capacity restricted to 1000 mA h g^{-1} at a current density of 200 mA g^{-1}.

13.3.2.2 Conductive Paper-Based Electrodes for Supercapacitors (SCs)

Recently, there has been a particular interest in developing supercapacitors for wearable devices, due to their fast charging and discharging speeds, as well as excellent cyclability. Paper-based supercapacitors have emerged because of the growing demand for thin, lightweight, flexible, and cost-effective devices.

SCs can be constructed in the configurations of sandwich-like devices and planar devices. Most paper-based and paper-like electrodes are assembled into a sandwich-like configuration for SCs. In this mode, conductive active materials combine with cellulose fibers to form electrodes. Yuan et al. (2012) assembled solid-state supercapacitors by sandwiching a PVA/H_3PO_4 film between two identical PANI-Au paper electrodes, as shown in Fig. 13.4a. The PVA/H_3PO_4 film served as both the electrolyte and the separator. The solid-state SCs exhibit a high energy density of around 0.01 W h cm^{-3} and a power density of around 3 W cm^{-3}. The highest areal capacitance of about 0.8 F cm^{-2} and a volumetric capacitance of 800 F cm^{-3} were achieved at a discharge current of 1 mA cm^{-2}, respectively. Both CV and galvanostatic charge-discharge curves show an ideal capacitive behavior of the SC (Fig. 13.4b, c). This configuration demonstrated good stability under various

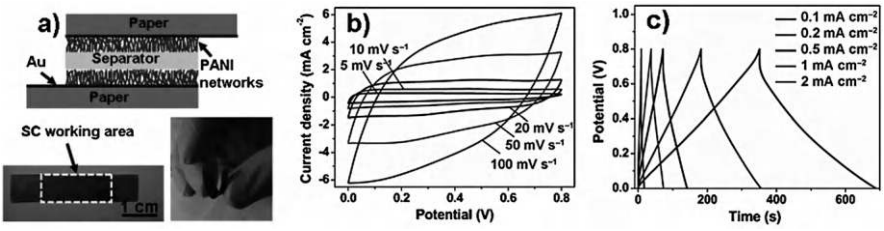

Fig. 13.4 Flexible conductive paper-based solid-state supercapacitors. (**a**) Scheme of the solid-state SCs (upper) and photographs of the SC (down). (**b**) CV and (**c**) galvanostatic charge–discharge curves of the solid-state supercapacitor. Reprinted with permission from Yuan et al. (2012). Copyright 2012, Wiley-VCH Verlag GmbH & Co

bending states. In a similar study, Yao et al. (2013) fabricated paper-based symmetric supercapacitors using two pencil-drawn graphite/polyaniline hybrid electrodes. The device exhibited a volumetric capacitance of 3.55 F cm^{-3} at a power density of 0.054 W cm^{-3}, and an energy density of approximately 0.32 mWh cm^{-3} at a power density of 0.054 W cm^{-3}, normalized to the total volume of the solid-state device. These characteristics highlight their potential for efficient energy storage applications.

13.3.2.3 Conductive Paper-Based Other Components for Energy Storage

In addition to electrode materials, paper substrates can also serve as the matrix for ionic and electron storage and transport in the battery or SC systems. Wang, Pan, et al. (2019b) developed a paper-based gel electrolyte (PBGE) for liquid-free Al-air batteries by infusing sodium polyacrylate and sodium hydroxide into paper. The PBGE enabled rechargeable and single-use Al-air batteries with an open circuit voltage of 1.5 V, a peak power density of 6.4 mW cm^{-2}, and a discharge capacity of 900 mA h g^{-1}. In 2023, Wang et al. (2023) also created a paper-based aqueous Al-ion battery that stored a highly concentrated $AlCl_3$ solution, achieving 1.6–1.8 V and 140 mA h g^{-1} at 1 A g^{-1}. This technology shows potential for powering RFID tags, smart packages, and biosensors.

The large porous network, low cost, and natural hydrophilicity could favor paper as an excellent separator in battery devices. Yang et al. (2022) developed a biodegradable zinc battery with hydrogel-reinforced cellulose paper (HCP) as the electrolyte and separator, enhancing mechanical strength and ionic conductivity (33 mS cm^{-1}). The HCP-based batteries exhibited excellent cycling performance and a volumetric energy density of 26 mW h cm^{-3}. Wang et al. (2020b) used lyocell fibrillated (LF) fibers as separators for lithium-ion batteries, achieving excellent cycling performance due to their large pores and high porosity. They further improved this by creating a polyvinyl alcohol/lyocell dual-layer (PDL) separator, offering superior discharge, high-temperature stability, and efficient electrolyte retention, making it a promising alternative for zinc-air batteries (Wang et al., 2021).

13.3.3 Conductive Paper-Based Sensors and Biosensors

Conductive paper is widely used in sensing and biosensing, enabling the monitoring of metrics like heart rate, respiration, stress, and biomarkers. Its advantages include cost-effectiveness, biodegradability, lightweight portability, and flexibility, making it ideal for wearable applications. The porous cellulose network stores reagents (e.g., antibodies, enzymes) and allows biofluid movement via capillary action. Several applications of conductive paper-based sensors are as follows.

13.3.3.1 Pressure Sensors

Flexible pressure sensors are gaining attention for applications in healthcare, human-machine interfaces, and prosthetics (Pierre Claver & Zhao, 2021). Conductive paper-based sensors are preferred over rigid materials like silicon and metal due to their flexibility, degradability, and porosity. A typical method for developing paper-based pressure sensors is to use a cellulose paper layer between conductive coatings, measuring the electrical resistance under varying pressure (Fig. 13.5). For example, Gong et al. (2014) mounted ultrathin Au NW-infused tissue paper between two PDMS sheets. Pressure reduces the air gap between the Au NW/paper layer and the PDMS electrodes, lowering the resistance. This sensor operates at a low voltage of 1.5 V, offering high sensitivity (1.14 kPa^{-1}), fast response time (<17 ms), and stability over 50,000 cycles with low power consumption

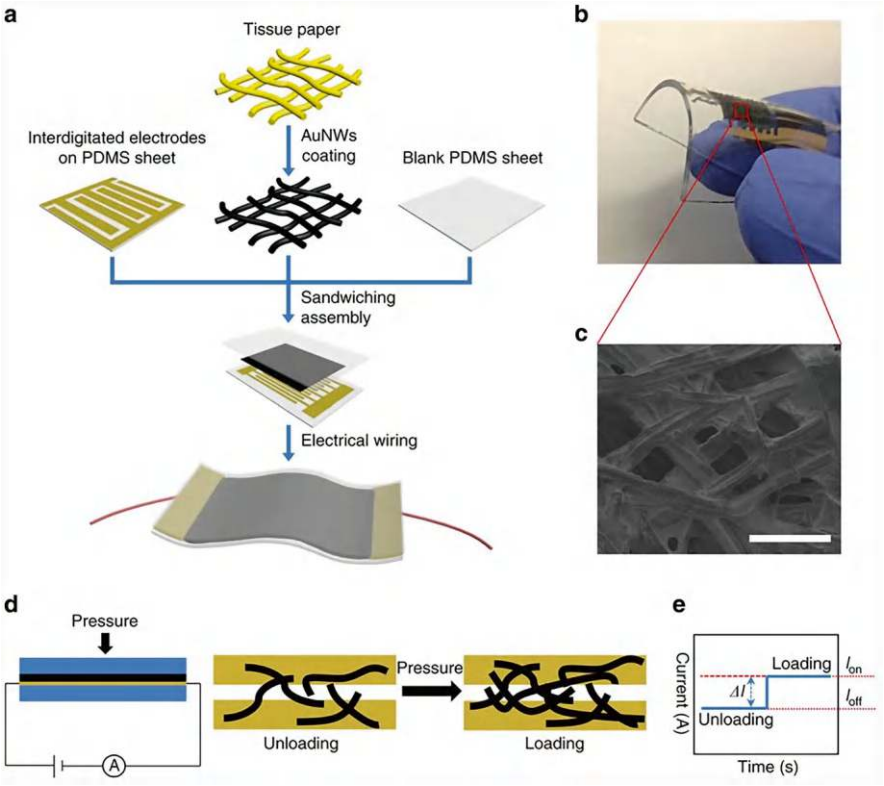

Fig. 13.5 (**a**) Schematic representation of the fabrication process for an AuNW-coated paper-based pressure sensor. (**b**) Photo showing the sensor's flexibility. (**c**) Scanning electron microscopy image depicting the porous structure of Au NWs-coated tissue fibers (scale bar: 100 μm). (**d**) Schematic illustration of the sensing mechanism and (**e**) current changes in response to loading and unloading (I_{off}: unloading, I_{on}: loading). Reprinted with permission from Gong et al. (2014). Copyright 2014, Springer Nature Limited

(<30 μW). It can detect a wide range of dynamic forces (13–50,000 Pa), including pressure, bending, torsion, and acoustic vibrations, making it suitable for real-time monitoring of blood pulses and acoustic vibrations.

Numerous paper-based pressure sensors have been developed by using different conductive materials, including Au NPs (Huang et al., 2020), Ag (Lee et al., 2022), CNTs (Lee et al., 2022; Wang, Hou, et al., 2020a; Zhan et al., 2017), MXenes (Guo et al., 2019; Pataniya et al., 2021), and metal chalcogenides (Aderu et al., 2022), either to offer better sensitivity or reduce the cost. These conductive materials are typical incorporated in the cellulose fibers using simply dip-coating. An alternative design uses paper origami, where Karmakar et al. (2024) combined two screen-printed conductive paper substrates with specific folds for optimization. This design achieved a sensitivity of 3.75 kPa^{-1} at low pressures (0–0.05 kPa).

Overall, conductive paper-based pressure sensors are cost-effective, scalable, and easy to produce, enabling real-time monitoring of forces like respiration, wrist pulses, and vibrations. Their use in sensors is expected to lead to seamless integration with smart wearables, such as flexible displays, human-machine interfaces, and prosthetic skins.

13.3.3.2 Electrochemical Sensors

A major application of conductive paper in recent decades has been the development of low-cost paper-based point-of-care (POC) electrochemical sensors for detecting substances and biomarkers in biofluids. Yager and Whiteside pioneered the development of POC paper-based microfluidic devices (μPAD) that were used in biosensing applications (Fu, Kauffman, et al., 2010a; Fu, Lutz, et al., 2010b; Martinez et al., 2007). The paper-based POC diagnostics are simple, rapid, and cost-effective, making them highly suitable for resource-limited environments. Initially, the μ-PADs can be analyzed via colorimetric method. However, the colorimetric analysis is imprecise and the limit of detection is also low. Dungchai et al. (2009) introduced the first electrochemical microfluidic paper-based analytical device for the simultaneous detection of glucose, lactate, and uric acid in human serum. Whiteside group further utilized microfluid patterns to guide the fluid transportation and developed a microfluidic paper-based electrochemical device termed as μPED for detecting glucose in artificial urine (Nie et al., 2010).

Paper-based electrochemical sensors replicate the traditional three-electrode system (counter, reference, and working electrodes) on paper (Fig. 13.6). Conductive inks like gold, platinum, carbon, graphene, or silver are used to print electrodes on paper (Xia et al., 2016). Silver/silver chloride paste is preferred for the reference electrode due to its stability, while carbon ink is used for the working and counter electrodes for its low cost and wide potential window in aqueous solvents (Dungchai et al., 2009; Xia et al., 2016). Bioreceptors, such as enzymes or antibodies, are immobilized on the working electrode to detect target analytes like glucose or antigens. Free electrons are produced via chemical reactions involving related enzyme

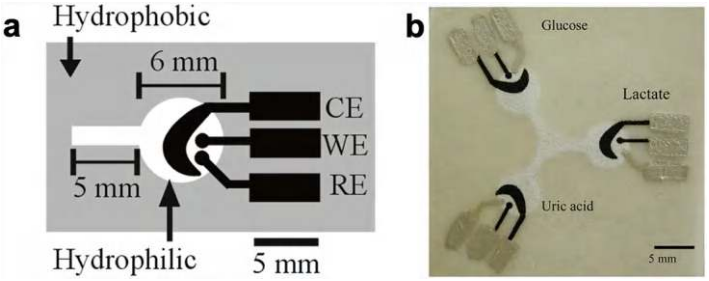

Fig. 13.6 (**a**) Basic design of the electrochemical detection cell on paper. *WE* working electrode, *RE* reference electrode, *CE* counter electrode. (**b**) Scheme of the paper-based electrodes in electrochemical sensors. Reprinted with permission from Dungchai et al. (2009). Copyright 2009, American Chemical Society

substrates and/or H_2O_2 (Wu et al., 2014; Zang et al., 2012). Signal detection is typically done using amperometry, measuring current and voltage changes in response to analyte concentration.

Other electrochemical analysis methods have also been explored, including potentiometric, voltammetric, photoelectrochemical, organic electrochemical transistors, and electro-chemiluminescent sensors (Fu & Wang, 2018). Among them, potentiometry, which is based on measurements of the difference in potential between an indicator electrode and a reference electrode, has been extensively used in label-free sensing. Bhardwaj et al. (2017) developed a low-cost electrochemical immunosensor on a paper substrate for label-free detection of *Staphylococcus aureus* using differential pulse voltammetry. The resulting paper-based electrochemical device-maintained stability for over a month and achieved a sensitive detection limit of 15 CFU mL^{-1}, with a concentration range from 10 to 10^7 CFU mL^{-1}. In recent years, electrochemical impedance spectroscopy (EIS), which offers a detailed view of the electrode/solution interface, measuring characteristics like capacitance and charge transfer resistance, has been used to construct paper-based electrochemical sensors (Li et al., 2021; Li & Liu, 2016). The label-free measurement makes it ideal for monitoring non-electroactive binding molecules, such as biomolecular interactions (e.g., antibody-antigen, DNA-DNA, DNA-protein, receptor-ligand) (Daniels & Pourmand, 2007).

Overall, conductive paper-based electrochemical sensors have great potential for POC diagnostics in resource-limited settings due to their affordability, sensitivity, specificity, user-friendliness, rapid results, robustness, and equipment-free design (collectively known as ASSURED). In the past decade, numerous studies have explored the use of conductive paper-based electrochemical sensor for sensing heavy metals, metabolic substances, protein biomarkers, virus, and cells (Sun et al., 2022). However, challenges remain for commercialization, including: (1) scaling up mass production, (2) ensuring reproducibility across varying testing conditions (such as humidity, temperature, ambient light, and sample complexity), and (3) facilitating accurate use by untrained individuals. The readers are referred to Ch 17 in Volume 2 of this handbook series or several recent reviews for detailed discussion (du Plooy et al., 2023; Sun et al., 2022).

13.3.3.3 Other Sensors

Conductive paper have also been extensively used as a substrates for developing other sensors, including temperature sensor (Zikulnig et al., 2019), bending strain sensor (Liu et al., 2017, 2021), light sensor (Gimenez et al., 2011), biopotential sensor (Das & Park, 2017; Guo et al., 2017; McKnight et al., 2015), pH sensor (Lei et al., 2012), gas sensor (Huang et al., 2014; Mirica et al., 2012, 2013; Noremberg et al., 2017; Quddious et al., 2016), and humidity and respiration (Güder et al., 2016). It is expected that research on the paper-based sensor will continue, and the applications will be further extended, particularly in resource-limited areas. Readers are referred to Volume 2 of this handbook series for more information.

13.4 Challenges and Conclusions

In conclusion, we highlighted the technology development in conductive paper substrates and the potential of these substrates for creating various low-cost, sustainable, and flexible electronic devices. The motivations of these technology developments align with the pursuit of more sustainable, disposable, and environmentally friendly alternatives to the currently used polymer or silicon-based electronics. Their applications span multiple fields, including energy storage, biochemical and motion sensing, and electronics, demonstrating their versatility.

However, challenges remain in advancing conductive paper-based devices. The porosity of cellulose-rich paper, while beneficial for adhesion and storage, can lower conductivity and affect resolution, particularly in high-capacity electronics. Additionally, the selection of active materials is crucial for enhancing performance, though it may involve trade-offs—for example, hydrophobic materials can improve electron mobility but hinder biofluid transport in biosensors. Further research is needed to address the stability and durability issues of paper-based devices, as cellulose fibers are weaker than traditional polymers and sensitive to moisture. Additionally, the lack of standardized manufacturing processes hampers reproducibility and scalability.

Despite these challenges, continued research and collaboration between academia and industry are essential to advancing these technologies and commercializing flexible paper electronics for practical, everyday use.

References

Aderu, V., Tathacharya, M., Raghuram, C. S., Mattela, V., & Sahatiya, P. (2022). TeNWs/$Ti_3C_2T_x$ nanohybrid-based flexible pressure sensors for personal safety applications using Morse code. *ACS Applied Nano Materials, 5*, 18209–18219. https://doi.org/10.1021/acsanm.2c04088

Aeby, X., Poulin, A., Siqueira, G., Hausmann, M. K., & Nyström, G. (2021). Fully 3D printed and disposable paper supercapacitors. *Advanced Materials, 33*, 2101328. https://doi.org/10.1002/adma.202101328

Andersson, H. A., Manuilskiy, A., Haller, S., Hummelgård, M., Sidén, J., Hummelgård, C., Olin, H., & Nilsson, H.-E. (2014). Assembling surface mounted components on ink-jet printed double sided paper circuit board. *Nanotechnology, 25*, 094002. https://doi.org/10.1088/0957-4484/25/9/094002

Ando, Y., Zhao, X., Shimoyama, H., Sakai, G., & Kaneto, K. (1999). Physical properties of multiwalled carbon nanotubes. *International Journal of Inorganic Materials, 1*, 77–82. https://doi.org/10.1016/S1463-0176(99)00012-5

Andò, B., Baglio, S., Lombardo, C. O., Marletta, V., & Pistorio, A. (2016). A low-cost accelerometer developed by inkjet printing technology. *IEEE Transactions on Instrumentation and Measurement, 65*, 1242–1248. https://doi.org/10.1109/TIM.2015.2490998

Bacon, W. S. (1968). Now they're printing transistors on paper. *Popular Science Magazines, 1968*, 124–125.

Bhardwaj, J., Devarakonda, S., Kumar, S., & Jang, J. (2017). Development of a paper-based electrochemical immunosensor using an antibody-single walled carbon nanotubes bio-conjugate modified electrode for label-free detection of foodborne pathogens. *Sensors & Actuators, B: Chemical, 253*, 115–123. https://doi.org/10.1016/j.snb.2017.06.108

Brody, T. P. (1984). The thin film transistor—A late flowering bloom. *IEEE Transactions on Electron Devices, 31*, 1614–1628. https://doi.org/10.1109/T-ED.1984.21762

Caratelli, V., Di Meo, E., Colozza, N., Fabiani, L., Fiore, L., Moscone, D., & Arduini, F. (2022). Nanomaterials and paper-based electrochemical devices: Merging strategies for fostering sustainable detection of biomarkers. *Journal of Materials Chemistry B, 10*, 9021–9039. https://doi.org/10.1039/D2TB00387B

Chang, F., Hampton, R. N., & Hobdell, S. B. (2000). The effect of paper properties on the temperature and stress dependence of the resistivity of impregnated laminates. In *Eighth international conference on dielectric materials, measurements and applications* (pp. 474–479). IEEE. https://doi.org/10.1049/cp:20000555

Chen, L., Ying, B., Song, P., & Liu, X. (2019). Nanopaper: A nanocellulose-paper-based SERS multiwell plate with high sensitivity and high signal homogeneity. *Advanced Materials Interfaces, 6*, 1970155. https://doi.org/10.1002/admi.201901346

Christie, J., Sylvander, S., Woodhead, I., & Irie, K. (2004). The dielectric properties of humid cellulose. *Journal of Non-Crystalline Solids, 341*, 115–123. https://doi.org/10.1016/j.jnoncrysol.2004.05.014

Chu, C.-L., Lee, J., Lee, T.-H., & Cheng, Y.-N. (2009). Oxidation behavior of metallic interconnect coated with La-Sr-Mn film by screen painting and plasma sputtering. *International Journal of Hydrogen Energy, 34*, 422–434. https://doi.org/10.1016/j.ijhydene.2008.09.091

Cimbala, R., Kruželák, L., & Sekelová, N. (2018). Impact of volume resistance on the surface resistance of paper. In *19th international scientific conference on electric power engineering*. IEEE. https://doi.org/10.1109/EPE.2018.8395988

Conti, S., Pimpolari, L., Calabrese, G., Worsley, R., Majee, S., Polyushkin, D. K., et al. (2020). Low-voltage 2D materials-based printed field-effect transistors for integrated digital and analog electronics on paper. *Nature Communications, 11*, 3566. https://doi.org/10.1038/s41467-020-17297-z

Costa, S. V., Pingel, P., Janietz, S., & Nogueira, A. F. (2016). Inverted organic solar cells using nanocellulose as substrate. *Journal of Applied Polymer Science, 133*, 43679. https://doi.org/10.1002/app.43679

Cunha, I., Barras, R., Grey, P., Gaspar, D., Fortunato, E., Martins, R., & Pereira, L. (2017). Reusable cellulose-based hydrogel sticker film applied as gate dielectric in paper electrolyte-gated transistors. *Advanced Functional Materials, 27*, 1606755. https://doi.org/10.1002/adfm.201606755

Cunha, I., Martins, J., Bahubalimdruni, P. G., Carvalho, J. T., Rodrigues, J., Rubin, S., et al. (2021). Handwritten and sustainable electronic logic circuits with fully printed paper transistors. *Advanced Materials Technologies, 6*, 2100633. https://doi.org/10.1002/admt.202100633

D'Andrade, B., Kattamis, A., & Murphy, P. (2014). Flexible organic electronic devices on metal foil substrates for lighting, photovoltaic, and other applications. In *Handbook of flexible organic electronics: Materials, manufacturing and applications* (p. 315). Elsevier.

Daniels, J. S., & Pourmand, N. (2007). Label-free impedance biosensors: Opportunities and challenges. Electroanalysis: *An International Journal Devoted to Fundamental and Practical Aspects of Electroanalysis, 19*(12), pp.1239–1257. https://doi.org/10.1002/elan.200603855

Das, P. S., & Park, J.-Y. (2017). A flexible touch sensor based on conductive elastomer for biopotential monitoring applications. *Biomedical Signal Processing and Control, 33*, 72–82. https://doi.org/10.1016/j.bspc.2016.11.008

Denneulin, A., Blayo, A., Bras, J., & Neuman, C. (2008). PEDOT:PSS coating on specialty papers: Process optimization and effects of surface properties on electrical performances. *Progress in Organic Coatings, 63*, 87–91. https://doi.org/10.1016/j.porgcoat.2008.04.009

Dillon, A. D., Ghidiou, M. J., Krick, A. L., Griggs, J., May, S. J., Gogotsi, Y., et al. (2016). Highly conductive optical quality solution-processed films of 2D titanium carbide. *Advanced Functional Materials, 26*, 4162–4168. https://doi.org/10.1002/adfm.201600357

Domaschke, M., Schmidt, M., & Peukert, W. (2018). A model for the particle mass yield in the aerosol synthesis of ultrafine monometallic nanoparticles by spark ablation. *Journal of Aerosol Science, 126*, 133–142. https://doi.org/10.1016/j.jaerosci.2018.09.004

Du Plooy, J., Jahed, N., Iwuoha, E., & Pokpas, K. (2023). Advances in paper-based electrochemical immunosensors: Review of fabrication strategies and biomedical applications. *Royal Society Open Science, 10*, 230940. https://doi.org/10.1098/rsos.230940

Dungchai, W., Chailapakul, O., & Hennry, C. S. (2009). Electrochemical detection for paper-based microfluidics. *Analytical Chemistry, 81*, 5821–5826. https://doi.org/10.1021/ac9007573

Fang, Z., Zhu, H., Yuan, Y., Ha, D., Zhu, S., Preston, C., et al. (2014). Novel nanostructured paper with ultrahigh transparency and ultrahigh haze for solar cells. *Nano Letters, 14*, 765–773.

Fortunato, E., Correia, N., Barquinha, P., Pereira, L., Gonçalves, G. & Martins, R. (2008). High-performance flexible hybrid field-effect transistors based on cellulose fiber paper. *IEEE Electron Device Letters, 29*(9), pp.988–990. https://doi.org/10.1109/LED.2008.2001549

Forrest, S. R. (2004). The path to ubiquitous and low-cost organic electronic appliances on plastic. *Nature, 428*, 911–918. https://doi.org/10.1038/nature02498

Fielding, L. A., Hillier, J. K., Burchell, M. J. and Armes, S. P., (2015). Space science applications for conducting polymer particles: synthetic mimics for cosmic dust and micrometeorites. *Chemical Communications, 51*(95), pp.16886–16899. https://doi.org/10.1039/C5CC07405C

Fu, L.-M., & Wang, Y.-N. (2018). Detection methods and applications of microfluidic paper-based analytical devices. *TrAC Trends in Analytical Chemistry, 107*, 196–211. https://doi.org/10.1016/j.trac.2018.08.018

Fu, E., Kauffman, P., Lutz, B., & Yager, P. (2010a). Chemical signal amplification in two-dimensional paper networks. *Sensors & Actuators, B: Chemical, 149*, 325–328. https://doi.org/10.1016/j.snb.2010.06.024

Fu, E., Lutz, B., Kauffman, P., & Yager, P. (2010b). Controlled reagent transport in disposable 2D paper networks. *Lab on a Chip, 10*, 918–920. https://doi.org/10.1039/B919614E

Fujisaki, Y., Koga, H., Nakajima, Y., Nakata, M., Tsuji, H., Yamamoto, T., et al. (2014). Transparent nanopaper-based flexible organic thin-film transistor array. *Advanced Functional Materials, 24*, 1657–1663. https://doi.org/10.1002/adfm.201303024

Fukuzumi, H., Saito, T., Iwata, T., Kumamoto, Y., & Isogai, A. (2009). Transparent and high gas barrier films of cellulose nanofibers prepared by TEMPO-mediated oxidation. *Biomacromolecules, 10*, 162–165. https://doi.org/10.1021/bm801065u

Garino, N., Lamberti, A., Stassi, S., Castellino, M., Fontana, M., Roppolo, I., et al. (2019). Multifunctional flexible membranes based on reduced graphene oxide/tin dioxide nanocomposite and cellulose fibers. *Electrochimica Acta, 306*, 420–426. https://doi.org/10.1016/j.electacta.2019.02.095

Gasser, H. P., Huser, J., Krause, C., Dahinden, V., & Emsley, A. M. (1999). Determining the ageing parameters of cellulosic insulation in a transformer. In *Proceedings of eleventh international*

symposium on high voltage engineering (Vol. 4, pp. 143–147). IEEE. https://doi.org/10.1049/cp:19990813

Gimenez, A. J., Yañez-Limón, J. M., & Seminario, J. M. (2011). ZnO-paper based photoconductive UV sensor. *Journal of Physical Chemistry C, 115*, 282–287. https://doi.org/10.1021/jp107812w

Gong, S., Schwalb, W., Wang, Y., Chen, Y., Tang, Y., Si, J., Shirinzadeh, B., & Cheng, W. (2014). A wearable and highly sensitive pressure sensor with ultrathin gold nanowires. *Nature Communications, 5*, 3132. https://doi.org/10.1038/ncomms4132

Grau, G., Frazier, E. J., & Subramanian, V. (2016). Printed unmanned aerial vehicles using paper-based electroactive polymer actuators and organic ion gel transistors. *Microsystems & Nanoengineering, 2*, 16032. https://doi.org/10.1038/micronano.2016.32

Guan, X., Cao, L., Huang, Q., Kong, D., Zhang, P., Lin, H., et al. (2019). Direct writing supercapacitors using a carbon nanotube/ag nanoparticle-based ink on cellulose acetate membrane paper. *Polymers, 11*, 973. https://doi.org/10.3390/polym11060973

Güder, F., Ainla, A., Redston, J., Mosadegh, B., Glavan, A., Martin, T. J., & Whitesides, G. M. (2016). Paper-based electrical respiration sensor. *Angewandte Chemie, International Edition, 55*, 5727–5732. https://doi.org/10.1002/anie.201511805

Guo, X., Pei, W., Wang, Y., Gong, Q., Zhang, H., Xing, X., et al. (2017). A self-wetting paper electrode for ubiquitous bio-potential monitoring. *IEEE Sensors Journal, 17*, 3645–3651. https://doi.org/10.1109/JSEN.2017.2684825

Guo, Y., Zhong, M., Fang, Z., Wan, P., & Yu, G. (2019). A wearable transient pressure sensor made with MXene nanosheets for sensitive broad-range human–machine interfacing. *Nano Letters, 19*, 1143–1150. https://doi.org/10.1021/acs.nanolett.8b04514

Ha, D. (2016). *Microscale dielectric anti-reflection coatings for photovoltaics*. University of Maryland.

Hamedi, M. M., Hajian, A., Fall, A. B., Håkansson, K., Salajkova, M., Lundell, F., et al. (2014). Highly conducting, strong nanocomposites based on nanocellulose-assisted aqueous dispersions of single-wall carbon nanotubes. *ACS Nano, 8*, 2467–2476. https://doi.org/10.1021/nn4060368

Han, J.-W., Kim, B., Li, J., & Meyyappan, M. (2014). Carbon nanotube ink for writing on cellulose paper. *Materials Research Bulletin, 50*, 249–253. https://doi.org/10.1016/j.materresbull.2013.10.048

Ho, T. D., Canestraro, A. J., & Anderson, J. L. (2011). Ionic liquids in solid-phase microextraction: A review. *Analytica Chimica Acta, 695*, 18–43. https://doi.org/10.1016/j.aca.2011.03.034

Hollertz, R., Wågberg, L., & Pitois, C. (2015). Effect of composition and morphology on the dielectric response of cellulose-based electrical insulation. *IEEE Transactions on Dielectrics and Electrical Insulation, 22*, 2339–2348. https://doi.org/10.1109/TDEI.2015.005017

Hu, L., Choi, J. W., Yang, Y., Jeong, S., La Mantia, F., Cui, L.-F., & Cui, Y. (2009). Highly conductive paper for energy-storage devices. *Proceedings of the National Academy of Sciences of the United States of America, 106*, 21490–21494. https://doi.org/10.1073/pnas.0908858106

Hu, C., Ding, Y., Ji, Y., Xu, J., & Hu, S. (2010a). Fabrication of thin-film electrochemical sensors from single-walled carbon nanotubes by vacuum filtration. *Carbon, 48*, 1345–1352. https://doi.org/10.1016/j.carbon.2009.12.024

Huang, J., Zhu, H., Chen, Y., Preston, C., Rohrbach, K., Cumings, J., & Hu, L. (2013a). Highly transparent and flexible nanopaper transistors. *ACS Nano, 7*, 2106–2113. https://doi.org/10.1021/nn304407r

Huang, X., Sun, B., Li, K., Chen, S., & Wang, G. (2013b). Mesoporous graphene paper immobilized sulfur as a flexible electrode for lithium–sulfur batteries. *Journal of Materials Chemistry A, 1*, 13484–13489. https://doi.org/10.1039/C3TA12826A

Huang, L., Jiang, P., Wang, D., Luo, Y., Li, M., Lee, H., & Gerhardt, R. A. (2014). A novel paper-based flexible ammonia gas sensor via silver and SWNT-PABS inkjet printing. *Sensors & Actuators, B: Chemical, 197*, 308–313. https://doi.org/10.1016/j.snb.2014.02.081

Huang, H., Chu, X., Su, H., Zhang, H., Xie, Y., Deng, W., et al. (2019). Massively manufactured paper-based all-solid-state flexible micro-supercapacitors with sprayable MXene conductive inks. *Journal of Power Sources, 415*, 1–7. https://doi.org/10.1016/j.jpowsour.2019.01.044

Huang, Y., Wang, Z., Zhou, H., Guo, X., Zhang, Y., Wang, Y., et al. (2020). Highly sensitive pressure sensor based on structurally modified tissue paper for human physiological activity monitoring. *Journal of Applied Polymer Science, 137*, 48973. https://doi.org/10.1002/app.48973

Hyun, W. J., Secor, E. B., Rojas, G. A., Hersam, M. C., Francis, L. F., & Frisbie, C. D. (2015). All-printed, foldable organic thin-film transistors on glassine paper. *Advanced Materials, 27*, 7058–7064. https://doi.org/10.1002/adma.201503478

Irimia-Vladu, M. (2014). "Green" electronics: Biodegradable and biocompatible materials and devices for a sustainable future. *Chemical Society Reviews, 43*, 588–610. https://doi.org/10.1021/acsabm.0c01139

Jansson, E., Lyytiäinen, J., Tanninen, P., Eiroma, K., Leminen, V., Immonen, K., & Hakola, L. (2022). Suitability of paper-based substrates for printed electronics. *Maternité, 15*, 957. https://doi.org/10.3390/ma15030957

Jiang, Z., Chen, L., Chen, J.-J., Wang, Y., Xu, Z.-Q., Sowade, E., et al. (2020). All-inkjet-printed MoS_2 field-effect transistors on paper for low-cost and flexible electronics. *Applied Nanoscience, 10*, 3649–3658. https://doi.org/10.1007/s13204-020-01438-3

Jiao, S., Zhou, A., Wu, M., & Hu, H. (2019). Kirigami patterning of MXene/bacterial cellulose composite paper for all-solid-state stretchable micro-supercapacitor arrays. *Advancement of Science, 6*, 1900529. https://doi.org/10.1002/advs.201900529

Jung, R., Kim, H.-S., Kim, Y., Kwon, S.-M., Lee, H. S., & Jin, H.-J. (2008). Electrically conductive transparent papers using multiwalled carbon nanotubes. *Journal of Polymer Science Part B: Polymer Physics, 46*, 1235–1242. https://doi.org/10.1002/polb.21457

Juqu, T., Willenberg, S. C., Pokpas, K., & Ross, N. (2022). Advances in paper-based battery research for biodegradable energy storage. *Advanced Sensor and Energy Materials, 1*, 100037. https://doi.org/10.1016/j.asems.2022.100037

Karmakar, R. S., Huang, J.-F., Chu, C.-P., Mai, M.-H., Chao, J.-I., Liao, Y.-C., & Lu, Y.-W. (2024). Origami-inspired conductive paper-based folded pressure sensor with interconnection scaling at the crease for novel wearable applications. *ACS Applied Materials & Interfaces, 16*, 4231–4241. https://doi.org/10.1021/acsami.3c15417

Kaur, G., Adhikari, R., Cass, P., Bown, M., & Gunatillake, P. (2015). Electrically conductive polymers and composites for biomedical applications. *RSC Advances, 5*, 37553–37567. https://doi.org/10.1039/C5RA01851J

Kava, A. A. and Henry, C. S. (2021). Exploring carbon particle type and plasma treatment to improve electrochemical properties of stencil-printed carbon electrodes. *Talanta, 221*, p.121553. https://doi.org/10.1016/j.talanta.2020.121553

Kim, P., Shi, L., Majumdar, A., & McEuen, P. L. (2001). Thermal transport measurements of individual multiwalled nanotubes. *Physical Review Letters, 87*, 215502. https://doi.org/10.1103/PhysRevLett.87.215502

Kim, M., Son, W.-S., Ahn, K. H., Kim, D. S., Lee, H.-S., & Lee, Y.-W. (2014). Hydrothermal synthesis of metal nanoparticles using glycerol as a reducing agent. *Journal of Supercritical Fluids, 90*, 53–59. https://doi.org/10.1016/j.supflu.2014.02.022

Kim, D., Ko, Y., Kwon, G., Kim, U.-J., & You, J. (2018). Micropatterning silver nanowire networks on cellulose nanopaper for transparent paper electronics. *ACS Applied Materials & Interfaces, 10*, 38517–38525. https://doi.org/10.1021/acsami.8b15230

Komoda, N., Nogi, M., Suganuma, K., Koga, H., & Otsuka, K. (2012). Silver nanowire antenna printed on polymer and paper substrates. In *Proceedings of 12th IEEE Int. Conf. Nanotechnol. (IEEE-NANO 2012)* (pp. 1336–1339). IEEE. https://doi.org/10.1109/NANO.2012.6322217

Kumar, S., Pandey, C. M., Hatamie, A., Simchi, A., Willander, M., & Malhotra, B. D. (2019). Nanomaterial-modified conducting paper: Fabrication, properties, and emerging biomedical applications. *Global Challenges, 3*, 1900041. https://doi.org/10.1002/gch2.201900041

Kurra, N., Ahmed, B., Gogotsi, Y., & Alshareef, H. N. (2016). MXene-on-paper coplanar microsupercapacitors. *Advanced Energy Materials, 6*, 1601372. https://doi.org/10.1002/aenm.201601372

Kyrylyuk, A. V., Hermant, M. C., Schilling, T., Klumperman, B., Koning, C. E., & Van der Schoot, P. (2011). Controlling electrical percolation in multicomponent carbon nanotube dispersions. *Nature Nanotechnology, 6*(6), 364–369. https://doi.org/10.1038/nnano.2011.40

Lee, J. H., Marroquin, J., Rhee, K. Y., Park, S. J., & Hui, D. (2013). Cryomilling application of graphene to improve material properties of graphene/chitosan nanocomposites. *Composites Part B: Engineering, 45*, 682–687. https://doi.org/10.1016/j.compositesb.2012.05.011

Lee, T.-W., Lee, S.-E., & Jeong, Y. G. (2016). Highly effective electromagnetic interference shielding materials based on silver nanowire/cellulose papers. *ACS Applied Materials & Interfaces, 8*, 13123–13132. https://doi.org/10.1021/acsami.6b02218

Lee, T., Kang, Y., Kim, K., Sim, S., Bae, K., Kwak, Y., et al. (2022). All paper-based, multilayered, inkjet-printed tactile sensor in wide pressure detection range with high sensitivity. *Advanced Materials Technologies, 7*, 2100428. https://doi.org/10.1002/admt.202100428

Lei, K. F., Lee, K.-F., & Yang, S.-I. (2012). Fabrication of carbon nanotube-based pH sensor for paper-based microfluidics. *Microelectronic Engineering, 100*, 1–5. https://doi.org/10.1016/j.mee.2012.07.113

Li, X., & Liu, X. (2016). A microfluidic paper-based origami nanobiosensor for label-free, ultrasensitive immunoassays. *Advanced Healthcare Materials, 5*, 1326–1335. https://doi.org/10.1002/adhm.201670056

Li, S., Huang, D., Yang, J., Zhang, B., Zhang, X., Yang, G., et al. (2014). Freestanding bacterial cellulose–polypyrrole nanofibres paper electrodes for advanced energy storage devices. *Nano Energy, 9*, 309–317. https://doi.org/10.1016/j.nanoen.2014.08.004

Li, L., Ma, Z., Xu, P., Zhou, B., Li, Q., Ma, J., et al. (2020). Flexible and alternant-layered cellulose nanofiber/graphene film with superior thermal conductivity and efficient electromagnetic interference shielding. *Composites Part A: Applied Science and Manufacturing, 139*, 106134. https://doi.org/10.1016/j.compositesa.2020.106134

Li, X., Qin, Z., Fu, H., Li, T., Peng, R., Li, Z., Rini, J. M., & Liu, X. (2021). Enhancing the performance of paper-based electrochemical impedance spectroscopy nanobiosensors: An experimental approach. *Biosensors & Bioelectronics, 177*, 112672. https://doi.org/10.1016/j.bios.2020.112672

Li, L., Han, L., Hu, H., & Zhang, R. (2023). A review on polymers and their composites for flexible electronics. *Materials Advances, 4*, 726–746. https://doi.org/10.1039/D2MA00940D

Liana, D. D., Raguse, B., Gooding, J. J., & Chow, E. (2012). Recent advances in paper-based sensors. *Sensors, 12*, 11505–11526. https://doi.org/10.3390/s120911505

Liao, X., Zhang, Z., Liao, Q., Liang, Q., Ou, Y., Xu, M., et al. (2016). Flexible and printable paper-based strain sensors for wearable and large-area green electronics. *Nanoscale, 8*, 13025–13032. https://doi.org/10.1039/C6NR02172G

Lim, W., Douglas, E. A., Norton, D. P., Pearton, S. J., Ren, F., Heo, Y.-W., et al. (2010). Low-voltage indium gallium zinc oxide thin film transistors on paper substrates. *Applied Physics Letters, 96*, 053510. https://doi.org/10.1063/1.3309753

Liu, Q. C., Li, L., Xu, J. J., Chang, Z. W., Xu, D., Yin, Y. B., et al. (2015). Flexible and foldable Li–O_2 battery based on paper-ink cathode. *Advanced Materials, 27*(48), 8095–8101. https://doi.org/10.1002/adma.201503025

Liu, H., Jiang, H., Du, F., Zhang, D., Li, Z., & Zhou, H. (2017). Flexible and degradable paper-based strain sensor with low cost. *ACS Sustainable Chemistry & Engineering, 5*, 10538–10543. https://doi.org/10.1021/acssuschemeng.7b02540

Liu, H., Zhao, G., Wu, M., Liu, Z., Xiang, D., Wu, C., et al. (2019). Ionogel infiltrated paper as flexible electrode for wearable all-paper-based sensors in active and passive modes. *Nano Energy, 66*, 104161. https://doi.org/10.1016/j.nanoen.2019.104161

Liu, L., Jiao, Z., Zhang, J., Wang, Y., Zhang, C., Meng, X., et al. (2021). Bioinspired, superhydrophobic, and paper-based strain sensors for wearable and underwater applications. *ACS Applied Materials & Interfaces, 13*, 1967–1978. https://doi.org/10.1021/acsami.0c18818

Ma, Y., Cheung, W., Wei, D., Bogozi, A., Chiu, P. L., Wang, L., et al. (2008). Improved conductivity of carbon nanotube networks by in situ polymerization of a thin skin of conducting polymer. *ACS Nano, 2*, 1197–1204. https://doi.org/10.1021/nn800201n

Magdassi, S., Grouchko, M., Berezin, O., & Kamyshny, A. (2010). Triggering the sintering of silver nanoparticles at room temperature. *ACS Nano, 4*, 1943–1948. https://doi.org/10.1021/nn901868t

Maldzius, R., Sirviö, P., Sidaravicius, J., Lozovski, T., Backfolk, K., & Rosenholm, J. B. (2010). Temperature-dependence of electrical and dielectric properties of papers for electrophotography. *Journal of Applied Physics, 107*, 114904. https://doi.org/10.1063/1.3386466

Martinez, A. W., Phillips, S. T., Butte, M. J., & Whitesides, G. M. (2007). Patterned paper as a platform for inexpensive, low-volume, portable bioassays. *Angewandte Chemie, 119*, 1340–1342. https://doi.org/10.1002/anie.200603817

Martins, R. F. P., Ahnood, A., Correia, N., Pereira, L. M. N. P., Barros, R., Barquinha, P. M. C. B., et al. (2013). Recyclable, flexible, low-power oxide electronics. *Advanced Functional Materials, 23*, 2153–2161. https://doi.org/10.1002/adfm.201202907

McKnight, M., Lin, F., Kauche, H., Ghosh, T., & Bozkurt, A. (2015). Towards paper-based diaper sensors. In *Proceedings of IEEE biomedical circuits and systems (BIOCAS)*. IEEE. https://doi.org/10.1109/BioCAS.2015.7348427

Meng, Q., & Manas-Zloczower, I. (2015). Carbon nanotubes enhanced cellulose nanocrystals films with tailorable electrical conductivity. *Composites Science and Technology, 120*, 1–8. https://doi.org/10.1016/j.compscitech.2015.10.008

Mirica, K. A., Weis, J. G., Schnorr, J. M., Esser, B., & Swager, T. M. (2012). Mechanical drawing of gas sensors on paper. *Angewandte Chemie, International Edition, 51*, 10740–10745. https://doi.org/10.1002/anie.201206069

Mirica, K. A., Azzarelli, J. M., Weis, J. G., Schnorr, J. M., & Swager, T. M. (2013). Rapid prototyping of carbon-based chemiresistive gas sensors on paper. *Proceedings of the National Academy of Sciences, 110*, E3265–E3270. https://doi.org/10.1073/pnas.1307251110

Mittal, G., Rhee, K. Y., Park, S. J., & Hui, D. (2017). Generation of the pores on graphene surface and their reinforcement effects on the thermal and mechanical properties of chitosan-based composites. *Composites Part B: Engineering, 114*, 348–355. https://doi.org/10.1016/j.compositesb.2017.02.018

Mo, L., Guo, Z., Wang, Z., Yang, L., Fang, Y., Xin, Z., et al. (2019). Nano-silver ink of high conductivity and low sintering temperature for paper electronics. *Nanoscale Research Letters, 14*, 197. https://doi.org/10.1186/s11671-019-3011-1

Montibon, E. (2011). *Modification of paper into conductive substrate for electronic functions: Deposition, characterization and demonstration*. Karlstad University.

Murphy, E. J. (1960). The dependence of the conductivity of cellulose, silk and wool on their water content. *Journal of Physics and Chemistry of Solids, 16*, 115–122. https://doi.org/10.1016/0022-3697(60)90081-0

Nie, Z., Nijhuis, C. A., Gong, J., Chen, X., Kumachev, A., Martinez, A. W., et al. (2010). Electrochemical sensing in paper-based microfluidic devices. *Lab on a Chip, 10*, 477–483. https://doi.org/10.1039/B917150A

Noremberg, B. S., Silva, R. M., Paniz, O. G., Alano, J. H., Gonçalves, M. R. F., Wolke, S. I., et al. (2017). From banana stem to conductive paper: A capacitive electrode and gas sensor. *Sensors & Actuators, B: Chemical, 240*, 459–467. https://doi.org/10.1016/j.snb.2016.09.014

Öhlund, T., Örtegren, J., Forsberg, S., & Nilsson, H.-E. (2012). Paper surfaces for metal nanoparticle inkjet printing. *Applied Surface Science, 259*, 731–739. https://doi.org/10.1016/j.apsusc.2012.07.112

Pan, T., Liu, S., Zhang, L., & Xie, W. (2022). Flexible organic optoelectronic devices on paper. *iScience, 25*(2), 103782. https://doi.org/10.1016/j.isci.2022.103782

Pang, Z., Sun, X., Wu, X., Nie, Y., Liu, Z., & Yue, L. (2015). Fabrication and application of carbon nanotubes/cellulose composite paper. *Vacuum, 122*, 135–142. https://doi.org/10.1016/j.vacuum.2015.09.020

Park, J., Seo, J. H., Yeom, S. W., Yao, C., Yang, V. W., Cai, Z., et al. (2018). Flexible and transparent organic phototransistors on biodegradable cellulose nanofibrillated fiber substrates. *Advanced Optical Materials, 6*, 1701140. https://doi.org/10.1002/adom.201701140

Pataniya, P. M., Bhakhar, S. A., Tannarana, M., Zankat, C., Patel, V., Solanki, G. K., et al. (2021). Highly sensitive and flexible pressure sensor based on two-dimensional $MoSe_2$ nanosheets for online wrist pulse monitoring. *Journal of Colloid and Interface Science, 584*, 495–504. https://doi.org/10.1016/j.jcis.2020.10.006

Pierre Claver, U., & Zhao, G. (2021). Recent progress in flexible pressure sensors based electronic skin. *Advanced Engineering Materials, 23*, 2001187. https://doi.org/10.1002/adem.202001187

Polat, E. O., Uzlu, H. B., Balci, O., Kakenov, N., Kovalska, E., & Kocabas, C. (2016). Graphene-enabled optoelectronics on paper. *ACS Photonics, 3*, 964–971. https://doi.org/10.1021/acsphotonics.6b00017

Preston, C., Fang, Z., Murray, J., Zhu, H., Dai, J., Munday, J. N., & Hu, L. (2014). Silver nanowire transparent conducting paper-based electrode with high optical haze. *Journal of Materials Chemistry C, 2*, 1248–1254. https://doi.org/10.1039/C3TC31726A

Quddious, A., Yang, S., Khan, M. M., Tahir, F. A., Shamim, A., Salama, K. N., & Cheema, H. M. (2016). Disposable, paper-based, inkjet-printed humidity and H_2S gas sensor for passive sensing applications. *Sensors, 16*, 2073. https://doi.org/10.3390/s16122073

Raut, N. C., & Al-Shamery, K. (2018). Inkjet printing metals on flexible materials for plastic and paper electronics. *Journal of Materials Chemistry C, 6*, 1618–1641. https://doi.org/10.1039/C7TC04804A

Ren, T.-L., Tian, H., Xie, D., & Yang, Y. (2012). *Sensors, 12*, 6685–6694. https://doi.org/10.3390/s120506685

Rida, A., Yang, L., Vyas, R., & Tentzeris, M. M. (2009). Conductive inkjet-printed antennas on flexible low-cost paper-based substrates for RFID and WSN applications. *IEEE Antennas and Propagation Magazine, 51*, 13–23. https://doi.org/10.1109/MAP.2009.5251188

Russo, A., Ahn, B. Y., Adams, J. J., Duoss, E. B., Bernhard, J. T., & Lewis, J. A. (2011). Pen-on-paper flexible electronics. *Advanced Materials, 23*, 3426–3430. https://doi.org/10.1002/adma.201101328

Salajkova, M., Valentini, L., Zhou, Q., & Berglund, L. A. (2013). Tough nanopaper structures based on cellulose nanofibers and carbon nanotubes. *Composites Science and Technology, 87*, 103–110. https://doi.org/10.1016/j.compscitech.2013.06.014

Santhiago, M., Corrêa, C. C., Bernardes, J. S., Pereira, M. P., Oliveira, L. J. M., Strauss, M., & Bufon, C. C. B. (2017). Flexible and foldable fully-printed carbon black conductive nanostructures on paper for high-performance electronic, electrochemical, and wearable devices. *ACS Applied Materials & Interfaces, 9*, 24365–24372. https://doi.org/10.1021/acsami.7b06598

Shah, J., & Malcolm Brown, R. (2005). Towards electronic paper displays made from microbial cellulose. *Applied Microbiology and Biotechnology, 66*, 352–355. https://doi.org/10.1007/s00253-004-1756-6

Shirakawa, H., Louis, E. J., MacDiarmid, A. G., Chiang, C. K., & Heeger, A. J. (1977). Synthesis of electrically conducting organic polymers: Halogen derivatives of polyacetylene, (CH) x. *Journal of the Chemical Society, Chemical Communications, 1977*, 578–580. https://doi.org/10.1039/C39770000578

Siegel, A. C., Phillips, S. T., Dickey, M. D., Lu, N., Suo, Z., & Whitesides, G. M. (2010). Foldable printed circuit boards on paper substrates. *Advanced Functional Materials, 20*, 28–35. https://doi.org/10.1002/adfm.200901363

Simula, S., & Niskanen, K. (2000). Electrical properties of viscose-Kraft fibre mixtures. In J. F. Kennedy, G. O. Phillips, & P. A. Williams (Eds.), *Cellulosic pulps, fibres and materials*. Woodhead Publishing.

Simula, S., Varpula, T., Ikäläinen, S., Seppä, H., Paukku, A., & Niskanen, K. (1998). Measurement of the dielectric properties of paper. *Journal of Imaging Science and Technology, 43*(5), 472–477. https://doi.org/10.2352/j.imagingsci.technol.1999.43.5.art00012

Sirviö, P., Backfolk, K., Maldzius, R., Sidaravicius, J., & Montrimas, E. (2008). Dependence of paper surface and volume resistivity on electric field strength. *Journal of Imaging Science and Technology, 52*, 30501.

Smeacetto, F., Salvo, M., Ferraris, M., Casalegno, V., & Asinari, P. (2008). Glass and composite seals for the joining of YSZ to metallic interconnect in solid oxide fuel cells. *Journal of the European Ceramic Society, 28*, 611–616. https://doi.org/10.1016/j.jeurceramsoc.2007.07.008

Spizzichino, V., & Fantoni, R. (2014). Laser induced breakdown spectroscopy in archeometry: A review of its application and future perspectives. *Spectrochimica Acta Part B: Atomic Spectroscopy, 99*, 201–209. https://doi.org/10.1016/j.sab.2014.07.003

Sudheshwar, A., Malinverno, N., Hischier, R., Nowack, B., & Som, C. (2023). The need for design-for-recycling of paper-based printed electronics—A prospective comparison with printed circuit boards. *Resources, Conservation and Recycling, 189*, 106757. https://doi.org/10.1016/j.resconrec.2022.106757

Sun, S., Duan, Z., Wang, X., Lai, G., Zhang, X., Wei, H., Liu, L., & Ma, N. (2017). Cheap, flexible, and thermal-sensitive paper sensor through writing with ionic liquids containing pencil leads. *ACS Applied Materials & Interfaces, 9*, 29140–29146. https://doi.org/10.1021/acsami.7b08737

Sun, Y., Jiang, Q.-Y., Chen, F., & Cao, Y. (2022). Paper-based electrochemical sensor. *Electrochemical Science Advances, 2*, e2100057. https://doi.org/10.1016/bs.coac.2019.11.001

Sung, J., Kang, B. J., & Oh, J. H. (2013). Fabrication of high-resolution conductive lines by combining inkjet printing with soft lithography. *Microelectronic Engineering, 110*, 219–223. https://doi.org/10.1016/j.mee.2013.04.004

Tian, W., Vahidmohammadi, A., Reid, M. S., Wang, Z., Ouyang, L., Erlandsson, J., et al. (2019). Multifunctional nanocomposites with high strength and capacitance using 2D MXene and 1D nanocellulose. *Advanced Materials, 31*, 1902977. https://doi.org/10.1002/adma.201902977

Tobjörk, D., & Österbacka, R. (2011). Paper electronics. *Advanced Materials, 23*, 1935–1961. https://doi.org/10.1002/adma.201004692

Tomiyama, T., Mukai, I., Yamazaki, H., & Takeda, Y. (2020). Optical properties of silver nanowire/polymer composite films: Absorption, scattering, and color difference. *Optical Materials Express, 10*, 3202–3214. https://doi.org/10.1364/OME.412015

Torvinen, K., Sievänen, J., Hjält, T., & Hellén, E. (2012). Smooth and flexible filler-nanocellulose composite structure for printed electronics applications. *Cellulose, 19*, 821–829. https://doi.org/10.1007/s10570-012-9677-5

Turkevich, J., Stevenson, P. C., & Hillier, J. (1951). A study of the nucleation and growth processes in the synthesis of colloidal gold. *Discussions of the Faraday Society, 11*, 55–75. https://doi.org/10.1039/DF9511100055

Valdec, D., Hajdek, K., Majnarić, I., & Čerepinko, D. (2021). Influence of printing substrate on quality of line and text reproduction in flexography. *Applied Sciences, 11*, 7827. https://doi.org/10.3390/app11177827

Wang, J.-Z., Zhong, C., Chou, S.-L., & Liu, H.-K. (2010). Flexible free-standing graphene-silicon composite film for lithium-ion batteries. *Electrochemistry Communications, 12*, 1467–1470. https://doi.org/10.1016/j.elecom.2010.08.008

Wang, J., Li, L., Wong, C. L., & Madhavi, S. (2012). Flexible single-walled carbon nanotube/polycellulose papers for lithium-ion batteries. *Nanotechnology, 23*, 495401. https://doi.org/10.1088/0957-4484/23/49/495401

Wang, B., Guo, R., Zheng, M., Liu, Z., Li, F., Meng, L., et al. (2018a). Embedded binary functional materials/cellulose-based paper as freestanding anode for lithium-ion batteries. *Electrochimica Acta, 260*, 1–10. https://doi.org/10.1016/j.electacta.2017.11.067

Wang, Y.-H., Song, P., Li, X., Ru, C., Ferrari, G., Balasubramanian, P., et al. (2018b). A paper-based piezoelectric accelerometer. *Micromachines, 9*, 19. https://doi.org/10.3390/mi9010019

Wang, Y., Du, D., Zhou, Z., Xie, H., Li, J., & Zhao, Y. (2019a). Reactive conductive ink capable of in situ and rapid synthesis of conductive patterns suitable for inkjet printing. *Molecules, 24*, 3548. https://doi.org/10.3390/molecules24193548

Wang, Y., Pan, W., Kwok, H. Y. H., Zhang, H., Lu, X., & Leung, D. Y. C. (2019b). Liquid-free Al-air batteries with paper-based gel electrolyte: A green energy technology for portable electronics. *Journal of Power Sources, 437*, 226896. https://doi.org/10.1016/j.jpowsour.2019.226896

Wang, Y., Yan, C., Cheng, S.-Y., Xu, Z.-Q., Sun, X., Xu, Y.-H., et al. (2019c). Flexible RFID tag metal antenna on paper-based substrate by inkjet printing technology. *Advanced Functional Materials, 29*, 1902579. https://doi.org/10.1002/adfm.201902579

Wang, C., Hou, X., Cui, M., Yu, J., Fan, X., Qian, J., et al. (2020a). An ultra-sensitive and wide measuring range pressure sensor with paper-based CNT film/interdigitated structure. *Science China Materials, 63*, 403–412. https://doi.org/10.1007/s40843-019-1173-3

Wang, Y., Long, J., Hu, J., Sun, Z., & Meng, L. (2020b). Polyvinyl alcohol/Lyocell dual-layer paper-based separator for primary zinc-air batteries. *Journal of Power Sources, 453*, 227853. https://doi.org/10.1016/j.jpowsour.2020.227853

Wang, Y., Luo, J., Chen, L., Long, J., Hu, J., & Meng, L. (2021). Effect of fibrillated fiber morphology on properties of paper-based separators for lithium-ion battery applications. *Journal of Power Sources, 482*, 228899. https://doi.org/10.1016/j.jpowsour.2020.228899

Wang, Y., Pan, W., Leong, K. W., Zhang, Y., Zhao, X., Luo, S., & Leung, D. Y. C. (2023). Paper-based aqueous Al ion battery with water-in-salt electrolyte. *Green Energy & Environment, 8*, 1380–1388. https://doi.org/10.1016/j.gee.2021.10.001

Weng, Z., Su, Y., Wang, D.-W., Li, F., Du, J., & Cheng, H.-M. (2011). Graphene–cellulose paper flexible supercapacitors. *Advanced Energy Materials, 1*, 917–922. https://doi.org/10.1002/aenm.201100312

Wu, Y., Xue, P., Hui, K. M., & Kang, Y. (2014). Electrochemical- and fluorescent-mediated signal amplifications for rapid detection of low-abundance circulating tumor cells on a paper-based microfluidic immunodevice. *ChemElectroChem, 1*, 722–727. https://doi.org/10.1002/celc.201300194

Wu, K., Zhang, Y., Wang, Y., Ge, S., Yan, M., Yu, J., & Song, X. (2015). Based analytical devices relying on visible-light-enhanced glucose/air biofuel cells. *ACS Applied Materials & Interfaces, 7*, 24330–24337. https://doi.org/10.1021/acsami.5b07698

Wu, J., Che, X., Hu, H.-C., Xu, H., Li, B., Liu, Y., et al. (2020). Organic solar cells based on cellulose nanopaper from agroforestry residues with an efficiency of over 16% and effectively wide-angle light capturing. *Journal of Materials Chemistry A, 8*, 5442–5448. https://doi.org/10.1039/C9TA14039E

Wu, H., Bi, J., Li, Y., Wang, L., Pang, X., Xiong, C., & Li, Z. (2021). Low-cost and low-density carbonized facial tissue supported uniform $NiCO_2S_4$ nanotubes for high capacity flexible solid-state supercapacitors. *Journal of Materiomics, 7*, 166–176. https://doi.org/10.1021/nl404008e

Xia, Y., Si, J., & Li, Z. (2016). Fabrication techniques for microfluidic paper-based analytical devices and their applications for biological testing: A review. *Biosensors & Bioelectronics, 77*, 774–789. https://doi.org/10.1016/j.bios.2015.10.032

Xiong, C., Wang, T., Han, J., Zhang, Z., & Ni, Y. (2024). Recent research progress of paper-based supercapacitors based on cellulose. *Energy and Environmental Materials, 7*, e12651. https://doi.org/10.1002/eem2.12651

Xu, Y., Fei, Q., Page, M., Zhao, G., Ling, Y., Stoll, S. B., & Yan, Z. (2021). Paper-based wearable electronics. *iScience, 24*, 102736. https://doi.org/10.1016/j.isci.2021.102736

Yadav, T. P., Yadav, R. M., & Singh, D. P. (2012). Mechanical milling: A top down approach for the synthesis of nanomaterials and nanocomposites. *Nanoscience and Nanotechnology, 2*, 22–48. https://doi.org/10.5923/j.nn.20120203.01

Yang, W., Zhao, Z., Wu, K., Huang, R., Liu, T., Jiang, H., et al. (2017). Ultrathin flexible reduced graphene oxide/cellulose nanofiber composite films with strongly anisotropic thermal conductivity and efficient electromagnetic interference shielding. *Journal of Materials Chemistry C, 5*, 3748–3756. https://doi.org/10.1039/C7TC00400A

Yang, P., Li, J., Lee, S. W., & Fan, H. J. (2022). Printed zinc paper batteries. *Advancement of Science, 9*, 2103894. https://doi.org/10.1002/advs.202103894

Yao, B., Yuan, L., Xiao, X., Zhang, J., Qi, Y., Zhou, J., et al. (2013). Solid-state supercapacitors with pencil-drawing graphite/polyaniline networks hybrid electrodes. *Nano Energy, 2*, 1071–1078. https://doi.org/10.1016/j.nanoen.2013.09.002

Yao, Y., Tao, J., Zou, J., Zhang, B., Li, T., Dai, J., et al. (2016). Light management in plastic–paper hybrid substrate towards high-performance optoelectronics. *Energy & Environmental Science, 9*, 2278–2285. https://doi.org/10.1039/C6EE01011C

Yu, Z., & Sun, L. (2018). Inorganic hole-transporting materials for perovskite solar cells. *Small Methods, 2*(2), 1700280. https://doi.org/10.1021/acs.jpcc.8b01177

Yuan, L., Xiao, X., Ding, T., Zhong, J., Zhang, X., Shen, Y., et al. (2012). Paper-based supercapacitors for self-powered nanosystems. *Angewandte Chemie, International Edition, 51*, 4934–4938. https://doi.org/10.1002/anie.201109142

Yuan, L., Yao, B., Hu, B., Huo, K., Chen, W., & Zhou, J. (2013). Polypyrrole-coated paper for flexible solid-state energy storage. *Energy & Environmental Science, 6*, 470–476. https://doi.org/10.1039/C2EE23977A

Yuan, M., Alocilja, E. C., & Chakrabartty, S. (2016). Self-powered wireless affinity-based biosensor based on integration of paper-based microfluidics and self-assembled RFID antennas. *IEEE Transactions on Biomedical Circuits and Systems, 10*, 799–806. https://doi.org/10.1109/TBCAS.2016.2535245

Yuan, B., Sun, X., Wang, Q., & Wang, H. (2023). Direct fabrication of liquid-metal multifunctional paper based on force-responsive adhesion. *Cell Reports Physical Science, 4*, 101419. https://doi.org/10.1016/j.xcrp.2023.101419

Zang, D., Ge, L., Yan, M., Song, X., & Yu, J. (2012). Electrochemical immunoassay on a 3D microfluidic paper-based device. *Chemical Communications, 48*, 4683–4685. https://doi.org/10.1039/C2CC16958D

Zhan, Z., Lin, R., Tran, V.-T., An, J., Wei, Y., Du, H., Tran, T., & Lu, W. (2017). Paper/carbon nanotube-based wearable pressure sensor for physiological signal acquisition and soft robotic skin. *ACS Applied Materials & Interfaces, 9*, 37921–37928. https://doi.org/10.1021/acsami.7b10820

Zhang, T. (2014). *Methods for fabricating printed electronics with high conductivity and high resolution*. The University of Western Ontario.

Zhang, Y., Li, L., Zhang, L., Ge, S., Yan, M., & Yu, J. (2017). In-situ synthesized polypyrrole-cellulose conductive networks for potential-tunable foldable power paper. *Nano Energy, 31*, 174–182. https://doi.org/10.1016/j.nanoen.2016.11.029

Zhang, Y., Zhang, L., Cui, K., Ge, S., Cheng, X., Yan, M., Yu, J., & Liu, H. (2018). Flexible electronics based on micro/nanostructured paper. *Advanced Materials, 30*, 1801588. https://doi.org/10.1002/adma.201801588

Zhang, D., Zhai, X., Wang, S., Li, X., Xu, P., Zhao, H., & Zhang, G.-J. (2024). Study on mechanical and electrical properties improvement of insulating paper modified by cellulose nanocrystals. *Journal of Applied Physics, 136*, 125108. https://doi.org/10.1063/5.0219452

Zheng, Y., He, Z., Gao, Y., & Liu, J. (2013). Direct desktop printed-circuits-on-paper flexible electronics. *Scientific Reports, 3*, 1786. https://doi.org/10.1038/srep01786

Zhou, Y., Fuentes-Hernandez, C., Khan, T. M., Liu, J. C., Hsu, J., Shim, J. W., et al. (2013). Recyclable organic solar cells on cellulose nanocrystal substrates. *Scientific Reports, 3*(1), 1536. https://doi.org/10.1038/srep01536

Zhu, H., Xiao, Z., Liu, D., Li, Y., Weadock, N. J., Fang, Z., Huang, J., & Hu, L. (2013). Biodegradable transparent substrates for flexible organic-light-emitting diodes. *Energy & Environmental Science, 6*, 2105. https://doi.org/10.1039/C3EE40492G

Zhu, C., Liu, P., & Mathew, A. P. (2017). Self-assembled TEMPO cellulose nanofibers: Graphene oxide-based biohybrids for water purification. *ACS Applied Materials & Interfaces, 9*, 21048–21058. https://doi.org/10.1021/acsami.7b06358

Zhu, M., Yan, X., Xu, H., Xu, Y., & Kong, L. (2021). Highly conductive and flexible bilayered MXene/cellulose paper sheet for efficient electromagnetic interference shielding applications. *Ceramics International, 47*, 17234–17244. https://doi.org/10.1016/j.ceramint.2021.03.034

Zikulnig, J., Hirschl, C., Rauter, L., Krivec, M., Lammer, H., Riemelmoser, F., & Roshanghias, A. (2019). Inkjet printing and characterisation of a resistive temperature sensor on paper substrate. *Flexible and Printed Electronics, 4*, 015008. https://doi.org/10.1088/2058-8585/ab0cea

Chapter 14
Hydrophobic Paper

Soraya Ghayempour, Mohammad Mazloum-Ardakani, and Hamid Dehghan-Manshadi

14.1 Introduction

Preparing biodegradable materials from renewable resources is an interesting field for researchers because it has no harmful effects on the environment or human life. Among known biodegradable materials, paper can be a good substitute for non-biodegradable materials such as plastic. The excellent features of paper such as low cost, abundance, biocompatibility, biodegradability, renewability, and good mechanical characterization lead to know it as an indispensable material in human life. Still, the hydrophilic properties of paper are the main obstacle in the application developments due to the hydrophilic nature of hydroxyl groups and the highly porous structure of cellulose, which is the main renewable and degradable component of paper. This leads to its ability to absorb water and moisture, reducing the positive properties of paper, decreasing the durability of cellulose fibers, and limiting its application in various fields (He et al., 2022; Samir et al., 2022).

Creating a hydrophobicity property can significantly improve the characterization of paper such as water repellency, moisture resistance, self-cleaning, antifouling, and friction reduction (Li, Kang, et al., 2021; Ghayempour et al. 2024; Li, Wang, et al., 2021). These features are of great importance in applied research. Water repellency and moisture resistance are the important properties of hydrophobic papers due to their role in stability, less damage, and preventing the growth of

S. Ghayempour
Department of Textile Engineering, Faculty of Engineering, Yazd University, Yazd, Iran

M. Mazloum-Ardakani (✉)
Department of Chemistry, Faculty of Science, Yazd University, Yazd, Iran
e-mail: mazloum@yazd.ac.ir

H. Dehghan-Manshadi
Thin Layer and Nanotechnology Laboratory, Department of Chemical Technologies, Iranian Research Organization for Science and Technology (IROST), Tehran, Iran

G. Korotcenkov (ed.), *The Handbook of Paper-Based Sensors and Devices*,
https://doi.org/10.1007/978-3-031-91080-7_14

microorganisms in humid environments as an ideal medium for their development. Contamination on the paper surface is usually unavoidable in their practical applications, so self-cleaning properties are useful in the paper's applications. The self-cleaning performance of hydrophobic papers is generally evaluated by placing soil and dust on their surface and falling water droplets on the contaminated surface. Antifouling property is another important characteristic of hydrophobic papers due to its role in inhibiting the undesirable attachment of microorganisms on their surface, which leads to obtaining an antibacterial and antifungal system. Friction reduction in hydrophobic papers leads to slipping a liquid over their surfaces. This property can be improved using a low surface energy material in the composition of the paper surface (Long et al., 2022; Saha et al., 2022; Teng et al., 2020).

Hydrophobic papers have been utilized in various fields such as packaging, sensors and biosensors, filters and membranes, protection of books and documents, etc. For instance, since food packaging plays a key role in food safety, the use of hydrophobic papers as green packaging can be useful for preventing spoilage of packaged materials through mold and the growth of various fungi and bacteria. The application of hydrophobic papers in the preparation of paper-based sensors and filters can improve their stability and durability. Also, a good approach to protecting books and documents, especially ancient books, is creating hydrophobic and moisture-proof properties on their surface (Lan & Duan, 2023; Mujtaba et al., 2022).

14.2 Principles of Hydrophobic Papers

The hydrophilicity/hydrophobicity of paper depends on how well water bonds to the paper surface compared with how well it bonds to itself. The surface of the hydrophilic paper is completely wet in the presence of water, forming a strong water–surface interaction, while water is repelled from the surface of the hydrophobic paper and forms a weak water–paper surface interaction. Water will form near-spherical droplets that roll across the paper surface. The movement behavior of the liquid droplet on a paper depends on the chemical properties and the surface roughness. The hydrophobicity of the paper surface is evaluated with the measurement of its water contact angle (WCA) which is calculated as the tangent angle of the liquid-vapor interface at the three-phase boundary (Fig. 14.1). The contact angle of a liquid droplet on a smooth surface can be calculated by the Young Equation:

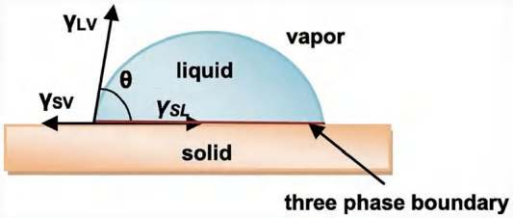

Fig. 14.1 The three-phase boundary of a liquid droplet on the surface. Reprinted with permission from Celia et al. (2013). Copyright 2013: Elsevier

$$\cos\theta = \frac{\gamma_{SV} - \gamma_{SL}}{\gamma_{LV}}, \tag{14.1}$$

where γ_{LV}, γ_{SL}, and γ_{SV} are the interfacial tensions between liquid and vapor, solid and liquid, and solid and vapor, respectively. A hydrophilic paper refers to a paper with contact angles less than 90°. Modifying the paper surface by various methods leads to an increase in the contact angle, which is between 90° and 150° called a hydrophobic paper, and if it is greater than 150°, the paper is described as a superhydrophobic paper (Celia et al., 2013; Nguyen-Tri et al., 2019).

The hydrophobic behavior of the surface can be explained with several models (Fig. 14.2). In the Wenzel model, the interpenetration of droplets into the asperities leads to increasing surface contact, and the contact angle is increased by drop contraction. In the Cassie-Baxter model, the droplet on top of the asperities cannot penetrate the surface, resulting in enhancing the hydrophobicity. In the lotus model, the asperities are nanostructured. There is a transitional state between the Wenzel and the Cassie-Baxter model. Also, a transitional state with partial wetting is called a "Gecko" state (Nguyen-Tri et al., 2019).

Generally, two factors are important to obtain a hydrophobic surface: (1) a low surface energy which requires a flat surface with a contact angle above 90° and (2) a high surface roughness which can amplify the surface hydrophobicity. Therefore, four main routes can be considered for the design of a hydrophobic property on the surface:

1. Application of a low-energy material to surface roughening. In this one-stage route, the surface roughens using a low-energy material with good adherence to the surface. The surface modifier's low adherence leads to its limited application.
2. Roughing up a surface composed of a low-energy material. In this route, the surface is a low-energy material with the ability to rough up and perdurability during the roughening process.
3. The use of a rough material on the surface, followed by coating with a low-energy material. In this route, the surface is modified using a rough material and a low-energy material during two stages.
4. Stabilizing a low-energy material on the surface, followed by roughing up the surface. In this route, the low energy of the material should be maintained during the roughing-up process.

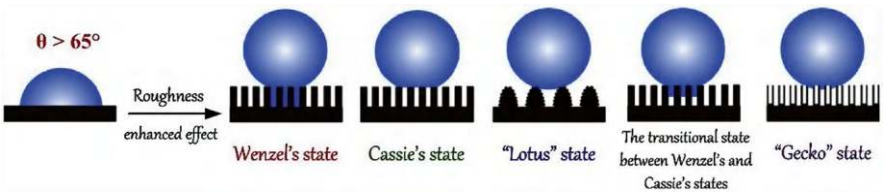

Fig. 14.2 Various models of the water droplet on the surface. Reprinted with permission from Nguyen-Tri et al. (2019). Copyright 2019: Elsevier

In the case of paper, although it has a rough surface, it has hydrophilic properties due to the presence of hydrophilic groups in its cellulose structure. Therefore, there are two ways to achieve hydrophobic paper. The first way is to modify the paper's surface in various ways. The hydrophobic features can begin on the paper surface by forming an external layer, which delays or prevents the diffusion of water into the paper. The second way is to modify the cellulose as the main component of paper using hydrophobic materials followed by preparing paper using the modified cellulose. Nevertheless, the modifications can hurt the recyclability and biodegradability of paper. Therefore, efforts are ongoing to produce hydrophobic paper using safe methods and biodegradable materials (Crick & Parkin, 2010; Li, Wang, et al., 2021).

14.3 Hydrophobic Coating Methods

There are several methods for coat substrate, but some of them are not applicable due to the nature of the paper. For instance, electrochemical deposition is not suitable for coating materials on paper due to its non-conductiveness. Some methods are expensive and are not economically viable. Methods based on harmful and non-biodegradable substances are not applicable. Among different coating methods, the immersion coating method is the most commonly reported technique for paper coating. In the next section, a brief explanation will be given about the most commonly used methods for hydrophobic paper coatings, such as immersion, spraying, layer-by-layer (LBL), sol-gel, metal-ion modification, lamination, and polymer coating.

14.3.1 Immersion Coating Method

The immersion method which is also known as the dip coating method or solution soaking method is the most commonly utilized method for hydrophobic coating of paper. This is a simple and green method without any complicated chemical reaction that has been usually applied to coat various materials on the surface. In this process, the surface immerses at a steady velocity in the solution containing the coating agent for a certain time and dries to evaporate its solvent. Figure 14.3 indicates the schematics of batch and continuous immersion coating methods. The continuous immersion method can only be used for coating materials on the surface of flexible substrates; therefore, it is suitable for coating the agents on the paper surface. The important parameter in this method is the pull-up velocity. A slow velocity is appropriate for the preparation of a thin layer and a high velocity and fast drying is suitable for the fabrication of a thick layer (Butt, 2022; He et al., 2022; Shakeel Ahmad et al., 2017).

Li et al. (2008) prepared a superhydrophobic surface on paper using coating potassium methyl siliconate through a solution-immersion method. The reported work was based on the formation of silanol through the interaction of potassium

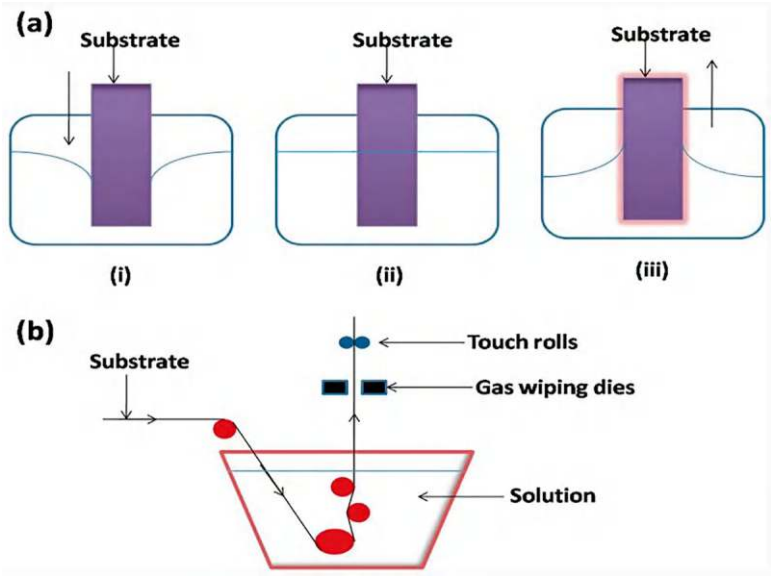

Fig. 14.3 The schematics of (**a**) batch and (**b**) continuous immersion coating method. Reprinted with permission from Shakeel Ahmad et al. (2017). Copyright 2017: Elsevier

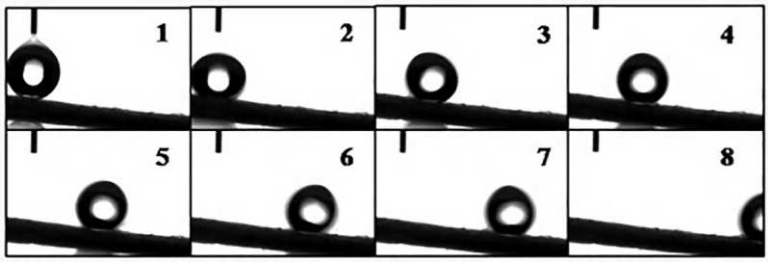

Fig. 14.4 Study of the water rolling-off angle using the video frames of water droplets placed on the tilted surface of superhydrophobic paper at different times (1–8). Reprinted with permission from Arbatan et al. (2012). Copyright 2012: Elsevier

methyl siliconate with CO_2 and followed by the preparation of polymethylsilsesquioxane through a polycondensation reaction of silanol with cellulose. Their results showed a superhydrophobic surface with a water contact angle of 157° obtained due to uniform coating of the synthesized nanoscale layer on the surface (Li et al., 2008).

A two-step dip coating method was reported by Arbatan et al. (2012) for the preparation of superhydrophobic filter paper. They prepared an aqueous suspension containing cellulose nanofibers and calcium carbonate pigment and coated it on the surface of filter paper. Then, the coated surface was treated with a solution of alkyl ketene dimer in n-heptane. As seen in Fig. 14.4, the water droplet began to roll off on the surface of the superhydrophobic paper as the tilting angle of the surface

reached 5°. The obtained superhydrophobic filter paper indicated a water contact angle of 160°. Based on their results, cellulose nanofiber plays an important role in the superhydrophobicity of the surface by helping in the retention of calcium carbonate clusters on the surface (Arbatan et al., 2012).

Gao et al. (2015) prepared a superhydrophobic paper through the stabilization of amorphous titanium dioxide using epoxy resin on the surface of filter paper. They used aminopropyltriethoxysilane (KH-550) as the coupling agent to bond the amorphous titanium dioxide to the epoxy resin. The obtained amorphous titanium dioxide/epoxy resin was coated on the filter paper using an immersion method based on the high viscosity of the epoxy resin. Therefore, epoxy resin plays an important role in forming the superhydrophobic surface, meanwhile, it also enhances the surface roughness. Finally, to obtain a superhydrophobic surface, the filter paper was modified using octadecyltrichlorosilane. The steps of producing the superhydrophobic paper and related chemical structure are indicated in Fig. 14.5. The water contact angle of 153 ± 1° indicated the superhydrophobicity of the surface. They utilized the

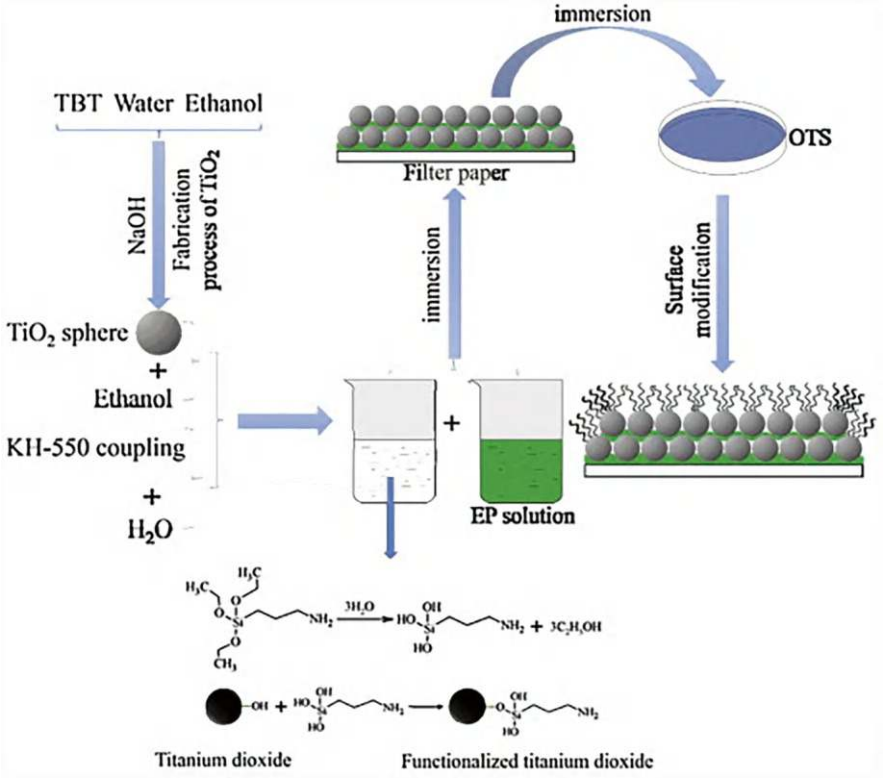

Fig. 14.5 A schematic of producing the superhydrophobic paper using amorphous titanium dioxide. Reprinted with permission from Gao et al. (2015). Copyright 2015: Elsevier

prepared superhydrophobic paper in water–oil separation and anti-UV applications (Gao et al., 2015).

Liu et al. (2018) prepared a hydrophobic paper using an immersion method based on the dehydrogenation of poly(methylhydrosiloxane) (PMHS) for application in water–oil separation. They immersed the filter paper into an n-hexane solution containing PMHS and Kastredt catalyst (platinum-1,3-divinyl-1,1,3,3-tetramethyldisiloxane). They confirmed the successful modification of the paper through evaluation of its hydrophobicity so that the water contact angle increased from 19.0° for the uncoated paper to 131.8° for the obtained hydrophobic paper. According to their statement, PMHS was grafted on the paper surface through covalent bonds. As shown in Fig. 14.6, the Si–H bonds in the structure of PMHS can interact with the hydroxyl groups of paper in the presence of Kastredt catalyst and produce hydrogen gas. They attributed the hydrophobicity of paper to the low surface energy of PMHS (Liu et al., 2018).

Gozutok et al. (2019) reported a dip-coating method for the hydrophobic coating of paper surfaces using hydrocarbon and fluorocarbon-based polymeric resins. The particle-free reactive silver inks were covered on the surface of fluorinated resin-coated paper through ink-jet printing to obtain a high-conductive surface. They proposed this approach for application as substrates in printed electronics due to the availability and eco-friendly nature of the used resins (fluorinated resin with alkyl chains of six carbons in length). For instance, they applied the modified paper as the substrate to prepare a radio frequency identification (RFID) tag (Gozutok et al., 2019). Guan et al. (2020) prepared a hydrophobic transparent paper through

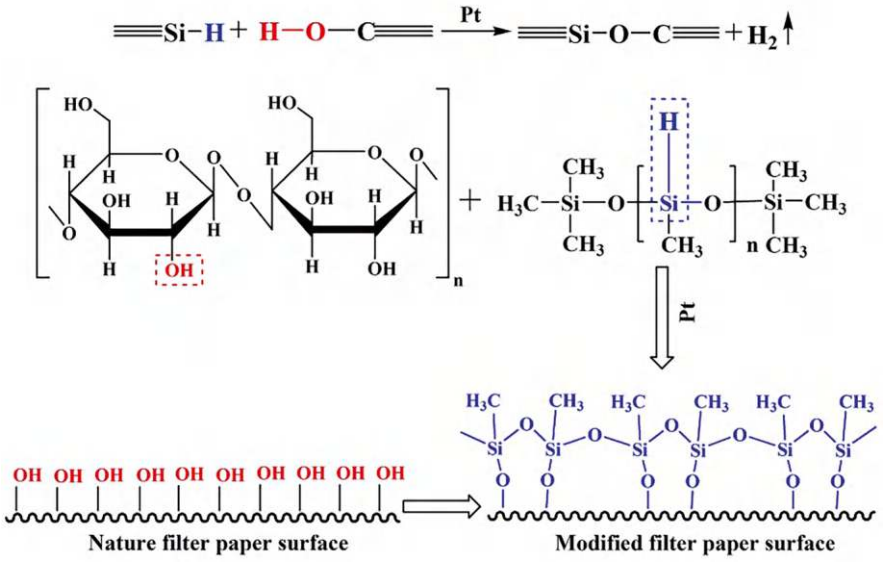

Fig. 14.6 Schematic of the preparation of hydrophobic paper using PMHS. Reprinted with permission from Liu et al. (2018). Copyright 2018: Elsevier

immersion of cellulose fiber paper in hydrolyzed tetraethyl orthosilicate followed by coating with hydrophobic polydimethylsiloxane. The synthesized silica nanoparticles improved the transparency and thermal stability of paper. Coating the paper with polydimethylsiloxane led to obtaining a transparent and hydrophobic paper with a transmittance of more than 90% at 550 nm and the water contact angle of the paper reached about 110° (Guan et al., 2020). Loesch-Zhang et al. (2022) utilized olive oil as the agent to fabricate a hydrophobic paper. Their approach was based on UV-induced thiol-ene photocrosslinking of olive oil on the paper's surface at a wavelength of 254 nm. They reported water contact angles of up to 120° (Loesch-Zhang et al., 2022). He et al. (2022) utilized a dip-coating method to coat the surface of paper by chitin nanocrystals and hexadecyltrimethoxysilane. The prepared hydrophobic paper indicated a high hydrophobic property with a water contact angle greater than 130°. They attributed this result to the low surface energy provided by hexadecyltrimethoxysilane. Also, adding chitin nanocrystals improved tensile strength and water vapor barrier. Figure 14.7 indicates SEM and AFM images of the uncoated paper and hydrophobic paper. As seen in SEM images, in the prepared hydrophobic paper, the pores were filled and the rough surface was turned into a smooth and uniform surface. AFM images also show a decrease in the arithmetic average roughness of hydrophobic paper compared to uncoated paper. They attributed it to coating low-lying parts of the fiber surface with chitin nanocrystals (He et al., 2022).

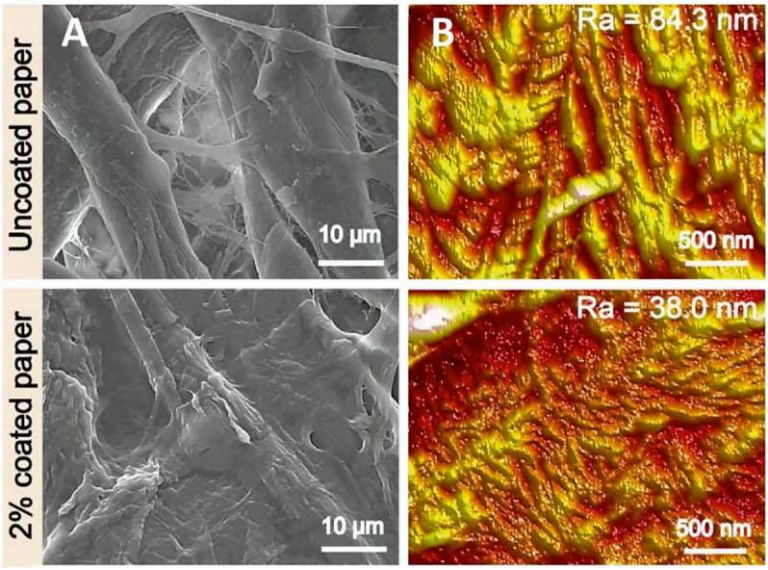

Fig. 14.7 (**a**) SEM and (**b**) AFM images of the uncoated paper and hydrophobic paper. Reprinted with permission from He et al. (2022). Copyright 2022: Elsevier

14.3.2 Spray Coating Method

The spray coating method is based on creating a thin layer on the surface of the substrate using different spraying methods. The most usual method is based on a mixture of the coating material with air followed by vaporizing the pressured air which leads to spraying them from the nozzle. Electrostatic spray and hot vapor-impelled spray are other common methods for creating sprays. Figure 14.8 indicates a schematic of the spray coating method. This method, which is very appropriate for coating the surface of non-flat papers, has disadvantages such as high cost and difficulty of creating the same thickness on substrates with wide width. However, this method provides suitable conditions for continual processing and controlled loading of coating material (Basak et al., 2024; Ghayempour & Montazer, 2016; Ghayempour & Mortazavi, 2013).

Ogihara et al. (2012) prepared a superhydrophobic and transparent paper using the spray coating method. They prepared an alcohol suspension of SiO_2 nanoparticles and sprayed it on the paper's surface. Based on their results, the superhydrophobic property of the modified paper depends on the aggregation conditions of SiO_2 nanoparticles, which is based on the type of the applied alcohol in the preparation of suspensions. Figure 14.9 indicates SEM images of SiO_2 nanoparticles coated on the paper surface using ethanol and 1-butanol. Figure 14.9a, d shows a uniform coating of SiO_2 nanoparticles on the paper using both alcohol due to low magnification of SEM images; however, SEM images of samples in higher-magnification (Fig. 14.9b, e) display their various morphology and rougher surface of the coated paper using ethanol suspension. Also, a comparison of Fig. 14.9c, f shows more clearly the uniform surface of the coated paper using 1-butanol suspension. The important features of the prepared superhydrophobic paper are a water contact angle of more than 150° and the retention of its properties after touching it with a finger (Ogihara et al., 2012). In another study, they prepared superhydrophobic paper using several oxide nanoparticles such as SiO_2, Al_2O_3, and TiO_2. Silane coupling agents were used to decrease their surface energy. According to their results, silane

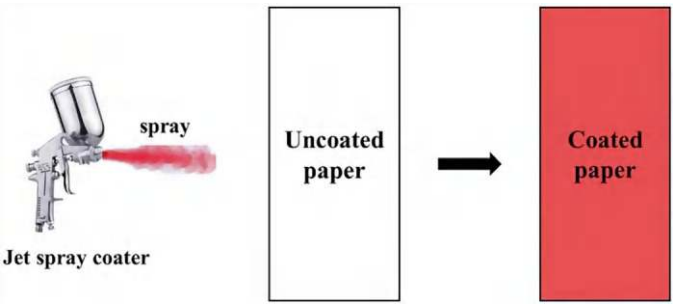

Fig. 14.8 Spray coating method. Reprinted with permission from Basak et al. (2024). Copyright 2024: Elsevier

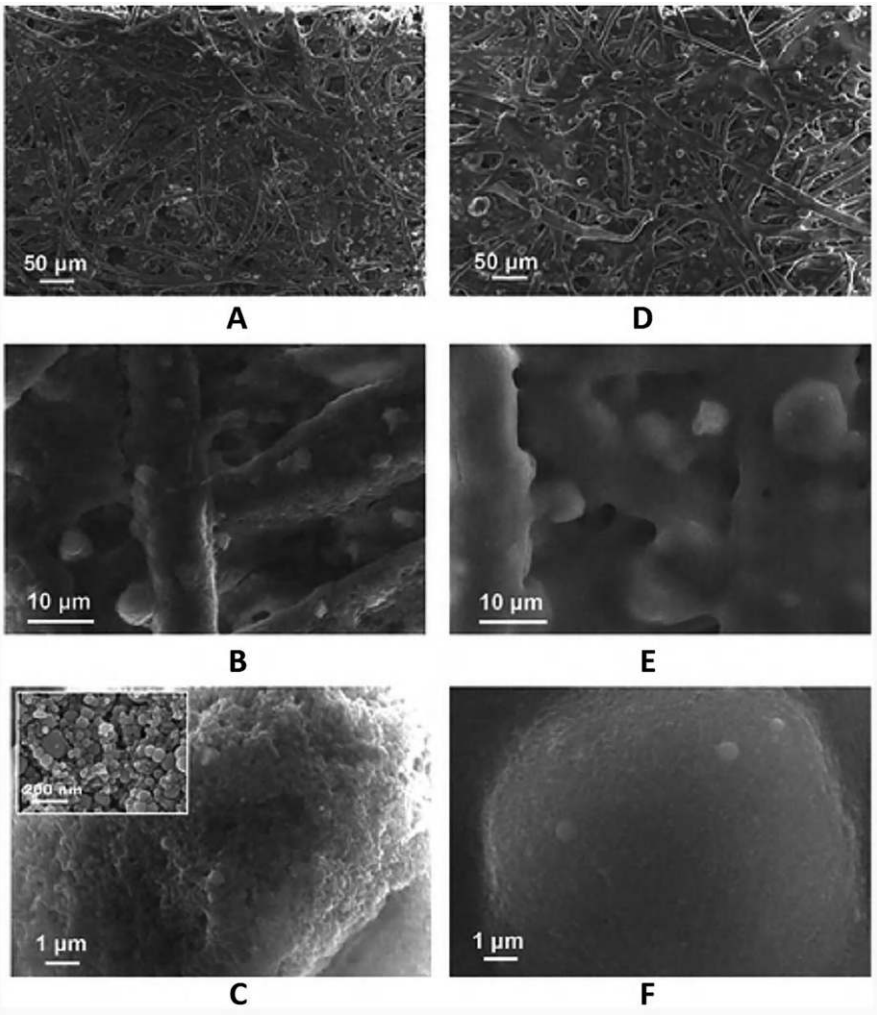

Fig. 14.9 SEM images of spray-coated SiO_2 nanoparticles on the paper using ethanol (**a**–**c**) and 1-butanol (**d**–**f**). Reprinted with permission from Ogihara et al. (2012). Copyright 2012: American Chemical Society

coupling agents with longer alkyl chains were more appropriate for obtaining superhydrophobic paper compared to silane coupling agents with a hexyl group. Also, among various used nanoparticles, the paper spray-coated with SiO_2 nanoparticles indicated a superhydrophobicity property. They attributed these results to low residual hydroxyl groups using SiO_2 nanoparticles (Ogihara et al., 2013).

14.3.3 Layer-by-Layer Coating Method

The layer-by-layer coating method is a useful coating technique for the preparation of customized profiles with the ability the simultaneously release two active agents of growth factor and antibiotic. This method is based on cyclic immersion of the substrate surface in the polyelectrolyte solutions with opposite charges which result in the certation of multiple layers on the surface. The stabilization of the layers on each other occurred using electrostatic forces and was followed by intermolecular interactions such as hydrophobic interactions and covalent bonding. This method provides the conditions for adjusting the thickness of layers from nanometers to micrometers. The important application of this method can be mentioned in the preparation of drug delivery systems and drug carriers (Amin Yavari et al., 2020; Min et al., 2016; Silva et al., 2016). Figure 14.10 displays the different carrier systems, where the layer-by-layer method is used to increase colloidal stability and protect active material. These systems involve nanobubbles, nanoporous templates, hydrogels, thin films and thin layers, micro-/nanocapsules, and liposomes (Shende et al., 2020).

Li et al. (2019) used a layer-by-layer coating method for the preparation of a superhydrophobic/superoleophilic paper. For this purpose, they coated a composition of chitosan and hexadecyltrimethoxysilane-g-TiO_2 on the paper surface followed by thermal operation. The coated paper displayed a superhydrophobicity property with a water contact angle of 167.4° and a superoleophilicity property with an oil contact angle of 0°. Since the modified paper indicated the ability to separate oil-water mixtures and water-in-oil emulsions, they proposed its application in oil cleanup and oily wastewater treatment (Li et al., 2019).

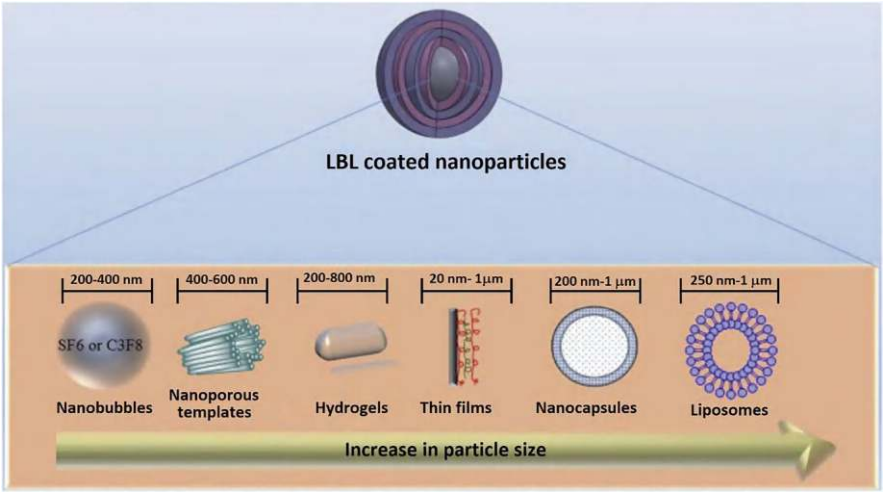

Fig. 14.10 The different carrier systems where the layer-by-layer method is used to coat their surface. Reprinted with permission from Shende et al. (2020). Copyright 2024: Elsevier

14.3.4 Sol-Gel Coating Method

The sol-gel coating method which is considered as a complementary method to the physical and chemical deposition methods is an effective technique for the preparation of high-quality and highly thermal stable hydrophobic paper. This method requires a thermal operation to convert the coating agents on the paper surface by hydrolysis and polycondensation reactions. The sol-gel coating method has been widely applied to produce superhydrophobic nanocoatings. However, this method has several disadvantages such as thickness limits and crackability (Lakshmi et al., 2011; Nguyen-Tri et al., 2019).

Wang et al. in 2014 prepared three hydrophobic papers based on sol-gel derived methylsilsesquioxane, wax, and alkyl ketene dimer as the barrier materials for the preparation of paper-based microfluidic devices. Among them, the paper coated with methylsilsesquioxane indicated a good performance against aggressive cell lysing solutions, surfactant solutions such as SDS, CTAB, and Triton X-100 as well as glycerol, toluene, and DMSO. The prepared hydrophobic paper using methylsilsesquioxane was used for the preparation of a colorimetric sensor for the detection of *Escherichia coli* (Wang et al., 2014). Zhang et al. (2016) prepared a hydrophobic/lipophobic paper using the sol-gel method and used it as the substrate to fabricate a sensor to detect metal ions and bacteria. They used fluoroalkyl-silica as the hydrophobic/lipophobic agent, which could retain organic solvents and surfactant solutions compared to surfaces coated with methyl-silica (Zhang et al., 2016).

Musikavanhu et al. in 2019 reported a sol-gel coating method based on SiO_2 to prepare a superhydrophobic filter paper. As seen in Fig. 14.11, they carried out a pretreatment on the paper surface using zinc chloride to activate the cellulose fibers. Then, SiO_2-based sol-gel was used to enhance the roughness. Finally, the surface

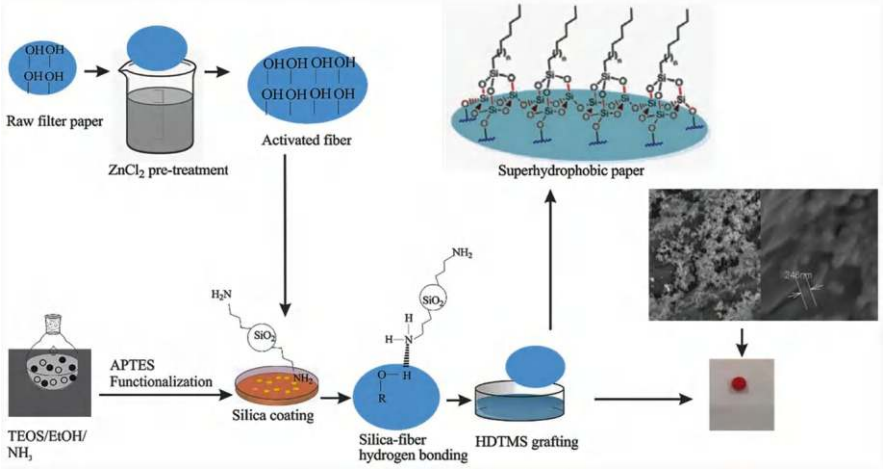

Fig. 14.11 A schematic of the preparation of superhydrophobic paper using sol-gel method. Reprinted with permission from Musikavanhu et al. (2019). Copyright 2024: Elsevier

was modified using hexadecyl trimethoxysilane to improve the hydrophobicity of the surface. They reported a water contact angle of 154.8° for the modified paper (Musikavanhu et al., 2019).

14.3.5 Metal-Ion Modification Method

The metal-ion modification method is a coating method based on swelling the paper in a dilute metal ion solution using immersion or spray. Figure 14.12a indicates a schematic of the hydrophobization of paper using the metal-ion-modification method. The interactions between the metal ion and the paper's functional groups (hydroxyl, carbonyl, and carboxylic) lead to obtaining a compressed structure. The fewer available hydroxyl groups of the created structure decrease the surface energy and increase hydrophobicity (Nayanathara et al., 2023, 2024; Wu et al., 2023). Nayanathara et al. in 2023 used the metal-ion modification method to prepare biodegradable hydrophobic papers. As seen in Fig. 14.12b, the process was based on swelling with aqueous metal ion solutions. They selected Fe^{3+} and Zr^{4+} ions as the best performance after testing various metal ions. They can interact with functional groups of fibers such as OH, C=O, and COOH. This leads to the self-assembly of surface fibrillated "hairy" cellulose nanofibrils which results in decreasing the

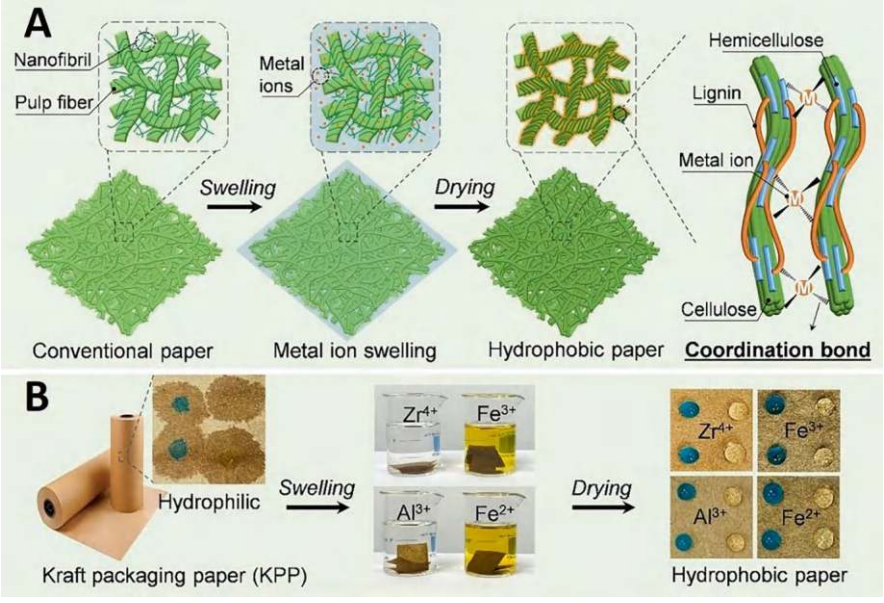

Fig. 14.12 (**a**) A schematic of the hydrophobization of lignocellulose paper using metal-ion modification method, and (**b**) the stages of metal-ion modification of paper. Reprinted with permission from Nayanathara et al. (2023). Copyright 2023: Elsevier

surface energy of fibers and obtaining a hydrophobic surface. They reported a water contact angle of 120–140° for the prepared hydrophobic paper (Nayanathara et al., 2023).

14.3.6 Lamination Coating Method

The lamination coating method is a process for preparing a stable multilayered structure in which the adhesion between the layers is provided by heat, adhesive, heat, pressure, or mechanical bonding (Shim, 2019). Chen et al. (2022) presented a laminating and spraying-based coupled method to fabricate a superhydrophobic paper as the packaging application. As seen in Fig. 14.13, they covered microfibrillated cellulose (MFC) on one side of cellulose paper using a lamination process. Then, they coated nano-silica on the other side of the paper by spraying method using an ethanol solution containing methyltrimethoxysilane and ammonia. The prepared multilayer paper indicated the low permeabilities of 3.17×10^{-3} μm·Pa^{-1}·s^{-1}, 9.687 cm^3·m^{-2}·day^{-1}·atm, and 378.24 g·m^{-2}·day^{-1} for air, oxygen, and water vapor, respectively. Also, the contact angle of 151.2° indicated good superhydrophobic performance of paper (Chen et al., 2022).

14.3.7 Polymer Coating Method

The most common method for preparing polymer-coated paper is the extrusion coating method. In this method, the melting plastic is transferred onto the paper roll and coated on the outer layer of the paper (Fig. 14.14). Although this coating method has some limitations such as unstable molten polymer and the need for a large coating weight, it is widely applied in the large-scale coating of paper due to its

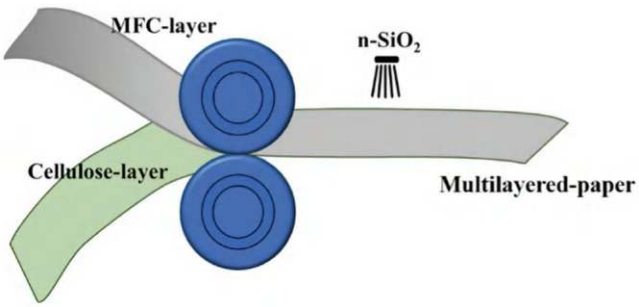

Fig. 14.13 The proposed laminating and spraying-based coupled method for preparation of a superhydrophobic paper. Reprinted with permission from Chen et al. (2022). Copyright 2022: Elsevier

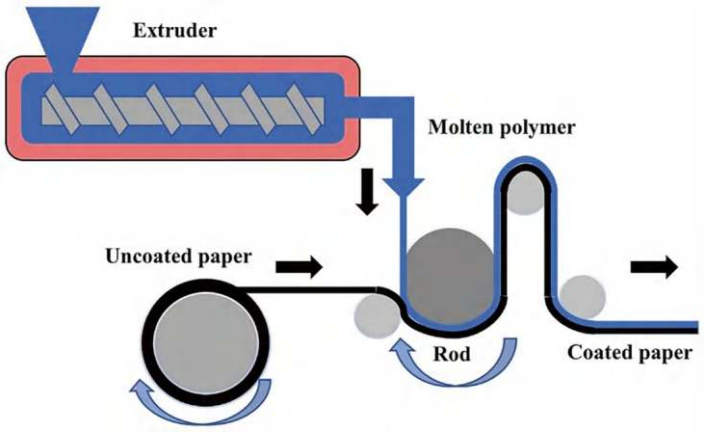

Fig. 14.14 A schematic of extrusion coating method. Reprinted with permission from Basak et al. (2024). Copyright 2024: Elsevier

advantages such as solvent-free process, uniform coated surface, non-stop processing, and others (Basak et al., 2024; Rastogi & Samyn, 2015). One of the disadvantages of this method is the limitation in the preparation of polymeric thin layers by some polymers. For example, the extrusion coating method can prepare polyethylene-based thin-film thicknesses down to 10–15 μm, while owing to their low melt strengths, poly(lactic acid) or polyhydroxyalkanoate cannot be made a thin film through the extrusion method. Also, extruding thinner films reduces the adhesion of the polymer to the paper surface (Calosi et al., 2024; Sängerlaub et al., 2019).

One of the chemical modification methods of the paper surface is the interaction between special functional groups of polymers and the existence of hydroxyl groups on the cellulosic paper surface. In this regard, the polymer coating method is based on precisely controlled chemical reactions with low efficiency. However, research has been continued to increase the efficiency of obtaining hydrophobic paper using this method (Bao et al., 2022; Yun et al., 2023).

Zhang et al. in 2020 prepared a superhydrophobic filter paper using a polymer coating method for application in oil/water separation. Their work was based on simultaneous esterification with stearoyl chloride and α-bromoisobutyryl bromide on the paper surface, followed by polymerization of superhydrophobic poly(styrene-co-acrylonitrile). A water contact angle of 153° and separation efficiency of 98.5% after 10 separation processes were the important results of the prepared superhydrophobic paper (Zhang et al., 2020).

14.3.8 Chemical Modification

Chemical modification of cellulose and its derivations such as cellulosic fibers, nanocelluloses, papers, and others usually carries out through high reactivity of available hydroxyl groups in their structure. This modification should be mildly performed to preserve their useful features without affecting their structure, morphology, and crystalline properties. Acetylation, isocyanate-hydroxyl reaction, and silylation are the important reported methods to prepare hydrophobic properties on the paper surface (Rodríguez-Fabià et al., 2022; Tortorella et al., 2020).

14.3.8.1 Acetylation Method

Acetylation is a special kind of esterification based on replacing the hydroxyl groups of cellulose with the acetyl groups. This process is one of the most used chemical modification methods for hydrophobization of the paper surface, which helps desorption of the modified molecules by weakening the inter-chain hydrogen bonds. The basic common acetylation process is an interaction between cellulose and a dry mixture of acetic acid and acetic anhydride in the presence of an acid catalyst. Figure 14.15 displays a schematic of typical homogeneous and heterogeneous

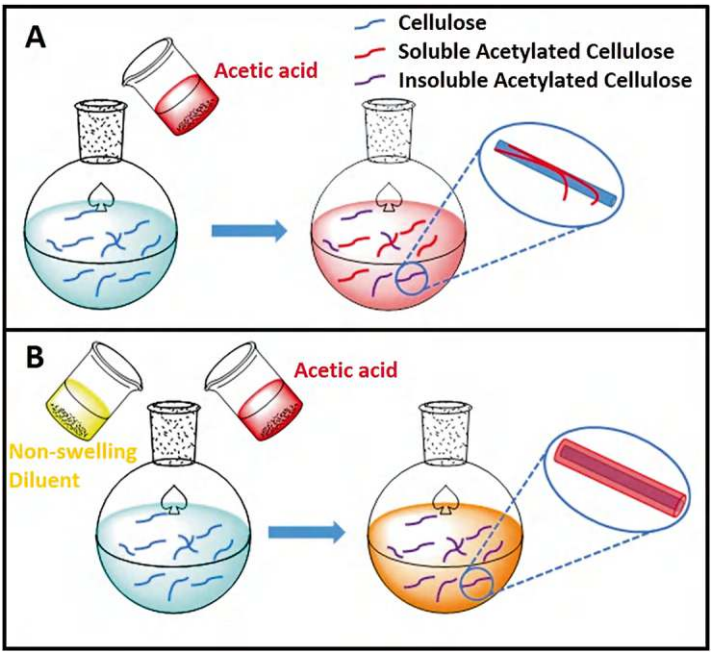

Fig. 14.15 A schematic of (**a**) homogeneous and (**b**) heterogeneous acetylation processes. Reprinted with permission from Rodríguez-Fabià et al. (2022). Copyright 2022: Springer

acetylation processes. In the homogeneous process, cellulose disperses in acetic acid solution as the acetylation medium and creates soluble and insoluble acetylated cellulose molecules. The surface molecules become soluble as soon as they are sufficiently acetylated. This leads to changing the fiber's morphology through the peeling-off effect. If the reaction continues, it can progress toward the substrate core until the fibers completely acetylate. In the heterogeneous process, a non-swelling diluent such as toluene, benzene, or amyl acetate adds to acetic acid and creates insoluble acetylated molecules. Therefore, the surface of the substrate modifies without affecting its morphology (Habibi, 2014; Rodríguez-Fabià et al., 2022; Tripathi et al., 2018; Wang et al., 2018). In this regard, Shin et al. in 2022 presented an acetylation process using a mixture of supercritical CO_2 and acetic anhydride as the reaction medium for the hydrophobization of a traditional Korean paper called Hanji. Good surface hydrophobicity properties obtained through acetylation for 4 h, enhanced tensile strength, and relatively low discoloration were some important results of this work (Shin et al., 2022).

14.3.8.2 Isocyanate-Hydroxyl Reaction

The available hydroxyl groups on the cellulose structure can act as nucleophiles to react with isocyanate groups and produce urethane groups. The reaction between isocyanate and hydroxyl groups of cellulose can be used to improve the hydrophobicity of papers.

Cellulosic materials can react with isocyanate groups through several mechanisms:

1. The reaction between cellulose and a mono-isocyanate having a hydrophobic group such as alkyl or aryl groups.
2. The reaction between cellulose and a di-isocyanate through one of its isocyanates. The second isocyanate can react with a functional group of a polymer or molecule. The application of non-functional alcohol in the reaction with isocyanate leads to obtaining a hydrophobic surface on the cellulosic material.
3. The reaction between a functional group of a polymer or molecule and a di-isocyanate through one of its isocyanates, followed by the reaction of second isocyanate with cellulose. This mechanism is more efficient than mechanism 2, due to the possibility of interaction between cellulose and both two isocyanates which leads to dysfunctionality of the second isocyanate for other stages of the reaction.
4. Simultaneous reaction of a mixture of cellulose, di-isocyanate, and polyol (Abushammala, 2019; Abushammala & Mao, 2019; Porto et al., 2023).

In a study, Saraji and Farajmand in 2013 modified the cellulose paper using various compounds such as octadecyltrichlorosilane, diphenyldichlorosilane, cyclohexyl isocyanate, and phenyl isocyanate. They examined the modified papers through their application as the sorbent in extracting several estrogenic hormones from aqueous samples. Their results indicated the best performance was obtained

using the paper modified with phenyl isocyanate (Saraji & Farajmand, 2013). In 2020, Zhou et al. (2020) prepared a tunable hydrophobic paper using the interaction of methylene diphenyl diisocyanate with hydroxyl groups of filter paper. The modified paper indicated a good hydrophobicity property with a high water contact angle of 137.0°, a suitable wet mechanical property with a wet tensile strength of 4.8 MPa, and good antibacterial activity against *Escherichia coli*. They attributed these results to the formation of urethane bonds during the isocyanate-hydroxyl reaction (Zhou et al., 2020). In another study reported by de Souza et al., they prepared a porous paper using eucalyptus pulp fibers and modified its surface by heating it in a blocked diisocyanate solution. They claimed the application of blocked isocyanates prevents its decomposition to urea and carbon dioxide in wet environments as well as reduces its toxicity. For this purpose, they heated isocyanate in the presence of phenol as the blocking agent at around 170 °C for a few minutes, recovered the reactants, and released the isocyanate groups. Their results indicated the prepared paper had a good hydrophobic property with a water contact angle of 144°, seven times reduction of water absorption, and good oil absorbance (Souza et al., 2020).

14.3.8.3 Silylation Reaction

A silylation reaction is based on replacing the active hydrogen of a material with a silicon atom. The disappearance of hydrogen bonds by a silylation reaction can improve the characterizations of materials by changing their reactivity, blocking reaction centers, increasing their solubility in non-polar solvents, and increasing their volatility. During the silylation of cellulosic materials, the surface free energy of cellulosic fibers reduces. Therefore, the hydrogen bond between their hydroxyl groups and water does not form, resulting in hydrophobicity property on the modified cellulosic surface (Arkles et al., 1982; Kashutina et al., 1975; Pacaphol et al., 2023).

Yu et al. in 2019 reported a gas-solid silylation reaction for hydrophobic modification of cellulosic filter paper. They used perfluorooctyltriethoxysilane as the reagent in the silylation reaction. The modified filter paper showed a water contact angle of 146° ± 3° and good chemical stability in acidic, alkaline, and saline solutions. The good performance of the modified filter paper was confirmed with a separation efficiency of over 99% in the separation of oil/water mixtures (Yu et al., 2019). Banyi and Hassett in 2021 applied chloro(dimethyl)octadecylsilane in a silylation reaction to obtain a hydrophobic paper straw. According to their results, the contact angle between water droplets and the modified paper straw was larger than that of unmodified paper straws. Also, the hydrophobic properties of the modified paper straw using dioxane as a solvent were better than the paper silylated using toluene as a solvent (Banyi & Hassett, 2020).

14.4 Outlooks

This chapter provided an overview of the hydrophobic papers, hydrophobic coating methods, and reported literature on the preparation of hydrophobic papers. As mentioned in sect. 14.3, the common method for obtaining hydrophobicity properties on paper surfaces is the immersion coating method. The outlook of progress in hydrophobic papers is an investigation of simple, efficient, low-cost, green, and safe coating methods and their application in designing and preparing multifunctional devices with a combination of sensors, solar cells, supercapacitors, fuel cells, and batteries.

References

Abushammala, H. (2019). A simple method for the quantification of free isocyanates on the surface of cellulose nanocrystals upon carbamation using toluene diisocyanate. *Surfaces, 2*(2), 444–454. https://doi.org/10.3390/surfaces2020032

Abushammala, H., & Mao, J. (2019). A review of the surface modification of cellulose and nanocellulose using aliphatic and aromatic mono- and di-isocyanates. *Molecules, 24*(15), 2782. https://doi.org/10.3390/molecules24152782

Amin Yavari, S., Croes, M., Akhavan, B., Jahanmard, F., Eigenhuis, C. C., Dadbakhsh, S., & Zadpoor, A. A. (2020). Layer by layer coating for bio-functionalization of additively manufactured meta-biomaterials. *Additive Manufacturing, 32*, 100991. https://doi.org/10.1016/j.addma.2019.100991

Arbatan, T., Zhang, L., Fang, X.-Y., & Shen, W. (2012). Cellulose nanofibers as binder for fabrication of superhydrophobic paper. *Chemical Engineering Journal, 210*, 74–79. https://doi.org/10.1016/j.cej.2012.08.074

Arkles, B. C., Peterson, W. R., & Anderson, R. (Eds.). (1982). *Silicon compounds: Register and review*. Petrarch Systems.

Banyi, N., & Hassett, J. (2020). Paper straws: An investigation into surface modification and hydrophobization of cellulose. *STEM Fellowship Journal, 6*(1), 24–33. https://doi.org/10.17975/sfj-2020-007

Bao, Y., Chang, J., Zhang, Y., & Chen, L. (2022). Robust superhydrophobic coating with hollow SiO_2/PAA-b-PS Janus microspheres for self-cleaning and oil–water separation. *Chemical Engineering Journal, 446*, 136959. https://doi.org/10.1016/j.cej.2022.136959

Basak, S., Dangate, M. S., & Samy, S. (2024). Oil- and water-resistant paper coatings: A review. *Progress in Organic Coating, 186*, 107938. https://doi.org/10.1016/j.porgcoat.2023.107938

Butt, M. A. (2022). Thin-film coating methods: A successful marriage of high-quality and cost-effectiveness—A brief exploration. *Coatings, 12*(8), 1115. https://doi.org/10.3390/coatings12081115

Calosi, M., D'Iorio, A., Buratti, E., Cortesi, R., Franco, S., Angelini, R., & Bertoldo, M. (2024). Preparation of high-solid PLA waterborne dispersions with PEG-PLA-PEG block copolymer as surfactant and their use as hydrophobic coating on paper. *Progress in Organic Coating, 193*, 108541. https://doi.org/10.1016/j.porgcoat.2024.108541

Celia, E., Darmanin, T., Taffin de Givenchy, E., Amigoni, S., & Guittard, F. (2013). Recent advances in designing superhydrophobic surfaces. *Journal of Colloid and Interface Science, 402*, 1–18. https://doi.org/10.1016/j.jcis.2013.03.041

Chen, H., Wang, B., Li, J., Ying, G., & Chen, K. (2022). High-strength and super-hydrophobic multilayered paper based on nano-silica coating and micro-fibrillated cellulose. *Carbohydrate Polymers, 288*, 119371. https://doi.org/10.1016/j.carbpol.2022.119371

Crick, C. R., & Parkin, I. P. (2010). Preparation and characterisation of super-hydrophobic surfaces. *Chemistry - A European Journal, 16*(12), 3568–3588. https://doi.org/10.1002/chem.200903335

Gao, Z., Zhai, X., Liu, F., Zhang, M., Zang, D., & Wang, C. (2015). Fabrication of TiO_2/EP super-hydrophobic thin film on filter paper surface. *Carbohydrate Polymers, 128*, 24–31. https://doi.org/10.1016/j.carbpol.2015.04.014

Ghayempour, S., & Montazer, M. (2016). Micro/nanoencapsulation of essential oils and fragrances: Focus on perfumed, antimicrobial, mosquito-repellent and medical textiles. *Journal of Microencapsulation, 33*(6), 497–510. https://doi.org/10.1080/02652048.2016.1216187

Ghayempour, S., & Mortazavi, S. M. (2013). Fabrication of micro–nanocapsules by a new electrospraying method using coaxial jets and examination of effective parameters on their production. *Journal of Electrostatics, 71*(4), 717–727. https://doi.org/10.1016/j.elstat.2013.04.001

Ghayempour, S., Mazloum-Ardakani, M., & Dehghan-Manshadi, H. (2024). Nanopaper-Based Biosensors: Diagnosis and Device Development. In: Azad, U.P. and Chandra, P. (Eds.) *Handbook of Material Engineering in Nanobiomedicine and Diagnostics* pp. 901–916. Singapore: Springer Nature Singapore. https://doi.org/10.1007/978-981-97-7445-6_38

Gozutok, Z., Kinj, O., Torun, I., Ozdemir, A. T., & Onses, M. S. (2019). One-step deposition of hydrophobic coatings on paper for printed-electronics applications. *Cellulose, 26*(5), 3503–3512. https://doi.org/10.1007/s10570-019-02326-y

Guan, F., Song, Z., Xin, F., Wang, H., Yu, D., Li, G., & Liu, W. (2020). Preparation of hydrophobic transparent paper via using polydimethylsiloxane as transparent agent. *Journal of Bioresources and Bioproducts, 5*(1), 37–43. https://doi.org/10.1016/j.jobab.2020.03.004

Habibi, Y. (2014). Key advances in the chemical modification of nanocelluloses. *Chemical Society Reviews, 43*(5), 1519–1542. https://doi.org/10.1039/C3CS60204D

He, Y., Zhou, Y., Cai, J., Feng, Y., Luo, B., & Liu, M. (2022). Facile fabrication of hydrophobic paper by HDTMS modified chitin nanocrystals coating for food packaging. *Food Hydrocolloids, 133*, 107915. https://doi.org/10.1016/j.foodhyd.2022.107915

Kashutina, M. V., Sema, L. I., & Vladimir, A. T. (1975). Silylation of organic compounds. *Russian Chemical Reviews, 44*(9), 733. https://doi.org/10.1070/RC1975v044n09ABEH002373

Lakshmi, R. V., Bharathidasan, T., & Basu, B. J. (2011). Superhydrophobic sol–gel nanocomposite coatings with enhanced hardness. *Applied Surface Science, 257*(24), 10421–10426. https://doi.org/10.1016/j.apsusc.2011.06.122

Lan, Z., & Duan, W. (2023). Achieving surface hydrophobic and moisture-proof properties of ancient-book paper by in-situ protection of epoxy-based POSS/PVDF composite coating. *Bulletin of Materials Science, 46*(2), 73. https://doi.org/10.1007/s12034-023-02910-w

Li, A., Kang, Q., Ren, S., Zhang, Y., Zhang, F., & He, Q. (2021). Preparation of superhydrophobic composite paper mulching film. *Arabian Journal of Chemistry, 14*(8), 103247. https://doi.org/10.1016/j.arabjc.2021.103247

Li, A., Wang, G., Zhang, Y., Zhang, J., He, W., Ren, S., & Ma, Y. (2021). Preparation methods and research progress of superhydrophobic paper. *Coordination Chemistry Reviews, 449*, 214207. https://doi.org/10.1016/j.ccr.2021.214207

Li, H., Wang, X., He, Y., & Peng, L. (2019). Facile preparation of fluorine-free superhydrophobic/superoleophilic paper via layer-by-layer deposition for self-cleaning and oil/water separation. *Cellulose, 26*(3), 2055–2074. https://doi.org/10.1007/s10570-018-2187-3

Li, S., Zhang, S., & Wang, X. (2008). Fabrication of superhydrophobic cellulose-based materials through a solution-immersion process. *Langmuir, 24*(10), 5585–5590. https://doi.org/10.1021/la800157t

Liu, Z., Yu, J., Lin, W., Yang, W., Li, R., Chen, H., & Zhang, X. (2018). Facile method for the hydrophobic modification of filter paper for applications in water-oil separation. *Surface and Coating Technology, 352*, 313–319. https://doi.org/10.1016/j.surfcoat.2018.08.026

Loesch-Zhang, A., Cordt, C., Geissler, A., & Biesalski, M. (2022). A solvent-free approach to crosslinked hydrophobic polymeric coatings on paper using vegetable oil. *Polymers, 14*(9), 1773. https://doi.org/10.3390/polym14091773

Long, C., Qing, Y., Long, X., Liu, N., Xu, X., An, K., & Liu, C. (2022). Synergistic reinforced superhydrophobic paper with green, durability, and antifouling function. *Applied Surface Science, 579*, 152144. https://doi.org/10.1016/j.apsusc.2021.152144

Min, J., Choi, K. Y., Dreaden, E. C., Padera, R. F., Braatz, R. D., Spector, M., & Hammond, P. T. (2016). Designer dual therapy nanolayered implant coatings eradicate biofilms and accelerate bone tissue repair. *ACS Nano, 10*(4), 4441–4450. https://doi.org/10.1021/acsnano.6b00087

Mujtaba, M., Lipponen, J., Ojanen, M., Puttonen, S., & Vaittinen, H. (2022). Trends and challenges in the development of bio-based barrier coating materials for paper/cardboard food packaging: A review. *Science of the Total Environment, 851*, 158328. https://doi.org/10.1016/j.scitotenv.2022.158328

Musikavanhu, B., Hu, Z., Dzapata, R. L., Xu, Y., Christie, P., Guo, D., & Li, J. (2019). Facile method for the preparation of superhydrophobic cellulosic paper. *Applied Surface Science, 496*, 143648. https://doi.org/10.1016/j.apsusc.2019.143648

Nayanathara, R. M. O., Leng, W., Liyanage, S. D., Wang, X., Wang, L., Wang, J., & Zhang, X. (2023). A general metal-ion-modification route for preparing hydrophobic paper and tableware from lignocellulose fibers. *Chemical Engineering Journal, 459*, 141596. https://doi.org/10.1016/j.cej.2023.141596

Nayanathara, R. M. O., Leng, W., Street, J., & Zhang, X. (2024). Wood dimensional stability enhancement by multivalent metal-cation-induced lignocellulosic microfibrils crosslinking. *International Journal of Biological Macromolecules, 269*, 131877. https://doi.org/10.1016/j.ijbiomac.2024.131877

Nguyen-Tri, P., Tran, H. N., Plamondon, C. O., Tuduri, L., Vo, D.-V. N., Nanda, S., & Bajpai, A. K. (2019). Recent progress in the preparation, properties and applications of superhydrophobic nano-based coatings and surfaces: A review. *Progress in Organic Coating, 132*, 235–256. https://doi.org/10.1016/j.porgcoat.2019.03.042

Ogihara, H., Xie, J., Okagaki, J., & Saji, T. (2012). Simple method for preparing superhydrophobic paper: Spray-deposited hydrophobic silica nanoparticle coatings exhibit high water-repellency and transparency. *Langmuir, 28*(10), 4605–4608. https://doi.org/10.1021/la204492q

Ogihara, H., Xie, J., & Saji, T. (2013). Factors determining wettability of superhydrophobic paper prepared by spraying nanoparticle suspensions. *Colloids and Surfaces A: Physicochemical and Engineering Aspects, 434*, 35–41. https://doi.org/10.1016/j.colsurfa.2013.05.034

Pacaphol, K., Seraypheap, K., & Aht-Ong, D. (2023). Extraction and silylation of cellulose nanofibers from agricultural bamboo leaf waste for hydrophobic coating on paper. *Journal of Natural Fibers, 20*(1), 2178581. https://doi.org/10.1080/15440478.2023.2178581

Porto, D. S., de Faria, C. M. G., Inada, N. M., & Frollini, E. (2023). Polyurethane films formation from microcrystalline cellulose as a polyol and cellulose nanocrystals as additive: Reactions favored by the low viscosity of the source of isocyanate groups used. *International Journal of Biological Macromolecules, 236*, 124035. https://doi.org/10.1016/j.ijbiomac.2023.124035

Rastogi, V. K., & Samyn, P. (2015). Bio-based coatings for paper applications. *Coatings, 5*(4), 887–930. https://doi.org/10.3390/coatings5040887

Rodríguez-Fabià, S., Torstensen, J., Johansson, L., & Syverud, K. (2022). Hydrophobization of lignocellulosic materials part II: Chemical modification. *Cellulose, 29*(17), 8957–8995. https://doi.org/10.1007/s10570-022-04824-y

Saha, R., Bhattacharya, D., & Mukhopadhyay, M. (2022). Advances in modified antimicrobial peptides as marine antifouling material. *Colloids and Surfaces. B, Biointerfaces, 220*, 112900. https://doi.org/10.1016/j.colsurfb.2022.112900

Samir, A., Ashour, F. H., Hakim, A. A. A., & Bassyouni, M. (2022). Recent advances in biodegradable polymers for sustainable applications. *npj Materials Degradation, 6*(1), 68. https://doi.org/10.1038/s41529-022-00277-7

Sängerlaub, S., Brüggemann, M., Rodler, N., Jost, V., & Bauer, K. D. (2019). Extrusion coating of paper with poly(3-hydroxybutyrate-co-3-hydroxyvalerate) (PHBV)—Packaging related functional properties. *Coatings, 9*(7), 457. https://doi.org/10.3390/coatings9070457

Saraji, M., & Farajmand, B. (2013). Chemically modified cellulose paper as a thin film microextraction phase. *Journal of Chromatography. A, 1314*, 24–30. https://doi.org/10.1016/j.chroma.2013.09.018

Shakeel Ahmad, M., Pandey, A. K., & Abd Rahim, N. (2017). Advancements in the development of TiO_2 photoanodes and its fabrication methods for dye sensitized solar cell (DSSC) applications. A review. *Renewable and Sustainable Energy Reviews, 77*, 89–108. https://doi.org/10.1016/j.rser.2017.03.129

Shende, P., Patil, A., & Prabhakar, B. (2020). Layer-by-layer technique for enhancing physico-chemical properties of actives. *Journal of Drug Delivery Science and Technology, 56*, 01519. https://doi.org/10.1016/j.jddst.2020.101519

Shim, E. (2019). 2 - coating and laminating processes and techniques for textiles. In W. C. Smith (Ed.), *Smart textile coatings and laminates* (2nd ed., pp. 11–45). Woodhead Publishing.

Shin, S., Lee, H.-S., Woo, H. S., Aregay, M. G., Yoon, T. J., & Lee, Y.-W. (2022). Improvement of mechanical strength and water repellency of Hanji (traditional Korean paper) through acetylation in supercritical CO_2. *Journal of Supercritical Fluids, 190*, 105735. https://doi.org/10.1016/j.supflu.2022.105735

Silva, J. M., Reis, R. L., & Mano, J. F. (2016). Biomimetic extracellular environment based on natural origin polyelectrolyte multilayers. *Small, 12*(32), 4308–4342. https://doi.org/10.1002/smll.201601355

Souza, G. D., Kramer, R. K., & Carvalho, A. J. F. (2020). Urethane modified hydrophobic compact wood pulp paper for oil spill cleanup: A preliminary study. *Journal of Renewable Materials, 8*(10), 1257–1268. https://doi.org/10.32604/jrm.2020.011906

Teng, Y., Wang, Y., Shi, B., Fan, W., Li, Z., & Chen, Y. (2020). Facile fabrication of superhydrophobic paper with durability, chemical stability and self-cleaning by roll coating with modified nano-TiO_2. *Applied Nanoscience, 10*(11), 4063–4073. https://doi.org/10.1007/s13204-020-01518-4

Tortorella, S., Vetri Buratti, V., Maturi, M., Sambri, L., Comes Franchini, M., & Locatelli, E. (2020). Surface-modified nanocellulose for application in biomedical engineering and nanomedicine: A review. *International Journal of Nanomedicine, 10*(15), 9909–9937. https://doi.org/10.2147/IJN.S266103

Tripathi, A., Ago, M., Khan, S. A., & Rojas, O. J. (2018). Heterogeneous acetylation of plant fibers into micro- and nanocelluloses for the synthesis of highly stretchable, tough, and water-resistant co-continuous filaments via wet-spinning. *ACS Applied Materials & Interfaces, 10*(51), 44776–44786. https://doi.org/10.1021/acsami.8b17790

Wang, J., Monton, M. R. N., Zhang, X., Filipe, C. D. M., Pelton, R., & Brennan, J. D. (2014). Hydrophobic sol–gel channel patterning strategies for paper-based microfluidics. *Lab on a Chip, 14*(4), 691–695. https://doi.org/10.1039/C3LC51313K

Wang, Y., Wang, X., Xie, Y., & Zhang, K. (2018). Functional nanomaterials through esterification of cellulose: A review of chemistry and application. *Cellulose, 25*(7), 3703–3731. https://doi.org/10.1007/s10570-018-1830-3

Wu, N., Gao, H., Wang, X., & Pei, X. (2023). Surface modification of titanium implants by metal ions and nanoparticles for biomedical application. *ACS Biomaterials Science & Engineering, 9*(6), 2970–2990. https://doi.org/10.1021/acsbiomaterials.2c00722

Yu, L., Zhang, Z., Tang, H., & Zhou, J. (2019). Fabrication of hydrophobic cellulosic materials via gas–solid silylation reaction for oil/water separation. *Cellulose, 26*(6), 4021–4037. https://doi.org/10.1007/s10570-019-02355-7

Yun, T., Tao, Y., Li, Q., Cheng, Y., Lu, J., Lv, Y., & Wang, H. (2023). Superhydrophobic modification of cellulosic paper-based materials: Fabrication, properties, and versatile applications. *Carbohydrate Polymers, 305*, 120570. https://doi.org/10.1016/j.carbpol.2023.120570

Zhang, K., Wang, M., Wu, M., Wu, Q., Liu, J., Yang, J., & Zhang, J. (2020). Fabrication of robust superhydrophobic filter paper for oil/water separation based on the combined octadecanoyl chain bonding and polymer grafting via surface-initiated ATRP. *Cellulose, 27*(1), 469–480. https://doi.org/10.1007/s10570-019-02810-5

Zhang, Y., Ren, T., Li, T., He, J., & Fang, D. (2016). Paper-based hydrophobic/lipophobic surface for sensing applications involving aggressive liquids. *Advanced Materials Interfaces, 3*(22), 1600672. https://doi.org/10.1002/admi.201600672

Zhou, X., Fu, Y., Chen, L., Wang, R., Wang, X., Miao, Y., & Dai, H. (2020). Diisocyanate modifiable commercial filter paper with tunable hydrophobicity, enhanced wet tensile strength and antibacterial activity. *Carbohydrate Polymers, 248*, 116791. https://doi.org/10.1016/j.carbpol.2020.116791

Chapter 15
Thermoconductive Paper

Mona T. Al-Shemy and Sawsan Dacrory

15.1 Introduction

The microelectronics sector has experienced significant and rapid advancement in the twenty-first century. Its efficacy relies on the fabrication of small components with exceptional thermal conductivity (TC), enabling rapid thermal energy dissipation. Thus, it is applicable in several sectors, including aircraft, automotive, military, computing, and telecommunications. Overheating in electronic devices is the primary cause of electronic equipment failures, specifically leading to printed circuit board (PCB) failures and significant malfunctions (Malekpour et al., 2014; Owais et al., 2021). This failure results in the fabrication of highly efficient thermal interface materials with reduced thickness to address the burgeoning development of electronic devices such as tablets and laptops, enhancing their longevity and reliability. Electronic packaging systems commonly utilize thermal interface materials (TIM) to improve thermal conduction. These materials are generally positioned between two solid surfaces to fill the voids, enhancing thermal conduction over the contact region (Owais et al., 2021). Thermal interface materials are categorized into several groups: solders, thermally conductive adhesives, thermal grease, gels, phase transition materials, and thermal pads. Despite their commendable thermal conductivities, MTI presents significant drawbacks, including potential messiness and environmental contamination when utilized in paste form. When subjected to pressure, the grease material extrudes at the edges; hence, it is not a suitable option for thermal interface materials (TIMs). Conversely, thermal pads are significantly more manageable but lack reusability. Consequently, alternative materials to thermal interface materials (TIM) are crucial; thermally conductive papers are increasingly favored due to their unique characteristics and cleaner alternative to TIM. These

M. T. Al-Shemy · S. Dacrory (✉)
Cellulose and Paper Department, National Research Centre, Giza, Egypt
e-mail: Sd.dacrory@nrc.sci.eg

G. Korotcenkov (ed.), *The Handbook of Paper-Based Sensors and Devices*,
https://doi.org/10.1007/978-3-031-91080-7_15

papers demonstrate high TC, superior mechanical properties, effective electrical insulation, satisfactory flame retardancy, and user-friendly characteristics (Hu et al., 2018; Sun et al., 2017; Wu et al., 2017; Zhu et al., 2014, 2019).

The rise of new applications, such as energy transfer and 5G communication, has rendered heat dissipation an increasingly significant concern (Hutchinson & Moradi, 2020). Epoxy resin (EPs) is extensively utilized in the energy, electrical, and electronics sectors due to its electrical insulation, thermal stability, high tensile strength, and superior performance properties. Nevertheless, its low TC of roughly 0.2 W $(mK)^{-1}$ limits its applicability across multiple domains, as it is predominantly regarded as a heat insulator. Consequently, the alteration and amalgamation of thermo-conductive (TC) materials with EPs to create TC epoxy composites have been established. However, augmenting TC materials as fillers diminishes mechanical characteristics and escalates costs (Han et al., 2018; Kubiak et al., 2022). This prompted the researcher to alter the molecular structure of EPs to enhance their TC and to investigate new filler structures to improve TC values. Carbon-based and boron nitride materials have recently been widely used to produce thermally conductive composites owing to their exceptional TC. The unique features of carbon-based materials have prompted extensive research to explore their functions due to their remarkable thermal, electrical, and mechanical advantages (Shen et al., 2014; Teng et al., 2017; Vu et al., 2021).

A growing number of electronic and electrical applications, such as high energy storage and capacitors, are drawing increased interest in materials with a high dielectric permittivity. Ceramic polymer composites have recently gained much attention as dielectric materials because of their low dielectric loss, low conductivity, ease of processing, and inexpensive cost (Almadhoun et al., 2012; Dacrory et al., 2021; Dang et al., 2012; Jia et al., 2015; Xu et al., 2014).

With good flexibility and short thickness, TC paper is emerging as a new class of materials for thermal management applications in electronics (Fig. 15.1). Contrary to popular belief, typical paper nanocomposites can attain high TC with more significant loading concentrations of thermally conductive fillers without compromising the paper's mechanical qualities. According to the literature, there are three main categories of paper/film-like thermally conductive composites: (1) composites and nanocomposites made of polymers, (2) carbonaceous materials with or without polymers, and (3) carbon/ceramic materials, which are discussed in depth later in this chapter.

15.2 Thermal Properties of Cellulose and Paper-Based on It

Cellulose is a macromolecular polysaccharide that is appealing as a renewable raw material. It is characterized by its non-toxic, biodegradable, and biocompatible properties. It has been reported as a material utilized in various applications (Dacrory et al., 2022; Elsayed et al., 2022; Hasanin et al., 2021). The unique molecular composition of this material, which is the structural framework of all green plant cells,

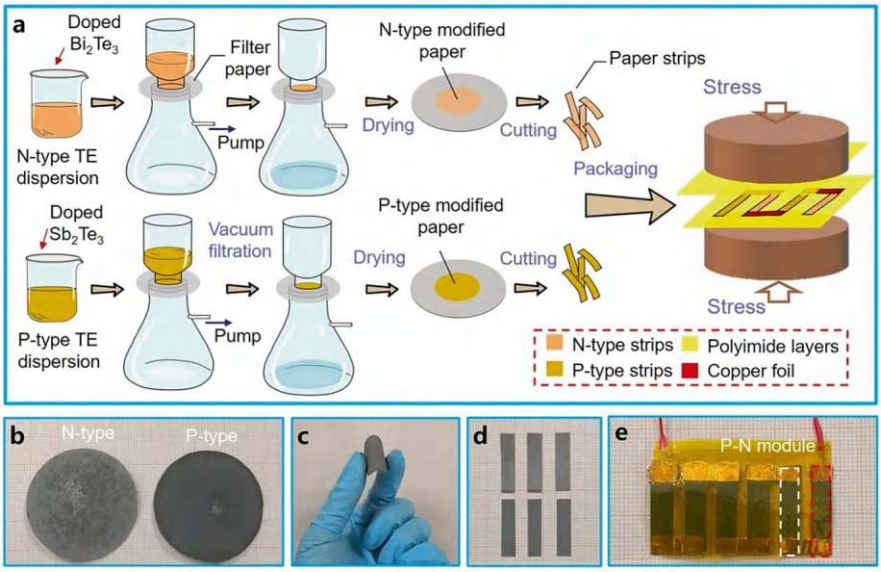

Fig. 15.1 Preparation process of flexible paper-based thermoelectric generator (PTG) and the photo displays. (**a**) Schematic diagram of the fabrication process for PTGs. The N- and P-type modified papers are prepared through the vacuum filtration method, cut into small strips, and connected with copper foil in an alternating sequence. (**b**–**e**) Photographs of the complete modified papers obtained by the vacuum filtration method (**b**), displaying their high flexibility (**c**), the small 5 × 20 mm strips (**d**), and the PTG with three units of P–N modules (**e**). The smallest grid point of the background grid paper represents 1 mm. Reprinted from Dong et al. (2021). Published 2021 by Nature with open access

is made up of linear chains connected by β(1 → 4) linked D-glucose units. There are many different uses for cellulose and paper made from it because of its unique thermal characteristics. Fiber type, density, moisture content, and additives are some of the most important elements determining the thermal characteristics of cellulose and paper. Due to its poor heat conductivity, cellulose is an excellent insulator. This quality comes in handy when thermal insulation is needed. Cellulose breaks down when exposed to high temperatures, usually between 200 and 300 °C. Char forms and volatile chemicals are released as a result. Different types of cellulose and their processing methods result in different precise breakdown temperatures. In addition, cellulose has a high specific heat capacity, so it can absorb much heat before its temperature rises dramatically.

Like cellulose, paper exhibits low TC. Under standard temperature and pressure conditions, its TC is approximately 0.05 W $(mK)^{-1}$. Paper exhibits high thermal resistivity, which is defined as the inverse of TC. This indicates its ability to impede heat transfer, rendering it an efficient insulator. The paper's specific heat capacity is approximately 1.4 kJ $(kg\ K)^{-1}$, reflecting its capacity for heat absorption. Because of its combustible cellulose content, paper's rate of combustion is affected by its density and other properties, such as additives like fire retardants.

Lightweight, optical transparency, specific surface area, and good mechanical qualities are all enhanced by cellulose's unique structure. Because of its compact structure and high-strength matrix, cellulose is insoluble in standard solvents and has peculiar features resulting from its strong inter- and intramolecular hydrogen bonding. Because of these qualities, cellulose is increasingly used in electrical devices, particularly those with high volumes that are not biodegradable, have poor durability, are not very flexible, and contribute to environmental contamination. The use of cellulose, which is abundant, lightweight, inexpensive, and good for the environment, has so garnered increased interest. Adding a conductive material to cellulose, chemically or by adsorption, can increase its conductivity (Lee & Jeong, 2015; Li et al., 2006; Li, Yang, Huang, et al., 2018). Many of these materials find widespread application, including metals, inorganic oxides, carbon compounds, and conductive polymers. Despite their advantages, these materials do have some defects. Metals are highly conductive but with low transmittance; inorganic oxides are highly conductive and have good transmittance but are inflexible; polymers are flexible but have low conductivity and transmittance (Lee & Jeong, 2015; Li et al., 2006; Li, Yang, Huang, et al., 2018).

15.3 Approaches to Developing Thermally Conductive Cellulose-Based Paper

15.3.1 Control of Paper Structure

Because of its potential usage in numerous applications, the behavior of cellulose's TC κ is both scientifically intriguing and practically significant. In most cases, the microstructure of a material is a crucial factor in determining κ and how it changes with critical variables like density and temperature. Here, the structure of cellulose seems to be closely related to its κ property. Although cellulose is essentially just an assembly of polymer chains, the natural nanofibrous structure that forms during its microstructure sets it apart from most manufactured polymers. The cellulose fibers consist of several microfibrils with a diameter ranging from around 5 to 50 nm. Furthermore, microfibrils are composed of elementary fibrils that range in diameter from 3 to 5 nm. These fibrils are formed by bundles of approximately 40 individual cellulose chains (Flity et al., 2024; Zhang, Kobayashi, et al., 2024). According to a popular structural model, the fibril of dry cellulose is made up of crystalline and amorphous parts repeated along the cellulose chains. Nanofibers (CNFs) or microfibrillated cellulose can be obtained by mechanically disintegrating fibers, while strong acid hydrolysis can be used to extract cellulose nanocrystals (CNCs) from cellulose fibers. CNFs can differ in shape from amorphous to crystalline. They can measure anywhere from 10 to 100 nm in diameter and many micrometers long, while CNCs consist of individual crystalline sections around 100 nm long (Horikawa et al., 2018).

Research on the conduction of heat in cellulose samples has revealed that the material exhibits good heat conduction along fibers but poor conduction in other directions. Thus, depending on the cellulose samples' porosity and structural arrangement, it can function as an excellent heat conductor or a thermal insulator. Research on cellulose sheets, papers, and films reveals κ anisotropy, with fibers ideally aligned with the sheet's plane (Antlauf et al., 2021; Diaz et al., 2014; Uetani et al., 2015; Uetani & Hatori, 2017).

Based on their review, Uetani et al. (2015) and Uetani and Hatori (2017) found that nanocellulose made from wood pulp, cotton, bacterial cellulose, and tunicate had through-plane κ values ranging from 0.3 to 0.5 W $(mK)^{-1}$, which were independent of the material used to make it, and in-plane values ranging from 0.6 to 2.5 W $(mK)^{-1}$, which were dependent on the material used to make it. Further, a study conducted by Antlauf et al. (2021) examined the impact of densification on samples of birch kraft pulp cellulose fibers and CNFs that were randomly orientated. A κ of 0.57 and 0.54 W $(mK)^{-1}$ were recorded along individual CNFs. The model for a dense random network of fibers, when used in conjunction with it, suggests that $\kappa = 1.7$ W $(mK)^{-1}$ along individual CNFs. Adachi et al. (2021) managed to measure κ along individual CNFs and reported $\kappa = (2.2 \pm 1.2)$ W $(mK)^{-1}$ at 300 K for nonporous cellulose fiber and CNF, respectively, despite the difficulty and large uncertainty in directly measuring κ of individual CNFs.

Prior research has also demonstrated that as temperature rises, κ of cellulose fiber and CNF increases. Amorphous polymers are typically linked to this behavior, while crystalline and semicrystalline polymers exhibit a temperature-dependent κ-decrease at ambient temperature. Above approximately 100 K, more precisely, in the low-temperature range where crystal sizes limit the transmission of phonons (heat quanta) (Adachi et al., 2021; Cao et al., 2021; Zhao et al., 2018).

κ decreases as temperature increases because the number of phonons increases, leading to an increase in phonon–phonon scattering. The amorphous-like κ increases with temperature due to rising heat capacity if the major phonon scattering mechanism originates from sources that are independent of temperature, like structural disorder (Cao et al., 2021; Tian et al., 2024).

The correlations between density, pressure, and temperature (κ) are quite similar for dense (nonporous) networks of randomly oriented cellulose fibers, CNCs, and CNFs, according to Antlauf and Andersson's study. There is a mere 10% difference in the value of κ. The value of κ is 0.60 ± 0.01 W $(mK)^{-1}$ at 295 K and atmospheric pressure, which is highest in a CNC sample. In cellulose fibers and CNF samples, it is 5% lower and 10% lower, respectively. One probable explanation for the discrepancy in κ between CNC and cellulose fiber samples is the presence of mostly amorphous hemicellulose in the latter. The mechanical disintegration of cellulose fibers into CNFs causes an increase in structural disorder, which may explain why the κ values of the two samples differ (Antlauf & Andersson, 2022).

Results showed that the thermal resistance in cellulose is mainly due to the random networks of cellulose fibers, CNCs, and CNFs, which limit the phonon mean free route to a few nanometers. All these κ values and their (almost universal) dependency on density, pressure, and temperature are explained by the nanoscale nature

of elementary fibrils and their inherent assemblages. The purest sample for the κ of a dense random network of thin fibers gives us 1.9 W $(mK)^{-1}$, which was the best estimate for κ along an elemental or microfibril fibril at ambient temperature and atmospheric pressure.

For cellulose fiber, CNC, and CNF samples, the pressure dependency of κ is 14% GPa^{-1}, lower than the often observed range of 30–160% GPa^{-1} for polymers. This surprising polymer conclusion seems to be caused by the combination of nano-sized fibrils with a high elastic modulus (i.e., stiffness) in the fiber direction, which cellulose possesses (Antlauf & Andersson, 2022). Figure 15.2 highlights the sources of cellulose, the methods used to enhance thermal conductivity, and the potential applications of TC paper.

15.3.2 Improvement of TC Through Formation of Cellulose-Based Composites

15.3.2.1 Cellulose/Metal Composites

Thermally conductive refers to a material's capacity to conduct or transfer heat. Heat transfer occurs through charge carriers such as electrons and holes within materials in solids. Heat transfer occurs through lattice vibrations, wherein vibrational energy is conveyed from one atom to its adjacent atom. Energy is transferred from high-energy electrons to low-energy electrons through electron motion. Recently, polymer composites have been utilized in electronic packaging and heat management applications owing to their versatile properties, which have evolved,

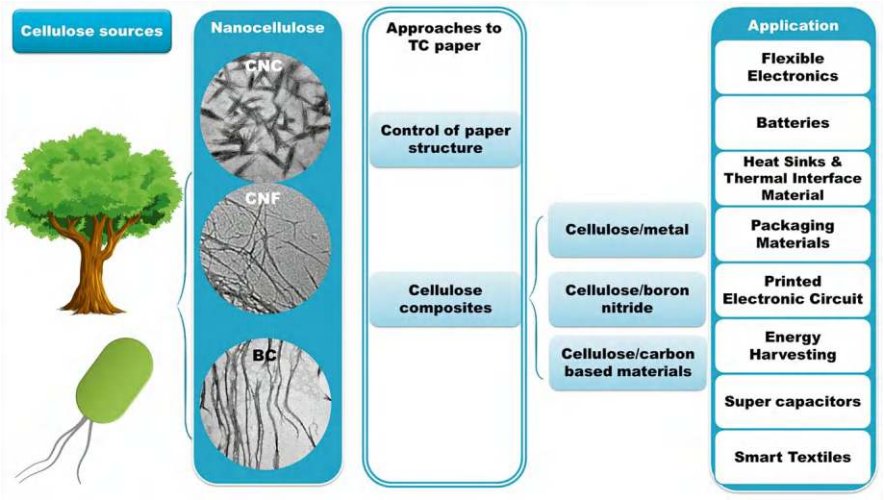

Fig. 15.2 Diagram for development and applications of TC cellulose-based paper

enhancing their importance in the electrical sector for electrical insulation, thermal conduction, and excess heat dissipation. Incorporating thermally conductive fillers into polymer compounds is a prevalent method to enhance TC, resulting in composites with superior thermal and mechanical properties. Incorporating numerous unique fillers in a polymer matrix presents scientific and technological challenges; specifically, the measured TC of the composites is diminished due to the presence of thermal resistances. More than choosing appropriate polymers and fillers, it is essential to consider these materials' structure and interactions (Mumtaz et al., 2024; Ouyang et al., 2022). Highly crystalline materials, including graphene, metals, and ceramics, demonstrate elevated TC. Metals, including silver, copper, and gold, along with their nanowire counterparts, serve as prevalent conductive materials. Materials possess a significant number of freely mobile electrons, resulting in high conductivity. Low transmittance is a defining characteristic of metals due to their metallic luster.

The preparation of cellulose composites incorporating metal particles, metal oxide particles, liquid metals, and inorganic compounds has increased significantly. Researchers have developed various effective strategies for conductive composites. Zou et al. (2019) prepared a self-supporting composite membrane of cellulose, reduced graphene oxide (RGO), and silver (Ag) nanoparticles. Cellulose filter paper, GO, and silver ammonia complexes were combined to form a slurry. Subsequently, silver ammonia was thermally reduced to Ag nanoparticles, and then a thin film was prepared via vacuum filtration. Hot hydrazine vapors were then employed to reduce GO to RGO, resulting in the final vimentin/RGO/Ag nanoparticle composite film, which exhibited a thickness of approximately 400 μm and an electrical resistivity as low as 0.17 Ω/sq. (Wang et al., 2023).

Fei et al. (2020) selected a metal–organic framework (MOF) as the source of metal particles, specifically anchoring ZIF-67 onto cellulose nanofibers (CNF). The composite structure underwent annealing to produce a cobalt/carbon@CNF aerogel.

15.3.2.2 Cellulose/Carbon-Based Materials

Renewable biomass as a sustainable carbon source to prepare materials with excellent electrochemical properties has been extensively investigated since it is an environmentally benign and cost-effective method. Cellulose, CNF, and BC can be used in the application of carbonization due to their unique network and pore size structure during the process. Cellulose has been processed through high-temperature pyrolysis ovens or high-pressure reactors, removing non-carbon elements. This process also provides high porosity, specific surface area, and electrical conductivity materials. Chen et al. (2018) prepared lightweight and highly compressible wood-derived carbon foam from natural wood where lignin and hemicellulose were removed by chemical treatment, and then by using pyrolysis, it was converted into a spring-like compressible layered structure. The conductivity of the final foam was 0.04–1.66 S cm^{-1}. Chen et al. (2021) also constructed aerogels with porous structures by mixing carbonized BC (which is very good at conducting electricity) with

CNF wood assembled by freeze-drying wood. Wang et al. (2021) reported a novel method for cellulose carbonization at a low temperature of 90 °C, resulting in the direct acquisition of conductive CNF (CNFene) with a carbon layer following the extraction of CNFs using dilute sulfuric acid. The acid serves as a hydrolysis reagent and initiator for carbonization, facilitating the production of carbonized CNF in a single step. The cellulose carbonization process involves a temperature reduction from 800 °C to 90 °C, resulting in an energy consumption decrease exceeding 80% per gram, while the conductivity of the final samples attained 1.1 S/cm.

Heat spreaders and films made of ultra-thin carbon nanotubes (CNTs) have also shown excellent heat dissipation and a high thermal conductance value (Fu et al., 2012). Researchers created carbon nanotube (CNT) micro-fins on a silicon chip, showing that the on-chip cooling fins and microchannel heat sink interfaced better with the CNTs. With the help of water and a high TC of over 1000 W $(mK)^{-1}$, CNT micro-fins could cool down electronic components by exhibiting a vast heat exchange area and an effective heat flux at 1000 W cm^{-2} scale. The VAF approach is the most common method for fabricating graphene films (100 wt %) (Owais et al., 2021; Xiang & Drzal, 2011). Several fabrication and post-fabrication procedures can affect the TC of rGO thin film sheets. Thermo-conductivity characteristics have been found to depend on regulating factors such as post-synthesis high-temperature annealing. One example is the synthesis and subsequent annealing of freestanding rGO films at temperatures as high as 2000 °C. The TC of rGO paper increased to 218 W $(mK)^{-1}$ as the annealing temperature was raised (Xia et al., 2023). The TC of flexible GNP papers was approximately 313 W $(mK)^{-1}$ (Liu et al., 2024), and that of GO films was approximately 1100 W $(mK)^{-1}$ (Song et al., 2017), compared to other carbonaceous fillers. The earlier method utilized the easy VAF technique followed by annealing, which may explain the significant disparity in results. In contrast, the latter method involved graphitization following the direct evaporation of GO solution under moderate heating, which added a bridging effect.

Wang, Samani, et al. (2018) have accomplished the most significant possible use of graphene's characteristics thus far. By utilizing the dry-bubbling technique, graphitization, and mechanical pressing method, they were able to produce the greatest TC of 3214 W $(mK)^{-1}$, thus maximizing the utilization of graphene's characteristics. Overly high-temperature annealing at 2850 °C resulted in the coalescence of neighboring GO sheets and increased grain size, leading to the fabrication and reduction of the film with an optimized thickness of around 0.8 μm. It was possible to create graphene sheets by reducing GO sheets. In this context, it was listed that when it comes to improving TC, the most critical elements are the average thickness and proper alignment of graphene layers.

In addition, two other study groups found that their graphene films had a TC of 1529 W $(mK)^{-1}$ and 2292 W $(mK)^{-1}$, respectively (Teng et al., 2017; Wang, Yu, et al., 2019). The films' high TC was achieved via a sequential combination of many fabrication procedures (Teng et al., 2017). These techniques included ball milling, sonication, quick vacuum filtering, thermal treatment, and mechanical compression. In contrast, using chemical vapor deposition and heat treatment at extreme temperatures, the researchers meticulously assembled 100 single-layer polycrystalline

graphene films layer by layer (Wang, Cunning, et al., 2019). Noteworthy here is that high-temperature heat treatments of films produced results even better than graphitization, and most researchers who found good TC for 100%wt carbonaceous papers concentrated on these treatments (Owais et al., 2021).

Many vital elements determine the success or failure of attempts to fabricate graphene-based thin films with very high TC. Many factors, including filler concentration, particle size, alignment, mechanical pressing, interfacial phonon scattering, and high-temperature heat treatment, decide the films' ultimate performance. Because there are fewer boundaries for a phonon to travel across in larger particles, the predicted increase in TC for polymer systems is proportional to the square of the particle size, which strongly affects the interfacial thermal resistance (Wang, Ou, et al., 2018). On the other hand, because there is a greater concentration of electrons in a more extensive system, the electrical resistivity is predicted to fall as particle size increases. Graphene nano-sheets that are in-plane aligned considerably improve the phonon-phonon transport chain, but the film's TC degrades due to formation-related wrinkling and misfit of both isolated nano-sheets and nano-sheet layers within the film. Recently, there has been a surge in interest in optimizing the TC characteristics of graphene by aligning it in thin films composed of hybrid graphene/metal composites. One study found that by using the vacuum-assisted flow (VAF) method in conjunction with the spark plasma sintering (SPS) technology, graphene/copper composite films were able to attain a high in-plane TC of 458 W $(mK)^{-1}$ and a low through-plane coefficient of thermal expansion (CTE) of 6.2 ppm K^{-1} (Chu et al., 2018). Thus, carbonaceous fillers like graphene have much promise for use in thermal management in electronics; nevertheless, when called upon, the well-known issue of electrical insulation for such fillers must be carefully considered.

15.3.2.3 Cellulose/Boron Nitride Composites

Because of its remarkable TC, structural stability, mechanical characteristics, and anti-oxidation ability, boron nitride (BN) is a material that is increasingly being studied as a functional filler for polymers. Due to its absence in nature, BN is a synthetically created refractory chemical molecule. As with other isoelectronic carbon structures, it has an equal number of boron (B) and nitrogen (N) atoms (Chari et al., 2023; Li, Yang, Xu, et al., 2018; Wang et al., 2022). There are three crystalline forms of BN: amorphous (a-BN) like amorphous carbon, cubic (c-BN) resembling diamond, and hexagonal (h-BN) resembling graphite. Graphite and h-BN are structurally comparable because they both have hexagonally packed layers of sp2-bonded layers (Zhang et al., 2022). The electron-conducting properties of graphite are due to its valence electrons being set in a conjugated system, whereas the electron-insulating properties of BN are due to the presence of two atoms with significantly different electronegativity values (boron = 2.04, nitrogen = 3.04) (Li, Liu, et al., 2024; Li, Zhang, et al., 2024). Graphite is black, while BN is transparent or white in bulk quantities, reflecting this structural variation in the optical characteristics of 2D

materials (Hattori et al., 2023; Roy et al., 2021). Also, graphite has its layers stacked in a Bernal sequence (AB), whereas BN has its sheets in a "registry," with the atoms of each layer being obscured by those of the higher and lower layers (Guerra et al., 2019).

One example of a nanostructure that can be created from h-BN is BN spherical nanoparticles (BNNP) (Li, Liu, et al., 2024; Li, Zhang, et al., 2024; Yang et al., 2022) or 2D BN nanosheets (BNNS) (Bondarev et al., 2020). Another option is to use air plasma treatment or chemical vapor deposition (CVD) to create BN nanotubes (BNNT) from h-BN (Hassan et al., 2021; Saji, 2023). Composites made of white or transparent polymers that are both highly conductive to heat and electrically insulating can be enhanced with the addition of BN nanostructures as fillers (Liu, Li, & Liu, 2020; Rasul et al., 2021). Adherence to the polymer matrix is more challenging with BNNT than with BNNS due to the high surface tension (26.7 mN/m) and the high interfacial heat resistance (Kang et al., 2023; Niu et al., 2020). Boron nitride nanosheets (BNNSs) have exceptional thermal conductivity but with a drawback, whereas unprocessed hexagonal boron nitride (h-BN) ligands tend to aggregate, reducing their efficiency. Zhang, Zhu, et al. (2024) could overcome this obstacle by involving ball-milling and amino-modifying h-BN before dispersing the BNNSs with carboxylated nanofibrillated cellulose (COOH-CNF). The BNNSs were evenly distributed throughout the CNF matrix via amide bonding, which decreased aggregation and inter-BNNS voids and facilitated the development of efficient thermal channels. The filtered composite film was made with a stably dispersed composite slurry that had a 30% BNNS loading and a TC of 9.00 W $(mK)^{-1}$ (compared to 1.88 W $(mK)^{-1}$for pure CNF). Moreover, the electrical strength was 22.67 kV mm (17.04 kV mm for CNF), and the volume resistivity was 9.38×10^{13} Ω cm, compared to 2.53×10^{13} Ω cm for pure CNF. The results demonstrated that the BNNS-CNF composite film exhibited high TC and outstanding insulating qualities.

The role of insulating paper in the power industry is paramount, influencing safety, equipment longevity, energy efficiency, environmental implications, and various other factors (Geng et al., 2022; Kamata et al., 1991). Nonetheless, as voltage levels increase, the thermal stability and insulation of cellulose insulation paper may become inadequate for high-voltage machinery. In particularly challenging conditions such as elevated humidity, high temperatures, and direct current bias, it is crucial for cellulose insulation paper to sustain its long-term insulation efficiency and thermal stability (Huang et al., 2017). Unfortunately, limited research focuses on improving essential characteristics in insulating paper, such as insulation performance, mechanical performance, and thermal stability (Wang, Cunning, et al., 2019; Wang, Yu, et al., 2019). While chemical modifications and the integration of synthetic fibers may exhibit promise in improving thermal stability, they can concurrently diminish mechanical performance (Fig. 15.3). Recently, according to research by Wei et al. (2024), cellulose-insulating paper with improved mechanical and thermal properties was successfully obtained by working in tandem with binary nano-BN and nano-cellulose.

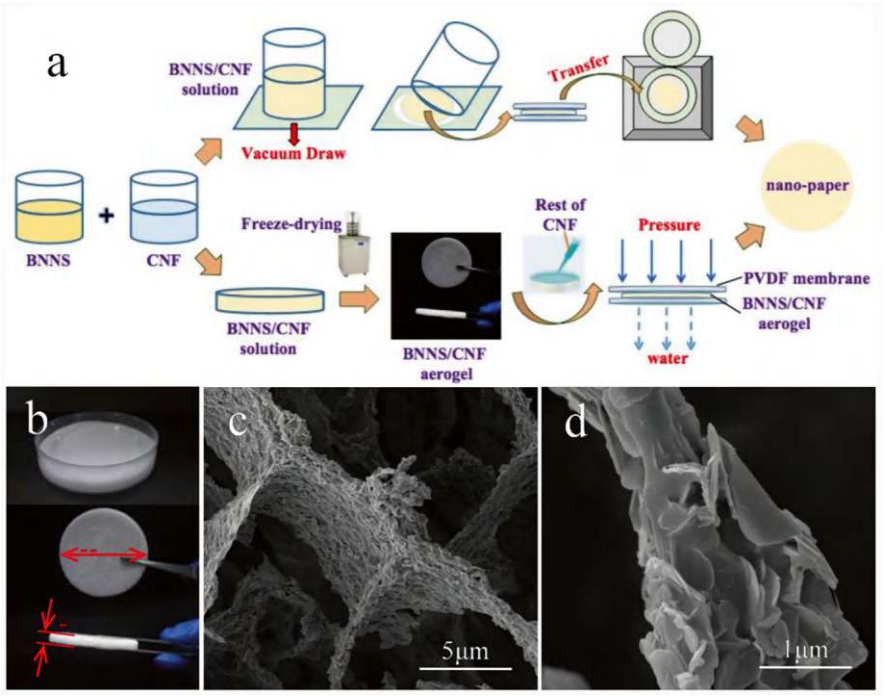

Fig. 15.3 (**a**) Scheme of preparation of BNNS/CNF nano-papers. (**b**) Images of BNNS/CNF mixing solution and aerogel. (**c**, **d**) SEM images under different magnifications of BNNS/CNF aerogel. Reprinted from Wang, Yu, et al. (2019). Published 2019 by MDPI with open access

15.4 Other Types of Thermally Conductive Paper

15.4.1 Graphene Paper

Carbonaceous fillers such as graphite, carbon nanotubes, graphene, graphene oxide, and reduced graphene oxide are well-known for their ability to improve the TC of thin films (Liang, 2024; Song et al., 2014; Wang, Samani, et al., 2018). While graphite and its family exhibit a somewhat strong heat conductivity, their notable electrical conduction poses a significant constraint on their application in industrial electronics. In response to this issue, a group of researchers proposed the concept of carbon papers based on polymers, taking into account the inherent electrical insulating properties of polymers (Li et al., 2017; Song et al., 2017). A recently developed, highly thermally conductive paper was fabricated by Li et al. (2017) using a durable, well-shed layered structure consisting of nano-fibrillated cellulose (NFC) and graphite nano-platelets (GNPs). The VAF approach was employed to self-assemble NFC into an interconnected network with the GNPs, where the platelets exhibited a tendency to align in the plane with respect to the paper. The resultant paper also exhibited remarkable mechanical strength and flexibility by achieving an

exceptional in-plane TC of 59.46 W $(mK)^{-1}$ with a loading concentration of 75 wt % GNPs. Therefore, these composite papers show great potential as substitute interface materials compared to silicone rubber thermal pads, which have substantially lower TC (0.26–4 W $(mK)^{-1}$) (Sim et al., 2005). In a separate investigation, Song's group successfully produced anisotropic thermally conductive films by sequentially assembling graphene oxide (GO) and nano-fibrillated cellulose (NFC) on a flexible NFC substrate (Song et al., 2017). The procedure entailed the chemical reduction and hydrogen bonding interactions, which subsequently led to the development of a hierarchical structure of nanosheets, composed of reduced graphene oxide (rGO). The nanosheets exhibited a significant level of in-plane alignment, increasing the hybrid film's in-plane TC to 12.6 W $(mK)^{-1}$. Furthermore, using the orientation and interface of natural nacre as inspiration, we successfully synthesized mechanically robust hybrid papers of BNNSs and GO via a straightforward VAF technique. The TC of papers was increased to 29.8 W $(mK)^{-1}$ by the synergistic and bridging impact of graphene oxide (GO) in boron nitride nanosheets in the presence of a mere 5 wt.% GO content (Yao et al., 2016).

Heat transport in polymer composite films/paper due to elastic vibration of the crystalline medium solid through the crystal lattice and mostly occurred by the transfer of phonons or phonons/electrons via the fillers in the composite, which are more concentrated than the polymer matrix. Increase heat flux due to increase TC in the filler material increases the thermal diffusivity in the composite system by reduced thermal resistance between the filler and the matrix, and the connecting adjacent pathways between filler and the matrix are created for the rapid transfer of phonons. Thus, the comprehensive TC increases in the system. Hence, therefore depending on the constituents of filler and matrix, scattering of phonons are classified into various types: (1) phonon scattering, (2) phonon-electron scattering, (3) phonon-impurity scattering, and (4) phonon-boundary scattering. So, an increase or reduction in TC of a composite system depends on these intrinsic and extrinsic defects (Owais et al., 2021). To understand the heat conduction mechanism in polymer composite paper-like material; a mixture reduced graphene oxide (RGO)/graphene oxide (GO) with nano-fibrillated cellulose (NFC) papery film has prepared. RGO nano-sheets were imbedded through a layered structured in the NFC polymer matrix (see Fig. 15.4). This hybrid structured showed an anisotropic high in-plane and out-of-plane thermal conductivities. With these sheets of RGO and GO, a structure was fabricated with various connecting pathways, where the heat conduction is increased and the thermal resistance is decreased to an extent (Song et al., 2016). In-plane TC was relatively high in compare to the out-of-plane TC due to presence of low TC NFC (0.034 W (mK^{-1})), restricted the thermal transport in the out-plane direction. Thus, the characteristics related to the dissipation of heat energy in thermal interface materials require a high TC in both directions.

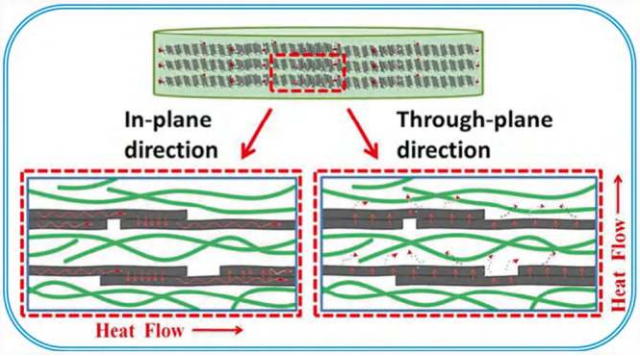

Fig. 15.4 The mechanism of the heat flow of graphene oxide (RGO)/graphene oxide (GO) (NFC) papery film along the in-plane and out-of-plane directions. Reprinted with permission from Song et al. (2016). Copyright 2016: RSC

15.4.2 Polymer-Based Composites

The conjugation of main electrons in the main chain of molecules makes conductive polymers electrically conductive themselves or doped with other materials that are also electrically conductive. Conductive polymers such as polyacetylene (PA), polythiophene (PT), polyaniline (PANI), polypyrrole (PPy), and poly (3,4-ethylenedioxythiophene) (PEDOT) added to cellulose to form flexible composite in form hydrogel, film and fibers. As well nanoparticles and elastomeric polymers can be used as the supporting substrate and to bridge the gaps and discontinuous regions of the cellulose/conducting polymer composite. Han et al. (2019) labeled a cellulose nanocrystal/carbon nanotube/polyvinyl alcohol CNC-CNT/PVA with polyacrylic acid (PAA) composite fibrous membrane using a classical spinning technique, and then polyaniline PANI was in situ synthesized on this membrane to obtain a composite conductive membrane. The in situ-grown PANI was spread out to form a shell on the surface of the fibers, and the whole membrane exhibited a large porosity and high specific surface area with good tensile strength. Chen et al. (2023) reported polydimethylsiloxanes (PDMS)-loaded CNF/MXene self-adhesive material using silicone foaming. The prepared PDMS composite CNF/MXene conductive foams have tunable electrical conductivity (10–8–10 S/m) and superhydrophobicity, stable compression cycling, and excellent flame retardancy due to presence of considerable oxygen groups in CNF and MXene that allows them to be impregnated into porous PDMS foams (Chen et al., 2023; Fei et al., 2020; Han et al., 2019; Wang et al., 2023). Many challenges arise with directly printing conductive inks containing nanoparticles onto paper substrates. For example, the nanoparticles tend to enter the paper's pores and partially segment, and the required low-temperature sintering process damages the paper's dimensional stability. Wu et al. (2014) prototyped the printed thermoplastic electrically conductive adhesives (ECA) and paper-based circuit substrate that took advantage of paper's capillarity to

significantly enhance the printed circuits' conductivity and mechanical robustness—all without resorting to the sintering process. The capillary force-assisted development of condensed conductive tracks of ECAs is schematically illustrated in Fig. 15.5.

15.4.3 Ceramic Fillers

In order to tackle the issue of low TC in polymer matrices, various strategies have been explored. These include incorporating high-TC liquid crystal groups or fillers into the polymer matrix, innovative design of three-dimensional thermal conductive networks, and optimizing the interface between fillers and the matrix. Among the various methodologies, the incorporation of high thermally conductive fillers to enhance the TC of the polymer matrix stands out as the most promising strategy for large-scale industrial production. Due to their exceptional electrical insulation and TC properties, ceramic-based thermal conductive materials have emerged as a prominent area of interest among researchers, positioning them as excellent candidates for electronic cooling substrates (Song et al., 2024). Furthermore, in contrast to conductive fillers like metals or carbon materials, polymer composites incorporating thermally conductive ceramic fillers such as alumina (Al_2O_3) (Sharma et al., 2024), aluminum nitride (AlN) (Yang et al., 2024), boron nitride (BN) (Wu et al., 2024), magnesium oxide (MgO) (Jung et al., 2024), silicon carbide (SiC) (Rout et al., 2024), and silicon nitride (Si_3N_4) (Prakash & Gnanavel, 2024) exhibit

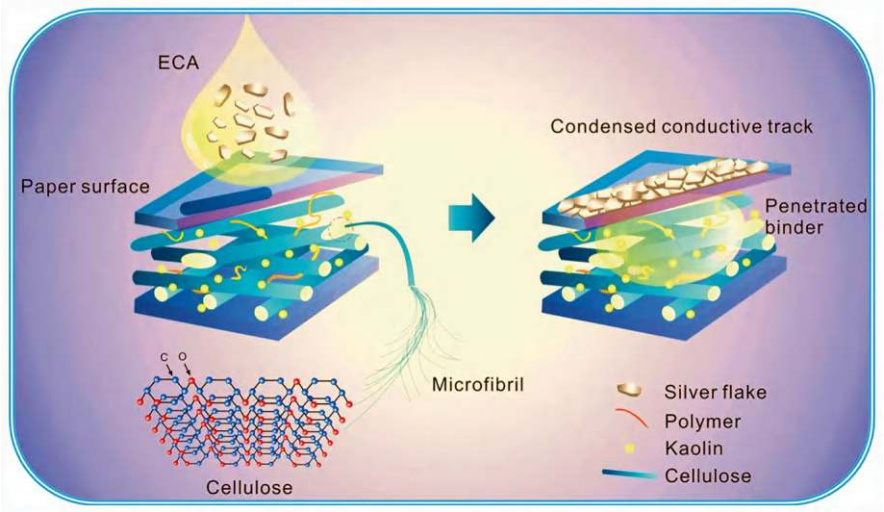

Fig. 15.5 A schematic illustration of capillary force-assisted formation of condensed conductive track of electrically conductive adhesives (ECAs). Reprinted from Wu et al. (2014). Published 2014 by Nature with open access

superior electrical insulating properties, making them more appropriate for high-voltage power equipment (Nie et al., 2020).

Generally, the enhancement of TC in composite materials is achieved through the incorporation of high TC fillers, albeit this often results in a compromise regarding the mechanical strength of the composite. This material encounters significant challenges in light of its thermal and mechanical properties. Consequently, numerous efforts have been made to address this issue; for example, Yang et al. (2024) used freeze casting and vacuum infiltration techniques to create a 3D-epoxy composite with CNF and two different diameters of AlN, which shows promise as a material for effective thermal management in a range of electronic devices. The 3D composite containing 7 wt% CNF content demonstrated enhanced thermal and mechanical conductivity attributable to various factors. The interaction of hydrogen bonding between the matrix and the filler, facilitated by the esterification of the filler, significantly improves compatibility and interfacial adhesion. The 3D CNF foam, featuring two distinct diameters of AlN achieved through freeze casting, established a continuous thermal pathway within the composite. The appropriate composition of the CNF for structural support and the ratio of AlN@CNF to AlN facilitated uniform dispersion within the matrix and reduced phonon scattering.

15.5 Application of Thermoconductive Papers

Thermally conductive papers have a range of applications due to their ability to efficiently transfer heat. The following are some key applications.

15.5.1 Flexible Electronics

One way to manage heat dissipation in flexible electronics is to employ thermally conductive papers. The papers are built from high-performance cellulose paper with excellent transparency, conductivity, and pliability. This aids in keeping components like folding cellphones, wearable electronics, and flexible screens functioning well and lasting a long time. Supercapacitors, solar cells, electromagnetic shielding appliances, sensors, chemical electrodes, actuators, antennas, and transistors are a few examples of high-value electronic devices that might be made using the prepared cellulose paper. In this regard, Liu, Xiao, et al. (2020) deposited TiO_2 on cellulose using a magnetron sputtering procedure to create a flexible, transparent cellulose paper that can serve as an electrode in a dye-sensitized solar cell.

Liang et al. (2022) developed high-performance electromagnetic shielding materials based on MOF-derived CoNi@C-silver nanowires/CNF composite in their study. These materials are ideal for aerospace, communication, artificial intelligence, and wearable electronics due to their exceptional thermal management capabilities and high flexibility.

15.5.2 Thermal Management in Batteries

Thermally conductive papers are useful for controlling the temperature of battery packs, an important consideration in many modern electric vehicles and portable gadgets. By keeping the batteries within safe operating temperatures, they prolong their life and efficiency.

The one-dimensional structure of anhydroglucose units in cellulose is organized to create a chain with a certain amount of oxygen-containing polar function groups, such as OH. They can stabilize the cycling performance of Li batteries, make modifications that make them more sustainable, and aid in the transfer of lithium ions. Composites with improved mechanical, thermal, optical, and barrier properties can be created by doping cellulose with fillers, which changes the electron configuration of the molecule. Electrode, separator, and electrolyte are the three main components of a battery. Cellulose conductive materials (CCMs) can be utilized for all three components because they decompose rapidly in the environment without chemical treatment (Deng et al., 2022; Wang et al., 2020). Yang et al. (2021) prepared high-performance cellulose-based solid polymer ionic conductors with molecular channel engineering and used them in a solid electrolyte/diaphragm for Li-ion batteries. These batteries are flexible, low-cost, and extensible. Cu^{2+} has inserted into the CNF structure, expanded the spacing of the polymer, and allowed for rapid Li^{+} doping and transport across the gaps. This composite Li-Cu-CNF has a high ionic conductivity of 1.5×10^{-3} S/cm and a transfer number up to 0.78 for Li^{+}. It also has a wide voltage window of 0–4.5 V.

15.5.3 Heat Sinks and Thermal Interface Materials

Thermally conductive papers can be used as heat sinks or thermal interface materials (TIMs) in electronic devices. They help in transferring heat away from critical components, preventing overheating and improving device reliability. This idea is based on flexible films with high in-plane κ used as heat spreaders, which can cool local hot spots via transferring heat through the basal plane of the films. In plane κ can be noticed most of the heat specially scatter from the hot resource along in-plane direction without affecting the neighboring devices. In many industrial fields, copper and aluminum films have been used as heater spreaders, but high density and easy corrosion make them unfavorable. Graphite-based film as a heat spreaders high in-plane with low density and low cost are a promising thermal solution for hot elimination on enclosure surfaces of electronics (Tao & He, 2018; Zhao et al., 2021). RGO films have higher κ than that of graphite films, thus, RGO heat spreaders show higher heat scattering ability, and commercial RGO films have been used as flexible heat spreaders in the smartphone of "Mate 20" (Fu et al., 2019). Feng et al. (2022) used phenylphosphonic acid@GNPs/PVA film as flexible heater spreader to cool smartphone without using the heater spreader, where the backside

temperature of the smartphone increased from 29.2 to 39.9 °C after game program for 5 min. After using thermally conductive as-fabricated films and commercial tinfoil, the temperature of the smartphone was reduced to 36.9 and 38.4 °C, respectively.

15.5.4 Packaging Materials

Thermally conductive sheets are a great way to keep products sensitive to temperature safe in packaging. The pharmaceutical, electronic, and food industries, where precise temperature control during shipping is of the utmost importance, find this feature very helpful (Abhang et al., 2024; Jin & Lu, 2024; Ma et al., 2024). Increasing the TC of antimicrobial packaging materials is crucial to transferring the respiratory heat produced by fruits and vegetables during the cold chain process to improve cooling efficiency and decrease postharvest losses. An attractive, environmentally conscious food packaging nanofibrous mat composed of boron nitride, polycaprolactone (PCL), and chitosan (CS) was quickly created using solution blow spinning (SBS) in the study by Shen et al. (2022). After 40 s of heating, the developed BNNS/PCL/CS mats exhibited in-plane and cross-plane thermal conductivities of 1.403 and 0.826 W $(mK)^{-1}$, respectively. These values were 2.4 and 1.4 times higher than the control group, indicating that the mats responded quickly to heat. Incorporating BNNSs into the created mats increased their thermal stability and water vapor barrier capability while reducing the average nanofiber diameter from 385.6 nm to 221.0 nm. Additionally, the created mats had hydrophobic surfaces and showed promising antibacterial action in laboratory tests. Research and advancements in thermal management are best accomplished using joints that use thermally conductive adhesive (TCA). The fast development of microelectronic technology has led to the widespread use of epoxy adhesive in electronic packaging (Wen et al., 2022). The work conducted by Yang et al. (2020) demonstrated the successful creation of an exceptional heat interface (a 94.4% decrease in interfacial heat resistance) with the substitution of an environmentally friendly polydopamine (PDA) during the metallization process for the reducing agent. PDA-nanodiamonds (NDs)-Ag NP composites with ternary heterostructures disseminate low interfacial thermal resistance in CNF, which enables these materials to have strong TC and electric insulation properties. The lower interfacial thermal resistance of CNF/Ag-PDA-ND (4.11×10^{-7} m^2 K W^{-1}) compared to CNF/Ag-ND (7.28×10^{-6} m^2 K W^{-1}) and CNF/ND (5.14×10^{-5} m^2 K W^{-1}), primarily because of the increased contact area between NDs that PDA-Ag and the bridging effect of AgNPs between NDs and CNFs. Composite paper made of CNF/Ag-PDA-ND has an in-plane TC of up to 16.36 W $(mK)^{-1}$, an increase of approximately 1202% over pure CNF, thanks to these ternary heterostructures. Aside from being very strong and durable, the flexible CNF/Ag-PDA-ND composite papers are also quite flexible. Thus, interfacial engineering may be applied to various materials, including carbon, polymers, metallic oxides, and more, paving the way for innovative,

environmentally friendly, high-performance transmetal metamorphic materials (TMMs) for smart, high-power electronics.

15.5.5 Printed Electronic Circuits (PECs)

Printed circuit boards (PCBs) with excellent TC, minimal high-frequency transmission loss, electrical insulation, and ideal mechanical flexibility are in great demand due to the proliferation of wearable and portable electronic devices. Thermally conductive papers can be integrated into PCBs to enhance heat dissipation. This is important for high-power electronic applications where efficient thermal management is necessary to prevent damage to components (Wang, Ou, et al., 2018). The printed electronics industry is showing much interest in paper due to its potential to produce inexpensive, biodegradable, lightweight, flexible, foldable, and low-voltage/frequency electronics (Sudheshwar et al., 2023). However, the circuit design cannot be printed directly onto paper using Ag-ink because of the high surface roughness, porosity, and wettability of the latter. The resultant circuit would exhibit subpar performance and have a limited lifespan (Wiklund et al., 2021). Therefore, it is appropriate to improve the paper's qualities and prepare it for printing the circuit design with Ag-ink by coating or laminating its surface (e.g., with CNC) (Sudheshwar et al., 2023). Compared to PECs, PCBs' utility and performance are important beyond sustainability. PECs have a higher resistivity than PCBs; hence, they may not be suitable for all applications. Because printed electronics technology is still in its early stages, it is also not possible to implement complicated multilayer circuit designs. The rapid breakdown of PEC's conductive tracks means a shorter operating life than conventional PCBs. However, the limited lifespan will not encourage frequent maintenance (Keskinen, 2012; Kunnari et al., 2009). Repairs and replacements are difficult because electronic components (microchips, batteries, displays, etc.) are mounted on the printed electronic substrate using a conductive adhesive (Ag-based). This adhesive effectively glues the components into place, making it impossible to gently remove them for replacement without risking circuit damage.

Nonetheless, printed electronics technology remains in its infancy and is anticipated to advance with time (Glogic et al., 2021). Additionally, specific low-voltage and low-frequency applications are manufactured in significant quantities yet possess brief lifespans and necessitate uncomplicated single-layer circuits; in these instances, PCBs will not be sustainable (Keskinen, 2012; Kunnari et al., 2009; Liu et al., 2014). In these particular applications, fire hazards would be minimal, and the "flame retardant-free" printed electronics might be regarded as technically feasible, secure, and sustainable substitutes for traditional PCBs. Figure 15.6 illustrates the practical use of the technique developed by Wu et al. (2014) who conducted a series of experiments to assess the prototypes' efficacy. Three prototypes comprised a light-emitting diode (LED) signaling device, a capacitive touchpad, and an ultra-high-frequency radio frequency identification (UHF-RFID) antenna. All were fabricated using screen-printed ECAs (50 wt% silver) on paper.

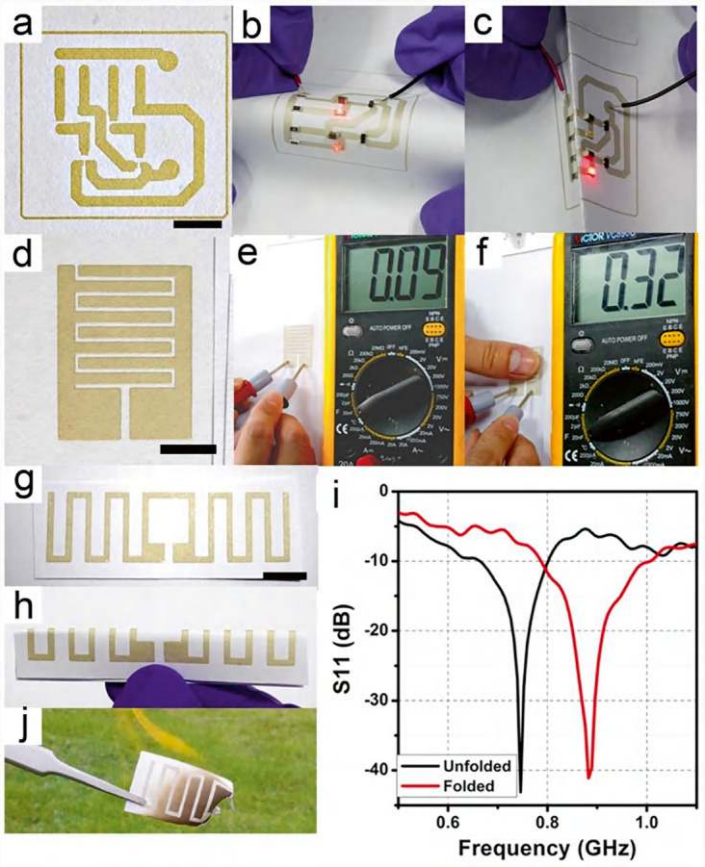

Fig. 15.6 (**a**) A prototype of the paper-based PCB for preparing an LED array winking circuit. (**b**) Working circuit with the placement of the necessary electronic components on the PCB. (**c**) Working circuit is being folded. (**d**) A prototype of paper-based capacitor. (**e**) The capacitance of this capacitor without finger-touch. (**f**) The capacitance of this capacitor under finger-touch. (**g**) The prototype of paper-based antenna. (**h**) The antenna in folding circumstance. (**i**) Operating frequency of the antenna measured in unfolded and folded circumstance. (**j**) Optical photograph of a piece of burning printed devices. The scale bars in the figures are 1 cm. Reprinted from Wu et al. (2014). Published 2014 by Nature with open access

15.5.6 Supercapacitors

Energy devices with high power density and good cycling stability, the charge are stored on the surface of the electrode, thus, the performance of electrode has an important role in supercapacitors. While binders in conventional electrodes affect the storage of charge or electrochemical substances, the high specific surface area and abundant chemical sites of sustainable cellulose can bind with electrochemically active substances to improve the performance of supercapacitors. Additional,

cellulose due to porous structure can provide high-speed channels for the diffusion of ions and charges with flexibility and excellent mechanical properties to supercapacitors (Bai et al., 2020; Chen et al., 2019; Meng et al., 2020).

Zhou et al. (2019) prepared conductive composite electrodes, metal–organic framework based on cellulose (c-MOF)/CNF for flexible supercapacitors. Combining the high specific surface area of conductive properties of c-MOF, and the self-crosslinking properties of CNF fabricated paper-like electrodes, that have an electrical conductivity up to 100 S/m, graded pores, with excellent mechanical properties. The capacitance retention of the fabricated supercapacitor was >99% after 10,000 cycles. Li et al. (2021) prepared an all-solid-state supercapacitor by RGO-encapsulated polyester fibers and loaded with PANI as flexible electrodes and BC-reinforced polyacrylamide as hydrogel electrolyte, the textile structure of the flexible electrode was deformable, and the BC-based electrolyte achieved an ionic conductivity of 125 mS/cm. The all-solid-state supercapacitor had a tensile strength of 330 kPa, an elastic tensile ratio of ~1300%, and a high area capacitance of 564 mF/cm^2, which can power a variety of small electronic devices.

15.5.7 Smart Textiles

In smart textiles, thermally conductive papers can be used to create fabrics that can manage heat effectively. This is useful in clothing designed for extreme temperatures, providing comfort and protection to the wearer. When the temperature of the human body is in the range of 23–26 °C and the humidity is in the range of 30–55%, they feel comfortable. Flexible thermally conductive films have excellent heat dissipation and can be used in personal thermal management to adjust the temperature and humidity of the body. The textiles with high κ and good cooling effect can provide thermal comfort in hot weather via heat exchange between the human body and the environment. Many efforts have been made to develop thermal regulation textiles with high in-plane κ, such as graphene-coated polyester textiles, CNT-coated cotton textiles (Mercado et al., 2021; Vu et al., 2020). Gao et al. (2017) fabricated a BNNS/PVA textile with a high in-plane κ for personal thermal cooling, and the textile fabricated by 3D printing can remove the body heat from the skin to the outside, 55% enhancement in personal cooling efficiency compared to commercial cotton textiles.

15.5.8 Energy Harvesting

Thermally conductive papers can be used in thermoelectric devices that convert heat into electrical energy. This application is particularly relevant for waste heat recovery systems, where excess heat from industrial processes can be converted into usable energy.

The production of flexible TC films with high in-plane became the research frontier, while the commercial applications of these films are still at the beginning of development. These films are suitable for applications such as flexible heat spreaders, energy storage devices, and electrocaloric cooling devices (Feng et al., 2022). Due to energy shortage resources, researchers now hotly sought to improve and develop new energy device systems that are fixable, stretchable, and wearable. CCMs play an important role in energy devices due to their unique pore size, network structure, and rich surface chemistry, where oxygen-containing groups on the surface of the fiber are considered as good moisturizing agent in the electrolyte solution with electrostatic reputation to prevent aggregation of the electrode material (Liu et al., 2021; Xu et al., 2021).

These applications highlight the versatility and importance of thermally conductive papers in various industries, from electronics to packaging and beyond.

15.6 Summary

Cellulose possesses distinct benefits over synthetic polymers, including relatively high thermal stability, low coefficients of thermal expansion, and considerable design flexibility, leading to its increasing appeal in flexible electronic systems. The cellulose polymer is anticipated to serve as a thermal management substrate for the forthcoming generation of flexible electronic products, addressing the issue of heat accumulation in these devices. Various methods exist to modify the structure of cellulose-based thermally conductive paper. These techniques aim to enhance the thermal conductivity of cellulose-based paper by refining its structure, rendering the material more appropriate for thermal management, flexible electronics, and various high-tech sectors. The thermal conductivity of a material is augmented as its fibers are larger; this increases the number of contact sites and pathways for heat transfer. The alignment of the fibers significantly influences thermal conductivity. Fibers aligned parallel to the heat flow direction enhance thermal conductivity by creating more direct pathways for heat transfer. Furthermore, the densification of cellulose fibers and the reduction of air gaps between them can be achieved by exerting pressure during the paper-making process. Consequently, the thermal conductivity of the paper is enhanced, and the interfacial area among the fibers is augmented.

Another method to enhance the paper's thermal conductivity is synthesizing cellulose composites with additional thermal conductivity elements, including metal/metal oxides, carbon-based substances, and boron nitride. TC cellulose-based paper is increasingly utilized in high-tech industries due to its biodegradability, flexibility, and lightweight properties. Nevertheless, novel obstacles have emerged for cellulose-based thermally conductive paper. The subsequent recommendations aim to broaden the utilization of these composites: Minimizing the quantity of thermally conductive filler in the composite material while enhancing its mechanical strength to achieve optimal thermal conductivity; devising an efficient three-dimensional

structure of the composite material to diminish the thermal resistance at the interface between the filler and the substrate, thereby establishing an effective heat conduction pathway; and reducing the spacing between fillers to ensure tight connections and lower the interface thermal resistance among the fillers. These factors influence the thermal conductivity of cellulose-based TC paper and are challenges that must be addressed. The effective design of the spatial configuration of thermally conductive fillers inside the cellulose matrix to optimize the heat conduction pathway represents the future trajectory for advancing flexible, high thermal conductivity materials.

References

Abhang, L. B., Subramanian, T., Nagabhooshanam, N., Sharma, K., Rao, P. V., Devi, K. M., & LakshmiLavanya, A. (2024). Biosynthesize of ZnO nanoparticle from orange fruit peel biomass and its PVA-based composite packaging material: A greener material for suitable packaging. *Biomass Conversion and Biorefinery*. https://doi.org/10.1007/s13399-024-06050-x

Adachi, K., Daicho, K., Furuta, M., Shiga, T., Saito, T., & Kodama, T. (2021). Thermal conduction through individual cellulose nanofibers. *Applied Physics Letters, 118*(5), 53701. https://doi.org/10.1063/5.0042463

Almadhoun, M. N., Bhansali, U. S., & Alshareef, H. N. (2012). Nanocomposites of ferroelectric polymers with surface-hydroxylated $BaTiO_3$ nanoparticles for energy storage applications. *Journal of Materials Chemistry, 22*(22), 11196–11200. https://doi.org/10.1039/C2JM30542A

Antlauf, M., & Andersson, O. (2022). Thermal conductivity of porous and dense networks of cellulose nanocrystals. *Macromolecules, 55*(13), 5326–5331. https://doi.org/10.1021/acs.macromol.2c00153

Antlauf, M., Boulanger, N., Berglund, L., Oksman, K., & Andersson, O. (2021). Thermal conductivity of cellulose fibers in different size scales and densities. *Biomacromolecules, 22*(9), 3800–3809. https://doi.org/10.1021/acs.biomac.1c00643

Bai, Q., Shen, Y., Asoh, T.-A., Li, C., Dan, Y., & Uyama, H. (2020). Controlled preparation of interconnected 3D hierarchical porous carbons from bacterial cellulose-based composite monoliths for supercapacitors. *Nanoscale, 12*(28), 15261–15274. https://doi.org/10.1039/D0NR03591B

Bondarev, A. V., Fraile, A., Polcar, T., & Shtansky, D. V. (2020). Mechanisms of friction and wear reduction by h-BN nanosheet and spherical W nanoparticle additives to base oil: Experimental study and molecular dynamics simulation. *Tribology International, 151*, 106493. https://doi.org/10.1016/j.triboint.2020.106493

Cao, T., Shi, X.-L., Zou, J., & Chen, Z.-G. (2021). Advances in conducting polymer-based thermoelectric materials and devices. *Microstructures, 1*(1), 2021007. https://doi.org/10.20517/microstructures.2021.06

Chari, C. S., McEnerney, B. W., Hofer, R. R., Wollmershauser, J. A., Gorzkowski, E. P., & Faber, K. T. (2023). High-temperature carbothermal synthesis and characterization of graphite/h-BN bimaterials. *Journal of the American Ceramic Society, 106*(4), 2225–2239. https://doi.org/10.1111/jace.18927

Chen, C., Song, J., Zhu, S., Li, Y., Kuang, Y., Wan, J., et al. (2018). Scalable and sustainable approach toward highly compressible, anisotropic, lamellar carbon sponge. *Chem, 4*(3), 544–554. https://doi.org/10.1016/j.chempr.2017.12.028

Chen, H.-Y., Chen, Z.-Y., Mao, M., Wu, Y.-Y., Yang, F., Gong, L.-X., et al. (2023). Self-adhesive polydimethylsiloxane foam materials decorated with MXene/cellulose nanofiber interconnected network for versatile functionalities. *Advanced Functional Materials, 33*(48), 2304927. https://doi.org/10.1002/adfm.202304927

Chen, L.-M., Yu, H.-Y., Wang, D.-C., Yang, T., Yao, J.-M., & Tam, K. C. (2019). Simple synthesis of flower-like manganese dioxide nanostructures on cellulose nanocrystals for high-performance supercapacitors and wearable electrodes. *ACS Sustainable Chemistry & Engineering, 7*(13), 11823–11831. https://doi.org/10.1021/acssuschemeng.9b02287

Chen, S., Chen, Y., Li, D., Xu, Y., & Xu, F. (2021). Flexible and sensitivity-adjustable pressure sensors based on carbonized bacterial nanocellulose/wood-derived cellulose nanofibril composite aerogels. *ACS Applied Materials & Interfaces, 13*(7), 8754–8763. https://doi.org/10.1021/acsami.0c21392

Chu, K., Wang, X., Li, Y., Huang, D., Geng, Z., Zhao, X., Liu, H., & Zhang, H. (2018). Thermal properties of graphene/metal composites with aligned graphene. *Materials & Design, 140*, 85–94. https://doi.org/10.1016/j.matdes.2017.11.048

Dacrory, S., Hammad, A. B. A., Nahrawy, A. M., Abou-Yousef, H., & Kamel, S. (2021). Cyanoethyl cellulose/$BaTiO_3$/GO flexible films with electroconductive properties. *ECS Journal of Solid State Science and Technology, 10*(8), 83004. https://doi.org/10.1149/2162-8777/ac1c56

Dacrory, S., Kamal, K. H., & Kamel, S. (2022). EDTA-functionalized magnetic graphene oxide/polyacrylamide grafted carboxymethyl cellulose hydrogel for removal of Pb^{+2} from aqueous solution. *Journal of Polymers and the Environment, 30*(5), 1833–1846. https://doi.org/10.1007/s10924-021-02310-3

Dang, Z.-M., Yuan, J.-K., Zha, J.-W., Zhou, T., Li, S.-T., & Hu, G.-H. (2012). Fundamentals, processes and applications of high-permittivity polymer–matrix composites. *Progress in Materials Science, 57*(4), 660–723. https://doi.org/10.1016/j.pmatsci.2011.08.001

Deng, J., Cao, D., Yang, X., & Zhang, G. (2022). Cross-linked cellulose/carboxylated polyimide nanofiber separator for lithium-ion battery application. *Chemical Engineering Journal, 433*, 133934. https://doi.org/10.1016/j.cej.2021.133934

Diaz, J. A., Ye, Z., Wu, X., Moore, A. L., Moon, R. J., Martini, A., Boday, D. J., & Youngblood, J. P. (2014). Thermal conductivity in nanostructured films: From single cellulose nanocrystals to bulk films. *Biomacromolecules, 15*(11), 4096–4101. https://doi.org/10.1021/bm501131a

Dong, Z., Liu, H., Yang, X., Fan, J., Bi, H., Wang, C., Zhang, Y., Luo, C., Chen, X., & Wu, X. (2021). Facile fabrication of paper-based flexible thermoelectric generator. *npj Flexible Electronics, 5*(1), 6. https://doi.org/10.1038/s41528-021-00103-1

Elsayed, G. H., Dacrory, S., & Fahim, A. M. (2022). Anti-proliferative action, molecular investigation and computational studies of novel fused heterocyclic cellulosic compounds on human cancer cells. *International Journal of Biological Macromolecules, 222*, 3077–3099. https://doi.org/10.1016/j.ijbiomac.2022.10.083

Fei, Y., Liang, M., Yan, L., Chen, Y., & Zou, H. (2020). Co/C@cellulose nanofiber aerogel derived from metal-organic frameworks for highly efficient electromagnetic interference shielding. *Chemical Engineering Journal, 392*, 124815. https://doi.org/10.1016/j.cej.2020.124815

Feng, C.-P., Wei, F., Sun, K.-Y., Wang, Y., Lan, H.-B., Shang, H.-J., et al. (2022). Emerging flexible thermally conductive films: Mechanism, fabrication, application. *Nano-Micro Letters, 14*(1), 127. https://doi.org/10.1007/s40820-022-00868-8

Flity, H., Jannot, Y., Terrei, L., Lardet, P., Schick, V., Acem, Z., & Parent, G. (2024). Thermal conductivity parallel and perpendicular to fibers direction and heat capacity measurements of eight wood species up to 160 °C. *International Journal of Thermal Sciences, 195*, 108661. https://doi.org/10.1016/j.ijthermalsci.2023.108661

Fu, Y., Hansson, J., Liu, Y., Chen, S., Zehri, A., Samani, M. K., et al. (2019). Graphene related materials for thermal management. *2D Materials, 7*(1), 12001. https://doi.org/10.1088/2053-1583/ab48d9

Fu, Y., Nabiollahi, N., Wang, T., Wang, S., Hu, Z., Carlberg, B., Zhang, Y., Wang, X., & Liu, J. (2012). A complete carbon-nanotube-based on-chip cooling solution with very high heat dissipation capacity. *Nanotechnology, 23*(4), 45304. https://doi.org/10.1088/0957-4484/23/4/045304

Gao, T., Yang, Z., Chen, C., Li, Y., Fu, K., Dai, J., et al. (2017). Three-dimensional printed thermal regulation textiles. *ACS Nano, 11*(11), 11513–11520. https://doi.org/10.1021/acsnano.7b06295

Geng, C., Liu, J., Zhang, H., Liu, C., Luo, Y., & Zhang, Y. (2022). Diffusion mechanism of furfural in transformer oil–paper insulation under moisture effect. *IEEE Transactions on Dielectrics and Electrical Insulation, 29*(2), 485–492. https://doi.org/10.1109/TDEI.2022.3157883

Glogic, E., Futsch, R., Thenot, V., Iglesias, A., Joyard-Pitiot, B., Depres, G., et al. (2021). Development of eco-efficient smart electronics for anticounterfeiting and shock detection based on printable inks. *ACS Sustainable Chemistry & Engineering, 9*(35), 11691–11704. https://doi.org/10.1021/acssuschemeng.1c02348

Guerra, V., Wan, C., & McNally, T. (2019). Thermal conductivity of 2D nano-structured boron nitride (BN) and its composites with polymers. *Progress in Materials Science, 100*, 170–186. https://doi.org/10.1016/j.pmatsci.2018.10.002

Han, J., Wang, S., Zhu, S., Huang, C., Yue, Y., Mei, C., Xu, X., & Xia, C. (2019). Electrospun core–shell nanofibrous membranes with nanocellulose-stabilized carbon nanotubes for use as high-performance flexible supercapacitor electrodes with enhanced water resistance, thermal stability, and mechanical toughness. *ACS Applied Materials & Interfaces, 11*(47), 44624–44635. https://doi.org/10.1021/acsami.9b16458

Han, X., Wang, T., Owuor, P. S., Hwang, S. H., Wang, C., Sha, J., et al. (2018). Ultra-stiff graphene foams as three-dimensional conductive fillers for epoxy resin. *ACS Nano, 12*(11), 11219–11228. https://doi.org/10.1021/acsnano.8b05822

Hasanin, M., Abdelhameed, R. M., Dacrory, S., Abou-Yousef, H., & Kamel, S. (2021). Photocatalytic degradation of pesticide intermediate using green eco-friendly amino functionalized cellulose nanocomposites. *Materials Science and Engineering B, 270*, 115231. https://doi.org/10.1016/j.mseb.2021.115231

Hassan, J., Naz, S., Haider, A., Raza, A., Ul-Hamid, A., Qumar, U., et al. (2021). H-BN nanosheets doped with transition metals for environmental remediation; a DFT approach and molecular docking analysis. *Materials Science and Engineering B, 272*, 115365. https://doi.org/10.1016/j.mseb.2021.115365

Hattori, Y., Taniguchi, T., Watanabe, K., & Kitamura, M. (2023). Identification of the monolayer thickness difference in a mechanically exfoliated thick flake of hexagonal boron nitride and graphite for van der Waals heterostructures. *Nanotechnology, 34*(29), 295701. https://doi.org/10.1088/1361-6528/accf23

Horikawa, Y., Shimizu, M., Saito, T., Isogai, A., Imai, T., & Sugiyama, J. (2018). Influence of drying of chara cellulose on length/length distribution of microfibrils after acid hydrolysis. *International Journal of Biological Macromolecules, 109*, 569–575. https://doi.org/10.1016/j.ijbiomac.2017.12.051

Hu, Z., Wang, S., Chen, G., Zhang, Q., Wu, K., Shi, J., Liang, L., & Lu, M. (2018). An aqueous-only, green route to exfoliate boron nitride for preparation of high thermal conductive boron nitride nanosheet/cellulose nanofiber flexible film. *Composites Science and Technology, 168*, 287–295. https://doi.org/10.1016/j.compscitech.2018.09.020

Huang, J., Zhou, Y., Dong, L., Zhou, Z., & Liu, R. (2017). Enhancement of mechanical and electrical performances of insulating presspaper by introduction of nanocellulose. *Composites Science and Technology, 138*, 40–48. https://doi.org/10.1016/j.compscitech.2016.11.020

Hutchinson, J. M., & Moradi, S. (2020). Thermal conductivity and cure kinetics of epoxy-boron nitride composites—A review. *Maternité, 13*(16), 3634. https://doi.org/10.3390/ma13163634

Jia, C., Shao, Z., & Wang, J. (2015). Preparation and dielectric property of cyanoethyl cellulose/$BaTiO_3$ flexible nanocomposite films. *RSC Advances, 5*, 15283–15291. https://doi.org/10.1039/C4RA13960G

Jin, Y., & Lu, Z. (2024). Preparation of carrageenan/konjac glucomannan/graphene oxide nanocomposite films with high mechanical and antistatic properties for food packaging. *Polymer Bulletin, 81*(2), 1373–1388. https://doi.org/10.1007/s00289-023-04784-8

Jung, H., Han, J.-H., & Jung, I.-C. (2024). Fabrication of silicone-based gap filler for electric vehicles using magnesium oxide thermally conductive fillers. *Journal of the Korean Ceramic Society, 61*, 713–721. https://doi.org/10.1007/s43207-024-00403-y

Kamata, Y., Ohe, E., Endoh, K., Furukawa, S., Tsukioka, H., Maejima, M., et al. (1991). Development of low-permittivity pressboard and its evaluation for insulation of oil-immersed

EHV power transformers. *IEEE Transactions on Electrical Insulation, 26*(4), 819–825. https://doi.org/10.1109/14.83708

Kang, M., Kim, J., Lim, H., Ko, J., Kim, H.-S., Joo, Y., et al. (2023). Eco-friendly dispersant-free purification method of boron nitride nanotubes through controlling surface tension and steric repulsion with solvents. *Nanomaterials, 13*(18), 2593. https://doi.org/10.3390/nano13182593

Keskinen, M. (2012). End-of-life options for printed electronics. In V. Goodship & A. Stevels (Eds.), *Waste electrical and electronic equipment (WEEE) handbook* (pp. 352–364). Elsevier. https://doi.org/10.1533/9780857096333.3.352

Kubiak, J. M., Li, B., Suazo, M., & Macfarlane, R. J. (2022). Polymer grafted nanoparticle composites with enhanced thermal and mechanical properties. *ACS Applied Materials & Interfaces, 14*(18), 21535–21543. https://doi.org/10.1021/acsami.2c03797

Kunnari, E., Valkama, J., Keskinen, M., & Mansikkamäki, P. (2009). Environmental evaluation of new technology: Printed electronics case study. *Journal of Cleaner Production, 17*(9), 791–799. https://doi.org/10.1016/j.jclepro.2008.11.020

Lee, T.-W., & Jeong, Y. G. (2015). Regenerated cellulose/multiwalled carbon nanotube composite films with efficient electric heating performance. *Carbohydrate Polymers, 133*, 456–463. https://doi.org/10.1016/j.carbpol.2015.06.053

Li, G., Tian, X., Xu, X., Zhou, C., Wu, J., Li, Q., Zhang, L., Yang, F., & Li, Y. (2017). Fabrication of robust and highly thermally conductive nanofibrillated cellulose/graphite nanoplatelets composite papers. *Composites Science and Technology, 138*, 179–185. https://doi.org/10.1016/j.compscitech.2016.12.001

Li, H., Liu, X., Zhang, C., & Zheng, W. (2024). Experimental study of thermal transport across metal/h-BN interfaces: Comparison with metal/graphite interfaces. *International Journal of Thermal Sciences, 205*, 109307. https://doi.org/10.1016/j.ijthermalsci.2024.109307

Li, H.-J., Cao, Y.-M., Qin, J.-J., Jie, X.-M., Wang, T.-H., Liu, J.-H., & Yuan, Q. (2006). Development and characterization of anti-fouling cellulose hollow fiber UF membranes for oil–water separation. *Journal of Membrane Science, 279*(1), 328–335. https://doi.org/10.1016/j.memsci.2005.12.025

Li, J., Yang, H., Huang, K., Cao, S., Ni, Y., Huang, L., Chen, L., & Ouyang, X. (2018). Conductive regenerated cellulose film as counter electrode for efficient dye-sensitized solar cells. *Cellulose, 25*(9), 5113–5122. https://doi.org/10.1007/s10570-018-1913-1

Li, Q., Zhang, K., Che, X., Gao, T., Wang, S., & Ni, G. (2024). Preparation of BN nanoparticle with high sintering activity and its formation mechanism. *Molecules, 29*(15), 3458. https://doi.org/10.3390/molecules29153458

Li, X., Yuan, L., Liu, R., He, H., Hao, J., Lu, Y., et al. (2021). Engineering textile electrode and bacterial cellulose nanofiber reinforced hydrogel electrolyte to enable high-performance flexible all-solid-state supercapacitors. *Advanced Energy Materials, 11*(12), 2003010. https://doi.org/10.1002/aenm.202003010

Li, Y., Yang, M., Xu, B., Sun, Q., Zhang, W., Zhang, Y., & Meng, F. (2018). Synthesis, structure and antioxidant performance of boron nitride (hexagonal) layers coating on carbon nanotubes (multi-walled). *Applied Surface Science, 450*, 284–291. https://doi.org/10.1016/j.apsusc.2018.04.205

Liang, C., He, J., Zhang, Y., Zhang, W., Liu, C., Ma, X., Liu, Y., & Gu, J. (2022). MOF-derived CoNi@ C-silver nanowires/cellulose nanofiber composite papers with excellent thermal management capability for outstanding electromagnetic interference shielding. *Composites Science and Technology, 224*, 109445. https://doi.org/10.1016/j.compscitech.2022.109445

Liang, H. (2024). Research progress of graphene thin films for heat dissipation applications in electronic devices. *Academic Journal of Science and Technology, 12*(1), 347–350. https://doi.org/10.54097/20shxr21

Liu, H., Du, H., Zheng, T., Liu, K., Ji, X., Xu, T., Zhang, X., & Si, C. (2021). Cellulose based composite foams and aerogels for advanced energy storage devices. *Chemical Engineering Journal, 426*, 130817. https://doi.org/10.1016/j.cej.2021.130817

Liu, J., Yang, C., Wu, H., Lin, Z., Zhang, Z., Wang, R., et al. (2014). Future paper based printed circuit boards for green electronics: Fabrication and life cycle assessment. *Energy & Environmental Science, 7*(11), 3674–3682. https://doi.org/10.1039/C4EE01995D

Liu, M., Lin, K., Zhou, M., Wallwork, A., Bissett, M. A., Young, R. J., & Kinloch, I. A. (2024). Mechanism of gas barrier improvement of graphene/polypropylene nanocomposites for new-generation light-weight hydrogen storage. *Composites Science and Technology, 249*, 110483. https://doi.org/10.1016/j.compscitech.2024.110483

Liu, X., Xiao, W., Ma, X., Huang, L., Ni, Y., Chen, L., Ouyang, X., & Li, J. (2020). Conductive regenerated cellulose film and its electronic devices–a review. *Carbohydrate Polymers, 250*, 116969. https://doi.org/10.1016/j.carbpol.2020.116969

Liu, Z., Li, J., & Liu, X. (2020). Novel functionalized BN nanosheets/epoxy composites with advanced thermal conductivity and mechanical properties. *ACS Applied Materials & Interfaces, 12*(5), 6503–6515. https://doi.org/10.1021/acsami.9b21467

Ma, L., Wang, Y., Jia, Q., Zhang, H., Wang, Y., Li, D., Zou, G., & Guo, F. (2024). Low-temperature-sintered nano-Ag film for power electronics packaging. *Journal of Electronic Materials, 53*(1), 228–237. https://doi.org/10.1007/s11664-023-10763-6

Malekpour, H., Chang, K.-H., Chen, J.-C., Lu, C.-Y., Nika, D. L., Novoselov, K. S., & Balandin, A. A. (2014). Thermal conductivity of graphene laminate. *Nano Letters, 14*(9), 5155–5161. https://doi.org/10.1021/nl501996v

Meng, X., Jia, S., Mo, L., Wei, J., Wang, F., & Shao, Z. (2020). O/N-co-doped hierarchically porous carbon from carboxymethyl cellulose ammonium for high-performance supercapacitors. *Journal of Materials Science, 55*(17), 7417–7431. https://doi.org/10.1007/s10853-020-04515-8

Mercado, E., Anaya, J., & Kuball, M. (2021). Impact of polymer residue level on the in-plane thermal conductivity of suspended large-area graphene sheets. *ACS Applied Materials & Interfaces, 13*(15), 17910–17919. https://doi.org/10.1021/acsami.1c00365

Mumtaz, N., Li, Y., Artiaga, R., Farooq, Z., Mumtaz, A., Guo, Q., & Nisa, F.-U. (2024). Fillers and methods to improve the effective (out-plane) thermal conductivity of polymeric thermal interface materials–a review. *Heliyon, 10*(3), e25381. https://doi.org/10.1016/j.heliyon.2024.e25381

Nie, S., Hao, N., Zhang, K., Xing, C., & Wang, S. (2020). Cellulose nanofibrils-based thermally conductive composites for flexible electronics: A mini review. *Cellulose, 27*(8), 4173–4187. https://doi.org/10.1007/s10570-020-03103-y

Niu, H., Ren, Y., Guo, H., Małycha, K., Orzechowski, K., & Bai, S.-L. (2020). Recent progress on thermally conductive and electrical insulating rubber composites: Design, processing and applications. *Computer Communications, 22*, 100430. https://doi.org/10.1016/j.coco.2020.100430

Ouyang, Y., Bai, L., Tian, H., Li, X., & Yuan, F. (2022). Recent progress of thermal conductive ploymer composites: Al_2O_3 fillers, properties and applications. *Composites. Part A, Applied Science and Manufacturing, 152*, 106685. https://doi.org/10.1016/j.compositesa.2021.106685

Owais, M., Javed, M. H., Akram, M. Z., Paxton, W. F., Akhatov, I. S., & Abaimov, S. G. (2021). Recent advances in thermally conductive paper-like films. *ECS Journal of Solid State Science and Technology, 10*(3), 33001. https://doi.org/10.1149/2162-8777/abea5b

Prakash, N. R., & Gnanavel, C. (2024). Effect of rice husk ash silicon nitride on mechanical, wear, thermal conductivity, and flammability behavior of aluminized glass-kenaf fiber-reinforced polyester composite. *Biomass Conversion and Biorefinery, 14*, 32229–32240. https://doi.org/10.1007/s13399-024-05335-5

Rasul, M. G., Kiziltas, A., Malliakas, C. D., Rojaee, R., Sharifi-Asl, S., Foroozan, T., et al. (2021). Polyethylene-BN nanosheets nanocomposites with enhanced thermal and mechanical properties. *Composites Science and Technology, 204*, 108631. https://doi.org/10.1016/j.compscitech.2020.108631

Rout, L. N., Mishra, D., & Swain, P. T. R. (2024). Physical, thermal, and mechanical characterization of ceramic (SiC) filled woven glass fiber reinforced hybrid polymer composites. *SILICON, 16*(4), 1731–1741. https://doi.org/10.1007/s12633-023-02792-x

Roy, S., Zhang, X., Puthirath, A. B., Meiyazhagan, A., Bhattacharyya, S., Rahman, M. M., et al. (2021). Structure, properties and applications of two-dimensional hexagonal boron nitride. *Advanced Materials, 33*(44), 2101589. https://doi.org/10.1002/adma.202101589

Saji, V. S. (2023). 2D hexagonal boron nitride (h-BN) nanosheets in protective coatings: A literature review. *Heliyon, 9*(9), e19362. https://doi.org/10.1016/j.heliyon.2023.e19362

Sharma, G. P., Bansal, A., & Singh, R. (2024). Thermal coefficients of fuller's earth reinforced with Al_2O_3 and TiO_2 micro-inclusions. *Indian Journal of Physics, 98*(6), 1951–1964. https://doi.org/10.1088/2632-959X/abe454

Shen, B., Zhai, W., & Zheng, W. (2014). Ultrathin flexible graphene film: An excellent thermal conducting material with efficient EMI shielding. *Advanced Functional Materials, 24*(28), 4542–4548. https://doi.org/10.1002/adfm.201400079

Shen, C., Yang, Z., Rao, J., Li, J., Wu, D., He, Y., & Chen, K. (2022). Development of a thermally conductive and antimicrobial nanofibrous mat for the cold chain packaging of fruits and vegetables. *Materials and Design, 221*, 110931. https://doi.org/10.1016/j.matdes.2022.110931

Sim, L., Ramanan, S. R., Ismail, H., Seetharamu, K. N., & Goh, T. J. (2005). Thermal characterization of Al_2O_3 and ZnO reinforced silicone rubber as thermal pads for heat dissipation purposes. *Thermochimica Acta, 430*(1–2), 155–165. https://doi.org/10.1016/j.tca.2004.12.024

Song, N., Jiao, D., Cui, S., Hou, X., Ding, P., & Shi, L. (2017). Highly anisotropic thermal conductivity of layer-by-layer assembled nanofibrillated cellulose/graphene nanosheets hybrid films for thermal management. *ACS Applied Materials & Interfaces, 9*(3), 2924–2932. https://doi.org/10.1021/acsami.6b11979

Song, N., Jiao, D., Ding, P., Cui, S., Tang, S., & Shi, L. (2016). Anisotropic thermally conductive flexible films based on nanofibrillated cellulose and aligned graphene nanosheets. *Journal of Materials Chemistry C, 4*(2), 305–314. https://doi.org/10.1039/C5TC02194D

Song, N.-J., Chen, C.-M., Lu, C., Liu, Z., Kong, Q.-Q., & Cai, R. (2014). Thermally reduced graphene oxide films as flexible lateral heat spreaders. *Journal of Materials Chemistry A, 2*(39), 16563–16568. https://doi.org/10.1039/C4TA02693D

Song, Y.-H., Yin, L.-J., Zhong, S.-L., Feng, Q.-K., Wang, H., Zhang, P., et al. (2024). A processable high thermal conductivity epoxy composites with multi-scale particles for high-frequency electrical insulation. *Advanced Composites and Hybrid Materials, 7*(4), 115. https://doi.org/10.1007/s42114-024-00914-6

Sudheshwar, A., Malinverno, N., Hischier, R., Nowack, B., & Som, C. (2023). The need for design-for-recycling of paper-based printed electronics—A prospective comparison with printed circuit boards. *Resources, Conservation and Recycling, 189*, 106757. https://doi.org/10.1016/j.resconrec.2022.106757

Sun, J., Yao, Y., Zeng, X., Pan, G., Hu, J., Huang, Y., Sun, R., Xu, J.-B., & Wong, C.-P. (2017). Preparation of boron nitride nanosheet/nanofibrillated cellulose nanocomposites with ultrahigh thermal conductivity via engineering interfacial thermal resistance. *Advanced Materials Interfaces, 4*(17), 1700563. https://doi.org/10.1002/admi.201700563

Tao, Y. B., & He, Y.-L. (2018). A review of phase change material and performance enhancement method for latent heat storage system. *Renewable and Sustainable Energy Reviews, 93*, 245–259. https://doi.org/10.1016/j.rser.2018.05.028

Teng, C., Xie, D., Wang, J., Yang, Z., Ren, G., & Zhu, Y. (2017). Ultrahigh conductive graphene paper based on ball-milling exfoliated graphene. *Advanced Functional Materials, 27*(20), 1700240. https://doi.org/10.1002/adfm.201700240

Tian, S., Wang, T., Chen, H., Ma, D., & Zhang, L. (2024). Phonon coherent transport leads to an anomalous boundary effect on the thermal conductivity of a rough graphene nanoribbon. *Physical Review Applied, 21*(6), 64005. https://doi.org/10.1103/PhysRevApplied.21.064005

Uetani, K., & Hatori, K. (2017). Thermal conductivity analysis and applications of nanocellulose materials. *Science and Technology of Advanced Materials, 18*(1), 877–892. https://doi.org/10.1080/14686996.2017.1390692

Uetani, K., Okada, T., & Oyama, H. T. (2015). Crystallite size effect on thermal conductive properties of nonwoven nanocellulose sheets. *Biomacromolecules, 16*(7), 2220–2227. https://doi.org/10.1021/acs.biomac.5b00617

Vu, M. C., Kim, I.-H., Choi, W. K., Lim, C.-S., Islam, M. A., & Kim, S.-R. (2020). Highly flexible graphene derivative hybrid film: An outstanding nonflammable thermally conductive yet electrically insulating material for efficient thermal management. *ACS Applied Materials & Interfaces, 12*(23), 26413–26423. https://doi.org/10.1021/acsami.0c02427

Vu, M. C., Mani, D., Kim, J.-B., Jeong, T.-H., Park, S., Murali, G., et al. (2021). Hybrid shell of MXene and reduced graphene oxide assembled on PMMA bead core towards tunable thermoconductive and EMI shielding nanocomposites. *Composites. Part A, Applied Science and Manufacturing, 149*, 106574. https://doi.org/10.1016/j.compositesa.2021.106574

Wang, B., Cunning, B. V., Kim, N. Y., Kargar, F., Park, S., Li, Z., et al. (2019). Ultrastiff, strong, and highly thermally conductive crystalline graphitic films with mixed stacking order. *Advanced Materials, 31*(29), 1903039. https://doi.org/10.1002/adma.201903039

Wang, D.-C., Lei, S.-N., Zhong, S., Xiao, X., & Guo, Q.-H. (2023). Cellulose-based conductive materials for energy and sensing applications. *Polymers, 15*(20), 4159. https://doi.org/10.3390/polym15204159

Wang, D.-C., Yu, H.-Y., Qi, D., Wu, Y., Chen, L., & Li, Z. (2021). Confined chemical transitions for direct extraction of conductive cellulose nanofibers with graphitized carbon shell at low temperature and pressure. *Journal of the American Chemical Society, 143*(30), 11620–11630. https://doi.org/10.1021/jacs.1c04710

Wang, J., Zhang, L., Wang, L., Lei, W., & Wu, Z. (2022). Two-dimensional boron nitride for electronics and energy applications. *Energy and Environmental Materials, 5*(1), 10–44. https://doi.org/10.1002/eem2.12159

Wang, N., Samani, M. K., Li, H., Dong, L., Zhang, Z., Su, P., et al. (2018). Tailoring the thermal and mechanical properties of graphene film by structural engineering. *Small, 14*(29), 1801346. https://doi.org/10.1002/smll.201801346

Wang, S., Zhang, L., Zeng, Q., Liu, X., Lai, W.-Y., & Zhang, L. (2020). Cellulose microcrystals with brush-like architectures as flexible all-solid-state polymer electrolyte for Lithium-ion battery. *ACS Sustainable Chemistry & Engineering, 8*(8), 3200–3207. https://doi.org/10.1021/acssuschemeng.9b06658

Wang, T., Ou, D., Liu, H., Jiang, S., Huang, W., Fang, X., Chen, X., & Lu, M. (2018). Thermally conductive boron nitride nanosheet composite paper as a flexible printed circuit board. *ACS Applied Nano Materials, 1*(4), 1705–1712. https://doi.org/10.1021/acsanm.8b00160

Wang, X., Yu, Z., Bian, H., Wu, W., Xiao, H., & Dai, H. (2019). Thermally conductive and electrical insulation BNNS/CNF aerogel nano-paper. *Polymers, 11*(4), 660. https://doi.org/10.3390/polym11040660

Wei, W., Zhang, Y., Chen, H., Su, Z., Lan, D., & Zha, J. (2024). Nano-BN and nano-cellulose synergistically enhanced the mechanical, thermal, and insulating properties of cellulose insulating paper. *Computer Science and Technology, 256*, 10748. https://doi.org/10.1016/j.compscitech.2024.110748

Wen, Y., Chen, C., Ye, Y., Xue, Z., Liu, H., Zhou, X., et al. (2022). Advances on thermally conductive epoxy-based composites as electronic packaging underfill materials—A review. *Advanced Materials, 34*(52), 2201023. https://doi.org/10.1002/adma.202201023

Wiklund, J., Karakoç, A., Palko, T., Yiğitler, H., Ruttik, K., Jäntti, R., & Paltakari, J. (2021). A review on printed electronics: Fabrication methods, inks, substrates, applications and environmental impacts. *Journal of Manufacturing and Materials Processing, 5*(3), 89. https://doi.org/10.3390/jmmp5030089

Wu, H., Chiang, S. W., Lin, W., Yang, C., Li, Z., Liu, J., et al. (2014). Towards practical application of paper based printed circuits: Capillarity effectively enhances conductivity of the thermoplastic electrically conductive adhesives. *Scientific Reports, 4*(1), 6275. https://doi.org/10.1038/srep06275

Wu, Y., Xue, Y., Qin, S., Liu, D., Wang, X., Hu, X., et al. (2017). BN nanosheet/polymer films with highly anisotropic thermal conductivity for thermal management applications. *ACS Applied Materials & Interfaces, 9*(49), 43163–43170. https://doi.org/10.1021/acsami.7b15264

Wu, Z., Gao, S., Wang, X., Ibrahim, M. M., Mersal, G. A. M., Ren, J., et al. (2024). Dielectric thermally conductive boron nitride/silica@ MWCNTs/polyvinylidene fluoride composites via a combined electrospinning and hot press method. *Journal of Materials Science: Materials in Electronics, 35*(15), 1032. https://doi.org/10.1007/s10854-024-12794-z

Xia, T., Cao, J., Bissett, M. A., Waring, H., Xiang, Y., Pinter, G., et al. (2023). Graphenization of graphene oxide films for strongly anisotropic thermal conduction and high electromagnetic interference shielding. *Carbon, 215*, 118496. https://doi.org/10.1016/j.carbon.2023.118496

Xiang, J., & Drzal, L. T. (2011). Thermal conductivity of exfoliated graphite nanoplatelet paper. *Carbon, 49*(3), 773–778. https://doi.org/10.1016/j.carbon.2010.10.003

Xu, T., Du, H., Liu, H., Liu, W., Zhang, X., Si, C., Liu, P., & Zhang, K. (2021). Advanced nanocellulose-based composites for flexible functional energy storage devices. *Advanced Materials, 33*(48), 2101368. https://doi.org/10.1002/adma.202101368

Xu, W., Ding, Y., Jiang, S., Chen, L., Liao, X., & Hou, H. (2014). Polyimide/$BaTiO_3$/MWCNTs three-phase nanocomposites fabricated by electrospinning with enhanced dielectric properties. *Materials Letters, 135*, 158–161. https://doi.org/10.1016/j.matlet.2014.07.157

Yang, C., Wu, Q., Xie, W., Zhang, X., Brozena, A., Zheng, J., et al. (2021). Copper-coordinated cellulose ion conductors for solid-state batteries. *Nature, 598*(7882), 590–596. https://doi.org/10.1038/s41586-021-03885-6

Yang, S., Sun, X., Shen, J., Li, Y., Xie, L., Qin, S., Xue, B., & Zheng, Q. (2020). Interface engineering based on polydopamine-assisted metallization in highly thermal conductive cellulose/nanodiamonds composite paper. *ACS Sustainable Chemistry & Engineering, 8*(48), 17639–17650. https://doi.org/10.1021/acssuschemeng.0c04427

Yang, S., Huang, Z., Hu, Q., Zhang, Y., Wang, F., Wang, H., & Shu, Y. (2022). Proportional optimization model of multiscale spherical BN for enhancing thermal conductivity. *ACS Applied Electronic Materials, 4*(9), 4659–4667. https://doi.org/10.1021/acsaelm.2c00878

Yang, W., Kim, J., & Kim, J. (2024). Improving thermal conductivity of epoxy composite by three-dimensional filler network constructed with two different diameters aluminum nitride and cellulose nanofiber. *Cellulose, 31*(4), 2461–2474. https://doi.org/10.1080/17439884.2020.1727501

Yao, Y., Zeng, X., Wang, F., Sun, R., Xu, J., & Wong, C.-P. (2016). Significant enhancement of thermal conductivity in bioinspired freestanding boron nitride papers filled with graphene oxide. *Chemistry of Materials, 28*(4), 1049–1057. https://doi.org/10.1021/acs.chemmater.5b04187

Zhang, S., Zhu, X., She, Y., Li, N., Li, L., & Deng, T. (2024). Highly exfoliated boron nitride nanosheets via carboxyl nanocellulose for thermally conductive nanocomposite films. *ACS Applied Nano Materials, 7*(3), 2971–2982. https://doi.org/10.1021/acsanm.3c05310

Zhang, X., Kang, L., & Zhu, M. (2022). Density functional theory study of low-dimensional (2D, 1D, 0D) boron nitride nanomaterials catalyzing acetylene acetate reaction. *International Journal of Molecular Sciences, 23*(17), 9997. https://doi.org/10.3390/ijms23179997

Zhang, Y., Kobayashi, K., Teramoto, Y., & Wada, M. (2024). Preparation of cellulose-paraffin composite foams by an emulsion–gelation method using aqueous inorganic salt solution for thermal energy regulation. *Composites. Part A, Applied Science and Manufacturing, 181*, 108158. https://doi.org/10.1016/j.compositesa.2024.108158

Zhao, X., Li, W., Wang, Y., Li, H., & Wang, J. (2021). Bioinspired modified graphite film with superb mechanical and thermoconductive properties. *Carbon, 181*, 40–47. https://doi.org/10.1016/j.carbon.2021.05.019

Zhao, X., Huang, C., Liu, Q., Smalyukh, I. I., & Yang, R. (2018). Thermal conductivity model for nanofiber networks. *Journal of Applied Physics, 123*(8), 85103. https://doi.org/10.1063/1.5008582

Zhou, S., Kong, X., Zheng, B., Huo, F., Strømme, M., & Xu, C. (2019). Cellulose nanofiber @ conductive metal–organic frameworks for high-performance flexible supercapacitors. *ACS Nano, 13*(8), 9578–9586. https://doi.org/10.1021/acsnano.9b04670

Zhu, H., Li, Y., Fang, Z., Xu, J., Cao, F., Wan, J., et al. (2014). Highly thermally conductive papers with percolative layered boron nitride nanosheets. *ACS Nano, 8*(4), 3606–3613. https://doi.org/10.1021/nn500134m

Zhu, Z., Li, C., Songfeng, E., Xie, L., Geng, R., Lin, C.-T., et al. (2019). Enhanced thermal conductivity of polyurethane composites via engineering small/large sizes interconnected boron nitride nanosheets. *Composites Science and Technology, 170*, 93–100. https://doi.org/10.1016/j.compscitech.2018.11.035

Zou, Z., Zhou, W., Zhang, Y., Yu, H., Hu, C., & Xiao, W. (2019). High-performance flexible all-solid-state supercapacitor constructed by free-standing cellulose/reduced graphene oxide/silver nanoparticles composite film. *Chemical Engineering Journal, 357*, 45–55. https://doi.org/10.1016/j.cej.2018.09.143

Chapter 16
Fire-Resistant Paper

Han-Ping Yu and Ying-Jie Zhu

16.1 Introduction

The traditional paper based on organic cellulose fibers is highly flammable and easy to burn. As a result, many precious paper-based artworks, books, and documents were ruined by fire disasters throughout the long history of mankind. Paper yellows with age and is also at risk of acid decay. In addition, papermaking consumes a large amount of precious trees and other natural resources and also causes environmental pollution. To solve these problems, it is necessary to explore new materials as building materials for the fire-resistant paper. The resistance to both high temperature and fire, and thermal insulation of paper are highly desirable for practical applications (Zhu, 2021a).

The addition of flame retardants can improve the fire-retardant performance of the traditional paper. In this case, phosphorus-based flame retardants are usually coated on the surface of cellulose fibers, or flame-retardant components are mixed with cellulose fibers for papermaking. Another strategy for the preparation of the fire-retardant paper is based on noncombustible organic fibers, such as aramid fibers as the raw materials. In addition, nonflammable inorganic nanofibers can be used to fabricate the fire-resistant paper.

H.-P. Yu
State Key Laboratory of High Performance Ceramics and Superfine Microstructure, Shanghai Institute of Ceramics, Chinese Academy of Sciences, Shanghai, China

Y.-J. Zhu (✉)
State Key Laboratory of High Performance Ceramics and Superfine Microstructure, Shanghai Institute of Ceramics, Chinese Academy of Sciences, Shanghai, China

Center of Materials Science and Optoelectronics Engineering, University of Chinese Academy of Sciences, Beijing, China
e-mail: y.j.zhu@mail.sic.ac.cn

G. Korotcenkov (ed.), *The Handbook of Paper-Based Sensors and Devices*,
https://doi.org/10.1007/978-3-031-91080-7_16

In this chapter, we will discuss the design principles, preparation strategies, structural characteristics, advantages and disadvantages of the fire-resistant paper, and recent advances in this innovative research field. We will introduce the wet end chemical properties for the preparation of the fire-resistant paper, which are the important theoretical basis for the mass production of the fire-resistant paper. Then, the wide applications of the fire-resistant paper will be summarized. Finally, we will discuss the challenges of the fire-resistant paper, proposed future research directions, and future outlook in the field of the fire-resistant paper.

16.2 Fire-Retardant Paper Based on Organic Fibers

The main raw building material for the traditional paper is flammable organic plant fibers (cellulose fibers). In order to enhance the high-temperature resistance of cellulose fibers, flame retardants are often used to modify cellulose fibers or incorporated into paper. In addition, with the rapid development of organic chemistry, some artificial organic fibers such as aramid fibers have been synthesized and commercialized, and they exhibit relatively good flame retardance and resistance to high temperatures. In this section, some examples of the fire-retardant paper based on flame retardants and organic fibers will be discussed.

16.2.1 Fire-Retardant Paper Based on Phosphorylated Cellulose Fibers

In general, flame retardants are used to modify cellulose fibers to achieve the flame-retardant ability. The flame-retardant mechanisms are usually described as follows: (1) reducing the surface temperature of combustible cellulose fibers; (2) diluting combustible gases and oxygen on the surface of cellulose fibers; and (3) accelerating the dehydration process of organic components to form a carbonized layer for oxygen barrier. The common flame retardants are phosphorus- and halogen-containing additives. However, halogenated flame retardants produce the dense and toxic smoke during combustion, which is harmful to human health (Azman Mohammad Taib et al., 2022). As a result, phosphorus-containing flame retardants are popular for the surface modification of cellulose fibers (Velencoso et al., 2018). The phosphorus-containing flame retardants decompose into non-volatile and glassy substances at the combustion temperature, which wrap around cellulose fibers to form a dense protective layer to block their combustion, and thus reduce the flammability of paper.

The common phosphorus-containing agents for the preparation of the flame-retardant paper include phosphorus pentoxide, diammonium hydrogen phosphate, phosphorus oxychloride, phosphoric acid, phytic acid, and ammonium phytate

(Fang, Chen, et al., 2022; Fang, Wu, et al., 2022; Ghanadpour et al., 2015; Patoary et al., 2023; Zhang, Wu, et al., 2020). The organic solvent such as urea, *N,N*-dimethylformamide, or pyridine is usually adopted for the phosphorylation of cellulose fibers using inorganic phosphorylating agents (Ghanadpour et al., 2015; Patoary et al., 2023). Urea is an effective solvent because it can break down the hydrogen bonds to promote the phosphorylation of cellulose fibers (Fiss et al., 2019). Urea and phosphoric acid are essential for the isolation of phosphorylated cellulose fibers. Urea can facilitate the swelling of cellulose fibers, thus increasing access for the phosphorylating agent (Etale et al., 2024). Ghanadpour et al. (2015) reported sulfite dissolving pulp cellulose fibers chemically modified by phosphorylation using $(NH_4)_2HPO_4$ and urea to enhance the flame retardancy. The paper prepared using phosphorylated cellulose nanofibrils exhibited a self-extinguishing behavior.

Phytic acid is an abundant and ecofriendly compound with a high phosphorus content and is a promising flame retardant for cellulose fibers. However, phytic acid is not efficient for the phosphorylation of cellulose fibers because of its strong acidity that leads to significantly decreased strength. The compounds with both phosphorous and nitrogen are efficient flame retardants and exhibit synergistic effect for the phosphorylation of cellulose fibers. Liu et al. (2018) synthesized a halogen-free flame retardant (ammonium phytate) containing a high level of phosphorus and nitrogen elements by reacting phytic acid with urea to improve the flame retardancy of lyocell fibers through the pad-dry-cure finishing process. The flame retardancy and durability of finished lyocell fabrics were significantly enhanced, with increased limiting oxygen index values up to 39.2% and still 29.7% after 30 washing cycles.

In addition, the modified lyocell fibers exhibited a good durable fire-retardant performance. Phytic acid is often used in combination with other flame retardants such as chitosan. Chitosan is rich in nitrogen element and has an excellent flame retardant effect. Fang, Chen, et al. (2022) prepared the antibacterial fire-retardant Chinese Xuan paper with the chitosan/phytic acid coating. With increasing number of coating bilayers, the Xuan paper showed better fire-retardant performance. The Xuan paper exhibited improved flame-retardant performance with a limiting oxygen index value of 36.4% with 20 coating bilayers on pulp fibers. In contrast, the limiting oxygen index value of the uncoated Xuan paper was only 18.7%. Fang, Wu, et al. (2022) adopted ammonium phytate for the flame-retardant treatment of Chinese Xuan paper by spray coating with limiting oxygen index values >40%. It was found that ammonium phytate could change the thermal decomposition process to promote char formation during the degradation of Xuan paper. The phosphorus component facilitated char formation in the condensed phase, and the nitrogen component released inert species to dilute the fuel load in the gas phase.

16.2.2 Fire-Retardant Paper Based on Cellulose Fibers with Inorganic Fillers

Generally, inorganic solid materials usually show much higher thermal stabilities than that of organic cellulose fibers; thus, inorganic fillers can be used to prepare the fire-retardant paper based on cellulose fibers. The challenges for the addition of inorganic fillers in paper are their agglomeration and poor dispersion. Wang et al. (2012) prepared Mg-Al hydrotalcite composed of layered hexagonal nanoparticles by co-precipitation and was used in flame-retardant paper as the inorganic filler. The flame-retardant paper prepared using Mg-Al hydrotalcite exhibited good fire-retarding performance, and its oxygen index was >25% at 20 wt.% Mg-Al hydrotalcite. Metal hydroxides, such as magnesium hydroxide, decompose by heat to form stabilized metal oxides and release water, which can decrease the temperature of the paper, isolate the paper from oxygen, or dilute the concentrations of oxygen and combustible gases during the combustion process. Many factors such as the type, particle size, loading content, and dispersity of inorganic fillers influence the properties of the composite paper. Kang et al. (2023) reported the preparation of the flame-retardant paper by in situ loading of magnesium hydroxide/basic magnesium chloride onto cellulose fibers based on the simultaneous dispersion of $MgCl_2$ and CaO in water followed by mixing with the cellulose fiber suspension before papermaking.

In addition to the fire resistance, some inorganic nanofillers are alkaline and can be concurrently used as deacidifying agents to endow paper with a long-term anti-acidification performance. Acidification of paper-based relics is a common problem, leading to their degradation and eventual loss. Paper deacidification is highly dependent on some alkaline materials. Wang et al. (2024) used layered double hydroxide and its calcined product (layered double oxide) with different acidities as protective materials for the deacidification of paper. The treatment of paper with Mg-Al layered double hydroxide and layered double oxide could effectively modify the pH value of the acidic paper (pH ~4.0–6.4) to a neutral or weakly basic state.

Wang, Yang, et al. (2022) reported $Mg(OH)_2$ nanoflakes with a high dispersion stability for paper protection and anti-acidification, and they were uniformly distributed on the paper fibers as an alkaline reserve (Fig. 16.1). $Mg(OH)_2$ nanoflakes with the surfactant-modified surface could homogeneously disperse in water to form a stable colloidal suspension and were directly used as a deacidifying agent. $Mg(OH)_2$ nanoflakes exhibited the superior paper protection performance demonstrated by its safe pH 7.29 for an aged bamboo paper (pH 5.03) and the long-term anti-acidification effect with pH 5.47 after accelerated aging at 105 °C for 5 months. In addition, $Mg(OH)_2$ nanoflakes with the surfactant-modified surface could be used as a flame retardant for paper protection.

The fire-resistant paper with a high thermal stability can be obtained by imitating the structure in organisms. Especially, some biomineralized tissues, such as nacre with the "brick-and-mortar" structure, usually exhibit the combination of superior mechanical properties and excellent fire/heat resistance (Yu & Zhu, 2024), enabling

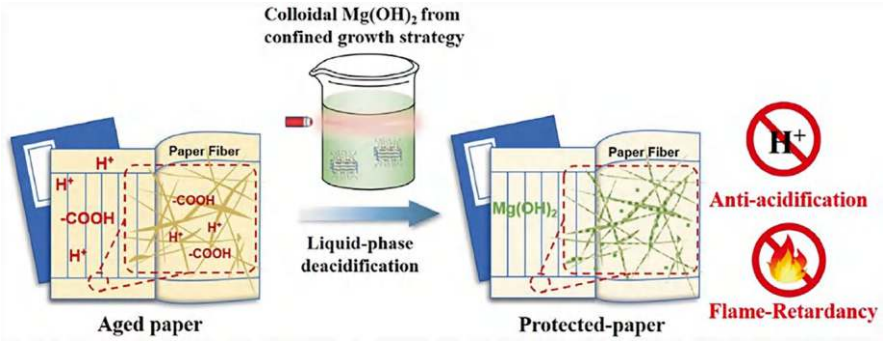

Fig. 16.1 Schematic illustration of the aged paper de-acidified and protected by $Mg(OH)_2$ nanoflakes to achieve anti-acidification and flame-retardancy. Reprinted with permission from Wang, Yang, et al. (2022). Copyright 2022, Elsevier

the design of high-performance flame-retardant paper. Fang et al. (2020) reported bio-inspired fabrication of nacre-mimetic hybrid nanocoating for ecofriendly fire-retardant cellulosic Chinese Xuan paper by layer-by-layer assembly of chitosan and montmorillonite. The flame retardancy of Xuan paper was greatly improved after the layer-by-layer coating of chitosan and montmorillonite with a limiting oxygen index value of >35% when the bilayers were over 10.

16.2.3 Fire-Retardant Paper Based on Organic Fibers

In addition to the fire-retardant paper based on surface-modified cellulose fibers and inorganic fillers, some kinds of synthetic organic fibers such as aramid fibers and polyarylsulphonamide fibers with high thermal stability can be used to fabricate the fire-retardant paper.

Aramid fiber family contains various members such as poly(*p*-phenylene terephthalamide) (Aramid 1414) and poly(*m*-phenylene isophthalamide) (Aramid 1313). Aramid fibers and their composites are widely used in various fields owing to their excellent properties, such as high mechanical properties, light-weight, high-temperature resistance, flame retardancy, chemical stability, and insulation. However, the ultraviolet radiation from the sunlight can deteriorate the structure of aramid fibers, and the dense, smooth, and inert surface of aramid fibers weakens the adhesion strength to other components in the composites (He et al., 2024).

In particular, aramid nanofibers exhibit excellent properties and are an ideal raw material for the preparation of the flame-retardant paper (Wang, Zhu, et al., 2022; Yang et al., 2020, 2024). Yang et al. (2024) prepared a high-performance ultrathin (5 μm) fire-retardant paper consisting of only aramid nanofibers, which exhibited excellent mechanical properties, and its tensile strength and Young's modulus were as high as 117.8 MPa and 41.6 GPa, respectively. Chen et al. (2023) reported the

preparation of high-performance fire-retardant paper made of para-aramid fibers by impregnating heterocyclic aramid solution into a para-aramid paper consisting of poly(*p*-phenylene terephthalamide) short fibers and polymerization-induced para-aramid nanofibers, and the fire-retardant paper exhibited a high thermal stability, good flame retardancy, high limiting oxygen index (40.5%), and high tensile strength (128.5 MPa).

Aramid fibers including nanofibers can also be hybridized with other nonflammable components, such as calcium hydroxyapatite (usually called as hydroxyapatite), and MXene, etc. to enhance the fire-retardant performance of the composite paper. Dong et al. (2019) reported a new kind of fire-retardant and high-temperature-resistant ultralong hydroxyapatite nanowire/aramid composite label paper with excellent properties. The tensile strength, smoothness, and oxygen index of the composite label paper with a hydroxyapatite/aramid weight ratio of 4:1 were 9.2 MPa, 904 s, and 76.8%, respectively, greatly higher than those of the pure aramid fiber paper (3.6 MPa, 62.2 s, and 27.6%). The composite label paper exhibited excellent fire-retardant and high-temperature-resistant performance. Compared with the commercial high-temperature-resistant label paper, which was carbonized heavily at 400 °C, the as-prepared composite label paper is promising for the application as the high-temperature-resistant and fire-retardant label paper in high-temperature environments. Wang, Zhu, et al. (2022) prepared a highly flexible, thermally stable, and fire-retardant nanocomposite paper consisting of ultralong hydroxyapatite nanowires and aramid nanofibers with excellent properties through the vacuum-assisted filtration method. Li et al. (2025) reported an ultrathin and highly flexible aramid nanofiber/MXene ($Ti_3C_2T_x$)/Ni composite paper prepared by the vacuum-assisted filtration and freeze-drying method, exhibiting excellent mechanical properties and flame retardancy.

Ma et al. (2020) reported a thermally conductive composite paper with a nacre-mimetic layered structure prepared by vacuum-assisted filtration followed by hot pressing, and it consisted of polydopamine-functionalized boron nitride nanosheets and aramid nanofibers. The composite paper exhibited anisotropic thermal conductivities, and its through-plane and in-plane values with 50 wt.% boron nitride nanosheets were 0.62 and 3.94 W m^{-1} K^{-1}, which were 181.8% and 196.2% higher than those of the aramid nanofiber paper, respectively, and its tensile strength was 36.8 MPa. Song et al. (2024) reported a nacre-inspired aramid nanofiber/basalt fiber composite paper with excellent flame retardance and thermal stability by constructing an organic-inorganic fiber alternating layered structure. The composite paper exhibited a high flexibility, low thermal conductivity (0.024 W m^{-1} K^{-1}), and high tensile strength (54.22 MPa), and its mechanical strength was still at a high level (92%) after heat treatment at 300 °C for 60 min.

16.3 Inorganic Fire-Resistant Paper

Many inorganic non-metallic fibers show much higher resistance to both high temperature and fire than those of organic fibers, which are promising for the preparation of the fire-resistant paper. However, one serious problem is the high brittleness and hardness of inorganic fibers. Fortunately, some kinds of flexible inorganic nanofibers such as ultralong hydroxyapatite nanowires with high aspect ratios have been successfully developed for the preparation of the flexible fire-resistant paper. In this section, recent advances in the preparation, properties, and applications of the advanced inorganic fire-resistant paper are discussed.

16.3.1 Fire-Resistant Paper Based on Ultralong Hydroxyapatite Nanowires

Hydroxyapatite ($Ca_{10}(PO_4)_6(OH)_2$) is the major inorganic component of human hard tissues such as tooth and bone. The content of hydroxyapatite in human tooth enamel is more than 90 wt.%, and is ~70 wt.% in bone. Hydroxyapatite has a high biocompatibility, high bioactivity, high whiteness, high-temperature resistance, and nonflammability. Unfortunately, hydroxyapatite is usually hard and brittle and is not suitable for making the flexible fire-resistant paper.

To address these challenges, the Zhu's research group (Lu et al., 2014) developed the calcium oleate precursor solvothermal method to synthesize highly flexible ultralong hydroxyapatite nanowires with diameters of about 10 nm and lengths of several hundred micrometers, which can solve the problem of high brittleness and hardness of traditional hydroxyapatite materials. Ultralong hydroxyapatite nanowires were synthesized using $CaCl_2$, oleic acid, $NaH_2PO_4{\cdot}2H_2O$, and NaOH in mixed solvents of water and ethanol by the calcium oleate precursor solvothermal method (Fig. 16.2a, b). The aspect ratios of ultralong hydroxyapatite nanowires are ultrahigh (>10,000), leading to their high flexibility. The calcium oleate precursor solvothermal method could be extended to the synthesis of ultralong hydroxyapatite nanowires using various monohydroxy alcohols (Jiang et al., 2015) and a variety of phosphate salts (Zhang et al., 2015). For example, ultralong hydroxyapatite nanowires with lengths of close to 1 mm could be synthesized by the calcium oleate precursor solvothermal method using methanol instead of ethanol (Jiang et al., 2015).

Later, the more environmentally friendly and low-cost calcium oleate precursor hydrothermal method was developed for the synthesis of ultralong hydroxyapatite nanowires in the only solvent of water without any organic solvent using water-soluble calcium salt, such as $CaCl_2$, sodium oleate, and water-soluble phosphate, such as NaH_2PO_4 (Li, Zhu, et al., 2017). Furthermore, ultralong hydroxyapatite nanowires could also be rapidly prepared by the microwave-assisted calcium oleate precursor hydrothermal method in a short period of heating time (within 20 min), greatly shortening the synthetic time by about two orders of magnitude compared

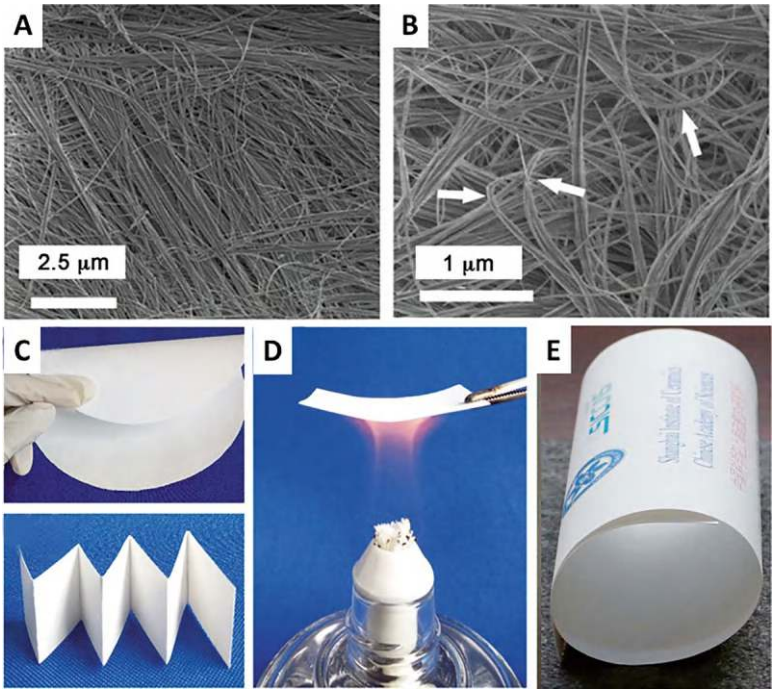

Fig. 16.2 (**a**, **b**) SEM images of ultralong hydroxyapatite nanowires. Reprinted with permission from Lu et al. (2014), Copyright 2014: Wiley-VCH. (**c**, **d**) Flexible fire-resistant paper based on ultralong hydroxyapatite nanowires. Reprinted with permission from Dong and Zhu (2017), Copyright 2017: Wiley-VCH. (**e**) The flexible fire-resistant paper based on ultralong hydroxyapatite nanowires can be used for writing and printing. Reprinted with permission from Li, Zhu, et al. (2017). Copyright 2017: Wiley-VCH

with the conventional hydrothermal method (Yu et al., 2018). The microwave heating is highly efficient, low-cost, and energy-saving, and can rapidly elevate the temperature of the polar solvent-containing reaction system (Zhu & Chen, 2014). Biocompatible organic biomolecules containing phosphorus such as adenosine 5′-triphosphate can also be used as the phosphorus sources for the rapid synthesis of ultralong hydroxyapatite nanowires by the microwave-assisted calcium oleate precursor hydrothermal method (Zhang et al., 2022).

The hydrophilicity and hydrophobicity of the as-prepared ultralong hydroxyapatite nanowires can be controlled by adjusting experimental parameters and post-washing process. In general, pure ultralong hydroxyapatite nanowires without any surface modification are hydrophilic. The adsorption of a certain amount of oleate groups on the surface of ultralong hydroxyapatite nanowires results in a hydrophobicity. Furthermore, the post-washing process can well control the surface properties of ultralong hydroxyapatite nanowires. Generally, thorough washing of the product using ethanol and water many times can produce hydrophilic ultralong hydroxyapatite nanowires; however, hydrophobic ultralong hydroxyapatite

nanowires can be obtained without washing or with less washing. In addition, the zeta potential measurement results showed that ultralong hydroxyapatite nanowires were negatively charged in aqueous solution (Zhu, 2021a).

The large-scale production of nanostructured materials is a universal challenge in the fields of nanotechnology and materials science. However, the large-scale production of nanostructured materials is a key factor for the realization of their practical applications. The laboratory synthesis of nanostructured materials is usually in a small scale of ≤100 mL volume reaction system. Nowadays, ultralong hydroxyapatite nanowires have been successfully synthesized in the author's laboratory by the calcium oleate precursor hydrothermal method using large stainless steel autoclaves with volumes of 10 L and 100 L, demonstrating the large-scale production potential of ultralong hydroxyapatite nanowires (Chen & Zhu, 2016).

The Zhu's research group put forward the innovative idea of using highly flexible ultralong hydroxyapatite nanowires as the raw material for making a new type of highly flexible inorganic fire-resistant paper (Lu et al., 2014). The as-prepared inorganic fire-resistant paper exhibited a high flexibility, porous and layered structure (Fig. 16.2c). More importantly, the as-prepared inorganic fire-resistant paper showed excellent resistance to both fire and high temperature (Dong & Zhu, 2017; Li, Zhu, et al., 2017; Lu et al., 2014), as shown in Fig. 16.2d. The advantages of the inorganic fire-resistant paper based on ultralong hydroxyapatite nanowires include (Zhu, 2021a, 2021b): (1) excellent biocompatibility and bioactivity; (2) high flexibility (Fig. 16.2e); (3) high whiteness without bleaching; (4) excellent resistance to both fire and high temperature; (5) excellent thermal insulation performance; (6) writable and printable function; (7) long-term safe preservation of important archives, artworks, books, and documents; (8) environmental protection because it is prepared from synthetic materials without consuming a large amount of natural resources such as trees; (9) easy functionalization for various applications; (10) ultralong hydroxyapatite nanowires exhibit a pH-responsive property, they are stable in weak acidic, neutral, and strong alkaline solutions, however, they are rapidly dissolved in a strong acidic solution, and this property can be used to destroy the ultralong hydroxyapatite nanowire-based fire-resistant paper when necessary; (11) high potential for the industry-scale production.

The waterproof fire-resistant paper consisting of superhydrophobic ultralong hydroxyapatite nanowires showed an excellent superhydrophobicity, with an excellent self-cleaning ability (Chen et al., 2016). In addition, the waterproof fire-resistant paper exhibited a highly stable superhydrophobicity after suffering from various surface damages, such as finger wipe, tape peeling, knife cutting, and sandpaper abrasion, because the waterproof fire-resistant paper was not only superhydrophobic on the surface layer but also on the interior with the layered structure. This novel waterproof fire-resistant paper could realize the multifunction of high resistance to both water and fire, which is favorable for protecting important archives, artworks, books, and documents from disasters of both floods and fire.

The pure fire-resistant paper consisting of only ultralong hydroxyapatite nanowires without any additives usually shows poor mechanical properties (the tensile strength is usually lower than 1 MPa). The author's research group designed and

optimized the structure of the fire-resistant paper and developed a new kind of inorganic adhesive (Na_2SiO_3, $AlCl_3$, etc.). In the fire-resistant paper, ultralong hydroxyapatite nanowires were interwoven to form a porous networked structure, coupled with the mechanical support and reinforcement of the micrometer-sized inorganic fibers and the binding effect of the inorganic adhesive, and the three synergistic effects could significantly enhance the mechanical properties of the fire-resistant paper (Zhu, 2021a). The tensile strengths of the fire-resistant paper based on ultralong hydroxyapatite nanowires could reach ~15 MPa after addition of glass fibers and inorganic adhesive (Li, Zhu, et al., 2017). In addition, the A4-sized (29.7 × 21 cm) fire-resistant paper based on ultralong hydroxyapatite nanowires was successfully prepared in the author's laboratory, and it could be used directly for writing and printing by a commercial ink-jet printer, as shown in Fig. 16.2e (Li, Zhu, et al., 2017).

The fire-resistant paper can be obtained by using ultralong hydroxyapatite nanowires as the main building material, and glass microfibers and a certain amount of aramid fibers or cellulose fibers as the minor building materials (Dong et al., 2019; Dong & Zhu, 2020; Wang, Zhu, et al., 2022). Dong et al. (2019) reported a new kind of fire-retardant and high-temperature-resistant label paper consisting of ultralong hydroxyapatite nanowires and aramid fibers. The tensile strength, smoothness, and oxygen index of the as-prepared label paper with a hydroxyapatite/aramid weight ratio of 4:1 were 9.2 MPa, 904 s and 76.8%, respectively, greatly higher than those of the pure aramid fiber paper (3.6 MPa, 62.2 s, and 27.6%). By addition of aramid nanofibers instead of aramid microfibers, the mechanical properties of the as-prepared fire-resistant paper can be further enhanced. Wang, Zhu, et al. (2022) prepared a highly flexible, thermally stable, and fire-retardant nanocomposite paper consisting of ultralong hydroxyapatite nanowires and aramid nanofibers with superior properties compared with the commercial Nomex T410 electrical insulation paper.

Dong and Zhu (2020) reported a highly smooth and glossy fire-retardant paper with ultrahigh smoothness and high glossiness consisting of ultralong hydroxyapatite nanowires, cellulose fibers, and inorganic adhesive (Fig. 16.3a). They found that

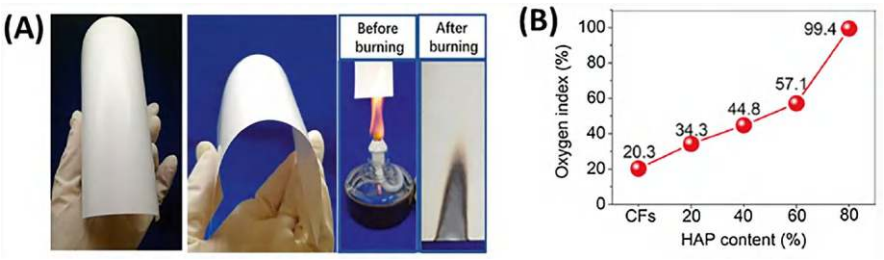

Fig. 16.3 The fire-retardant paper with ultrahigh smoothness and high glossiness consisting of ultralong hydroxyapatite nanowires, cellulose fibers, and inorganic adhesive. (**a**) Digital images. (**b**) Oxygen index values. Reprinted with permission from Dong and Zhu (2020). Copyright 2020: American Chemical Society

the addition of ultralong hydroxyapatite nanowires could enhance the fire-retardant performance, smoothness, and glossiness of the cellulose fiber paper. The oxygen index of the highly smooth and glossy fire-retardant paper increased with increasing content of ultralong hydroxyapatite nanowires, as shown in Fig. 16.3b. The smoothness and oxygen index of the highly smooth and glossy fire-retardant paper with 80 wt.% ultralong hydroxyapatite nanowires could reach as high as 1250 s and 99.4%, respectively. When the content of ultralong hydroxyapatite nanowires was 20% and 80%, the tensile strength of the highly smooth and glossy fire-retardant paper was 38.5 and 22.9 MPa, respectively.

Although the chemical composition of hydroxyapatite is different from those of plant fibers, the hydroxyl groups on the surface of ultralong hydroxyapatite nanowires can form hydrogen bonds between nanowires, similar to hydrogen bonds formed between cellulose fibers. The wet-end chemical properties of the ultralong hydroxyapatite nanowire pulp are crucial to the papermaking and properties of the as-prepared fire-resistant paper. It is necessary to investigate how these factors affect the dispersion and flocculation properties of the ultralong hydroxyapatite nanowire paper pulp, as these will influence the working ability of the paper machine, and determine the properties of the fire-resistant paper, such as the basis weight, thickness, tightness, mechanical strength, thermal conductivity, electrical insulation property, etc. (Dong et al., 2022).

In order to expand the applications, the functionalization of the fire-resistant paper based on ultralong hydroxyapatite nanowires is a useful strategy. Up until now, the author's research group has successfully developed more than 20 new types of fire-resistant paper based on ultralong hydroxyapatite nanowires with various functions. For example, the waterproof fire-resistant paper, fire-resistant "Xuan paper," high-temperature-resistant label paper, antibacterial fire-resistant paper, waterproof photoluminescent fire-resistant paper, waterproof electrically conductive fire-resistant paper, catalytic fire-resistant paper, waterproof magnetic fire-resistant paper, automatic fire-alarm fire-resistant wallpaper, photothermal fire-resistant paper, high-temperature-resistant battery separator, fire-resistant paper tape for electric cables and fiber-optic cables, secret information encryption and decryption fire-resistant paper, light-driven self-propelled waterproof fire-resistant paper, water purification filter paper, air purification filter paper, biomedical paper, antibacterial biomedical paper, rapid test paper, etc. (Zhu, 2021a, 2021b). More details of these functionalized fire-resistant paper based on ultralong hydroxyapatite nanowires will be discussed in Sect. 16.4.

16.3.2 Fire-Resistant Paper Based on Ultralong Nanowires of Cadmium Phosphate Hydroxide

Cadmium phosphate hydroxide ($Cd_5(PO_4)_3(OH)$) (cadmium hydroxyapatite) is formed by the complete substitution of Ca^{2+} ions of calcium hydroxyapatite with Cd^{2+} ions. The radius of Cd^{2+} ion is 0.095 nm and is slightly smaller than Ca^{2+} ion (0.100 nm). Cadmium phosphate hydroxide shows a similar structure to calcium hydroxyapatite, but its structure is slightly contracted due to the smaller diameter of Cd^{2+} ion than Ca^{2+} ion (Yasukawa et al., 2001).

Recently, the Zhu's research group developed the cadmium oleate precursor hydrothermal method for the synthesis of ultralong nanowires of cadmium phosphate hydroxide (Chen, Zhu, & Xiong, 2024). In this method, water-soluble cadmium salt is used as the cadmium source, water-soluble phosphate is used as the phosphorus source, and sodium oleate is adopted as a reactant to form cadmium oleate precursor and as a structure-directing agent. By using this method, ultralong nanowires of cadmium phosphate hydroxide were synthesized using $CdCl_2$, sodium oleate, and NaH_2PO_4 as reactants in an aqueous solution by hydrothermal treatment at 180 °C for 24 h. The as-prepared ultralong nanowires of cadmium phosphate hydroxide possessed diameters of <100 nm and lengths of several hundred micrometers, and their aspect ratios were high (>1000) with a high flexibility. In addition, a flexible inorganic fire-resistant paper was prepared using ultralong nanowires of cadmium phosphate hydroxide as the building material by the vacuum-assisted filtration method, and it exhibited a high whiteness without bleaching, and it was nonflammable and could maintain its structural integrity even after heating by the alcohol lamp (Chen, Zhu, & Xiong, 2024).

16.3.3 Fire-Resistant Paper Based on Barium Sulfate Nanofibers

As one of the members of calcium phosphate family, hydroxyapatite is stable in the neutral, weakly acidic, and alkali environments; however, it is soluble in the strongly acidic aqueous solution. Although the fire-resistant paper based on ultralong hydroxyapatite nanowires shows a high resistance to strong alkalis, it is susceptible to the attack of strong acids, and this weakness limits its applications in strong acid environments.

Barium sulfate is a promising building material for the acid/alkali-proof fire-resistant paper because it has a high melting point of 1580 °C and high chemical stability in strong acids and strong alkalis. Furthermore, barium sulfate exhibits a good biosecurity, and it is widely used as a gastrointestinal contrast agent in medical tests. The author's research group developed the barium oleate precursor hydrothermal method for the synthesis of barium sulfate fibers self-assembled with nanorods in a large scale (using a 10-L stainless steel autoclave) (Wu & Zhu, 2021). The

as-prepared barium sulfate fibers were constructed by parallel self-assembled nanorods with diameters of ~20 nm and lengths of 50–150 nm. The barium sulfate fibers had lengths up to several hundred micrometers and diameters of ~1 μm.

The acid/alkali-proof inorganic fire-resistant paper was prepared using barium sulfate fibers constructed by self-assembly of barium sulfate nanorods along the longitudinal direction. The as-prepared acid/alkali-proof inorganic fire-resistant paper exhibited high flexibility, high whiteness, smooth surface, good mechanical strength, and excellent resistance to harsh conditions such as fire, high temperature, strong acid, and strong alkali. In addition, the acid/alkali-proof inorganic fire-resistant paper could be used for writing and color printing by a commercial ink-jet printer. The text and graphic pattern with various colors could be finely printed on the acid/alkali-proof inorganic fire-resistant paper. The acid/alkali-proof inorganic fire-resistant paper consisting of pure barium sulfate nanorods-assembled fibers exhibited a low mechanical strength. Therefore, glass fibers and inorganic adhesive developed by the authors' laboratory were adopted to fabricate the high-strength acid/alkali-proof inorganic fire-resistant paper. The mechanical properties of the acid/alkali-proof inorganic fire-resistant paper could be adjusted by varying the composition of the paper. The tensile strength and fracture strain of the as-prepared acid/alkali-proof inorganic fire-resistant paper were 11.9 MPa and 4%, respectively.

The acid/alkali-proof inorganic fire-resistant paper was nonflammable. The acid/alkali-proof inorganic fire-resistant paper caught fire in 0.5 s once it was placed on the flame of a spirit lamp due to adsorbed oleate groups on the surface of barium sulfate fibers. The fire extinguished rapidly after adsorbed oleate groups were burned out. The color of the acid/alkali-proof inorganic fire-resistant paper turned from white to gray because of the formation of carbon particles. The experimental results demonstrated that the acid/alkali-proof inorganic fire-resistant paper possessed excellent fire-resistant performance and high thermal stability.

The acid/alkali-proof inorganic fire-resistant paper exhibited excellent acid-resistant performance. The acid/alkali-proof inorganic fire-resistant paper could be preserved well in the strong acid (1 mol L^{-1} HCl aqueous solution). In comparison, the ultralong hydroxyapatite nanowire fire-resistant paper dissolved within 52 s, and only insoluble glass fibers remained, indicating that the acid/alkali-proof inorganic fire-resistant paper possessed excellent corrosion resistance to strong acids. In addition, the acid/alkali-proof inorganic fire-resistant paper could be well preserved in 1 mol L^{-1} NaOH aqueous solution after 217 s, demonstrating that the acid/alkali-proof inorganic fire-resistant paper exhibited excellent corrosion resistance to strong alkalis (Wu & Zhu, 2021). Therefore, this novel kind of acid/alkali-proof inorganic fire-resistant paper has promising applications under various extreme conditions, such as high temperatures, strongly acidic environments, and strongly alkali circumstances.

16.3.4 Fire-Resistant Paper Based on Silicon Compound Fibers

Zhang, Xu, et al. (2020) reported a superhydrophobic and fire-retardant paper using electrospun fluorinated SiO_2 fibers and methyl silicone resin as building materials by vacuum filtration, and it exhibited a good writing performance using a commercial ink of inorganic pigment. Liu et al. (2023) reported a flexible fire-retardant and hydrophobic paper consisting of Si_3N_4@polydimethylsiloxane core-shell fibers with a tensile strength of 6.19 MPa. The Si_3N_4@polydimethylsiloxane paper exhibited water contact angles of larger than 110° after mechanical damage, chemical corrosion, and thermal treatment, and could be applied in oil/water separation and oil collection.

16.4 Applications of the Fire-Resistant Paper

Among various kinds of the fire-resistant paper reported in the literature, the fire-resistant paper based on ultralong hydroxyapatite nanowires is especially important, and it has many advantages, such as high flexibility, high biocompatibility, high-quality natural white color without bleaching, high surface smoothness without surface sizing, environment friendliness, excellent resistance to both fire and high temperature, etc. The fire-resistant paper based on ultralong hydroxyapatite nanowires has the same functions as the traditional paper based on cellulose fibers, such as writing and printing. Furthermore, the fire-resistant paper based on ultralong hydroxyapatite nanowires has functions such as excellent resistance to both high temperature and fire, which the traditional paper does not have. Thus, the fire-resistant paper based on ultralong hydroxyapatite nanowires has promising applications in various fields such as biomedical, environmental, energy, electronics, and information technology. In order to expand its applications, the functionalization of the fire-resistant paper is a useful strategy. Next, we will focus on the applications of the fire-resistant paper based on ultralong hydroxyapatite nanowires.

16.4.1 Long-Term Safe Preservation of Important Archives, Art Works, and Books

In contrast to the flammable traditional paper based on cellulose fibers, the fire-resistant paper based on ultralong hydroxyapatite nanowires is nonflammable and high-temperature-resistant and can be used for writing and printing. Therefore, the fire-resistant paper based on ultralong hydroxyapatite nanowires can be used for long-term safe preservation of important archives, documents, art works, and books. In addition to excellent resistance to both fire and high temperature, the fire-resistant

paper based on ultralong hydroxyapatite nanowires has excellent heat insulation performance, thus, it can be used as the fire-resistant cover for traditional flammable paper-based archives, documents, books, and art works, to protect these flammable paper products from being ruined by fire and high temperature.

Among various kinds of paper, Xuan paper is an excellent representative of traditional handmade paper sheets. Xuan paper is the most durable paper and enjoys a great reputation as "the king of paper that lasts for a 1000 years." Xuan paper is the best material carrier for calligraphy and paintings. Many famous ancient calligraphy and painting works and books using Xuan paper have been well preserved and survive even today. The organic origin of Xuan paper leads to the paper degradation, yellowing, and deteriorating during the long-term natural aging process. One main problem of the traditional Xuan paper is its high flammability, and numerous precious calligraphy and painting works and books were burned to ashes in fire in the past centuries (Dong & Zhu, 2018).

The author's research group developed a new kind of highly flexible inorganic fire-resistant analogous Xuan paper based on ultralong hydroxyapatite nanowires with high whiteness, excellent resistance to fire and high temperature, superdurability of thousands of years, unique ink wetting, and excellent anti-mildew benefiting from its 100% inorganic origin, which are far superior over the traditional Xuan paper (Fig. 16.4) (Dong & Zhu, 2018). The thermal stability tests showed that the traditional Xuan paper turned yellow at 200 °C and heavily carbonized to ashes at 400 °C after 30 min. However, the inorganic fire-resistant analogous Xuan paper had no obvious change in both color and dimension at temperatures ranging from

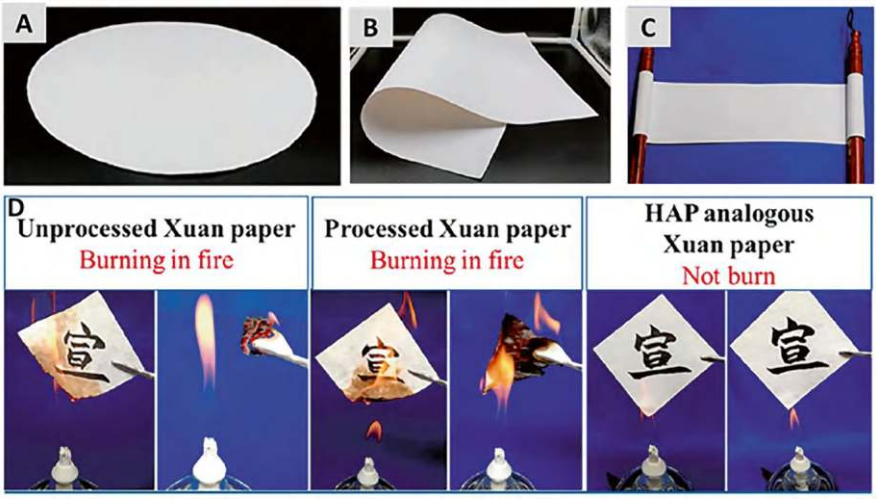

Fig. 16.4 (**a**–**c**) Digital images of the highly flexible inorganic fire-resistant analogous Xuan paper sheets based on ultralong hydroxyapatite nanowires with a diameter of 20 cm and the A3 size (297 × 420 mm). (**d**) Fire resistance tests of the commercial unprocessed Xuan paper, commercial processed Xuan paper, and inorganic fire-resistant analogous Xuan paper. Reprinted with permission from Dong and Zhu (2018), Copyright 2018: American Chemical Society

200 °C to 1000 °C. Although the tensile strength of the inorganic fire-resistant analogous Xuan paper decreased after heat treatment at high temperatures, a tensile strength retention rate of 98.4% was achieved after heat treatment at 200 °C for 30 min, and 77.5% after heat treatment at 400 °C for 30 min (Dong & Zhu, 2018).

The as-prepared inorganic fire-resistant analogous Xuan paper exhibited the unique ink wetting behavior and different from those on the traditional Xuan paper. The ink droplet spread slightly on the inorganic fire-resistant analogous Xuan paper but did not penetrate through the paper, and no ink was observed on the back side of the paper, and the edges of ink and strokes were smooth. The inorganic fire-resistant analogous Xuan paper was superhydrophilic with a water contact angle of 0° and an ink contact angle of 36.9°, and the diffusion of water and ink constituents was not simultaneous, and the water in the ink diffused more rapidly than the ink constituents. This unique phenomenon could lead to faster drying of the ink on the inorganic fire-resistant analogous Xuan paper than on the traditional processed Xuan paper (Dong & Zhu, 2018). In addition, a nanocomposite Xuan paper comprising ultralong hydroxyapatite nanowires and plant cellulose fibers was reported with unique ink wetting performance, high whiteness, and excellent durability (Shao et al., 2019).

Mold is an important factor for the deterioration of traditional Xuan paper. The prevention of mold growth on the paper is vital for its long-term safe preservation. During the normal storage of calligraphy works and paintings, the surface of Xuan paper is easily polluted by the organic pollutants in air. The experiments indicated that three kinds of mold spores could not breed and spread on the inorganic fire-resistant analogous Xuan paper, and it could preserve a clean surface without the growth of mold, indicating its excellent anti-mildew performance even in the presence of external nutrients. On the contrary, mold could grow and spread on both commercial unprocessed and processed Xuan paper sheets in Bengal culture medium, indicating that the anti-mildew performance of the traditional Xuan paper was not satisfactory in the presence of external nutrients (Dong & Zhu, 2018; Shao et al., 2021).

The durable performance of paper is extremely important for its long-term safe preservation. It was estimated that the lifetime of newspapers was about 150–300 years. Although Xuan paper was more durable, it showed significant degradation and deteriorated properties during the long-term natural aging process. In contrast, the inorganic fire-resistant analogous Xuan paper exhibited isotropic mechanical properties, and the tensile strength was the same along different directions. The tensile strength retention rate of the inorganic fire-resistant analogous Xuan paper was 95.2% after simulated aging for 2000 years and was 81.3% after simulated aging for 3000 years. The tensile strength of the traditional Xuan paper usually depends on the orientation along the longitudinal direction (LD) or transverse direction (TD). The tensile strength retention rate of the commercial unprocessed Xuan paper was only 61.2% (TD) and 48.6% (LD) after simulated aging for 2000 years and was only 38% (TD) and 42.8% (LD) after simulated aging for 3000 years. For commercial processed Xuan paper, the tensile strength retention rate was 56.7% (TD) and 81.5% (LD) after simulated aging for 2000 years, and 52.7% (TD) and 58.9% (LD) after simulated aging for 3000 years. The inorganic

fire-resistant analogous Xuan paper exhibited a much higher tensile strength retention rate (95.2%) than commercial unprocessed Xuan paper (average 54.9%) and processed Xuan paper (average 69.1%) after simulated aging for 2000 years. The tensile strength retention rate for the inorganic fire-resistant analogous Xuan paper was 81.3% after simulated aging for 3000 years; however, it was 40.4% on average for the commercial unprocessed Xuan paper and 55.8% for the commercial processed Xuan paper (Dong & Zhu, 2018).

The stability of whiteness is another important factor for the paper. The whiteness of the inorganic fire-resistant analogous Xuan paper before aging was very high (92%), much higher than that of traditional Xuan paper (~70%). The whiteness of the traditional Xuan paper obviously reduced during the simulated aging process. The whiteness decreased from an initial 70.5% to 47.3% and to 42.2% with a whiteness retention rate of 67.1% and 59.9% for the commercial unprocessed Xuan paper after simulated aging for 2000 and 3000 years, respectively, and from an initial 70.1% to 46.4% and to 40.6% with a whiteness retention rate of 66.2% and 57.9% for the commercial processed Xuan paper after simulated aging for 2000 and 3000 years, respectively. However, the whiteness of the inorganic fire-resistant analogous Xuan paper exhibited a slight decrease from the initial 92% to 91.6% and to 86.7% with a whiteness retention rate as high as 99.6% and 94.2% after simulated aging for 2000 and 3000 years, respectively. The whiteness (86.7%) of the inorganic fire-resistant analogous Xuan paper after simulated aging for 3000 years was still much higher than that of the traditional Xuan paper before aging (~70%), indicating the excellent whiteness stability of the inorganic fire-resistant analogous Xuan paper even after the simulated aging for thousands of years (Dong & Zhu, 2018).

16.4.2 Fire-Resistant Wallpaper for Interior Decoration of Houses

Nowadays, wallpaper is more and more popular in the interior decoration of houses. However, many kinds of wallpaper currently on the market are usually made from flammable plant fibers or synthetic polymers and have safety concerns. Furthermore, fire alarm systems are essential for fire warning and rescue. If the fire alarm system can be integrated on the fire-resistant wallpaper, the fire alarm can be sent out in a timely manner to avoid personnel casualties and property loss. Therefore, the smart fire alarm fire-resistant wallpaper is desirable because it can simultaneously prevent the fire from spreading and send out immediate alerts in a fire disaster.

Recently, the author's research group developed a smart automatic fire alarm fire-resistant wallpaper consisting of the inorganic fire-resistant paper based on ultralong hydroxyapatite nanowires, and a graphene oxide thermosensitive sensor that could rapidly respond to the high temperature of fire (Chen et al., 2018). Graphene oxide possessed abundant oxygen-containing groups, thus the graphene oxide thermosensitive sensor was in a state of electrical insulation at room

temperature, however, at high temperatures it became electrically conductive because the oxygen-containing groups of graphene oxide could be rapidly removed, resulting in the transformation of graphene oxide from an electrically insulated state into a highly conductive one. In this way, the alarm lamp and buzzer connected with the graphene oxide thermosensitive sensor could send out the alerts to people immediately for taking emergency actions. The thermal responsive temperature of the polydopamine-modified graphene oxide thermosensitive sensor was 126.9 °C, which was much lower than that of the graphene oxide thermosensitive sensor (231.3 °C). Furthermore, the polydopamine-modified graphene oxide thermosensitive sensor could rapidly respond to the high temperature of fire (only several seconds), and it could steadily work and send out an alarm in the flame for at least 5 min.

He et al. (2023) improved the performance of the graphene oxide fire warning sensor. They prepared an asymmetric nanocomposite paper based on color and resistance switching. The top surface of the nanocomposite paper was composed of ultralong hydroxyapatite nanowires and poly(pentacosadiynoic acid), which could send out the alarm by a color change from purple to red at 55 °C due to the conformational distortion of the poly(pentacosadiynoic acid) backbone. Furthermore, the bottom surface of the nanocomposite paper consisted of ultralong hydroxyapatite nanowires and 3-aminopropyltriethoxysilane-modified graphene oxide nanosheets, which could give the alarm within 1 s in fire by electrical resistance change due to the thermal reduction of graphene oxide. It was found that 3-aminopropyltriethoxysilane could significantly improve the flame retardancy of graphene oxide by releasing nonflammable gases and producing a protective solid barrier.

16.4.3 High-Temperature-Resistant Label Paper

High-temperature-resistant label paper is usually used in high-temperature environments. The commercial high-temperature-resistant label paper products are usually made of polymers and other organic substances, which have disadvantages such as poor high-temperature resistance and unsatisfactory fire-resistant properties. In some cases, the surface of the paper made from cellulose fibers is coated with the high-temperature-resistant coating to prepare the high-temperature-resistant label paper.

The fire-resistant paper made from ultralong hydroxyapatite nanowires has excellent resistance to both fire and high temperature with excellent thermal stability and can be used as the high-performance high-temperature-resistant label paper, which can withstand high temperatures (>1000 °C). Moreover, the authors' research group also developed a high-temperature-resistant label paper consisting of ultralong hydroxyapatite nanowires, aramid fibers, and inorganic adhesive. The as-prepared high-temperature-resistant label paper exhibited excellent fire-retardant and high-temperature-resistant properties. The oxygen index of the pure aramid fiber paper without ultralong hydroxyapatite nanowires was 27.6%, and the oxygen index of the high-temperature-resistant label paper significantly increased with increasing

hydroxyapatite/aramid weight ratio, and it was 32.2%, 34.9%, 43.4%, and 76.8% when the hydroxyapatite/aramid weight ratio was 1:4, 2:3, 3:2, and 4:1, respectively (Dong et al., 2019).

The thermal stability performance of the as-prepared high-temperature-resistant label paper was compared with that of the commercial high-temperature-resistant label paper. During the heating process, the whiteness of the as-prepared high-temperature-resistant label paper gradually decreased with increasing heating temperature for 30 min, but the dimension of the label paper had no obvious change. However, the white color of the commercial high-temperature-resistant label paper greatly deteriorated at 300 °C; it was totally carbonized and turned black at 400 °C for 30 min and burned to ashes at 500 °C for 30 min. The as-prepared high-temperature-resistant label paper exhibited excellent thermal stability and is promising for applications in various high-temperature environments.

16.4.4 Protection for Fiber Optic/Electric Cables

With the rapid development of the communication technology, electric cables and fiber-optic cables are widely used in various fields. In recent years, fire-resistant electric cables and fiber-optic cables are in high demand. Recently, the authors' research group developed a fire-resistant paper tape made from ultralong hydroxyapatite nanowires, glass fibers, and inorganic adhesive as the fireproof and heat insulation protection layer for fireproof electric cables and fiber-optic cables (Dong & Zhu, 2017). Compared with conventional heat insulation materials, such as the glass fiber paper and aluminum silicate fiber paper, the as-prepared fire-resistant paper tape exhibited superior mechanical properties (tensile strength ~16 MPa) and smooth surface. In addition, the fire-resistant paper tape possessed excellent nonflammability, high thermal stability, low thermal conductivity, and excellent heat insulation performance. The thermal conductivity of the fire-resistant paper tape with 80 wt.% ultralong hydroxyapatite nanowires was 0.10 W m^{-1} K^{-1} (25 °C) and 0.14 W m^{-1} K^{-1} (600 °C).

Compared with other kinds of protection materials for the fire-retardant electric cables and fiber-optic cables, the fire-resistant paper tape exhibited much better fire-resistant and heat insulation properties. Without the heat insulation protection layer, the temperature increased rapidly with increasing heating time by an alcohol lamp, and the temperature was ~687 °C after heating for 5 min. In comparison, using the fire-resistant paper tape as the protection layer, the temperature increased slowly and was 376 °C after heating for 5 min, which is 311 °C lower than that without using the fire-resistant paper tape as a protection layer. Other kinds of the protection materials were also tested, such as the glass fiber paper, polyolefin fire-retardant belt, and mica tape, which possessed similar thickness to that of the fire-resistant paper tape. The temperatures for the glass fiber paper, polyolefin fire-retardant belt, and mica tape were 589 °C, 580 °C, and 525 °C, respectively, after heating for 5 min. In addition, the fire-resistant paper tape was intact after

heating, but other traditional protection materials were damaged to some extent (Dong & Zhu, 2017).

16.4.5 Energy-Related Applications

The current commercial lithium-ion battery separators are mainly organic polyolefin separators. However, the polyolefin battery separators exhibit poor wettability with the electrolytes, low porosity, high internal electric resistance, poor thermal stability, and potential risks of short circuit, fire, or even explosion accidents.

Recently, the authors' research group investigated the energy-related applications of the fire-resistant paper based on ultralong hydroxyapatite nanowires, for example, as a high-temperature-resistant separator for advanced lithium-ion batteries (Li, Wu, et al., 2017). The as-prepared high-temperature-resistant separator exhibited a high flexibility, high porosity (~81%), narrow pore size distribution (~110–130 nm), high thermal stability, good fire resistance, excellent electrolyte wettability, high electrolyte absorption capacity (253%), and superior electrochemical properties, which can ensure high safety of the battery. The tensile strength of the polypropylene separator decreased rapidly with increasing temperature, and the thermal shrinkage rate for the polypropylene separator was more than 90% at 200 °C. In comparison, the ultralong hydroxyapatite nanowire-based high-temperature-resistant separators showed nearly zero shrinkage from room temperature to 200 °C. The ionic conductivity was 3.05 mS cm^{-1} for the high-temperature-resistant separator based on ultralong hydroxyapatite nanowires, which was about seven times that of the commercial polypropylene separator (0.43 mS cm^{-1}). The lithium-ion transport number of the polypropylene separator, high-temperature-resistant separator was 0.35 and 0.54, respectively. The higher lithium-ion transport number of the separator based on ultralong hydroxyapatite nanowires indicated the higher Li^+ ion transport ability.

The cycling performance and rate capability of the $LiFePO_4$/separator/Li half cells assembled using the high-temperature-resistant separator and commercial polypropylene separator were investigated. The cell with the high-temperature-resistant separator exhibited an initial discharge capacity of 138 mA h g^{-1}, which was higher than that using the polypropylene separator (130.1 mA h g^{-1}) at 0.5 °C. During the cycling process, the cell with the high-temperature-resistant separator exhibited a higher discharge capacity of 135.4 mA h g^{-1} than that of the polypropylene separator (129.5 mA h g^{-1}) after 145 cycles at 1 °C, revealing superior cyclability of the high-temperature-resistant separator. The $LiFePO_4$/separator/Li half cells at different current densities indicated that a capacity retention of 85.7% was obtained for the cell with the high-temperature-resistant separator at 5 °C. In comparison, the capacity retention was only 65.7% for the cell with the polypropylene separator. The discharge capacity of the cell with the high-temperature-resistant separator was ~117.2 mA h g^{-1}, which was 1.4 times that of the cell

with the polypropylene separator (83 mA h g^{-1}) at 5 °C. Furthermore, the cell with the high-temperature-resistant separator showed a better recycling performance and rate capability using the working electrode of graphite compared with the commercial polypropylene separator. The discharge capacity of the cell with the high-temperature-resistant separator was ~421 mA h g^{-1}, which was higher than that with the polypropylene separator (386 mA h g^{-1}) after 150 cycles at 0.5 °C. The cell with the high-temperature-resistant separator exhibited a much better rate capability (175 mA h g^{-1} at 5 °C) than that with the polypropylene separator (101.5 mA h g^{-1}).

The open-circuit voltage of the $LiFePO_4$/separator/Li battery with the commercial polypropylene separator rapidly reduced to zero in 20 min at 150 °C because of the internal short circuit caused by thermal shrinkage of the polypropylene separator. However, the $LiFePO_4$/separator/Li battery with the high-temperature-resistant separator could maintain its initial voltage throughout the whole testing process at 150 °C for 2 h. The high-safety batteries that can work at high temperatures above 100 °C are urgently needed for applications in various special fields. The battery prepared using the high-temperature-resistant separator showed a high thermal stability and good recycling performance at 150 °C, and the average Coulombic efficiency was >98%. Furthermore, a higher discharge capacity of 157.8 mA h g^{-1} was obtained for the battery with the high-temperature-resistant separator compared with that at room temperature (138 mA h g^{-1}) owing to increased ion diffusion rate and reduced interfacial resistance at high temperatures. The battery prepared with the high-temperature-resistant separator could continuously light up two 3.0 V small lamps at 150 °C, indicating the excellent thermal stability of the high-temperature-resistant separator based on ultralong hydroxyapatite nanowires and the great potential for the application in high-temperature-resistant and high-safety advanced batteries (Li, Wu, et al., 2017). The high thermal stability of the high-temperature-resistant separators based on ultralong hydroxyapatite nanowires can greatly enhance the safety of the batteries working at high temperatures and significantly widen their applications of lithium-ion batteries and other kinds of batteries, especially in high-temperature environments.

The reliability and durability of lithium-ion capacitors are severely limited by the kinetic imbalance between capacitive and Faradaic electrodes. Efficient charge storage in lithium-ion capacitors is still a great challenge, particularly for thick electrodes with high mass loading, fast charge delivery, and harsh working conditions. Recently, the authors' research group reported a superior thermally stable high-energy-density lithium-ion capacitor with an ultralong hydroxyapatite nanowire-based separator and electrodes ($Li_4Ti_5O_{12}$-based anode and activated carbon-based cathode), which showed much enhanced electrochemical kinetics and properties, especially at high current rates and temperatures, and could achieve a long cycling lifetime, high energy density, high power density, and high areal energy density at a high active material mass loading of 30 mg cm^{-2}, and it possessed a high thermal durability and could work at high temperatures (Li et al., 2019).

16.4.6 Fire-Resistant and Thermally Stable Flexible Electronic Devices

With the increasing popularity of modern electronic devices, high-performance and high-safety electrically insulating materials with good mechanical flexibility and strength, high thermal stability and fire resistance are urgently needed. Recently, the authors' research group reported a highly flexible, thermally stable, and fire-retardant nanocomposite paper with high dielectric breakdown strength and mechanical strength prepared using ultralong hydroxyapatite nanowires and aramid nanofibers as building materials by the vacuum-assisted filtration method. The as-prepared fire-retardant nanocomposite paper exhibited a nanowire/nanofiber networked porous framework and layered structure, excellent flexibility, high tensile strength (73.5 MPa), fracture strain (7.4%), folding durability (1396 times under a loading weight of 9.8 N), and good processibility. In addition, the fire-retardant nanocomposite paper showed a superior dielectric breakdown strength (92.4 kV mm^{-1}), high thermal stability, and flame retardancy in comparison with the commercial Nomex T410 electrical insulation paper (Wang, Zhu, et al., 2022). The as-prepared multifunctional fire-retardant nanocomposite paper is promising for applications in miniaturized and flexible electronic devices, high-voltage electrical insulation equipments, and fire-retardant and high-temperature fields.

A specific scene was designed to verify the potential application of the fire-retardant nanocomposite paper consisting of ultralong hydroxyapatite nanowires and aramid nanofibers in the protection of electronic devices in a simulative fire environment. A thermistor with the negative temperature coefficient was placed on the surface of the fire-retardant nanocomposite paper, and the thermistor was connected with the electrical circuit. Subsequently, the thermistor was protected by the fire-retardant nanocomposite paper from the alcohol flame, and the electrical current in the circuit was measured by a multimeter during the testing process. The electrical current increased until it reached the maximum value with increasing heating time under the protection of the fire-retardant nanocomposite paper, and the electrical current reached ~183 mA after heating for 10 min. In comparison, the electrical current increased more rapidly when the thermistor was unprotected by the fire-retardant nanocomposite paper. The surface topography and color of the thermistor without the protection of the fire-retardant nanocomposite paper significantly changed after the heating test. The back side of the thermistor was scorched and cracked, and the color of the front surface changed from black to grey. In contrast, the thermistor maintained its full shape and initial surface, and the color of the front and back surfaces of the thermistor was still black with the protection of the fire-retardant nanocomposite paper after the heating test, indicating the excellent flame-retardant and heat-insulating performance of the fire-retardant nanocomposite paper. The temperature of the thermocouple increased rapidly with the heating time in the alcohol flame, and the temperature was ~619 °C after heating for 10 min without the heat-insulation protection of the fire-retardant nanocomposite paper. In contrast, using the fire-retardant nanocomposite paper as the protection layer, the

temperature of the thermocouple increased more slowly and was ~376 °C after heating for 10 min. Thus, the nanocomposite paper is promising for the applications as the electric packaging paper, high temperature-resistant and fire-retardant paper in flexible electronic devices, high-power electrical equipment, and fire-retardant fields, etc. (Wang, Zhu, et al., 2022).

16.4.7 Anti-Counterfeiting

The authors' research group reported the waterproof photoluminescent fire-resistant paper prepared using rare earth ion-doped sodium oleate-modified ultralong hydroxyapatite nanowires for the application in multimode anti-counterfeiting (Yang et al., 2017). The waterproof photoluminescent fire-resistant paper sheets were white under visible light; however, they exhibited different colors under UV irradiation (~365 nm), they showed a strong green color (doped with Tb^{3+} ions) or red color (doped with Eu^{3+} ions) under irradiation with a UV lamp (~365 nm), and their photoluminescence properties could be tuned through adjusting the weight ratio of Eu^{3+}-doped ultralong hydroxyapatite nanowires to Tb^{3+}-doped ultralong hydroxyapatite nanowires. Furthermore, predesigned special patterns could be hidden in the waterproof photoluminescent fire-resistant paper, and these hidden patterns were not visible under visible light, but they could be seen under UV irradiation, that is, the visibility of the predesigned patterns could be turned on and off using a single UV lamp for the anti-counterfeiting purpose. In addition, the waterproof photoluminescent fire-resistant paper exhibited a high thermal stability and fire resistance, and its photoluminescence intensity and whiteness showed almost no change after thermal treatment at 300 °C for 1 h (Yang et al., 2017).

Security inks based on photoluminescent materials are mostly investigated for security applications, such as information encryption and decryption, and anti-counterfeiting. Although security inks are invisible to the naked eyes under ambient light, they can be detected under ultraviolet or near-infrared light. Zhu's research group reported a new kind of secret paper consisting of ultralong hydroxyapatite nanowires and cellulose fibers. They adopted white vinegar, a common cooking ingredient, as an invisible security ink. The information written with white vinegar on the secret paper was totally invisible under natural light, but it was decrypted and clearly read after exposure to fire, and the response time to fire was short (<10 s). The writing on the secret paper was easy and could be realized using various pens loaded with white vinegar (Chen et al., 2019).

16.4.8 Environment-Related Applications

16.4.8.1 Recyclable Adsorption Paper for Removal of Organic Compounds and Rapid Separation of Water and Oil

The hydrophobic fire-resistant paper consisting of oleate-adsorbed ultralong hydroxyapatite nanowires exhibited high adsorption capacities for various organic pollutants, for example, a high adsorption capacity of 7.3 g g^{-1} for chloroform, and it could also be used as a filler to make a filtration column for the treatment of a mixture of organic pollutants and water. When a mixture of toluene and water was added into the filtration column, water went through the fire-resistant paper filler, whereas toluene was adsorbed completely by the filler. By this simple and rapid procedure, toluene could be completely separated from water and the polluted water was effectively purified (Lu et al., 2014). Furthermore, the fire-resistant paper with adsorbed organic compounds could be easily recovered and regenerated by heating in a distillation unit or by burning in fire, and the adsorbed organic solvents could be completely removed from the fire-resistant paper for recycling. No visible damage to the fire-resistant paper was observed after many cycles of organic solvent removal. The regenerated fire-resistant paper could be reused for the adsorption of organic pollutants and exhibited similar adsorption capacities compared with the freshly prepared fire-resistant paper, exhibiting excellent recyclability, and has promising applications in treating various organic pollutants (Lu et al., 2014). The superhydrophobic fire-resistant paper based on oleate-adsorbed ultralong hydroxyapatite nanowires could effectively adsorb organic solvents such as cyclohexane. For instance, when cyclohexane was dropped onto the water surface in a culture dish, and a piece of the superhydrophobic fire-resistant paper was put on the cyclohexane, cyclohexane could be completely adsorbed by the superhydrophobic fire-resistant paper rapidly, and there was no residual cyclohexane on water after the oil-water separation. In addition, the sizes of the nanopores in the superhydrophobic fire-resistant paper were small enough to prevent solid contaminants from penetrating into the interior space, and the tiny contact area could significantly minimize the adhesion between solid contaminants and the paper surface owing to the superhydrophobicity. Both effects could result in enhanced adhesion between water droplets and solid contaminants; thus, water droplets and water flow could carry and wash away solid contaminants completely on the superhydrophobic fire-resistant paper surface, exhibiting the excellent self-cleaning performance (Chen et al., 2016).

The superhydrophobic mini-paper boat as an oil-collecting device made from the superhydrophobic magnetic fire-resistant paper consisting of magnetic Fe_3O_4 nanoparticles decorated ultralong hydroxyapatite nanowires coated by a polydimethylsiloxane showed a high separation selectivity (>99.0%), high permeation water flux (2924.3 L m^{-2} h^{-1}), and good recycling ability (Yang et al., 2018). The paper mini-boat could be magnetically driven to the oil-polluted region, and the selective collection, convenient transportation, and recovery of oil from water could be realized with a high separation efficiency and good reusability. The superhydrophobic

property could prevent water from permeating into the paper mini-boat and enabled the paper mini-paper boat to float on the water surface. Furthermore, the paper mini-boat could be magnetically driven to the oil-polluted region, and oil could be absorbed and collected automatically by the paper mini-boat. After the oil collection, the paper mini-boat loaded with oil could be actuated by a magnet and transported to the edge of the glass dish. The oil loaded in the paper mini-boat could be easily recovered, and the paper mini-boat could be efficiently recycled for repeated use. The separation efficiencies for isooctane, toluene, petroleum ether, soybean oil, and vacuum pump oil were higher than 99.2%. The superhydrophobic magnetic paper mini-boat could be washed with ethanol and dried for recycling. The high separation efficiency of the superhydrophobic magnetic paper mini-boat for cyclohexane could be well maintained after 10 cycles (Yang et al., 2018).

16.4.8.2 Solar Energy-Driven Photothermal Water Evaporation for Seawater Desalination and Wastewater Purification

The authors' research group developed a photothermal fire-resistant paper composed of ultralong hydroxyapatite nanowires as the thermal insulation support and the light absorber for solar energy-driven photothermal seawater desalination and wastewater purification (Xiong et al., 2018). The highly porous networked structure, excellent high-temperature stability, and fire-resistance merits of the photothermal fire-resistant paper are favorable for solar energy-driven water evaporation. The thermal conductivity of the fire-resistant paper was ~0.1 W m^{-1} K^{-1}, which were significantly lower than that of water (0.6 W m^{-1} K^{-1}). The excellent thermal insulation property of the photothermal fire-resistant paper could effectively minimize the heat loss from the paper surface to bulk water, which could realize the high-performance solar energy-driven water evaporation. The photothermal fire-resistant paper could be used for the generation of fresh drinkable water from seawater and wastewater. The concentrations of sodium chloride in the generated condensed water obtained from five simulated seawater samples after solar energy-driven photothermal desalination using the photothermal fire-resistant paper decreased by three orders of magnitude compared with those of the original solutions, and the ion rejection percentages were >99.95%. The collected clean water using the photothermal fire-resistant paper could meet the standards of healthy drinkable water as defined by the World Health Organization and U.S. Environmental Protection Agency. The photothermal fire-resistant paper could also be used for solar photothermal purification of wastewater containing heavy metal ions, and the concentrations of metal ions in the collected purified water after solar energy-driven photothermal purification using the photothermal fire-resistant paper were <2 μg L^{-1} with metal ion rejection percentages >99.99%. In addition, the photothermal fire-resistant paper could also be used for high-performance solar energy-driven photothermal purification of wastewater containing organic dyes and bacteria (Xiong et al., 2018).

One of the problems for the photothermal water evaporators is the accumulation of salt crystals on the water evaporation surface, which can deteriorate water evaporation performance. Using a hydrophobic surface can prevent the infiltration of salt aqueous solution, and salt ions can be blocked underneath the hydrophobic layer and further diffuse to the bulk solution, resulting in salt rejection and clean water evaporation surface. Zhu's research group developed a flexible salt-rejecting photothermal fire-resistant paper for high-performance solar energy-driven water evaporation and stable seawater desalination without salt accumulation. The salt-rejecting photothermal fire-resistant paper exhibited advantages such as a porous structure, interconnected channels, high mechanical strength, high efficiencies of solar light absorption and photothermal conversion, fast water transportation, good heat insulation, and excellent salt-rejecting ability, which could efficiently produce clean water from seawater and wastewater. Chen, Zhu, Wang, et al. (2024) reported a hydrophilic bilayer photothermal paper-based 3D cone flowing evaporator for stable high-performance seawater desalination with a high salt-rejecting ability. The bilayer photothermal paper consisted of ultralong hydroxyapatite nanowires, MXene ($Ti_3C_2T_x$), poly(acrylic acid), and poly(acrylic acid-2-hydroxyethyl ester). A siphon effect-driven unidirectional fluid transportation unit in the 3D cone flowing evaporator could guide the concentrated saline flowing away from the evaporating surface to prevent salt deposition on the water evaporation surface. Owing to high solar light absorption efficiency, high photothermal conversion efficiency, low water evaporation enthalpy (1838 ± 11 J g^{-1}), and additional energy taken from the ambient environment, the as-prepared cone flowing evaporator exhibited a high water evaporation rate of 3.22 ± 0.20 kg m^{-2} h^{-1} for real seawater under one sun illumination (1 kW m^{-2}), which was significantly higher than many values reported in the literature. Qin et al. (2020) reported a Janus photothermal fire-resistant paper comprising hydrophobic sodium oleate-modified ultralong hydroxyapatite nanowires, glass fibers, and black nickel oxide (NiO) nanoparticles for high-performance salt-rejecting solar energy-driven seawater desalination. With the bottom hydrophobic ultralong hydroxyapatite nanowire layer and water-transporting channels in the air-laid paper to facilitate salt exchange, the as-prepared Janus photothermal evaporator showed no salt accumulation on the evaporation surface, high performance and long-time stable seawater desalination. In addition, the Janus photothermal evaporator with the hydrophobic ultralong hydroxyapatite nanowire substrate could be extended to support other photothermal materials such as black titanium oxide (Ti_2O_3) and Ketjen black carbon with the salt-resistant desalination function.

16.4.8.3 Fire-Resistant Filter Paper for Wastewater Purification

Recently, an environmentally friendly filter paper based on ultralong hydroxyapatite nanowires and cellulose fibers with excellent filtration and adsorption properties was developed for high-performance water purification. The addition of polyamidoamine-epichlorohydrin resin could enhance the wet mechanical strength

of the filter paper, and the addition of cellulose fibers could increase the mechanical strength of the filter paper. Because of the porous structure and superhydrophilicity of the filter paper, the pure water flux was 287.28 L m^{-2} h^{-1} bar^{-1} under cross-flow conditions, which was about 3200 times higher than that of the cellulose fiber paper with addition of polyamidoamine-epichlorohydrin resin. Furthermore, the filter paper exhibited a superior performance in the removal of TiO_2 nanoparticles (>98.61%) and bacteria (up to 100%) in water. The filter paper also showed high adsorption capacities for methyl blue (273.97 mg g^{-1}) and Pb^{2+} ions (508.16 mg g^{-1}) (Zhang, Zhu, Wu, Shao, et al., 2019). In addition, a filter paper with a large number of nanopores and channels is important for highly efficient nanofiltration to significantly increase the water flux without sacrificing the separation efficiency. Zhu's research group (Zhang, Zhu, Wu, & Dong, 2019) reported a nanofiltration filter paper consisting of a cellulose nanofiber barrier layer on the cellulose fiber/ultralong hydroxyapatite nanowire substrate. The porous network formed by the interweaving of cellulose fibers and ultralong hydroxyapatite nanowires provided channels for rapid water transportation. The pure water flux of the cellulose fiber/ultralong hydroxyapatite nanowire filter paper was as high as 544.4 L m^{-2} h^{-1} bar^{-1}, which was about 50 times that of the cellulose nanofiber/ultralong hydroxyapatite nanowire filter paper. Compared with the nanofiltration filter paper based on cellulose nanofibers and ultralong hydroxyapatite nanowires, the pure water flux of the nanofiltration filter paper based on cellulose nanofibers, cellulose fibers, and ultralong hydroxyapatite nanowires was enhanced by 20% with rejection rates above 95% for different dyes. In another work, they prepared a filter paper composed of ultralong hydroxyapatite nanowires, cellulose fibers, and double metal oxide nanosheets to achieve the simultaneous enhancement of both water flux and removal efficiency for high-performance dye separation. Positively charged double metal oxide nanosheets could adsorb negatively charged ultralong hydroxyapatite nanowires and adjust the pore size and water flux of the nanocomposite filter paper. The optimized pure water flux of the nanocomposite filter paper was as high as 783.6 L m^{-2} h^{-1} bar^{-1}, and the optimized rejection percentage and water flux for Congo red were high (98.3% and 736.8 L m^{-2} h^{-1} bar^{-1}, respectively) (Zhang, Zhu, et al., 2020).

16.4.8.4 Filter Paper for Air Purification and Anti-Haze Face Mask

Recently, Zhu's research group (Xiong, Yang, Zhu, Chen, & Dong, 2017) developed an air filter paper consisting of ultralong hydroxyapatite nanowires and cotton fibers by a vacuum-assisted filtration process, and it exhibited high removal efficiencies for $PM_{2.5}$ and PM_{10}. Ultralong hydroxyapatite nanowires intertwined with cotton fibers and formed a highly porous structure of the air filter paper. By optimizing the weight ratio of ultralong hydroxyapatite nanowires and cotton fibers, the air filter paper showed high removal efficiencies of >95% for $PM_{2.5}$ and PM_{10}, and a lower pressure drop and a smaller thickness than commercial breathing masks.

16.4.9 Biomedical Applications

Recently, Zhu's research group proposed a new concept of deformable biomaterials based on highly flexible ultralong hydroxyapatite nanowires, which can overcome the high brittleness and high hardness of the traditional hydroxyapatite biomaterials (Zhu & Lu, 2019). Ultralong hydroxyapatite nanowire-based deformable biomaterials have many advantages, such as excellent deformability, high biocompatibility/bioactivity, good biodegradation, excellent ability for cell adhesion/spreading/proliferation, excellent osteoinduction/osteogenesis/neovascularization, excellent ability of loading and releasing drugs/proteins/growth factors, etc. Deformable biomaterials based on ultralong hydroxyapatite nanowires will extend the range of biomedical applications of hydroxyapatite biomaterials to various fields, such as bone regeneration, artificial periosteum, skin wound healing, biomedical paper, medical test paper, drug delivery, diagnosis, and therapy.

Sun, Zhu, and Chen (2017) prepared highly flexible composite biopaper sheets composed of ultralong hydroxyapatite nanowires and chitosan with ultralong hydroxyapatite nanowires weight ratios ranging from 0 to 100 wt.%. The as-prepared composite biopaper showed excellent mechanical properties (tensile strength 98.93 MPa at 50 wt.% hydroxyapatite nanowires, and 3.53 GPa Young's modulus at 66.7 wt.% hydroxyapatite nanowires). Furthermore, the surface wettability, swelling ratio, and water vapor transmission rate of the biopaper could be adjusted by the weight ratio of ultralong hydroxyapatite nanowires. Therefore, the as-prepared composite biopaper is promising for biomedical applications, such as wound dressing, bone-fracture fixation, bone defect repair, and artificial periosteum. Similarly, a highly flexible biopaper composed of ultralong hydroxyapatite nanowires and collagen with excellent mechanical properties and cellular attachment performance was also reported (Sun, Zhu, Chen, & Zhang, 2017).

The biopaper consisting of ultralong hydroxyapatite nanowires exhibited a high performance in bone regeneration; thus, it is a promising candidate for novel bone therapies; for example, covering a large-sized bone defect area with the biopaper after filling the defect with a conventional bone substitute may prohibit soft tissues from invading to the bone defect area and promote the new bone formation. In addition, the ultralong hydroxyapatite nanowire biopaper may be used as a high-performance artificial periosteum for bone defect repair (Kashiwada et al., 2021). In another research work, a highly flexible biopaper consisting of selenium-doped ultralong hydroxyapatite nanowires and chitosan was investigated for high-performance anti-bone tumor application, which could effectively inhibit the growth of bone tumor. The possible anti-tumor mechanisms of the biopaper were studied in terms of accumulation of reactive oxygen species, activation of apoptosis, and the underlying signal pathway involved. In addition, in vivo evaluations performed using a patient-derived xenograft animal model further revealed the obvious anti-tumor effects of the biopaper (Zhou et al., 2019).

In addition, the highly flexible antibacterial biopaper consisting of ultralong hydroxyapatite nanowires and antibacterial components was developed for

biomedical applications (Xiong et al., 2016; Xiong, Yang, Zhu, Chen, Zhang, & Yang, 2017). In addition, a flexible recyclable rapid test biopaper based on ultralong hydroxyapatite nanowires and metal-organic framework with peroxidase-like activity was developed for the detection of H_2O_2 and glucose, and it could be recovered easily for reuse by simply dipping in absolute ethanol for just 30 min (Chen et al., 2017). Moreover, the highly flexible photothermal antibacterial biopaper composed of Cu^{2+}-doped ultralong hydroxyapatite nanowires and black phosphorus nanosheets was also investigated for the biomedical application as the dressing for accelerated healing of infected wound (Zeng et al., 2022).

16.5 Conclusions and Outlook

In this chapter, we highlight the significance and high values of the advanced fire-resistant paper. Fire-resistant paper is a kind of high added value product, which can be regarded as a milestone in the development of paper, it changes our common perception that paper is flammable. The fire retardancy of the organic fiber-based paper can be obtained by the use of phosphorylated cellulose fibers, fire-retardant organic fibers, and addition of inorganic fillers for papermaking. However, the dominant components of the organic fiber-based paper are still flammable organic fibers, and thus, it cannot acquire high resistance to fire and high temperature. In comparison, the inorganic nanofibers, such as ultralong hydroxyapatite nanowires, ultralong nanowires of cadmium phosphate hydroxide, $BaSO_4$ nanofibers, and silicon compound (SiC, SiO_2, and Si_3N_4) nanowires, have high melting points, high thermal stability, and good flexibility, and thus, the paper made from these inorganic nanofibers is nonflammable with excellent resistance to both fire and high temperature.

Among various inorganic nanofibers, ultralong hydroxyapatite nanowires are promising for making the fire-resistant paper. Ultralong hydroxyapatite nanowires have high flexibility, ultrahigh aspect ratios (more than 10,000), high thermal stability, and excellent resistance to both fire and high temperature. Furthermore, ultralong hydroxyapatite nanowires possess a large number of hydroxyl groups, which can form hydrogen bonds between nanowires to strengthen the fire-resistant paper. The fire-resistant paper based on ultralong hydroxyapatite nanowires has many advantages, which the traditional paper does not possess; for instance, the fire-resistant paper based on ultralong hydroxyapatite nanowires is environment friendly and has a high-quality natural white color without bleaching and sizing. The fire-resistant paper based on ultralong hydroxyapatite nanowires is promising for the application in long-term safe preservation of important documents, such as archives, art works, and books. In addition, the fire-resistant paper based on ultralong hydroxyapatite nanowires also has many other uses and has good application prospects in various fields. Ultralong hydroxyapatite nanowires can be synthesized artificially using common chemicals without consuming valuable natural resources such as trees. The whole manufacturing process of the fire-resistant paper based on ultralong hydroxyapatite nanowires is environment friendly and will not pollute the

environment. Thus, the fire-resistant paper based on ultralong hydroxyapatite nanowires has a tempting prospect for commercialization and large-scale applications.

Although great progress has achieved in the field of the fire-resistant paper, there are still some challenging issues which need to be addressed. Firstly, the wet-end chemical properties of the paper pulp for the fire-resistant paper should be highlighted. The wet-end chemical properties such as flocculation, retention, draining, and white water circulation of the fire-resistant paper pulp are very important for papermaking and mechanical performance of the paper, which play a guiding role in the practical production of the fire-resistant paper. The experimental results indicated that the wet end chemical properties of the fire-resistant paper pulp based on ultralong hydroxyapatite nanowires were unique and entirely different from those of the traditional paper pulp based on plant fibers (Dong et al., 2022). The wet-end chemical properties of the fire-resistant paper pulp were also significantly influenced by the inorganic adhesive and its content, which affected the runnability of the paper machine and the properties of the as-prepared fire-resistant paper. The addition of the inorganic adhesive in the fire-resistant paper pulp based on ultralong hydroxyapatite nanowires could increase the conductivity of the fire-resistant paper pulp, reduce the particle size of paper pulp floccules, and increase the tensile strength of the fire-resistant paper. Secondly, the thermal stability and fire resistance of the fire-retardant paper based on organic fibers are still not satisfactory and need to be enhanced. Thirdly, in the case of the inorganic fire-resistant paper based on ultralong hydroxyapatite nanowires, the large-scale production of ultralong hydroxyapatite nanowires with high yield, high throughput, and low cost is still really challenging, and more research on this issue should be conducted. It is important to develop environmentally friendly, low-cost, and large-scale synthetic technologies to produce high-quality ultralong hydroxyapatite nanowires with high yield and high throughput. Last but not least, the applications of the fire-resistant paper in various fields should be further investigated.

References

Azman Mohammad Taib, M. N., Hamidon, T. S., Garba, Z. N., Trache, D., Uyama, H., & Hussin, M. H. (2022). Recent progress in cellulose-based composites towards flame retardancy applications. *Polymer, 244*, 124677. https://doi.org/10.1016/j.polymer.2022.124677

Chen, F., & Zhu, Y. J. (2016). Large-scale automated production of highly ordered ultralong hydroxyapatite nanowires and construction of various fire-resistant flexible ordered architectures. *ACS Nano, 10*(12), 11483–11495. https://doi.org/10.1021/acsnano.6b07239

Chen, F. F., Zhu, Y. J., Chen, F., Dong, L. Y., Yang, R. L., & Xiong, Z. C. (2018). Fire alarm wallpaper based on fire-resistant hydroxyapatite nanowire inorganic paper and graphene oxide thermosensitive sensor. *ACS Nano, 12*(4), 3159–3171. https://doi.org/10.1021/acsnano.8b00047

Chen, F. F., Zhu, Y. J., Xiong, Z. C., & Sun, T. W. (2017). Hydroxyapatite nanowires@metal–organic framework core/shell nanofibers: Templated synthesis, peroxidase-like activity, and derived flexible recyclable test paper. *Chemistry - A European Journal, 23*, 3328–3337. https://doi.org/10.1002/chem.201605968

Chen, F. F., Zhu, Y. J., Xiong, Z. C., Sun, T. W., & Shen, Y. Q. (2016). Highly flexible superhydrophobic and fire-resistant layered inorganic paper. *ACS Applied Materials & Interfaces, 8*(50), 34715–34724. https://doi.org/10.1021/acsami.6b12838

Chen, F. F., Zhu, Y. J., Zhang, Q. Q., Yang, R. L., Qin, D. D., & Xiong, Z. C. (2019). Secret paper with vinegar as an invisible security ink and fire as a decryption key for information protection. *Chemistry - A European Journal, 25*(46), 10918–10925. https://doi.org/10.1002/chem.201902093

Chen, Y., Xie, C., Yang, S., He, R., Guo, Y., Guo, Z.-X., Guo, B., Qiu, T., & Tuo, X. (2023). High performance all-Para-aramid paper prepared by impregnating heterocyclic aramid into poly(p-phenylene terephthalamide) microfiber/nanofiber-based paper. *Composites Science and Technology, 242*, 110203. https://doi.org/10.1016/j.compscitech.2023.110203

Chen, Y. Q., Zhu, Y. J., Wang, Z. Y., Yu, H. P., & Xiong, Z. C. (2024). Salt-rejecting 3D cone flowing evaporator based on bilayer photothermal paper for high-performance solar seawater desalination. *Journal of Colloid and Interface Science, 660*, 370–380. https://doi.org/10.1016/j.jcis.2024.01.035

Chen, Y. Q., Zhu, Y. J., & Xiong, Z. C. (2024). Ultralong nanowires of cadmium phosphate hydroxide synthesized using a cadmium oleate precursor hydrothermal method and sulfidation conversion to ultralong cds nanowires. *Molecules, 29*(2), 549. https://doi.org/10.3390/molecules29020549

Dong, L. Y., & Zhu, Y. J. (2017). A new kind of fireproof, flexible, inorganic, nanocomposite paper and its application to the protection layer in flame-retardant fiber-optic cables. *Chemistry - A European Journal, 23*(19), 4597–4604. https://doi.org/10.1002/chem.201604552

Dong, L.-Y., & Zhu, Y.-J. (2018). Fire-resistant inorganic analogous Xuan paper with thousands of years' super-durability. *ACS Sustainable Chemistry & Engineering, 6*(12), 17239–17251. https://doi.org/10.1021/acssuschemeng.8b04630

Dong, L.-Y., & Zhu, Y.-J. (2020). Fire-retardant paper with ultrahigh smoothness and glossiness. *ACS Sustainable Chemistry & Engineering, 8*(47), 17500–17507. https://doi.org/10.1021/acssuschemeng.0c06665

Dong, L.-Y., Zhu, Y.-J., & Wu, J. (2022). Wet end chemical properties of a new kind of fire-resistant paper pulp based on ultralong hydroxyapatite nanowires. *Molecules, 27*(20), 6808. https://doi.org/10.3390/molecules27206808

Dong, L. Y., Zhu, Y. J., Zhang, Q. Q., & Shao, Y. T. (2019). Fire-retardant and high-temperature-resistant label paper and its potential applications. *ChemNanoMat, 5*(11), 1418–1427. https://doi.org/10.1002/cnma.201900456

Etale, A., Onyianta, A. J., Eloi, J. C., Rowlandson, J., & Eichhorn, S. J. (2024). Phosphorylated cellulose nanocrystals: Optimizing production by decoupling hydrolysis and surface modification. *Carbohydrate Polymers, 325*, 121560. https://doi.org/10.1016/j.carbpol.2023.121560

Fang, Y., Chen, L., Wu, J., & Liu, X. (2022). Fire-resistant and antibacterial Chinese Xuan paper by fully bio-based chitosan/phytic acid coating on pulp fibers. *Industrial Crops and Products, 187*, 115456. https://doi.org/10.1016/j.indcrop.2022.115456

Fang, Y., Liu, X., Zheng, H., & Shang, W. (2020). Bio-inspired fabrication of nacre-mimetic hybrid nanocoating for eco-friendly fire-resistant precious cellulosic Chinese Xuan paper. *Carbohydrate Polymers, 235*, 115782. https://doi.org/10.1016/j.carbpol.2019.115782

Fang, Y., Wu, J., Sun, W., & Liu, X. (2022). Pyrolysis of precious Chinese Xuan paper containing ammonium phytate as a flame retardant. *ACS Omega, 7*(42), 37971–37979. https://doi.org/10.1021/acsomega.2c05138

Fiss, B. G., Hatherly, L., Stein, R. S., Friščić, T., & Moores, A. (2019). Mechanochemical phosphorylation of polymers and synthesis of flame-retardant cellulose nanocrystals. *ACS Sustainable Chemistry & Engineering, 7*(8), 7951–7959. https://doi.org/10.1021/acssuschemeng.9b00764

Ghanadpour, M., Carosio, F., Larsson, P. T., & Wågberg, L. (2015). Phosphorylated cellulose nanofibrils: A renewable nanomaterial for the preparation of intrinsically flame-retardant materials. *Biomacromolecules, 16*(10), 3399–3410. https://doi.org/10.1021/acs.biomac.5b01117

He, A., Xing, T., Liang, Z., Luo, Y., Zhang, Y., Wang, M., Huang, Z., Bai, J., Wu, L., Shi, Z., Zuo, H., Zhang, W., Chen, F., & Xu, W. (2024). Advanced aramid fibrous materials: Fundamentals, advances, and beyond. *Advanced Fiber Materials, 6*, 3–35. https://doi.org/10.1007/s42765-023-00332-1

He, X., Xu, F., Chen, F.-F., Zhu, Y.-J., & Yu, Y. (2023). Graphene oxide and hydroxyapatite nanowire-based asymmetric nanocomposite papers with heat-induced color and resistance switching for dual-mode early fire warning. *ACS Applied Nano Materials, 6*(24), 23390–23400. https://doi.org/10.1021/acsanm.3c04723

Jiang, Y. Y., Zhu, Y. J., Chen, F., & Wu, J. (2015). Solvothermal synthesis of submillimeter ultralong hydroxyapatite nanowires using a calcium oleate precursor in a series of monohydroxy alcohols. *Ceramics International, 41*(4), 6098–6102. https://doi.org/10.1016/j.ceramint.2014.12.122

Kang, M., Wang, G., Liu, W., Yu, D., Li, G., Song, Z., Liu, X., & Wang, H. (2023). Fabrication of highly flame-retardant paper by in situ loading of magnesium hydroxide/basic magnesium chloride onto cellulose fibers. *Cellulose, 30*(11), 7295–7312. https://doi.org/10.1007/s10570-023-05319-0

Kashiwada, H., Shimizu, Y., Sano, Y., Yamauchi, K., Guang, H., Kumamoto, H., et al. (2021). In vivo behaviors of highly flexible paper consisting of ultralong hydroxyapatite nanowires. *Journal of Biomedial Materials Research Part B Applied Biomaterials, 109*, 1611–1621. https://doi.org/10.1002/jbm.b.34819

Li, H., Guo, S., Wang, L., Wu, J., Zhu, Y. J., & Hu, X. (2019). Thermally durable lithium-ion capacitors with high energy density from all hydroxyapatite nanowire-enabled fire-resistant electrodes and separators. *Advanced Energy Materials, 9*(46), 1902497. https://doi.org/10.1002/aenm.201902497

Li, H., Wu, D., Wu, J., Dong, L. Y., Zhu, Y. J., & Hu, X. (2017). Flexible, high-wettability and fire-resistant separators based on hydroxyapatite nanowires for advanced lithium-ion batteries. *Advanced Materials, 29*(44), 1703548. https://doi.org/10.1002/adma.201703548

Li, H., Zhu, Y. J., Jiang, Y. Y., Yu, Y. D., Chen, F., Dong, L. Y., & Wu, J. (2017). Hierarchical assembly of monodisperse hydroxyapatite nanowires and construction of high-strength fire-resistant inorganic paper with high-temperature flexibility. *ChemNanoMat, 3*(4), 259–268. https://doi.org/10.1002/cnma.201700027

Li, Z., Chen, Y., Hang, T., Xu, C., Shen, J., Li, X., Zheng, J., & Wu, Z. (2025). Highly flexible and flame-retardant aramid nanofiber composite papers for energy harvesting. *Journal of Materials Science and Technology, 204*, 81–90. https://doi.org/10.1016/j.jmst.2024.02.076

Liu, X.-H., Zhang, Q.-Y., Cheng, B.-W., Ren, Y.-L., Zhang, Y.-G., & Ding, C. (2018). Durable flame retardant cellulosic fibers modified with novel, facile and efficient phytic acid-based finishing agent. *Cellulose, 25*(1), 799–811. https://doi.org/10.1007/s10570-017-1550-0

Liu, Y., Zhang, L., Zhao, F., Li, C., Sheng, H., & Li, H. (2023). Fire-resistant and hydrophobic paper based on Si_3N_4@PDMS core-shell nanowires with 3d interlocking structure. *Ceramics International, 49*(17), 28002–28010. https://doi.org/10.1016/j.ceramint.2023.06.043

Lu, B. Q., Zhu, Y. J., & Chen, F. (2014). Highly flexible and nonflammable inorganic hydroxyapatite paper. *Chemistry - A European Journal, 20*(5), 1242–1246. https://doi.org/10.1002/chem.201304439

Ma, T., Zhao, Y., Ruan, K., Liu, X., Zhang, J., Guo, Y., et al. (2020). Highly thermal conductivities, excellent mechanical robustness and flexibility, and outstanding thermal stabilities of aramid nanofiber composite papers with nacre-mimetic layered structures. *ACS Applied Materials & Interfaces, 12*(1), 1677–1686. https://doi.org/10.1021/acsami.9b19844

Patoary, M. K., Islam, S. R., Farooq, A., Rashid, M. A., Sarker, S., Hossain, M. Y., et al. (2023). Phosphorylation of nanocellulose: State of the art and prospects. *Industrial Crops and Products, 201*, 116965. https://doi.org/10.1016/j.indcrop.2023.116965

Qin, D. D., Zhu, Y. J., Yang, R. L., & Xiong, Z. C. (2020). A salt-resistant janus evaporator assembled from ultralong hydroxyapatite nanowires and nickel oxide for efficient and recyclable solar desalination. *Nanoscale, 12*, 6717–6728. https://doi.org/10.1039/C9NR10357K

Shao, Y. T., Zhu, Y. J., Dong, L. Y., & Cai, A. Y. (2021). Nanocomposite "Xuan paper" made from ultralong hydroxyapatite nanowires and cellulose fibers and its anti-mildew properties. *Journal of Inorganic Materials, 36*(1), 107–112. https://doi.org/10.15541/jim20200087

Shao, Y. T., Zhu, Y. J., Dong, L. Y., & Zhang, Q. Q. (2019). A new kind of nanocomposite Xuan paper comprising ultralong hydroxyapatite nanowires and cellulose fibers with a unique ink wetting performance. *RSC Advances, 9*(69), 40750–40757. https://doi.org/10.1039/c9ra08349a

Song, S., Wang, Q., Ji, D., Li, L., Tan, J., Wu, Q., Lyu, Y., & Zhang, M. (2024). Nacre-inspired aramid nanofibers/basalt fibers composite paper with excellent flame retardance and thermal stability by constructing an organic-inorganic fiber alternating layered structure. *ACS Applied Materials & Interfaces, 16*(3), 4045–4055. https://doi.org/10.1021/acsami.3c16614

Sun, T. W., Zhu, Y. J., & Chen, F. (2017). Highly flexible multifunctional biopaper comprising chitosan reinforced by ultralong hydroxyapatite nanowires. *Chemistry - A European Journal, 23*, 3850–3862. https://doi.org/10.1002/chem.201605165

Sun, T. W., Zhu, Y. J., Chen, F., & Zhang, Y. G. (2017). Ultralong hydroxyapatite nanowire/collagen biopaper with high flexibility, improved mechanical properties and cellular attachment. *Chemistry, an Asian Journal, 12*, 655–664. https://doi.org/10.1002/asia.201601592

Velencoso, M. M., Battig, A., Markwart, J. C., Schartel, B., & Wurm, F. R. (2018). Molecular firefighting—How modern phosphorus chemistry can help solve the challenge of flame retardancy. *Angewandte Chemie, International Edition, 57*(33), 10450–10467. https://doi.org/10.1002/anie.201711735

Wang, S., Jin, S., Yang, X., Huang, Y., Liu, P., Tang, Y., & Yang, Y. (2024). Development of Mg-Al LDH and LDO as novel protective materials for deacidification of paper-based relics. *Chinese Chemical Letters, 35*(9), 109890. https://doi.org/10.1016/j.cclet.2024.109890

Wang, S., Yang, X., Li, Y., Gao, B., Jin, S., Yu, R., Zhang, Y., & Tang, Y. (2022). Colloidal magnesium hydroxide nanoflake: One-step surfactant-assisted preparation and paper-based relics protection with long-term anti-acidification and flame-retardancy. *Journal of Colloid and Interface Science, 607*, 992–1004. https://doi.org/10.1016/j.jcis.2021.09.041

Wang, S. L., Huang, J. L., & Chen, F. S. (2012). Study on Mg-Al hydrotalcites in flame-retardant paper preparation. *BioResources, 7*(1), 997–1007. https://doi.org/10.15376/biores.7.1.997-1007

Wang, Z.-Y., Zhu, Y.-J., Chen, Y.-Q., Yu, H.-P., & Xiong, Z.-C. (2022). Flexible nanocomposite paper with superior fire retardance, mechanical properties and electrical insulation by engineering ultralong hydroxyapatite nanowires and aramid nanofibers. *Chemical Engineering Journal, 444*, 136470. https://doi.org/10.1016/j.cej.2022.136470

Wu, J., & Zhu, Y. J. (2021). Acid/alkali-proof fire-resistant inorganic paper comprising fibers assembled from barium sulfate nanorods. *European Journal of Inorganic Chemistry, 5*, 492–499. https://doi.org/10.1002/ejic.202000940

Xiong, Z. C., Yang, R. L., Zhu, Y. J., Chen, F. F., & Dong, L. Y. (2017). Flexible hydroxyapatite ultralong nanowire-based paper for highly efficient and multifunctional air filtration. *Journal of Materials Chemistry A, 5*, 17482–17491. https://doi.org/10.1039/C7TA03870D

Xiong, Z. C., Yang, Z. Y., Zhu, Y. J., Chen, F. F., Zhang, Y. G., & Yang, R. L. (2017). Ultralong hydroxyapatite nanowires-based paper co-loaded with silver nanoparticles and antibiotic for long-term antibacterial benefit. *ACS Applied Materials & Interfaces, 9*, 22212–22222. https://doi.org/10.1021/acsami.7b05208

Xiong, Z. C., Zhu, Y. J., Chen, F. F., Sun, T. W., & Shen, Y. Q. (2016). One-step synthesis of silver nanoparticle-decorated hydroxyapatite nanowires for the construction of highly flexible free-standing paper with high antibacterial activity. *Chemistry - A European Journal, 22*, 11224–11231. https://doi.org/10.1002/chem.201601438

Xiong, Z. C., Zhu, Y. J., Qin, D. D., Chen, F. F., & Yang, R. L. (2018). Flexible fire-resistant photothermal paper comprising ultralong hydroxyapatite nanowires and carbon nanotubes for solar energy-driven water purification. *Small, 14*(50), 1803387. https://doi.org/10.1002/smll.201803387

Yang, B., Wang, L., Zhang, M., Luo, J., Lu, Z., & Ding, X. (2020). Fabrication, applications, and prospects of aramid nanofiber. *Advanced Functional Materials, 30*(22), 2000186. https://doi.org/10.1002/adfm.202000186

Yang, L., Zhu, Y. J., Yu, H. P., Wang, Z. Y., Cheng, L., Li, D. D., et al. (2024). A five micron thick aramid nanofiber separator enables highly reversible Zn anode for energy-dense aqueous zinc-ion batteries. *Advanced Energy Materials, 14*, 2401858. https://doi.org/10.1002/aenm.20240185

Yang, R. L., Zhu, Y. J., Chen, F. F., Dong, L. Y., & Xiong, Z. C. (2017). Luminescent, fire-resistant, and water-proof ultralong hydroxyapatite nanowire-based paper for multimode anticounterfeiting applications. *ACS Applied Materials & Interfaces, 9*(30), 25455–25464. https://doi.org/10.1021/acsami.7b06835

Yang, R.-L., Zhu, Y.-J., Chen, F.-F., Qin, D.-D., & Xiong, Z.-C. (2018). Recyclable, fire-resistant, superhydrophobic, and magnetic paper based on ultralong hydroxyapatite nanowires for continuous oil/water separation and oil collection. *ACS Sustainable Chemistry & Engineering, 6*(8), 10140–10150. https://doi.org/10.1021/acssuschemeng.8b01463

Yasukawa, A., Yokoyama, T., & Ishikawa, T. (2001). Preparation of cadmium hydroxyapatite particles using acetamide. *Materials Research Bulletin, 36*(3–4), 775–786. https://doi.org/10.1016/S0025-5408(01)00536-0

Yu, H. P., & Zhu, Y. J. (2024). Guidelines derived from biomineralized tissues for design and construction of high-performance biomimetic materials: From weak to strong. *Chemical Society Reviews, 53*(9), 4490–4606. https://doi.org/10.1039/d2cs00513a

Yu, H.-P., Zhu, Y.-J., & Lu, B.-Q. (2018). Highly efficient and environmentally friendly microwave-assisted hydrothermal rapid synthesis of ultralong hydroxyapatite nanowires. *Ceramics International, 44*(11), 12352–12356. https://doi.org/10.1016/j.ceramint.2018.04.022

Zeng, J., Geng, X., Tang, Y., Xiong, Z. C., Zhu, Y. J., & Chen, X. (2022). Flexible photothermal biopaper comprising Cu^{2+}-doped ultralong hydroxyapatite nanowires and black phosphorus nanosheets for accelerated healing of infected wound. *Chemical Engineering Journal, 437*, 135347. https://doi.org/10.1016/j.cej.2022.135347

Zhang, Q.-Q., Zhu, Y.-J., Wu, J., & Dong, L.-Y. (2019). Nanofiltration filter paper based on ultralong hydroxyapatite nanowires and cellulose fibers/nanofibers. *ACS Sustainable Chemistry & Engineering, 7*(20), 17198–17209. https://doi.org/10.1021/acssuschemeng.9b03793

Zhang, Q. Q., Zhu, Y. J., Wu, J., Shao, Y. T., Cai, A. Y., & Dong, L. Y. (2019). Ultralong hydroxyapatite nanowire-based filter paper for high-performance water purification. *ACS Applied Materials & Interfaces, 11*(4), 4288–4301. https://doi.org/10.1021/acsami.8b20703

Zhang, Q. Q., Zhu, Y. J., Wu, J., Shao, Y. T., & Dong, L. Y. (2020). A new kind of filter paper comprising ultralong hydroxyapatite nanowires and double metal oxide nanosheets for high-performance dye separation. *Journal of Colloid and Interface Science, 575*, 78–87. https://doi.org/10.1016/j.jcis.2020.04.079

Zhang, T., Wu, M., Kuga, S., Ewulonu, C. M., & Huang, Y. (2020). Cellulose nanofibril-based flame retardant and its application to paper. *ACS Sustainable Chemistry & Engineering, 8*(27), 10222–10229. https://doi.org/10.1021/acssuschemeng.0c02892

Zhang, Y., Xu, Q., Jiang, B., & Ma, Z. (2020). Flame-retardant paper with robust hydrophobicity enabled by perfluorodecane doped SiO_2 nanofibers. *Journal of Sol-Gel Science and Technology, 93*(2), 309–314. https://doi.org/10.1007/s10971-019-05206-w

Zhang, Y., Zhu, Y. J., & Yu, H. P. (2022). Microwave-assisted hydrothermal rapid synthesis of ultralong hydroxyapatite nanowires using adenosine 5′-triphosphate. *Molecules, 27*(15), 5020. https://doi.org/10.3390/molecules27155020

Zhang, Y. G., Zhu, Y. J., Chen, F., & Wu, J. (2015). Ultralong hydroxyapatite nanowires synthesized by solvothermal treatment using a series of phosphate sodium salts. *Materials Letters, 144*, 135–137. https://doi.org/10.1016/j.matlet.2015.01.031

Zhou, Z. F., Sun, T. W., Qin, Y. H., Zhu, Y. J., Jiang, Y. Y., Zhang, Y., et al. (2019). Selenium-doped hydroxyapatite biopaper with anti-bone tumor effect by inducing apoptosis. *Biomaterials Science, 7*, 5044–5053. https://doi.org/10.1039/C9BM00953A

Zhu, Y. J. (2021a). *Fire-resistant paper: Materials, technologies, and applications*. CRC Press.
Zhu, Y. J. (2021b). Multifunctional fire-resistant paper based on ultralong hydroxyapatite nanowires. *Chinese Journal of Chemistry, 39*(8), 2296–2314. https://doi.org/10.1002/cjoc.202100170
Zhu, Y. J., & Chen, F. (2014). Microwave-assisted preparation of inorganic nanostructures in liquid phase. *Chemical Reviews, 114*(12), 6462–6555. https://doi.org/10.1021/cr400366s
Zhu, Y. J., & Lu, B. Q. (2019). Deformable biomaterials based on ultralong hydroxyapatite nanowires. *ACS Biomaterials Science & Engineering, 5*, 4951–4961. https://doi.org/10.1021/acsbiomaterials.9b01183

Chapter 17
Synthesis of Magnetic Materials Using Bacterial Cellulose and Iron Oxides

Thaís Cavalcante de Souza, Claudio José Galdino da Silva Junior, Alexandre D'Lamare Maia de Medeiros, Andréa Fernanda de Santana Costa, Glória Maria Vinhas, and Leonie Asfora Sarubbo

17.1 Introduction

Cellulose is the most common polymer on Earth and is a linear organic chain of glucose monomers. It is found in a variety of sources, such as algae and plants, and can be produced by fermentative (biotechnological) processes (Esa et al., 2014; Medeiros et al., 2022). Although less commonly used than plant cellulose, bacterial cellulose (BC) has been the object of an increasing number of studies due to its acquisition process, versatility, and unique characteristics (Nascimento et al., 2021,

T. C. de Souza
Universidade Federal de Pernambuco (UFPE), Recife, PE, Brazil

Instituto Avançado de Tecnologia e Inovação (IATI), Recife, PE, Brazil
e-mail: thais.csouza@ufpe.br

C. J. G. da Silva Junior · A. D'Lamare Maia de Medeiros
Instituto Avançado de Tecnologia e Inovação (IATI), Recife, PE, Brazil
e-mail: claudio.junior@iati.org.br; alexandre.medeiros@iati.org.br

A. F. de Santana Costa
Instituto Avançado de Tecnologia e Inovação (IATI), Recife, PE, Brazil

Universidade Federal de Pernambuco (UFPE), Centro Acadêmico da Região Agreste, Caruaru, PE, Brazil
e-mail: andrea.costa@iati.org.br; andrea.santana@ufpe.br

G. M. Vinhas
Universidade Federal de Pernambuco (UFPE), Recife, PE, Brazil
e-mail: gloria.vinhas@ufpe.br

L. A. Sarubbo (✉)
Instituto Avançado de Tecnologia e Inovação (IATI), Recife, PE, Brazil

Escola de Tecnologia e Comunicação, Universidade Católica de Pernambuco (UNICAP), Recife, PE, Brazil
e-mail: leonie.sarubbo@unicap.br; leonie.sarubbo@iati.org.br

G. Korotcenkov (ed.), *The Handbook of Paper-Based Sensors and Devices*,
https://doi.org/10.1007/978-3-031-91080-7_17

2022; Ul-Islam et al., 2017, 2020). Fermentation for the obtainment of BC can be performed with bacteria and/or microbial consortia (Hestrin & Schramm, 1954). At the end of the process, the BC is in the form of a biofilm (when static fermentation is employed) or pellets (when shaking occurs during fermentation) (Betlej et al., 2021; Medeiros et al., 2023; Sharma et al., 2019; Silva Jr et al., 2022).

Besides lowering production costs, such changes to the culture medium can lead to biopolymers with novel characteristics and properties, such as antioxidant and antimicrobial activities (Albuquerque et al., 2021; Amorim et al. 2022a, b; Huang et al., 2010; Hussain et al., 2019; Kurosumi et al., 2019; Sperotto et al., 2021; Huo et al., 2022). Due to the considerable versatility, BC has potential applications in a variety of fields, such as the pharmaceutical, medical, food, textile, wastewater treatment, and electronic industries, as this biopolymer can be combined with other materials using different methods, including magnetic materials (Medeiros et al., 2023; Moon et al., 2011; Silva Jr et al., 2022; Urbina et al., 2021).

Magnetic materials are an important part of modern life, with applications in a variety of common devices and playing a crucial role in technological advancement and innovation. However, the production of such materials generally involves the use of chemical compounds and petroleum derivatives, which substantially contribute to global pollution and require specific disposal methods (Chen et al., 2022). In contrast, studies have been conducted to obtain biotechnological materials with magnetic properties ("smart materials"), the production of which does not generate waste that is harmful to the environment (or greatly reduces the generation of such waste). Moreover, these materials are created from renewable sources (Merazzo et al., 2021; Safarik & Safarikova, 2009). Such novel materials, including those involving BC, are obtained using different production processes and different inputs and used for diverse purposes (Souza et al. 2023a; Sriplai & Pinitsoontorn, 2020).

Various studies have been conducted on the magnetisation of BC with the addition of different types of magnetic particles, such as ferrites, magnetite, and nickel. Magnetised BC has considerable technological potential, is adaptable to various production environments, and is capable of meeting the demand for magnetic biomaterials (Kumar et al., 2022; Souza et al. 2023b). Considering this technological potential and the variety of methods used for the acquisition of magnetic BC, this chapter offers a review of the literature on the production and applications of this material.

17.2 Preparations for the Production of Magnetic Bacterial Cellulose

During the production of magnetic BC, many authors begin additivation soon after purification of the fermentative product (Amorim et al., 2020). The processing/treatment of BC prior to the incorporation of other compounds is sometimes needed to impart specific properties to the final material or improve the distribution of the added particles in the interior of the material. These operations may be mechanical,

such as the shredding of the biofilm, or chemical, such as acid hydrolysis (Amarasekara et al., 2020; Costa et al., 2017, 2020). Shredding enables a more even distribution of the added particles, whereas acid hydrolysis makes the structure of BC more pliable for the addition of other materials. These methods are crucial to enhancing the functionality and applicability of BC in different products, such as electronic devices and biomaterials (Arias et al., 2016; Chanthiwong et al., 2020; Mira-Cuenca et al., 2021; Patwa et al., 2020; Souza et al. 2023b).

With acid hydrolysis, BC is added to a solution containing a strong acid, which breaks down the glycosidic bonds of the fibres into simpler units of glucose and oligosaccharides. This leads to the obtainment of cellulose nanowhiskers/nanocrystals (Eichhorn, 2011). Prior to the addition of the acid, some researchers shred/cut the BC to increase the surface area, thus enhancing hydrolytic efficiency. After this treatment, the biomaterial undergoes filtration and centrifugation and the nanowhiskers measure 200 to 500 nm in length and 3 to 30 nm in diameter (Purnama et al., 2022). The effects of different variables, such as the type of acid used, its concentration, time, temperature, and pH of the reaction, on the crystallinity and dimensions of the material have been the topic of discussion in various studies (Arserim-Uçar et al., 2021; Martínez-Sanz et al., 2011; Vasconcelos et al., 2017).

Mechanical processing occurs with the shredding of BC in a knife mill, blender, or mixer or by cutting to achieve specific shapes. This is the simplest way to prepare BC films. In the study conducted by Salleh et al. (2023), BC membranes were shredded in a high-speed blender prior to the incorporation of magnetite. Silva et al. (2023) shredded BC and then diluted it in N-methylmorpholine-N-oxide (NMMO), which is commonly used in cellulose industries to obtain a stiffer material. In the work of Souza et al. (2024), the authors incorporated magnetite nanoparticles into intact BC membranes and into biopolymer with mechanical processing, and when checking the percentage of incorporated material, they noticed that there was a slight increase in the percentage of nanoparticles added in the samples which were processed, due to the increase in its disposal area. Figure 17.1 demonstrates the visual aspects of BC before and after mechanical processing.

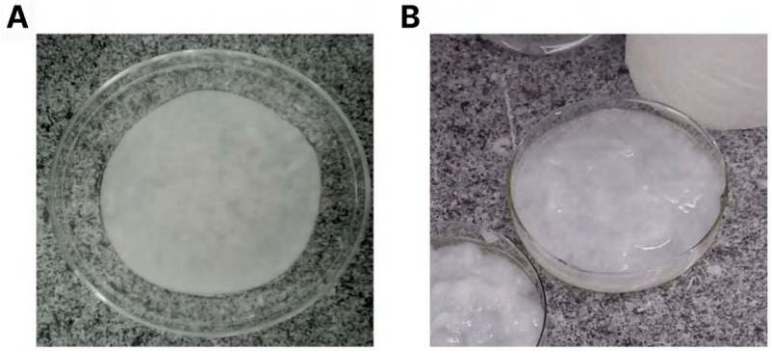

Fig. 17.1 Visual aspect of moist biocellulose (BC) without processing (**a**) and with mechanical processing (**b**). (Reprinted from Souza et al. (2024). Published 2024 by MDPI with open access)

17.3 Magnetism: General Concepts

Magnetism is a phenomenon originating from the movement of electrons and is inherent to each material, resulting from the interaction and alignment of electrons when exposed to an external magnetic field and causing the attraction or repulsion of other materials (Callister & Rethwisch, 2016). The two types of electron movements are denominated magnetic moments. The orbital angular moment of an electron is determined by its movement around the nucleus of an atom, whereas spin is the angular moment defined by the rotation of the electron on its own axis (Cullity & Graham, 2009).

Materials can exhibit different behaviours when subjected to an external magnetic field. The spins of electrons can align in specific ways. Portions of a material in which all spins are aligned in the same direction are denominated "domains" (Guimarães, 2009; Spaldin, 2010). Based on the spin alignment and the organisation of the domains, during and after exposure to an external magnetic field, materials are classified as ferromagnetic, ferrimagnetic, paramagnetic, diamagnetic, or antiferromagnetic (Halliday & Resnick, 2021; Shackelford, 2022).

17.3.1 Magnetic Domains in Nanoparticles

As discussed above, groups of spins arrange themselves in a similar way throughout their lengths in a given material due to exposure to a magnetic field, forming magnetic domains, as illustrated in Fig. 17.2a (Francisquini et al., 2014). These domains function as tiny magnets within ferromagnetic and ferrimagnetic materials separated by walls, which are regions in which the transition between neighbouring domains occurs. In the domain walls, magnetic moment vectors spin from one direction to another, as illustrated in Fig. 17.2b (Guimarães, 2009). In particles on the nanoscale, however, there is no formation of walls or multiple domains.

Due to their stabilised molecular state, nanoparticles have differentiated properties that are dependent on morphology, crystallinity, and size (Yusoff et al., 2017). As shown in Fig. 17.2, the number of domains in particles depends on their size. Nanoparticles have a large surface area in relation to volume, with the possibility of being used as additives and their spins forming magnetic monodomains. As the dimensions of a material diminish, the energy costs related to the maintenance of the domain walls increase. Thus, when the material reaches a critical size, it becomes

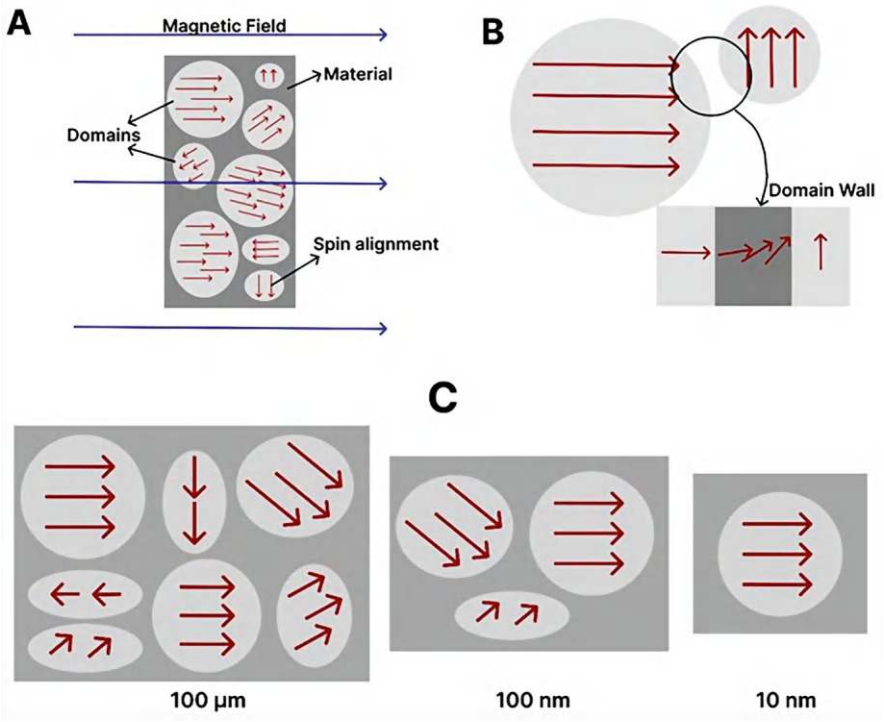

Fig. 17.2 Magnetic domains within a material. Material with multiple domains and tendencies to align with an external magnetic field (**a**). Domain walls among multiple domains (**b**). Materials in decreasing size until the formation of a magnetic monodomain (**c**)

energetically more favourable to maintain a single domain rather than multiple domains. Consequently, the reduction in particle dimensions until reaching a critical size or diameter results in the formation of magnetic monodomains (Fig. 17.2c) (Francisquini et al., 2014).

Particles with magnetic monodomains can respond more quickly and efficiently to an external field (Francisquini et al., 2014; Souza et al. 2023b). In some cases, particles of certain materials with dimensions smaller than the critical size have spontaneous magnetisation, but the direction of magnetisation can be changed by thermal fluctuations, which is behaviour similar to paramagnetism, but with a greater intensity of the magnetic moment. This behaviour is denominated superparamagnetic (Bustamante-Torres et al., 2022; Samrot et al., 2021).

Iron oxides, such as magnetite, maghemite, and hematite, are among the most widely studied nanomaterials with magnetic properties. Moreover, a wide area of research is devoted to superparamagnetic iron oxide nanoparticles (SPIONs) with a size of less than 20 nm (Bustamante-Torres et al., 2022).

17.4 Features of the Preparation of Magnetic Biocellulose

To impart magnetic characteristics to BC, magnetic particles are added to the biopolymer. Nanometric particles have greater adhesion, since BC fibres are of nanometric order, and nanoparticles of compounds such as nickel and cobalt, known to have good magnetic properties, are used as additives (Menchaca-Nal et al., 2023; Vitta et al., 2010). Meanwhile, there is a group of compounds that stands out and is the most used as magnetic dopants in the literature, iron oxides.

17.4.1 Iron Oxides

From the end of the Neolithic period to the present day, iron and its derivatives have been widely used by humans. In its most common form, iron is found in the form of oxides and oxyhydroxides, which constitute an extensive group of materials. This category includes different types of oxides and hydroxides, which vary in accordance with the oxidation state of iron (+2 or +3) and quantity of Fe^{2+} and Fe^{3+} ions in its structure (Schwertmann & Cornell, 2008). Each component acquires different crystalline structures and properties. Magnetic properties vary in accordance with the proportion of Fe^{3+} and Fe^{2+} ions in each component together with the vacancies in oxygen atoms and its corresponding crystalline structure (Yusoff et al., 2017).

Most research on the production of magnetic materials derived from BC uses iron oxide particles as additives, with ferromagnetic or ferrimagnetic characteristics (total or partial alignment of spins in the same direction as an external field, and their temporary or definitive conservation), and also superparamagnetic particles (Samrot et al., 2021; Vangijzegem et al., 2023). Examples of iron oxides and oxyhydroxides, with some of these magnetical proprieties, are magnetite, hematite, and maghemite, the crystalline structures of which are shown in Fig. 17.3.

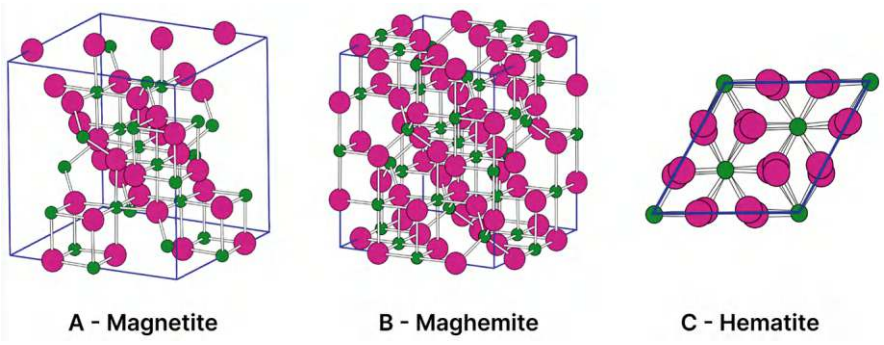

Fig. 17.3 Crystalline structures of magnetite (**a**), maghemite (**b**), and hematite (**c**). Iron atoms are in green and oxygen atoms are in pink

Figure 17.3a shows the crystalline structure of magnetite, which has an inverse spinel structure and differs from other oxides by containing both Fe^{3+} and Fe^{2+} ions in its composition. Within its network, Fe^{3+} ions occupy octahedral interstices, where bonds are formed with six O^{2-} ions, and tetrahedral interstices, where bonds are formed with four O^{2-} ions. In contrast, Fe^{2+} ions are only found in tetrahedral interstices, attaching to four O^{2-} ions (Bhateria & Singh, 2019). This difference in the oxidation of iron ions and interactions among spins results in distinct zero magnetic moments, giving magnetite ferrimagnetic properties (Oliveira et al., 2013). Moreover, its critical diameter is 126 nm; smaller particles form magnetic monodomains, which has motivated studies on production within this size range (Francisquini et al., 2014; Souza et al. 2023b).

Maghemite also has an inverse spinel crystalline structure, as shown in Fig. 17.3b. This mineral is composed of Fe^{3+} ions occupying octahedral interstices, where each iron ion forms bonds with six O^{2-} ions, and tetrahedral interstices, where each iron ion forms bonds with four O^{2-} ions (Oliveira et al., 2013). Due to the exclusive presence of Fe^{3+} ions, the formation of cationic vacancies occurs in its structure, giving it ferrimagnetic behaviour (Bhateria & Singh, 2019).

Hematite (Fig. 17.3c) has a hexagonal crystalline structure, in which each Fe^{3+} ion forms bonds with six O^{2-} ions. However, each iron ion carries a magnetic spin that can interact with the spins of neighbouring atoms, resulting in the formation of regions of magnetic domains. The interaction among these domains is responsible for the ferromagnetism in hematite (Oliveira et al., 2013).

In industries, iron oxides and oxyhydroxides play a fundamental role in the extraction of metallic iron, the fabrication of dyes, and the production of magnetic alloys for the fabrication of magnets, among other uses. Due to their distinct magnetic properties, iron oxide nanoparticles are widely employed in different applications and have been the object of numerous studies, with suggestions for applications in electronic devices, enzyme immobilisation systems, water treatment process, data storage devices, sound amplification equipment, sensors, and medical applications, such as the controlled release of medications (Dudchenko et al., 2023; Niculescu et al., 2021).

Numerous studies have investigated the obtainment of iron oxide nanoparticles with magnetic monodomains due to the unique magnetic characteristics. However, studies have also focused on the obtainment of SPIONs, which are particles with diameters much smaller than their critical radius. According to Girardet et al. (2022), magnetite and maghemite have magnetic monodomains when the nanoparticles are smaller than 30 ± 5 nm and exhibit superparamagnetic behaviour when smaller than 20 ± 5 nm. The synthesis of SPIONs and nanoparticles with monodomains can be quite challenging due to the different production methods, the variables of which exert an impact on the magnetic characteristics and final dimensions of the particles (Akhtar et al., 2022; Narayanaswamy et al., 2021).

Metallic ferrites constitute an extensive group of magnetic materials that are widely used in industries and studies. These materials are derived from iron oxides, with the addition of other metals, such as cobalt, aluminium, and nickel. The crystalline structure varies depending on the specific type. However, the most common

is the spinel structure, in which metal ions alternately occupy tetrahedral and octahedral positions in a cubic crystalline matrix, in which iron and cobalt ions are present in tetrahedral and octahedral sites. The arrangement of the metal irons influences the magnetic properties of ferrites (Menchaca-Nal et al., 2023).

The choice of the type of oxide that will be added to BC will depend on the objective of each study and application, and there are cases where the authors need particles with stronger ferromagnetic characteristics, such as cobalt and nickel ferrites, and magnetite in monodomain size (Salidkul et al., 2021), and in other cases, SPIONS (Mira-Cuenca et al., 2021) are necessary, as will be discussed later. The most widely used iron oxides for the production of magnetic BC are magnetite, maghemite, and ferrites. The graph in Fig. 17.4 illustrates the recurrence of these iron oxides in works produced from 2010 to 2024, available on Google Scholar.

17.4.2 Incorporation Methods

Among the various iron oxide incorporation methods, a specific process or set of specific methods may be adopted, exerting an influence on the final characteristics of the material (Stumpf et al., 2018). The most widely used incorporation methods are in situ reactions (co-precipitation and thermal decomposition techniques) and processes involving the addition of particles synthesised ex situ (Menchaca-Nal et al., 2023; Souza et al. 2023a). These methods vary depending on the oxide particle synthesis route adopted. The graph in Fig. 17.5 shows the occurrence of methods described in the literature (works produced from 2010 to 2024, available on Google Scholar) for the doping of BC with iron oxides. Figure 17.6 is a schematic of the two co-precipitation processes, made by authors in 2024.

With in situ processes, the reaction for the obtainment of iron oxides occurs in the interior of the BC. With co-precipitation, BC is immersed in a solution containing precursor reagents, which are absorbed. Next, the impregnated BC is immersed

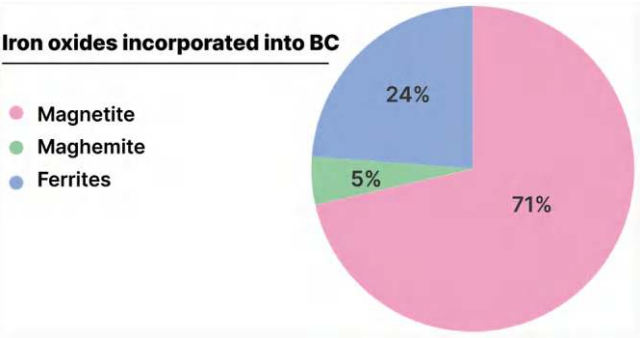

Fig. 17.4 Graph with percentage of iron oxide particles used in the doping of BC, according to the literature

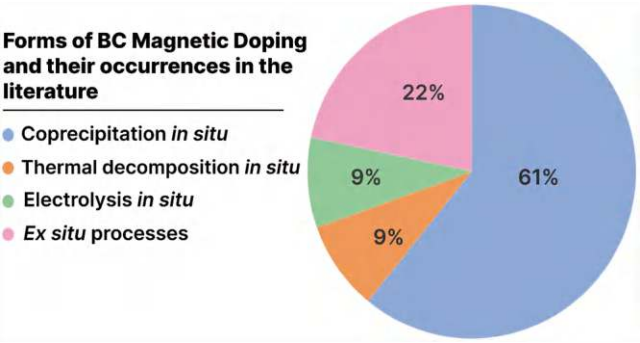

Fig. 17.5 Graph showing the percentage of methods of BC doping with iron oxides described in the literature

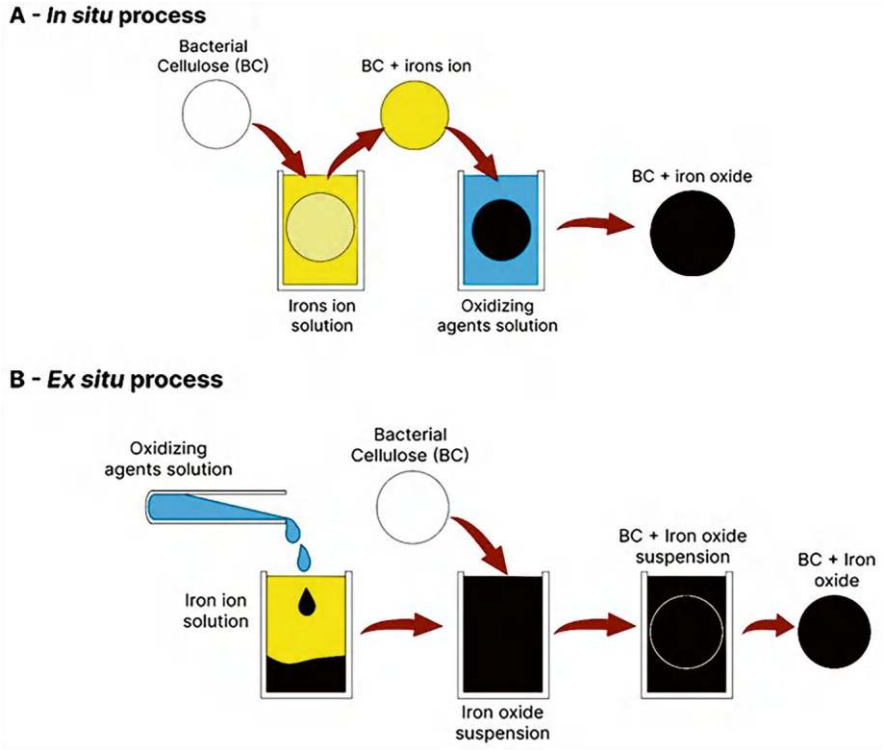

Fig. 17.6 In situ (**a**) and ex situ (**b**) iron oxide co-precipitation processes

in an oxidising medium, in which the reagents are converted into oxides. In situ co-precipitation (Fig. 17.6a) is described in studies conducted by Chanthiwong et al. (2020), Chen et al. (2021, 2022), Menchaca-Nal et al. (2023), Qiao et al. (2022), and Usawattanakul et al. (2021). With in situ thermal decomposition, the

reagents are added to the BC matrix and decomposed, thus forming iron oxides within the BC. This route is described in studies conducted by Zeng et al. (2014) and Mira-Cuenca et al. (2021). With in situ electrolysis, the BC matrix is loaded with a solution of iron salts and then submitted to an electrical current through electrodes. This process causes the oxidation of the iron ions, producing the desired iron oxide within the BC. This method is described in studies conducted by Zhou et al. (2009) and Yang et al. (2022).

With the ex situ process (Fig. 17.6b), iron oxide particles are first obtained and then added to the BC matrix. Ex situ co-precipitation is described in studies conducted by Salidkul et al. (2021), Salles et al. (2022), Sriplai et al. (2018), Zhang et al. (2022), and Zhu et al. (2011).

There are several ways to incorporate iron oxides into BC. Each researcher chooses the most feasible route depending on the objectives and applications of the final material or the context and availability of materials and equipment. The graph in Fig. 17.5 demonstrates a greater occurrence of studies involving incorporation via in situ co-precipitation. According to Chanthiwong et al. (2020), this route provides a good distribution of particles in BC and can be easily adapted with the adjustment of the reagents.

The ex situ synthesis of particles prior to incorporation into BC is also widely used. Researchers often adopt ex situ methods when particles should be synthesised without the interference of the cellulose or when synthesis would degrade the biomaterial. For instance, Salidkul et al. (2021) used the ex situ route because the desired nanoparticles were synthesised at a temperature higher than 800 °C, which would have degraded the BC if synthesis were performed in situ.

Another point to take into consideration is the control of the characteristics of the iron oxide particles and distribution within the BC matrix. Synthesis temperature, agitation, the choice of reagents, pH, etc. exert an influence on these aspects and specific applications require differentiated particle control (Dudchenko et al., 2023). For instance, Mira-Cuenca et al. (2021) needed SPIONs for the final application (magnetic resonance contrast) and adopted thermal decomposition, with specific temperature, time reagents, and proportions to achieve a controlled particle formation mechanism and a final product with the necessary characteristics for the target application. Souza et al. (2023b) investigated the impact of each reactional variable on the final characteristics of iron oxides in different particle synthesis methods. With in situ synthesis, an assessment must be performed to determine whether the variation in each of the variables will affect the BC structure.

The choice of iron oxide particle synthesis route, forms of incorporation into BC, or in situ synthesis is a factor of extreme importance to the final characteristics of the product. For the successful obtainment of a BC material with iron oxides, one should take into account the final application and all variables in the method selected.

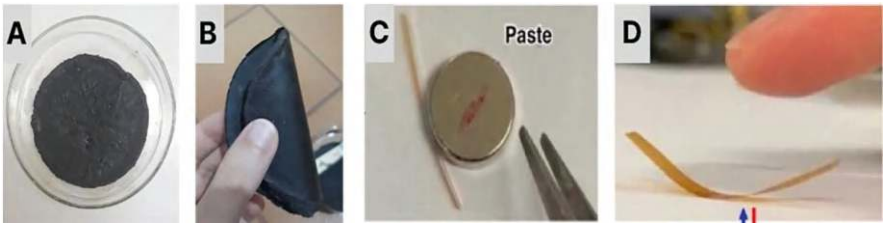

Fig. 17.7 (**a**, **b**) BC biofilm with magnetite (corresponding to 90% of total mass) incorporated by in situ coprecipitation in a Petri dish (**a**) and folded (**b**); (**c**) Magnetic responsive bending of bacterial cellulose nanocrystals (bCNC) films in the presence of the permanent magnet. (**d**) Reversible humidity responsive actuation in the presence of a finger. (Figures c and d reprinted from Zhang et al. (2022). Published 2022 by Nature Portfolio with open access)

17.5 General Characteristics of Magnetic BC

Some characteristics of BC impregnated with iron oxides vary depending on the type of oxide used, the proportion of the materials, and the methods employed for its production. Most studies in the literature report flexibility, a change in colour, the acquisition of magnetic properties, and enhanced tensile strength (Chen et al., 2022; Kumar et al., 2022; Menchaca-Nal et al., 2023; Qiao et al., 2022; Salidkul et al., 2021; Zeng et al., 2014; Zhang et al., 2022; Zhu et al., 2011). Figure 17.7 shows a BC membrane with magnetite obtained by in situ coprecipitation, in which the Fe_3O_4 incorporated accounted for 90% of the total mass of the material, made by the authorship group, and a magnetic biomaterial made by Zhang et al. (2022).

Figure 17.7b displays the flexibility of the material. Chen et al. (2022), Salidkul et al. (2021), Zeng et al. (2014), and Zhang et al. (2022), also show the flexibility of BC materials with different iron oxide through images of folding and origami. Fig. 17.7a, b also show the dark colour of the material due to the addition of magnetite. Katepetch and Rujiravanit (2011) and Barud et al. (2015) obtained different colours as the researchers tested different proportions of iron oxide and BC, with lower quantities of magnetite resulting in lighter biofilms and greater quantities resulting in darker biofilms. The colour of these materials is generally dark and on a grey scale or in brown tones. However, Zhang et al. (2022) were able to produce a transparent biofilm due to treatments of the BC prior to the addition of the iron oxide (acid hydrolysis of dried films and dilution in water) (Fig. 17.7c, d), the form of incorporation, and specific concentrations (mixture of aqueous solutions in which BC accounted for 22% of the weight in one and others had 63, 129, and 318 ppm of magnetite). The objective of the study was the creation of a photonic material.

Regarding the magnetic properties, they may vary depending on the type and size of the added particle. The most commonly used magnetic characterisation is the magnetic hysteresis curve, obtained through Vibrating Sample Magnetometry (VSM) analysis, which provides data such as the sample's saturation magnetisation (Ms) and its coercive field (H). Ms. is defined as the point at which all spins and domains of a material align in the same direction as an external magnetic field

(Cullity & Graham, 2009; Souza et al. 2023a, b). After reaching saturation, an additional increase in the intensity of the external field will not result in any change in the magnetisation of the material. Coercivity indicates the point to which a material can resist an external magnetic field without being de-magnetised (Shackelford, 2022). Materials used in the fabrication of permanent magnets have very high coercivity, whereas those with a greater adaptation capacity to changes in the field have lower coercivity (Guimarães, 2009).

In a VSM analysis, the material is exposed to a magnetic field gradually until reaching saturation. The field is then gradually reversed to determine the remanence of magnetism in the material (Ganapathe et al., 2020). The analysis of this method produces a hysteresis curve, as illustrated in Fig. 17.8.

Table 17.1 demonstrates the diversity of saturation magnetisation (Ms) and coercive field (H) values of magnetic BC samples reported in selected literature works, where authors have produced magnetic BC biopolymers with iron oxides.

As can be observed, there is a significant variation in Ms. and H values depending on the selected material and methodology. Other factors influencing these values include the final particle size and their percentage in the sample. For instance, Zhang et al. (2022) and Zhu et al. (2011) used the same type of particle (magnetite) and incorporation methodology into BC (ex situ process), as shown in Table 17.1. However, the achieved Ms. and H values were markedly different. This effect stemmed from the size disparity between the particles obtained in the two studies; in Zhang et al. (2022), the average particle diameter was 3.3 ± 1.2 nm, whereas in Zhu et al. (2011), it was 15 nm. Despite employing the same methodology, the production parameters differed between the studies, leading to distinct particle sizes.

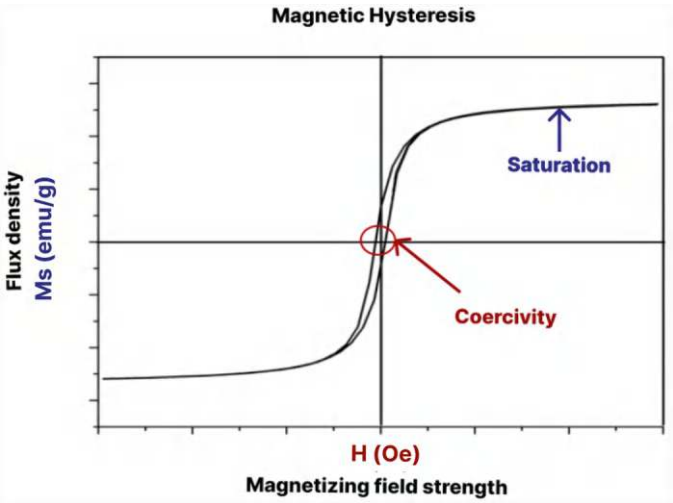

Fig. 17.8 Magnetic hysteresis curve highlighting coercivity and saturation magnetisation. (Adapted from Souza et al. (2023b). Published 2013 by MDPI with open access)

Table 17.1 Summary of saturation magnetisation (Ms) and coercive field (H) values in samples from selected literature works, along with their respective added particles and synthesis methodologies

Ref.	Added particle	Methodology used	Saturation magnetisation—Ms (emulg)[a]	Coercive field—H (Oe)[a]
Qiao et al. (2022)	Magnetite	In situ coprecipitation	34.07	[b]
Chaabane et al. (2020)			23.63	0.042
Usawattanakul et al. (2021)			5.14–11.56	[b]
Marins et al. (2013)			60.0	15
Souza et al. (2024)			3–17	1.04–6.23
Zhu et al. (2011)		Ex situ process	41	27
Zhang et al. (2022)			0.14	[b]
Souza et al. (2024)			8–10	3.80–22.07
Sriplai et al. (2018)			53.6	[b]
Olsson et al. (2010)	Cobalt ferrite	In situ coprecipitation	3.769–5.026	5000
Salidkul et al. (2021)	Barium ferrite	Ex situ process	24.1–49.5	5.31
Zeng et al. (2014)	Maghemite	Thermal decomposition in situ	60	[b]

[a] Measurements taken at room temperature
[b] Values very close to 0

The final dimensions of the particles to be added to BC can vary according to the synthesis parameters. Specific studies on the production of iron oxide nanoparticles highlight the influence of conditions such as pH, time, temperature, agitation, and reagents on the final particle size and consequently on their magnetic parameters (Koo et al., 2019; Riaz et al., 2013; Souza et al., 2023b, Yazdani & Seddigh, 2016).

In the work presented by Souza et al. (2024), there were also discrepancies in the magnetic values of the final materials, due to the adoption of different magnetite incorporation methodologies for each sample. In this study, in situ coprecipitation and ex situ process methodologies were employed with processed and intact films, respectively, each method influencing the final sizes of the nanoparticles, resulting in samples containing SPIONs and ferromagnetic nanoparticles.

17.6 Application of Magnetic BC

One of the main advantages in the production of magnetic BC is the diversity of possibilities in terms of the materials that can be added, methods that can be employed, with adaptations and variations for production, and applications, enabling the production of distinct biotechnological materials (Nypelö, 2022).

The literature describes the different applications of BC materials with iron oxides in the medical field, electronics, sensors, catalytic processes, and water treatment systems (Andriani et al., 2020; Campano et al., 2016; Chaabane et al., 2020; Chanthiwong et al., 2020; Kumar et al., 2022; Qiao et al., 2022; Salidkul et al., 2021; Zhu et al., 2011). The graph in Fig. 17.9 illustrates the proportion of applications for BC materials with iron oxides in different fields described in the literature (Works produced from 2010 to 2024, available on Google Scholar), and Fig. 17.10 shows some magnetic materials, found in the work of Mira-Cuenca et al. (2021) and Galland et al. (2013), where the authors directed their work to the medical and electronics areas, respectively.

17.6.1 Medical and Pharmaceutical Applications

The biocompatibility of BC enables the creation of novel materials and products with applications in the medical and pharmaceutical fields (Amorim et al. 2022a), such as the creation of advanced healing bandages, drug delivery systems, biomedical implants, and tissue engineering (Aditya et al., 2022; Eslahi et al., 2019).

In the fabrication of advanced healing bandages, BC is promising due to its moisture retention capacity and permeability to oxygen. BC bandages are able to retain medications for the treatment of conditions without impeding the circulation of air while protecting regions of the body from contaminants. The addition of iron

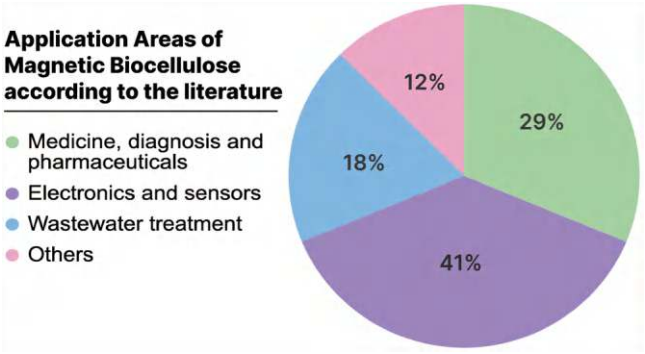

Fig. 17.9 Fields of application of magnetic bacterial cellulose suggested by articles in the literature (percentages of occurrence of suggestions)

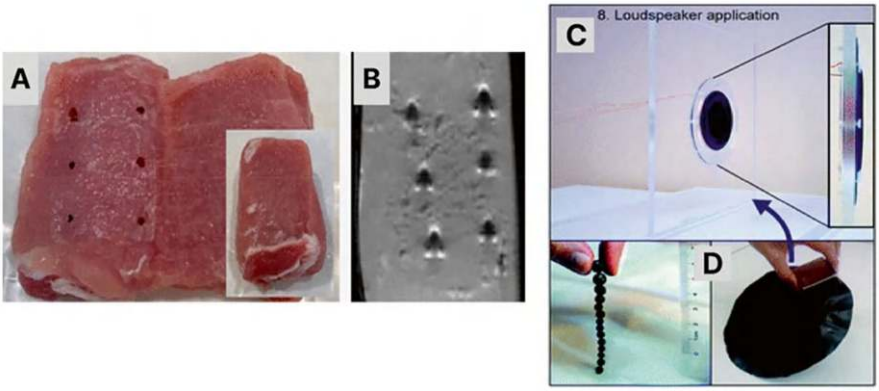

Fig. 17.10 (**a**, **b**) These pictures illustrate the possibility of the positioning of an implant in the human body. For this purpose, magnetic biotechnological materials produced by Mira-Cuenca et al. (2021) were applied to a piece of pork (**a**) and magnetic resonance imaging was performed (**b**). Detection of implanted material by MRI is made possible by the magnetic properties of the implant, visible as black areas in sharp contrast to the surrounding tissue. (Reprinted from Mira-Cuenca et al. (2021). Published 2021 by ACS as open access). (**c**) Large magnetic membranes (20 cm diameter) prepared by vacuum filtration of the decorated cellulose nanofibril suspension and adapted in a thin prototype loudspeaker without external magnet. (Reprinted from Galland et al. (2013). Published 2013 by RSC with open access)

oxide nanoparticles can also impart an antibiotic effect to the bandage (Ameen & Majrashi, 2024; Chaabane et al., 2020). Maruthupandy et al. (2021) produced a BC composite with graphene and magnetite and tested its antimicrobial activity against pathogens, such as *E. coli* and *P. mirabilis*, reporting an excellent performance.

In drug delivery systems, the magnetic properties of iron oxide particles incorporated into BC assist in the delivery of drugs to specific regions of the body. For instance, Chaabane et al. (2020) produced a complex with modified BC and magnetite for a drug delivery system that proved effective in the treatment of tumours in mice.

In the field of biomedical implants, the advantages of BC over other materials include its strength and capacity to be moulded into different shapes, serving as a basis for the creation of sutures, stents, and fixation devices. With the addition of iron oxides, these materials can be seen better in magnetic resonance images, thus dispensing the need for invasive surgical procedures. Mira-Cuenca et al. (2021) developed a paint with shredded BC fibres and magnetite nanoparticles for implants. The paint exhibited excellent performance as a transverse relaxation contrast agent that was detected by magnetic resonance in tests involving pig meat (Fig. 17.10a, b).

Another application reported in the literature is the use of iron oxide particles in chemotherapy for combatting cancer. Chaabane et al. (2020) modified the BC structure and added magnetite nanoparticles. The resulting material had antimicrobial properties and was also used as a chemotherapeutic agent in mice with tumours, achieving an excellent result in inhibiting tumour growth.

17.6.2 Electronic Applications

Advances in the field of electronics exert direct and indirect impacts on other fields, as all fields require electronic devices to perform tasks. BC materials with iron oxides are used in the production and optimisation of different parts and appliances, such as sensors, electric actuators, data storage systems, and sound amplification systems (Choi et al., 2022; Guan & Guo, 2021; Kumar et al., 2022; Zhang et al., 2022).

The use of BC materials with iron oxides is proposed and/or tested in studies conducted by Marins et al. (2013), Sriplai et al. (2020), and Chen et al. (2022). Flexibility, lightness, and the possibility of moulding the material into any shape are described as some of the major advantages for electronic applications. Sriplai et al. (2020) also discuss the piezoelectrical properties of BC films with iron oxides, which are important to the development of a broad variety of highly sensitive piezoelectric sensors. In the study, the authors created BC films with manganese ferrites. Chen et al. (2022) developed a wearable BC sensor with cobalt ferrites capable of monitoring oscillation frequency and motion velocity embedded in an "intelligent" jacket.

Other applications include use in sound amplifiers due to the flexibility and magnetisation, as described by Zeng et al. (2014), and in data storage systems due to the magnetic coercivity that can be achieved, as described by Salidkul et al. (2021). Sriplai et al. (2018) also suggest the application of a magnetic BC material in data storage systems as well as electric actuators due to the good response to external magnetic fields. Usawattanakul et al. (2021) suggest the application of BC films with magnetite in the design of novel electronic devices. Olsson et al. (2010) created a BC aerogel with cobalt ferrite with high coercivity and magnetic saturation, suggesting its use in electric actuators.

Various studies suggest applications in the field of electronics. However, few describe operating prototypes. Galland et al. (2013) and Tarrés et al. (2017) created prototype sound amplifiers using material made with nanofibres of treated plant cellulose (material similar to BC) embedded with magnetic iron oxides and obtained good results (Fig. 17.10c, d). The researchers state that similar prototypes could be made with magnetic BC and have satisfactory results.

17.6.3 Applications in Wastewater Treatment Systems

Nanometric fibres make BC films an excellent filtering medium (Galdino Jr et al., 2020). For selective filtering, studies have used dopants in the BC matrix, including iron oxides. Salleh et al. (2023) produced a BC composite with magnetite capable of cleaning wastewater with methyl orange, which is a dye used in the textile industry. The composite was capable of absorbing and inactivating the dye due to the structure of the BC and the interaction with the Fe^{3+} ions in magnetite. Chen et al.

(2021) also tested a BC composite embedded with magnetite and reported satisfactory results in the removal of Congo Red from wastewater.

There are also reports of the removal of heavy metals. The magnetic characteristics also assist in the applicability of BC composites, facilitating removal from the medium. In a review performed by Mikhailidi et al. (2023), a schematic demonstrates heavy metal removal and the recovery of magnetic BC biopolymers in treatment tanks. The operation occurs with the transference of the material between absorption and desorption tanks with the aid of an electromagnetic device.

17.7 Conclusions

This chapter shows that materials produced with BC and iron oxides constitute a significant innovation. The unique characteristics make these materials highly versatile, with enormous potential in various applications in the most diverse sectors of industry and research. Various studies have been conducted that explore the production and applications of these materials. However, there are still challenges that need to be overcome, such as the production of prototypes on a commercial scale.

To overcome these challenges, continued research is needed for the constant improvement of the materials and the expansion of the gamut of potential applications. Moreover, it is necessary to focus on more practical issues, such as the efficient production of devices and the investigation of applications in different fields.

New and continuous investment in research, development, and innovation is essential to addressing the challenges and exploring the full potential of these materials. We could then blaze the trail for new discoveries and applications that could benefit different fields of science and technology.

References

Aditya, T., Allain, J. P., Jaramillo, C., & Restrepo, A. M. (2022). Surface modification of bacterial cellulose for biomedical applications. *International Journal of Molecular Sciences, 23*, 610. https://doi.org/10.3390/ijms23020610

Akhtar, N., Mohammed, H. A., Yusuf, M., Al-Subaiyel, A., Sulaiman, G. M., & Khan, R. A. (2022). SPIONs conjugate supported anticancer drug doxorubicin's delivery: Current status, challenges, and prospects. *Nanomaterials, 12*, 3686. https://doi.org/10.3390/nano12203686

Albuquerque, R. M. P., Meira, H. M., Silva, I. D. L., Silva Jr, C. J. G., Almeida, F. C. G., et al. (2021). Production of a bacterial cellulose/poly (3-hydroxybutyrate) blend activated with clove essential oil for food packaging. *Polymers and Polymer Composites, 29*(4), 259–270. https://doi.org/10.1177/0967391120912098

Amarasekara, A. S., Wang, D., & Grady, T. L. (2020). A comparison of kombucha SCOBY bacterial cellulose purification methods. *SN Applied Sciences, 2*, 240. https://doi.org/10.1007/s42452-020-1982-2

Ameen, F., & Majrashi, N. (2024). Recent trends in the use of cobalt ferrite nanoparticles as an antimicrobial agent for disability infections: A review. *Inorganic Chemistry Communications, 156*, 111187. https://doi.org/10.1016/j.inoche.2023.111187

Amorim, J. D. P., Souza, K. C., Duarte, C. R., Duarte, I. S., Ribeiro, F. A. S., Silva, G. S., et al. (2020). Plant and bacterial nanocellulose: Production, properties and applications in medicine, food, cosmetics, electronics and engineering. A review. *Environmental Chemistry Letters, 18*(3), 851–869. https://doi.org/10.1007/s10311-020-00989-9

Amorim, J. D. P., Nascimento, H. A., Silva Jr, C. J. G., Medeiros, A. D. M., Silva, I. D. L., Costa, A. F. S., et al. (2022a). Obtainment of bacterial cellulose with added propolis extract for cosmetic applications. *Polymer Engineering and Science, 62*(2), 565–575. https://doi.org/10.1002/pen.25868

Amorim, J. D. P., Silva Jr, C. J. G., Medeiros, A. D. M., Nascimento, H. A., Sarubbo, M., Medeiros, T. P. M., et al. (2022b). Bacterial cellulose as a versatile biomaterial for wound dressing application. *Molecules, 27*(17), 5580–5605. https://doi.org/10.3390/molecules27175580

Andriani, D., Yuthi, A. A., & Karina, M. (2020). The optimization of bacterial cellulose production and its applications: A review. *Cellulose, 27*(12), 6747–6766. https://doi.org/10.1007/s10570-020-03273-9

Arias, S. L., Shetty, A. R., Senpan, A., Echeverry-Rendón, M., Reece, L. M., & Allain, J. P. (2016). Fabrication of a functionalized magnetic bacterial nanocellulose with iron oxide nanoparticles. *Journal of Visualized Experiments, 111*, 52951. https://doi.org/10.3791/52951

Arserim-Uçar, D. K., Korel, F., Liu, L. S., & Inhame, K. L. (2021). Characterization of bacterial cellulose nanocrystals: Effect of acid treatments and neutralization. *Food Chemistry, 336*, 127597. https://doi.org/10.1016/j.foodchem.2020.127597

Barud, H. S., Tercjak, A., Gutierrez, J., Viali, W. R., Nunes, E. S., Ribeiro, S. J. L., et al. (2015). Biocellulose-based flexible magnetic paper. *Journal of Applied Physics, 117*, 17B734. https://doi.org/10.1063/1.4917261

Betlej, I., Zakaria, S., Krajewski, K. J., & BoruszewskIi, P. (2021). Bacterial cellulose properties and its potential application. *Sains Malaysiana, 50*, 493–505. https://doi.org/10.17576/jsm-2021-5002-20

Bhateria, R., & Singh, R. (2019). A review on nanotechnological application of magnetic iron oxides for heavy metal removal. *Journal of Water Process Engineering, 31*, 100845. https://doi.org/10.1016/j.jwpe.2019.100845

Bustamante-Torres, M., Romero-Fierro, D., Estrella-Nuñez, J., Arcentales-Vera, B., Chichande-Proaño, E., & Bucio, E. (2022). Polymeric composite of magnetite iron oxide nanoparticles and their application in biomedicine: A review. *Polymers, 14*, 752. https://doi.org/10.3390/polym14040752

Callister, W. D., & Rethwisch, D. G. (2016). *Ciência e Engenharia De Materiais: Uma Introdução* (9th ed.). LTC.

Campano, C., Balea, A., Blanco, A., & Negro, C. (2016). Enhancement of the fermentation process and properties of bacterial cellulose: A review. *Cellulose, 23*(1), 57–91. https://doi.org/10.1007/s10570-015-0802-0

Chaabane, L., Chahdoura, H., Mehdaoui, R., Snoussi, M., Beyou, E., Lahcini, M., & Baouab, M. H. V. (2020). Functionalization of developed bacterial cellulose with magnetite nanoparticles for nanobiotechnology and nanomedicine applications. *Carbohydrate Polymers, 247*, 116707. https://doi.org/10.1016/j.carbpol.2020.116707

Chanthiwong, M., Mongkolthanaruk, W., Eichhorn, S. J., & Pinitsoontorn, S. (2020). Controlling the processing of co-precipitated magnetic bacterial cellulose/iron oxide nanocomposites. *Materials and Design, 196*, 109148. https://doi.org/10.1016/j.matdes.2020.109148

Chen, X., Huang, Z., & Luo, S. (2021). Multi-functional magnetic hydrogels based on Millettia speciosa Champ residue cellulose and Chitosan: Highly efficient and reusable adsorbent for Congo red and Cu^{2+} removal. *Chemical Engineering Journal, 423*, 130198. https://doi.org/10.1016/j.cej.2021.130198

Chen, K., Li, Y., Du, Z., Hu, S., Huang, J., Shi, Z., Su, B., & Yang, G. (2022). $CoFe_2O_4$ embedded bacterial cellulose for flexible, biodegradable, and self-powered electromagnetic sensor. *Nano Energy, 102*, 107740. https://doi.org/10.1016/j.nanoen.2022.107740

Choi, S. M., Rao, K. M., Zo, S. M., Shin, E. J., & Han, S. S. (2022). Bacterial cellulose and its applications. *Polymers, 14*(6), 1080. https://doi.org/10.3390/polym14061080

Costa, A. F. S., Almeida, F. C. G., Vinhas, G. M., & Sarubbo, L. A. (2017). Production of bacterial cellulose by *Gluconacetobacter Hansenii* using corn steep liquor as nutrient sources. *Frontiers in Microbiology, 8*, 2007. https://doi.org/10.3389/fmicb.2017.02027

Costa, A. F. S., Silva Jr, C. J. G., Meira, H. M., Amorim, J. D. P., Silva, I., Gomes, E. S., & Sarubbo, L. A. (2020). Production of paper using bacterial cellulose and residue from the sugar and alcohol industry. *Chemical Engineering Transactions, 79*, 85–90. https://doi.org/10.3303/CET2079015

Cullity, B. D., & Graham, C. D. (2009). *Introduction to magnetic materials* (2nd ed.). Wiley.

Dudchenko, N., Pawar, S., Perelshtein, I., & Fixler, D. (2023). Magnetite-based biosensors and molecular logic gates: From magnetite synthesis to application. *Biosensors, 13*, 304. https://doi.org/10.3390/bios13030304

Eichhorn, S. J. (2011). Cellulose nanowhiskers: Promising materials for advanced applications. *Soft Matter, 7*(2), 303. https://doi.org/10.1039/c0sm00142b

Esa, F., Tasirin, S. M., & Rahman, N. A. (2014). Overview of bacterial cellulose production and application. *Agriculture and Agricultural Science Procedia, 2*, 113–119. https://doi.org/10.1016/j.aaspro.2014.11.017

Eslahi, N., Mahmoodi, A., Mahmoudi, N., Zandi, N., & Simchi, A. (2019). Processing and properties of nanofibrous bacterial cellulose-containing polymer composites: A review of recent advances for biomedical applications. *Polymer Reviews, 60*(1), 144–170. https://doi.org/10.1080/15583724.2019.1663210

Francisquini, E., Schoenmaker, J., & Souza, J. A. (2014). Nanopartículas magnéticas e suas aplicações. *Química Supramolecular e Nanotecnologia, 1*, 269–288. https://doi.org/10.1590/1806-9126-RBEF-2020-0374

Galdino Jr, C. J. S., Maia, A. D., Meira, H. M., Souza, T. C., Amorim, J. D. P., Almeida, F. C. G., et al. (2020). Use of a bacterial cellulose filter for the removal of oil from wastewater. *Process Biochemistry, 91*, 288–296. https://doi.org/10.1016/j.procbio.2019.12.020

Galland, S., Andersson, R. L., Salajková, M., Ström, V., Olsson, R. T., & Berglund, L. A. (2013). Cellulose nanofibers decorated with magnetic nanoparticles–synthesis, structure and use in magnetized high toughness membranes for a prototype loudspeaker. *Journal of Materials Chemistry C, 1*(47), 7963–7972. https://doi.org/10.1039/C3TC31748J

Ganapathe, L. S., Mohamed, M. A., Yunus, M. R., & Berhanuddin, D. D. (2020). Magnetite (Fe_3O_4) nanoparticles in biomedical application: From synthesis to surface functionalisation. *Magnetochemistry, 6*(4), 68. https://doi.org/10.3390/magnetochemistry6040068

Girardet, T., Venturini, P., Martinez, H., Dupin, J. C., Cleymand, F., & Fleutot, S. (2022). Spinel magnetic iron oxide nanoparticles: Properties, synthesis and washing methods. *Applied Sciences, 12*, 8127. https://doi.org/10.3390/app12168127

Guan, F., & Guo, C. F. (2021). Flexible, high-strength, and porous nano-nano composites based on bacterial cellulose for wearable electronics: A review. *Soft Science, 1*, 16. https://doi.org/10.20517/ss.2021.19

Guimarães, A. P. (2009). *Magnetismo e Ressonância Magnética em Sólidos* (1st ed.). Ed USP.

Halliday, D., & Resnick, R. (2021). *Fundamentals of physics* (Vol. 3, 11th ed.). Wiley.

Hestrin, S., & Schramm, M. (1954). Synthesis of cellulose by *Acetobacter xylinum*: II. Preparation of freeze—Dried cells capable of polymerized glucose to cellulose. *The Biochemical Journal, 58*, 345–352. https://doi.org/10.1042/bj0580345

Huang, H. C., Chen, L. C., Lin, S. B., Hsu, C. P., & Chen, H. H. (2010). In situ modification of bacterial cellulose network structure by adding interfering substances during fermentation. *Bioresource Technology, 101*(15), 6084–6091. https://doi.org/10.1016/j.biortech.2010.03.031

Huo, Y., Guo, D., Yang, J., Chang, Y., Wang, B., Mu, C., et al. (2022). Multifunctional bacterial cellulose nanofibers/polypyrrole (PPy) composite films for joule heating and electromagnetic interference shielding. *ACS Applied Electronic Materials, 4*(5), 2552–2560. https://doi.org/10.1021/acsaelm.2c00316

Hussain, Z., Sajjad, W., Khan, T., & Wahid, F. (2019). Production of bacterial cellulose from industrial wastes: A review. *Cellulose, 26*(5), 2895–2911. https://doi.org/10.1007/s10570-019-02307-1

Katepetch, C., & Rujiravanit, R. (2011). Synthesis of magnetic nanoparticle into bacterial cellulose matrix by ammonia gas-enhancing *in situ* co-precipitation method. *Carbohydrate Polymers, 86*(1), 162–170. https://doi.org/10.1016/j.carbpol.2011.04.024

Koo, K. N., Ismail, A. F., Othman, M. H. D., Bidin, N., & Rahman, M. A. (2019). Preparation and characterization of superparamagnetic magnetite (Fe_3O_4) nanoparticles: A short review. *Malaysian Journal of Fundamental and Applied Sciences, 15*(1), 23–31. https://doi.org/10.11113/MJFAS.V15N2019.1224

Kumar, A., Sood, A., & Han, S. S. (2022). Potential of magnetic nano cellulose in biomedical applications: Recent advances. *Biomaterials and Polymers Horizon, 1*(1), 32–47. https://doi.org/10.37819/bph.001.01.0133

Kurosumi, A., Sasaki, C., Yamashita, Y., & Nakamura, Y. (2019). Utilization of various fruit juices as carbon source for production of bacterial cellulose by *Acetobacter xylinum* NBRC 13693. *Carbohydrate Polymers, 76*, 333–335. https://doi.org/10.1016/j.carbpol.2008.11.009

Marins, J. A., Soares, B. G., Barud, H. S., & Ribeiro, S. J. L. (2013). Flexible magnetic membranes based on bacterial cellulose and its evaluation as electromagnetic interference shielding material. *Materials Science and Engineering: C, 33*(7), 3994–4001. https://doi.org/10.1016/j.msec.2013.05.035

Martínez-Sanz, M., López-Rubio, A., & Lagarón, J. M. (2011). Optimization of the nanofabrication by acid hydrolysis of bacterial cellulose nanowhiskers. *Carbohydrate Polymers, 85*(1), 228–236. https://doi.org/10.1016/j.carbpol.2011.02.021

Maruthupandy, M., Riquelme, D., Rajivgandhi, G., Muneeswaran, T., Cho, W. S., Anand, M., et al. (2021). Dual-role of graphene/bacterial cellulose/magnetite nanocomposites as highly effective antibacterial agent and visible-light-driven photocatalyst. *Journal of Environmental Chemical Engineering, 9*(5), 106014. https://doi.org/10.1016/j.jece.2021.106014

Medeiros, A. D. M. d., Silva Junior, C. J. G. d., Amorim, J. D. P. d., Durval, I. J. B., Costa, A. F. d. S., & Sarubbo, L. A. (2022). Oily wastewater treatment: Methods, challenges, and trends. *Processes*, *10*, 743. https://doi.org/10.3390/pr10040743

Medeiros, A. D. M. d., Silva Junior, C. J. G. d., Amorim, J. D. P. d., Durval, I. J. B., Damian, R. B., Cavalcanti, Y. d. F., et al. (2023). Design and modeling of a biotechnological nanofiltration module using bacterial cellulose membranes for the separation of oily mixtures. *Water*, *15*, 2025. https://doi.org/10.3390/w15112025

Menchaca-Nal, S., Jativa-Herrera, J. A., Moscoso-Londoño, O., Pampillo, L. G., Martínez-García, L., Knobel, M., & Londoño-Calderón, C. L. (2023). Composite magnetic properties of cobalt ferrite nanoparticles embedded in bacterial nanocellulose of different porosity levels. *Materials Chemistry and Physics, 303*, 127798. https://doi.org/10.1016/j.matchemphys.2023.127798

Merazzo, K. J., Lima, A. C., Rincón-Iglesias, M., Fernandes, L. C., Pereira, N., Lanceros-Mendez, S., & Martins, P. (2021). Magnetic materials: A journey from finding north to an exciting printed future. *Materials Horizons, 8*(10), 2654–2684. https://doi.org/10.1039/D1MH00641J

Mikhailidi, A., Ungureanu, E., & Belosinschi, D. (2023). Cellulose-based metallogels—Part 3: Multifunctional materials. *Gels, 9*, 878. https://doi.org/10.3390/gels9110878

Mira-Cuenca, C., Meslier, T., Roig-Sanchez, S., Laromaine, A., & Roig, A. (2021). Patterning bacterial cellulose films with iron oxide nanoparticles and magnetic resonance imaging monitoring. *ACS Applied Polymer Materials, 3*(10), 4959–4965. https://doi.org/10.1021/acsapm.1c00723

Moon, R. J., Martini, A., Nairn, J., Simonsen, J., & Youngblood, J. (2011). Cellulose nanomaterials review: Structure, properties and nanocomposites. *Chemical Society Reviews, 40*, 3941–3994. https://doi.org/10.1039/C0CS00108B

Narayanaswamy, V., Sambasivam, S., Saj, A., Alaabed, S., Issa, B., Al-Omari, I. A., & Obaidat, I. M. (2021). Role of magnetite nanoparticles size and concentration on hyperthermia under various field frequencies and strengths. *Molecules, 26*(4), 796. https://doi.org/10.3390/molecules26040796

Nascimento, H. A., Converti, A., Costa, A. F. S., & Sarubbo, L. A. (2021). Bacterial cellulose biotextiles for the future of sustainable fashion: A review. *Environmental Chemistry Letters, 19*(4), 2967–2980. https://doi.org/10.1007/s10311-021-01214-x

Nascimento, H. A., Amorim, J. D. P., Filho, L. E. P. T. M., Costa, A. F. S., Sarubbo, L. A., Napoleão, D. C., & Vinhas, G. M. (2022). Production of bacterial cellulose with antioxidant additive from grape residue with promising cosmetic applications. *Polymer Engineering and Science, 62*(9), 2826–2839. https://doi.org/10.1002/pen.26065

Niculescu, A. G., Chircov, C., & Grumezescu, A. M. (2021). Magnetite nanoparticles: Synthesis methods–A comparative review. *Methods, 199*, 16–27. https://doi.org/10.1016/j.ymeth.2021.04.018

Nypelö, T. (2022). Magnetic cellulose: Does extending cellulose versatility with magnetic functionality facilitate its use in devices? *Journal of Materials Chemistry C, 10*, 805–818. https://doi.org/10.1039/D1TC02105B

Oliveira, L. C., Fabris, J. D., & Pereira, M. C. (2013). Óxidos de ferro e suas aplicações em processos catalíticos: uma revisão. *Química Nova, 36*, 123–130. https://doi.org/10.1590/S0100-40422013000100022

Olsson, R. T., Azizi Samir, M. A. S., Salazar-Alvarez, G., Belova, L., Ström, V., Berglund, L. A., et al. (2010). Making flexible magnetic aerogels and stiff magnetic nanopaper using cellulose nanofibrils as templates. *Nature Nanotechnology, 5*(8), 584–588. https://doi.org/10.1038/nnano.2010.155

Patwa, R., Zandraa, O., Capáková, Z., Saha, N., & Sáha, P. (2020). Effect of iron-oxide nanoparticles impregnated bacterial cellulose on overall properties of alginate/casein hydrogels: Potential injectable biomaterial for wound healing applications. *Polymers, 12*(11), 2690. https://doi.org/10.3390/polym12112690

Purnama, P., Samsuri, M., & Iswaldi, I. (2022). A review on fully bio-based materials development from polylactide and cellulose nanowhiskers. *Polymers, 14*(19), 4009. https://doi.org/10.3390/polym14194009

Qiao, W., Zhang, Z., Qian, Y., Xu, L., & Guo, H. (2022). Bacterial laccase immobilized on a magnetic dialdehyde cellulose without cross-linking agents for decolorization. *Colloids and Surfaces A: Physicochemical and Engineering Aspects, 632*, 127818. https://doi.org/10.1016/j.colsurfa.2021.127818

Riaz, S., Bashir, M., & Naseem, S. (2013). Iron oxide nanoparticles prepared by modified co-precipitation method. *IEEE Transactions on Magnetics, 50*(1), 4003304. https://doi.org/10.1109/TMAG.2013.2277614

Safarik, I., & Safarikova, M. (2009). Magnetic nano-and microparticles in biotechnology. *Chemical Papers, 63*(5), 497–505. https://doi.org/10.2478/s11696-009-0054-2

Salidkul, N., Mongkolthanaruk, W., Faungnawakij, K., & Pinitsoontorn, S. (2021). Hard magnetic membrane based on bacterial cellulose–barium ferrite nanocomposites. *Carbohydrate Polymers, 264*, 118016. https://doi.org/10.1016/j.carbpol.2021.118016

Salleh, A. K., Salama, A., Badawy, A. S., Diab, M. A., & El-Gendiet, H. (2023). Paper sludge saccharification for batch and fed-batch production of bacterial cellulose decorated with magnetite for dye decolorization by experimental design. *Cellulose, 30*, 10841–10866. https://doi.org/10.1007/s10570-023-05545-6

Salles, T. R., Bruckamann, F. S., Viana, A. R., Krause, L. M. F., Mortari, S. R., & Rhoden, C. R. B. (2022). Magnetic nanocrystalline cellulose: Azithromycin adsorption and in vitro biological activity against melanoma cells. *Journal of Polymers and the Environment, 30*(7), 2695–2713. https://doi.org/10.1007/s10924-022-02388-3

Samrot, A. V., Sahithy, C. S., Selvarani, J., Purayi, S. K., & Ponnaiah, P. (2021). A review on synthesis, characterization and potential biological applications of superparamagnetic iron oxide nanoparticles. *Current Research in Green and Sustainable Chemistry, 4*, 100042. https://doi.org/10.1016/j.crgsc.2020.100042

Schwertmann, U., & Cornell, R. M. (2008). *Iron oxides in the laboratory: Preparation and characterization* (2nd ed.). Wiley.

Shackelford, J. F. (2022). *Introduction to materials science for engineers* (9th ed.). Pearson Prentice Hall.

Sharma, A., Thakur, M., Bhattacharya, M., Mandal, T., & Saswata, G. (2019). Commercial application of cellulose nano-composites—A review. *Biotechnology Reports, 21*, e00316. https://doi.org/10.1016/j.btre.2019.e00316

Silva Jr, C. J. G., de Amorim, J. D. P., de Medeiros, A. D. M., de Holanda Cavalcanti, A. K. L., do Nascimento, H. A., Henrique, M. A., et al. (2022). Design of a naturally dyed and waterproof biotechnological leather from reconstituted cellulose. *Journal of Functional Biomaterials, 13*, 49. https://doi.org/10.3390/jfb13020049

Silva, F. A. G. S., Meister, F., Dourado, F., & Gama, M. (2023). Regenerated bacterial cellulose fibres. *International Journal of Biological Macromolecules, 253*(7), 127310. https://doi.org/10.1016/j.ijbiomac.2023.127310

Souza, T. C., Amorim, J. D. P., Silva Jr, C. J. G., Medeiros, A. D. M., Costa, A. F. S., Vinhas, G. M., & Sarubbo, L. A. (2023a). Magnetic bacterial cellulose biopolymers: Production and potential applications in the electronics sector. *Polymers, 15*(4), 853. https://doi.org/10.3390/polym15040853

Souza, T. C., Costa, A. F. S., Vinhas, G. M., & Sarubbo, L. A. (2023b). Synthesis of iron oxides and influence on final sizes and distribution in bacterial cellulose applications. *Polymers, 15*(15), 3284. https://doi.org/10.3390/polym15153284

Souza, T. C., Santos, A. R., Chacon, J. L. S. P., Durval, I. J. B., Costa, A. F. S., Hernández, E. P., et al. (2024). Innovation in methods for incorporating magnetite into biocellulose for electromagnetic interference shielding effectiveness applications. *Energies, 17*(13), 3202. https://doi.org/10.3390/en17133202

Spaldin, N. A. (2010). *Magnetic materials: Fundamentals and applications* (2nd ed.). Cambridge University Press.

Sperotto, G., Stasiak, L. G., Godoi, J. P. M. G., Gabiatti, N. C., & Souza, S. S. (2021). A review of culture media for bacterial cellulose production: Complex, chemically defined and minimal media modulations. *Cellulose, 28*(5), 2649–2673. https://doi.org/10.1007/s10570-021-03754-5

Sriplai, N., & Pinitsoontorn, S. (2020). Bacterial cellulose-based magnetic nanocomposites: A review. *Carbohydrate Polymers, 254*, 117228. https://doi.org/10.1016/j.carbpol.2020.117228

Sriplai, N., Mongkolthanaruk, W., Eichhorn, S. J., & Pinitsoontorn, S. (2018). Magnetically responsive and flexible bacterial cellulose membranes. *Carbohydrate Polymers, 192*, 251–262. https://doi.org/10.1016/j.carbpol.2018.03.072

Sriplai, N., Mangayil, R., Pammo, A., Santala, V., Tuukkanen, S., & Pinitsoontorn, S. (2020). Enhancing piezoelectric properties of bacterial cellulose films by incorporation of $MnFe_2O_4$ nanoparticles. *Carbohydrate Polymers, 231*, 115730. https://doi.org/10.1016/j.carbpol.2019.115730

Stumpf, T. R., Yang, X., Zhang, J., & Cao, X. (2018). In situ and ex situ modifications of bacterial cellulose for applications in tissue engineering. *Materials Science and Engineering: C, 82*, 372–383. https://doi.org/10.1016/j.msec.2016.11.121

Tarrés, Q., Deltell, A., Espinach, F. X., Pèlach, M. À., Delgado-Aguilar, M., & Mutjé, P. (2017). Magnetic bionanocomposites from cellulose nanofibers: Fast, simple and effective production method. *International Journal of Biological Macromolecules, 99*, 29–36. https://doi.org/10.1016/j.ijbiomac.2017.02.072

Ul-Islam, M., Ullah, M. W., Khan, S., & Park, J. K. (2017). Strategies for cost-effective and enhanced production of bacterial cellulose. *International Journal of Biological Macromolecules, 102*, 1166–1173. https://doi.org/10.1007/s11814-020-0524-3

Ul-Islam, M., Ullah, M. W., Khan, S., & Park, J. K. (2020). Production of bacterial cellulose from alternative cheap and waste resources: A step for cost reduction with positive environmental aspects. *Korean Journal of Chemical Engineering, 37*(6), 925–937. https://doi.org/10.1007/s11814-020-0524-3

Urbina, L., Corcuera, M. A., Gabilondo, N., Eceiza, A., & Retegi, A. (2021). A review of bacterial cellulose: Sustainable production from agricultural waste and applications in various fields. *Cellulose, 28*(13), 8229–8253. https://doi.org/10.1007/s10570-021-04020-4

Usawattanakul, N., Torgbo, S., Sukyai, P., Khantayanuwong, S., Puangsin, B., & Srichola, P. (2021). Development of nanocomposite film comprising of polyvinyl alcohol (PVA) incorporated with bacterial cellulose nanocrystals and magnetite nanoparticles. *Polymers, 13*(11), 1778. https://doi.org/10.3390/polym13111778

Vangijzegem, T., Lecomte, V., Ternad, I., Van Leuven, L., Muller, R. N., Stanicki, D., & Laurent, S. (2023). Superparamagnetic iron oxide nanoparticles (SPION): From fundamentals to state-of-the-art innovative applications for cancer therapy. *Pharmaceutics, 15*(1), 236. https://doi.org/10.3390/pharmaceutics15010236

Vasconcelos, N. F., Feitosa, J. P. A., Gama, F. M. P., Morais, J. P. S., Andrade, F. K., Souza Filho, M. S. M., & Rosa, M. F. (2017). Bacterial cellulose nanocrystals produced under different hydrolysis conditions: Properties and morphological features. *Carbohydrate Polymers, 155*(2), 425–431. https://doi.org/10.1016/j.carbpol.2016.08.090

Vitta, S., Drillon, M., & Derory, A. (2010). Magnetically responsive bacterial cellulose: Synthesis and magnetic studies. *Journal of Applied Physics, 108*(5), 053905. https://doi.org/10.1063/1.3476058

Yang, P., Li, E., Xiao, F., Zhou, P., Wang, Y., Tang, W., He, P., & Jia, B. (2022). Nanostructure Fe-Co-B/bacterial cellulose based carbon nanofibers: An extremely efficient electrocatalyst toward oxygen evolution reaction. *International Journal of Hydrogen Energy, 47*, 12953–12963. https://doi.org/10.1016/j.ijhydene.2022.02.053

Yazdani, F., & Seddigh, M. (2016). Magnetite nanoparticles synthesized by co-precipitation method: The effects of various iron anions on specifications. *Materials Chemistry and Physics, 184*, 318–323. https://doi.org/10.1016/j.matchemphys.2016.09.058

Yusoff, A. H. M., Salimi, M. N., & Jamlos, M. F. (2017). A review: Synthetic strategy control of magnetite nanoparticles production. *Advances in Nano Research, 6*(1), 1–19. https://doi.org/10.12989/anr.2018.6.1.001

Zeng, M., Laromaine, A., Feng, W., Levkinb, A. P., & Roig, A. (2014). Origami magnetic cellulose: Controlled magnetic fraction and patterning of flexible bacterial cellulose. *Journal of Materials Chemistry C, 2*, 6312–6318. https://doi.org/10.1039/C4TC00787E

Zhang, X., Kang, S., Adstedt, K., Kim, M., Xiong, R., Yu, J., et al. (2022). Uniformly aligned flexible magnetic films from bacterial nanocelluloses for fast actuating optical materials. *Nature Communications, 13*, 5804. https://doi.org/10.1038/s41467-022-33615-z

Zhou, J., Li, R., Liu, S., Li, Q., Zhang, L., Zhang, L., & Guan, J. (2009). Structure and magnetic properties of regenerated cellulose/Fe_3O_4 nanocomposite films. *Journal of Applied Polymer Science, 111*(5), 2477–2484. https://doi.org/10.1002/app.29236

Zhu, H., Jia, S., Wan, T., Jia, Y., Yang, H., Li, J., Yan, L., & Zhong, C. (2011). Biosynthesis of spherical Fe_3O_4/bacterial cellulose nanocomposites as adsorbents for heavy metal ions. *Carbohydrate Polymers, 86*(4), 1558–1564. https://doi.org/10.1016/j.carbpol.2011.06.061

Chapter 18
Nanocellulose-Based Hydrogels

Falk Liebner and Nurali Alaudini

18.1 Introduction

Coined by the nineteenth-century Scottish chemist Thomas Graham, the term "gel" refers to a material characterized by a non-fluid colloidal or polymer network that is permeated by a fluid. According to the International Union of Pure and Applied Chemistry (IUPAC), the properties of a gel are influenced by three primary factors: (1) the nature of the colloidal particles or polymers constituting the non-fluid fraction, (2) the interparticle or intermolecular bonding present within the network, and (3) the characteristics of the fluid phase occupying the interstitial spaces of the network. Key properties that affect the interaction with the fluid include chemical composition, surface functional groups, crosslinking density, molecular weight, crystallinity, size, geometry, and the topology of the particle surfaces (Alemán et al., 2007).

This chapter focuses on nanocellulose hydrogels, defining them as containing water as the sole expanding fluid, distinguishing them from organogels. The composition of hydrogels primarily consists of hydrophilic polymers crosslinked by physical and/or chemical means, creating stable soft materials. Hydration begins with the most polar groups at the surface of the dry hydrogel, leading to "primary bound water." As hydration progresses, the networks swell, exposing less polar and hydrophobic groups, forming "secondary bound water" (Hoffman, 2002). This results in a cumulative "total bound water," and swelling reaches equilibrium when osmotic pressure balances the elastic retraction from crosslinking (Deng et al., 2022). Water absorbed before this equilibrium is termed "free water" or "bulk water."

F. Liebner (✉) · N. Alaudini
Institute of Chemistry of Renewable Resources, BOKU University Vienna, Tulln an der Donau, Austria
e-mail: falk.liebner@boku.ac.at

G. Korotcenkov (ed.), *The Handbook of Paper-Based Sensors and Devices*,
https://doi.org/10.1007/978-3-031-91080-7_18

The kinetics of swelling and quantitative features related to water interaction can be tailored through network design and the choice of monomers, oligomers, and polymers. Hydrogels can also be modified to respond to external stimuli by reconfiguring crosslinks or altering polymer segment conformations, enabling changes in shape, polarity, and morphology (Deng et al., 2022). Stimuli-responsive hydrogels may utilize physical (e.g., temperature, pressure) or chemical triggers (e.g., pH, metal ions), making them suitable for diverse applications such as sensing, controlled release of compounds (Gunathilake et al., 2020), tissue engineering, shape-memory materials, and self-healing materials (Wang et al., 2018).

Hydrogels have been developed from various synthetic polymers, including polyacrylic acid and polyoxyethylene, polyacrylamide and (methacrylic acid), polyvinylpyrrolidone, polyethyleneimine, polyamine, polyamide, and polyvinyl alcohol. However, these synthetic polymers may contain trace amounts of harmful unreacted monomers, oligomers, crosslinking agents, by-products, or solvent residues (Deng et al., 2022).

In response to these concerns and growing emphasis on a bio-based economy aligned with Green Chemistry principles, there is increasing interest in biopolymer hydrogels. Biopolymers are biocompatible, biodegradable, and suited for humid environments, and they are inherently free from harmful unreacted monomers or solvent residues, depending of course on the extraction and purification methods employed.

Among various biopolymers suitable for hydrogel applications, cellulose occupies a prominent position due to its environmental friendliness, affordability, and versatility. As the most abundant biopolymer on Earth, cellulose is widely accessible and high in purity. Its hydrophilic nature arises from the numerous hydroxyl groups distributed along its unbranched backbone (three hydroxyl groups per anhydroglucose repeating unit, AGU) and its supramolecular structure, which relies on both intra- and intermolecular hydrogen bonding. The natural "sugar" pattern imparts two key properties to cellulose: biocompatibility and biodegradability. Biocompatibility results from the similarity of its (1→4)-β-D-pyranoglucan structure to the glycoproteins and polysaccharides (glucosaminoglycans) found in the extracellular matrix of living tissues. Biodegradability is primarily due to its polar surface, which supports biofilm formation and allows enzymes to hydrolyze β-(1→4)-glycosidic bonds. This process can be enhanced by radical depolymerization, a phenomenon observed during the aerobic degradation of lignocellulosic biomass in soils, mediated by fungal enzymes, for example (Datta, 2024).

Comparative biodegradability studies of various non-derivatized and derivatized cellulose products have confirmed that native cellulose, including bacterial cellulose (Ruka et al., 2015), nanocrystalline cellulose (Bading et al., 2024), and cellulose fibrils (Vikman et al., 2015), is readily biodegradable, as assessed by EN 13432 and OEC 1992 standards. Based on these fundamental properties and the ability to modify cellulose through mechanical, physical, and chemical means, nanocellulose hydrogels have found diverse applications in recent decades.

These properties, combined with the ability to modify cellulose through mechanical, physical, and chemical means, have led to the diverse applications across various sectors including biomedicine, food industry, environmental protection, or

flexible electronics (Tang et al., 2024). A more comprehensive overview of nanocellulose hydrogel applications is provided at the end of this chapter.

18.2 Hydrogels from Different Types of Nanocelluloses

The term "nanocellulose" designates a class of materials that possess a dimension not exceeding 100 nm in at least one spatial direction. Despite variations in aspect ratio, morphology, crystallinity, cellulose allomorphs, supramolecular ordering, and surface charge, these distinctions can be leveraged to develop both simple and complex (composite) nanocellulose hydrogels tailored for specific applications. Numerous methods have been established to obtain the requisite nanocellulose building blocks for hydrogel fabrication.

It is essential to recognize that nanocellulose materials are commonly classified into two categories: nanostructured materials and nanocellulose materials (Trache et al., 2020). Although this classification is scientifically sound, it may lead to confusion among processors and customers. Generally, nanostructured materials are produced from non-nanoscale starting materials (e.g., pulp cellulose, microcrystalline cellulose) but exhibit nanoscale substructures in the final product. In contrast, nanocellulose materials are derived from fibrillar nanocellulose building blocks with varying aspect ratios and degrees of crystallinity, including cellulose nanocrystals (CNCs), cellulose nanofibrils (CNFs), bacterial nanocellulose (BNC), and cellulose nanospheres (CNS). This chapter concentrates on hydrogels formed from these nanoscale building blocks.

Bottom-Up Approach Nanocellulose hydrogels can be synthesized through sol-gel processes, similar to silica gel preparation. Until recently, this was thought unattainable, but advances in chemical, enzymatic, and biosynthetic synthesis have enabled the generation of cellulose from monosaccharides or oligosaccharides (e.g., α-D-glucose). With sufficient polymerization and supramolecular assembly, nanoscale fibrils form three-dimensional networks, resulting in nanocellulose hydrogel structures.

Top-Down Approach Alternatively, nanocellulose hydrogels can be produced by gelation of aqueous dispersions of anisometric cellulose nanoparticles, an approach recently advanced through nanocellulose production and characterization. This process involves disintegrating cellulosic fibers using mechanical, chemical, or enzymatic methods to yield CNCs or CNFs. Both CNCs and CNFs exhibit excellent self-assembly in aqueous systems due to strong hydrogen bonding, even in highly diluted dispersions. Additionally, cellulose nanoparticles can be functionalized before or after top-down processing, allowing for a broader range of physical and chemical crosslinking opportunities and network architectures. Interest in cellulose nanospheres (CNS), which are thicker and shorter than CNCs, has increased due to their ability to enhance the performance of cellulose nanoparticles in various applications. CNS can be sourced from both native (cellulose I) and mercerized or regen-

erated (cellulose II) materials;,however harsher conditions are often required for cellulose I (Tian et al., 2022).

Biosynthesis Approach BNC as a "ready-to-go" nanocellulose hydrogel can be produced in batch or continuous processes by inoculating nutrient media with specific aerobic bacterial strains. It can be disintegrated to obtain cellulose nanoribbons, thicker and longer than plant-derived CNC and CNF. BNC is used in medical applications, such as for healing burns and skin lesions caused by basal-cell carcinoma or radiation therapy (Portela et al., 2019) (Fig. 18.1).

18.2.1 Bottom-Up Synthesis of Nanocellulose: A Challenge

In situ polymerization of cellulose and sol-gel synthesis from low-molecular-weight precursor compounds were long considered impractical due to the complex stereochemical and regioselective requirements for chemical activation, modification, and β-(1→4)-D-glycosidic bond formation. However, recent pioneering work has now made chemical, enzymatic, and microbial engineering tools available to create nanocellulose hydrogels through in situ polymerization and subsequent self-assembly as reviewed elsewhere (Lehrhofer et al., 2022).

18.2.1.1 Chemical Bottom-Up Synthesis

Chemical synthesis faces significant challenges in replicating the stereoselective (strictly β-configured anomeric carbons) and regioselective (1→4)-D-glucosidic linkages specific to the (1→4)-β-D-pyranoglucan structure of cellulose. Achieving

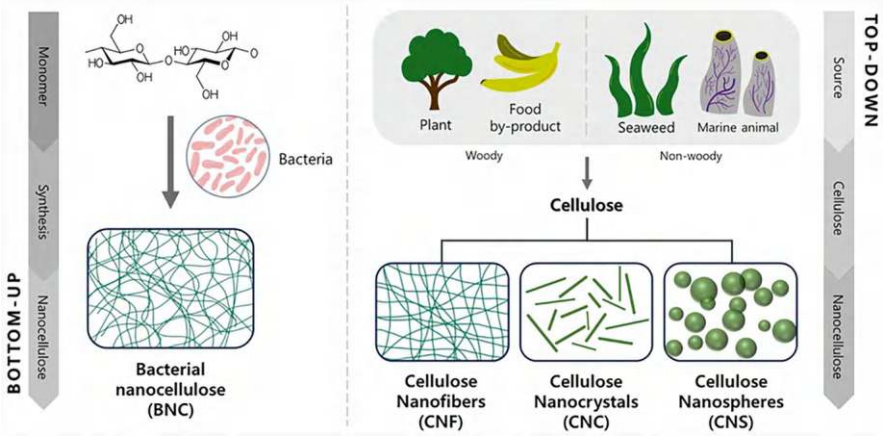

Fig. 18.1 Bottom-up (biosynthetic) and top-down (mechanical, chemical, enzymatic) processes to yield nanocellulose. (Reproduced from Kim and Doh (2023). Copyright 2024, Wiley-VCH GmbH)

this while simultaneously controlling the degree of polymerization (DP) and maintaining low dispersity is critical. Notably, it is commendable that various chemical strategies, such as stepwise addition (Kawada et al., 1994; Nishimura & Nakatsubo, 1997; Takano et al., 1990) and cationic ring-opening polymerization (Ikegami et al., 2021; Nakatsubo et al., 1996; Yagura et al., 2020), have succeeded in synthesizing cello-oligomers that closely resemble natural cellulose. In some cases, short-chain cellulose derivatives with DPs of up to 63 have been successfully produced.

18.2.1.2 Enzymatic Bottom-Up Synthesis

In vitro polymerization utilizing the catalytic activity of isolated enzymes represents a non-biosynthetic (non-metabolic) approach that is gaining traction in material chemistry (Kobayashi et al., 2001). Native enzymes exhibit remarkable capabilities for regioselective and stereoregular synthesis, particularly in the formation of β-(1→4)-D-glycosidic bonds. Consequently, numerous efforts have been undertaken to achieve enzymatic in vitro synthesis of cellulose, categorized based on the type of enzyme employed: (1) glycosylases, (2) glycosyltransferases, (3) phosphorylases, and (4) artificial glycosynthases, which are engineered glycosylases designed to eliminate hydrolytic activity (Ichikawa et al., 1992).

18.2.1.3 Glycosylases

Glycosylases, also known as glycoside hydrolases, are renowned for their ability to cleave glycosidic bonds. However, they can also function in reverse through thermodynamically controlled equilibrium displacement or when activated sugars are present, facilitating kinetically controlled transglycosylation (Bulmer et al., 2021). This latter pathway was crucial in the first enzymatic cellulose synthesis using the activated sugar β-cellobiosyl fluoride (with β-cellobiose as the repeating unit of cellulose) in conjunction with cellulase as a glycosylase. Additionally, the E197A mutant of cellulase Cel7B (derived from *Humicola insolens*) demonstrated tolerance for α-cellobiosyl fluorides with various functional groups at the C-6 position, enabling the synthesis of regioselectively modified oligo- and polysaccharides.

18.2.1.4 Glycosyltransferases

Glycosyltransferases efficiently form glycosidic linkages between non-activated acceptor carbohydrates (e.g., monosaccharides, oligosaccharides) and activated sugar donors (Ban et al., 2012). Those utilizing activated nucleotide sugars, such as CMP, GDP, or UDP, are classified as Leloir glycosyltransferases and are important for synthesizing medically relevant glycans, including antibacterial drugs and compounds for treating diabetes, inflammation, and cancer (Priebe et al., 2018).

Cellulose synthase is a key glycosyltransferase involved in the natural production of cellulose from UDP-glucose. Early experiments isolating cellulose synthase

for in vitro synthesis of β-(1→4)-D-glucans (Aloni et al., 1982) were milestones toward enzymatic cellulose production, despite the small size of microfibrils obtained compared to in vivo-produced bacterial cellulose. Enzyme deactivation and product precipitation limited UDP-glucose polymerization to low DPs (Kobayashi et al., 2001).

Later studies revealed that the absence of the membrane-bound cellulose synthase complex (CSC) contributed to small microfibril aggregates. CSC-rich plant extracts were more effective in achieving higher DP values and better supramolecular self-assembly (Cho et al., 2015). Crystal structure analysis of bacterial cellulose synthase (BCSA) showed that each of the 18 cellulose synthase (CESA) proteins forms a rosette-type structure that catalyzes cellulose chain synthesis while providing a pore for chain passage, leading to the formation of elementary fibrils.

Recent efforts to functionally reconstitute cellulose synthases from both plants (CesA8 from *Populus tremula x tremuloides*) and bacteria (BcsA from *Rhodobacter sphaeroides*) have enabled in vitro synthesis of cellulose (Purushotham et al., 2016). For BcsA, both the purified enzyme and the periplasmic subunit BcsB, along with the allosteric activator cyclic-di-GMP, are necessary to maintain catalytic activity in non-denaturing detergents (Omadjela et al., 2013). This approach achieved cellulose with a DP of 200–300, comparable to moderately degraded pulp cellulose and slightly lower than the average DP of Lyocell fibers.

18.2.1.5 Glycoside Phosphorylases

Glycoside phosphorylases, like glycoside hydrolases, can catalyze the synthesis of glycosides, enabling regio- and stereospecific synthesis. Cellodextrin phosphorylase (CDP) is particularly noteworthy for enzymatic cellulose synthesis, as it synthesizes cellulose oligomers from natural donor compounds, such as α-D-glycosyl-1-phosphate (α-D-Glc-1P) and acceptor substrates like D-cellobiose (Bulmer et al., 2021). CDP demonstrates tolerance for functionalized acceptors and exhibits stability across various pH levels (5.0–8.6), temperatures (37–60 °C), and organic solvents (O'Neill et al., 2017). This stability facilitates the production of cellulose nanostructures through iterative glycosylation and post-modification using introduced functional groups.

Research by Takeshi Serizawa's group at the Tokyo Institute of Technology has explored the in situ self-assembly of cellulose oligomers into nanostructures influenced by reaction conditions and functionalized acceptors. One promising strategy involves molecular crowding, akin to intracellular environments, where high concentrations of macromolecular compounds slow diffusion rates and enhance self-assembly. This concept has promoted the formation of stable hydrogels from cello-oligomers synthesized from α-D-Glc-1P and D-glucose, resulting in crystalline nanoribbon networks regardless of additional water-soluble polymers like dextran and PEG. In contrast, without these polymers, only rectangular sheet-like precipitates formed (Hata et al., 2018).

Temperature and organic solvents (Hata et al., 2019) also significantly influence self-assembly. Lowering the temperature from 40–60 °C to 20–30 °C resulted in reduced DP and increased crystallinity, facilitating the formation of nanoribbon networks instead of precipitated nanosheets. Organic solvents, such as ethanol and dimethyl sulfoxide, further promoted the formation of well-structured nanoribbon networks. Additionally, substituting D-Glc with D-cellobiose influenced assembly, yielding cellulose II hydrogels with nanoribbon networks (Pylkkanen et al., 2020; Serizawa et al., 2017).

In summary, significant advancements have been made in the bottom-up synthesis of cellulose via chemical and enzymatic means. However, challenges such as high costs of reagents, complex synthesis of intermediates, and limited availability of nucleotide sugars must be addressed before these technologies can be scaled for large-scale nanocellulose hydrogel production (Frohnmeyer & Elling, 2023).

18.2.2 Nanocellulose Building Blocks from Top-Down Processes

Many natural inorganic and organic materials result from the inherent ability of nanoscale building blocks to self-assemble under physiological conditions into long-range anisotropic nanostructures. Typical examples include iridescent iron oxide layers (Schiller layers) formed from rod-like particles of β-FeOOH, secondary clay minerals such as smectite or montmorillonite, and organic structures like lipid membranes, higher-order proteins, or nucleic acids. Biomimicry, which utilizes natural design principles, presents an attractive and cost-effective strategy for developing new functional materials and devices (Majerle et al., 2019).

Cellulose, the most abundant biopolymer on Earth, begins to align during its biosynthesis, producing nanoscale elemental fibrils that further self-assemble into supramolecular structures and fibers, driven primarily by hydrogen bonding. Depending on their crystallinity and integration into a composite matrix, these fibers can exhibit varying degrees of stiffness and flexibility, while generally maintaining high tensile strength. In addition to bottom-up processes (see Sect. 18.2.1), several efficient top-down technologies are available to disrupt supramolecular structures, yielding anisometric cellulose nanoparticles with differing aspect ratios, crystallinity, and surface properties, depending on whether mechanical, enzymatic, chemical, or hybrid methods are employed.

Several types of particulate nanocellulose building blocks exist, each differing in shape, aspect ratio, degree of crystallinity, dominant allomorph, surface charge, and origin. The primary plant-derived forms include cellulose nanocrystals (CNCs), cellulose nanofibrils (CNFs), and cellulose nanospheres (CNSs). Additionally, cellulose nanoribbons can be produced through the disintegration of bacterial nanocellulose (BNC). These anisometric nanoparticles, obtained via top-down

processes, exhibit distinct properties that are influenced by their specific structural characteristics.

Besides spatial dimension and surface charge, the latter are strongly related to their share in crystalline domains and crystal lattice configuration. It may be briefly reminded that the cellulose Iα allomorph dominates in BNC, cellulose Iβ allomorph in native plant cellulose and hence in CNC and CNF, while the cellulose II allomorph is formed upon mercerization, coagulation (from molecular-dispersing solutions of non-derivatized cellulose), or regeneration of cellulose from solutions of respective cellulose derivatives (reversion of derivatization). These different polymorphs differ in the arrangement of the reducing end groups (parallel: cellulose I; anti-parallel: cellulose II, thermodynamically favored), and unit cell geometry (Iα: triclinic P1 with one chain per cell; Iβ and II: monoclinic $P2_1$ with 2 chains per cell) which translates into different packing density, polarity, and hydrogen bond formation (Zlenko et al., 2021).

A range of methods are nowadays available for liberation of nanocellulose building blocks as reviewed for CNC (Singh et al., 2024), CNF (Anusiya & Jaiganesh, 2022), and CNS (Tian et al., 2022) or BNC (Klemm et al., 2018). However, significant differences exist among these various types of nanocellulose building blocks concerning large-scale applications, particularly regarding their availability, economic considerations, and manufacturing complexity.

18.2.2.1 Cellulose Nanocrystals (CNC)

Cellulose nanocrystals (CNCs) are considered one of the most significant types of nanocellulose. In addition to their role in polymer reinforcement, CNCs can be applied in various fields, including sensing, packaging, separation, tissue engineering, and security and anti-forgery applications, the latter owing to their photonic properties. CNC particles exhibit high crystallinity, typically ranging from 54% to 88%, and their dimensions generally fall between 5 to 15 nm in width and 77 to 503 nm in length. Additionally, CNC substrates possess both hydrophobic and hydrophilic binding sites, enabling interactions with a wide range of compounds.

Cellulose nanocrystals (CNCs) can be extracted from native cellulose, typically sourced from wood pulp, through the hydrolytic cleavage of amorphous domains using strong mineral acids, such as H_2SO_4, a method commonly employed in large-scale production (Reid et al., 2017). This extraction process imparts an electrical surface charge, which enhances both hydrophilicity and colloidal stability. Further improvements in surface charge density, hydrophilicity, and colloidal stability can be achieved through post-hydrolysis treatments. Colloidal stability depends on electrostatic forces, which can be modulated by the adsorption of counter ions from electrolyte solutions. This adsorption contributes to the formation of electric double layers, thereby increasing the effective diameter of CNCs (Lewis et al., 2016). Such adjustments can be utilized to modulate both gel formation and the architecture of aerogels.

Interestingly, CNCs exhibit left-handed, chiral-nematic self-assembly beyond a critical concentration, resulting in helical structures that reflect circularly polarized light. This configuration creates iridescent effects when the pitch of the structures approaches the wavelengths of visible light (de Vries, 1951). The pitch length can be controlled by factors such as CNC length, surface charge density, ion strength, and mechanical forces applied to compress a cholesteric CNC gel or flexible transparent CNC aerogel, thus facilitating a wide range of sensing applications. Notably, the chiral nematic order can be preserved during the conversion of gels into aerogel films, which has generated considerable interest in CNC-based solid materials with stimuli-responsive properties.

18.2.2.2 Cellulose Nanofibers (CNF)

Cellulose nanofibers (CNFs) are characterized by a higher aspect ratio compared to CNCs, with dimensions typically ranging from 2 to 3 nm in width and 300 to 1000 nm in length. This increased aspect ratio, along with their greater hydrophilicity, results from the lower crystallinity of CNFs, which diminishes the contribution of the crystallographic (200) surface plane to hydrophobicity (Habibi et al., 2010). Consequently, CNFs exhibit enhanced flexibility, allowing for the formation of robust three-dimensional porous networks upon drying, whereas CNC materials tend to be relatively brittle.

In contrast to the selective cleavage of amorphous domains used to liberate CNCs, CNFs are produced through mechanical delamination of cellulose fibers, primarily obtained from biomass pulping and integrated bleaching processes. This fibrillation significantly increases the surface area of liberated CNFs, making methods such as high-pressure homogenization, microfluidization, grinding, and ultrasonication highly energy-intensive (Trigui et al., 2022). However, energy consumption can be reduced through various fiber pretreatments, including swelling in deep eutectic solvents (Sirviö et al., 2015) or aqueous NaOH (Abe, 2016), enzyme treatments (Henríquez-Gallegos et al., 2021), or chemical methods designed to introduce repulsive surface charges (Isogai & Bergström, 2018). Each of these methods has its own advantages and drawbacks, necessitating careful selection for specific applications. For instance, enzymatic treatments may reduce the degree of polymerization, resulting in width variability and non-transparent gels. Moreover, the application of shear force alone without pretreatments can yield micro-fibrillated cellulose (MFC) particles, which are coarser and not the desired CNF (Osong et al., 2015).

Chemical pretreatments that introduce electrically charged functional groups can promote the complete individualization of cellulose elemental fibrils with low diametrical polydispersity, a vital characteristic for applications such as the production of thermal super-insulating aerogel panels (see Chap. 19). Among the most common methods for this purpose are oxidation processes utilizing the metastable 2,2,6,6-tetramethylpiperidinyloxyl (TEMPO) nitroxyl radical in combination with sodium hypochlorite (Isogai et al., 2011) or sodium periodate oxidation (Guigo

et al., 2014). TEMPO oxidation selectively converts primary hydroxyl groups to carboxylate groups, while periodate oxidation targets vicinal secondary hydroxyls, resulting in the creation of 2,3-dialdehyde cellulose (DAC), which can be further functionalized or oxidized.

TEMPO oxidation is recognized as a green, cost-effective method, used industrially (Isogai & Bergström, 2018) by companies like Nippon Paper Industries, producing 500 tons of CNF annually. Periodate oxidation facilitates surface modifications while preserving the microfibrillar cellulose I structure (Guigo et al., 2014). Treatment with chlorite, sulfonation, or reductive amination further enhances electrical surface charge.

18.2.2.3 Cellulose Nanospheres (CNSs)

Cellulose nanospheres (CNSs) are spherical particles that are shorter and thicker than CNCs. They can be derived from both cellulose I and cellulose II source materials. The production of CNS from native cellulose requires harsher conditions compared to CNCs, involving hydrolysis with H_2SO_4 in combination with H_2O_2 or IO_4^- treatments. In contrast, CNS derived from cellulose II can be produced using methods similar to those for CNCs, including acid or oxidative hydrolysis, enzymatic treatment, and mechanical processing of mercerized materials or regenerated cellulose derivatives. The most common approach involves degrading cellulose II prepared from coagulated solutions (Beaumont et al., 2016), with the crystallinity of the resulting CNS adjustable by varying the solvent system and coagulation conditions.

However, as research on CNS is still in its early stages and involves complex production processes, the potential role of CNS in the realm of nanocellulose materials remains uncertain. Therefore, further discussion on this topic is not provided here; however, a comprehensive review is available for those interested (Tian et al., 2022).

18.2.3 Biosynthesis and Bacterial Nanocellulose (BNC)

Bacterial nanocellulose (BNC) could also be discussed in Sect. 18.2.2, which covers top-down processes, as it can be disintegrated similarly to plant cellulose through mechanical, enzymatic, or chemical methods to yield cellulose nanocrystals (CNCs), cellulose nanofibers (CNFs), or cellulose nanospheres (CNSs). However, it is warranted to introduce BNC separately here, as it is most commonly utilized in its "as-produced" hydrogel or pellicle form, following the removal of residual proteinaceous materials, nutrient residues, or additives. The primary reason for this focus is that relatively costly biosynthetic BNC serves as an intriguing "ready-to-go" material, characterized by its high purity and lack of impurities. BNC is one of the stiffest organic materials produced in nature. Created through the metabolic

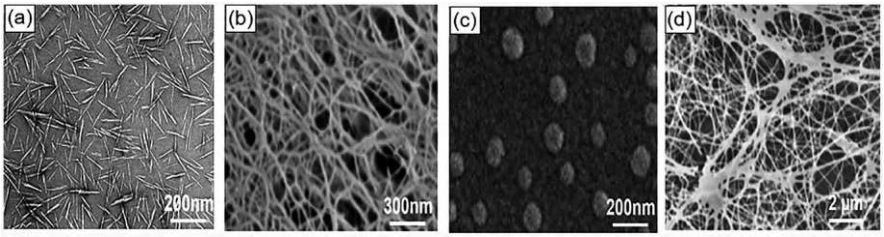

Fig. 18.2 Transmission (**a**) and scanning (**b**–**d**) electron micrographs of different nanocelluloses obtained by top-down (**a**: CNC, **b**: CNF, **c**: CNS) and biosynthetic (**d**: BNC) processes. ((**a**-**c**) Reproduced with permission from (**a**) (Arai et al., 2018). Copyright 2018:ACS; (**b**) (Prakobna et al., 2015). Copyright 2015: Elsevier; (c) (Meyabadi et al., 2014). Copyright 2014: Elsevier. (**d**) Reproduced from Ataide et al. (2017). Published 2017 by Springer Nature with open access)

activity of various bacterial strains, predominantly *Komagataeibacter xylinus*, BNC comprises highly entangled nanoribbons that are longer and thicker than those found in CNCs and CNFs (Lee et al., 2014). Its open nanoscale porosity, high water-holding capacity (up to 99%), and excellent biocompatibility render it ideal for various biomedical and cosmetic applications (Jonas & Farah, 1998).

Key factors influencing the morphology and yield of bacterial nanocellulose (BNC) include the composition of the culture medium, pH, temperature, and oxygen levels. Significant advancements have been made in the genetic modification of bacteria and large-scale production techniques, utilizing various bioreactors such as stirred tank, airlift, and horizontal lift reactors, which enhance efficiency by permitting the continuous extraction of BNC sheets (Lee et al., 2013). Nevertheless, challenges persist in achieving commercial-scale BNC production, including low yield, microbial strain instability, and cost constraints (Samyn et al., 2023).

To address these challenges, strategies have been proposed that involve genetic modifications to enhance production and develop value-added BNC-based biomaterials. Despite BNC's exceptional properties, further modifications are often required to improve cellular compatibility, protein interactions, and antimicrobial properties (Samyn et al., 2023). Given the limited production sites in Europe, high resource demands, transportation difficulties, and the overall cost of BNC, its widespread adoption in mass applications remains uncertain, with its primary market likely to be concentrated in the medical field (Fig. 18.2).

18.2.4 Further Types of Nanocelluloses

For the sake of completeness, it is important to acknowledge the existence of other types of nanocellulose. Amorphous nanocellulose (ANC), for instance, is produced through acid hydrolysis, ultrasonic disintegration, and coagulation (or "regeneration") from a molecular-dispersing solution state (Wang et al., 2016). ANC is characterized by a spherical to elliptical shape, with diameters ranging from 80 to

120 nm, and exhibits high hydrophilicity, surface accessibility, and sorption capacities. These properties make it a valuable thickening agent and carrier material for bioactive compounds in aqueous systems (Kargarzadeh et al., 2017). Cellulose nanoyarn (CNY) is another type of nanocellulose that can be obtained through electrospinning, with diameters ranging from 500 to 800 nm and low crystallinity, making it suitable for use in wound dressings (Ioelovich, 2016). Additionally, cellulose nanoplatelets (CNP), approximately 80 nm thick and composed of entangled nanofibrils (around 3 nm in diameter), have been prepared from agave powder through mild oxidation (Chávez-Guerrero et al., 2018). Furthermore, cellulose II nanofibrils with high crystallinity (CrI $\approx$ 72%) have been regenerated from isotropic, highly viscous supercooled solutions of cellulose in the power-law ionic liquid 1,1,3,3-tetramethylguanidinium acetate via the slow infusion of ethanol. These nanofibrils, comparable in width (approximately 2.5 nm) and length to CNFs, have been demonstrated to self-assemble in a nematic, liquid crystalline manner, as evidenced by synchrotron X-ray scattering experiments (Plappert et al., 2018a; Rennhofer et al., 2019).

18.3 Nanocellulose Hydrogel Architecture

The properties and applications of nanocellulose hydrogels are largely influenced by the nature and extent of interactions within their macromolecular or nanoparticulate networks.

- ***Physical gels*** behave as viscoelastic solids and rely on physicochemical interactions forming extended junction zones between polymer chains, such as in cellulose solutions (Burchard, 1985) or dispersions of colloidal particles (e.g., CNC, CNF, CNS). Gelation mechanisms include crystallization, amphiphilic copolymer interactions, charge interactions, hydrogen bonding, stereocomplexation, and protein interactions (Bustamante-Torres et al., 2021). These interactions (molecular entanglement, ion-ion, ion-dipole, dipole-dipole attractions, hydrogen bonding, and van der Waals forces) are susceptible to changes in temperature, pH, electrolyte composition, and ionic strength, potentially causing partial solubilization through disruption of intermolecular bonding (Nasution et al., 2022). This sensitivity makes physical gels, also termed "non-permanent" or "pseudogels," inherently inhomogeneous, exhibiting domains with varying degrees of molecular entanglement and transient network defects. Consequently, their functional characteristics are less predictable than those of chemical gels.
- ***Chemical gels*** on the contrary are referred to as "true" or "permanent gels," since their non-fluid component exclusively consists of covalent bonds (crosslinks) connecting macromolecules of a certain polymer type (linear, branched, star-shaped, etc.) in all spatial directions with each other or with macromolecules of a different polymer type. These crosslinks formed in the course of common chemical/enzymatic graft polymerization approaches using respective functional

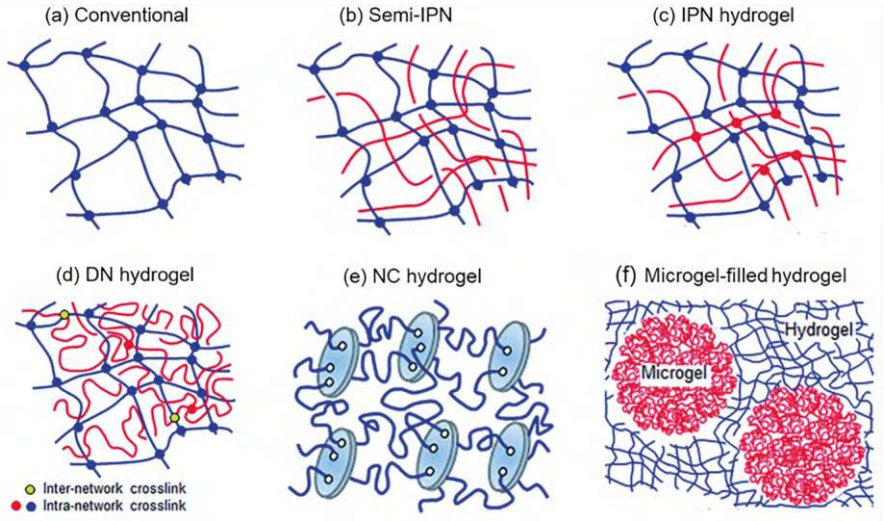

Fig. 18.3 Selection of important network architectures in hydrogels. *IPN* interpenetrating network, *DN* double network, *NC* nanocomposite. (Adapted with permission from Richtering and Saunders (2014). Copyright 2014: RSC Publishing)

groups as anchor sites are typically not sensitive toward changes in temperature, electrolyte composition, or ion strength and are, therefore, preferred in applications requiring constant properties independent of physicochemical alterations of the fluid phase. However, an increasing number of chemical crosslinking approaches exist that provide on-demand reversible bonding capabilities, such as thermal or photoinitiated cycloaddition, redox coupling, imine/Schiff-base formation, transesterification, boronate ester formation, and oximation (Jarach et al., 2021). In smart gels, similarly, chemical or physical networks can be additionally equipped with structural moieties allowing for on-demand permanent double crosslinking, i.e., complementing of physical by chemical crosslinking and vice versa. The most common network architectures found in nanocellulose hydrogels are represented in Fig. 18.3.

18.3.1 Hydrogels with Low Structural Complexity

Common NCN, CNF, or BNC hydrogels are often considered to have low structural complexity, as their networks of aligned (rod-like) nanocrystals or entangled nanofibrils and nanoribbons lack chemical crosslinking and the presence of a secondary, property-modulating, polymeric component. Like many natural polymers, cellulose has a great ability to form physical networks through extended hydrogen bonding, being the driving force for supramolecular self-assembly to afford nano-size crystals, fibrils, or ribbons. However, Van der Waals forces, specifically dipole-dipole

interactions, also contribute to through-space interaction and orientation in respective nanocellulose hydrogels (Burchard, 1985). Chemical modification of cellulose, such as occurring under sulfuric acid treatment to release CNCs (formation of negatively charged sulfate half-ester groups) or oxidation to facilitate delamination of fibers to yield CNFs (formation of carboxylate groups), significantly increases the opportunities for self-alignment or physical crosslinking. This can significantly modulate the viscoelastic nature of the modified physical gel. Uniaxial or chiral nematic alignment of CNC for example can be achieved under shear force or by application of (even weak) external electromagnetic fields as reviewed elsewhere (De France et al., 2016). However, different from CNFs, which reach uniaxial alignment in water already at concentrations as low as 0.1 wt.%, CNC dispersions require a critical concentration of about 4.5 wt.% for chiral nematic liquid crystals self-assembly (Revol et al., 1994) and start to gel only at concentrations beyond 10 wt.% (De France et al., 2017). This is also different for CNF dispersions which start to gel at about 1.5 wt.% depending on their degree of oxidation and, hence, surface charge density.

A high degree of surface coverage by (repulsive) electrically negative charges is not supportive for gelation of aqueous CNC and CNF dispersions due to the high colloidal stability of the nanoparticles. This, however, can be changed by screening, compensating, or depleting surface charge by protonation, addition of salts, or surface derivatization, all leading to reduced electrostatic repulsion and colloidal stability, hence increasing the propensity for gelation (De France et al., 2017). CNF gel panels (300 mm × 150 mm × 40 mm)—intended for $scCO_2$-assisted production of uniaxially densified aerogel panels—have been prepared from 1 wt.% dispersions of nearly fully individualized cellulose nanofibrils (Ø 2–3 nm, 500–800 nm long) that were prepared by TEMPO-mediated oxidation of beech sulfite dissolving pulp and subsequent multi-pass high-pressure homogenization following the protocol reported elsewhere (Plappert et al., 2018b). Gelation after molding of the transparent low-viscous dispersion was accomplished by immersion in an acidic medium. Like other physical gels, CNF hydrogels be viewed as viscoelastic solids.

BNC hydrogels also fall into the category of architecturally simple hydrogels which derive their remarkable mechanical and water-retaining properties from the highly entangled and crystalline networks of robust cellulose nanoribbons, and the abundance of hydroxyl groups being probably better accessible due to the rigidity of the BNC networks.

Despite their architectural simplicity, nanocellulose hydrogels of low complexity are considerable value for biomedical applications, such as wound dressings for burns or lesions caused by cancer or radiation treatments (Portela et al., 2019), artificial blood vessels (Gatenholm & Klemm, 2010), or suppression of foreign body responses towards implant materials (Costa et al., 2024). With regard to potential production numbers, however, the biggest interest currently is to use nanocellulose hydrogels as source materials for cellulosic aerogels—open-porous solids obtained from gels by replacing the continuous liquid phase with air under far-reaching preservation of the gel shape—for large-scale thermal superinsulation, such as in buildings or textiles. With regard to applications, it is also worth noting that CNF

hydrogels behave as viscoelastic solids as long as the shear stress applied is below the yield stress, but they behave like viscous liquids above the yield stress (Hermans Jr., 1965) which is important for processing of nanocellulose hydrogels, such as in 3D-printing (see applications).

18.3.2 Semi-Interpenetrating and Interpenetrating Networks

- ***Semi-interpenetrating polymer networks (semi-IPN)*** consist of linear polymer chains intertwined with crosslinked networks of a secondary polymer. This principle can be illustrated by the example of a semi-IP hydrogel adsorbent material for anionic dyes. It was formed by one-pot amino-anhydride "click" crosslinking of a maleic anhydride-acrylamide copolymer with poly(allylamine hydrochloride) performed within a solution of a cationic cellulose derivative, representing the linear, unbranched polymer in the formed semi-IPN (Liu et al., 2022).
- ***Interpenetrating polymer networks (IPNs)*** comprise two independent, crosslinked polymer networks formed via orthogonal chemistries, either simultaneously or sequentially. A prime example is alginate-modified bacterial nanocellulose (BNC), exhibiting enhanced moisture retention compared to pristine BNC, making it a promising wound dressing (Sulaeva et al., 2015). The developed approach has been adapted for scalable fabrication and relies on two simple process steps: BNC pellicles are soaked in 0.5% (w/v) sodium alginate (25 °C, 24 h), then immersed in 1% (w/v) $CaCl_2$ (25 °C, 40 min) to crosslink the alginate, creating an IPN where the BNC forms a physical network (hydrogen bonds) and the alginate forms an ionic network (Sulaeva et al., 2020). Similarly, double crosslinked SA/G hydrogels reinforced with 50 wt.% CNC are produced via freeze-drying (Abraham et al., 2023).

18.3.3 Double Network Hydrogels

Double network (DN) hydrogels, introduced by Gong et al. (2003), consist of a rigid, brittle, strongly crosslinked polyelectrolyte primary network and a softer, more ductile, secondary network with longer chain segments between crosslinks (Richtering & Saunders, 2014). The high molar concentration of the secondary network monomer is critical for achieving their exceptional toughness. DN hydrogels are exemplified by recyclable, electroconductive hydrogels, combining a conductive cellulose/Zn^{2+}/Ca^{2+} primary network with a stretchable, thermo-reversible poly(vinyl alcohol)-borax secondary network, used in triboelectric nanogenerators (TENGs) and sensors (Wang et al., 2024b). Biocompatible DN hydrogels for vascular and cartilage tissue engineering utilize bacterial nanocellulose (BNC) as the rigid primary network and UV-photopolymerized poly(acrylic acid) as the secondary network (Roig-Sanchez et al., 2022). The commercial availability of high-purity

BNC allows for one-step hydrogel formation. Furthermore, DN hydrogels overcome limitations in additive manufacturing. For example, the instability of gelatin hydrogels at mild conditions, hindering 3D printing at physiological temperatures, is addressed by a self-healing nanocomposite DN gelatin hydrogel incorporating carboxymethyl chitosan (CMCh) and periodate-oxidized BNC nanofibers (Heidarian & Kouzani, 2023). Dynamic imine bond formation between the amino groups of gelatin/CMCh and the carbonyl groups of the oxidized BNC nanofibers significantly enhances the hydrogel's properties, making it a promising bioink for 3D-printed tissue engineering scaffolds.

18.3.4 Hydrogels Containing Microgels

Microgels are colloidal dispersions of individual gel-like particles, exhibiting network architectures similar to those of larger gels, i.e., low complexity networks, semi-IPNs, IPNs, DN hydrogels, and nanocomposite hydrogels (Pelton & Hoare, 2011). Incorporation into hydrogels either without or with crosslinking introduces additional length scales (particle size) and affects mechanical properties; "hard" microgels can strengthen "soft" hydrogels, and dangling chains facilitate entanglement with the parent hydrogel. Microgels can be "responsive" or "intelligent," exhibiting swelling changes controlled by stimuli such as pH or temperature (Dickinson, 2015), making them useful for long-term stabilization in various industries. Preparation methods include bottom-up synthesis (homogeneous nucleation, emulsion/precipitation polymerization) and top-down approaches, such as macrogel fragmentation (Bertsch et al., 2019). Their high surface-to-volume ratio and sensitivity to swelling/shrinkage enable rapid responses to environmental changes, making them attractive for smart colloids and hydrogels. The food industry extensively utilizes top-down produced polysaccharide microgels, which find applications in Janus particle assembly, responsive systems, and biocatalysis (Wiese et al., 2016). Nanocellulose microgels are currently produced mainly via top-down methods (Lefroy et al., 2021), but a recently developed bottom-up method offers better control over particle characteristics, surface properties, and microgel formation (Yang et al., 2021).

18.4 Crosslinking: The Key to Nanocellulose Nanocomposite Hydrogels

Nanocomposites contain at least one constituent with dimensions below 100 nm. The incorporation of nanocellulose, via physical or chemical means, into a secondary network of a different material forms a nanocellulose nanocomposite (Fig. 18.4).

The combination of nanocellulose with secondary constituents, linked by physical, chemical, or physicochemical crosslinks, significantly modulates the properties

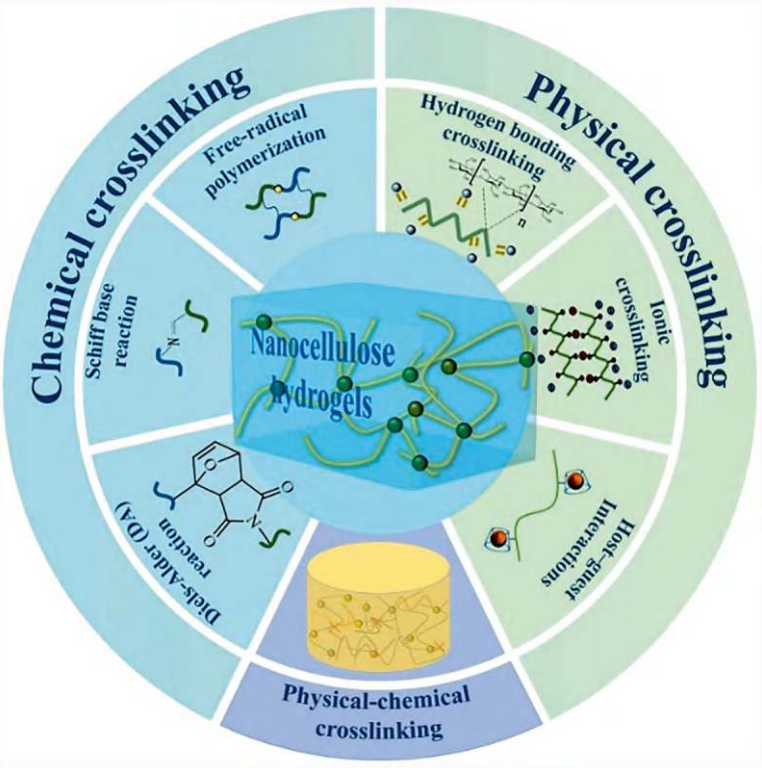

Fig. 18.4 Major crosslinking methods of nanocellulose hydrogels for advanced applications. (Adapted with permission from Lv et al. (2024). Copyright 2024: Elsevier)

of the individual components. Reversible crosslinking, achieved via non-covalent interactions or dynamic covalent chemistry, for example, can impart self-healing capabilities, mitigating damage from breakage or cutting (Taylor & Panhuis, 2016). Bio-based and synthetic hydrogel constituents, like all polymers, undergo aging processes (photo-oxidation, thermal degradation), resulting in polymer degradation, altered functionality, crosslink cleavage/rearrangement, and compromised performance. Consequently, the incorporation of self-healing mechanisms—inspired by natural systems—into polymeric materials has been a significant area of research since the early 2000s.

Crosslinks within hydrogels can be permanent or reversible. Reversible crosslinking enables the creation of self-healing and stimuli-responsive hydrogels, whose properties are modulated by external stimuli (pH, temperature, humidity, redox potential, pressure, electromagnetic irradiation, magnetism, or chemical environment). Nanocellulose-based smart hydrogels are increasingly prevalent, with significant research growth in the last decade, and a broad variety of processing techniques have been developed which include solution casting, melt extrusion, ball milling, injection molding, compression molding, precipitation routes, 3D printing,

layer-by-layer assembly, wet- and elector-spinning, and micro-pattering techniques (Trache et al., 2020). The following section summarizes physical, chemical, and physicochemical crosslinking strategies in nanocellulose hydrogels, referencing a comprehensive review (Lv et al., 2024).

18.4.1 Physical Crosslinking

18.4.1.1 Hydrogen Bonding

Hydrogen bonding, as prevalent in biological systems, confers biocompatibility and self-healing properties to hydrogels (Heidarian et al., 2021). However, the inherent weakness of hydrogen bonds limits their structural stability and susceptibility to environmental influences. While nanocellulose, particularly cellulose nanofibrils (CNF), forms hydrogels at low concentrations via hydrogen bonding, these hydrogels are often mechanically weak and sensitive to environmental changes (Heise et al., 2021). Introducing negatively charged carboxylates, as in TEMPO-oxidized CNF, enhances the stability of acid-induced gels (Isogai, 2021). Nanocellulose readily forms hydrogen bonds with various polymers, such as polyvinyl alcohol (PVA), polyacrylic acid, proteins, and polysaccharides, creating physical composite hydrogels. The extensive study of nanocellulose-PVA hydrogels is mainly due to their self-healing properties. For example, one such hydrogel utilizes borax as a crosslinker, exploiting strong, dynamic hydrogen bonding between the hydroxyl groups of graphene (GN)-CNF, PVA, and borax to achieve repeated remolding, room-temperature self-healing, and high extensibility (Zheng et al., 2019).

18.4.1.2 Ionic Crosslinking

Ionic crosslinking, connecting polymer chains via oppositely charged ions, provides a rapid and responsive method for hydrogel fabrication (You et al., 2021). Hydrogel properties (mechanical strength and responsiveness) are tunable via ion type and concentration, although susceptibility to ionic interference exists. Nanocellulose particles liberated through sulfuric acid hydrolysis or TEMPO oxidation carry electrical surface charges, enabling ionic crosslinking. Ionic crosslinking of sulfuric acid-hydrolyzed cellulose nanocrystals (CNC) with quaternized xylan, for example, was demonstrated to significantly enhance the mechanical properties by electrostatic interaction compared to gels formed solely by hydrogen bonding (Ren et al., 2018). Similar ionically crosslinked hydrogels have been created using TEMPO-oxidized CNC, CNF, and BNC. As an example of CNF obtained by TEMPO oxidation/fibrillation of sugar can bagasse, it was shown that both hydrogel structure and compressive strength can be tuned by varying the concentration of CNF, Zn^{2+}, and carboxyl group content (Lu et al., 2018). Also, a biocompatible, pH-responsive hydrogel was obtained by ionic crosslinking of carboxylated CNC with dopamine and 5-aminolevulinic acid using Fe^{3+} coordination chemistry (You et al., 2021).

18.4.1.3 Host-Guest Interactions

This type of interaction is based on non-covalent binding between macrocyclic hosts and guest molecules (Heidarian et al., 2021), which are not intrinsic to nanocellulose and require modification. Cyclodextrins (CD) are commonly employed to create these interactions, often resulting in hydrogels with enhanced mechanical properties and self-healing due to the reversible nature of supramolecular bonding (Zhou et al., 2020). This was demonstrated by modifying CNC with adamantane and incorporating β-CD, forming host-guest interactions within the resulting hydrogel. Inhibition tests disrupting these interactions significantly reduced the hydrogel's maximum stress (from 34 to 11 kPa), highlighting their importance in regulating nanocellulose hydrogel network structure and mechanical properties through guest/host molecule selection (May et al., 2023). However, this approach requires the synthesis of specific molecules, potentially increasing complexity and cost.

18.4.2 Chemical Crosslinking

Chemical crosslinking can impart significantly better mechanical performance, network stability, and durability to gels, including nanocellulose hydrogels. The abundance of cellulose hydroxyl groups and the tools nowadays available for cellulose modification and crosslinking, combined with the multiple options for adjusting crosslinker density, spacer length, composition, conformal flexibility, and polarity, allows for almost infinite options to fine-tune the properties of nanocellulose hydrogels for specific requirements in applications like food packaging, 3D printing, tissue engineering, or sensing.

Aiming to employ the multitude of surface hydroxyl groups, the majority of chemical crosslinking approaches for pristine cellulose are centered around esterification using bifunctional or polyfunctional carboxylic acids like citric acid (Golor et al., 2020) and boronic acids (Daniels et al., 2023). Acetalization with low-molecular (e.g., glutaraldehyde) or polymeric aldehydes, reaction with dialdehyde cellulose (Plappert et al., 2018c), or Williamson etherification/alkali-catalyzed oxyalkylation with epichlorohydrin is also common (Fig. 18.5).

Each of these crosslinking agents has pros and cons. While remaining dialdehydes are toxic, citric acid would not be harmful to health but requires high weight fractions to form gels (Nasution et al., 2022) and would feature excellent swelling capabilities next to biodegradability. Comparative studies have shown that addition of 40% citric acid forms cellulose hydrogels with a mechanical strength comparable to that of a similar hydrogel crosslinked with 5% ECH (Golor et al., 2020). Dimethylol-dihydroxy-ethylene urea (DMDHEU) is another highly efficient crosslinking reagent (Xin & Lu, 2018) that is used at large scale to impart wrinkle resistance to cellulosic garments, such as shirt fabrics, due to suppressed hydrogen bonding (İlleez et al., 2017).

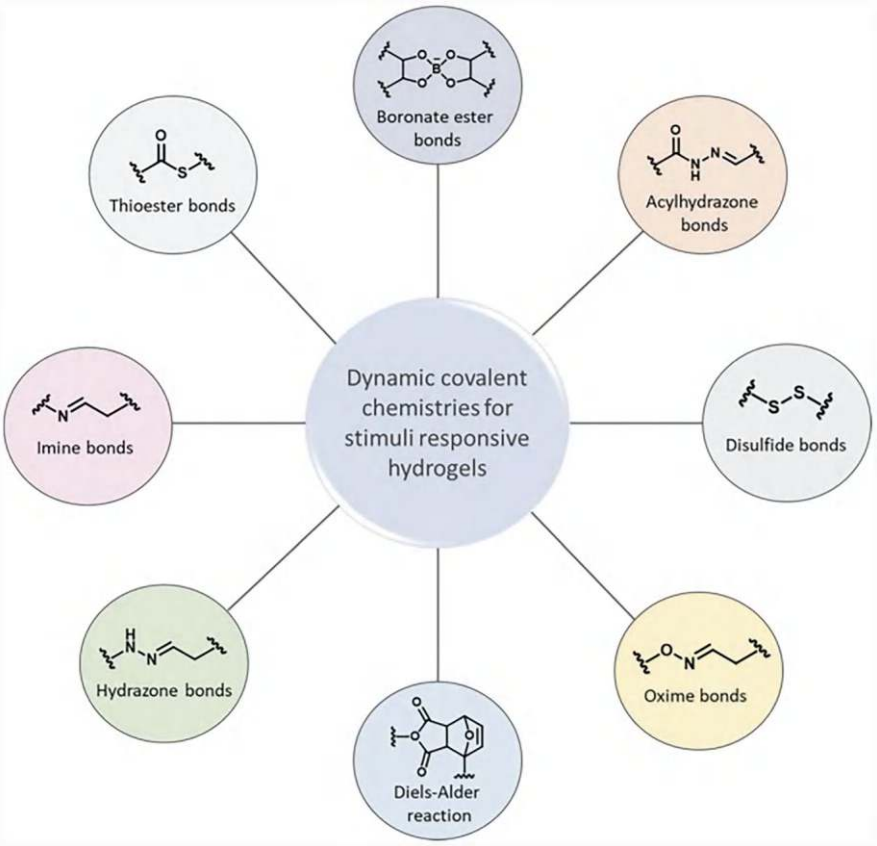

Fig. 18.5 Dynamic covalent crosslinking approaches employed for creation of smart stimuli-responsive hydrogels. (Adapted with permission from Perera and Ayres (2020). Copyright 2020: RSC Publishing)

Surface modification of (nano)cellulose prior to hydrogel formation vastly increases the opportunities for chemical crosslinking. Respective modifications can be accomplished by plasma, corona discharge, and laser treatments, as well as by UV irradiation, or chemical reactions. The latter include a multitude of protocols for oxidation, esterification, etherification, amidation, carbamation, or nucleophilic substitution reactions as comprehensively reviewed elsewhere (Eyley & Thielemans, 2014).

18.4.2.1 Oxidation Reactions

Oxidation reactions are paramount to the use of nanocelluloses, specifically CNF, in advanced hydrogels, such as for imparting stimuli responsiveness, as the targeted introduction of carbonyl and carboxyl groups provides a plethora of further

opportunities for crosslinking. Oxidation reactions can be non-selective (as in the case of using perchloric acid or hydrogen peroxide) or selective, as summarized elsewhere (Toshikj et al., 2019). Periodate oxidation using $NaIO_4$ or KIO_4 and oxidations using nitroxyl radicals in combination with an appropriate co-oxidant, such as the TEMPO/NaOCl system (see Sect. 18.2.2.2), are the most prominently applied protocols for equipping cellulosic surfaces with carbonyl (periodate oxidation) or carboxyl groups (TEMPO oxidation). Carboxymethylation of (nano)cellulose dispersions in aqueous NaOH (swelling, mercerization) and subsequent treatment with chloroacetic acid in aqueous isopropanol would be another option for introducing carboxyl groups and has been used to enhance the water-dispersibility of nanofibrillated bacterial cellulose, for example (Kono et al., 2021).

18.4.2.2 Esterification (Including Transesterification)

Esterification is a widely used method for modifying and crosslinking cellulose nanoparticles. Base-catalyzed reactions with acid anhydrides readily achieve this, altering surface polarity, charge density, or charge type. Applications include "grafting from" ring-opening polymerization (e.g., using lactones to attach poly(lactic acid) or poly(ε-caprolactone) chains to CNC surfaces), free radical polymerization following the introduction of unsaturated ester moieties, and the creation of functional groups for stimuli-responsive bonding/debonding. A recent approach uses N-succinyl-imidazole to achieve highly regioselective esterification of cellulose in a never-dried state, largely preserving physicochemical properties (Beaumont et al., 2021). Similar to TEMPO oxidation, this method introduces negative surface charge and facilitates fiber disintegration into individualized nanofibrils, but unlike TEMPO, it avoids chemical degradation and is reversible via mild saponification. This allows for the restoration of native intra-, inter-, and supramolecular interactions post-processing. A refined two-step process involving swelling in DMAc/LiCl followed by esterification using cyclic anhydrides (succinic or phthalic anhydride) further improves fibril length preservation during high-pressure homogenization (Zhou et al., 2024). While other esterification methods exist (e.g., tosylation, chemical vapor deposition, acid halide reactions for atom transfer radical polymerization), they are primarily used for incorporating non-polar materials and are less relevant for hydrogel applications.

18.4.2.3 Etherification

Etherification often employs alkali-catalyzed reactions with bifunctional or polyfunctional glycidyl ethers or epichlorohydrin, which is another significant chemical crosslinking approach. Modifying cellulose nanoparticles with glycidyl ether derivatives bearing secondary functional groups, such as epoxypropyl trimethyl ammonium chloride (EPTAC), introduces quaternary ammonium groups, imparting positive surface charge and antimicrobial properties to CNC or CNF (Vel et al.,

2022). Similarly, tertiary amines like diethyl aminoethyl cellulose (DEAE-C), a weak basic anion exchanger, can be synthesized and used to adjust viscosity and shear-thinning properties in bioinks for extrusion 3D printing, enhancing stability and cell adhesion in alginate/gelatin mixtures (Vel et al., 2022). While EPTAC is toxic, 3-chloro-2-hydroxypropyl-trimethylammonium chloride (CHPTAC) offers a safer alternative, formed in situ as a readily consumed intermediate. Both epichlorohydrin and CHPTAC can be produced via the environmentally friendly Dow GTE process, a solvent-less, atom-efficient method starting from glycerol, a low-cost renewable resource derived from sugar fermentation or biodiesel production (Bell et al., 2008).

18.4.2.4 Amidation

This approach is frequently used for direct crosslinking of TEMPO-oxidized (nano) cellulose or for grafting amino-functional moieties, modulating properties, and enabling "click" chemistry (Filpponen & Argyropoulos, 2010). This carboxyl-amine reaction also facilitates the conjugation of reporter systems, such as photoluminescent nanoparticles, to oxidized (nano)cellulosic substrates for sensing applications (Guo et al., 2017). To maintain the advantages of using (nano)cellulose in its never-dried state, amidation often employs 1-ethyl-3-(3-dimethylaminopropyl)-carbodiimide (EDC) and *N*-hydroxysuccinimide (NHS) to promote amide bond formation under mild conditions. EDC, a water-soluble carbodiimide, reacts with carboxyl groups, forming an active O-acylisourea intermediate readily displaced by primary amines. Optimal reaction conditions are at pH 4.5 (e.g., MES buffer), and efficiency can be improved using the water-soluble sulfo-NHS derivative, which converts the unstable O-acylisourea intermediate into a stable, amine-reactive sulfo-NHS ester.

18.4.2.5 Carbamation

In carbamation reactions, bifunctional or polyfunctional isocyanates like tolylene-2,4-diisocyanate (TDI) or polymeric 4,4′-methylene diphenyl isocyanate (PMDI) are used to react with the abundant hydroxyl groups of cellulose. A comprehensive review can be found elsewhere (Abushammala & Mao, 2019).

18.4.2.6 Dynamic Imine Bond Formation

Imine bond formation is a viable crosslinking strategy when network constituents possess free aldehyde and amino groups (Heidarian et al., 2021). The reversibility of imine bonds enables the creation of multifunctional hydrogels exhibiting self-healing and shape memory properties (Deng et al., 2020; Heidarian et al., 2021). Periodate oxidation of cellulose, a common method for introducing carbonyl

groups, is frequently employed to crosslink cellulose with amine-rich polymers like chitosan or polyethyleneimine (Deng et al., 2020; Heidarian et al., 2021).

18.4.2.7 Diels-Alder (DA) Reactions

DA reactions offer a valuable approach for on-demand, stimuli-responsive bonding/debonding in hydrogels. This pericyclic reaction involves heat-induced ring formation between a conjugated diene and a dienophile. The reaction's reversibility, coupled with the significant temperature difference between bonding and debonding, is advantageous. Additional benefits include mild reaction conditions (aqueous, catalyst- and initiator-free), high efficiency and selectivity, and the absence of byproducts (Morozova, 2023). The furan/maleimide diene/dienophile pair is frequently used in Diels-Alder "click" reactions to synthesize thermally reversible nanocellulose-based hydrogels (Kramer et al., 2019).

18.4.2.8 Energy-Rich Electromagnetic Radiation

It is well-known that ionizing radiation, as used in e-beam treatments of synthetic polymer films, can enhance mechanical properties of materials by crosslinking. However, energy-rich electromagnetic radiation requires careful optimization to balance crosslinking and degradation, influenced by polymer structure and radiation parameters. Quaternary carbons favor β-scission, while phenyl groups enhance stability, and double bonds promote crosslinking. Oxygen accelerates chain scission, especially with e-beam or gamma radiation (Sonnier & Rouif, 2012). Gamma irradiation has been used to crosslink pH-sensitive gelatin/CNC hydrogels (from rice husk), enhancing thermal and dynamic mechanical properties for drug delivery applications, with optimal swelling and porosity at pH 3 and 4 wt.% CNC, respectively (Ishak et al., 2021). Similarly, electron-beam irradiation has been used to create thermo- and pH-responsive bacterial cellulose/acrylic acid hydrogels (Mohd Amin et al., 2012).

18.4.3 Physical-Chemical Crosslinking

Physicochemical crosslinking combines physical and chemical approaches to enhance nanocellulose hydrogel properties. This strategy often creates temporary and permanent crosslinks between two or more network constituents, resulting in sophisticated architectures like double networks. Physicochemical crosslinking leverages diverse reaction types, including pericyclic (e.g., Diels-Alder), condensation (e.g., ester, amide, imine), and redox reactions (e.g., thiol/disulfide), to achieve on-demand bonding/debonding (Zhang et al., 2018). For example, a tough hydrogel for oilfield water control was created by copolymerizing acrylamide, acrylic acid,

and *N,N′*-methylene-bis(acrylamide) amino-functionalized CNF, achieving a sevenfold increase in compressive strength and enhanced thermal stability (Li et al., 2022) compared to unmodified CNF. Transparent, crack-free nanocellulose gels of high compression strength and swelling capacity were obtained by combined physical (e.g., Fe^{3+}) and chemical (epichlorohydrin) crosslinking (Xu et al., 2019). A self-healing nanocellulose hydrogel was created by connecting nanocellulose and flexible PVA networks via reversible diol-borate bonds (Zhang et al., 2022).

18.5 Nanocellulose Hybrid Hydrogels

Nanocellulose hybrid hydrogels, combining nanocellulose with functional nanoparticles, offer synergistic properties for diverse applications (medicine, food, catalysis, agriculture). Nanostructured matrices prevent nanoparticle aggregation, crucial for maintaining activity (Kaushik & Moores, 2016), using strategies such as physical adsorption (Guan et al., 2018), covalent bonding (Wu et al., 2018), and surface graft polymerization (Wu et al., 2015). Incorporated nanoparticles include metals, metal oxides, mineral salts, nanocarbons, and quantum dots, providing catalytic, antimicrobial, and other functionalities (Zhang et al., 2020). Metal nanoparticles are often incorporated via physical adsorption or in situ reduction, influenced by the nanocellulose surface charge (Hoeng et al., 2015), while metal oxides are incorporated using sol-gel, co-precipitation, or electrostatic methods (Zhang et al., 2020). A representative example is a wastewater purification hydrogel comprising a δ-Bi_2O_3-modified titanate nanofiber core and a TEMPO-oxidized CNF shell, effectively removing oils, cations (Cs^+, Cu^{2+}, Pb^{2+}, Sr^{2+}), and anions (I^-, Br^-, SeO_4^{2-}, SeO_3^{2-}) (Xiong et al., 2018). Mineral nanoparticles like hydroxyapatite are incorporated via biomimetic mineralization (Qi et al., 2019). Incorporating carbon nanoparticles (carbon dots, nanotubes, graphene) requires different approaches due to harsh synthesis conditions, often involving mixing with precursors or post-gelation infiltration with subsequent physical or chemical bonding (Guo et al., 2017; Jiang et al., 2017; Quraishi et al., 2018). Covalent bonding, often employing EDC/sulfo-NHS coupling, offers superior durability compared to physical adsorption (Guo et al., 2017; Quraishi et al., 2018).

18.6 Applications of Nanocellulose Hydrogels

Twenty years ago, research and development in the field of nanocellulose hydrogels was focused primarily on bacterial cellulose for biomedical applications as reflected in a joint paper by pioneers in this field (Gatenholm & Klemm, 2010) who referred BNC at that time as “an emerging biomaterial with great potential as a biological implant, wound and burn dressing material, and scaffolds for tissue regeneration.” Since then, the enormous progress in nanocellulose hydrogel research, extending to

plant-derived nanocellulose like CNF, CNC, CNS, their derivatives, combination with other materials in nanocellulose nanocomposite and hybrid materials, as well as the development of advanced technologies for manufacture, modification, and processing of nanocelluloses into hydrogels, has vastly extended their range of applications. This progress has been further fueled by initiatives promoting bio-based economies and green chemistry principles.

This chapter focuses on major applications of nanocellulose hydrogels, given that a comprehensive overview is beyond its scope. Key areas include food preservation packaging, sensing, sorption, tissue engineering, controlled drug release, iontronics, and soft actuators. Many applications utilize the self-assembly properties of cellulose nanoparticles and the stimuli-responsiveness of modified hybrids and composites (Bustamante-Torres et al., 2021; Trache et al., 2020). Furthermore, nanocellulose, nanocomposite, and hybrid hydrogels can be processed into nanocellulose aerogels (see Chap. 19), open-porous, lightweight materials with potential applications in thermal and acoustic insulation, passive daytime radiative cooling, interfacial solar steam generation, water desalination, atmospheric water harvesting, solar energy conversion, (bio)sensing, catalysis, environmental pollution control, and energy technologies.

18.6.1 Food Applications

Given the potential of nanocellulose hydrogels for a positive environmental impact, their use in food packaging is a key application. Along with other biopolymers, they offer a crucial alternative to petroleum-based packaging, addressing the significant global plastic waste problem (Singh et al., 2023). Packaging consumes over one-third of global plastic production and accounts for 40% of plastic waste (56 million tons annually), with a large portion of food packaging discarded within the same year (Geyer et al., 2017). While efforts focus on replacing oil-based plastics with renewable materials or improving biodegradability, biopolymer hydrogels, including nanocellulose-based hydrogels, offer a promising solution (Singh et al., 2023). These hydrogels exhibit cost-effectiveness, moldability, stimuli-responsiveness, biocompatibility, biodegradability, good mechanical properties (especially after crosslinking), thermal stability, and UV absorption/scattering (Dai et al., 2019; Deshmukh et al., 2022; Thivya et al., 2022).

18.6.1.1 Pads and Sachets

The above food-safe properties and large specific surface, combined with high water-adsorption capacity under retention of structural integrity even at a fully swollen state (Batista et al., 2019), render nanocelluloses promising additives for active food packaging materials, such as pads or sachets. The latter are designed to ensure fast uptake of excess moisture from high-water-content food to establish a reduced,

constant moisture level, concomitantly inhibiting microbial growth and extending the shelf life of food (Nath et al., 2022). Highly adsorbent nanocellulose hydrogel pads, for example, placed inside the packaging material beneath high-water-content food (e.g., fresh meat, fish, fresh-cut fruits and vegetables) readily allow for gradual exudate uptake (Singh et al., 2023). Similarly, sachets filled with hygroscopic gels can be used to preserve the crispiness of products, such as fried potatoes, dried fruits, or cookies. Besides water affinity and swelling performance which can be adjusted by type and extent of crosslinking, the abundance of hydroxyl groups allows—if necessary, after further modification (see section about chemical modification and crosslinking)—the integration of functional materials. The latter can impart specific sorption or release capabilities to nanocellulose pads or sachets beneficial for adsorption of malodorous compounds or release of antioxidants, such as allyl isothiocyanate, essential oils, in situ-generated chlorine dioxide, ethanol (Otoni et al., 2016), antimicrobial agents, bacteriophages, volatile flavoring compounds, or oxygen scavengers (Almeida et al., 2018). Furthermore, nanocellulose hydrogels can be equipped with smart sensing features, i.e., molecules or nanoparticles, able to emit a signal when a critical humidity or gas concentration (O_2, CO_2, ClO_2) is reached. Other sensors provide temperature monitoring, able to give a visible response to the temperature history, when exceeding a threshold temperature limit, or visualize time periods when the product exceeds a certain specified temperature (Yousefi et al., 2019).

18.6.1.2 Edible Coatings

Edible coatings, applied via spraying, electrospraying, dipping, brushing, or layer-by-layer deposition, enhance the postharvest quality of fruits and vegetables. These coatings, composed of proteins, polysaccharides, or lipids, act as primary packaging materials by reducing respiration, water loss, and oxidation, thereby simplifying secondary packaging (Pirozzi et al., 2021). Nanocellulose incorporation significantly improves the gas barrier properties and mechanical performance of these coatings. However, crosslinking is often necessary to achieve adequate mechanical strength, chemical resistance, and thermal stability for storage and handling (Guo et al., 2015). For example, a corn nanostarch nanocomposite hydrogel coating incorporating double-crosslinked cellulose nanocrystals (CNC)—achieved via citric acid esterification and chitosan amidation using DCC/NHS in dimethylformamide—exhibited enhanced tensile strength, water contact angle, reduced water vapor permeability, and improved antimicrobial activity against *E. coli* and *S. aureus* compared to a CNC-free control (Chen et al., 2019).

18.6.2 Biomedical Applications

Nanocellulose hydrogels are increasingly utilized in biomedical applications, including tissue engineering, regenerative medicine, wound dressings, and controlled drug delivery (Athukoralalage et al., 2019; Varghese et al., 2023; Wang et al.,

2021). While bacterial nanocellulose (BNC) is often cited for its superior biocompatibility, evidenced by the lack of foreign body reactions in animal studies (Athukoralalage et al., 2019), plant-derived nanocelluloses also exhibit excellent biocompatibility (Koivuniemi et al., 2020). Nanocellulose hydrogels are fabricated using various methods including homogenization, freeze-thawing, polymerization, and 3D printing (Du et al., 2019). CNF/alginate hydrogels are widely used in wound healing due to their biocompatibility, ability to maintain a moist environment, liquid absorption capacity, and antibacterial properties (Zhang et al., 2020). These composites also demonstrate sustained drug release capabilities, enabling the controlled delivery of antibiotics and analgesics alongside wound healing (Rana et al., 2024). Sodium alginate and CMC are frequently used components in composite hydrogels for drug encapsulation (Rana et al., 2024).

18.6.2.1 Wound Dressing Materials

Bacterial nanocellulose (BNC), with its biocompatibility, low immunogenicity, positive effects on skin regeneration, biodegradability, high strength, hydrophilicity, and purity, is a valuable material for biomedical and cosmetic applications. Commercial BNC products are available for wound healing (Suprasorb®X, Bioprocess®, XCell®, Biofill®) and skincare (Nanomasque®), with applications extending to hemodialysis, vascular grafts, bone tissue engineering, drug delivery, and artificial skin (Liebner et al., 2015). Laser processing techniques, such as 3D perforation and femtosecond texturing, further enhance BNC's properties, improving cell attachment and hydrophilicity and reducing fibrotic tissue formation on implants (Samyn et al., 2023). Clinical studies demonstrate BNC's efficacy in wound healing, showing faster closure times and improved patient outcomes compared to standard care (references needed for specific clinical studies). Similarly, nanofibrillated cellulose (CNF)-based dressings show promise in skin graft donor site treatment, promoting adherence and self-detaching after re-epithelialization (Koivuniemi et al., 2020), with commercial examples such as FibDex™ being now available.

18.6.2.2 Tissue Engineering and Bioink 3D Printing

Three-dimensional (3D) printing of nanocellulose scaffolds, mimicking the extracellular matrix, is rapidly advancing in regenerative medicine and cell culture (Yang et al., 2020). The ability to create morphological and compositional gradients using bioinks containing both scaffold components and cells is particularly advantageous for cell culture applications. CNF is a key bioink component; respective CNF-based bioinks are commercially available, such as GrowInk-N™ (CNF), GrowInk-T™ (anionic CNF), and GrowInk-ALG™ (CNF/alginate). Often CNF bioinks are blended with CNC or BNC to optimize mechanical properties. While the shear-thinning behavior of nanocellulose dispersions facilitates printability, preventing nozzle clogging necessitates low CNF concentrations and post-printing crosslinking to maintain shape fidelity (Xu et al., 2018). Crosslinking can be achieved using

physical methods (e.g., sodium alginate/calcium salt ionic crosslinking) or chemical/photochemical approaches. Photocrosslinking, while fast and energy-efficient, requires transparent bioinks, such as those made from fully individualized, oxidized CNF, or CNF modified with photoactive groups. Dynamic crosslinking strategies, such as imine chemistry—favored for its mild conditions, rapid equilibration, and biocompatibility (Ulrich, 2019)—are also employed, as exemplified by bioinks based on gelatin, carboxymethyl chitosan, and dialdehyde-BNC (Heidarian & Kouzani, 2023). Combined dynamic (imine and Diels-Alder chemistries) and permanent crosslinking can create reversibly crosslinked hydrogels (Zhang et al., 2021). Beyond scaffold materials, bioinks incorporate biological components such as cells, growth factors, nutrients, and other additives. Post-proliferation/differentiation, enzymes like GrowDase™ can liquefy the scaffold to release cells while preserving viability and geometry. Furthermore, surface modification of CNF with avidin or streptavidin (GrowDex®-A bioinks) allows for the selective binding of biotinylated biomolecules for cell-specific matrix creation.

18.6.2.3 Drug Delivery

The high surface area and facile chemical modification of nanocellulose hydrogels, rich in hydroxyl groups, make them well-suited for controlled drug release via sorption/desorption mechanisms. Stimuli-responsiveness (e.g., pH, temperature, ionic strength), leading to swelling/contraction or altered bonding, enables controlled release. Incorporating responsive nanoparticles, such as quantum dots utilizing Förster resonance energy transfer (FRET) with drug molecules, offers additional control and sensing capabilities, for example, monitoring drug loading in transdermal patches. Drug release is governed by matrix properties (structure, expandability, degradability), the release medium (pH, temperature, ionic strength, enzymes), and drug characteristics (solubility, stability, charge, matrix interactions); hydrogel swelling kinetics are particularly important, influencing drug release rates, penetrant diffusion, and dissolution (Gunathilake et al., 2020). Release mechanisms include diffusion-controlled release (obeying Fick's first law) when pore size exceeds drug size (Ghasemiyeh & Mohammadi-Samani, 2019), swelling-controlled release where water absorption increases pore size, and degradation-controlled release via enzymatic or hydrolytic processes (Rana et al., 2024). Stimuli-responsive hydrogels utilize chemical (pH, redox reagents, metal ions) and physical (temperature, pressure, light, magnetic fields) triggers to control crosslinking, structure, and permeability (Deng et al., 2022). Nanocellulose-based hydrogels have shown efficacy in various drug delivery routes: oral (e.g., ibuprofen via paramagnetic nanocellulose/alginate beads), local injection (e.g., doxorubicin via pH-responsive CNC hydrogels), and transdermal (e.g., ketorolac tromethamine via CNF/chitosan films) (Varghese et al., 2023).

18.6.3 Sensing Applications

18.6.3.1 pH-Responsiveness

Poly(vinyl alcohol), owing to its biocompatibility and compatibility with nanocellulose, is a promising material for stimuli-responsive composite hydrogels. pH-sensitive CNF/PVA hydrogels have demonstrated sustained in vitro release of cisplatin, with both CNF content and pH influencing swelling and drug release rates. At pH 7.4, a hydrogel containing 1 wt.% CNF effectively sustained drug release, potentially mitigating side effects (Azhar et al., 2017). Another pH-sensitive hydrogel utilized bacterial nanocellulose (BNC) modified via microwave-assisted grafting of poly[(acrylic acid)-co-acrylamide]. Poly(acrylic acid), like poly(methacrylic acid), offers advantages for oral protein delivery, including mucoadhesion, enzyme inhibition, and epithelial tight junction opening (Ahmad et al., 2016). Microwave-assisted grafting onto BNC facilitated drug release in the lower digestive tract (Kuang et al., 2019), while the BNC reinforcement enhanced gastric retention (Lim et al., 2017). Superporous, swellable, pH-sensitive hydrogels, created via CO_2 gas foaming to eliminate organic solvents, have been developed using nanocellulose-reinforced chitosan for the delivery of poorly water-soluble curcumin (Sionkowska et al., 2019) and its degradation products for antimicrobial applications (Bacakova et al., 2019).

18.6.3.2 Thermo-Responsiveness

Incorporation of cellulose nanocrystals (CNC) into thermoresponsive poly(N-isopropylacrylamide) (PNIPAm) hydrogels enhances their mechanical properties, increasing elastic and viscous moduli. This was achieved by grafting PNIPAm onto CNC surfaces and subsequent free-radical polymerization, creating injectable hydrogels without added crosslinkers (Zubik et al., 2017). The resulting PNIPAm/CNC composites exhibited excellent drug loading capacity (metronidazole) at room temperature and sustained drug release at 37 °C.

18.6.3.3 Magnetic Responsiveness

Magnetically responsive nanocellulose hydrogels integrate the biocompatibility and tunable properties of nanocellulose with the responsiveness of embedded magnetic nanoparticles, typically iron oxides like magnetite (Fe_3O_4). These composites exhibit controlled swelling and/or release of encapsulated molecules upon exposure to an external magnetic field, offering potential for targeted drug delivery and magnetically guided tissue engineering (Gonçalves & Gomes, 2023). The precise control over both magnetic nanoparticle incorporation and nanocellulose network architecture allows for fine-tuning of the material's responsiveness and

biocompatibility. This is exemplified by green pH/magnetic hydrogels that were prepared by freeze-thawing gelation of a mixture of CNC, CMC, and PVA, immersion of the resulting nanocomposite gel in aqueous acidic Fe^{2+}/Fe^{3+} solution, and formation of magnetic Fe_3O_4 nanoparticles by infusion of aqueous NaOH (Dai et al., 2019).

18.6.4 Smart Materials

18.6.4.1 Iontronics

Iontronics are materials that bridge solid-state electronics and biological systems, utilize controlled ion transport for signal processing, and mirror natural processes like neuronal polarization (Nyamayaro et al., 2023). Aqueous iontronic devices offer biocompatibility and biodegradability, enabling applications in sensing, environmental monitoring, and brain-machine interfaces. Hybrid circuits combining ionic and electronic conduction transmit signals at the ionic/electronic interface (Nyamayaro et al., 2023), enabling diverse device architectures including diodes and transistors. Flexible iontronics often employ ionic conductive hydrogels (ICHs), whose tunable mechanical properties (1 Pa–0.1 GPa Young's modulus) can match those of biological tissues (0.5–500 kPa), potentially minimizing scarring (Wang et al., 2024a). Cellulose nanocrystals (CNCs) enhance ICH properties, improving water retention and ionic conductivity through hydroxyl and carboxyl/sulfonate group interactions (Mittal et al., 2022). Furthermore, dynamic crosslinking strategies are being explored to achieve self-healing and adhesive properties, such as by incorporating tannic acid-coated CNCs and metal ions into poly(acrylic acid) hydrogels (Shao et al., 2018).

18.6.4.2 Soft Actuators

Soft actuators, mimicking natural muscle tissue, generate mechanical work in response to external stimuli (e.g., pressure, temperature, light, electric or magnetic fields). Their versatility and ease of design make them attractive for diverse applications including microfluidics, robotics, and responsive textiles (Huang et al., 2023). Key design principles focus on material selection (elasticity, flexibility, responsiveness) and geometry optimization (force, displacement, energy efficiency) (Abitbol et al., 2016). Nanocellulose hydrogels, exhibiting stimuli-responsive changes in size and shape, are particularly valuable for mechanical reinforcement in soft actuators and bionic robots (Pilz da Cunha et al., 2020). For instance, CNF hydrogel membranes incorporated into stimuli-responsive silk-elastin-like protein hydrogels create a bilayer actuator system responding to underwater temperature and ionic strength. In this system, the hydrogel provides the active element responding by reversible 3D folding mechanisms, while the vacuum-formed CNF membrane, with

its interwoven nanofiber bundles, provides crucial passive mechanical strength (Wang et al., 2020). This actuator consists entirely of biocompatible and biodegradable materials, providing a choice for constructing stimulus response systems for in-vivo biomedical, soft robot, and bionic research (Deng et al., 2022).

18.6.5 Environmental Applications

Nanocellulose hydrogels are emerging as environmentally friendly materials for water purification and pollution control due to their biodegradability, biocompatibility, and non-toxicity (Batista et al., 2019; Koneru et al., 2020). Their high porosity and large surface area make them effective adsorbents for a wide range of contaminants. Specific examples include the use of nanocellulose-polyvinylamine microgels for the removal of anionic dyes (Jin et al., 2015) and crosslinked cellulose dialdehyde for the adsorption of Congo red (Kumari et al., 2016). Furthermore, the physicochemical properties of nanocellulose hydrogels can be tailored for enhanced performance through modifications such as crosslinking with collagen (Pietrucha & Safandowska, 2015), opening possibilities for targeted pollutant removal.

References

Abe, K. (2016). Nanofibrillation of dried pulp in NaOH solutions using bead milling. *Cellulose, 23*(2), 1257–1261. https://doi.org/10.1007/s10570-016-0891-4

Abitbol, T., Rivkin, A., Cao, Y., Nevo, Y., Abraham, E., Ben-Shalom, T., et al. (2016). Nanocellulose, a tiny fiber with huge applications. *Current Opinion in Biotechnology, 39*, 76–88. https://doi.org/10.1016/j.copbio.2016.01.002

Abraham, E., Cherpak, V., Senyuk, B., ten Hove, J. B., Lee, T., et al. (2023). Highly transparent silanized cellulose aerogels for boosting energy efficiency of glazing in buildings. *Nature Energy, 8*(4), 381–396. https://doi.org/10.1038/s41560-023-01226-7

Abushammala, H., & Mao, J. (2019). A review of the surface modification of cellulose and nanocellulose using aliphatic and aromatic mono- and di-isocyanates. *Molecules, 24*(15), 2782. https://doi.org/10.3390/molecules24152782

Ahmad, N., Mohd Amin, M. C. I., Ismail, I., & Buang, F. (2016). Enhancement of oral insulin bioavailability: In vitro and in vivo assessment of nanoporous stimuli-responsive hydrogel microparticles. *Expert Opinion on Drug Delivery, 13*(5), 621–632. https://doi.org/10.1517/17425247.2016.1160889

Alemán, J. V., Chadwick, A. V., He, J., Hess, M., Horie, K., Jones, R. G., et al. (2007). Definitions of terms relating to the structure and processing of sols, gels, networks, and inorganic-organic hybrid materials (IUPAC Recommendations 2007). *Pure and Applied Chemistry, 79*(10), 1801–1829. https://doi.org/10.1351/pac200779101801

Almeida, A. P. C., Canejo, J. P., Fernandes, S. N., Echeverria, C., Almeida, P. L., & Godinho, M. H. (2018). Cellulose-based biomimetics and their applications. *Advanced Materials, 30*(19), e1703655. https://doi.org/10.1002/adma.201703655

Aloni, Y., Delmer, D. P., & Benziman, M. (1982). Achievement of high rates of in vitro synthesis of 1, 4-beta-D-glucan: Activation by cooperative interaction of the Acetobacter xylinum enzyme system with GTP, polyethylene glycol, and a protein factor. *Proceedings of the*

National Academy of Sciences of the United States of America, 79(21), 6448–6452. https://doi.org/10.1073/pnas.79.21.6448

Anusiya, G., & Jaiganesh, R. (2022). A review on fabrication methods of nanofibers and a special focus on application of cellulose nanofibers. *Carbohydrate Polymer Technologies and Applications, 4*, 100262. https://doi.org/10.1016/j.carpta.2022.100262

Arai, K., Horikawa, Y., & Shikata, T. (2018). Transport properties of commercial cellulose nanocrystals in aqueous suspension prepared from chemical pulp via sulfuric acid hydrolysis. *ACS Omega, 3*, 13944–13951. https://doi.org/10.1021/acsomega.8b01760

Ataide, J. A., de Carvalho, N. M., Rebelo, M.d.A., Chaud, M.V., Grotto, D., Gerenutti, M., et al. (2017). Bacterial nanocellulose loaded with bromelain: Assessment of antimicrobial, antioxidant and physical-chemical properties. *Scientific Reports, 7*(1), 18031. https://doi.org/10.1038/s41598-017-18271-4

Athukoralalage, S. S., Balu, R., Dutta, N. K., & Roy Choudhury, N. (2019). 3D bioprinted nanocellulose-based hydrogels for tissue engineering applications: A brief review. *Polymers, 11*(5), 898. https://doi.org/10.3390/polym11050898

Azhar, F. F., Shahbazpour, E., & Olad, A. (2017). pH sensitive and controlled release system based on cellulose nanofibers-poly vinyl alcohol hydrogels for cisplatin delivery. *Fibers and Polymers, 18*, 416–423. https://doi.org/10.1007/s12221-017-6958-5

Bacakova, L., Pajorova, J., Bacakova, M., Skogberg, A., Kallio, P., Kolarova, K., et al. (2019). Versatile application of nanocellulose: From industry to skin tissue engineering and wound healing. *Nanomaterials (Basel), 9*(2), 164. https://doi.org/10.3390/nano9020164

Bading, M., Olsson, O., & Kümmerer, K. (2024). Analysis of environmental biodegradability of cellulose-based pharmaceutical excipients in aqueous media. *Chemosphere, 352*, 141298. https://doi.org/10.1016/j.chemosphere.2024.141298

Ban, L., Pettit, N., Li, L., Stuparu, A. D., Cai, L., Chen, W., et al. (2012). Discovery of glycosyltransferases using carbohydrate arrays and mass spectrometry. *Nature Chemical Biology, 8*(9), 769–773. https://doi.org/10.1038/nchembio.1022

Batista, R. A., Espitia, P. J. P., Quintans, J. d. S. S., Freitas, M. M., Cerqueira, M. Â., Teixeira, J. A., et al. (2019). Hydrogel as an alternative structure for food packaging systems. *Carbohydrate Polymers*, *205*, 106–116. https://doi.org/10.1016/j.carbpol.2018.10.006

Beaumont, M., Rennhofer, H., Opietnik, M., Lichtenegger, H. C., Potthast, A., & Rosenau, T. (2016). Nanostructured cellulose II gel consisting of spherical particles. *ACS Sustainable Chemistry & Engineering, 4*(8), 4424–4432. https://doi.org/10.1021/acssuschemeng.6b01036

Beaumont, M., Tardy, B. L., Reyes, G., Koso, T. V., Schaubmayr, E., Jusner, P., et al. (2021). Assembling native elementary cellulose nanofibrils via a reversible and regioselective surface functionalization. *Journal of the American Chemical Society, 143*(41), 17040–17046. https://doi.org/10.1021/jacs.1c06502

Bell, B. M., Briggs, J. R., Campbell, R. M., Chambers, S. M., Gaarenstroom, P. D., Hippler, J. G., et al. (2008). Glycerin as a renewable feedstock for epichlorohydrin production. The GTE process. *CLEAN—Soil, Air, Water, 36*(8), 657–661. https://doi.org/10.1002/clen.200800067

Bertsch, P., Arcari, M., Geue, T., Mezzenga, R., Nyström, G., & Fischer, P. (2019). Designing cellulose nanofibrils for stabilization of fluid interfaces. *Biomacromolecules, 20*(12), 4574–4580. https://doi.org/10.1021/acs.biomac.9b01384

Bulmer, G. S., de Andrade, P., Field, R. A., & van Munster, J. M. (2021). Recent advances in enzymatic synthesis of β-glucan and cellulose. *Carbohydrate Research, 508*, 108411. https://doi.org/10.1016/j.carres.2021.108411

Burchard, W. (1985). Networks in nature. *British Polymer Journa, 17*(2), 154–163. https://doi.org/10.1002/pi.4980170213

Bustamante-Torres, M., Romero-Fierro, D., Arcentales-Vera, B., Palomino, K., Magaña, H., & Bucio, E. (2021). Hydrogels classification according to the physical or chemical interactions and as stimuli-sensitive materials. *Gels, 7*(4), 182. https://doi.org/10.3390/gels7040182

Chávez-Guerrero, L., Sepúlveda-Guzmán, S., Silva-Mendoza, J., Aguilar-Flores, C., & Pérez-Camacho, O. (2018). Eco-friendly isolation of cellulose nanoplatelets through oxidation under mild conditions. *Carbohydrate Polymers, 181*, 642–649. https://doi.org/10.1016/j.carbpol.2017.11.100

Chen, Q.-J., Zhou, L.-L., Zou, J.-Q. & Gao, X. (2019). The preparation and characterization of nanocomposite film reinforced by modified cellulose nanocrystals. *International Journal of Biological Macromolecules, 132*, 1155–1162. https://doi.org/10.1016/j.ijbiomac.2019.04.063

Cho, S. H., Du, J., Sines, I., Poosarla, V. G., Vepachedu, V., Kafle, K., et al. (2015). In vitro synthesis of cellulose microfibrils by a membrane protein from protoplasts of the non-vascular plant Physcomitrella patens. *The Biochemical Journal, 470*(2), 195–205. https://doi.org/10.1042/bj20141391

Costa, L., Carvalho, A. F., Silva-Carvalho, R., Rodrigues, A. C., Dourado, F., Deuermeier, J., et al. (2024). Laser-patterning bacterial nanocellulose for cell-controlled interaction. *Cellulose, 31*(14), 8479–8499. https://doi.org/10.1007/s10570-024-06131-0

Dai, H., Zhang, H., Ma, L., Zhou, H., Yu, Y., Guo, T., et al. (2019). Green pH/magnetic sensitive hydrogels based on pineapple peel cellulose and polyvinyl alcohol: Synthesis, characterization and naringin prolonged release. *Carbohydrate Polymers, 209*, 51–61. https://doi.org/10.1016/j.carbpol.2019.01.014

Daniels, E. L., Runge, J. R., Oshinowo, M., Leese, H. S., & Buchard, A. (2023). Cross-linking of sugar-derived polyethers and boronic acids for renewable, self-healing, and single-ion conducting organogel polymer electrolytes. *ACS Applied Energy Materials, 6*(5), 2924–2935. https://doi.org/10.1021/acsaem.2c03937

Datta, R. (2024). Enzymatic degradation of cellulose in soil: A review. *Heliyon, 10*(1), e24022. https://doi.org/10.1016/j.heliyon.2024.e24022

De France, K. J., Yager, K. G., Hoare, T., & Cranston, E. D. (2016). Cooperative ordering and kinetics of cellulose nanocrystal alignment in a magnetic field. *Langmuir, 32*(30), 7564–7571. https://doi.org/10.1021/acs.langmuir.6b01827

De France, K. J., Hoare, T., & Cranston, E. D. (2017). Review of hydrogels and aerogels containing nanocellulose. *Chemistry of Materials, 29*(11), 4609–4631. https://doi.org/10.1021/acs.chemmater.7b00531

De Vries, H. (1951). Rotatory power and other optical properties of certain liquid crystals. *Acta Crystallographica, 4*(3), 219–226. https://doi.org/10.1107/s0365110x51000751

Deng, Z., Wang, H., Ma, P. X., & Guo, B. (2020). Self-healing conductive hydrogels: Preparation, properties and applications. *Nanoscale, 12*(3), 1224–1246. https://doi.org/10.1039/C9NR09283H

Deng, Y., Xi, J., Meng, L., Lou, Y., Seidi, F., Wu, W., et al. (2022). Stimuli-responsive nanocellulose hydrogels: An overview. *European Polymer Journal, 180*, 111591. https://doi.org/10.1016/j.eurpolymj.2022.111591

Deshmukh, R. K., Akhila, K., Ramakanth, D., & Gaikwad, K. K. (2022). Guar gum/carboxymethyl cellulose based antioxidant film incorporated with halloysite nanotubes and litchi shell waste extract for active packaging. *International Journal of Biological Macromolecules, 201*, 1–13. https://doi.org/10.1016/j.ijbiomac.2021.12.198

Dickinson, E. (2015). Microgels—An alternative colloidal ingredient for stabilization of food emulsions. *Trends in Food Science and Technology, 43*(2), 178–188. https://doi.org/10.1016/j.tifs.2015.02.006

Du, H., Liu, W., Zhang, M., Si, C., Zhang, X., & Li, B. (2019). Cellulose nanocrystals and cellulose nanofibrils based hydrogels for biomedical applications. *Carbohydrate Polymers, 209*, 130–144.

Eyley, S., & Thielemans, W. (2014). Surface modification of cellulose nanocrystals. *Nanoscale, 6*(14), 7764–7779. https://doi.org/10.1039/c4nr01756k

Filpponen, I., & Argyropoulos, D. S. (2010). Regular linking of cellulose nanocrystals via click chemistry: Synthesis and formation of cellulose nanoplatelet gels. *Biomacromolecules, 11*(4), 1060–1066. https://doi.org/10.1021/bm1000247

Frohnmeyer, H., & Elling, L. (2023). Enzyme cascades for the synthesis of nucleotide sugars: Updates to recent production strategies. *Carbohydrate Research, 523*, 108727. https://doi.org/10.1016/j.carres.2022.108727

Gatenholm, P., & Klemm, D. (2010). Bacterial nanocellulose as a renewable material for biomedical applications. *MRS Bulletin, 35*(3), 208–213. https://doi.org/10.1557/mrs2010.653

Geyer, R., Jambeck, J. R., & Law, K. L. (2017). Production, use, and fate of all plastics ever made. *Science Advances, 3*(7), e1700782. https://doi.org/10.1126/sciadv.1700782

Ghasemiyeh, P., & Mohammadi-Samani, S. (2019). Hydrogels as drug delivery systems; pros and cons. *Trends in Pharmaceutical Sciences, 5*(1), 7–24. https://doi.org/10.30476/tips.2019.81604.1002

Golor, M., Rosma, D., Santoso, S., Soetaredjo, F., Yuliana, M., Ismadji, S., et al. (2020). Citric acid-crosslinked cellulosic hydrogel from sugarcane bagasse: Preparation, characterization, and adsorption study. *Journal of the Indonesian Chemical Society, 3*, 59. https://doi.org/10.34311/jics.2020.03.1.68

Gonçalves, A. I., & Gomes, M. E. (2023). Outlook in tissue-engineered magnetic systems and biomagnetic control. *Current Opinion in Biomedical Engineering, 25*, 100431. https://doi.org/10.1016/j.cobme.2022.100431

Gong, J. P., Katsuyama, Y., Kurokawa, T., & Osada, Y. (2003). Double-network hydrogels with extremely high mechanical strength. *Advanced Materials, 15*(14), 1155–1158. https://doi.org/10.1002/adma.200304907

Guan, Q., Song, R., Wu, W., Zhang, L., Jing, Y., Dai, H., et al. (2018). Fluorescent CdTe-QD-encoded nanocellulose microspheres by green spraying method. *Cellulose, 25*, 7017–7029. https://doi.org/10.1007/s10570-018-2065-z

Guigo, N., Mazeau, K., Putaux, J.-L., & Heux, L. (2014). Surface modification of cellulose microfibrils by periodate oxidation and subsequent reductive amination with benzylamine: A topochemical study. *Cellulose, 21*(6), 4119–4133. https://doi.org/10.1007/s10570-014-0459-0

Gunathilake, T. M. S. U., Ching, Y. C., Chuah, C. H., Abd Rahman, N., & Liou, N.-S. (2020). Recent advances in celluloses and their hybrids for stimuli-responsive drug delivery. *International Journal of Biological Macromolecules, 158*, 670–688. https://doi.org/10.1016/j.ijbiomac.2020.05.010

Guo, J., Liu, D., Filpponen, I., Johansson, L. S., Malho, J. M., Quraishi, S., et al. (2017). Photoluminescent hybrids of cellulose nanocrystals and carbon quantum dots as cytocompatible probes for in vitro bio-imaging. *Biomacromolecules, 18*(7), 2045–2055. https://doi.org/10.1021/acs.biomac.7b00306

Guo, Q., Paliy, M., Kobe, B., Trebicky, T., Suhan, N., Arsenault, G., et al. (2015). Characterization of cross-linking depth for thin polymeric films using atomic force microscopy. *Journal of Applied Polymer Science, 132*(8), 41493. https://doi.org/10.1002/app.41493

Habibi, Y., Lucia, L. A., & Rojas, O. J. (2010). Cellulose nanocrystals: Chemistry, self-assembly, and applications. *Chemical Reviews, 110*(6), 3479–3500. https://doi.org/10.1021/cr900339w

Hata, Y., Sawada, T., & Serizawa, T. (2018). Macromolecular crowding for materials-directed controlled self-assembly. *Journal of Materials Chemistry B, 6*(40), 6344–6359. https://doi.org/10.1039/C8TB02201A

Hata, Y., Fukaya, Y., Sawada, T., Nishiura, M., & Serizawa, T. (2019). Biocatalytic oligomerization-induced self-assembly of crystalline cellulose oligomers into nanoribbon networks assisted by organic solvents. *Beilstein Journal of Nanotechnology, 10*(1), 1778–1788. https://doi.org/10.3762/bjnano.10.173

Heidarian, P., & Kouzani, A. Z. (2023). A self-healing nanocomposite double network bacterial nanocellulose/gelatin hydrogel for three dimensional printing. *Carbohydrate Polymers, 313*, 120879. https://doi.org/10.1016/j.carbpol.2023.120879

Heidarian, P., Kaynak, A., Paulino, M., Zolfagharian, A., Varley, R. J., & Kouzani, A. Z. (2021). Dynamic nanocellulose hydrogels: Recent advancements and future outlook. *Carbohydrate Polymers, 270*, 118357. https://doi.org/10.1016/j.carbpol.2021.118357

Heise, K., Kontturi, E., Allahverdiyeva, Y., Tammelin, T., Linder, M. B., Nonappa, et al. (2021). Nanocellulose: Recent fundamental advances and emerging biological and biomimicking applications. *Advanced Materials, 33*(3), 2004349. https://doi.org/10.1002/adma.202004349

Henríquez-Gallegos, S., Albornoz-Palma, G., Andrade, A., Soto, C., & Pereira, M. (2021). Impact of the enzyme charge on the production and morphological features of cellulose nanofibrils. *Polymers, 13*(19), 3238. https://doi.org/10.3390/polym13193238

Hermans, J., Jr. (1965). Investigation of the elastic properties of the particle network in gelled solutions of hydrocolloids. I. Carboxymethyl cellulose. *Journal of Polymer Science, Part A: General Papers, 3*(5), 1859–1868. https://doi.org/10.1002/pol.1965.100030517

Hoeng, F., Denneulin, A., Neuman, C., & Bras, J. (2015). Charge density modification of carboxylated cellulose nanocrystals for stable silver nanoparticles suspension preparation. *Journal of Nanoparticle Research, 17*, 1–14. https://doi.org/10.1007/s11051-015-3044-z

Hoffman, A. S. (2002). Hydrogels for biomedical applications. *Advanced Drug Delivery Reviews, 54*(1), 3–12. https://doi.org/10.1016/S0169-409X(01)00239-3

Huang, R., Guo, H., Gu, Z., & Ling, Y. (2023). Advances in laser processed material of soft sensing and soft actuation. *Materials Today Communications, 37*, 107187. https://doi.org/10.1016/j.mtcomm.2023.107187

Ichikawa, Y., Look, G. C., & Wong, C.-H. (1992). Enzyme-catalyzed oligosaccharide synthesis. *Analytical Biochemistry, 202*(2), 215–238. https://doi.org/10.1016/0003-2697(92)90099-S

Ikegami, W., Kamitakahara, H., Teramoto, Y., & Takano, T. (2021). Synthesis of optically inactive cellulose via cationic ring-opening polymerization. *Cellulose, 28*(10), 6125–6132. https://doi.org/10.1007/s10570-021-03970-z

İlleez, A. A., Dalbaşıi, E. S., & Kayseri, G. Ö. (2017). Seam properties and sewability of crease resistant shirt fabrics. *AATCC Journal of Research, 4*(1), 28–34. https://doi.org/10.14504/ajr.4.1.4

Ioelovich, M. (2016). Chapter 9: Nanocellulose—Fabrication, structure, properties, and application in the area of care and cure. In M. Grumezescu (Ed.), *Fabrication and self-assembly of nanobiomaterials. Applications of nanobiomaterials* (Vol. 1, pp. 243–288). William Andrew. https://doi.org/10.1016/B978-0-323-41533-0.00009-X

Ishak, W. H. W., Rosli, N. A., Ahmad, I., Ramli, S., & Amin, M. C. I. M. (2021). Drug delivery and in vitro biocompatibility studies of gelatin-nanocellulose smart hydrogels cross-linked with gamma radiation. *Journal of Materials Research and Technology, 15*, 7145–7157. https://doi.org/10.1016/j.jmrt.2021.11.095

Isogai, A. (2021). Emerging nanocellulose technologies: Recent developments. *Advanced Materials, 33*(28), 2000630. https://doi.org/10.1002/adma.202000630

Isogai, A., & Bergström, L. (2018). Preparation of cellulose nanofibers using green and sustainable chemistry. *Current Opinion in Green and Sustainable Chemistry, 12*, 15–21. https://doi.org/10.1016/j.cogsc.2018.04.008

Isogai, A., Saito, T., & Fukuzumi, H. (2011). TEMPO-oxidized cellulose nanofibers. *Nanoscale, 3*(1), 71–85. https://doi.org/10.1039/c0nr00583e

Jarach, N., Zuckerman, R., Naveh, N., Dodiuk, H., & Kenig, S. (2021). Bio- and water-based reversible covalent bonds containing polymers (vitrimers) and their relevance to adhesives—A critical review. *Progress in Adhesion and Adhesives, 6*, 587–619. https://doi.org/10.1002/9781119846703.ch13

Jiang, Q., Kacica, C., Soundappan, T., Liu, K.-k., Tadepalli, S., Biswas, P., et al. (2017). An in situ grown bacterial nanocellulose/graphene oxide composite for flexible supercapacitors. *Journal of Materials Chemistry A, 5*(27), 13976–13982. https://doi.org/10.1039/C7TA03824K

Jin, L. Q., Sun, Q. C., Xu, Q. H., & Xu, Y. J. (2015). Adsorptive removal of anionic dyes from aqueous solutions using microgel based on nanocellulose and polyvinylamine. *Bioresource Technology, 197*, 348–355. https://doi.org/10.1016/j.biortech.2015.08.093

Jonas, R. & Farah, L.F. (1998). Production and application of microbial cellulose. *Polymer Degradation and Stability, 59*(1), 101–106. https://doi.org/10.1016/S0141-3910(97)00197-3

Kargarzadeh, H., Ahmad, I., Thomas, S., & Dufresne, A. (2017). *Handbook of nanocellulose and cellulose nanocomposites*. Wiley. https://doi.org/10.1002/9783527689972

Kaushik, M., & Moores, A. (2016). Review: Nanocelluloses as versatile supports for metal nanoparticles and their applications in catalysis. *Green Chemistry, 18*(3), 622–637. https://doi.org/10.1039/c5gc02500a

Kawada, T., Nakatsubo, F., Umezawa, T., Murakami, K., & Sakuno, T. (1994). Synthetic studies of cellulose. XII. First chemical synthesis of cellooctaose acetate. *Mokuzai Gakkaishi, 40*(7), 738–743.

Kim, M., & Doh, H. (2023). Upcycling food by-products: Characteristics and applications of nanocellulose. *Chemistry, an Asian Journal, 19*, e202301068. https://doi.org/10.1002/asia.202301068

Klemm, D., Cranston, E. D., Fischer, D., Gama, M., Kedzior, S. A., Kralisch, D., et al. (2018). Nanocellulose as a natural source for groundbreaking applications in materials science: Today's state. *Materials Today, 21*(7), 720–748. https://doi.org/10.1016/j.mattod.2018.02.001

Kobayashi, S., Sakamoto, J., & Kimura, S. (2001). In vitro synthesis of cellulose and related polysaccharides. *Progress in Polymer Science, 26*(9), 1525–1560. https://doi.org/10.1016/S0079-6700(01)00026-0

Koivuniemi, R., Hakkarainen, T., Kiiskinen, J., Kosonen, M., Vuola, J., Valtonen, J., et al. (2020). Clinical study of nanofibrillar cellulose hydrogel dressing for skin graft donor site treatment. *Advances in Wound Care, 9*(4), 199–210. https://doi.org/10.1089/wound.2019.0982

Koneru, A., Dharmalingam, K., & Anandalakshmi, R. (2020). Cellulose based nanocomposite hydrogel films consisting of sodium carboxymethylcellulose–grapefruit seed extract nanoparticles for potential wound healing applications. *International Journal of Biological Macromolecules, 148*, 833–842. https://doi.org/10.1016/j.ijbiomac.2020.01.018

Kono, H., Tsukamoto, E., & Tajima, K. (2021). Facile post-carboxymethylation of cellulose nanofiber surfaces for enhanced water dispersibility. *ACS Omega, 6*(49), 34107–34114. https://doi.org/10.1021/acsomega.1c05603

Kramer, R. K., Belgacem, M. N., Carvalho, A. J. F., & Gandini, A. (2019). Thermally reversible nanocellulose hydrogels synthesized via the furan/maleimide Diels-Alder click reaction in water. *International Journal of Biological Macromolecules, 141*, 493–498. https://doi.org/10.1016/j.ijbiomac.2019.09.027

Kuang, Y., Chen, C., Cheng, J., Pastel, G., Li, T., Song, J., et al. (2019). Selectively aligned cellulose nanofibers towards high-performance soft actuators. *Extreme Mechanics Letters, 29*, 100463. https://doi.org/10.1016/j.eml.2019.100463

Kumari, S., Mankotia, D., & Chauhan, G. S. (2016). Crosslinked cellulose dialdehyde for Congo red removal from its aqueous solutions. *Journal of Environmental Chemical Engineering, 4*, 1126–1136. https://doi.org/10.1016/j.jece.2016.01.008

Lee, K.-Y., Buldum, G., Mantalaris, A., & Bismarck, A. (2013). More than meets the eye in bacterial cellulose: Biosynthesis, bioprocessing, and applications in advanced fiber composites. *Macromolecular Bioscience, 14*(1), 10–32. https://doi.org/10.1002/mabi.201300298

Lee, K.-Y., Buldum, G., Mantalaris, A. & Bismarck, A. (2014). More Than Meets the Eye in Bacterial Cellulose: Biosynthesis, Bioprocessing, and Applications in Advanced Fiber Composites. *Macromolecular Bioscience, 14*(1), 10–32. https://doi.org/10.1002/mabi.201300298

Lefroy, K. S., Murray, B. S., & Ries, M. E. (2021). Advances in the use of microgels as emulsion stabilisers and as a strategy for cellulose functionalisation. *Cellulose, 28*, 647–670. https://doi.org/10.1007/s10570-020-03595-8

Lehrhofer, A. F., Goto, T., Kawada, T., Rosenau, T., & Hettegger, H. (2022). The in vitro synthesis of cellulose—A mini-review. *Carbohydrate Polymers, 285*, 119222. https://doi.org/10.1016/j.carbpol.2022.119222

Lewis, L., Derakhshandeh, M., Hatzikiriakos, S. G., Hamad, W. Y., & MacLachlan, M. J. (2016). Hydrothermal gelation of aqueous cellulose nanocrystal suspensions. *Biomacromolecules, 17*(8), 2747–2754. https://doi.org/10.1021/acs.biomac.6b00906

Li, J., Wei, P., Xie, Y., Liu, Z., Chen, H., & He, L. (2022). Conjoined-network induced highly tough hydrogels by using copolymer and nano-cellulose for oilfield water plugging. *Journal of Industrial and Engineering Chemistry, 109*, 161–172. https://doi.org/10.1016/j.jiec.2022.01.038

Liebner, F., Pircher, N., Schimper, C., Haimer, E., & Rosenau, T. (2015). Aerogels: Cellulose-based. In *Encyclopedia of biomedical polymers and polymer biomaterials* (1st ed., pp. 37–75). https://doi.org/10.1201/9781351237970

Lim, L. S., Rosli, N. A., Ahmad, I., Mat Lazim, A., & Mohd Amin, M. C. I. (2017). Synthesis and swelling behavior of pH-sensitive semi-IPN superabsorbent hydrogels based on poly

(acrylic acid) reinforced with cellulose nanocrystals. *Nanomaterials, 7*(11), 399. https://doi.org/10.3390/nano7110399

Liu, Y., Wei, H., Li, S., Wang, G., Guo, T., & Han, H. (2022). Facile fabrication of semi-IPN hydrogel adsorbent based on quaternary cellulose via amino-anhydride click reaction in water. *International Journal of Biological Macromolecules, 207*, 622–634. https://doi.org/10.1016/j.ijbiomac.2022.03.032

Lu, P., Liu, R., Liu, X., & Wu, M. (2018). Preparation of self-supporting bagasse cellulose nanofibrils hydrogels induced by zinc ions. *Nanomaterials, 8*(10), 800. https://doi.org/10.3390/nano8100800

Lv, X., Huang, Y., Hu, M., Wang, Y., Dai, D., Ma, L., et al. (2024). Recent advances in nanocellulose based hydrogels: Preparation strategy, typical properties and food application. *International Journal of Biological Macromolecules, 277*, 134015. https://doi.org/10.1016/j.ijbiomac.2024.134015

Majerle, A., Schmieden, D. T., Jerala, R., & Meyer, A. S. (2019). Synthetic biology for multiscale designed biomimetic assemblies: From designed self-assembling biopolymers to bacterial bioprinting. *Biochemistry, 58*(16), 2095–2104. https://doi.org/10.1021/acs.biochem.8b00922

May, M. N., Sugawara, A., Asoh, T.-A., Takashima, Y., Harada, A., & Uyama, H. (2023). Composite hydrogels with host–guest interaction using cellulose nanocrystal as supramolecular filler. *Polymer, 277*, 125979. https://doi.org/10.1016/j.polymer.2023.125979

Meyabadi, T. F., Dadashian, F., Sadeghi, G. M. M., & Asl, H. E. Z. (2014). Spherical cellulose nanoparticles preparation from waste cotton using a green method. *Powder Technology, 261*, 232–240. https://doi.org/10.1016/j.powtec.2014.04.039

Mittal, N., Tien, S., Lizundia, E., & Niederberger, M. (2022). Hierarchical nanocellulose-based gel polymer electrolytes for stable Na electrodeposition in sodium ion batteries. *Small, 18*(43), 2107183. https://doi.org/10.1002/smll.202107183

Mohd Amin, M. C. I., Ahmad, N., Halib, N., & Ahmad, I. (2012). Synthesis and characterization of thermo- and pH-responsive bacterial cellulose/acrylic acid hydrogels for drug delivery. *Carbohydrate Polymers, 88*(2), 465–473. https://doi.org/10.1016/j.carbpol.2011.12.022

Morozova, S. M. (2023). Recent advances in hydrogels via Diels–Alder crosslinking: Design and applications. *Gels, 9*(2), 102. https://doi.org/10.3390/gels9020102

Nakatsubo, F., Kamitakahara, H., & Hori, M. (1996). Cationic ring-opening polymerization of 3, 6-di-O-benzyl-α-D-glucose 1, 2, 4-orthopivalate and the first chemical synthesis of cellulose. *Journal of the American Chemical Society, 118*(7), 1677–1681. https://doi.org/10.1021/ja953286u

Nasution, H., Harahap, H., Dalimunthe, N. F., Ginting, M. H. S., Jaafar, M., Tan, O. O. H., et al. (2022). Hydrogel and effects of crosslinking agent on cellulose-based hydrogels: A review. *Gels, 8*(9), 568. https://doi.org/10.3390/gels8090568

Nath, P. C., Debnath, S., Sridhar, K., Inbaraj, B. S., Nayak, P. K., & Sharma, M. (2022). A comprehensive review of food hydrogels: Principles, formation mechanisms, microstructure, and its applications. *Gels, 9*(1), 1. https://doi.org/10.3390/gels9010001

Nishimura, T., & Nakatsubo, F. (1997). Chemical synthesis of cellulose derivatives by a convergent synthetic method and several of their properties. *Cellulose, 4*(2), 109–130. https://doi.org/10.1023/A:1018423503762

Nyamayaro, K., Hatzikiriakos, S. G., & Mehrkhodavandi, P. (2023). Utilizing cellulose-based conducting hydrogels in iontronics. *RSC Sustainability, 1*(6), 1369–1385. https://doi.org/10.1039/D3SU00139C

O'Neill, E. C., Pergolizzi, G., Stevenson, C. E. M., Lawson, D. M., Nepogodiev, S. A., & Field, R. A. (2017). Cellodextrin phosphorylase from Ruminiclostridium thermocellum: X-ray crystal structure and substrate specificity analysis. *Carbohydrate Research, 451*, 118–132. https://doi.org/10.1016/j.carres.2017.07.005

Osong, S. H., Norgren, S., & Engstrand, P. (2015). Processing of wood-based microfibrillated cellulose and nanofibrillated cellulose, and applications relating to papermaking: A review. *Cellulose, 23*(1), 93–123. https://doi.org/10.1007/s10570-015-0798-5

Otoni, C. G., Espitia, P. J., Avena-Bustillos, R. J., & McHugh, T. H. (2016). Trends in antimicrobial food packaging systems: Emitting sachets and absorbent pads. *Food Research International, 83*, 60–73. https://doi.org/10.1016/j.foodres.2016.02.018

Omadjela, A., Narahari, J., Strumillo, H., Mélida, O., Mazur, V., Bulone, V. & Zimmer, J. (2013). BcsA and BcsB form the catalytically active core of bacterial cellulose synthase sufficient for in vitro cellulose synthesis. *Proceedings of the National Academy of Sciences, 110*(44), 17856–17861. https://doi.org/10.1073/pnas.1314063110

Pelton, R., & Hoare, T. (2011). Microgels and their synthesis: An introduction. In A. Fernandez-Nieves, H. M. Wyss, J. Mattsson, & D. A. Weitz (Eds.), *Microgel suspensions: Fundamentals and applications* (pp. 1–32). Wiley. https://doi.org/10.1002/9783527632992.ch1

Perera, M. M., & Ayres, N. (2020). Dynamic covalent bonds in self-healing, shape memory, and controllable stiffness hydrogels. *Polymer Chemistry, 11*(8), 1410–1423. https://doi.org/10.1039/C9PY01694E

Pietrucha, K., & Safandowska, M. (2015). Dialdehyde cellulose-crosslinked collagen and its physicochemical properties. *Process Biochemistry, 50*, 2015–2111. https://doi.org/10.1016/j.procbio.2015.09.025

Pilz da Cunha, M., Debije, M. G., & Schenning, A. P. H. J. (2020). Bioinspired light-driven soft robots based on liquid crystal polymers. *Chemical Society Reviews, 49*(18), 6568–6578. https://doi.org/10.1039/D0CS00363H

Pirozzi, A., Ferrari, G. & Donsì, F. (2021). The Use of Nanocellulose in Edible Coatings for the Preservation of Perishable Fruits and Vegetables. *Coatings, 11*(8), 990. https://doi.org/10.3390/coatings11080990

Plappert, S. F., Nedelec, J. M., Rennhofer, H., Lichtenegger, H. C., Bernstorff, S., & Liebner, F. W. (2018a). Self-assembly of cellulose in super-cooled ionic liquid under the impact of decelerated antisolvent infusion: An approach toward anisotropic gels and aerogels. *Biomacromolecules, 19*(11), 4411–4422. https://doi.org/10.1021/acs.biomac.8b01278

Plappert, S. F., Quraishi, S., Nedelec, J.-M., Konnerth, J., Rennhofer, H., Lichtenegger, H. C., et al. (2018b). Conformal ultrathin coating by $scCO_2$-mediated PMMA deposition: A facile approach to add moisture resistance to lightweight ordered nanocellulose aerogels. *Chemistry of Materials, 30*(7), 2322–2330. https://doi.org/10.1021/acs.chemmater.7b05226

Plappert, S. F., Quraishi, S., Pircher, N., Mikkonen, K. S., Veigel, S., Klinger, K. M., et al. (2018c). Transparent, flexible, and strong 2,3-dialdehyde cellulose films with high oxygen barrier properties. *Biomacromolecules, 19*(7), 2969–2978. https://doi.org/10.1021/acs.biomac.8b00536

Portela, R., Leal, C. R., Almeida, P. L., & Sobral, R. G. (2019). Bacterial cellulose: A versatile biopolymer for wound dressing applications. *Microbial Biotechnology, 12*(4), 586–610. https://doi.org/10.1111/1751-7915.13392

Prakobna, K., Terenzi, C., Zhou, Q., Furó, I., & Berglund, L. A. (2015). Core–shell cellulose nanofibers for biocomposites–Nanostructural effects in hydrated state. *Carbohydrate Polymers, 125*, 92–102. https://doi.org/10.1016/j.carbpol.2015.02.059

Priebe, X., Daschner, M., Schwab, W., & Weuster-Botz, D. (2018). Rational selection of biphasic reaction systems for geranyl glucoside production by Escherichia coli whole-cell biocatalysts. *Enzyme and Microbial Technology, 112*, 79–87. https://doi.org/10.1016/j.enzmictec.2017.11.003

Purushotham, P., Cho, S. H., Díaz-Moreno, S. M., Kumar, M., Nixon, B. T., Bulone, V., & Zimmer, J. (2016). A single heterologously expressed plant cellulose synthase isoform is sufficient for cellulose microfibril formation in vitro. *Proceedings of the National Academy of Sciences, 113*(40), 11360–11365. https://doi.org/10.1073/pnas.1606210113

Pylkkanen, R., Mohammadi, P., Arola, S., de Ruijter, J. C., Sunagawa, N., Igarashi, K., et al. (2020). In vitro synthesis and self-assembly of cellulose II nanofibrils catalyzed by the reverse reaction of Clostridium thermocellum cellodextrin phosphorylase. *Biomacromolecules, 21*(10), 4355–4364. https://doi.org/10.1021/acs.biomac.0c01162

Qi, Y., Cheng, Z., Ye, Z., Zhu, H., & Aparicio, C. (2019). Bioinspired mineralization with hydroxyapatite and hierarchical naturally aligned nanofibrillar cellulose. *ACS Applied Materials & Interfaces, 11*(31), 27598–27604. https://doi.org/10.1021/acsami.9b09443

Quraishi, S., Plappert, S., Griesser, T., Gindl-Altmutter, W., & Liebner, F. (2018). Chemical vs. physical grafting of photoluminescent amino-functional carbon dots onto transparent nematic nanocellulose gels and aerogels. *Cellulose, 26*, 7781–7796. https://doi.org/10.1007/s10570-019-02619-2

Rana, A. K., Gupta, V. K., Hart, P., & Thakur, V. K. (2024). Cellulose-alginate hydrogels and their nanocomposites for water remediation and biomedical applications. *Environmental Research, 243*, 117889. https://doi.org/10.1016/j.envres.2023.117889

Reid, M. S., Villalobos, M., & Cranston, E. D. (2017). Benchmarking cellulose nanocrystals: From the laboratory to industrial production. *Langmuir, 33*(7), 1583–1598. https://doi.org/10.1021/acs.langmuir.6b03765

Ren, J., Dai, Q., Zhong, H., Liu, X., Meng, L., Wang, X., et al. (2018). Quaternized xylan/cellulose nanocrystal reinforced magnetic hydrogels with high strength. *Cellulose, 25*, 4537–4549. https://doi.org/10.1007/s10570-018-1858-4

Rennhofer, H., Plappert, S. F., Lichtenegger, H. C., Bernstorff, S., Fitzka, M., Nedelec, J.-M., & Liebner, F. W. (2019). Insight into the nanostructure of anisotropic cellulose aerogels upon compression. *Soft Matter, 15*(41), 8372–8380. https://doi.org/10.1039/C9SM01422E

Revol, J.-F., Godbout, L., Dong, X.-M., Gray, D. G., Chanzy, H., & Maret, G. (1994). Chiral nematic suspensions of cellulose crystallites; phase separation and magnetic field orientation. *Liquid Crystals, 16*(1), 127–134. https://doi.org/10.1080/02678299408036525

Richtering, W., & Saunders, B. R. (2014). Gel architectures and their complexity. *Soft Matter, 10*(21), 3695–3702. https://doi.org/10.1039/c4sm00208c

Roig-Sanchez, S., Kam, D., Malandain, N., Sachyani-Keneth, E., Shoseyov, O., Magdassi, S., et al. (2022). One-step double network hydrogels of photocurable monomers and bacterial cellulose fibers. *Carbohydrate Polymers, 294*, 119778. https://doi.org/10.1016/j.carbpol.2022.119778

Ruka, D. R., Sangwan, P., Garvey, C. J., Simon, G. P., & Dean, K. M. (2015). Biodegradability of poly-3-hydroxybutyrate/bacterial cellulose composites under aerobic conditions, measured via evolution of carbon dioxide and spectroscopic and diffraction methods. *Environmental Science & Technology, 49*(16), 9979–9986. https://doi.org/10.1021/es5044485

Samyn, P., Meftahi, A., Geravand, S. A., Heravi, M. E. M., Najarzadeh, H., Sabery, M. S. K., et al. (2023). Opportunities for bacterial nanocellulose in biomedical applications: Review on biosynthesis, modification and challenges. *International Journal of Biological Macromolecules, 231*, 123316. https://doi.org/10.1016/j.ijbiomac.2023.123316

Serizawa, T., Fukaya, Y., & Sawada, T. (2017). Self-assembly of cellulose oligomers into nanoribbon network structures based on kinetic control of enzymatic oligomerization. *Langmuir, 33*(46), 13415–13422. https://doi.org/10.1021/acs.langmuir.7b03653

Shao, C., Wang, M., Meng, L., Chang, H., Wang, B., Xu, F., et al. (2018). Mussel-inspired cellulose nanocomposite tough hydrogels with synergistic self-healing, adhesive, and strain-sensitive properties. *Chemistry of Materials, 30*(9), 3110–3121. https://doi.org/10.1021/acs.chemmater.8b01172

Singh, A. K., Itkor, P., & Lee, Y. S. (2023). State-of-the-art insights and potential applications of cellulose-based hydrogels in food packaging: Advances towards sustainable trends. *Gels, 9*(6), 433. https://doi.org/10.3390/gels9060433

Singh, S., Bhardwaj, S., Tiwari, P., Dev, K., Ghosh, K., & Maji, P. K. (2024). Recent advances in cellulose nanocrystals-based sensors: A review. *Materials Advances, 5*(7), 2622–2654. https://doi.org/10.1039/D3MA00601H

Sionkowska, A., Mężykowska, O., & Piątek, J. (2019). Bacterial nanocelullose in biomedical applications: A review. *Polymer International, 68*(11), 1841–1847. https://doi.org/10.1002/pi.5882

Sirviö, J. A., Visanko, M., & Liimatainen, H. (2015). Deep eutectic solvent system based on choline chloride-urea as a pre-treatment for nanofibrillation of wood cellulose. *Green Chemistry, 17*(6), 3401–3406. https://doi.org/10.1039/C5GC00398A

Sonnier, R. A. T., & Rouif, S. (2012). Modification of polymer blends by E-beam and γ-irradiation. In V. Mittal (Ed.), *Functional polymer blends: Synthesis, properties, and performance* (pp. 261–304). CRC Press. https://doi.org/10.1201/b11799

Sulaeva, I., Henniges, U., Rosenau, T., & Potthast, A. (2015). Bacterial cellulose as a material for wound treatment: Properties and modifications. A review. *Biotechnology Advances, 33*(8), 1547–1571. https://doi.org/10.1016/j.biotechadv.2015.07.009

Sulaeva, I., Hettegger, H., Bergen, A., Rohrer, C., Kostic, M., Konnerth, J., et al. (2020). Fabrication of bacterial cellulose-based wound dressings with improved performance by impregnation with alginate. *Materials Science and Engineering: C, 110*, 110619. https://doi.org/10.1016/j.msec.2019.110619

Takano, T., Harada, Y., Nakatsubo, F., & Murakami, K. (1990). Synthetic studies of cellulose. VI: Effect of the substituent groups of glycon on β-glycosylation. *Cellulose Chemistry and Technology, 24*(3), 333–341.

Tang, Y., Fang, Z., & Lee, H.-J. (2024). Exploring applications and preparation techniques for cellulose hydrogels: A comprehensive review. *Gels., 10*(6), 365. https://doi.org/10.3390/gels10060365

Taylor, D. L., & Panhuis, M. (2016). Self-healing hydrogels. *Advanced Materials, 28*(41), 9060–9093. https://doi.org/10.1002/adma.201601613

Thivya, P., Akalya, S., & Sinija, V. (2022). A comprehensive review on cellulose-based hydrogel and its potential application in the food industry. *Applied Food Research, 2*(2), 100161. https://doi.org/10.1016/j.afres.2022.100161

Tian, W., Gao, X., Zhang, J., Yu, J., & Zhang, J. (2022). Cellulose nanosphere: Preparation and applications of the novel nanocellulose. *Carbohydrate Polymers, 277*, 118863. https://doi.org/10.1016/j.carbpol.2021.118863

Toshikj, E., Tarbuk, A., Grgić, K., Mangovska, B., & Jordanov, I. (2019). Influence of different oxidizing systems on cellulose oxidation level: Introduced groups versus degradation model. *Cellulose, 26*(2), 777–794. https://doi.org/10.1007/s10570-018-2133-4

Trache, D., Tarchoun, A. F., Derradji, M., Hamidon, T. S., Masruchin, N., Brosse, N., et al. (2020). Nanocellulose: From fundamentals to advanced applications. *Frontiers in Chemistry, 8*, 392. https://doi.org/10.3389/fchem.2020.00392

Trigui, K., Magnin, A., Putaux, J.-L., & Boufi, S. (2022). Twin-screw extrusion for the production of nanocellulose-PVA gels with a high solid content. *Carbohydrate Polymers, 286*, 119308. https://doi.org/10.1016/j.carbpol.2022.119308

Ulrich, S. (2019). Growing prospects of dynamic covalent chemistry in delivery applications. *Accounts of Chemical Research, 52*(2), 510–519. https://doi.org/10.1021/acs.accounts.8b00591

Varghese, R. T., Cherian, R. M., Chirayil, C. J., Antony, T., Kargarzadeh, H., & Thomas, S. (2023). Nanocellulose as an avenue for drug delivery applications: A mini-review. *Journal Of Composites Science, 7*(6), 210. https://doi.org/10.3390/jcs7060210

Vel, R., Bhatt, A., Priyanka, A., Gauthaman, A., Anilkumar, V., & Safeena, A. S. (2022). DEAE-cellulose-based composite hydrogel for 3D printing application: Physicochemical, mechanical, and biological optimization. *Materials Today Communications, 33*, 104335. https://doi.org/10.1016/j.mtcomm.2022.104335

Vikman, M., Vartiainen, J., Tsitko, I., & Korhonen, P. (2015). Biodegradability and compostability of nanofibrillar cellulose-based products. *Journal of Polymers and the Environment, 23*(2), 206–215. https://doi.org/10.1007/s10924-014-0694-3

Wang, S., Lu, A., & Zhang, L. (2016). Recent advances in regenerated cellulose materials. *Progress in Polymer Science, 53*, 169–206. https://doi.org/10.1016/j.progpolymsci.2015.07.003

Wang, C., Fadeev, M., Vázquez-González, M., & Willner, I. (2018). Stimuli-responsive donor–acceptor and DNA-crosslinked hydrogels: Application as shape-memory and self-healing materials. *Advanced Functional Materials, 28*(35), 1803111. https://doi.org/10.1002/adfm.201803111

Wang, Y., Huang, W., Wang, Y., Mu, X., Ling, S., Yu, H. et al. (2020). Stimuli-responsive composite biopolymer actuators with selective spatial deformation behavior. *Proceedings of the National Academy of Sciences, 117*(25), 14602–14608. https://doi.org/10.1073/pnas.200299611

Wang, C., Bai, J., Tian, P., Xie, R., Duan, Z., Lv, Q., & Tao, Y. (2021). The application status of nanoscale cellulose-based hydrogels in tissue engineering and regenerative biomedicine.

Frontiers in Bioengineering and Biotechnology, 18(9), 732513. https://doi.org/10.3389/fbioe.2021.732513

Wang, J., Yang, B., Jiang, Z., Liu, Y., Zhou, L., Liu, Z., & Tang, L. (2024a). Recent advances of conductive hydrogels for flexible electronics. *Electronic Materials, 5*(3), 101–131. https://doi.org/10.3390/electronicmat5030008

Wang, Y., Zhang, Y., Ren, P., Yu, S., Cui, P., Nielsen, C. B., Abrahams, I., et al. (2024b). Versatile and recyclable double-network PVA/cellulose hydrogels for strain sensors and triboelectric nanogenerators under harsh conditions. *Nano Energy, 125*, 109599. https://doi.org/10.1016/j.nanoen.2024.109599

Wiese, S., Tsvetkova, Y., Daleiden, N. J., Spieß, A. C., & Richtering, W. (2016). Microgel stabilized emulsions: Breaking on demand. *Colloids and Surfaces A: Physicochemical and Engineering Aspects, 495*, 193–199. https://doi.org/10.1016/j.colsurfa.2016.02.003

Wu, W., Huang, F., Pan, S., Mu, W., Meng, X., Yang, H., et al. (2015). Thermo-responsive and fluorescent cellulose nanocrystals grafted with polymer brushes. *Journal of Materials Chemistry A, 3*(5), 1995–2005. https://doi.org/10.1039/C4TA04761C

Wu, W., Song, R., Xu, Z., Jing, Y., Dai, H., & Fang, G. (2018). Fluorescent cellulose nanocrystals with responsiveness to solvent polarity and ionic strength. *Sensors and Actuators B: Chemical, 275*, 490–498. https://doi.org/10.1016/j.snb.2018.07.085

Xin, J. H., & Lu, H. F. (2018). 8—Easy-care treatments for fabrics and garments. In M. Miao & J. H. Xin (Eds.), *Engineering of high-performance textiles* (pp. 187–215). Woodhead Publishing. https://doi.org/10.1016/B978-0-08-101273-4.00025-1

Xiong, Y., Wang, C., Wang, H., Jin, C., Sun, Q., & Xu, X. (2018). Nano-cellulose hydrogel coated flexible titanate-bismuth oxide membrane for trinity synergistic treatment of super-intricate anion/cation/oily-water. *Chemical Engineering Journal, 337*, 143–151. https://doi.org/10.1016/j.cej.2017.12.080

Xu, W., Wang, X., Sandler, N., Willfor, S., & Xu, C. (2018). Three-dimensional printing of wood-derived biopolymers: A review focused on biomedical applications. *ACS Sustainable Chemistry & Engineering, 6*(5), 5663–5680. https://doi.org/10.1021/acssuschemeng.7b03924

Xu, H., Liu, Y., Xie, Y., Zhu, E., Shi, Z., Yang, Q., et al. (2019). Doubly cross-linked nanocellulose hydrogels with excellent mechanical properties. *Cellulose, 26*, 8645–8654. https://doi.org/10.1007/s10570-019-02689-2

Yagura, T., Ikegami, W., Kamitakahara, H., & Takano, T. (2020). Synthesis of an enantiomer of cellulose via cationic ring-opening polymerization. *Cellulose, 27*, 9755–9766. https://doi.org/10.1007/s10570-020-03512-z

Yang, J., An, X., Liu, L., Tang, S., Cao, H., Xu, Q., & Liu, H. (2020). Cellulose, hemicellulose, lignin, and their derivatives as multi-components of bio-based feedstocks for 3D printing. *Carbohydrate Polymers, 250*, 116881. https://doi.org/10.1016/j.carbpol.2020.116881

Yang, Y., Zhang, M., Sha, L., Lu, P., & Wu, M. (2021). "Bottom-Up" assembly of nanocellulose microgels as stabilizer for pickering foam forming. *Biomacromolecules, 22*(9), 3960–3970. https://doi.org/10.1021/acs.biomac.1c00766

You, C., Ning, L., Wu, H., Huang, C., & Wang, F. (2021). A biocompatible and pH-responsive nanohydrogel based on cellulose nanocrystal for enhanced toxic reactive oxygen species generation. *Carbohydrate Polymers, 258*, 117685. https://doi.org/10.1016/j.carbpol.2021.117685

Yousefi, H., Su, H.-M., Imani, S. M., Alkhaldi, K., Filipe, C. D. M., & Didar, T. F. (2019). Intelligent food packaging: A review of smart sensing technologies for monitoring food quality. *ACS Sensors, 4*(4), 808–821. https://doi.org/10.1021/acssensors.9b00440

Zhang, Z. P., Rong, M. Z., & Zhang, M. Q. (2018). Polymer engineering based on reversible covalent chemistry: A promising innovative pathway towards new materials and new functionalities. *Progress in Polymer Science, 80*, 39–93. https://doi.org/10.1016/j.progpolymsci.2018.03.002

Zhang, Q., Zhang, L., Wu, W., & Xiao, H. (2020). Methods and applications of nanocellulose loaded with inorganic nanomaterials: A review. *Carbohydrate Polymers, 229*, 115454. https://doi.org/10.1016/j.carbpol.2019.115454

Zhang, Y., Wang, Q., Wang, Z., Zhang, D., Gu, J., Ye, K., et al. (2021). Strong, self-healing gelatin hydrogels cross-linked by double dynamic covalent chemistry. *ChemPlusChem, 86*(11), 1524–1529. https://doi.org/10.1002/cplu.202100474

Zhang, L., Wan, C., Su, J., Zhang, C., Wei, S., Tian, W., et al. (2022). A dual-crosslinked self-healing and antibacterial nanocellulose hydrogel for monitoring of human motions. *Materials and Design, 215*, 110464. https://doi.org/10.1016/j.matdes.2022.110464

Zheng, C., Yue, Y., Gan, L., Xu, X., Mei, C., & Han, J. (2019). Highly stretchable and self-healing strain sensors based on nanocellulose-supported graphene dispersed in electro-conductive hydrogels. *Nanomaterials, 9*(7), 937. https://doi.org/10.3390/nano9070937

Zhou, Y., Zhang, Y., Dai, Z., Jiang, F., Tian, J., & Zhang, W. (2020). A super-stretchable, self-healing and injectable supramolecular hydrogel constructed by a host–guest crosslinker. *Biomaterials Science, 8*(12), 3359–3369. https://doi.org/10.1039/D0BM00290A

Zhou, M., Chen, D., Chen, Q., Chen, P., Song, G., & Chang, C. (2024). Reversible surface engineering of cellulose elementary fibrils: From ultralong nanocelluloses to advanced cellulosic materials. *Advanced Materials, 36*(21), 2312220. https://doi.org/10.1002/adma.202312220

Zlenko, D. V., Vtyurina, D. N., Usachev, S. V., Skoblin, A. A., Mikhaleva, M. G., Politenkova, G. G., et al. (2021). On the orientation of the chains in the mercerized cellulose. *Scientific Reports, 11*(1), 8765. https://doi.org/10.1038/s41598-021-88040-x

Zubik, K., Singhsa, P., Wang, Y., Manuspiya, H., & Narain, R. (2017). Thermo-responsive poly(N-isopropylacrylamide)-cellulose nanocrystals hybrid hydrogels for wound dressing. *Polymers, 9*(4), 119. https://doi.org/10.3390/polym9040119

Chapter 19
Nanocellulose-Based Aerogels

Falk Liebner and Sven Plappert

19.1 Introduction

The discovery of aerogels, a novel subclass of lightweight, highly porous materials, arose from a combination of dedication, competition, and scientific curiosity among inventors. Legend has it that in the late 1920s, two chemistry colleagues at the College of the Pacific wagered whether it was possible to replace the liquid in a jelly jar without causing shrinkage, essentially transforming a pectin hydrogel into an aerogel while preserving its network architecture. Samuel Stevens Kistler won the bet by demonstrating that delicate polymer networks could be "dried" without collapsing by avoiding capillary forces, using extraction agents that coexist with the gel's continuous liquid phase in a supercritical state.

Despite Kistler's groundbreaking work in the 1940s to commercialize silica aerogels, they struggled to enter the market due to complex, costly production processes and safety incidents, like a catastrophic methanol leak in 1984. However, two key discoveries greatly shifted aerogel production: the invention of sol-gel synthesis in 1971 (Teichner & Nicolaon, 1972), which eliminated problematic salt extraction, and the introduction of supercritical carbon dioxide ($scCO_2$) technology in the 1980s, which improved extraction methods and laid the groundwork for wider commercial acceptance (Grimmett, 1982).

Since then, silica aerogels have been utilized in various NASA projects due to their thermal insulating properties (Domínguez et al., 2003), while aerogels made from synthetic polymers emerged in the 1990s (Pekala et al., 1995), expanding to include significant classes such as polyimides (Rhine et al., 2006). By the early 2000s, research into cellulose and other biopolymer aerogels began to flourish,

F. Liebner (✉) · S. Plappert
Institute of Chemistry of Renewable Resources, BOKU University Vienna, Tulln an der Donau, Austria
e-mail: falk.liebner@boku.ac.at

G. Korotcenkov (ed.), *The Handbook of Paper-Based Sensors and Devices*,
https://doi.org/10.1007/978-3-031-91080-7_19

demonstrating that lightweight, open-nanoporous materials could be made from cellulose using various solvents and processes (Gavillon & Budtova, 2008; Hoepfner et al., 2008; Innerlohinger et al., 2006).

Recent advancements in the use of anisometric cellulose nanoparticles as self-assembling building blocks have revitalized cellulose aerogel research. A pivotal study in "Angewandte" showcased aerogels with 3D ordered nanofiber structures, indicating promising applications in thermal insulation, air and water treatment, energy harvesting, and tissue engineering (Kobayashi et al., 2014).

Fueled by a push for a bio-based circular economy, numerous studies have explored the manufacture and modification of various nanocellulose types, leading to an exponential increase in applications. This growth played a role in the International Union for Pure and Applied Chemistry (IUPAC) recognizing aerogels as an emerging technology in its 2022 top ten list, reflecting their vast potential across diverse fields.

19.2 Nanocellulose Building Blocks

Nature often employs the self-assembly of biopolymers into long-range anisotropic nanostructures, exemplified by tobacco mosaic virus, clay minerals, and iridescent iron oxide layers. Self-assembly of individual cellulose molecules to nanofibrils and their sophisticated packing into fibers composed of amorphous and crystalline domains is the target of cellulose biosynthesis, as it gives rise to intriguing mechanical and chemical properties which are required to withstand harsh environmental influences. These natural principles are employed in biomimicry efforts, to create advanced bio-based materials, using similar concepts for precise tailoring of material properties for advanced smart applications in sensing, sorption, controlled release, or tissue engineering (Bai et al., 2024), that often rely on periodic regular arrangements of network forming entities, homogeneous availability of certain functional groups, high specific surface, or defined pore geometries. Besides the largely improved possibilities to synthesize cellulose fibrils, sheets, and volumetric hydrogels by bottom-up sol-gel synthesis, efficient technologies have been made available to produce anisometric cellulose nanoparticles of different aspect ratios, crystallinity, and surface properties. These nanocelluloses can self-assemble in various ways, specifically in aqueous media, giving rise to different forms of liquid-crystallinity which largely broadens the application spectrum, specifically for sensing applications.

Nanocelluloses can be distinguished in cellulose nanocrystals (CNC), cellulose nanofibrils (CNF, from cellulose I), bacterial nanocellulose (BNC), cellulose nanospheres (CNS, from cellulose I and II), and cellulose II nanofibrils formed by very slow alignment from highly viscous molecular-dispersing solution state under the influence of an antisolvent. All of these nanocellulose building blocks have in common that their size does not exceed 100 nm at least in one spatial direction. Otherwise, they all differ in shape, aspect ratio, crystallinity, surface charge, and

ability for hydrogen bonding, which collectively leads to different macroscopic properties.

The processes used to synthesize nanocelluloses by bottom-up chemistry, bioengineering, or liberation from bulk cellulosic substrates by top-down processes have been comprehensively introduced in the previous chapter on cellulose-based hydrogels (Chap. 18).

From a large-scale production perspective, significant differences exist between these nanocellulose types regarding availability, cost, and manufacturing complexity. Therefore, this chapter focuses mainly on the processing of CNC and CNF into respective nanocellulose aerogels and gives a very brief overview of BNC aerogel production and properties but will not address CNS and cellulose II nanofibrils as it remains uncertain whether these research directions can be implemented on a larger scale.

19.3 Shaping and Post-processing of Nanocellulose Hydrogels

This section discusses shaping nanocellulose dispersions, focusing on cellulose nanofibers (CNF), the most widely used building block for nanocellulose aerogels. However, similar manipulation techniques can apply to CNC, CNS, and BNC, with variations in processability and properties due to differences in aspect ratio, crystallinity, and surface charge.

Nanoscale cellulose colloids, obtained through chemical and mechanical liberation, can exhibit entropy-driven self-assembly into liquid crystalline phases (Guccini et al., 2018; Marchessault et al., 1959) or be oriented by external forces (Brouzet et al., 2018). Utilizing these mechanisms in material formation allows for precise nanoscale structures, leading to unique physical properties. Depleting self-organizing forces through protonation or electrostatic screening enables physical gel formation at higher nanoparticle volume fractions, preserving the specific anisotropic assembly throughout the gelation process (Kobayashi et al., 2014; Plappert et al., 2017). High electrolyte concentrations can also shield electrostatic forces, promoting gelation rather than flocculation (Nordenstrom et al., 2017).

The high aspect ratio of nanofibers helps align them and restricts their kinetic mobility. At volume fractions above 0.5 wt.%, competing processes of nematic self-assembly and kinetic arrest may occur (Guccini et al., 2018). Effective self-assembly may require balanced attractive and repulsive forces (Bertsch et al., 2017). Before gelation, nanofibers are in a nematic arrangement and likely in a partially arrested kinetic state. While developing kinetically arrested states in CNF dispersions is undesirable for dispersion casting due to increased viscosity, which complicates processing beyond 1 wt.%, resulting CNF aerogels are ultra-lightweight but have limited mechanical properties and pore structures.

Despite increased research on technologies like spinning (Lundahl et al., 2018) and additive manufacturing (Feng et al., 2021) that can cope with higher dispersion viscosity, this section will briefly describe a typical dispersion casting approach for creating nematic ultralightweight CNF aerogels, illustrating the principles of CNF aerogel formation and strategies for enhancing mechanical performance, moisture sensitivity, transparency, and thermal superinsulation. Additionally, an aerogel manufactured from 2,3-dicarboxyl-cellulose will be presented, as periodate pretreatment has been shown to significantly reduce energy demands compared to TEMPO-mediated oxidation.

19.3.1 Dispersion-Casting and Manufacture of Nematic Transparent 2,3-DCC Aerogels

Heterogeneous oxidation of never-dried sulfite dissolving pulp using sodium metaperiodate (at 50 °C for 3 h) yields 2,3-dialdehyde cellulose (DAC). The subsequent oxidation of the aldehyde groups to produce 2,3-dicarboxyl cellulose (2,3-DCC) (1.02 mmol g^{-1}) is achieved using sodium chlorite in an acidic medium. Following this, nanofibrillation of the DCC is performed in a dilute aqueous suspension (0.25 wt.%, pH 7.5) using a high-pressure homogenizer, with results obtained after two passes at 50 MPa and two additional passes at 80 MPa. Centrifugation at 5000 rpm for 1 h eliminates any non-fibrillated residues. Notably, the resulting clear and transparent dispersions display lower viscosity compared to their 6-carboxyl cellulose (6-CC) counterparts obtained through TEMPO-mediated oxidation. This difference aligns with the dimensions of the corresponding individualized CNFs, with measurements of 2.08 ± 0.4 nm and 525 ± 160 nm for the 2,3-DCC CNFs, in contrast to 2.4 ± 0.5 nm and 940 ± 250 nm for the 6-CC, despite the latter undergoing twice as many fibrillation cycles.

As illustrated in Fig. 19.1a, cellulose nanofibers (CNFs) possess the ability to self-assemble into a nematic orientation of anisometric, rod-like particles beyond a critical concentration, as observed through their birefringence using polarized light microscopy. Before casting, the solid content of the 2,3-DCC nanofiber dispersions is adjusted to 0.25–2.1 w/v % utilizing a vacuum rotavapor. Within this concentration range, the viscosity of the DCC dispersions remains sufficiently low for effective solution casting. Acid-induced gelation is achieved by immersing the cast 2,3-DCC dispersions in aqueous HCl, which stabilizes the liquid-crystalline ordering through extensive hydrogen bonding, resulting in transparent, free-standing gelatinous hydrogels. Notably, the nematic arrangement of the 2,3-DCC particles is preserved during the acid-induced gelation process (Plappert et al., 2017), similar to 6-CC (Kobayashi et al., 2014). Incrementally replacing water with ethanol, as is necessary for the conversion to aerogels via supercritical CO_2 ($scCO_2$) drying, significantly increases the stiffness of the gels. This increase primarily results from the removal of structural water, which acts as a plasticizer for the 2,3-DCC nanofibril

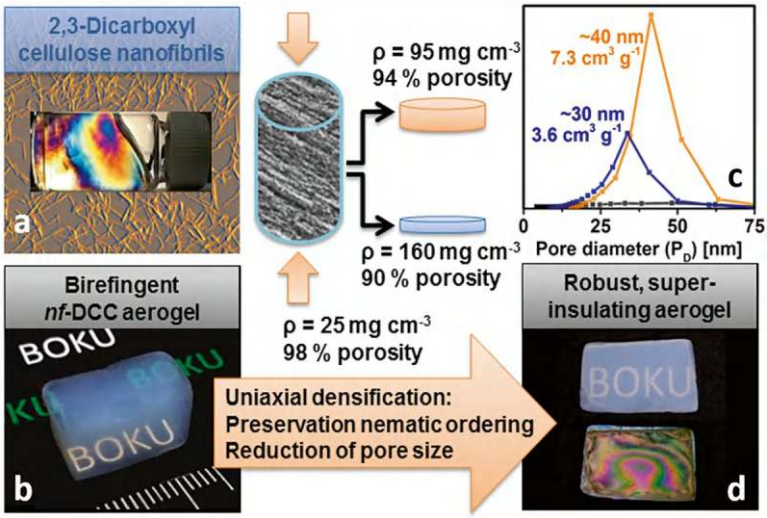

Fig. 19.1 Preparation of mechanically robust, transparent, thermal super-insulating CNF aerogels obtained from 2,3-dicarboxyl cellulose (2,3-DCC). Preservation of nematic CNF fibril orientation from dispersion state (**a**) through solvent exchange and $scCO_2$ drying (**b**). Uniaxial densification (from 25 mg cm^{-3} to 95 and 160 mg cm^{-3}) increases robustness and imparts the panels' thermal super-insulating properties by pore-size harmonization (**c**) which occurs in favor of mesopores and at the expense of pores larger than 70 nm. Reduction of inter-fibril angle by uniaxial folding largely preserves preferential nematic orientation, transparency, (**d**) and porosity (98% vs. 94 and 90%). (Reprinted with permission from Plappert et al. (2017). Copyright 2017 American Chemical Society)

network, akin to the behavior observed in bacterial cellulose (Pircher et al., 2014). The extraction of ethanol from the 2,3-DCC alcogels using $scCO_2$ yields highly transparent (Fig. 19.1b), birefringent aerogels with well-preserved nematic CNF orientation. While the resulting aerogels are lightweight (e.g., 18 mg cm^{-3}), highly porous (98.8%), and have a large specific surface area (448 m^2 g^{-1}), they remain fragile and sensitive to mechanical impacts and moisture-induced shrinkage. Therefore, additional strategies are needed to address these limitations for practical applications (Plappert et al., 2017).

19.3.2 Improving Mechanical Performance by Uniaxial Densification

Uniaxial densification of the 2,3-DCC aerogels increased their density from 18 to 90 mg cm^{-3}, resulting in nearly a 30-fold increase in Young's modulus and a sixfold increase in specific modulus. Concurrently, the specific surface area increased from 448 to 588 m^2 g^{-1} (Plappert et al., 2017). Nitrogen sorption analysis further

indicated significant capillary condensation at higher relative pressures for the densified material, suggesting a narrow pore size distribution with considerable volumes contributed by pores smaller than 100 nm. In the uncompressed sample at 25 mg cm^{-3} (porosity 98.4%), only 2.8% of the total pore volume consisted of pores smaller than 100 nm; this figure rose to 99% for the densified sample (density 95 mg cm^{-3}, porosity 94.1%). These findings emphasize the creation of smaller nanopores at the expense of larger ones, illustrating pore size harmonization (Plappert et al., 2017) as shown in Fig. 19.1c.

Additionally, small-angle X-ray scattering revealed that network compaction during uniaxial densification primarily occurs through a reduction in the inter-fibril angle rather than the sliding of 2,3-DCC fibrils over one another to form thicker network strands, which was not observed here. The abundant presence of pores smaller than the mean free path of air molecules (approximately 70 nm) at atmospheric pressure (Baillis et al., 2015) resulted in very low thermal conductivities down to 17.7 mW m^{-1} K^{-1} for the strain-hardened 2,3-DCC aerogels, attributed to the Knudsen effect (Baetens et al., 2011). Notably, nematic ordering and transparency were unaffected by uniaxial compression and pore size harmonization, enhancing their appeal for various applications (Fig. 19.1d).

19.3.3 Improving Moisture Resistance by Conformal Ultrathin Coating Through scCO$_2$-Mediated Antisolvent Deposition of Poly(Methyl Methacrylate)

The hydrophilicity of cellulose and other polysaccharide-based biopolymers presents a major challenge for applications requiring dry solid materials, particularly relevant for lightweight, soft cellulose nanofiber (CNF) aerogels. Their inherent fragility, extensive nanocapillary networks, and large internal surface areas make them susceptible to moisture absorption and shrinkage due to capillary forces. To ensure the viability of aerogels for practical use, effective techniques to impart moisture resistance while preserving chemical integrity, open porosity, high specific surface area, nematic orientation, and transparency are essential. While various methods exist to enhance hydrophobicity, maintaining these critical features can be challenging.

Recently, a scCO$_2$-assisted hydrophobization method has been developed, enabling conformal ultrathin coatings on nearly any moisture-sensitive aerogel while avoiding the complexities associated with chemical vapor deposition or wet-chemical derivatization. This method combines scCO$_2$ antisolvent precipitation of the secondary polymer poly (methyl methacrylate) (PMMA) with scCO$_2$ drying of the CNF/PMMA hybrid aerogels in a single batch process, utilizing isothermal variations in CO$_2$ pressure. This takes advantage of the sharp decrease in solvent power of many solvents in mixtures with CO$_2$ as they transition into a supercritical state, allowing CO$_2$ to act as an antisolvent (Mukhopadhyay, 2003). PMMA was

chosen for its non-foaming behavior in $scCO_2$, strong adhesion to cellulosic surfaces, and biocompatibility compared to other polymers.

As proof of concept, this method was applied to create lightweight, transparent bulk 6-CC aerogels (Fig. 19.2). Similar to 2,3-DCC (see above), nematic orientation of 6-CC fibrils in both dispersion and gel state (Fig. 19.2a, b) is observed. Immersion of alcogels in a solution of PMMA in acetone followed by consecutive but single-batch $scCO_2$ antisolvent precipitation and $scCO_2$ drying afforded highly transparent, nematic, and hydrophobic CNF composite aerogels (Fig. 19.2c–f) featuring specific surface areas as high as 500 $m^2\ g^{-1}$ (Plappert et al., 2018).

Birefringence studies demonstrated that the nematic ordering of the individualized CNF remained intact after surface modification (Fig. 19.2d). Small-angle X-ray scattering (SAXS) and scanning electron microscopy confirmed the presence of a uniform ultrathin PMMA layer that did not significantly alter the aerogel's high porosity (≥99%) and transparency (over 77% transmission at 600 nm, thickness 2.13 mm).

PMMA enhances the stiffness and hydrophobicity of the fragile aerogel structure, preventing nanofibril aggregation in moist environments or under vacuum

Fig. 19.2 Visualized appearance and properties of CNF alcogels (**a**, **b**) obtained from an aqueous dispersion of 2-CC (9.5 mg mL^{-1}) by acid-induced gelation and solvent exchange. Immersion in a solution of PMMA in acetone and consecutive $scCO_2$ antisolvent precipitation and $scCO_2$ drying in a single batch afforded CNF/PMMA composite aerogels (**c**–**f**; ρ_B = 14.8 mg cm^{-3}) with conformal ultrathin PMMA coating (**c**). Birefringence patterns under crossed polarizers confirmed preservation of nematic orientation throughout all conducted manipulations (**b**, **d**). The obtained materials were transparent (**e**, thickness 2 mm) and hydrophobic (water contact angle of 119.4° ± 7.5°) as seen from the shape of four water droplets resting on an aerogel disc illuminated by a light source (**f**). (Reprinted with permission from Plappert et al. (2018). Copyright 2018 American Chemical Society)

conditions, even at densities as low as 9.6 mg cm^{-3}. The combination of uniaxial densification and pore size harmonization with $scCO_2$-assisted PMMA coating is a promising strategy to enhance the potential of CNF aerogels for applications in thermal and acoustic insulation, volumetric displays, and sensing technologies (Plappert et al., 2018).

19.3.4 3D/4D-Printing and Microfluidics

In the last decade, additive manufacturing of aerogels has emerged as a promising technique, enabling the creation of application-specific characteristics such as gradients in density, composition, and pore size, which are particularly beneficial for cell culture, sensing, and fractionation applications. Reviews detailing recent advancements in 3D printing of biopolymers, including cellulose and its derivatives, are available (Dai et al., 2019; Yang et al., 2020).

Cellulose nanoparticles, particularly CNF, are vital components of many bio-inks. By blending them with varying proportions of CNC or BNC, the mechanical properties of both the printed gel and final aerogel can be effectively modulated. The shear-thinning behavior of aqueous CNF, CNC, and BNC dispersions ensures good flowability through the printing nozzle while returning to an elastic gel state afterward. Notably, CNF/BNC blends exhibit greater viscosity than CNF/CNC blends at equal ratios due to their higher aspect ratio and propensity for mechanical entanglement, which can aid sustainability by requiring less BNC for the same aerogel volume.

Low CNF content in nanocellulose bio-inks is often needed to prevent clogging, necessitating post-printing crosslinking to maintain shape fidelity. This can be achieved through dynamic or permanent crosslinking chemistry, with substantial permanent crosslinking typically occurring after printing. Mixtures of gelatin, carboxymethyl chitosan, and dialdehyde-BNC exemplify pre-modified bio-inks that demonstrate shear-thinning and dynamic crosslinking via imine bond formation (Heidarian & Kouzani, 2023). Additionally, dynamic covalent bonds can be formed using acylhydrazone, boronic ester, and disulfide bridges, as well as Diels-Alder click chemistry (Zheng et al., 2021). Among these, imine chemistry is commonly favored for its mild conditions, rapid equilibration, and good biocompatibility (Ulrich, 2019). These reactions can also be combined to develop double reversibly cross-linked hydrogels, such as a gelatin-based bio-ink that incorporates both imine and Diels-Alder bonds, producing multifunctional porous materials (Zhang et al., 2021).

Recently, a bioinspired 3D freeze-printing (3DFP) method for CNC aerogels was developed (Yang et al., 2024b), facilitating two-dimensional pore orientation. This technique combines freeze-casting with extrusion-based additive manufacturing on a chilled bed, utilizing wedges with significantly different thermal conductivities to create a thermal gradient. Following freeze-drying and thermal crosslinking of CNC with 1,2,3,4-butanetetracarboxylic acid, the resulting aerogels exhibited

significantly higher sound transmission loss compared to existing acoustic materials while maintaining superior stiffness-to-density ratios.

Integration of 3D printing with microfluidics represents another emerging area of aerogel technology (Abbasi Moud, 2022). This approach enables simultaneous control of flow characteristics and materials in microscale channels, enhancing the capabilities of both techniques (Nguyen et al., 2019). At the microfluidic scale, mass and heat transfer effects are amplified, leading to behaviors that differ considerably from macroscopic systems. Aerogels produced through microfluidics contrast with those from 3D printing; while the latter focuses on crafting precise objects with predetermined dimensions, microfluidics aims to align particles or mass-produce adsorbent aerogels with specific diameters. Both methods can facilitate bottom-up production of intricate designs, including multilayer core-shell microcapsules and responsive 4D-printed aerogels that react predictably to external stimuli. For a comprehensive overview of cellulose in bio-derived formulations for 3D/4D printing, excellent reviews are available (Abbasi Moud, 2022; Gauss et al., 2021).

19.4 Drying of Nanocellulose Hydrogels: A Critical Step

The conversion of hydrogels into aerogels is a crucial process that determines the extent to which the original gel network structure can be preserved. Many natural cellular materials evolved to thrive in humid environments can withstand dehydration without significant changes to their appearance or network morphology. However, this is not the case for physical nanocellulose hydrogels, which are sensitive to ambient pressure and thermal drying due to their low solid content (e.g., 1 wt.%) and delicate network architecture. Given that low densities and the preferential orientation of anisometric nanoparticles are essential for various applications, specific methods are necessary to maintain the integrity of their original network structures to a large extent.

During air drying, these soft precursor hydrogels experience significant shrinkage during ambient pressure and thermal drying due to inward capillary forces at the solvent menisci, as described by the Young-Laplace equation. The hydrostatic pressure (Ψp) is inversely proportional to the capillary radius (r) and directly proportional to the fluid's surface tension (σ), which for water can be as high as 72.75 mN m^{-1} at 20 °C. With an average void radius of about 50 nm, the inward tension in the pores of such hydrogels can reach approximately 2.9 MPa, leading to pore collapse and substantial gel shrinkage.

Freeze-drying, which utilizes vacuum-assisted sublimation of water from a frozen state, is an effective method to prevent the formation of solvent menisci and destructive capillary forces during the transition from nanocellulose hydrogels to aerogels. Unlike air drying, freeze-drying eliminates phase boundaries and the energy differences between liquid and vapor phases. However, the expansion of water into hexagonal ice crystals (up to 9 vol-%) during freezing can lead to

templating effects that alter gel architecture (Gun'ko et al., 2013; Smirnova & Gurikov, 2017). Unidirectional freeze-casting, initiated from one side of the gel, promotes anisotropic structuring, resulting in nanocellulosic dual-porous materials with prominent tubular macropores measuring several micrometers in diameter (Gun'ko et al., 2013; Smirnova & Gurikov, 2017). These tubular macropores, reminiscent of honeycombs, form at the expense of larger nanopores and are integrated into thick, dense sheets featuring single-digit nanoporosity (Lavoine & Bergström, 2017).

Nucleation and kinetics of ice crystal formation significantly influence the extent of network damage in soft gels and the quality of frozen aquatic products (Tan et al., 2021). Slow freezing (e.g., −20 °C to −60 °C) from a few nucleation sites typically results in large, uneven ice crystals that severely damage fragile gel structures. Although cyclic freeze-thaw processes can strengthen these networks (Huang et al., 2023), rapid freezing with low boiling point liquids like liquid nitrogen (−196 °C) minimizes damage by favoring the formation of smaller ice crystals, as demonstrated in cellulose II hydrogels (Hoepfner et al., 2008).

This effect can be enhanced using techniques such as the ice fog method, which generates numerous nucleation sites in supercooled solutions within seconds (Kasper & Friess, 2011). Cryoprotectants like antifreeze proteins, glycerol, or sucrose can also help maintain small crystal sizes; antifreeze proteins inhibit growth by binding to ice crystal surfaces and lowering the freezing point.

High-pressure shift freezing is another effective method, reducing water's freezing point from 0 to −21 °C at 210 MPa, allowing for rapid formation of small, uniform ice crystals upon pressure release (Tan et al., 2021). Alternative gentle freezing methods, such as ultrasound or electric and magnetic field-assisted freezing, have shown promise in preserving the cellular structure of food materials (Li et al., 2018), though they have not yet been widely applied to freeze-drying soft nanocellulose gels.

Additionally, replacing water with solvents that have lower thermal expansion coefficients, like tert-butanol, could help reduce shrinkage. This would necessitate a solvent exchange step, which could induce shrinkage, particularly with anhydrous solvents, as the cellulose network's architecture relies on tightly bonded surface water for effective hydrogen bonding. Nevertheless, CNF aerogels obtained via vacuum-assisted sublimation of tert-butanol from deep-frozen gels (−20 °C for 48 h) experienced minimal volumetric shrinkage (about 5%) and exhibited a specific surface area of 165 $m^2 g^{-1}$ with an average porosity of 10 nm (Wang et al., 2017).

Supercritical fluid drying (SCF-drying) remains the preferred method for converting soft physical gels into lightweight, highly porous aerogels, particularly when preserving the arrangement of network building blocks is crucial for directional properties. Like freeze-drying, SCF-drying avoids crossing the liquid/vapor phase boundary, thus eliminating capillary forces (Fig. 19.3 left). This method also avoids network compaction and destruction from sharp ice crystal formation, as no prior solidification is needed. Supercritical drying operates on the principle that the phase boundary of fluids disappears once critical conditions are reached.

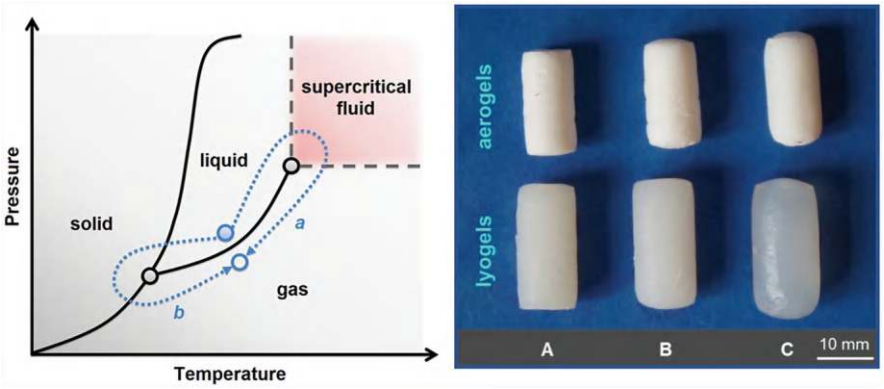

Fig. 19.3 Left: Phase diagram with dotted lines depicting the pathes of the gel's fluid phase during $scCO_2$ drying (a) and freeze-drying (b), both methods circumventing the liquid-vapor phase transition that leads to capillary forces. Right: Comparison of cellulose II alcogels derived from unmodified hardwood pre-hydrolysis kraft pulp (hw-PHK; A) and phosphorylated hw-PHK (B: $DS_{PO4} = 0.01$, C: $DS_{PO4} = 0.15$; 3 wt.% solids) before (bottom) and after $scCO_2$ drying (top)

Liquid carbon dioxide is the most commonly used fluid for SCF drying due to its abundance, low cost, chemical inertness, and excellent recyclability (Zhang et al., 2014). Its mild critical conditions (30.98 °C, 7.375 MPa) make it particularly suitable for thermally sensitive materials like cellulose. CO_2's properties as a transport medium are noteworthy; below its critical temperature, it behaves like a typical liquid, while above it, increasing pressure leads to continuous density increases without a distinct vapor-liquid transition. At typical drying conditions (40 °C, 10 MPa), CO_2 exhibits a density (628 kg/m^3) that falls between liquid and gas states.

To convert hydrogels to aerogels, an intermediate step is necessary where water is replaced with an organic solvent that is well-miscible with liquid CO_2. This step must be carefully managed to prevent significant reductions in volume and porosity due to solvent-polymer interactions, particularly the hydrogen bonding influences tied to cellulose's hydroxyl groups. The Hansen model demonstrates that replacing water with solvents like ethanol, acetone, or THF considerably reduces the cohesive energy density (δ_{SI}) and hydrogen bonding component (δ_H). For example, δ_H decreases from 42.3 MPa$^{1/2}$ (water) to 19.4 MPa$^{1/2}$ (ethanol), 8.0 MPa$^{1/2}$ (THF), and 7.0 MPa$^{1/2}$ (acetone). Solvents with δ_{SI} and δ_H values similar to those of water are preferable and have been validated for BNC hydrogels (Pircher et al., 2014).

Using ethanol as a precursor solvent before $scCO_2$ drying (40 °C, 10 MPa) resulted in lower-density aerogels (7.8 ± 0.5 mg cm^{-3}) compared to those obtained using acetone (9.4 ± 0.6 mg cm^{-3}) or THF (9.6 ± 0.8 mg cm^{-3}). Ethanol's favorable properties—such as miscibility with $scCO_2$, low viscosity, ease of recovery, environmental compatibility, and cost-effectiveness—make it an optimal choice for converting cellulose hydrogels to aerogels at far-reaching preservation of the original shape and network morphology (Fig. 19.3 right).

Supercritical CO_2 extraction of ethanol (or other miscible solvents) requires careful process control to prevent crossing the binary ethanol/CO_2 phase envelope (Fig. 19.4 left) during drying (Mukhopadhyay & Rao, 2008). This envelope, defined by the boiling and dew point curves, indicates the vapor pressure of ethanol and its critical point at high CO_2 concentrations.

During the drying process, the alcogel is placed in a high-pressure stainless-steel vessel connected to a dual-piston pump and preheating unit at the inlet, and to a backpressure valve at the outlet. The drying vessel should be pre-saturated with ethanol vapor to prevent ambient pressure drying. Initially, the pores of the gel are filled with ethanol (Point A, Fig. 19.4 left).

Subsequent pressurization with preheated CO_2 (40 °C) facilitates the diffusion of CO_2 into the pore liquid ethanol, increasing its volume and density while reducing its surface tension (Jessop et al., 2005). As the CO_2/ethanol phase expands, it begins to exit the pores, and CO_2 solubilization in ethanol increases with pressure, provided the binary system remains below its critical pressure (Fig. 19.4 right). During this phase, convective transport should be avoided until CO_2 diffusion is complete, ensuring uniform concentration within the gel and negligible density differences affecting surface tension.

Once this equilibrium is achieved and operating pressure exceeds the mixture's critical pressure, convective removal of the ethanol/CO_2 phase using supercritical CO_2 can commence (Point B, Fig. 19.4 left). This process continues until the remaining ethanol content in the pores is low enough to prevent re-condensation upon depressurization, which would create capillary forces. The time it takes to reach this state (Point C, Fig. 19.4 left) varies due to mass transfer resistances represented by an effective diffusion coefficient (D_{eff}) (Masmoudi et al., 2006). These resistances depend on various gel properties, such as network architecture, pore size

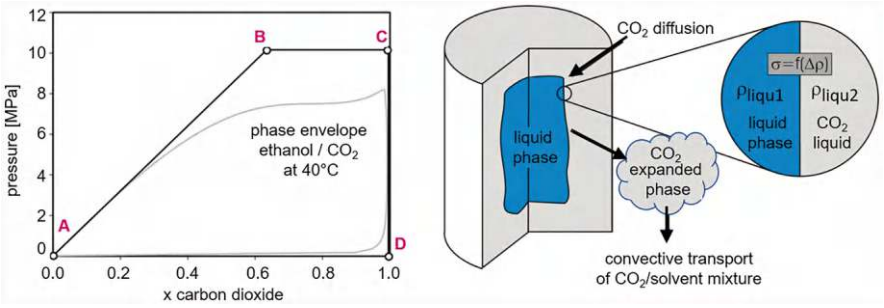

Fig. 19.4 Left: Phase envelope of the binary system ethanol/CO_2 at 40 °C (capital letters represent the main process steps of scCO_2 drying). A: Alcogel at ambient conditions. B: Convective removal of alcohol under scCO_2 conditions starts. C: Extraction of ethanol is concluded, depressurization starts. D: Return to ambient conditions after depressurization. Right: Schematic representation of the mass transfer pathways associated with pressurization of the alcogel with carbon dioxide. The interfacial tension σ between the liquid ethanol phase and the CO_2/ethanol mixture within the pores of the gel upon pressurization is marginal. (Reprinted with permission from Liebner et al. (2015). Copyright 2015 CRC Press, Taylor & Francis Group)

distribution, tortuosity, and the preservation of tightly bound surface water after solvent exchange. A comprehensive model for the supercritical drying of silica aerogels has been proposed earlier (Mukhopadhyay & Rao, 2008). Based on the author's experience, a drying time of approximately 2 h is sufficient for cylindrical mesoporous cellulose alcogels with bulk densities of up to 100 mg cm^{-3} and an aerogel volume of 1 cm^3.

Finally, depressurization to atmospheric pressure yields the dried product (Point D, Fig. 19.4 left). It is essential to ensure slow depressurization rates (typically 0.1–0.2 MPa min^{-1}) to prevent damage to the fragile open-cellular materials, particularly critical when transitioning through the supercritical pressure range, as small relative pressure changes can lead to substantial volume alterations.

Considering the complexities of $scCO_2$ drying—especially for larger monoliths or molded parts, which involve multiple solvent exchange steps, limited batch processing, and inefficient use of drying vessel space and carbon dioxide—there has been a significant push to develop simpler drying methods. Currently, ambient-pressure drying is regarded as one of the most viable technologies for the large-scale production of inorganic and organic silica aerogels due to its energy and cost-effectiveness. This evaporative drying method utilizes solvents with low surface tension, such as *n*-hexane, to replace the fluid phase in gels formed by sol-gel synthesis, allowing for substantial preservation of the inorganic or organosilicon network architecture.

Applying ambient pressure drying to soft nanocellulose gels requires additional strengthening of the networks. Given that the morphology of CNF networks in hydrogels can be controlled by freezing conditions, various techniques have been developed to enhance their structure. For example, dual ice-templating assembly (DITA) of aqueous CNF dispersions (0.05 wt.%) derived from TEMPO-oxidized cellulose results in isotropically super-elastic aerogels that quickly recover from large compressive strains (80%) even in extremely cold liquid nitrogen. This method involves a simple two-step freezing process: (1) rapid freezing at −196 °C to assemble CNF into sub-micrometer fibers (131 ± 40 nm) and (2) slow freezing (−20 °C) to form an elastic network architecture. After chemical vapor deposition of methyltrimethoxysilane for hydrophobization, the resulting aerogels exhibit superhydrophobic properties, high sorption capacities for non-polar solvents, excellent thermal insulation (23 mW m^{-1} K^{-1}), and infrared shielding (Qin et al., 2021).

Freeze-linking is another recent technique aiming to strengthen the gel networks during aerogel conversion. This method involves the pre-modification of nanoparticulate cellulose, such as treating an aqueous BNC dispersion with 3-aminopropyltriethoxysilane (APTES) before freeze-casting. In frozen state, a solvent exchange is performed using a bifunctional crosslinker solution, such as glutaraldehyde, which facilitates melting of the ice, Schiff-base crosslinking, and gradual water replacement with ethanol. This process can yield minimal shrinkage (3.3% ± 1.4%) during ambient pressure drying at 60 °C (Hu et al., 2023). However, the high amount of APTES required and the slow freezing involved may lead to significant templating of BNC, which could be seen as disadvantages of this approach.

19.5 Current Challenges

19.5.1 To Be or Not to Be … Am I Considered an Aerogel or Not?

The aerogel community has increasingly faced a critical issue: despite significant advancements in aerogel research and numerous commercial production sites, many materials marketed as aerogels do not adhere to the IUPAC definition established when aerogel research was still nascent (Jones, 2007). According to IUPAC, an aerogel is defined as a "gel comprised of a microporous solid in which the dispersed phase is a gas." Since "micropores" are defined as pores with diameters ≤2 nm, most current aerogels, although open-porous, lightweight, and having high specific surface areas, do not qualify as aerogels because their solid network architectures typically exhibit multiscale porosity, including micro (≤2 nm), meso ($2 < x \leq 50$ nm), and larger macropores ($x \geq 50$ nm).

Many aerogels exhibit multiscale porosity necessary for various applications. For example, the thermal conductivity of (bio)aerogels varies with bulk density and can achieve superinsulation—conductivity lower than air—only at specific combinations of low density and mesoporosity, which minimizes heat transfer. Furthermore, hybrid aerogels used in environmental and medical applications require sufficiently large pores for the transport of analytes, proteins, or bioactive compounds, a function that microporous aerogels cannot perform.

The existing definition's focus on microporosity is inconsistent, as it does not impose size limitations on the "non-fluid colloidal or polymer networks" that serve as the precursors to aerogels (Jones, 2007). In response, a project has recently been drafted, requesting IUPAC to revise the aerogel definition, supported by over 45 countries participating in the European Cooperation in Science and Technology project CA18125 "AERoGELS" (2019–2023) and IG18125 "ECO-AERoGELS" (2023–2024). The envisaged revision aims to provide better clarity for aerogel producers, distributors, customers, researchers, funding bodies, and decision-makers regarding the nature of aerogels, which is vital for strategic planning, investment, product promotion, and scientific advancement.

19.5.2 Nanocellulose Aerogel Monoliths Versus Nanocellulose Particle Aerogels

Until recently, many aerogel applications, especially for thermal and acoustic insulation, relied on monolithic tiles and panels. However, these monoliths, like silica aerogels, are prone to cracking and defects (Baudron et al., 2019). Biopolymer aerogels, particularly those from nanocellulose, require time-consuming multiple solvent exchanges before supercritical CO_2 drying, along with expensive high-pressure drying equipment and limitations to batch processing. This inefficiency hinders

mass production for uses such as thermal superinsulation, passive cooling, and air filtration.

While alternative drying methods and chemical crosslinking might address some commercialization challenges, they involve additional modification steps, solvent recovery, and possible recyclability issues. As a result, there has been a shift from monolithic to particulate biopolymer aerogels (Smirnova & Gurikov, 2017), which can be integrated into thermal insulating materials using roll-to-roll technologies. Particulate aerogels, particularly silica microspheres, outperform monoliths in air filtration and exhibit excellent thermal and acoustic insulation properties. They are also favored in cosmetic and pharmaceutical applications as carriers for bioactive compounds.

Inspired by the continuous fluidized bed drying of silica particles (≤40 μm) using hot air (Bhagat et al., 2008), a novel co-current drying process with supercritical CO_2 has been developed, where CO_2 functions as both the drying fluid and fluidization medium. Dried particles with lower apparent density exit the fluidized bed with the drying fluid (Ruiz & Clavier, 2016). However, continuous drying processes still face challenges, such as high CO_2 consumption in co-current systems and elevated pressures in countercurrent systems, leading to agglomeration. Recent advancements have effectively addressed these challenges, demonstrated by successful drying of alginate aerogel particles (≤500 μm) at 120 bar and 60 °C, significantly reducing CO_2 use compared to traditional batch methods (Mißfeldt et al., 2020).

To further explore and adapt continuous drying methods for biopolymer aerogel particles, the "NanoHybrids" program has been launched, aiming to develop technologies for producing aerogel particles from both biopolymers and synthetic polymers (European Commission, 2019; Paraskevopoulou et al., 2019).

19.5.3 Advancing CNF Production by Extrusion

The energy required to disintegrate cellulosic fibers and liberate nanofibrils is linked to the significant increase in surface area, necessitating sufficient mechanical energy to overcome interfacial binding forces. Common delamination methods include high-pressure homogenization, microfluidization, grinding, and ultrasonication. However, these techniques often have high energy consumption (10–40 $kW•h•kg^{-1}$) and typically yield low solid content, often not exceeding 2 wt.%, posing challenges for scalable industrial production of cellulose nanofibrils (Trigui et al., 2022).

Depending on the intended application, varying amounts of water must be removed after production. For shipping, low water content is preferred, but air-drying and freeze-drying are impractical due to high energy and time demands and potential irreversible aggregation of CNFs. While aggregation can be mitigated to certain extent by carboxymethylation (Eyholzer et al., 2010) or incorporating water-soluble polymers like maltodextrin (Velásquez-Cock et al., 2018), these methods come with cost and property implications.

Recently, twin-screw extrusion (TSE) has emerged as an energy-efficient method for producing CNFs at much higher solid contents (10–20 wt.%) compared to traditional methods (Banvillet et al., 2021). Still, pretreatments to introduce electrical surface charges for effective delamination are required, as well as the addition of plasticizers for flowability. For example, TEMPO-oxidized cellulose fibers from eucalyptus pulp underwent TSE at 15 wt.% solid content with 20 wt.% poly (vinyl alcohol). However, over 50% of the fibers remained partially fibrillated only, limiting conversion to CNFs. A brief secondary ultrasonic treatment improved yield to 70% at a mild oxidation level (350 μmol·g^{-1} COOH). Notably, TSE has successfully produced CNF particles with fire-retardant and antibacterial properties by incorporating phosphate (Rol et al., 2019a) or quaternary ammonium groups (Rol et al., 2019b).

In summary, twin-screw extrusion (TSE) offers a promising alternative to traditional mechanical methods for CNF production. However, further research is needed to ensure nanofibrils are fully individualized for applications relying on liquid-crystalline self-assembly, formation of defect-free gels and aerogels of homogeneous nanostructure.

19.6 Applications

It is probably not an overstatement to say that the significant achievements in aerogel technology—as recognized by IUPAC as one of the top 10 emerging technologies in chemistry—have now reached a level that allows these materials to conquer a virtually limitless range of applications. Among the extensive variety of precursor compounds for aerogels, their hybrids, and composite derivatives, biopolymers have gained tremendous interest in recent years. The increasing awareness of the intriguing properties of nanocellulose building blocks has significantly expanded opportunities for both mainstream and niche market applications. Some of them will be briefly introduced, drawn from a selection of recent reports and reviews, and intended to serve as a valuable starting point for a more thorough literature search.

19.6.1 High-Performance Thermal Insulation

About 40% of the world's annual energy production is consumed by buildings for maintaining comfortable indoor conditions, prompting a search for efficient heating and cooling systems. Thermal superinsulation, utilizing materials with thermal conductivity values lower than that of air (25 mW m^{-1} K^{-1}), is a promising approach, particularly for nanocellulose aerogels. These materials have the potential to protect buildings from overheating and excessive cooling, with a mesoporous architecture that minimizes heat transfer through convection. Research has successfully developed 3–4 mm thick CNF tiles, featuring thermal superinsulation through processes such as dispersion casting, scCO_2 drying, and uniaxial densification (Plappert et al.,

2017). Concomitant $scCO_2$-mediated antisolvent conformal ultrathin coating with PMMA (Plappert et al., 2018), introduction of secondary networks of a silicone resin for flexible BNC/silica composite aerogels (Birdsong et al., 2024), or post-synthesis incorporation of microporous MOF nanoparticles (Li et al., 2024) can further improve properties like hydrophobicity and fire retardance.

19.6.2 Passive Daytime Radiative Cooling (PDRC)

PDRC is an emerging strategy to combat global warming and the urban heat island effect in cities. PDRC systems use sky-facing white surfaces that reflect significant solar radiation to minimize heat gain and convert thermal radiation into long-wave infrared radiation aligning with the atmospheric window (8–18 μm), stabilizing tropospheric temperatures. Thin cellulose nanofiber (CNF) aerogel films are particularly promising for PDRC due to their reflective surfaces and good emissivity in the mid-infrared range (Sun et al., 2023). Mechanical robustness of these films, produced by freeze-casting, can be enhanced through uniaxial compaction. Additionally, incorporating finely dispersed zinc oxide improves reflectivity, while alkoxysilane chemistry provides self-cleaning and anti-dust properties (Cai et al., 2023).

19.6.3 Interfacial Solar Steam Generation (ISSG)

Solar energy utilization and water desalination are emerging areas of aerogel research, exemplified by a cost-effective bilayer eggplant composite aerogel design (Zhu et al., 2022). Janus-type ISSG materials feature a hydrophilic bottom layer with low heat conductivity and a hydrophobic top layer with photothermal conversion material like carbon black (CB). When placed on saline water, the hydrophilic layer transports water to the hydrophobic interface, where solar energy generates steam, while the remaining concentrate is replaced by incoming water. Recently, an ISSG was developed using a robust bacterial nanocellulose aerogel composite (BNC/agar with CB) and a hydrophobic top layer created from a binary siloxane formulation. Testing in the Yellow Sea demonstrated a maximum desalination performance of 8.1 kg m^{-2} under daylight conditions (Wang et al., 2024).

19.6.4 Atmospheric Water Harvesting (AWH) and Release by Solar Energy

Freshwater scarcity is a pressing environmental challenge, leading to extensive AWH research. Recent studies have introduced hierarchical scaffolds made from cellulose nanofibers (CNF) fabricated through 3D printing of CNF gels (up to

10 wt.%), followed by freeze-drying, immersion in aqueous LiCl, and final freeze drying. The obtained materials feature open micrometer-sized pores that trap hygroscopic LiCl, while the vertical millimeter-sized grid enhances sorption (mainly at night) and water delivery to the entrapped LiCl. Additionally, solar-driven evaporation of the adsorbed water has been achieved in closed transparent compartments by coating the CNF/LiCl scaffolds with a thin film of equal parts CNF and carbon nanotubes. This coating generates sufficient heat for effective water evaporation (Zhu et al., 2024).

19.6.5 Acoustic Insulation

The high-performance acoustic insulation market is rapidly evolving, driven by the swift expansion of densely populated areas. A notable example that illustrates the current advancements in nanocellulose 3D freeze-printing (3DFP) for acoustic insulation materials involves a combination of layer-by-layer extrusion printing and bidirectional freeze-casting. This process utilizes a heterogeneous printing substrate with a horizontal temperature gradient to manipulate the thermal gradient within the print volume. As a result, this technique achieves bidirectional laminated pore orientation, leading to materials that exhibit significantly higher sound transmission loss performance compared to existing acoustic materials, while also enabling targeted sound absorption at specific frequencies (Yang et al., 2024b).

19.6.6 Nanostructured Transparent Solutions for UV-Shielding

Ultraviolet (UV) radiation poses health risks, including aging, sunburn, skin cancer, and adverse effects on medications, as well as altering the taste, color, and texture of food. This has led to research on UV-shielding materials for applications in UV-resistant packaging, sunscreens, contact lenses, coatings, and clothing. These materials typically involve dispersing UV absorbers, which can be inorganic (e.g., ZnO, TiO_2, or CeO_2) or organic (e.g., lignin or nanocellulose), into a transparent polymer or glass matrix, with common UV absorbers including semiconductor particles and quantum dots (Silva et al., 2023). Transparent CNF aerogels are suitable candidates for the integration of down-converting photoluminescent nanoparticles (Plappert & Liebner, 2020) and could be embedded into transparent polymers like PMMA.

19.6.7 Matrices for Selective Sorption of Environmental Pollutants

Nanocellulose aerogels are highly attractive adsorbent materials for a wide range of compounds due to their high specific surface area, tunable surface chemistry, and open-porous hierarchical architecture. While CNF and CNC are extensively researched, bacterial nanocellulose (BNC) and CNS are less prominent. To satisfy the requirements for aerogels in aqueous environments and ensure compression resistance for repeated use, these materials are typically prepared through freeze templating, cross-linking, and freeze-drying processes. Some examples of the wide range of CNC and CNF composite aerogels for environmental protection (Yang et al., 2023) are given below:

- *Selective capture of gases and gas purification:* A comprehensive review of nanocellulose aerogels for CO_2 absorption (such as in passenger cabins on long-haul flights) is available (Baraka & Labidi, 2024). Removal of volatile organic pollutants by a biomimetic light-driven aerogel passive pump has been also the subject of a recent research paper (Drdova et al., 2022).
- *Oil/water separation:* Hydrophobic nanocellulose composite aerogels have been tailored for oil spill applications. A most recent study summarizes these advances focusing on new trends in hydrophobization and techniques facilitating oil collection and recyclability of the adsorbent materials (Chhajed et al., 2024).
- *Organic compounds*: CNF aerogels (after TEMPO oxidation) are particularly effective in removing cationic dyes from wastewater due to their anionic surface. Reversing polarity for adsorption of anionic compounds can be achieved through quaternization of CNF, for example (Rol et al., 2019b).
- *Inorganic compounds*: Heavy metal "harvesting" is probably one of the most prominent fields. CNC aerogels grafted with acrylamide (AA) and CNF/chitosan/montmorillonite composite aerogels produced via directional freeze-drying of aqueous dispersions, for example, are highly efficient sorbents for Pb^{2+}, Cd^{2+}, and Cu^{2+} ions (Rong et al., 2021). Grafting of 3-mercaptopropyl groups imparts largely pH-independent, high specific sorption capacities for Hg^{2+} ions to CNF aerogels (Geng et al., 2017).

19.6.8 Catalysis

The nanoarchitecture of CNF and CNC aerogels literally invites to be used in green catalysis. Photocatalytic oxidative conversion of nitrogen oxides (NOx) by CNF/TiO_2 hybrid aerogels (Carrasco et al., 2023) and the photocatalytic reduction of Cr^{6+} ions (99.8% efficiency) using a CNF composite aerogel containing a titanium-based MOF (MIL-125-NH_2) are two prominent examples (Yang et al., 2024a).

19.6.9 Sensing

Sensors typically consist of responsive molecules, nanoparticles, or layers immobilized within a solid matrix. Major requirements of such transducer platforms are a readily accessible, high specific surface for extensive sensor-analyte interactions. Among all nanocellulose aerogels, CNC clearly dominates the field of nanocellulose transducer platforms for bioimaging, photonic, optical, and electrical (bio) sensing, as well as gas, humidity, or mechanoresponsive sensors, as reviewed recently (Dai et al., 2020; Singh et al., 2024). Considering the vast variety of sensor types, only three of the more prominent chemo-analytical techniques should be briefly mentioned.

- *Local surface plasmon resonance:* LSPR occurs when conductive nanoparticles, such as gold or silver, oscillate collectively at specific wavelengths of light, enhancing their electromagnetic fields. This resonance leads to a strong interaction with surrounding molecules, causing changes in the nanoparticles' optical properties, which can be measured as shifts in color or intensity, making it useful for sensing applications. This color shift must be observable with transparent materials. Both CNC aerogel films (Campbell et al., 2014) and BNC nanopapers have been explored as plasmonic platforms. BNC, for instance, has served as a template and reducing agent for in situ synthesis of Ag and Au nanoparticles for sensitive tracing of drugs and toxic compounds down to 2 ppm (Morales-Narvaez et al., 2015). Volumetric transparent nematic CNF aerogels have been equipped with gold nanorods to advance three-dimensional plasmonic devices for optical sensing or metamaterials, which manipulate light around objects (Liu et al., 2020).
- *On-demand surface-enhanced Raman spectroscopy (ON-SERS):* LSPR, occurring in metallic nanostructures like Au and Ag nanoparticles, significantly enhances Raman signals, enabling single-molecule SERS (Maher, 2012). A recent 3D ON-SERS matrix was developed via nonaqueous, seedless synthesis of AuNPs in CNC dispersion, resulting in free-standing CNC aerogels with immobilized Au nanoparticles, which allow for rapid analyte uptake and increased signal intensity through pore collapsing (Panikar et al., 2022). These plasmonic aerogels have demonstrated sensitivity for detecting organophosphorus pesticides in rice and tea extracts down to one nanomole per liter. A review on the use of nanocellulose aerogels for SERS is available (Ogundare & van Zyl, 2019).
- *Sensing by photoluminescence (PL):* Transparent nanocellulose aerogels can be used to integrate various photoluminescent (PL) nanoscale materials like organic dyes, carbon nanodots, semiconductor quantum dots (QDs), or lanthanide-doped nanocrystals, which respond differently to excitation by electromagnetic radiation. For instance, low-energy photons excite QDs, leading to Stokes-type down-conversion of the emitted light, while shell modifications can enhance their PL properties and enable ligand binding for tracing metal ions. A major application of these nanoparticles is fluorescence resonance energy transfer (FRET), which allows nonradiative energy transfer between donor and acceptor fluorophores,

with systems that either activate energy transfer or quench luminescence based on target analytes. Lanthanide-doped nanoparticles, combined with cellulose, achieve detection limits as low as a few femtomoles in immunoassays and nucleotide detection. For a more comprehensive overview of the potential of PL nanoparticles, reference is made to recent reviews (Giese & Spengler, 2019; Plappert & Liebner, 2020).

19.6.10 Medical Applications

Among nanocellulose materials, BNC stands out in the biomedical field due to its high purity, hydrophilicity, water retention, biocompatibility, and mechanical properties. Key applications include wound care (temporary epidermal substitute), tissue engineering (e.g., dental tissue for treating necrotic teeth) (Jain et al., 2024), medical implants like artificial blood vessels, drug delivery systems, bioactive compound carriers, and biosensor platforms (Samyn et al., 2023). Efficient measures to control BNC's properties (e.g., bacteria strain, cultivation conditions, reactor design, additives) are essential (Lee et al., 2014; Reshmy et al., 2021). Chemical and physical surface modifications are often needed to enhance cell compatibility and antimicrobial properties. Three-dimensional laser perforation of BNC, for instance, enhances cell attachment and proliferation (Ahrem et al., 2014), femtosecond laser texturing the hydrophilicity of nanocellulose films (Samyn et al., 2024), while microstructured and micro-engineered BNC coatings reduce the formation of fibrotic tissue on implants (Robotti et al., 2020). Recently, synthetic biology (SynBio) and engineered living materials (ELM) have emerged as strategies for sustainably creating products traditionally derived from petrochemicals, involving genetic modifications of microorganisms for tailored biological properties (Malcı et al., 2024).

However, also CNC and CNF aerogels have been explored for a range of medical and cosmetic applications. Cotton CNC and pulp cellulose aerogels, for instance, have been equipped with a specific tripeptide motif linked to a fluorophore. The latter is released upon bonding to human neutrophil elastase (HNE) and creates a color response (Fontenot et al., 2017), which could be used in theragnostic applications upon further modification. In another study, controlled release has been demonstrated for a stimuli-responsive biomimetic cellulose nanofiber (CNF) hybrid aerogel, functionalized with a metal-organic framework (MOF) that forms coordinative bonds with proteins, allowing for release upon slight pH changes. These aerogels are created by freeze-casting an aqueous mixture of carboxymethylated CNF, sodium alginate, and $CaCO_3$, followed by solvent exchange, physical crosslinking, and infiltration with zinc acetate to form a zeolitic imidazolate framework-8 (ZIF-8) structure, which accommodates the proteins bonded by coordination chemistry. Release of the proteins or bioactive compounds is triggered by pH changes, leading to disassembly of the coordination bonds (Rostami et al., 2021). For a more comprehensive overview of various nanocellulose aerogels prepared for controlled release applications, reference is made to a recent review (Das et al., 2022).

19.6.11 Energy Technologies

- *Triboelectric nanogenerators (TENG):* Triboelectric nanogenerators (TENGs) convert mechanical into electrical energy through triboelectric effects and electrostatic induction, making them suitable for energy harvesting and wearable health devices. Repeated contact and separation of different materials generate an electric field that produces current to power devices, recharge batteries, or store energy. Recent findings indicate that adding of ZnO, a common enhancer for CNF-based TENGs, results in significant crosslinking with poly (ethylene imine), a secondary constituent. This is due to the formation of $[Zn(OH)_2(NH_2)_2]^{2+}$ ions in the created alkaline medium, leading to increased intermolecular cohesion and boosted electrical conductivity, achieving a peak power density of 54.4 μW/cm^2 at a load resistance of 107 Ω (Xie et al., 2024).
- *Self-powered moisture-electricity generation (SMEG):* Aerogels prepared by directional freeze-drying of mixtures of quaternized CNF, CMC, and single-walled carbon nanotubes have been recently demonstrated to generate ionic ionization and a directional flow, creating a potential difference when exposed to humid air. A single SMEG unit had a continuous voltage and current output of up to 668 mV and 6.4 μA, with a power density of 0.871 μW cm^{-2} at high humidity (90%). Connecting multiple SMEG devices can directly power various commercial electronics, including LED lights and calculators (Zhong et al., 2024).

References

Abbasi Moud, A. (2022). Advanced cellulose nanocrystals (CNC) and cellulose nanofibrils (CNF) aerogels: Bottom-up assembly perspective for production of adsorbents. *International Journal of Biological Macromolecules, 222*, 1–29. https://doi.org/10.1016/j.ijbiomac.2022.09.148

Ahrem, H., Pretzel, D., Endres, M., Conrad, D., Courseau, J., Muller, H., et al. (2014). Laser-structured bacterial nanocellulose hydrogels support ingrowth and differentiation of chondrocytes and show potential as cartilage implants. *Acta Biomaterialia, 10*(3), 1341–1353. https://doi.org/10.1016/j.actbio.2013.12.004

Baetens, R., Jelle, B. P., & Gustavsen, A. (2011). Aerogel insulation for building applications: A state-of-the-art review. *Energy and Build, 43*(4), 761–769. https://doi.org/10.1016/j.enbuild.2010.12.012

Bai, Y., Tan, R., Yan, Y., Chen, T., Feng, Y., Sun, Q., et al. (2024). Effect of addition of γ-poly glutamic acid on bacterial nanocellulose production under agitated culture conditions. *Biotechnology for Biofuels and Bioproducts, 17*(1), 68. https://doi.org/10.1186/s13068-024-02515-3

Baillis, D., Coquard, R., & Moura, L. M. (2015). Heat transfer in cellulose-based aerogels: Analytical modelling and measurements. *Energy, 84*, 732–744. https://doi.org/10.1016/j.energy.2015.03.039

Banvillet, G., Gatt, E., Belgacem, N., & Bras, J. (2021). Cellulose fibers deconstruction by twin-screw extrusion with in situ enzymatic hydrolysis via bioextrusion. *Bioresource Technology, 327*, 124819.

Baraka, F., & Labidi, J. (2024). The emergence of nanocellulose aerogels in CO(2) adsorption. *Science of The Total Environment, 912*, 169093. https://doi.org/10.1016/j.scitotenv.2023.169093

Baudron, V., Gurikov, P., & Smirnova, I. (2019). A continuous approach to the emulsion gelation method for the production of aerogel micro-particle. *Colloids and Surfaces A: Physicochemical and Engineering Aspects, 566*, 58–69. https://doi.org/10.1016/j.colsurfa.2018.12.055

Bertsch, P., Isabettini, S., & Fischer, P. (2017). Ion-induced hydrogel formation and nematic ordering of nanocrystalline cellulose suspensions. *Biomacromolecules, 18*(12), 4060–4066. https://doi.org/10.1021/acs.biomac.7b01119

Bhagat, S. D., Park, K.-T., Kim, Y.-H., Kim, J.-S., & Han, J.-H. (2008). A continuous production process for silica aerogel powders based on sodium silicate by fluidized bed drying of wet-gel slurry. *Solid State Sciences, 10*(9), 1113–1116. https://doi.org/10.1016/j.solidstatesciences.2007.11.016

Birdsong, B. K., Wu, Q., Hedenqvist, M. S., Capezza, A. J., Andersson, R. L., Svagan, A. J., et al. (2024). Flexible and fire-retardant silica/cellulose aerogel using bacterial cellulose nanofibrils as template material. *Materials Advances, 5*(12), 5041–5051. https://doi.org/10.1039/D3MA01090B

Brouzet, C., Mittal, N., Söderberg, L. D., & Lundell, F. (2018). Size-dependent orientational dynamics of Brownian nanorods. *ACS Macro Letters, 7*(8), 1022–1027. https://doi.org/10.1021/acsmacrolett.8b00487

Cai, C., Sun, Y., Chen, Y., Wei, Z., Wang, Y., Chen, F., et al. (2023). Large scalable, ultrathin and self-cleaning cellulose aerogel film for daytime radiative cooling. *Journal of Bioresources and Bioproducts, 8*(4), 421–429. https://doi.org/10.1016/j.jobab.2023.06.004

Campbell, M., Liu, Q., Sanders, A., Evans, J., & Smalyukh, I. (2014). Preparation of nanocomposite Plasmonic films made from cellulose nanocrystals or mesoporous silica decorated with unidirectionally aligned gold nanorods. *Materials (Basel), 7*(4), 3021–3033. https://doi.org/10.3390/ma7043021

Carrasco, S., Espinosa, E., González, Z., Cruz-Yusta, M., Sánchez, L., & Rodríguez, A. (2023). Simple route to prepare composite nanocellulose aerogels: A case of photocatalytic de-NO_x materials application. *ACS Sustainable Chemistry & Engineering, 11*(6), 2354–2363. https://doi.org/10.1021/acssuschemeng.2c06170

Chhajed, M., Verma, C., & Maji, P. K. (2024). Recent advances in hydrophobic nanocellulose aerogels for oil spill applications: A review. *Marine Pollution Bulletin, 199*, 116024. https://doi.org/10.1016/j.marpolbul.2024.116024

Dai, H., Zhang, H., Ma, L., Zhou, H., Yu, Y., & Guo, T. (2019). Green pH/magnetic sensitive hydrogels based on pineapple peel cellulose and polyvinyl alcohol: Synthesis, characterization and naringin prolonged release. *Carbohydr. Polym., 209* 51–61. https://doi.org/10.1016/j.carbpol.2019.01.014

Dai, L., Wang, Y., Zou, X., Chen, Z., Liu, H., & Ni, Y. (2020). Ultrasensitive physical, bio, and chemical sensors derived from 1-, 2-, and 3-D nanocellulosic materials. *Small, 16*(13), 1906567. https://doi.org/10.1002/smll.201906567

Das, S., Ghosh, B., & Sarkar, K. (2022). Nanocellulose as sustainable biomaterials for drug delivery. *Sensors International, 3*, 100135. https://doi.org/10.1016/j.sintl.2021.100135

Domínguez, G., Westphal, A. J., Phillips, M. L. F., & Jones, S. M. (2003). A fluorescent aerogel for capture and identification of interplanetary and interstellar dust. *The Astrophysical Journal, 592*, 631–635. https://doi.org/10.1086/375549

Drdova, S., Zhao, S., Giannakou, M., Sivaraman, D., Guerrero-Alburquerque, N., Bonnin, A., et al. (2022). Biomimetic light-driven aerogel passive pump for volatile organic pollutant removal. *Advanced Science, 9*(11), e2105819. https://doi.org/10.1002/advs.202105819

European Commission. (2019). *New generation of nanoporous organic and hybrid aerogels for industrial applications.* https://cordis.europa.eu/project/rcn/199829/factsheet/en. Accessed 31 Dec 2024.

Eyholzer, C., Bordeanu, N., Lopez-Suevos, F., Rentsch, D., Zimmermann, T., & Oksman, K. (2010). Preparation and characterization of water-redispersible nanofibrillated cellulose in powder form. *Cellulose, 17*, 19–30. https://doi.org/10.1007/s10570-009-9372-3

Feng, J., Su, B.-L., Xia, H., Zhao, S., Gao, C., Wang, L., et al. (2021). Printed aerogels: Chemistry, processing, and applications. *Chemical Society Reviews, 50*(6), 3842–3888. https://doi.org/10.1039/C9CS00757A

Fontenot, K. R., Edwards, J. V., Haldane, D., Pircher, N., Liebner, F., Condon, B. D., et al. (2017). Designing cellulosic and nanocellulosic sensors for interface with a protease sequestrant wound-dressing prototype: Implications of material selection for dressing and protease sensor design. *Journal of Biomaterials Applications, 32*(5), 622–637. https://doi.org/10.1177/0885328217735049

Gauss, C., Pickering, K. L., & Muthe, L. P. (2021). The use of cellulose in bio-derived formulations for 3D/4D printing: A review. *Composites Part C: Open Access, 4*, 100113. https://doi.org/10.1016/j.jcomc.2021.100113

Gavillon, R., & Budtova, T. (2008). Aerocellulose: New highly porous cellulose prepared from cellulose-NaOH aqueous solutions. *Biomacromolecules, 9*, 269–277. https://doi.org/10.1021/bm700972k

Geng, B., Wang, H., Wu, S., Ru, J., Tong, C., Chen, Y., et al. (2017). Surface-tailored nanocellulose aerogels with thiol-functional moieties for highly efficient and selective removal of Hg(II) ions from water. *ACS Sustainable Chemistry & Engineering, 5*(12), 11715–11726. https://doi.org/10.1021/acssuschemeng.7b03188

Giese, M., & Spengler, M. (2019). Cellulose nanocrystals in nanoarchitectonics—Towards photonic functional materials. *Molecular Systems Design and Engineering, 4*(1), 29–48. https://doi.org/10.1039/C8ME00065D

Grimmett, C. (1982). The use of liquid carbon dioxide for extracting natural products. *Chemistry & Industry, 15*, 359.

Guccini, V., Yu, S., Agthe, M., Gordeyeva, K., Trushkina, Y., Fall, A., Schutz, C., & Salazar-Alvarez, G. (2018). Inducing nematic ordering of cellulose nanofibers using osmotic dehydration. *Nanoscale, 10*(48), 23157–23163. https://doi.org/10.1039/c8nr08194h

Gun'ko, V. M., Savina, I. N., & Mikhalovsky, S. V. (2013). Cryogels: Morphological, structural and adsorption characterisation. *Advances in Colloid and Interface Science, 187-188*, 1–46. https://doi.org/10.1016/j.cis.2012.11.001

Heidarian, P., & Kouzani, A. Z. (2023). A self-healing nanocomposite double network bacterial nanocellulose/gelatin hydrogel for three dimensional printing. *Carbohydrate Polymers, 313*, 120879. https://doi.org/10.1016/j.carbpol.2023.120879

Hoepfner, S., Ratke, L., & Milow, B. (2008). Synthesis and characterisation of nanofibrillar cellulose aerogels. *Cellulose, 15*(1), 121–129. https://doi.org/10.1007/s10570-007-9146-8

Hu, X., Zhang, S., Yang, B., Hao, M., Chen, Z., Liu, Y., Wang, X., & Yao, J. (2023). Preparation of ambient-dried multifunctional cellulose aerogel by freeze-linking technique. *Journal of Chemical Engineering, 477*, 147044. https://doi.org/10.1016/j.cej.2023.147044

Huang, Z., Qin, R., Zhang, H., Guo, M., Zhang, D., Gao, C., et al. (2023). Ambient-drying to construct unidirectional cellulose nanofibers/carbon nanotubes aerogel with ultra-lightweight, robust, and superior microwave absorption performance. *Carbon, 212*, 118150. https://doi.org/10.1016/j.carbon.2023.118150

Innerlohinger, J., Weber, H. K., & Kraft, G. (2006). Aerocellulose: Aerogels and aerogel-like materials made from cellulose. *Macromolecular Symposia, 244*(1), 126–135. https://doi.org/10.1002/masy.200651212

Jain, P., Lin, R. Y.-T., Mishra, K., Handral, H., & Dubey, N. (2024). Three-dimensional eco-friendly bacterial nanocellulose (BNC) scaffold for regenerative dentistry: Characterization, cytocompatibility and differentiation potential. *Dental Materials, 40*(1), 151–157. https://doi.org/10.1016/j.dental.2023.11.001

Jessop, P. G., Heldebrant, D. J., Li, X., Eckert, C. A., & Liotta, C. L. (2005). Green chemistry: Reversible nonpolar-to-polar solvent. *Nature, 436*(7054), 1102. https://doi.org/10.1038/4361102a

Jones, G. (2007) Definitions of terms relating to the structure and processing of sols, gels, networks, and inorganicorganic hybrid materials (IUPAC Recommendations 2007). *Pure Appl. Chem. 79(10)* 1801–1829. https://doi.org/10.1351/pac200779101801

Kasper, J. C., & Friess, W. (2011). The freezing step in lyophilization: Physico-chemical fundamentals, freezing methods and consequences on process performance and quality attributes of biopharmaceuticals. *European Journal of Pharmaceutics and Biopharmaceutics, 78*(2), 248–263. https://doi.org/10.1016/j.ejpb.2011.03.010

Kobayashi, Y., Saito, T., & Isogai, A. (2014). Aerogels with 3D ordered nanofiber skeletons of liquid-crystalline nanocellulose derivatives as tough and transparent insulators. *Angewandte Chemie (International Ed. in English), 53*(39), 10394–10397. https://doi.org/10.1002/anie.201405123

Lavoine, N., & Bergström, L. (2017). Nanocellulose-based foams and aerogels: Processing, properties, and applications. *Journal of Materials Chemistry A, 5*(31), 16105–16117. https://doi.org/10.1039/c7ta02807e

Lee, K.-Y., Buldum, G., Mantalaris, A., & Bismarck, A. (2014). More than meets the eye in bacterial cellulose: Biosynthesis, bioprocessing, and applications in advanced fiber composites. *Macromolecular Bioscience, 14*(1), 10–32. https://doi.org/10.1002/mabi.201300298

Li, D., Zhu, Z., & Sun, D.-W. (2018). Effects of freezing on cell structure of fresh cellular food materials: A review. *Trends in Food Science & Technology, 75*, 46–55. https://doi.org/10.1016/j.tifs.2018.02.019

Li, Z., Chen, Z., Huang, Q., Zhang, S., Wang, W., & Li, W. (2024). MOF@lignocellulosic nanofibril aerogel designed by carboxymethylated nanocellulose bridging for thermal insulation and fire retardancy. *Advanced Composites and Hybrid Materials, 7*(1), 28. https://doi.org/10.1007/s42114-024-00844-3

Liebner, F., Pircher, N., Schimper, C., Haimer, E., & Rosenau, T. (2015). Aerogels: Cellulose-based. In M. Mishra (Ed.), *Encyclopedia of biomedical polymers and polymeric biomaterials*. CRC Press.

Liu, Q., Mundoor, H., Sheetah, G., & Smalyukh, I. (2020). Plasmonic gold-cellulose nanofiber aerogels. *Optics Express, 28*, 34237. https://doi.org/10.1364/OE.399181

Lundahl, M. J., Klar, V., Ajdary, R., Norberg, N., Ago, M., Cunha, A. G., & Rojas, O. J. (2018). Absorbent filaments from cellulose nanofibril hydrogels through continuous coaxial wet spinning. *ACS Applied Materials & Interfaces, 10*(32), 27287–27296. https://doi.org/10.1021/acsami.8b08153

Maher, R. C. (2012). SERS hot spots. In C. S. S. R. Kumar (Ed.), *Raman spectroscopy for nanomaterials characterization* (pp. 215–260). Springer. https://doi.org/10.1007/978-3-642-20620-7_10

Malcı, K., Li, I. S., Kisseroudis, N., & Ellis, T. (2024). Modulating microbial materials—Engineering bacterial cellulose with synthetic biology. *ACS Synthetic Biology, 13*(12), 3857–3875. https://doi.org/10.1021/acssynbio.4c00615

Marchessault, R. H., Morehead, F. F., & Walter, N. M. (1959). Liquid crystal systems from fibrillar polysaccharides. *Nature, 184*(4686), 632–633. https://doi.org/10.1038/184632a0

Masmoudi, Y., Rigacci, A., Ilbizian, P., Cauneau, F., & Achard, P. (2006). Diffusion during the supercritical drying of silica gels. *Drying Technology, 24*(9), 1121–1125. https://doi.org/10.1080/07373930600778270

Mißfeldt, F., Gurikov, P., Lölsberg, W., Weinrich, D., Lied, F., Fricke, M., & Smirnova, I. (2020). Continuous supercritical drying of aerogel particles: Proof of concept. *Industrial and Engineering Chemistry Research, 59*(24), 11284–11295. https://doi.org/10.1021/acs.iecr.0c01356

Morales-Narvaez, E., Golmohammadi, H., Naghdi, T., Yousefi, H., Kostiv, U., Horak, D., et al. (2015). Nanopaper as an optical sensing platform. *ACS Nano, 9*(7), 7296–7305. https://doi.org/10.1021/acsnano.5b03097

Mukhopadhyay, M. (2003) Partial molar volume reduction of solvent for solute crystallization using carbon dioxide as antisolvent. *J. Supercrit. Fluids 25*(3) 213–223. https://doi.org/10.1016/S0896-8446(02)00147-X

Mukhopadhyay, M., & Rao, B. S. (2008). Modeling of supercritical drying of ethanol-soaked silica aerogels with carbon dioxide. *Journal of Chemical Technology and Biotechnology, 83*(8), 1101–1109. https://doi.org/10.1002/jctb.1996

Nguyen, N.-T., Wereley, S. T., & Shaegh, S. A. M. (2019). *Fundamentals and applications of microfluidics*. Artech house.

Nordenstrom, M., Fall, A., Nystrom, G., & Wagberg, L. (2017). Formation of colloidal nanocellulose glasses and gels. *Langmuir, 33*(38), 9772–9780. https://doi.org/10.1021/acs.langmuir.7b01832

Ogundare, S. A., & van Zyl, W. E. (2019). A review of cellulose-based substrates for SERS: Fundamentals, design principles, applications. *Cellulose, 26*, 6489–6528. https://doi.org/10.1007/s10570-019-02580-0

Panikar, S. S., Sekhar Reddy, K. C., Gonzalez, A. L., Ramírez-García, G., Rodríguez, Á. G., Mondragon Sosa, M. A., Salas, P., Mota-Morales, J. D., et al. (2022). Deep eutectic solvent-enabled Plasmonic nanocellulose aerogel: On-demand three-dimensional (3D) SERS hotspot based on collapsing mechanism. *Analytical Chemistry, 94*(47), 16470–16480. https://doi.org/10.1021/acs.analchem.2c03964

Paraskevopoulou, P., Chriti, D., Raptopoulos, G., & Anyfantis, G. C. (2019). Synthetic polymer aerogels in particulate form. *Materials (Basel), 12*(9), 1543. https://doi.org/10.3390/ma12091543

Pekala, R. W., Alviso, C. T., Lu, X., Gross, J., & Fricke, J. (1995). New organic aerogels based upon a phenolic-furfural reaction. *Journal of Non-Crystalline Solids, 188*(1), 34–40. https://doi.org/10.1016/0022-3093(95)00027-5

Pircher, N., Veigel, S., Aigner, N., Nedelec, J. M., Rosenau, T., & Liebner, F. (2014). Reinforcement of bacterial cellulose aerogels with biocompatible polymers. *Carbohydrate Polymers, 111*, 505–513. https://doi.org/10.1016/j.carbpol.2014.04.029

Plappert, S., & Liebner, F. (2020). Chapter 5—Cellulose-based photoluminescent nanocomposites. In I. Filpponen, M. S. Peresin, & T. Nypelö (Eds.), *Lignocellulosics* (pp. 117–170). Elsevier. https://doi.org/10.1016/B978-0-12-804077-5.00010-5

Plappert, S. F., Nedelec, J. M., Rennhofer, H., Lichtenegger, H. C., & Liebner, F. W. (2017). Strain hardening and pore size harmonization by uniaxial densification: A facile approach toward superinsulating aerogels from nematic nanofibrillated 2,3-dicarboxyl cellulose. *Chemistry of Materials, 29*(16), 6630–6641. https://doi.org/10.1021/acs.chemmater.7b00787

Plappert, S. F., Quraishi, S., Nedelec, J.-M., Konnerth, J., Rennhofer, H., Lichtenegger, H. C., & Liebner, F. W. (2018). Conformal ultrathin coating by $scCO_2$-mediated PMMA deposition: A facile approach to add moisture resistance to lightweight ordered nanocellulose aerogels. *Chemistry of Materials, 30*(7), 2322–2330. https://doi.org/10.1021/acs.chemmater.7b05226

Qin, H., Zhang, Y., Jiang, J., Wang, L., Song, M., Bi, R., Zhu, P., & Jiang, F. (2021). Multifunctional superelastic cellulose nanofibrils aerogel by dual ice-templating assembly. *Advanced Functional Materials, 31*(46), 2106269. https://doi.org/10.1002/adfm.202106269

Reshmy, R., Philip, E., Thomas, D., Madhavan, A., Sindhu, R., Binod, P., et al. (2021). Bacterial nanocellulose: Engineering, production, and applications. *Bioengineered, 12*(2), 11463–11483. https://doi.org/10.1080/21655979.2021.2009753

Rhine, W., Wang, J., & Begag, R. (2006). *Polyimide aerogels, carbon aerogels, and metal carbide aerogels and methods of making same.* Google Patents. WO2004009673A1.

Robotti, F., Sterner, I., Bottan, S., Monné Rodríguez, J. M., Pellegrini, G., Schmidt, T., et al. (2020). Microengineered biosynthesized cellulose as anti-fibrotic in vivo protection for cardiac implantable electronic devices. *Biomaterials, 229*, 119583. https://doi.org/10.1016/j.biomaterials.2019.119583

Rol, F., Belgacem, M. N., Gandini, A., & Bras, J. (2019a). Recent advances in surface-modified cellulose nanofibrils. *Progress in Polymer Science, 88*, 241–264. https://doi.org/10.1016/j.progpolymsci.2018.09.002

Rol, F., Saini, S., Meyer, V., Petit-Conil, M., & Bras, J. (2019b). Production of cationic nanofibrils of cellulose by twin-screw extrusion. *Industrial Crops and Products, 137*, 81–88. https://doi.org/10.1016/j.indcrop.2019.04.031

Rong, N., Chen, C., Ouyang, K., Zhang, K., Wang, X., & Xu, Z. (2021). Adsorption characteristics of directional cellulose nanofiber/chitosan/montmorillonite aerogel as adsorbent for wastewa-

ter treatment. *Separation and Purification Technology, 274*, 119120. https://doi.org/10.1016/j.seppur.2021.119120

Rostami, J., Gordeyeva, J., Benselfelt, K., Lahchaichi, T., Hall, E., & Riazanova, S. A. (2021) Hierarchical build-up of bio-based nanofibrous materials with tunable metal–organic framework biofunctionality. *Mater., (48)* 47–58. https://doi.org/10.1016/j.mattod.2021.04.013

Ruiz, F., & Clavier, J.-Y. (2016). *Method for continuous aerogel production*. (Patent). US11542169B2.

Samyn, P., Meftahi, A., Geravand, S. A., Heravi, M. E. M., Najarzadeh, H., Sabery, M. S. K., & Barhoum, A. (2023). Opportunities for bacterial nanocellulose in biomedical applications: Review on biosynthesis, modification and challenges. *International Journal of Biological Macromolecules, 231*, 123316. https://doi.org/10.1016/j.ijbiomac.2023.123316

Samyn, P., Everaerts, J., Chandroth, A. M., Cosemans, P., & Malek, O. (2024). A feasibility study on femtosecond laser texturing of sprayed nanocellulose coatings. *Carbohydrate Polymers, 340*, 122307. https://doi.org/10.1016/j.carbpol.2024.122307

Silva, M. R. F., Alves, M. F. R. P., Cunha, J. P. G. Q., Costa, J. L., Silva, C. A., Fernandes, M. H. V., Vilarinho, P. M., & Ferreira, P. (2023). Nanostructured transparent solutions for UV-shielding: Recent developments and future challenges. *Materials Today Physics, 35*, 101131. https://doi.org/10.1016/j.mtphys.2023.101131

Singh, S., Bhardwaj, S., Tiwari, P., Dev, K., Ghosh, K., & Maji, P. K. (2024). Recent advances in cellulose nanocrystals-based sensors: A review. *Materials Advances, 5*(7), 2622–2654. https://doi.org/10.1039/D3MA00601H

Smirnova, I., & Gurikov, P. (2017). Aerogels in chemical engineering: Strategies toward tailor-made aerogels. *Annual Review of Chemical and Biomolecular Engineering, 8*, 307–334. https://doi.org/10.1146/annurev-chembioeng-060816-101458

Sun, H., Tang, F., Chen, Q., Xia, L., Guo, C., Liu, H., et al. (2023). A recyclable, up-scalable and eco-friendly radiative cooling material for all-day sub-ambient comfort. *Journal of Chemical Engineering, 455*, 139786. https://doi.org/10.1016/j.cej.2022.139786

Tan, M., Mei, J., & Xie, J. (2021). The formation and control of ice crystal and its impact on the quality of frozen aquatic products: A review. *Crystals, 11*(1), 68. https://doi.org/10.3390/cryst11010068

Teichner, S. J., & Nicolaon, G. A. (1972). *Method of preparing inorganic aerogels*. US 3672833-A (Patent).

Trigui, K., Magnin, A., Putaux, J.-L., & Boufi, S. (2022). Twin-screw extrusion for the production of nanocellulose-PVA gels with a high solid content. *Carbohydrate Polymers, 286*, 119308. https://doi.org/10.1016/j.carbpol.2022.119308

Ulrich, S. (2019). Growing prospects of dynamic covalent chemistry in delivery applications. *Accounts of Chemical Research, 52*(2), 510–519. https://doi.org/10.1021/acs.accounts.8b00591

Velásquez-Cock, J., Gañán, P., Posada, P., Castro, C., Dufresne, A., & Zuluaga, R. (2018). Improved redispersibility of cellulose nanofibrils in water using maltodextrin as a green, easily removable and non-toxic additive. *Food Hydrocolloids, 79*, 30–39. https://doi.org/10.1016/j.foodhyd.2017.12.024

Wang, X., Zhang, Y., Jiang, H., Song, Y., Zhou, Z., & Zhao, H. (2017). Tert-butyl alcohol used to fabricate nano-cellulose aerogels via freeze-drying technology. *Materials Research Express, 4*(6), 065006. https://doi.org/10.1088/2053-1591/aa72bc

Wang, F., Zhao, S., Jiang, Y., Zhang, X., Zhang, K., & Su, Z. (2024). Bacterial cellulose-based porous Janus aerogels for efficient interfacial solar steam generation. *Desalination, 579*, 117506. https://doi.org/10.1016/j.desal.2024.117506

Xie, B., Ma, Y., Wang, J., Liu, Y., & Yin, R. (2024). Chemical cross-linking cellulose aerogel-based triboelectric nanogenerators for energy harvesting and sensing human activities. *ACS Applied Materials & Interfaces, 16*(15), 19411–19420. https://doi.org/10.1021/acsami.4c02671

Yang, J., An, X., Liu, L., Tang, S., Cao, H., Xu, Q., & Liu, H. (2020). Cellulose, hemicellulose, lignin, and their derivatives as multi-components of bio-based feedstocks for 3D printing. *Carbohydrate Polymers, 250*, 116881. https://doi.org/10.1016/j.carbpol.2020.116881

Yang, J., Han, X., Yang, W., Hu, J., Zhang, C., Liu, K., & Jiang, S. (2023). Nanocellulose-based composite aerogels toward the environmental protection: Preparation, modification and applications. *Environmental Research, 236*, 116736. https://doi.org/10.1016/j.envres.2023.116736

Yang, F., Hao, D., Wu, M., Fu, B., & Zhang, X. (2024a). Amino-functionalized metal–organic framework-mediated cellulose aerogels for efficient Cr(VI) reduction. *Polymers, 16*(22), 3162. https://doi.org/10.3390/polym16223162

Yang, G., Lomte, A., Sharma, B., Lei, S., & Lin, D. (2024b). Sustainable multifunctionality: Bio-inspired printing of nanocellulose aerogel acoustical materials. *Advanced Materials Technologies, 9*(16), 2400232. https://doi.org/10.1002/admt.202400232

Zhang, X., Heinonen, S., & Levänen, E. (2014). Applications of supercritical carbon dioxide in materials processing and synthesis. *RSC Advances, 4*(105), 61137–61152. https://doi.org/10.1039/c4ra10662h

Zhang, Y., Wang, Q., Wang, Z., Zhang, D., Gu, J., Ye, K., et al. (2021). Strong, self-healing gelatin hydrogels cross-linked by double dynamic covalent chemistry. *ChemPlusChem, 86*(11), 1524–1529. https://doi.org/10.1002/cplu.202100474

Zheng, N., Xu, Y., Zhao, Q., & Xie, T. (2021). Dynamic covalent polymer networks: A molecular platform for designing functions beyond chemical recycling and self-healing. *Chemical Reviews, 121*(3), 1716–1745. https://doi.org/10.1021/acs.chemrev.0c00938

Zhong, H., Wang, S., Wang, Z., & Jiang, J. (2024). Asymmetric self-powered cellulose-based aerogel for moisture-electricity generation and humidity sensing. *Chemical Engineering Journal, 486*, 150203. https://doi.org/10.1016/j.cej.2024.150203

Zhu, R., Wang, D., Zhang, J., Yu, Z., Liu, M., & Fu, S. (2022). Biomass eggplant-derived photothermal aerogels with Janus wettability for cost-effective seawater desalination. *Desalination, 527*, 115585. https://doi.org/10.1016/j.desal.2022.115585

Zhu, P., Yu, Z., Sun, H., Zheng, D., Zheng, Y., Qian, Y., et al. (2024). 3D printed cellulose nanofiber aerogel scaffold with hierarchical porous structures for fast solar-driven atmospheric water harvesting. *Advanced Materials, 36*(1), 2306653. https://doi.org/10.1002/adma.202306653

Chapter 20
Cellulose-Based Nanocomposites

Angelica Corpuz, Tabkrich Khumsap, and Loc Thai Nguyen

20.1 Current Status

The universal quest for progressive improvement of all possible aspects of life at the same time the demand for sustainable development and green circular economy coupled with the advancements in nanotechnology has put forth the exploration of cellulose-based nanomaterials (CNMs) for a myriad of applications in energy, electronics, biomedical, health, environment, and many other fields (Fu et al., 2023; Joseph et al., 2020; Kumar et al., 2022; Sadi & Kumpikaitė, 2023; Wang et al., 2022). The past few decades have seen the rise of high-tech fields such as Internet of Things (IoTs), artificial intelligence, and smart robots transforming our society into one dominated by electronics (Chen et al., 2021; Kadumudi et al., 2020; Tachibana et al., 2022). This has naturally revolutionized the electronics industry, shifting from the rather unsustainable conventional electronics technologies, which are highly polluting in nature across the whole life cycle, and bulky and rigid in design, to sustainable electronics, which promotes scalability, cost-effectiveness, and harmonious integration of device technologies into our ecology (Brooke et al., 2021; Fu et al., 2023; Sadi & Kumpikaitė, 2023; Thi et al., 2022). Similarly, the quest for sustainability leads to innovative solutions such as self-powered and multifunctional devices, biodegradable materials and eco-friendly manufacturing, waste

A. Corpuz (✉)
Cagayan State University, Tuguegarao, Cagayan, Philippines

Hongkong University of Science and Technology, Kowloon, Hongkong
e-mail: arcorpuz@csu.edu.ph

T. Khumsap
Chiang Mai University, Tambon Chang Puak, Maung, Chiangmai, Thailand

L. T. Nguyen
Asian Institute of Technology, Pathum Thani, Thailand

G. Korotcenkov (ed.), *The Handbook of Paper-Based Sensors and Devices*,
https://doi.org/10.1007/978-3-031-91080-7_20

remediation technologies, among others. To this end, sustainable manufacturing approaches and challenges alike, including Fleco (flexible and eco-friendly), fully recyclable electronics, transient electronics, and the concept of trillion sensor universe, emerge in the field. More recently, research and industrial interests in wearable electronics, flexible electronics, and printed electronics, among others, have surfaced (Feng et al., 2021; Kadumudi et al., 2020; Koga et al., 2019; Lay et al., 2023; Thi et al., 2022; Williams et al., 2021).

Thus, the development of sustainable high-performance functional nanomaterials for a myriad of industries is put in the spotlight. This calls for mass production of low-cost devices and components, utilization of environmentally friendly materials, synthetic methodologies and handling, and robust design for a superb performance at the point of use. Cellulose is an emerging and desirable bio-material that holds the highest hallmark for green materials. More recently, further modification of cellulose with the nanostructures into composites leads to its application as a matrix or a support material for (bio)sensor and electronic devices construction, which is generally called "nanocellulose." Nanocellulose (NC) materials or cellulose nanomaterials are recognized for several useful properties such as mechanical strength, low density, biodegradability, large surface area, distinct optical and electrochemical properties, and low thermal expansion (Chen et al., 2018; Kumar et al., 2022). The surface modification ability and versatile nature of nanocellulose offer several opportunities for hybrid materials in the sensing and electronics field. This is supported by the commercial production of CNMs including cellulose nanocrystals (CNCs) and cellulose nanofibers (CNFs) that have been set up in the last decade (Divya et al., 2021; Kumar et al., 2022). As such CNMs, which also include the bacterial (nano)cellulose (BNC) and cellulose-based nanocomposites, have been instrumental in the remarkable advancements of the development of various types of sensors (physical sensors, chemosensors, biosensors) and other modern advanced devices in the last two decades with superb analytical performance, portability, and/or respective electrical function (Ansari et al., 2020; Kummari et al., 2023; Teodoro et al., 2021). Cellulose nanocomposites may be engineered by top-down synthetic methodologies from a nanocellulose precursor followed by any or a combination of various chemical and physical functionalization techniques and may be configured as a high surface-area membrane, nanopaper, hydrogels, aerogels, liquid crystals, and thin films. These can be applied as excellent carrier substrates or supporting matrixes for the immobilization and stabilization of other nanostructures and/or bioreceptor molecules in the sensing or electronic platform or as a transducer material. The incorporation of CNMs in functional material composites enhances the analytical and functional performance of materials as shown in the improved physical, electrical, mechanical, thermal, and/or catalytic properties of the device or product. The sustainability of nanocellulosic materials and derivatives along with its ease of functionalization and formulation is seen to replace plastic, metal, and ceramic substrates in electronics and other material fabrication and expand their applications in a sustainable manner (Gabrielli & Frasconi, 2022). The discussion in the next sections focuses on various nanocellulose-based composite architectures and their

multifunctionality, promising fabrication techniques, applications, and future outlooks in the field of NC-based composites.

20.2 Materials and Technologies Used to Form Cellulose-Based Composites

A wide variety of materials can be used to form cellulose-based composites, including polymers, metals, carbon-based materials, and metal oxides. In some cases, the formation of such composites improves the functional properties of cellulose, and in others, it improves the properties of the second component of the composite being formed. For example, adding cellulose to a polymer can significantly improve the mechanical properties of the polymer. Cellulose is most effective as a component of various composites in the form of nanocellulose, which is divided into two main classes depending on its shape and size: CNCs and CNFs. The effectiveness of NC is due to the fact that this form of cellulose has a high aspect ratio, high specific strength, and low density. In addition, it can be chemically modified to adapt its properties for use in various fields. As a result, when well dispersed, nanocellulose provides a large surface area for interaction with composite components, which contributes to the formation of a composite with high mechanical and functional properties.

Efficient interfacial interaction between the nanocellulose and other composite component/s must be achieved to realize the desired synergistic effects of the nanocomposite. Thus, careful control and fine-tuning of the interfacial properties of nanocellulose is a vital step in maximizing its full potential in the development of high-performing hybrid materials. This is achieved by optimization of the physical and chemical compatibility of the various components involved in composite formation. On one hand, varied surface-modification routes have been proposed to improve its miscibility and interfacial compatibility with hosting matrices or nanofillers and to award new functionalities (Abdel-Hakim & Mourad, 2023; Ghasemlou et al., 2021). For example, diverse oxidation techniques are applied as chemical pretreatment techniques to increase the surface charge density and hydrophilic groups of the hydroxyl-rich nanocellulose surface and form carboxylated-NCs including the increasingly preferred 2,2,6,6 tetramethyl-1-piperidinyloxy (TEMPO)-oxidation (Bandi et al., 2021; Ma et al., 2018; Tang et al., 2020), potassium permanganate oxidation (Liu et al., 2024), carboxymethylation (Belaineh et al., 2019; Brooke et al., 2021; Lay et al., 2023; Martinez-Crespiera et al., 2022), acid treatment under microwave irradiation (Pasupuleti et al., 2021), and sulfated CNCs by sulfonation (Feng et al., 2021; Williams et al., 2021). In addition, substitution of the carboxyl groups by sulfhydryl groups using cysteine has also been employed (Yu et al., 2021). Hydrophobic moieties can also be introduced by esterification (acetylation) by deep eutectic solvent treatment with ultrasonication (Gong et al., 2022) and by silylation, etc. (Thomas et al., 2018). On the other hand, chemical

functionalization is also applied to hybridizing components for increased compatibility with nanocellulose such as the grafting of amino-rich polydopamine (PDA) on GO nanofiller (Ma et al., 2018) and fractionation and epoxidization of lignin (Jia et al., 2022). Moreover, physical techniques such as ultrasonication (Liu et al., 2024) are employed to disrupt strong intramolecular forces in at least one of the components and to favor a stronger intermolecular attraction between composite components. As regards physical compatibility, good dimensional matching between two materials is also important in achieving interfacial compatibility in nanocomposite fabrication. For instance, high aspect ratio of one-dimensional carbon nanotubes (CNTs) and CNFs (Liu et al., 2024), ZnO nanowires (NWs), and CNFs (Koga et al., 2019) allows for their favorable entanglement whereas the combination of smaller sized Ag nanoparticles (AgNPs) and CNC nanorods effected to beneficial protrusion of nanoparticles on nanorods (Martinez-Crespiera et al., 2022). It is noteworthy that the synthesis conditions could limit the extent of interaction(s) achievable for a given composite system (Li et al., 2023; Yu et al., 2021).

Tunability of the nanocomposite properties is achieved by composition adjustments. A trade-off analysis is often needed to arrive at the desired physicochemical properties of the product. As much as a higher concentration of the first component would mean a more pronounced display of its associated properties in the resulting composite, care must be ensured not to exceed the dispersion limit of a nanofiller in the composite, thus conserving the molecular assembly and hence the resulting modulated functional properties such as mechanical strength (Ma et al., 2018; Liu et al., 2024), rheology (Brooke et al., 2021), and optical properties (Celi et al., 2023; Yu et al., 2021; Zhang et al., 2022), among other controlled functional parameters; meanwhile, a percolation threshold must be achieved in which conductive nanofillers effectively form a conductive network in the nanohybrid structure (Brooke et al., 2021; Koga et al., 2019; Ma et al., 2018; Pinto et al., 2020;).

To date, a large number of different fabrication techniques have been tested to form nanocellulose-based composites, including in situ chemical synthesis, electrospinning, printing, transfer patterning, liquid-phase blending, impregnation, solvent casting, and vacuum filtration. Meanwhile, a layer-by-layer assembly process may combine various techniques. These different strategies are summarized in Fig. 20.1, and detailed information can be found elsewhere (Dufresne, 2012). Let us consider the most commonly used methods.

20.2.1 Blending

Blending is a preparatory step in the synthesis of nanocomposites that combines two or more nanomaterials in a suitable solvent, including water, alcohol, and propylene glycol, to facilitate intermolecular interactions between components and bring about proper nanomaterial dispersion aided by deagglomeration techniques such as mechanical and ultrasonic agitation (Dandegaonkar et al., 2022). It is often succeeded by or coupled with other preparation techniques such as vacuum filtration in

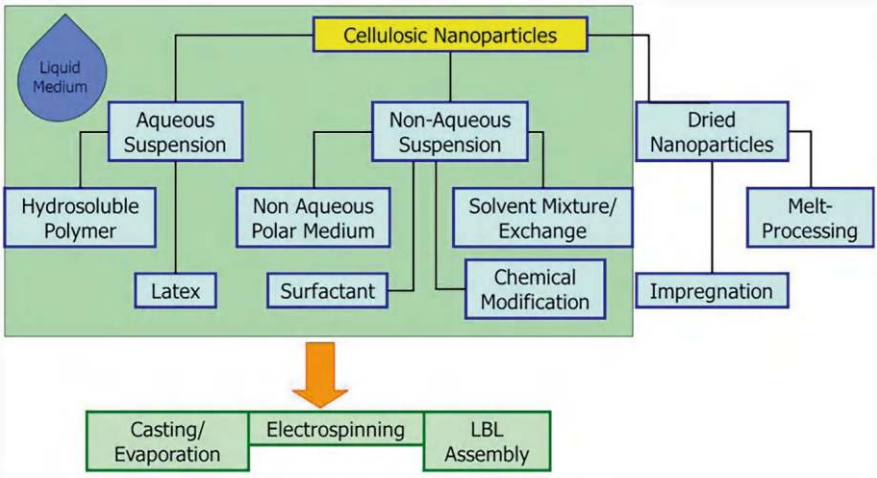

Fig. 20.1 The different strategies applied for the processing of nanocellulose reinforced polymer nanocomposites. (Reprinted from Dufresne (2013). Published 2013 by Elsevier with open access)

nanopaper fabrication (Bandi et al., 2021; Celi et al., 2023; Gong et al., 2022; Pinto et al., 2020) and other thin film deposition techniques including screen printing (Brooke et al., 2021; Martinez-Crespiera et al., 2022), aerosol jet printing (Williams et al., 2021), syringe deposition and 3D printing (Lay et al., 2023), dip coating (Pasupuleti et al., 2021), and solvent casting. The high surface area and rich hydroxyl groups (and corresponding tunability) of nanocellulose is especially helpful in blended ink formulations for printing applications, serving as a stabilizing, capping, binding, and templating agent. The dispersion composition which may include other additives are carefully controlled to achieve the proper dispersion and printability (Brooke et al., 2021; Martinez-Crespiera et al., 2022; Williams et al., 2021).

20.2.2 Impregnation

Impregnation is a straightforward technique used to incorporate functional materials into a nanocellulosic matrix, often improving the composite's mechanical, thermal, and barrier properties. The method involves immersing cellulose-based substrates, such as NC films or fibers, into a solution containing the desired additive or precursor material. This technique allows for the uniform deposition of functional agents, such as polymers, metals, or other nanoparticles, onto or within the cellulose structure. The primary advantage of impregnation lies in its simplicity and adaptability to a wide range of functional materials. It typically includes steps like soaking, drying, and sometimes additional curing to achieve effective adhesion or interaction between the impregnated material and the cellulose matrix. The efficiency of impregnation is influenced by parameters such as concentration, pH of the

solution, temperature, and impregnation time. Recent studies have demonstrated the effectiveness of this method in synthesizing nanocomposites with enhanced properties. For instance, Abdel-Hakim and Mourad (2023) utilized impregnation to incorporate silver nanoparticles into bacterial cellulose for antimicrobial applications, achieving a high degree of nanoparticle distribution and stability. Similarly, Kumar et al. (2022) reported the use of impregnation to functionalize CNFs with metal oxides, improving their photocatalytic and UV-blocking properties. These examples highlight the versatility of impregnation as a technique in the development of cellulose-based nanocomposites.

20.2.3 In Situ Synthesis of Nanofiller on Nanocellulosic Matrix

In situ synthesis techniques of nanofillers such as metallic, polymeric, or carbonaceous nanomaterials on the surface of nanocellulose rods or fibrils are increasingly utilized in nanocellulose composites. These processes commonly involve the oxidation of monomeric precursors of polymers or the reduction of metallic or carbonaceous material species from an aqueous solution or a deposited precursor nanomaterial. The objective is to coat the NC biotemplate with a high loading of evenly distributed polymeric, metallic, or carbonaceous nanoarchitectures for a high-performance nanohybrid. Several studies have explored the in situ chemical reduction of metallic species (AgNPs) using different oxidation agents such as $NaBH_4$ (Chen et al., 2019) and sodium citrate (Xian et al., 2020) and may also be coupled to visible light (Xian et al., 2020). Similarly, in situ chemical and thermal reduction of pre-deposited GO film has been used to create a conductive paper. In addition, the facile and low-cost electrodeposition technique has been employed to deposit metal nanofractal structures on the graphene (Gr)-NC paper (Burrs et al., 2016) and reduce pre-coated GO to RGO on the NC-based template (Ahmadi et al., 2021; Wang et al., 2019). As regards in situ polymerization, oxidative polymerization in basic and acidic conditions has been applied to dopamine, thiophene, and pyrrole to coat CNF-based support or template, respectively (Dias et al., 2019; Han et al., 2019; Ma et al., 2018). Figure 20.2 illustrates the process of the fabrication of CNF/polythiophene composite. This process includes grafting and in situ polymerization of CNF.

It must be noted that optimization of polymerization or reduction conditions such as monomer:oxidant ratio and pH is crucial to achieve the desired morphology of nanocomposite (Xiong et al., 2024). Finally, the use of metallic organic coordination polymers was also found effective in resolving agglomeration of deposited polymeric nanoparticles during in situ synthesis (Chang et al., 2024).

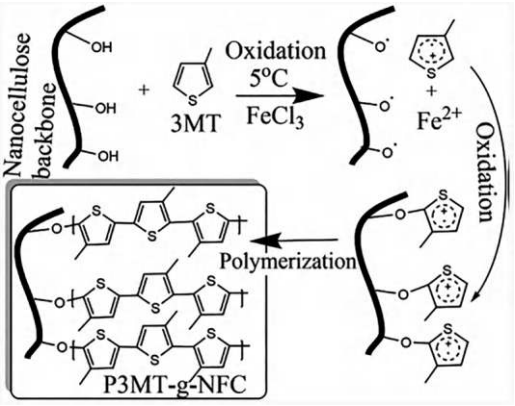

Fig. 20.2 Grafting and polymerization mechanism between polythiophene, conductive polymer, and CNF. A longer polymerization time achieved a higher yield of CNF composites. Upon grafting with polythiophene, the insulator characteristics of CNF were converted to conductive. (Reprinted with permission from Dias et al. (2019). Copyright 2019: Elsevier)

20.2.4 Vacuum-Assisted Filtration or Assembly Process

Vacuum-assisted filtration is the preferred preparation tool for composite nanopapers, thin films, or membranes based on nanocellulose attributed to its facile operation. Generally, an aqueous suspension of the nanomaterials containing the nanofibrils (CNF or BNC) and functional nanomaterials is prepared and subjected to vacuum filtration unto a filter membrane, commonly a microporous one, peeled off from the substrate, and then dried via oven or at ambient conditions to become a self-standing functional film, membrane, or nanopaper (Bandi et al., 2021; Celi et al., 2023; Pinto et al., 2020; Wang et al., 2018; Zhu et al., 2022a). In some instances, a layer-by-layer assembly may be prepared by first depositing a BNC or CNF-based membrane or another polymeric membrane to be covered by the nanomaterial suspension or the CNF-based solution via vacuum filtration (Wang et al., 2022; Zhang et al., 2022). On a less frequent basis, supported membranes are fabricated using this simple process. For example, a paper-based surface-enhanced Raman scattering (SERS) substrate was prepared using a filter paper support for the CNC-AgNP nanocomposite (Xian et al., 2020).

20.2.5 Low-Cost Thin Film Printing Techniques

Printed electronics is an emerging field that often comes with flexible electronics. This promising field integrates the development of functional inks and the conventional and more novel deposition techniques onto (nano)paper or NC membrane substrates to create more sustainable and cheaper electronic products

(Martinez-Crespiera et al., 2022; Pan et al., 2022; Williams et al., 2021). Ink jet printing and screen printing are conventional techniques relied upon for fast, low-cost, and eco-friendly fabrication of electronic devices, whereas printable ink must have shear thinning behavior and sufficient viscosity within 1000–10,000 cP. In addition, additional post-printing processes are normally required, including sintering at high temperatures, which is not environmentally friendly and energy efficient (Latonen et al., 2017; Li et al., 2023). Hence, novel printing and deposition techniques circumventing high temperature processing and/or accommodating viscous inks and high-surface tension fluids onto thin paper/membrane substrates are proposed. Aerosol jet-printing is a direct-writing technique that creates an ink suspension of 1–5 μm droplets by ultrasonication (Williams et al., 2021). Another method is stencil printing that gives easy patterning and good uniformity by virtue of a digitally designed pattern in the stencil mask. Both could cater to more viscous fluids that ink jet printing cannot process. However, the latter requires annealing at high temperature (Tachibana et al., 2022). Flexographic printing and light-induced printing, on the other hand, may be operated at room temperature. Whereas the former operates with a high-speed rotary functionality to transfer ink to the substrate while using a printing plate containing a relief pattern fit for a large-scale production (Latonen et al., 2017), the latter uses a "digital" mask, defining the pattern that is projected by visible light from a commercial projector to the substrate containing the metal nanoparticle precursor solution which is successively reduced in the process (Pan et al., 2022). Finally, an evaporation-induced transfer printing technique allows for the transfer printing of fluids with high surface tension such as liquid metal onto thin film substrate by first printing onto a sacrificial thicker substrate and then spreading of the thin film substrate precursor solution (c-CNF aqueous dispersion) and followed by successive solvent evaporation resulting to deposition, aggregation, and tight coverage of CNFs substrate onto liquid metal (LM) matrix. Finally, the process is completed by peeling off the sacrificial substrate (Mao et al., 2021).

20.2.6 Solvent Casting

Solvent casting, also known as solution casting, is another simple technique commonly employed for preparing cellulose nanocomposite films, membranes, or nanopaper (Abdel-Hakim & Mourad, 2023; Manimaran et al., 2024). This involves preparing a dispersion of aqueous nanocellulose suspension combined with the hydrophilic polymer or other nanomaterials including polyaniline (PANI) (Fan et al., 2023), (Poly(3,4-ethylenedioxythiophene):Polystyrene sulfonate) (PEDOT:PSS) (Belaineh et al., 2019), polyvinyl alcohol (PVA) (Han et al., 2019), polymer-coated nanofillers such as PDA-coated GO (Ma et al., 2018), and nanosilicates (Kadumudi et al., 2020) aided by mechanical or ultrasonic agitation followed

by casting on a mold or substrate for subsequent solvent evaporation. The evaporation process may be done in ventilated areas at ambient or heated conditions using an oven. For water-insoluble polymers, it is crucial to prevent NC aggregation due to the incompatibility between the hydrophilic cellulose filler and the hydrophobic polymeric matrix (Abdel-Hakim & Mourad, 2023). Similarly, the aggregation of nanofillers in the NC matrix must also be controlled and one way is modulation of its concentration in the matrix. Whereas the generated nanocellulose network facilitated by proper dispersion reinforces the polymer nanocomposite, the incorporation of nanosilicate in NC polymer matrix also enhances the mechanical strength of the cellulose nanocomposite. The solid nanocomposite is finally peeled off from the mold, which is normally a glass petri dish or Teflon mold. It has been shown that the substrate may influence on the surface morphology of the generated nanocomposite (Belaineh et al., 2019). The thickness must also be sufficiently thick (control of solids concentration) to ensure intact removal from the substrate (Fan et al., 2023).

20.2.7 Electrospinning

Electrospinning is a versatile and scalable technique for fabricating nanofiber-based cellulose composites with tailored properties. This process uses an electric field to draw charged polymer solutions or melts into fine fibers, which are subsequently deposited on a collector to form a nanofibrous mat. For cellulose-based composites, electrospinning can be employed to produce membranes, scaffolds, or films with high surface area, porosity, and mechanical strength. The key to successful electrospinning lies in optimizing parameters such as solution viscosity, electrical conductivity, and applied voltage. Cellulose is often dissolved in suitable solvents or modified into derivatives like cellulose acetate (CA) to facilitate electrospinning. These nanofibers can then be further treated, such as through deacetylation, to restore cellulose properties. Electrospinning has been extensively studied for its potential in creating nanocomposites for applications ranging from filtration to biomedical devices. For example, Ahmadi et al. (2021) electrospun CA nanofibers loaded with graphene oxide (GO) to develop a highly sensitive glucose sensor. In another study, Kadumudi et al. (2020) used electrospinning to create cellulose nanofiber-based membranes functionalized with nanosilicates, resulting in improved mechanical and barrier properties. These findings underscore the role of electrospinning in advancing the functionality and application spectrum of cellulose-based nanocomposites.

20.3 Cellulose-Based Nanocomposites and Their Applications

As we have indicated earlier, cellulose-based nanocomposites are mainly formed on the basis of CNCs and CNFs. Let us consider composites based on them in more detail.

20.3.1 Cellulose-Polymer Nanocomposites and Their Applications

Nanocellulose materials and their derivatives have recently gained a lot of interest as potential fillers for reinforcing and reducing the environmental impact of both natural and synthetic polymeric materials for various applications (Abdel-Hakim & Mourad, 2023; Nhi et al., 2024; Uusi-Tarkka et al., 2021). The superior properties of CNCs and CNFs including high surface area, mechanical strength, lower occurrence of defects, abundance, low density, and biodegradability make them a suitable alternative to the conventional reinforcements such as synthetic fibers and other micrometer-sized additives in polymeric nanocomposites (Thomas et al., 2018). In order to attain effective reinforcement from nanoparticles or nanofibers (fillers) in a polymer matrix, compatible interfacial properties associated to specific favorable interactions between the nanofiller and the matrix and good nanomaterial dispersibility must be achieved (Wohlert et al., 2024). As discussed earlier, tailoring the surface chemistry of either of the nanocomposite components or phases is crucial to achieve the superior mechanical strength and other desired performance of the nanocomposite.

20.3.1.1 Sensors and Other Electronic Devices

Nanocellulose is being used as base substrates, acting as reinforcing or supporting scaffolds, in cellulose-polymer nanocomposite-based functional structures in the fabrication of a wide array of electronic devices including physical and chemical sensors, energy devices, memory devices, and displays. Several examples of polymer/nanocellulose-based composites intended for use in sensors and electronic devices are given in Table 20.1.

NC reinforcement can also significantly improve the overall physical and mechanical properties of polymer nanocomposites taking part in the electrode, substrate, and/or sensing component of the device. In addition, NC is often combined with functional polymeric materials such as conductive (Belaineh et al., 2019; Brett et al., 2021; Chang et al., 2024; Han et al., 2019; Lay et al., 2023; Wang et al., 2020), piezoelectric (Wang et al., 2022), piezoresistive (Han et al., 2019), triboelectric (Zhu et al., 2022b), elastic (Ye et al., 2020), and bio materials (Jia

Table 20.1 Examples of polymer/nanocellulose-based composites and their applications

Composite	Polymer matrix	Preparation technique	Application	Ref.
PANI/CNF/PVA-H_2SO_4	PANI	In situ chemical polymerization, drop-casting	Integrated paper-based supercapacitor, stress sensor	Xiong et al. (2024)
PANI/(PA + ARS)/Zr-CNFs	PANI	Chemical precipitation, doping and coordination processes, in situ polymerization	Paper-based electrode material	Chang et al. (2024)
CNF/PEDOT:PSS	PEDOT:PSS	Core-shell structure by blending; syringe deposition, 3D printing	Conductive paper-based electrode, supercapacitor paper	Lay et al. (2023)
CNF/PEDOT:PSS	PEDOT:PSS	Large-scale spray deposition	Biobased organic electronics	Brett et al. (2021)
CNF/PEDOT:PSS	PEDOT:PSS	Film casting	Supercapacitor electrodes	Belaineh et al. (2019)
PEI-CNFs/CP	PEI	Microwave-assisted acid treatment, electrostatic interactions, dip-coating	Paper-based solid phase extraction technique coupled to UHPLC-PDA method for environmental monitoring	Pasupuleti et al. (2021)
pBT@CNF/PVDF-g-MA	PVDF-g-MA	Vacuum-assisted layer assembly	Piezoelectric nanogenerator, self-powered pressure sensor	Wang et al. (2022)
PDA/CNF film	PDA	Chemical grafting, vacuum filtration	Triboelectric nanogenerator for a motion sensor	Zhu et al. (2022b)
CNF/PPy/PVA	PVA	In situ co-polymerization, solvent casting	Piezoresistive strain sensor (human motions)	Han et al. (2019)
CNF/lignin	Lignin	Crosslinking	Green composite substrates for flexible electronics	Jia et al. (2022)
CNF/PLA	PLA	Solvent casting	Electrochemical sensor for nitrates	Yan et al. (2014)

Abbreviations: *PANI* polyaniline, *CNF* cellulose nanofiber, *PVA* polyvinyl alcohol, *PA* phytic acid, ARS alizarin red S, *Zr* zirconium, *PEDOT* poly(3,4-ethylenedioxythiophene), *PSS* polystyrene sulfonate, *PEI* polyethylenimine, *CP* cellulose paper, *pBT* polydopamine@BaTiO3, *PVDF-g-MA* maleic-anhydride-grafted polyvinylidene fluoride, *PDA* polydopamine, *PPy* polypyrrole, *PLA* polylactic acid

et al., 2022; Nhi et al., 2024; Uusi-Tarkka et al., 2021) to endow functional properties. For instance, a multifunctional nanocomposite material was fabricated that can be assembled into a symmetrical supercapacitor (energy density of 11.49 W.h/kg at a high power density of 413.55 W/kg) with an excellent electromagnetic (EM) shielding performance (34.75 dB in X-band) thanks to the conductive PANI

coated onto the CNF aerogel, and stress sensing capability (pressure and human motion signals) attributed to the increased strength and deformation from the coating of flexible PVA-H_2SO_4 (Xiong et al., 2024). In this electronic platform, the CNF aerogel serves as a nanoporous, flexible substrate which also helps in ionic mobility of the electrolytes in the electrode. Dandegaonkar et al. (2022) have previously reported various forms of polymeric-nanocellulose composite structures including functional hydrogels and aerogels, films and membranes, fibers, and hybrids for the development of multifunctional sensors. As for the hydrogels, extensive crosslinking of hydrogen bonds, covalent bonds, or ionic interactions in an array of polymers, different metals, and organic species into 3-D networks awards the composite with its remarkable mechanical strength that can be modulated by the crosslinking density (Thomas et al., 2018). In addition, self-healing hydrogels and nanocomposite films that can easily recover their thermal, mechanical, and electrical properties are of particular importance in wearable devices for utility in continuous monitoring in dynamic application conditions. Thus, dynamic coordination interactions such as reversible hydrogen- and metal-coordination bonds have been introduced in their structures (Han et al., 2019; Shao et al., 2018). Conductive cellulose nanopaper-based composites are also on the rise due to their self-standing and flexible nature ideal to Fleco electronics (Belaineh et al., 2019; Chang et al., 2024). More recently, all-cellulose nanocomposites, a fully cellulosic single-polymer composite, are deemed alternatives to overcome weak interfacial compatibility and recyclability challenges in conventional composites and biocomposites supporting sustainable and fully recyclable electronics (Uusi-Tarkka et al., 2021).

20.3.1.2 Food Packaging

The increasing clamor for green packaging materials also puts forward NC reinforcement and barrier coatings in food packaging materials, normally in the form of natural fiber-reinforced biopolymer composites and nanocellulose-coated films. The optical transparency of the nanocellulosic composite films also positively provides customers with a clear visibility of the content (Nguyen et al., 2021). The inherent weakness in any one or combination of poor mechanical properties (flexibility, toughness, etc.), poor oxygen impermeability, moisture sensitivity, and poor thermal properties of commonly used biopolymers such as thermoplastic starch (TPS) (Souza et al., 2021), PVA (Sarwar et al., 2018), polylactic acid (PLA) (Jacob et al., 2024), and polybutylene succinate (PBS) (Nazrin et al., 2020) can be enhanced by the reinforcement of NC dense crystalline structure, entangled nanoporous network, and nanoscale dimensions while moisture sensitivity may be addressed by hydrophobic modification, layered design, or increased crosslinking (Thomas et al., 2018). To be effective, interfacial adhesion between the matrix and the reinforcing materials is important for enhanced thermal, mechanical, and barrier performance, especially under high humidity conditions (Abdel-Hakim & Mourad, 2023; Nazrin et al., 2020; Thomas et al., 2018). To illustrate, a novel biofilm based on protein

isolates extracted from sunflower meal (SFMPI) matrix reinforced with BNC biofillers was developed as innovative food packaging material. The hydrophilic nature of both BNC and SFMPI facilitates the miscibility between these two components reminiscent to H-bonding interactions of filler-filler and filler-matrix, while nanosized network of BNC enables efficient stress transfer from the polymeric chains to the nanoparticles of BNC. These have improved overall mechanical behavior, water barrier properties, and decreased water solubility of the nanocomposite films that demonstrated effective fresh fruit preservation at 10 °C over a 15-day period (Efthymiou et al., 2022). In another study, the thermal stability of TPS films was greatly enhanced due to the strong molecular interactions among starch chains and NC-stabilized Pickering emulsions in the developed active packaging (Souza et al., 2021). Meanwhile, researchers have also documented the efficacy of CNC composite coatings in decreasing oxygen permeability of coated plastic film (Ji et al., 2023) and reducing water absorptivity, enhancing tensile strength of coated paper, and coating recyclability (Jin et al., 2021), offering a sustainable solution for the production of food packages. Easy functionalization of active materials for smart functionality, its low cost, and light weight also add up to its wide utility (Sarwar et al., 2018; Zhang et al., 2023a).

20.3.1.3 Solid, Water, and Air Remediation

Nanocellulose has been used as a part of a composite to improve the solid, water, and gas purification efficiency via adsorption or membrane filtration technique. Altogether, crystallinity, hydrophilic-tunable surface chemistry, low density, and highly porous 3D structure of NC, in addition to nontoxicity, abundance, biodegradability, flexibility, and mechanical strength, lead to the development of functional composite hydrogels, aerogels, and membranes for efficient separation of contaminants from solid, liquid, and gas systems (Abdel-Hakim & Mourad, 2023; Ibrahim et al., 2019; Paul & Ahankari, 2023; Shaghaleh et al., 2024). Nanocellulose composite-based hydrogel adsorbents (ANCHs) containing interpenetrating polymer networks (IPNs) with poly(2-(dimethylamino) ethyl methacrylate) (PDMAEMA), PVA, polyacrylamide (PAM), chitosan (CS), collagen, alginate, among others, can function as stabilizer amendments and adsorbent hydrogels for in situ and ex situ soil remediation and wastewater remediation techniques from heavy metal ions. On one hand, the 3D-porous scaffold of NC participates in the high adsorption capacity of the ANCHs and hydrophilic nature allows the transfer of pollutants from aqueous wastes, whereas mechanical strength and chemical stability contribute to regeneration ability of the hydrogel (Shaghaleh et al., 2024). On the other hand, the additional functional groups and structural alterations from IPNs extend the adsorption range of these ANCHs. NC-based aerogels are also gaining importance in the field of water and air purification due to their excellent adsorptive capacity and water flux rates compared to conventional thin membranes (Paul & Ahankari, 2023). This also addresses poor separation capacity and recyclability of the powdered form due to a lack of 3D structure and the poor surface area (Zubair

et al., 2024). NC-based aerogels find application in the removal of dyes, metal ions, emerging pollutants, and oils/organic solvents. In addition to adding polymers such as chitin and polyethylenimine, the use of nontoxic crosslinking agents can also add to the available functional groups of the nanocomposite for increased adsorption (Nan et al., 2023; Zhang et al., 2019). As regards membrane-based separation technologies, nanocelluloses are suitable additives in enhancing the performance of conventional polymeric membranes for carbon dioxide (CO_2) and nitrogen (N_2) capture, attributed to their high surface charges and high surface area (Ibrahim et al., 2019).

20.3.1.4 Biomedical Applications

There is a growing interest in BNC in the biomedical field due to its nontoxicity, excellent high aspect ratio, biocompatibility, biodegradability, large water holding capacity, and mechanical properties. It is combined with other biopolymers to attain important functionalities needed for applications in wound dressings, scaffolding in tissue engineering, and drug delivery carriers (Liu et al., 2021; Norizan et al., 2022; Wang et al., 2024). For instance, the antimicrobial properties of CS complement the flexibility and mechanical strength of BNC in BNC/CS composites in the development of advanced biomedical materials with effective antimicrobial and biological activities (Liu et al., 2024). PVA may be added to improve the optical transparency and regulate the mechanical and biological properties of the BNC films (Mbituyimana et al., 2021). The poor durability and flexibility of gelatin but with rich amino and carboxyl groups on the side chains is strategically combined with the robust toughness and water retention of NC for an improved performance of the functional biomaterial (Li et al., 2024). Scaffolds with excellent mechanical properties and structural stability were made based on BNC hydrogel with poly(2-hydroxyethyl methacrylate) (PHEMA) (Saleh et al., 2024) and CNF composite with collagen in tissue engineering (Wang et al., 2024). Patch conductivity may also be achieved with polypyrrole NPs and BNC composite in cardiac patches to simulate the natural microenvironment (Wang et al., 2024).

20.3.1.5 Automotive and Aerospace

The automotive and aerospace industries are met with ever-increasing fuel prices, depletion of petroleum resources, and environmentally friendly demands causing the shift to nanobiocomposites such as CNF- and CNC-reinforced polymer composites as alternative materials (Chowdhury et al., 2022; Mansor et al., 2019; Oladele et al., 2024; Sebagala et al., 2024). The myriad of mechanical and physical properties of these cellulose-nanocomposites are significantly influenced by molecular-level interactions between NC and polymer matrix as well as the presence of a very extensive NC–polymer interfacial region (Norizan et al., 2022) which far exceeds the performance of typical micro-sized fillers in polymeric composites (Chowdhury

et al., 2022) and is at par with metallic materials that have previously dominated the automobile and aerospace equipment manufacture (Muhammad et al., 2020). Lightweight features, mechanical strength, and thermal stability are among the coveted characteristics for possible translation in the manufacture of both automobiles and aircraft parts. For instance, the combination of enzymatically treated CNFs and lignin reinforced the rigid bio-polyurethane (PU) foams for enhanced impact and compression properties suitable for use as automotive parts. In another study, a nanofibrillated cellulose reinforced low-density polyethylene (LDPE) nanocomposite showed excellent thermal stability, degree of crystallinity, elastic modulus, tensile strength, and transparency applicable for automotive application (Ali & Hoque, 2022). The impregnation of nanocellulose in hybrid barkcloth-banana fiber-reinforced polyester resin biocomposites increased the surface reaction sites for resin adherence resulting to thermal stability in temperatures below 220 °C for possible application in the automotive interior panels (Sebagala et al., 2024). CNF-reinforced PVA composites have also been previously proposed for aerospace and automotive sector applications due to the lightweight and high-strength features (Mansor et al., 2019).

20.3.2 Nanocomposites Based on Cellulose and Inorganic Materials and Their Applications

20.3.2.1 Cellulose-Carbon Nanocomposites and Their Applications

Carbonaceous nanomaterials and derivatives such as CNTs, Gr, MXene, GO, reduced graphene oxide (RGO), carbon fiber, carbon dots (CDs), and carbon black are known for their mechanical strength, chemical stability, large surface area, and extraordinary electrical conductivity. In addition, they possess p-type semiconductor feature. Their good processability, low cost, and scalability make them an interesting nanofiller alternative in many nanocomposite fabrications (Ahmadi et al., 2021; Bacakova et al., 2020; Durairaj, 2022; Li et al., 2021; Liu et al., 2024; Zheng et al., 2024; Zhu et al., 2022a). The incorporation of carbon-based materials into NC-based composites overcomes many of the disadvantages of cellulose and even adds new functionalities to it (Durairaj, 2022), thus forming promising smart hybrid materials in the form of 2D free-standing or supported films, papers or membranes, or in the form of 3D aerogels, foams, or sponges (Bacakova et al., 2020). For example, as it is shown in Fig. 20.3, incorporation of graphene makes the cellulose-based composite highly conductive. Several examples of carbon/cellulose composites are listed in Table 20.2.

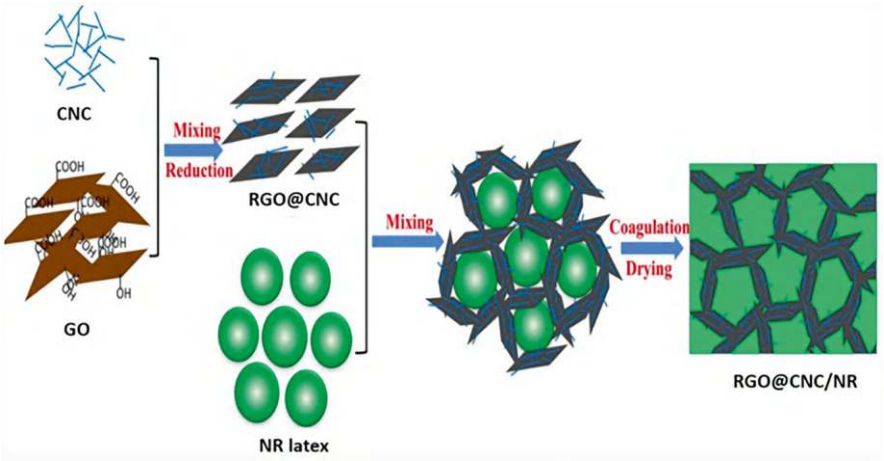

Fig. 20.3 Schematic illustration of the formation of a 3D conductive network during the preparation of RGO/CNC/NR composite. (Reprinted with permission from Cao et al. (2016). Copyright 2016: Elsevier)

20.3.2.1.1 Sensors and Other Electronic Devices

Conductive water-based ink dispersions are increasingly used in creating standalone or supported films and nanopapers in multifunctional flexible electronic devices. In most cases, the CNMs serve as the conductive nanofiller while CNF or CNC serve as the reinforcing agent, scaffold component, or carrier matrix with film forming ability. In the process, NC disperses the CNMs to prevent aggregation and achieve a uniform dispersion with good interfacial interactions. The high-density negative charges of the NC contribute to the repulsion of CNMs while intra- and inter-hydrogen bonding interactions further stabilize the structure. Furthermore, this hydrophilic nature enables hygroscopic swelling of NC-composite which is humidity sensitive. Nanocellulose composites with single-walled CNTs (SWCNTs) (Feng et al., 2021), multi-walled CNTs (MWCNTs) (Durairaj, 2022; Liu et al., 2024), RGO (Gong et al., 2022), Gr (Trache et al., 2024; Yan et al., 2014), carbon black (Brooke et al., 2021; Tachibana et al., 2022), and carbon NFs (Wang et al., 2018) have been printed, casted, or filtered onto temporary or permanent substrates to fabricate nanopaper or thin film layers for various applications such as electrodes in sensors and wearable electronics (piezoresistive, electrothermal), electrochromic displays, EM shielding, and energy harvesting and storage devices (supercapacitors, current collectors in batteries, thermal energy collection device). In some cases, the CNMs including RGO (Ahmadi et al., 2021), C flakes and C nanoballs (Silva et al., 2020), GO-MWCNTs (Wang et al., 2019), and Fe-doped CDs (Bandi et al., 2021) may be deposited directly onto the cellulose-based nanopaper or electrode. Zheng et al. (2024) also reported multifunctional aerogels from dispersed linear carbon materials, carbon NF and CNT, in CCNF matrix with thermal insulation, thermoelectric, Joule heating, and photothermal capabilities.

Table 20.2 Examples of carbon/nanocellulose-based composites and their applications

Composite	Substrate	Preparation techniques	Application	Ref.
CNF/CB	PEN film	Blending, stencil printing	Flexible humidity sensor	Tachibana et al. (2022)
CNF/FeCDs	CNF paper	Vacuum filtration	Smartphone-based colorimetric sensor for H_2O_2 and glucose	Bandi et al. (2021)
CNF/RGO	CNF paper	Esterification, intercalation, filtration	Flexible humidity sensor	Gong et al. (2022)
Bi/ Gr-MWCNTs/ PBE	NC paper	Layer-by-layer assembly, drop casting, electrochemical reduction, and plating	Electrochemical sensor for Cd(II) and Pb(II)	Wang et al. (2019)
BNC/C/SPCE	BC sheet	Screen printing	Electrochemical sensor for Cd(II) and Pb(II), biomarkers	Silva et al. (2020)
Gr/CNF/PDMS	PDMS	Vacuum filtration	Flexible nanopaper for piezoresistive strain sensor	Yan et al. (2014)
CBNC/CNF aerogels	Paper	Directional ice templating, freeze-drying	Pressure sensor	Chen et al. (2021)
SWCNT/SNC	Paper, glass, PET film	Screen printing	Conductive ink for humidity sensing	Feng et al. (2021)
MWCNTs/c--CNFs	Paper	Screen printing (stencil printing)	Thermoelectric generator	Li et al. (2021)
PDMS/ cellulose/ MWCNT	Hybrid film	Mixing, drying	Piezoelectric nanogenerator	Alam and Mandal (2016)
C/CNFs	Paper, PET film, Al foil	Screen printing	Supercapacitor	Brooke et al. (2021)
CNF/ CarbonNF/Li	CNFs	Vacuum filtration	Energy storage (Li-ion battery)	Wang et al. (2018)
CNF/TMC/Au/ RGO	CNF paper	Wax patterning, sputtering, electrochemical reduction, and deposition	Impedimetric paper-based enzymatic biosensor	Ahmadi et al. (2021)
CNF/CNT	Filter paper, printing paper	Filtration, ink printing	Flexible electronics, piezoresistive strain sensors	Liu et al. (2024)

Abbreviations: *CNF* cellulose nanofiber, *CB* carbon black, *FeCDs* iron-doped carbon dots, *RGO* reduced graphene oxide, *Bi* bismuth, *Gr* graphene, *MWCNTs* multiwall carbon nanotubes, *PBE* paper-based electrode, *BNC* bacterial nanocellulose, *C* carbon, *SPCE* screen-printed carbon electrode, *PDMS* Polydimethylsiloxane, *CBNC* carbonized bacterial nanocellulose, *SWCNT* single-walled carbon nanotube, *SNC* sulfated nanocellulose, *c-CNFs* carboxylated carbon nanotubes, *Li* lithium, *TMC* trimethyl chitosan

20.3.2.1.2 Biomedical Applications

The great biological properties including low toxicity, biocompatibility, and biodegradability along with surface functionality of NC has made it one of the most researched biomedical materials (Mokhena et al., 2024). As such, cellulose-based nanostructures such as fibers, films, and aerogels have been widely explored in drug delivery systems with cellulose as a base and are then modified to increase drug-loading capacity, acquire antimicrobial properties, improve biocompatibility and mechanical property, and achieve sustained drug release, among others (Wang et al., 2024). CNTs are excellent nanofillers due to their chemical stability, inner-cavity encapsulation, target specificity, drug load capacity, cell membrane permeability, and the ability to reversibly interact with therapeutic molecules. Nanofillers can be used as drug carriers. For instance, carboxylic acid-functionalized SWCNTs were covalently linked with fluorescein, folic acid targeting agent, and anti-cancer drug. This SWCNT/CNC-based theragnostic colloidal nanohybrid demonstrated high intrinsic selective chemotherapeutic activity against colon cancer cells, even in the absence of a therapeutic drug. In addition, the CNCs efficiently dispersed and stabilized the functionalized SWCNTs leading to their disentangling and individual wrapping by rod-shaped CNCs, hence the minimal to no toxicity (de Almeida Barcelos et al., 2023). Graphene-based nanomaterials may also be used as drug nanocarriers to improve the functionality of cellulose-based drug delivery systems. As an example, integration of GO into 3D porous bacterial BNC greatly enhances the ibuprofen drug loading capacity and cell viability of BNC. A sustained drug release following a non-Fickian diffusion mechanism was achieved (Luo et al., 2017). Unlike BNC, CNF and CNC are underexplored relative to BNC in this biomedical field. Another application of BNC is in the fabrication of biomimetic scaffolds for tissue engineering. Its excellent mechanical strength, purity, and similar porous structure to the extracellular matrix allow cellular attachment and migration as well as diffusion of nutrients and metabolites. However, the limited electrical conductivity and bioactivity, and unmatching mechanical properties with that of natural tissues limit their applications. Reinforcement with conductive nanofillers such as Gr helps solve this problem endowing the composite with electrical conductivity and enhanced thermal stability and mechanical properties (Mokhena et al., 2024). Furthermore, hydrophilicity plays a crucial role in the bioactivity of the surface. It was shown that the more hydrophilic GO-reinforced porous BC nanofibrous nanocomposite scaffolds are more biocompatible and bioactive than the Gr/BNC scaffold (Luo et al., 2019) and that the hydrophilicity of nanocomposite hydrogels can help promote cell adhesion, proliferation, and maturation (Shi et al., 2023). For GO/CNC-based scaffolds, carrier material in the form of polymeric matrix is needed to enhance brittle behavior (Mokhena et al., 2024). Nanocellulose-based wound dressings also find important application as eco-friendly alternatives in the growing wound care industry. The lacking antimicrobial properties of BC, CNC, and other cellulose derivatives needed for wound healing may be addressed by the substantial antimicrobial activity of CNM fillers such as MWCNT (Khalid et al., 2022) and GrQDs, while the electrical conductivity also helps accelerate the wound healing

process. Nanohydrogels, composite films, and electrospun 3D porous patch primary and secondary wound dressings have been developed. More recently, active wound dressings containing bioactive nanofillers have been reported for improved performance (Mokhena et al., 2024).

20.3.2.1.3 Water Remediation

NC-2D nanostructured hybrid membranes are emerging as next-generation water purification membranes for applications in reverse osmosis, nanofiltration, ultrafiltration, adsorption, and photocatalytic degradation due to their remarkable processability, economic viability, and performance. The hydrophilic nature of NC endowed in the nanocomposite can overcome the problematic hydrophobic nature of conventional polymeric membranes. In this membrane design, the 1D NC uniformly disperses and strongly interacts with 2D nanomaterials including Gr, GO, and MXenes, leading to enhanced physicochemical features such as well-connected structure, hydrophilicity, surface roughness, porosity, and better membrane performance. For instance, GO/CNF hybrid membranes showed better mechanical stability in both dry and wet states relative to a CNF membrane or a comparable hydrophilic commercial reference membrane. Applications in remediation of different inorganic and organic pollutants from water and wastewater; filtration of salt, dyes, and several antibiotics; and water remediation by advanced oxidation processes have been demonstrated by NC-based Gr and GO 2D membranes, NC-MXene membranes, and NC-carbon nitride membranes, respectively (Mokhena et al., 2024; Zubair et al., 2024).

20.3.2.2 Nanocellulose-Metal Based Composites and Their Applications

Mechanical strength, excellent conductivity, catalytic properties, and optical properties are some of the inherent properties of various metallic nanomaterials. In addition, various archetypes such as nanowires, nanoparticles, thin films, and fractal structures enhance these characteristics. Recently, nanocellulose materials have been used as a green template or substrate for producing metal nanoarchitectures. As a result, multifunctional nanocellulose/metal hybrid nanomaterials have been prepared for various applications. Several examples of such composites are given in Table 20.3.

20.3.2.2.1 Sensors and Other Electronic Devices

With IoT development, a diverse range of complex electronic equipment arises with complicated environmental application and working functionality. The rise of smart, intelligent devices leads us to the miniaturization and flexibilization of electronic devices. Thus, the traditional rigid and bulky devices based on metals and

Table 20.3 Examples of metal/nanocellulose-based composites and their applications

Substrate	Nanocomposite	Fabrication technique	Application	Ref.
CNF nanopaper	CNF/AgNP	Light-induced printing	Flexible electronics, electrochemical biosensor	Pan et al. (2022)
CNC paper	CNC/RGO/PtNP	Pulsed sonoelectro-deposition	Electrochemical biosensor for small molecules	Burrs et al. (2016)
CNF paper	CNF/AgNP	Successive ionic layer adsorption and reaction (SILAR)	SERS-based chemical sensor	Chen et al. (2019)
CNF paper	CNF/CuNWs	Vacuum filtration	Paper electrodes for flexible electric materials	Pinto et al. (2020)
BNC paper	BNC/M-AgNPs	Vacuum filtration	SERS-based sensor for pesticide residue	Zhang et al. (2022)
NC-coated paper	CNC/AgNP	In situ chemical reduction and deposition, screen printing	Conductive ink for printed electronics	Martinez-Crespiera et al. (2022)
CNF-HS paper	CNF-HS/AgNW	EDC-NHS chemistry, spin-coating	Flexible touch screen panels	Yu et al. (2021)
CNF membrane	CNF/EGaIn	Evaporation-induced transfer printing	Conductive ink for printed electronics	Mao et al. (2021)
CNF paper	CNF/CuNP	Screen printing	Liquid metal ink for electro-thermal electronics	Li et al. (2023)
NC paper	NC/Ti/Ni	RF magnetron sputtering	Flexible piezoresistive strain sensors	Koval et al. (2021)
CNF paper	CNF/NS	Solvent casting	Flexible, electro-thermal electronics	Kadumudi et al. (2020)
CNF paper	CNF/ZnO NW	Pressure filtration, hot pressing	Disposable molecular sensor for volatile gases	Koga et al. (2019)
BNC paper	BNC/CdTe QDs	Magnetic and vacuum filtration	Fluorescence-based chemosensor for Hg^{2+}	Celi et al. (2023)
Paper	ZnO:Au NWs/ paper	ZnO NWs in-situ synthesis	Stretchable and wearable electronics	Liao et al. (2014)
Paper	$BaTiO_3$ NPs/ wood cellulose	Layer by layer	Microelectromechanical systems; sensors and actuators	Mahadeva et al. (2014)

Abbreviations: CNF cellulose nanofiber, *AgNP* silver nanoparticle, *CNC* cellulose nanocrystal, *RGO* reduced graphene oxide, *PtNP* platinum nanoparticle, *CuNWs* copper nanowires, *BNC* bacterial nanocellulose, *M-AgNPs* monodisperse silver nanoparticles, *CdTe QDs* cadmium tellurium quantum dots, *CNF-HS* thiol-modified nanofibrillated cellulose, *AgNW* silver nanowire, *EGaIn* eutectic gallium indium, *CuNP* copper nanoparticle, *NC* nanocellulose, *Ti* titanium, *Ni* nickel, *NS* nanosilicate, *ZnO NW* zinc oxide nanowire

semiconductors fall short. More recently, nanomaterials have been proposed as an alternative in sensor and electronics fabrication to achieve gains in sensitivity, selectivity, improved functional performance, and portability. In this direction, the use of ultra-thin and flexible soft materials like nanocellulose has encountered rapid growth in electronics fabrication. However, the poor electrical conductivity limits the applications of NC. Thus, surface functionalization through its hydroxyl groups with conductive materials such as metal nanostructures is often done (Teodoro et al., 2021; Jiao et al., 2024). First, electrochemical sensors detect analytes by the electrical signals generated from oxidation or reduction of analytes or redox probes. Second, electromechanical sensors detect pressure and/or strain by the variations of electrical properties in the sensing interface. Both require electroactive and conductive transducing surfaces to enhance analytical performance. For instance, a conductive silver-printed nanocellulose paper electrode-based electrochemical sensor was fabricated to detect glucose molecules via glucose oxidase (GOx) enzymatic reaction in the sample, giving a limit of detection (LOD) of 0.84 mM in PBS (Pan et al., 2022). This sensor however encounters instability issue by virtue of pure Ag oxidation in the electrode surface. In another work, platinum (Pt) nanocauliflower structure-modified Gr-functionalized cellulose nanopaper was used as an electrode for the electrochemical detection of glucose and pathogen. Adaptability of the transducer platform was demonstrated by robust performance of either GOx-immobilized (0.0870.02 μM) or an aptamer-immobilized receptor on transducer (4 CFU mL^{-1} *E. coli* O157:H7)(Burrs et al., 2016). Flexible strain sensors based on cellulose need piezoelectric or piezoresistive materials such as Ni busbars (Koval et al., 2021). Optical sensors, on the other hand, detect analytes by changes in optical signals at the transducer. SERS, fluorescence, surface plasmon resonance (SPR), and colorimetric methods are among the detection techniques utilized (Gabrielli & Frasconi, 2022). SERS and SPR are usually based on SERS-active or plasmonic metal nanostructures particles such as Ag (Chen et al., 2019; Zhang et al., 2022), Au, and Cu. In these systems, negative functionalities of CNF or BNC such as carboxyl groups facilitate the adsorption of the cations and stabilization of the reduced NPs on the substrate. Fluorescence is another optical sensing technique. Fluorophores are immobilized on the biopolymetric matrix to give fluorescent signals reminiscent to analyte concentration. Quantum dots such as cadmium telluride (CdTe) (Celi et al., 2023) and Mn-doped ZnS (Qin et al., 2022) and metal nanoclusters including gold nanoclusters (NC) (Lei et al., 2021) and AgNC (Díez et al., 2011) have been modified onto NC to realize photoluminescence behavior.

Optoelectronic devices such as flexible touch screen panels (f-TSP) need transparent conductive electrodes (TCEs). Among the metal NWs used as TCEs, AgNWs have been bonded to NC substrate layer to form a TCE that was subsequently integrated into f-TSP devices with striking durability. TCEs also find utility in other multifunctional flexible electronics such as antenna materials, radio-frequency identification (RFID), electronic paper, solar cells, liquid crystal display (LCD), and organic light-emitting diodes (OLED) display (Yu et al., 2021).

Electrothermal electronics in the form of stretchable and wearable heating generators is also gaining traction. Such conformal paper heaters normally comprise of a thermally insulating substrate like nanocellulose and strain-resistant patterns of conductive materials such as serpentine gold pattern on cellulose-based substrate (Kadumudi et al., 2020) and conductive Cu traces on kirigami-patterned cellulose-based paper substrate (Li et al., 2023). Joule heating enables heat radiation due to resistance from current flow through the conductive material. Aside from thermal management, EM radiation management, such as in EM interference (EMI) shielding, is also important in realizing robust performance of multifunctional electronic devices. This has been demonstrated by the previously mentioned copper-nanocellulose paper heater. Conductive inks and electrodes are also increasingly investigated for their prospective applications in flexible and printed electronics, energy storage, and sensors. These could be made of NC-metal NP dispersion such as AgNP-CNC (Martinez-Crespiera et al., 2022) and CNF-CuNW (Pinto et al., 2020) and conductive fillers like liquid metal inks (Mao et al., 2021) that can be easily deposited onto the NC substrate. In all applications mentioned, the excellent eco-friendliness, biodegradability, low thermal expansion coefficient, and high maximum thermal degradation temperature of the nanocellulose make it a suitable substrate.

20.3.2.2.2 Biomedical Applications

As an established antimicrobial agent, Ag nanomaterials find application in antimicrobial celluloses for wound healing and microbial infections mitigation. The potential cytotoxicity to eukaryotic cells of isolated nanometals is alleviated by combining with biocompatible biopolymers such as nanocellulose aided by functionalization via the hydroxyl groups (Ong et al., 2023). For wound healing, a novel multifunctional dressing containing AgNWs, BNC, and collagen was developed with the latter controlling the release of silver ions. Ag+ can also be used in electrostimulation therapy. To illustrate, a transparent, ultra-thin, sandwich-structured BNC/AgNWs bandage fabricated by vacuum filtration demonstrated superior tensile strength, antibacterial activity, biocompatibility, and conductivity. The latter enabled capability of electrical stimulation therapy to promote wound healing by increasing the secretion of vascular endothelial growth factor (VEGF) (Wang et al., 2024). In addition to AgNPs, Gold NPs were also loaded onto pristine BNC for treating infected wounds (Mbituyimana et al., 2021). As regards microbial infections mitigation, NC-AgNP composites have been reported to be effective in killing various bacteria, including multidrug-resistant strains, as well as fungi. More recently, researchers have found interest in using green reducing agents in lieu of strong solvents for the in situ growth nanocellulose-AgNPs fabrication (Ong et al., 2023).

20.3.2.2.3 Active Food Packaging

NC-based metal nanohybrids are nanosized fillers that can enhance the active functions of food packaging materials. Metal NPs such as AgNPs are well-established antimicrobial agents and UV blockers. The released silver ions tend to disrupt the proteins, microbial membranes, and microbial nucleic acids. However, their incorporation into the biopolymeric packaging film may reduce the mechanical properties. Hence, nanocellulose is used as the reinforcement and templating material for the nanofiller. NC-AgNP nanohybrids have demonstrated to have synergistic reinforcing and antimicrobial effects toward PLA, PVA, poly(3-hydroxybutyrate-co-3-hydroxyvalerate) (PHBV), and PU. For instance, a CNF/AgNP composite exhibited inhibitory effects on *E. coli O157:H7* and *L. monocytogenes*, and the uptake of AgNPs by endosomal mechanism were shown demonstrating its potential in active packaging (Yu et al., 2019). Improvement in crystallization ability, mechanical, barrier, and thermal properties, and overall migration in the packaging film were also reported using these nanohybrids (Abdalkarim et al., 2021; Jiao et al., 2024; Oun et al., 2020;).

20.3.2.2.4 Wastewater Treatment

AgNPs are important non-toxic and antibacterial inorganic NPs integrated with cellulose-based materials for water purification. These NC-AgNP nanohybrids are widely studied and used in the functionalization of filtration membranes for waste remediation. Other hybrids such as BNC-PdNPs, CNC-PdNPs, CA-CdSe/AgNPs, and BNC-CdS have also been explored for wastewater treatment. To improve adsorptive and catalytic abilities, other inorganic NPs such as metal oxides are often integrated as discussed in Sect. 20.3.2.3.3 (Zhang et al., 2023b).

20.3.2.3 Nanocellulose-Based Composites with Other Types of Inorganic Particles

20.3.2.3.1 Sensors and Other Electronic Devices

Nanostructures of metal oxides have interesting optical and electrical properties, large specific surface area, tunable chemical reactivity, and thermal stability; hence, they are studied extensively in sensing applications. The porous structure, firm-forming ability, rich hydroxyl groups, low density, abundance, environmental friendliness, mechanical strength, and flexibility of NC complement them for the fabrication of nanocomposite-based sensing layer, transducers, or electrodes for low-cost, high-performance, and disposable or flexible optical (Sukhavattanakul & Manuspiya, 2020), electrochemical (Norrrahim et al., 2022), or electrical (Zhu et al., 2023) (bio)chemical or physical sensors and energy storage devices (Palem et al., 2022). Their semiconducting properties allow them to participate in

chemiresistive sensing by the change in resistance, in capacitive sensing by change of dielectric constant, and in field effect transistor-based sensing by change in surface charges. For instance, the piezoelectricity and affinity to NO_2 gas molecules of ZnO enable its use as a transducer component in strain sensing (NC/ZnO nanocomposite electrode) for motion monitoring (Teodoro et al., 2021) and in chemical sensing (ZnO NW@CNF paper electrode) (Koga et al., 2019). As part of the sensing layer, Fe_3O_4 catalyst was immobilized in a self-supporting and translucent NC film of a colorimetric enzymatic sensor (Teodoro et al., 2021). Other inorganic materials such as perovskite-structured ceramic and metal organic frameworks (MOFs) have interesting tunable electrical and chemical properties and a porous feature, wherein NC often serves as the shaping component or porous framework of the functional nanocomposite. Their piezoelectric effect and excellent electroactivity and conductivity have been demonstrated in reported strain or pressure sensors for prospective applications in the field of medical rehabilitation training and sports injury detection (Zhu et al., 2023), electrode, interlayer, and gel electrolytes of supercapacitors and batteries (Mai et al., 2023). More recently, self-powered wearable sensors utilizing these capabilities of NC-inorganic composites are on the rise for longer use.

20.3.2.3.2 Active Food Packaging

NC-based metal oxide nanohybrids are also widely used nanofillers in active food packaging. The NC serves as a scaffolding matrix of dispersible inorganic NPs. The rich surface hydroxyl groups interact with these NPs, or in some cases, further surface modification is done to stabilize the adhesion or attachment of NPs on the surface. It has been shown to improve the mechanical properties of the biopolymeric packaging film by serving as heterogeneous nucleating agents. Inorganic NPs like ZnO, CuO, and Fe_3O_4 have been loaded onto NC template. Antimicrobial effects are one special features of active packaging. First, ZnO and TiO2 NPs can form highly active free radicals under light exposure which harm bacterial cells. Second, the accumulation of NPs in the microbial membrane could result in membrane disorganization and cellular uptake. Fourth, Fe-Cu alloy can produce superoxide radicals that permanently harm the cell membrane surface. UV-shielding effect is also required in active packaging. ZnO NPs have been mostly used as UV absorbers due to their catalytic effects, low bandgap, and refractive index. Other inorganic UV absorbers including Ag, ZnO, TiO_2, and ZnS NPs were also proposed. Finally, biodegradation behavior is also important for sustainability in food packaging. The hydrolytic degradation of ZnO in CNC-ZnO nanohybrids produces the Zn^{2+} and water, speeding up the degradation ability of the composite film (Abdalkarim et al., 2021; Oun et al., 2020).

20.3.2.3.3 Water and Air Remediation

Membrane technology for water purification encounters limitations such as slow purification, fouling, poor mechanical, and thermal stability. Surface functionalization with specialized nanostructured materials can improve their treatment performance. To this end, inorganic NPs including TiO_2, CuO, Fe_2O_3, Fe_3O_4, MnO_2, MoS_2/ZnO, Ru/HfO_2, Pt/HfO_2, C_3N_4/NiO/ZnO, Bi_2MoO_6, WO_3, and Ag have been increasingly explored owing to their high specific surface area and pollutant specificity for the targeted remediation of pollutants from wastewater. Nanocellulose is combined with the NPs into nanohybrid to ensure dispersion of the NPs and colloid stability for increased surface exposure. In addition, the functionalization of the nanohybrid in the membrane scaffolding will minimize the release of free nanoparticles into the water channels. Moreover, easy isolation of nanocomposite after use will be realized with the incorporation of magnetic NPs. Material hybridization involves in situ growth of NPs from precursor solution (by reduction) or in situ immobilization of pre-synthesized inorganic NPs in the solution onto the anionic- or cationic-functionalized NC. These anionic or cationic functionalized NCs both aid in the reduction and immobilization of NPs and act as pollutant receptor. More recently, stand-alone and supported filter membranes or composite films based on 3D porous structure of NC containing unitary and binary metal MOFs composites, with inorganic metals or metal oxides and organic ligands, have been studied for sewage treatment. The remediation mechanism is governed by adsorption using different kinds of MOFs via ion exchange, electrostatic interaction, coordination, and/or by cationic or anionic surface groups of NC. Alternatively, remediation is achieved by photocatalytic activity of carbonized ZIF or catalytic activity of ZIFs (Mai et al., 2023). Interestingly, incorporation of hydrophobic MOFs ensures the possibility of oil contaminants removal. A wide array of organic and inorganic pollutants such as dyes, myoglobin, heavy metals (As (III), As(V), Cu(II), Pb(II), Zn(II), Cr(VI), Cd(II)), pharmaceutical wastes (para nitro phenol, tetracycline, nitrofurantoin, ciprofloxacin, esomeprazole), and pathogens (*E. coli*, *S. aureus*) have been reportedly remediated (Elumalai et al., 2023; Oun et al., 2020; Zhang et al., 2023b; Zubair et al., 2024). Moving on to air purification, solgel aminosilane-coated or MOF-modified NC aerogel membrane filters have also been reported for the particulate pollutants or volatile organic compounds (formaldehyde, etc.) filtration from air, wherein the aminosilanes and MOFs serve as the separation medium and NC provides the filter membrane structure (Mai et al., 2023; Sepahvand et al., 2023).

20.3.2.3.4 Biomedical Applications

Along with metal NPs, metal oxide-based NPs are also widely explored in antimicrobial celluloses. In wound healing, BNC/ZnO composites showed broad-spectrum antibacterial activity against *E. coli, P. aeruginosa*, *S. aureus,* and *Citrobacter freundii* as well as significantly faster healing than treatments with

pristine BNC (Ong et al., 2023). This antibacterial activity of ZnO-NPs against *S. aureus* and *E. coli* was also demonstrated by hydroxypropyl methylcellulose (HPMC)/carboxymethyl starch (CMS)/ZnO-NPs composite film (Wang et al., 2024). The antimicrobial efficacy of TiO_2 NPs in BNC-based wound dressings has also been shown (Mbituyimana et al., 2021). In another antimicrobial material, the antibacterial activity against *Klebsiella pneumonia* and *S. aureus* of BNC aerogels decorated with Ag, CuO, and ZnO NPs correlated with the amount and size of metal NPs formed. MOF-based NPs also find utility in biomedical applications. A PDA-functionalized CNF composite hydrogel was conjugated with MOFs for high-density loading and tunable release of the hydrophobic curcumin drug delivery (Ong et al., 2023). Leveraging its superb mechanical strength, physicochemical properties, and biocompatibility, nanocellulosic base materials are also employed as natural scaffolding biomaterial. A BNC-based scaffold loaded with hydroxyapatite (HAP) promoted bone regeneration, manifesting increased mineralization of human osteoblast-like cells (SaOs-2) and cell migration (Ong et al., 2023).

20.4 Outlook

Over the years, cellulose-based nanocomposites have earned a spot in the rapidly evolving electronics industry and are arising as an innovative solution to sustainable and biocompatible material alternatives in material fabrications, waste remediation, food packaging, and biomedical tools. On one hand, their abundance and biodegradability make them suitable materials in low-cost, environmentally friendly, fully recyclable, and/or transient or degradable materials. On the other hand, their lightweight, flexibility, and multidimensional properties afford them their functional performance in an adaptable environment. As such, multifunctional and adaptable devices from these nanocomposites, including self-powered electronic devices and flexible devices with easy tunability of desired functions, are on the rise. Recently, the development of free-standing nanocellulose composite-based films, membranes, or nanopapers has increasingly replaced the bulky and inorganic substrates such as polymers, metals, and ceramics in electronics and other applications. More recently, the rise of water-based conductive, semiconductive, or dielectric inks has spurred research attention to NC-based printable ink supporting both the printed and flexible electronics field. With the ever-expanding Internet of Things, wearable devices and integrated electronic sensors and devices are anticipated to prosper. This calls for scalable routes, thus the rise of novel, green, and scalable synthesis processes such as printing and in situ synthesis techniques for nanocomposite processing. However, sustainability must extend beyond the end-of-life of the engineered materials. This creates demand for sustainable and fully recyclable devices wherein components are either biodegradable and soluble or easily recoverable for recycling back into the process. All-cellulose composites or bionanocomposites are anticipated to prosper in the near future. In the electronics perspective,

this should not contradict the need for transient electronics and the concept of trillion sensor universe which push for high-performing devices, low-cost, and disposable design. In the sensing field, smartphone readouts and data analysis have been gaining interest, complementing the application of NC hybrids in the field of point-of-care and/or on-body sensors. In material synthesis, there is a quest to the use of renewable materials and the maximization of machine learning and computational tools in optimizing synthesis parameters and materials for desired functionalities. Finally, it is foreseen that the demand for NC-based composites in multifunctional devices, high-performing material solutions will be sustained in the next years.

References

Abdalkarim, S. Y. H., Chen, L. M., Yu, H. Y., Li, F., Chen, X., Zhou, Y., & Tam, K. C. (2021). Versatile nanocellulose-based nanohybrids: A promising-new class for active packaging applications. *International Journal of Biological Macromolecules, 182*, 1915–1930. https://doi.org/10.1016/j.ijbiomac.2021.05.169

Abdel-Hakim, A., & Mourad, R. (2023). Nanocellulose and its polymer composites: Preparation, characterization, and applications. *Russian Chemical Reviews, 92*(4), 5076. https://doi.org/10.57634/rcr5076

Ahmadi, A., Khoshfetrat, S. M., Kabiri, S., Fotouhi, L., Dorraji, P. S., & Omidfar, K. (2021). Impedimetric paper-based enzymatic biosensor using electrospun cellulose acetate nanofiber and reduced graphene oxide for detection of glucose from whole blood. *IEEE Sensors Journal, 21*(7), 9210–9217. https://doi.org/10.1109/JSEN.2021.3053033

Alam, M. M., & Mandal, D. (2016). Native cellulose microfiber-based hybrid piezoelectric generator for mechanical energy harvesting utility. *ACS applied materials & interfaces, 8* (3), 1555–1558. https://doi.org/10.1021/acsami.5b08168

Ali, N., & Hoque, M. E. (2022). Bionanocomposites in the automotive and aerospace applications. In C. Muthukumar, S. Muthu, K. Thiagamani, S. Krishnasamy, R. Nagarajan, & S. Siengchin (Eds.), *Polymer based bio-nanocomposites properties, durability and applications* (pp. 237–253). Springer Nature. https://doi.org/10.1007/978-981-16-8578-1

Ansari, J. R., Hegazy, S. M., Houkan, M. T., Kannan, K., Aly, A., & Sadasivuni, K. K. (2020). Nanocellulose-based materials/composites for sensors. In S. Thomas & Y. B. Pottathara (Eds.), *Nanocellulose based composites for electronics* (pp. 185–214). Elsevier. https://doi.org/10.1016/B978-0-12-822350-5.00008-4

Bacakova, L., Pajorova, J., Tomkova, M., Matejka, R., Broz, A., Stepanovska, J., et al. (2020). Applications of nanocellulose/nanocarbon composites: Focus on biotechnology and medicine. *Nanomaterials, 10*(2), 196. https://doi.org/10.3390/nano10020196

Bandi, R., Alle, M., Park, C. W., Han, S. Y., Kwon, G. J., Kim, J. C., et al. (2021). Cellulose nanofibrils/carbon dots composite nanopapers for the smartphone-based colorimetric detection of hydrogen peroxide and glucose. *Sensors and Actuators B: Chemical, 330*, 129330. https://doi.org/10.1016/j.snb.2020.129330

Belaineh, D., Andreasen, J. W., Palisaitis, J., Malti, A., Håkansson, K., Wågberg, L., et al. (2019). Controlling the organization of PEDOT:PSS on cellulose structures. *ACS Applied Polymer Materials, 1*(9), 2342–2351. https://doi.org/10.1021/acsapm.9b00444

Brett, C. J., Forslund, O. K., Nocerino, E., Kreuzer, L. P., Widmann, T., Porcar, L., et al. (2021). Humidity-induced nanoscale restructuring in PEDOT:PSS and cellulose nanofibrils reinforced biobased organic electronics. *Advanced Electronic Materials, 7*(6), 2100137. https://doi.org/10.1002/aelm.202100137

Brooke, R., Fall, A., Borras, M., Yilma, D. B., Edberg, J., Martinez-Crespiera, S., et al. (2021). Nanocellulose based carbon ink and its application in electrochromic displays and supercapacitors. *Flexible and Printed Electronics, 6*(4), 045011. https://doi.org/10.1088/2058-8585/ac3ddb

Burrs, S. L., Bhargava, M., Sidhu, R., Kiernan-Lewis, J., Gomes, C., Claussen, J. C., & McLamore, E. S. (2016). A paper based graphene-nanocauliflower hybrid composite for point of care biosensing. *Biosensors & Bioelectronics, 85*, 479–487. https://doi.org/10.1016/j.bios.2016.05.037

Cao, J., Zhang, X., Wu, X., Wang, S., & Lu, C. (2016). Cellulose nanocrystals mediated assembly of graphene in rubber composites for chemical sensing applications. *Carbohydrate Polymers, 140*, 88–95. https://doi.org/10.1016/j.carbpol.2015.12.042

Celi, I. H., Peña González, P. T., & Martínez Bonilla, C. A. (2023). Bacterial nanocellulose and CdTe quantum dots: Assembled nanopaper for heavy metal detection in aqueous solution. *Journal of Materials Chemistry C, 11*(44), 15690–15699. https://doi.org/10.1039/d3tc02927a

Chang, Z., Liang, D., Sun, S., Zheng, S., Sun, K., Wang, H., et al. (2024). Innovative modification of cellulose fibers for paper-based electrode materials using metal-organic coordination polymers. *International Journal of Biological Macromolecules, 264*(1), 130599. https://doi.org/10.1016/j.ijbiomac.2024.130599

Chen, C., Bu, X., Feng, Q., & Li, D. (2018). Cellulose nanofiber/carbon nanotube conductive nano-network as a reinforcement template for polydimethylsiloxane nanocomposite. *Polymers, 10*(9), 1000. https://doi.org/10.3390/polym10091000

Chen, L., Ying, B., Song, P., & Liu, X. (2019). A nanocellulose-paper-based SERS multiwell plate with high sensitivity and high signal homogeneity. *Advanced Materials Interfaces, 6*(24), 1901346. https://doi.org/10.1002/admi.201901346

Chen, S., Chen, Y., Li, D., Xu, Y., & Xu, F. (2021). Flexible and sensitivity-adjustable pressure sensors based on carbonized bacterial nanocellulose/wood-derived cellulose nanofibril composite aerogels. *ACS Applied Materials & Interfaces, 13*(7), 8754–8763. https://doi.org/10.1021/acsami.0c21392

Chowdhury, M. I. S., Autul, Y. S., Rahman, S., & Hoque, M. E. (2022). Polymer nanocomposites for automotiveapplications. *In Advanced Polymer Nanocomposites*, 267–317. Woodhead Publishing. https://doi.org/10.1016/B978-0-12-824492-0.00010-6

Dandegaonkar, G., Ahmed, A., Sun, L., Adak, B., & Mukhopadhyay, S. (2022). Cellulose based flexible and wearable sensors for health monitoring. *Materials Advances, 3*, 3766–3783. https://doi.org/10.1039/d1ma01210j

de Almeida Barcelos, K., Garg, J., Ferreira Soares, D. C., de Barros, A. L. B., Zhao, Y., & Alisaraie, L. (2023). Recent advances in the applications of CNT-based nanomaterials in pharmaceutical nanotechnology and biomedical engineering. *Journal of Drug Delivery Science and Technology, 87*, 104834. https://doi.org/10.1016/j.jddst.2023.104834

Dias, O. A. T., Konar, S., Leão, A. L., & Sain, M. (2019). Flexible electrically conductive films based on nanofibrillated cellulose and polythiophene prepared via oxidative polymerization. *Carbohydrate Polymers, 220*, 79–85. https://doi.org/10.1016/j.carbpol.2019.05.057

Díez, I., Eronen, P., Österberg, M., Linder, M. B., Ikkala, O., & Ras, R. H. A. (2011). Functionalization of nanofibrillated cellulose with silver nanoclusters: Fluorescence and antibacterial activity. *Macromolecular Bioscience, 11*(9), 1185–1191. https://doi.org/10.1002/mabi.201100099

Divya, Mahapatra, S., Srivastava, V. R., & Chandra, P. (2021). Nanobioengineered sensing technologies based on cellulose matrices for detection of small molecules, macromolecules, and cells. *Biosensors, 11*(6), 168. https://doi.org/10.3390/bios11060168

Dufresne, A. (2012). Processing of polymer nanocomposites reinforced with cellulose nanocrystals: A challenge. *International Polymer Processing, 27*, 557–564. https://doi.org/10.3139/217.2603

Dufresne, A. (2013). Nanocellulose: A new ageless bionanomaterial. *Materials Today, 16*, 220–227. https://doi.org/10.1016/j.mattod.2013.06.004

Durairaj, V. (2022). *Nanocellulose/nanocarbon composites for direct electrochemical detection of small molecules* (pp. 1–35). Aalto University. Available at: www.aalto.fi

Efthymiou, M. N., Tsouko, E., Papagiannopoulos, A., Athanasoulia, I. G., Georgiadou, M., Pispas, S., et al. (2022). Development of biodegradable films using sunflower protein isolates and bacterial nanocellulose as innovative food packaging materials for fresh fruit preservation. *Scientific Reports, 12*(1), 6935. https://doi.org/10.1038/s41598-022-10913-6

Elumalai, P., Muthukumar, B., Dhandapani, P., Parthiba Karthikeyan, O., & Huang, M. (2023). Role of bionanohybrids for pollutant removal in wastewater environment. *Current Opinion in Environmental Science & Health, 35*, 100504. https://doi.org/10.1016/j.coesh.2023.100504

Fan, J., Xu, M., Xu, Y. T., Hamad, W. Y., Meng, Z., & MacLachlan, M. J. (2023). A visible multi-response electrochemical sensor based on cellulose nanocrystals. *Chemical Engineering Journal, 457*, 141175. https://doi.org/10.1016/j.cej.2022.141175

Feng, X., Wang, X., Zhang, C., Dang, C., Chen, Y., & Qi, H. (2021). Highly conductive and multifunctional nanocomposites based on sulfated nanocellulose-assisted high dispersion limit of single-walled carbon nanotubes. *Carbon, 183*, 187–195. https://doi.org/10.1016/j.carbon.2021.07.022

Fu, D., Yang, R., Wang, R., Wang, Y., & Li, Z. (2023). Comparative study of various nanocellulose enhanced freezing-tolerant, stretchable organohydrogels for versatile sensors. *Cellulose, 30*(11), 7095–7111. https://doi.org/10.1007/s10570-023-05312-7

Gabrielli, V., & Frasconi, M. (2022). Cellulose-based functional materials for sensing. *Chemosensors, 10*(9), 352. https://doi.org/10.3390/chemosensors10090352

Ghasemlou, M., Daver, F., Ivanova, E. P., Habibi, Y., & Adhikari, B. (2021). Surface modifications of nanocellulose: From synthesis to high-performance nanocomposites. *Progress in Polymer Science, 119*, 101418. https://doi.org/10.1016/j.progpolymsci.2021.101418

Gong, L., Fu, H., Liu, L., Li, Z., Guo, J., Cao, Z., et al. (2022). Construction and performance of a nanocellulose−graphene-based humidity sensor with a fast response and excellent stability. *ACS Applied Polymer Materials, 4*(5), 3656–3666. https://doi.org/10.1021/acsapm.2c00188

Han, L., Cui, S., Yu, H. Y., Song, M., Zhang, H., Grishkewich, N., et al. (2019). Self-healable conductive nanocellulose nanocomposites for biocompatible electronic skin sensor systems. *ACS Applied Materials & Interfaces, 11*(47), 44642–44651. https://doi.org/10.1021/acsami.9b17030

Ibrahim, H., Sazali, N., Salleh, W. N. W., & Zainal Abidin, M. N. (2019). A short review on recent utilization of nanocellulose for wastewater remediation and gas separation. In *Materials today: Proceedings* (pp. 45–49). Elsevier Ltd. https://doi.org/10.1016/j.matpr.2020.09.245

Jacob, J., Linson, N., Mavelil-Sam, R., Maria, H. J., Pothan, L. A., Thomas, S., et al. (2024). Poly(lactic acid)/nanocellulose biocomposites for sustainable food packaging. *Cellulose, 31*(10), 5997–6042. https://doi.org/10.1007/s10570-024-05975-w

Ji, Y., Shen, D. E., Lu, Y., Schueneman, G. T., Shofner, M. L., & Meredith, J. C. (2023). Aqueous-based recycling of cellulose nanocrystal/chitin nanowhisker barrier coatings. *ACS Sustainable Chemistry & Engineering, 11*(29), 10874–10883. https://doi.org/10.1021/acssuschemeng.3c02457

Jia, D., Xie, J., Dirican, M., Fang, D., Yan, C., Liu, Y., et al. (2022). Highly smooth, robust, degradable and cost-effective modified lignin-nanocellulose green composite substrates for flexible and green electronics. *Composites, Part B: Engineering, 236*, 109803. https://doi.org/10.1016/j.compositesb.2022.109803

Jiao, K., Cao, W., Yuan, W., Yuan, H., Zhu, J., Gao, X., et al. (2024). Cellulose nanostructures as tunable substrates for nanocellulose-metal hybrid flexible composites. *ChemPlusChem, 89*(5), e202300704. https://doi.org/10.1002/cplu.202300704

Jin, K., Tang, Y., Liu, J., Wang, J., & Ye, C. (2021). Nanofibrillated cellulose as coating agent for food packaging paper. *International Journal of Biological Macromolecules, 168*, 331–338. https://doi.org/10.1016/j.ijbiomac.2020.12.066

Joseph, B., Sagarika, V. K., Sabu, C., Kalarikkal, N., & Thomas, S. (2020). Cellulose nanocomposites: Fabrication and biomedical applications. *Journal of Bioresources and Bioproducts, 5*(4), 223–237. https://doi.org/10.1016/j.jobab.2020.10.001

Kadumudi, F. B., Trifol, J., Jahanshahi, M., Zsurzsan, T. G., Mehrali, M., Zeqiraj, E., et al. (2020). Flexible and green electronics manufactured by origami folding of nanosilicate-reinforced cellulose paper. *ACS Applied Materials & Interfaces, 12*(42), 48027–48039. https://doi.org/10.1021/acsami.0c15326

Khalid, A., Madni, A., Raza, B., Islam, M., Hassan, A., Ahmad, F., et al. (2022). Multiwalled carbon nanotubes functionalized bacterial cellulose as an efficient healing material for diabetic wounds. *International Journal of Biological Macromolecules, 203*, 256–267. https://doi.org/10.1016/j.ijbiomac.2022.01.146

Koga, H., Nagashima, K., Huang, Y., Zhang, G., Wang, C., Takahashi, T., et al. (2019). Paper-based disposable molecular sensor constructed from oxide nanowires, cellulose nanofibers, and pencil-drawn electrodes. *ACS Applied Materials & Interfaces, 11*(16), 15044–15050. https://doi.org/10.1021/acsami.9b01287

Koval, V., Barbash, V., Dusheyko, M., Lapshuda, V., Yashchenko, O., & Naidonov, A. (2021). Nickel-based piezoresistive sensors obtained on flexible nanocellulose substrate. In *Proceedings of the 2021 IEEE 11th international conference "Nanomaterials: Applications and Properties", NAP 2021*. Institute of Electrical and Electronics Engineers Inc. https://doi.org/10.1109/NAP51885.2021.9568610

Kumar, S., Ngasainao, M. R., Sharma, D., Sengar, M., Gahlot, A. P. S., Shukla, S., & Kumari, P. (2022). Contemporary nanocellulose-composites: A new paradigm for sensing applications. *Carbohydrate Polymers, 298*, 120052. https://doi.org/10.1016/j.carbpol.2022.120052

Kummari, S., Panicker, L. R., Rao Bommi, J., Karingula, S., Sunil Kumar, V., Mahato, K., & Goud, K. Y. (2023). Trends in paper-based sensing devices for clinical and environmental monitoring. *Biosensors, 13*(4), 420. https://doi.org/10.3390/bios13040420

Latonen, R. M., Määttänen, A., Ihalainen, P., Xu, W., Pesonen, M., Nurmi, M., & Xu, C. (2017). Conducting ink based on cellulose nanocrystals and polyaniline for flexographical printing. *Journal of Materials Chemistry C, 5*(46), 12172–12181. https://doi.org/10.1039/c7tc03729e

Lay, M., Say, M. G., & Engquist, I. (2023). Direct ink writing of nanocellulose and PEDOT:PSS for flexible electronic patterned and supercapacitor papers. *Advanced Materials Technologies, 8*(18), 2300652. https://doi.org/10.1002/admt.202300652

Lei, X., Li, H., Luo, Y., Sun, X., Guo, X., Hu, Y., & Wen, R. (2021). Novel fluorescent nanocellulose hydrogel based on gold nanoclusters for the effective adsorption and sensitive detection of mercury ions. *Journal of the Taiwan Institute of Chemical Engineers, 123*, 79–86. https://doi.org/10.1016/j.jtice.2021.05.044

Li, H., Zong, Y., Ding, Q., Han, W., & Li, X. (2021). Paper-based thermoelectric generator based on multi-walled carbon nanotube/carboxylated nanocellulose. *Journal of Power Sources, 500*, 229992. https://doi.org/10.1016/j.jpowsour.2021.229992

Li, Z., Islam, A., Di Luigi, M., Huang, Y., & Ren, S. (2023). Stretchable copper-nanocellulose paper heater. *Applied Materials Today, 31*, 101740. https://doi.org/10.1016/j.apmt.2023.101740

Li, X., Jiang, G., Wang, G., Zhou, J., Zhang, Y., & Zhao, D. (2024). Promising cellulose–based functional gels for advanced biomedical applications: A review. *International Journal of Biological Macromolecules, 260*(2), 129600. https://doi.org/10.1016/j.ijbiomac.2024.129600

Liao, Q., Zhang, Z., Zhang, X., Mohr, M., Zhang, Y., & Fecht, H.-J. (2014). Flexible piezoelectric nanogenerators based on a fiber/ZnO nanowires/paper hybrid structure for energy harvesting. *Nano Research, 7*, 917–928. https://doi.org/10.1007/s12274-014-0453-8

Liu, H., Du, H., Zheng, T., Liu, K., Ji, X., Xu, T., et al. (2021). Cellulose based composite foams and aerogels for advanced energy storage devices. *Chemical Engineering Journal, 426*, 130817. https://doi.org/10.1016/j.cej.2021.130817

Liu, Y., Zhang, S., Li, L., & Li, N. (2024). High-performance cellulose nanofibers/carbon nanotubes composite for constructing multifunctional sensors and wearable electronics. *Advanced Fiber Materials, 6*(3), 758–771. https://doi.org/10.1007/s42765-024-00388-7

Luo, H., Ao, H., Li, G., Li, W., Xiong, G., Zhu, Y., et al. (2017). Bacterial cellulose/graphene oxide nanocomposite as a novel drug delivery system. *Current Applied Physics, 17*(2), 249–254. https://doi.org/10.1016/j.cap.2016.12.001

Luo, H., Ao, H., Peng, M., Yao, F., Yang, Z., & Wan, Y. (2019). Effect of highly dispersed graphene and graphene oxide in 3D nanofibrous bacterial cellulose scaffold on cell responses: A comparative study. *Materials Chemistry and Physics, 235*, 121774. https://doi.org/10.1016/j.matchemphys.2019.121774

Ma, X., Chen, Y., Chang, P. R., & Huang, J. (2018). Facile fabrication of conductive paper-based materials from tunicate cellulose nanocrystals and polydopamine-decorated graphene oxide. *Paper and Biomaterials, 3*(4), 19–25. https://doi.org/10.26599/pbm.2018.9260024

Mahadeva, S. K., Walus, K., & Stoeber, B. (2014). Piezoelectric paper fabricated via nanostructured Barium Titanate functionalization of wood cellulose fibers. *ACS Applied Materials & Interfaces, 6*(10), 7547. https://doi.org/10.1021/am5008968

Mai, T., Li, D. D., Chen, L., & Ma, M. G. (2023). Collaboration of two-star nanomaterials: The applications of nanocellulose-based metal organic frameworks composites. *Carbohydrate Polymers, 302*, 120359. https://doi.org/10.1016/j.carbpol.2022.120359

Manimaran, M., Norizan, M. N., Mohamad Kassim, M. H., Adam, M. R., Norrrahim, M. N. F., & Knight, V. F. (2024). Critical assessment of the thermal stability and degradation of chemically functionalized nanocellulose-based polymer nanocomposites. *Nanotechnology Reviews, 13*(1), 20240005. https://doi.org/10.1515/ntrev-2024-0005

Mansor, M. R., Nurfaizey, A. H., Tamaldin, N., & Nordin, M. N. A. (2019). Natural fiber polymer composites: Utilization in aerospace engineering. In *Biomass, biopolymer-based materials, and bioenergy: Construction, biomedical, and other industrial applications* (pp. 203–224). Elsevier. https://doi.org/10.1016/B978-0-08-102426-3.00011-4

Mao, Y., Wu, Y., Zhang, P., Yu, Y., He, Z., & Wang, Q. (2021). Nanocellulose-based reusable liquid metal printed electronics fabricated by evaporation-induced transfer printing. *Journal of Materials Science and Technology, 61*, 132–137. https://doi.org/10.1016/j.jmst.2020.05.040

Martinez-Crespiera, S., Pepió-Tàrrega, B., González-Gil, R. M., Cecilia-Morillo, F., Palmer, J., Escobar, A. M., et al. (2022). Use of nanocellulose to produce water-based conductive inks with Ag NPs for printed electronics. *International Journal of Molecular Sciences, 23*(6), 2946. https://doi.org/10.3390/ijms23062946

Mbituyimana, B., Liu, L., Ye, W., Ode Boni, B. O., Zhang, K., Chen, J., et al. (2021). Bacterial cellulose-based composites for biomedical and cosmetic applications: Research progress and existing products. *Carbohydrate Polymers, 273*, 118565. https://doi.org/10.1016/j.carbpol.2021.118565

Mokhena, T. C., Mochane, M. J., Mtibe, A., Sigonya, S., Ntsendwana, B., Masibi, E. G., et al. (2024). Recent advances on nanocellulose-graphene oxide composites: A review. *Cellulose, 31*, 7207–7249. https://doi.org/10.1007/s10570-024-06055-9

Muhammad, A., Rahman, M. R., Baini, R., & Bin Bakri, M. K. (2020). Applications of sustainable polymer composites in automobile and aerospace industry. In M. R. Rahman (Ed.), *Advances in sustainable polymer composites* (pp. 185–207). Elsevier. https://doi.org/10.1016/B978-0-12-820338-5.00008-4

Nan, Y., Gomez-Maldonado, D., Whitehead, D. C., Yang, M., & Peresin, M. S. (2023). Comparison between nanocellulose-polyethylenimine composites synthesis methods towards multiple water pollutants removal: A review. *International Journal of Biological Macromolecules, 232*, 123342. https://doi.org/10.1016/j.ijbiomac.2023.123342

Nazrin, A., Sapuan, S. M., Zuhri, M. Y. M., Ilyas, R. A., Syafiq, R., & Sherwani, S. F. K. (2020). Nanocellulose reinforced thermoplastic starch (TPS), polylactic acid (PLA), and polybutylene succinate (PBS) for food packaging applications. *Frontiers in Chemistry, 8*, 213. https://doi.org/10.3389/fchem.2020.00213

Nguyen, H. L., Tran, T. H., Hao, L. T., Jeon, H., Koo, J. M., Shin, G., et al. (2021). Biorenewable, transparent, and oxygen/moisture barrier nanocellulose/nanochitin-based coating on polypropylene for food packaging applications. *Carbohydrate Polymers, 271*, 118421. https://doi.org/10.1016/j.carbpol.2021.118421

Nhi, T. T. Y., Cong, T. D., Hop, T. T. T., Mai, D. T., & Tung, N. T. (2024). Nanocellulose as promising reinforcement materials for biopolymer nanocomposites: A review. *Vietnam Journal of Science and Technology, 62*(2), 197–221. https://doi.org/10.15625/2525-2518/18831

Norizan, M. N., Shazleen, S. S., Alias, A. H., Sabaruddin, F. A., Asyraf, M. R. M., Zainudin, E. S., et al. (2022). Nanocellulose-based nanocomposites for sustainable applications: A review. *Nanomaterials, 12*(19), 3483. https://doi.org/10.3390/nano12193483

Norrrahim, M. N. F., Knight, V. F., Nurazzi, N. M., Jenol, M. A., Misenan, M. S. M., Janudin, N., et al. (2022). The frontiers of functionalized nanocellulose-based composites and their application as chemical sensors. *Polymers, 14*(20), 4461. https://doi.org/10.3390/polym14204461

Oladele, I. O., Bichang'a, D. O., Borisade, S. G., Isola-Makinde, B. A., Akinbamiyorin, I., & Githinji, D. N. (2024). Recent advancements in the application of natural fibre/particulate based polymer composites in automotive industry: a review on sustainable development. *Matériaux & Techniques, 112*(4), 402. https://doi.org/10.1051/mattech/2024020

Ong, X. R., Chen, A. X., Li, N., Yang, Y. Y., & Luo, H. K. (2023). Nanocellulose: Recent advances toward biomedical applications. *Small Science, 3*(2), 2200076. https://doi.org/10.1002/smsc.202200076

Oun, A. A., Shankar, S., & Rhim, J. W. (2020). Multifunctional nanocellulose/metal and metal oxide nanoparticle hybrid nanomaterials. *Critical Reviews in Food Science and Nutrition, 60*(3), 435–460. https://doi.org/10.1080/10408398.2018.1536966

Palem, R. R., Ramesh, S., Rabani, I., Shimoga, G., Bathula, C., Kim, H. S., et al. (2022). Microstructurally assembled transition metal oxides with cellulose nanocrystals for high-performance supercapacitors. *Journal of Energy Storage, 50*, 104712. https://doi.org/10.1016/j.est.2022.104712

Pan, Y., Qin, Z., Kheiri, S., Ying, B., Pan, P., Peng, R., & Liu, X. (2022). Optical printing of conductive silver on ultrasmooth nanocellulose paper for flexible electronics. *Advanced Engineering Materials, 24*(7), 2101598. https://doi.org/10.1002/adem.202101598

Pasupuleti, R. R., Tsai, P. C., & Ponnusamy, V. K. (2021). Low-cost disposable poly(ethyleneimine)-functionalized carbon nanofibers coated cellulose paper as efficient solid phase extraction sorbent material for the extraction of parahydroxybenzoates from environmental waters. *Chemosphere, 267*, 129274. https://doi.org/10.1016/j.chemosphere.2020.129274

Paul, J., & Ahankari, S. S. (2023). Nanocellulose-based aerogels for water purification: A review. *Carbohydrate Polymers, 309*, 120677. https://doi.org/10.1016/j.carbpol.2023.120677

Pinto, R. J. B., Martins, M. A., Lucas, J. M. F., Vilela, C., Sales, A. J. M., Costa, L. C., et al. (2020). Highly electroconductive nanopapers based on nanocellulose and copper nanowires: A new generation of flexible and sustainable electrical materials. *ACS Applied Materials & Interfaces, 12*(30), 34208–34216. https://doi.org/10.1021/acsami.0c09257

Qin, X., Zhang, Z., Yang, T., Yuan, L., Guo, Y., & Yang, X. (2022). Auto-fluorescence of cellulose paper with spatial solid phrase dispersion-induced fluorescence enhancement behavior for three heavy metal ions detection. *Food Chemistry, 389*, 133093. https://doi.org/10.1016/j.foodchem.2022.133093

Sadi, M. S., & Kumpikaitė, E. (2023). Highly conductive composites using polypyrrole and carbon nanotubes on polydopamine functionalized cotton fabric for wearable sensing and heating applications. *Cellulose, 30*(12), 7981–7999. https://doi.org/10.1007/s10570-023-05356-9

Saleh, A. K., Ray, J. B., El-Sayed, M. H., Alalawy, A. I., Omer, N., Abdelaziz, M. A., & Abouzeid, R. (2024). Functionalization of bacterial cellulose: Exploring diverse applications and biomedical innovations: A review. *International Journal of Biological Macromolecules, 264*, 130454. https://doi.org/10.1016/j.ijbiomac.2024.130454

Sarwar, M. S., Niazi, M. B. K., Jahan, Z., Ahmad, T., & Hussain, A. (2018). Preparation and characterization of PVA/nanocellulose/ag nanocomposite films for antimicrobial food packaging. *Carbohydrate Polymers, 184*, 453–464. https://doi.org/10.1016/j.carbpol.2017.12.068

Sebagala, I., Rwahwire, S., & Tumusiime, G. (2024). The effect of nanocellulose and alkali treatment on the thermal and mechanical properties of hybrid barkcloth-banana fiber reinforced polyester bio composites. *Polymer Bulletin, 81*, 14547–14560. https://doi.org/10.1007/s00289-024-05390-y

Sepahvand, S., Kargarzadeh, H., Jonoobi, M., Ashori, A., Ismaeilimoghadam, S., Varghese, R. T., et al. (2023). Recent developments in nanocellulose-based aerogels as air filters: A review.

International Journal of Biological Macromolecules, 246, 125721. https://doi.org/10.1016/j.ijbiomac.2023.125721

Shaghaleh, H., Alhaj Hamoud, Y., & Sun, Q. (2024). Functionalized nanocellulose nanocomposite hydrogels for soil and water pollution prevention, remediation, and monitoring: A critical review on fabrication, application properties, and potential mechanisms. *Journal of Environmental Chemical Engineering, 12*(1), 111892. https://doi.org/10.1016/j.jece.2024.111892

Shao, C., Wang, M., Meng, L., Chang, H., Wang, B., Xu, F., et al. (2018). Mussel-inspired cellulose nanocomposite tough hydrogels with synergistic self-healing, adhesive, and strain-sensitive properties. *Chemistry of Materials, 30*(9), 3110–3121. https://doi.org/10.1021/acs.chemmater.8b01172

Shi, L., Hong, G., Chen, C., Li, X., Zhang, H., Chai, R., & Sun, D. (2023). Growth of spiral ganglion neurons induced by graphene oxide/oxidized bacterial cellulose composite hydrogel. *Carbohydrate Polymers, 311*, 120749. https://doi.org/10.1016/j.carbpol.2023.120749

Silva, R. R., Raymundo-Pereira, P. a., Campos, A. m., Wilson, D., Otoni, C. G., Barud, H. S., et al. (2020). Microbial nanocellulose adherent to human skin used in electrochemical sensors to detect metal ions and biomarkers in sweat. *Talanta*, *218*, 121153. https://doi.org/10.1016/j.talanta.2020.121153

Souza, A. G., Ferreira, R. R., Paula, L. C., Mitra, S. K., & Rosa, D. S. (2021). Starch-based films enriched with nanocellulose-stabilized pickering emulsions containing different essential oils for possible applications in food packaging. *Food Packaging and Shelf Life, 27*, 100615. https://doi.org/10.1016/j.fpsl.2020.100615

Sukhavattanakul, P., & Manuspiya, H. (2020). Fabrication of hybrid thin film based on bacterial cellulose nanocrystals and metal nanoparticles with hydrogen sulfide gas sensor ability. *Carbohydrate Polymers, 230*, 115566. https://doi.org/10.1016/j.carbpol.2019.115566

Tachibana, S., Wang, Y. F., Sekine, T., Takeda, Y., Hong, J., Yoshida, A., et al. (2022). A printed flexible humidity sensor with high sensitivity and fast response using a cellulose nanofiber/carbon black composite. *ACS Applied Materials & Interfaces, 14*(4), 5721–5728. https://doi.org/10.1021/acsami.1c20918

Tang, Y., Petropoulos, K., Kurth, F., Gao, H., Migliorelli, D., Guenat, O., et al. (2020). Screen-printed glucose sensors modified with cellulose nanocrystals (CNCs) for cell culture monitoring. *Biosensors, 10*(9), 125. https://doi.org/10.3390/bios10090125

Teodoro, K. B. R., Sanfelice, R. C., Migliorini, F. L., Pavinatto, A., Facure, M. H. M., & Correa, D. S. (2021). A review on the role and performance of cellulose nanomaterials in sensors. *ACS Sensors, 6*(7), 2473–2496. https://doi.org/10.1021/acssensors.1c00473

Thi, Q. V., Ko, J., Jo, Y., & Joo, Y. (2022). Ion-incorporative, degradable nanocellulose crystal substrate for sustainable carbon-based electronics. *ACS Applied Materials & Interfaces, 14*(38), 43538–43546. https://doi.org/10.1021/acsami.2c10437

Thomas, B., Raj, M. C., Joy, J., Moores, A., Drisko, G. L., & Sanchez, C. (2018). Nanocellulose, a versatile green platform: From biosources to materials and their applications. *Chemical Reviews, 118*(24), 11575–11625. https://doi.org/10.1021/acs.chemrev.7b00627

Trache, D., Tarchoun, A. F., Abdelaziz, A., Bessa, W., Thakur, S., Hussin, M. H., et al. (2024). A comprehensive review on processing, characteristics, and applications of cellulose nanofibrils/graphene hybrid-based nanocomposites: Toward a synergy between two-star nanomaterials. *International Journal of Biological Macromolecules, 268*, 131633. https://doi.org/10.1016/j.ijbiomac.2024.131633

Uusi-Tarkka, E. K., Skrifvars, M., & Haapala, A. (2021). Fabricating sustainable all-cellulose composites. *Applied Sciences (Switzerland), 11*(21), 10069. https://doi.org/10.3390/app112110069

Wang, Z., Pan, R., Sun, R., Edström, K., Strømme, M., & Nyholm, L. (2018). Nanocellulose structured paper-based Lithium metal batteries. *ACS Applied Energy Materials, 1*(8), 4341–4350. https://doi.org/10.1021/acsaem.8b00961

Wang, H., Wang, J., Liu, G., Zhang, Z., & Hou, X. (2019). Electrochemical sensing of Pb(II) and Cd(II) in decorative material of wood panel using nano-cellulose paper-based electrode

modified using graphene/multi-walled carbon nanotubes/bismuth film. *International Journal of Electrochemical Science, 14*, 11253–11266. https://doi.org/10.20964/2019.12.13

Wang, M., Li, R., Feng, X., Dang, C., Dai, F., Yin, X., et al. (2020). Cellulose nanofiber-reinforced ionic conductors for multifunctional sensors and devices. *ACS Applied Materials & Interfaces, 12*(24), 27545–27554. https://doi.org/10.1021/acsami.0c04907

Wang, L., Cheng, T., Lian, W., Zhang, M., Lu, B., Dong, B., et al. (2022). Flexible layered cotton cellulose-based nanofibrous membranes for piezoelectric energy harvesting and self-powered sensing. *Carbohydrate Polymers, 275*, 118740. https://doi.org/10.1016/j.carbpol.2021.118740

Wang, Y., Qi, J., Zhang, M., Xu, T., Zheng, C., Yuan, Z., et al. (2024). Cellulose-based aerogels, films, and fibers for advanced biomedical applications. *Chemical Engineering Journal, 497*, 154434. https://doi.org/10.1016/j.cej.2024.154434

Williams, N. X., Bullard, G., Brooke, N., Therien, M. J., & Franklin, A. D. (2021). Printable and recyclable carbon electronics using crystalline nanocellulose dielectrics. *Nature Electronics, 4*(4), 261–268. https://doi.org/10.1038/s41928-021-00574-0

Wohlert, J., Chen, P., Berglund, L. A., & Lo Re, G. (2024). Acetylation of nanocellulose: Miscibility and reinforcement mechanisms in polymer nanocomposites. *ACS Nano, 18*(3), 1882–1891. https://doi.org/10.1021/acsnano.3c04872

Xian, L., You, R., Lu, D., Wu, C., Feng, S., & Lu, Y. (2020). Surface-modified paper-based SERS substrates for direct-droplet quantitative determination of trace substances. *Cellulose, 27*(3), 1483–1495. https://doi.org/10.1007/s10570-019-02855-6

Xiong, C., Zheng, C., Zhang, Z., Xiong, Q., Zhou, Q., Li, D., et al. (2024). Polyaniline @ cellulose nanofibers multifunctional composite material for supercapacitors, electromagnetic interference shielding and sensing. *Journal of Materiomics, 11*(1), 100841. https://doi.org/10.1016/j.jmat.2024.01.015

Yan, C., Wang, J., Kang, W., Cui, M., Wang, X., Foo, C. Y., et al. (2014). Highly stretchable piezoresistive graphene-nanocellulose nanopaper for strain sensors. *Advanced Materials, 26*(13), 2022–2027. https://doi.org/10.1002/adma.201304742

Ye, Y., Zhang, Y., Chen, Y., Han, X., & Jiang, F. (2020). Cellulose nanofibrils enhanced, strong, stretchable, freezing-tolerant ionic conductive organohydrogel for multi-functional sensors. *Advanced Functional Materials, 30*(35), 200340. https://doi.org/10.1002/adfm.202003430

Yu, Z., Wang, W., Kong, F., Lin, M., & Mustapha, A. (2019). Cellulose nanofibril/silver nanoparticle composite as an active food packaging system and its toxicity to human colon cells. *International Journal of Biological Macromolecules, 129*, 887–894. https://doi.org/10.1016/j.ijbiomac.2019.02.084

Yu, H., Tian, Y., Dirican, M., Fang, D., Yan, C., Xie, J., et al. (2021). Flexible, transparent and tough silver nanowire/nanocellulose electrodes for flexible touch screen panels. *Carbohydrate Polymers, 273*, 118539. https://doi.org/10.1016/j.carbpol.2021.118539

Zhang, S., Xu, J., Huang, Y., Liu, Z., & Jiang, S. (2022). Monodisperse Ag nanoparticle-decorated bacterial nanocellulose as flexible surface-enhanced Raman scattering sensors for trace detection of toxic thiram. *ACS Applied Nano Materials, 5*(12), 18519–18530. https://doi.org/10.1021/acsanm.2c04325

Zhang, F., Xu, K., Bai, Y., & Wang, P. (2023a). Multifunctional cellulose paper-based materials. *Cellulose, 30*(14), 8539–8569. https://doi.org/10.1007/s10570-023-05426-y

Zhang, X., Elsayed, I., Navarathna, C., Schueneman, G. T., & Hassan, E. B. (2019). Biohybrid hydrogel and aerogel from self-assembled nanocellulose and nanochitin as a high-efficiency adsorbent for water purification. *ACS applied materials & interfaces, 11*(50), 46714–46725. https://doi.org/10.1021/acsami.9b15139

Zhang, Z., Ahmed, A. I. S., Malik, M. Z., Ali, N., Khan, A., Ali, F., et al. (2023b). Cellulose/inorganic nanoparticles-based nano-biocomposite for abatement of water and wastewater pollutants. *Chemosphere, 313*, 137483. https://doi.org/10.1016/j.chemosphere.2022.137483

Zheng, Z., Zhang, R., Song, Y., Zhao, Q., Qu, M., Tang, P., et al. (2024). Cellulose/nanocarbon composite based multifunctional aerogels for thermal management. *Materials Today Communications, 38*, 107701. https://doi.org/10.1016/j.mtcomm.2023.107701

Zhu, P., Wei, Y., Kuang, Y., Qian, Y., Liu, Y., Jiang, F., et al. (2022a). Porous and conductive cellulose nanofiber/carbon nanotube foam as a humidity sensor with high sensitivity. *Carbohydrate Polymers, 292*, 119684. https://doi.org/10.1016/j.carbpol.2022.119684

Zhu, Q., Wang, T., Wei, Y., Sun, X., Zhang, S., Wang, X., et al. (2022b). Low-cost, environmentally friendly and high-performance cellulose-based triboelectric nanogenerator for self-powered human motion monitoring. *Cellulose, 29*(16), 8733–8747. https://doi.org/10.1007/s10570-022-04800-6

Zhu, M., Zhang, J., Xu, W., Xiong, R., & Huang, C. (2023). Cellulose-based fibrous materials for self-powered wearable pressure sensor: A mini review. *Cellulose, 30*(4), 1981–1998. https://doi.org/10.1007/s10570-022-05023-5

Zubair, M., Yasir, M., Ponnamma, D., Mazhar, H., Sedlarik, V., Hawari, A. H., et al. (2024). Recent advances in nanocellulose-based two-dimensional nanostructured membranes for sustainable water purification: A review. *Carbohydrate Polymers, 329*, 121775. https://doi.org/10.1016/j.carbpol.2024.121775

Part IV
Paper-Based Device Technology

Chapter 21
Advantages and Limitations of Using Paper in Sensors and Electronic Devices

Ghenadii Korotcenkov

21.1 Introduction

Currently, paper technology is considered as a new alternative technology for manufacturing simple, low-cost, and flexible sensors and electronic devices (Korotcenkov, 2025; Liu et al., 2017; Tai et al., 2020; Tobjörk & Österbacka, 2011; Zhang et al., 2018; Zhu et al., 2016). Compared to other commonly used materials such as polyethylene terephthalate (PET) and glass, paper is 200 times cheaper than PET and 1000 times cheaper than glass (Nery & Kubota, 2013). The wide variety of existing forms of cellulose, the high molecular weight of the polymer, and its ability to form three-dimensional networks lead to the emergence of paper-based materials of different morphology and assembly in the form of sheets, fibers, and globular particles (Fig. 21.1). In addition, various processes of cellulose treatment make it possible to transform it into a hydrogel or aerogel state. Each of these forms of cellulose has characteristic properties that are important for different applications. In particular, the unique properties of paper (Cabrera et al., 2011; Han et al., 2021; Nery & Kubota, 2013; Romanholo et al., 2020; Santhiago et al., 2018), such as its versatility, commercial availability, high quantity, low cost, light weight (~10 mg/cm^2), small thickness, available in a wide range of thicknesses (0.07–1 mm), high porosity, sufficient biocompatibility for bioassays, high thermal stability for reliable application, high mechanical strength to resist wear and tear, and increased Young's modulus values make paper a promising platform for the development of flexible wearable electronics, portable and disposable analytical devices for many applications including clinical diagnostics, food quality control, safety, healthcare and environmental monitoring (Costa et al., 2014; Khan et al., 2021; Martinez et al., 2010; Nguyen & Kim, 2020; Singh et al., 2018; Tai et al., 2020; Yao et al., 2022).

G. Korotcenkov (✉)
Department of Physics and Engineering, Moldova State University, Chisinau, Moldova

G. Korotcenkov (ed.), *The Handbook of Paper-Based Sensors and Devices*,
https://doi.org/10.1007/978-3-031-91080-7_21

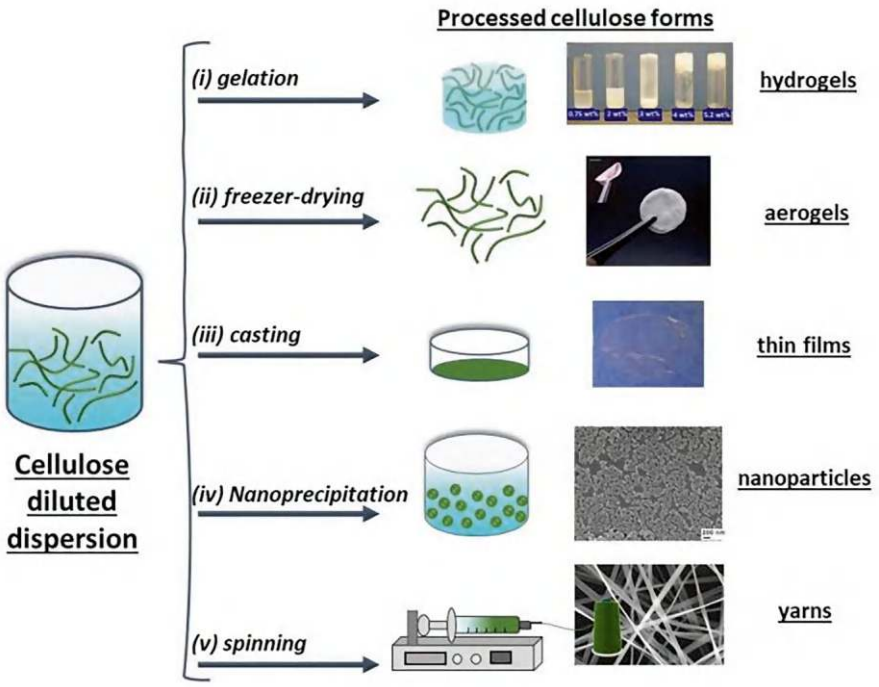

Fig. 21.1 Representation of different approaches for processing cellulose dispersions resulting in (i) hydrogels from cotton CNC suspensions at different CNC concentrations (Wu et al., 2014), (ii) highly flexible CNF aerogel formed by freezer-drying of a CNF hydrogel (Chen et al., 2011), (iii) thin films prepared from a 10 times homogenized dispersion of MFC 0.13 wt% (Aulin et al., 2010), (iv) nanoparticles of cellulose acetate (CA) formed by the dropwise adding of water into an 4 mg CA/mL acetone solution (Hornig & Heinze, 2008), and (v) SEM images of cellulose acetate (CA) yarns prepared by electrospinning 17 wt% CA solution in acetone/water (85/15 v/v) solution (Son et al., 2004). (Reprinted from Gabrielli and Frasconi (2022). Published 2022 by MDPI as open access. All images used in this Figure have been adapted and reproduced with permission from: (i) © 2014 Wiley Periodicals, Inc. (ii) © The Royal Society of Chemistry 2011, (iii) © Springer Science+Business Media B.V. 2010, (iv) © 2008, American Chemical Society, (v) © 2004, American Chemical Society)

The main advantages of paper as a substrate compared to traditional materials used in the development of sensors and electronic devices are summarized in Table 21.1.

In addition, the porous nature of the paper allows it to be used as a filter paper through which liquids or particles smaller than the pore size can pass while larger particles are retained. Cellulose also has good sorption properties. As a result, cellulose-based membranes can be used for absorption of organic and inorganic toxins, filtration of bacteria, viruses, and ionic contaminants, photocatalytic dye removal, and detection of aqueous toxins (Chen et al., 2016; Khan et al., 2021).

It is important to note that the use of paper as a tool for analytical research has a long history. For example, already at the beginning of the twentieth century, paper began to be used in chromatography (Clegg, 1950), and in 1956 the first

Table 21.1 Comparison of paper with traditional materials as substrates

			Material	
Property	Glass	Silicon	Polydimethylsiloxane (PDMS)	Paper
Surface profile	Very low	Very low	Very low	Moderate
Flexibility	No	No	Yes	Yes
Structure	Solid	Solid	Solid, gas permeable	Fibrous
Surface-to-volume ration	Low	Low	Low	High
Fluid flow	Forced	Forced	Forced	Capillary action
Sensitivity to moisture	No	No	No	Yes
Biocompatibility	Yes	Yes	Yes	Yes
Disposability	No	No	No	Yes
Biodegradability	No	No	To some extent	Yes
High-throughput fabrication	Yes	Yes	No	Yes
Functionalization	Difficult	Moderate	Difficult	Easy
Spatial resolution	High	Very high	High	Low to moderate
Homogeneity of the material	Yes	Yes	Yes	No
Price	Moderate	High	Moderate	Low
Initial investment	Moderate	High	Moderate	Low

Source: Reprinted with permission from Nery and Kubota (2013). Copyright 2013; Springer

paper-based sensors were developed (Comer, 1956). It was a device for the semi-quantitative determination of glucose in urine. Since then, such detection devices have been further developed. Paper-based pregnancy tests were developed by Valanis and Perlman (1982), and in 2007, a paper microfluidic device was developed by Martinez et al. (2007) that could simultaneously detect both glucose and protein in urine. However, the first evidence of the use of lab-on-paper technology dates back to 1902, when a patent was issued for paper strips impregnated with hydrophobic materials (Dieterich, 1902). Earlier diagnostic applications of paper-based laboratory testing included determination of nickel and copper salt concentrations (Yagoda, 1937), determination of pH for water analysis, and biological analysis of urine and blood composition (Johnson, 1967). These stages up to 2003 are reflected in more detail in Table 21.2. As we can see, the use of paper as an element of analytical methods begins at the beginning of our era, with the first written reports of Pliny the Elder, who in his book *Natural History* described papyrus-based methods for estimation of the quality of Tyrian purple dye and a spot test for ferrous sulfate (Bostock & Riley, 1855).

Let us now consider in more detail those areas where the advantages of paper are most fully realized, the greatest effect is achieved, and significant progress is ensured in the development of commercially attractive instruments and devices.

Table 21.2 Milestones in the history of paper-based sensing

Year	Milestone
~79	Pliny the Elder presents a method for assessing the quality of Tyrian purple dye using a method similar to papyrus chromatography and a papyrus-based ferrous sulfate spot test (Morgan & Wilson, 2004)
Early 1800s	Gay–Lussac describes the litmus paper test for acids (Crosland, 1978)
1834	The first report on radial paper chromatography was published by Runge, who was working on methods for dye characterization (Weil, 1953)
Nineteenth century	A number of researchers develop papers and dipsticks for dry chemistry tests (Rocco, 2006)
1859	Hugo Schiff reports the first spot test for uric acid that can be detected as a gray precipitate using silver carbonate
1883	G. Oliver describes a paper-based sensor for detecting glucose and protein in urine that is stable at room temperature (Rocco, 2006)
1906	Plesch presents a chromatography-based spot test for bilirubin from urine (Morgan & Wilson, 2004)
1917	F. Feigl and R. Stern proposed a new color detection, culminating in the paper spot-test reaction (Anger, 1971)
1937	Yagoda reports a spot test with defined walls made by paraffin embossing method (Yagoda, 1937)
1949	R.H. Müller and D.L. Clegg describe a paper-based device with walls defined by paraffin embossing for chromatographic separation and reflectance-based detection of dyes and pigments (Muller et al., 1949)
1950s	Electrophoresis on paper becomes a breakthrough in protein separation (Kunkel & Tiselius, 1951; Müller & Clegg, 1949)
1952	A.J.P. Martin and R.L.M. Synge are awarded the Nobel Prize in chemistry for the invention of paper chromatography
1956	A. Keston presents the first colorimetric enzymatic glucose assay on filter paper, based on reaction of o-toluidine with hydrogen peroxide (Rocco, 2006)
1957	J. Kohn describes the first application of reported earlier urine glucose test strips with blood samples (Rocco, 2006)
1964	The first commercial paper test is introduced by the Ames company; an enzymatic blood glucose dipstick called Dextrostix (Rocco, 2006)
1970	The first commercial, battery-powered, portable reflectance meter from Ames company (Rocco, 2006)
1988	First commercial immunoassay; Unipath launches home pregnancy test kits (Chard, 1992; Liu et al., 2012)
1995	US Patent 5,409,664 describes a laminated assay device for detection of cholesterol with walls made by hydrophobic printing or cutting (Allen, 1995)
2003	US Patent 6,573,108 presents the first example of a tangential flow device, incorporating multiple channels, timers indicating the end of analysis, and a filtration step for sample pretreatment. Walls can be made by screen printing, dipping in polymer with a template pressed onto paper, or by a computer-controlled deposition system. Researchers have proposed the use of polymers such as heteropolysaccharides, acrylic polymers and copolymers, and silanes (Hardman et al., 2003)

Source. Data extracted from Nery and Kubota (2013)

21.2 Chemical and Optical Paper-Based Sensors

Research has shown that paper, and especially transparent nanocellulose (read Chap. 12), is an excellent platform for the development of various optical, chemical, electrochemical, optoelectronic, optoelectrochemical, and electro-opto-mechanical devices (Eynaki et al., 2020; Khan et al., 2021; Korotcenkov, 2025; Zhai et al., 2021), where flexible, transparent, and conductive substrates or biocompatible transparent membranes capable of finely dispersing various nanomaterials and biomaterials are needed.

21.2.1 Optoelectrochemical Sensors

Due to its unique properties, cellulose is an important component in the development of substrates for SERS applications. Cellulose is also an exceptional material for making the interface of surface plasmon resonance (SPR) immunosensors. Cellulose, in addition to minimal SERS signal interference, is capable of controlling the growth of metal nanoparticles such as Au, Pd, Ag, and Cu, with various shapes and dimensions (Wu et al., 2013; Yan et al., 2016; Xie et al., 2020). For example, it was shown that negatively charged celluloses, sulfuric acid-hydrolyzed CNC (Padalkar et al., 2010), and TEMPO-oxidized nanofibrillated celluloses (Ifuku et al., 2009) are able to act as capping agents in the synthesis of spherical Ag nanoparticles. These noble metal nanoparticles generate strong surface plasmon resonance (SPR) in the visible and near-infrared regions, used in various biosensors. The three-dimensional structure of cellulose with defined porosity and morphology is an excellent platform for preventing agglomeration/aggregation of metal NPs and controlling the distance between particles (see Fig. 21.2). Cellulose can also form films/membranes with defined porosity (as in the case of cellulose acetate), which is especially important in SPR analysis as it allows the control of analyte binding on

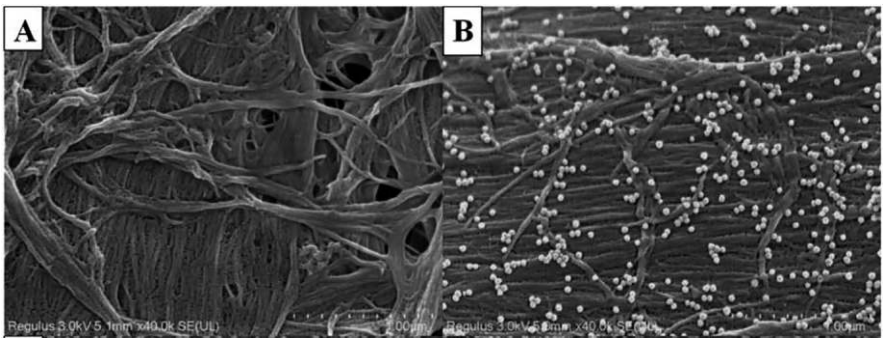

Fig. 21.2 SEM images of filter paper with Au nanoparticles adsorbed on the surface. (Reprinted with permission from Xie et al. (2020). Copyright 2020: Elsevier)

multilayer immobilized antibodies with high sensitivity (Miura et al., 2012). The initiation of capillary flow is another rationale for the use of cellulose acetate and nitrocellulose in the development of certain types of biosensors (Miura et al., 2012).

Paper has the innate ability to adsorb and retain small amounts of liquid on its surface. Researchers have taken advantage of this property to detect chemicals that change color or fluorescence intensity in response to certain stimuli. Moreover, the simple technology of immobilizing fluorophores and chromophores in a cellulose matrix can impart assay-dependent optical properties to the polymer, necessary for the development of highly sensitive colorimetric and fluorescent sensors for specific applications. At the same time, the high hydroxyl content makes it possible to improve the binding of chromophore and fluorophores (Li et al., 2017; Yang et al., 2020) and provide high yields of fluorescent groups in the cellulose matrix. Cellulose can also be used as a scaffold for biomolecules responsible for the sensory response of paper biosensors to various analytical studies. For example, the anchoring of red cabbage pigment (RC) in CNF (Devarayan & Kim, 2015) and carboxymethylcellulose (CMC) (Liang et al., 2019) provides sensor sensitivity to pH and NH_3. The high processability and large surface area of cellulose also lead to improved interactions between analytes, fluorophores, and biomolecules, leading to improved sensor performance (Davis et al., 2010).

It should be emphasized that in addition to its ability to immobilize chromophores and fluorophores in the cellulose matrix, cellulose can also play an active role in the recognition process. For example, the natural chirality of cellulose has been exploited in the development of a chiral fluorescent sensor for aromatic nitro compounds, such as π-basic or π-acid aromatic compounds (Ikai & Okamoto, 2009), which exhibit central and axial chirality (Ikai et al., 2016). The chiral nematic phase of cellulose nanocrystals (CNCs) also allows for the implementation of chiral reflectors or polarized light detectors (Grey et al., 2019). Such characteristics can also be used as a photonic pigment or polarization and wavelength filter by adapting mesoscopic structures (Wei et al., 2019).

21.2.2 Electrochemical Sensors

Research has shown that cellulose paper can serve as an excellent platform for supporting catalysts and enzymes as it can provide both the required surface geometry and optimal hydrophilic/hydrophobic balance (Mahapatra et al., 2021). Thus, the fine fiber pulp and paper matrix, together with its inherent hydrophilicity, provides an excellent biocompatible microenvironment to maintain the catalytic activity of enzymes (Lawrence et al., 2014). The introduction of hydrophobic functionalization of the cellulose surface allows efficient absorption and immobilization of enzymes also through hydrophobic interactions (Koga et al., 2012). Such properties of cellulose contribute to the successful development of high-performance biosensors for various applications (Sun et al., 2021). Several examples of paper-based electrochemical biosensors are shown in Fig. 21.3. Constructions of biosensors

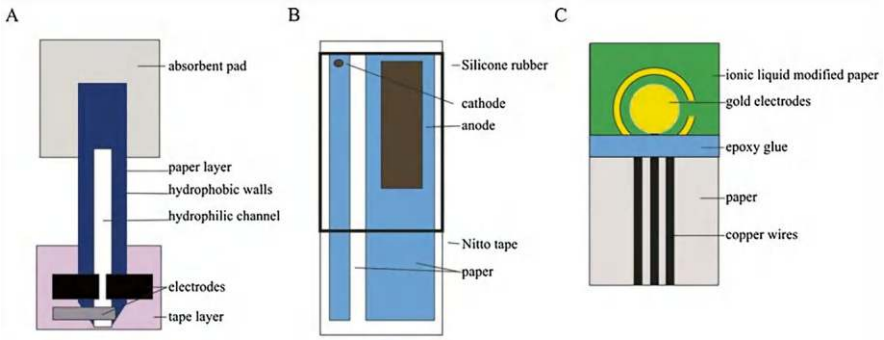

Fig. 21.3 Examples of voltammetric sensors: (**a**) stripping voltammetry measurement of Pb(II); (**b**) Clark-type oxygen electrode; (**c**) oxygen sensor based on nanoporous gold. (Reprinted with permission from Nery and Kubota (2013). Copyright 2013: Springer)

shown in Fig. 21.3 were developed by Nie et al. (2010) (Fig. 21.3a), Yang et al. (1997) (Fig. 21.3b), and Hu et al. (2012) (Fig. 21.3c). The manufacturing features and operating principles of these sensors are described in the relevant articles. It is important to note that these are very cheap sensors. For example, the price of a three-electrode device for analysis of Pb(II), developed by the Whitesides group (Nie et al., 2010) and having a limit of detection of 1.0 ppb, was only $0.02 per device.

The ability to retain metal nanoparticles or carbon-based nanomaterials, such as CNTs or graphene, makes nanocellulose a very promising material for the development of electrodes for various electrochemical devices (Gabrielli & Frasconi, 2022). Nanomaterials used to coat cellulose directly affect the specific surface area of the electrode and the immobilization of the receptor, and hence its interaction with the analyte, which directly affects the electrical conductivity and electrocatalytic properties of the electrodes and helps to increase the sensitivity threshold of sensors and improve the selectivity of their sensory response. The large surface-to-volume ratio that allows storage of reagents in large quantities, the mesoporous structure with tunable porosity in which electrolytes and ions can diffuse, and the stable electrochemical and mechanical properties of nanocellulose are an additional bonus to its use in electrochemical sensors and biosensors (Migliorini et al., 2019).

It is important to note that the emergence of conductive cellulose based on nanocomposites, containing graphene (Chen et al., 2018), graphene oxide (GO) (El Miri et al., 2016), single-walled carbon nanotubes (SWCNT) (Koga et al., 2013), multiwalled carbon nanotubes (MWCNTS) (Durairaj et al., 2021), and nanodiamonds (Morimune-Moriya et al., 2018), further expands the use of cellulose in the development of electrochemical sensors (Kumar et al., 2019). Thus, due to their excellent electrochemical properties, various nanocomposites containing nanocelluloses and MWCNTs or SWCNTs have been proposed as electrode materials for amperometric detection of biomolecules. For example, a composite membrane assembled from MWCNTs and sulfated nanofibrillar cellulose (SNFC) has been used for selective

and sensitive detection of various analytes in pharmaceutical products and biological fluids (Durairaj et al., 2021; Shalauddin et al., 2019).

21.2.3 Gas and Humidity Sensors

Gas and humidity sensors are another promising area of application for paper, which has important properties for these applications such as a large active surface area, an extremely high surface-to-volume ratio combined with a porous structure that provides high gas permeability, and good adsorption capacity (Korotcenkov, 2023; Korotcenkov et al., 2023). Moreover, in these applications, paper can act as both a substrate for gas and humidity sensitive material (Mirica et al., 2013; Toniolo et al., 2013), and an active material, the properties of which can be chemically functionalized in order to adapt to specific applications (Bracher et al., 2010; Güder et al., 2016) In particular, cellulose molecules contain three hydroxyl (-OH) groups that can be modified to achieve high chemical reactivity. Typically, to achieve the required sensitivity to certain gases, cellulose is functionalized with conductive materials such as CNTs, graphene, conductive polymers, or metal oxides (Korotcenkov et al., 2023; Mirica et al., 2012, 2013). In addition, the surface properties of the paper can also be easily manipulated by changing the printing, coating, and impregnation conditions.

The mechanism of gas and humidity paper-based sensors operation is based on the fact that cellulose fibers of paper tend to absorb moisture from the environment or interact with active gas components that are hazardous to human health (Korotcenkov, 2023). The result of this interaction is a change in dielectric constant, i.e., capacity, and ionic conductivity of paper, for example, increase/decrease in resistance with decreasing/increasing concentration of gas or water vapor in the atmosphere (see Fig. 21.4a).

Paper-based gas sensors have proven sensitive to hazardous gases such as ammonia, acetonitrile, toluene, cyclohexanone, and nitrogen dioxide (Han et al., 2014b; Mirica et al., 2012, 2013). However, from a practical point of view, the results obtained during the development of humidity sensors are more significant (Korotcenkov et al., 2023). It turned out that with the help of such sensors, it is possible to easily monitor a person's respiratory activity, as evidenced by the ability to distinguish between different breathing patterns. Additionally, paper sensors can be integrated into a general face mask, detecting breathing status in a wearable manner and transmitting signals to the client's mobile device (e.g., phone and tablet) to store, analyze, and display the information (Fig. 21.4b). Gas sensors and humidity sensors can also be integrated into the paper skin multisensory platform for simultaneous environmental monitoring (Nassar et al., 2016). These same sensors can also be built into diapers to signal the presence of moisture in the diapers. The use of paper ensures that such disposable sensors have a very low cost.

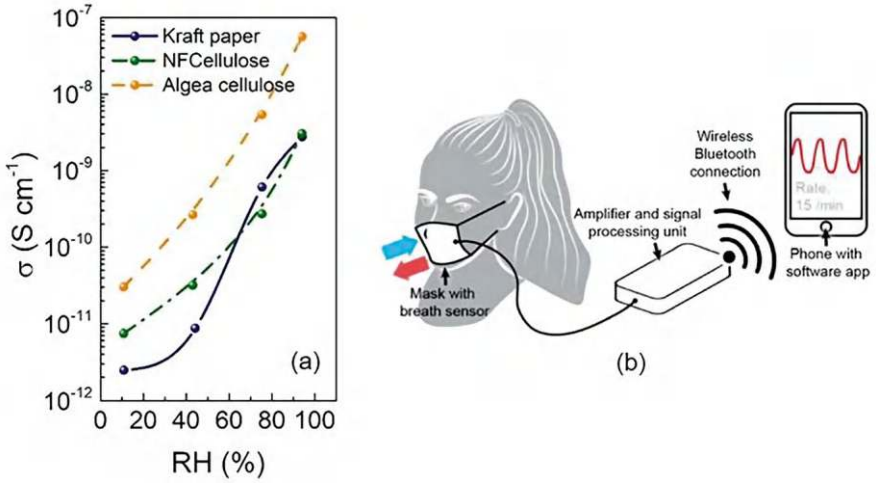

Fig. 21.4 (**a**) Conductivity variation with the RH for kraft paper, wood nanofibrillated, and algae cellulose. (Reprinted with permission from Le Bras et al. (2015). Copyright 2015: ACS); (**b**) Promising wearable applications of RH sensors as respiration sensors. The entire respiration monitoring system consisting of a facemask embedded with a paper respiration sensor, a signal processing circuit, and a mobile device for data display and analysis. (Reprinted with permission from Güder et al. (2016). Copyright 2016: Wiley)

21.2.4 Microfluidic Analytical Devices

Another important property of paper that makes it widely used is the ability of paper to be used for the development of microfluidic devices (commonly known as μPAD (microfluidic paper-based analytical device)), which in many cases are basic analytical instruments for human measurement and disease diagnosis (Gong & Sinton, 2017; Santhiago et al., 2014; Xu et al., 2014). One example of such μPADs is shown in Fig. 21.5. Typically, when making μPADs, a border is applied to a paper substrate, thereby creating a physical barrier to pattern hydrophilic channels, as well as the sample and test zones (see Fig. 21.6). Each test zone is coated with appropriate bioreceptors to detect target analytes, and microfluidic channels are responsible for the autonomous transfer of target analytes from the sample to the test zones through capillary forces (Nandy et al., 2021).

Due to the natural properties of paper, liquid substances can flow through certain channels formed in the paper through capillary action without relying on external forces (Gong & Sinton, 2017; Yang et al., 2017). At the same time, the properties of the paper matrix such as thickness, porosity, hydrophilicity, permeability, roughness, and wettability allow microfluidic behavior to be fine-tuned to meet different requirements that arise when developing sensors for various purposes (Bohm & Biesalski, 2017; Renault et al., 2014; Shen et al., 2019). In addition, thicknesses of tens and hundreds of micrometers result in a small overall volume of solutions required for analysis. Mechanical flexibility also allows the paper to form complex

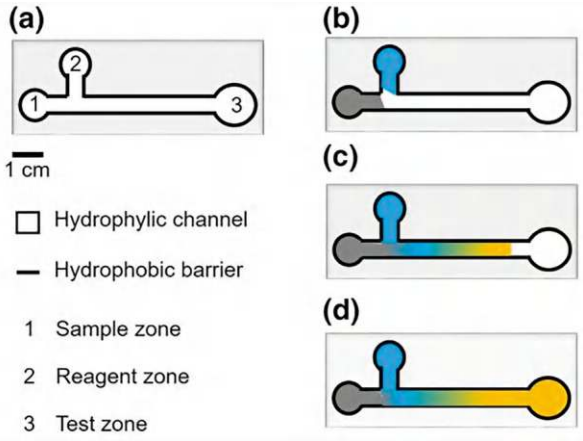

Fig. 21.5 Scheme of a simple wax-based ink printed μPAD. (**a**) Description of the different zones of the device; (**b**) initial stage of the assay with sample and reagent confined in their zones; (**c**) sample and reagent flow through the hydrophilic channel and start to react; (d) end of the assay with the end-product of the reaction reaching the test zone. (Reprinted with permission from Doménech-Carbó and Doménech-Carbó (2022). Copyright 2022: Springer)

2D and 3D structures. These characteristics make paper an ideal platform for the development of microfluidic analytical devices with high sensitivity, low cost, small size, portability, ease of operation, and short analysis time (Santhiago et al., 2014). The integration of such devices into wearable electronics opens up opportunities for new functions such as micrototal analysis (Son et al., 2014). Various analytical operations typically performed in the laboratory, including sample pretreatment, transport, mixing, separation, reaction, filtration, and determination, can be easily adapted to paper-based microfluidics using smart instruments such as smartphones (Wang et al., 2017). Leveraging the existing mobile phone infrastructure for health and environmental monitoring will speed up the diagnostic process and also help expand affordable healthcare options for existing and emerging diseases (Khan et al., 2021). Such microfluidic devices are especially needed in kindergartens where there is limited access to advanced analytical equipment (Hu et al. 2014b; Yao et al., 2022). The use of paper sensors will also allow low-income regions to significantly expand the range of medical services provided at a low cost. Standard medical tests performed in centralized laboratories are either unavailable in such countries or are too expensive for most citizens. At the same time, paper-based sensors, which are inexpensive and easy to use, can be used in resource-limited settings. Paper-based detection platforms also have great potential for use in remote areas and during emergency situations where fully equipped facilities and highly trained medical personnel are not available. Finally, paper/cellulose, as a widely available, lightweight, easy-to-process, and inexpensive material, allows its use as substrate for disposable sensors (Nandy et al., 2021).

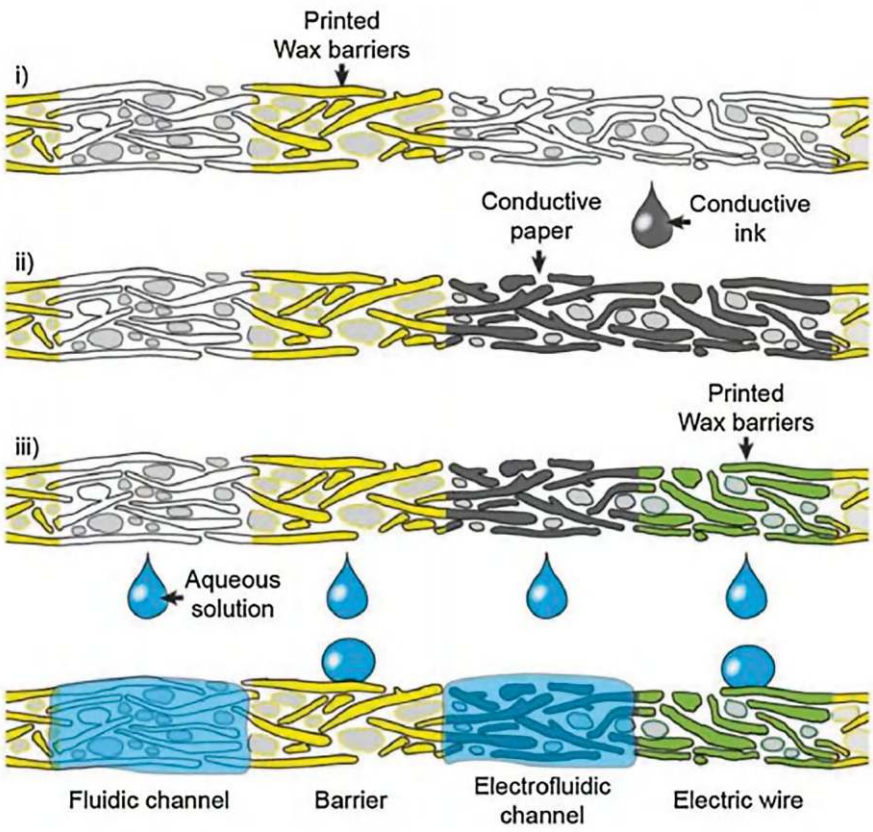

Fig. 21.6 Schematic diagram illustrating the principles of fabrication of microfluidic sensors with the help of wax barriers: (i) Printing wax on paper to form a channel for conductive materials inside the paper. (ii) Adding inks to the wax-defined channels. (iii) Another round of wax printing to further confine the liquid microfluidic channel and fix the conductive network. (Reprinted with permission from Liu et al. (2017). Copyright 2017: Elsevier)

21.3 Physical Sensors

Conductive paper, which has a fibrous structure, is also of interest for the development of electromechanical sensors capable of measuring mechanical stress, pressure, or displacement (Zhang et al., 2018). For these systems, the measurement is based on the change in capacitance or conductivity of the nanocellulose under mechanical stress. Under the influence of a tensile or compressive force, a change in the contact area between the fibers occurs, which leads to an increase or decrease in the resistance of the material, or a change in the distance between the metal electrodes applied to the paper on both sides. Nanocellulose is particularly useful due to its inherent anisotropy of properties (Dieter et al., 2005; Perez & Samain, 2010). This feature of nanocellulose has found application in a strain sensor capable of

responding differently to forces applied parallel or perpendicular to aligned cellulose fibers (Chen et al., 2018).

As shown by Mun et al. (2016) and Gao et al. (2019), strain sensors can also be created based on thin Ag NW films deposited on the surface of flexible nanocellulose substrates. The amount of deformation in this case is estimated by measuring the change in the resistance of the surface layer of the Ag NW film. According to Gao et al. (2019), by using conventional tissue paper, NCP, AgNW, and nanosilver conductive ink, such pressure sensors are characterized by low cost, easy fabrication, quick preparation for use, and easy disposal by incineration. The working mechanism of such sensors and examples of their application are shown in Fig. 21.7. Nanocellulose substrates, unlike traditional flexible substrates (De et al., 2009), also

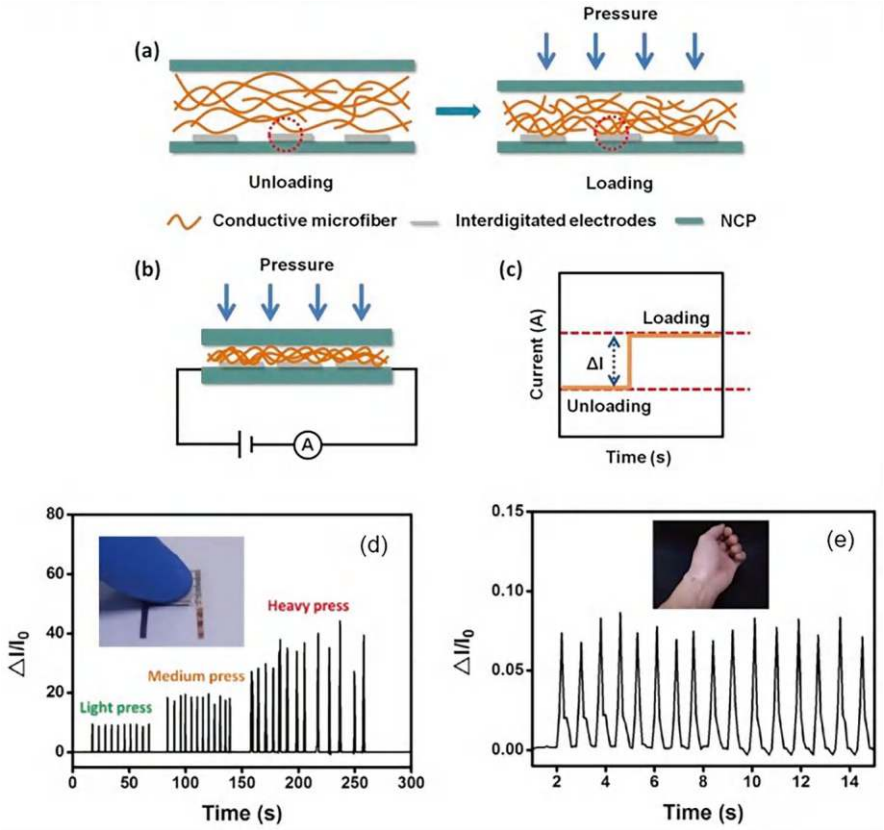

Fig. 21.7 Working mechanism of all paper-based piezoresistive (APBP) pressure sensor. (**a**) Compressive deformation of a sensitive material under external pressure. (**b**) The device connection during characterizing performance of the APBP pressure sensor. (**c**) Increasing the ADBP sensor current under external pressure; (**d**) Real-time pressure sensor response. (**e**) Detection of the arterial heart pulse on the wrist, with the heart beats of 75 times per minute. (Reprinted with permission from Gao et al. (2019). Copyright 2019: ACS)

promote better adhesion of the metal film. Research shows that pressure sensors can also be created based on cellulose in the hydrogel state. It was found that both compressive and tensile strains are accompanied by changes in the conductivity of the hydrogel. In (Chen et al., 2020), the observed decrease in conductivity under the influence of compressive and tensile deformations was explained by the narrowing of channels for water molecules and an increase in the resistance to ion movement.

Notably, paper-based pressure sensor designs are simple, cost-effective, scalable, and do not require complex equipment. With such devices, driving forces in different directions can be sensed and various movements involving stretching, torsion, and bending can be controlled (Zhang et al., 2018). These sensors allow real-time and on-site monitoring of reactions to breathing, heart rate on the wrist, and even acoustic vibrations caused by external influences. Paper can also be the basis for the manufacture of temperature sensors. In particular, Nassar and Hussain (2017) used the change in resistance of a silver film deposited on the surface of paper to measure temperature. The rough structure of the paper ensured good adhesion of the film and, as a result, no peeling off of the silver ink was observed. It is important to note that paper-based temperature, pressure, and stress sensors attached to a person can be easily integrated with smart wearable electronics (Takei et al., 2010; Yamada et al., 2011). At the same time, paper-based temperature sensors integrated with humidity sensors can be used to monitor the state of the atmosphere inside food or medicine containers (Khan et al., 2019).

The good mechanical properties of nanocellulose make it possible to create soft electronic muscle actuators based on it (Haldi et al., 2014; Kim et al., 2012, 2015). In particular, in (Kim et al., 2010, 2015) electroactive artificial muscles were created on a paper basis. Such soft electronic muscle actuators are very promising in the era of portable consumer electronics (Liu et al., 2017), since the tactile sensing capabilities, they provide to users, can be used in human-machine interaction, as well as in the development of headset reality and wearable exoskeletons. Desirable actuators for these applications must conform to human motion and be biocompatible. The use of nanocellulose achieves these requirements (Hu et al., 2014a; Zhao et al., 2013).

21.4 Paper-Based Electronics and Optoelectronics

As demonstrated in previous chapters, cellulose is renewable, biodegradable, nontoxic, biocompatible, industrially available at low cost, heat-resistant, printable, and capable of forming highly transparent, flexible, and foldable films suitable for a variety of electronic applications. In addition, cellulose is one of the most common materials in nature. It is important to note that paper substrates make it possible to use printing and writing technologies in the manufacture of various devices, which is an important advantage of paper-based electronics (Sudheshwar et al., 2023; Tobjörk & Österbacka, 2011; Zhang et al., 2018). Writing technology is a promising method for manufacturing paper-based electronics due to its advantages of

simplicity, low cost, speed, and portability. It can be realized using brush pen, fountain pen, and ballpoint pen, which are compatible with various conductive inks, both carbon-based (Han et al., 2014a) and metal-based (Zheng et al., 2013; Li et al., 2014; Russo et al., 2011; Yang et al., 2013). Pencil writing can also be used, which fits well with the fabrication of carbon electronics on paper without the use of any solvents (Kurra & Kulkarni, 2013).

All of these properties characterize cellulose as a powerful alternative to petroleum-based polymers in the development of both highly sensitive sensors and high-performance electronic and optoelectronic devices (Lee et al., 2020). In recent years, a large number of various devices have been developed based on paper, such as supercapacitors, batteries, fuels cells, generators, actuators, RFID tags, and thin film transistors (read corresponding chapters in Vol. 3), which have such important functional properties as bendability and increased efficiency. As is known, the flexibility and stretchability of electronics are critical for wearable electronic devices that involve contact of sensors and therapeutic devices with human skin (Gabrielli & Frasconi, 2022). Rigid electronics pose integration challenges in certain applications where space is limited or electronics must be mounted on curved surfaces such as the human body. Flexible and stretchable electronics transform rigid electronics into a flexible form, allowing them to be integrated into narrow curved spaces (Khan et al., 2021). As a natural dielectric material, paper can also be used as the dielectric substrate or gate of field-effect transistors, the main active element of paper-based electronics (Fortunato et al., 2008; Gaspar et al., 2014; Zschieschang & Klauk, 2019).

Paper, especially transparent paper, is also a successful platform for green photonics (Lee et al., 2020; Pan et al., 2022). Photonic devices based on paper and nanocellulose-based materials, such as light diodes (LEDs), including organic LEDs (OLEDs) (see Fig. 21.8), solar cells, and photodetectors, have been widely studied in recent decades. For example, Barr et al. (2011) developed paper photovoltaic cells that produced enough voltage to power conventional electronic displays in natural indoor light and could be bent and folded without loss of functionality. The optical transparency of nanopaper also allows its use in unique photonic device applications, such as polarization-dependent reflectors, optical resonators, optical sensing, random lasing, and color conversion filtration for light-emitting diodes (LED) (Dumanli et al., 2014; Kim et al., 2016; Orelma et al., 2020).

Since paper is not an inherently active material, the use of cellulose in active photonic devices is typically achieved by embedding semiconductor quantum dots (QDs) into cellulose-based materials. For example, using this approach, Wu and Lin (2017) developed an ultrathin UV photodetector. By embedding ZnO QDs into paper, they were able to achieve increased absorption of UV radiation by the paper. As discussed earlier, the structure of the paper facilitates efficient capture and retention of QDs. There have also been several attempts to develop traditional optical elements such as nanocellulose-based optical fiber (Orelma et al., 2020). The manufacturing process of such an optical fiber and its use as a humidity sensor is shown schematically in Fig. 21.9.

It is important to note that paper also offers the opportunity to develop hybrid electronic circuits (Hamedi et al., 2016). One example of such hybrid circuits is

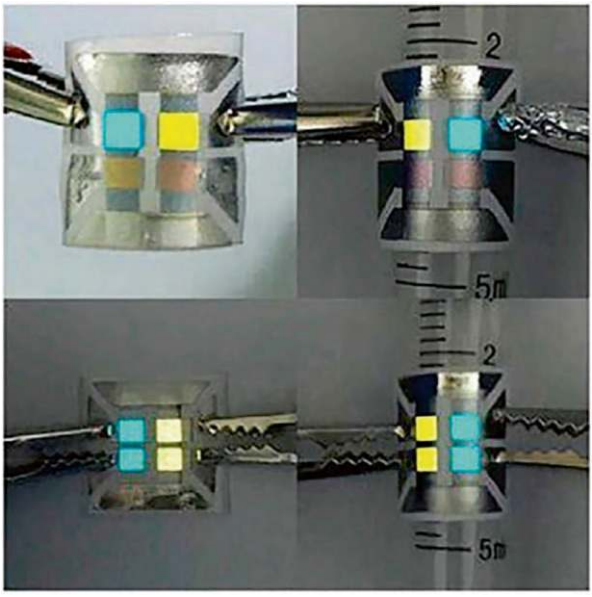

Fig. 21.8 Pictures of dual-microcavity top-emitting (DMT)-OLEDs based on paper substrates. A cross-linked poly(4-vinylphenol) layer was deposited by spin coating and subsequently cross-linked at 160 °C for 2 h; the polypropylene (PVP) layer acts as a buffer. (Reprinted with permission from Zhang et al. (2019). Copyright 2019: American Chemical Society)

shown in Fig. 21.10. The circuit contains several off-the-shelf electronic components (including a microprocessor, transistors, and LEDs) mounted on cellulose nanopaper. The device was folded in the middle (Fig. 21.10b) to form a two-layer structure and provide contact between the resistive heater and the fluid channel. The device's microprocessor was programmed to detect the presence of liquid within the microfluidic channel and execute the programmed thermal cycle.

21.5 Wearable Paper-Based Electronics

Wearable electronics, which include a series of smart electronic accessories and systems that can be conveniently placed on the human body, have recently attracted significant attention from developers around the world (Liu et al., 2017). To reduce the discomfort caused by devices worn directly on the body, lightweight and flexible substrate materials are needed. Until now, various soft materials such as polymers (Hyun et al., 2017) and silicone elastomers (Lu et al., 2014; Viry et al., 2014) have been used as substrates for wearable electronics. Metal foil can also be used for this purpose (Kim et al., 2017). However, these materials, which require an expensive production process (King et al., 1997), have adverse environmental impacts (Powell et al., 1999). Plastic litter is known to be a major source of marine pollution, leading to a rapid decline in global biodiversity (Derraik, 2002).

Other disadvantages of these substrates include poor stability of the formed systems (Hamedi et al., 2016; Yao et al., 2017). Active materials applied to the top

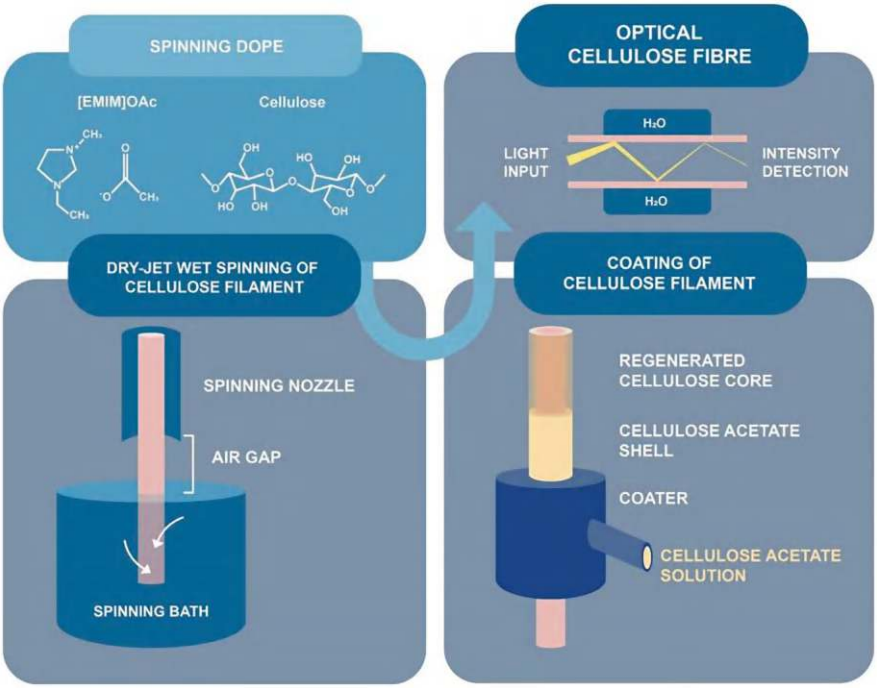

Fig. 21.9 Manufacturing process of optical cellulose fiber. Cellulose was first dissolved in [EMIM]OAc and dry-jet wet spun into water. The water was then evaporated from the filament in a room atmosphere. The optical cladding was produced by coating the cellulose core with cellulose acetate dissolved in acetone. The prepared cellulose optical fiber was connected to a light source and tested as humidity sensors. (Reprinted from Orelma et al. (2020). Published 2020 by Springer as open access)

surface of such substrates cannot adhere firmly to the untreated substrate, and even miniature structures can crack or tear when the substrate is flexed. Another disadvantage is related to the complexity of interconnection and integration of electronic circuit elements manufactured on such substrates. Components formed on opposite sides of the substrate cannot be connected except by cutting holes in the substrate or using external circuits. These substrates are also characterized by a small active surface area. Functional layers are formed on the surface of the substrate and therefore do not exploit the internal architecture of the substrate material (Zhang et al., 2018).

In this regard, the paper substrate does not have these disadvantages (Liu et al., 2017). Paper is made from unprocessed plant (e.g., wood or cotton) cellulose fibers and is therefore recyclable and renewable (Liu et al., 2014). In addition, thanks to good mechanical deformability and biocompatibility, paper provides minimal harmful effects on human skin. Moreover, the low cost, availability, environmental friendliness, and three-dimensional porous structure of paper, which facilitates the manufacturing process (Lessing et al., 2014) and significantly increases the active

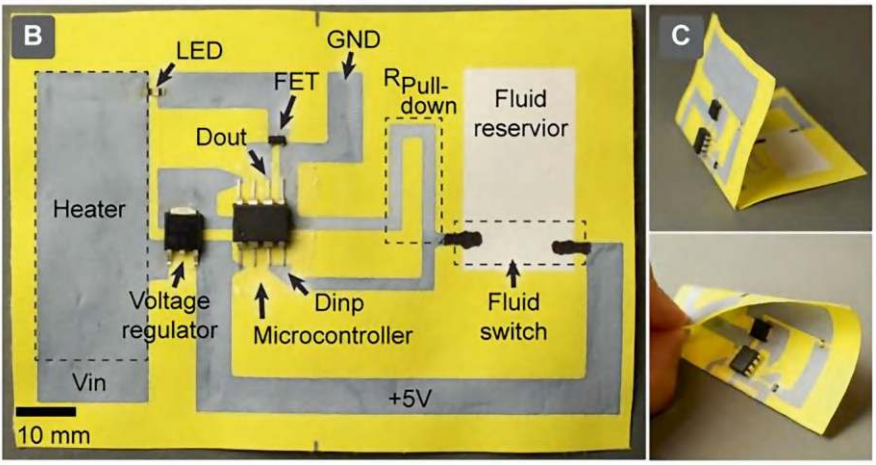

Fig. 21.10 (**a**) Photo of the printed microcontroller-based heater. All the wires are printed on paper, using wax printing and PEDOT inks. The electrical components are mounted on one side using electrically conductive adhesive tapes. (**b**) Photos showing the folding of the paper circuit to form the final device. (Reprinted with permission from Hamedi et al. (2016). Copyright 2016: Wiley)

surface area, pave the way for a fast, simple, and inexpensive process of mastering paper-based electronics technology (Liu et al., 2017). For example, the structure of paper makes it easy to absorb functional reagents and, most importantly, allows the two sides of the paper to be selectively processed to give them different or the same functions (Zheng et al., 2018). Since paper is biocompatible, biodegradable, and flammable, it can be safely disposed of (Nassar et al., 2017), such as by incineration, saving space in e-waste disposal.

Paper products, widely known as recyclable materials, have a recovery rate of about 70%. According to the U.S. Environmental Protection Agency's report on municipal solid waste (MSW), paper waste accounts for 27.4% of total MSW in the United States. However, paper dominates MSW disposal—51% (US EPA, 2014). Paper recycling has improved significantly over the past decades. This saves huge amounts of energy and reduces deforestation. In addition, the paper can be easily stored and transported. Moreover, since paper-based electronics are made from natural substrates of plant origin and do not contain harmful materials, they do not have a toxic effect on natural ecosystems when disposed of.

All of the above suggest that the use of paper and cellulose-based materials is an essential step in the transition to green technologies and green electronics (Cantarella et al., 2023; Liu et al., 2014; Nandy et al., 2021; Prenzel et al., 2021; Scandurra et al., 2023). A key aspect of green technology is reintroduction of electronic devices to nature through repair or recycling methods (Stahel, 2016). How important this is can be judged by the following facts. According to a United Nations report, the world generated a total of more than 50 million tons of e-waste in 2016 alone (Baldé et al., 2020). It is important to note that e-waste is the fastest-growing type of waste

in the world today, of which only 20% is officially recycled (WEF, 2019). This is why it is very important to develop new technologies to prevent the uncontrolled growth of electronic waste. The use of paper and paper electronics is one such solution. Table 21.3 shows a comparison of paper and plastic materials, which are the most commonly used substrates, in terms of impact on climate change and resource use (Prenzel et al., 2021).

Paper properties such as resistance to classical organic solvents can also be highlighted, which gives the paper excellent chemical stability (Budtova & Navard, 2016), as well as higher dimensional stability with temperature changes, and lower thermal expansion compared to most plastics (Hsieh et al., 2013; Huang et al., 2014). This feature of paper substrates allows them to be used at elevated temperatures and reduces the likelihood of complex thermal parasitic effects in the behavior of electronic devices (Zhang et al., 2018).

As it was shown in previous chapters, over the past decades, significant progress has been made in the development of new paper materials based on bacterial cellulose, graphene, as well as carbon microfibers and nanotubes (Kim et al., 2009; Kong et al., 2014) (read Chapters 11–15). These new types of paper demonstrate comparable mechanical flexibility, biosafety, and environmental friendliness, as well as some advantages over traditional cellulose in the manufacture of paper-based electronics. In particular, such nanocomposites containing graphene or carbon fibers are electrically conductive, which facilitates or even eliminates the procedure for increasing the conductivity of paper, which in many cases is mandatory when developing devices for paper-based electronics (Tobjörk & Österbacka, 2011). That is why, recently, nanopaper, graphene paper, and carbon microfiber paper are increasingly used in the development of various paper-based devices (Liu et al., 2017).

Paper has another important advantage. The ease of cutting paper into complex shapes using a laser cutter, paper cutter, or even simple scissors allows the fabrication of complex 3D structures that do not break or tear when bent (Han et al., 2021). Moreover, many researchers have taken advantage of this property of paper to fabricate complex 3D devices inspired by origami (Cybulski et al., 2014). For example, in some laboratories, researchers have used such origami to develop paper-based

Table 21.3 Comparison between paper and the most used plastic substrates, in terms of the impact on climate change and resource use

Substrate material	Climate change impact kg CO_2 eq.[a]/Sheet	Resource use kg Sb eq.[b]/Sheet
Paper[c]	1.3×10^{-4}	5.2×10^{-11}
PET (polyethylene terephthalate)	1.5×10^{-3}	1.8×10^{-10}
PEI (polyetherimide)	1.3×10^{-2}	2.0×10^{-9}
PEEK (polyether ether ketone)	7.4×10^{-3}	2.2×10^{-9}

Source: Reprinted from Scandurra et al. (2023). Published 2023 by MDPI as open access. Data extracted from Prenzel et al. (2021)

[a] Indicator of potential global warming due to emissions of greenhouse gases to the air

[b] Indicator of the depletion of natural non-fossil resources

[c] Sheet with 25 cm^2 surface area, 125 μm thickness

analytical devices (Hamedi et al., 2016) and paper-based energy storage and harvesting devices (Choi et al., 2011; Fraiwan & Choi, 2016). One example of such analytical devices is shown in Fig. 21.11. Such devices cannot be manufactured with either semiconductor or polymer-based substrates.

As shown earlier, paper can be given a variety of properties. Paper may have dielectric properties or be conductive with hydrophobic or hydrophilic surface properties, etc. On this basis, it can be assumed that the existing technology makes it possible to develop a new approach to the manufacture of paper-based devices, which, depending on the processing method, will allow the use of the same locally modified paper as a substrate for electronic circuits, as a matrix for electrolyte, as dielectric or element that provides the device with the necessary functionality. This feature of paper makes it particularly attractive for the development of complex multifunctional electronic devices. For example, as shown in Fig. 21.12, in addition to sensors used for monitoring and active electronic devices such as thin film transistors (Mattana et al., 2017) used to process incoming information, paper can serve as a medium for storage devices. Such paper memory with ultra-low cost and impact on a person during movement was implemented on the basis of thin films of TiO_2 (Acharyya et al., 2014). The manufactured paper memory was mechanically quite strong and resistant to bending. The results showed that paper memory labels attached to the human body remained stable for 10,000 switching cycles and functioned normally under tension and compression, providing the potential for paper memory to be used in wearable electronics. Resistive nonvolatile memory that was developed by Nagashima et al. (2014) using Ag-decorated cellulose nanofiber paper (CNP) also exhibited superflexibility. It was shown that the memory performance of CNP devices was maintained without any degradation when bending up to a radius of 350 μm. At the same time, the devices demonstrated stable effects of non-volatile memory with 6 orders of magnitude of the ON/OFF resistance ratio and a small standard deviation of the switching voltage distribution.

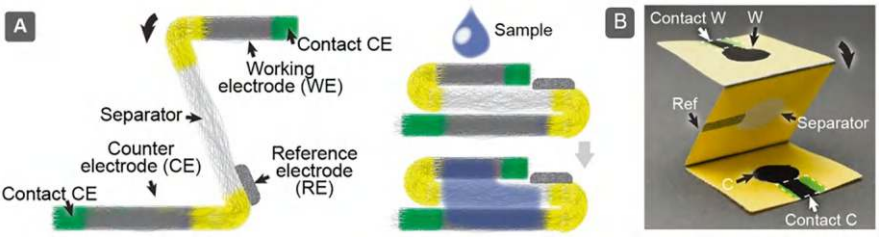

Fig. 21.11 Vertical-flow 3D electroanalytical paper device. (**a**) Schematic side view diagram of the assembly and operation of an electroanalytical device. The device is first printed on a single piece paper using wax printing and contacting inks to form electrofluidic working- and counter electrodes, and electrical contact points. A Ag/AgCl ink is printed in the middle layer as a reference electrode. The paper is then folded to form the device. The device works by adding a sample on the working electrode. The fluid containing the sample then wicks through the electrodes and forms an electrochemical circuit. (**b**) Photo of the device before folding into the final structure. (Reprinted with permission from Hamedi et al. (2016). Copyright 2016: Wiley)

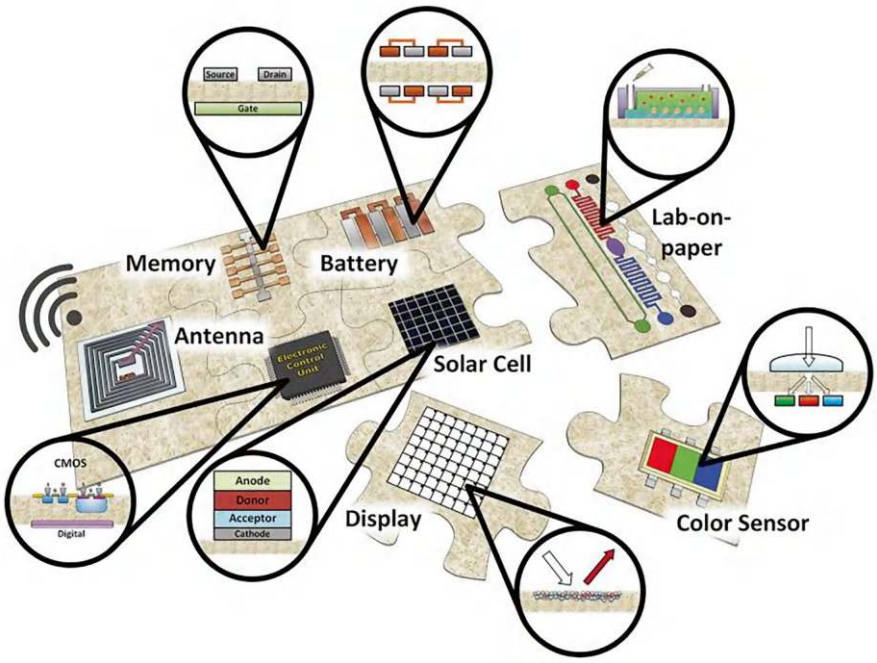

Fig. 21.12 Concept of the multiple integration of devices built with or on paper to perform complex functions. A solar cell coupled with a battery assures full autonomy to a device that requires energy to perform logic operations at the electronic control unit (CMOS), given the signals received from the sensor unit, and then distributes the processed information to be saved in a paper memory or transmitted by a radio frequency identification (RFID) antenna to another device. Other devices/functions can be added according to the final application, such as a display to visually convey messages to the user, or a lab-on-paper diagnostic device. (Reprinted from Vicente et al. (2016). Published 2016 by INTECH as open access)

Experiments have shown that paper memory devices are also compatible with other electronic components, providing a significant expansion of the functions of wearable electronics. For example, they can be integrated with radio frequency identification (RFID) paper tags (Alimenti et al., 2011; Lakafosis et al., 2010) for portable ticketing and security identification. In addition, memory devices can be combined with a paper-based antenna (Inui et al., 2015; Russo et al., 2011) for wireless transmission of data collected from wearable devices.

Another type of paper devices that holds great promise for wearable electronics is paper devices with power storage and delivery functions (Liu et al., 2017; Zhang et al., 2022). These include supercapacitors (Nyholm et al., 2011), various batteries (Nguyen et al., 2014), including lithium-ion batteries (Wang et al., 2018), and fuel cells (Hu & Cui, 2012). In these devices, conductive paper modified with noble metal nanoparticles or carbon-based nanomaterials serves as electrodes (Malti et al., 2015). Moreover, due to its excellent electrical conductivity (55 S/m (He et al., 2012)), large active surface area (1.52 m^2/mg (El-Kady et al., 2012)), and

mechanical stability, graphene paper is the most suitable for these applications. These unique properties allow graphene paper to act as both an active electrode and a current collector. This simplifies the manufacturing process by eliminating the addition of active materials and metal for current collection, which are usually required during the standard production of these devices. Paper materials with a porous structure, which can provide sufficient transport pathways for ionic charge carriers, also have significant potential to be used as a separating component to provide mechanical support and electrochemical functionality (Chun et al., 2012; Hu et al., 2009, 2010).

Other properties of cellulose, such as capillarity and biocompatibility, can also be used in energy storage and generation devices. For example, Wang et al. (2019) showed that due to its capillarity, cellulose paper can be used to absorb and store electrolyte in aluminum-air batteries. At the same time, Mohammadifar et al. (2018), exploiting the biocompatibility of cellulose, developed hybrid paper-polymer microbial fuel cells that can automatically biodegrade in water without further processing. The microporous hydrophilic network of interwoven cellulose fibers of the paper provides rapid adsorption of bacterial cells and promotes their accumulation.

The mechanical and structural properties of paper also make it possible to develop various types of nanogenerators based on it (Feng et al., 2016; Zhang et al., 2022). For example, the pores of paper can promote the embedding and adhesion of thermoelectric materials (Jin et al., 2018) and conductive composites (Gao et al., 2018) to produce high-performance thermoelectric generators (Zhao et al., 2019). Moreover, rough paper is good for fabricating high-performance triboelectric nanogenerator (TENG) (Chen et al., 2019). A schematic diagram illustrating the fabrication and operation principle of TENG is shown in Fig. 21.13. Due to the unique heterogeneous structure of the paper, Yang and Lu (2019) used its two sides as the friction pair of wearable TENG. Their rough surface and special triboelectric properties greatly enhance the triboelectric effect, resulting in exceptional output characteristics.

It is important to note that the development of these paper-based devices with functions of storing and supplying electricity made possible the implementation of the concept of self-powered, fully paper-based wearable electronics (Hu & Cui, 2012). Such flexible and lightweight paper-based energy storage devices can also be used in other applications, such as identification tags and functional packaging, that require built-in flexible power sources.

21.6 Limitations

Of course, paper substrates are inferior to plastic ones in terms of mechanical strength, resistance to aggressive environments, and manufacturability. The inherent roughness and porosity of the surface make it difficult to fabricate devices on paper, especially as their size decreases. High surface roughness of the paper is

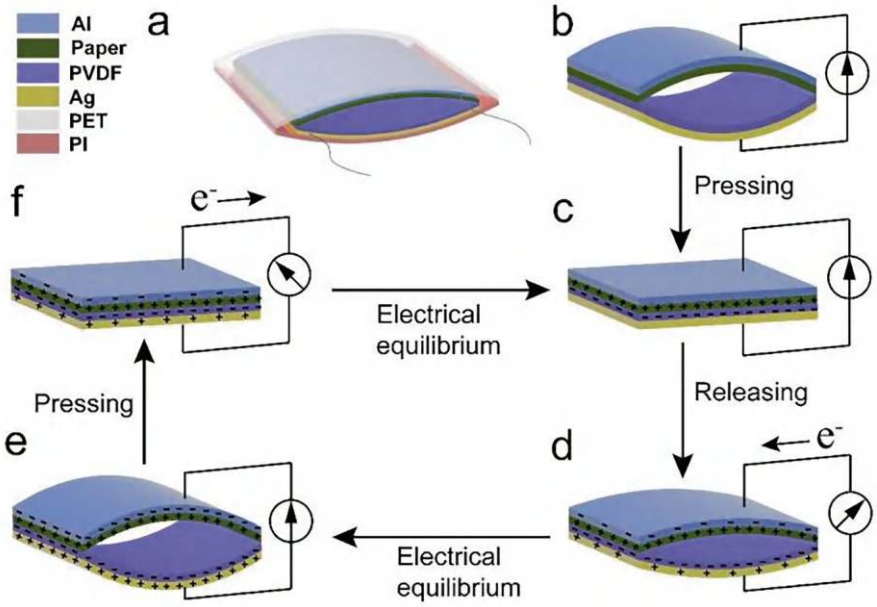

Fig. 21.13 Schematic diagrams of the structure (**a**) and power generation process (**b**–**f**) of paper-based TENG. (**b**) Before contact; (**c**) fully contacted, the electric charges are generated on paper and PVDF surfaces; (**d**) releasing, electrons flow from PVDF electrode to paper electrode; (**e**) fully separated and reaches an electrical equilibrium, no current flows; (**f**) pressing, electrons flow from the paper electrode to PVDF electrode generated on paper and PVDF surfaces; (**d**) releasing, electrons flow from PVDF electrode to paper electrode; (**e**) fully separated and reaches an electrical equilibrium, no current flows; (**f**) pressing, electrons flow from the paper electrode to PVDF electrode. (Reprinted with permission from Feng et al. (2016). Copyright 2016: the Royal Society of Chemistry)

especially dangerous in multi-layer devices, where one protrusion on the surface can cause a short circuit between conductors at different levels and render the device inoperable (Tobjörk & Österbacka, 2011). However, there are paper processing methods that can significantly improve its surface properties (Jalkanen et al., 2015). For example, it has been shown that laser ablation (Chitnis & Ziaie, 2012) can be used to improve paper surface morphology and alter surface energy, and plasma polymerization can be used to create hydrophobic polymer chains on the paper surface to make it water-repellent (Song et al., 2013). Other interesting approaches to control paper properties include the ability to improve the hydrophobicity of paper surfaces by coating with organic or inorganic nanoparticles (Bollstrom et al., 2014; Ogihara et al., 2012; Stanssens et al., 2011).

In addition, the large pore size of paper results in poor thermal performance (Salmen & Back, 1980). Moreover, cellulose itself is also prone to decomposition at temperatures above 100 °C (Clark, 1942; Soares et al., 2001; Tang et al., 2017). Excessive heating easily warps the paper and degrades the quality of the cellulose structure. The upper limit of temperatures used in the production process of

paper-based devices must be below 150 °C, and this limit can only be exceeded for a very short period of time. Decomposition of cellulose leads to a decrease in the mechanical strength of paper (Emsley & Stevens, 1994). This means that paper cannot be used in the high-temperature processes often used to deposit functional materials such as metal oxides. This severely limits the types of deposition processes that can be applied to paper and the amount of sensitive and active materials that can be used in paper sensors and electronic devices.

For paper electronics, a significant disadvantage is also the exceptional sensitivity of paper to moisture, and therefore to environmental conditions (Salmen & Back, 1980). Changes in humidity and temperature have a profound effect on the fibers, the connections between them, as well as their size and length. It is reported that an increase in relative humidity from 25% RH to 65% RH can lead to hygroexpansion in the range of 0.1–0.4% (Tobjörk & Österbacka, 2011). Dimensional instability, which can cause cracks and separations in printed tracks, is considered one of the important problems when using fiber-based materials. In addition to changes in geometric parameters, changes in humidity lead to deterioration of the mechanical properties of paper (Zhang et al., 2018) and changes in electrical conductivity and dielectric constant. The moisture content of the paper also affects the elastic modulus. High moisture content softens the material, thereby reducing the elastic modulus of the paper (Östlund & Kaarlo Niskanen, 2021; Zauscher et al., 1996). Moreover, the tendency of paper to absorb solvents results in ink permeation throughout its thickness, which reduces the lateral resolution of the printing process and causes short-circuiting of electrical connections when printing on both sides of the paper (Sala de Medeiros et al., 2020). This necessitates either monitoring the operating conditions of paper-based devices or using additional protective layers to seal paper-based devices from external influences such as air (Mo et al., 2020). The thickness of this protective coating often compromises the flexibility and foldability of these paper devices, making them difficult to use (Gwon et al., 2014). Without any doubt, to reduce the negative effects of encapsulation, these protective barriers should be thin, soft, transparent, and, most importantly, not interfere with the smooth operation of paper-based electronics (Liu et al., 2017).

Currently, the best results in the development of paper-based electronics, optoelectronics, and photonics elements are achieved using nanopaper substrates. However, the complex synthesis method of nanopaper substrates limits their wide range of applications (Pan et al., 2022). Therefore, simple and efficient methods for processing paper substrates, as well as simple and inexpensive methods for synthesizing nanopapers, are very important for the future of paper-based electronic and optoelectronic devices.

The pronounced surface roughness of the fibrous paper structure can also create difficulties in the manufacture of devices, since roughness can create defects in the active layers and, as a result, deteriorate their electrical conductivity (Vicente et al., 2016). Similar problems are more relevant for solar cells and thin-film transistors fabricated using inorganic materials. For organic devices, paper surface roughness has less of an impact, as they are more tolerant of the surface quality of the substrates (Polman et al., 2016; Zschieschang & Klauk, 2019).

However, more significant limitations to bringing paper-based electronics to market are current approaches to paper-based electronics manufacturing, which in many cases are not compatible with mass production (Liu et al., 2017). Many electronic functions, including sensing, actuation, and power supply, have been successfully implemented on paper, but it must be recognized that the fully integrated paper-based circuitry required for real-world, practical applications is still in development. This means that there is a need to develop both more advanced elements that make up electronic devices and new scalable technologies for their manufacture that meet the requirements of mass production. In addition, the low-resolution technologies used and the properties of the paper itself limit the size of the devices produced, which creates difficulties in microminiaturizing these devices.

It is also worth noting that in real-world use, electronic devices made from paper may not be as reliable as tested in a research lab. Chemical corrosion in humid atmospheres and mechanical overload of the fragile layers on the paper surface can lead to cracking of the active layers, which can be accompanied by reduced device performance and failure, thereby further reducing the life of such paper electronics.

Of course, it should also be recognized that paper sensors and electronic devices based on it have parameters worse than those of devices made using traditional materials and technologies (Khan et al., 2021). For example, paper has a lower Young's modulus (2 GPa) than silicon (130–170 GPa), resulting in a low natural resonant frequency (~25 Hz), limiting the use of low frequency or static force measurements (Liu et al., 2011). Paper is also much less resistant than silicon-based devices to heat and atmospheric components such as water vapor, ozone, oxygen, and peroxides. Paper devices also cannot be compared to commercial devices in terms of reliability and repeatability. However, it can be assumed that the performance/cost ratio may be higher for paper-based sensors and electronics. Such sensors and instruments can be targeted at low-performance applications and can significantly reduce their manufacturing costs (Khan et al., 2021).

21.7 Summary

Studies have shown that paper substrates cannot replace plastic substrates and silicon in all applications. But in specific applications, paper substrates can certainly be used as a viable alternative to traditional materials. For example, the high porosity of paper allows it to incorporate materials that have properties that are important for sensing applications but that are difficult to attach to plastic and silicon substrates. In addition, continuous pore channels allowing efficient diffusion of gases and biomolecules throughout the film matrix ensure maximum exposure of the analytes to the sensing material and thus improve the sensor signal and accuracy of the measurements (Xu et al., 2011).

Moreover, despite all the difficulties encountered in the development of paper electronics, Liu et al. (2017) are confident that paper-based electronics will bring

revolutionary development to the wearable electronics industry and will help improve people's quality of life. It is confident that the next decade will bring breakthroughs in the accuracy, efficiency of paper-based biosensors, and portability of wearable electronic monitoring systems, and many of the challenges limiting the accuracy, consistency, and speed of real-time data collection will be addressed (Khan et al., 2021). All this will contribute to the personalization of medicine and the improvement of the primary healthcare system.

Acknowledgments G.K. is grateful to the Moldova State University (research program no. 011208) for supporting his research.

References

Acharyya, D., Hazra, A., & Bhattacharyya, P. (2014). A journey towards reliability improvement of TiO_2 based resistive random access memory: A review. *Microelectronics and Reliability, 54*(3), 541–560. https://doi.org/10.1016/j.microrel.2013.11.013

Alimenti, F., Virili, M., Orecchini, G., Mezzanotte, P., Palazzari, V., Tentzeris, M. M., & Roselli, L. (2011). A new contactless assembly method for paper substrate antennas and UHF RFID chips. *IEEE Transactions on Microwave Theory and Techniques, 59*, 627–637. https://doi.org/10.1109/TMTT.2010.210321

Allen, M. P. (1995). Laminated assay device. ChemTrack, Inc., U.S. patent 5,409,664.

Anger, V. (1971). Prof. Dr. Dr. h. c. Fritz Feigl zum 70. Geburtstag. *Zeitschrift für Analytische Chemie, 184*, 1–3. https://doi.org/10.1007/BF00693989

Aulin, C., Gällstedt, M., & Lindström, T. (2010). Oxygen and oil barrier properties of microfibrillated cellulose films and coatings. *Cellulose, 17*, 559–574.

Baldé, C. P., Forti, V., Gray, V., Kuehr, R., & Stegmann, P. (2020). The Global E-waste Monitor—2017, United Nations Univ. (UNU), Int. Telecommun. Union Int. Solid Waste Assoc. (ISWA), Bonn/Geneva/Vienna.

Barr, M. C., Rowehl, J. A., Lunt, R. R., Xu, J., Wang, A., Boyce, C. M., et al. (2011). Direct monolithic integration of organic photovoltaic circuits on unmodified paper. *Advanced Materials, 23*(31), 3500–3505. https://doi.org/10.1002/adma.201101263

Bohm, A., & Biesalski, M. (2017). Paper-based microfluidic devices: A complex low-cost material in high-tech applications. *MRS Bulletin, 42*, 356–364. https://doi.org/10.1557/mrs.2017.92

Bollstrom, R., Pettersson, F., Dolietis, P., Preston, J., Osterbacka, R., & Toivakka, M. (2014). Impact of humidity on functionality of on-paper printed electronics. *Nanotechnology, 25*, 094003. https://doi.org/10.1088/0957-4484/25/9/094003

Bostock, J., & Riley, H. T. (Eds.). (1855). *The natural history of Pliny*. Taylor & Francis.

Bracher, P. J., Gupta, M., & Whitesides, G. M. (2010). Patterning precipitates of reactions in paper. *Journal of Materials Chemistry, 20*, 5117–5122. https://doi.org/10.1039/C000358A

Budtova, T., & Navard, P. (2016). Cellulose in NaOH-water based solvents: A review. *Cellulose, 23*, 5–55. https://doi.org/10.1007/s10570-015-0779-8

Cabrera, R. Q., Meersman, F., McMillan, P. F., & Dmitriev, V. (2011). Nanomechanical and structural properties of native cellulose under compressive stress. *Biomacromolecules, 12*, 2178–2183. https://doi.org/10.1021/bm200253h

Cantarella, G., Madagalam, M., Merino, I., Ebner, C., Ciocca, M., Polo, A., et al. (2023). Laser-induced, green and biocompatible paper-based devices for circular electronics. *Advanced Functional Materials, 33*, 2210422. https://doi.org/10.1002/adfm.202210422

Chard, T. (1992). Pregnancy tests: A review. *Human Reproduction, 7*(5), 701–710. https://doi.org/10.1093/oxfordjournals.humrep.a137722

Chen, W., Yu, H., Li, Q., Liu, Y., & Li, J. (2011). Ultralight and highly flexible aerogels with long cellulose I nanofibers. *Soft Matter, 11*(7), 10360–10368. https://doi.org/10.1039/C1SM06179H

Chen, S., Song, Y., Ding, D., Ling, Z., & Xu, F. (2018). Flexible and anisotropic strain sensor based on carbonized crepe paper with aligned cellulose fibers. *Advanced Functional Materials, 28*, 1802547. https://doi.org/10.1002/adfm.201802547

Chen, S., Jiang, J., Xu, F., & Gong, S. (2019). Crepe cellulose paper and nitrocellulose membrane-based triboelectric nanogenerators for energy harvesting and self-powered human-machine interaction. *Nano Energy, 61*, 69–77. https://doi.org/10.1016/j.nanoen.2019.04.043

Chen, D., Zhao, X., Wei, X., Zhang, J., Wang, D., Lu, H., & Jia, P. (2020). Ultrastretchable, tough, antifreezing, and conductive cellulose hydrogel for wearable strain sensor. *ACS Applied Materials & Interfaces, 12*, 53247–53256. https://doi.org/10.1021/acsami.0c14935

Chitnis, G., & Ziaie, B. (2012). Waterproof active paper via laser surface micropatterning of magnetic nanoparticles. *ACS Applied Materials & Interfaces, 4*, 4435–4439. https://doi.org/10.1021/am3011065

Choi, S., Lee, H.-S., Yang, Y., Parameswaran, P., Torres, C. L., Rittmann, B. E., & Chae, J. (2011). A μL-scale micromachined microbial fuel cell having high power density. *Lab on a Chip, 11*(6), 1110–1117. https://doi.org/10.1039/C0LC00494D

Chun, S.-J., Choi, E.-S., Lee, E.-H., Kim, J. H., & Lee, S.-Y. (2012). Eco-friendly cellulose nanofiber paper-derived separator membranes featuring tunable nanoporous network channels for lithium-ion batteries. *Journal of Materials Chemistry, 22*, 16618–16626. https://doi.org/10.1039/C2JM32415F

Clark, F. (1942). Factors affecting the mechanical deterioration of cellulose insulation. *Electrical Engineering, 61*(10), 742–749. https://doi.org/10.1109/EE.1942.6435499

Clegg, D. L. (1950). Paper chromatography. *Analytical Chemistry, 22*, 48–59. https://doi.org/10.1021/ac60037a014

Comer, J. (1956). Semi-quantitative specific test paper for glucose in urine. *Analytical Chemistry, 28*, 1748–1750. https://doi.org/10.1021/ac60119a030

Costa, M., Veigas, B., Jacob, J., Santos, D., Gomes, J., Baptista, P., et al. (2014). A low cost, safe, disposable, rapid and self-sustainable paper-based platform for diagnostic testing: Lab-on-paper. *Nanotechnology, 25*, 094006. https://doi.org/10.1088/0957-4484/25/9/094006

Crosland, M. (1978). *Gay-Lussac scientist and bourgeois*. Cambridge University Press.

Cybulski, J. S., Clements, J., & Prakash, M. (2014). Foldscope: Origami-based paper microscope. *PLoS One, 9*(6), e98781. https://doi.org/10.1371/journal.pone.0098781

Davis, B. W., Niamnont, N., Hare, C. D., Sukwattanasinitt, M., & Cheng, Q. (2010). Nanofibers doped with dendritic fluorophores for protein detection. *ACS Applied Materials & Interfaces, 2*, 1798–1803. https://doi.org/10.1021/am100345g

De, S., Higgins, T. M., Lyons, P. E., Doherty, E. M., Nirmalraj, P. N., Blau, W. J., Boland, J. J., & Coleman, J. N. (2009). Silver nanowire networks as flexible, transparent, conducting films: Extremely high DC to optical conductivity ratios. *ACS Nano, 3*, 1767–1774. https://doi.org/10.1021/nn900348c

Derraik, J. G. (2002). The pollution of the marine environment by plastic debris: A review. *Marine Pollution Bulletin, 44*, 842–852. https://doi.org/10.1016/S0025-326X(02)00220-5

Devarayan, K., & Kim, B. S. (2015). Reversible and universal pH sensing cellulose nanofibers for health monitor. *Sensors and Actuators B: Chemical, 209*, 281–286. https://doi.org/10.1016/j.snb.2014.11.120

Dieter, K., Heublein, B., Fink, H. P., & Bohn, A. (2005). Cellulose: Fascinating biopolymer and sustainable raw material. *Angewandte Chemie, International Edition, 44*, 3358–3393. https://doi.org/10.1002/anie.200460587

Dieterich, K. (1902). Testing-paper and method of making same. Patent US 691249 A.

Doménech-Carbó, M. T., & Doménech-Carbó, A. (2022). Spot tests: Past and present. *ChemTexts, 8*, 4. https://doi.org/10.1007/s40828-021-00152-z

Dumanli, A. G., Kamita, G., Landman, J., van der Kooij, H., Glover, B. J., Baumberg, J. J., J.J., et al. (2014). Controlled, bio-inspired self-assembly of cellulose-based chiral reflectors. *Advanced Optical Materials, 2*, 646–650. https://doi.org/10.1002/adom.201400112

Durairaj, V., Li, P., Liljeström, T., Wester, N., Etula, J., Leppänen, I., et al. (2021). Functionalized nanocellulose/multiwalled carbon nanotube composites for electrochemical applications. *ACS Applied Nano Materials, 4*, 5842–5853. https://doi.org/10.1021/acsanm.1c00774

El Miri, N., El Achaby, M., Fihri, A., Larzek, M., Zahouily, M., Abdelouahdi, K., Barakat, A., & Solhy, A. (2016). Synergistic effect of cellulose nanocrystals/graphene oxide nanosheets as functional hybrid nanofiller for enhancing properties of PVA nanocomposites. *Carbohydrate Polymers, 137*, 239–248. https://doi.org/10.1016/j.carbpol.2015.10.072

El-Kady, M. F., Strong, V., Dubin, S., & Kaner, R. B. (2012). Laser scribing of high-performance and flexible graphene-based electrochemical capacitors. *Science, 335*, 1326–1330. https://doi.org/10.1126/science.1216744

Emsley, A., & Stevens, G. (1994). Kinetics and mechanisms of the low-temperature degradation of cellulose. *Cellulose, 1*(1), 26–56. https://doi.org/10.1007/BF00818797

Eynaki, H., Kiani, M. A., & Golmohammadi, H. (2020). Nanopaper-based screen-printed electrodes: A hybrid sensing bioplatform for dual opto-electrochemical sensing applications. *Nanoscale, 12*, 18409–18417. https://doi.org/10.1039/D0NR03505J

Feng, Y., Zheng, Y., Rahman, Z. U., Wang, D., Zhou, F., & Liu, W. (2016). Paper-based triboelectric nanogenerators and their application in self-powered anticorrosion and antifouling. *Journal of Materials Chemistry A, 4*, 18022. https://doi.org/10.1039/C6TA07288G

Fraiwan, A., & Choi, S. (2016). A stackable, two-chambered, paper-based microbial fuel cell. *Biosensors & Bioelectronics, 83*, 27–32. https://doi.org/10.1016/j.bios.2016.04.025

Gabrielli, V., & Frasconi, M. (2022). Cellulose-based functional materials for sensing. *Chem, 10*, 352. https://doi.org/10.3390/chemosensors10090352

Gao, C., Gao, J., Shao, C., Xiao, Y., Zhao, Y., & Qu, L. (2018). Versatile origami microsupercapacitors array as a wind energy harvester. *Journal of Materials Chemistry A, 6*, 19750–19756. https://doi.org/10.1039/C8TA05148H

Gao, L., Zhu, C., Li, L., Zhang, C.-W., Liu, J., Yu, H.-D., & Huang, W. (2019). All paper-based flexible and wearable piezoresistive pressure sensor. *ACS Applied Materials & Interfaces, 11*(28), 25034–25042. https://doi.org/10.1021/acsami.9b07465

Gong, M. M., & Sinton, D. (2017). Turning the page: Advancing paper-based microfluidics for broad diagnostic application. *Chemical Reviews, 117*, 8447. https://doi.org/10.1021/acs.chemrev.7b00024

Grey, P., Fernandes, S. N., Gaspar, D., Fortunato, E., Martins, R., Godinho, M. H., & Pereira, L. (2019). Field-effect transistors on photonic cellulose nanocrystal solid electrolyte for circular polarized light sensing. *Advanced Functional Materials, 29*, 1805279. https://doi.org/10.1002/adfm.201805279

Güder, F., Ainla, A., Redston, J., Mosadegh, B., Glavan, A., Martin, T. J., & Whitesides, G. M. (2016). Paper-based electrical respiration sensor. *Angewandte Chemie, 128*, 5821–5826. https://doi.org/10.1002/ange.201511805

Gwon, H., Hong, J., Kim, H., Seo, D.-H., Jeon, S., & Kang, K. (2014). Recent progress on flexible lithium rechargeable batteries. *Energy & Environmental Science, 7*, 538–551. https://doi.org/10.1039/C3EE42927J

Hamedi, M. M., Ainla, A., Guder, F., Christodouleas, D. C., Fernandez-Abedul, M. T., & Whitesides, G. M. (2016). Integrating electronics and microfluidics on paper. *Advanced Materials, 28*, 5054. https://doi.org/10.1002/adma.201505823

Han, J. W., Kim, B., Li, J., & Meyyappan, M. (2014a). Carbon nanotube ink for writing on cellulose paper. *Materials Research Bulletin, 50*, 249–253. https://doi.org/10.1016/j.materresbull.2013.10.048

Han, J. W., Kim, B., Li, J., & Meyyappan, M. (2014b). A carbon nanotube-based ammonia sensor on cellulose paper. *RSC Advances, 4*, 549–553. https://doi.org/10.1039/c3ra46347h

Hardman, D. J., Slater, J. H., Reid, A. G., Lang, W. K., & Jackson, J. R. (2003). Biochemical and immunochemical assay device. US Patent, 6,573,108.

He, Y., Chen, W., Li, X., Zhang, Z., Fu, J., Zhao, C., & Xie, E. (2012). Assessment of methodological quality and outcome measures of acute stroke randomized controlled trials in China in recent 15 years. *ACS Nano, 7*, 174–182. https://doi.org/10.1111/j.1756-5391.2012.01190.x

Hornig, S., & Heinze, T. (2008). Efficient approach to design stable water-dispersible nanoparticles of hydrophobic cellulose esters. *Biomacromolecules, 9*, 1487–1492. https://doi.org/10.1021/bm8000155

Hsieh, M.-C., Kim, C., Nogi, M., & Suganuma, K. (2013). Electrically conductive lines on cellulose nanopaper for flexible electrical devices. *Nanoscale, 5*, 9289–9295. https://doi.org/10.1039/C3NR01951A

Hu, L., & Cui, Y. (2012). Energy and environmental nanotechnology in conductive paper and textiles. *Energy & Environmental Science, 5*, 6423–6435. https://doi.org/10.1039/c2ee02414d

Hu, L., Choi, J. W., Yang, Y., Jeong, S., La Mantia, F., Cui, L. F., & Cui, Y. (2009). Highly conductive paper for energy-storage devices. *Proceedings of the National Academy of Sciences of the United States of America, 106*, 21490–21494. https://doi.org/10.1073/pnas.0908858106

Hu, L., Wu, H., La Mantia, F., Yang, Y., & Cui, Y. (2010). Thin, flexible secondary Li-ion paper batteries. *ACS Nano, 4*, 5843–5848. https://doi.org/10.1021/nn1018158

Hu, C., Bai, X., Wang, Y., Jin, W., Zhang, X., & Hu, S. (2012). Inkjet printing of nanoporous gold electrode arrays on cellulose membranes for high-sensitive paper-like electrochemical oxygen sensors using ionic liquid electrolytes. *Analytical Chemistry, 84*, 3745–3750. https://doi.org/10.1021/ac3003243

Hu, Y., Lan, T., Wu, G., Zhu, Z., Tao, X., & Chen, W. (2014a). Novel electromechanical actuation based on a spongy graphene paper. *Chemical Communications, 50*, 4951–4954. https://doi.org/10.1039/C3CC49376H

Hu, J., Wang, S., Wang, L., Li, F., Pingguan-Murphy, B., Lu, T. J., & Xu, F. (2014b). Advances in paper-based point-of-care diagnostics. *Biosensors & Bioelectronics, 54*, 585–597. https://doi.org/10.1016/j.bios.2013.10.075

Huang, G.-W., Xiao, H.-M., & Fu, S.-Y. (2014). Paper-based silver-nanowire electronic circuits with outstanding electrical conductivity and extreme bending stability. *Nanoscale, 6*, 8495–8502. https://doi.org/10.1039/C4NR00846D

Hyun, W. J., Secor, E. B., Kim, C.-H., Hersam, M. C., Francis, L. F., & Frisbie, C. D. (2017). Scalable, self-aligned printing of flexible graphene micro-supercapacitors. *Advanced Energy Materials, 7*, 1700285. https://doi.org/10.1002/aenm.201700285

Ifuku, S., Tsuji, M., Morimoto, M., Saimoto, H., & Yano, H. (2009). Synthesis of silver nanoparticles templated by tempo-mediated oxidized bacterial cellulose nanofibers. *Biomacromolecules, 10*, 2714–2717. https://doi.org/10.1021/bm9006979

Ikai, T., & Okamoto, Y. (2009). Structure control of polysaccharide derivatives for efficient separation of enantiomers by chromatography. *Chemical Reviews, 109*, 6077–6101. https://doi.org/10.1021/cr8005558

Ikai, T., Suzuki, D., Kojima, Y., Yun, C., Maeda, K., & Kanoh, S. (2016). Chiral fluorescent sensors based on cellulose derivatives bearing terthienyl pendants. *Polymer Chemistry, 7*, 4793–4801. https://doi.org/10.1039/C6PY00967K

Inui, T., Koga, H., Nogi, M., Komoda, N., & Suganuma, K. (2015). A miniaturized flexible antenna printed on a high dielectric constant nanopaper composite. *Advanced Materials, 27*, 1112–1116. https://doi.org/10.1002/adma.201404555

Jalkanen, T., Määttänen, A., Mäkilä, E., Tuura, J., Kaasalainen, M., Lehto, V.-P., et al. (2015). Fabrication of porous silicon-based humidity sensing elements on paper. *Journal of Sensors, 2015*, 927396. https://doi.org/10.1155/2015/927396

Jin, Q., Shi, W., Zhao, Y., Qiao, J., Qiu, J., Sun, C., et al. (2018). Cellulose fiber-based hierarchical porous bismuth telluride for high-performance flexible and tailorable thermoelectrics. *ACS Applied Materials & Interfaces, 10*, 1743–1751. https://doi.org/10.1021/acsami.7b16356

Johnson, J. L. (1967). Microchemical techniques in solving industrial problems. *Mikrochimica Acta., 55*(4), 756–762. https://doi.org/10.1007/BF01224400

Khan, S. M., Qaiser, N., Shaikh, S. F., Ding, L. J., & Hussain, M. M. (2019). Do-it-yourself integration of a paper sensor in a smart lid for medication adherence. *Flexible and Printed Electronics, 4*(2), 025001. https://doi.org/10.1088/2058-8585/ab10f5

Khan, S. M., Nassar, J. M., & Hussain, M. M. (2021). Paper as a substrate and an active material in paper electronics. *ACS Applied Electronic Materials, 3*(1), 30–52. https://doi.org/10.1021/acsaelm.0c00484

Kim, K. S., Zhao, Y., Jang, H., Lee, S. Y., Kim, J. M., Kim, K. S., et al. (2009). Large-scale pattern growth of graphene films for stretchable transparent electrodes. *Nature, 457*, 706–710. https://doi.org/10.1038/nature077

Kim, J., Yun, S., Mahadeva, S. K., Yun, K., Yang, S. Y., & Maniruzzaman, M. (2010). Paper actuators made with cellulose and hybrid materials. *Sensors (Basel), 10*, 1473–1485. https://doi.org/10.3390/s100301473

Kim, D.-H., Ghaffari, R., Lu, N., Wang, S., Lee, S. P., Keum, H., et al. (2012). Electronic sensor and actuator webs for large-area complex geometry cardiac mapping and therapy. *Proceedings of the National Academy of Sciences of the United States of America, 109*, 19910–19915. https://doi.org/10.1073/pnas.1205923109

Kim, S.-S., Jeon, J.-H., Kim, H.-I., Kee, C. D., & Oh, I.-K. (2015). High-fidelity bioelectronic muscular actuator based on graphene-mediated and TEMPO-oxidized bacterial cellulose. *Advanced Functional Materials, 25*, 3560–3570. https://doi.org/10.1002/adfm.201500673

Kim, S., Ko, H., Lee, C., Kim, M., Kim, K. S., Lee, Y. H., et al. (2016). Semiconductor photonic nanocavity on a paper substrate. *Advanced Materials, 28*, 9765–9769. https://doi.org/10.1002/adma.201603368

Kim, H.-J., Yim, E.-C., Kim, J.-H., Kim, S.-J., Park, J.-Y., & Oh, I.-K. (2017). Bacterial nanocellulose triboelectric nanogenerator. *Nano Energy, 33*, 130–137. https://doi.org/10.1016/j.nanoen.2017.01.035

King, E., Xia, Y., Zhao, X. M., & Whitesides, G. M. (1997). Solvent-assisted microcontact molding: A convenient method for fabricating three-dimensional structures on surfaces of polymers. *Advanced Materials, 9*, 651–654. https://doi.org/10.1002/adma.19970090814

Koga, H., Kitaoka, T., & Isogai, A. (2012). Paper-immobilized enzyme as a green microstructured catalyst. *Journal of Materials Chemistry, 12*, 11591–11597. https://doi.org/10.1039/C2JM30759F

Koga, H., Saito, T., Kitaoka, T., Nogi, M., Suganuma, K., & Isogai, A. (2013). Transparent, conductive, and printable composites consisting of tempo-oxidized nanocellulose and carbon nanotube. *Biomacromolecules, 14*, 1160–1165. https://doi.org/10.1021/bm400075f

Kong, D., Wang, H., Lu, Z., & Cui, Y. (2014). $CoSe_2$ nanoparticles grown on carbon fiber paper: An efficient and stable electrocatalyst for hydrogen evolution reaction. *Journal of the American Chemical Society, 136*, 4897–4900. https://doi.org/10.1021/ja501497n

Korotcenkov, G. (2023). Paper-based humidity sensors as promising flexible devices: State of the art. Part 1. General consideration. *Nanomaterials, 13*, 1110. https://doi.org/10.3390/nano13061110

Korotcenkov, G. (2025). Paper-based sensors: Fantasy or reality? *Nanomaterials, 15*(2), 89. https://doi.org/10.3390/nano15020089

Korotcenkov, G., Simonenko, N. P., Simonenko, E. P., Sysoev, V. V., & Brinzari, V. (2023). Paper-based humidity sensors as promising flexible devices: State of the art. Part 2. Humidity sensors performances. *Nanomaterials, 13*(8), 1381. https://doi.org/10.3390/nano13081381

Kumar, S., Pandey, C. M., Hatamie, A., Simchi, A., Willander, M., & Malhotra, B. D. (2019). Nanomaterial-modified conducting paper: Fabrication, properties, and emerging biomedical applications. *Global Challenges, 3*, 1900041. https://doi.org/10.1002/gch2.201900041

Kunkel, H. G., & Tiselius, A. (1951). Electrophoresis of proteins on filter paper. *The Journal of General Physiology, 35*, 89–118. https://doi.org/10.1085/jgp.35.1.89

Kurra, N., & Kulkarni, G. (2013). Field effect transistors and RC filters from pencil-trace on paper. *Physical Chemistry Chemical Physics, 15*, 8367–8372. https://doi.org/10.1039/C3CP50675D

Lakafosis, V., Rida, A., Vyas, R., Yang, L., Nikolaou, S., & Tentzeris, M. M. (2010). Progress towards the first wireless sensor networks consisting of inkjet-printed, paper-based RFID-enabled sensor tags. *Proceedings of the IEEE, 98*, 1601–1609. https://doi.org/10.1109/JPROC.2010.2049622

Lawrence, C. S. K., Tan, S. N., & Floresca, C. Z. (2014). A "green" cellulose paper based glucose amperometric biosensor. *Sensors and Actuators B: Chemical, 193*, 536–541. https://doi.org/10.1016/j.snb.2013.11.054

Le Bras, D., Stromme, M., & Mihranyan, A. (2015). Characterization of dielectric properties of nanocellulose from wood and algae for electrical insulator applications. *The Journal of Physical Chemistry. B, 119*(18), 5911–5917. https://doi.org/10.1021/acs.jpcb.5b00715

Lessing, J., Glavan, A. C., Walker, S. B., Keplinger, C., Lewis, J. A., & Whitesides, G. M. (2014). Inkjet printing of conductive inks with high lateral resolution on omniphobic "R^F Paper" for paper-based electronics and MEMS. *Advanced Materials, 26*, 4677–4682. https://doi.org/10.1002/adma.201401053

Li, W., Li, W., Wei, J., Tan, J., & Chen, M. (2014). Preparation of conductive Cu patterns by directly writing using nano-Cu ink. *Materials Chemistry and Physics, 146*, 82–87. https://doi.org/10.1088/1361-6528/ab925c

Li, M., Li, X., Xiao, H. N., & James, T. D. (2017). Fluorescence sensing with cellulose-based materials. *Chemistry Open, 6*, 685–696. https://doi.org/10.1002/open.201700133

Liang, T., Sun, G., Cao, L., Li, J., & Wang, L. (2019). A pH and NH_3 sensing intelligent film based on Artemisia sphaerocephala Krasch. gum and red cabbage anthocyanins anchored by carboxymethyl cellulose sodium added as a host complex. *Food Hydrocolloids, 87*, 858–868. https://doi.org/10.1016/j.foodhyd.2018.08.028

Liu, X., O'Brien, M., Mwangi, M., Li, X., & Whitesides, G. (2011). Paper-based piezoresistive MEMS force sensors. In *Proceedings of the 24th IEEE International Conference on Micro Electro Mechanical Systems*, 23–27 January, Cancún, Quintana Roo, Mexico, pp. 133–136. https://doi.org/10.1109/MEMSYS.2011.5734379

Liu, J., Yang, C., Wu, H., Lin, Z., Zhang, Z., Wang, R., R., et al. (2014). Future paper based printed circuit boards for green electronics: Fabrication and life cycle assessment. *Energy & Environmental Science, 7*, 3674–3682. https://doi.org/10.1039/C4EE01995D

Liu, H., Qing, H., Li, Z., Han, Y. L., Lin, M., Yang, H., et al. (2017). Paper: A promising material for human-friendly functional wearable electronics. *Materials Science and Engineering: R: Reports, 112*, 1–22. https://doi.org/10.1016/j.mser.2017.01.001

Lu, T., Finkenauer, L., Wissman, J., & Majidi, C. (2014). Embedded 3D printing of strain sensors within highly stretchable. *Advanced Functional Materials, 24*, 3351–3356. https://doi.org/10.1002/adma.201400334

Mahapatra, S., Srivastava, V. R., & Chandra, P. (2021). Nanobioengineered sensing technologies based on cellulose matrices for detection of small molecules, macromolecules, and cells. *Biosensors, 11*, 168. https://doi.org/10.3390/bios11060168

Malti, A., Edberg, J., Granberg, H., Khan, Z. U., Andreasen, J. W., Liu, X., et al. (2015). An organic mixed ion-electron conductor for power electronics. *Advancement of Science, 3*, 1500305. https://doi.org/10.1002/advs.201500305

Martinez, A. W., Phillips, S. T., Butte, M. J., & Whitesides, G. M. (2007). Patterned paper as a platform for inexpensive, low-volume, portable bioassays. *Angewandte Chemie, International Edition, 46*, 1318–1320. https://doi.org/10.1002/anie.200603817

Martinez, A. W., Phillips, S. T., Whitesides, G. M., & Carrilho, E. (2010). Diagnostics for the developing world: Microfluidic paper-based analytical devices. *Analytical Chemistry, 82*, 3–10. https://doi.org/10.1021/ac9013989

Mattana, G., Loi, A., Woytasik, M., Barbaro, M., Noel, V., & Piro, B. (2017). Inkjet-printing: A new fabrication technology for organic transistors. *Advanced Materials Technologies, 2*, 1700063. https://doi.org/10.1002/admt.201700063

Migliorini, F. L., Teodoro, K. B., Scagion, V. P., dos Santos, D. M., Fonseca, F. J., Mattoso, L. H., & Correa, D. S. (2019). Tuning the electrical properties of electrospun nanofibers with hybrid nanomaterials for detecting isoborneol in water using an electronic tongue. *Surfaces, 2*, 432–443. https://doi.org/10.3390/surfaces2020031

Mirica, K. A., Weis, J. G., Schnorr, J. M., Esser, B., & Swager, T. M. (2012). Mechanical drawing of gas sensors on paper. *Angewandte Chemie, 51*, 10740–10745. https://doi.org/10.1002/anie.201206069

Mirica, K. A., Azzarelli, J. M., Weis, J. G., Schnorr, J. M., & Swager, T. M. (2013). Rapid prototyping of carbon-based chemiresistive gas sensors on paper. *Proceedings of the National Academy of Sciences of the United States of America, 110*, E3265–E3270. https://doi.org/10.1073/pnas.1307251110

Miura, T., Horiuchi, T., Iwasaki, Y., Seyama, M., Camou, S., Takahashi, J. I., & Haga, T. (2012). Patterned cellulose membrane for surface plasmon resonance measurement. *Sensors and Actuators B: Chemical, 173*, 354–360. https://doi.org/10.1016/j.snb.2012.07.019

Mo, F., Liang, G., Huang, Z., Li, H., Wang, D., & Zhi, C. (2020). An overview of fiber-shaped batteries with a focus on multifunctionality, scalability, and technical difficulties. *Advanced Materials, 32*, 1902151. https://doi.org/10.1002/adma.201902151

Mohammadifar, M., Yazgan, I., Zhang, J., Kariuki, V., Sadik, O. A., & Choi, S. (2018). Green biobatteries: Hybrid paper–polymer microbial fuel cells. *Advanced Sustainable Systems, 2*, 1800041. https://doi.org/10.1002/adsu.201800041

Morgan, E. D., & Wilson, I. D. (2004). An early description of paper chromatography? *Chromatographia, 60*, 135–136. https://doi.org/10.1365/s10337-004-0316-7

Morimune-Moriya, S., Salajkova, M., Zhou, Q., Nishino, T., & Berglund, L. A. (2018). Reinforcement effects from nanodiamond in cellulose nanofibril films. *Biomacromolecules, 19*, 2423–2431. https://doi.org/10.1021/acs.biomac.8b00010

Müller, R., & Clegg, D. (1949). Automatic paper chromatography. *Analytical Chemistry, 21*(9), 1123–1125. https://doi.org/10.1021/ac60033a032

Mun, S., Zhai, L., Min, S. K., Yun, Y., & Kim, J. (2016). Flexible and transparent strain sensor made with silver nanowire–coated cellulose. *Journal of Intelligent Material Systems and Structures, 27*, 1011–1018. https://doi.org/10.1177/1045389X15577651

Nagashima, K., Koga, H., Celano, U., Zhuge, F., Kanai, M., Rahong, S., et al. (2014). Cellulose nanofiber paper as an ultra flexible nonvolatile memory. *Scientific Reports, 4*, 5532. https://doi.org/10.1038/srep05532

Nandy, S., Goswami, S., Marques, A., Gaspar, D., Grey, P., Cunha, I., et al. (2021). Cellulose: A contribution for the zero e-waste challenge. *Advanced Materials Technologies, 2021*, 2000994. https://doi.org/10.1002/admt.202000994

Nassar, J. M., & Hussain, M. M. (2017). Impact of physical deformation on electrical performance of paper-based sensors. *IEEE Transactions on Electron Devices, 64*(5), 2022–2029. https://doi.org/10.1109/TED.2017.2650981

Nassar, J. M., Cordero, M. D., Kutbee, A. T., Karimi, M. A., Sevilla, G. A. T., Hussain, A. M., et al. (2016). Paper skin multisensory platform for simultaneous environmental monitoring. *Advanced Materials Technologies, 1*(1), 1600004. https://doi.org/10.1002/admt.201600004

Nassar, J. M., Mishra, K., Lau, K., Aguirre-Pablo, A. A., & Hussain, M. M. (2017). Recyclable nonfunctionalized paper-based ultralow-cost wearable health monitoring system. *Advanced Materials Technologies, 2*(4), 1600228. https://doi.org/10.1002/admt.201600228

Nery, E. W., & Kubota, L. T. (2013). Sensing approaches on paper-based devices: A review. *Analytical and Bioanalytical Chemistry, 405*, 7573–7595. https://doi.org/10.1007/s00216-013-6911-4

Nguyen, Q. H., & Kim, M. I. (2020). Nanomaterial-mediated paper-based biosensors for colorimetric pathogen detection. *TrAC, Trends in Analytical Chemistry, 132*, 116038. https://doi.org/10.1016/j.trac.2020.116038

Nguyen, T. H., Fraiwan, A., & Choi, S. (2014). Paper-based batteries: A review. *Biosensors & Bioelectronics, 54*, 640–649. https://doi.org/10.1016/j.bios.2013.11.007

Nie, Z., Nijhuis, C. A., Gong, J., Chen, X., Kumachev, A., Martinez, A. W., Narovlyansky, M., & Whitesides, G. M. (2010). Electrochemical sensing in paper-based microfluidic devices. *Lab on a Chip, 10*, 477–483. https://doi.org/10.1039/B917150A

Nyholm, L., Nystrom, G., Mihranyan, A., & Stromme, M. (2011). Toward flexible polymer and paper-based energy storage devices. *Advanced Materials, 23*, 3751–3769. https://doi.org/10.1002/adma.201004134

Ogihara, H., Xie, J., Okagaki, J., & Saji, T. (2012). Simple method for preparing superhydrophobic paper: Spray-deposited hydrophobic silica nanoparticle coatings exhibit high water-repellency and transparency. *Langmuir, 28*, 4605–4608. https://doi.org/10.1021/la204492q

Orelma, H., Hokkanen, A., Leppänen, I., Kammiovirta, K., Kapulainen, M., & Harlin, A. (2020). Optical cellulose fiber made from regenerated cellulose and cellulose acetate for water sensor applications. *Cellulose, 27*, 1543–1553. https://doi.org/10.1007/s10570-019-02882-3

Östlund, S., & Kaarlo Niskanen, K. (Eds.). (2021). *Mechanics of paper products*. De Gruyter. https://doi.org/10.1515/9783110619386

Padalkar, S., Capadona, J. R., Rowan, S. J., Weder, C., Won, Y. H., Stanciu, L. A., & Moon, R. J. (2010). Natural biopolymers: Novel templates for the synthesis of nanostructures. *Langmuir, 26*, 8497–84502. https://doi.org/10.1021/la904439p

Pan, T., Liu, S., Zhang, L., & Xie, W. (2022). Flexible organic optoelectronic devices on paper. *iScience, 25*, 103782. https://doi.org/10.1016/j.isci.2022.103782

Perez, S., & Samain, D. (2010). Structure and engineering of celluloses. *Advances in Carbohydrate Chemistry and Biochemistry, 64*, 25–116. https://doi.org/10.1016/S0065-2318(10)64003-6

Polman, A., Knight, M., Garnett, E. C., Ehrler, B., & Sinke, W. C. (2016). Photovoltaic materials: Present efficiencies and future challenges. *Science, 352*(6283), aad4424. https://doi.org/10.1126/science.aad4424

Powell, D. E., Annelin, R. B., & Gallavan, R. H. (1999). Silicone in the environment: A worst-case assessment of poly(dimethylsiloxane) (PDMS) in sediments. *Environmental Science & Technology, 33*, 3706–3710. https://doi.org/10.1021/es9903476

Prenzel, T. M., Gehring, F., Fuhs, F., & Albrecht, S. (2021). Influence of design properties of printed electronics on their environmental profile. *Matériaux & Techniques, 109*, 506. https://doi.org/10.1051/mattech/2022016

Renault, C., Anderson, M. J., & Crooks, R. M. (2014). Electrochemistry in hollow-channel paper analytical devices. *Journal of the American Chemical Society, 136*, 4616. https://doi.org/10.1021/ja4118544

Rocco, R. M. (2006). *Landmark papers in clinical chemistry*. Elsevier.

Romanholo, P. V. V., Sgobbi, L. F., & Carrilho, E. (2020). Exploring paper as a substrate for electrochemical micro-devices. *Comprehensive Analytical Chemistry, 89*, 1–29. https://doi.org/10.1016/bs.coac.2020.03.001

Russo, A., Ahn, B. Y., Adams, J. J., Duoss, E. B., Bernhard, J. T., & Lewis, J. A. (2011). Pen-on-paper flexible electronics pen-on-paper flexible electronics. *Advanced Materials, 23*, 3426–3430. https://doi.org/10.1002/adma.20110132

Sala de Medeiros, M., Chanci, D., & Martinez, R. V. (2020). Moisture-insensitive, self-powered paper-based flexible electronics. *Nano Energy, 78*, 105301. https://doi.org/10.1016/j.nanoen.2020.105301

Salmen, N. L., & Back, E. L. (1980). Moisture-dependent thermal softening of paper, evaluated by its elastic modulus. *TAPPI, 63*(6), 117–120.

Santhiago, M., Nery, E. W., Santos, G. P., & Kubota, L. T. (2014). Microfluidic paper-based devices for bioanalytical applications. *Bioanalysis, 6*(1), 89–106. https://doi.org/10.4155/BIO.13.296

Santhiago, M., da Costa, P. G., Pereira, M. P., Correa, C. C., de Morais, V. B., & Bufon, C. C. B. (2018). Versatile and robust integrated sensors to locally assess humidity changes in fully enclosed paper-based devices. *ACS Applied Materials & Interfaces, 10*, 35631–35638. https://doi.org/10.1021/acsami.8b12780

Scandurra, G., Arena, A., & Ciofi, C. (2023). A brief review on flexible electronics for IoT: Solutions for sustainability and new perspectives for designers. *Sensors, 23*, 5264. https://doi.org/10.3390/s23115264

Shalauddin, M., Akhter, S., Basirun, W. J., Bagheri, S., Anuar, N. S., & Johan, M. R. (2019). Hybrid nanocellulose/F-Mwcnts nanocomposite for the electrochemical sensing of diclofenac sodium in pharmaceutical drugs and biological fluids. *Electrochimica Acta, 304*, 323–333. https://doi.org/10.1016/j.electacta.2019.03.003

Shen, L. L., Zhang, G. R., & Etzold, B. J. M. (2019). Paper-based microfluidics for electrochemical applications. *ChemElectroChem, 7*, 10–30. https://doi.org/10.1002/celc.201901495

Singh, A. T., Lantigua, D., Meka, A., Taing, S., Pandher, M., & Camci-Unal, G. (2018). Paper-based sensors: Emerging themes and applications. *Sensors, 18*, 2838. https://doi.org/10.3390/s18092838

Soares, S., Ricardo, N. M., Jones, S., & Heatley, F. (2001). High temperature thermal degradation of cellulose in air studied using FTIR and 1H and 13C solid-state NMR. *European Polymer Journal, 37*(4), 737–745. https://doi.org/10.1016/S0014-3057(00)00181-6

Son, W. K., Youk, J. H., & Park, W. H. (2004). Preparation of ultrafine oxidized cellulose mats via electrospinning. *Biomacromolecules, 5*, 197–201. https://doi.org/10.1021/bm034312g

Son, D., Lee, J., Qiao, S., Ghaffari, R., Kim, J., Lee, J. E., et al. (2014). Multifunctional wearable devices for diagnosis and therapy of movement disorders. *Nature Nanotechnology, 9*, 397–404. https://doi.org/10.1038/nnano.2014.38

Song, Z., Tang, J., Li, J., & Xiao, H. (2013). Plasma-induced polymerization for enhancing paper hydrophobicity. *Carbohydrate Polymers, 92*, 928–933. https://doi.org/10.1016/j.carbpol.2012.09.089

Stahel, W. R. (2016). The circular economy. *Nature, 531*, 435–438. https://doi.org/10.1038/531435a

Stanssens, D., Van den Abbeele, H., Vonck, L., Schoukens, G., Deconinck, M., & Samyn, P. (2011). Creating water-repellent and super-hydrophobic cellulose substrates by deposition of organic nanoparticle. *Materials Letters, 65*, 1781–1784. https://doi.org/10.1016/j.matlet.2011.03.057

Sudheshwar, A., Malinverno, N., Hischier, R., Nowack, B., & Som, C. (2023). The need for design-for-recycling of paper-based printed electronics—A prospective comparison with printed circuit boards. *Resources, Conservation and Recycling, 189*, 106757. https://doi.org/10.1016/j.resconrec.2022.106757

Sun, B., Wang, Z., Wang, X., Qiu, M., Zhang, Z., Wang, Z., Cui, J., & Jia, S. (2021). Paper-based biosensor based on phenylalnine ammonia lyase hybrid nanoflowers for urinary phenylalanine measurement. *International Journal of Biological Macromolecules, 166*, 601–610. https://doi.org/10.1016/j.ijbiomac.2020.10.218

Tai, H., Duan, Z., Wang, Y., Wang, S., & Jiang, Y. (2020). Paper-based sensors for gas, humidity, and strain detections: A review. *ACS Applied Materials & Interfaces, 12*, 31037–31053. https://doi.org/10.1021/acsami.0c06435

Takei, K., Takahashi, T., Ho, J. C., Ko, H., Gillies, A. G., Leu, P. W., et al. (2010). Nanowire active-matrix circuitry for low-voltage macroscale artificial skin. *Nature Materials, 9*, 821–826. https://doi.org/10.1038/nmat2835

Tang, C., Zhang, S., Wang, Q., Wang, X., & Hao, J. (2017). Thermal stability of modified insulation paper cellulose based on molecular dynamics simulation. *Energies, 10*(3), 397. https://doi.org/10.3390/en10030397

Tobjörk, D., & Österbacka, R. (2011). Paper electronics. *Advanced Materials, 23*, 1935–1961. https://doi.org/10.1002/adma.201004692

Toniolo, R., Dossi, N., Pizzariello, A., Casagrande, A., & Bontempelli, G. (2013). Electrochemical gas sensors based on paper-supported room-temperature ionic liquids for improved analysis of acid vapours. *Analytical and Bioanalytical Chemistry, 405*, 3571–3577. https://doi.org/10.1007/s00216-012-6588-0

US EPA (US Environmental Protection Agency). (2014). Municipal solid waste generation, recycling, and disposal in the United States: Facts and figures for 2012. *US Environ. Prot. Agency, 2014*, 1–13.

Valanis, B. G., & Perlman, C. S. (1982). Home pregnancy testing kits: Prevalance of use, false-negative rates, and compliance with instructions. *American Journal of Public Health, 72*, 1034–1036. https://doi.org/10.2105/ajph.72.9.1034

Vicente, A. T., Araújo, A., Gaspar, D., Santos, L., Marques, A. C., Mendes, M. J., et al. (2016). Optoelectronics and bio devices on paper powered by solar cells. In N. Das (Ed.), *Nanostructured sola cells* (pp. 33–65). INTECH. https://doi.org/10.5772/66695

Viry, L., Levi, A., Totaro, M., Mondini, A., Mattoli, V., Mazzolai, B., & Beccai, L. (2014). Flexible three-axial force sensor for soft and highly sensitive artificial touch. *Advanced Materials, 26*, 2659–2664. https://doi.org/10.1002/adma.201305064

Wang, X., Lin, G., Cui, G., Zhou, X., & Liu, G. L. (2017). White blood cell counting on smartphone paper electrochemical sensor. *Biosensors & Bioelectronics, 90*, 549–557. https://doi.org/10.1016/j.bios.2016.10.017

Wang, Z., Pan, R., Sun, R., Edström, K., Strømme, M., & Nyholm, L. (2018). Nanocellulose structured paper-based lithium metal batteries. *ACS Applied Energy Materials, 1*, 4341–4350. https://doi.org/10.1021/acsaem.8b00961

Wang, Y., Kwok, H., Pan, W., Zhang, H., & Leung, D. Y. (2019). Innovative paper-based Al-air batteries as a low-cost and green energy technology for the miniwatt market. *Journal of Power Sources, 414*, 278–282. https://doi.org/10.1016/j.jpowsour.2019.01.018

WEF. (2019). World Economic Forum Annual Meeting. www.weforum.org/events/world-economic-forum-annual-meeting-2019

Wei, Y., Cheng, Z., & Lin, J. (2019). An overview on enhancing the stability of lead halide perovskite quantum dots and their applications in phosphor-converted LEDs. *Chemical Society Reviews, 48*, 310–350. https://doi.org/10.1039/C8CS00740C

Weil, H. (1953). The evolution of paper chromatography. *Kolloid-Zeitschrift, 132*(2–3), 149–162. https://doi.org/10.1007/BF01513715

Wu, J., & Lin, L. Y. (2017). Ultrathin (<1 μm) substrate-free flexible photodetector on quantum dot-nanocellulose paper. *Scientific Reports, 7*, 43898. https://doi.org/10.1038/srep43898

Wu, X., Lu, C., Zhang, W., Yuan, G., Xiong, R., & Zhang, X. (2013). A novel reagentless approach for synthesizing cellulose nanocrystal-supported palladium nanoparticles with enhanced catalytic performance. *Journal of Materials Chemistry A, 1*, 8645–8652. https://doi.org/10.1039/C3TA11236E

Wu, Q., Meng, Y., Wang, S., Li, Y., Fu, S., Ma, L., & Harper, D. (2014). Rheological behavior of cellulose nanocrystal suspension: Influence of concentration and aspect ratio. *Journal of Applied Polymer Science, 131*, 40525–40532. https://doi.org/10.1002/app.40525

Xie, J., Li, L., Khan, I. M., Wang, Z., & Ma, K. (2020). Flexible paper-based SERS substrate strategy for rapid detection of methyl parathion on the surface of fruit. *Spectrochimica Acta A, 231*, 118104. https://doi.org/10.1016/j.saa.2020.118104

Xu, M., Bunes, B. R., & Zang, L. (2011). Paper based vapor detection of hydrogen peroxide: Colorimetric sensing with tunable interface. *ACS Applied Materials & Interfaces, 3*(3), 642–647. https://doi.org/10.1021/am1012535

Xu, S., Zhang, Y., Jia, L., Mathewson, K. E., Jang, K.-I., Kim, J., et al. (2014). Soft microfluidic assemblies of sensors, circuits, and radios for the skin. *Science, 344*, 70–74. https://doi.org/10.1126/science.1250169

Yagoda, H. (1937). Applications of confined spot tests in analytical chemistry: Preliminary paper. *Industrial and Engineering Chemistry Research, 9*, 79–82. https://doi.org/10.1021/ac50106a012

Yamada, T., Hayamizu, Y., Yamamoto, Y., Yomogida, Y., Izadi-Najafabadi, A., Futaba, D. N., & Hata, K. (2011). A stretchable carbon nanotube strain sensor for human-motion detection. *Nature Nanotechnology, 6*, 296–301. https://doi.org/10.1038/nnano.2011.36

Yan, W., Chen, C., Wang, L., Zhang, D., Li, A. J., Yao, Z., & Shi, L. Y. (2016). Facile and green synthesis of cellulose nanocrystal-supported gold nanoparticles with superior catalytic activity. *Carbohydrate Polymers, 140*, 66–73. https://doi.org/10.1016/j.carbpol.2015.12.049

Yang, W., & Lu, X. (2019). Triboelectric power generation from heterostructured air-laid paper for breathable and wearable self-charging power system. *Advanced Materials Technologies, 4*, 1900745. https://doi.org/10.1002/admt.201900745

Yang, Z., Suzuki, H., Sasaki, S., & Karube, I. (1997). Design and validation of a low-cost paper-based oxygen electrode. *Analytical Letters, 30*, 1797–1807. https://doi.org/10.1080/00032719708001698

Yang, W., Liu, C., Zhang, Z., Liu, Y., & Nie, S. (2013). Paper-based nanosilver conductive ink. *Journal of Materials Science: Materials in Electronics, 24*, 628–634. https://doi.org/10.1007/s10854-012-0777-7

Yang, Y., Noviana, E., Nguyen, M. P., Geiss, B. J., Dandy, D. S., & Henry, C. S. (2017). Paper-based microfluidic devices: Emerging themes and applications. *Analytical Chemistry, 89*, 71–91. https://doi.org/10.1021/acs.analchem.6b04581

Yao, B., Zhang, J., Kou, T., Song, Y., Liu, T., & Li, Y. (2017). Paper-based electrodes for flexible energy storage devices. *Advancement of Science, 4*, 1700107. https://doi.org/10.1002/advs.201700107

Yao, Z., Coatsworth, P., Shi, X., Zhi, J., Hu, L., Yan, R., et al. (2022). Paper-based sensors for diagnostics, human activity monitoring, food safety and environmental detection. *Sensors & Diagnostics, 1*, 312–342. https://doi.org/10.1039/D2SD00017B

Zauscher, S., Caulfield, D. F., & Nissan, A. H. (1996). The influence of water on the elastic modulus of paper. *Tappi Journal, 79*(12), 178–182.

Zhai, L., Kim, H. C., Muthoka, R. M., Latif, M., Alrobei, H., Malik, R. A., & Kim, J. (2021). Environment-friendly zinc oxide nanorods grown cellulose nanofiber nanocomposite and its electromechanical and UV sensing behaviors. *Nanomaterials, 11*, 1419. https://doi.org/10.3390/nano11061419

Zhang, Y., Zhang, L., Cui, K., Ge, S., Cheng, X., Yan, M., et al. (2018). Flexible electronics based on micro/nanostructured paper. *Advanced Materials, 30*(51), 1801588. https://doi.org/10.1002/adma.201801588

Zhang, X., Pan, T., Zhang, J., Zhang, L., Liu, S., & Xie, W. (2019). Color-tunable, spectra-stable flexible white top-emitting organic light-emitting devices based on alternating current driven and dual-microcavity technology. *ACS Photonics, 6*(9), 2350–2357. https://doi.org/10.1021/acsphotonics.9b00900

Zhang, Y., Zhang, T., Huang, Z., & Yang, J. (2022). A new class of electronic devices based on flexible porous substrates. *Advancement of Science, 9*, 2105084. https://doi.org/10.1002/advs.202105084

Zhao, Y., Song, L., Zhang, Z., & Qu, L. (2013). Stimulus-responsive graphene systems towards actuator applications. *Energy & Environmental Science, 6*, 3520. https://doi.org/10.1039/C3EE42812E

Zhao, X., Han, W., Zhao, C., Wang, S., Kong, F., Ji, X., et al. (2019). Fabrication of transparent paper-based flexible thermoelectric generator for wearable energy harvester using modified distributor printing technology. *ACS Applied Materials & Interfaces, 11*, 10301–11309. https://doi.org/10.1021/acsami.8b21716

Zheng, Y., Zhang, Q., & Liu, J. (2013). Pervasive liquid metal direct writing electronics with roller-ball pen. *AIP Advances, 3*, 112117. https://doi.org/10.1063/1.4832220

Zheng, X., Li, L., Cui, K., Zhang, Y., Zhang, L., Ge, S., & Yu, J. (2018). Ultrasensitive enzyme-free biosensor by coupling cyclodextrin functionalized Au nanoparticles and high-performance Au-paper electrode. *ACS Applied Materials & Interfaces, 10*, 3333–3340. https://doi.org/10.1021/acsami.7b17037

Zhu, H., Luo, W., Ciesielski, P. N., Fang, Z., Zhu, J. Y., Henriksson, G., Himmel, M. E., & Hu, L. (2016). Wood-derived materials for green electronics, biological devices, and energy applications. *Chemical Reviews, 116*, 9305–9374. https://doi.org/10.1021/acs.chemrev.6b00225

Zschieschang, U., & Klauk, H. (2019). Organic transistors on paper: A brief review. *Journal of Materials Chemistry C, 7*, 5522–5533. https://doi.org/10.1039/c9tc00793h

Chapter 22
Flexible Functional Materials

Bharath Gunaseelan, Ghenadii Korotcenkov, and Andrews Nirmala Grace

22.1 Introduction

Every year, paper electronics finds wider application. The unique properties of paper (see Fig. 22.1) allow to implement various paper sensors on its basis, such as humidity sensors, pressure sensors, etc., electronic devices, including such devices as thin-film transistors, photodetectors and light-emitting diodes, and even electronic circuits (Khan et al., 2021; Yokota, 2024; Zhang et al., 2018). All these applications are based on different principles and often use electrophysical properties of materials that paper does not have. As is known, paper is a dielectric due to its properties. High surface roughness and porosity of paper can also create limitations on its application in complex electronic circuits. Therefore, it is quite natural that in order to implement all the possibilities of paper in the development of paper sensors and devices, various functional materials are widely used, which, on the one hand, can level out the disadvantages of paper, and on the other, give the paper the required functionality.

Recent studies have shown that the most promising area of paper application is flexible electronics, which makes it possible to implement complex portable and wearable systems for monitoring the environment and human health based on paper (Hussain & Hussain, 2016; Lipomi, 2016; Ma et al., 2019). Many are confident that, thanks to growing demand, flexible, functional electronics with human-friendly interfaces and conformal compactness will soon appear on the market (Li et al., 2012b, 2018; Lv et al., 2018; Wang et al., 2019). This means that the development

B. Gunaseelan · A. N. Grace (✉)
Centre for Nanotechnology Research, Vellore Institute of Technology, Vellore, Tamil Nadu, India
e-mail: anirmalagrace@vit.ac.in

G. Korotcenkov
Department of Physics and Engineering, Moldova State University, Chisinau, Moldova

G. Korotcenkov (ed.), *The Handbook of Paper-Based Sensors and Devices*,
https://doi.org/10.1007/978-3-031-91080-7_22

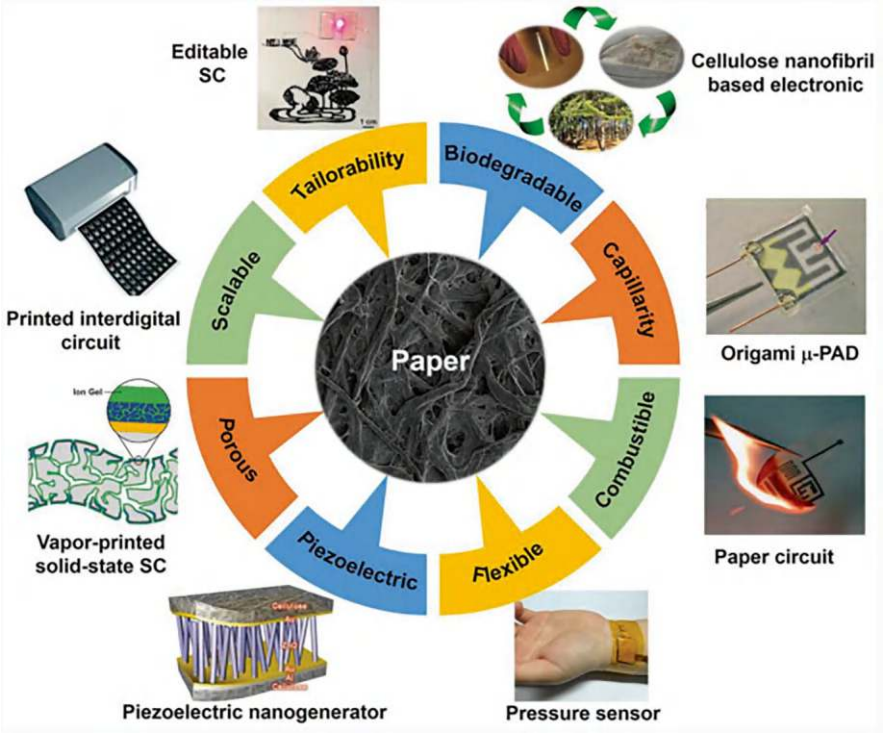

Fig. 22.1 Distinctive qualities and a variety of paper-based flexible electronics devices or applications. (Reproduced with permission from Zhang et al. (2018). Copyright 2018: Wiley and Sons)

of such devices requires not just functional materials, but functional materials that have the ability to bend and stretch.

The possibility of using paper in the development of disposable analytical devices for biomedical applications, which significantly reduce the cost of diagnostics at the point of care, also raises the issue of recycling these devices. Therefore, biocompatibility, biodegradability, and the possibility of their waste-free recycling are also of great importance for functional materials used in paper electronics (Nassajfar et al., 2021; Wang et al., 2017).

22.2 Flexible Functional Materials

Flexible functional materials refer to materials that possess both flexibility and certain functional properties required for the development of specific flexible sensors and electronic devices (Channon et al., 2018; Fu et al., 2011; Li et al., 2012a; Yu & Zhang, 2017; Xu et al., 2021; Zhang et al., 2017, Zhao et al., 2017). For example, they can be semiconductors, metals or dielectrics, have increased electronic or ionic

conductivity, be catalytically active, exhibit high gas sensitivity, etc. Their flexibility and stretchability allow them to be easily manipulated or bent while maintaining their functionality (Hyun et al., 2013). Of particular value in this regard are flexible functional materials that are compatible with basic manufacturing technologies such as printing and painting used to make paper-based sensors and devices (Cate et al., 2015; Liu et al., 2017; Zhang et al., 2015). Such materials with adaptive and versatile properties are of interest for a wide range of applications where traditional rigid materials may be unsuitable. For example, the flexibility and stretchability of functional materials allow them to conform to a variety of shapes and surfaces, making them ideal for wearable electronics and biomedical research (Rojas et al., 2017; Zhong et al., 2013). It is important to note that most bulk materials, with a few exceptions, are not flexible, which would seem to prevent their use in flexible electronics. However, if the thickness of these materials is reduced to micron thicknesses, these materials usually become flexible to some extent. A striking example of such materials is metals. Another approach to imparting flexibility to functional materials is to use these materials in the form of nanomaterials (Son & Bao, 2018; Xiang et al., 2018). Some examples of flexible functional materials used in paper-based sensors and devices are listed in Table 22.1. Let us consider in more detail these functional materials.

Table 22.1 Advantages and disadvantages of common functional materials currently used in different applications

Common material	Advantages	Disadvantages
Ecoflex	Low cost; nontoxic; good adhesive	Low transparency
Polydimethylsiloxane (PDMS)	Low cost; biocompatible; nontoxic; chemical inertness; high transparency; high stretchability	Difficult to integrate electrodes or to carry out deposition directly on its surface
Polyimide (PI)	High adhesiveness; outstanding thermal stability; good mechanical and insulating properties	Ability to absorb small hydrophobic molecules
Polyethylene (PE)	Proper bendability; low cost; good bendability	No recovery under large deformations; nontransparency
Polyethylene terephthalate (PET)	Low cost; good bendability; high transparency	No recovery under large deformations; low stretchability; low adhesiveness
Polystyrene (PS)-polybutadiene-PS	Good organic solubility	Low stretchability
PS-poly(isoprene)-PS	High adhesiveness	Complex preparation
PS-poly(ethylene butylene)-PS	Good viscoelasticity and fluidity	Low adhesiveness

(continued)

Table 22.1 (continued)

Common material	Advantages	Disadvantages
PS-poly(isobutylene)-PS	Capability to bind various substrate materials (e.g., glass, metals, polymers)	Toxicity
Poly(pyrrole) (PPy)	Stability in air- room temperature; biocompatibility; ease of synthesis and surface modification	Non-thermoplastic; brittle, rigid, and nondegradable properties; insoluble in common solvents
Polyaniline (PANI)	High-temperature resistance; good environmental stability; excellent electrical conductivity	Instability in biological environments
Poly(2,3-dihydrothieno-1,4-dioxin)-poly(styrene sulfonate) (PEDOT: PSS)	Water dispersible; different deposition techniques can be used	Poor solubility; high rigidity; low conductivity; poor environmental stability; functionalization hampered owing to PSS
Graphene	Easy to scale up; excellent electric conductivity	Difficult to form chain aggregates
Carbon black; activated carbon	Low cost; easy to prepare; high and stable electricity	Easy to reunite
CNTs	Excellent electricity; rich in variety; large surface area.	Complex preparation; high cost
Metal nanoparticles (NPs)	Excellent electrical conductivity; high stability; high surface area/volume ratio; good biocompatibility	Easy oxidization; high hardness; difficult forming; expensive
Metal nanowires (NWs)	Easy functionalization; excellent transparency, conductivity, catalytic activity, and mechanical flexibility; high surface area/volume ratio; good stability	Nonabundant in natural sources; expensive

Source: Adapted with permission from Vo and Kim (2024). Copyright 2023: Wiley-VCH

22.3 Flexible and Stretchable Conductive Materials

Conductive materials are an important element of electronic devices because they provide electrical contact between the various components of the device. Paper cannot perform this function because paper is an insulator. In addition, the parameters of conductive materials affect the ability of chemical and electrochemical sensors to achieve high sensitivity. They also contribute to the achievement of high efficiency in electronic devices. Therefore, when developing flexible devices, conductive materials, in addition to good mechanical properties that ensure good bendability and stretchability, must have high conductivity, chemical stability, and, preferably, good compatibility with the technological processes used in the large-scale production of sensor devices. Currently, these requirements can be met by metals, various nanomaterials, including conductive metal oxides, carbon-based nanomaterials

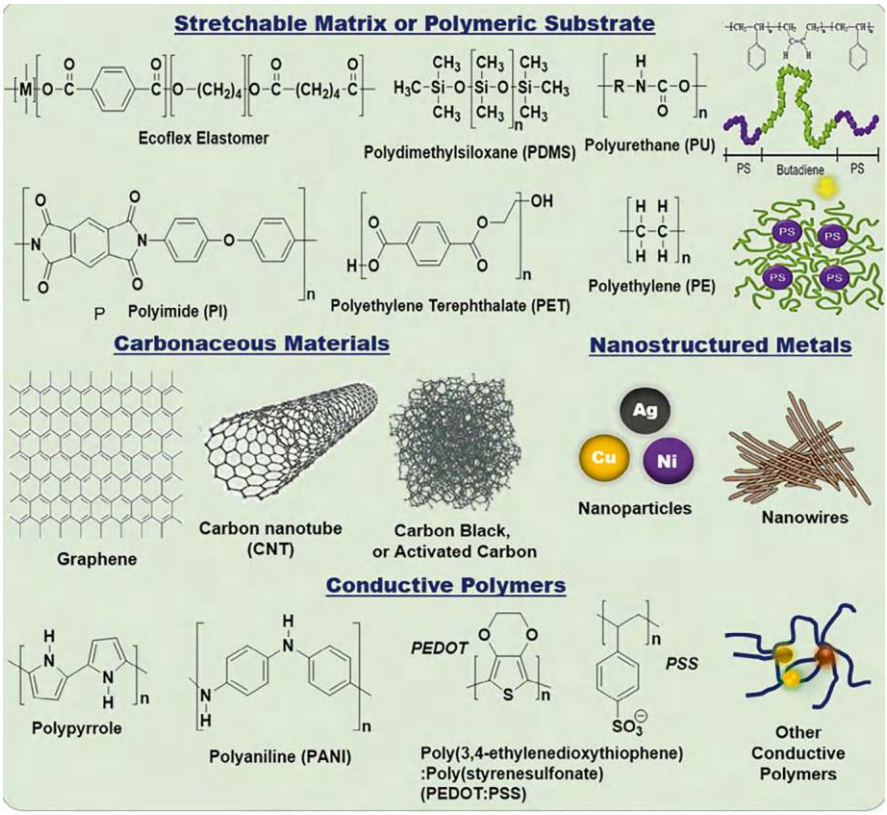

Fig. 22.2 Chemical structure and morphology of common functional materials. (Reproduced with permission from Vo and Kim (2024). Copyright 2023: Wiley-VCH)

such as graphene and carbon nanotubes, and various 2D nanostructures (Fig. 22.2). Conductive polymers can also be used for these purposes. Chapter 27 provides a detailed analysis of the process of fabricating electrodes on a paper surface. Therefore, in this chapter, we consider only some points concerning conductive functional materials.

22.3.1 Metals

Thin film and nanostructured metals are widely used as electrodes or conductive materials to create flexible electronics due to their excellent conductivity and ability to form flexible coatings. Various nanostructures such as metal nanowires (Joo et al., 2015), metal nanoparticles (NPs) (Kim et al., 2018a), metal thin films (Park et al., 2015), and liquid metals are able to establish and maintain their percolation

networks at relatively low concentrations even under large tensile strains. Among the potential candidates, metal nanoparticles (e.g., Al, Ag, Au, and Cu) are considered the best for electrical wiring and printing processes due to their ability to form films at low temperatures while providing good conductivity. Moreover, nanoparticle-based inks can create precise patterns. However, an experiment showed that 1D nanostructured metals with high aspect ratios are generally more effective in stretchable and flexible devices than 2D and 3D metals (Choi et al., 2018a). It was found that 1D metal nanomaterials may not crack when stretched, but rather slide into each other, maintaining percolation pathways.

Among 1D nanomaterials, the most studied are Ag-NWs, which have good mechanical flexibility, high conductivity, and transparency, making them suitable materials for many applications. The efficient performance of conductive networks under repeated mechanical deformation is ensured by the strong interaction between Ag-NWs and the supporting substrates (Akter & Kim, 2012). This property of Ag-NWs embedded in PDMS enabled the fabrication of a highly sensitive electronic pressure sensor. However, the natural sources of Ag-NWs are limited and relatively expensive (Wei et al., 2016). Therefore, in recent years, there has been great interest in the use of Cu-NWs in flexible electronics due to their low cost and excellent performance. However, they react very quickly to oxygen or moisture, which may cause oxidation of Cu-NWs, deterioration of conductivity, and unwanted chemical corrosion.

It is important to note that conductive networks based on metallic nanoparticles and 1D nanostructures can be fabricated using various manufacturing techniques, including screen printing and inkjet printing, which are widely used in paper-based sensors and devices. In addition, flexible metal electrodes can exhibit exceptional stability and high conductivity under high strain. Metal electrodes are usually formed as thin films (less than 100 nm). Stretching these thin film-like products can lead to cracks, but folding or bending at bending usually does not harm them. Using thin films of metals formed from nanoparticles and nanowires, researchers have successfully fabricated flexible and transparent electronics (Nam et al., 2021).

22.3.2 Carbon-Based Nanomaterials

Flexible carbon-based functional materials show great potential in the development of paper-based electronic devices and sensors. These materials, including graphene, carbon fibers (CF), carbon nanotubes (CNT), activated carbon (AC), and carbon-based composites, exhibit outstanding mechanical, electrical, and thermal properties that make them ideal for incorporation into flexible and eco-friendly electronic components (Hosseini et al., 2025).

22.3.2.1 Graphene

Graphene, a two-dimensional (2D) honeycomb lattice carbon sheet, exhibits exceptional mechanical strength, high electrical conductivity and optical transmittance, large surface area, and large aspect ratio (Iijima, 1991), making it very promising for a wide range of applications. For example, the use of graphene allows the development of extremely sensitive sensors (Shin et al., 2024) and efficient devices. In particular, López-Naranjo et al. (2016) used graphene to fabricate electrodes in devices such as flexible displays, solar cells, and electronic devices. Hyun et al. (2013) used graphene nanoplatelets to create foldable electronic circuits on paper substrates. Wang et al. (2009a, b) developed a graphene electrode for a lithium-ion battery and a supercapacitor. The above films are shown in Fig. 22.3a, b. In most cases, graphene electrodes have been fabricated by selectively transferring graphene dispersion using pen laying and vacuum filtration of the mixture. However, the widespread use of graphene still faces significant problems such as the quality and scalability of production, as well as the inconvenience of the graphene transfer step, which is actually a serious drawback to obtaining an effective electrode.

22.3.2.2 Carbon Nanotube (CNT)

Carbon nanotubes (CNTs) are among the first 1D nanostructures that have found wide application in various industries. In particular, the high conductivity and mechanical strength of CNTs make them attractive for the manufacture of electrodes in flexible electronics. Various electronic devices, such as digital logic circuits, resonators, and antennas, are developed using these components. In addition to electronic circuits, carbon nanotubes are used in the development of various physical and chemical sensors and biosensors, photovoltaic converters, and solar

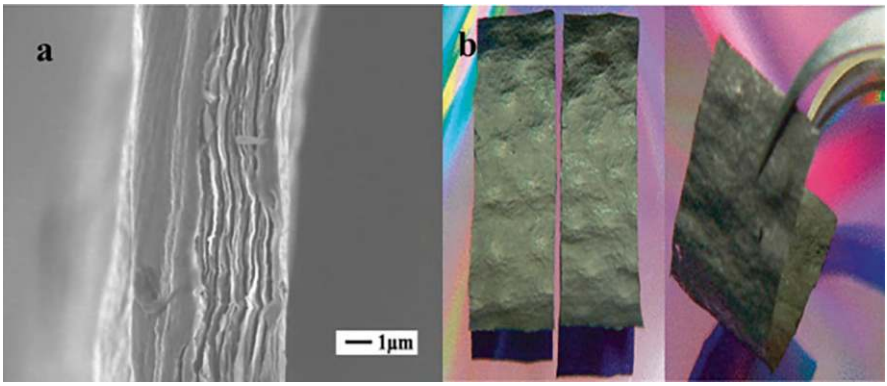

Fig. 22.3 (**a**) SEM image of freestanding graphene sheet. (**b**) Camera image of freestanding graphene paper. (Reprinted with permission from Wang et al. (2009a). Copyright 2009: ACS)

cells. Due to their high porosity and surface area, CNTs are useful in the manufacture of electrodes in energy storage devices.

22.3.3 Metal Carbides/Nitrides (MXenes)

MXenes are the new class of 2D inorganic metal carbides or nitrides formed when MAX (M—transition metals; A—elements of the 13th and 14th group of the periodic table; X—carbide or nitride or carbonitride) phase compounds are etched to create MXenes. Because of their terminal functional groups, MXenes exhibit hydrophilic properties (Yu & Breslin, 2020). MXenes can be synthesized and used as clay, colloidal, or film form in their pure form, or combined with polymer matrices to form nanocomposites thanks to their special hydrophilic behavior. This is one of MXenes' main advantages over nanomaterials based on carbon.

MXene compounds, after exfoliation and transformation into individual flakes (Fig. 22.4), exhibit excellent elasticity and conductivity, making them promising for the fabrication of electrodes. By changing the chemistry of the compound, the electrical and chemical properties of MXene can be changed. Using the unique properties of MXene, various chemical sensors have been developed based on them in recent years (Harley et al., 2010; Jerome & Sundramoorthy, 2019). However, during

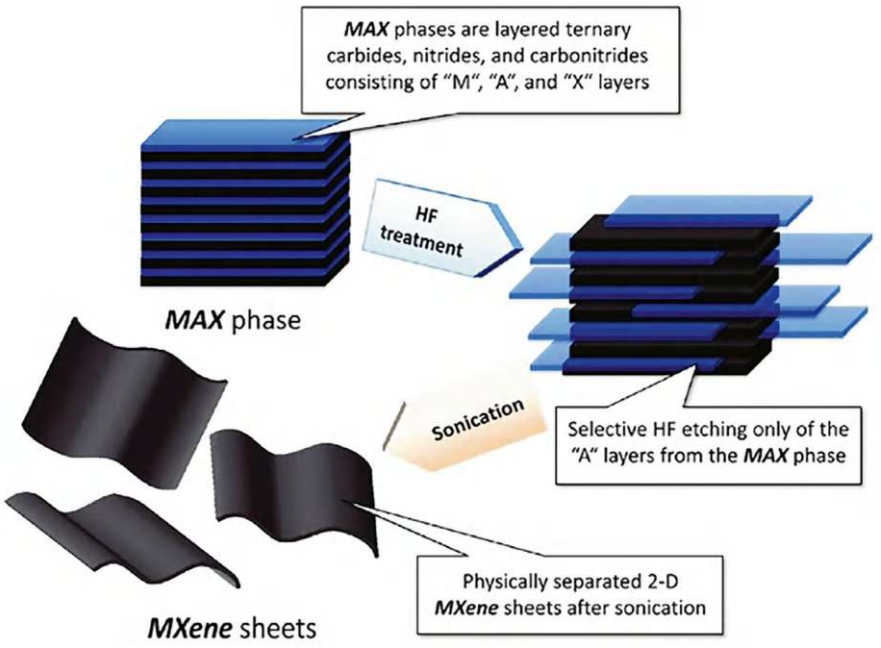

Fig. 22.4 Schematic representation of MXene formation from MAX phase. (Reprinted from Biswas and Prashant (2021). Published 2021 by MDPI with open access)

the research, it was found that MXene are susceptible to oxidation. This means that the problem of temporal instability of MXene parameters needs to be addressed.

22.3.4 Metal Oxides

Metal oxides are almost never used to make conductive contacts. Only In_2O_3 doped with Sn (ITO) can be found in photodetectors, displays, solar cells, touch screens, and light-emitting diodes, where the electrodes are required to be transparent in addition to conductivity.

22.3.5 Conductive Polymers

Conductive polymers form another group of materials that can be used in the manufacture of conductive electrodes. They exhibit exceptional mechanical properties, effectively maintaining electrical properties under stretching and bending. This is why conductive polymers have become the focus of attention in the production of stretchable and flexible electronic devices.

The most well-known and widely used conductive polymers are polypyrrole (PPy), polyaniline (PANI), polythiophenes (PTS), polyacetylene, and PEDOT:PSS (the chemical structure is shown in Fig. 22.2) and their derivatives (Hwang et al., 2015; Sun et al., 2014). They are widely used as conductive polymers in the production of electronic devices and sensors for various purposes. Due to their exceptional compatibility with solution processing methods, these polymers are easily produced by printing and spraying methods and are often used in the production of large-scale, low-cost electronic and sensor arrays. Due to their mechanical properties, which are more similar to those of soft human skin, the polymers are well suited for use as skin-like sensors in wearable devices for health and motion monitoring.

22.3.6 Composites

As is known, when applying inorganic materials to bendable substrates, including paper, it is not always possible to achieve the required adhesion and mechanical strength of the coating. Therefore, methods are being developed to help solve this problem. The experiment showed that the best solution to this problem is the use of polymer-based composites that will provide bendability and good adhesion, and inorganic fillers will provide the necessary functionality. In the manufacture of conductive coatings, this approach is used quite often in the development of paper-based flexible sensors and electronic devices (Al-Ghamdi et al., 2016; Gong et al., 2015a, b; Guo et al., 2022). The same highly conductive materials, such as metal

nanoparticles (NPs), graphene, and CNTs, are used as fillers. In this case, the polymer matrix can be both conductive and insulating. In the case of an insulating matrix, at a concentration of NPs close to the conductivity threshold, conditions are created that allow the development of highly sensitive chemical and physical sensors (Choi et al., 2018a; Lee et al., 2015).

By combining carbon materials with biodegradable matrices such as ethyl cellulose, carbon-based composites provide eco-friendly solutions that adhere well to paper substrates and facilitate the development of next-generation paper-based sensors and electronic devices for advanced wearables and environmental and health monitoring applications that offer superior performance, adaptability, and environmental sustainability.

Of course, metal NPs can also form composites with one-dimensional (1D) and two-dimensional (2D) functional nanomaterials. For example, Xia et al. (2018) fabricated conductive hybrids based on Ag-NWs/Cu-NPs, Ag-NPs/CNT, PEDOT:PSS/graphene, and Ag-NWs/poly(pyrrole) and found that these hybrids have demonstrated exceptional stretchability and conductivity, making them suitable for use in various electromechanical sensors and devices. Peng et al. (2015) developed a novel label-free electrochemical DNA biosensor based on Au NPs/toluidine blue (TB)-graphene oxide (GO) composite electrode for simple, efficient, and convenient detection of MDR1 gene, which showed a detection limit of 2.95 pM. Lin et al. (2015) developed a reusable biosensor for cancer detection by detecting vascular endothelial growth factor (VEGF) in human plasma using magnetic graphene oxide (MGO)-modified Au electrode.

22.3.6.1 Flexible and Stretchable Polymeric Matrix

As we have mentioned earlier, in many cases the most effective method of using functional nanomaterials in the development of flexible paper-based devices is the creation of composites in which polymers provide bendability and good adhesion to the substrate, and nanomaterials impart the required functionality to the composite. Experiments have shown that elastomers perform this role best of all polymers, as they can guarantee the required bendability and stretchability of the formed composite (Wu et al., 2021). Depending on their properties, elastomers are divided into thermosetting (e.g., poly(dimethylsiloxane) (PDMS) and Ecoflex), thermoplastic (e.g., polyurethane (PU) and block copolymer elastomers), and gels. Various inter- and intramolecular interactions, such as ionic (as in gels), physical (as in thermoplastic elastomers), and chemical (as in thermosetting elastomers) crosslinks, are responsible for their characteristics. Due to these interactions, elastomers exhibit ultra-high elasticity, making them ideal for use in stretchable electronics (Wu et al., 2018). For example, Ecoflex elastomers, whose chemical structure is shown in Fig. 22.2, are extremely elastic and can withstand strains of up to 900% (Lu et al., 2019). In addition, they are safe for the environment and human health. Therefore, they are suitable candidates for the fabrication of tactile sensors, which, in addition to Ecoflex, include a mixture of graphene and molybdenum disulfide (MoS_2) (Kim

et al., 2018b; Li & Guo, 2020). In addition, Ecoflex layers are used to develop a triboelectric nanogenerator (TENG) (Gunasekara et al., 2021; Oliveira et al., 2022). Schwartz et al. (2013) showed that a composite containing reduced graphene oxide (rGO)@nickel nanowires (magnetic rGO@Ni-NW) incorporated into an Ecoflex matrix could be used to develop a pressure sensor with high sensitivity for application in electronic skin and health monitoring.

In addition to Ecoflex elastomers, silicone films such as PDMS have been widely used recently. Due to its non-toxicity, chemical inertness, ease of use, high transparency (>95%), and stretchability (>100%), it is also a promising candidate for flexible and stretchable sensors and electronics (Jin et al., 2022; Ko et al., 2014). The chemical structure of PDMS is shown in Fig. 22.2. The flexible cross-linked molecular chains of PDMS allow it to recover after torsion, stretching, or compression. PDMS-based sensors can be implanted into the human body due to their non-toxic nature, and their potential for biological applications on human skin has been explored. In addition, due to its high transparency, PDMS can serve as an ideal substrate for photoelectronic devices. It can be mixed and combined with various functional materials to create composites that enable the development of incredibly elastic and flexible sensors. (Rovisco et al., 2020; Yu et al., 2020).

Currently, there are also many synthetic polymer materials available in the market, such as self-healing materials (Parida et al., 2019), block copolymer elastomers (You et al., 2019), hydrogels, and UV-cross-linkable materials (Liu et al., 2019b; Wang et al., 2018). Polyethylene (PE), polyethylene terephthalate (PET), polyimide (PI), and polyurethane (PU) are the most commercially available polymers from this list (Fig. 22.2) (Hong et al., 2016; Kaltenbrunner et al., 2013; Zhou et al., 2021). The exceptional mechanical properties, insulating properties, and thermal stability of PI substrates have made them the most popular films for flexible sensors. In particular, PIs have high glass transition temperatures (360–410 °C), which allows the fabrication and use of corresponding sensors at elevated temperatures (Kuribara et al., 2012; Rim et al., 2016). These polymeric materials can also be used as possible support materials for flexible electromechanical sensors due to their elastic nature (Sekitani et al., 2010b).

As for thermoplastic elastomers (TPE), including triblock copolymer elastomers, they can also be used in flexible devices, including as a flexible matrix for nanomaterials. Thermoplastic elastomers combine elasticity, easy thermal processing, and recyclability. Unlike conventional rubbers, TPEs are recyclable and can be produced in large volumes. In addition, they exhibit good adhesion, viscoelasticity, organic solubility, and flowability. Triblock copolymer elastomers are usually assembled with a long soft chain in the middle and two short hard chains at the ends, consisting of SBS, SIS, poly(styrene)–poly(ethylene butylene)–poly(styrene), and poly(styrene)–poly(isobutylene)–poly(styrene), as shown in Fig. 22.2. As a result, they are able to successfully achieve the desired physical characteristics of sensors, including compatibility with printing technologies and the ability to bond to various materials, including metals, metal oxides, and polymers (You et al., 2019). Moreover, even for low-cost mass production, UV-cross-linkable elastomer materials can be used with advanced technologies such as photolithography and 3D printing (Liu

et al., 2019b; Wang et al., 2018). However, weak interface interactions, modulus mismatch between elastomers and active nanomaterials in the matrix, and viscoelastic behavior of the used elastomers are the main reasons for the strain hysteresis in elastomer-based physical strain sensors under cyclic loading (Cai et al., 2018).

Hydrogels, which are composed of soft conductive materials, can also be a very interesting matrix for bendable electronics. They can bind living tissues and metal electrodes as biocompatible materials (Ge et al., 2018). In addition, their elastic moduli are comparable to those of living tissues. They also have softness and self-healing properties that reproduce the mechanical properties of human skin. Various hydrogel-based sensors have been developed. For example, a transparent, highly biocompatible, and stretchable hydrogel-based pressure sensor that was self-structured was fabricated by Sekitani et al. (2010a). However, the development of hydrogel devices faces challenges in achieving the intended results regarding fatigue resistance as well as strong and flexible adhesion similar to that found in human skin (Liu et al., 2019b; Wang et al., 2018).

22.4 Semiconductors

A semiconductor is a material that has electrical conductivity between that of a conductor (such as a metal) and an insulator. Our current understanding of the properties of a semiconductor is based on quantum physics, which explains the motion of charge carriers in a crystal lattice. A semiconductor can conduct electricity under certain conditions, but not under other conditions. This unique property makes it an excellent material for conducting electricity in a controlled manner as needed. Moreover, semiconductors can be modified by doping, making semiconductor devices suitable for a variety of applications. For example, semiconductors form the basis of modern electronic devices such as computers, smartphones, and televisions. Without semiconductors, it would be impossible to develop many fundamental components in electronics such as diodes, transistors, memory devices, and integrated circuits. Power generation using, for example, solar cells and light-emitting diodes (LEDs) also requires the use of materials with semiconductor properties.

22.4.1 Metal Oxides

Nanostructured metal oxide semiconductors and thin films have garnered significant attention in recent years due to their potential applications in flexible and stretchable electronic devices and sensors (see Fig. 22.5).

A wide bandgap metal oxide semiconductors represent a class of unique materials due to their electronic charge transport properties when compared to conventional covalent semiconductors such as silicon (Si). Metal oxide semiconductors are valence compounds with a high degree of ionic bonding. Their conduction band

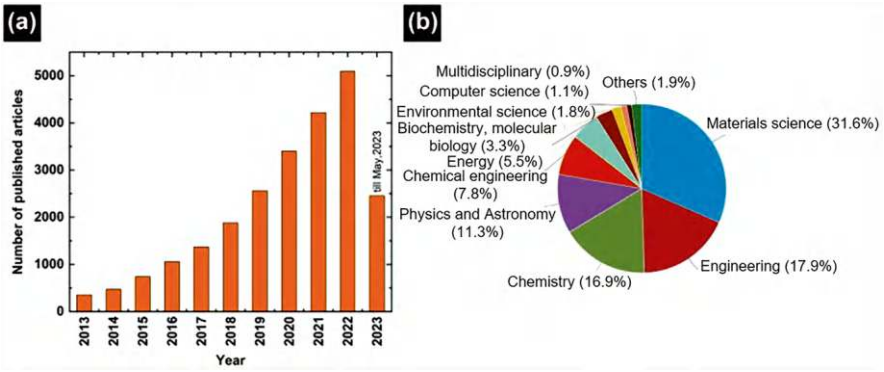

Fig. 22.5 Statistical report of metal oxide thin film-based soft electronic devices. (**a**) The number of metal oxide-based soft electronic device articles published in the last 10 years. (**b**) The percentage of articles on metal oxides published in different fields. (Reprinted from Dong et al. (2023). Published 2023 by AIP with open access)

minimum (CBM) and valence band maximum (VBM) mainly consist of the metal (M) and oxygen (O)2p orbital, respectively. These materials are divided into two groups: transition-metal oxides, such as TiO_2, V_2O_5, and WO_3, and non-transition-metal oxides, such as In_2O_3, ZnO, and SnO_2. Typical metal oxide semiconductors, as well as their solid solutions, are predominantly n-type conductivity. Metal oxides of p-type conductivity include nickel oxide (NiO) and Cu(I)-based oxides, such as Cu_2O and $CuMO_2$.

Metal oxides with superior electrical, optical, chemical, and mechanical properties are used as photoanodes, catalysts, photocatalysts, and chemical detectors (Petti et al., 2016). In addition to the high sensitivity, resistance to humidity, and aging effects, different metals can change these sensors' selectivity. They can also be heavily doped to act as conductors with very low resistivity, some of which are known as transparent conducting oxides. Such materials can form the channel layer for the transistors and are useful for photovoltaic, energy harvesting, and storage, foldable displays, antimicrobial agents, fuel cells, and solar cells (Dong et al., 2023). Metal oxides also have the advantage of providing fast film deposition over large areas using simple methods. Another advantage of nanostructured metal oxides, especially in the form of polymer-metal oxide composites, is their ability to adhere to various substrates, including flexible and stretchable polymeric materials, including cellulose paper. These unique properties of metal oxides and the compatibility of their fabrication technology with both traditional semiconductor processes and emerging printing technologies make them ideal candidates for next-generation electronic devices (Jeon et al., 2022; Ha et al., 2015). Moreover, the high flexibility of polymer/metal oxide composites enables the development of wearable electronics that can be easily integrated into clothing or directly attached to human skin, providing continuous and accurate health monitoring (Wang et al., 2009b).

Of the metal oxide semiconductors, nanostructured TiO_2 and ZnO with wide bandgap are the most widely used in the development of various devices, possessing an optimal set of properties. They have corrosion resistance, low cost, abundance of their constituent elements, non-toxicity, high transparency, and stability of parameters. In addition, obtaining TiO_2 and ZnO is cheap, and there are many methods for depositing a solution for preparing thin films. That is why they can be suitable for the development of cheap sensors and devices manufactured in mass production.

Another metal oxide that is promising for application primarily in new flexible and wearable electronic devices is amorphous indium gallium zinc oxide (IGZO) (Rim et al., 2016). Due to the spherical symmetry of the s-orbital, amorphous states can provide electron mobility comparable to crystalline states, which can be considered a major advantage of these amorphous metal oxide semiconductors. In addition, high tolerance to structural defects makes low-temperature solution processing a convenient and feasible approach to their deposition on paper substrates.

Despite the promising potential of nanostructured metal oxides and their thin films, several challenges remain to be addressed, including optimization of fabrication methods, improvement of device stability, and integration with other materials. Continued research and development in this area is essential to overcome these challenges and realize the full potential of flexible and stretchable metal oxide-based electronic devices and sensors.

22.4.2 Organic and Polymeric Semiconductors

In contrast to classical inorganic semiconductors, which are usually used in single-crystal forms, organic semiconductors, consisting of either oligomer or polymer chain molecules, are usually deposited as thin films over large areas, resulting in amorphous or polycrystalline structures. Organic semiconductors are characterized by relatively weak van der Waals bonding, resulting in soft materials and narrow energy bands. The π-conjugated network of carbon chemical structures in organic semiconductors, i.e., the overlap of molecular orbitals of neighboring molecules, provides the electron delocalization necessary for electrical conductivity of the materials (Facchetti, 2007). In single crystals, band transport is observed. However, in thin films of organic semiconductors, disorder plays an important role, and hopping transport is usually observed with mobilities well below 1 $cm^2/V{\cdot}s$. In most organic polymers, carrier mobility lies in the range of 0.001–3 $cm^2/V{\cdot}s$. Such low mobility is a significant limitation for the production of efficient devices.

Organic semiconductors can be deposited by vacuum evaporation or solution processes, which are suitable for low-cost, large-area deposition. Unlike inorganic semiconductors, which require high processing temperatures, organic semiconductors only require solvent evaporation after solution deposition. Compatibility with a variety of substrates, including paper, and low processing temperatures, combined

with intrinsic mechanical flexibility, make organic semiconductors suitable for flexible electronics (Rim et al., 2016; Xu et al., 2019). In particular, using organic semiconductors, it is possible to fabricate large-area flexible devices that are very lightweight and can be manufactured at room temperature with very low manufacturing costs, including printing technologies. Examples of organic semiconductors used in flexible electronics include pentacene ($C_{22}H_{14}$), two hexyl-substituted quinquethiophenes (DH5T), poly(3-hexylthiophene) (P3HT), poly(triarylamines) (PTAAs), and many more. These organic semiconductors are used in flexible organic light-emitting diodes (OLEDs), organic solar cells (OSCs), organic field-effect transistors (OFETs), and various sensors (Facchetti, 2007).

The main disadvantage of organic semiconductors is their high sensitivity to oxidation. For this reason, these compounds are slowly destroyed by exposure to air and light. Therefore, in the process of developing organic semiconductors for real applications, much attention is paid to their engineering in such a way as to ensure rigidity in the molecular framework and the ability to resist oxidation.

22.4.3 Graphene and Carbon Nanotubes

Experiments and modeling have shown that carbon nanotubes (CNTs) have semiconductor properties in addition to high conductivity, which is why they receive considerable attention in the development of various devices. The potential of SWNT thin films has been demonstrated by testing analog circuits and complex functional circuits consisting of nearly 100 SWNT components operating at frequencies including the GHz range (Cao et al., 2008; Sun et al., 2011). Thus, in (Cao et al., 2017; Han et al., 2017), high-mobility CNT field-effect transistors (FET) and a five-stage CNT FET ring oscillator with an amazing operating frequency of 2.8 GHz were demonstrated. Thin-film transistors using coordinated single-walled CNT (SWNT) arrays have been reported to achieve mobilities of about 2000 cm^2/V s, which compares favorably with thin-film transistors fabricated using many inorganic and, especially, organic semiconductors (Derycke et al., 2009). Applications of CNTs as the active matrix in OLED displays and active material in various sensors have also been demonstrated (Zhang et al., 2011). It is also important to note that CNTs were introduced into flexible electronics more than 15 years ago.

Graphene is the earliest 2D material. However, its bandgap is 0. But researchers have found ways to produce sizable bandgap in graphene by doping, stacking and making graphene to nanoribbons (Jiao et al., 2009). The semiconducting graphene has been employed in sensing devices like strain sensor, chemical sensors, and photodetector. However, as a high-mobility semiconducting material, its full potential lies in logic devices. The reported highest electro mobility tested in a graphene FET is over 10^5 $cm^2/V{\cdot}s$ (Lee et al., 2014a). There is also reported inverter made of graphene which exhibits a gain of 1.9 (Li et al., 2010).

22.4.4 Dihalcogenides and Other 2D Nanomaterials

Since the discovery of 2D graphene, many other 2D materials have emerged (Lin et al., 2018; Zhu et al., 2017). 2D materials were initially fabricated by mechanical exfoliation. Now, CVD is used to fabricate 2D materials, which is a cost-effective, scalable process. In recent years, inks based on 2D materials have also been invented, making it possible to fabricate flexible electronic devices based on them (Lin et al., 2018).

Among the most studied and promising 2D materials are transition metal dichalcogenide (TMD) monolayers. Transition metal dichalcogenides, with their unique properties, hold great promise for a variety of new electrical, optical, and mechanical devices and applications. For example, a MoS_2 monolayer is known for its enormous on-off ratio of up to 10^7 (Jin et al., 2014). This unique property makes it potentially attractive as gate dielectrics and semiconductor channel for high-performance field-effect transistors and low-power electronic systems. In particular, Zhang et al. (2016) fabricated a phototransistor with MoS_2 semiconductor channels on a flexible and transparent cellulose paper substrate, which demonstrated excellent photosensitivity of ~1.5 kA/W. The device simultaneously exhibited high transparency with an average optical transmittance of 82%. Flexible MoS_2 TFTs have also been applied as the backplane of LED displays in wearable systems (Choi et al., 2018b). The successful fabrication of phototransistors and TFTs on flexible cellulose nanopaper with excellent performance and transparency suggests that dichalcogenides are suitable for the fabrication of environmentally friendly and biodegradable phototransistor with high photosensitivity, wide spectral range, and durable flexibility.

Black phosphorus (BP) is another popular 2D material, which has attracted interest due to its high mobility (>1000 $cm^2/V{\cdot}s$) and adjustable band gap (0.3 eV–2 eV) (Korotcenkov, 2019; Zhu et al., 2017). Of course, BP is not as popular as MoS_2. However, there are reports that flexible transistors have been made using it (Zhu et al., 2015).

It should be noted that 2D nanomaterials can also be used in the development of various flexible chemical sensors, biosensors, humidity, and gas sensors (Korotcenkov, 2019).

22.4.5 Quantum Dots

QDs are a class of semiconductor materials with zero dimensions. This condition is satisfied by semiconductor crystals with particle sizes smaller than their Bohr radius in all dimensions. QDs have many advantages. The application of QDs is mainly based on their exquisite optical properties and their role in the emission, conversion, and detection of light (Agarwal et al., 2023; Cotta, 2020). Unlike simple atomic structures, quantum dots have an unusual property: their energy levels are highly

dependent on their size. For example, the light emission of CdSe QDs can be tuned from the red (5 nm QD) to the violet range (1.5 nm QD). In addition to sharp emission, QD technology can use solution processing, which is extremely simple and applicable for flexible electronics.

While the initial research on QDs was largely focused on group IV and III-V compounds, advances in QD synthesis over the years have expanded their elemental composition (Agarwal et al., 2023). Nowadays, in addition to III-V compounds, QDs are also based on II-VI and I-III-VI compounds, as well as transition metal dichalcogenides, perovskites, and carbon, among others (Cotta, 2020).

QDs have been utilized in various flexible devices, including field-effect transistors (FETs) (CdSe QDs, PbSe QDs, HgTe QDs, InAs QDs, InP QDs), displays (CdSe QDs, InP QDs, InGaN QDs, InZnP QDs), solar cells (CdS QDs, CdSe and CdSe/CdS QDs, PbS QDs, CdS/ZnS QDs), LEDs (InAs/GaAs QDs, InGaN QDs, ZnSe/ZnS QDs, CdSe/CdS, $CsPbX_3$ QDs, $CuInS_2$/ZnS QDs), sensors (CdTe QDs, CdSe/ZnS QDs, CdS QDs, CdSe QDs, CdTe/Cds QDs), photodetectors (PbS QDs, Ag_2Se QDs, WS_2 QDs, $CsPbBr_3$ QDs), catalysis (Carbon QDs, CdS QDs, CdSe/CdZnS/ZnS QDs, CdSe/ZnS QDs, PbS and PbS/CdS QDs), biomedical and environmental applications ($CuInS_2$/ZnS QDs, MoS_2 QDS, Fe_3O_4 QDs, CdTe QDs, ZnSe QDs), etc. (Agarwal et al., 2023; Cotta, 2020; Kramer et al., 2014; Kim et al., 2011; Liu et al., 2014). Flexible QD display is the most promising one in all those applications (Kim et al., 2011). Several technological giants, Samsung, LG, and TCL, all released their prototype flexible QD displays.

22.4.6 Photovoltaic Materials

Photovoltaic (PV) applications require semiconductor materials with a high absorption coefficient in the required spectral region. In particular, the absorption spectra of solar cells should cover the solar spectrum as much as possible to achieve high efficiency. The most successful flexible solar cell to date is the amorphous silicon solar cell. The efficiency of amorphous silicon solar cells has a theoretical limit of about 15%. However, the realized efficiency has currently increased to about 6–8% (Qarony et al., 2017). Of course, this is very low in comparison with crystalline silicon solar cells. But this is the price for flexibility and low absorption coefficient of amorphous silicon. Crystalline compound semiconductor materials, such as CdTe, $CuInSe_2$ (CIS), $Cu(In,Ga)Se_2$ (CIGS), and III–V semiconductors, have also been intensively studied for low-cost PV modules with high efficiency and excellent stability (Lin et al., 2014). Moreover, of the indicated semiconductors, the most promising are CIGS compounds. CIGS has an amazing ability to absorb 99% of energy at a thickness of less than 1 μm, which makes its power conversion efficiency (PCE) (20.3%) comparable to crystalline silicon solar cells (Jackson et al., 2011). It is important to note that the PCE of flexible CIGS solar cells approaches 20%. There are reports of solar cells on PI substrates with a conversion efficiency of 18.7% (Chirila et al., 2011).

Organic semiconductors, such as P3HT, phenyl-C61-butyric-acid-methyl-ester (PCBM), are also used for flexible solar cells (Huang et al., 2015; Kim et al., 2015; Na et al., 2008), in which the most efficient one can achieve a PCE of 10.4% (Huang et al., 2015). However, the stability of organic solar cells is still a big problem. Quantum dot-based solar cells are more stable. Colloidal quantum dots are of interest as a photovoltaic material because of their solution processability, high durability post-processing, and tunable optical absorption and emission spectra through quantum size effects. But the efficiency of such solar cells is still low. A sputter-printed flexible colloidal QD solar cell with a PCE of 7.2% has been reported (Kramer et al., 2014). In recent years, perovskite-based flexible solar cells have attracted considerable interest. Perovskite compounds have a chemical formula ABX_3, where "A" and "B" represent cations and X is an anion. $CsPbI_3$, $CsPbI_2Br$, $CH_3NH_3PbI_3$ ($MAPbI_3$), and other perovskites were tested (El-Atab & Hussain, 2020). A flexible perovskite solar cell was reported to achieve a PCE of more than 18% (Subbiah et al., 2018). However, the hygroscopicity of perovskite materials makes them highly sensitive to moisture. Thermal instability is another issue that can affect the stability of perovskite solar cells.

Meanwhile, the experiment showed that flexible solar cells can be applied not only to wearable devices but also to large-scale building-integrated photovoltaics (BIPV) (Pagliaro et al., 2008).

22.5 Dielectric Materials

Dielectric flexible functional materials are crucial for creating technologies and devices that rely on paper. Because of their exceptional electrical insulation, flexibility, and biodegradability, these materials are perfect for use in flexible electronics. Dielectric materials are used in displays, field-effect transistors, energy-storage capacitors, radio frequency (RF) chips, microwave resonators, passive elements of integrated circuits, organic light-emitting diodes (OLEDs), solar cells, etc. (see Fig. 22.6). Additionally, the dielectric is also used in sensors for various applications. It is used in temperature sensors, touch screens, humidity sensors, pressure sensors, and as position sensors. Due to its feature of flexibility, flexible dielectrics are also used in smart watches and wearable electronics for health monitoring. Strong electric breakdown strength, low dielectric losses, and a high dielectric constant are essential for any dielectric material, just like other physical characteristics.

Various materials can be used as dielectrics. In particular, inorganic dielectrics are most widely used in traditional electronics (Rim et al., 2016), the parameters of which are given in Table 22.2. However, it turned out that these materials are mostly not applicable for flexible electronics. Due to the low dielectric constant of SiO_2, thin films have to be used, which, when applied to substrates with high roughness, leads to a loss of the insulating ability of the coatings. Al_2O_3, ZrO_2, and HfO_2 have a significantly higher dielectric constant, which allows the use of thicker

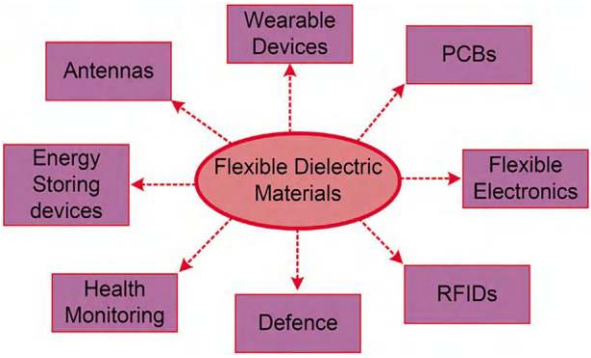

Fig. 22.6 Applications of flexible dielectric materials. (Reprinted from Hussain et al. (2024). Published 2024 by Wiley with open access)

Table 22.2 Comparison of dielectric constants of different inorganic materials

Material	Dielectric constant
SiO_2	3.9
Si_3N_4	6.2
Al_2O_3	7–10
$BaSr_xTi_{1-x}O_3$	16
$BaZr_xTi_{1-x}O_3$	17.3
Ta_2O_5	23
CeO_2	23
ZrO_2	25
HfO_2	22–25
La_2O_3	30
TiO_2	41

films. However, these materials have problems with the deposition of high-quality layers at low temperatures. These dielectrics require a high-temperature annealing process that is incompatible with paper substrates, due to the need for high-density films and low leakage currents. In addition, these coatings typically have poor mechanical properties, which complicates their use in flexible electronics. In this regard, easily processable organic dielectrics perform much better (Hussain et al., 2024).

According to Hussain et al. (2024) and Ortiz et al. (2010), polyethylene terephthalate (PET) is a commonly used flexible dielectric material in printed circuits. Polyimide (PI) is used in biomedical applications due to its chemical resistance and mechanical properties similar to natural human skin. In addition, PI finds application in thin-film transistors, flexible heaters, and sensors such as strain, shear, pressure, and crack sensors due to its high resistance, stability, and electrical insulation. Polyethylene naphtholate (PEN) has an accommodating tolerance at high temperatures. Polydimethylsiloxane (PDMS) is used in flexible electronics for antenna and soft robotics applications. PS, PI, PMMA, and other polymers are also used in various devices of organic electronics.

Natural polymers, such as cellulose, silk, shellac, and gelatine, can also be used as dielectrics in flexible electronics. In particular, Dai et al. (2018) fabricated a class of all solid-state ionic dielectrics using cellulose nanopaper. These dielectrics show high transparency, low surface roughness, good thermal durability, and excellent mechanical properties. Silk, due to its outstanding mechanical properties, flexibility, processability, and chemical stability, is also an ideal backbone for flexible and stretchable electronics (Zhu et al., 2016). Irimia-Vladu et al. (2013) have shown that, similar to the aforementioned biopolymers, shellac is biodegradable and can be used as a dielectric. The successful applications of natural polymers as substrates and dielectric materials demonstrate its potential for use in flexible, environmentally friendly, and biodegradable sensors and electronic devices.

As for transparent flexible dielectric materials, these include polymethyl methacrylate (PMMA, acrylic), polycarbonate (PC), polyamide, and polystyrene (Hussain et al., 2024). Their transparency can exceed 80–85%. The transparency of PDMS can also reach 80%. These materials are widely used in flexible displays, optical devices, flexible electronics, packaging, and biomedical devices, as well as in sensors.

As can be seen from the data presented in Table 22.3, polymer dielectrics have a small permittivity, which creates certain difficulties in the manufacture of high-performance devices requiring high capacity. The experiment showed that this problem is successfully solved through the use of nanocomposites (Ortiz et al., 2010). Interestingly, both metal oxide powders with high permittivity, such as high-*k* $BaTiO_3$ or TiO_2 (Ortiz et al., 2010), and various nanomaterials, such as CNTs and graphene, which do not have insulating properties, can be used as polymer fillers (Li et al., 2015). The experiment showed that such composite materials ideally combine the high dielectric constant of inorganic inclusions and the high mechanical flexibility and easy processability of organic analogues. For example, Chen et al. (2004)

Table 22.3 Commonly used flexible organic dielectric materials and their dielectric constant and losses

Flexible dielectric materials	Dielectric constant (ε_r)	Dielectric loss (tan δ)
Polyethylene Terephthalate (PET)	3.2	0.0071
Polyethylene Naphthalate (PEN)	2.9	0.025
Polyethylene (PE)	2.8	0.005
Poly Tetrafluoroethylene (PTFE)	2.2	0.0009
Polyamide (PI)	2.9–3.5	0.005
Polydimethylsiloxane (PDMS)	2.6–3	0.02
Kapton Polyimide (KP)	3.4–3.5	0.002
Poly(methyl methacrylate) (PMMA)	3.6	0.094
Polycarbonate (PC)	2.9–3	0.0005
Polysterene (PS)	1.9	0.02
Photo Paper	3.2	0.05
Kodak Paper	2.8	0.05
Synthetic Paper	2	0.0022

prepared nanocomposite dielectric layers using cross-linked poly-4-vinylphenol (PVP) and TiO_2 nanoparticles, which could be deposited by spin-coating. Almafie et al. (2022) developed polyacrylonitrile and reduced graphene oxide (PAN/GO) composite by electrospinning and studied their dielectric properties. The dielectric properties of the composite material exhibited the relative permittivity of 86 with a dielectric loss (tan δ) of ~5 at 10^2 Hz, and the maximum conductivity was achieved at 34.9×10^{-6} Sm^{-1} at high frequencies.

22.6 Other Functional Materials

It is clear that in this chapter we cannot adequately consider all the functional materials that can be used in the development and manufacture of paper-based sensors and devices. These are chromogenic materials, plasmonic materials, fluorophores, various biomaterials, etc. These materials will be discussed in detail in the corresponding chapters of our issue. For example, chromogenic materials will be discussed in Chap. 23 (Vol. 1). Other materials will be discussed in Vol. 2 and Vol. 3 of our Handbook. Therefore, in this chapter, we will not focus on these specific functional materials. Let's consider only piezoelectric materials and materials used for encapsulation of flexible devices.

22.6.1 Piezoelectric Materials

In addition to what was said in Sect. 22.4.1, ZnO also has pronounced piezoelectric properties, which makes it possible to fabricate piezoelectric-type strain sensors and nanogenerators based on it (Rim et al., 2016). Other metal oxides, such as $PbZr_xTi_{1-x}O_3$ (PZT), $BaTiO_3$ (BTO), and $Pb(Mg_{1/3}Nb_{2/3})O_3$-$PbTiO_3$ (PMN-PT), also belong to piezoelectric materials. Moreover, the piezoelectric coefficient of these materials is even higher than that of ZnO, which provides nanogenerators based on them with higher efficiency (Lee et al., 2014b). There are also polymer-based piezoelectric materials such as poly(vinylidene fluoride) (PVDF) and its copolymers that can work as piezoelectric-type sensors in flexible electronics (Bae et al., 2013). In the case of polymer-based piezoelectric materials, more stress is allowed due to the intrinsic flexible material properties. However, the piezoelectric coefficient is not high compared with that of piezoelectric inorganic materials. Thus, the performance of the PVDF-based sensors and copolymers is not that high compared with those based on inorganic piezoelectric materials. To overcome this limitation, some composites such as PVDF/multiwall carbon nanotubes, PVDF/ZnO, and PVDF/PZT were developed to improve performances of sensors and nanogeterators (Bae et al., 2013).

The experiment showed that some two-dimensional materials, such as MoS_2, also have strong piezoelectricity, which disappears in the volume due to the

opposite orientation of dipole moments in neighboring atomic layers (Wu et al., 2014). In particular, MoS_2 flakes with an odd number of atomic layers produce electricity under voltage, while flakes with an even number do not. This feature of MoS_2 was used in the development of piezoelectric transducers based on MoS_2.

22.6.2 Encapsulation Materials

As mentioned in many chapters of our book, paper and many functional materials are sensitive to external influences and therefore almost all devices made on a paper substrate need encapsulation to extend the lifetime of the devices. For traditional rigid devices, the encapsulation is usually a glass cover or a metal cover filled with nitrogen and CaO to prevent contact with oxygen and moisture. However, this is not applicable to flexible devices. To solve this problem, it is proposed to use a polymer cover with an oxide barrier layer on top. However, since this technology is complex, many are switching to thin-film encapsulation (TFE). Generally, a polymeric encapsulation is employed including polyvinyl fluoride films, Teflon ethylene tetrafluoroethylene, or "EVA" resin encapsulant. Currently, the encapsulation of flexible devices with polymers makes the resulting module very costly. However, the search for inexpensive polymers that exhibit excellent transparency, low oxygen and water vapor transmission rates, good stability, and UV resistance continues (El-Atab & Hussain, 2020).

Multilayers of organic/inorganic films have also been used (Spee et al., 2012). For example, Vitex developed the Barix™ technology, which included alternating layers of AlO_x and UV-cross-linked polymers. This coating can effectively block oxygen and water while maintaining flexibility. Of course, there are other approaches to protecting flexible devices. For example, much attention is currently being paid to finding an acceptable biodegradable coating (Sun et al., 2019). It has been shown that an adequate biodegradable packaging polymer is poly(L-lactide) (PLLA), which provides gas and vapor barrier properties and can be easily produced by melt casting or using common organic solvents. Moreover, adding nanofillers to polymers can be an effective method to improve gas and vapor barrier properties. Many nanofillers have been found to be useful for this purpose, including organophilic layered double hydroxide (OLDH) nanosheets, montmorillonite, and GO (Liu et al., 2019a).

22.7 Summary

The analysis showed that for the development of the whole range of flexible sensors and electronic devices on a paper basis, a large number of the most diverse functional materials are required, capable of maintaining their properties during bending and stretching. It was found that under certain conditions, such as a decrease in

thickness and the transition to nanosizes, such properties to one degree or another can be possessed by a variety of materials, including metals, metal oxides, conventional semiconductors, dichalcogenides, polymers, carbon-based materials, and MXenes.

It is clear that not all materials have good electrical, physical, and chemical properties and can be used on large continuous areas at low cost. In addition, not all materials are able to provide the required mechanical stability of devices when folding or bending. All this undoubtedly stimulates the search for new functional materials. The experiment showed that, as a rule, the greatest success in this direction is achieved in the formation of hybrid composites based on the use of nanomaterials.

Acknowledgments G.K. is grateful to the Moldova State University (research program no. 011208) for supporting his research.

References

Agarwal, K., Rai, H., & Mondal, S. (2023). Quantum dots: An overview of synthesis, properties, and applications. *Materials Research Express, 10*, 062001. https://doi.org/10.1088/2053-1591/acda17

Akter, T., & Kim, W. S. (2012). Reversibly stretchable transparent conductive coatings of spray-deposited Silver nanowires. *ACS Applied Materials & Interfaces, 4*(4), 1855–1859. https://doi.org/10.1021/am300058j

Al-Ghamdi, A. A., Al-Hartomy, O. A., Al-Solamy, F. R., Dishovsky, N., Zaimova, D., Shtarkova, R., & Iliev, V. (2016). Some factors influencing the dielectric properties of natural rubber composites containing different carbon nanostructures. *Materials Sciences and Applications, 7*(2), 108–118. https://doi.org/10.4236/msa.2016.72011

Almafie, M. R., Marlina, L., Riyanto, R., Jauhari, J., Nawawi, Z., & Sriyanti, I. (2022). Dielectric properties and flexibility of polyacrylonitrile/graphene oxide composite nanofibers. *ACS Omega, 7*(37), 33087–33096. https://doi.org/10.1021/acsomega.2c03144

Bae, S.-H., Kahya, O., Sharma, B. K., Kwon, J., Cho, H. J., Ozyilmaz, B., & Ahn, J.-H. (2013). Graphene-P(VDF-TrFE) multilayer film for flexible applications. *ACS Nano, 7*, 3130. https://doi.org/10.1021/nn400848j

Biswas, S., & Prashant, S. A. (2021). MXene: Evolutions in chemical synthesis and recent advances in applications. *Surfaces, 5*(1), 1–34. https://doi.org/10.3390/surfaces5010001

Cai, Y., Shen, J., Ge, G., Zhang, Y., Jin, W., Huang, W., et al. (2018). Stretchable $Ti_3C_2T_x$ MXene/carbon nanotube composite based strain sensor with ultrahigh sensitivity and tunable sensing range. *ACS Nano, 12*(1), 56–62. https://doi.org/10.1021/acsnano.7b06251

Cao, Q., Kim, H.-S., Pimparkar, N., Kulkarni, J. P., Wang, C., Shim, M., et al. (2008). Medium-scale carbon nanotube thin-film integrated circuits on flexible plastic substrates. *Nature, 454*(7203), 495–500. https://doi.org/10.1038/nature07110

Cao, Q., Tersoff, J., Farmer, D. B., Zhu, Y., & Han, S.-J. (2017). Carbon nanotube transistors scaled to a 40-nanometer footprint. *Science, 356*(6345), 1369–1372. https://doi.org/10.1126/science.aan2476

Cate, D. M., Adkins, J. A., Mettakoonpitak, J., & Henry, C. S. (2015). Recent developments in paper-based microfluidic devices. *Analytical Chemistry, 87*(1), 19–41. https://doi.org/10.1021/ac503968p

Channon, R. B., Nguyen, M. P., Scorzelli, A. G., Henry, E. M., Volckens, J., Dandy, D. S., & Henry, C. S. (2018). Rapid flow in multilayer microfluidic paper-based analytical devices. *Lab on a Chip, 18*(5), 793–802. https://doi.org/10.1039/C7LC01300K

Chen, F.-C., Chu, C.-W., He, J., Yang, Y., & Lin, J.-L. (2004). Organic thin-film transistors with nanocomposite dielectric gate insulator. *Applied Physics Letters, 85*, 3295–3297. https://doi.org/10.1063/1.1806283

Chirila, A., Buecheler, S., Pianezzi, F., Bloesch, P., Gretener, C., Uhl, A. R., et al. (2011). Highly efficient cu (in,Ga)Se_2 solar cells grown on flexible polymer films. *Nature Materials, 10*(11), 857–861. https://doi.org/10.1038/nmat3122

Choi, S., Han, S. I., Jung, D., Hwang, H. J., Lim, C., Bae, S., et al. (2018a). Highly conductive, stretchable and biocompatible Ag–Au core–sheath nanowire composite for wearable and implantable bioelectronics. *Nature Nanotechnology, 13*(11), 1048–1056. https://doi.org/10.1038/s41565-018-0226-8

Choi, M., Park, Y. J., Sharma, B. K., Bae, S.-R., Kim, S. Y., & Ahn, J.-H. (2018b). Flexible active-matrix organic light-emitting diode display enabled by MoS_2 thin-film transistor. *Science Advances, 4*(4), eaas8721. https://doi.org/10.1126/sciadv.aas8721

Cotta, M. N. (2020). Quantum dots and their applications: What lies ahead? *ACS Applied Nano Materials, 3*, 4920–4924. https://doi.org/10.1021/acsanm.0c01386

Dai, S. L., Chu, Y. L., Liu, D. P., Cao, F., Wu, X. H., Zhou, J. C., et al. (2018). Intrinsically ionic conductive cellulose nanopapers applied as all solid dielectrics for low voltage organic transistors. *Nature Communications, 9*, 2737. https://doi.org/10.1038/s41467-018-05155-y

Derycke, V., Auvray, S., Borghetti, J., Chung, C.-L., Lefèvre, R., Lopez-Bezanilla, A., et al. (2009). Carbon nanotube chemistry and assembly for electronic devices. *Comptes Rendus Physique, 10*(4), 330–347. https://doi.org/10.1016/j.crhy.2009.05.006

Dong, D., Dhanabalan, S. S., Elango, P. F. M., Yang, M., Walia, S., Sriram, S., & Bhaskaran, M. (2023). Emerging applications of metal-oxide thin films for flexible and stretchable electronic devices. *Applied Physics Reviews, 10*(3), 031314. https://doi.org/10.1063/5.0151297

El-Atab, N., & Hussain, M. M. (2020). Flexible and stretchable inorganic solar cells: Progress, challenges, and opportunities. *MRS Energy & Sustainability, 7*, e19. https://doi.org/10.1557/mre.2020.22

Facchetti, A. (2007). Semiconductors for organic transistors. *Materials Today, 10*(3), 28–37. https://doi.org/10.1016/S1369-7021(07)70017-2

Fu, E., Ramsey, S. A., Kauffman, P., Lutz, B., & Yager, P. (2011). Transport in two-dimensional paper networks. *Microfluidics and Nanofluidics, 10*(1), 29–35. https://doi.org/10.1007/s10404-010-0643-y

Ge, G., Zhang, Y., Shao, J., Wang, W., Si, W., Huang, W., & Dong, X. (2018). Stretchable, transparent, and self-patterned hydrogel-based pressure sensor for human motions detection. *Advanced Functional Materials, 28*(32), 1802576. https://doi.org/10.1002/adfm.201802576

Gong, S., Lai, D. T. H., Su, B., Si, K. J., Ma, Z., Yap, L. W., et al. (2015a). Highly stretchy black Gold E-skin nanopatches as highly sensitive wearable biomedical sensors. *Advanced Electronic Materials, 1*(4), 1400063. https://doi.org/10.1002/aelm.201400063

Gong, S., Lai, D. T. H., Wang, Y., Yap, L. W., Si, K. J., Shi, Q., et al. (2015b). Tattoolike polyaniline microparticle-doped Gold nanowire patches as highly durable wearable sensors. *ACS Applied Materials & Interfaces, 7*(35), 19700–19708. https://doi.org/10.1021/acsami.5b05001

Gunasekara, D. S. W., He, Y., Liu, H., & Liu, L. (2021). Smart wearable, highly sensitive pressure sensor with MWNTs/PPy aerogel composite. *Fibers and Polymers, 22*(8), 2102–2111. https://doi.org/10.1007/s12221-021-0787-2

Guo, J., Si, M., Zhao, X., Wang, L., Wang, K., Hao, J., et al. (2022). Altering interfacial properties through the integration of C60 into ZnO ceramic via cold sintering process. *Carbon, 190*, 255–261. https://doi.org/10.1016/j.carbon.2022.01.017

Ha, M., Lim, S., Park, J., Um, D.-S., Lee, Y., & Ko, H. (2015). Bioinspired interlocked and hierarchical design of ZnO nanowire arrays for static and dynamic pressure-sensitive electronic skins. *Advanced Functional Materials, 25*(19), 2841–2849. https://doi.org/10.1002/adfm.201500453

Han, S.-J., Tang, J., Kumar, B., Falk, A., Farmer, D., Tulevski, G., et al. (2017). High-speed logic integrated circuits with solution-processed self-assembled carbon nanotubes. *Nature Nanotechnology, 12*(9), 861–865. https://doi.org/10.1038/nnano.2017.115

Harley, C. C., Rooney, A. D., & Breslin, C. B. (2010). The selective detection of dopamine at a polypyrrole film doped with sulfonated β-Cyclodextrins. *Sensors and Actuators B: Chemical, 150*(2), 498–504. https://doi.org/10.1016/j.snb.2010.09.012

Hong, S. Y., Lee, Y. H., Park, H., Jin, S. W., Jeong, Y. R., Yun, J., et al. (2016). Stretchable active matrix temperature sensor array of polyaniline nanofibers for electronic skin. *Advanced Materials, 28*(5), 930–935. https://doi.org/10.1002/adma.201504659

Hosseini, Z., Dongmin Shi, D., & Jie, Y. J. (2025). A flexible multiplexed electrochemical biosensing platform with Graphene and Gold nanoparticle modification for enhanced E-ELISA point-of-care biomarker detection. *Microchemical Journal, 208*, 112437. https://doi.org/10.1016/j.microc.2024.112437

Huang, J., Li, C.-Z., Chueh, C.-C., Liu, S.-Q., Yu, J.-S., & Jen, A. K.-Y. (2015). 10.4% power conversion efficiency of ito-free organic photovoltaics through enhanced light trapping configuration. *Advanced Energy Materials, 5*(15), 1500406. https://doi.org/10.1002/aenm.201500406

Hussain, A. M., & Hussain, M. M. (2016). CMOS-technology-enabled flexible and stretchable electronics for internet of everything applications. *Advanced Materials, 28*(22), 4219–4249. https://doi.org/10.1002/adma.201504236

Hussain, M., Zahra, H., Abbas, S. M., & Zhu, Y. (2024). Flexible dielectric materials: Potential and applications in antennas and RF sensors. *Advanced Electronic Materials, 10*, 2400240. https://doi.org/10.1002/aelm.202400240

Hwang, B.-U., Lee, J.-H., Trung, T. Q., Roh, E., Kim, D.-I., Kim, S.-W., & Lee, N.-E. (2015). Transparent stretchable self-powered patchable sensor platform with ultrasensitive recognition of human activities. *ACS Nano, 9*(9), 8801–8810. https://doi.org/10.1021/acsnano.5b01835

Hyun, W. J., Park, O. O., & Chin, B. D. (2013). Foldable Graphene electronic circuits based on paper substrates. *Advanced Materials, 25*(34), 4729–4734. https://doi.org/10.1002/adma.201302063

Iijima, S. (1991). Helical microtubules of graphitic carbon. *Nature, 354*(6348), 56–58. https://doi.org/10.1038/354056a0

Irimia-Vladu, M., Glowacki, E. D., Schwabegger, G., Leonat, L., Akpinar, H. Z., Sitter, H., et al. (2013). Natural resin shellac as a substrate and a dielectric layer for organic field-effect transistors. *Green Chemistry, 15*, 1473–1476. https://doi.org/10.1039/C3GC40388B

Jackson, P., Hariskos, D., Lotter, E., Paetel, S., Wuerz, R., Menner, R., et al. (2011). New world record efficiency for Cu(In,Ga)Se_2 thin-film solar cells beyond 20%. *Progress in Photovoltaics: Research and Applications, 19*(7), 894–897. https://doi.org/10.1002/pip.1078

Jeon, Y., Lee, D., & Yoo, H. (2022). Recent advances in metal-oxide thin-film transistors: Flexible/stretchable devices, integrated circuits, biosensors, and neuromorphic applications. *Coatings, 12*(2), 204. https://doi.org/10.3390/coatings12020204

Jerome, R., & Sundramoorthy, A. K. (2019). Hydrothermal synthesis of Boron nitride quantum dots/poly(Luminol) nanocomposite for selective detection of ascorbic acid. *Journal of the Electrochemical Society, 166*(9), B3017–B3024. https://doi.org/10.1149/2.0041909jes

Jiao, L., Zhang, L., Wang, X., Diankov, G., & Dai, H. (2009). Narrow graphene nanoribbons from carbon nanotubes. *Nature, 458*(7240), 877–880. https://doi.org/10.1038/nature07919

Jin, Z., Li, X., Mullen, J. T., & Kim, K. W. (2014). Intrinsic transport properties of electrons and holes in monolayer transition-metal dichalcogenides. *Physical Review B, 90*(4), 045422. https://doi.org/10.1103/PhysRevB.90.045422

Jin, T., Park, S.-H. K., & Fang, D.-W. (2022). Highly-stable flexible pressure sensor using piezoelectric polymer film on metal oxide TFT. *RSC Advances, 12*(33), 21014–21021. https://doi.org/10.1039/D2RA02613A

Joo, Y., Byun, J., Seong, N., Ha, J., Kim, H., Kim, S., et al. (2015). Silver nanowire-embedded PDMS with a multiscale structure for a highly sensitive and robust flexible pressure sensor. *Nanoscale, 7*(14), 6208–6215. https://doi.org/10.1039/C5NR00313J

Kaltenbrunner, M., Sekitani, T., Reeder, J., Yokota, T., Kuribara, K., Tokuhara, T., et al. (2013). An ultra-lightweight design for imperceptible plastic electronics. *Nature, 499*(7459), 458–463. https://doi.org/10.1038/nature12314

Khan, S. M., Nassar, J. M., & Hussain, M. M. (2021). Paper as a substrate and an active material in paper electronics. *ACS Applied Electronic Materials, 3*(1), 30–52. https://doi.org/10.1021/acsaelm.0c00484

Kim, T.-H., Cho, K.-S., Lee, E. K., Lee, S. J., Chae, J., Kim, J. W., et al. (2011). Full-colour quantum dot displays fabricated by transfer printing. *Nature Photonics, 5*(3), 176–182. https://doi.org/10.1038/nphoton.2011.12

Kim, T., Kim, J.-H., Kang, T. E., Lee, C., Kang, Y., Shin, M., et al. (2015). Flexible, highly efficient all-polymer solar cells. *Nature Communications, 6*, 8547. https://doi.org/10.1038/ncomms9547

Kim, H., Kim, G., Kim, T., Lee, S., Kang, D., Hwang, M.-S., et al. (2018a). Transparent, flexible, conformal capacitive pressure sensors with nanoparticles. *Small, 14*(8), 1703432. https://doi.org/10.1002/smll.201703432

Kim, S. J., Mondal, S., Min, B. K., & Choi, C.-G. (2018b). Highly sensitive and flexible strain–pressure sensors with cracked paddy-shaped MoS_2/Graphene foam/Ecoflex hybrid nanostructures. *ACS Applied Materials & Interfaces, 10*(42), 36377–36384. https://doi.org/10.1021/acsami.8b11233

Ko, Y. H., Nagaraju, G., Lee, S. H., & Yu, J. S. (2014). PDMS-based triboelectric and transparent nanogenerators with ZnO nanorod arrays. *ACS Applied Materials & Interfaces, 6*(9), 6631–6637. https://doi.org/10.1021/am5018072

Korotcenkov, G. (2019). Black phosphorus—New nanostructured material for humidity sensors: Achievements and limitations. *Sensors (MDPI), 19*, 1010. https://doi.org/10.3390/s19051010

Kramer, I. J., Moreno-Bautista, G., Minor, J. C., Kopilovic, D., & Sargent, E. H. (2014). Colloidal quantum dot solar cells on curved and flexible substrates. *Applied Physics Letters, 105*(16), 163902. https://doi.org/10.1063/1.4898635

Kuribara, K., Wang, H., Uchiyama, N., Fukuda, K., Yokota, T., Zschieschang, U., et al. (2012). Organic transistors with high thermal stability for medical applications. *Nature Communications, 3*(1), 723. https://doi.org/10.1038/ncomms1721

Lee, S., Iyore, O. D., Park, S., Lee, Y. G., Jandhyala, S., Kang, C. G., et al. (2014a). Rigid substrate process to achieve high mobility in graphene field-effect transistors on a flexible substrate. *Carbon, 68*, 791–797. https://doi.org/10.1016/j.carbon.2013.11.071

Lee, H. S., Jeong, C. K., Hwang, G.-T., & Lee, K. J. (2014b). Self-powered flexible inorganic electronic system. *Nano Energy, 14*, 111–125. https://doi.org/10.1016/j.nanoen.2014.12.003

Lee, S., Shin, S., Lee, S., Seo, J., Lee, J., Son, S., et al. (2015). Ag nanowire reinforced highly stretchable conductive fibers for wearable electronics. *Advanced Functional Materials, 25*(21), 3114–3121. https://doi.org/10.1002/adfm.201500628

Li, S.-L., Miyazaki, H., Kumatani, A., Kanda, A., & Tsukagoshi, K. (2010). Low operating bias and matched input-output characteristics in graphene logic inverters. *Nano Letters, 10*(7), 2357–2362. https://doi.org/10.1021/nl100031x

Li, M., Tian, J., Al-Tamimi, M., & Shen, W. (2012a). Paper-based blood typing device that reports patient's blood type 'in writing'. *Angewandte Chemie International Edition, 51*(22), 5497–5501. https://doi.org/10.1002/anie.201201822

Li, X., Ballerini, D. R., & Shen, W. (2012b). A perspective on paper-based microfluidics: Current status and future trends. *Biomicrofluidics, 6*(1), 11301–1130113. https://doi.org/10.1063/1.3687398

Li, Q., Chen, L., Gadinski, M. R., Zhang, S., Zhang, G., Li, H. U., et al. (2015). Flexible high-temperature dielectric materials from polymer nanocomposites. *Nature, 523*(7562), 576–579. https://doi.org/10.1038/nature14647

Li, J., Bao, R., Tao, J., Peng, Y., & Pan, C. (2018). Recent progress in flexible pressure sensor arrays: From design to applications. *Journal of Materials Chemistry C, 6*(44), 11878–11892. https://doi.org/10.1039/C8TC02946F

Li, Z., and Guo, Z. (2020). Flexible 3D porous superhydrophobic composites for oil-water separation and organic solvent detection. *Materials & Design, 196*, 109144. https://doi.org/10.1016/j.matdes.2020.109144

Lin, Q., Huang, H., Jing, Y., Fu, H., Chang, P., Li, D., Yao, Y., & Fan, Z. (2014). Flexible photovoltaic technologies. *Journal of Materials Chemistry C, 2*, 1233. https://doi.org/10.1039/c3tc32197e

Lin, C.-W., Wei, K.-C., Liao, S.-S., Huang, C.-Y., Sun, C.-L., Wu, P.-J., et al. (2015). A reusable magnetic graphene oxide-modified biosensor for vascular endothelial growth factor detection in cancer diagnosis. *Biosensors & Bioelectronics, 67*, 431–437. https://doi.org/10.1016/j.bios.2014.08.080

Lin, Z., Liu, Y., Halim, U., Ding, M., Liu, Y., Wang, Y., et al. (2018). Solution-processable 2D semiconductors for high-performance large-area electronics. *Nature, 562*(7726), 254–258. https://doi.org/10.1038/s41586-018-0574-4

Lipomi, D. J. (2016). Stretchable figures of merit in deformable electronics. *Advanced Materials, 28*(22), 4180–4183. https://doi.org/10.1002/adma.201504196

Liu, H., Li, M., Voznyy, O., Hu, L., Fu, Q., Zhou, D., et al. (2014). Physically flexible, rapid-response gas sensor based on colloidal quantum dot solids. *Advanced Materials, 26*(17), 2718–2724. https://doi.org/10.1002/adma.201304366

Liu, A., Kovacik, P., Peard, N., Tian, W., Goktas, H., Lau, J., et al. (2017). Monolithic flexible supercapacitors integrated into single sheets of paper and membrane via vapor printing. *Advanced Materials, 29*(19), 1606091. https://doi.org/10.1002/adma.201606091

Liu, H., Jian, R., Chen, H., Tian, X., Sun, C., Zhu, J., et al. (2019a). Application of biodegradable and biocompatible nanocomposites in electronics: Current status and future directions. *Nanomaterials, 9*, 950. https://doi.org/10.3390/nano9070950

Liu, Y., Liu, J., Chen, S., Lei, T., Kim, Y., Niu, S., et al. (2019b). Soft and elastic hydrogel-based microelectronics for localized low-voltage neuromodulation. *Nature Biomedical Engineering, 3*(1), 58–68. https://doi.org/10.1038/s41551-018-0335-6

López-Naranjo, E. J., González-Ortiz, L. J., Apátiga, L. M., Rivera-Muñoz, E. M., & Manzano-Ramírez, A. (2016). Transparent electrodes: A review of the use of carbon-based nanomaterials. *Journal of Nanomaterials, 2016*(1), 4928365. https://doi.org/10.1155/2016/4928365

Lu, Z., Song, J., Pan, K., Meng, J., Xin, Z., Liu, Y., et al. (2019). EcoFlex sponge with ultrahigh oil absorption capacity. *ACS Applied Materials & Interfaces, 11*(22), 20037–20044. https://doi.org/10.1021/acsami.9b04446

Lv, T., Liu, M., Zhu, D., Gan, L., & Chen, T. (2018). Nanocarbon-based materials for flexible all-solid-state supercapacitors. *Advanced Materials, 30*(17), 1705489. https://doi.org/10.1002/adma.201705489

Ma, L., Wu, R., Patil, A., Zhu, S., Meng, Z., Meng, H., et al. (2019). Full-textile wireless flexible humidity sensor for human physiological monitoring. *Advanced Functional Materials, 29*(43), 1904549. https://doi.org/10.1002/adfm.201904549

Na, S.-I., Kim, S.-S., Jo, J., & Kim, D.-Y. (2008). Efficient and flexible ITO-free organic solar cells using highly conductive polymer anodes. *Advanced Materials, 20*(21), 4061–4067. https://doi.org/10.1002/adma.200800338

Nam, V. B., Shin, J., Choi, A., Choi, H., Ko, S. H., & Lee, D. (2021). High-temperature, thin, flexible and transparent Ni-based heaters patterned by laser-induced reductive sintering on colorless polyimide. *Journal of Materials Chemistry C, 9*(17), 5652–5661. https://doi.org/10.1039/D1TC00435B

Nassajfar, M. N., Deviatkin, I., Leminen, V., & Horttanainen, M. (2021). Alternative materials for printed circuit board production: An environmental perspective. *Sustainability, 13*(21), 12126. https://doi.org/10.3390/su132112126

Oliveira, G. S., Candido, I. C. M., & de Oliveira, H. P. (2022). Metal-free triboelectric nanogenerators for application in wearable electronics. *Materials Advances, 3*(11), 4460–4470. https://doi.org/10.1039/D2MA00195K

Ortiz, R. P., Facchetti, A., & Marks, T. J. (2010). High-k organic, inorganic, and hybrid dielectrics for low-voltage organic field-effect transistors. *Chemical Reviews, 110*, 205–239. https://doi.org/10.1021/cr9001275

Pagliaro, M., Ciriminna, R., & Palmisano, G. (2008). Flexible solar cells. *ChemSusChem: Chemistry–Sustainability–Energy–Materials, 1*(11), 880–891. https://doi.org/10.1002/cssc.200800127

Parida, K., Thangavel, G., Cai, G., Zhou, X., Park, S., Xiong, J., & Lee, P. S. (2019). Extremely stretchable and self-healing conductor based on thermoplastic elastomer for all-three-dimensional printed triboelectric nanogenerator. *Nature Communications, 10*(1), 2158. https://doi.org/10.1038/s41467-019-10061-y

Park, H., Jeong, Y. R., Yun, J., Hong, S. Y., Jin, S., Lee, S.-J., et al. (2015). Stretchable array of highly sensitive pressure sensors consisting of polyaniline nanofibers and Au-coated polydimethylsiloxane micropillars. *ACS Nano, 9*(10), 9974–9985. https://doi.org/10.1021/acsnano.5b03510

Peng, H.-P., Hu, Y., Liu, P., Deng, Y.-N., Wang, P., Chen, W., et al. (2015). Label-free electrochemical DNA biosensor for rapid detection of mutidrug resistance gene based on Au nanoparticles/toluidine blue–graphene oxide nanocomposites. *Sensors and Actuators B: Chemical, 207*, 269–276. https://doi.org/10.1016/j.snb.2014.10.059

Petti, L., Münzenrieder, N., Vogt, C., Faber, H., Büthe, L., Cantarella, G., et al. (2016). Metal oxide semiconductor thin-film transistors for flexible electronics. *Applied Physics Reviews, 3*(2), 021303. https://doi.org/10.1063/1.4953034

Qarony, W., Hossain, M. I., Hossain, M. K., Uddin, M. J., Haque, A., Saad, A. R., & Tsang, Y. H. (2017). Efficient amorphous silicon solar cells: Characterization, optimization, and optical loss analysis. *Results in Physics, 7*, 4287–4293. https://doi.org/10.1016/j.rinp.2017.09.030

Rim, Y. S., Bae, S.-H., Chen, H., De Marco, N., & Yang, Y. (2016). Recent progress in materials and devices toward printable and flexible sensors. *Advanced Materials, 28*(22), 4415–4440. https://doi.org/10.1002/adma.201505118

Rojas, J. P., Conchouso, D., Arevalo, A., Singh, D., Foulds, I. G., & Hussain, M. M. (2017). Paper-based origami flexible and foldable thermoelectric nanogenerator. *Nano Energy, 31*, 296–301. https://doi.org/10.1016/j.nanoen.2016.11.012

Rovisco, A., dos Santos, A., Cramer, T., Martins, J., Branquinho, R., Águas, H., et al. (2020). Piezoelectricity enhancement of nanogenerators based on PDMS and $ZnSnO_3$ nanowires through microstructuration. *ACS Applied Materials & Interfaces, 12*(16), 18421–18430. https://doi.org/10.1021/acsami.9b21636

Schwartz, G., Tee, B. C. K., Mei, J., Appleton, A. L., Kim, D. H., Wang, H., & Bao, Z. (2013). Flexible polymer transistors with high pressure sensitivity for application in electronic skin and health monitoring. *Nature Communications, 4*(1), 1859. https://doi.org/10.1038/ncomms2832

Sekitani, T., Zschieschang, U., Klauk, H., & Someya, T. (2010a). Flexible organic transistors and circuits with extreme bending stability. *Nature Materials, 9*(12), 1015–1022. https://doi.org/10.1038/nmat2896

Sekitani, T., Ute Zschieschang, U., Klauk, H., & Someya, T. (2010b). Flexible organic transistors and circuits with extreme bending stability. *Nature Materials, 9*(12), 1015–1022. https://doi.org/10.1038/nmat2896

Shin, M., Lim, J., Park, Y., Lee, J.-Y., Yoon, J., & Choi, J.-W. (2024). Carbon-based nanocomposites for biomedical applications. *RSC Advances, 14*(10), 7142–7156. https://doi.org/10.1039/D3RA08946K

Son, D., & Bao, Z. (2018). Nanomaterials in skin-inspired electronics: Toward soft and robust skin-like electronic nanosystems. *ACS Nano, 12*(12), 11731–11739. https://doi.org/10.1021/acsnano.8b07738

Spee, D., van der Werf, K., Rath, J. K., & Schropp, R. (2012). Excellent organic/inorganic transparent thin film moisture barrier entirely made by hot wire CVD at 100°C. *Physica Status Solidi (RRL), 6*, 151–153. https://doi.org/10.1002/pssr.201206035

Subbiah, A. S., Mathews, N., Mhaisalkar, S., & Sarkar, S. K. (2018). Novel plasma-assisted low-temperature-processed SnO_2 thin films for efficient flexible perovskite photovoltaics. *ACS Energy Letters, 3*(7), 1482–1491. https://doi.org/10.1021/acsenergylett.8b00692

Sun, D.-M., Timmermans, M. Y., Tian, Y., Nasibulin, A. G., Kauppinen, E. I., Kishimoto, S., et al. (2011). Flexible high-performance carbon nanotube integrated circuits. *Nature Nanotechnology, 6*(3), 156–161. https://doi.org/10.1038/nnano.2011.1

Sun, J.-Y., Keplinger, C., Whitesides, G. M., & Suo, Z. (2014). Ionic skin. *Advanced Materials, 26*(45), 7608–7614. https://doi.org/10.1002/adma.201403441

Sun, J., Li, H., Huang, Y., Zheng, X., Liu, Y., Zhuang, J., & Wu, D. (2019). Simple and affordable way to achieve polymeric superhydrophobic surfaces with biomimetic hierarchical roughness. *ACS Omega, 4*, 2750–2757. https://doi.org/10.1021/acsomega.8b03138

Vo, T. S., & Kim, K. (2024). Recent trends of functional composites and structures for electro-mechanical sensors: A review. *Advanced Intelligent Systems, 6*(5), 2300730. https://doi.org/10.1002/aisy.202300730

Wang, C., Li, D., Too, C. O., & Wallace, G. G. (2009a). Electrochemical properties of graphene paper electrodes used in Lithium batteries. *Chemistry of Materials, 21*(13), 2604–2606. https://doi.org/10.1021/cm900764n

Wang, D.-W., Li, F., Zhao, J., Ren, W., Chen, Z.-G., Tan, J., et al. (2009b). Fabrication of graphene/polyaniline composite paper *via in situ* anodic electropolymerization for high-performance flexible electrode. *ACS Nano, 3*(7), 1745–1752. https://doi.org/10.1021/nn900297m

Wang, L., Chen, D., Jiang, K., & Shen, G. (2017). New insights and perspectives into biological materials for flexible electronics. *Chemical Society Reviews, 46*(22), 6764–6815. https://doi.org/10.1039/C7CS00278E

Wang, S., Xu, J., Wang, W., Wang, G.-J. N., Rastak, R., Molina-Lopez, F., et al. (2018). Skin electronics from scalable fabrication of an intrinsically stretchable transistor array. *Nature, 555*(7694), 83–88. https://doi.org/10.1038/nature25494

Wang, Y., Yang, Q., Zhao, Y., Du, S., & Zhi, C. (2019). Recent advances in electrode fabrication for flexible energy-storage devices. *Advanced Materials Technologies, 4*(7), 1900083. https://doi.org/10.1002/admt.201900083

Wei, Y., Chen, S., Yuan, X., Wang, P., & Liu, L. (2016). Multiscale wrinkled microstructures for piezoresistive fibers. *Advanced Functional Materials, 26*(28), 5078–5085. https://doi.org/10.1002/adfm.201600580

Wu, W., Wang, L., Li, Y., Zhang, F., Lin, L., Niu, S., et al. (2014). Piezoelectricity of single-atomic-layer MoS_2 for energy conversion and piezotronics. *Nature, 514*, 470–474. https://doi.org/10.1038/nature13792

Wu, J., Han, S., Yang, T., Li, Z., Wu, Z., Gui, X., et al. (2018). Highly stretchable and transparent thermistor based on self-healing double network hydrogel. *ACS Applied Materials & Interfaces, 10*(22), 19097–19105. https://doi.org/10.1021/acsami.8b03524

Wu, Z., Yang, X., & Wu, J. (2021). Conductive hydrogel- and organohydrogel-based stretchable sensors. *ACS Applied Materials & Interfaces, 13*(2), 2128–2144. https://doi.org/10.1021/acsami.0c21841

Xia, K., Wang, C., Jian, M., Wang, Q., & Zhang, Y. (2018). CVD growth of fingerprint-like patterned 3D Graphene film for an ultrasensitive pressure sensor. *Nano Research, 11*(2), 1124–1134. https://doi.org/10.1007/s12274-017-1731-z

Xiang, L., Zhang, H., Hu, Y., & Peng, L.-M. (2018). Carbon nanotube-based flexible electronics. *Journal of Materials Chemistry C, 6*(29), 7714–7727. https://doi.org/10.1039/C8TC02280A

Xu, J., Wu, H.-C., Zhu, C., Ehrlich, A., Shaw, L., Nikolka, M., et al. (2019). Multi-scale ordering in highly stretchable polymer semiconducting films. *Nature Materials, 18*(6), 594–601. https://doi.org/10.1038/s41563-019-0340-5

Xu, Y., Fei, Q., Page, M., Zhao, G., Ling, Y., Stoll, S. B., & Yan, Z. (2021). Paper-based wearable electronics. *iScience, 24*(7), 102736. https://doi.org/10.1016/j.isci.2021.102736

Yokota, T. (2024). Ultra-flexible organic electronics. In S. Ogawa (Ed.), *Organic electronics materials and devices* (pp. 185–219). Springer. https://doi.org/10.1007/978-4-431-56936-7_5

You, I., Kong, M., & Jeong, U. (2019). Block copolymer elastomers for stretchable electronics. *Accounts of Chemical Research, 52*(1), 63–72. https://doi.org/10.1021/acs.accounts.8b00488

Yu, T., & Breslin, C. B. (2020). Review—Two-dimensional Titanium Carbide MXenes and their emerging applications as electrochemical sensors. *Journal of the Electrochemical Society, 167*(3), 037514. https://doi.org/10.1149/2.0142003JES

Yu, Y., & Zhang, J. (2017). Pencil-drawing assembly to prepare Graphite/MWNT hybrids for high performance integrated paper supercapacitors. *Journal of Materials Chemistry A, 5*(9), 4719–4725. https://doi.org/10.1039/C6TA10076G

Yu, Y., Peng, S., Blanloeuil, P., Wu, S., & Wang, C. H. (2020). Wearable temperature sensors with enhanced sensitivity by engineering microcrack morphology in PEDOT:PSS–PDMS sensors. *ACS Applied Materials & Interfaces, 12*(32), 36578–36588. https://doi.org/10.1021/acsami.0c07649

Zhang, J., Fu, Y., Wang, C., Chen, P.-C., Liu, Z., Wei, W., et al. (2011). Separated carbon nanotube macroelectronics for active matrix organic light-emitting diode displays. *Nano Letters, 11*(11), 4852–4858. https://doi.org/10.1021/nl202695v

Zhang, Y.-Z., Wang, Y., Cheng, T., Lai, W.-Y., Pang, H., & Huang, W. (2015). Flexible supercapacitors based on paper substrates: A new paradigm for low-cost energy storage. *Chemical Society Reviews, 44*(15), 5181–5199. https://doi.org/10.1039/C5CS00174A

Zhang, Q., Bao, W., Gong, A., Gong, T., Ma, D., Wan, J., et al. (2016). High-sensitivity, highly transparent, gel-gated MoS_2 phototransistor on biodegradable nanopaper. *Nanoscale, 8*(29), 14237–14242. https://doi.org/10.1039/C6NR01534D

Zhang, X.-S., Su, M., Brugger, J., & Kim, B. (2017). Penciling a triboelectric nanogenerator on paper for autonomous power MEMS applications. *Nano Energy, 33*, 393–401. https://doi.org/10.1016/j.nanoen.2017.01.053

Zhang, Y., Zhang, L., Cui, K., Ge, S., Cheng, X., Yan, M., Yu, J., & Liu, H. (2018). Flexible electronics based on micro/nanostructured paper. *Advanced Materials, 30*(51), 1801588. https://doi.org/10.1002/adma.201801588

Zhao, S., Li, J., Cao, D., Zhang, G., Li, J., Li, K., et al. (2017). Recent advancements in flexible and stretchable electrodes for electromechanical sensors: Strategies, materials, and features. *ACS Applied Materials & Interfaces, 9*(14), 12147–12164. https://doi.org/10.1021/acsami.6b13800

Zhong, Q., Zhong, J., Hu, B., Hu, Q., Zhou, J., & Wang, Z. L. (2013). A paper-based nanogenerator as a power source and active sensor. *Energy & Environmental Science, 6*(6), 1779. https://doi.org/10.1039/c3ee40592c

Zhou, Z., Walker, S. B., LeMieux, M., & Leu, P. W. (2021). Polymer-embedded Silver microgrids by particle-free reactive inks for flexible high-performance transparent conducting electrodes. *ACS Applied Electronic Materials, 3*(5), 2079–2086. https://doi.org/10.1021/acsaelm.1c00107

Zhu, W., Yogeesh, M. N., Yang, S., Aldave, S. H., Kim, J.-S., Sonde, S., et al. (2015). Flexible black phosphorus ambipolar transistors, circuits and am demodulator. *Nano Letters, 15*(3), 1883–1890. https://doi.org/10.1021/nl5047329

Zhu, B., Wang, H., Leow, W. R., Cai, Y., Loh, X. J., Han, M.-Y., & Chen, X. (2016). Silk fibroin for flexible electronic devices. *Advanced Materials, 28*, 4250–4265. https://doi.org/10.1002/adma.201504276

Zhu, W., Park, S., Yogeesh, M. N., & Akinwande, D. (2017). Advancements in 2D flexible nanoelectronics: From material perspectives to rf applications. *Flexible and Printed Electronics, 2*(4), 043001. https://doi.org/10.1088/2058-8585/aa84a4

Chapter 23
Functional Materials for Paper-Based Chromogenic Sensors and Devices

Ghenadii Korotcenkov

23.1 Chromism: General Consideration

Chromogenic materials comprise another large group of materials used in paper sensors and devices. The main advantage of these materials is the ability to change color, often reversibly, under the influence of various irritants, which can be both chemical and physical. This process is called chromism. It should be noted that chromism has a long history. A diagram of the evolution of the chromogenic effect and chromogenic materials is presented in Fig. 23.1.

Chromogenics covers switchable technology used in glazing, mirrors, transparent displays, sensors, and a variety of other applications (Bamfield, 2001; Lampert, 2004; Sadeghi et al., 2020; Seok et al., 2022). Possible applications of chromogenic materials are shown in Fig. 23.2.

Chromism is classified according to the type of stimuli used. Examples of chromism are photochromism, electrochromism, thermochromism, piezochromism, ionochromism, halochromism, solvatochromism, mechanochromism, magnetochromism, hydrochromism, biochromism, and others. Various names indicate that physicochemical changes are caused by light, electric current, temperature, pressure, ions, pH, nature of the solvent, mechanical action, magnetic field, water or humidity, and biochemical reaction, respectively. It has been established that there are many natural organic or inorganic compounds that have chromism. In addition, many artificial compounds with specific chromism have been synthesized. However, experiment has shown that for practical devices it is desirable that chromogenic materials have the following parameters (Lampert, 2004).

(a) High contrast ratio, defined as the difference in transmittance across the visible spectrum.

G. Korotcenkov (✉)
Department of Physics and Engineering, Moldova State University, Chisinau, Moldova

G. Korotcenkov (ed.), *The Handbook of Paper-Based Sensors and Devices*,
https://doi.org/10.1007/978-3-031-91080-7_23

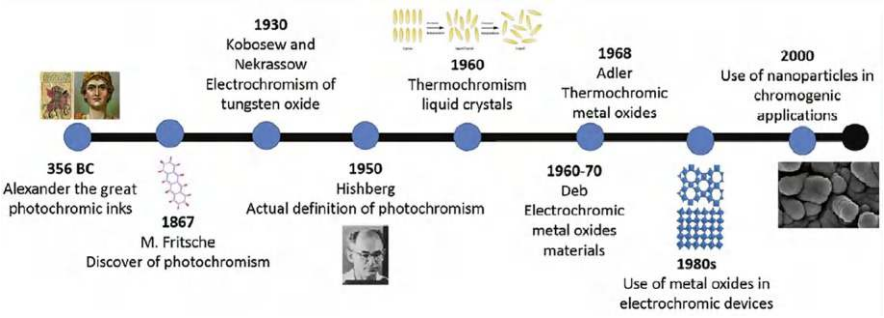

Fig. 23.1 Historic events in the development of chromogenic materials. (Reprinted with permission from Nunes et al. (2019). Copyright 2019: Elsevier)

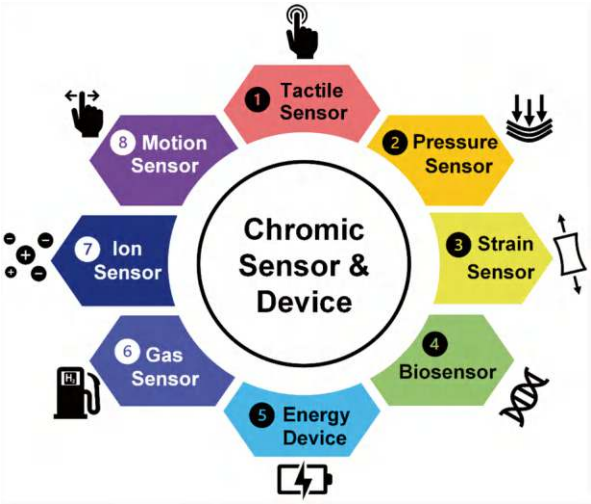

Fig. 23.2 Schematic representation of the areas of application of chromium systems as a visual indicator in various types of sensors. (Reprinted from Seok et al. (2022). Published 2022 by MDPI with open access)

(b) Low response time, which is defined as the time it takes for the color change to reach 95% of the final change.
(c) High coloration efficiency, defined as the change in optical density per unit electrode area for a given wavelength.
(d) Write-erase efficiency, defined as the fraction of the originally formed color state that can be electrochemically bleached.
(e) Good service life: Lifetime is defined as the number of write-erase cycles that can be completed before significant degradation occurs.

Let us now take a closer look at the main types of chromism that are found in paper sensors and other paper applications, such as packaging applications, where

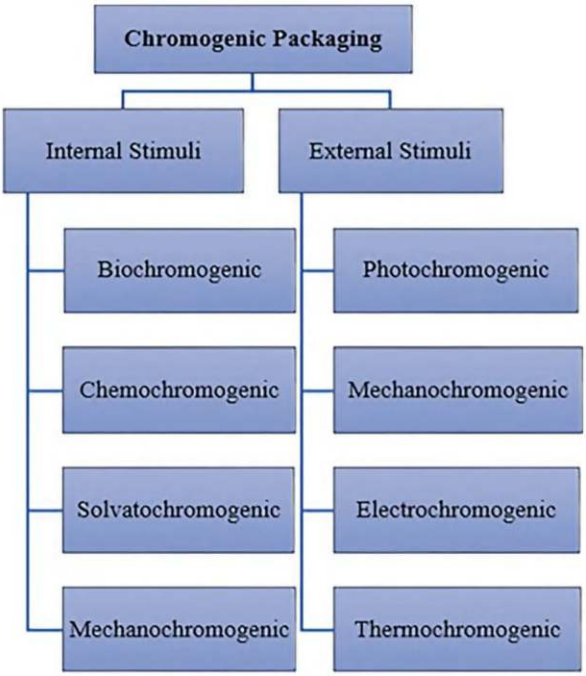

Fig. 23.3 Stimuli in smart packaging. (Reprinted with permission from Sadeghi et al. (2020). Copyright 2020: Taylor and Francis group)

changing color depending on food stimuli can be a smart method of communication between consumers and food products (Sadeghi et al., 2020). Stimuli that can cause color change in chromogenic materials during food storage are shown in Fig. 23.3. As can be seen, during food storage, the phenomenon of color change is usually associated with an energy source, such as an external or internal stimulus. It must be borne in mind that each mechanism may be associated with several different chromisms. For example, Ntoi et al. (2017) showed that dithizone, its derivatives, and complexes respond to at least seven different external stimuli that cause color changes. In these materials they observed concentratochromism, solvatochromism, halochromism, thermochromism, chronochromism, and photochromism.

23.2 Thermochromism

Thermochromism is chromism caused by heat, that is, a change in temperature (Day, 1963). This is the most common chromism of all. Thermochromic (TC) materials change their optical behavior when they reach a certain critical temperature (T_c). Upon reaching T_c, TC materials undergo a reversible phase transition with corresponding changes in physical properties such as transmittance and resistivity.

Thermochromism is observed in many organic compounds, ionic liquids, inorganic materials, and composite materials (Granqvist et al., 2009; Seeboth et al., 2014). At the same time, inorganic materials, such as metal oxides, demonstrate higher stability compared to other materials. They retain their properties even at temperatures above 200 °C (Day, 1968). The most widely studied metal oxide TC material to date is vanadium dioxide (VO_2). VO_2 at temperatures below T_c (68 °C) is a monoclinic material with semiconducting properties, relatively transparent to infrared radiation, while at temperatures above T_c it becomes a tetragonal material with metallic properties, reflecting infrared radiation (Warwick & Binions, 2014). Below are some additional examples of inorganic thermochromic materials (Suhag & Singh, 2015):

- Cu_2HgI_4 is red at 20 °C but black at 70 °C.
- ZnO is white at room temperature but yellow at higher temperatures.
- In_2O_3 is yellow at a lower temperature but yellow-brown at a high temperature.
- Cr_2O_3-Al_2O_3 is red at 20 °C but gray at 400 °C.
- $(Et_2NH_2)_2CuCl_4$ is bright green at 20 °C but yellow at 43 °C.
- $CoCl_2$ is pink at 25 °C but blue at 75 °C.

For these compounds, thermochromism commonly occurs based on the chemical equilibrium between two different forms of a molecular structure or between different crystalline phases.

Organic thermochromic materials are typically leuco-dye mixtures consisting of a color former, a color developer, and a solvent (White & Leblanc, 1999). The color former is usually a cyclic ether and determines the base color. The color developer is a weak acid and causes color change and final color intensity. The melting point of the solvent (alcohol or ester) influences the color transition temperature (Karlessi et al., 2009). Thus, the thermochromic transition temperature of an organic compound can be calculated depending on the specific application (Granqvist et al., 2009). For example, some devices switch over a very narrow temperature range, while others exhibit TC behavior over a wide temperature range. A typical example of organic thermochromic materials is poly(N-isopropylacrylamide) (PNIPAm), whose lower critical solution temperature (LCST) is 32 °C.

Organic thermochromic materials can change color reversibly or irreversibly when heated or cooled through various direct (intrinsic) or indirect mechanisms (Burkinshaw et al., 1998). The direct mechanism requires relatively high energy, which causes molecular changes such as the breaking of a covalent bond or a change in the conformation of the molecule (for example, acid-base, keto-enol, or lactim-lactam tautomerism). Heat triggers a change in molecular structure and a change in color, but once the heat source is removed, the system returns to a thermally more stable form. Color changes can also result from various structural changes, such as in crystalline liquid crystals. This change occurs when a liquid crystalline compound transitions from an equilibrium state of a crystalline solid to an isotropic liquid state upon reaching a certain critical temperature (MacLaren & White, 2003).

Several commercial dyes that are produced as TC compounds have shown potential for various applications (Pardo et al., 2011; Seeboth et al., 2014). The

availability of thermochromic dyes/inks and the convenient process of their synthesis and application make them suitable thermochromic agents with a wide range of applications. These materials can be applied directly to a paper substrate for use as temperature-sensitive color-changing paper strips or temperature indicators on beer or beverage cans or bottles, milk cartons, frozen foods, etc. (Bašnec et al., 2014). Such TC materials can convey information to consumers about optimal temperature levels and alert them to safety or other potential problems (see Chapter 14, Volume 2).

Thin, lightweight, and foldable thermochromic displays can also be created from paper (Siegel et al., 2009). These electronic displays are made by applying micron-sized electrically conductive wires (heaters) to one side of a sheet of paper and thermochromic ink applied to the opposite side. According to their design, the passage of electric current through the wires heats the paper, causing the thermochromic ink to change color (black, green, or other colors) to transparent. This change in ink color reveals any messages printed on the paper before the ink is applied. In these displays, thermochromic ink acts as a two-state "gate." Leuco dye is used as a TC material in such displays. Siegel et al. (2009) believe that such displays can be used in various fields for one-time applications. Several examples of such applications are shown in Fig. 23.4.

23.3 Photochromism

Photochromism is caused by light irradiation. Photochromic (PC) materials undergo reversible photoinduced switching between different states (or isomers) that have completely different absorption spectra (Du et al., 2024; Irie, 2000; Wang & Li, 2018; Zhang et al., 2013). To activate the color change process, PC materials must be exposed to light of a specific wavelength. The change in the state PC materials caused by irradiation is accompanied by a simultaneous change in the chemical and physical properties of PC materials (refractive index, polarizability, and often also electrical, magnetic, and mechanical properties). Photochromism may or may not be reversible, and the kinetics of PC is highly dependent on the compound used, wavelength, and light intensity.

An important requirement for photochromism is the presence of two states of the molecule, A and B, that are thermally stable under ambient conditions for a reasonable time. The thermodynamically stable form A turns into form B when irradiated. Typical metastability of the B state is associated with a longer time to return to the stable A state. The typically colorless form A is thermodynamically stable and can be converted to the colored state B upon exposure to ultraviolet (UV) irradiation. State B can be isomerized back to A naturally or through a process of visible light activation or thermal activation. During isomerization, chemical bonds are rearranged, usually in the form of cyclization reactions or E/Z transformations. In most cases, positive photochromism, the colorless isomer, is thermally stable, in contrast to negative photochromism (Hatano et al., 2013), where the color form exhibits the

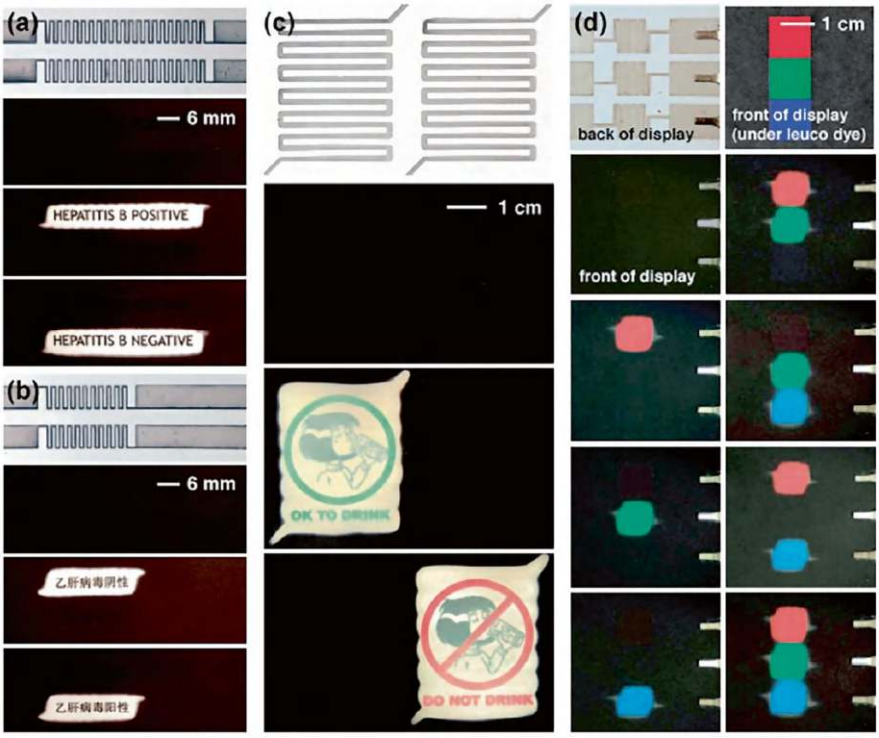

Fig. 23.4 Paper displays as simple, low-cost, textual indicators for diagnostic tests. All displays comprised a 50-μm thick layer of thermochromic ink on Xerox 32 lb. photo paper; 1.5 μm thick 100% Zn metallic wires patterned on the non-ink side of the paper formed the heating elements. (**a**) An example of a display that could show the result of a Hepatitis B test (Hepatitis B positive vs. Hepatitis B negative) in English; the textual message is activated by passing current (140 mA) through one of the two heating elements (wire resistance = 26 Ω). (**b**) A display that shows the same textual message in Chinese (current = 160 mA, wire resistance = 15 Ω). (**c**) A display that indicates safe vs. unsafe drinking water using pictures; the display allows the communication of complex messages to populations with high illiteracy, or populations where multiple languages are used (current = 300 mA, wire resistance = 15 Ω). (**d**) A multi-color red-green-blue (RGB) shutter display. The back side of the display comprises three heating elements, one behind each color. The sequence of photographs shows activation of all eight combinations of colors by passing current through heating elements. (Reprinted with permission from Siegel et al. (2009). Copyright 2009: RSC)

greatest stability. This mechanism of positive photochromism is shown schematically in Fig. 23.5. A and B states are separated by a potential barrier (ΔE). If this barrier is low, B state is metastable and can spontaneously return to A state. Such systems are called T-type, referring to the thermally induced reaction from B to A. In contrast, a high barrier characterizes a bistable system. In this case, only photons are capable of causing a reaction, and such systems are called P-type. In other words, in the absence of light, nothing changes (Nakatani et al., 2016).

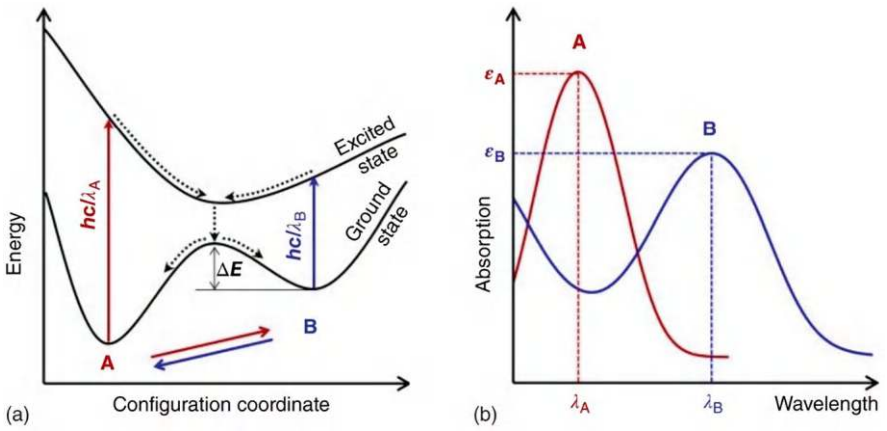

Fig. 23.5 Bidirectional reaction induced by an electromagnetic excitation between two molecular/crystal states, A and B: (**a**) Diagram of potential energies and (**b**) associated absorption spectra. (Reprinted with permission from Nakatani et al. (2016). Copyright 2016: Wiley)

Currently, many inorganic substances have been studied, such as oxides of various metals WO_3, TiO_2, V_2O_5, MoO_3, sulfides of alkaline earth metals, titanates, copper compounds, mercury compounds, some minerals, and transition metal compounds (Badour et al., 2021; Du et al., 2024). Many organic substances also exhibit photochromic properties (Nakatani et al., 2016). The most important organic photochromic dyes belong to the families of spiropyrans, spirooxazines, chromenes, fulgides, fulgimides, and diarylethenes (Barachevsky & Butenko, 2018; Li et al., 2017a; Lvov et al., 2017; Wu et al., 2016). Of these photochromic dyes, spiropyrans and spirooxazines belong to the T-type group, i.e., they return to a colorless state when exposed to heat or visible light. Fulgides and diarylethenes belong to the P-type group (photochemical reversibility), which become discolored when exposed to visible light. The advantages of diarylethenes over many other organic photochromes are the high thermal stability of both isomeric forms, high photochemical fatigue resistance, and reversible photo switching in the solid state. The main disadvantage of diarylethenes is the complexity of their structural modifications, which are necessary to obtain PC compounds with optimal properties (Krayushkin & Kalik, 2011). There is also a large group of hybrid photochromic structures. For example, many hybrid PC molecules consist of one (or more) organic photochromic antenna(s) linked to a metal ion. Among the best-described photochromic antennas are derivatives of azobenzene, spiropyran, diarylethene, or quinone. Ligands used to connect the metal complex are often bipyridine, terpyridine, and cyclopentadienyl substituted with an azobenzene group.

The processes that occur during lighting and lead to color changes are numerous. This can be either a structural transition (photoisomerization around double bonds, proton transfer, ring opening and closing) or a redox reaction (Bamfield, 2001). For example, upon UV excitation, MoO_3 changes color from pale yellow to intense

blue. The color change is due to photoreduction of the metal cations Mo^{6+} ($4d^0$ configuration) to Mo^{5+} ($4d^1$ configuration) under the influence of illumination. In organic PC materials, the color change is the result of a rearrangement of chemical bonds, causing a change in their structural and electronic properties.

Despite the wide range of organic and inorganic PC materials synthesized, only a small number of PC materials have been commercialized. Currently, organic photochromic materials such as spiropyrans, spirooxazines, and naphthopyrans are commonly used as commercial organic photochromic dyes (Fleischmann et al., 2015; Mortimer et al., 2006). The photochromic properties of these materials are very often due to the presence of functional groups associated with their aromatic rings, as well as ring opening or closing reactions caused by light stimuli, which can create a wide range of colors with different color spectra. For example, after irradiation with UV irradiation, the bond between spiro-carbon and oxazine is broken and the carbon-oxygen ring opens (Fleischmann et al., 2015; Zhang et al., 2013).

It should be noted that each of these families of PC materials has its own advantages and disadvantages. For example, organic photochromic materials are not stable enough when exposed to light for long periods of time, especially when used outdoors. Loss of performance over time due to chemical degradation of the material is called "fatigue." Typically, the main cause of damage to photochromic organic substances is oxidation (Malatesta, 1999). In other words, the main disadvantage of organic photochromic materials is related to their durability. However, there are also fairly stable organic PC materials. In particular, photochromic compounds considered "thermostable" include some diarylethenes, which do not undergo reverse isomerization even after heating at 80 °C for 3 months. Therefore, when choosing PC dyes, it is necessary to take into account many factors, which include:

- Intensity and nature of the required optical source: wavelength, continuous or intermittent radiation, laser, LED
- Rate of transition from the ground state to the photostationary state
- Lifetime of the photostationary state
- Permissible operating temperature range
- Materials and processes that can be used: powder, crystal, polymer, solution, ink, paint, and technological process used

Photochromic materials can be used in many paper-based devices, including smart packaging, various sensors, and indicators (Sadeghi et al., 2020). One such indicator is the OnVuTM printed Time/Temperature Indicator (TTI) for determining the freshness of frozen and perishable foods (Ciba Specialty Chemicals and FreshPoint, Inc.). OnVuTM labels contain a UV filter, filter paper as a substrate, a reference color, and a color base prepared using a heat-sensitive photochromic ink (spiropyran) (Fig. 23.6a). In general, spiropyrans are more desirable materials for applications than spirooxazines due to their convenient preparation procedure and the ability to exhibit intense visual color changes. After activation by UV radiation, resulting in a change in color from the colorless core to dark blue, the indicator is placed in the package. Using such a label, you can determine the time and temperature of storage of fresh products, since the time to return to their original state after

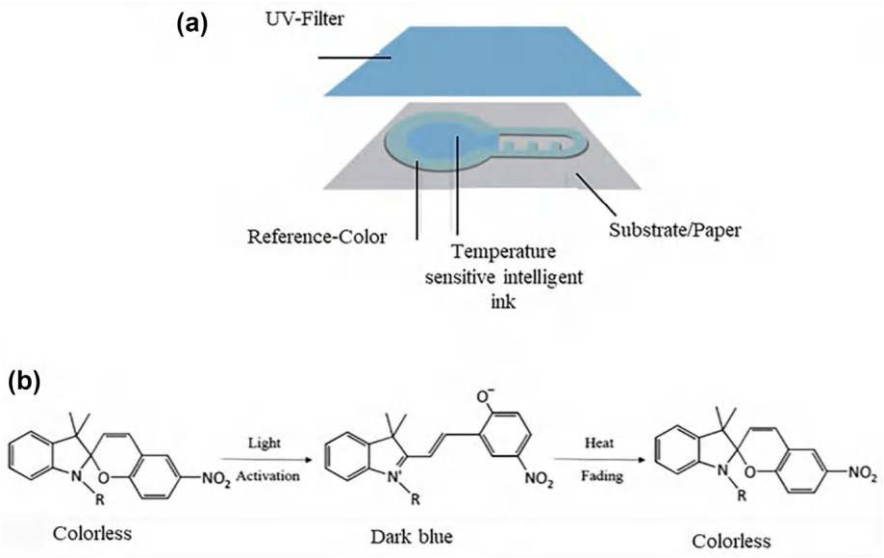

Fig. 23.6 (**a**) Structure of OnVuTM TTI in the shape of a bulb and (**b**) interconversion chemical reaction of the photochromic compound by exposure to UV irradiation and heat release. (Reprinted with permission from Sadeghi et al. (2020). Copyright 2020: Taylor and Francis group)

UV activation depends not only on time but also on temperature, which accelerates this process as it increases. Storing food above the optimum temperature over time causes the core to gradually change color to light blue and finally to a colorless state. Products are considered spoiled if the specified color change process occurs on their label. The color change phenomenon of PC connections is shown in Fig. 23.6b. Depending on the shelf life of the product, the OnVuTM TTI label can be optimized by changing the ink composition (Ahn et al., 2003; Brizio & Prentice, 2014).

Li et al. (2016) showed that it is also possible to develop paper-based colorimetric UV sensors. UV-sensitive photochromic paper was prepared by covalently immobilizing functional polymer networks with spiropyran moieties on paper sheets. Li et al. (2016) believe that due to its simplicity of design and the fact that no additional equipment or power source is required, this paper indicator can be used to quantify unknown UV radiation doses in situations where no instrumentation is possible or desirable.

There are other applications for photochromic materials. For example, Ma et al. (2020) proposed using a photochromic dye to make security paper. Increased security of securities was achieved through the use of various zinc salts as ink for recording classified information. To realize this possibility, they used zinc complexes based on the crystalline violet lactone salicylaldehyde hydrazine (CVLSH) as a photochromic dye. By varying the counterions of zinc complexes (CVLSH-Zn-X,X = CH_3COO^-, $CF_3SO_3^-$, NO_3^-, Cl^-, or Br^-), the colorability and coloration rate of these photochromic molecules can be precisely controlled on demand. The

recorded information cannot be seen under natural visible light. However, when the paper is exposed to ultraviolet light, the safety information becomes clearly visible. A similar application for photochromic materials was proposed by Shen et al. (2023). They believe that the use of luminescent and photochromic fiber based on cellulose acetate is very promising in the field of modern information encryption. In their developments they used the spiropyran photochromic dye. It is important to note that the covalent incorporation of spiropyran (SP) into the polymer upon simple mixing leads to a decrease in SP aggregation and, as a consequence, to an increase in physicochemical stability and fatigue strength. This statement can also be applied to other photochromic dyes. Bretel et al. (2019) also believe that photochromic patterns of dibenzothienylethenes (DBE) on cellulose paper can be used to combat counterfeiting. They justified the use of DBE as a photochrome by the following properties of this material: (i) an efficient and rapid dyeing-bleaching process under appropriate light irradiation; (ii) thermal stability of DBE isomers, as shown by theory and experiment; (iii) good color contrast; and (iv) high fatigue resistance, allowing many cycles to be completed without significant loss of performance.

23.4 Electrochromism

Electrochromism is caused by the gain or loss of electrons through redox reactions involving electrochromic (EC) films (Mortimer et al., 2013). EC materials change color depending on the application of external bias to the device in which they are embedded. This phenomenon occurs in compounds with redox active sites such as metal ions or organic radicals. Typically, changing the optical properties of EC materials results in a reversible transition from colored to transparent (bleached) or between two or more colored states. Compared to thermochromic materials, electrochromic materials can change their properties in a shorter time and have a more flexible transition (Granqvist, 2014).

The most widely studied EC materials are inorganic transition metal oxides (Jensen & Krebs, 2014), such as tungsten oxide (WO_3), molybdenum oxide (MoO_3), titanium dioxide (TiO_2), and nickel oxide (NiO). Electrochromic materials can also be oxides of other metals, such as Bi_2O_3, CeO_2, CoO, CuO, Fe_3O_4, Fe_2O_3, FeO, MnO_2, etc. (Granqvist, 2012; Yu et al., 2024). Organic EC compounds also undergo reversible coloration (and bleaching) as a result of certain redox reactions. The most common organic EC materials are bipyrylidyl systems (viologen family), quinones, cyanobiphenyls, phthalocyanines, and Prussian blue. These materials, with a small amount of electrolyte, exhibit a reversible and intense color change when a direct current (DC) electric field is applied or removed. Research has shown that electrochromic effects can also be observed in conjugated and electroactive polymers such as polythiophene, polypyrrole, and pyrazoline (Bamfield, 2001; Mortimer et al., 2013). Interest in their use is due not only to their high color fastness and optical contrast but also to the ease of synthesis and the ability to form thin films.

Electrochromic color switching in these materials occurs through different mechanisms (Mortimer, 2011). Although there is still controversy regarding the detailed color mechanism of transition metal oxides, it is generally accepted that the injection and extraction of electrons, protons, or monovalent noble metal cations play a key role in the process. At the same time, optical charge transfer between the +1 and 0 valence nitrogen atoms is responsible for redox color switching in transition metal coordination complexes such as bipyrylidyl systems. The optical band gap between the valence band and the conduction band determines the electrochromic properties of conducting conjugated polymers. Electrochromism in metal complexes and related coordination complexes such as metal phthalocynines and Prussian blue involves several electron transfer processes, including metal-to-ligand charge transfer (MLCT), inter-valence charge transfer (IVCT), intra-ligand excitation, and coupled electronic transitions in the visible region.

In general, organic EC materials with color-changing properties exhibit faster response time and higher coloring efficiency than inorganic ones. However, they have a low UV protection index and exhibit lower electrochemical stability. Research has shown that many metal complexes and related coordination complexes also have low to moderate efficiency, and poor redox, photochemical, and cyclic stability, resulting in reduced efficiency in their use. However, the use of nanomolecule-based metal-organic assemblies as homogeneous thin-film electrochromic materials in the development of solid-state electrochromic devices (SEDs) is still very promising (Mortimer et al., 2013). The possibilities of polymerization, dip coating, spin coating, drop casting, spray coating, layer deposition, and printing make this class of materials very advantageous in terms of processability and film production. Moreover, small changes in ligand configuration or choice of metal salts can result in color tuning, resulting in almost complete coverage of the red, green, and blue (RGB) color space (Elool Dov et al., 2017; Shankar et al., 2015).

Liquid crystals can also be classified as EC materials. In liquid crystal devices, when voltage is applied, randomly oriented elements are aligned in one direction, resulting in a transition from a translucent light-scattering state to a transparent state. These devices are characterized by two on-off states without any color modulation between the two states. When the power is turned off, the "off" state is the light scattering state. Additionally, Koga et al. (2017) showed that [bmim]-based ionic liquids supported by cellulose fibers can be used as a solvent layer for functional molecules such as $LiClO_4$ electrolyte. Such paper containing $LiClO_4$/[bmim]BF_4 can act as a flexible electrolyte for paper-based electrochromic devices, in particular, an electrochromic paper display (see Fig. 23.7).

In general, electrochromism is used in many devices, from smart mirrors and windows to thermal control of spacecraft, optical diaphragm for camera lenses, optical information, and data storage (Granqvist, 2014; Mortimer et al., 2013; Sadeghi et al., 2020; Yang et al., 2015; Yu et al., 2024). EC films can be divided into three types depending on their color scheme (Granqvist, 2014):

– EC film showing one color, for example, transition metal oxides, Prussian blue
– EC film showing two colors, for example, polythiophene

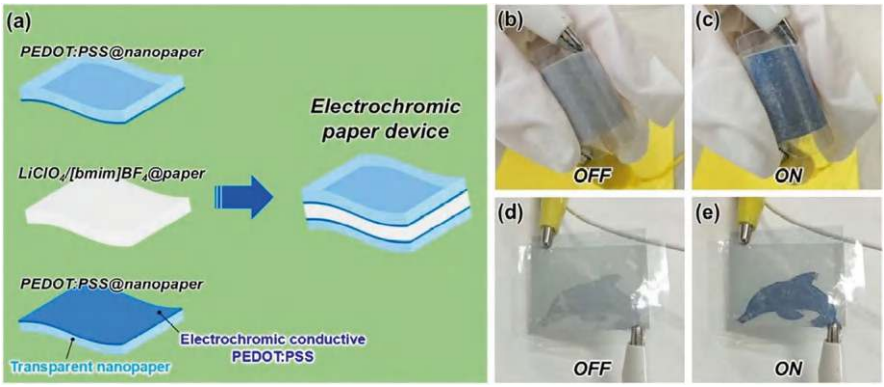

Fig. 23.7 Electrochromic paper device: (**a**) Schematic illustration of the electrochromic paper device fabricated using two pieces of PEDOT:PSS@nanopaper and one piece of $LiClO_4$/[bmim]BF_4@paper as transparent electrochromic electrodes and an electrolyte, respectively, (**b**, **c**) flexibility and corresponding performance of the electrochromic paper device, (**d**, **e**) dolphin-patterned electrochromism of the paper device. Operating voltage and current were 2.0 V and 0.06 A, respectively. (Reprinted with permission from Koga et al. (2017). Copyright 2017: ACS)

– EC film showing multiple colors, for example, poly(3,4-propylenedioxypyrrole)

An important advantage of electrochromic devices is the fact that these devices do not consume power between write and erase cycles. This color retention is called the "memory effect." For example, the intense color of a viologen radical cation sample remains unchanged for many months in the absence of chemical oxidizing agents such as molecular oxygen (Monk et al., 2009).

Electrochromic devices that can use paper or cellulose include paper flexible displays (see Fig. 23.7d, e), electronic skins, battery charge indicator strips, electrochemical sensors, biosensors, tactile sensors, strain sensors, and pressure sensors (Malti et al., 2016; Seok et al., 2022). For example, Liana et al. (2016) developed a simple and portable paper-based integrated platform using a piezoresistive electrochromic pressure sensor to visually read applied pressure during patient bandaging. A paper-based sensing system was developed using gold nanoparticle-coated film, EC-Prussian blue/polyaniline film, and graphite (as resistive material separators). The gradual coloring of the EC material allows end users to easily and quickly interpret applied pressure.

Yeon et al. (2022) developed another type of paper-based electrochemical sensor. This was a paper-based EC glucose sensor using redox-based colorimetric visual detection. Prussian blue and glucose oxidase (GOx) were used to detect hydrogen peroxide (H_2O_2) and glucose. There are other developments in this area. In particular, Sun et al. (2019) developed a self-powered paper-based enzymatic biosensor (ESPB) for formaldehyde detection using electrochromism for visualization. As a sensitive, simple, cost-effective, and highly selective inspection system, this ESPB colorimetric sensor can replace disposable test paper. Chow et al. (2017) showed

that paper-based potentiometric pH sensors integrated with an electrochromic sensing system can also be fabricated on paper. The readout system in this sensor consists of four segments of electrochromic Prussian blue/polyaniline on conductive gold nanoparticle films connected by graphite resistive separators. Whatman® No. 1 paper was used as a substrate.

23.5 Solvatochromism

Solvatochromism is a reversible change in the absorption or emission spectrum of a material caused by the action of solvents (Rijavec & Bračko, 2007). The color change is a consequence of a shift in the absorption maximum, which occurs due to the difference in the solvation energy of the initial and excited states in different solvents. The effect depends on the polarity of the solvent. An excited state that is more polar than the initial state is more stable in more polar solvents. Most solvatochromic compounds are metal complexes.

The process of color change in a solvatochromic system occurs due to changes in the position, intensity, and shape of the absorption spectra as a result of the interaction of the solvatochromic material with the solvent. In general, the spectral properties of most of the solvatochromic compounds are based on a donor–acceptor mechanism. Changing the polarity of the solvent leads to stabilization of the ground or excited states of the chromophore, which leads to a change in the energy gaps (dipole moment) between these electronic states (Bamfield, 2001; Marini et al., 2010).

The polarity of a solution can be changed by dissolving certain materials, such as gas or solvent vapors. This means that this effect can be used for colorimetric detection of these gases and vapors. The solvatochromic phenomenon can also be utilized in a wide range of gas sensor applications, including biosensors. For example, enzyme-labeled fluorescence as a solvatochromic indicator can detect the proteins and nucleic acids in normal and cancer cells by binding to the cell sites as an external fluorescent (Bamfield, 2001).

23.6 Gasochromism

Gasochromism is the result of exposure of gasochromic (GC) material to reducing or oxidizing gases such as hydrogen and oxygen. This is why this effect underlies the operation of many colorimetric gas sensors (Seok et al., 2022). The effect is carried out through the redox reaction. It is important to note that redox reactions underlie both gasochromism and electrochromism.

The gasochromism process uses an electrochromic material, usually a transition metal oxide such as tungsten oxide, which reacts with oxidizing or reducing gases, most commonly hydrogen and oxygen, to produce reversible color changes. Due to

the rapid and reversible intercalation of protons, WO_3 exhibits active gasochromic behavior and good reversibility. The gasochromic properties of WO_3 films are significantly improved when they are coated with a thin catalytic layer of platinum or palladium (Liu et al., 2014). The catalyst dissociates hydrogen molecules into protons and electrons, which then diffuse into the WO_3 layer. This causes a change in optical transmittance due to low-polarity transitions, similar to the electrochromic process (Bamfield, 2001). In addition to WO_3, MoO_3, VO_X, and Nb_2O_5 can also be used to develop colorimetric gas sensors (Seok et al., 2022). Unfortunately, the use of metal oxides in paper-based gas sensors has limited application. As is known, metal oxides as gas-sensitive materials are most effective at temperatures above the maximum permissible temperature for paper.

In colorimetric gas sensors, in addition to metal oxides, various organic compounds, including dyes, organometallic complexes, and polymers, can of course be used to capture target gas molecules (Annisa et al., 2020; Hu et al., 2016; Ordronneau et al., 2013; Wallace et al., 2007; Zhang & Jin, 2012). For example, Gu and Huang (2013) used a thin polyaniline film on cellulose paper to fabricate a paper-based sensor that could detect 100 ppm ammonia gas in nitrogen or 10 ppm evaporated ammonia from aqueous solution. This NH_3 responsive paper is a colorimetric sensor that changes color from green to blue when exposed to ammonia. Da Silveira Petruci et al. (2018) developed a microfluidic paper assay for the selective detection of hydrogen cyanide gas. Detection is based on the reaction of the cyanide anion with palladium dimethylglyoximate (DMG) followed by the colorimetric reaction of DMG with nickel. For the above materials, the mechanism responsible for the colorimetric sensory response may differ from that inherent in metal oxides. These possible mechanisms are shown in Fig. 23.8. These include (i) ring opening or closing

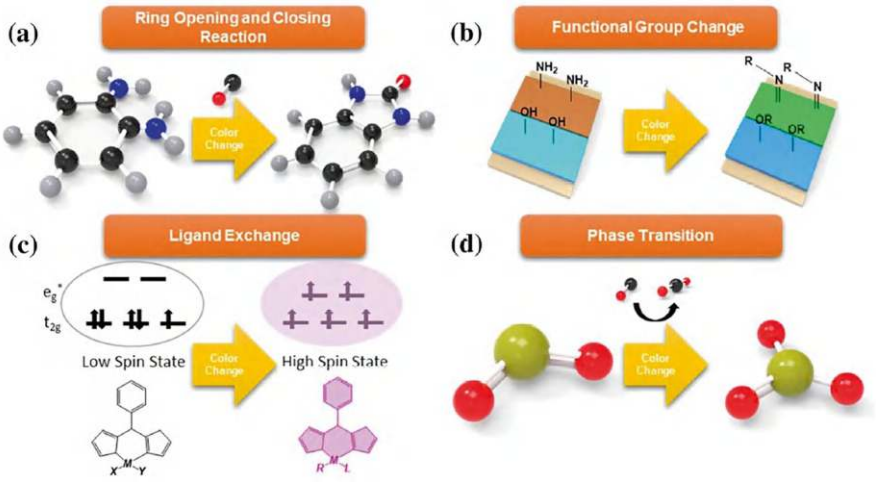

Fig. 23.8 Schematic illustration of four major colorimetric gas sensor mechanisms: (**a**) ring opening and closing reaction, (**b**) functional group change, (**c**) ligand exchange, and (**d**) phase transition. (Reprinted with permission from Cho et al. (2020). Copyright 2020: Springer)

reaction of sensitive materials (dyes, organic polymers), (ii) change of functional groups (organic compounds with hydroxyl groups), (iii) ligand exchange (transition metal complexes), and (iv) phase transition (inorganic materials) (Cho et al., 2020). For a more detailed introduction to colorimetric paper gas sensors using the gasochromic effect, you can refer to Chapter 12 (Volume 2).

23.7 Vaporchromism

Vaporchromism occurs in materials when they interact with vapors of organic compounds. In most cases, this effect is associated with polarization and the chemical polarity of organic compounds condensing on the surface of colorimetric indicator dyes. Analysis shows that vaporchromism, solvatochromism, and adsorbochromism are largely of the same nature. However, it must not be forgotten that vapors from volatile organic compounds (VOCs) when interacting with inorganic materials, such as metal oxides, at elevated temperatures can exhibit reducing properties and, therefore, they can also cause gasochromism.

Vaporchromism, like gasochromism, is used to develop sensors for analytes in the vapor phase (Kingsborough et al., 2021). Practical colorimetric sensor matrices were first developed by Rakow and Suslick (2000). They used arrays of different metalloporphyrins to visually identify different classes of volatile organic chemicals (VOCs). These dyes act by changing color by coordinating the analyte with the metalloporphyrin. Subsequently, numerous other types of colorimetric indicator dyes have been used to take advantage of other physical and chemical properties of the analytes (Rakow et al., 2005). In addition, indicator arrays have been prepared that allow the discrimination of various volatile organic compounds (Janzen et al., 2006; Lin et al., 2011) and toxic industrial chemicals (TICs) (Feng et al., 2010), as well as the identification of specific organic amines (Janzen et al., 2006) and aldehydes and ketones (Li et al., 2017b) from each other. Commercial uses of colorimetric sensor arrays include the identification of automotive fuels (Li et al., 2015), liquor vapors (Li & Suslick, 2018), etc. Although it should be admitted that we are not sure that when detecting vapors of various substances, for example, such as vapors from nitroaromatic explosives (Aguado et al., 2022), vaporchromism is actually used, and not some other mechanism.

One example of visualization of the sensory response to the appearance of VOCs in the atmosphere is shown in Fig. 23.9. Three vapochromic dyes named DiMo, MoMe, and DiMe, synthesized by Lee et al. (2022), were used as a sensitive material. As can be seen in Fig. 23.9, the dyes changed color when VOCs vapor appeared. Lee et al. (2022) concluded that the sensing performance of the cotton-based VOC sensors is affected by the three factors together: solvatochromism, aggregative properties of the dyes, and adsorption amount of VOCs on to substrates. But the predominant factor is still solvatochromism. Eaidkong et al. (2012) also reported a VOC-responsive paper array. Sensors were fabricated by drop-casting of polydiacetylene (PDA) as colorimetric molecules on paper substrates. The papers showed

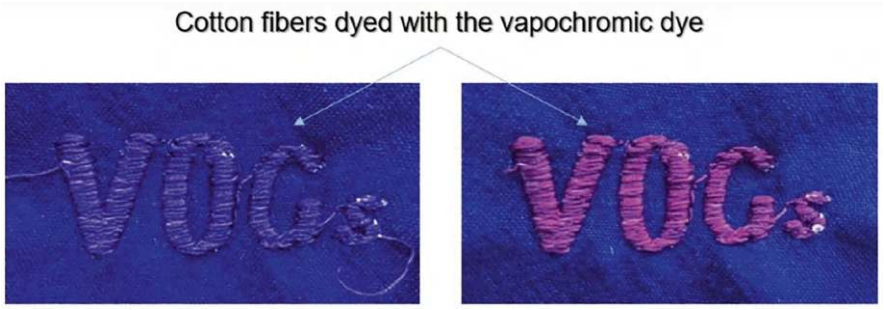

Fig. 23.9 Visualization of the concept of cotton-based VOCs sensor. (Reprinted with permission from Lee et al. (2022). Copyright 2022: Springer)

solvent-induced irreversible color transition upon exposure to VOC vapors. Optimally, a paper array containing three chosen PDAs was capable of classifying 18 VOCs with a high reproducibility and discriminating ability.

23.8 Hydrochromism

Reversible solid-state hydrochromism (HC), associated with dehydration-hydration as a result of interaction with bulk water or moisture, has long been known in transition metal compounds. The best-known examples of hydrochromic materials are cobalt chloride dehydrate, copper sulfate pentahydrate, cobalt nitrate hexahydrate, copper(II) chloride, and potassium lead iodide (Burneo et al., 2015). Hydrochromism has also been observed in organic materials (Park et al., 2016). More recently, some oxazolidines and oxazines have been shown to be hydrochromic due to water-initiated reversible ring-opening isomerization. These hydrochromic dyes have been tested for water-jet rewritable printing (Sheng et al., 2014).

The use of hydrochromic (HC) materials is mainly concentrated on the development of paper moisture indicators, which are described in detail in Chapter 14, Vol. 2. Humidity indicators are widely used in various fields such as pharmaceutical, food, packaging industries, etc.

23.9 Halochromism

Halochromism (HaC) is an effect where a material changes color when the pH of a solution changes. Color change in halochromic (HaC) materials occurs when a chemical substance binds to existing hydrogen and hydroxide ions in solution. Such bonds lead to changes in the conjugated systems of the molecule or the flow of electrons. This changes the wavelength of light absorbed, which in turn results in a

visible color change. HaC materials do not display a full spectrum of color over the entire pH range because beyond a certain acidity the conjugated system will not change. The different shades are due to different concentrations of halochromic molecules with different conjugated systems.

Halochromism is sometimes also defined as any change in color resulting from a chemical reaction. In principle, this is true for many cases, since a change in pH very often changes the chemical reaction in one direction or another, with a corresponding change in the color of the compounds that form. The compounds themselves are weak acids or bases and undergo acid-base reactions. A change in pH causes a change in the ratio of ionized and nonionized states, and since these two states have different colors, the color of the solution also changes.

There are various chemical structures in pH-sensitive dyes that can react with a wide range of pH levels. Typically, these materials are prepared from various combinations of monomers and polymers, such as methacrylic acid, methylmethacrylate, carboxy methyl ethyl cellulose, cellulose acetate, cellulose phthalate, hydroxyl propyl methylcellulose phthalate, hydroxyl propyl methyl cellulose acetate, hydroxyl propyl methyl cellulose succinate, diethyl amino ethyl methacrylate, and butyl methacrylate (Mattila, 2006).

Today, the well-known chemical classes of pH-sensitive materials are acid and base indicators. As shown in Table 23.1, various phthaleins and sulfophthaleins with different chemical functional groups, as well as azo dyes, can be used to produce paper-based analytical indicators (Hutchings & Bamfield, 2010). Paper pH

Table 23.1 Phthaleins, sulfophthaleins, and azo dyes used as pH indicators

Name	Formula	pH range	Color change
Phenolphthalein	$C_{20}H_{14}O_4$	8.5–9.0	Colorless–red
Cresolphthalein	$C_{22}H_{18}O_4$	8.2–9.8	Colorless–red
Thymolphthalein	$C_{28}H_{30}O_4$	9.3–10.5	Colorless–blue
Phenol Red	$C_{19}H_{14}O_5S$	6.8–8.4	Yellow–red
Thymol Blue	$C_{27}H_{30}O_5S$	1.2–2.8 8.0–9.6	Red–yellow Yellow–blue
Xylenol Blue	$C_{23}H_{22}O_5S$	1.2–2.8 8.0–9.6	Red–yellow Yellow–blue
Cresol Red	$C_{21}H_{17}NaO_5S$	7.2–8.8	Yellow–red
Chlorophenol Red	$C_{19}H_{12}Cl_2O_5S$	4.8–6.4	Yellow–red
Bromophenol Red	$C_{19}H_{12}Br_2O_5S$	5.2–6.8	Yellow–red
Bromophenol Blue	$C_{19}H_{10}Br_4O_5S$	3.0–4.6	Yellow–blue
Bromothymol Blue	$C_{27}H_{28}Br_2O_5S$	6.0–7.6	Yellow–blue
Bromocresol Green	$C_{21}H_{14}Br_4O_5S$	3.8–5.4	Yellow–blue
Bromocresol Purple	$C_{21}H_{16}Br_2O_5S$	5.2–6.8	Yellow–purple
Congo Red	$C_{32}H_{22}N_6Na_2O_6S_2$	3.0–5.2	Blue–red
Methyl yellow	$C_{14}H_{15}N_3$	2.9–4.0	Red–yellow
Methyl Orange	$C_{14}H_{14}N_3NaO_3S$	3.1–4.4	Red–yellow
Methyl Red	$C_{15}H_{15}N_3O_2$	4.4–6.2	Red–yellow

Source: Data extracted from Sadeghi et al. (2020)

indicators are described in more detail in chapter (Vol. 2). Although pH-sensitive azo dyes are commonly produced as commercial products, some azo dyes, due to their carcinogenic potential, such as methyl yellow and Congo red, despite their unique pH ranges, are no longer used in the production of pH indicators (De Campos Ventura-Camargo & Marin-Morales, 2013).

In addition, pH-sensitive dyes with a wide range of pH levels can be used as optical alteration agents in various chemical sensors and paper-based biosensors, where detection is based on a reaction accompanied by a change in the pH of the solution (Han & Burgess, 2010). For example, Rai et al. (2022) developed a paper-based chromogenic strip for the detection of tannic acid in beverages using this principle. The work of various indicators of product quality during storage is based on the same principle (see Chapter 14, Volume 2). pH-sensitive materials are also widely used when irreversible ionochromes are required, such as in heat- or pressure-sensitive fax paper. In addition, commercial pH-sensitive dyes can be a good replacement for thermochromic pigments (Van der Schueren & De Clerck, 2012). Important note: Many chromogenic materials are pH sensitive. For example, Genovese et al. (2018), using the pH or acidity sensitivity of photochromic spiropyrans (SPs), developed photochromic paper indicators to detect acidic spoilage in foods.

23.10 Ionochromism

Ionochromism (IC) is a reversible process of changing the color of a material caused by the flow of ions through that material. In other words, it is a phenomenon involving the interaction of a compound or material with an ionic species. This means that the halochromism discussed earlier must also be classified as this type of chromism. Both cations and anions can participate in the process of ionochromism. Anions are more effective because they have greater polarizability than cations. Important note: IC materials are similar in many ways to electrochromic materials, which change color when electrons pass through them. Electrons, like anions, carry a negative charge. Depending on the type of ions involved in the color change process, ionochromy is often divided into subgroups (Hutchings & Bamfield, 2010; Suhag & Singh, 2015):

1. Halochromism owing to a change in acidic or basic pH
2. Acidochromism stimulated by acid
3. Metallochromism from the formation of colored complexes from metal ions and chelating ligands

There is a wide range of organic molecules with ionochromic properties. Organic materials that change color when interacting with ions are called ionochromes or ionophores. The color change can be from colorless to colored or from colored to colorless and is usually reversible. These IC materials include commercial dyes and pH indicators such as phthalides, leukotriarylmethanes, fluoranes, cresolphthalein,

thymolphthalein, phenol red, cresol red, thymol blue, methyl orange, and methyl red. In addition, materials such as azo dyes and styryl dyes, merocyanines and indophenols, metal ions, and especially transition metal ions, which are capable of forming metallochromism complexes by reaction with chelating ligands leading to a color change, are also considered as IC materials (Arman, 2001; Sengupta & Behera, 2014). Some chromophores, such as azo- and indoanilines, as mentioned earlier, can also be used as IC materials and pH indicators. The ionochromic process can be observed in polythiophene and poly(p-phenylenevinylene) derivatives substituted with ether or crown ether groups (Wang & Li, 2018).

Ionochromic compounds have many technological applications. In addition to applications based on measuring the pH of a solution, ionochromic compounds can be used in analytical chemistry. The properties of IC materials provide the basis for the development of various paper-based colorimetric gas sensors (Chapters 7 and 12, Volume 2), metal ion sensors (Kaur et al., 2011) (Chapter 25, Volume 2), and biosensors (Chapter 19, Volume 2). Selectivity and high sensitivity are the main advantages of ion sensors, especially electrochemical heavy metal ion sensors. These paper sensors are discussed in detail in Vol. 2 of this issue and in several reviews on this topic (Bendicho et al., 2021). In most cases, the basis of these sensors is filter paper. Specifically, Rahbar et al. (2019), using ion exchange (IE) filter paper to immobilize anionic chromogenic reagents through ion exchange interactions, developed microfluidic paper analytical devices (μPADs) with dynamically forming a color band along the length of paper microfluidic channels. Cai et al. (2017) also developed a paper-based microfluidic analytical device (μPAD) but for the detection of Hg ions. Dithizone in a NaOH solution applied to filter paper was used as a chromogenic reagent. Reactions occurred between mercury ions and dithizone to form an insoluble colored complex, resulting in the formation of a colored precipitate on the paper channel. The length of the sediment increases linearly with increasing mercury concentration. The amount of mercury in a sample solution can be quantified by measuring the length of the colored precipitate. A schematic diagram of this distance-based detection method is shown in Fig. 23.10.

Carbon-free copying and printing papers and direct thermal printing are still one of the important applications of IC materials (Selektor & Shokurov, 2015). Ionochromic printing papers were developed based on the ionochromic concept (Bamfield, 2001). Double-ply carbon-free paper is made by coating the top layer of paper with a microencapsulated pH dye or ink and the bottom layer with an acidic compound. To achieve microencapsulation, various resins are used, such as urea/formaldehyde, polyester, or polyurethane, as well as acidic materials including acid clay, zinc salicylate, and zinc-modified phenolic resins. When pressure is applied (by writing or impact printing), the broken microcapsules release dyes that react with the acidic clay on the bottom sheet to form a colored symbol to be duplicated on the top sheet. Heat-sensitive ionochromic transfer paper also creates a digitized image on coated paper containing a dye and an acid co-reagent using thermal stimuli. The heat-sensitive paper and heating stimulus provide a sensitive surface for the ionic reaction and color change process (Hutchings & Bamfield, 2010).

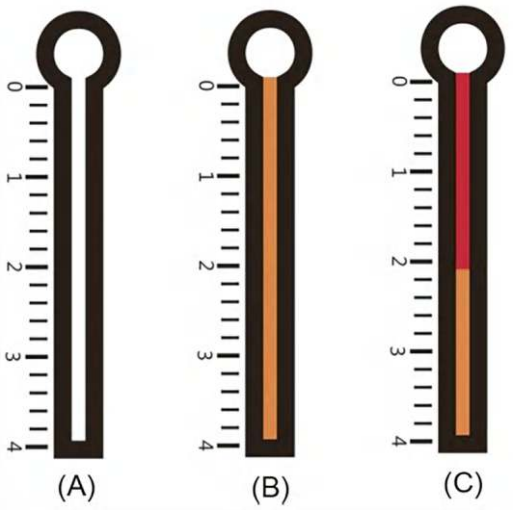

Fig. 23.10 Schematic diagrams illustrating mercury concentration determination on a μPAD microplate using a distance-based detection strategy. (**a**) μPAD with a circular reservoir and a straight channel. (**b**) μPAD with chromogenic reagents deposited on the channel. (**c**) A colored product forms and precipitates in the channel after adding a sample solution containing mercury ions to a circular reservoir. (Reprinted with permission from Cai et al. (2017). Copyright 2017: AIP)

23.11 Piezochromism

Piezochromism refers to the reversible color change of a solid in response to external pressure. Piezochromic materials display a change in color or opacity upon application (or variation) of various types of stress. Piezochromic materials can respond to compressive, tensile, or more complex forms of stress. Piezochromic compounds are mostly prepared from conjugated polymeric materials: polydiacetylenes, polythiophenes, and polysilanes. Piezochromism has also been observed for materials, such as metal oxides/complexes (such as molybdates, Cu(II) complexes, Ni(II) glyoximates, and Fe(II) spin-crossover compounds), organic molecules in polymer matrices, and crystalline organic molecular solids (Sui et al., 2017). Some inorganic materials are also known to exhibit piezochromism, including LiF and NaCl single crystals, $CuMoO_4$, and palladium complexes (Hernándeza et al., 1999).

Pressure and compression cause perturbations of the ground and excited states, a change in the crystal structure through a first-order phase transition, or a change in the molecular geometry in species that comprise the solid (Bamfield, 2001; Ferrara & Bengisu, 2014). Since covalent bonds are rather resistant to the effects of pressure, organic molecular solids respond to high pressure mainly by reducing intermolecular space and/or changing molecular conformations (if flexible) (Caruso et al., 2009; Wang et al., 2015). In the presence of appropriate chromophores, the pressure-forced structural changes may lead to a color change through modulation of electronic energy gaps.

Piezochromic materials are not yet widely used. But research shows that integrating piezochromic materials into mechanically sensitive objects can easily make it easier to obtain information about damage that has occurred to determine whether repair or replacement is required (Seeboth et al., 2012). Mechanical color change systems, such as those found in food and pharmaceutical packaging, may indicate problems with accidental damage, tampering, and counterfeiting, since any mechanical stress on the packaging can be observed visually (Suslick, 1998). In addition, visualization of mechanical stress by changing the optical properties (absorption, emission, and/or reflection) in piezochromic materials may find applications in paper health monitoring systems and piezochromic paper pressure sensors (Chan et al., 2013).

23.12 Magnetochromism

Magnetochromism (MC) is the term used when chemical compounds change color when exposed to a magnetic field. Magnetochromic materials are typically inorganic in chemical composition and are alloys of iron and nickel doped with rare earth elements (Harvey, 2006). Of course, this type of chromism is of limited use. However, research in this direction is underway. For example, Wang et al. (2018) propose using this effect to develop a color display that responds to a magnetic field. To address this issue, a novel solid magnetochromic photonic hydrogel has been developed to respond colorimetrically to an alternating magnetic field (AMF). According to Wang et al. (2018), these outstanding magnetochromic performances are attributed to the superior magnetothermal effect of the one-dimensional aggregates of magnetic-sensitive chains fixed in the hydrogel.

23.13 Biochromism

A biochromic (BC) compound is a type of chromogenic material that changes color to a new color when exposed to a biological stimulus. This change occurs as a result of biochemical reactions or hydrolysis reactions. Numerous studies can be found in this area. For example, it has been reported that modified conjugated polymers such as polydiacetylenes (PDA) and polythiophenes can be used as biosensors in the form of liposomes (vesicles), thin films on solid supports, and membranes (Bamfield, 2001; Sun et al., 2004). Natural lipids embedded in a polydiacetylenes (PDA) matrix can also serve as a platform exhibiting chromium transition due to alternating configurational structural modifications of double and triple bonds in the backbones of the conjugated PDA polymer during biochromism. The mechanism of this system is that lipids as recognition elements interact with environmental factors such as biomolecules and subsequently change the arrangement of double and triple bond chains as well as the electrical properties of the polymer matrix from acetylene to

butatriene, and finally cause a color transition of liposomes from blue to red (Charych et al., 1993). Of course, there are other mechanisms of biochromism. For example, in Pomili et al. (2021), the color change from blue to pink occurred due to a change in the shape of AuNPs caused by the interaction of AuNPs with the products of a biochemical reaction.

The development of biochromogenic systems is considered a popular area of research in the food industry, especially in the field of detection of foodborne microorganisms. As a result, the application of biochromogenic materials in packaging can be used to alert the consumer about a potential toxic agent or quality issue related to a food product. Biochromogenic systems also allow the development of colorimetric paper-based biosensors for detection of a wide range of biological agents, such as parasites, viruses, bacteria, neurotoxins, and other pathogens (Asif et al., 2020; Lathwal & Sikes, 2016; Morbioli et al., 2017). In particular, Asif et al. (2020) developed paper-based analytical devices for the colorimetric detection of *S. aureus* and *E. coli*. The μPADs were fabricated on filter paper using wax printing and then impregnated with a chromogenic substance, which reacted with bacterial enzymes to produce colored products. The chromogenic substance used was 5-bromo-6-chloro-3-indolyl phosphate p-toluidine salt (BCIP, purple phosphate) and HMRZ-86, a new chromogenic cephalosporin. *S. aureus* was identified by the color change of BCIP embedded in the μPAD from colorless to purple/violet. The color change of HMRZ-86 embedded in the μPAD from yellow to red indicated the presence of ESBL-positive bacteria.

Another approach to develop biochromogenic biosensors was used in Pomili et al. (2021). A multiplexed PAD for simultaneous detection of salivary biomarkers, i.e., glucose, cholesterol, and lactate, is shown in Fig. 23.11. μPAD is fabricated on chromatography paper and contains a small central saliva sampling region connected to three microfluidic channels. Each channel contains a detection zone

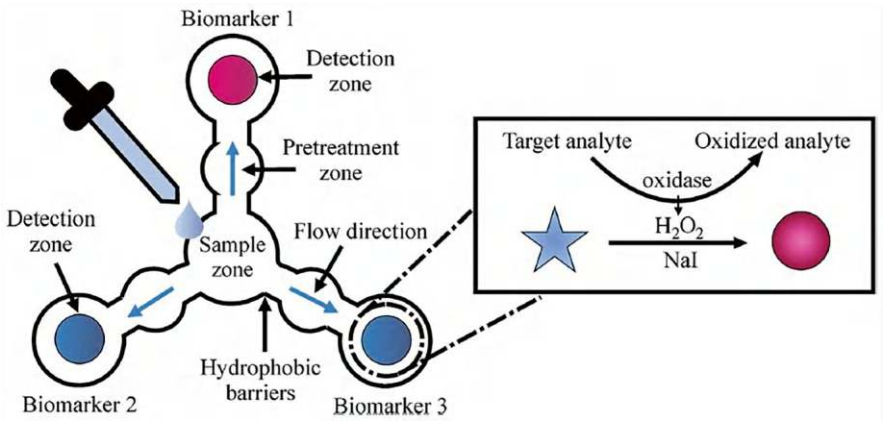

Fig. 23.11 Schematic illustration of the colorimetric paper-based device for the simultaneous detection of three salivary biomarkers. The inset shows the colorimetric reaction mediated by the H_2O_2 by-product in the presence of NaI, which leads to a visible color change from blue to pink of the target analyte. (Reprinted from Pomili et al. (2021). Published 2021 by MDPI with open access)

Table 23.2 Summary of recent PADs found associated with colorimetric detection for point-of-need applications

Paper type	Analyte	Diagnostic	Sample
Whatman chromatography No 1	Glucose, cholesterol, lactate	Diabetes	Saliva
	Glucose and lactate	Diabetes	Human serum
Whatman filter No 4	hCG hormone	Pregnancy	Urine
	Creatinine	Renal disorders	Artificial urine
Whatman chromatography No 1 and 3	HIV-1	AIDS	Human blood plasma
Ahlstrom chromatography Grade 222	SARS-CoV-2 200 genomic copies	COVID-19	Saliva
Whatman chromatography No 1	Dengue virus serotypes	Dengue	Plasmids
Whatman chromatography No 3	Tuberculosis DNA	Tuberculosis	Human disc tissue
Cellulose paper	*E. coli*	Bacterial infection, drug resistance	Mice wound tissue
Whatman filter No 1	PCA3 antigen	Prostate cancer	RNA from cancer cells
	Citrate	Prostate cancer	Urine
	Cytochrome	Hematologic cancer	Human serum
Nitrocellulose membrane	AFP and MUC16 proteins	Liver and ovarian cancer	Synthetic serum

Source: Adapted with permission from Pradela-Filho et al. (2023). Copyright 2023: Springer
hCG human chorionic gonadotropin, *HIV* human immunodeficiency virus, *AIDS* acquired immunodeficiency syndrome, *CFU* colony-forming unit, *PCA3* prostate cancer antigen 3, *AFP* alpha-fetoprotein, *MUC16* mucin-16

spotted with gold nanoparticles (AuNPs) and a layer of corresponding enzymes (glucose (GOx), cholesterol (ChOx), and lactate oxidase (LOx)) for the corresponding analytes. In addition, halogen (NaI) functionalized pretreatment zones were located between the sample and test zones. Colorimetric detection is based on the oxidation of the biomarker by its specific enzyme, which produces hydrogen peroxide (H_2O_2) as a by-product, leading to morphological changes in AuNPs, thereby promoting a color change from blue to pink. A more detailed description of such sensors can be found in the chapter (volume 2). Some other examples of colorimetric biosensors are listed in Table 23.2.

23.14 Summary

In this chapter, we have shown that chromism is a promising direction in the development of both paper-based sensors for the detection of gases, vapors, metal ions and biomolecules, and paper-based devices for smart packaging, energy storage/conversion, wearable electronics, medical monitoring, etc. The change in color of

chromogenic materials under the influence of various stimuli acts as a visual indicator of these external conditions (pressure, deformation, biomolecules, energy, gas, ion, irradiation, movement, etc.), which allows the development of devices that are convenient to use.

Of course, as with any development, there are obstacles that must be overcome. For example, as mentioned in the introduction, the same material can exhibit different chromogenic effects, which complicates the process of detecting a specific stimulus if the object is in an uncontrolled environment. There are also problems associated with the stability of some chromogenic materials. A number of studies have concluded that to improve the stability of chromogenic materials, it is necessary to encapsulate them to prevent oxygen from entering the device. To achieve this, it is proposed to use barrier layers and manufacture devices in an inert atmosphere (Bulloch & Reynolds, 2015; Jensen et al., 2013). The high hydrophilicity of paper also requires the use of hydrophobic barrier films to protect devices from rapid degradation when exposed to high humidity environments or water. In some cases, it is also necessary to solve the problem of increasing the performance of devices using chromism, namely, making them faster.

Acknowledgments G.K. is grateful to the Moldova State University (research program no. 011208) for supporting his research.

References

Aguado, R., Santos, A. R. M. G., Vallejos, S., & Valente, A. J. M. (2022). Paper-based probes with visual response to vapors from nitroaromatic explosives: Polyfluorenes and tertiary amines. *Molecules, 27*, 2900. https://doi.org/10.3390/molecules27092900

Ahn, D. J., Chae, E. H., Lee, G. S., Shim, H. Y., Chang, T. E., Ahn, K. D., & Kim, J. M. (2003). Colorimetric reversibility of polydiacetylene supramolecules having enhanced hydrogen-bonding under thermal and pH stimuli. *Journal of the American Chemical Society, 125*, 8976–8977. https://doi.org/10.1021/ja0299001

Annisa, T. N., Jung, S.-H., Gupta, M., Bae, J. Y., Park, J. M., & Lee, H. (2020). A reusable polymeric film for the alternating colorimetric detection of a nerve agent mimic and ammonia vapor with subparts-per-million sensitivity. *ACS Applied Materials & Interfaces, 12*, 11055–11062. https://doi.org/10.1021/acsami.0c00042

Arman, S. (2001). Electrochromic materials for display applications: An introduction. *Journal of New Materials for Electrochemical Systems, 4*, 173–180.

Asif, M., Awan, F. R., Khan, Q. M., Ngamsom, B., & Pamme, N. (2020). Paper-based analytical devices for colorimetric detection of *S. aureus* and *E. coli* and their antibiotic resistant strains in milk. *Analyst, 145*, 7320–7329. https://doi.org/10.1039/d0an01075h

Badour, Y., Jubera, V., Andron, I., Frayret, C., & Gaudon, M. (2021). Photochromism in inorganic crystallised compounds. *Optical Materials: X, 12*, 100110. https://doi.org/10.1016/j.omx.2021.100110

Bamfield, P. (2001). *Chromic phenomena, technological applications of color chemistry*. Royal Society of Chemistry. https://doi.org/10.1039/9781849731034

Barachevsky, V. A., & Butenko, V. G. (2018). Photoelectrochromic organic systems. *Russian Journal of General Chemistry, 88*, 2747–2772. https://doi.org/10.1134/S1070363218120459

Bašnec, K., Bezek, K., Hajzeri, M., Raspor, P., & Klanjšek Gunde, M. (2014). Chromogenic indicators for temperature control in the food cold chain. *Journal of Hygienic Engineering and Design, 8*, 53–59.

Bendicho, C., Lavilla, I., Pena-Pereira, F., de la Calle, I., & Romero, V. (2021). Paper-based analytical devices for colorimetric and luminescent detection of mercury in waters: An overview. *Sensors, 21*, 7571. https://doi.org/10.3390/s21227571

Bretel, G., Le Grognec, E., Jacquemin, D., Hirose, T., Matsuda, K., & Felpin, F.-X. (2019). Fabrication of robust spatially-resolved photochromic patterns on cellulose papers by covalent printing for anti-counterfeiting applications. *ACS Applied Polymer Materials, 1*(5), 1240–1250. https://doi.org/10.1021/acsapm.9b00266.hal-03016826

Brizio, A. P. D. R., & Prentice, C. (2014). Use of smart photochromic indicator for dynamic monitoring of the shelf life of chilled chicken based products. *Meat Science, 96*, 1219–1226. https://doi.org/10.1016/j.meatsci.2013.11.006

Bulloch, R. H., & Reynolds, J. R. (2015). Photostability in dioxyheterocycle electrochromic polymers. *Journal of Materials Chemistry C, 4*, 603–610. https://doi.org/10.1039/C5TC03536H

Burkinshaw, S. M., Griffiths, J., & Towns, A. D. (1998). Reversibly thermochromic systems based on pH-sensitive spirolactone-derived functional dyes. *Journal of Materials Chemistry, 8*, 2677–2683. https://doi.org/10.1039/A805994B

Burneo, I., Stylianou, K. C., Rodriguez-Hermida, S., Juanhuix, J., Fontrodona, X., Imaz, I., & Maspoch, D. (2015). Two new adenine-based Co(II) coordination polymers: Synthesis, crystal structure, coordination modes, and reversible hydrochromic behavior. *Crystal Growth & Design, 15*, 3182–3189. https://doi.org/10.1021/acs.cgd.5b00218

Cai, L., Fang, Y., Mo, Y., Huang, Y., Xu, C., Zhang, Z., & Wang, M. (2017). Visual quantification of Hg on a microfluidic paper-based analytical device using distance-based detection technique. *AIP Advances, 7*, 085214. https://doi.org/10.1063/1.4999784

Caruso, M., Davis, D. A., Shen, Q., Odom, S. A., Sottos, N. R., White, S. R., & Moore, J. S. (2009). Mechanically-induced chemical changes in polymeric materials. *Chemical Reviews, 109*(11), 5755–5798. https://doi.org/10.1021/cr9001353

Chan, E. P., Walish, J. J., Urbas, A. M., & Thomas, E. L. (2013). Mechanochromic photonic gels. *Advanced Materials, 25*, 3934–3947. https://doi.org/10.1002/adma.201300692

Charych, D. H., Nagy, J. O., Spevak, W., & Bednarski, M. D. (1993). Direct colorimetric detection of a receptor-ligand interaction by a polymerized bilayer assembly. *Science, 261*, 585–588. https://doi.org/10.1126/science.8342021

Cho, S. H., Suh, J. M., Eom, T. H., Kim, T., & Jang, H. W. (2020). Colorimetric sensors for toxic and hazardous gas detection: A review. *Electronic Materials Letters, 17*, 1–17. https://doi.org/10.1007/s13391-020-00254-9

Chow, E., Liana, D. D., Raguse, B., & Gooding, J. J. (2017). A potentiometric sensor for pH monitoring with an integrated electrochromic readout on paper. *Australian Journal of Chemistry, 70*(9), 979–984. https://doi.org/10.1071/CH17191

Da Silveira Petruci, J. F., Hauser, P. C., & Cardoso, A. A. (2018). Colorimetric paper-based device for gaseous hydrogen cyanide quantification based on absorbance measurements. *Sensors and Actuators B: Chemical, 268*, 392–397. https://doi.org/10.1016/j.snb.2018.04.101

Day, J. H. (1963). Thermochromism. *Chemical Reviews, 63*, 65–80. https://doi.org/10.1021/cr60221a005

Day, J. H. (1968). Thermochromism of inorganic compounds. *Chemical Reviews, 68*(6), 649–657. https://doi.org/10.1021/cr60256a001

De Campos Ventura-Camargo, B., & Marin-Morales, M. A. (2013). Azo dyes: Characterization and toxicity–A review. *Textiles and Light Industrial Science and Technology, 2*, 85–103.

Du, J., Yang, Z., Lin, H., & Poelman, D. (2024). Inorganic photochromic materials: Recent advances, mechanism, and emerging applications. *Responsive Materials, 2*, e20240004. https://doi.org/10.1002/rpm.20240004

Eaidkong, T., Mungkarndee, R., Phollookin, C., Tumcharern, G., Sukwattanasinitt, M., & Wacharasindhu, S. (2012). Polydiacetylene paper-based colorimetric sensor array for vapor

phase detection and identification of volatile organic compounds. *Journal of Materials Chemistry, 22*(13), 5970–5977. https://doi.org/10.1039/C2JM16273C

Elool Dov, N., Shankar, S., Cohen, D., Bendikov, T., Rechav, K., Shimon, L. J. W., et al. (2017). Electrochromic metallo-organic nanoscale films: Fabrication, color range, and devices. *Journal of the American Chemical Society, 139*, 11471–11281. https://doi.org/10.1021/jacs.7b04217

Feng, L., Musto, C. J., Kemling, J. W., Lim, S. H., & Suslick, K. S. (2010). A colorimetric sensor array for identification of toxic gases below permissible exposure limits. *Chemical Communications, 46*(12), 2037–2039. https://doi.org/10.1039/B926848K

Ferrara, M., & Bengisu, M. (2014). *Materials that change color* (pp. 9–60). Springer. https://doi.org/10.1007/978-3-319-00290-3

Fleischmann, C., Lievenbruck, M., & Ritter, H. (2015). Polymers and dyes: Developments and applications. *Polymers, 7*, 717–746. https://doi.org/10.3390/polym7040717

Genovese, M. E., Abraham, S., Caputo, G., Nanni, G., Kumaran, S. K., Montemagno, C. D., et al. (2018). Photochromic paper indicators for acidic food spoilage detection. *ACS Omega, 3*, 13484–13493. https://doi.org/10.1021/acsomega.8b02570

Granqvist, C. G. (2012). Oxide electrochromics: An introduction to devices and materials. *Solar Energy Materials and Solar Cells, 99*, 1–13. https://doi.org/10.1016/j.solmat.2011.08.021

Granqvist, C. G. (2014). Electrochromics for smart windows: Oxide-based thin films and devices. *Thin Solid Films, 564*, 1–38. https://doi.org/10.1016/j.tsf.2014.02.002

Granqvist, C. G., Lansåker, P. C., Mlyuka, N. R., Niklasson, G. A., & Avendaño, E. (2009). Progress in chromogenics: New results for electrochromic and thermochromic materials and devices. *Solar Energy Materials & Solar Cells, 93*, 2032–2039. https://doi.org/10.1016/j.solmat.2009.02.026

Gu, Y., & Huang, J. (2013). Colorimetric detection of gaseous ammonia by polyaniline nanocoating of natural cellulose substances. *Colloids and Surfaces, A: Physicochemical and Engineering Aspects, 433*, 166–172. https://doi.org/10.1016/j.colsurfa.2013.05.016

Han, J., & Burgess, K. (2010). Fluorescent indicators for intracellular pH. *Chemical Reviews, 110*, 2709–2728. https://doi.org/10.1021/cr900249z

Harvey, J. A. (2006). Smart materials. In M. Kutz (Ed.), *Mechanical engineers' handbook: Materials and mechanical design* (Vol. 1, 3rd ed.). Wiley. Chapter 11.

Hatano, S., Horino, T., Tokita, A., Oshima, T., & Abe, J. (2013). Unusual negative photochromism via a short-lived imidazolyl radical of 1,1′-binaphthyl-bridged imidazole dimer. *Journal of the American Chemical Society, 135*(8), 3164. https://doi.org/10.1021/ja311344u

Hernándeza, D., Rodríguezа, F., Garcia-Jacab, J., Ehrenbergc, H., & Weitzelc, H. (1999). Pressure-dependence on the absorption spectrum of $CuMoO_4$: Study of the green to brownish-red piezochromic phase transition at 2.5 kbar. *Physica B: Condensed Matter, 265*, 181–185. https://doi.org/10.1016/S0921-4526(98)01366-0

Hu, Y., Chen, L., Jung, H., Zeng, Y., Lee, S., Swamy, K. M. K., et al. (2016). Effective strategy for colorimetric and fluorescence sensing of phosgene based on small organic dyes and nanofiber platforms. *ACS Applied Materials & Interfaces, 8*, 22246–22252. https://doi.org/10.1021/acsami.6b07138

Hutchings, M., & Bamfield, P. (2010). *Chromic phenomena: Technological applications of colour chemistry*. Royal Society of Chemistry. https://doi.org/10.1039/9781849731034

Irie, M. (2000). Photochromism: Memories and switches—Introduction. *Chemical Reviews, 100*(5), 1683–1684. https://doi.org/10.1021/cr980068l. PMID 11777415.

Janzen, M. C., Ponder, J. B., Bailey, D. P., Ingison, C. K., & Suslick, K. S. (2006). Colorimetric sensor arrays for volatile organic compounds. *Analytical Chemistry, 78*(11), 3591–3600. https://doi.org/10.1021/ac052111s

Jensen, J., & Krebs, F. C. (2014). From the bottom up—Flexible solid state electrochromic devices. *Advanced Materials, 26*, 7231–7234. https://doi.org/10.1002/adma.201402771

Jensen, J., Madsen, M. V., & Krebs, F. C. (2013). Photochemical stability of electrochromic polymers and devices. *Journal of Materials Chemistry C, 1*, 4826–4835. https://doi.org/10.1039/C3TC30751D

Karlessi, T., Santamouris, M., Apostolakis, K., Synnefa, A., & Livada, I. (2009). Development and testing of thermochromic coatings for buildings and urban structures. *Solar Energy, 83*(4), 538–551. https://doi.org/10.1016/j.solener.2008.10.005

Kaur, B., Kaur, N., & Kumar, S. (2011). Colorimetric metal ion sensors. *Tetrahedron, 48*, 9233–9264. https://doi.org/10.1016/j.tet.2011.09.003

Kingsborough, R. P., Wrobel, A. T., & Kunz, R. R. (2021). Colourimetry for the sensitive detection of vapour-phase chemicals: State of the art and future trends. *Trends in Analytical Chemistry, 143*, 116397. https://doi.org/10.1016/j.trac.2021.116397

Koga, H., Nogi, M., & Isogai, A. (2017). Ionic liquid mediated dispersion and support of functional molecules on cellulose fibers for stimuli-responsive chromic paper devices. *ACS Applied Materials & Interfaces, 9*(46), 40914–40920. https://doi.org/10.1021/acsami.7b14827

Krayushkin, M. M., & Kalik, M. A. (2011). Syntheses of photochromic diarylethenes. In A. Katritzky (Ed.), *Advances in heterocyclic chemistry* (Vol. 103, pp. 1–59). Academic Press.

Lampert, C. M. (2004). Chromogenic smart materials. *Materials Today, 7*(3), 28–35. https://doi.org/10.1016/S1369-7021(04)00123-3

Lathwal, S., & Sikes, H. D. (2016). Assessment of colorimetric amplification methods in a paper-based immunoassay for diagnosis of malaria. *Lab on a Chip, 16*, 1374–1382. https://doi.org/10.1039/C6LC00058D

Lee, J., Park, N., & Kim, T. (2022). Synthesis of VOC-sensing dyes for fabrication of cotton-based chromogenic sensors. *Cellulose, 29*, 8937–8956. https://doi.org/10.1007/s10570-022-04775-4

Li, Z., & Suslick, K. S. (2018). A hand-held optoelectronic nose for the identification of liquors. *ACS Sensors, 3*(1), 121–127. https://doi.org/10.1021/acssensors.7b00709

Li, Z., Jang, M., Askim, J. R., & Suslick, K. S. (2015). Identification of accelerants, fuels and post-combustion residues using a colorimetric sensor array. *Analyst, 140*(17), 5929–5935. https://doi.org/10.1039/C5AN00806A

Li, W., Trosien, S., Schenderlein, H., Graf, M., & Biesalski, M. (2016). Preparation of photochromic paper, using fibre-attached spiropyran polymer networks. *RSC Advances, 6*, 109514. https://doi.org/10.1039/c6ra23673a

Li, X., Li, C., Wang, S., Dong, H., Ma, X., & Cao, D. (2017a). Synthesis and properties of photochromic spirooxazine with aggregation-induced emission fluorophores polymeric nanoparticles. *Dyes and Pigments, 142*, 481–490. https://doi.org/10.1016/j.dyepig.2017.03.068

Li, Z., Fang, M., La Gasse, M. K., Askim, J. R., & Suslick, K. S. (2017b). Colorimetric recognition of aldehydes and ketones. *Angewandte Chemie, International Edition, 56*(33), 9860–9863. https://doi.org/10.1002/anie.201705264

Liana, D. D., Raguse, B., Gooding, J. J., & Chow, E. (2016). An integrated paper-based readout system and piezoresistive pressure sensor for measuring bandage compression. *Advanced Materials Technologies, 1*, 1600143. https://doi.org/10.1002/admt.201600143

Lin, H., Jang, M., & Suslick, K. S. (2011). Preoxidation for colorimetric sensor array detection of VOCs. *Journal of the American Chemical Society, 133*(42), 16786e16789. https://doi.org/10.1021/ja207718t

Liu, B., Cai, D., Liu, Y., Wang, D., Wang, L., Wang, Y., Li, H., Li, Q., & Wang, T. (2014). Improved room-temperature hydrogen sensing performance of directly formed Pd/WO_3 nanocomposite. *Sensors and Actuators B: Chemical, 193*, 28–34. https://doi.org/10.1016/j.snb.2013.11.057

Lvov, A. G., Kavun, A. M., Kachala, V. V., Nelyubina, Y. V., Metelitsa, A. V., & Shirinian, V. Z. (2017). Structural and spectral properties of photochromic diarylethenes: Size effect of the ethene bridge. *The Journal of Organic Chemistry, 82*, 1477–1486. https://doi.org/10.1021/acs.joc.6b02665

Ma, Y., Yu, Y., She, P., Lu, J., Liu, S., Wei Huang, W., & Qiang Zhao, Q. (2020). On-demand regulation of photochromic behavior through various counterions for high-level security printing. *Science Advances, 6*(16), eaaz2386. https://doi.org/10.1126/sciadv.aaz2386

MacLaren, D. C., & White, M. A. (2003). Competition between dye-developer and solvent-developer interactions in a reversible thermochromic system. *Journal of Materials Chemistry, 13*, 1701–1704. https://doi.org/10.1039/B302250A

Malatesta, V. (1999). Photodegradation of organic photochromes. In J. R. Crano & R. J. Guglielmetti (Eds.), *Organic photochromic and thermochromic compounds* (Vol. 2, Ch. 2). Plenum.

Malti, A., Brooke, R., Liu, X., Zhao, D., Ersman, P. A., Fahlman, M., et al. (2016). Freestanding electrochromic paper. *Journal of Materials Chemistry C, 4*, 9680–9686. https://doi.org/10.1039/C6TC03542F

Marini, A., Munoz-Losa, A., Biancardi, A., & Mennucci, B. (2010). What is solvatochromism? *The Journal of Physical Chemistry. B, 114*, 17128–17135. https://doi.org/10.1021/jp1097487

Mattila, H. (Ed.). (2006). *Intelligent textiles and clothing*. Woodhead Publishing.

Monk, P. M. S., Mortimer, R. J., & Rosseinsky, D. R. (Eds.). (2009). *Electrochromism and electrochromic devices*. Cambridge University Press.

Morbioli, G. G., Mazzu-Nascimento, T., Stockton, A. M., & Carrilho, E. (2017). Technical aspects and challenges of colorimetric detection with microfluidic paper-based analytical devices (μPADs)—A review. *Analytica Chimica Acta, 970*, 1–22. https://doi.org/10.1016/j.aca.2017.03.037

Mortimer, R. J. (2011). Electrochromic materials. *Annual Review of Materials Research, 4*, 241–268. https://doi.org/10.1146/annurev-matsci-062910-100344

Mortimer, R. J., Dyer, A. L., & Reynolds, J. (2006). Electrochromic organic and polymeric materials for display applications. *Displays, 27*, 2–18. https://doi.org/10.1016/j.displa.2005.03.003

Mortimer, R. J., Rosseinsky, D. R., & Monk, P. M. S. (Eds.). (2013). *Electrochromic materials and devices*. Wiley-VCH Verlag GmbH & Co..

Nakatani, K., Piard, J., Yu, P., & Metivier, R. (2016). Introduction: Organic photochromic molecules. In H. Tian & J. Zhang (Eds.), *Photochromic materials: Preparation, properties and applications* (pp. 1–45). Wiley-VCH Verlag GmbH & Co. KGaA.

Ntoi, L. L. A., Buitendach, B. E., & von Eschwege, K. G. (2017). Seven chromisms associated with Dithizone. *The Journal of Physical Chemistry. A, 121*(48), 9243–9251. https://doi.org/10.1021/acs.jpca.7b09490

Nunes, D., Pimentel, A., Santos, L., Barquinha, P., Pereira, L., Fortunato, E., & Martins, R. (2019). *Metal oxide nanostructures* (pp. 103–147). Elsevier. https://doi.org/10.1016/B978-0-12-811512-1.00004-7

Ordronneau, L., Carella, A., Pohanka, M., & Simonato, J. P. (2013). Chromogenic detection of Sarin by discolouring decomplexation of a metal coordination complex. *Chemical Communications, 49*, 8946–8948. https://doi.org/10.1039/c3cc45029e

Pardo, R., Zayat, M., & Levy, D. (2011). Photochromic organic–inorganic hybrid materials. *Chemical Society Reviews, 40*, 672–687. https://doi.org/10.1039/c0cs00065e

Park, D.-H., Park, B. J., & Kim, J.-M. (2016). Hydrochromic approaches to mapping human sweat pores. *Accounts of Chemical Research, 49*, 1211–1222. https://doi.org/10.1021/acs.accounts.6b00128

Pomili, T., Donati, P., & Pompa, P. P. (2021). Paper-based multiplexed colorimetric device for the simultaneous detection of salivary biomarkers. *Biosensors, 11*(11), 443. https://doi.org/10.3390/bios11110443

Pradela-Filho, L. A., Veloso, W. B., Arantes, I. V. S., Gongoni, J. L. M., de Farias, D. M., Araujo, D. A. G., et al. (2023). Paper-based analytical devices for point-of-need applications. *Microchimica Acta, 190*, 179. https://doi.org/10.1007/s00604-023-05764-5

Rahbar, M., Wheeler, A. R., Paull, B., & Macka, M. (2019). Ion-exchange based immobilization of chromogenic reagents on microfluidic paper analytical devices. *Analytical Chemistry, 14*, 8756–8761. https://doi.org/10.1021/acs.analchem.9b01288

Rai, P., Mehrotra, S., & Sharma, S. K. (2022). Development of a paper-based chromogenic strip and electrochemical sensor for the detection of tannic acid in beverages. *LWT—Food Science and Technology, 169*, 113999. https://doi.org/10.1016/j.lwt.2022.113999

Rakow, N. A., & Suslick, K. S. (2000). A colorimetric sensor array for odour visualization. *Nature, 406*, 710–713. https://doi.org/10.1038/35021028

Rakow, N. A., Sen, A., Janzen, M. C., Ponder, J. B., & Suslick, K. S. (2005). Molecular recognition and discrimination of amines with a colorimetric array. *Angewandte Chemie, International Edition, 44*(29), 4528–4532. https://doi.org/10.1002/anie.200500939

Rijavec, T., & Bračko, S. (2007). Smart dyes for medical and other textiles. In L. Van Langenhove (Ed.), *Smart textiles for medicine and healthcare: Materials, systems and applications* (pp. 123–149). Woodhead Publishing.

Sadeghi, K., Yoon, J.-Y., & Seo, J. (2020). Chromogenic polymers and their packaging applications: A review. *Polymer Reviews, 60*(3), 442–492. https://doi.org/10.1080/15583724.2019.1676775

Seeboth, A., Loetzsch, D., & Ruhmann, R. (2012). Piezochromic polymer materials displaying pressure changes in bar-ranges. *Materials, 1*, 139–142. https://doi.org/10.5923/j.materials.20110102.23

Seeboth, A., Lotzsch, D., Ruhmann, R., & Muehling, O. (2014). Thermochromic polymers function by design. *Chemical Reviews, 114*, 3037–3068. https://doi.org/10.1021/cr400462e

Selektor, S., & Shokurov, A. (2015). Conjugated compounds in supramolecular informational systems: A review. *Protection of Metals and Physical Chemistry of Surfaces, 51*, 171–203. https://doi.org/10.1134/S2070205115020161

Sengupta, A., & Behera, J. (2014). Smart chromic colorants draw wide attention for the growth of future intelligent textile materials. *Journal of Advanced Research in Manufacturing, Material Science & Metallurgical Engineering, 1*, 89–112.

Seok, H., Son, S., Cho, J., Choi, S., Park, K., Kim, C., et al. (2022). Chromism-integrated sensors and devices for visual indicators. *Sensors, 22*, 4288. https://doi.org/10.3390/s22114288

Shankar, S., Lahav, M., & van der Boom, M. E. (2015). Coordination-based molecular assemblies as electrochromic materials: Ultra-high switching stability and coloration efficiencies. *Journal of the American Chemical Society, 137*, 4050–4053. https://doi.org/10.1021/jacs.5b00429

Shen, X., Hu, Q., Jin, Y., & Ge, M. (2023). Long-lived luminescence and photochromic cellulose acetate-based fiber: Preparation, characterization, and potential applications. *Cellulose, 30*, 2181–2195. https://doi.org/10.1007/s10570-022-05034-2

Sheng, L., Li, M., Zhu, S., Li, H., Xi, G., Li, Y. G., et al. (2014). Hydrochromic molecular switches for water-jet rewritable paper. *Nature Communications, 5*, 4044. https://doi.org/10.1038/ncomms4044

Siegel, A. C., Phillips, S. T., Wiley, B. J., & Whitesides, G. M. (2009). Thin, lightweight, foldable thermochromic displays on paper. *Lab on a Chip, 9*, 2775–2781. https://doi.org/10.1039/b905832j

Suhag, N., & Singh, S. (2015). Types of chromism & its applications in fashion & textile designing. *International Journal of Enhanced Research in Science, Technology & Engineering, 4*(8), 28–36.

Sui, Q., Ren, X.-T., Dai, Y.-X., Wang, K., Li, W.-T., Gong, T., et al. (2017). Piezochromism and hydrochromism through electron transfer: New stories for viologen materials. *Chemical Science, 8*, 2758. https://doi.org/10.1039/c6sc04579k

Sun, C., Zhang, Y., Fan, Y., Li, Y., & Li, J. (2004). Mannose–Escherichia coli interaction in the presence of metal cations studied in vitro by colorimetric polydiacetylene/glycolipid liposomes. *Journal of Inorganic Biochemistry, 98*, 925–930. https://doi.org/10.1016/j.jinorgbio.2004.03.006

Sun, X., Zhang, H., Hao, S., Zhai, J., & Dong, S. (2019). A self-powered biosensor with a flake electrochromic display for electrochemical and colorimetric formaldehyde detection. *ACS Sensors, 4*, 2631–2637. https://doi.org/10.1021/acssensors.9b00917

Suslick, K. S. (1998). *Kirk-Othmer encyclopedia of chemical technology* (Vol. 26, pp. 517–541). Wiley. https://doi.org/10.1002/0471238961.herbduke.a01.pub2

Van der Schueren, L., & De Clerck, K. (2012). Coloration and application of pH-sensitive dyes on textile materials. *Coloration Technology, 128*, 82–90. https://doi.org/10.1111/j.1478-4408.2011.00361.x

Wallace, K. J., Cordero, S. R., Tan, C. P., Lynch, V. M., & Anslyn, E. V. (2007). A colorimetric response to hydrogen sulfide. *Sensors and Actuators B: Chemical, 120*, 362–367. https://doi.org/10.1016/j.snb.2006.02.031

Wang, L., & Li, Q. (2018). Photochromism into nanosystems: Towards lighting up the future nanoworld. *Chemical Society Reviews, 47*, 1044–1097. https://doi.org/10.1039/C7CS00630F

Wang, L., Wang, K., Zou, B., Ye, K., Zhang, H., & Wang, Y. (2015). Luminescent chromism of boron diketonate crystals: Distinct responses to different stresses. *Advanced Materials, 27*, 2918–2922. https://doi.org/10.1002/adma.201500589

Wang, W., Fan, X., Li, F., Qiu, J., Ren, W., Ju, B., et al. (2018). Magnetochromic photonic hydrogel for an alternating magnetic field-responsive color display. *Advanced Optical Materials, 6*(4), 1701093. https://doi.org/10.1002/adom.201701093

Warwick, M. E. A., & Binions, R. (2014). Advances in thermochromic vanadium dioxide films. *Journal of Materials Chemistry A, 2*, 3275–3292. https://doi.org/10.1039/C3TA14124A

White, M. A., & Leblanc, M. (1999). Thermochromism in commercial products. *Journal of Chemical Education, 76*, 1201–1205. https://doi.org/10.1021/ed076p1201

Wu, L., Zhang, S., Gao, J., Qiang, P., & Lei, J. (2016). Preparation of a spirooxazine grafted PMMA and its photochromic properties. *Synthetic Communications, 46*, 818–830. https://doi.org/10.1080/00397911.2016.1178296

Yang, P., Sun, P., & Mai, W. (2015). Electrochromic energy storage devices. *Materials Today, 19*, 394–402. https://doi.org/10.1016/j.mattod.2015.11.007

Yeon, S. Y., Seo, M., Kim, Y., Hong, H., & Chung, T. D. (2022). Paper-based electrochromic glucose sensor with polyaniline on indium tin oxide nanoparticle layer as the optical readout. *Biosensors & Bioelectronics, 203*, 114002. https://doi.org/10.1016/j.bios.2022.114002

Yu, X., Guo, P., Chen, J., Li, S., & Li, H. (2024). Recent advances in multifunctional electrochromic devices. *Responsive Materials, 2*, e20240013. https://doi.org/10.1002/rpm.20240013

Zhang, D., & Jin, W. (2012). Highly selective and sensitive colorimetric probe for hydrogen sulfide by a copper (II) complex of azo-dye based on chemosensing ensemble approach. *Spectrochimica Acta Part A: Molecular and Biomolecular Spectroscopy, 90*, 35–39. https://doi.org/10.1016/j.saa.2012.01.013

Zhang, J., Zou, Q., & Tian, H. (2013). Photochromic materials: More than meets the eye. *Advanced Materials, 25*, 378–399. https://doi.org/10.1002/adma.201201521

Chapter 24
Printing Technology Used in Fabrication of Paper-Based Sensors and Devices

Philipp Yu. Gorobtsov, Tatiana L. Simonenko, Nikolay P. Simonenko, Elizaveta P. Simonenko, and Ghenadii Korotcenkov

24.1 Introduction

Today it is impossible to discuss various technologies for forming films of various compositions on substrates of any type and creating devices based on such coatings without mentioning printing technologies. This group of methods is very widely used in the creation of devices for a large number of areas due to the low cost, ease of automation and scaling of the printing process, high reproducibility provided by their use, and the ability to set the most complex geometry of printed structures and apply the material selectively to different areas of the substrate. In addition, there are a large number of printing methods, each of which differs in process parameters, requirements for inks, characteristics of the resulting films, etc., making it convenient to select a printing method for a particular task. A number of printing technologies (flexography, gravure printing, etc.) also make it possible to produce large batches of devices with high reproducibility and degree of automation. All these factors are common advantages of printing technologies compared to classical technologies.

In the context of creating devices in which paper is the primary construction material, acting as the substrate on which functional elements are applied, the use of printing techniques is also the most intuitive, along with writing methods (discussed below in a separate Chap. 26). After all, the use of various printing methods to record information on paper and similar media is centuries old and to create functional devices in this way requires only adapting the process by using, for example, different inks, employing additional printing methods beyond those commonly used

P. Y. Gorobtsov · T. L. Simonenko (✉) · N. P. Simonenko · E. P. Simonenko
Kurnakov Institute of General and Inorganic Chemistry, Russian Academy of Sciences, Moscow, Russia

G. Korotcenkov
Department of Physics and Engineering, Moldova State University, Chisinau, Moldova

G. Korotcenkov (ed.), *The Handbook of Paper-Based Sensors and Devices*,
https://doi.org/10.1007/978-3-031-91080-7_24

to produce so-called printed matter, and so on. It is therefore not surprising that printing technologies are often used in the creation of paper-based devices. Furthermore, it can be stated that paper is a substrate ideally suited for the creation of various devices using printing technologies—its fibrous structure promotes ink absorption, which improves the adhesion of printed coatings and especially facilitates the creation of microfluidic chips on its basis (it makes it possible to apply impermeable hydrophobic barriers). In addition, most printing methods were originally developed to apply ink to paper.

This chapter will summarize the general features of the various printing techniques used in obtaining various sensors and electronics using paper as a substrate for the deposition of electrodes and other functional coatings, then review selected of the most notable technologies in use, noting their advantages and disadvantages.

24.2 General Features of Printing Technology

Printing technology is an extremely broad field, comprising a large number of considerably different methods and approaches for the production of coatings (as well as three-dimensional products in the case of 3D printing). What they all have in common, however, is that they are primarily additive manufacturing (hence the name "additive technologies" sometimes used interchangeably with "printing technologies"), i.e., the final product is obtained by adding new material to it, rather than, for example, removing parts from the original raw material. The material is added initially in the form of an ink, which may, depending on the particular printing method, be liquid or solid, or it may be transferred to the substrate as an aerosol, i.e., a dispersion in the gas phase. Liquid inks can be either true solutions or dispersions—usually of solid particles (Al-Amri, 2023; Dahiya et al., 2020; Han et al., 2023; Yu et al., 2018). The composition of inks, as well as their aggregate state, can be very different: depending on the combination of the task to be solved and the chosen specific printing method, polymer inks, true solutions of various organic or inorganic compounds (which can also enter into chemical reactions with each other or with atmospheric species during drying), dispersions of polymer particles or inorganic, and the latter can be metals, oxides, or, in principle, any other stable inks (Batet et al., 2023; Hoeng et al., 2016; Liu et al., 2017; Nandy et al., 2021). Printing processes are almost never carried out manually either, in the sense that a person cannot (even hypothetically) take the tool that directly applies the ink and use it to draw the required structure with his or her own hands during the ink application itself: the "drawing" is usually already pre-determined, either by a manufactured gravure cylinder (in the case of gravure printing), a stencil (screen printing), or a plate cylinder (flexography), or digitally programmed (in the case of inkjet printing, laser printing, etc.). Because of this factor in particular, the writing of structures with markers or pens does not belong to printing but is recognized as a separate group of methods (see Chap. 26).

The text of the previous paragraph clearly demonstrates the variety of methods included within the framework of printing methods: on the one hand, by listing the differences in the inks that can be used in them, and on the other hand, by the extreme breadth in the notions of the factors that bring these methods together into a family of printing technologies. It is therefore hypothetically possible to define many classifications of printing methods—at least in terms of the viscosity of the ink used, or the maximum achievable resolution—but the most fundamental is the one classification that is usually mentioned in the literature. This is a division into contact and non-contact printing methods. In contact methods, a roller or other surface on which ink is applied, or an opening through which ink is to be transferred to the substrate, comes into direct mechanical contact with the substrate to transfer the ink. In non-contact methods, this does not happen—the substrate is only in contact with the ink, which, for example, flies out of the nozzle of an inkjet or aerosol printer that is removed from the substrate. Contact methods (screen printing, flexography, gravure printing, etc.) are generally considered to use more material, have lower resolution, and are more limited in ink selection than non-contact methods (inkjet printing, spray printing, etc.) (Cruz et al., 2018; Khan et al., 2015). However, at the same time, contact methods possess high productivity and simplicity, so they are extremely common in modern printing and industry, especially when it is necessary to produce large batches of products (Liang et al., 2016). In general, however, all these methods have the merits of simplicity, low cost, easy automation, high reproducibility, and the ability to selectively apply material to different areas of the substrate without masking layers.

It is also necessary to briefly mention several points concerning the paper requirements for printing devices based on it. Firstly, the choice of a particular type of paper is naturally determined by the device itself and the function that the substrate has to fulfill in it. For example, if it is necessary to apply some voltage to a functional coating, then instead of applying electrodes to cellulose paper, using conductive carbon paper (see example below in Sect. 24.3.10) might be more appropriate. For microfluidic chips on the other hand, where paper acts as a hydrophilic medium in which the liquid spreads, there is no need for such a special substrate, and when creating transistors, ordinary paper can play the role of an insulator. Secondly, the porosity of the paper and its ability to absorb ink is an important factor—this is especially important when working with low-viscosity inks (Nandy et al., 2021). If the paper substrate absorbs ink too well, there will be a discrepancy between the geometry of the device as specified during printing and the area where the coating was actually applied. The roughness of the paper also affects the uniformity of the resulting coating. For this reason, coated paper is often used as a substrate, as it is less absorbent and less rough. Nanopaper can also be used instead of coated paper. As for the compatibility of different types of paper with individual printing methods, in general, almost any paper is compatible with any method, especially unpretentious are microplotter printing, flexography, gravure printing, and screen printing. In general, when obtaining paper-based devices by printing techniques, filter paper (e.g., Whatman brand), chromatography paper, and coated paper are generally used.

Having thus noted the general features of printing technologies and their basic classification, we next turn to the specific printing techniques used in the literature to produce paper-based devices, limiting ourselves to a brief description of the principles underlying them and a few specific examples of their application from the scientific literature, since a more thorough examination would require an extensive review for each of the techniques with the volume of each being the same as the size of this chapter, which is out of the intended scope of this Handbook—we direct the readers to the publications referenced in the text if they desire a more in-depth insight into any specific technique.

24.3 Main Printing Techniques in Paper-Based Device Fabrication

24.3.1 Inkjet Printing

Inkjet printing belongs to non-contact printing methods: it is based on the application of ink in the form of droplets falling on the substrate through the nozzle of the print head (Kwon et al., 2021; Li et al., 2019; Xi et al., 2024; Yan et al., 2020; Zea, 2021; Zhang et al., 2018). Two modifications of inkjet printing can be distinguished: continuous and drop-on-demand (DoD). In the first case, droplets flow out of the liquid column under the action of gravity, continuously, as long as there is the necessary amount of ink. This modification is the most technically simple but does not have the same high resolution, as well as worse suited for the application of complex structures consisting, for example, of several phases, or of discrete geometric elements than drop-on-demand, although these disadvantages can be leveled by using the reflection of "extra" drops by an external electric field and their collection in a separate container. However, it is the DoD that is most commonly used today for printing on paper, even in the case of everyday applications—to apply text or images to paper. In the case of DoD inkjet printing, droplets are specifically generated rather than falling in a continuous stream (hence the name drop-on-demand). Either a heating or piezoelectric element in the printhead is used to generate the droplets. In the first case the ink drop falls due to pressure from bubbles appearing in the liquid, in the second case—due to mechanical vibrations of the piezo element (Fig. 24.1) (Kwon et al., 2021; Yamada et al., 2015; Yan et al., 2020; Zea, 2021). In general, inkjet printing has a fairly high resolution (mostly 15–50 μm, but in some cases a resolution of 100 nm and below is possible (Godard et al., 2019; Zhao et al., 2007)), it can use both true solutions and nanoparticle dispersions as inks, but the latter can clog cartridges and printheads relatively easily; in addition, parallel printing from multiple printheads has to be used to ensure fast and mass production with this technology (Simonenko et al., 2022; Yan et al., 2020; Zea, 2021). Also, while inkjet printing, one must take into account the "coffee stain" effect, which results in uneven distribution of material after drying with higher concentrations closer to the

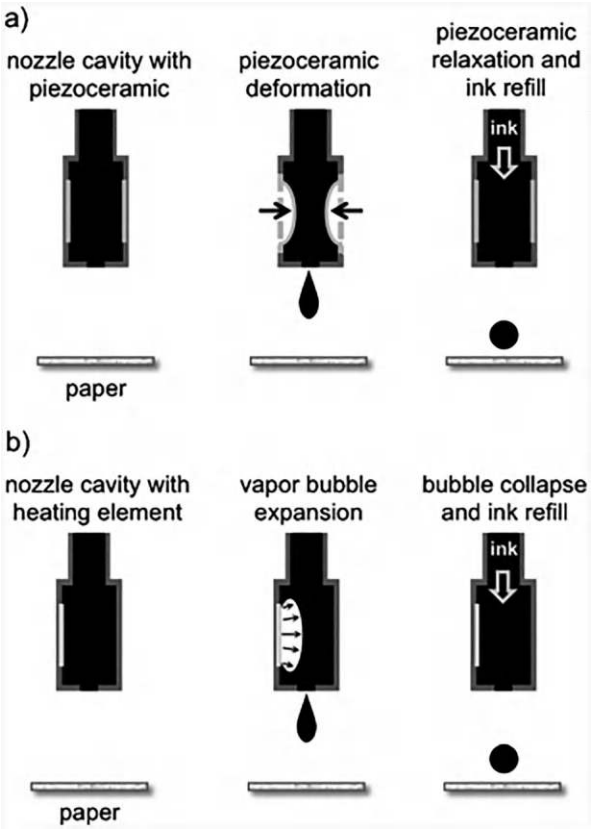

Fig. 24.1 Basic working principle of drop-on-demand (DOD) inkjet printing: (**a**) piezoelectric inkjet and (**b**) thermal inkjet. (Reproduced with permission from Yamada et al. (2015); Copyright 2015: Wiley)

edges of the dried ink drop (Yan et al., 2020). Inkjet printing is often used in the creation of various devices with functional coatings on flexible substrates; for example, Layani et al. (2014) utilized it in preparation of electrochromic film of WO_3 on plastic with transparent silver electrodes, clearly showing prospective of the technique. Inkjet printing is very widely used in the development of paper-based devices due to its advantages and the prevalence of the corresponding printers. It is also possible to use a wide variety of inks and to obtain the most original coatings.

Thus, using inkjet printing on paper substrates, organometallic frameworks (MOFs) attached to the surface (SURMOFs) can be formed. In Zhuang et al. (2013) a solution of precursors of the target SURMOF ($Cu_3(btc)_2$, also called HKUST-1) in a mixture of dimethyl sulfoxide (DMSO), ethanol, and ethylene glycol was used as an ink. The importance of solvent and dispersion medium composition for obtaining suitable systems for printing should be noted here: the authors note that previously used solutions (such as the same starting reagents in pure DMSO (Ameloot et al.,

2010)) were unsuitable for inkjet printing due to their viscosity and surface tension (Zhuang et al., 2013). The introduction of ethanol reduced the viscosity sufficiently for inkjet printing, but additional introduction of ethylene glycol into the solvent composition was required to obtain ink stability for a long time (8 months). Using these inks, HKUST-1 coatings were successfully obtained on the surface of ordinary office paper, but the authors note one of the characteristics of such a substrate. This substrate, as formed by intersecting fibers, has a large roughness and significant voids between the fibers, where the ink mainly leaks and where, as a result, there is a predominant concentration of the material after drying. Overall, the authors of the study (Zhuang et al., 2013) were able to demonstrate the promising potential of inkjet printing for the deposition of various SURMOFs on paper—in addition to HKUST-1, they used the same approach to form a working luminescent coating of $[Zn_2(adc)_2(dabco)_2]$ (adc = 9,10-anthracenedicarboxylate, dabco = 1,4-diazabicyclo[2.2.2]octane).

Equally interesting and original coatings produced by inkjet printing on paper are components for electronics—such as RFID antenna, inductive coil, etc.—consisting of liquid metal. In Zheng et al. (2013), $GaIn_{24.5}$ alloy was used as an ink, which was applied to coated paper. Then the obtained structures were stabilized by printing over them liquid silicone rubber, which hardens at room temperature under the effect of air moisture. The liquid metal screened in this way does not spread out during bending and further manipulation of the paper product. The authors of the study note that in addition to choosing the right paper, it is important to monitor the optimal oxygen content in the alloy that acts as an ink: the higher it is, the better the adhesion of the metal to the substrate, viscosity, and wettability. At the same time, too high a viscosity can lead to a difficult exit of the ink from the printhead. As a result, in the present work Zheng et al. settled on an oxygen content of 0.1% (wt.) in the alloy (Zheng et al., 2013).

However, it is still much more common to use inkjet printing on paper substrates to produce various paper analytical devices (PADs), primarily microfluidic, electrochemical sensors using less exotic inks. First of all, in such devices, the microfluidic chips themselves are constructed by inkjet printing by coating the hydrophobic "walls" of the channels with appropriate inks (polystyrene, hydrophobic sols and gels, polyacrylates, silicone), or the hydrophilic channels are etched into the hydrophobic layer on the substrate by inkjet printing with an appropriate agent as ink (toluene, for example) (Le et al., 2020; Prabhu et al., 2020; Yamada et al., 2015). In addition, it is also possible to deposit analytes inside the microfluidic PADs directly by inkjet printing method (Yamada et al., 2015). In addition to such devices, inkjet printing is also used to create sensors for mechanical pressure and voltage, supercapacitors, in which, for example, a layer of graphene is applied by this technique (Yan et al., 2020). In order to obtain metal electrode layers, however, not liquid metals but inks based on dispersions of silver or gold nanoparticles are used first (Tortorich et al., 2018).

24.3.2 Aerosol Printing

Aerosol printing is also a non-contact method. In this technology, also called Aerosol jet printing (AJP), an aerosol is generated from an ink, which is a true solution or dispersion of solid particles in a liquid, when the ink is atomized and a carrier gas is injected; the resulting aerosol jet is directed onto the substrate by the carrier gas stream (Fig. 24.2) (Agarwala et al., 2017; Cooper & Hughes, 2020; Wilkinson et al., 2019). Commercially available setups allow generating aerosol from ink with viscosity of up to 1000 cP (Wilkinson et al., 2019), which is one of the advantages of this printing method over others. The most important technical nuances in aerosol printing are aerosol generation (more precisely, ink atomization) and focusing of its jet. Atomization can be performed by ultrasound if the initial ink has a relatively low viscosity, up to about 20 cP. In such a case, as a rule, the liquid phase in the aerosol has a size of 2–5 microns. Another aerosol generation process, the so-called "pneumatic" process, is based on passing a high-speed flow of carrier gas over a narrow channel leading into the ink reservoir. As a result, a portion of the ink is sucked through the channel into the carrier gas and carried away by the gas, forming an aerosol. In this way it is possible to produce an aerosol from more viscous inks, up to 500–1000 cP. Then, as a rule, additional droplets of the required size and energy are selected by means of a virtual impactor before the jet is sent directly to the printhead. The sheath gases then focus the jet inside the printhead (Cooper & Hughes, 2020; Wilkinson et al., 2019).

When creating paper-based devices, aerosol printing is used in the application of conductive electrodes, particularly silver electrodes, to paper substrates (Chen et al.,

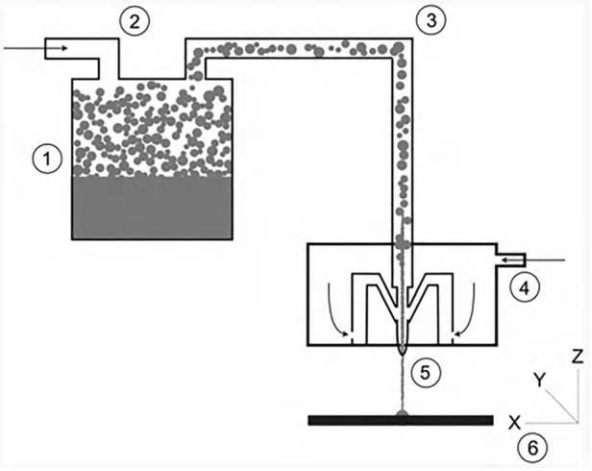

Fig. 24.2 An overview of AJP: (*1*) aerosol generation using either ultrasonic or pneumatic atomizer, (*2*) introduction of a carrier gas to transport the aerosol, (*3*) transportation and refinement, (*4*) focusing, (*5*) deposition, and (*6*) computer-controlled translation of the substrate. (Reproduced from Wilkinson et al. (2019). Published 2019 by Springer with open access)

2020; Serpelloni et al., 2020). It is important to note a feature that has received special attention in some papers: for better adhesion between the printed coating and the substrate (in this case paper, but this is also true for other materials), additional treatment is required after aerosol printing (in the case of metal electrodes, this also helps to increase their conductivity). Thus, in Chen et al. (2020) the deposited layers were treated with hot air flow (T = 80 °C), and in Serpelloni et al. (2020), oven heat treatment at 140 °C was used to dry the metal tracks. Serpelloni et al. (2020) in their work showed in general the possibility of creating a smart device based on paper and photopolymer with extensive involvement of aerosol printing—including the creation of insulative layers on the chip under construction.

In addition, aerosol printing has also been used to create paper-based photodetectors (Aga et al., 2014), chemical sensors for detection of water and volatile organic substances (Lombardi et al., 2017; Wilkinson et al., 2019), and ammonia (Borghetti et al., 2022). In (Borghetti et al., 2022), in particular, this technology was used to apply carbon interdigital electrodes for an ammonia sensor promising for application in the food industry (in "smart" food packaging). Aerosol printing also has great potential in terms of creating microfluidic chips, although glass substrates are more often used for this purpose than paper substrates (Ćatić et al., 2020).

Although aerosol printing has such advantages as the ability to work with more viscous inks, sufficiently high resolution, and the possibility of easy application even on non-planar substrates, there are certain disadvantages. Firstly, the phenomenon of overspray is observed during such printing, when drops or particles of aerosol continue to be in contact with the material already applied just from it on the substrate, which can cause even the removal of this material from the substrate. Secondly, the processes of aerosol generation and focusing of its jet are quite complex and require a lot of attention from the technical point of view, while very much affecting the application process and its results (Cooper & Hughes, 2020; Wilkinson et al., 2019).

24.3.3 Screen Printing

Screen printing is a contact printing method. As a rule, very viscous inks in the form of pastes are used, and it is possible to use compositions with viscosity at the level of tens of thousands of cP and with an extremely high content of solid phase (more than 70–80% wt.). The principle is quite simple (Fig. 24.3): a stencil is pressed to the substrate, which can be made of any sufficiently dense and impermeable material, usually cardboard or a network of metallic threads; then a paste is applied to this stencil, which is pressed onto the substrate through the holes in the stencil with a squeegee (Hong et al., 2023; Jansson et al., 2022; Khan et al., 2015; Le Borgne et al., 2019; Malik et al., 2024; Shen et al., 2024). Besides, it is possible to realize a rotary realization of screen printing, where the squeegee is stationary and the ink is squeezed out through holes in a rotating cylinder; the substrate can also move under the cylinder at the same speed (Simonenko et al., 2022). This option allows printing

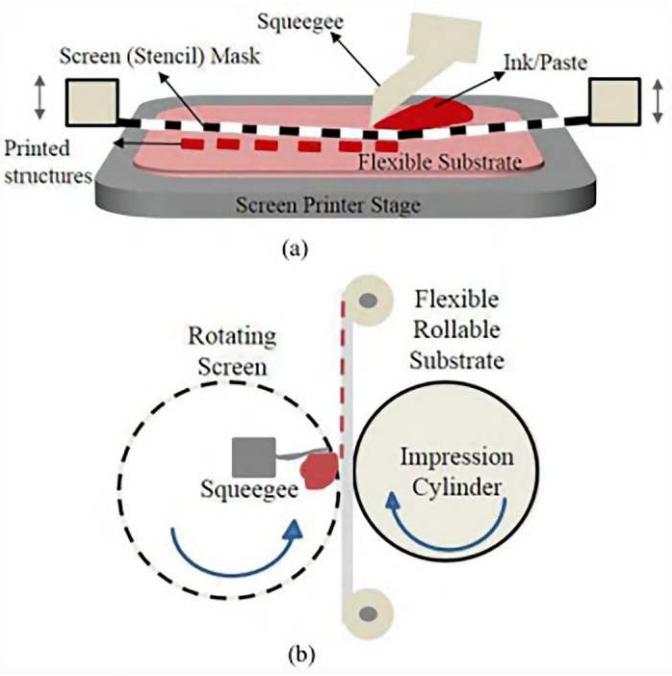

Fig. 24.3 (**a**) The flatbed Screen printing with planar substrates under screen and squeegee for solution dispensing. (**b**) Rotary screen printer with moving substrate (web) between cylindrical mask and impression cylinder. (Reproduced from Khan et al. (2015). Published 2015 by IEEE with open access)

at a much higher speed and throughput. Coating may be followed by an additional heat treatment step to dry the ink and improve adhesion of the material to the substrate. Screen printing is a widespread technique in science and industry due to its simplicity and wide capabilities, relatively low ink requirements, and ease of automation. However, it has disadvantages related to resolution—viscous ink tends to clog the rather small gaps between the filaments in the stencil (thus blocking coating outside the required area of the substrate). Nevertheless, it is possible to achieve a resolution of 100–200 μm with screen printing (Tseng et al., 2021).

The most common use of screen printing for paper-based devices is to produce electrodes and hydrophobic layers of microfluidic chips. In Jansson et al. (2022) researchers applied silver conductor lines using a viscous paste (22 Pa•s, or 22,000 cP, silver content 75% wt. %) through a stainless steel stencil. The authors of the study focused on the comparison between different types of paper and polymer substrates; it was found that the best detailing of the applied structures was observed on coated paper because on conventional paper there is more smearing of ink along the surface irregularities and its fibers. In general, the screen-printed silver electrodes had lower resistivity compared to those applied by flexographic method, which, however, may be due to the use of microdispersed silver particles in the ink

in the former case and nanodispersed ones in the latter. An interesting study was performed by Brooke et al. (2023), in which, in addition to screen printing on paper electrodes based on the well-known conjugated poly(3,4-ethylenedoxythiophene) (PEDOT) polymer and demonstration of their conductivity when connected to LED cells, a complete electrochromic display was created using only screen printing to apply layers of different materials, from electrochromic (PEDOT) to electrolyte and insulator. Thus, in addition to pastes with PEDOT, inks with silver, carbon (auxiliary electrodes and voltage lines), and polymer electrolyte and insulator were used. The resulting device showed excellent stability of the colored state.

As already mentioned, many works are devoted to the creation of microfluidic chips using screen printing, which is used in them for the application of hydrophobic layers. Thus, in Lamas-Ardisana et al. (2017) a three-electrode amperometric hexocyanoferrate(III) detector was fabricated, in which this printing method was used both for the application of electrodes (carbon, silver, and comparison—silver/chlorosilver) and for the creation of hydrophobic barriers (based on a mixture of different dyes). In Silva-Neto et al. (2024), a paper sensor on α-amylase was constructed in a similar manner; screen printing is also widely used to obtain various other sensors for medicine related to immunosorption and microRNA detection (Lin et al., 2022; Raucci et al., 2024; Silva-Neto et al., 2024). The study by Tseng et al. (2021) is devoted to attempts at optimizing the process of applying hydrophobic coatings to paper using screen printing in a single layer by adjusting the thickness of the substrate and the temperature of the subsequent heat treatment. The authors found that for paper thicknesses of 150 μm and less, the hydrophobic agent completely impregnates the substrate, while a thicker sheet (210 μm) was not impregnated by one layer of the ink used. However, it should be noted that the thickest paper (210 μm) was of a different brand (Whatman) and, as a consequence, was produced using a slightly different technology with a slightly different composition from the thinner paper (Xuan brand).

In addition to extremely viscous pastes, fairly well-flowing inks can also be used in screen printing. For example, in Le Borgne et al. (2019), albumin with a viscosity of only 20.1 cP was used to apply an insulator layer between two carbon electrodes.

24.3.4 Flexographic Printing

Flexography is a contact printing method. Several rollers are used in the respective machines. The first roller (anilox roller) is fed with ink, which is then applied to the elevations of the raised second roller (plate cylinder) (Fig. 24.4). The highest points of this roller are already in direct contact with the substrate, leaving a corresponding trace on the substrate. At the same time, the impression cylinder on the opposite side of the plate cylinder exerts additional pressure on the substrate (Anushka et al., 2023; Hu et al., 2018; Khan et al., 2015; Olsson, 2007; Soman et al., 2024). Flexographic inks can have relatively high viscosity—pastes with viscosities up to 300–600 cP are found in the literature (Jansson et al., 2022). The main advantage of

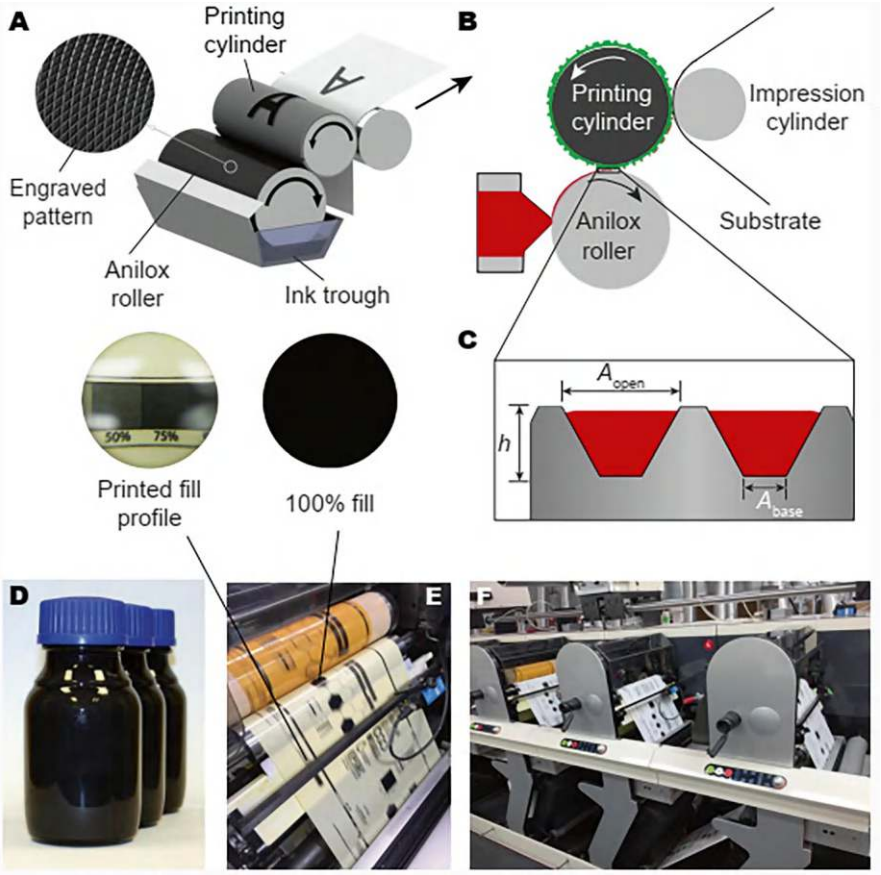

Fig. 24.4 Flexographic printing: (**a**–**c**) Schematic figures showing flexographic printing principles. (**d**) Photograph of graphene/carbon flexographic ink. Printing trials of the ink shown in (**d**) on (**e**) PET and (**f**) paper substrates using a commercial graphic printing press. Inset: zoomed-in photographs of the printed fill profiles. (Reproduced with permission from Hu et al. (2018). Copyright 2018: Royal Society of Chemistry)

this process is its high speed and, therefore, high productivity, which is why it is actively used for printing large batches of products. However, this method requires the production of a separate plate cylinder for each device or typographic product, which is usually appropriate for printing large batches. Nevertheless, this method, as a potentially highly desirable method for the production of paper products, needs to be investigated, and there are papers on the production of various paper-based electronic and sensor devices using flexography in the scientific literature.

For example, in Jansson et al. (2022) silver electrodes were applied using the flexographic printing method, and it was found that the best properties were those applied on coated paper compared to polyethylene terephthalate (PET) and uncoated paper. The authors attributed this to the fact that, on the one hand, PET is too smooth,

which impairs ink transfer from the plate cylinder, while on the contrary, a slightly higher roughness contributes to the transfer. However, too high roughness, on the contrary, is detrimental to uniform ink transfer according to this study. The role of substrate roughness in the case of this printing method was found to be greater than in the case of screen printing. At the same time, this comparison should be taken carefully, since screen printing uses inks based on less highly dispersed silver particles. The flexographic method can also be used to create fluidic chips for the application of a hydrophobic layer (Olkkonen et al., 2010).

24.3.5 Wax Printing

Another printing process is wax printing, which, depending on the specific technical design, can be classified as either contact or non-contact technique. This process is based on the application of molten ink to the substrate, which, based on the temperature of the substrate, either solidifies on it or continues to be absorbed inside it (in the case of heated paper) (Altundemir et al., 2017; Das et al., 2022; Lim et al., 2019; Mustafa et al., 2020). If special printers capable of handling solid ink are used for coating (Xerox Phaser 8560N, Xerox ColorQube 8570, Xerox Phaser 8000DP, etc. (Altundemir et al., 2017; Carrilho et al., 2009; Potter et al., 2019)), then the printing is more of a non-contact printing, as the molten wax droplets are applied to the substrate surface using the same principle as in DoD ink. In cases where wax is applied to a heated substrate by stamping, printing is a contact technique (Borah et al., 2022).

The inks for this printing method are waxes that are solid at room temperature and may contain various other organic components, such as dyes. This feature determines the main application of wax printing in the creation of paper-based devices, namely, the application of hydrophobic layers for various fluidic chips (Altundemir et al., 2017; Borah et al., 2022; Carrilho et al., 2009; Liang et al., 2021). When designing such chips, however, it must be taken into account that in the case of non-contact wax printing of hydrophobic layers, additional heat treatment of the sample is required to melt the applied wax and impregnate the paper with it, which will cause the area of the hydrophobic layer to differ by a large margin from the area originally inked. This process was clearly demonstrated and studied by Carrilho et al. (2009). In the case of contact wax printing, in which the ink is normally heated in contact with a hot paper substrate, it is important to optimize the temperature of the substrate and the contact time of the stamp in order to achieve the necessary impregnation of the substrate with a hydrophobic agent (Borah et al., 2022).

It should be noted that since 2016, many solid ink printers convenient for wax printing are no longer commercially available, making it necessary to switch to contact wax printing or other methods in research. However, in Ruiz et al. (2022) the feasibility of moving from wax printing with no longer available printers to thermal transfer printing is demonstrated.

24.3.6 Laser Printing

Printing with laser printers, also quite common in everyday life just like inkjet printers, refers to contact methods. In laser printing, a negative electrical charge is first induced on the surface of a photosensitive roller. The desired points on its surface are then irradiated with a laser, which removes the charge from them. Next, the section of the photosensitive roller with laser-treated dots contacts the developer roll, on which a uniform layer of toner is applied. The toner particles themselves have a negative electrical charge, so they adhere only to the laser-treated parts of the photoreceptor roll. Next, the photoreceptor with the adhered toner contacts the paper (or other flexible substrate) to which the image is transferred. An additional positively charged roller underneath the paper may also be used for better toner transfer to the paper. The printed paper is then heat-treated in the device itself to improve adhesion of the toner to the substrate. In the context of creating paper-based devices, laser printing has attracted attention for several reasons. First, it is a widely available printing method due to the ubiquity of laser printers in everyday life. Second, commercially available laser printing inks, or toner, typically comprise mixtures including styrene-acrylate copolymer, iron oxide, amorphous silicon oxide, or other similar compositions (Moulahoum, 2023). Due to the presence of polymer, almost any toner can be used to create hydrophobic layers on paper (Ghosh et al., 2019), thus printing microfluidic chips. In addition, some researchers became interested in laser printing of μPADs after printers mainly used in wax printing disappeared from the market (Ng & Hashimoto, 2020)—thus, laser printing is offered by them as an alternative.

Indeed, there are a number of works dedicated to the creation of paper microlufidic chips with the application of a hydrophobic layer by laser printing method (Ghosh et al., 2019; Liu et al., 2023; Moulahoum, 2023; Ng & Hashimoto, 2020). It is interesting to note the researchers' tendency to cover almost the entire substrate surface with a hydrophobic layer, except for the supposed hydrophilic channel, without saving ink. As a result, because the toner is black in color, the resulting paper devices have easily distinguishable front and back sides, since the former is almost entirely black. This may make working with such μPADs somewhat easier in practice. However, an important conclusion clearly follows from this observation: conventional laser printing without additional heat treatment may generally not completely impregnate the paper substrate with the hydrophobic agent, even if it penetrates deeper than the black dye itself. The works of researchers confirm this (Ghosh et al., 2019; Ng & Hashimoto, 2020) and indicate that after printing an additional step of holding the product for 10–30 min at temperatures of 100–160 °C is necessary—then the softened polymer in the toner composition will soak the paper deeper.

Despite the suitability of commercially available toners for creating microfluidic chips, the hydrophobicity of their organic components is not optimal. Therefore, there are studies in which scientists prepare their own toners specifically for tasks related to the application of hydrophobic barriers in μPADs. Liu et al. (2023)

developed a so-called functional toner based on Fe_3O_4 modified with oleic acid and octadecylamine, clearly demonstrated the enhancement of hydrophobic properties in it compared to commercially available toner, and successfully printed μPAD for nitrite ion analysis using it.

In addition, laser printing can be used in a kind of lithographic process in the creation of paper-based devices with conductive metal electrodes. For example, in the paper by Harper et al. (2019), toner was used as a mask for aerosol application of metallic and carbon inks in negative lithography, and as a substrate on which these inks were also applied from aerosol in positive lithography.

24.3.7 Gravure Printing

Gravure printing is very similar to flexography and is therefore also a contact printing method. However, there are a few differences. In gravure printing, instead of anilox roller and plate cylinder, there is a single gravure cylinder that directly draws ink from a reservoir (Fig. 24.5). Whereas on the plate cylinder in flexography the ink remains on the elevated parts of the relief, on the gravure cylinder there are recessed cells inside which the ink must remain—the rest of the cylinder surface is removed by the doctor blade. Next, the ink cells come into contact with the substrate, which is also affected by the impression cylinder, and the ink is transferred to it (Cen et al., 2014; Chung, 2011; Grau et al., 2015, 2016; Kopola et al., 2009; Rivadeneyra et al., 2018; Sico et al., 2022). Typically, the resolution of this method is up to a few tens of μm (Grau et al., 2016). As in the case of flexography, the advantages of gravure printing include the high speed and productivity of the process and its greater simplicity compared to flexography, and the disadvantage is also the need to manufacture a unique gravure cylinder for each task.

Due to its advantages, this printing method is very promising for mass production of various devices. For example, its application in printing conductive silver and other electrodes on various substrates (Hrehorova et al., 2011) and deposition of pyroelectric structures (Sico et al., 2022) has been investigated. Interestingly, in publications that use paper as a substrate, gravure printing is also used mainly for depositing conductive structures rather than hydrophobic layers for microfluidic chips. For example, Zhu et al. (2014) have gravure printed an RFID (Radio Frequency Identification) antenna on transparent nanopaper. This work is generally interesting for the substrate used as much as for the printing method and the final device—the authors created a nanopaper stable under solution processing. However, consideration of this material is the subject of another chapter (see Chap. 11). Also, the thesis of Grau (2016) is devoted to the creation of field effect transistors on paper using gravure printing to apply a dielectric layer (polyvinylpyrrolidone).

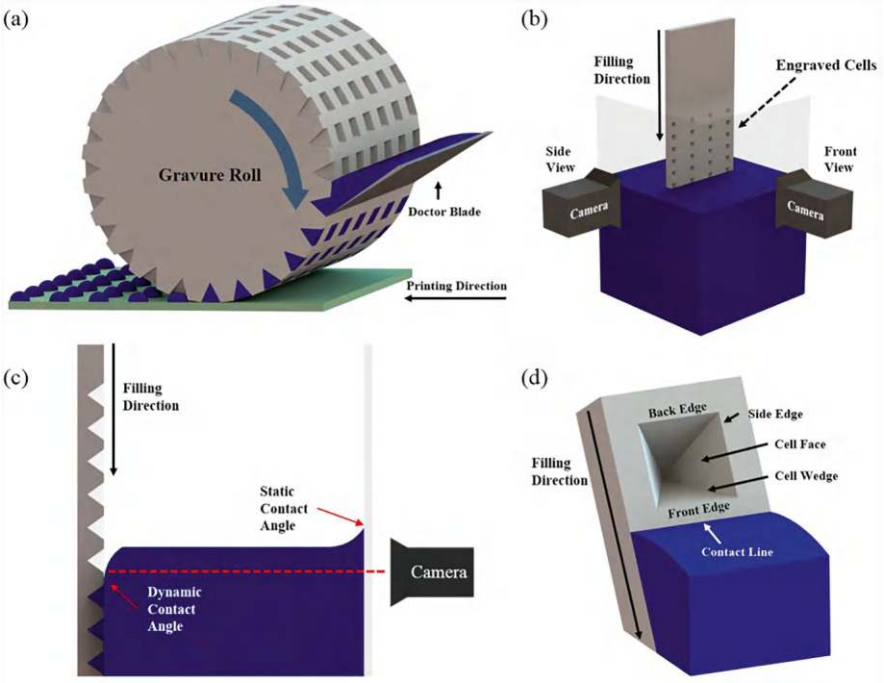

Fig. 24.5 (**a**) Typical gravure printing process. (**b**) Overview of filling experiment setup. (**c**) Cross-sectional schematic of filling experiment, showing deformation of the liquid−air interface and observational optical path. (**d**) Close-up of filling process with an engraved cell rolling toward the liquid−air interface and definition of the cell features. (Reproduced with permission from Cen et al. (2014). Copyright 2014: American Chemical Society)

24.3.8 Roll-to-Roll Printing

Roll-to-roll printing is a well-known way of producing electronic devices and components in large quantities, a convenient method for production. It would be somewhat more correct, however, to speak of the roll-to-roll process, since it is precisely a process of organizing production, the steps which may be various methods of coating, both printing and lithography, or writing, etc. The main feature of the roll-to-roll process is the movement of a sheet of flexible material, called web, between two rollers—one unwinds the roll of raw web, the other winds and sometimes cuts the web with already applied elements (Fig. 24.6). In the course of movement from one roller to another, the web is printed with the required structures by any technically compatible methods, and as a rule, the movement is not interrupted (Bollström et al., 2012; Du, 2020; Phung et al., 2021, 2023; Schwartz, 2006). Accordingly, roll-to-roll printing is a particular case of organizing a roll-to-roll process in which at least one printing method, among others, is used to create the final device. In web printing it is possible to use almost all the technologies discussed earlier in this

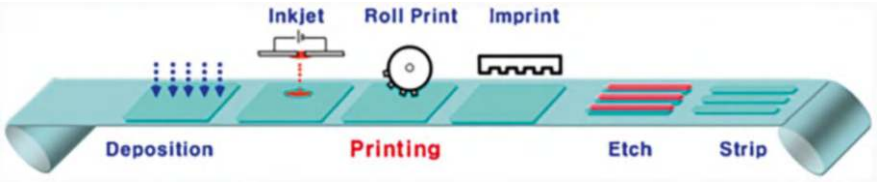

Fig. 24.6 Schematic of printing processes based on the R2R system. (Reproduced with permission from Chang et al. (2015). Copyright 2015: AIP Publishing LLC)

chapter: flexography, inkjet printing, wax printing, aerosol printing, screen printing, gravure printing, etc. (Bariya et al., 2018; Bollström et al., 2012; Kang et al., 2014; Kim et al., 2017, 2018; Lee et al., 2015; Palavesam et al., 2018; Park et al., 2012; Phung et al., 2021; Shan et al., 2020; Zhang et al., 2016). Some authors, however, note that contact printing methods (such as flexography and gravure printing) are better compatible with the web process, producing devices faster and with higher productivity than non-contact methods (Tiara et al., 2022). Roll-to-roll printing is an extremely promising way to organize industrial production of large batches of paper devices, precisely because of the high productivity of the process. However, it requires a preliminary study of the application of the individual printing methods to be used in production, although it is extremely useful in prototyping the final devices, to study the reproducibility of the application methods included in a particular roll-to-roll process. In addition, roll-to-roll printing is convenient for combining several film-forming steps with different methods within a common process, but this requires organizing the maximum accuracy of structure deposition by one of the involved printing methods with respect to the position of previously deposited structures. This seems particularly relevant when non-contact methods, such as inkjet printing, are involved in web printing, and there are studies specifically addressing the issue of maximizing the accuracy of layer deposition in such cases (Chang et al., 2015).

Roll-to-roll printing is used to produce both paper-based microfluidic devices and various electrochemical devices such as electrochromic devices. Thus, in Kim et al. (2018) the authors printed a batch of μPADs for glucose determination using gravure printing, and Liu et al. (2020) developed a roll-to-roll process combined with wax printing to produce up to 10 microfluidic chips per second. Bollström et al. (2012) demonstrated the possibility of producing a number of electronic devices on paper by means of web printing combining flexography, inkjet printing and gravure printing: hygroscopic field effect transistor (HIFET), a sensor for hydrogen sulfide in air, ion-selective electrodes, and an electrochromic device (based on PEDOT).

24.3.9 3D Printing

The term 3D printing can be applied to any of a whole family of printing methods that differ significantly in their operating principles, ink materials, and capabilities. This family includes fused deposition modeling, powder bed fusion, direct ink writing, stereolithography, vat photopolymerization, laminated object manufacturing, and others (Bas et al., 2024; Fu & Wentland, 2022; Ma et al., 2024; Ngo et al., 2018; Prabhakar et al., 2021; Saha et al., 2024). However, only one of the above methods is primarily used to obtain paper-based devices, so a description of the others is omitted in this chapter. For instance, in papers by Espinosa et al. (2022), Suvanasuthi et al. (2022), and Zargaryan et al. (2020) microfluidic chips have been fabricated using fused deposition modeling. Espinosa et al. (2022) demonstrated an electrochemical sensor for dopamine based on the printed chip, and Zargaryan et al. (2020) formed by the same method valves and reservoirs, additionally allowing to control fluids in hydrophilic channels limited by printed hydrophobic fiber Fused deposition modeling is based on the use of thermoplastic polymer filament as "ink." In a heated zone at the nozzle, the filament is heated to a semi-liquid state and then extruded onto the substrate or previously printed layers. The filament fuses with the previous layers and solidifies again at room temperature. This non-contact method is quite simple, fast, and cheap, but has a limited set of filaments that can be used for printing, and volumetric products obtained in this way do not have the best mechanical properties. However, thermoplastic polymers are suitable for creating microfluidic chips because they have hydrophobic properties, and in addition, wax can be used in their place as well (Espinosa et al., 2022). As a result, by applying only one layer on paper and additionally subjecting the product to heat treatment at about 150 °C for better adhesion, as well as impregnating the substrate with a hydrophobic agent, it is easy to obtain a finished chip. Thus, the method of 3D printing with fused deposition modeling, which is found in the literature for the creation of paper-based devices, currently appears to be close to wax printing and laser printing in terms of its capabilities.

24.3.10 Other Printing Techniques

The above printing technologies are the most common ones used in the creation and research of paper-based devices, so a separate subsection is devoted to each of them. However, in addition to them, there are many other printing techniques that can be used for these purposes in principle, but there is very limited research on them. Among such promising technologies is microplotter printing. This contact method is based on shaking a drop of ink from the capillary onto the substrate by vibrations transmitted from the piezoelectric generator, or by transferring the liquid onto the substrate as a result of touching it with a meniscus of ink at the tip of the capillary. Its advantages include not needing a special cartridge (which can be difficult to

change and is prone to clogging with solid phase inks), unlike inkjet printing, and the ability to use relatively viscous inks (up to 450 cP) (Simonenko et al., 2021, 2022). In the study by Simonenko et al. (2023) using this method, $NiCo_2O_4$ was coated on carbon paper using a functional ink, which was a dispersion of spinel nanopowder (with a solid phase weight percentage of 5%), and the promising potential of the resulting device as a supercapacitor component was shown.

The so-called "atom stamp printing" is also a curious technology (Guan & Sun, 2020). In some ways, it resembles flexography, but instead of a rotating cylinder, a stationary "atomic stamp" is used, on which depressions corresponding to the places where ink will not be applied. Guan and Sun (2020) propose to use as a stamp a special microporous structure, the volume of which can act as a reservoir for ink; unfortunately, the researchers did not report data on the nature of the material of this stamp. In addition to the simplicity of the method, it is noted that when using a laser for patterning on the atomic stamp, it is possible to achieve both the width of the hydrophobic barrier and the width of the hydrophilic channel ~300 μm when creating microfluidic chips, which was demonstrated experimentally by the authors. They further used the paper microfluidic chip as a component of a device for extraction of heavy ions from solutions.

24.4 Summary

Printing technologies, which are an example of additive technologies in a broad sense, are based on the application of films of ink (which can be solid or liquid) using equipment in which the specific geometry of the coating to be obtained is predetermined. This approach has been used for centuries to apply various coatings to paper, originally for the purpose of conveying information. Recently, however, printing techniques have begun to attract a great deal of research attention in obtaining functional paper-based devices. This is observed because of the advantages of printing technologies, such as the simplicity of most of them, the low cost of manufacturing products, the ease of scaling and automation, the ability to create the most complex structures in terms of geometry without the use of masks (e.g., when applying hydrophobic barriers for a microfluidic chip), the ability to use the widest range of functional inks, and the high compatibility of these technologies with virtually any type of paper (although filter, chromatography, and coated papers are the most commonly used). For instance, many types of printing are extremely convenient for applying hydrophobic barriers to paper, which makes it possible to create microfluidic chips of different architectures for μPADs. There are also a number of works in which printing technologies are used to obtain electrochromic devices, gas sensors, transistors, electrodes for supercapacitors, etc. The most diverse range of printing methods is used depending on the specific task—inkjet printing, screen printing, wax printing (although this particular method is somewhat backward due to the disappearance of the corresponding printers from the market), laser printing, flexography, gravure printing, etc. The advantages of printing technologies are

premises for a further increase in the number of studies devoted to the creation of paper-based devices using them and the implementation of their findings in the mass production of paper-based devices using printing methods.

Acknowledgments Ph. Yu. thanks RSF for funding, since the study was funded by Russian Science Foundation grant №23-73-01249, https://rscf.ru/project/23-73-01249/. G.K. is grateful to the Moldova State University (research program no. 011208) for supporting his research.

References

Aga, R. S., Lombardi, J. P., Bartsch, C. M., & Heckman, E. M. (2014). Performance of a printed photodetector on a paper substrate. *IEEE Photonics Technology Letters, 26*, 305–308. https://doi.org/10.1109/LPT.2013.2292830

Agarwala, S., Goh, G. L., & Yeong, W. Y. (2017). Optimizing aerosol jet printing process of silver ink for printed electronics. *IOP Conference Series: Materials Science and Engineering, 191*, 012027. https://doi.org/10.1088/1757-899X/191/1/012027

Al-Amri, A. M. (2023). Recent progress in printed photonic devices: A brief review of materials, devices, and applications. *Polymers (Basel), 15*, 3234. https://doi.org/10.3390/polym15153234

Altundemir, S., Uguz, A. K., & Ulgen, K. (2017). A review on wax printed microfluidic paper-based devices for international health. *Biomicrofluidics, 11*, 041501. https://doi.org/10.1063/1.4991504

Ameloot, R., Cobechiya, E., Uji-i, H., Martens, J. A., Hofkens, J., Alaerts, L., et al. (2010). Direct patterning of oriented metal-organic framework crystals via control over crystallization kinetics in clear precursor solutions. *Advanced Materials, 22*, 2685–2688. https://doi.org/10.1002/adma.200903867

Anushka, Bandopadhyay, A., & Das, P. K. (2023). Paper based microfluidic devices: A review of fabrication techniques and applications. *The European Physical Journal Special Topics, 232*, 781–815. https://doi.org/10.1140/epjs/s11734-022-00727-y

Bariya, M., Shahpar, Z., Park, H., Sun, J., Jung, Y., Gao, W., et al. (2018). Roll-to-roll gravure printed electrochemical sensors for wearable and medical devices. *ACS Nano, 12*, 6978–6987. https://doi.org/10.1021/acsnano.8b02505

Bas, J., Dutta, T., Llamas Garro, I., Velázquez-González, J. S., Dubey, R., & Mishra, S. K. (2024). Embedded sensors with 3D printing technology: Review. *Sensors, 24*, 1955. https://doi.org/10.3390/s24061955

Batet, D., Vilaseca, F., Ramon, E., Esquivel, J. P., & Gabriel, G. (2023). Experimental overview for green printed electronics: Inks, substrates, and printing techniques. *Flexible and Printed Electronics, 8*, 024001. https://doi.org/10.1088/2058-8585/acd8cc

Bollström, R., Tobjörk, D., Dolietis, P., Remonen, T., Wikman, C., Viljanen, S., & Sarfraz, J. (2012). Roll-to-roll printed electronics on paper. In *Proceedings of paper conference 2012*, 22–25 April, New Orleans, USA.

Borah, M., Maheswari, D., & Dutta, H. S. (2022). Fabrication of microtiter plate on paper using 96-well plates for wax stamping. *Microfluidics and Nanofluidics, 26*, 99. https://doi.org/10.1007/s10404-022-02606-3

Borghetti, M., Cantù, E., Ponzoni, A., Sardini, E., & Serpelloni, M. (2022). Aerosol jet printed and photonic cured paper-based ammonia sensor for food smart packaging. *IEEE Transactions on Instrumentation and Measurement, 71*, 9504810. https://doi.org/10.1109/TIM.2022.3161695

Brooke, R., Edberg, J., Petsagkourakis, I., Freitag, K., Mulla, M. Y., Nilsson, M., et al. (2023). Paper electronics utilizing screen printing and vapor phase polymerization. *Advanced Sustainable Systems, 7*, 2300058. https://doi.org/10.1002/adsu.202300058

Carrilho, E., Martinez, A. W., & Whitesides, G. M. (2009). Understanding wax printing: A simple micropatterning process for paper-based microfluidics. *Analytical Chemistry, 81*, 7091–7095. https://doi.org/10.1021/ac901071p

Ćatić, N., Wells, L., Al Nahas, K., Smith, M., Jing, Q., Keyser, U. F., et al. (2020). Aerosol-jet printing facilitates the rapid prototyping of microfluidic devices with versatile geometries and precise channel functionalization. *Applied Materials Today, 19*, 100618. https://doi.org/10.1016/j.apmt.2020.100618

Cen, J., Kitsomboonloha, R., & Subramanian, V. (2014). Cell filling in gravure printing for printed electronics. *Langmuir, 30*, 13716–13726. https://doi.org/10.1021/la503180a

Chang, J., Lee, S., Lee, K. B., Lee, S., Cho, Y. T., Seo, J., et al. (2015). Overlay accuracy on a flexible web with a roll printing process based on a roll-to-roll system. *The Review of Scientific Instruments, 86*, 055108. https://doi.org/10.1063/1.4921495

Chen, Y. D., Nagarajan, V., Rosen, D. W., Yu, W., & Huang, S. Y. (2020). Aerosol jet printing on paper substrate with conductive silver nano material. *Journal of Manufacturing Processes, 58*, 55–66. https://doi.org/10.1016/j.jmapro.2020.07.064

Chung, D. (2011). *Gravure printed and solution-processed polymer semiconductor devices*. PhD Thesis, Imperial College London, UK.

Cooper, C., & Hughes, B. (2020). Aerosol jet printing of electronics: An enabling technology for wearable devices. In *Proceedings of 2020 Pan Pacific microelectronics symposium*, 10–13 February 2020, HI, USA. https://doi.org/10.23919/PanPacific48324.2020.9059444

Cruz, S. M. F., Rocha, L. A., & Viana, J. C. (2018). Printing technologies on flexible substrates for printed electronics. In S. Rackauskas (Ed.), *Flexible electronics* (pp. 46–70). IntechOpen. https://doi.org/10.5772/intechopen.76161

Dahiya, A. S., Shakthivel, D., Kumaresan, Y., Zumeit, A., Christou, A., & Dahiya, R. (2020). High-performance printed electronics based on inorganic semiconducting nano to chip scale structures. *Nano Convergence, 7*, 33. https://doi.org/10.1186/s40580-020-00243-6

Das, S., Gagandeep, & Bhatia, R. (2022). Paper-based microfluidic devices: Fabrication, detection, and significant applications in various fields. *Reviews in Analytical Chemistry, 41*, 112–136. https://doi.org/10.1515/revac-2022-0037

Du, X. (2020). Roll-to-roll printing of wearable sensors and devices for personalized health monitoring. *American Journal of Biomedical Science & Research, 7*, 495–498. https://doi.org/10.34297/ajbsr.2020.07.001208

Espinosa, A., Diaz, J., Vazquez, E., Acosta, L., Santiago, A., & Cunci, L. (2022). Fabrication of paper-based microfluidic devices using a 3D printer and a commercially-available wax filament. *Talanta Open, 6*, 100142. https://doi.org/10.1016/j.talo.2022.100142

Fu, E., & Wentland, L. (2022). A survey of 3D printing technology applied to paper microfluidics. *Lab on a Chip, 22*, 9–25. https://doi.org/10.1039/D1LC00768H

Ghosh, R., Gopalakrishnan, S., Savitha, R., Renganathan, T., & Pushpavanam, S. (2019). Fabrication of laser printed microfluidic paper-based analytical devices (LP-μPADs) for point-of-care applications. *Scientific Reports, 9*, 7896. https://doi.org/10.1038/s41598-019-44455-1

Godard, N., Glinšek, S., Matavž, A., Bobnar, V., & Defay, E. (2019). Direct patterning of piezoelectric thin films by inkjet printing. *Advanced Materials Technologies, 4*, 1800168. https://doi.org/10.1002/admt.201800168

Grau, G. (2016). *Gravure-printed electronics: Devices, technology development and design*. PhD Thesis, University of California, Berkley, USA.

Grau, G., Kitsomboonloha, R., & Subramanian, V. (2015). Fabrication of a high-resolution roll for gravure printing of 2 μm features. *SPIE Proceedings, 9568*, 95680M. https://doi.org/10.1117/12.2187280

Grau, G., Cen, J., Kang, H., Kitsomboonloha, R., Scheideler, W. J., & Subramanian, V. (2016). Gravure-printed electronics: Recent progress in tooling development, understanding of printing physics, and realization of printed devices. *Flexible and Printed Electronics, 1*, 023002. https://doi.org/10.1088/2058-8585/1/2/023002

Guan, Y., & Sun, B. (2020). Detection and extraction of heavy metal ions using paper-based analytical devices fabricated via atom stamp printing. *Microsystems & Nanoengineering, 6*, 14. https://doi.org/10.1038/s41378-019-0123-9

Han, Y., Cui, Y., Liu, X., & Wang, Y. (2023). A review of manufacturing methods for flexible devices and energy storage devices. *Biosensors (Basel), 13*, 896. https://doi.org/10.3390/bios13090896

Harper, A. F., Diemer, P. J., & Jurchescu, O. D. (2019). Contact patterning by laser printing for flexible electronics on paper. *npj Flexible Electronics, 3*, 11. https://doi.org/10.1038/s41528-019-0055-3

Hoeng, F., Denneulin, A., & Bras, J. (2016). Use of nanocellulose in printed electronics: A review. *Nanoscale, 8*, 13131–13154. https://doi.org/10.1039/c6nr03054h

Hong, M., Sun, S., Lyu, W., Li, M., Liu, W., Shi, X. L., & Chen, Z. G. (2023). Advances in printing techniques for thermoelectric materials and devices. *Soft Science, 3*, 29. https://doi.org/10.20517/ss.2023.20

Hrehorova, E., Rebros, M., Pekarovicova, A., Bazuin, B., Ranganathan, A., Garner, S., Merz, G., Tosch, J., & Boudreau, R. (2011). Gravure printing of conductive inks on glass substrates for applications in printed electronics. *IEEE/OSA Journal of Display Technology, 7*, 318–324. https://doi.org/10.1109/JDT.2010.2065214

Hu, G., Kang, J., Ng, L. W. T., Zhu, X., Howe, R. C. T., Jones, C. G., Hersam, M. C., & Hasan, T. (2018). Functional inks and printing of two-dimensional materials. *Chemical Society Reviews, 47*, 3265–3300. https://doi.org/10.1039/C8CS00084K

Jansson, E., Lyytikäinen, J., Tanninen, P., Eiroma, K., Leminen, V., Immonen, K., & Hakola, L. (2022). Suitability of paper-based substrates for printed electronics. *Materials, 15*, 957. https://doi.org/10.3390/ma15030957

Kang, H., Park, H., Park, Y., Jung, M., Kim, B. C., Wallace, G., & Cho, G. (2014). Fully roll-to-roll gravure printable wireless (13.56 MHz) sensor-signage tags for smart packaging. *Scientific Reports, 4*, 5387. https://doi.org/10.1038/srep05387

Khan, S., Lorenzelli, L., & Dahiya, R. S. (2015). Technologies for printing sensors and electronics over large flexible substrates: A review. *IEEE Sensors Journal, 15*, 3164–3185. https://doi.org/10.1109/JSEN.2014.2375203

Kim, J., Hassinen, T., Lee, W. H., & Ko, S. (2017). Fully solution-processed organic thin-film transistors by consecutive roll-to-roll gravure printing. *Organic Electronics, 42*, 361–366. https://doi.org/10.1016/j.orgel.2016.12.061

Kim, K., Kim, J., Kim, B., & Ko, S. (2018). Fabrication of microfluidic structure based biosensor using roll-to-roll gravure printing. *International Journal of Precision Engineering and Manufacturing-Green Technology, 5*, 369–374. https://doi.org/10.1007/s40684-018-0039-0

Kopola, P., Tuomikoski, M., Suhonen, R., & Maaninen, A. (2009). Gravure printed organic light emitting diodes for lighting applications. *Thin Solid Films, 517*, 5757–5762. https://doi.org/10.1016/j.tsf.2009.03.209

Kwon, K. S., Rahman, M. K., Phung, T. H., Hoath, S. D., Jeong, S., & Kim, J. S. (2021). Review of digital printing technologies for electronic materials. *Flexible and Printed Electronics, 6*, 015001. https://doi.org/10.1088/2058-8585/abd29e

Lamas-Ardisana, P. J., Casuso, P., Fernandez-Gauna, I., Martínez-Paredes, G., Jubete, E., Añorga, L., Cabañero, G., & Grande, H. J. (2017). Disposable electrochemical paper-based devices fully fabricated by screen-printing technique. *Electrochemistry Communications, 75*, 25–28. https://doi.org/10.1016/j.elecom.2016.11.015

Layani, M., Darmawan, P., Foo, W. L., Liu, L., Kamyshny, A., Mandler, D., Magdassi, S., & Lee, P. S. (2014). Nanostructured electrochromic films by inkjet printing on large area and flexible transparent silver electrodes. *Nanoscale, 6*, 4572–4576. https://doi.org/10.1039/c3nr06890k

Le Borgne, B., Chung, B.-Y., Tas, M. O., King, S. G., Harnois, M., & Sporea, R. A. (2019). Eco-friendly materials for daily-life inexpensive printed passive devices: Towards "do-it-yourself" electronics. *Electronics (Basel), 8*, 699. https://doi.org/10.3390/electronics8060699

Le, N. N., Phan, H. C. T., Tran, H. K., Dang, D. M. T., & Dang, C. M. (2020). Fabrication of paper-based microfluidic channels by electrohydrodynamic inkjet printing technology for analytical biochemistry applications. *International Journal of Nanotechnology, 17*, 673–688. https://doi.org/10.1504/IJNT.2020.111333

Lee, W., Koo, H., Sun, J., Noh, J., Kwon, K. S., Yeom, C., et al. (2015). A fully roll-to-roll gravure-printed carbon nanotube-based active matrix for multi-touch sensors. *Scientific Reports, 5*, 17707. https://doi.org/10.1038/srep17707

Li, Q., Zhang, J., Li, Q., Li, G., Tian, X., Luo, Z., Qiao, F., Wu, X., & Zhang, J. (2019). Review of printed electrodes for flexible devices. *Frontiers in Materials, 5*, 77. https://doi.org/10.3389/fmats.2018.00077

Liang, T., Zou, X., & Mazzeo, A. D. (2016). A flexible future for paper-based electronics. *Proceedings of SPIE, 9836*, 98361D. https://doi.org/10.1117/12.2224391

Liang, Q., Zhao, M., Chiu, G. T. C., & Allebach, J. P. (2021). Design and fabrication of microfluidics paper-based devices for contaminant detection using a wax printer. In *Proceedings of IS and T international symposium on electronic imaging science and technology* (pp. 339-1–339-8). https://doi.org/10.2352/ISSN.2470-1173.2021.16.COLOR-339

Lim, H., Jafry, A. T., & Lee, J. (2019). Fabrication, flow control, and applications of microfluidic paper-based analytical devices. *Molecules, 24*, 2869. https://doi.org/10.3390/molecules24162869

Lin, D., Li, B., Fu, L., Qi, J., Xia, C., Zhang, Y., et al. (2022). A novel polymer-based nitrocellulose platform for implementing a multiplexed microfluidic paper-based enzyme-linked immunosorbent assay. *Microsystems & Nanoengineering, 8*, 53. https://doi.org/10.1038/s41378-022-00385-z

Liu, H., Qing, H., Li, Z., Han, Y. L., Lin, M., Yang, H., et al. (2017). Paper: A promising material for human-friendly functional wearable electronics. *Materials Science and Engineering: R: Reports, 112*, 1–22. https://doi.org/10.1016/j.mser.2017.01.001

Liu, J., Kong, X., Wang, H., Zhang, Y., & Fan, Y. (2020). Roll-to-roll wax transfer for rapid and batch fabrication of paper-based microfluidics. *Microfluidics and Nanofluidics, 24*, 6. https://doi.org/10.1007/s10404-019-2310-2

Liu, Y., Liu, X., Chen, J., Zhang, Z., & Feng, L. (2023). Functional toner for office laser printer and its application for printing of paper-based superwettable patterns and devices. *Scientific Reports, 13*, 12592. https://doi.org/10.1038/s41598-023-39729-8

Lombardi, J., Poliks, M. D., Zhao, W., Yan, S., Kang, N., Li, J., et al. (2017). Nanoparticle based printed sensors on paper for detecting chemical species. In *Proceedings of electronic components and technology conference,* 30 May–2 June 2017, Orlando, FL, USA, pp. 764–771. https://doi.org/10.1109/ECTC.2017.320

Ma, T., Zhang, Y., Ruan, K., Guo, H., He, M., Shi, X., et al. (2024). Advances in 3D printing for polymer composites: A review. *InfoMat, 6*, e12568. https://doi.org/10.1002/inf2.12568

Malik, S., Singh, J., Saini, K., Chaudhary, V., Umar, A., Ibrahim, A. A., et al. (2024). Paper-based sensors: Affordable, versatile, and emerging analyte detection platforms. *Analytical Methods, 16*, 2777–2809. https://doi.org/10.1039/d3ay02258g

Moulahoum, H. (2023). Dual chromatic laser-printed microfluidic paper-based analytical device (μPAD) for the detection of Atrazine in water. *ACS Omega, 8*, 41194–41203. https://doi.org/10.1021/acsomega.3c04387

Mustafa, F., Finny, A. S., Kirk, K. A., & Andreescu, S. (2020). Printed paper-based (bio)sensors: Design, fabrication and applications. In A. Merkoçi (Ed.), *Comprehensive analytical chemistry* (Vol. 89, pp. 63–89). Elsevier.

Nandy, S., Goswami, S., Marques, A., Gaspar, D., Grey, P., Cunha, I., Nunes, D., Pimentel, A., Igreja, R., Barquinha, P., Pereira, L., Fortunato, E., & Martins, R. (2021). Cellulose: A contribution for the zero e-waste challenge. *Advanced Materials Technologies, 6*, 2000994. https://doi.org/10.1002/admt.202000994

Ng, J. S., & Hashimoto, M. (2020). Fabrication of paper microfluidic devices using a toner laser printer. *RSC Advances, 10*, 29797–29807. https://doi.org/10.1039/d0ra04301j

Ngo, T. D., Kashani, A., Imbalzano, G., Nguyen, K. T. Q., & Hui, D. (2018). Additive manufacturing (3D printing): A review of materials, methods, applications and challenges. *Composites Part B: Engineering, 143*, 172–196. https://doi.org/10.1016/j.compositesb.2018.02.012

Olkkonen, J., Lehtinen, K., & Erho, T. (2010). Flexographically printed fluidic structures in paper. *Analytical Chemistry, 82*, 10246–10250. https://doi.org/10.1021/ac1027066

Olsson, R. (2007). *Some aspects on flexographic ink-paper and paperboard coating interaction*. PhD Thesis, Karlstad University, Sweden.

Palavesam, N., Marin, S., Hemmetzberger, D., Landesberger, C., Bock, K., & Kutter, C. (2018). Roll-to-roll processing of film substrates for hybrid integrated flexible electronics. *Flexible and Printed Electronics, 3*, 014002. https://doi.org/10.1088/2058-8585/aaaa04

Park, H., Kang, H., Lee, Y., Park, Y., Noh, J., & Cho, G. (2012). Fully roll-to-roll gravure printed rectenna on plastic foils for wireless power transmission at 13.56MHz. *Nanotechnology, 23*, 344006. https://doi.org/10.1088/0957-4484/23/34/344006

Phung, T. H., Gafurov, A. N., Kim, I., Kim, S. Y., Kim, K. M., & Lee, T. M. (2021). IoT device fabrication using roll-to-roll printing process. *Scientific Reports, 11*, 19982. https://doi.org/10.1038/s41598-021-99436-0

Phung, T. H., Gafurov, A. N., Kim, I., Kim, S. Y., Kim, K. M., & Lee, T. M. (2023). Hybrid device fabrication using roll-to-roll printing for personal environmental monitoring. *Polymers (Basel), 15*, 2687. https://doi.org/10.3390/polym15122687

Potter, J., Brisk, P., & Grover, W. H. (2019). Using printer ink color to control the behavior of paper microfluidics. *Lab on a Chip, 19*, 2000–2008. https://doi.org/10.1039/C9LC00083F

Prabhakar, P., Sen, R. K., Dwivedi, N., Khan, R., Solanki, P. R., Srivastava, A. K., & Dhand, C. (2021). 3D-printed microfluidics and potential biomedical applications. *Frontiers in Nanotechnology, 3*, 609355. https://doi.org/10.3389/fnano.2021.609355

Prabhu, A., Giri Nandagopal, M. S., Peralam Yegneswaran, P., Singhal, H. R., & Mani, N. K. (2020). Inkjet printing of paraffin on paper allows low-cost point-of-care diagnostics for pathogenic fungi. *Cellulose, 27*, 7691–7701. https://doi.org/10.1007/s10570-020-03314-3

Raucci, A., Cimmino, W., Grosso, S. P., Normanno, N., Giordano, A., & Cinti, S. (2024). Paper-based screen-printed electrode to detect miRNA-652 associated to triple-negative breast cancer. *Electrochimica Acta, 487*, 144205. https://doi.org/10.1016/j.electacta.2024.144205

Rivadeneyra, A., Loghin, F. C., & Falco, A. (2018). Technological integration in printed electronics. In S. Rackauskas (Ed.), *Flexible electronics*. IntechOpen. https://doi.org/10.5772/intechopen.76520

Ruiz, R. A., Gonzalez, J. L., Vazquez-Alvarado, M., Martinez, N. W., & Martinez, A. W. (2022). Beyond wax printing: Fabrication of paper-based microfluidic devices using a thermal transfer printer. *Analytical Chemistry, 94*, 8833–8837. https://doi.org/10.1021/acs.analchem.2c01534

Saha, R., Sarkar, M., Choudhury, S. S., Kumar, H., Bhatt, G., & Bhattacharya, S. (2024). Evolution of 3d printing technology in fabrication of microfluidic devices and biological applications: A comprehensive review. *Journal of Micromanufacturing, 7*, 110–140. https://doi.org/10.1177/25165984241237357

Schwartz, E. (2006). Roll to roll processing for flexible electronics. MSE 542: Flexible Electronic, Cornell University, USA, pp. 1–24.

Serpelloni, M., Cantù, E., Borghetti, M., & Sardini, E. (2020). Printed smart devices on cellulose-based materials by means of aerosol-jet printing and photonic curing. *Sensors (Switzerland), 20*, 841. https://doi.org/10.3390/s20030841

Shan, X. C., Sunappan, V., Salam, B., & Lok, B. K. (2020). Roll-to-roll gravure printing of electric heaters on polymeric substrates. In *Proceedings of IEEE 22nd Electronics Packaging Technology Conference* (EPTC), 2–4 December 2020, Singapore, pp. 210–212. https://doi.org/10.1109/EPTC50525.2020.9315005.

Shen, Y., Sun, Z., Zhao, S., Chen, F., Shi, P., Zhao, N., Sun, K., Ye, C., Lin, C., & Fu, L. (2024). Screen-printed electrodes as low-cost sensors for breast cancer biomarker detection. *Sensors, 24*, 5679. https://doi.org/10.3390/s24175679

Sico, G., Montanino, M., Loffredo, F., Borriello, C., & Miscioscia, R. (2022). Gravure printing for PVDF thin-film pyroelectric device manufacture. *Coatings, 12*, 1020. https://doi.org/10.3390/coatings12071020

Silva-Neto, H. A., Jaime, J. C., Rocha, D. S., Sgobbi, L. F., & Coltro, W. K. T. (2024). Fabrication of paper-based analytical devices using stencil-printed glass varnish barriers for colorimetric detection of salivary α-amylase. *Analytica Chimica Acta, 1297*, 342336. https://doi.org/10.1016/j.aca.2024.342336

Simonenko, T. L., Simonenko, N. P., Gorobtsov, P. Y., Vlasov, I. S., Solovey, V. R., Shelaev, A. V., et al. (2021). Microplotter printing of planar solid electrolytes in the CeO_2–Y_2O_3 system. *Journal of Colloid and Interface Science, 588*, 209–220. https://doi.org/10.1016/j.jcis.2020.12.052

Simonenko, N. P., Fisenko, N. A., Fedorov, F. S., Simonenko, T. L., Mokrushin, A. S., Simonenko, E. P., Korotcenkov, G., Sysoev, V. V., Sevastyanov, V. G., & Kuznetsov, N. T. (2022). Printing technologies as an emerging approach in gas sensors: Survey of literature. *Sensors, 22*, 3473. https://doi.org/10.3390/s22093473

Simonenko, T. L., Simonenko, N. P., Gorobtsov, P. Y., Simonenko, E. P., & Kuznetsov, N. T. (2023). Microplotter printing of a miniature flexible supercapacitor electrode based on hierarchically organized $NiCo_2O_4$ nanostructures. *Materials, 16*, 4202. https://doi.org/10.3390/ma16124202

Soman, S. S., Samad, S. A., Venugopalan, P., Kumawat, N., & Kumar, S. (2024). Microfluidic paper analytic device (μPAD) technology for food safety applications. *Biomicrofluidics, 18*, 031501. https://doi.org/10.1063/5.0192295

Suvanasuthi, R., Chimnaronk, S., & Promptmas, C. (2022). 3D printed hydrophobic barriers in a paper-based biosensor for point-of-care detection of dengue virus serotypes. *Talanta, 237*, 122962. https://doi.org/10.1016/j.talanta.2021.122962

Tiara, A. M., Moon, H., Cho, G., & Lee, J. (2022). Fully roll-to-roll gravure printed electronics: Challenges and the way to integrating logic gates. *Japanese Journal of Applied Physics, 61*, SE0802. https://doi.org/10.35848/1347-4065/ac575e

Tortorich, R. P., Shamkhalichenar, H., & Choi, J. W. (2018). Inkjet-printed and paper-based electrochemical sensors. *Applied Sciences (Switzerland), 8*, 288. https://doi.org/10.3390/app8020288

Tseng, H. Y., Lizama, J. H., Shen, Y. W., & Chen, C. J. (2021). The pursuit of further miniaturization of screen printed micro paper-based analytical devices utilizing controlled penetration towards optimized channel patterning. *Scientific Reports, 11*, 21496. https://doi.org/10.1038/s41598-021-01048-1

Wilkinson, N. J., Smith, M. A. A., Kay, R. W., & Harris, R. A. (2019). A review of aerosol jet printing—A non-traditional hybrid process for micro-manufacturing. *The International Journal of Advanced Manufacturing Technology, 105*, 4599–4619. https://doi.org/10.1007/s00170-019-03438-2

Xi, J., Yang, H., Li, X., Wei, R., Zhang, T., Dong, L., et al. (2024). Recent advances in tactile sensory systems: Mechanisms, fabrication, and applications. *Nanomaterials, 14*, 465. https://doi.org/10.3390/nano14050465

Yamada, K., Henares, T. G., Suzuki, K., & Citterio, D. (2015). Paper-based inkjet-printed microfluidic analytical devices. *Angewandte Chemie International Edition, 54*, 5294–5310. https://doi.org/10.1002/anie.201411508

Yan, K., Li, J., Pan, L., & Shi, Y. (2020). Inkjet printing for flexible and wearable electronics. *APL Materials, 8*, 120705. https://doi.org/10.1063/5.0031669

Yu, X., Shou, W., Mahajan, B. K., Huang, X., & Pan, H. (2018). Materials, processes, and facile manufacturing for bioresorbable electronics: A review. *Advanced Materials, 30*, 1707624. https://doi.org/10.1002/adma.201707624

Zargaryan, A., Farhoudi, N., Haworth, G., Ashby, J. F., & Au, S. H. (2020). Hybrid 3D printed-paper microfluidics. *Scientific Reports, 10*, 18379. https://doi.org/10.1038/s41598-020-75489-5

Zea, M. (2021). *Inkjet printing technology is driving the innovation of sensors for point-of-care devices*. PhD Thesis, Universitat Autònoma de Barcelona, Barcelona, Spain.

Zhang, Z., Qiu, J., & Wang, S. (2016). Roll-to-roll printing of flexible thin-film organic thermoelectric devices. *Manufacturing Letters, 8*, 6–10. https://doi.org/10.1016/j.mfglet.2016.04.002

Zhang, Y., Zhang, L., Cui, K., Ge, S., Cheng, X., Yan, M., Yu, J., & Liu, H. (2018). Flexible electronics based on micro/nanostructured paper. *Advanced Materials, 30*, 1801588. https://doi.org/10.1002/adma.201801588

Zhao, N., Chiesa, M., Sirringhaus, H., Li, Y., Wu, Y., & Ong, B. (2007). Self-aligned inkjet printing of highly conducting gold electrodes with submicron resolution. *Journal of Applied Physics, 101*, 064513. https://doi.org/10.1063/1.2496249

Zheng, Y., He, Z., Gao, Y., & Liu, J. (2013). Direct desktop printed-circuits-on-paper flexible electronics. *Scientific Reports, 3*, 1786. https://doi.org/10.1038/srep01786

Zhu, H., Narakathu, B. B., Fang, Z., Tausif Aijazi, A., Joyce, M., Atashbar, M., & Hu, L. (2014). A gravure printed antenna on shape-stable transparent nanopaper. *Nanoscale, 6*, 9110–9115. https://doi.org/10.1039/c4nr02036g

Zhuang, J. L., Ar, D., Yu, X. J., Liu, J. X., & Terfort, A. (2013). Patterned deposition of metal-organic frameworks onto plastic, paper, and textile substrates by inkjet printing of a precursor solution. *Advanced Materials, 25*, 4631–4635. https://doi.org/10.1002/adma.201301626

Chapter 25
Deposition Technologies for Paper-Based Sensors and Devices

Shriswaroop Sathyanarayanan, Tamilselvi Gopal, Sathish Marimuthu, and Andrews Nirmala Grace

25.1 Introduction

Deposition technologies play a crucial role in controlling material properties and device architecture. Various deposition technologies, including vapor deposition, electrodeposition, vacuum deposition, and spray coating, have been employed in paper-based device fabrication (Yao et al., 2017). An overall schematic representation of different coating techniques for paper-based substrates is shown in Fig. 25.1. Each deposition technology has its advantages and limitations, and the choice of technology depends on the specific application and device requirements. The unique benefits of paper as substrate, such as flexibility, biodegradability, and low cost, make it an attractive material for device fabrication (Sharifi et al., 2015). However, the fabrication of paper-based devices requires precise control over material properties and device architecture.

This chapter provides a comprehensive overview of deposition technologies employed in paper-based sensor and device fabrication. The principles, advantages, and limitations of various deposition technologies are discussed, along with material considerations and applications. Recent advancements in nanotechnology and materials science have enabled the development of high-performance paper-based devices. It gives way for various applications, including biosensing, energy storage, and flexible electronics. Deposition technologies play a crucial role in controlling material properties and device architecture.

S. Sathyanarayanan · T. Gopal · S. Marimuthu · A. N. Grace (✉)
Centre for Nanotechnology Research, Vellore Institute of Technology, Vellore, Tamil Nadu, India

G. Korotcenkov (ed.), *The Handbook of Paper-Based Sensors and Devices*,
https://doi.org/10.1007/978-3-031-91080-7_25

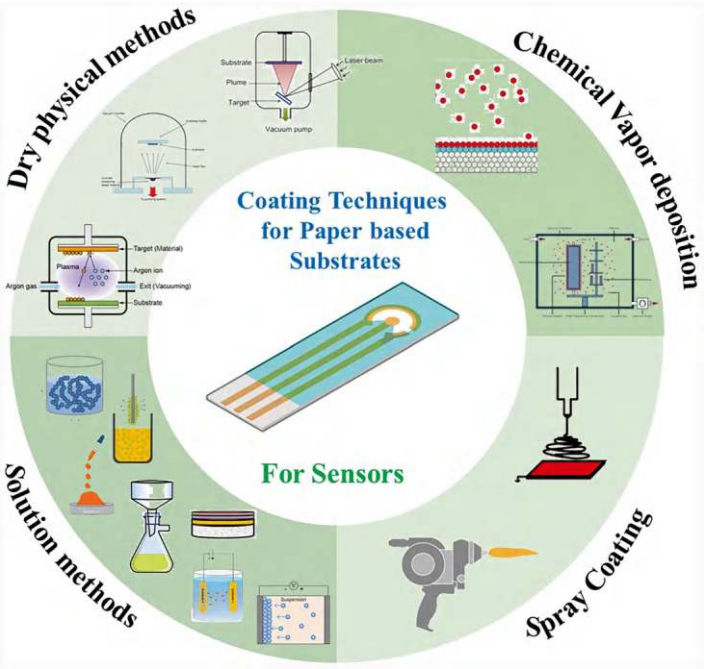

Fig. 25.1 Various deposition techniques for paper-based substrates

25.2 Dry Physical Methods

Dry physical methods of deposition for paper-based substrates are a clean approach of sensor fabrication. It facilitates large-scale production, offering high control over material deposition. It is also compatible with a variety of nanomaterials and substrate types. Avoiding many harmful solvents for deposition, dry physical methods can be eco-friendly alternatives to conventional deposition methods. Some dry deposition methods suitable for paper substrates are discussed below.

25.2.1 Sputtering for Paper-Based Applications

Sputtering involves ejecting atoms from a target material by bombarding it with energetic ions, typically Argon, within a vacuum chamber. These ejected atoms then travel and deposit onto a substrate, forming a thin film. It is a viable method for fabricating thin films on paper substrates for sensors and electronic devices. This deposition method is commonly used to create aluminized or conductive paper. Aluminum is used as the target material, and DC magnetron sputtering film is employed to deposit a thin aluminum film coating onto the paper substrate (Zhou

et al., 2023). This creates a barrier layer that can improve the paper's resistance to moisture, oxygen, and light. By carefully controlling the sputtering parameters and selecting appropriate paper substrates, high-quality thin films can be successfully deposited onto paper for a variety of applications.

Substrate selection and preparation play a crucial role in the deposition and its suitability for various applications. Kaidatzis et al. (2017) used standard printing paper and glossy photo paper for the sputtering of gold and silver while Zhou et al. (2023) used specialty high-strength paper. Several properties of the paper including its weight, pH, tensile strength, moisture content, porosity, and deformation temperature influence the quality of the deposition.

For paper-based substrates DC magnetron mode of sputtering is often preferred offering uniform deposition at lower temperatures, crucial for avoiding paper damage. It uses an ultra-high vacuum environment, needed to create plasma by applying a DC voltage. Sputtering ions are generated by the glow discharge, with the help of gas flow, typically Argon, which then bombards the target material, ejecting atoms that deposit onto the paper substrate. The discharge ionizes the Ar gas which helps in separating the atoms from the target material. Sputtering parameters such as power, time, and pressure need to be optimized to achieve the desired film thickness, uniformity, and adhesion to the paper substrate. Sputtering offers a highly precise control over the thickness of the coating. Kaidatzis et al. (2017) have shown a deposition rate of 0.48 nm/s for Au and Ag on the paper substrate. Complex sensor designs on flexible paper substrates can be achieved through sputtering as it doesn't restrict the usage of masks for easy patterning and precise control over thickness. Nanocomposites can also be used as target materials depending on the application making it an ideal deposition technique for paper-based substrates (Diop et al., 2015).

Post-deposition treatments help optimize the performance and functionality of the sputtered films on paper-based sensors and devices. Annealing, encapsulation, surface functionalization, and integrating with other components are few of the various treatment options that can be applied based on the application the sensor is designed for. By adapting sputtering technique, functional thin films on paper substrates for low-cost, flexible sensors and electronic devices can be fabricated.

Although sputtering offers a clean uniform coating, it has a few drawbacks. A prolonged deposition period can cause heat damage deteriorating the paper's structural integrity. Plasma has a direct effect on the fibers of paper, altering its properties or degradation. On rough surfaces, uniform film thickness can be challenging to achieve and may sometimes lead to shadowing effect. Porosity of the paper may cause variation in the thickness of the coating as it may allow some target material to penetrate the pores affecting the sensor performance. It should be noted that not all materials are suitable for sputtering thus limiting the range of materials. Although the deposition process is cheaper comparatively, the equipment and maintaining ultra-high vacuum can be expensive and complex. This method can be relatively slow which can be a disadvantage for high-volume production. Despite these drawbacks, sputtering remains a viable technique for depositing thin films on paper, especially for applications where precise control over thickness of the film is

required. Optimization of sputtering parameters can mitigate some of these disadvantages.

25.2.2 Thermal Evaporation

Thermal evaporation is a physical vapor deposition technique where a source material such as Au, Ag, etc., is heated in a high vacuum until it vaporizes. This vapor then travels to the substrate which is kept at a lower temperature, where it condenses and forms a thin film. Thermal evaporation is conducted in a high vacuum chamber in order to minimize the collisions between the air molecules and vaporized material, facilitating the material to travel directly to the substrate. The material can be heated with a variety of heat sources such as resistive heating (passing a current through a filament or boat holding the source material), electron beam evaporation (using a focused beam of electrons to heat the source), or laser ablation. Quartz crystal microbalances, located inside the deposition chamber, are often used to monitor the deposition rate in real time. By monitoring the duration of the evaporation process and the deposition rate, the thickness of the deposited film can be measured and controlled.

25.2.3 Laser Ablation

Laser ablation technique can selectively remove materials from a substrate by directing a high-energy laser beam at it. Selection of laser source is vital for paper-based devices as the heat generated by the laser beam can have devastating effects on the paper. Schematic illustration of (a) steps involved in pulsed laser deposition (PLD) technique and (b) tailored parameters during the PLD process is shown in Fig. 25.2. Lasers like Nd:YAG (1.06 μm) can selectively remove Al metal efficiently as it has higher absorption coefficients for the metal film than the paper substrate (Rahimi et al., 2018). Thus, the thermal effect on the paper substrate is reduced greatly as compared to CO_2 laser (10.6 μm) which is more suitable for polymeric substrates. This process is termed as Direct Laser ablation (DLA). Metallic films such as Al do not absorb the radiation from CO_2 laser well enough to be etched, thus it can cause a partial depletion of the cellulose layer, destabilizing the integrity of the paper substrate, changing the hydrophobicity or other surface properties of the paper. This process is termed as indirect laser ablation (ILA). Any paper-based sensor that benefits from the high surface area can utilize DLA method as it maintains the porous structure and fibrous nature of the paper while selectively removing the metallic film layer (Rahimi et al., 2018).

Wavelength, power, and scanning speed are significant parameters that are sensitive to the paper substrate. Calibrating and fine-tuning these parameters can help achieve the desired outcome. Excessive energy can cause damage to the substrate by

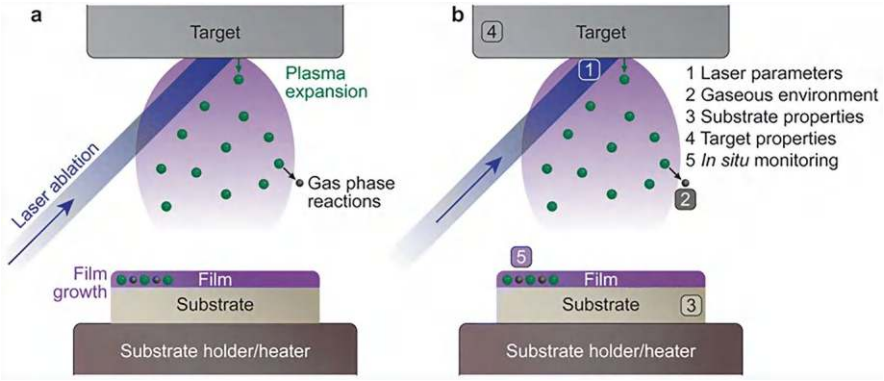

Fig. 25.2 Schematic illustration of (**a**) steps involved in pulsed laser deposition (PLD) technique, (**b**) tailored parameters during the PLD process. (Reprinted from Shepelin et al. (2023). Published 2023 by RSC with open access)

creating holes. Similarly, if the energy imparted is low, the laser may not entirely remove the metal atoms resulting in an uneven deposition. Thus, finding a balance in the laser parameters is essential to ensure precision and avoid damaging the delicate paper substrates.

Laser ablation allows for quick patterning for prototyping and large-scale production while maintaining high level of precision. Intricate patterns with complex designs, such as interdigitated sensors and circuits, can be fed to be patterned through the laser ablation method (Rahimi et al., 2018). Laser ablation removes the need for masks or toxic chemical etching, thus simplifying the production process. This method does have its drawbacks such as that it is limited to materials that can absorb the laser's energy and requires precise control over laser power and speed, and unoptimized laser parameters can damage the substrate.

Pulsed laser deposition (PLD) is a physical vapor deposition technique where laser is used to form a plasma plume by ejecting particles from the solid target materials. This plume transports the material to the paper substrate forming a thin film. Metals or oxides can be used as targets, and they need to be tested for laser absorption for specific wavelengths. Laser pulses between 10 and 25 ns have shown to be optimal windows considering the thin film growth and the plasma properties. Pulse rate and shape have an effect on the film growth as well (Shepelin et al., 2023). Pulsed laser ablation can have pulse lengths in femtoseconds, picoseconds, nanoseconds, or microseconds, and depending on the length, different physical reaction occurs on the incident target such as cold ablation, hot ablation, and melt expulsion taking place respectively as shown in Fig. 25.3. For proper ablation the intensity has to be around the ablation threshold, below which very little material is exuded while a bulk of the energy is dissipated as heat energy (Shepelin et al., 2023). By optimizing the parameters, the nucleation process can be controlled leading to a uniform coating of the film avoiding cluster formation or re-evaporation from the substrate.

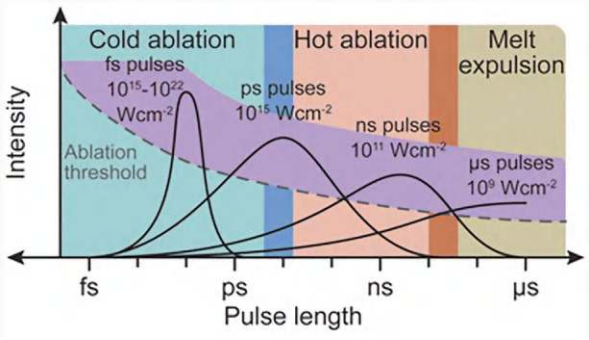

Fig. 25.3 Different ablation domains with corresponding pulse lengths along with the ablation threshold. (Reprinted from Shepelin et al. (2023). Published 2023 by RSC with open access)

25.3 Vapor Phase Deposition

25.3.1 Conventional CVD and PECVD

Chemical vapor deposition (CVD) is a method where volatile precursor gases are transported in a high vacuum chamber with the help of carrier gases (e.g., nitrogen, argon) to the substrate where the precursor gets adsorbed on to the surface. Heterogenous surface-catalyzed reaction is induced on the surface either by thermal application or can be plasma-enhanced (PECVD). Products that are formed as a result of this reaction diffuse across the surface forming nucleation sites where films can grow as more material gets deposited. Once the desired thickness is achieved, the gaseous reaction products are desorbed from the surface to stop further deposition on the substrate. Thermally activated CVD uses heat to break down the precursor gases. For paper substrates the temperature must remain below its usual thermal degradation threshold, which is around 200 °C. PECVD is better suited for paper-based substrates as it initiates the necessary chemical reactions through plasma resulting in deposition at lower temperatures minimizing substrate damage from higher temperatures. Plasma treatment also enhances the adhesion of the paper substrate assisting in improving film uniformity.

Highly reactive chemicals/reaction by-products can degrade the paper substrates or damage its structure, affecting its properties. Reaction by-products are usually removed from the chamber through vents. Monomers can be vaporized (through heating or plasma) and transported to the paper substrates to be polymerized layer-by-layer with high uniformity through CVD/PECVD while simultaneously forming thin films (Asatekin et al., 2010; Byranvand et al., 2020). CVD process can result in forming a variety of shapes and structures on the substrate like hexagons, triangles, and truncated triangles as shown in Fig. 25.4. Variation in these shapes occurs due to various factors during the deposition process including the temperature and pressure, precursor gas composition, orientation of the substrate, and deposition time. For example, deposition of graphene through CVD often produces hexagonal

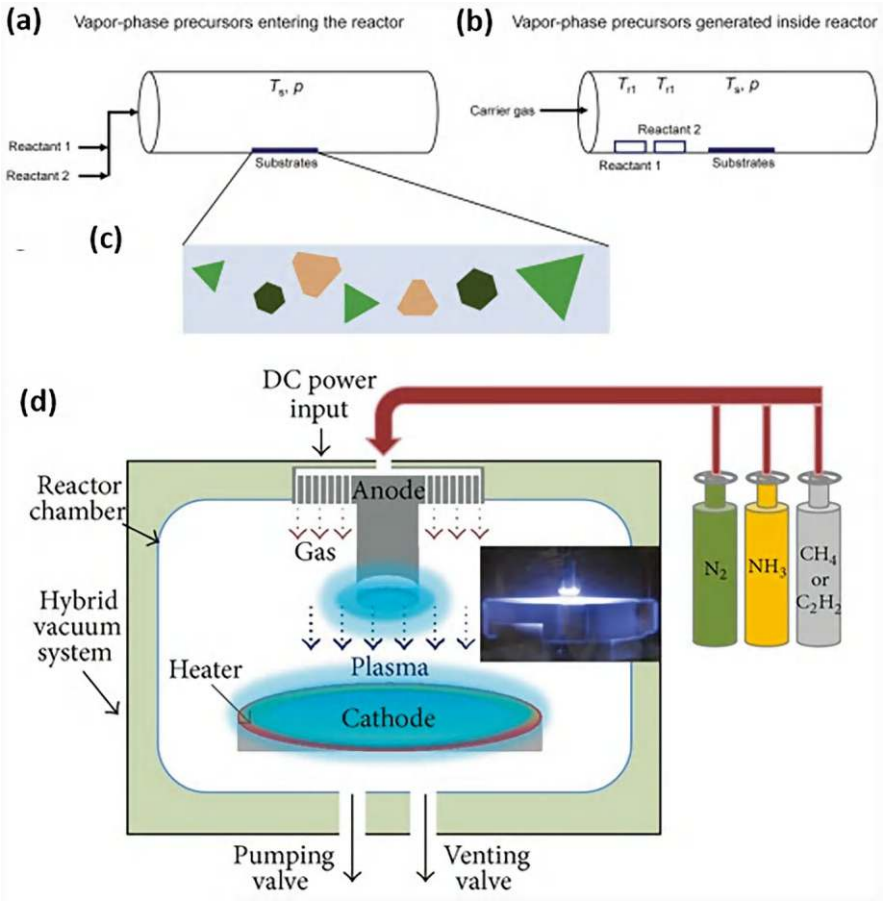

Fig. 25.4 Processes involved in (**a**–**c**) chemical vapor deposition, and (**d**) plasma-enhanced chemical vapor deposition (Inset: generated plasma). ((**a**–**c**) Reprinted from Bhowmik and Rajan (2022). Published 2022 by Cell Press with open access. (**d**) Reprinted from Oke and Jen (2022). Published 2022 by Elsevier with open access)

shapes due to the hexagonal lattice structure of graphene (Li et al., 2018). In addition to monomers, by supplying an oxidant, conducting polymers like PEDOT, PPy, and PTAA can be formed which is known as oxidative chemical vapor deposition (oCVD). Initiators such as tert-butyl peroxide can be introduced along with the monomers to help form free radicals in low temperatures; this process is called initiated CVD (iCVD). This method is versatile for chain growth polymers. Film growth can be adjusting the initiator species (Asatekin et al., 2010).

25.3.2 Atomic Layer Deposition

Atomic layer deposition is a thin-film deposition technique that relies on sequential, self-limiting surface chemical reactions to achieve atomic-level control over film thickness. Monolayer-level precision can be obtained through ALD process. The process is more effective for conformal coatings on complex geometric substrates. The desired primary chemical precursor is introduced into the reaction chamber, reacting with the substrate surface (hydroxyl groups on cellulose) to form the base for the monolayer to attach on. It is temperature controlled to preserve the substrate's integrity. Due to the finite number of reactive sites on the substrate surface, this reaction is self-limiting. Unreacted precursor and the by-products are purged from the reaction chamber to prevent phase change reactions in the following steps. The secondary precursor is introduced after purging which can react with the surface bound layer completing the monolayer. Unreacted by-products and co-reactants are cleared out of the chamber through purging again. This cycle is repeated until the desired thickness is obtained (George, 2010; Shen et al., 2022).

Highly uniform coatings can be deposited even on high-aspect-ratio structures. Paper substrates are highly compatible with ALD even with the fibrous and porous nature of the paper. This process can coat individual fibers or fill voids within the structure of the substrate while preserving the substrate's flexibility and breathability (George, 2010). Plasma-enhanced techniques can reduce the maximum temperature needed for a uniform ALD process. The precursors for ALD must be volatile, thermally stable, and reactive at lower temperatures, thus limiting the range of usable materials to certain oxides, nitrides, or organic-inorganic hybrids (Jur et al., 2011). ALD is ideal for creating ultrathin coatings. It can also be used to impart properties such as barrier characteristics, hydrophobicity, or conductivity to paper. Optimization of exposure time and proper substrate selection has to be done to avoid excessive penetration of precursors into the substrate and a nonuniform coating or even substrate damage. For better adhesion, the paper substrates can also be coated with aluminum oxide (Jur et al., 2011). ALD can be used to create advanced functional paper-based sensors and electronic devices. Although it is ideal for many applications, it can be a very slow process for large-scale production or thicker film coatings. Some of the coatings such as ZnO may crack under mechanical stress, reducing their effectiveness (Jur et al., 2011). Despite the drawbacks, ALD can be used for deposition with ultra-high precision and conformality for paper-based substrates.

Atomic layer deposition (ALD) technique comprises several steps of self-limiting surface reactions between gaseous precursors at the chosen substrate's interface. In this approach, alternating pulse and purge sequences along with an inert carrier gas help in providing selective reactions among different precursor reactants as shown in Fig. 25.5a. However, the number of ALD cycles and the growth temperatures influence the deposition capabilities of the ALD process as shown in Fig. 25.5b, c. This ultimately results in precise control over film thickness

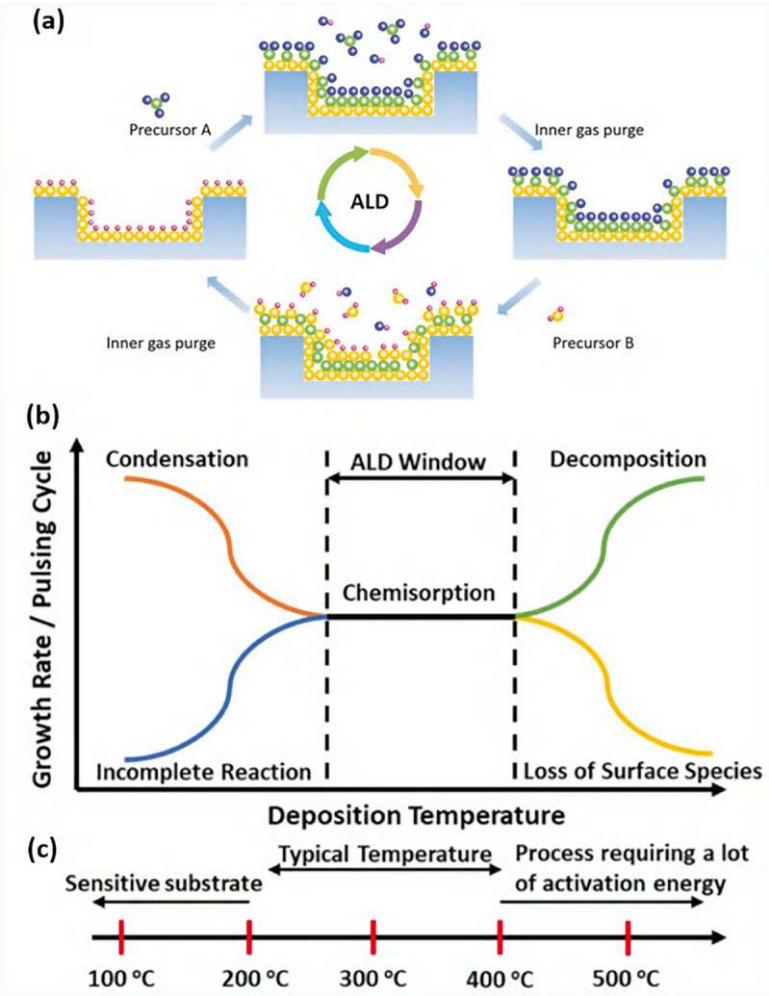

Fig. 25.5 Atomic layer deposition process: (**a**) steps involved in the ALD process, (**b**) influence of growth cycle, (**c**) deposition temperature effect. ((**a**) Reprinted from Bhowmik and Rajan (2022). Published 2022 by Cell Press with open access. (**b**, **c**) Reprinted from Oke and Jen (2022). Published 2022 by Elsevier with open access)

and composition through layered deposition, highlighting the inherent scalability and uniformity.

25.4 Solution Methods

25.4.1 Sol-Gel Method

The sol-gel method involves the transition of a system from a liquid (sol) to a solid (gel) phase, often used for the deposition of thin films. In this method, metal alkoxides or salts are hydrolyzed and polycondensed to form a gel, which can then be processed into a thin film. The sol-gel method allows for the deposition of materials such as metal oxides, semiconductors, and polymers onto various substrates, including paper (Chaudhury et al., 2007).

The sol-gel method is commonly used to deposit materials like titanium dioxide (TiO_2), silica, and zinc oxide (ZnO) onto paper substrates, imparting properties such as photocatalysis, hydrophobicity, and piezoelectricity, which are critical for paper-based sensors and energy devices.

The sol-gel method offers the advantage of high control over the film thickness and composition, making it a versatile technique for depositing a wide range of materials such as metal oxides (TiO_2, ZnO) and polymers on paper substrates. This method allows for the creation of uniform thin films with precise composition control, which is particularly valuable in applications like sensor coatings, photovoltaic devices, and catalysis. However, one major disadvantage of the sol-gel process is the time-consuming drying and curing stages, which can limit throughput. Additionally, the films produced can sometimes be brittle and prone to cracking, particularly on flexible substrates like paper. Despite these challenges, sol-gel remains a popular choice due to its versatility and precision in depositing functional coatings (Chaudhury et al., 2007; Mac Craith et al., 1997).

25.4.2 Dip Coating

Dip coating is a simple and widely used technique where a substrate is immersed in a solution and withdrawn at a controlled speed to create a uniform coating. The solution may contain functional materials such as metals, polymers, or nanoparticles. The thickness of the film can be controlled by the speed at which the substrate is withdrawn and the concentration of the solution (Huang et al., 2017; Lee et al., 2016; Zhan et al., 2021).

Dip coating is commonly used to deposit conductive polymers (such as polyaniline), nanoparticles (like gold or silver), and organic materials (such as polythiophene) onto paper substrates. This technique is frequently employed for the

development of paper-based sensors and devices such as electrochemical sensors, capacitive sensors, and bio-sensors.

The primary advantage of this technique is its scalability, making it suitable for large-area applications. The process creates uniform films with good adhesion to paper. It allows for good uniformity in coating thickness, which can be controlled by adjusting the withdrawal speed of the substrate. This method is commonly used for depositing conductive polymers like polyaniline and nanoparticles on paper substrates, which are essential for sensor applications. However, dip coating has some limitations, including limited control over extremely thin films and the need for a drying stage, which can result in cracking or nonuniform coatings if not done carefully. Despite these challenges, dip coating is still favored for its ease of use and efficiency in covering large areas (Lee et al., 2016).

25.4.3 Drop Coating

Drop coating involves applying small droplets of a solution containing functional materials directly onto a substrate, where they spread and dry to form a thin film. The method is relatively simple, requiring only a pipette or syringe for material deposition (Cho et al., 2019). Drop coating is often used to deposit organic semiconductors, biomolecules, or nanoparticle suspensions on paper substrates. This method is suitable for fabricating sensors or biosensors with well-defined sensing regions on paper-based platforms.

Drop coating involves applying small droplets of solution onto a substrate and allowing them to spread and dry, which allows for precise localization of material deposition. One of its key advantages is its ability to deposit materials with high precision, making it ideal for organic semiconductors, biomolecules, and nanoparticles on paper-based sensors and devices. Drop coating is also relatively easy to implement and does not require complex equipment, making it suitable for small-scale or prototype work. However, this method is limited in scalability, and the drying process can sometimes cause cracks or nonuniformities in the coating, especially when dealing with large-area substrates. Additionally, while drop coating offers high precision, it may not be as suitable for large-scale production compared to other methods like dip coating (Malik et al., 2024).

25.4.4 Vacuum Filtration

Vacuum filtration involves filtering a solution through a porous membrane under vacuum pressure, allowing the solid phase to accumulate on the membrane. This technique is often used to create thin films or coatings of nanoparticles, polymers, or other materials that can be applied to various substrates (Wang et al., 2022, 2023; Zhan et al., 2021). Vacuum filtration is widely used to deposit carbon nanotubes

(CNTs), graphene oxide (GO), and other nanomaterials onto paper. This method is especially advantageous for creating conductive or sensor-active layers on paper for use in flexible sensors, energy storage devices, or wearable electronics. Vacuum filtration is a technique that involves filtering a solution through a membrane, allowing materials like carbon nanotubes (CNTs), graphene, and ceramics to be deposited onto a substrate. The primary advantage of this method is the creation of dense, uniform layers, which is particularly useful when working with high-surface-area materials like CNTs or graphene for sensor applications. This method provides high uniformity in the deposited material, which is crucial for ensuring consistent sensor performance. However, the setup required for vacuum filtration can be complex, and scaling up the process for larger areas can pose challenges. Additionally, vacuum filtration is typically limited to materials that can be effectively filtered through a membrane, which may restrict its versatility compared to other deposition methods (Dong et al., 2021).

25.4.5 Layer-by-Layer Deposition

Layer-by-layer (LbL) deposition involves sequentially depositing alternating layers of positively and negatively charged materials. This method is based on electrostatic or chemical interactions between the layers, allowing the formation of multilayer films with precise control over thickness (Nery & Kubota, 2013). This method is often employed for the deposition of polyelectrolyte films, conductive polymers, or nanoparticles on paper substrates. LbL is especially useful in creating functional coatings for sensors, drug delivery systems, or capacitors.

Layer-by-layer (LbL) deposition is a versatile technique that involves the sequential deposition of alternating layers of materials with opposite charges, creating multilayered structures. One of the main advantages of LbL is the precise control it offers over the composition and thickness of each layer, making it ideal for applications where customized functionalities are required, such as in supercapacitors, sensors, and multifunctional coatings. The method allows for high precision and the creation of complex structures that cannot be achieved with other deposition techniques. However, LbL is a time-consuming process that requires multiple deposition cycles, which can make it less efficient for large-scale production. Additionally, the technique is somewhat limited by the properties of the substrate and may not be suitable for all materials (Nohria et al., 2006).

25.4.6 Electrochemical Deposition

Electrochemical deposition involves the reduction of metal ions onto a substrate via an applied electrical current. This method can be used to deposit metals, alloys, and conductive polymers onto substrates (Klem et al., 2024). Electrochemical

deposition is used for depositing conductive materials, such as gold, silver, and copper, onto paper substrates, enabling the development of paper-based electrodes for sensors and energy devices.

The primary advantage of electrochemical deposition is its high precision and ability to produce uniform, highly adherent films on substrates like paper. This method is particularly useful for depositing electrodes for sensors, batteries, and other electronic applications. Electrochemically deposited materials, such as Ni_2O_3 on carbon paper, have been utilized for electrocatalytic processes, enhancing energy conversion efficiency (Du et al., 2024). In sensors, Devices fabricated using electrodeposition have shown improved detection limits for analytes like mercury and organic compounds (Economou et al., 2023; González-Martínez et al., 2023). This technique can significantly increase the electrochemically active surface area (ECSA), improving sensitivity and performance in sensing applications (Du et al., 2024; Ghanbari & Etzold, 2023).

It also allows for precise control over the thickness and composition of the deposited films, which is crucial for optimizing the performance of electrochemical devices. However, electrochemical deposition requires specialized electrical equipment, and it is limited to materials that can undergo reduction in an electrolytic solution. Despite these limitations, electrochemical deposition remains a preferred choice for creating conductive coatings on paper-based substrates (Serfőző et al., 2023).

25.4.7 Electrophoretic Deposition

Electrophoretic deposition (EPD) uses an electric field to move charged particles suspended in a solution onto a substrate. The deposition process continues as long as the electric field is applied, and the particles are attracted to the electrode (Amrollahi et al., 2015). EPD is used for depositing nanoparticles, ceramics, and polymers onto paper, making it a promising technique for creating sensors, actuators, or coatings with specific properties such as hydrophobicity or conductivity. Electrophoretic deposition (EPD) uses an electric field to move charged particles onto a substrate, allowing for the deposition of materials like nanoparticles, ceramics, and conductive polymers. The main advantages of EPD include a high deposition rate and excellent control over the thickness of the deposited films by adjusting parameters such as voltage, particle concentration, and deposition time, which is beneficial for sensor fabrication and coating applications. The process also provides a uniform deposition of materials, which is essential for achieving consistent performance in sensors and other devices. However, one of the challenges of EPD is that it requires the particles to be charged or functionalized, which may not be suitable for all materials. Additionally, the composition of the solution must be carefully controlled to avoid inconsistencies in the deposition process. Despite these challenges, EPD is a powerful technique for high-throughput and uniform material deposition (Chavez-Valdez et al., 2013; Nery & Kubota, 2013).

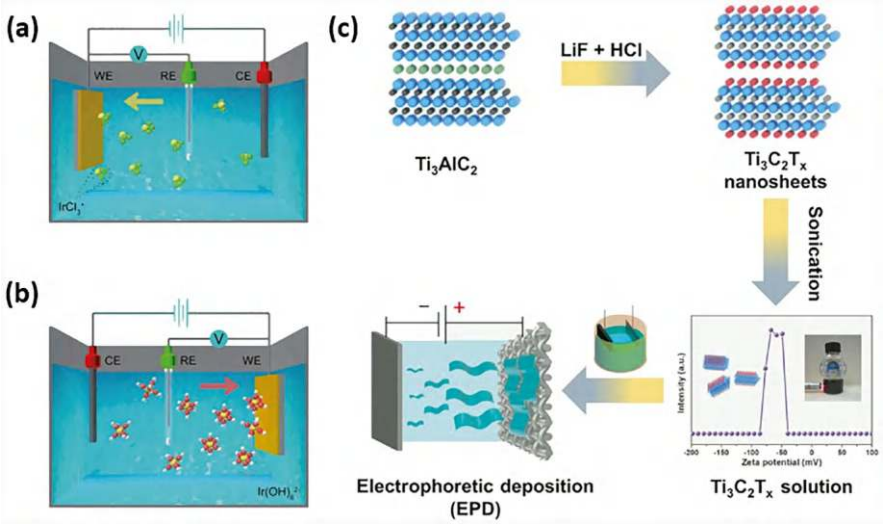

Fig. 25.6 Mechanism of electrochemical deposition. (**a**) Cathodic deposition, (**b**) anodic deposition of Ir species; [yellow (Ir), green (Cl), red (O), and white (H) spheres]. A three-electrode system is employed with $Co(OH)_2$ nanosheets on glassy carbon electrode (WE), a carbon rod counter electrode (CE), and Ag/AgCl electrode (RE). (**c**) Synthesis of MXene and process of electrophoretic deposition on graphite paper substrate. ((**a**, **b**) Reprinted from Zhang et al. (2020). Published 2020 by Nature with open access. (**c**) Reprinted with permission from Deng et al. (2021). Copyright 2021: Elsevier)

Zhang et al. (2020) have described the mechanism of electrochemical deposition with a schematic for cathodic and anodic deposition of Ir species in KOH electrolyte as shown in Fig. 25.6. Figure 25.6a shows the cathodic deposition, where upon applying the required electric field the iridium cations are driven towards the cathode leading to deposition onto the supports, coordinating with three O atoms on $Co(OH)_2$. This process involves the reduction of Ir ions, resulting in an oxidation state of Ir lower than +4 C-Ir_1/$Co(OH)_2$. Similarly, Fig. 25.6b depicts anodic deposition where iridium anions were derived due to the reaction of Ir^{4+} precursors and OH^- in the electrolyte resulting in deposition on the anode. This deposition occurs alongside the oxidation of anions, leading to an oxidation state of Ir higher than +4 in A-Ir_1/$Co(OH)_2$.

Synthesis of MXene via electrophoretic deposition was reported by Deng et al. (2021). In this the synthesis process involves Al etching and its dispersion in water. Here, two electrodes stainless steel mesh act as anode and carbon paper as cathode resulting in electrophoretic deposition upon supplying the electrode with a constant voltage. Schematic of electrophoretic deposition is as shown in Fig. 25.6c.

25.5 Spray Coating

Spray coating is a technique for depositing films on preheated substrates by spraying a precursor solution, where components react to form desired compounds due to the temperature gradient across the substrate. This method offers versatility for depositing various materials and eliminates the need for high vacuum conditions. Key aspects of the procedure include precursor composition, aerosol generation, and deposition. Variation of this technique includes the following methods.

25.5.1 Thermal Spray

Thermal spraying involves heating a material to a molten or semi-molten state and spraying it onto a substrate (see Fig. 25.7). This technique is commonly used to deposit metallic coatings, ceramics, or composites (Maho et al., 2023). Thermal spray can be used to apply conductive, insulating, or protective coatings onto paper substrates for the development of sensors, wearables, or protective films.

Thermal spray is a process where materials are heated to a molten or semi-molten state and then sprayed onto a substrate to form a coating. The primary advantage of thermal spray is its high material deposition rate, which makes it suitable for applications where thick, protective layers are required. However, the high temperatures involved in thermal spray can damage the paper substrate, limiting its applicability

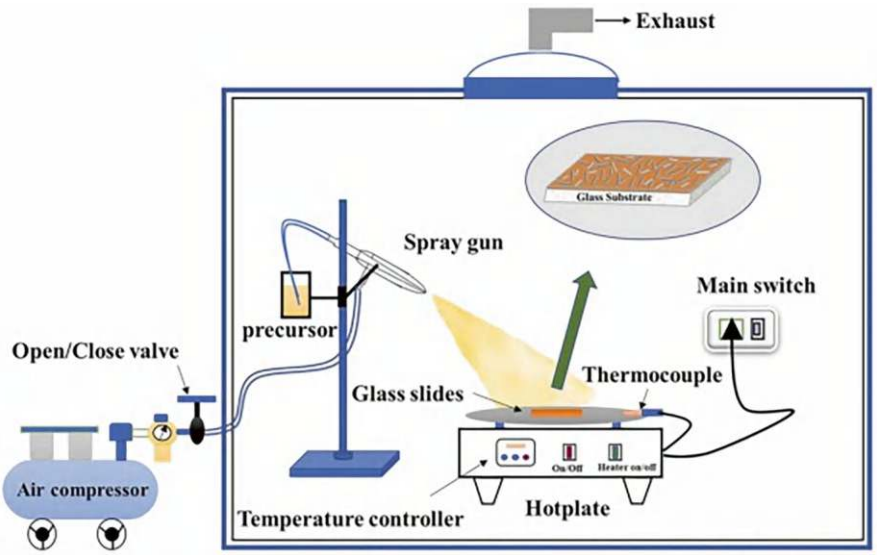

Fig. 25.7 Schematic representation of the spray coating technique. (Reprinted with permission from Ravikumar et al. (2023). Copyright 2023: Elsevier)

in some cases. Additionally, the setup for thermal spray can be complex, requiring specialized equipment such as spray guns, heat sources, and compressors. Despite these challenges, thermal spray remains a popular choice for applications that demand fast deposition rates and durable coatings (Du et al., 2022).

25.5.2 Lacquer Spraying

Another easy way to fabricate paper analytic devices (PADs) quickly and affordably is via lacquer spraying. For this process, a paper, a spray-on lacquer, and a mold were used. The mold can consist of either a basic metal or a laminate sheet that acts as a barrier, preventing the paper from coming into contact with lacquer (Deng et al., 2019). Paper is positioned between the magnet and the metal mold to hold it in place, while appropriate adhesive is used to hold laminating sheets in place. Next, a lacquer solution is evenly sprayed onto the paper using a spray bottle and the exposed parts will result in hydrophobic zones. After, drying the sprayed lacquer solution, the mold was removed. The resulting paper will generate alternative regions of hydrophobic-hydrophilic in a single paper. This process and application of lacquer spraying are illustrated in Fig. 25.8 (Lin et al., 2020; Nurak et al., 2013).

25.5.3 Electrospinning

Electrospinning uses an electric field to draw a polymer melt or solution into fibers, which are deposited onto a substrate. The result is a nonwoven mat of fibers with high surface area (Cao et al., 2023).

Electrospinning is a technique that uses an electric field to draw fibers from a polymer solution onto a substrate, creating fine, nanometer-scale fibers. The primary advantage of electrospinning is its ability to produce fibers with high surface area, making it ideal for applications in sensors, energy storage devices, and filtration. The resulting nanofibers are highly porous, which can enhance the performance of paper-based sensors by providing more surface area for interaction with target molecules. However, electrospinning requires high-voltage power supplies and specialized equipment, making it less accessible for some applications. Additionally, scalability can be an issue, as producing large quantities of nanofibers can be challenging. Despite these limitations, electrospinning is a powerful method for producing fine fibers with unique properties that are ideal for advanced sensor applications (Table 25.1).

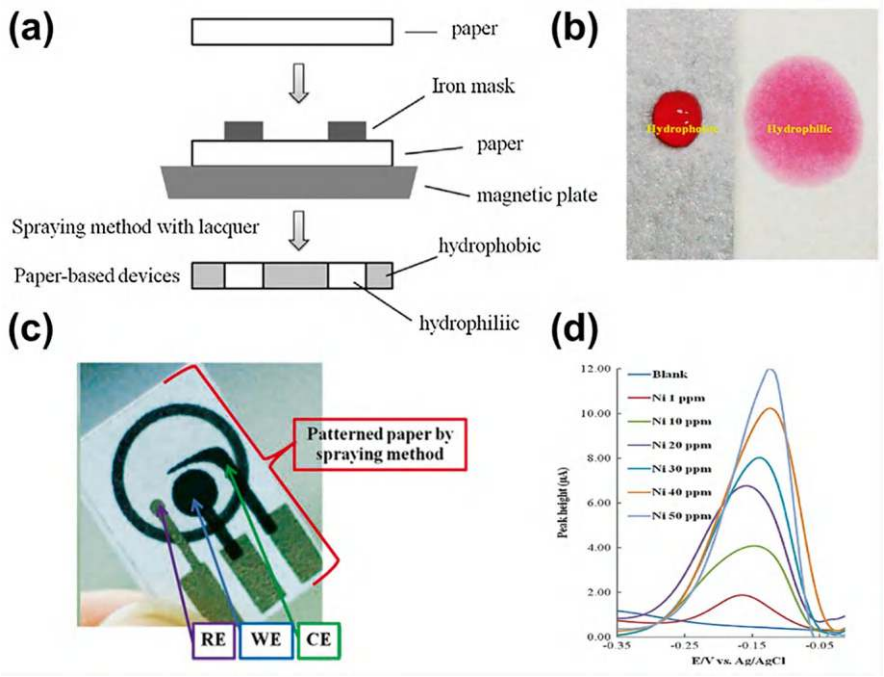

Fig. 25.8 (**a**) Schematic of hydrophobic-hydrophilic layer formation by lacquer spraying, (**b**) optical image of droplets on hydrophobic and hydrophilic region, (**c**) picture of electrochemical sensor prepared by the lacquer spraying, and (**d**) DPV response of nickel concentration variation of the prepared device. (Reprinted with permission from Nurak et al. (2013). Copyright 2013: Elsevier)

25.6 In Situ Synthesis

In situ synthesis method integrates the synthesis of functional materials directly onto or within the paper substrate. This process relies on thermal or chemical reactions started directly on the substrate to form the desired material coating. Chemical precursors that are introduced onto the substrate react and deposit functional coatings in situ. The fibrous and porous nature of paper, serving as a matrix, allow precursors to efficiently infiltrate and react in controlled environments (Aouay et al., 2024). Conductive polymers, metal nanoparticles, or oxides can be directly synthesized on the paper substrates through chemical reactions, thermal treatments, or photonic activation through in situ method. In situ method reduces material waste and aids in sustainable manufacturing practices (Pinheiro et al., 2020). Material formation is limited to desired areas, providing more freedom for complex device designs. It is a cost-effective process of simultaneously synthesizing and depositing in one step. Porosity variation across the paper's surface may affect the distribution of deposition of functional materials creating nonuniformity. In situ methods can be easily used for scalable production of paper-based sensors and devices.

Table 25.1 Comparison of dry and wet methods for deposition of functional materials on paper substrates

Deposition method	Materials deposited	Features of deposition	Advantages	Disadvantages	Equipment required	Typical applications	Examples of application
Sol-gel	Used to deposit metal oxides and composites for functional coatings	Uniform thin films with precise control over thickness	High control over film thickness and composition; versatile for various materials	Time-consuming drying and curing process; films can be brittle	Furnace, hot plates for curing	Sensor coatings, photovoltaic applications, catalysis	Chaudhury et al. (2007), Mac Craith et al. (1997)
Dip coating (immersing)	Deposits conductive polymers and metal and metal oxide NPs	Uniform coating; thickness control via withdrawal speed	Simple, cost-effective, scalable for large areas	Limited control over very thin films; requires drying	Dip tank, drying oven	Coating for sensors, membranes, electrodes	Huang et al. (2017)
Drop coating	Suitable for organic semiconductors, biomolecules, and metal and metal oxide NPs	Precise localization of deposition; control over droplet size	High precision; easy to implement.	Limited scalability; drying may lead to cracks or nonuniformity	Micropipettes, dropper system	Organic electronics, bio-sensors, coatings	Cho et al. (2019)
Vacuum filtration	Used for various nanomaterials	Dense, uniform layers; good for high-surface-area materials	High uniformity; ideal for nanomaterials	Requires complex setup; scaling up for large areas can be challenging	Vacuum chamber, filtration setup	Nanomaterial deposition, sensor electrodes	Wang et al. (2022, 2023)
Layer-by-layer (LbL)	Used for polyelectrolytes, conductive polymers, metals and metal oxides	High precision; customizable multilayer structures	Precise control over composition and thickness; customizable functionalities	Time-consuming; requires multiple cycles; limited by substrate properties	Solution reservoirs, syringe pumps, electrode setups	Multilayer coatings, sensors, supercapacitors	Nery and Kubota (2013), Nohria et al. (2006)

Deposition method	Materials deposited	Features of deposition	Advantages	Disadvantages	Equipment required	Typical applications	Examples of application
Electro-chemical deposition	Deposits conductive metals and metal oxides	Uniform, highly adherent films; controlled by current and voltage	High precision; ideal for conductive coatings	Requires electrical equipment; limited to reducible materials	Power supply, electrochemical cell	Electrodes for sensors, batteries, corrosion protection	Klem et al. (2024), Serfőző et al. (2023)
Electro-phoretic deposition	Used for metal nanoparticles, metal oxides, and polymers	Uniform deposition; controllable by voltage and solution composition	High deposition rate; excellent control over film thickness	Requires charged or functionalized materials; needs careful solution control	Power supply, electrophoretic cell	Ceramic and metal coatings, sensor fabrication	Amrollahi et al. (2015)
Thermal spray	Deposits metal oxides, or composite	Rapid deposition; creates dense, protective layers	High material deposition rate; suitable for various materials	High temperatures can damage paper; complex setup	Spray gun, heat source, compressor	Coating for protective layers, sensors, energy storage	Maho et al. (2023)
Electro-spinning	Deposits polymers and metal oxides	Fine, nanometer-scale fibers with high surface area	Produces fine fibers; ideal for sensitive sensor applications	Requires high voltage and specific equipment; scalability issues	High-voltage power supply, syringe pump, collector	Nanofiber coatings for sensors, energy storage, filters	Cao et al. (2023)

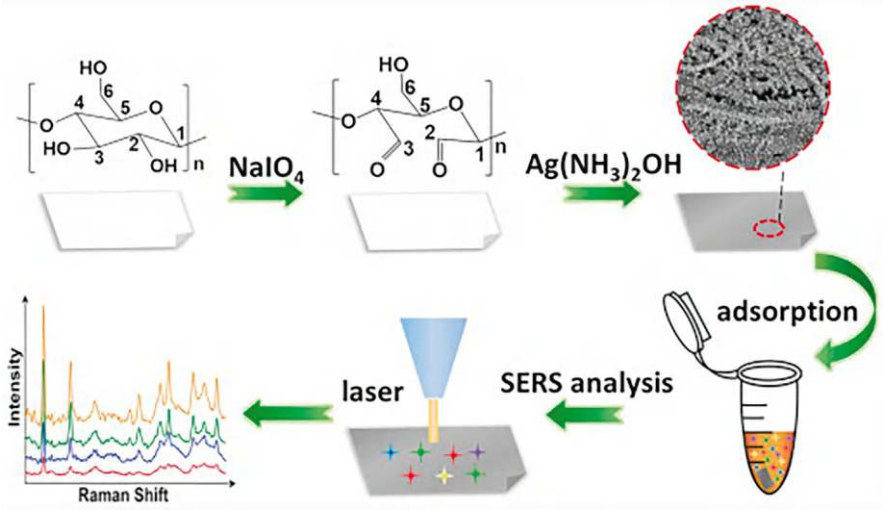

Fig. 25.9 An illustration of the integration of the synthesized AgNPs within the porous structure of the paper showing improved molecular signal detection for analytical applications. (Reprinted with permission from Li et al. (2016). Copyright 2016: Elsevier)

Fast-wicking paper membranes are stacked on top of a slow-wicking paper membrane containing dried reagents. The dried reagents are rehydrated uniformly across the area by the fast-wicking paper, and this process is termed as paper stacking. This method can be used to fabricate sensors, such as for diagnosing cystic fibrosis (Chauhan et al., 2022). A major advantage of in situ synthesis is that it eliminates the need for patterning steps, making it suitable for large-scale manufacturing. Metal salts such as $AgNO_3$ and $HAuCl_3$ can be directly reduced with $NaBH_4$ on the paper surface resulting in the reduced metal particles being deposited on the cellulose surface (Mekonnen et al., 2021). The density of the deposited nanoparticles on the substrate depends on the reaction time and initial salt concentration, which has to be optimized to get the desired results. In situ reduction can be made eco-friendly by using cellulose self-sacrifice reduction, removing the requirement for stabilizing and reducing agents (Desmonda et al., 2016).

Li et al. (2016) developed a simple three-dimensional (3D) paper-based substrate for Surface-Enhanced Raman Spectroscopy (SERS) via the silver mirror reaction to obtain plasmonic silver nanoparticles (AgNPs). These AgNPs were then distributed in situ on the paper strip and were found to show enhanced SERS performance due to their active plasmonic properties as shown in Fig. 25.9.

25.7 Summary

With increasing development of deposition techniques, paper-based devices are being developed for a diverse set of applications. These techniques have also helped evolve the paper devices to transition from 1D to 3D devices that are able to process multiple reactions and functions easily (Cate et al., 2015). With its rapid growth in recent years, problems that require attention also rise at a steady rate such as material selection, substrate choices that are more versatile and functional than a form of filter paper. Synthesizing compatible solvents for different deposition techniques continues to prove to be a challenge as improvement in material compatibility could increase repeatability and high precision. As paper-based devices get implemented in more applications, the demand for low-cost, high-throughput, in situ methods of deposition techniques would ascent.

Acknowledgments The author Shriswaroop Sathyanarayanan thanks the DST-SERB project, India (CRG/2020/005273) and Sathish Marimuthu thanks the DST-PURSE project, India, for funding this research work through the project number [File.no. SR/PURSE/2020/34], and Dr. Andrews Nirmala Grace extends their appreciation to DST-TDT (DST/TDT/AM/2022/75), Government of India, and Vellore Institute of Technology (VIT), Vellore, India, for supporting the chapter work.

References

Amrollahi, P., Krasinski, J. S., Vaidyanathan, R., Tayebi, L., & Vashaee, D. (2015). Electrophoretic deposition (EPD): Fundamentals and applications from nano- to microscale structures. In M. Aliofkhazraei & A. S. H. Makhlouf (Eds.), *Handbook of nanoelectrochemistry* (pp. 561–591). Springer International Publishing. https://doi.org/10.1007/978-3-319-15266-0_7

Aouay, M., Aguado, R. J., Bayés, G., Fiol, N., Putaux, J.-L., Boufi, S., & Delgado-Aguilar, M. (2024). In-situ synthesis and binding of silver nanoparticles to dialdehyde and carboxylated cellulose nanofibrils, and active packaging therewith. *Cellulose, 31*, 5687–5706. https://doi.org/10.1007/s10570-024-05918-5

Asatekin, A., Barr, M. C., Baxamusa, S. H., Lau, K. K. S., Tenhaeff, W., Xu, J., & Gleason, K. K. (2010). Designing polymer surfaces via vapor deposition. *Materials Today, 13*, 26–33. https://doi.org/10.1016/S1369-7021(10)70081-X

Bhowmik, S., & Rajan, A. G. (2022). Chemical vapor deposition of 2D materials: A review of modeling, simulation, and machine *iScience, 25*, 103832. https://doi.org/10.1016/j.isci.2022.103832

Byranvand, M. M., Behboodi-Sadabad, F., Eliwi, A. A., Trouillet, V., Welle, A., Ternes, S., et al. (2020). Chemical vapor deposited polymer layer for efficient passivation of planar perovskite solar cells. *Journal of Materials Chemistry A, 8*, 20122. https://doi.org/10.1039/D0TA06646J

Cao, H., Chai, S., Tan, Z., Wu, H., Mao, X., Wei, L., et al. (2023). Recent advances in physical sensors based on electrospinning technology. *ACS Materials Letters, 5*, 1627. https://doi.org/10.1021/acsmaterialslett.3c00144

Cate, D. M., Adkins, J. A., Mettakoonpitak, J., & Henry, C. S. (2015). Recent developments in paper-based microfluidic devices. *Analytical Chemistry, 87*, 19–41. https://doi.org/10.1021/ac503968p

Chaudhury, N. K., Gupta, R., & Gulia, S. (2007). Sol-gel technology for sensor applications. *Defence Science Journal, 57*, 241–253. https://doi.org/10.14429/dsj.57.1765

Chauhan, A., Mittal, M., & Toley, B. J. (2022). *In situ* synthesis of reagents in paper-based analytical devices using paper stacking. *Analytical Methods, 14*, 4021. https://doi.org/10.1039/D2AY00924B

Chavez-Valdez, A., Shaffer, M. S. P., & Boccaccini, A. R. (2013). Applications of graphene electrophoretic deposition. A review. *The Journal of Physical Chemistry. B, 117*, 1502–1515. https://doi.org/10.1021/jp3064917

Cho, H. H., Kim, S. J., Jafry, A. T., Lee, B., Heo, J. H., Yoon, S., et al. (2019). A paper-based platform for long-term deposition of nanoparticles with exceptional redispersibility, stability, and functionality. *Particle and Particle Systems Characterization, 36*, 1800483. https://doi.org/10.1002/ppsc.201800483

Deng, M., Liao, C., Wang, X., Chen, S., Qi, F., Zhao, X., & Yu, P. (2019). A paper-based colorimetric microfluidic sensor fabricated by a novel spray painting prototyping process for iron analysis. *Canadian Journal of Chemistry, 97*, 373–377. https://doi.org/10.1139/cjc-2018-0346

Deng, J., Lu, Z., Ding, L., Li, Z.-K., Wei, Y., Caro, J., & Wang, H. (2021). Fast electrophoretic preparation of large-area twodimensional titanium carbide membranes for ion sieving. *Chemical Engineering Journal, 408*, 127806. https://doi.org/10.1016/j.cej.2020.127806

Desmonda, C., Kar, S., & Tai, Y. (2016). Formation of gold nanostructures on copier paper surface for cost effective SERS active substrate—Effect of halide additives. *Applied Surface Science, 367*, 362–369. https://doi.org/10.1016/j.apsusc.2016.01.154

Diop, D. K., Simonot, L., Destouches, N., Abadias, G., Pailloux, F., Guérin, P., & Babonneau, D. (2015). Magnetron sputtering deposition of Ag/TiO_2 nanocomposite thin films for repeatable and multicolor photochromic applications on flexible substrates. *Advanced Materials Interfaces, 2*, 1500134. https://doi.org/10.1002/admi.201500134

Dong, Z., Liu, H., Yang, X., Fan, J., Bi, H., Wang, C., et al. (2021). Facile fabrication of paper-based flexible thermoelectric generator. *Npj Flexible Electronics, 5*, 6. https://doi.org/10.1038/s41528-021-00103-1

Du, J.-B., Yang, L., Jin, X., Liu, C.-L., Wang, H.-H., & Wang, X.-F. (2022). Spray deposition of vinyl tris (2-methoxyethoxy) silane-doped Ti3C2Tx MXene hole transporting layer for planar perovskite solar cells. *Journal of Alloys and Compounds, 900*, 163372. https://doi.org/10.1016/j.jallcom.2021.163372

Du, R., Zhong, Q., Tan, X., Liao, L., Tang, Z., Chen, S., et al. (2024). Optimized electrodeposition of Ni2O3 on carbon paper for enhanced electrocatalytic oxidation of ethanol. *ACS Omega, 9*, 30404–30414. https://doi.org/10.1021/acsomega.4c01658

Economou, A., Kokkinos, C., Soulis, D., Pagkali, V., & Prodromidis, M. (2023). Development of electrochemical paper-based devices for field assays. *ECS Meeting Abstracts, MA2023-02*, 2937. https://doi.org/10.1149/MA2023-02622937mtgabs

George, S. M. (2010). Atomic layer deposition: An overview. *Chemical Reviews, 110*, 111–131. https://doi.org/10.1021/cr900056b

Ghanbari, M. H., & Etzold, B. J. M. (2023). Direct electrode modification of paper-based microfluidic sensors through electrodeposition and electropolymerization, In *Proceedings of 2023 IEEE SENSORS Conference,* 29 October–1 November, Vienna, Austria, pp. 1-3. https://doi.org/10.1109/SENSORS56945.2023.10324932

González-Martínez, E., Rekas, A., & Moran-Mirabal, J. (2023). Shrinking devices: Shape-memory polymer fabrication of micro-and nanostructured electrodes. *ACS Applied Materials & Interfaces, 15*, 55183. https://doi.org/10.1002/cphc.202300535

Huang, L., Li, C., Sun, X., Xu, R., Du, Y., Ni, J., et al. (2017). Efficient and hysteresis- less pseudo-planar heterojunction perovskite solar cells fabricated by a facile and solution-saving one-step dip-coating method. *Organic Electronics, 40*, 13–23. https://doi.org/10.1016/j.orgel.2016.10.035

Jur, J. S., Sweet, W. J., Oldham, C. J., & Parsons, G. N. (2011). Atomic layer deposition of conductive coatings on cotton, paper, and synthetic fibers: Conductivity analysis and functional

chemical sensing using "all-fiber" capacitors. *Advanced Functional Materials, 21*, 1993–2002. https://doi.org/10.1002/adfm.201001756

Kaidatzis, A., Psycharis, V., González Sagardoy, M. U., García Martín, J. M., & Niarchos, D. (2017). Au and Ag sputter deposition on printer paper. *Journal of Physics: Conference Series, 939*, 012032. https://doi.org/10.1088/1742-6596/939/1/012032

Klem, M. D. S., Abreu, R., Pinheiro, T., Coelho, J., Alves, N., & Martins, R. (2024). Electrochemical deposition of manganese oxide on paper-based laser-induced graphene for the fabrication of sustainable high-energy-density supercapacitors. *Advanced Sustainable Systems, 8*, 2400254. https://doi.org/10.1002/adsu.202400254

Lee, T.-W., Lee, S.-E., & Jeong, Y. G. (2016). Highly effective electromagnetic interference shielding materials based on silver nanowire/cellulose papers. *ACS Applied Materials & Interfaces, 8*, 13123–13132. https://doi.org/10.1021/acsami.6b02218

Li, Y., Zhang, K., Zhao, J., Ji, J., Ji, C., & Liu, B. (2016). A three-dimensional silver nanoparticles decorated plasmonic paper strip for SERS detection of low-abundance molecules. *Talanta, 147*, 493–500. https://doi.org/10.1016/j.talanta.2015.10.025

Li, M., Xiong, P., Yan, F., Li, S., Ren, C., Yin, Z., et al. (2018). An overview of graphene-based hydroxyapatite composites for orthopedic applications. *Bioactive Materials, 3*, 1–18. https://doi.org/10.1016/j.bioactmat.2018.01.001

Lin, D., Li, B., Qi, J., Ji, X., Yang, S., Wang, W., & Chen, L. (2020). Low cost fabrication of microfluidic paper-based analytical devices with water-based polyurethane acrylate and their application for bacterial detection. *Sensors and Actuators B: Chemical, 303*, 127213. https://doi.org/10.1016/j.snb.2019.127213

Mac Craith, B. D., Mc Donagh, C., McEvoy, A. K., Butler, T., O'keeffe, G., & Murphy, V. (1997). Optical chemical sensors based on sol-gel materials: Recent advances and critical issues. *Journal of Sol-Gel Science and Technology, 8*, 1053–1061. https://doi.org/10.1023/A:1018338426081

Maho, A., Nayak, S., Gillissen, F., Cloots, R., & Rougier, A. (2023). Film deposition of electrochromic metal oxides through spray coating: A descriptive review. *Coatings, 13*, 1879. https://doi.org/10.3390/coatings13111879

Malik, S., Singh, J., Saini, K., Chaudhary, V., Umar, A., Ibrahim, A. A., et al. (2024). Paper-based sensors: Affordable, versatile, and emerging analyte detection platforms. *Analytical Methods, 16*, 2777–2809. https://doi.org/10.1039/D3AY02258G

Mekonnen, M. L., Workie, Y. A., Su, W.-N., & Hwang, B. J. (2021). Plasmonic paper substrates for point-of-need applications: Recent developments and fabrication methods. *Sensors and Actuators B: Chemical, 345*, 130401. https://doi.org/10.1016/j.snb.2021.130401

Nery, E. W., & Kubota, L. T. (2013). Sensing approaches on paper-based devices: A review. *Analytical and Bioanalytical Chemistry, 405*, 7573–7595. https://doi.org/10.1007/s00216-013-6911-4

Nohria, R., Khillan, R. K., Su, Y., Dikshit, R., Lvov, Y., & Varahramyan, K. (2006). Humidity sensor based on ultrathin polyaniline film deposited using layer-by-layer nano-assembly. *Sensors and Actuators B: Chemical, 114*, 218–222. https://doi.org/10.1016/j.snb.2005.04.034

Nurak, T., Praphairaksit, N., & Chailapakul, O. (2013). Fabrication of paper-based devices by lacquer spraying method for the determination of nickel (II) ion in waste water. *Talanta, 114*, 291–296. https://doi.org/10.1016/j.talanta.2013.05.037

Oke, J. A., & Jen, T.-C. (2022). Atomic layer deposition and other thin film deposition techniques: From principles to film properties. *Journal of Materials Research and Technology, 21*, 2481–2514. https://doi.org/10.1016/j.jmrt.2022.10.064

Pinheiro, T., Ferrão, J., Marques, A. C., Oliveira, M. J., Batra, N. M., Costa, P. M. F. J., et al. (2020). Paper-based in-situ gold nanoparticle synthesis for colorimetric, non-enzymatic glucose level determination. *Nanomaterials, 10*, 2027. https://doi.org/10.3390/nano10102027

Rahimi, R., Ochoa, M., & Ziaie, B. (2018). Comparison of direct and indirect laser ablation of metallized paper for inexpensive paper-based sensors. *ACS Applied Materials & Interfaces, 10*, 36332–36341. https://doi.org/10.1021/acsami.8b09598

Ravikumar, T., Thirumalaisamy, L., Madanagurusamy, S., & Sivaperuman, K. (2023). Substrate temperature dependent ammonia gas sensing performance of zinc ferrite thin films prepared by spray pyrolysis technique. *Journal of Alloys and Compounds, 959*, 170568. https://doi.org/10.1016/j.jallcom.2023.170568

Serfőző, A., Csík, G. A., Kormányos, A., Balog, A., Janáky, C., & Endrődi, B. (2023). One-step electrodeposition of binder-containing Cu nanocube catalyst layers for carbon dioxide reduction. *Nanoscale, 15*, 16734–16740. https://doi.org/10.1039/D3NR03834C

Sharifi, F., Ghobadian, S., Cavalcanti, F. R., & Hashemi, N. (2015). Paper-based devices for energy applications. *Renewable and Sustainable Energy Reviews, 52*, 1453–1472. https://doi.org/10.1016/j.rser.2015.08.027

Shen, C., Yin, Z., Collins, F., & Pinna, N. (2022). Atomic layer deposition of metal oxides and chalcogenides for high performance transistors. *Advancement of Science, 9*, e2104599. https://doi.org/10.1002/advs.202104599

Shepelin, N. A., Tehrani, Z. P., Ohannessian, N., Schneider, C. W., Pergolesi, D., & Lippert, T. (2023). A practical guide to pulsed laser deposition. *Chemical Society Reviews, 52*, 2294–2321. https://doi.org/10.1039/D2CS00938B

Wang, J., He, J., Kan, D., Chen, K., Song, M., & Huo, W. (2022). MXene film prepared by vacuum-assisted filtration: Properties and applications. *Crystals, 12*, 1034. https://doi.org/10.3390/cryst12081034

Wang, C., Liu, Q., Song, H., & Jiang, Q. (2023). Vacuum filtration method towards flexible thermoelectric films. *Soft Science, 3*, 34. https://doi.org/10.20517/ss.2023.25

Yao, B., Zhang, J., Kou, T., Song, Y., Liu, T., & Li, Y. (2017). Paper-based electrodes for flexible energy storage devices. *Advancement of Science, 4*(7), 1700107. https://doi.org/10.1002/advs.201700107

Zhan, Y., Hao, X., Wang, L., Jiang, X., Cheng, Y., Wang, C., et al. (2021). Superhydrophobic and flexible silver nanowire-coated cellulose filter papers with sputter-deposited nickel nanoparticles for ultrahigh electromagnetic interference shielding. *ACS Applied Materials & Interfaces, 13*, 4623–14633. https://doi.org/10.1021/acsami.1c03692

Zhang, Z., Feng, C., Liu, C., Zuo, M., Qin, L., Yan, X., et al. (2020). Electrochemical deposition as a universal route for fabricating single-atom catalysts. *Nature Communications, 11*, 1215. https://doi.org/10.1038/s41467-020-14917-6

Zhou, Y., Zhou, W., & Xia, G. (2023). Preparation and innovative design applications of paper-based aluminized film. *Coatings, 13*, 1751. https://doi.org/10.3390/coatings13101751

Chapter 26
Writing of Paper Electronics

Tatiana L. Simonenko, Nikolay P. Simonenko, Philipp Yu. Gorobtsov, Elizaveta P. Simonenko, and Ghenadii Korotcenkov

26.1 Introduction

Growing digitalization of all life aspects, the Internet of Things (IoT) and artificial intelligence development serve as a powerful motivation for researches devoted to the creation of various intelligent electronic systems for household and specialized applications. Consumption rates of electronic devices are steadily increasing every year, which requires intensification of their production, resulting in a significant environmental impact associated with the production of electronic components and devices, as well as with the recycling of such residues, the so-called electronic waste. One of the crucial steps toward careful environmental management while maintaining sustainable technological development and quality of life is the transition to a circular economy that maximizes the use of renewable resources and their eco-friendly conversion. In this context, paper/cellulose draws attention as one of the most widespread and accessible materials, being 100% biodegradable and characterized by the highest recyclability compared to other solid wastes (Liu et al., 2017a; Nandy et al., 2021). Furthermore, the development of cellulose industry allows the creation of many different types of paper with the required density and degree of transparency, which makes paper a promising alternative to plastic, glass, and silicon in modern electronic design. This chapter will discuss approaches to manual and automated writing of paper-based electronic components and devices, illustrated by successful examples of their implementation by various research groups.

T. L. Simonenko (✉) · N. P. Simonenko · P. Y. Gorobtsov · E. P. Simonenko
Kurnakov Institute of General and Inorganic Chemistry of the Russian Academy of Sciences, Moscow, Russia

G. Korotcenkov
Department of Physics and Engineering, Moldova State University, Chisinau, Moldova

G. Korotcenkov (ed.), *The Handbook of Paper-Based Sensors and Devices*,
https://doi.org/10.1007/978-3-031-91080-7_26

26.2 Handwriting

Writing is undoubtedly one of the civilization cornerstones, as an essential tool for information transfer, cultural and historical heritage conservation, and humankind's progress. Over time, not only writing systems have evolved and changed but also writing utensils themselves. Modern electronics demands in the context of miniaturization of its components, development of flexible/stretchable and wearable devices, which manufacture does not require large financial expenses and causes minimal harm to the environment (zero "e-waste" paradigm (Nandy et al., 2021)), made the scientific community reconsider the possibilities offered by handwriting. For instance, this technology, with no need for expensive high-tech production equipment and a considerable amount of time, allows a wide range of users to apply functional layers having different compositions of the required, including complex geometry, in the manufacture of customizable ("Do-it-Yourself" concept, DIY) prototypes of components (e.g., capacitors, resistors, diodes) (Costa et al., 2018), circuits (Liu et al., 2017b), and devices for specialized electronics in the fields of electromechanical/electrochemical and gas sensing (Loghin et al., 2018; Stefano et al., 2022), microfluidics (Ghaderinezhad et al., 2017; Rao et al., 2020), memory systems (Park et al., 2017), and alternative energy (Rao et al., 2022; Yeasmin et al., 2021). The undoubted advantage of handwriting is also the possibility of employing a variety of inexpensive and easy-to-use writing tools (brush pen, pencil, fountain pen, marker pen, ball pen, and rollerball pen) as well as available flexible biodegradable substrates, primarily paper-based.

26.2.1 Pens

Writing instruments used for the application of functional coatings to paper substrates by handwriting can be categorized into two main groups: (1) solid-lead-based pencils, consisting of solid phase particles and binders; (2) ink-based pens, providing application of inks, which are true solutions or disperse systems (Liu et al., 2020b). One of the most prominent representatives of the first group is graphite pencil, characterized by commercial availability and a wide variety of hardness (marked by the letter H) and blackness (indicated by the letter B) depending on the concentration ratio of graphite and binder in its composition (designated by a number before the corresponding letter, e.g., 2H, 9B), which in turn affects the electrical conductivity of the structures formed (Li et al., 2016). In addition, this parameter also depends on the quality of contact between graphite particles in the patterns applied with a pencil, which makes them vulnerable, in particular, to mechanical effects on the substrate (expansion/compression). For example, pencils labeled 9B allow to obtain the most conductive structures (Yao et al., 2017), while patterns based on "hard" pencils (e.g., HB) are the most sensitive to substrate deformation and show the most significant decrease in conductivity compared to samples applied

with “soft” pencils (Lin et al., 2014). Considering the features of pencils with different hardness and blackness levels, a variety of pencil-on-paper devices such as resistors (Kurra & Kulkarni, 2013), capacitors (Thompson, 2017), strain gauges and chemiresistors (Lin et al., 2014), as well as electrochemical sensor electrodes (Santhiago et al., 2017) and LED electrodes (Kim et al., 2021) can be created. Commercial pencils provide an opportunity to generate patterns characterized by high chemical stability, resistance to moisture and ultraviolet radiation, simple in terms of their fabrication and subsequent processing; however, they are limited regarding the composition and microstructure of the resulting coatings. The solution to the above problem is possible with the shift toward home-made pencils, allowing to optimize the characteristics of pencils in each specific case and adapt this technology to the individual task. For example, Park et al. (2017) reported the formation of highly conductive electrode structures deposited on two types of paper (A4-size copy and print paper) using a composite pencil consisting of silver nanoparticles and reduced graphene oxide (AgNPs/rGO). The sheet resistance value of the AgNPs/rGO lines thus formed was about 0.32 Ω/sq. Evaluation of mechanical stability showed that after 35 folding cycles the resistance of electrode structures increased from 0.6 to 1.4 Ohm. At the same time, exposure of the studied samples in the media of polar (water, ethanol) and nonpolar (toluene) solvents for 6 h had almost no effect on the discussed parameter, which indicates high chemical stability of the conductive coatings obtained. In addition, Park et al. (2017) demonstrated the promising potential of the developed hybrid AgNPs/rGO pencil for memory device creation (Fig. 26.1, left). For this purpose, two lines for electrodes and one for the resistive switching layer (the specified layer was formed using a pencil containing a reduced amount of silver nanoparticles) were applied on the paper. Within 38 operating cycles, the fabricated device showed stable operation even in the folded state and a quite clear set and reset process with a consistent on/off ratio of about 100. Additionally, it is noted that the option of rapid recycling (e.g., combustion) of such a portable flexible device allows for a high protection level of the data stored. The applicability of homemade pencils for the creation of paper-based microfluidic devices (microPADs), in particular the fabrication of simple platforms for point-of-care diagnostic assays, was investigated by Mitchell et al. (2015). In this case, enzymes serving as reagents for biochemical assays were distributed in solid matrices based on 75% poly(ethylene glycol) methyl ether and 25% graphite powder (Fig. 26.1, right). In each case, up to 15% w/w of the reagent was added to the matrix composition, and then, by pressing (25 kN), custom pencils were formed and the corresponding coatings were applied in different zones of microPADs obtained by the wax printing method. It was found that the pressing process practically does not affect the enzyme activity, which remains for 63 days regardless of the method of their storage (in the pencil itself or as a coating applied on paper), which is an important factor for this type of sensitive biological reagents. At the same time, the accuracy of glucose detection in the composition of test samples using receptor layers obtained with the developed pencils was not inferior to the results obtained by the traditional application of enzymes from solutions. Besides, Mitchell et al. (2015) pointed to the universal use of such pencils both in automated scaling of microPADs

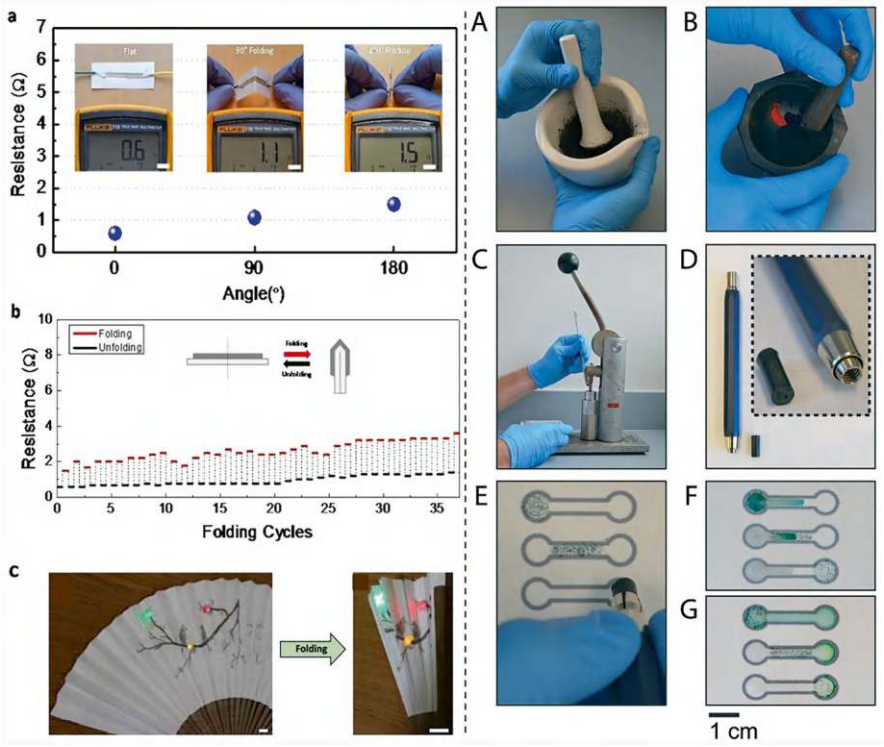

Fig. 26.1 (Left) Electrical and mechanical properties of conductive lines drawn by a hand-written conductive pencil on papers. (**a**) Resistance measurement of the drawn conductive line (length of 4 cm and width of 3 mm) for unfolded, 90°-folded, and entirely-folded (180°) states. (**b**) Measured resistance data with multiple folding cycles. Both unfolded (black line) and folded (red line) resistances were measured with the number of folding cycles. (**c**) Pencil drawing art on a handheld folding fan. (Reproduced with permission from Park et al. (2017). Copyright 2017, Royal Society of Chemistry). (Right) Fabrication and use of reagent pencils. (**a**) The matrix for the pencil composed of 75% PEGME and 25% graphite is pulverized. (**b**) Reagents (blue and yellow dye) are added to the matrix, pulverized, and mixed. (**c**) The resulting mixture is added to a pellet press and pressed into a pellet. (**d**) The pellet is loaded into a mechanical pencil holder. (**e**) The reagent pencil is used to deposit reagents on microPADs in three distinct areas: the sample zone, channel, and test zone. (**f**) When water is added to the sample zone of the devices, it dissolves the reagents from the pencil traces and transports them into the test zone. (**g**) The final appearance of the reagents in the test zone depends on the location of the pencil trace on the device. (Reproduced with permission from Mitchell et al. (2015). Copyright 2015, Royal Society of Chemistry)

using pen plotters and in small-scale manual production of devices at the point of care.

The group of ink-based pens includes such varieties of writing instruments as brush pen, fountain pen, marker pen, ball pen, and rollerball pen. The earliest of these was the brush pen (which can also include the paintbrush), which is a simple tool in the form of a filament bundle (natural and synthetic fibers can be used) attached to a handle. The tip of the brush pen can have different size and shape

(conical, flat), which allows to form lines of different geometry. Before coating the substrate surface (in this case both flexible substrates like paper and more "rigid," for example, glass, plastic can be used), it is necessary to dip the tip of the brush pen in a container with ink, the viscosity of which can vary within a fairly wide range (from true solutions to concentrated pastes). It is noted that the speed of line formation by this method should not exceed 1–2 cm/s to ensure their continuity and uniformity (Li et al., 2016). Other types of pens, unlike the brush pen, do not need to be immersed in a vessel with ink, as they contain a cartridge or reservoir, which is filled with the necessary solution to create patterns. In the case of the fountain pen, the ink flows from the cartridge to the nib slit through a feeder consisting of two capillaries, one for the ink supply and the other for the air supply from the nib slit, compensating for the pressure differential in the ink reservoir. The operation of this writing device is based on the gravity and capillary force balance, preventing the ink from leaking beyond the writing process. Upon contact with the substrate, the nib slit expands, thus reducing the effect of capillary forces on the ink, allowing it to flow out under the influence of gravity (Liu et al., 2017a). Despite the possibility of using different types of inks and substrates, this technology is not widespread today due to the difficulties in applying functional inks. For example, the imbalance that occurs between the air holding pressure in the cartridge and the pressure drop across the capillary valve during use can lead to unstable and uneven ink application as well as ink spattering (Nikolov et al., 2020).

One of the most popular and widespread tools for drawing structures on paper is the ball pen (its roller ball pen version, filled with water-based ink, is also actively used). This type of pen has a simpler and more reliable design compared to a fountain pen, and the distribution of ink on the substrate surface is made by a ball rotating on the tip of the rod filled with ink. The widespread popularity of ballpoint pens in various fields of human activity provides a wide range of commercial variants of these writing devices, which can easily form lines with a thickness of several tens of microns, with width ranging from 250 μm to 1 mm (Li et al., 2016). In addition, ballpoint pens are compatible with different types of inks: carbon (Li et al., 2015), metal (Ghosale et al., 2016; Russo et al., 2011), as well as inks based on organic semiconducting crystals (Zhang et al., 2017) and immunoreagents (Russo et al., 2024). However, the considered variant of pens may have limitations in terms of drawing uniform continuous lines on hard substrates and also requires optimization of ink viscosity in such a way that its uncontrolled flow or, on the contrary, clogging of the pen tip does not occur. Also, Lee et al. (2023) noted that drawing patterns with ballpoint pens is not absolutely even, as a close look at the texture of the written lines reveals a narrow white band (an area not completely saturated with ink), which requires a more detailed examination of the wetting of the pen's ball with different inks to optimize the writing performance of this particular type of writing utensil.

Marker pens (capillary pens can be included in this type) also find application in the formation of various paper electronics components. In this case, the low-viscosity ink in the reservoir impregnates the fiber tip of the marker, providing convenient coating on substrates of different nature (Jeong et al., 2019). Furthermore, commercial markers can form even finer lines compared to ballpoint pens, reaching

a resolution of 100 μm. It is also worth noting that changing ink in such a pen is quite convenient and fast, while good compatibility with water- and oil-based inks is observed. Zhao et al. (2017) considered an example of using a marker pen filled with ink based on oxidized multi-walled nanotubes dispersed in water. With the help of such a marker, a receptor layer of the corresponding composition for a humidity sensor was drawn on the paper surface, the response of which was about five times higher than the analogous parameter for sensors on ceramic substrates. At the same time, the response drop in the case of the obtained paper sensor was only 6.7% even when it was half-folded.

26.2.2 Inks

Due to the considerable diversity of commercially available pens and their features, it becomes possible to use a wide variety of functional inks with different viscosities (true solutions, suspensions, and pastes) and electrical conductivity (materials with metallic and semiconductor conductivity, as well as dielectrics) in the formation of electronic and microfluidic devices on paper. The materials used in the manufacture of functional inks for the above purpose can be divided into the following groups: (a) carbon materials; (b) metals; (c) metal oxides; (d) quantum dots (QDs); (e) organic and inorganic halide perovskites; (f) polymers; and (g) reagents for biochemical assays.

In the case of carbon-based functional inks, the most commonly used solid phase components are carbon nanotubes (CNTs) (Liao et al., 2019; Zhao et al., 2017), graphite (Li et al., 2015; Pradela-Filho et al., 2017, 2020), carbon black (Sritapunya et al., 2011), and graphene-based materials (Polychronopoulos & Brouzgou, 2024), while water (Liao et al., 2019; Zhao et al., 2017), alcohols (Amjadi et al., 2015; Chaya Devi et al., 2017), acetone (Pradela-Filho et al., 2017), and dimethylformamide (DMF) (Htwe et al., 2021) are used as solvent. Various surfactants (e.g., sodium dodecyl sulfate (Loghin et al., 2018), Triton X-100 and sodium dodecylbenzene sulfonate (Zhang et al., 2019)) and binders (vinyl resin (Li et al., 2015), aqueous acrylic resin (Liao et al., 2019), nail polish (Pradela-Filho et al., 2017), and glass varnish (Pradela-Filho et al., 2020)) are often employed to achieve sedimentation stability of the resulting inks and increase the adhesion of the coatings applied. Carbon-based materials remain among the most popular in the development of various paper electronic devices. As noted above, they can be used as components of moisture sensors, as well as in the creation of proximity sensors, as, for example, it was shown by Liao et al. (2019), when a functional ink based on dihydroxyphenyl-functionalized multi-walled carbon nanotubes/carbon black/graphite filled in a marker was used to draw conductive ring structures on paper coupled with a commercial capacitive sensing chip (MTCH112). In this case, with a line thickness of 40 μm, the surface resistivity reached 29 Ω/sq., and the fabricated structures could withstand more than 2000 folding cycles with only 11% increase in the resistance

value of the flexible circuit. The formation of flexible electrochemical sensors also requires the use of carbon electrodes. The possibility of three-electrode sensor systems patterning by means of graphite-based ink-brushing with glass varnish and nail polish as binders was demonstrated by Pradela-Filho et al. (2017, 2020). The results for the devices obtained (Pradela-Filho et al., 2020) indicate the ability to detect analytes such as dopamine (15–100 μmol/L; limit of detection (LOD), 4.1 μmol/L), catechol (10–1000 μmol/L; LOD, 9.0 μmol/L), hydroquinone (10–1000 μmol/L; LOD, 5.3 μmol/L), and in the case of sensors drawn with graphite powder/nail polish functional ink (Pradela-Filho et al., 2017), the LOD value of dopamine increases slightly to 5.2 μmol/L. Ferreira de Oliveira et al. (2022) used a marker with CNT-based ink (8 mg/mL) to draw an amperometric electrode. They found that the ohmic resistance value of the final coating decreased by about two orders of magnitude when the number of layers increased from 5 (~580 kΩ) to 25 (18.62 kΩ). The chronoamperometry results for the final analytical system based on CNT electrode by introducing $K_4[Fe(CN)_6]$ as the redox probe showed that there was a linear relationship between the current response and analyte concentration in the range of 0.5–3.5 mmol/L, and the linearity coefficient was 0.09981.

Metal-based inks are an indispensable component of electronic devices printed or drawn on flexible substrates. In order to produce them, noble metals (platinum, gold, silver) or copper particles (Liu et al., 2020b) dispersed in water (Russo et al., 2011), ethanol, glycerol, ethylene glycol (Li & Chen, 2014), or toluene (Terzi et al., 2017) are most frequently used. Additionally, binders (e.g., polystyrene (Terzi et al., 2017)) or viscosity regulators (e.g., hydroxyethyl cellulose (Russo et al., 2011)) can further be added to the ink composition. Studies proposing gallium-indium alloys as inks for flexible electronics (Zheng et al., 2013) as well as their mixtures with nickel nanoparticles (Chang et al., 2018) are also encountered. The considered type of inks allows achieving high values of electrical conductivity, but can significantly increase the cost of the final devices (primarily when using Pt and Au inks), and in some cases (Ag- and Cu-ink) requires additional encapsulating layers to prevent undesirable metal particles oxidation. It should be taken into account that the presence of such antioxidant additives can adversely affect the conductivity of the drawn patterns, which necessitates their subsequent heat treatment at rather high temperatures (150–200 °C). This factor is especially critical considering the low thermal stability of paper substrates. In particular, Ghosale et al. (2016) report the formation of inks based on silver nanoparticles encapsulated with oleylamine (AgNPs/OLA) to create flexible conducting electrode structures for electroanalytical applications. Using roller balls filled with AgNPs/OLA-ink, a coating of appropriate composition with 8.0 cm × 0.20 cm dimensions and 1 × 1 cm^2 bottom area, of 5.5 μm thickness, was manually applied on the surface. It was shown that heat treatment at 150 °C for 1 h allowed to achieve the conductivity value of 0.11–105 S/cm, whereas at higher temperatures the paper substrates started to deform or degrade.

Creation of effective low-cost semiconductor devices also demands approaches to the formation of inks based on metal oxides with different conductivity types and quantum dots of different compositions, suitable in their microstructure and rheological characteristics for coating on paper substrates using available writing

instruments. Grey et al. (2017) proposed to use a parallel metal plate pen, which allows the formation of lines from 0.5 to 5.7 mm wide, for the deposition of zinc oxide layers when forming UV sensors and field effect transistors. In the first step, source and drain contacts were screen-printed in the form of interdigitated structures on one side of the paper and gate contacts on the backside. Further, a layer of zinc oxide was applied over the interdigitated electrodes using a parallel metal plate pen filled with two-phase inks (a mixture of 50 wt% ZnO aqueous suspension and zinc nitrate-hexamethylenetetramine (HMT) aqueous system). According to Grey et al. (2017), the use of the described system as a functional ink increases its final viscosity while avoiding cracking of the final film (which was observed when using only ZnO suspension without the addition of a mixture of zinc salt and base). The obtained final zinc oxide film was homogeneous, did not contain any defects in the form of breaks, and its thickness was about 1.5 μm. The photocurrent generated by the sensor on its basis under UV irradiation reached 3.4 mA cm^{-2} with a switching time of about several seconds. Transistors based on ZnO film, in which the paper simultaneously plays the role of substrate and dielectric, demonstrated on/off current ratios (I_{On}/I_{Off}) of about two orders of magnitude and field effect mobility close to 5×10^{-3} cm^2 V^{-1} s^{-1}. Ersu et al. (2023) evaluated the performance of marker pens (1.3 mm line width) in the context of applying various types of inks to paper, including molybdenum oxide (MoO_3 was dispersed in a mixture of ethanol:water = 85:15 v/v with 0.1 mL Fairy liquid added as a surfactant) and quantum dots (CdS_xSe_{1-x}/ZnS in chloroform and Ag_2S in toluene). After deposition, the coatings showed generally expected optical characteristics: MoO_3 lines, almost indistinguishable on paper in the visible range, darkened under UV irradiation (365 nm), whereas Ag_2S coatings exhibited IR photoluminescence. In the case of CdS_xSe_{1-x}/ZnS lines, the observed photoluminescence color deviated from the classical one (the characteristic maximum at 515 nm was absent), which is due to the superposition of signals from quantum dots with paper blue emission caused by the presence of bleaching components in it. With application of a pen plotter and markers filled with ink based on molybdenum oxide and silver sulfide, the possibility of quick (within 5 min) drawing of QR codes, easily readable by a smartphone, to paper carriers was demonstrated.

Perovskite-based materials play an important role among different types of functional inks, which are actively used in the development of various optoelectronic devices (in particular, photodetectors and light-emitting diodes (Zhao et al., 2023)). The efforts of many scientific groups are focused on designing an affordable and efficient approach to create perovskite-based coatings with competitive performance parameters (e.g., high on/off ratio and responsivity, as well as satisfactory detectivity) on flexible substrates. In particular, the formation of a perovskite-based photosensitive layer on various types of paper (weighing paper, office-copy paper, and filter paper) was demonstrated by Stefano et al. (2022). The application was carried out using a commercial marker pen filled with $CH_3NH_3PbBr_3$-based ink (0.5 mol/L) in a DMF medium. It was revealed that after the first ink layer was applied, as the solvent evaporated, a seed layer was formed, on which crystal growth occurred during the application of subsequent layers, resulting in the formation of

an integrated single-crystal perovskite film. The final photodetector on its basis demonstrated responsivity of 4.2 mA W^{-1} at a low operational bias voltage of 4 V. One of the serious problems of halide perovskite nanocrystals (PNC) is the instability of their characteristics when exposed to moisture, oxygen, light, heating, and polar solvents, leading to active degradation of the whole device. Karabel Ocal et al. (2022) tried to solve this problem by using natural carnauba wax (CW) as an encapsulating layer for perovskite structures. It was added to the reaction system during the synthesis of green-emitting $CsPbBr_3$, after which the resulting final material (PNC-CW) was then employed both in solid form (as a stand-alone pencil, glue pen cartridge, or playdough) and as a colloidal system in toluene medium. It was shown that the films formed with PNC-CW exhibit satisfactory stability in ambient atmosphere, in particular after 3 months the material retained about 83% of the photoluminescent (PL) signal intensity compared to the initial measurements, and withstood short-term heating up to 150 °C with retention of 80% PL intensity. In addition, a study of the moisture resistance of PNC-CW film at 60 °C also showed encouraging results (after 20 days, about 50% PL signal was retained).

Functional inks based on polymers, depending on their conductivity, can be used either to create contact pads and electrodes or to form hydrophobic barriers, for example, in the fabrication of microfluidic devices (Mani et al., 2019). In this case, the process of obtaining such inks can be quite simple, as it was shown by Prestowitz et al. (2021), when a standard technique for obtaining polyaniline nanofibers (polymerization of aniline using ammonium persulfate in HCl) with their subsequent dispersion in a water-alcohol mixture to obtain the corresponding functional ink is proposed. It is noted that this technique is convenient and illustrative for teaching students of technical and engineering specialties to prepare inks of different viscosity, as well as to study the influence of their characteristics on the process of coating (smoothness of writing, drying rate, wettability on paper) with a ballpoint pen in the manufacture of paper-based chemical and mechanical sensors or simple circuits as well as LED-enhanced art. In the case of hydrophobic barrier formation, it is also possible to use inexpensive available polymers, as has been shown, in particular, by Mani et al. (2019), when the capabilities of a commercial correction fluid were tested in this context. Although the precise composition of such products is obscure, they typically include titanium dioxide, resins (most commonly polyvinyl chloride), solvents (water, alcohols), and colorants. After application, the correction fluid does not require an additional heating stage. According to test results, the hydrophobic ring barriers formed in this way showed high chemical resistance to various solvents (water, dimethyl sulfoxide (DMSO), acetone, ethanol, DMF, acetonitrile, phosphate-buffered saline, 1N HCl, glycerol, and Tween-20) after drying, and scanning electron microscopy results indicate reliable overlap of paper pores in the area of the correction fluid application. Standard colorimetric assays for glucose and protein determination performed with the drawn hydrophobic regions confirmed correct coloration of the receptor regions according to the analytes concentration, indicating the promising potential of the approach described for manual rapid preparation of microPADs for bioassays. A more environmentally friendly type of ink for hydrophobic barriers of paper-based analytical devices tested by

Romanholo et al. (2024) is based on the use of "bio-ink" on a rosin solution in ethanol (0.8–1.2 g/mL). The chemical resistance of the drawn barriers to aqueous systems containing sulfuric acid, sodium hydroxide, phosphoric acid, cetyltrimethylammonium bromide, and TRITON X-100, as well as to a number of organic solvents (DMSO and acetone) was found to be the highest, while the resistance to alcohols (ethanol and isopropanol) was 9/10, and in the case of DMF 8/10. Moreover, the chemical resistance of the barriers applied with bio-ink was higher compared to those formed with wax or commercial markers. The barrier structures obtained using rosin-based inks showed promise in the development of pH PADs and colorimetric sensors for cholecalciferol. Comparison of the characteristics of a commercial pH meter and the fabricated pH PAD showed no statistically significant difference between these devices (correlation coefficient was 0.985). In turn, the final colorimetric sensor was characterized by the limits of detection and quantification of analyte 0.08 and 0.26 g/L, respectively.

The possibilities of handwriting also attract attention of biochemistry specialists, since it opens perspectives for the development of affordable yet sufficiently accurate and sensitive paper biosensors and bioarrays, which is especially important from the point of view of developing low-cost point-of-care (POC) testing capabilities. A recent study by Russo et al. (2024) emphasizes the importance of designing not only paper-based lateral flow immunoassays (LFIAs) that allow qualitative assessment of various analytes in biological fluids, as well as environmental and food quality analysis, but also highlights the need to develop Surface Enhanced Resonance Raman Scattering (SERRS)-based LFIAs that enable the transition to quantitative analysis of the samples under study. In particular, this work describes an approach to apply penicillin-bovine serum albumin (1 mg-ml^{-1}) and anti-rabbit antibody (0.7 mg-ml^{-1}) dissolved in phosphate buffer (pH 7.4) using fountain pens to the test (T) and control (C) lines of a fabricated SERRS-LFIA device for the determination of penicillin G in milk. It was shown that this type of writing instrument enables uniform lines of biochemical reagents to be applied while maintaining their activity and avoiding damage to the sensitive nitrocellulose-based membrane. The final SERRS-LFIA assay demonstrated a visual LOD of 20 ppm and a range of quantification (IC_{10}-IC_{90}) of 0.03–97.5 ppm, which indicates the potential of the proposed methodology for the development of portable test pads for other practically relevant analytes.

26.2.3 Robot-Writing

As discussed above, handwriting with a variety of pens and pencils (both commercial and home-made) offers significant potential for the fabrication of a broad class of electronic devices on flexible substrates (including various paper types). Nevertheless, the quality and accuracy of handwriting patterns may vary considerably among different performers of the task. At the same time, low-cost pen plotters or positioning systems with the possibility of holding writing instruments in them

can significantly increase process reproducibility when it comes to the targeted formation of coatings of various, including complex, geometries in the prototyping process (Ersu et al., 2023; Simonenko et al., 2021, 2023). Moreover, automation of this process helps to significantly reduce its duration and, if necessary, to proceed to large-scale production of pen-on-paper electronics (Singhal et al., 2021). The use of supplementary software makes it possible to build digital models of patterns before transferring them to paper, to set the necessary distance between the lines to be drawn while studying the influence of various writing parameters (pressure force, movement speed of the writing instrument, spatial resolution, and the number of layers to be formed) along with the type of pens/pencils used on the resulting coating characteristics (uniformity, continuity, roughness, thickness), which, in turn, significantly affect its functional performance (Franke & Rose, 2004; Franke et al., 2005; Loghin et al., 2021). Thus, the involvement of robotic systems makes it possible to choose the optimal conditions for patterning, taking into account the characteristics of the ink, writing tools, and substrates used, while the possibility of quick pen replacement (unlike, for example, household printers) facilitates and accelerates the formation of multilayer structures of different composition and purpose. In particular, Jeong et al. (2019) demonstrated the successful creation of QD-LED displays on the surface of glass, plastic (polyethylene naphthalate), and photopaper (260 g/m^2; thickness, 0.25 mm) using a custom-built three-axis micropositioning system and eight felt-tip pens filled with different inks (Fig. 26.2). The layers were applied in six consecutive steps: (1) first, an anode layer was applied (PEDOT:PSS (1:2.5 by weight) in aqueous solution with the addition of 5 wt% DMSO), (2) then a hole injection layer (PEDOT:PSS (1:6 by weight) in aqueous solution), (3) followed by hole transfer layer (poly(N-vinylcarbazole) solution in chlorobenzene), (4) after that emission layer was formed (dispersions of CdSeS@ZnS (Red), CdZnSeS@ZnS (Green), and CdZnS@ZnS (Blue) QDs in hexane) and (5) electron transfer layer (dispersion of zinc oxide nanoparticles in ethanol (30 mg/mL)) was drawn, and finally (6) the cathode layer (dispersion of silver nanowires (0.5 wt%) in isopropanol) was fabricated. The device formation was carried out using felt-tip pens with different line widths (0.4 mm and 4 mm), and in order to optimize the drawing parameters, the influence of writing speed (10–30 mm/s) and substrate temperature (20–80 °C) on the thickness and microstructure of the resulting layers was investigated at the first stage of the experiment. It was found that with higher writing speed their thickness increases due to the formation of a supersaturated wet film by capillary flow in the meniscus area (between the substrate and the ink). At the same time, heating the substrate to 60 °C allowed to obtain the most uniform (in terms of microstructure, as well as optical transparency and surface resistivity) polymer films (PEDOT:PSS), which in ordinary cases have the greatest tendency to aggregate compared to other materials used in the described work. In addition, the optimum number of layers (number of drawing cycles - from 1 half cycle to 5 full cycles) for each type of ink used was selected, given their nature and rheology. Evaluation of the luminescent properties of the final QD-LED device showed turn-on voltages of ~7 (R), ~7 (G), and ~ 9 (B) V and maximum luminance values of 125 (Red), 72 (Green), and 5.6 (Blue) cd/m^2 at 9.4, 9.25, and 10.4 V,

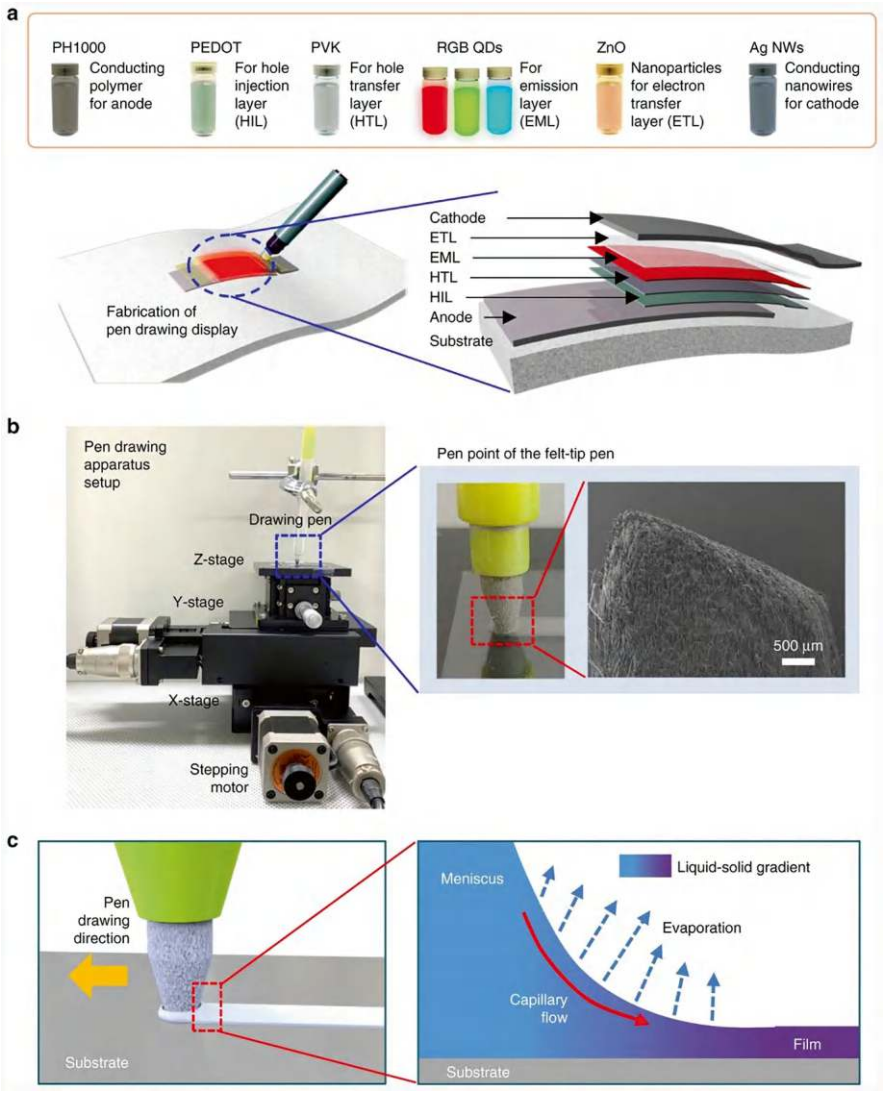

Fig. 26.2 Pen-drawing display. (**a**) Schematic diagram of pen-drawing display with six drawing pens containing anode, hole injection layer (HIL), hole transfer layer (HTL), emission layer (EML), electron transfer layer (ETL), and cathode solutions. A quantum dot light-emitting diode (QD-LED) display fabricated using the pen-drawing method consists of PH1000 (anode), PEDOT:PSS (HIL), PVK (HTL), CdSeS@ZnS (red (R), EML), CdZnSeS@ZnS (green (G), EML), CdZnS@ZnS (blue (B), EML), zinc oxide nanoparticles (ZnO NPs, ETL), and silver nanowires (Ag NWs, cathode). (**b**) Optical image (left) of the pen-drawing apparatus setup. The pen drawing was performed using a custom-built three-axis micropositioning system controlled by a computer-programmable motion controller. Field emission scanning electron microscopy (FE-SEM) image (right) of the pen point of the felt-tip pen. (**c**) Schematic diagram and working principle of film formation through pen drawing. (Reproduced from Jeong et al. (2019). Published 2019 by Springer Nature with open access)

respectively. The current efficiencies were 0.031 (R), 0.020 (G), and 0.004 (B) cd/A at 9.3, 9.25, and 10 V, respectively.

Improving the productivity of the paper electronics manufacturing process can be achieved not only by increasing the drawing speed but also by extending the number of pens used within a single plotter. An example of such an approach was demonstrated by Amin et al. (2017), describing the integration of a pen plotter with a custom-designed multipen holder that allows simultaneous installation of eight marker pens involved in the drawing patterns of a given geometry. Additional optimization of the process was achieved by connecting a continuous ink supply system to the markers fixed in the holder to solve their refilling issue. As a result, 550 hydrophobic barriers in the form of circular areas were applied to the paper in 12 min (if several pens are used, this time can be reduced to 3 min), with a water resistance of about 95%. The colorimetric biological assays produced in this way showed high efficiency in clinical analysis of urine for nitrite, urobilinogen, protein, blood, as well as allowed to estimate the pH value of the liquid under study.

26.3 Direct Laser Writing

When creating modern flexible and wearable electronics, a wide variety of additive technologies and handwriting certainly take an important place; however, many technological stages of functional layers formation within multi-material processing systems currently require laser technologies. The capabilities of lasers allow their active implementation at various steps of miniature electronic and microfluidic device fabrication, including synthesis (Averchenko et al., 2023), doping (Lamberti et al., 2017; Zhu et al., 2021), functionalization (Wei et al., 2020), polymerization (Sones et al., 2014), etching (Kalish et al., 2020), curing (Gao et al., 2020), as well as assembly of the final devices (Bian et al., 2019). Thus, to date, direct laser writing (DLW) has found its application in such fields as micromachining (Mahmud et al., 2016, 2018), lithographic-based techniques (Ocier et al., 2020), and 3D printing approaches (Young et al., 2024), allowing the fabrication of both planar and three-dimensional structures (He et al., 2016; Thekkekara, 2018). According to the review paper by Pinheiro et al. (2024), depending on the final result obtained when laser radiation interacts with a material, three variations of this method are distinguished (Fig. 26.3): subtractive DLW, based on ablation and etching processes to remove material in a selected area (often used for micromachining or material drilling); additive DLW, which includes synthesis procedures with simultaneous patterning of material of the required geometry using precursors (realized in the framework of photon-induced chemical reactions); and transformative DLW, which implies involving direct irradiation of materials with subsequent transformation of their chemical or structural characteristics without significant ablation or the need to introduce additional precursors (examples include crystallization of amorphous materials or laser doping of semiconductors). When using the DLW method, it is important to consider parameters such as wavelength, laser energy and power, laser

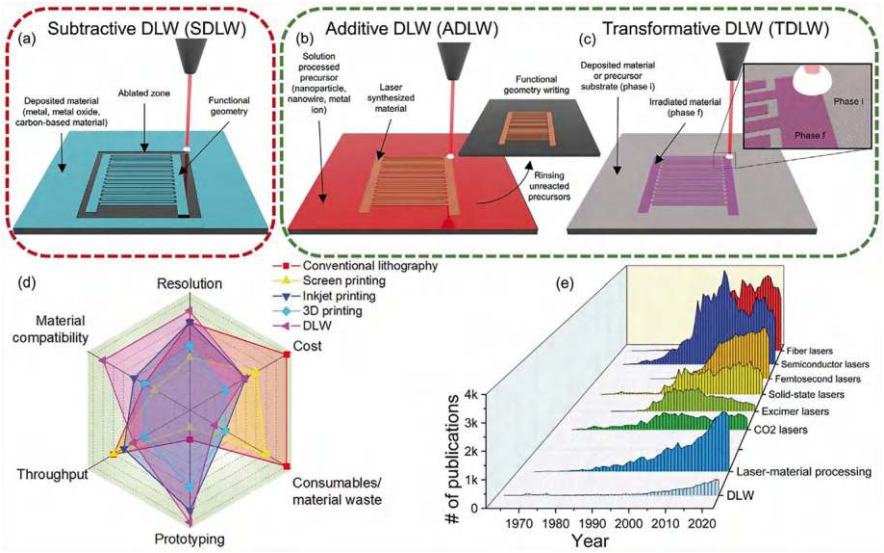

Fig. 26.3 Modalities of DLW, comparison with established microfabrication technologies, and literature outlook. (**a**) Schematic of subtractive DLW (ADLW) for ablation-based geometry writing. (**b**) Schematic of additive DLW (ADLW) for simultaneous material synthesis and patterning. (**c**) Schematic of transformative DLW (TDLW), characterized by selective chemical and structural material transformation. (**d**) Spider chart comparing DLW with lithography techniques, inkjet, screen, and 3D printing, in relation to key fabrication and implementation characteristics. (**e**) Scopus literature survey, portraying the evolution of publication for various laser systems, laser-material processing, and DLW. (Reproduced from Pinheiro et al. (2024). Published 2024 by Wiley with open access)

writing speed, pulse width and pulse repetition frequency, laser beam focus and spot size, and irradiation atmosphere. Laser wavelength determines the nature of the initiated reactions, for example, in the case of lower wavelengths, the level of absorption of the incident radiation by the material is determined mainly by its chemical and electronic structure, promoting photochemical phenomena, while in the case of higher wavelengths, photothermal effects become dominant, leading to high energy accumulation and temperature rise, thus providing rapid reorganization and structural transitions of the irradiated chemical structures during accumulation and after the heat. Laser energy and power is crucial to establish the threshold at which photochemical or photothermal effects are dominant. Writing speed is usually chosen with respect to the laser power in order to dose the energy received by the irradiated material: low speeds lead to higher temperatures at the irradiation point and more heat accumulation in neighboring regions and in the depth of the material, while higher speeds contribute to less heat accumulation due to energy dissipation caused by the movement of the laser spot (He et al., 2015).

Depending on the laser setup used, the pulse width can vary widely from milliseconds (10^{-3} s) to femtoseconds (10^{-15} s), determining the interaction time of the laser pulse with the material and allowing to control the radial profile of heat

dissipation and its penetration depth. In the case of continuous wave (c.w.) lasers and short-pulsed lasers, characterized by increased energy storage, higher speeds are usually used to provide the conditions necessary for the desired type of reaction and correct patterning. In turn, ultrashort pulsed lasers give the opportunity to create milder conditions, favoring the predominance of photochemical processes over thermally induced ones. In this context, a special role is played by femtosecond lasers (Wang et al., 2024), which have gained great popularity due to the possibility of use in two-photon DLW processes, allowing to achieve submicron resolution and to form objects with developed surface topology (Brown et al., 2023; Yang et al., 2015). At the same time, for some ultrashort lasers, there is an additional option to adjust the pulse repetition frequency in the high-frequency range (10^6–10^9 Hz), which allows to further optimize the structure patterning process. Additionally, it is possible to control the DLW process by changing the laser beam focus state, thus manipulating the irradiation spot size (in particular, in the most focused position the laser spot size is minimal and vice versa) and focusing the laser beam in different positions relative to the surface of the processed material. The composition of the surrounding atmosphere, although not directly related to the laser system, is still an important parameter of DLW (Ludvigsen et al., 2021). The use of inert media makes it possible to avoid contamination of the film and substrate, and the absence of reactive volatiles suppresses possible oxidation or combustion in the presence of oxygen. Nevertheless, the need for gas injection systems makes the DLW technique more expensive, so in cases where this does not significantly disrupt the synthesis and conversion of materials, DLW protocols in air are preferred.

Currently, the optimization of DLW technology is in progress in order to adapt it to the creation of functional coatings not only on solid (glass (Yang et al., 2023) or fused silica (Chen et al., 2022)) and polymer substrates (Huang et al., 2020) but also on paper. In the following sections, examples of successful use of direct laser writing in the forming of carbon-based and polymer-based structures will be discussed regarding paper electronics devices.

26.4 Carbon and Graphene Patterning

Approaches to the graphene-based structures formation using direct laser writing can be divided into photothermal as well as photochemical synthesis depending on the nature of the processes taking place. When using lasers with wavelengths above 390 nm, as a rule, photothermal processes dominate, when the energy of photons absorbed by the material leads to atomic vibration and heating of the adjacent region, which eventually results in the breaking of chemical bonds (e.g., C–O, C–N, or C=O when irradiating polymers, as well as -COOH and -OH when using graphene oxide as a starting material for synthesis) (Li, 2020). In the case of laser irradiation with a wavelength below 390 nm, the photochemical processes taking place become more significant during synthesis, since higher photon energies are already capable of directly breaking chemical bonds. It should be noted that at low

laser fluence (<1 J/cm^2) the ablation rate predicted considering the realization of only photochemical effect is in good agreement with experimental data; however, as the laser fluence increases, the discrepancy between theory and experiment becomes more pronounced due to the effect of temperature increase caused by molecular energy levels and radiation-free leap processes (Yu et al., 2023). Therefore, in this case one should refer to a combined photothermal-photochemical synthesis mechanism.

In order to obtain laser-induced graphene (LIG) different types of starting materials can be used: graphene oxide (Chen et al., 2022), polymers (the most popular is polyimide, but there is also phenolic resin, photoresists, and others (Yu et al., 2023)), wood (Ye et al., 2017), textiles, food and paper (Chyan et al., 2018). The variety of carbon sources offers new opportunities in terms of waste recycling; however, it should be kept in mind that the nature of the source material significantly affects the grade of laser-induced graphene (in some cases it is possible to obtain only amorphous carbon). In general, the quality (primarily in terms of composition and structure) of such laser-induced graphene is significantly inferior to that of graphene formed using solution methods or CVD (Yu et al., 2023). The CO_2 lasers used at the initial stage of LIG technologies development still remain appropriate in this context (Liu et al., 2020a), although today excimer and near IR solid-state lasers (Li, 2020), UV lasers (Wang et al., 2021), laser diodes (Burke et al., 2020), and femtosecond lasers (Wang et al., 2024; Yang et al., 2023) are also used to optimize the patterning process of graphene structures.

DLW-derived carbon structures, including laser-induced graphene, are effectively used in various paper electronics devices. In particular, Cantarella et al. (2023) demonstrated an interesting example of circular electronics concept realization, when the paper made of recycled materials (fruit leftovers) was used to form electrochemical sensor and parallel plate capacitor by DLW method, which then could be utilized in eco-friendly ways—either by dissolution in natural solutions or used in the process of plant germination. The process of carbon structures patterning on the paper substrate surface was carried out using CO_2 pulsed laser (wavelength 10.6 μm; power varied from 3 to 4.2 W, laser speed varied from 210 to 1050 mm/s, with 42 mm/s step while keeping constant defocus of 5 mm). In order to achieve optimal sheet resistance values, which in turn depended on the carbonization degree of the material, the initial substrates were pre-soaked in flame retardant solution (BBT Antiflame) from 10 min to 8 h. The best results with respect to sheet resistance (366 Ω/sq. ± 25 Ω/sq) were demonstrated by carbonized layers (amorphous carbon was obtained) on the surface of apple-based paper (laser speed, power, and immersion time equal to 378 mm/s, 3 W, and 2.5 h, respectively). The final parallel plate capacitors formed on the mentioned paper with different plate areas (1.5–45 mm^2), characterized by capacitance from 0.5 to 16 pF, loss tangent from 0.46 to 0.90, and dielectric constant value of 2.9 at 5 MHz. The DLW-carbonized layers were also integrated within a three-electrode electrochemical sensor, and the results of ferrocene determination by cyclic voltammetry

were almost as good as those for the commercial carbon-based one (the maximum oxidation peak was recorded at 226 μA on the cellulose substrate and at 239 μA on the commercial one; the potential difference between the oxidation and reduction peaks ΔEp was 0.14 and 0.22 V). Zhu et al. (2022) reported a procedure for the DLW formation of conductive (sheet resistance varied from 10^8 to 10^2 Ω/sq) moisture-resistant electrodes based on ordered and disordered graphitic carbon structures by (10.6 μm CO_2 laser) on the surface of TEMPO (2,2,6,6,6-tetramethylpiperidine-1-oxyl radical)-oxidized paper. It has been shown that the electrodes thus obtained can be used to create a resistive-type humidity sensor due to the presence of sodium-ion conductivity due to the presence of COONa groups on the surface of TEMPO-oxidized paper. The sensitivity and response/recovery time of the final all-cellulose-derived sensor at 30 and 75% humidity conditions were $1.19 \cdot 10^5$ and 60/495 s, respectively. Stability tests showed that the sensor performance remained unchanged over 100 bending cycles and a minimum of 3 months of storage. Additionally, it was demonstrated that sensors formed in this way can be used for positional localization of moist objects (e.g., when a human finger approaches the sensor, its resistance decreases by about 70% due to skin moistening), synchronous detection of biological activities (breathing-behavioral analysis, sweating process from the human body), and plant transpiration monitoring (Fig. 26.4). It is also worth mentioning the work on laser-induced graphene-based planar micro-supercapacitors (MSCs) realized on paper substrates. In particular, successful deposition of LIG interdigital electrodes is described by Coelho et al. (2023). The finger dimensions of the deposited electrodes were 0.5 cm × 0.08 cm with an interspacing distance of 0.06 cm, and the lateral dimensions of the whole device were 1.8 × 2 cm. The surface resistivity of the LIG structures reached 30 Ω/sq. A layer of PVA/H_2SO_4 aqueous gel was deposited on the formed electrode structures as an electrolyte. The final MSC showed a capacitance of 4.6 mF/cm^2 at a current density of 0.015 mA/cm^2 and also exhibited significant cyclic stability (over 10,000 cycles at a current density of 0.5 mA/cm^2). Unfortunately, after 1000 bending cycles at 180°, significant losses of device capacitance (about 60%) were observed, which, according to Coelho et al. (2023) predictions, can be adjusted by proper sealing of the device for its stabilization under mechanical loads. In turn, Abreu et al. (2024) compared the electrochemical performance of LIG-based MSC as well as composite (LIG-MnO_x) electrodes. In order to form LIG-MnO_x, manganese acetate ($C_4H_6MnO_4$, 1 mol/L) was pre-applied on the paper substrate, and after drying, DLW process was carried out according to the given interdigital geometry. Silver layers served as contact pads for both devices (based on LIG electrodes, as well as on LIG-MnO_x). It was found that the introduction of MnO_x into the electrode composition contributed to a significant increase (about 10 times) in the specific capacitance of the resulting device. Thus, in the case of LIG-MSC, this parameter was 1.18 mF/cm^2 (at 0.05 mA/cm^2), whereas for LIG-MnO_x-MSC the capacitance value at a similar current density reached 12.30 mF/cm^2 with 60% retention at 1000 bending cycles (30°).

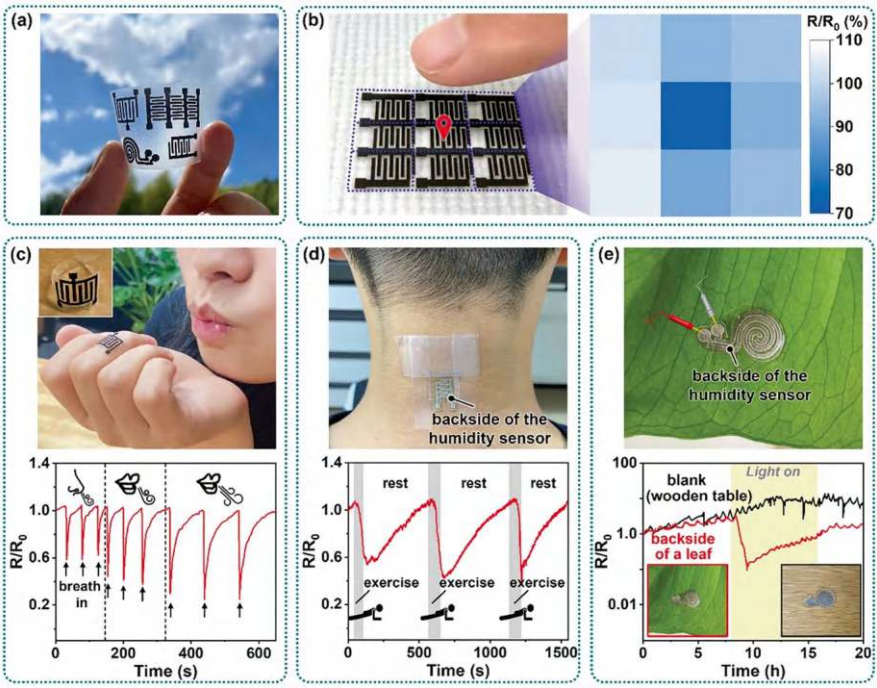

Fig. 26.4 Applicability of the all-cellulose-derived humidity sensor. (**a**) Optical image of all-cellulose-derived humidity sensors with various patterned electrodes, (**b**) positional localization of an approaching finger using a 3 × 3 sensor array, (**c**) sensor response for different extents of human exhalation (breathing from the nose and mouth (soft and hard)), (**d**) monitoring of human-body sweating process during plank exercise and rest periods, and (**e**) monitoring of the transpiration process of a Monstera leaf in comparison with monitoring of a wooden table surface. In all cases, the electrodes were prepared at a laser power of 3.2 W. All demonstrations were conducted at room temperature. (Reproduced from Zhu et al. (2022). Published 2022 by RSC Publishing with open access)

26.5 Polymer Writing

Formation of hydrophobic barriers is an important issue in the fabrication of efficient microfluidic devices. Unlike glass, silicon, or polymer substrates, where the fluid channels are relief structures embedded in these substrates, in paper-based microfluidic devices the fluid channels are formed within the substrate and can extend through the entire thickness of the substrate. The barriers required to delimit individual fluid channels to introduce and direct fluid flow have been successfully formed using polymeric materials such as SU8, PDMS, polystyrene (PS), alkyl ketene dimer (AKD), and wax (Sones et al., 2014). In this context, the DLW method can be highly promising because it is a non-contact approach to structure patterning, avoiding possible cross-contamination when the deposition tool is in contact with the substrate, which is a significant advantage in the manufacturing of biological or

biomedical microfluidic devices. In addition, no masks or complex lithographic steps are required in this case, which increases the usability of DLW for both prototyping and transition to reproducible mass production. Also, as mentioned above, this technology allows controlling the patterning process by optimizing a wide range of laser setup parameters, achieving quite high resolutions (50 μm and below). When forming hydrophobic barriers by DLW method, paper substrates are first impregnated with photopolymer, and then under the influence of laser radiation the process of its local curing with the formation of channels of the desired geometry is induced. A similar approach was demonstrated in studies (He et al., 2015; Sones et al., 2014), where irradiation of paper substrates impregnated with a solution of photopolymers (DeSolite 3471-3-14 and Substance G (SubG) dissolved in isopropanol) was carried on using Nd:YVO4 laser (266 nm; pulse duration, 10 ns; maximum single pulse energy, 2 mJ; repetition rate, 20 Hz) and continuous semiconductor lasers (Omicron, operating at 375 nm with a maximum output of 70 mW and Cobolt MLD, operating at 405 nm; maximum output power ~110 mW). In the study by Sones et al. (2014), the influence of laser wavelength and power and the type of photopolymer on the width of the barriers formed were considered. It was shown that the minimum width of hydrophobic barriers successfully preventing liquid leakage was ~120 μm, and the minimum width of formed liquid channels was ~80 μm. He et al. (2015) used two approaches to create delay barriers: (1) by controlling the depth of solid/impermeable barriers applied across the fluid flow by reducing the depth of photopolymerization, or (2) by forming porous barriers that provide controlled fluid flow by varying the degree of polymerization. The formation of the described barriers was realized by varying the laser output power (5–50 mW) and writing speed (0.1–1.5 mm/s), which finally allowed to achieve flow delays ranging from a few minutes, to over half an hour. It is possible to implement laser-induced photopolymerization not only within a single paper layer but also when fabricating multilayer paper microfluidic devices, as it was illustrated by He et al. (2016). In this case, by controlling the penetration depth of laser radiation, a three-layer stack of cellulose paper (each 180 μm thick) was bonded after its impregnation with a polymer solution (SubG solution in acetone) and subsequent irradiation with a c.w. laser (405 nm; output power, 100 mW; scan speed of 10 mm/s). Increasing the number of layers in the formed stack, although permitted to bond them together, resulted in significant leakage of test liquids. Nevertheless, the idea of using intermediate sealing layers of polyvinylidene fluoride (PVDF) between the paper sheets (the whole three-layer assembly was bonded by photopolymerization using DLW) allowed to achieve the desired result. Testing of the final device confirmed that inks of different types injected into the top and bottom layers of this stack flow only within the corresponding layers and do not penetrate into the opposite layer due to the presence of an intermediate blocking PVDF layer. The described concept is promising both in terms of isolating heterogeneous paper layers and in developing three-dimensional trajectories by elaborately assembling multiple layers, possibly in combination with holes and voids in some layers.

It is possible to provide additional localization of photopolymer application (in order to exclude the stage of substrate impregnation with its solution, as well as the

subsequent removal of its untreated residues) by using dispensing devices. In particular, Galanis et al. (2019) presented an example of the local polymer (DeSolite 3471-3-14) deposition on a nitrocellulose substrate followed (30 s after polymer application) by c.w. laser irradiation (405 nm). The width of the polymer lines formed in this way was about 1 mm before laser treatment, whereas the minimum width of the wall formed by photopolymerization was about 200 μm. The barriers obtained allowed effective filtration of different particle types—Au nanoparticles of 40–200 nm, as well as latex microbeads of 200 nm and 1 μm size dispersed in aqueous solution.

26.6 3D Electrodes Formation

When creating modern electronics and microfluidics devices, it is necessary to form not only 2D but also 3D structures. Particularly, in the case of electrochemical energy and sensor devices, it allows achieving enhanced electrochemical responses due to the formation of highly conductive pathways, which in turn facilitate mass and charge transfer. From this point of view, attention is attracted to 3D direct ink writing, which involves dosing of high-viscosity ink or polymer filament through a dispenser in the process of forming a coating of the desired geometry. 3D pens (Singhal et al., 2021), various syringe dispensing systems (Li et al., 2015), and positioning systems based on 3D printers (Wei et al., 2017) can be used as auxiliary tools in this case. Similarly, structures of different compositions can be obtained on the surface of flexible substrates of different nature. For example, in a paper (Lee et al., 2022), the formation of conductive structures was demonstrated by sequentially applying two types of inks based on PEDOT:PSS (aqueous solution, 5.0 wt.%) and electrochemically exfoliated graphene (aqueous dispersion, 1.0 wt.%), each filled into a plastic syringe with a needle of about 1.27 mm in diameter. The syringes were integrated into a 3D printer system that pressurizes the syringe plunger with the desired force and moves them along a predetermined path. First, the pattern of the desired geometry was printed using polymer ink, and then graphene-based ink layers were applied in the same geometry. After removing the solvent, the developed composite layers exhibited a resistance of 1.23 (four-layer structure) to 5.63 kΩ (three-layer structure). De Oliveira et al. (2020) showed the possibility of shaping conductive 3D structures based on carbon black and polylactic acid formed using a commercial 3D pen (nozzle diameter 0.7 mm, nozzle temperatures 160–230 °C, extrusion speeds 3.2–20.3 mg/s). The final electrochemical sensor designed with such electrodes allowed to detect organic (paracetamol and ascorbic acid) and inorganic (Cd^{2+} and Pb^{2+} ions) analytes within stationary and hydrodynamic systems with accuracy not inferior to similar variants fabricated using a 3D printer.

The need for high-density neural recording in animal studies and human clinical devices requires the development of three-dimensional electrode structures similar to microwire arrays in a “bed of nails” design. In this context, it is worth noting the

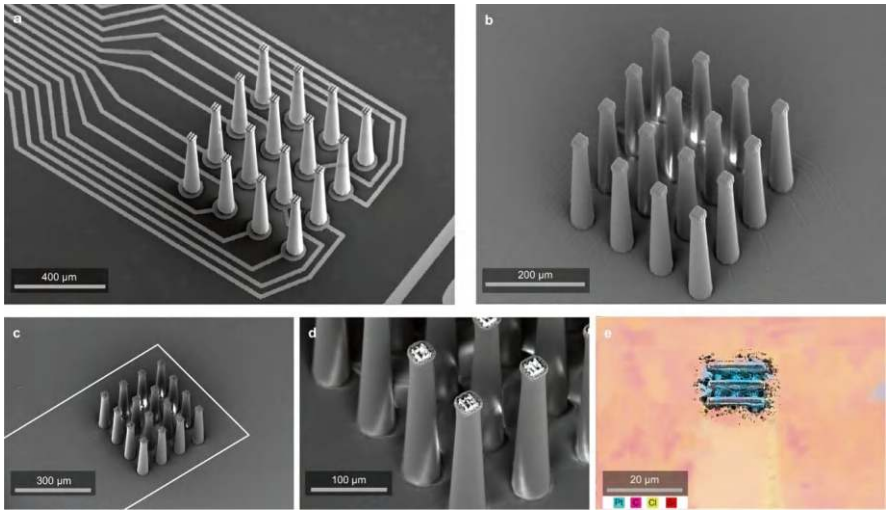

Fig. 26.5 (**a**) Platinum-coated array on the wafer before insulation. (**b**) Array coated in 3 µm of parylene C insulation. (**c**–**e**) Images taken post tip exposure. The connecting traces are outlined with a dashed line (c). The exposed platinum is evident in (**d**), and (**e**) shows an EDX of the exposed tip with platinum in blue. (Reproduced from Brown et al. (2023). Published 2023 by Springer Nature with open access)

approach proposed by Brown et al. (2023), which yields miniaturized 3D electrodes (16-channel array with 300 µm pitch) on the surface of flexible substrates using two-photon DLW (Fig. 26.5). Despite a rather complicated and multistage procedure (at different stages of the experiment methods of spin coating, sputtering, etching, focused ion beam milling, as well as photolithography technologies were also applied), it was possible to create an effective device based on the described electrodes, correctly measuring electrophysiological signals during the monitoring of birds and mice brain activity. Additionally, there were also fabricated devices based on biomimetic electrode arrays similar to mosquito needles with a pitch of 90 µm, capable of penetrating through the dura of birds, as well as porous 3D pyramids with a developed surface area (0.076–0.391 mm^2), promising for stable multi-unit registration and reduced thresholds for stimulation of ingrown axons or dendrites during monitoring.

26.7 Advantages and Limitations of Writing Methods on Paper

Features of the above-discussed writing methods enable to create structures of different thickness, geometry, and composition, opening up opportunities to design a wide spectrum of devices for multiple purposes. In order to competently use each of

the described methods and achieve the best result, it is necessary to take into account their specific features. From the point of view of possible compositions, handwriting and 3D direct ink writing methods are superior to direct laser writing, allowing to employ both commercial and customized inks of required chemical composition, type (true solutions and dispersions of different viscosity), concentration, and microstructure (particle size, shape, degree of self-organization) of the solid phase. In turn, the possibilities of DLW on the surface of paper substrates are limited by the low thermal and chemical stability of the substrates themselves, so in cases where the required coatings composition requires elevated temperatures or the use of aggressive precursor solutions, there may be risks of paper deformation or degradation. In an attempt to solve this problem, a group of authors (Abreu et al., 2024; Coelho et al., 2023) suggests using flame retardant-based protective coatings, which, however, is not always convenient and may also affect the functional characteristics of the final devices. In this regard, DLW is primarily applied on paper substrates to obtain carbon and polymer structures. Also, as noted above, the process of paper surface carbonization often produces amorphous rather than crystalline carbon (Cantarella et al., 2023). In those cases where graphene-based materials can still be obtained by this approach, its quality (chemical composition and structure) is significantly inferior to materials obtained by other methods (Yu et al., 2023). An undeniable advantage of DLW over handwriting and robot-writing techniques (using writing accessories) is the high resolution of the applied patterns (50 μm and below (Sones et al., 2014), while for the discussed contact methods the minimum resolution is about 250 μm (Li et al., 2016)), which allows local processing of the substrate surface, providing miniaturization of manufactured devices with different geometries. In addition, the DLW method is non-contact, which eliminates possible contamination or mechanical damage of the substrate or the applied coating upon contact with a writing instrument. Elimination of using pens/pencils/dispensers solves the problem related to the reproducibility of patterning due to the gradual deformation of the tips of pens/pencils used. Also, a notable feature of DLW is the ability to control the depth of laser penetration, thereby adjusting the thickness and porosity of the resulting structures (He et al., 2016), which is quite difficult to achieve in contact writing (meaning the depth of ink penetration into paper substrates). It is worth noting that in terms of availability, convenience of use, and the cost of the necessary equipment (and thus the final cost of the target device), the advantage lies on the side of handwriting or robot-writing, which allows users to quickly start applying functional coatings and prototyping without acquiring special knowledge in the field of laser technologies.

26.8 Summary

Diversity of direct writing methods, possible writing devices, inks, and technological equipment opens wide horizons for researchers in the field of portable low-cost paper-based devices designed for health care, environmental monitoring, services

and entertainment, industrial, and military applications. Nevertheless, the prospects for mass production and widespread use of paper-based electronics remain relatively distant due to a number of significant limitations. First of all, it should be noted that the considered methods require either complex and expensive equipment requiring specialized skills for addressed formation of paper-based structures (including large-scale), or experience limitations in terms of reproducibility and resolution of the final patterns. Additional stages involving vacuum, long drying time or high post-processing temperatures also result in additional energy and labor costs, making the final devices more expensive. An important parameter is the low chemical and thermal stability of paper, which calls for the development of effective protective coatings that do not adversely affect the functional characteristics of the final components for reliable device operation under real-life conditions. The integrity of paper electronics also remains an open question. Despite the successful realization of various paper-based components for multiple applications, there is no comprehensive implementation of fully integrated paper-based circuits, which are crucial for today's electronics.

Therefore, the development of paper-based electronics needs the elaboration of new materials to create functional inks on their basis, combining both the required level of performance (e.g., electrical conductivity, optical transparency, magnetic properties, and thermal stability) and high compatibility with paper. There is also a demand for improved paper coating approaches to increase their accessibility, as well as to reduce the cost and time required for manufacturing, to enable the transition to mass production of targeted devices. A further prospect lies in the integration of functional elements with interconnects, power sources, and more advanced logic programmable blocks made entirely on paper to effectively move towards the concept of paper electronics and its practical application. Summarizing the above, it should be stated that the achievement of the outlined ambitious tasks is a challenge for modern materials science, chemical, and technological engineering, capable of giving the key to the high-tech future of humankind being in harmony with nature.

Acknowledgments This work was supported by the Ministry of Science and Higher Education of the Russian Federation within the framework of the state assignment for the Kurnakov Institute of General and Inorganic Chemistry. G.K. is grateful to the Moldova State University (research program no. 011208) for supporting his research.

References

Abreu, R., dos Santos, K. M., Pinheiro, T., Vaz Pinto, J., Alves, N., Martins, R., Carlos, E., & Coelho, J. (2024). Direct laser writing of MnO_x decorated laser-induced graphene on paper for sustainable microsupercapacitor fabrication. *FlatChem, 46*, 100672. https://doi.org/10.1016/j.flatc.2024.100672

Amin, R., Ghaderinezhad, F., Li, L., Lepowsky, E., Yenilmez, B., Knowlton, S., & Tasoglu, S. (2017). Continuous-ink, multiplexed pen-plotter approach for low-cost, high-throughput fabrication of paper-based microfluidics. *Analytical Chemistry, 89*, 6351–6357. https://doi.org/10.1021/acs.analchem.7b01418

Amjadi, M., Yoon, Y. J., & Park, I. (2015). Ultra-stretchable and skin-mountable strain sensors using carbon nanotubes–Ecoflex nanocomposites. *Nanotechnology, 26*, 375501. https://doi.org/10.1088/0957-4484/26/37/375501

Averchenko, A. V., Salimon, I. A., Zharkova, E. V., Lipovskikh, S., Somov, P., Abbas, O. A., et al. (2023). Laser-enabled localized synthesis of $Mo_{1-x}WxS_2$ alloys with tunable composition. *Materials Today Advances, 17*, 100351. https://doi.org/10.1016/j.mtadv.2023.100351

Bian, J., Zhou, L., Wan, X., Zhu, C., Yang, B., & Huang, Y. (2019). Laser transfer, printing, and assembly techniques for flexible electronics. *Advanced Electronic Materials, 5*, 1800900. https://doi.org/10.1002/aelm.201800900

Brown, M. A., Zappitelli, K. M., Singh, L., Yuan, R. C., Bemrose, M., Brogden, V., et al. (2023). Direct laser writing of 3D electrodes on flexible substrates. *Nature Communications, 14*, 3610. https://doi.org/10.1038/s41467-023-39152-7

Burke, M., Larrigy, C., Vaughan, E., Paterakis, G., Sygellou, L., Quinn, A. J., et al. (2020). Fabrication and electrochemical properties of three-dimensional (3D) porous graphitic and graphenelike electrodes obtained by low-cost direct laser writing methods. *ACS Omega, 5*, 1540–1548. https://doi.org/10.1021/acsomega.9b03418

Cantarella, G., Madagalam, M., Merino, I., Ebner, C., Ciocca, M., Polo, A., et al. (2023). Laser-induced, green and biocompatible paper-based devices for circular electronics. *Advanced Functional Materials, 33*, 2210422. https://doi.org/10.1002/adfm.202210422

Chang, H., Guo, R., Sun, Z., Wang, H., Hou, Y., Wang, Q., Rao, W., & Liu, J. (2018). Direct writing and repairable paper flexible electronics using nickel–liquid metal ink. *Advanced Materials Interfaces, 5*, 1800571. https://doi.org/10.1002/admi.201800571

Chaya Devi, K. S., Angadi, B., & Mahesh, H. M. (2017). Multiwalled carbon nanotube-based patch antenna for bandwidth enhancement. *Materials Science and Engineering B, 224*, 56–60. https://doi.org/10.1016/j.mseb.2017.07.005

Chen, M., Wan, Z., Dong, H., Chen, Q., Gu, M., & Zhang, Q. (2022). Direct laser writing of graphene oxide for ultra-low power consumption memristors in reservoir computing for digital recognition. *National Science Open, 1*, 20220020. https://doi.org/10.1360/nso/20220020

Chyan, Y., Ye, R., Li, Y., Singh, S. P., Arnusch, C. J., & Tour, J. M. (2018). Laser-induced graphene by multiple lasing: Toward electronics on cloth, paper, and food. *ACS Nano, 12*, 2176–2183. https://doi.org/10.1021/acsnano.7b08539

Coelho, J., Correia, R. F., Silvestre, S., Pinheiro, T., Marques, A. C., Correia, M. R. P., et al. (2023). Paper-based laser-induced graphene for sustainable and flexible microsupercapacitor applications. *Microchimica Acta, 190*, 40. https://doi.org/10.1007/s00604-022-05610-0

Costa, J. C., Wishahi, A., Pouryazdan, A., Nock, M., & Münzenrieder, N. (2018). Hand-drawn resistors, capacitors, diodes, and circuits for a pressure sensor system on paper. *Advanced Electronic Materials, 4*, 1700600. https://doi.org/10.1002/aelm.201700600

de Oliveira, F. M., de Melo, E. I., & da Silva, R. A. B. (2020). 3D Pen: A low-cost and portable tool for manufacture of 3D-printed sensors. *Sensors and Actuators B: Chemical, 321*, 128528. https://doi.org/10.1016/j.snb.2020.128528

Ersu, G., Sozen, Y., Sánchez-Viso, E., Kuriakose, S., Juárez, B. H., Mompean, F. J., et al. (2023). Pen plotter as a low-cost platform for rapid device prototyping with solution-processable nanomaterials. *Advanced Engineering Materials, 25*, 2300226. https://doi.org/10.1002/adem.202300226

Ferreira de Oliveira, A. E., César Pereira, A., & Ferreira, L. F. (2022). Fully handwritten electrodes on paper substrate using rollerball pen with silver nanoparticle ink, marker pen with carbon nanotube ink and graphite pencil. *Analytical Methods, 14*, 1880–1888. https://doi.org/10.1039/D2AY00373B

Franke, K., & Rose, S. (2004). Ink-deposition model: The relation of writing and ink deposition processes. In: *Proceedings of Ninth International Workshop on Frontiers in Handwriting Recognitio*n (IEEE), 26–29 October 2004, Kokubunji, Japan, pp 173–178. https://doi.org/10.1109/IWFHR.2004.59

Franke, K., Schomaker, L., & Koppen, M. (2005). Pen force emulating robotic writing device and its application. In: *Proceedings of IEEE Workshop on Advanced Robotics and its Social Impacts*, 12–15 June 2005, Nagoya, IEEE, pp 36–46. https://doi.org/10.1109/ARSO.2005.1511616

Galanis, P., He, .P, Katis, I., Thomas, M. R., Xianyu, Y., Stevens, M. M., Eason, R. W, & Sones, C. L. (2019). Laser-direct-writing to enable filtration in paper-based devices. In B. L. Gray, & H. Becker (Eds.), *Microfluidics, BioMEMS, and Medical Microsystems XVII*. Proc. SPIE, 10875, 108750P. https://doi.org/10.1117/12.2508753

Gao, L., Wang, X., Dai, W., Bagheri, R., Wang, C., Tian, Z., Dai, X., & Zou, G. (2020). Laser direct writing assisted fabrication of skin compatible metal electrodes. *Advanced Materials Technologies, 5*, 2000012. https://doi.org/10.1002/admt.202000012

Ghaderinezhad, F., Amin, R., Temirel, M., Yenilmez, B., Wentworth, A., & Tasoglu, S. (2017). High-throughput rapid-prototyping of low-cost paper-based microfluidics. *Scientific Reports, 7*, 3553. https://doi.org/10.1038/s41598-017-02931-6

Ghosale, A., Shankar, R., Ganesan, V., & Shrivas, K. (2016). Direct-writing of paper based conductive track using silver nano-ink for electroanalytical application. *Electrochimica Acta, 209*, 511–520. https://doi.org/10.1016/j.electacta.2016.05.109

Grey, P., Gaspar, D., Cunha, I., Barras, R., Carvalho, J. T., Ribas, J. R., et al. (2017). Handwritten oxide electronics on paper. *Advanced Materials Technologies, 2*, 1700009. https://doi.org/10.1002/admt.201700009

He, P. J. W., Katis, I. N., Eason, R. W., & Sones, C. L. (2015). Engineering fluidic delays in paper-based devices using laser direct-writing. *Lab on a Chip, 15*, 4054–4061. https://doi.org/10.1039/C5LC00590F

He, P. J. W., Katis, I. N., Eason, R. W., & Sones, C. L. (2016). Laser direct-write for fabrication of three-dimensional paper-based devices. *Lab on a Chip, 16*, 3296–3303. https://doi.org/10.1039/C6LC00789A

Htwe, Y. Z. N., Abdullah, M. K., & Mariatti, M. (2021). Optimization of graphene conductive ink using solvent exchange techniques for flexible electronics applications. *Synthetic Metals, 274*, 116719. https://doi.org/10.1016/j.synthmet.2021.116719

Huang, F., Feng, G., Yin, J., Zhou, S., Shen, L., Wang, S., & Luo, Y. (2020). Direct laser writing of transparent polyimide film for supercapacitor. *Nanomaterials, 10*, 2547. https://doi.org/10.3390/nano10122547

Jeong, S.-M., Lim, T., Park, J., Han, C.-Y., Yang, H., & Ju, S. (2019). Pen drawing display. *Nature Communications, 10*, 4334. https://doi.org/10.1038/s41467-019-12395-z

Kalish, B., Tan, M. K., & Tsutsui, H. (2020). Modifying wicking speeds in paper-based microfluidic devices by laser-etching. *Micromachines, 11*, 773. https://doi.org/10.3390/mi11080773

Karabel Ocal, S., Kiremitler, N. B., Yazici, A. F., Celik, N., Mutlugun, E., & Onses, M. S. (2022). Natural wax-stabilized perovskite nanocrystals as pen-on-paper inks and doughs. *ACS Applied Nano Materials, 5*, 6201–6212. https://doi.org/10.1021/acsanm.2c00224

Kim, J., Ahn, D., Sun, J., Park, S., Cho, Y., Park, S., et al. (2021). Vertically and horizontally drawing formation of graphite pencil electrodes on paper by frictional sliding for a disposable and foldable electronic device. *ACS Omega, 6*, 1960–1970. https://doi.org/10.1021/acsomega.0c04792

Kurra, N., & Kulkarni, G. U. (2013). Pencil-on-paper: electronic devices. *Lab on a Chip, 13*, 2866. https://doi.org/10.1039/c3lc50406a

Lamberti, A., Perrucci, F., Caprioli, M., Serrapede, M., Fontana, M., Bianco, S., et al. (2017). New insights on laser-induced graphene electrodes for flexible supercapacitors: Tunable morphology and physical properties. *Nanotechnology, 28*, 174002. https://doi.org/10.1088/1361-6528/aa6615

Lee, H., Kim, Y., Kim, J., Moon, S. Y., & Lee, J. U. (2022). Consecutive ink writing of conducting polymer and graphene composite electrodes for foldable electronics-related applications. *Polymers (Basel), 14*, 5294. https://doi.org/10.3390/polym14235294

Lee, J., Murad, S., & Nikolov, A. (2023). Ballpoint/rollerball pens: Writing performance and evaluation. *Colloids Interfaces, 7*, 29. https://doi.org/10.3390/colloids7020029

Li, G. (2020). Direct laser writing of graphene electrodes. *Journal of Applied Physics, 127*, 010901. https://doi.org/10.1063/1.5120056

Li, W., & Chen, M. (2014). Synthesis of stable ultra-small Cu nanoparticles for direct writing flexible electronics. *Applied Surface Science, 290*, 240–245. https://doi.org/10.1016/j.apsusc.2013.11.057

Li, Z., Li, F., Hu, J., Wee, W. H., Han, Y. L., Pingguan-Murphy, B., Lu, T. J., & Xu, F. (2015). Direct writing electrodes using a ball pen for paper-based point-of-care testing. *Analyst, 140*, 5526–5535. https://doi.org/10.1039/C5AN00620A

Li, Z., Liu, H., Ouyang, C., Hong, W. W., Cui, X., Jian, L. T., et al. (2016). Recent advances in pen-based writing electronics and their emerging applications. *Advanced Functional Materials, 26*, 165–180. https://doi.org/10.1002/adfm.201503405

Liao, Y., Zhang, R., Wang, H., Ye, S., Zhou, Y., Ma, T., et al. (2019). Highly conductive carbon-based aqueous inks toward electroluminescent devices, printed capacitive sensors and flexible wearable electronics. *RSC Advances, 9*, 15184–15189. https://doi.org/10.1039/C9RA01721F

Lin, C.-W., Zhao, Z., Kim, J., & Huang, J. (2014). Pencil drawn strain gauges and chemiresistors on paper. *Scientific Reports, 4*, 3812. https://doi.org/10.1038/srep03812

Liu, H., Qing, H., Li, Z., Han, Y. L., Lin, M., Yang, H., et al. (2017a). Paper: A promising material for human-friendly functional wearable electronics. *Materials Science & Engineering R: Reports, 112*, 1–22. https://doi.org/10.1016/j.mser.2017.01.001

Liu, S., Li, J., Shi, X., Gao, E., Xu, Z., Tang, H., et al. (2017b). Rollerball-pen-drawing technology for extremely foldable paper-based electronics. *Advanced Electronic Materials, 3*, 1700098. https://doi.org/10.1002/aelm.201700098

Liu, H., Xie, Y., Liu, J., Moon, K., Lu, L., Lin, Z., et al. (2020a). Laser-induced and KOH-activated 3D graphene: A flexible activated electrode fabricated via direct laser writing for in-plane micro-supercapacitors. *Chemical Engineering Journal, 393*, 124672. https://doi.org/10.1016/j.cej.2020.124672

Liu, Y., Mo, S., Shang, S., Wang, P., Zhao, W., & Li, L. (2020b). Handwriting flexible electronics: Tools, materials and emerging applications. *Journal of Science: Advanced Materials and Devices, 5*, 451–467. https://doi.org/10.1016/j.jsamd.2020.09.006

Loghin, F. C., Falco, A., Albrecht, A., Salmerón, J. F., Becherer, M., Lugli, P., & Rivandeneyra, A. (2018). A handwriting method for low-cost gas sensors. *ACS Applied Materials & Interfaces, 10*, 34683–34689. https://doi.org/10.1021/acsami.8b08050

Loghin, F. C., Salmerón, J. F., Lugli, P., Becherer, M., Falco, A., & Rivadeneyra, A. (2021). Optimization of a handwriting method by an automated ink pen for cost-effective and sustainable sensors. *Chemosensors, 9*, 264. https://doi.org/10.3390/chemosensors9090264

Ludvigsen, E., Pedersen, N. R., Zhu, X., Marie, R., Mackenzie, D. M. A., Emnéus, J., et al. (2021). Selective direct laser writing of pyrolytic carbon microelectrodes in absorber-modified SU-8. *Micromachines, 12*, 564. https://doi.org/10.3390/mi12050564

Mahmud, M. A., Blondeel, E. J. M., Kaddoura, M., & MacDonald, B. D. (2016). Creating compact and microscale features in paper-based devices by laser cutting. *Analyst, 141*, 6449–6454. https://doi.org/10.1039/C6AN02208A

Mahmud, M. A., Blondeel, E. J. M., Kaddoura, M., & MacDonald, B. D. (2018). Features in microfluidic paper-based devices made by laser cutting: How small can they be? *Micromachines, 9*, 220. https://doi.org/10.3390/mi9050220

Mani, N. K., Prabhu, A., Biswas, S. K., & Chakraborty, S. (2019). Fabricating paper based devices using correction pens. *Scientific Reports, 9*, 1752. https://doi.org/10.1038/s41598-018-38308-6

Mitchell, H. T., Noxon, I. C., Chaplan, C. A., Carlton, S. J., Liu, C. H., Ganaja, K. A., et al. (2015). Reagent pencils: A new technique for solvent-free deposition of reagents onto paper-based microfluidic devices. *Lab on a Chip, 15*, 2213–2220. https://doi.org/10.1039/C5LC00297D

Nandy, S., Goswami, S., Marques, A., Gaspar, D., Grey, P., Cunha, I., et al. (2021). Cellulose: A contribution for the zero e-waste challenge. *Advanced Materials Technologies, 6*, 2000994. https://doi.org/10.1002/admt.202000994

Nikolov, A., Murad, S., Wasan, D., & Wu, P. (2020). How the capillarity and ink-air flow govern the performance of a fountain pen. *Journal of Colloid and Interface Science, 578*, 660–667. https://doi.org/10.1016/j.jcis.2020.04.123

Ocier, C. R., Richards, C. A., Bacon-Brown, D. A., Ding, Q., Kumar, R., Garcia, T. J., et al. (2020). Direct laser writing of volumetric gradient index lenses and waveguides. *Light: Science & Applications, 9*, 196. https://doi.org/10.1038/s41377-020-00431-3

Park, J.-H., Park, M.-J., & Lee, J.-S. (2017). Dry writing of highly conductive electrodes on papers by using silver nanoparticle–graphene hybrid pencils. *Nanoscale, 9*, 555–561. https://doi.org/10.1039/C6NR07616E

Pinheiro, T., Morais, M., Silvestre, S., Carlos, E., Coelho, J., Almeida, H. V., et al. (2024). Direct laser writing: From materials synthesis and conversion to electronic device processing. *Advanced Materials, 36*, 2402014. https://doi.org/10.1002/adma.202402014

Polychronopoulos, N. D., & Brouzgou, A. (2024). Direct ink writing for electrochemical device fabrication: A review of 3D-printed electrodes and ink rheology. *Catalysts, 14*, 110. https://doi.org/10.3390/catal14020110

Pradela-Filho, L. A., Araújo, D. A. G., Takeuchi, R. M., & Santos, A. L. (2017). Nail polish and carbon powder: An attractive mixture to prepare paper-based electrodes. *Electrochimica Acta, 258*, 786–792. https://doi.org/10.1016/j.electacta.2017.11.127

Pradela-Filho, L. A., Andreotti, I. A. A., Carvalho, J. H. S., Araújo, D. A. G., Orzari, L. O., Gatti, A., Takeuchi, R. M., Santos, A. L., & Janegitz, B. C. (2020). Glass varnish-based carbon conductive ink: A new way to produce disposable electrochemical sensors. *Sensors and Actuators B: Chemical, 305*, 127433. https://doi.org/10.1016/j.snb.2019.127433

Prestowitz, L. C. O., Emery, J. D., & Huang, J. (2021). Polysketch pen: Drawing from materials chemistry to create interactive art and sensors using a polyaniline ink. *Journal of Chemical Education, 98*, 2055–2061. https://doi.org/10.1021/acs.jchemed.0c01330

Rao, L. T., Rewatkar, P., Dubey, S. K., Javed, A., & Goel, S. (2020). Automated pencil electrode formation platform to realize uniform and reproducible graphite electrodes on paper for microfluidic fuel cells. *Scientific Reports, 10*, 11675. https://doi.org/10.1038/s41598-020-68579-x

Rao, L. T., Jayapiriya, U. S., Dubey, S. K., Javed, A., & Goel, S. (2022). Portable paper-based hydrogen fuel cell with automated pencil-stroked electrodes: Development, analysis, and performance investigation. *International Journal of Energy Research, 46*, 24008–24020. https://doi.org/10.1002/er.8699

Romanholo, P. V. V., de Andrade, L. M., Silva-Neto, H. A., Coltro, W. K. T., & Sgobbi, L. F. (2024). Digitally controlled printing of bioink barriers for paper-based analytical devices: An environmentally friendly one-step approach. *Analytical Chemistry, 96*, 5349–5356. https://doi.org/10.1021/acs.analchem.3c03801

Russo, A., Ahn, B. Y., Adams, J. J., Duoss, E. B., Bernhard, J. T., & Lewis, J. A. (2011). Pen-on-paper flexible electronics. *Advanced Materials, 23*, 3426–3430. https://doi.org/10.1002/adma.201101328

Russo, A., Cavalera, S., Murray, R., Lovera, P., Quinn, A., Anfossi, L., & Iacopino, D. (2024). Pen direct writing of SERRS-based lateral flow assays for detection of penicillin G in milk. *Nanoscale Advances, 6*, 1524–1534. https://doi.org/10.1039/D3NA00846K

Santhiago, M., Strauss, M., Pereira, M. P., Chagas, A. S., & Bufon, C. C. B. (2017). Direct drawing method of graphite onto paper for high-performance flexible electrochemical sensors. *ACS Applied Materials & Interfaces, 9*, 11959–11966. https://doi.org/10.1021/acsami.6b15646

Simonenko, T. L., Simonenko, N. P., Gorobtsov, P. Y., Pozharnitskaya, V. M., Simonenko, E. P., Glumov, O. V., et al. (2021). Pen plotter printing of MnO_x thin films using manganese alkoxoacetylacetonate. *Russian Journal of Inorganic Chemistry, 66*, 1416–1424. https://doi.org/10.1134/S0036023621090138

Simonenko, T. L., Simonenko, N. P., Gorobtsov, P. Y., Simonenko, E. P., & Kuznetsov, N. T. (2023). Current trends and promising electrode materials in micro-supercapacitor printing. *Materials (Basel), 16*, 6133. https://doi.org/10.3390/ma16186133

Singhal, H. R., Prabhu, A., Giri Nandagopal, M. S., Dheivasigamani, T., & Mani, N. K. (2021). One-dollar microfluidic paper-based analytical devices: Do-it-yourself approaches. *Microchemical Journal, 165*, 106126. https://doi.org/10.1016/j.microc.2021.106126

Sones, C. L., Katis, I. N., He, P. J. W., Mills, B., Namiq, M. F., Shardlow, P., et al. (2014). Laser-induced photo-polymerisation for creation of paper-based fluidic devices. *Lab on a Chip, 14*, 4567–4574. https://doi.org/10.1039/C4LC00850B

Sritapunya, T., Jairakdee, S., Kornprapakul, T., Somabutr, S., Siemanond, K., Bunyakiat, K., et al. (2011). Adsorption of surfactants on carbon black and paper fiber in the presence of calcium ions. *Colloids and Surfaces A: Physicochemical and Engineering Aspects, 389*, 206–212. https://doi.org/10.1016/j.colsurfa.2011.08.025

Stefano, J. S., Orzari, L. O., Silva-Neto, H. A., de Ataíde, V. N., Mendes, L. F., Coltro, W. K. T., et al. (2022). Different approaches for fabrication of low-cost electrochemical sensors. *Current Opinion in Electrochemistry, 32*, 100893. https://doi.org/10.1016/j.coelec.2021.100893

Terzi, F., Zanfrognini, B., Ruggeri, S., Dossi, N., Casagrande, G. M., & Piccin, E. (2017). Amperometric paper sensor based on Cu nanoparticles for the determination of carbohydrates. *Sensors and Actuators B: Chemical, 245*, 352–358. https://doi.org/10.1016/j.snb.2017.01.064

Thekkekara, L. V. (2018). Direct laser writing of supercapacitors. In L. Liudvinavičius (Ed.), *Supercapacitors—Theoretical and practical solutions*. InTechOpen. https://doi.org/10.5772/intechopen.73000

Thompson, J. E. (2017). Pencil-on-paper capacitors for hand-drawn RC circuits and capacitive sensing. *Journal of Chemistry, 2017*, 909327. https://doi.org/10.1155/2017/4909327

Wang, M., Yang, Y., & Gao, W. (2021). Laser-engraved graphene for flexible and wearable electronics. *Trends in Chemistry, 3*, 969–981. https://doi.org/10.1016/j.trechm.2021.09.001

Wang, S., Yang, J., Deng, G., & Zhou, S. (2024). Femtosecond laser direct writing of flexible electronic devices: A mini review. *Materials (Basel), 17*, 557. https://doi.org/10.3390/ma17030557

Wei, M., Zhang, F., Wang, W., Alexandridis, P., Zhou, C., & Wu, G. (2017). 3D direct writing fabrication of electrodes for electrochemical storage devices. *Journal of Power Sources, 354*, 134–147. https://doi.org/10.1016/j.jpowsour.2017.04.042

Wei, T., Al-Fogra, S., Hauke, F., & Hirsch, A. (2020). Direct laser writing on graphene with unprecedented efficiency of covalent two-dimensional functionalization. *Journal of the American Chemical Society, 142*, 21926–21931. https://doi.org/10.1021/jacs.0c11153

Yang, L., El-Tamer, A., Hinze, U., Li, J., Hu, Y., Huang, W., Chu, J., & Chichkov, B. N. (2015). Parallel direct laser writing of micro-optical and photonic structures using spatial light modulator. *Optics and Lasers in Engineering, 70*, 26–32. https://doi.org/10.1016/j.optlaseng.2015.02.006

Yang, L., Hu, H., Scholz, A., Feist, F., Cadilha, M. G., Kraus, S., et al. (2023). Laser printed microelectronics. *Nature Communications, 14*, 1103. https://doi.org/10.1038/s41467-023-36722-7

Yao, B., Zhang, J., Kou, T., Song, Y., Liu, T., & Li, Y. (2017). Paper-based electrodes for flexible energy storage devices. *Advancement of Science, 4*, 1700107. https://doi.org/10.1002/advs.201700107

Ye, R., Chyan, Y., Zhang, J., Li, Y., Han, X., Kittrell, C., & Tour, J. M. (2017). Laser-induced graphene formation on wood. *Advanced Materials, 29*, 1702211. https://doi.org/10.1002/adma.201702211

Yeasmin, S., Talukdar, S., & Mahanta, D. (2021). Paper based pencil drawn multilayer graphene-polyaniline nanofiber electrodes for all-solid-state symmetric supercapacitors with enhanced cyclic stabilities. *Electrochimica Acta, 389*, 138660. https://doi.org/10.1016/j.electacta.2021.138660

Young, O. M., Xu, X., Sarker, S., & Sochol, R. D. (2024). Direct laser writing-enabled 3D printing strategies for microfluidic applications. *Lab on a Chip, 24*, 2371–2396. https://doi.org/10.1039/D3LC00743J

Yu, H., Gai, M., Liu, L., Chen, F., Bian, J., & Huang, Y. (2023). Laser-induced direct graphene patterning: From formation mechanism to flexible applications. *Soft Science, 3*, 4. https://doi.org/10.20517/ss.2022.26

Zhang, Y., Guo, Y., Song, L., Qian, J., Jiang, S., Wang, Q., et al. (2017). Directly writing 2D organic semiconducting crystals for high-performance field-effect transistors. *Journal of Materials Chemistry C, 5*, 11246–11251. https://doi.org/10.1039/C7TC02348K

Zhang, X., Song, K., Liu, J., Zhang, Z., Wang, C., & Li, H. (2019). Sorption of triclosan by carbon nanotubes in dispersion: The importance of dispersing properties using different surfactants. *Colloids and Surfaces A: Physicochemical and Engineering Aspects, 562*, 280–288. https://doi.org/10.1016/j.colsurfa.2018.11.037

Zhao, H., Zhang, T., Qi, R., Dai, J., Liu, S., & Fei, T. (2017). Drawn on paper: A reproducible humidity sensitive device by handwriting. *ACS Applied Materials & Interfaces, 9*, 28002–28009. https://doi.org/10.1021/acsami.7b05181

Zhao, J., Lo, L.-W., Yu, Z., & Wang, C. (2023). Handwriting of perovskite optoelectronic devices on diverse substrates. *Nature Photonics, 17*, 964–971. https://doi.org/10.1038/s41566-023-01266-1

Zheng, Y., Zhang, Q., & Liu, J. (2013). Pervasive liquid metal based direct writing electronics with roller-ball pen. *AIP Advances, 3*, 112117. https://doi.org/10.1063/1.4832220

Zhu, C., Zhao, X., Wang, X., Chen, J., Yu, P., Liu, S., et al. (2021). Direct laser patterning of a 2D WSe_2 logic circuit. *Advanced Functional Materials, 31*, 2009549. https://doi.org/10.1002/adfm.202009549

Zhu, L., Li, X., Kasuga, T., Uetani, K., Nogi, M., & Koga, H. (2022). All-cellulose-derived humidity sensor prepared via direct laser writing of conductive and moisture-stable electrodes on TEMPO-oxidized cellulose paper. *Journal of Materials Chemistry C, 10*, 3712–3719. https://doi.org/10.1039/D1TC05339F

Chapter 27
Paper-Supported Electrodes

Ghenadii Korotcenkov

27.1 Introduction

Electrodes play an important role in all types of paper-based sensors and electronic devices (Elbadawi et al., 2021; Korotcenkov, 2023; Sakata et al., 2020). For example, to achieve the maximum sensory signal, the resistance of the electrodes themselves should be as low as possible. Therefore, for their manufacture, it is necessary to use highly conductive materials. As it is known, metals, carbon-based materials, metal nitrides, metal carbides, and conductive polymers are such materials (Yao et al., 2017; Xu et al., 2022).

27.2 Metal-Based Electrodes

Metal conductors are key elements of all electronic and optoelectronic devices, including sensors of all types (Elbadawi et al., 2021; Lu et al., 2021). Metals are much more malleable than other typical materials used to make the electrodes in these devices. For example, thin metal films become quite flexible, allowing them to be used to fabricate strong and conductive electrodes on bendable or stretchable substrates used in flexible electronics (Merilampi et al., 2009). At that, experiment and simulation showed that reducing the thickness of both the metal film and the substrate used provides a significant improvement in the bendability of the manufactured devices. The thinner the structure, the smaller the radius of curvature that it can withstand without damaging the electrodes deposited on its surface. For example, simulations have shown that at a damage threshold of 2% (Gray et al., 2004), metal films applied to a 100-μm-thick flexible substrate can withstand bending up to

G. Korotcenkov (✉)
Department of Physics and Engineering, Moldova State University, Chisinau, Moldova

G. Korotcenkov (ed.), *The Handbook of Paper-Based Sensors and Devices*,
https://doi.org/10.1007/978-3-031-91080-7_27

a radius of curvature of 2.5 mm (Graz & Rosset, 2021). It is important to note that this finding applies to all materials used to make electrodes (Kim et al., 2008). Optimizing the geometry of metal electrodes also helps improve their flexibility and stretchability (Guo et al., 2015).

Thin films of metals such as Ag, Au, Pt, Ni, Sn, Zn, and Pd are commonly used to make electrodes on the paper substrate (Siegel et al., 2010). Platinum is a widely used electrode material due to its high electrical conductivity, stability, and low reactivity with most chemicals. Pt is used in electrochemical sensors for gas detection, including oxygen, and pH measurement. Au is also a popular electrode material due to its high conductivity, biocompatibility, and stability. Au is commonly used in biosensors to detect biological molecules such as proteins, DNA, and viruses. However, in paper-based devices, silver electrodes remain the most common metal used in the production of various sensors (Cinti et al., 2018; De Araujo & Paixao, 2014; Molina-Lopez et al., 2012). Silver is by far the most widely used metal due to its high volume conductivity and high oxidation resistance. Depending on process parameters and materials, the surface resistance of printed conductive electrodes varied from 0.04 Ω/□ to 0.13 Ω/□ (Merilampi et al., 2009). Most conductive silver inks are based on the use of spherical nanoparticles or flakes. Silver nanoparticle inks have excellent low electrical resistance when printed and cured onto paper substrates, but the resulting printed tracks and layers are typically opaque and brittle.

Copper was also of interest due to its high conductivity and lower price compared to silver, and especially to Au and Pt. However, the instability of copper particles under environmental conditions is a major disadvantage of using copper in conductive metallic inks. Several studies have focused on protecting copper particles, but without apparent success (Zhang et al., 2014a).

Ink with metal particles provides the highest level of electrical conductivity of the electrode. However, to obtain a high level of electrical conductivity, additional post-treatment is usually required by annealing at a temperature of 100–250 °C for several minutes. This results in the elimination of all insulating components present in the ink (stabilizers, other additives, etc.) that promote the formation of a continuous interconnected phase between the metal nanoparticles.

Regarding energy storage devices, metal materials such as copper, nickel, aluminum, and gold are still the most commonly used current collectors for flexible supercapacitors due to their good mechanical properties and electrical conductivity (Ko et al., 2017; Nguyen et al., 2022; Zhang et al., 2021).

27.3 Carbon-Based Electrodes

Carbon-based materials such as carbon nanotubes (CNTs), graphite, and graphene are another group of materials successfully used to make electrodes on the surface of paper (Elbadawi et al., 2021). Carbon-based materials have become a popular choice in sensor electrodes due to their low cost, high conductivity, and availability.

In addition, carbonaceous materials have a larger surface area-to-volume ratio, high chemical stability, and a wide potential window and are chemically inert. Furthermore, they exhibit a rich surface chemistry that provides a variety of redox reactions (Villarreal et al., 2017).

Although the electrochemical performance varies among allotropes and is highly dependent on the hybridization state and its structure, all types of carbon nanomaterials are widely used as electrode material in the development of paper-based devices. For example, Arena et al. (2010) used multi-walled carbon nanotube-based interdigital (ID) electrodes. Hu et al. (2009) fabricated a high-performance conductive paper electrode with reliable chemical and mechanical stability using a simple conformal coating of CNT ink on commercial photocopy paper. The electrical conductivity of CNTs is about 10^7 S/m for pure CNTs (Wang & Weng, 2018). In addition, CNTs have a large specific surface area, which allows the immobilization of a number of biofunctional molecules (Tîlmaciu & Morris, 2015). However, we must not forget that immobilization can damage the activity of biomolecules, as well as their structural stability. Moreover, the production of CNTs of desired sizes is difficult and is an expensive method that does not provide high purity yield (Sireesha et al., 2018). We must also keep in mind that the conductivity of CNTs varies depending on their diameter and chirality and can be either semiconducting or semi-metallic.

Steffens et al. (2009) developed a low-cost sensor with graphite interdigitated electrodes. The advantages of graphite include low price and good conductivity (Kongkaew et al., 2022; Li et al., 2022). For example, Ferreira de Oliveira et al. (2022) compared the sheet resistance of CNT, AgNP, and graphite electrodes and found that electrodes with similar geometries had a resistance of 18.62 kΩ for CNT ink, 1.53 Ω for AgNP ink, and 3.53 kOhm for graphite tracks. In addition, graphite has a stable dispersion without further processing and can be used to immobilize organic molecules on it.

Weng et al. (2011) reported a simple and scalable method for making conductive paper from graphene and cellulose. Graphene, a two-dimensional conducting carbon-based material is currently attracting much attention for electronic applications due to its fascinating advantages such as high electrical conductivity (~10^8 S/m), optical transparency (>97%), gas barrier property, robustness, flexibility, and environmental stability (Bonaccorso et al., 2010; Elbadawi et al., 2021; Geim, 2009; Stankovich et al., 2006). The combination of these remarkable electrical and mechanical properties suggests that graphene can be used as a stable conductor under any kind of substrate deformation. For example, Hyun et al. (2013) developed foldable electronic circuits for paper substrates by using graphene nanoplates. The graphene circuits have been prepared via vacuum filtration of a graphene dispersion and a selective transfer process with a pen. The polystyrene sulfonate (PSS) surfactant used was effective in both dispersion stability and the formation of a hydrophilic surface on the graphene nanoplatelets, which ensured a clear selective transfer process and favorable adhesion between the graphene and the paper substrate. The thickness was directly proportional to the graphene dispersion, and the sheet resistance was decreased with increasing thickness. The electronic circuits

revealed a small change in conductance under various folding angles and maintained an electronic path on the paper substrate after repetitive folding and unfolding. The effect of bending on the change in conductivity of graphene-based conductive traces is shown in Fig. 27.1. The ratio of measured conductance (G) to initial conductance (G_0) was obtained under various kinds of deformation shown in Fig. 27.1a. It is seen that the graphene circuits showed a small change in conductance under various folding angles and retained more than 80% of their conductance compared to their initial conductance, even after 1000 folding cycles. One limitation of graphene is that it is difficult to synthesize and disperse in solvents. Another limitation of graphene is the complex and expensive process to ensure pure graphene has been obtained.

Some groups have demonstrated ink-jet printed circuits using graphene (Huang et al., 2011; Tölle et al., 2012). The challenge in graphene printing lies in the development of ink formulation since the various rheological properties such as density, surface tension, and viscosity have a strong effect on the printing process (Banerjee et al., 2017). The nature of the binder material is also critical in determining sediment flexibility (Chen et al., 2003). A key advantage of 2D graphene is its high aspect ratio flake structure, which results in a much lower percolation conductivity threshold than in the case of 1D nanomaterials such as nanowires or nanotubes. If the graphene loading is too small, below the percolation threshold of the system,

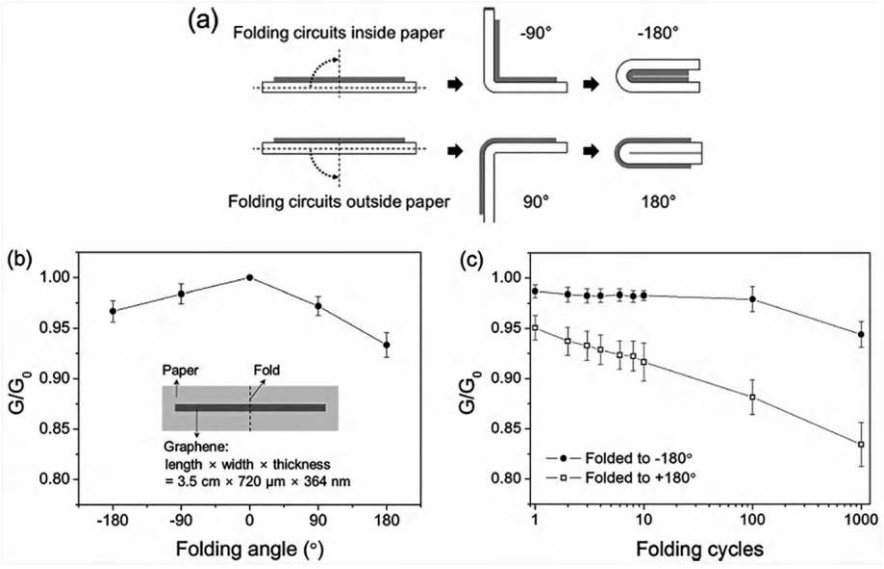

Fig. 27.1 (**a**) Schematic diagrams of the folding angles. (**b**) Relative conductance of the graphene circuits obtained on paper substrates and folded under various folding angles (inset: schematic diagram of the graphene circuits used for the measurement). (**c**) Relative conductance of the graphene circuits after repetition of folding and unfolding. These data were collected from seven samples, and error bars are the standard deviation. (Reprinted with permission from Hyun et al. (2013). Copyright 2013: Wiley)

there will be no conductivity. Above the percolation threshold, the conductivity will improve slightly as the load increases, but this improvement will be accompanied by a deterioration in the mechanical properties of the coating, such as flexibility and extensibility. Poor mechanical stability can lead to film cracks and loss of conductivity.

Another carbon-based material that can be used in paper-based electrochemical sensors as analytical electrodes, but as a bulk material, is glassy carbon (GC) (Elbadawi et al., 2021). GC is a non-graphitic glassy carbon formed by the pyrolysis of some polymer precursors (Yi et al., 2017). GC electrodes (GCE) are a suitable replacement for metal-based electrodes such as platinum or gold, since the latter have a smaller cathodic potential window due to the low hydrogen overpotential and are therefore not suitable for redox reactions that occur at more negative potentials. In addition, the formation of oxides on the surface of platinum and gold electrodes causes high background noise (Cheng et al., 2000; Han & Tachikawa, 2005; Li et al., 2015a). GCEs have good electrical conductivity, a wide potential window, high hardness, low porosity, low gas and liquid permeability, low oxidation rate, and high chemical inertness. Therefore, GCEs are suitable as inert electrodes. However, GCE has a limited number of active sites, which leads to low electrochemical sensitivity and selectivity to the analyte in trace measurements. For this reason, ECSs are rarely used in their pure form. Typically, GCEs are pretreated to overcome their limitations (Wang et al., 2019) or used as a substrate for chemically modified electrodes. For example, Sun et al. (2019) proposed to modify a GO/MnO_2 glassy carbon electrode for simultaneous electrochemical determination of trace Cu(II) and Pb(II) in water. Various GC pretreatment or activation procedures are used to increase the specific surface area, improve electron transfer kinetics, and introduce functional groups personalized to the analyte of interest (Abdel-Aziz et al., 2022).

Carbon materials are also widely used in the development of flexible energy storage devices (Zhang et al., 2021). Similar to conventional supercapacitors for energy storage, the development of electrode materials for flexible supercapacitors began with carbon materials. Carbon-based materials such as activated carbon (AC), carbon nanotubes (CNT), graphene, and carbon fibers (CF) have become a research hotspot due to their large surface area, excellent electrical conductivity, high stability, as well as good electrochemical performance and mechanical properties (Bellani et al., 2019; Jiang et al., 2021). As one of the most classical carbon materials, graphene has been widely studied and applied in various fields. However, when graphene flakes are deposited, they are prone to stacking, causing re-stacking effects, resulting in reduced specific surface area, clogging of ion transport channels, etc., which reduces the overall electrochemical performance of the devices.

Experiments have shown that mixing graphene and single-walled carbon nanotubes (SWCNTs) can solve many problems of carbon-based electrodes. In particular, SWCNTs in this composite can act as both a connecting element and a spacer between single-layer graphene sheets. In addition, the addition of SWCNTs can improve the conductivity of the electrode. The complex network structure formed by CNTs also provides better mechanical properties, since after deformation it can return to its original state relatively smoothly, without major structural changes.

Therefore, this structure can be used in flexible carbon-based supercapacitors. Supercapacitors using such electrodes have shown good resistance to stretching, bending, and other mechanical stresses (Bellani et al., 2019).

Although SWCNT is more suitable as an electrode material, the preparation process of SWCNTs is complicated and therefore expensive. Therefore, in many studies, cheaper multi-walled carbon nanotubes (MWNTs) doped with elements B and N are used as raw materials. Doping leads to the appearance of defect sites in the structure of the CNTs, which improves the charge storage performance. The use of MWCNT in energy storage materials can effectively reduce production costs (Kang et al., 2012).

Flexible activated carbon also is a cheap material that after wet chemical treatment can have high surface area and improved electrochemical performance. It is known that increasing the specific surface area is the most effective strategy for improving energy storage capacity. Carbon cloth due to lower capacitance usually is used in supercapacitors as a current collector (Zhang et al., 2021).

In the course of research, it was found that supercapacitors based on carbon materials have advantages such as good cyclic stability and high electrical conductivity, but their energy storage efficiency is relatively low. In general, carbon-based materials intended for electrical double-layer capacitors (EDLC) have low capacitance, which is a huge obstacle to increasing the energy density of supercapacitors. Therefore, after step-by-step research, metal oxides, conductive polymers, MXene, and various carbon-based hybrid materials are beginning to be used as electrode materials (Han & Dai, 2019; Zhang et al., 2009, 2021). At that, it is believed that the use of composite materials is the most promising direction in this research.

27.4 MAX Phase-Based Electrodes

MAX phases are a new class of materials that combine the properties of metal and ceramic (Gonzalez-Julian, 2020). These are materials with the $M_{n+1}AX_n$ phase, where M is an early transition metal; A represents a group A element, usually Al or Si; X represents a carbon and/or nitrogen group; and *n* ranges from 1 to 6 (Magnus et al., 2019). Ti_3AlC_2, NB_4AlC_3, Ti_3C_2, and Cr_2AlC are examples of such materials (Ghosh & Harimkar, 2012; Magnus et al., 2019; Zhao et al., 2015). MXene is a two-dimensional (2D) derivative of MAX phases (Biswas & Alegaonkar, 2022; Yu & Breslin, 2020). These phases have unusual and exceptional properties, including electrical properties. For example, MXene under optimal synthesis conditions can have a conductivity of up to 1.5×10^6 S/m (Levitt et al., 2020). Moreover, compared with graphene and its derivatives, the multilayer structure of MXene provides a larger specific surface area, which facilitates the immobilization of various materials and biological molecules on the electrode surface (Neampet et al., 2019). For example, MXenes have been found to retain enzymatic activity on the surface of electrodes (Neampet et al., 2019). In addition, MXenes inherently exhibit good stability in liquids, eliminating the need to use surfactants or dispersants to form stable

inks, as would be the case with other conductive particles (Zhang et al., 2020). According to Zhang et al. (2019), even 12 months after ink preparation, no sedimentation was observed. This is causing increased interest in these compounds. For example, MXenes have been shown to have great potential for energy storage devices such as supercapacitors, Li-ion batteries, Li-S batteries, catalysis, H_2 storage, and selective ion sieving (Ahmed et al., 2020; Biswas & Alegaonkar, 2022; Xie et al., 2016; Zhao et al., 2015). Levitt et al. (2020) found that MXenes can have volumetric capacities up to 1500 F/cm^3. The computational results showed that MXenes also have a low diffusion barrier for Na^+-ion on their surface, which favors rapid charging/discharging. These characteristics make MXenes attractive candidates for Na-ion storage. Wang et al. (2015a) reported that multilayer Ti_2CTx as a negative electrode showed a capacity of 175 mAh/g and good recharging rate.

Very good conductivity, large surface area, excellent hydrophilic properties, ease of combination with other materials, and easy surface modification make MXenes attractive for the development of various electrochemical sensors and biosensors (Biswas & Alegaonkar, 2022; Szuplewska et al., 2020; Yu & Breslin, 2020), as well as portable bendable technologies (Levitt et al., 2020; Zhang et al., 2018c). Zhang et al. (2019) showed that the conductivity of the MXene electrode decreased by only 2.5 times after 1000 bending cycles. It is important to note that in many published papers where comparisons are made with graphene or carbon nanotubes, MXenes demonstrate higher sensitivity and lower detection limits, outperforming graphene and carbon nanotube-based sensors (Yu & Breslin, 2020).

Examples of using MXenes in paper devices can be found in (Jiao et al., 2019; Tang et al., 2022; Wang et al., 2021a). Wang et al. (2021a) used an MXene (Ti_3C_2) modified working electrode to develop an electrochemical immunosensor. The modified paper-based electrochemical sensor was prepared according to the process shown in Fig. 27.2. First, f-Ti_3C_2-MXene was screen-printed on the electrode surface, and dried at room temperature. Then, 60 μg/ml anti-cTnI was applied to the modified MXene electrode and incubated for 30 min. Subsequently, 10 μL of 1% bovine serum albumin (BSA) was added to minimize nonspecific adsorption by blocking the remaining active sites. Finally, the immunosensors were stored at 4 °C before use. According to Wang et al. (2021a), the large surface area of MXene nanosheets promoted the immobilization of antibodies, and the excellent conductivity promoted electron transfer between the electrochemical particles and the underlying electrode surface. As a result, the paper-based immunosensor could detect cTnI over a wide range of 5–100 ng/mL with a detection limit of 0.58 ng/mL.

Jiao et al. (2019) prepared bacterial cellulose (BC)/MXene composite electrodes with excellent mechanical and electrochemical properties using vacuum filtration. From these electrodes, an all-solid flexible paper-based supercapacitor was assembled. This supercapacitor showed a specific capacitance of 115 mF/cm^2 and good mechanical stability under bending. Similarly, Tian et al. (2019) and Tang et al. (2022) prepared paper-based electrodes by vacuum filtration method using CNF/MXene and MXene/AgNW composites, which also showed excellent electrochemical performance of 298 F/g and 505 F/g, respectively. The works (Xie et al., 2016; Zhao et al., 2015) also mention CNT/MXene paper, which showed good volumetric

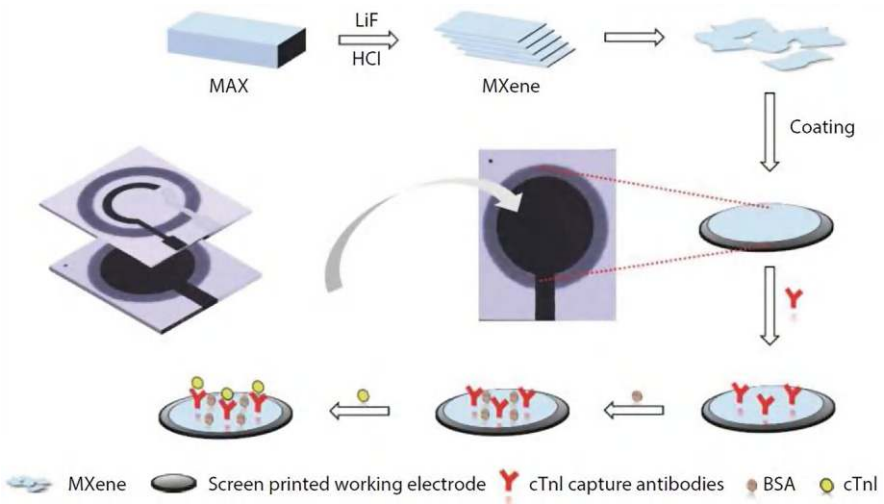

Fig. 27.2 Schematic diagram illustrating the fabrication of the paper-based immunosensor and its usage in the detection of cTnI. (Reprinted with permission from Wang et al. (2021a). Copyright 2021: Chinese Institute of Electronics)

capacity and speed characteristics for storing Na-ions. However, in these electrodes, the CNT/MXene had a paper-like structure that did not use cellulose.

27.5 Transition Metal Chalcogenides-Based Electrodes

Transition metal chalcogenides (VS_2, CuS, CoE_2, NiE_2, E = S, Se), rare earth metal sulfides (La_2S_3 and Sm_2S_3), and chalcogenides with a layered structure (MoS_2, $MoSe_2$, WS_2, and SnSe) form another class of electrode materials that are promising for flexible devices energy storage. This is due to their chemically rich surface, which promotes redox reactions (Cao et al., 2013; Feng et al., 2011; Jiang et al., 2014; Lin et al., 2019; Ramasamy et al., 2015; Ratha & Rout, 2013; Peng et al., 2014; Tanwar et al., 2021; Wei et al., 2014; Zhang et al., 2014b). At that, the most suitable alternative to graphene are 2D TMDs with a graphene-like planar structure, which are characterized by high fluorescence (FL) emission and quenching, high carrier mobility, high surface-to-volume ratio, and compatibility with modern manufacturing technologies. In addition, all TMD materials exist in the semiconductor (2H) and metallic phase (1T). Another important advantage of these materials is that 2D TMDs are mechanically flexible and therefore can be integrated with next-generation flexible wearable devices (He et al., 2012; Lyu et al., 2021). The high flexibility of ultrathin TMDC nanomaterials allows them to be easily applied to flexible substrates. The mechanical strength of TMDCs also allows them to adapt well to the human body.

Transition metal dichalcogenides (TMDs) with layered structures have also recently attracted considerable attention from supercapacitor developers due to their unique properties (Cherusseri et al., 2019; Chhowalla et al., 2013; Choi et al., 2017; Mukherjee & Singh, 2019). This class of materials can have two-dimensional (2D) layered morphologies that exhibit large surface areas and improved electrochemical kinetics coupled with small volume changes upon ion intercalation. For example, Balasingam et al. (2015) studied multilayer $MoSe_2$ nanosheets prepared by hydrothermal methods for supercapacitor applications. An optimal capacity of 49.7 F/g was obtained with a capacity retention of 75% after 10,000 operating cycles. Acerce et al. (2015) successfully synthesized 1T phase MoS_2 nanosheets and used a vacuum filtration method to prepare free-standing pure MoS_2 paper. These paper-like electrodes achieved high volumetric capacitances ranging from 400 to 700 F/cm^3 in a variety of aqueous electrolytes. These MoS_2 paper-like electrodes achieved an even higher energy density (0.11 W/cm^3) and power density (51 W/cm^3) in organic electrolyte with operating working window up to 3.5 V (Fig. 27.3). WS_2 "nanoribbons" were also studied as a supercapacitor electrode in potassium electrolyte, and the results showed that such electrodes had an optimal capacitance area of 2813 μF/cm^2 (Khalil et al., 2016). Ternary and higher-order chalcogenides are also promising for applications. These materials are attractive for supercapacitor electrodes because they contain different metal ions to facilitate rich redox reactions and the tunable gap between the layers can host a wide range of ions from the electrolyte to enhance the specific capacitance. For example, the $CuSbS_2$, $CuSbSe_xS_{2-x}$, $Zn_xCo_{1-x}S$, $NiFe_2Se_4$-based electrodes provided exceptional cyclic stability at high current densities, making them attractive for fast charging applications (Lyu et al., 2021; Ramasamy et al., 2014, 2015).

Another promising area of application for dichalcogenides is Na-ion batteries (David et al., 2014). David et al. (2014) reported that Na-ion batteries with MoS_2 electrodes demonstrated a capacity value that was twice the value theoretically calculated for Na/MoS_2 electrodes. It has been suggested that a conversion type reaction may be responsible for such high capacity. In comparison, graphite, which can also have a two-dimensional layered morphology, exhibits almost negligible

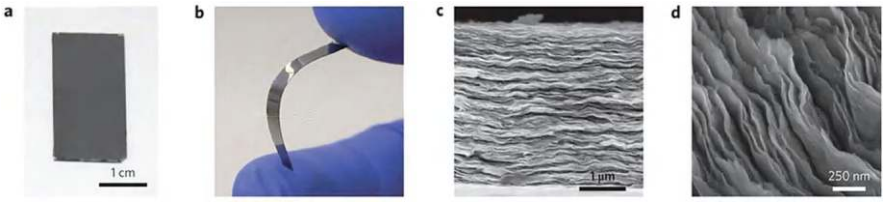

Fig. 27.3 Chemically exfoliated 1T MoS_2 electrodes. (**a**, **b**) Photographs of electrodes consisting of a thick film of chemically exfoliated 1T MoS_2 prepared by vacuum filtration and transferred onto rigid glass (**a**) and a flexible polyimide substrate (**b**). (**c**) Side view of the electrode observed by scanning electron microscopy (SEM) showing the layered nature of the film made by restacking exfoliated MoS_2 nanosheets. (**d**) High-magnification image of restacked MoS_2 nanosheets. (Reproduced with permission from Acerce et al. (2015) Copyright 2015: Nature Publishing Group)

capacity and cycling ability with respect to Na (Ge & Fouletier, 1988). $MoSe_2$ nanoplatelets have also been tested as anodes in sodium-ion batteries (SIB) (Wang et al., 2015b). The nanoplates were produced by pyrolysis, and the initial charging and discharging capacity of the batteries reached 1846.8 C/g. However, after 50 operating cycles, the capacity dropped to approximately 1400 C/g. The decrease in capacity was explained by a change in the $MoSe_2$ lattice structure from octahedral to tetrahedral due to the intercalation of Na ions (Wang et al., 2015b). David et al. (2014) studied also self-contained MoS_2/graphene composite anodes in sodium-ion battery systems. Their composite anode demonstrated a stable charging capacity of 828 C/g with a coulombic efficiency of 99%. TMDs can also be used as electrodes in Li-ion batteries (Lai et al., 2023; Mi et al., 2013; Miao et al., 2015). For example, recent theoretical calculations demonstrated that the covalently bonded S-Re-S layers of ReS_2 show a large interlayer distance (0.61 nm) and much weaker interlayer Van der Waals force (approximately 18 m eV) compared with those of other TMDs, e.g., MoS_2 (460 m eV). This exotic bond structure is highly appreciated for the transfer and storage of electrolyte ions, e.g., the de-intercalation, diffusion, and intercalation of lithium ions (Lai et al., 2023).

Research has shown that the layer-dependent tunable band structure, biocompatibility, low toxicity, and properties mentioned above make TMDs suitable candidates for the development of various sensors, primarily biosensors, where TMDs can be used both active materials and electrodes (Mia et al., 2023; Sun et al., 2022; Wang et al., 2020). In particular, Irandoost et al. (2023) have shown that nickel sulfide (NiS) due to its exceptional conductivity and stability has great potential for use as an electrode in electrochemical sensors. Due to their lower cost and outstanding electrochemical properties, TMDs can replace noble metals. With advanced synthesis methods and transfer processes, TMD heterostructures with other 2D materials show improved properties suitable for selective detection. The use of composites can also improve parameter stability of TMDs. For example, reduced graphene oxide (rGO) is used as an auxiliary material to effectively stabilize NiS in redox reactions to solve the instability problem of NiS-based electrodes (Irandoost et al., 2023). Surface modification of TMDs with the help of defect engineering by various methods, such as plasma treatment and thermal annealing, helps in suitable surface functionalization with specific receptors (Kirubasankar et al., 2022; Sun et al., 2022). The increase in the active surface site density increases the probability of binding of analytes to the sites of the sensing transducer elements, hence causing the modulation of opto-electronic properties, which results in highly sensitive biosensors with improved detection limit (Lee et al., 2014).

However, despite the promise of transition metal chalcogenides for flexible devices, these materials are practically not used in the development of paper-based devices. There are only a few works done in this direction (Lee & Choi, 2019; Pataniya et al., 2022). Some of the limitations in the use of TMDC appear to be the technology for the synthesis of these compounds, low catalytic activity and low conductivity of 2H TMDC. However, it is possible that TMDCs will be more widely used as electrodes in paper-based devices in the near future, as 1T TMDs have been found to be typically metallic and highly conductive. For example, a single-layer 1T

MoS_2 sheet at room temperature has an electrical conductivity of 10–100 S/cm, which is 10^7 times higher than the electrical conductivity of 1H MoS_2 monolayers. These values are close to the conductivity of reduced graphene oxide sheets (~100 S/cm) (Acerce et al., 2015). All these indicate that the use of certain metallic 1T TMDs that are stable in certain electrochemical processes may have a great future in energy storage devices (Lin et al., 2019). Recent experiments confirm this conclusion. Pataniya et al. (2022) reported a flexible, large area, and durable paper-based electrode functionalized with electrochemically active 1T rhenium disulfide (ReS_2) nanocrystals. ReS_2 has a very stable 1T phase and exhibits efficient electron transport characteristics. Pataniya et al. (2022) fabricated a paper-based ReS_2 electrode without using a binder. Extremely low series resistances of 2 ohms and charge transfer resistances of 5 ohms were achieved for the fabricated electrodes. The paper-based electrode also showed a high specific capacitance of 133 F/g. The ReS_2-based low-mass electrode also demonstrated more than 95% capacity retention after 3000 cycles.

27.6 Metal Oxides

Metal oxides are usually not used in sensors and many electronic devices for the manufacture of electrodes. An exception is ITO, which is used as transparent conductive contacts in many flexible optoelectronic devices such as displays, organic LEDs, and solar cells (Cao et al., 2014). At the same time, in the development of flexible energy storage devices, conductive transparent metal oxides, such as MnO_2 (Yao et al., 2014), MoO_3 (Yao et al., 2016), Fe_2O_3 (Hu et al., 2016), Co_3O_4 (Yang et al., 2013), TiO_2 (Zhao & Shao, 2012), V_2O_5, RuO_2 (Hwang et al., 2015), and In_2O_3 (Chen et al., 2009), are quite common. They are used to make electrodes in supercapacitors and batteries. In a basic form, a supercapacitor consists of two electrodes isolated from electrical contact by a semipermeable membrane functioning as a separator. The advantages of metal oxides include large energy and power density, low cost, manufacturability, and stability (Lyu et al., 2021; Palchoudhury et al., 2019).

Metal oxide usually has a complex microstructure and larger specific surface area, and this leads to a large number of active sites and ion channels, which can accelerate the redox reaction and improve the charge storage capacity. Indeed, metal oxides have high theoretical specific capacity: Fe_2O_3 (1005 mAh/g) (Zhu et al., 2011); Co_3O_4 (890 mAh/g) (Wu et al., 2010); MnO_2 (838 mAh/g) (Sun et al., 2011); SnO_2 (781 mAh/g) (Meduri et al., 2009); CuO (674 mAh/g) (Ko et al., 2012); V_2O_5 (294 mAh/g) (Zeng et al., 2015). By comparison, carbon allotropes, which have been widely studied as electrode materials for energy storage devices, have relatively low theoretical capacitance/capacity. The theoretical capacitance of graphene for supercapacitor is 550 F/g, and the theoretical capacity of graphite for Li-ion battery is 372 mAh/g (El-Kady et al., 2016; Zhang & Qi, 2016). For comparison,

theoretical capacitance for Fe_2O_3 and Co_3O_4 is 3625 F/g and 3560 F/g, respectively (Lyu et al., 2021).

However, due to the complex structure, the active materials are easy to fall off and bond in the process of cycling, thereby reducing the cycle stability (Zhang et al., 2021). Therefore, the formation of a composite with structurally stable carbon materials is a promising approach that can both improve the stability of metal oxide supercapacitors and increase the capacity of carbon-based supercapacitors (Yao et al., 2017). Examples of such composites are MnO_2/Ni/graphite (Feng et al., 2014), Fe_2O_3/graphene (Hu et al., 2016), SnO_2/graphene (Liang et al., 2012), MnO_2/CNT (Dong et al., 2016), graphene oxide/MnO_2 (Sundriyal & Bhattacharya, 2017), and V_2O_5-CNT (Wu et al., 2016). Nanocomposites with metals also are used. In particular, Ko et al. (2017) reported a new ligand-mediated layer-by-layer technique to assemble metal (Au) and metal oxide (MnO) pseudocapacitive nanoparticles on flexible paper substrate to form supercapacitor electrodes. The device showed substantially high energy (15.1 mW/cm^2) and power (267.3 μWh/cm^2) densities.

Research has shown that ternary metal oxides are also very attractive for energy storage applications, because they provide additional sites for pseudocapacitive redox processes to facilitate higher capacity. For example, ternary metal oxide $NiCo_2O_4$ is very suitable for supporting a variety of electrochemical processes because it contains mixed-valence metals (Zhang et al., 2014c). In addition, $NiCo_2O_4$ nanocrystals grown on carbon fiber paper have shown good cyclic stability and high capacitance (Huang et al., 2013).

27.7 Polymer-Based Electrodes

27.7.1 Polymers as Conductive Electrodes

In some publications, conductive polymers such as poly(3,4-ethylenedioxythiophene) (PEDOT) (Bihar et al., 2017), polypyrrole (*PPy*) (Yuan et al., 2013), polyacetylene (Wang et al., 2018), or polyaniline (PANI) (Jagadeesan et al., 2012) are also used to form conductive layer and electrodes on paper substrates. Conductive polymers can be easily processed at lower temperatures and at lower costs (Stejskal et al., 2016). Thus, conductive polymers can replace metals and ceramics in electrodes for some applications (Amanat et al., 2010; Carrión et al., 2011). For example, Yuan et al. (2013) successfully fabricated highly conductive paper electrodes using a PPy layer. The electrical conductivity of polypropylene-coated paper electrodes increased with increasing polymerization time and polypropylene mass loading. Yuan et al. (2013) showed that the surface resistance of such electrodes can be as low as 4.5 Ω/□. These same polymers can be used to make electrodes based on composites such as CNTs/PANI (Niu et al., 2012), CNTs/PEDOT (Shin et al., 2011), or graphene/PEDOT:PSS (Lee et al., 2017b; Liu et al., 2015).

Among conductive polymers, PEDOT is of particular interest due to its high conductivity, mechanical flexibility, transparency, catalytic ability, high specific capacity, flexibility, biocompatibility, acceptable potential window for electrochemical operations, small bandgap, and stability in the oxidized state (Chiang & Wu, 2013; Sappia et al., 2021; Shin et al., 2011). In the case of PEDOT, metal-free electrodes can be produced by depositing conductive polymer films on insulating plastic or paper substrates with excellent performance in electrochemical applications such as nanofluidics, biosensing, and even for flexible electrodes (Sappia et al., 2021). Figure 27.4 shows the effect of electrode type on the bending resistance of dye-sensitized solar cells. It can be seen that the use of graphene dot (GD)/PEDOT:PSS composite instead of Pt significantly improves the stability of parameters of flexible solar cells.

However, PEDOT is not soluble in most solvents, making the solution processing problematic. To improve the material's processability for industrial production, the researchers incorporated poly(styrene sulfonate) (PSS) as a counter anion to dope PEDOT. The resulting PEDOT:PSS product can be easily dispersed in water, allowing the formation of conductive layers on various substrates using solution coating methods (Chiang & Wu, 2013; Xu et al., 2009). However, pristine PEDOT:PSS exhibits low conductivity (below 1 S/cm) due to non-conducting PSS-16-rich layers encapsulating PEDOT conductive chains (Kim et al., 2019). The experiment showed that conductivity can be significantly increased by doping, solution processing, or incorporating conductive materials such as carbon nanotubes and graphene into the polymer. For example, Lee et al. (2017b) compared parameters of Pt electrodes fabricated by sputtering and graphene dot (GD)/PEDOT:PSS-based electrodes fabricated by solution method. They found that the polymer/GDs-based ink was better able to fill the pores of the paper substrate, while

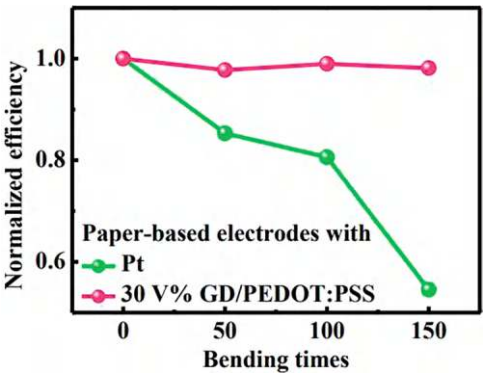

Fig. 27.4 Normalized efficiency of the flexible DSSCs using the two types of paper-based counter electrodes after being bent up to 150 times. Pt electrode was deposited by sputtering. To prepare the paper-based counter electrodes, commercially available A4 printing paper (Double A) was used as the substrate. The paper was immersed in the optimal 30 Vol% GD/PEDOT:PSS solution for 10 min and then dried at 60 °C for a few hours. (Reprinted with permission from Lee et al. (2017b). Copyright 2017: Elsevier)

sputtered Pt coating was unable to sufficiently reach all the surfaces and coat the metal inside all the voids. After bending the paper electrodes 150 times, it was found that the performance of the solar cell with the GD/PEDOT:PSS paper electrode was well preserved, while in contrast, the device made using sputtered Pt drastically lost its initial cell performance after the same test. A significant increase in the conductivity of PEDOT:PSS was also achieved through post-treatment with sulfuric acid (Kim et al., 2014). A value of 4380 S/cm was reported for PEDOT:PSS after such treatment. Recently, the polymer was solution-processed using a combination of an organic acid-organic solvent which yielded a polymer film thereof with a conductivity of ~3500 S/cm, yet maintaining a high transparency of 94% (Mukherjee et al., 2014).

Given the aforementioned advantages, PEDOT:PSS has been widely researched in biosensors (Distler & Boccaccini, 2020; Elbadawi et al., 2021; Moon et al., 2018). The polymer displays both excellent electrochemical stability and reliability (Liu et al., 2008). Additionally, the polymer's surface has been found to be suitable for the electrodeposition of nickel nanoparticles, which is a cheap, selective, and sensitive non-enzyme electrode (Mazloum-Ardakani et al., 2016), and glucose oxidase immobilization (Liu et al., 2008).

However, it must be recognized that although significant progress has been made in the development of flexible conductive electrodes (CE) based on PEDOT:PSS in terms of their electrical conductivity, the electrical conductivity of PEDOT:PSS is still low compared to conventional ITO, Ag NWs, and graphene CEs.

27.7.2 Polymers in Energy-Storage Devices

Research has shown that the following problems exist when using electronically conducting polymers (ECPs), such as polypyrrole (PPy), polyaniline (PANI), and polythiophene (PTP), in the manufacture of electrodes for batteries, fuel cells, and supercapacitors (Nyholm et al., 2011): (1) poor cycling stabilities, (2) high self-discharge rates, (3) low capacities due to the low attainable doping degrees, and (4) mass transport limitations within thick polymer layers. Other disadvantages associated with the use of ECPs in flexible energy storage devices include their limited processability once synthesized due to their poor solubility, refractoriness, and mechanical brittleness. It was to solve these problems that it was proposed to use polymer composites containing carbon nanotubes (CNTs) or graphene (El-Kady et al., 2016; Li et al., 2009; Yao et al., 2017) or deposit ECP in the form of a thin film on high surface area substrates such as cellulose (Fan et al., 2007; Nyström et al., 2009). The polymer binders in such composites are used to glue the active materials and conducting agents as well as the current collector, whereas the conductive agent network helps to transfer electrons from active materials to current collector. Regarding the deposition of thin layers of conductive polymer on cellulose fibers, several methods have been proposed in the literature for coating of cellulose fibers with ECP, which include (i) lean base solution deposition (Huang et al., 2005), (ii)

vapor polymerization (Winther-Jensen et al., 2007), and (iii) deposition from polymer solutions in organic solvents (Pääkkö et al., 2008).

Thanks to these approaches, it was possible to improve the parameters of energy storage devices. In particular, recent work indicates significant progress in overcoming the limitation associated with the cyclic instability of electrodes. Nyholm et al. (2011) showed that reinforcing conductive polymers with cellulose fibers also provided improvements in cycling stability, mechanical flexibility, and strength of electrodes. In particular, Van Den Berg et al. (2007) found that the inclusion of small amounts of cellulose whiskers was beneficial for PPy, since reinforcing the conductive polymer with cellulose whiskers resulted in a significant increase in Young's modulus, decrease in elongation at break, and increase in tensile strength. Moreover, cellulose-ECP composites can be formed into various shapes, which is a great advantage for the development of energy storage devices. Such composites can either be used directly as a working electrode or used as a conductive material for the electrochemical deposition of various metals, such as Cu or Ag (Kelly et al., 2007).

In energy storage devices, the electrode structure also plays an important role in improving charge storage performance. Open pore electrodes allow rapid ion diffusion and help achieve both high capacity and high recharge rate. In particular, by polymerizing polypropylene in the presence of cellulose nanofibers, a highly porous, mechanically strong conductive paper material with a large charge capacity can be obtained (Mihranyan et al., 2008; Nyström et al., 2009). In these electrodes, polypropylene provides rapid mass transfer of ions required for the oxidation and reduction of polypropylene, and the cellulose base provides good overall flexibility of the material.

In addition to these composites, composites such as PEDOT/graphene (Liu et al., 2015), PPy/MnO_2/CNT (Liang et al., 2014b), PANI/Au (Yuan et al., 2012), PANI/MnO_2/graphene (Li et al., 2015b), and MXene/PEDOT:PSS (Bora et al., 2020) can also be used in the manufacture of paper-based energy-storage devices.

27.8 Electrodes Based on Composites Containing Ag Nanowires

As previously shown, metal and carbon-based electrodes often cannot meet all the requirements of electrodes designed for specific applications. In this regard, electrodes based on composites demonstrate significantly better parameters. Thus, Liu et al. (2017a) compared the properties of electrodes made on paper using aqueous inks based on silver microflakes (AgMF), silver nanoparticles (AgNP), Ag nanowires-PVP (AgNW-PVP) composite, and AgNW-graphene (AgNW-GO) composite. As a result of the studies conducted by Liu et al. (2017a), it was concluded that AgNW-GO-Ink (AgNWs: ≈4.7 wt% or ≈0.48 vol%; GO: ≈0.59 wt% or ≈0.3 vol%) provides the most optimal parameters for electrode coatings. The drawn

AgNW-GO-Ink conductive lines on paper can achieve conductivity as high as 2.3×10^4 S/cm and sheet resistance as low as 0.44 Ω/□ upon drying for only ≈5 min at 25 °C. In addition, AgNW-GO-Ink electrodes have excellent stability (Fig. 27.5a) and foldability (Fig. 27.5b). AgNW-GO-Ink conductive lines drawn on paper can be repeatedly folded with a permanent non-elastic crease at the fold line of the paper without significant deterioration in conductivity even after 1000 cycles. According to Liu et al. (2017a), monolayer graphene oxide (GO) sheets in AgNW-GO ink act as dispersing, thickening, stabilizing, adhesive, oxidation resistance, and mechanical strengthening agents simultaneously (Fig. 27.6).

Regarding the stability of contacts based on AgNW-GO inks, studies by Liu et al. (2017a) showed that electrodes fabricated using AgNW-GO inks have not only low resistance, but also increased stability compared to electrodes based on AgNW-PVP, AgNP, and AgMF inks. As can be seen from Fig. 27.5b, after accelerated tests at 60 °C in air for 30 days, the resistance of electrodes made using AgNP-ink and AgMF-ink tends to slightly increase during the test and reaches values 1.8 and 1.6 times higher than the initial values. At the same time, the resistance of the electrode based on AgNW-PVP-ink demonstrates a much greater increase. After 30 days, it increases by 4.3 times compared to the initial values. It was found that the increase in resistance is mainly due to the problem of surface oxidation of nanosized or microsized silver fillers caused by exposure to oxygen and sulfur from the environment (Lee et al., 2013; Moon et al., 2013). In contrast, the resistance of the AgNW-GO-ink electrode increased by only ≈15% after 30 days. It is assumed that GO wrapping AgNW can act as a barrier layer that prevents the reaction of AgNW with oxygen and sulfur from the environment (Lee et al., 2013; Liang et al., 2014a; Moon et al., 2013). This long-term storage stability is an important advantage of AgNW-GO electrodes for paper electronics and sensor applications.

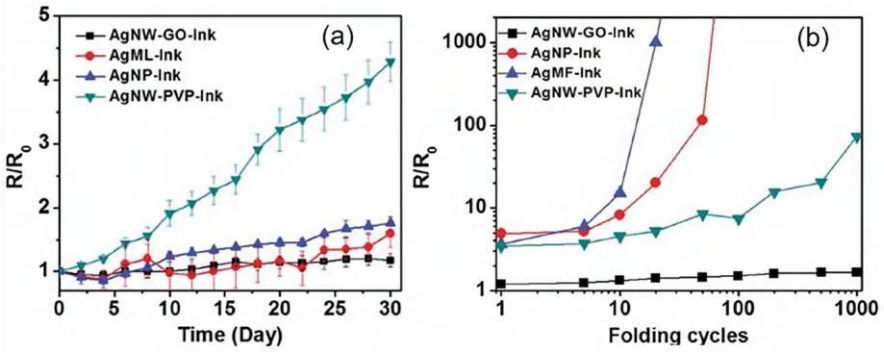

Fig. 27.5 (**a**) Plots of relative resistance change versus time for AgNW-GO-Ink, AgNWPVP-Ink, AgNP-Ink, and AgMF-Ink electrodes drawn on paper substrates after exposure to hot air at 60 °C for 30 days. (**b**) Relative resistance changes of AgNW-GO-Ink, AgNW-PVP-Ink, AgNP-Ink, and AgMF-Ink electrodes drawn on paper substrates during 1000 repeated folding–unfolding cycles. More than five samples for each electrode were measured for the electrical conductivity and stability tests. (Reprinted with permission from Liu et al. (2017a). Copyright 2017: Wiley)

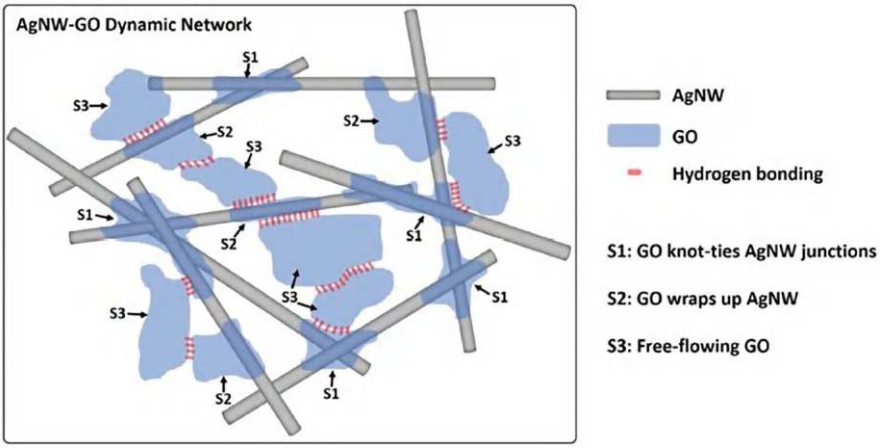

Fig. 27.6 Schematic illustration of associative thickening of AgNW-GO-Ink via dynamic AgNW-GO network. GO is present in the inks as three states: S1, GO knot-ties and solders the AgNW junctions; S2, GO warps up the AgNWs; S3, GO free flows in the ink. The cohesion of the AgNW-GO dynamic network stems from the hydrogen bonding. (Reprinted with permission from (Liu et al., 2017a). Copyright 2027, Wiley)

Kim et al. (2017) also showed that protective layers such as rGO and CNTs enhance the durability of the electrical conductivity of the AgNW layer. In particular, highly flexible transparent conductive multilayer electrode coatings based on rGO, CNTs, and AgNWs exhibited excellent mechanical, chemical, and thermal properties. Moreover, they showed superior flexibility and durability, as well as lower friction and wear characteristics compared to a single AgNW layer. Applying a polyacrylate or polyimide film to the AgNW layer has an even greater effect in improving the bending durability of AgNW electrode (Li et al., 2014b; You et al., 2016). Molina-Lopez et al. (2012) found that the stability of Ag-based electrodes could also be improved by passivation of printed silver electrodes with nickel. Choi et al. (2019) have shown that Ag fiber/IZO composite electrodes also exhibited chemical and thermal stability.

Another promising material for flexible electrodes is AgNW/polymer composite film, which takes advantage of the high electrical conductivity of Ag NWs and the flexibility of the polymer film (Han et al., 2015). The random distribution of Ag NW/polymer composite film can be produced by a solution-based process and is suitable for roll-to-roll production. The diameter and length of the AgNWs, as well as the percolation of the Ag NW network, have a strong influence on the R_{sh} and optical transparency of the Ag NW/polymer composite film. The small diameter of the AgNW can reduce its light scattering, and its long length ensures good connectivity with the AgNW network and low R_{sh}. Moreover, the incorporation of Ag NWs into the polymer film can significantly reduce the surface roughness of the Ag NW electrode, which is a critical disadvantage. PVA (polyvinyl alcohol) film can also be used as a transparent polymer matrix for Ag NWs (Han et al., 2015).

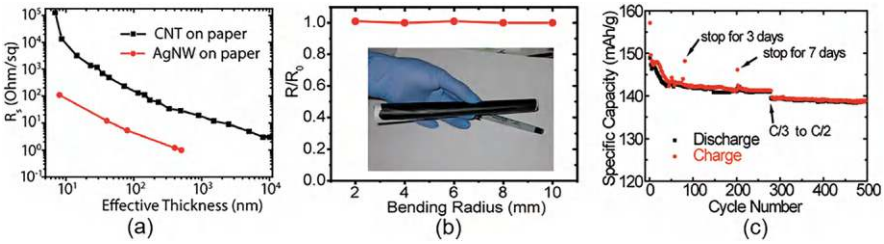

Fig. 27.7 (**a–c**) Electrical performance of conducting paper based on CNTs and Ag. (Reprinted from Hu et al. (2009). Published 2009 by the National Academy of Sciences with open access)

Hu et al. (2013) fabricated a highly conducting porous composite of nanocellulose (NC) fibers and CNTs for application as high-performance electrodes by simply uniformly mixing CNTs and NC with Ag nanowires. Hu et al. (2009) also showed that, due to the continuous electrical conduction pathways formed by combining CNTs with silver nanowires, composite CNT-AgNWs make it possible to form electrodes with very good electrical parameters and mechanical flexibility (see Fig. 27.7). The sheet resistance of the electrodes increased insignificantly (<5%) even after 100-fold bending to a radius of 2 mm. Hu et al. (2009) believe that this encouraging result is likely due to the combined effect of the flexibility of individual CNTs, the strong bond between CNTs and cellulose, and the porous structure of cellulose paper, which can greatly reduce the applied bending stress. In addition, the strong attraction of the cellulose fiber to the CNTs makes the film highly resistant to damage (e.g., scratches and peeling). Weng et al. (2011) showed that conductive paper electrodes made of graphene and cellulose are also suitable for fabricating sensors. After 1000 repeated bending tests, only a 6% decrease in conductivity was found.

27.9 Transparent Flexible Electrodes

As it will be shown in Vol. 3, optoelectronic devices such as solar cells, photodetectors, light diodes, and various optical sensors occupy a central spot among the wide array of applications that benefit from flexibility. All of these examples require electrodes that, in addition to being flexible, must be able to let light go through them.

There are two main classes of transparent flexible electrodes: electrodes that are intrinsically transparent, and electrodes made thin enough to be transparent (Graz & Rosset, 2021). Many of the flexible electrodes mentioned in the previous sections can be made partially transparent if their thickness is reduced (McCoul et al., 2016). For example, metal films, when sufficiently thin (<10 nm), become transparent to light, still maintaining continuity, thus having good electrical properties (Yun, 2017). However, you should always keep in mind that there is an inverse relationship between light transmission and electrode conductivity. For example, De et al.

(2009) studied the relationship between optical transmittance at λ = 550 nm and sheet resistance of silver nanowire films. They tested conductive films that ranged from 0.5 ohm/□ sheet resistance and 30% transmittance to 100 ohm/□ sheet resistance and 90% transmittance. It was found that the greater the thickness and the lower the resistance, the lower the transparency of the electrodes (see Fig. 27.8). This means that in the process of developing transparent devices, when choosing the thickness of the conductive film, a compromise must be made between transparency and electrical conductivity of the electrode. The surface roughness and structure of the transparent electrodes should also be taken into account, since these electrode parameters can negatively affect the quality of the transmitted image, even if the overall transmitted intensity is high.

The experiment showed that metal electrodes can provide both high electrical conductivity and good optical transparency (Lu et al., 2021). Although conventional metal thin films of gold and palladium can achieve transparency of about 50% (Rosset et al., 2009), flexible transparent metal electrodes are still mainly based on a network of silver (AgNW) or copper nanowires (CuNW). At the same time, silver is most often used in transparent electrodes, since it has the lowest electrical resistivity and optical losses in the visible region of the spectrum among known metals. In the case of nanotubes and nanowires, their high aspect ratio allows the percolation threshold to be reached at a very low nanowire concentration, resulting in a conductive electrode with extremely low material density and thus a high degree of transparency. Moreover, as the length of the nanowires increases, this effect

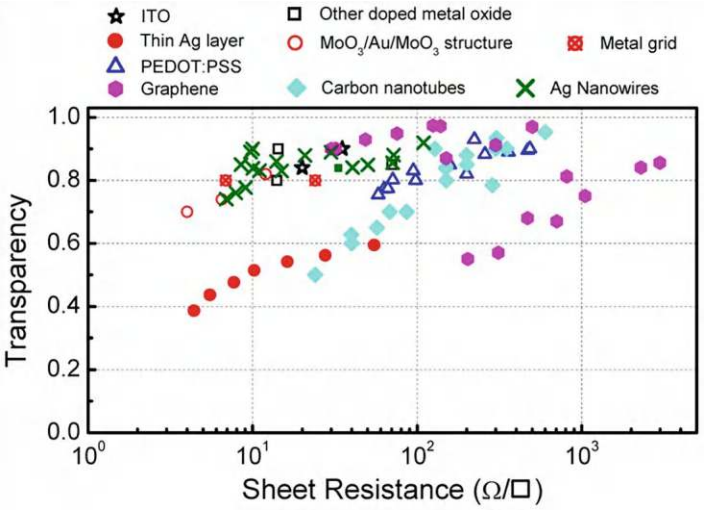

Fig. 27.8 Literature-reported transparency values in the visible spectral range as a function of the sheet resistance for transparent conductive materials: indium-tin oxide (ITO), other doped metal oxides, thin metal layers, dielectric/metal/dielectric multilayers, metal grids, poly(3,4-ethylene dioxythiophene):polystyrene sulfonic acid layers, graphene, carbon nanotube films, and Ag nanowires. (Reprinted from Cao et al. (2014). Published 2014 by SPIE with open access)

intensifies. In particular, Lee et al. (2012b) found that very long metallic nanowire conductors combined with a low-temperature laser nano-welding process can produce superior transparent flexible conductors with high transmittance and high electrical conductivity. The experiment showed that typically transparent (T > 50%) nanowire electrodes have sheet resistances in the range of 5–100 Ω/□ (McCoul et al., 2016). Cho et al. (2017) found that the performance of large-area transparent contacts can be significantly improved if random AgNW networks are replaced by cross-aligned AgNW arrays. Cross-oriented AgNW arrays fabricated using the developed technology demonstrated excellent electrical conductivity (Rs ~ 21 Ω/□), as well as high optical transmittance (T = 95%) over a large film area (area 20 × 20 cm^2). Cho et al. (2017) believe that this technology can be used to make touch panels, organic solar cells, and organic light-emitting diodes.

Similar to metal nanowires, carbon nanotubes and graphene can also be used to fabricate flexible transparent electrodes with the same trade-off between electrical conductivity and optical transparency (Cao et al., 2014). Specifically, single-layer graphene absorbs only 2.3% of visible light and can withstand 4% strain with negligible cracking. Single-walled carbon nanotubes spray-coated onto PET substrates at various surface densities exhibit transmittances ranging from 70% to 99% with sheet resistances ranging from 100 Ω/□ to 40 kΩ/□ (Scardaci et al., 2010). Although transmittance similar to that which can be achieved with metal nanowires is possible, the sheet resistance of the carbon nanotube-based layer is typically 1–3 orders of magnitude higher (Lessing et al., 2014; Li et al., 2015a). Typically, the Rs of films based on synthesized graphene usually exceeds several hundred Ohm/□.

Formation of macroscopic metal meshes (MMG) (Fig. 27.9a–c) is another approach of using metal to fabricate flexible transparent electrodes (Lee et al., 2019). Macroscopic metal meshes composed of ordered metal lines that are <1 μm wide are considered as a potential replacement for semitransparent continuous metal films and transparent metal oxide films (ITO) (Wu et al., 2013). One of the advantages of metal meshes is the increased transparency compared to continuous metal layers, where the gaps between metal lines are blank (100% in transparency) and contribute to the high transparency. The transmittance of metal meshes is determined by the percentage of the blank areas on the film, which is related to the metal line width, spacing between lines, and the number of total lines within a unit area. This means that different combinations of transmittance and conductance can be configured simply by adjusting the width and spacing of the lines. The low sheet resistance of the metal meshes can be achieved by using thick metal lines, 100 nm or even thicker. In addition, such electrodes have better bending and stretching durability (see Fig. 27.9d–f). They can withstand heavy bending and stretching stresses.

Table 27.1 provides a comprehensive evaluation of three types of flexible metal-based TCEs. Metallic meshes are seen to exhibit a better balance between optical and electrical performance due to their highly tunable architecture. However, although the use of macroscopic metal meshes offers great opportunities for the development of flexible paper-based devices (Lee et al., 2019), there are a number of factors affecting their large-scale application. The main one is the extremely rough surface. In addition, the production of metal mesh is still expensive. More

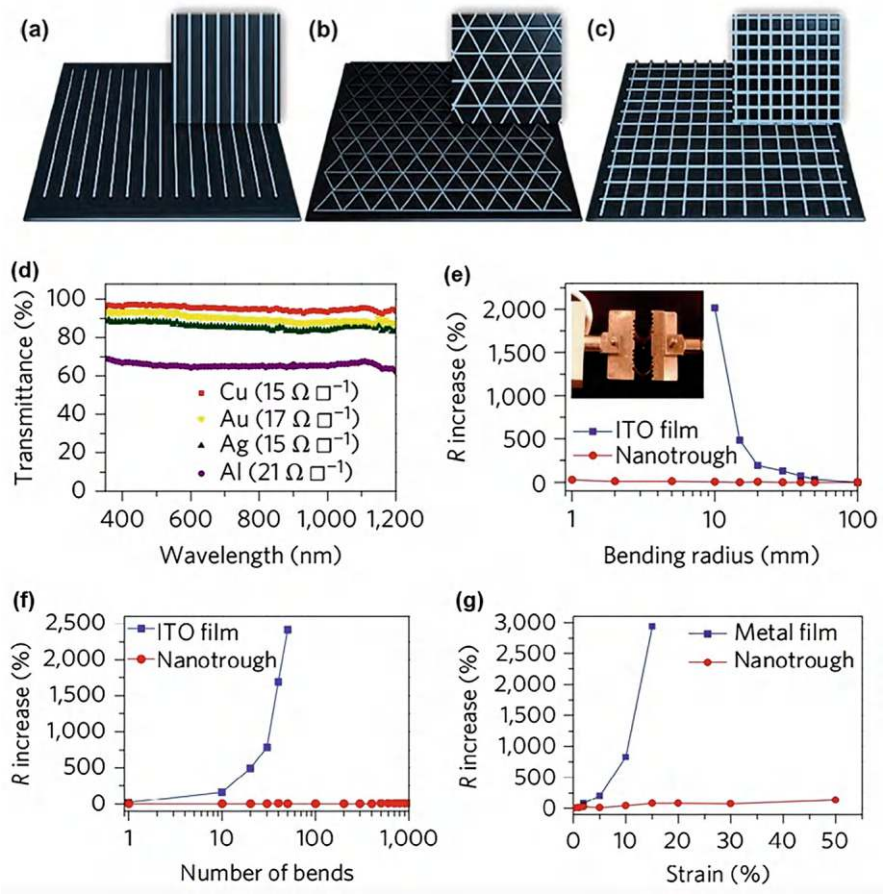

Fig. 27.9 Metal nanotrough networks as transparent, flexible electrodes. (**a**, **b**, **c**) Schematic metal-mesh electrodes with different geometries and aspect ratios: (**a**) lines, (**b**) pyramids, (**c**) grids. Reprinted with permission from Lee et al. (2019). Copyright 2019: RSC; (**d**) UV–vis spectra of metal nanotrough networks on glass substrates, showing a very flat spectrum for the entire wavelength range. (**e**) Rs versus bending radius for bendable transparent electrodes consisting of gold nanotrough networks or ITO films on 178-mm-thick PET substrates. (**f**) Variations in resistance of a gold nanotrough electrode and an ITO electrode on PET film as a function of the number of cycles of repeated bending to a radius of 10 mm. (**g**) Rs versus uniaxial strain for a stretchable transparent electrode consisting of gold nanotrough networks on 0.5-mm-thick PDMS substrate. The rapid degradation of a gold thin film with a thickness similar to the nanotroughs (80 nm) is shown. (Reprinted with permission from Wu et al. (2013). Copyright 2013: Springer Nature)

efforts are also needed to integrate MMG manufacturing technology with roll-to-roll processing (Cao et al., 2014).

Another approach to fabrication of transparent flexible electrodes is to use materials that are inherently transparent (Graz and Rosset, 2021). Such materials are, for example, heavily doped semiconductors with large band gaps, such as metal oxides

Table 27.1 Comparison of metal-based flexible transparent electrodes with ITO films

	Ultrathin metal film	Metal nanowire network	Metal mesh	ITO
Sheet resistance (Ω/□)	12–57	9–100	0.07–10	3–60
Transmittance (%)	80–93	89–95	70–95	80–90
Mechanical flexibility	Good	Good	Good	Poor
Chemical stability	Average	Average	Good	Good
Surface smoothness	Good	Average	Average	Good
Cost efficiency	Average	Good	Good	Average

Source: Reprinted with permission from Lu et al. (2021). Copyright 2021: Wiley

known as transparent conducting oxides (TCO) (Ong et al., 2015; Vosgueritchian et al., 2011). Of these metal oxides, the most famous is the previously mentioned indium tin oxide (ITO), with its excellent electronic conductivity and optical transparency in the visible range of light. ITO is usually deposited on transparent substrates as a bottom electrode and light window. Commercially available polycrystalline ITO with thicknesses in the range of 100–200 nm on glass substrates shows transmittance of more than 80% in the visible spectral range (Betz et al., 2006; Cao et al., 2014). However, ITO has poor mechanical properties. Microcracks have been observed in thin ITO layers after repeated bending and high-angle bending, resulting in a drastic reduction in film conductivity as well as device performance (Cao et al., 2014). In addition, when producing transparent electrodes on flexible substrates, it is necessary to use amorphous ITO, which has significantly lower conductivity compared to polycrystalline films. Therefore, to improve the conductivity of amorphous ITO, it is necessary to increase the thickness of the ITO layers. However, even in this case, the conductivity of amorphous ITO layers is still inferior to that of much thinner crystalline ITO films. This poses many technical limitations when applying ITO to mechanically flexible and thermally responsive polymers, which is critical for the recently emerging portable, bendable, and even wearable organic optoelectronic devices based on polymer and paper substrates. The use of relatively thick amorphous ITO in such flexible devices carries the risk of microscopic cracks and a corresponding catastrophic reduction in conductivity during mechanical deformation of the device (Leterrier et al., 2004; Lewis, 2006). These changes are clearly shown in Fig. 27.10. It can be seen that the resistance of the ITO film increases sharply as the bending cycle increases. On the other hand, the resistances of Ag fiber electrode, Ag fiber/IZO composite electrode (Fig. 27.10a), and PEDOT electrode (Fig. 27.10b) did not increase with the bending cycle.

Conducting polymers such as poly(3,4-ethylenedioxythiophene) doped with polystyrene sulfonic acid (PEDOT:PSS) can also be used as transparent conductive electrodes in flexible optoelectronics. Thin films of PEDOT:PSS dispersed in water as gel particles can be easily produced by simple and low-cost solution-based processes such as spin coating, dip coating, inkjet printing, and stamping printing (Han et al., 2015). For example, Vosgueritchian et al. (2011) tested spin-coated PEDOT:PSS layers. They obtained sheet resistances ranging from 230 Ω/□ (95%

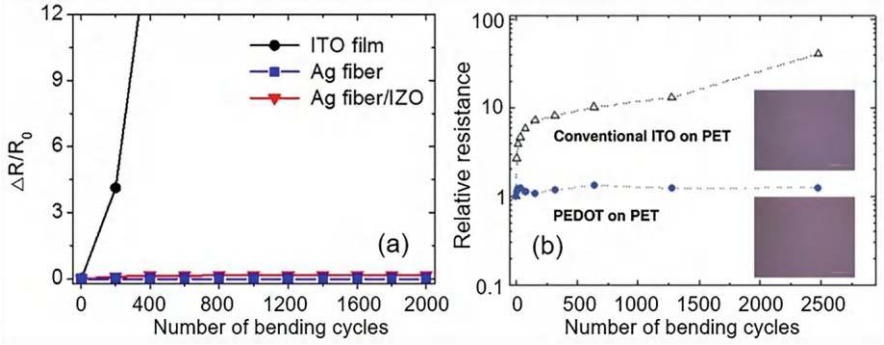

Fig. 27.10 (**a**) Resistance changes in the cyclic bending test for ITO, Ag, and Ag/ZnO-based electrodes. (Choi et al., 2019. Springer Nature. Open access) (**b**) Relative resistance of ITO and PEDOT:PSS films on PET substrates as a function of number of bending cycles. (Reprinted with permission from Na et al. (2008). Copyright 2008, John Wiley and Sons)

transmittance) to 46 Ω/□ (82% transmission), depending on the number of spin-coated layers. In addition, as shown in Fig. 27.10b, the resistance of PEDOT:PSS films remained almost constant after 2500 bending cycles, while the resistance of conventional ITO films on a PET substrate increased by more than 10 times after bending, resulting in a sharp deterioration in device performance. (Na et al., 2008).

27.10 Technologies Used for Fabrication of Flexible Electrodes

As with conventional substrates, various methods can be used to fabricate paper-based electrodes (Elbadawi et al., 2021; Li et al., 2019; Yao et al., 2017). For example, magnetron sputtering (Sakata et al., 2020; Wang et al., 2013), sintering (Liana et al., 2013), thermal evaporation (Yuan et al., 2012), laser etching (Santhiago et al., 2013), spray coating (Gilje et al., 2007), dip coating (Secor et al., 2014), drop casting (Liang et al., 2009), Langmiur-Blodgett deposition (Li et al., 2008), layer-by-layer assembly (Ko et al., 2017; Yu & Dai, 2010), soaking and polymerization method (Yuan et al., 2013), as well as various printing technologies (Simonenko et al., 2022; Yuan et al., 2016; Zhang et al., 2015) can be used. In particular, Nie et al. (2010) and Dungchai et al. (2009) used electrodes printed by screen printing on paper in the development of electrochemical sensors. Cinti et al. (2018) used inkjet technology to fabricate carbon black-based electrodes. Inkjet technology has also been used by Gaspar et al. (2017) for the formation of silver interdigital electrodes in the production of capacitive humidity sensors (see Fig. 27.11). Hu et al. (2012) used inkjet printing to fabricate arrays of nanoporous gold electrodes on cellulose membranes. Some details about specific conductive materials suitable for

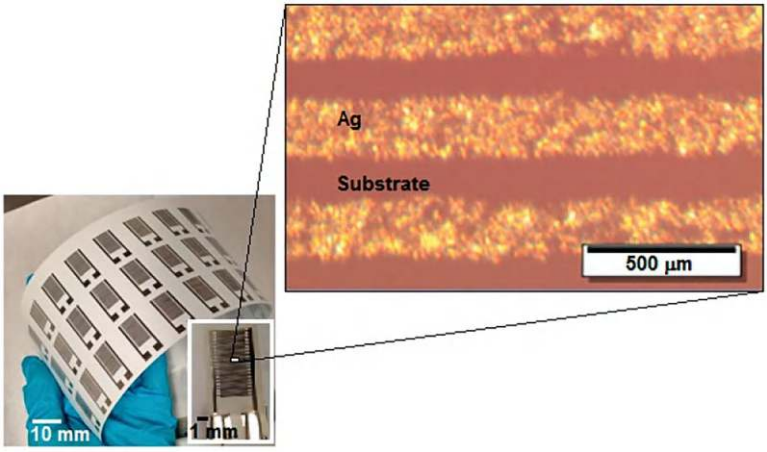

Fig. 27.11 Digital picture of an array of inkjet-printed Ag-interdigitated finger electrodes structure and the magnified view of one device and the electrodes (5× magnification). The printed structures showed average width of ~208 µm, a gap between fingers of ~140 µm, and average thickness of ~185 nm. Silver (Ag) nanoparticle colloidal ink (ANP 40LT15C) was used. (Reprinted from Gaspar et al. (2017). Published 2017 by MDPI with open access)

use in inkjet printers are discussed in (Cummins & Desmulliez, 2012; Hoeng et al., 2016; Sui & Zorman, 2020).

An advantage of inkjet printing in electrode fabrication is that the thickness of the electrode can be controlled by printing multiple layers. Due to this, it is possible to achieve a decrease in the resistance of the electrodes, an increase in their robustness, and an increase in the reliability of devices (Shamkhalichenar & Choi, 2017). Inkjet printing also eliminates some of the drawbacks of screen and stencil printing and provides better resolution, which can be important for complex patterns. Inks with the needed properties are applied to the desired areas, eliminating the need for masks, and the thickness of the applied materials can be precisely controlled (Bihar et al., 2017; Sui & Zorman, 2020). Production waste is also significantly reduced. Due to the already automated nature of this method, inkjet printing can be used effectively in large-scale production. Gaspar et al. (2017) also noted that usually during the process of applying ink to the surface of a paper substrate, some of the ink immediately impregnates the paper fibers and penetrates the paper. This not only promotes the drying process by increasing the evaporation rate of the ink solvent, but also improves adhesion. The porosity of the paper also improves the resolution of the print. Due to the absence of ink bleeding on the surface of the substrate, the definition of the roughness of the edge line is improved.

The limitations of inkjet printing are especially due to the specific ink physicochemical properties requirements for allowing droplet ejection and the restriction in the particle size (<1 µm) for avoiding nozzle clogging (Lee et al., 2012a). In these technologies, a wide range of carbon and silver inks can be used to produce electrodes (De Araujo & Paixao, 2014; Dungchai et al., 2009; Nie et al., 2010). In

particular, commercial CCI-300 Ag-ink (Cabot, Inc.) having an Ag nanoparticle diameter in the range of 30 ~ 50 nm in ethylene glycol/ethanol as the main solvent can be used to form electrodes. You can also use silver nanoparticle ink (DGP 40LT-15C from Anapro). Au, Cu, and Pt nanoparticle inks can also be used to form electrodes (Cummins & Desmulliez, 2012; Pavithra et al., 2018).

Yao et al. (2013) found that in order to produce high-quality electrodes using printing technology on an office paper substrate, pretreatment of the paper is necessary to remove inactive additives and increase its porosity. They suggested the following procedure: immerse a sheet of printing paper in an aqueous solution containing 0.3 M hydrochloric acid (HCl) for about 10 min, then rinse thoroughly with deionized water and allow to dry at room temperature. Pretreatment typically results in a reduction in both weight and thickness due to the removal of mineral fillers and fluorescent bleaching agents, resulting in a more porous open structure, which is often useful for paper-backed electrodes (Yao et al., 2017). To improve the quality of the electrodes before printing with Ag ink, Courbat et al. (2011) dehydrated the paper at 110 °C for 2 h, without any surface pretreatment.

It was also found that in the manufacture of silver contacts, post-treatment drying at room temperature of about 25 °C followed by treatment at T ~ 150 °C is necessary to achieve maximum conductivity. At that, only less than 2 min of drying time at this temperature was required to achieve the best electrical conductivity (Liu et al., 2017b). It was also found that photon annealing may be a better option in the manufacture of Ag-based electrodes (Gaspar et al., 2016). When using photon sintering methods, the effect of nanoparticle displacement during annealing is practically absent. The photon energy is more localized and efficient, which means that solvent evaporation and nanoparticle coalescence occur at almost the same rate, preventing nanoparticles from moving to the edges of the printed lines, providing a more uniform electrode thickness. Another common effect when using thermal sintering is crack formation, or microcracking (Tobjörk et al., 2012), resulting in disruptive and non-conductive structures. Paper has a low thermal expansion when compared to polymers, and that is the main reason why the crack formation due to substrate shrinkage is almost non-existent (Lewis et al., 2006). It was also found that electrodes made with other materials also require heat treatment at 60–90 °C for several minutes after printing.

The experiment showed that in addition to surface pretreatment and heat treatment after deposition (Lewis et al., 2006; Wakuda et al., 2007), there are many additional factors that need to be clarified for the successful fabrication of electrodes on paper substrates using printing technology. The wetting, spreading, or permeability of nanoparticle inks is very different from plastic substrates. It is necessary to control the spreading or penetration of inks. Another issue is interface reaction or paper-ink compatibility during curing. The paper must retain its structure, forming a strong interface during curing.

Vacuum filtration is another popular method in making paper-supported electrodes because of its fast and scalable characteristics. Vacuum filtration is highly scalable, low-cost, and easy process. Vacuum filtration setup usually consists of Buchner funnel, filter membrane, and vacuum system. Owing to its intrinsic 3D

porous structure, paper can be used as a "filter" to block the materials with the size larger than its pore size and at the same time coat the surface of fibers and fill its pores with these materials. Vacuum filtration method has been used to prepare carbon-based (e.g., graphene, graphite, CNT) paper-supported electrodes (Jabbour et al., 2012; Li et al., 2014a; Olsson et al., 2011; Weng et al., 2011). For example, Weng et al. (2011) fabricated the graphene paper by simply filtering a graphene nanosheets (GNSs) suspension through a filter paper. The strong binding between cellulose fibers and graphene was ascribed to the strong electrostatic interaction between the functional groups on the fibers and the negatively charged GNSs. The resistivity of this graphene paper was 6 Ω·cm and only decreased 6% after being bent 1000 times.

Ball pen as another writing technique has also shown great ability to write conductive materials (e.g., silver ink, carbon ink, and Cu-metal ink) on papers, since ball pens are compatible with various conductive inks and well suited to mark various patterns on papers (Li et al., 2015a; Liu et al., 2017a; Russo et al., 2011). Liu et al. (2017a) believe that this method can quickly prepare electrodes without any expensive equipment. But the main disadvantages of this approach include painter influence, low repeatability, and inability to be used in large-scale production. In addition, different conducive inks have different viscosities, which have a direct effect on their conductivity during writing. However, for direct writing technique with ball pen, there is a strict requirement of the ink viscosity (~1–10 Pa·s) for the ink to smoothly flow through the roller ball. Therefore, it needs an additional step of special pretreatment of conductive inks (e.g., dilution) to tune their viscosity (Li et al., 2015a).

Due to the rough surface of the paper, electrodes for paper-based (PB) sensors and devices can be made by simple, inexpensive, and solvent-free processing methods such as pencil drawing (Kano & Fujii, 2018; Liao et al., 2015; Zhao et al., 2017, 2019). Conductive graphite is the main component of a pencil, and this is what makes it possible to use a pencil drawing for the manufacture of conductive elements of PB electronic devices (Tai et al., 2020). When pencil traces are drawn on paper, the friction between pencil lead and paper rubs off graphite particles which in turn adhere to the paper fibers. Thus, pencil traces can be considered as conductive films made of percolated graphite particle network on paper. Figure 27.12a–c shows electrodes drawn with a pencil for PB sensors and devices (Tai et al., 2020). It has been established that the sheet resistances of the electrodes fabricated using different types of pencils are different due to the different content of graphite and clay in the pencil shaft (Zhang et al., 2018b; Zhao et al., 2017). In particular, it was found that pencil rods HB (6B–12B) are more suitable for the manufacture of electrodes for PB sensors and devices (Table 27.2) (Zhao et al., 2017). Typically, the pattern is repeated 8–10 times to ensure the continuity of the conductive graphite film on the paper. There is no chemical interaction between paper and graphite flakes, but graphite flakes adhere to paper due to a weak van der Waals interaction. Although pencil electrodes have the advantages of ease of manufacture, low cost, and environmental friendliness, they are influenced by the types of pencils used for drawing (Zhang et al., 2018b; Zhao et al., 2017), and the manufacturing process is

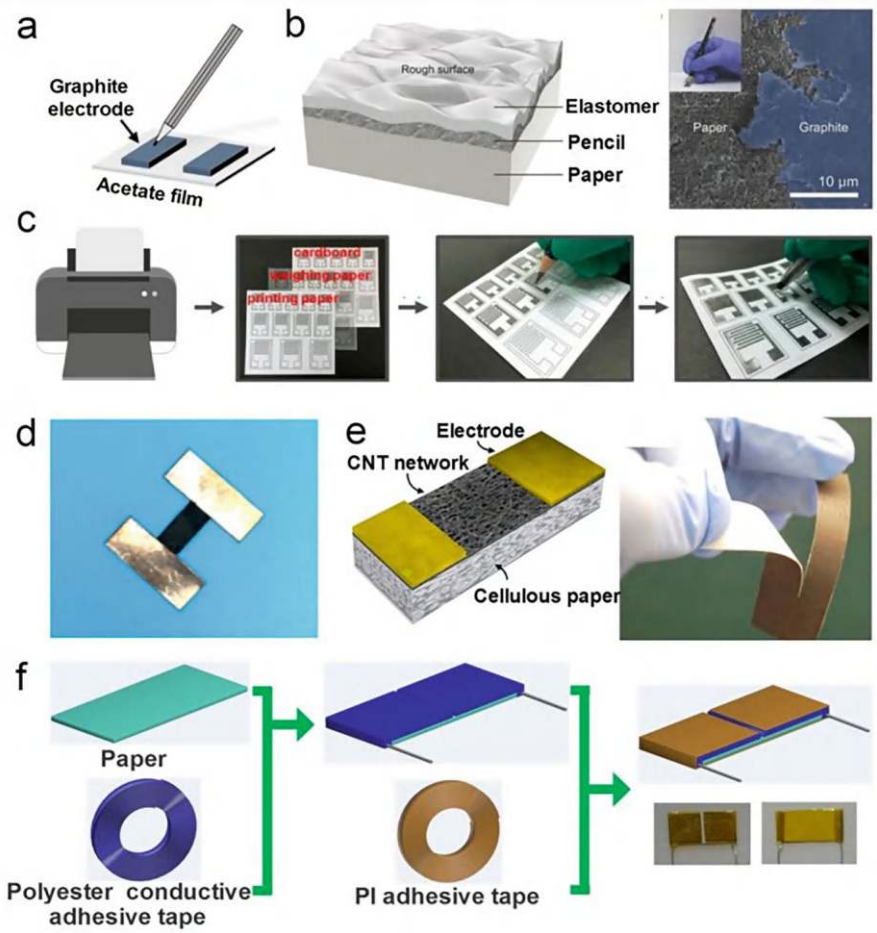

Fig. 27.12 (**a**) Fabrication schematic illustration of the pencil electrodes. (Reproduced with permission from Kano and Fujii (2018). Copyright 2018: American Chemical Society). (**b**) Schematic illustration of the microstructure-like randomly rough surface. (Reproduced with permission from Lee et al. (2017a). Copyright 2017: Wiley-VCH). (**c**) Fabrication schematic illustration of the PB electrodes using drawing method. (Reproduced with permission from Zhao et al. (2017). Copyright 2017: American Chemical Society). (**d**) Photograph of the PB humidity sensor based on copper electrodes. (Reproduced with permission from Zhu et al. (2019). Copyright 2019: American Chemical Society). (**e**) Schematic illustration of the humidity sensor built on a cellulose paper substrate using copper electrodes. (Reproduced with permission from Han et al. (2012). Copyright 2012: American Chemical Society). (**f**) Fabrication process of the PB humidity sensor using pasting method. (Reproduced with permission from Duan et al. (2019). Copyright 2019: American Chemical Society. Reprinted from Tai et al. (2020). Published 2020 by ACS with open access)

quite lengthy due to the need for repeated repetition (Zhang et al., 2018b). In addition, the process depends on the painter and is not reproducible. The conductive properties of such electrodes are also affected by bending deformation (Liao et al.,

Table 27.2 The bulk conductance of pencil leads from 1B to 12B and square resistances of pencil trace on the printing paper. The preparation of pencil trace is analogous to the fabrication of electrodes

Pencil	B	2B	3B	4B	5B	6B	8B	10B	12B
Square resistance (Ω)	8717	6776	4163	2168	509	368	332	410	643

Source: Reprinted with permission from Zhao et al. (2017). Copyright 2017: ACS

2015), which can affect the stability and performance of fabricated sensors and devices (Kurra & Kulkarni, 2013).

Therefore, in a number of publications, another simple approach to the manufacture of paper-based electrodes has been proposed. This approach was based on the use of conductive adhesive tapes (Duan et al., 2019; Han et al., 2012; Tai et al., 2020; Zhu et al., 2019). Adhesive copper foil and adhesive tape based on conductive polyester fibers were tested (see Fig. 27.12d, e). The experiment showed that the electrode rigids of adhesive copper foil tapes cannot resist continuous bending and twisting, resulting in poor wearable flexibility and even damage to the sensors (Duan et al., 2019). At the same time, it was found that the flexible conductive tape based on polyester fibers is helpful to solve the compatibility problem between the rigid electrodes and paper. In addition to the direct formation of electrodes, such a tape, applied to the surface of electrodes formed by various methods, significantly improves their mechanical stability when bending paper substrates. Using this approach, a multifunctional PB humidity sensor (see Fig. 27.12f) was fabricated (Duan et al., 2019).

Some developers believe that it is not economically feasible to use noble metals in paper-based sensors, as they are expensive and non-renewable. To solve this problem, a method was proposed for preparing conductive electrodes by directly forming electrodes with CO_2-laser writing on TEMPO-oxidized cellulose paper (Zhao et al., 2020; Zhu et al., 2022). As seen in Fig. 27.13, if the original paper from TEMPO-oxidized cellulose had a high sheet resistance of approximately 10^9 Ω sq.$^{-1}$, then the area of the paper after laser irradiation had a sheet resistance varying in the range of 10^8–10^2 Ω sq.$^{-1}$, depending on the time and intensity of the laser radiation. The carbonization of polymeric materials under the action of a CO_2 laser can be associated with the release of thermal energy due to the photothermal effect caused by vibrations of their lattice (Lin et al., 2014). Under the influence of a CO_2 laser, the polymer material is heated to a high temperature, which causes the breaking of chemical bonds, such as C–O and C=O, inside the polymer and their rearrangement with the formation of a graphite structure (Fig. 27.14). This approach made it possible to implement a humidity sensor made entirely from cellulose. Experiments have shown that paper-based sensors made from TEMPO-oxidized cellulose with sodium carboxylate groups provided satisfactory humidity-sensing performance (Zhu et al., 2022). Zhu et al. (2022) and Lin et al. (2014) believe that the process of electrode forming using CO_2 laser irradiation is extremely attractive for industrial use, since it can be carried out completely in atmospheric air without any reagents.

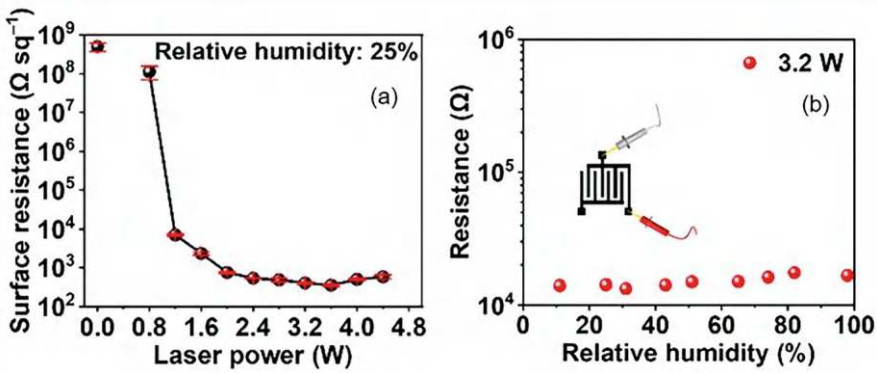

Fig. 27.13 CO_2-laser-induced direct formation of electrodes on TEMPO-oxidized cellulose paper: (**a**) surface resistance as a function of laser power used for laser irradiation; (**b**) relationship between relative humidity and electrical resistance of laser-induced electrodes prepared at laser powers of 3.2 W. Laser scan speed: 10 cm s^{-1}. The resistance was measured at room temperature. (Reprinted from Zhu et al. (2022). Published 2022 by RSC with open access)

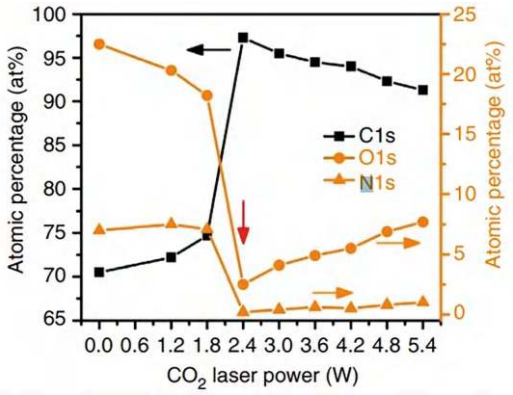

Fig. 27.14 Characterizations of laser-induced graphene (LIG) prepared with different laser powers. Atomic percentages of carbon, oxygen, and nitrogen as a function of laser power. These values are obtained from high-resolution XPS. The threshold power is 2.4 W, at which conversion from PI to LIG occurs. (Reprinted from Lin et al. (2014). Published 2014 by Natio Portfolio with open access)

If electrodes are required that are conductive over the whole area of the paper, then commercially available carbon paper can be used for this purpose, or metals, such as Au, can be deposited on the whole area of the paper. Another possibility to achieve this goal is to pyrolyze the paper by heating it to ~900–1000 °C in an inert atmosphere. However, the resulting material is rather brittle (Mazurkiewicz et al., 2020). It was shown that pyrolysis can also be carried out locally using a laser (de Araujo et al., 2017). It is also possible to make conductive paper by mixing

conductive materials with cellulose or by coating the surface of the paper with conductive polymers such as PEDOT/PSS (Ha et al., 2018; Yao et al., 2017).

As previously shown, many conductive materials are well suited for the development of various paper sensors and energy storage devices. To expand the range of applications of these materials, electrodes are often functionalized by depositing or growing other materials on their surface, such as oxides, polymers, and biomolecules (Määttänen et al., 2013; Sjöberg et al., 2016; Zea et al., 2019). For this purpose, chemical functionalization, physical functionalization, and biochemical functionalization can be used (Sui & Zorman, 2020). The functional material can be applied to the electrode to be functionalized by various methods, including drop casting, electrodeposition, and inkjet printing. At the same time, drop casting is the simplest way to functionalize electrodes. For example, copper oxide (CuO) has been used as a functional material in a non-enzymatic glucose sensor (Romeo et al., 2018). Drop casting is also widely used to deposit organic polymer materials because the method does not require special ink formulations or chemical reactions (Le et al., 2016). Biochemical functionalization is typically used in biosensors intended to use an enzymatic reaction or perform some kind of immunoassay. Coupling enzymes with electrochemical sensors allows for rapid detection of metabolites and proteins. For example, in a paper-based glucose sensor design, an inkjet-printed Au electrode was functionalized with the glucose enzyme glucose oxidase (GOx) (Määttänen et al., 2013). Ihalainen et al. (2013) proposed the use of homogeneous self-assembled monolayers (SAMs) of thiols on printed metal electrodes to fabricate biorecognition layers for flexible bioaffinity sensors. More details on electrode functionalization processes can be found in (Sui & Zorman, 2020).

27.11 Summary

To summarize the discussion, we can state that there are quite a lot of possibilities for the production of flexible and transparent conductive electrodes on paper. However, it must be kept in mind that each approach that can be used to fabricate electrodes has its own characteristics, advantages, and limitations (Kulkarni et al., 2015), which are reflected in Figs. 27.15 and 27.16. Figure 27.15 shows SEM images of conductive particles and their length scale compared to nanocellulose. The conductivity, flexibility, and transparency of polymer, carbon, and metal-based electrodes are different (Hoeng et al., 2016). Inks with conductive polymers and carbon nanoparticles differ from metallic inks by being moderately conductive (about 100 times lower than silver), but can exhibit layer transparency and greater flexibility. In addition, carbon- and polymer-based inks do not require annealing, allowing conductive electrodes to print on flexible substrates such as plastic and paper that cannot withstand high temperatures (Cho et al., 2011; Denneulin et al., 2009).

Figure 27.16a is a graph showing schematic trends of transmittance versus sheet resistance for various families of transparent conductive electrodes (TCE). It is seen

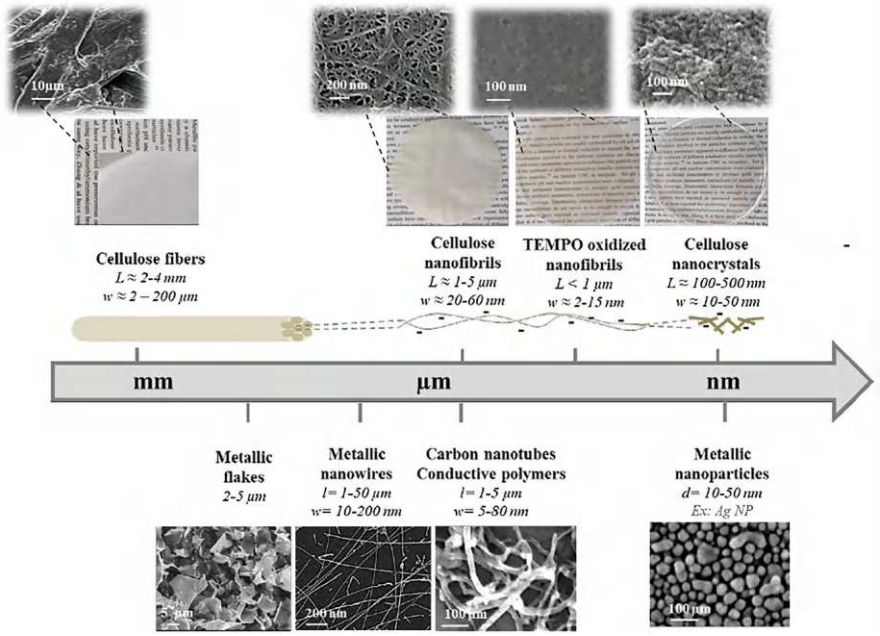

Fig. 27.15 Schematic length-scale representation of networks obtained with different cellulosic materials (up) compared to specific dimensions of different conductive particles (down). (Reprinted with permission from Hoeng et al. (2016). Copyright 2016: RSC)

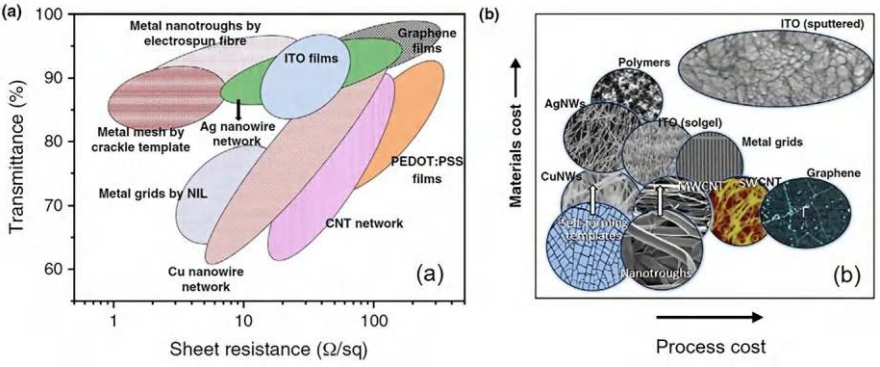

Fig. 27.16 (**a**) Schematic shows the clear trade-off between transparence and sheet resistance for different categories of electrodes. Lowering Rs compromises transmittance, in general. (**b**) Comparison plot of materials cost versus process cost for different categories of transparent conductive electrode materials. Upward arrows shown on nanotroughs and self-forming processes indicate that material cost may fluctuate with the choice of metal. (Reprinted with permission from Kulkarni et al. (2015). Copyright 2015: Elsevier)

that decreasing Rs deteriorates the transmittance (Kulkarni et al., 2015). Metal meshes fabricated using self-assembled crackle and electrospun nanofibers, ultralong silver nanowires, and thin graphene films typically show minimal reduction in transmittance, while sheet resistance is dramatically reduced. Copper nanowires and CNT-based electrodes are in another category, whose sheet resistance is typically high for the higher transparency regime due to the sparse density of shorter conductive paths. Organic TCE exhibits moderate transmission with relatively high surface resistance compared to metal-based TCE.

The cost of TCE is determined mainly by material and process costs (Fig. 27.16b). The cost of the substrate is relatively much less. Process costs are minimal for Cu nanowires, Ag nanowires, PEDOT:PSS, nanotroughs, and self-forming processes, while their material costs vary widely. At the same time, the sputtering process for applying ITO is an expensive process. On the other hand, ITO synthesized by sol-gel process is cost-effective. This explains the wide price range of ITO wafers in the market. In the case of carbon nanostructures, carbon as a source may be cheap, but the synthesis of nanostructures, whether CNTs or graphene, is usually expensive, especially if high purity is required, which increases the cost of production. The most successful TCE is based on metal nanowires grown using solution routes that reduce the cost of the process, since coating the nanowires can be done in a single-step roll-to-roll process, reducing production costs. The cost of the material can be reduced if expensive metals such as Pt, Pd, and Au are not used. However, in this case, additional processing may be required to improve the stability of the parameters of electrodes using cheap metals such as Ag, Cu, and Al. For example, Ag, Cu, and Al have a low resistance to corrosion. Post-deposition treatments with sealants and additive layers can increase the cost of TCEs based on nanowires of these metals (Kulkarni et al., 2015). Therefore, conductive ink particles and their size should be selected based on the specific physicochemical properties of the ink required for a particular printer and the characteristics of the electrodes required for the end application in terms of flexibility, transparency, conductivity, and cost of the finished product. However, it must be borne in mind that one of the most important criteria for choosing a particular material for the manufacture of electrodes in large-scale production is the suitability of the synthesis and deposition recipes for roll-to-roll conditions (Kulkarni et al., 2015). Therefore, new materials and processes need to be developed in the near future to overcome this trade-off between transparency, conductivity, stability, and cost.

Additional information regarding the formation of electrodes on paper can be found in the reviews by Cummins and Desmulliez (2012), Hoeng et al. (2016), Liu et al. (2017a, 2017b), Yao et al. (2017, 2022), Zhang et al. (2018a), Noviana et al. (2020), and Mazurkiewicz et al. (2020). Cummins and Desmulliez (2012) and Sui and Zorman (2020) considered inkjet printing of conductive materials. Yao et al. (2017) summarized the advances of paper-based electrodes for flexible energy storage devices. Zhang et al. (2021) discussed electrode materials for flexible supercapacitors. Mazurkiewicz et al. (2020) analyzed the features of the formation of electrodes for paper-based electrochemical sensors. Xu et al. (2022) reviewed the approaches used in the manufacture of electrodes for flexible solar cells. Hoeng

et al. (2016) and Zhang et al. (2018a) analyzed devices based on nanopaper and features of using printing technology for their manufacture. Graz and Rosset (2021) considered manufacturing features of stretchable electrodes. Cao et al. (2014), López-Naranjo et al. (2016), Lu et al. (2021), Luo et al. (2017), Nguyen et al. (2022), Qin et al. (2021), and Wang et al. (2021b) analyzed various approaches for developing flexible transparent electrodes.

Acknowledgments G.K. is grateful to the Moldova State University (research program no. 011208) for supporting his research.

References

Abdel-Aziz, A. M., Hassan, H. H., & Badr, I. H. A. (2022). Activated glassy carbon electrode as an electrochemical sensing platform for the determination of 4-Nitrophenol and dopamine in real samples. *ACS Omega, 7*, 34127–34135. https://doi.org/10.1021/acsomega.2c03427

Acerce, M., Voiry, D., & Chhowalla, M. (2015). Metallic 1T phase MoS_2 nanosheets as supercapacitor electrode materials. *Nature Nanotechnology, 10*, 313–318. https://doi.org/10.1038/nnano.2015.40

Ahmed, B., El Ghazaly, A., & Rosen, J. (2020). *i*-MXenes for energy storage and catalysis. *Advanced Functional Materials, 30*, 2000894. https://doi.org/10.1002/adfm.202000894

Amanat, N., James, N. L., & McKenzie, D. R. (2010). Welding methods for joining thermoplastic polymers for the hermetic enclosure of medical devices. *Medical Engineering & Physics, 32*, 690–699. https://doi.org/10.1016/j.medengphy.2010.04.011

Arena, A., Donato, N., Saitta, G., Bonavita, A., Rizzo, G., & Neri, G. (2010). Flexible ethanol sensors on glossy paper substrates operating at room temperature. *Sensors and Actuators B: Chemical, 14*, 488–494. https://doi.org/10.1016/j.snb.2009.12.053

Balasingam, S. K., Lee, J. S., & Jun, Y. (2015). Few-layered $MoSe_2$ nanosheets as an advanced electrode material for supercapacitors. *Dalton Transactions, 44*(35), 15491–15498. https://doi.org/10.1039/c5dt01985k

Banerjee, I., Faris, T., Stoeva, Z., Harris, P., Chen, J., Sharma, A. K., & Ray, A. K. (2017). Graphene films printable on flexible substrates for sensor applications Graphene films printable on flexible substrates for sensor applications. *2D Materials, 4*, 015036. https://doi.org/10.1088/2053-1583/aa50f0

Bellani, S., Petroni, E., Del Rio Castillo, A. E., Curreli, N., Martín-García, B., Oropesa-Nuñez, R., et al. (2019). Scalable production of graphene inks via wet-jet milling exfoliation for screen-printed micro-supercapacitors. *Advanced Functional Materials, 29*, 1807659. https://doi.org/10.1002/adfm.201807659

Betz, U., Kharrazi Olsson, M., Marthy, J., Escola, M. F., & Atammny, F. (2006). Thin films engineering of indium tin oxide: Large area flat panel displays application. *Surface and Coating Technology, 200*, 5751–5759. https://doi.org/10.1016/j.surfcoat.2005.08.144

Bihar, E., Roberts, T., Saadaoui, M., Hervé, T., De Graaf, J. B., & Malliaras, G. G. (2017). Inkjet-printed PEDOT: PSS electrodes on paper for electrocardiography. *Advanced Healthcare Materials, 6*(6), 1601167. https://doi.org/10.1002/adhm.201601167

Biswas, S., & Alegaonkar, P. S. (2022). MXene: Evolutions in chemical synthesis and recent advances in applications. *Surfaces, 4*, 1–36. https://doi.org/10.3390/surfaces5010001

Bonaccorso, F., Sun, Z., Hansan, T., & Ferrari, A. C. (2010). Graphene photonics and optoelectronics. *Nature Photonics, 4*, 611–622. https://doi.org/10.1038/nphoton.2010.186

Bora, P. J., Anil, A. G., Ramamurthy, P. C., & Tan, D. Q. (2020). MXene interlayered crosslinked conducting polymer film for highly specific absorption and electromagnetic interference shielding. *Materials Advances, 1*, 177–183. https://doi.org/10.1039/D0MA00005A

Cao, L., Yang, S., Gao, W., Liu, Z., Gong, Y., Ma, L., et al. (2013). Direct laser-patterned micro-supercapacitors from paintable MoS_2 films. *Small, 9*, 2905–2910. https://doi.org/10.1002/smll.201203164

Cao, W., Li, J., Chen, H., & Xue, J. (2014). Transparent electrodes for organic optoelectronic devices: A review. *Journal of Photonics for Energy, 4*, 040990. https://doi.org/10.1117/1.JPE.4.040990

Carrión, F. J., Sanes, J., Bermúdez, M.-D., & Arribas, A. (2011). New single-walled carbon nanotubes–ionic liquid lubricant. Application to polycarbonate–stainless steel sliding contact. *Tribology Letters, 41*, 199–207. https://doi.org/10.1007/s11249-010-9700-7

Chen, G. H., Wu, D. J., Weng, W. U., & Wu, C. L. (2003). Exfoliation of graphite flake and its nanocomposites. *Carbon, 41*, 619–621. https://doi.org/10.1016/S0008-6223(02)00409-8

Chen, P. C., Shen, G., Sukcharoenchoke, S., & Zhou, C. (2009). Flexible and transparent supercapacitor based on In_2O_3 nanowire/carbon nanotube heterogeneous films. *Applied Physics Letters, 94*, 043113. https://doi.org/10.1063/1.3069277

Cheng, L., Liu, J., & Dong, S. (2000). Layer-by-layer assembly of multilayer films consisting of silicotungstate and a cationic redox polymer on 4-aminobenzoic acid modified glassy carbon electrode and their electrocatalytic effects. *Analytica Chimica Acta, 41*, 133–142. https://doi.org/10.1016/S0003-2670(00)00931-4

Cherusseri, J., Choudhary, N., Kumar, K. S., Jung, Y., & Thomas, J. (2019). Recent trends in transition metal dichalcogenides based supercapacitor electrodes. *Nanoscale Horizons, 4*, 840–858. https://doi.org/10.1039/C9NH00152B

Chhowalla, M., Shin, H. S., Eda, G., Li, L. J., Loh, K. P., & Zhang, H. (2013). The chemistry of two-dimensional layered transition metal dichalcogenide nanosheets. *Nature Chemistry, 5*, 263–275. https://doi.org/10.1038/nchem.1589

Chiang, C.-H., & Wu, C.-C. (2013). High-efficient dye-sensitized solar cell based on highly conducting and thermally stable PEDOT:PSS/glass counter electrode. *Organic Electronics, 14*, 1769–1776. https://doi.org/10.1016/j.orgel.2013.03.020

Cho, C.-K., Hwang, W.-J., Eun, K., Choa, S.-H., Na, S.-I., & Kim, H.-K. (2011). Mechanical flexibility of transparent PEDOT:PSS electrodes prepared by gravure printing for flexible organic solar cells. *Solar Energy Materials & Solar Cells, 95*, 3269–3275. https://doi.org/10.1016/j.solmat.2011.07.009

Cho, S., Kang, S., Pandya, A., Shanker, R., Khan, Z., Lee, Y., et al. (2017). Large-area cross-aligned silver nanowire electrodes for flexible, transparent, and force-sensitive mechanochromic touch screens. *ACS Nano, 11*(4), 4346–4357. https://doi.org/10.1021/acsnano.7b01714

Choi, W., Choudhary, N., Han, G. H., Park, J., Akinwande, D., & Lee, Y. H. (2017). Recent development of two-dimensional transition metal dichalcogenides and their applications. *Materials Today, 20*, 116–130. https://doi.org/10.1016/j.mattod.2016.10.002

Choi, J., Park, C. H., Kwack, J. H., Lee, D. J., Kim, J. G., Choi, J., et al. (2019). Ag fiber/IZO composite electrodes: Improved chemical and thermal stability and uniform light emission in flexible organic light-emitting diodes. *Scientific Reports, 9*, 738. https://doi.org/10.1038/s41598-018-37105-5

Cinti, S., Colozza, N., Cacciotti, I., Moscone, D., Polomoshnov, M., Sowade, E., et al. (2018). Electroanalysis moves towards paper-based printed electronics: Carbon black nanomodified inkjet-printed sensor for ascorbic acid detection as a case study. *Sensors and Actuators B: Chemical, 265*, 155–160. https://doi.org/10.1016/j.snb.2018.03.006

Courbat, J., Kim, Y. B., Briand, D., & de Rooij, N. F. (2011). Inkjet printing on paper for the realization of humidity and temperature sensors. In *Proceedings of 16th International Solid-State Sensors, Actuators and Microsystems Conference*, 5–9 June 2011, Beijing, China, 12169626. https://doi.org/10.1109/TRANSDUCERS.2011.5969506

Cummins, G., & Desmulliez, M. P. Y. (2012). Inkjet printing of conductive materials: A review Inkjet printing of conductive materials: A review. *Circuit World, 38*, 193–213. https://doi.org/10.1108/03056121211280413

David, L., Bhandavat, R., & Singh, G. (2014). MoS_2/Graphene composite paper for sodium-ion battery electrodes. *ACS Nano, 8*, 1759–1770. https://doi.org/10.1021/nn406156b

De Araujo, W. R., & Paixao, T. R. L. C. (2014). Fabrication of disposable electrochemical devices using silver ink and office paper. *Analyst, 139*, 2742–2747. https://doi.org/10.1039/C4AN00097H

De Araujo, W. R., Frasson, C. M. R., Ameku, W. A., Silva, J. R., Angnes, L., & Paixao, T. (2017). Single-step reagentless laser scribing fabrication of electrochemical paper-based analytical devices. *Angewandte Chemie (International Ed. in English), 56*, 15113–15117. https://doi.org/10.1002/anie.201708527

De, S., Higgins, T. M., Lyons, P. E., Doherty, E. M., Nirmalraj, P. N., Blau, W. J., et al. (2009). Silver nanowire networks as flexible, transparent, conducting films: Extremely high DC to optical conductivity ratios. *ACS Nano, 3*(7), 1767–1774. https://doi.org/10.1021/nn900348c

Denneulin, A., Bras, J., Blayo, A., Khelifi, B., Roussel-Dherbey, F., & Neuman, C. (2009). The influence of carbon nanotubes in inkjet printing of conductive polymer suspensions. *Nanotechnology, 20*, 385701. https://doi.org/10.1088/0957-4484/20/38/385701

Distler, T., & Boccaccini, A. R. (2020). 3D printing of electrically conductive hydrogels for tissue engineering and biosensors—A review. *Acta Biomaterialia, 101*, 1–13. https://doi.org/10.1016/j.actbio.2019.08.044

Dong, L., Xu, C., Li, Y., Pan, Z., Liang, G., Zhou, E., et al. (2016). Breathable and wearable energy storage based on highly flexible paper electrodes. *Advanced Materials, 28*, 9313–9319. https://doi.org/10.1002/adma.201602541

Duan, Z., Jiang, Y., Yan, M., Wang, S., Yuan, Z., Zhao, Q., et al. (2019). Facile, flexible, cost-saving, and environment-friendly paper-based humidity sensor for multifunctional applications. *ACS Applied Materials & Interfaces, 11*(24), 21840–21849. https://doi.org/10.1021/acsami.9b05709

Dungchai, W., Chailapakul, O., & Henry, C. S. (2009). Electrochemical detection for paper-based microfluidics. *Analytical Chemistry, 81*, 5821–5826. https://doi.org/10.1021/ac9007573

Elbadawi, M., Ong, J. J., Pollard, T. D., Gaisford, S., & Basit, A. W. (2021). Additive manufacturable materials for electrochemical biosensor electrodes. *Advanced Materials, 31*(10), 2006407. https://doi.org/10.1002/adfm.202006407

El-Kady, M. F., Shao, Y., & Kaner, R. B. (2016). Graphene for batteries, supercapacitors and beyond. *Nature Reviews Materials, 1*, 16033. https://doi.org/10.1038/natrevmats.2016.33

Fan, L. Z., Hu, Y. S., Maier, J., Adelhelm, P., Smarsly, B., & Antonietti, M. (2007). High electroactivity of polyaniline in supercapacitors by using a hierarchically porous carbon monolith as a support. *Advanced Functional Materials, 17*, 3083. https://doi.org/10.1002/adfm.200700518

Feng, J., Sun, X., Wu, C., Peng, L., Lin, C., Hu, S., et al. (2011). Metallic few-layered VS_2 ultrathin nanosheets: High two-dimensional conductivity for in-plane supercapacitors. *Journal of the American Chemical Society, 133*, 17832–17838. https://doi.org/10.1021/ja207176c

Feng, J. X., Li, Q., Lu, X. F., Tong, Y. X., & Li, G. R. (2014). Flexible symmetrical planar supercapacitors based on multi-layered MnO_2/Ni/graphite/paper electrodes with high-efficient electrochemical energy storage. *Journal of Materials Chemistry A, 2*, 2985–2992. https://doi.org/10.1039/C3TA14695B

Ferreira de Oliveira, A. E., Pereira, A. C., & Ferreira, L. F. (2022). Fully handwritten electrodes on paper substrate using rollerball pen with silver nanoparticle ink, marker pen with carbon nanotube ink and graphite pencil. *Analytical Methods, 14*(19), 1880–1888. https://doi.org/10.1039/d2ay00373b

Gaspar, C., Passoja, S., Olkkonen, J., & Smolander, M. (2016). IR-sintering efficiency on inkjet-printed conductive structures on paper. *Microelectronic Engineering, 149*, 135–140. https://doi.org/10.1016/j.mee.2015.10.006

Gaspar, C., Olkkonen, J., Passoja, S., & Smolander, M. (2017). Paper as active layer in inkjet-printed capacitive humidity sensors. *Sensors, 17*(7), 1464. https://doi.org/10.3390/s17071464

Ge, P., & Fouletier, M. (1988). Electrochemical intercalation of sodium in graphite. *Solid State Ionics, 28-30*, 1172–1175. https://doi.org/10.1016/0167-2738(88)90351-7

Geim, A. K. (2009). Graphene: Status and prospects. *Science, 324*(5934), 1530–1534. https://doi.org/10.1126/science.1158877

Ghosh, N. C., & Harimkar, S. P. (2012). Consolidation and synthesis of MAX phases by spark plasma sintering (SPS): A review. In I. M. Low (Ed.), *Advances in science and technology of $M_{n+1}AX_n$ phases* (pp. 47–80). Woodhead Publishing. https://doi.org/10.1533/9780857096012.47

Gilje, S., Han, S., Wang, M., Wang, K. L., & Kaner, R. B. (2007). A chemical route to graphene for device applications. *Nano Letters, 7*, 3394–3398. https://doi.org/10.1021/nl0717715

Gonzalez-Julian, J. (2020). Processing of MAX phases: From synthesis to applications. *Journal of the American Ceramic Society, 104*(2), 659–690. https://doi.org/10.1111/jace.17544

Gray, D. S., Tien, J., & Chen, C. S. (2004). High conductivity elastomeric electronic. *Advanced Materials, 16*, 393–397. https://doi.org/10.1002/adma.200306107

Graz, I. M., & Rosset, S. (2021). Stretchable electrodes for highly flexible electronics. In P. Cosseddu & M. Caironi (Eds.), *Organic flexible electronics* (pp. 479–500). Elsevier. https://doi.org/10.1016/B978-0-12-818890-3.00016-3

Guo, C. F., Liu, Q., Wang, G., Wang, Y., Shi, Z., Suo, Z., et al. (2015). Fatigue-free, superstretchable, transparent, and biocompatible metal electrodes. *PNAS, 112*(40), 12332–12337. https://doi.org/10.1073/pnas.1516873112

Ha, D., Fang, Z., & Zhitenev, N. B. (2018). Paper in electronic and optoelectronic devices. *Advanced Electronic Materials, 4*(5), 1700593. https://doi.org/10.1002/aelm.201700593

Han, Y., & Dai, L. (2019). Conducting polymers for flexible supercapacitors. *Macromolecular Chemistry and Physics, 220*, 1800355. https://doi.org/10.1002/macp.201800355

Han, H., & Tachikawa, H. (2005). Electrochemical determination of thiols at single-wall carbon nanotubes and PQQ modified electrodes. *Frontiers in Bioscience, 10*, 931–939. https://doi.org/10.2741/1587

Han, J. W., Kim, B., Li, J., & Meyyappan, M. (2012). Carbon nanotube based humidity sensor on cellulose paper. *Journal of Physical Chemistry C, 116*(41), 22094–22097. https://doi.org/10.1021/jp3080223

Han, T.-H., Jeong, S.-H., Lee, Y., Seo, H.-K., Kwon, S.-J., Park, M.-H., & Lee, T.-W. (2015). Flexible transparent electrodes for organic light-emitting diodes. *Journal of Information Display, 16*(2), 71–84. https://doi.org/10.1080/15980316.2015.1016127

He, Q., Zeng, Z., Yin, Z., Li, H., Wu, S., Huang, X., & Zhang, H. (2012). Fabrication of flexible MoS_2 thin-film transistor arrays for practical gas-sensing applications. *Small, 8*, 2994–2999. https://doi.org/10.1002/smll.201201224

Hoeng, F., Denneulin, A., & Bras, J. (2016). Use of nanocellulose in printed electronics: A review. *Nanoscale, 8*, 13131–13154. https://doi.org/10.1039/C6NR03054H

Hu, L., Choi, J. W., Yang, Y., Jeong, S., La Mantia, F., Cui, L. F., & Cui, Y. (2009). Highly conductive paper for energy-storage devices. *Proceedings of the National Academy of Sciences of the United States of America, 106*(51), 21490–21494. https://doi.org/10.1073/pnas.0908858106

Hu, C., Bai, X., Wang, Y., Jin, W., Zhang, X., & Hu, S. (2012). Inkjet printing of nanoporous gold electrode arrays on cellulose membranes for high-sensitive paper-like electrochemical oxygen sensors using ionic liquid electrolytes. *Analytical Chemistry, 84*, 3745–3750. https://doi.org/10.1021/ac3003243

Hu, L., Liu, N., Eskilsson, M., Zheng, G., McDonough, J., Wagberg, L., & Cui, Y. (2013). Silicon-conductive nanopaper for Li-ion batteries. *Nano Energy, 2*, 138–145. https://doi.org/10.1016/j.nanoen.2012.08.008

Hu, Y., Guan, C., Ke, Q., Yow, Z. F., Cheng, C., & Wang, J. (2016). Hybrid Fe_2O_3 nanoparticle clusters/rGO paper as an effective negative electrode for flexible supercapacitors. *Chemistry of Materials, 28*, 7296–7303. https://doi.org/10.1021/acs.chemmater.6b02585

Huang, J. G., Ichinose, I., & Kunitake, T. (2005). Nanocoating of natural cellulose fibers with conjugated polymer: Hierarchical polypyrrole composite materials. *Chemical Communications, 2005*, 1717–1719. https://doi.org/10.1039/B415339A

Huang, L., Liang, J., Wan, X., & Chen, Y. (2011). Graphene-based conducting inks for direct inkjet printing of flexible conductive patterns and their applications in electric circuits and chemical sensors. *Nano Research, 4*, 675–684. https://doi.org/10.1007/s12274-011-0123-z

Huang, L., Chen, D., Ding, Y., Feng, S., Wang, Z. L., & Liu, M. (2013). Nickelcobalt hydroxide nanosheets coated on $NiCo_2O_4$ nanowires grown on carbon fiber paper for high-performance pseudocapacitors. *Nano Letters, 13*, 3135–3139. https://doi.org/10.1021/nl401086t

Hwang, J. Y., El-Kady, M.-F., Wang, Y., Wang, L. S., Shao, Y. L., Marsh, K., et al. (2015). Direct preparation and processing of graphene/RuO_2 nanocomposite electrodes for high-performance capacitive energy storage. *Nano Energy, 18*, 57–70. https://doi.org/10.1016/j.nanoen.2015.09.009

Hyun, W. J., Park, O. O., & Chin, B. D. (2013). Foldable graphene electronic circuits based on paper substrates. *Advanced Materials, 25*, 4729–4734. https://doi.org/10.1002/adma.201302063

Ihalainen, P., Majumdar, H., Määttänen, A., Wang, S., Österbacka, R., & Peltonen, J. (2013). Versatile characterization of thiol-functionalized printed metal electrodes on flexible substrates for cheap diagnostic applications. *Biochimica et Biophysica Acta, 1830*(9), 4391–4397. https://doi.org/10.1016/j.bbagen.2012.09.007

Irandoost, M., Kumari, B., Truong, T., Kark, B., & Miah, R. (2023). Nickel sulfide-based composite as electrodes in electrochemical sensors: A review. *Journal of Composites and Compounds, 5*, 38–50. https://doi.org/10.52547/jcc.5.1.6

Jabbour, L., Destro, M., Gerbaldi, C., Chaussy, D., Penazzi, N., & Beneventi, D. (2012). Aqueous processing of cellulose based paper-anodes for flexible Li-ion batteries. *Journal of Materials Chemistry, 22*, 3227–3233. https://doi.org/10.1039/C2JM15117K

Jagadeesan, K. K., Kumar, S., Sumana, G. (2012) Application of conducting paper for selective detection of troponin. *Electrochem. Commun, 20*, 71–74. https://doi.org/10.1016/j.elecom.2012.03.041

Jiang, Z., Lu, W., Li, Z., Ho, K., Li, X., Jiao, X., et al. (2014). Synthesis of amorphous cobalt sulfide polyhedral nanocages for high performance supercapacitors. *Journal of Materials Chemistry A, 2*, 8603–8606. https://doi.org/10.1039/C3TA14430E

Jiang, S., Zhou, X., Xiao, H., Chen, W., Xu, X., & Liu, Z. (2021). Robust and durable flexible micro-supercapacitors enabled by graphene nanoscrolls. *Chemical Engineering Journal, 405*, 127009. https://doi.org/10.1016/j.cej.2020.127009

Jiao, S., Zhou, A., Wu, M., & Hu, H. (2019). Kirigami patterning of MXene/bacterial cellulose composite paper for all-solid-state stretchable micro-supercapacitor arrays. *Advancement of Science, 6*, 1900529. https://doi.org/10.1002/advs.201900529

Kang, Y. J., Chung, H., Han, C.-H., & Kim, W. (2012). All-solid-state flexible supercapacitors based on papers coated with carbon nanotubes and ionic-liquid-based gel electrolytes. *Nanotechnology, 23*, 065401. https://doi.org/10.1088/0957-4484/23/6/065401

Kano, S., & Fujii, M. (2018). All-painting process to produce respiration sensor using humidity-sensitive nanoparticle film and graphite trace. *ACS Sustainable Chemistry & Engineering, 6*(9), 12217–12223. https://doi.org/10.1021/acssuschemeng.8b02550

Kelly, F. M., Johnston, J. H., Borrmann, T., & Richardson, M. J. (2007). Functionalised hybrid materials of conducting polymers with individual fibres of cellulose. *European Journal of Inorganic Chemistry, 35*, 5571–5577. https://doi.org/10.1002/ejic.200700608

Khalil, A., Liu, Q., He, Q., Xiang, T., Liu, D., Wang, C., Fang, Q., & Song, L. (2016). Metallic 1T-WS_2 nanoribbons as highly conductive electrodes for supercapacitors. *RSC Advances, 6*, 48788–48791. https://doi.org/10.1039/C6RA08975E

Kim, D.-H., Ahn, J.-H., Choi, W. M., Kim, H.-S., Kim, T.-H., Song, J., et al. (2008). Stretchable and foldable silicon integrated circuits. *Science, 320*, 507–511. https://doi.org/10.1126/science.1154367

Kim, N., Kee, S., Lee, S. H., Lee, B. H., Kahng, Y. H., Jo, Y.-R., et al. (2014). Highly conductive PEDOT:PSS nanofibrils induced by solution-processed crystallization. *Advanced Materials, 26*, 2268–2272. https://doi.org/10.1002/adma.201304611

Kim, C.-L., Jung, C.-W., Oh, Y.-J., & Kim, D. E. (2017). A highly flexible transparent conductive electrode based on nanomaterials. *NPG Asia Materials, 9*, e438. https://doi.org/10.1038/am.2017.177

Kim, T., Park, S., Seo, J., Lee, C. W., & Kim, J.-M. (2019). Highly conductive PEDOT:PSS with enhanced chemical stability. *Organic Electronics, 74*, 77–81. https://doi.org/10.1016/j.orgel.2019.06.033

Kirubasankar, B., Won, Y. S., Adofo, L. A., Choi, S. H., Kim, S. M., & Kim, K. K. (2022). Atomic and structural modifications of two-dimensional transition metal dichalcogenides for various advanced applications. *Chemical Science, 13*, 7707–7738. https://doi.org/10.1039/D2SC01398C

Ko, S., Lee, J.-I., Yang, H. S., Park, S., & Jeong, U. (2012). Mesoporous CuO particles threaded with CNTs for high-performance Lithium-ion battery anodes. *Advanced Materials, 24*, 4451–4456. https://doi.org/10.1002/adma.201201821

Ko, Y., Kwon, M., Bae, W. K., Lee, B., Lee, S. W., & Cho, J. (2017). Flexible supercapacitor electrodes based on real metal-like cellulose papers. *Nature Communications, 8*, 536. https://doi.org/10.1038/s41467-017-00550-3

Kongkaew, S., Tubtimtong, S., Thavarungkul, P., Kanatharana, P., Chang, K. H., Abdullah, A. F. L., & Limbut, W. (2022). A fabrication of multichannel graphite electrode using low-cost stencil-printing technique. *Sensors, 22*, 3034. https://doi.org/10.3390/s22083034

Korotcenkov, G. (2023). Paper-based humidity sensors as promising flexible devices: State of the art. Part 1. General consideration. *Nanomaterials, 13*, 1110. https://doi.org/10.3390/nano13061110

Kulkarni, G. U., Kiruthika, S., Gupta, R., & Rao, K. D. M. (2015). Towards low cost materials and methods for transparent electrodes. *Current Opinion in Chemical Engineering, 8*, 60–68. https://doi.org/10.1016/j.coche.2015.03.001

Kurra, N., & Kulkarni, G. (2013). Pencil-on-paper: electronic devices. *Lab on a Chip, 13*, 2866–2873. https://doi.org/10.1039/C3LC50406A

Lai, Z., Rong, S., Huang, S., Qin, M., Huang, J., Zhang, X., et al. (2023). 2D ReS_2 nanosheets embedded on porous carbon framework for efficient and stable all-solid-state flexible supercapacitor. *Surfaces and Interfaces, 42*(Part B), 103494. https://doi.org/10.1016/j.surfin.2023.103494

Le, D. D., Nguyen, T. N. N., Doan, D. C. T., Dang, T. M. D., & Dang, M. C. (2016). Fabrication of interdigitated electrodes by inkjet printing technology for apllication in ammonia sensing. *Advances in Natural Sciences: Nanoscience and Nanotechnology, 7*, 025002. https://doi.org/10.1088/2043-6262/7/2/025002

Lee, W. S., & Choi, J. (2019). Hybrid integration of carbon nanotubes and transition metal dichalcogenides on cellulose paper for highly sensitive and extremely deformable chemical sensor. *ACS Applied Materials & Interfaces, 11*(21), 19363–19371. https://doi.org/10.1021/acsami.9b03296

Lee, A., Sudau, K., Ahn, K. H., Lee, S. J., & Willenbacher, N. (2012a). Optimization of experimental parameters to suppress nozzle clogging in inkjet printing. *Industrial and Engineering Chemistry Research, 51*(40), 13195–13204. https://doi.org/10.1021/ie301403g

Lee, J., Lee, P., Lee, H., Lee, D., Lee, S. S., & Ko, S. H. (2012b). Very long Ag nanowire synthesis and its application in a highly transparent, conductive and flexible metal electrode touch panel. *Nanoscale, 4*, 6408–6414. https://doi.org/10.1039/c2nr31254a

Lee, M.-S., Lee, K., Kim, S.-Y., Lee, H., Park, J., Choi, K.-H., et al. (2013). High-performance, transparent, and stretchable electrodes using graphene–metal nanowire hybrid structures. *Nano Letters, 13*, 2814–2821. https://doi.org/10.1021/nl401070p

Lee, J., Dak, P., Lee, Y., Park, H., Choi, W., Alam, M. A., & Kim, S. (2014). Two-dimensional layered MoS_2 biosensors enable highly sensitive detection of biomolecules. *Scientific Reports, 4*, 7352. https://doi.org/10.1038/srep07352

Lee, K., Lee, J., Kim, G., Kim, Y., Kang, S., Cho, S., et al. (2017a). Rough-surface-enabled capacitive pressure sensors with 3D touch capability. *Small, 13*(43), 1700368. https://doi.org/10.1002/smll.201700368

Lee, C.-P., Lai, K.-Y., Lin, C.-A., Li, C.-T., Ho, K.-C., et al. (2017b). A paper-based electrode using a graphene dot/PEDOT:PSS composite for flexible solar cells. *Nano Energy, 36*, 260–267. https://doi.org/10.1016/j.nanoen.2017.04.044

Lee, H.-B., Jin, W.-Y., Ovhal, M. M., Kumar, N., & Kang, J.-W. (2019). Flexible transparent conducting electrodes based on metal meshes for organic optoelectronic device applications: A review. *Journal of Materials Chemistry C, 7*, 1087–1110. https://doi.org/10.1039/c8tc04423f

Lessing, J., Glavan, A. C., Brett Walker, S., Keplinger, C., Lewis, J. A., & Whitesides, G. M. (2014). Inkjet printing of conductive inks with high lateral resolution on omniphobic "RF Paper" for paper-based electronics and MEMS. *Advanced Materials, 26*, 4677–4682. https://doi.org/10.1002/adma.201401053

Leterrier, Y., Medico, L., Demarco, F., Manson, J.-A. E., Betz, U., Scola, M. F., et al. (2004). Mechanical integrity of transparent conductive oxide films for flexible polymer-based displays. *Thin Solid Films, 460*, 156–166. https://doi.org/10.1016/j.tsf.2004.01.052

Levitt, A., Zhang, J., Dion, G., Gogotsi, Y., & Razal, J. M. (2020). MXene-based fibers, yarns, and fabrics for wearable energy storage devices. *Advanced Functional Materials, 30*(47), 2000739. https://doi.org/10.1002/adfm.202000739

Lewis, J. (2006). Material challenge for flexible organic devices. *Materials Today, 9*, 38–45. https://doi.org/10.1016/S1369-7021(06)71446-8

Lewis, L. N., Spivack, J. L., Gasaway, S., Williams, E. D., Gui, J. Y., Manivannan, V., & Siclovan, O. P. (2006). A novel UV-mediated low temperature sintering of TiO_2 for dye-sensitized solar cells. *Solar Energy Materials and Solar Cells, 90*, 1041–1051. https://doi.org/10.1016/j.solmat.2005.05.019

Li, X., Zhang, G., Bai, X., Sun, X., Wang, X., Wang, E., & Dai, H. (2008). Highly conducting graphene sheets and Langmuir–Blodgett films. *Nature Nanotechnology, 3*, 538–542. https://doi.org/10.1038/nnano.2008.210

Li, C., Bai, H., & Shi, G. Q. (2009). Conducting polymer nanomaterials: Electrosynthesis and applications. *Chemical Society Reviews, 38*, 2397–2409. https://doi.org/10.1039/B816681C

Li, S., Huang, D., Yang, J., Zhang, B., Zhang, X., Yang, G., et al. (2014a). Freestanding bacterial cellulose–polypyrrole nanofibres paper electrodes for advanced energy storage devices. *Nano Energy, 9*, 309–317. https://doi.org/10.1016/j.nanoen.2014.08.004

Li, J., Liang, J., Jian, X., Hu, W., Li, J., & Pei, Q. (2014b). A flexible and transparent thin film heater based on a silver nanowire/heat-resistant polymer composite. *Macromolecular Materials and Engineering, 299*, 1403–1409. https://doi.org/10.1002/mame.201400097

Li, Z., Li, F., Hu, J., Wee, W. H., Han, Y. L., Pingguan-Murphy, B., et al. (2015a). Direct writing electrodes using ball pen for paper-based point-of-care testing. *Analyst, 140*, 5526–5535. https://doi.org/10.1039/C5AN00620A

Li, H., He, Y., Pavlinek, V., Cheng, Q., Saha, P., & Li, C. (2015b). MnO_2 nanoflake/polyaniline nanorod hybrid nanostructures on graphene paper for high-performance flexible supercapacitor electrodes. *Journal of Materials Chemistry A, 3*, 17165–17171. https://doi.org/10.1039/C5TA04008F

Li, Q., Zhang, J., Li, Q., Li, G., Tian, X., Luo, Z., et al. (2019). Review of printed electrodes for flexible devices. *Frontiers in Materials, 5*, 77. https://doi.org/10.3389/fmats.2018.00077

Li, G., Ren, M., & Zhou, H. (2022). Observably boosted electrochemical performances of roughened graphite sheet/polyaniline electrodes for use in flexible supercapacitors. *Surfaces and Interfaces, 30*, 101874. https://doi.org/10.1016/j.surfin.2022.101874

Liana, D. D., Raguse, B., Wieczorek, L., Baxter, G. R., Chuah, K., Gooding, J. J., & Chow, E. (2013). Sintered gold nanoparticles as an electrode material for paper-based electrochemical sensors. *RSC Advances, 3*, 8683–8691. https://doi.org/10.1039/C3RA00102D

Liang, Y., Wu, D., Feng, X., & Mullen, K. (2009). Dispersion of graphene sheets in organic solvent supported by ionic interactions. *Advanced Materials, 21*, 1679–1683. https://doi.org/10.1002/adma.200803160

Liang, J., Zhao, Y., Guo, L., & Li, L. (2012). Flexible free-standing graphene/SnO_2 nanocomposites paper for Li-ion battery. *ACS Applied Materials & Interfaces, 4*, 5742–5748. https://doi.org/10.1021/am301962d

Liang, J., Li, L., Tong, K., Ren, Z., Hu, W., Niu, X., et al. (2014a). Silver nanowire percolation network soldered with graphene oxide at room temperature and its application for fully stretchable polymer light-emitting diodes. *ACS Nano, 8*, 1590–1600. https://doi.org/10.1021/nn405887k

Liang, K., Gu, T. L., Cao, Z. Y., Tang, X. Z., Hu, W. C., & Wei, B. Q. (2014b). *In situ* synthesis of SWNTs@MnO_2/polypyrrole hybrid film as binder-free supercapacitor electrode. *Nano Energy, 9*, 245–251. https://doi.org/10.1016/j.nanoen.2014.07.017

Liao, X., Liao, Q., Yan, X., Liang, Q., Si, H., Li, M., et al. (2015). Flexible and highly sensitive strain sensors fabricated by pencil drawn for wearable monitor. *Advanced Functional Materials, 25*(16), 2395–2401. https://doi.org/10.1002/adfm.201500094

Lin, J., Peng, Z., Liu, Y., Ruiz-Zepeda, F., Ye, R., Samuel, E. L. G., et al. (2014). Laser-induced porous graphene films from commercial polymers. *Nature Communications, 5*, 5–12. https://doi.org/10.1038/ncomms6714

Lin, L., Lei, W., Zhang, S., Liu, Y., Wallace, G. G., & Chen, J. (2019). Two-dimensional transition metal dichalcogenides in supercapacitors and secondary batteries. *Energy Storage Materials, 19*, 408–423. https://doi.org/10.1016/j.ensm.2019.02.023

Liu, J., Agarwal, M., & Varahramyan, K. (2008). Glucose sensor based on organic thin film transistor using glucose oxidase and conducting polymer. *Sensors and Actuators B: Chemical, 135*, 195–199. https://doi.org/10.1016/j.snb.2008.08.009

Liu, Y., Weng, B., Razal, J. M., Xu, Q., Zhao, C., Hou, Y., et al. (2015). High-performance flexible all-solid-state supercapacitor from large free-standing graphene-PEDOT/PSS films. *Scientific Reports, 5*, 17045. https://doi.org/10.1038/srep17045

Liu, S., Li, J., Shi, X., Gao, E., Xu, Z., Tang, H., et al. (2017a). Rollerball-pen-drawing technology for extremely foldable paper-based electronics. *Advanced Electronic Materials, 3*, 1700098. https://doi.org/10.1002/aelm.201700098

Liu, H., Qing, H., Li, Z., Han, Y. L., Lin, M., Yang, H., et al. (2017b). Paper: A promising material for human-friendly functional wearable electronics. *Materials Science and Engineering: R: Reports, 112*, 1–22. https://doi.org/10.1016/j.mser.2017.01.001

López-Naranjo, E. J., González-Ortiz, L. J., Apátiga, L. M., Rivera-Muñoz, E. M., & Manzano-Ramírez, A. (2016). Transparent electrodes: A review of the use of carbon-based nanomaterials. *Journal of Nanomaterials, 2016*, 4928365. https://doi.org/10.1155/2016/4928365

Lu, X., Zhang, Y., & Zheng, Z. (2021). Metal-based flexible transparent electrodes: Challenges and recent advances. *Advanced Electronic Materials, 7*, 2001121. https://doi.org/10.1002/aelm.202001121

Luo, M., Liu, Y., Huang, W., Qiao, W., Zhou, Y., Ye, Y., & Chen, L.-S. (2017). Towards flexible transparent electrodes based on carbon and metallic materials. *Micromachines, 8*, 12. https://doi.org/10.3390/mi8010012

Lyu, L., Antink, W. H., Kim, Y. S., Kim, C. W., Hyeon, T., & Piao, Y. (2021). Recent development of flexible and stretchable supercapacitors using transition metal compounds as electrode materials. *Small, 17*, 2101974. https://doi.org/10.1002/smll.202101974

Määttänen, A., Vanamo, U., Ihalainen, P., Pulkkinen, P., Tenhu, H., Bobacka, J., & Peltonen, J. (2013). A low-cost paper-based inkjet-printed platform for electrochemical analyses. *Sensors and Actuators B: Chemical, 177*, 153–162. https://doi.org/10.1016/j.snb.2012.10.113

Magnus, C., Cooper, D., Sharp, J., & Rainforth, W. M. (2019). Microstructural evolution and wear mechanism of Ti_3AlC_2—Ti_2AlC dual MAX phase composite consolidated by spark plasma sintering (SPS). *Wear, 438–439*, 203013. https://doi.org/10.1016/j.wear.2019.203013

Mazloum-Ardakani, M., Amin-Sadrabadi, E., & Khoshroo, A. (2016). Enhanced activity for non-enzymatic glucose oxidation on nickel nanostructure supported on PEDOT:PSS. *Journal of Electroanalytical Chemistry, 775*, 116–120. https://doi.org/10.1016/j.jelechem.2016.05.044

Mazurkiewicz, W., Podrażka, M., Jarosińska, E., Valapil, K. K., Wiloch, M., Jönsson-Niedziółka, M., & Witkowska Nery, E. (2020). Paper-based electrochemical sensors and how to make them (work). *ChemElectronChem, 7*(14), 2939–2956. https://doi.org/10.1002/celc.202000512

McCoul, D., Hu, W., Gao, M., Mehta, V., & Pei, Q. (2016). Recent advances in stretchable and transparent electronic materials. *Advanced Electronic Materials, 2*, 1500407. https://doi.org/10.1002/aelm.201500407

Meduri, P., Pendyala, C., Kumar, V., Sumanasekera, G. U., & Sunkara, M. K. (2009). Hybrid tin oxide nanowires as stable and high capacity anodes for Li-ion batteries. *Nano Letters, 9*, 612–616. https://doi.org/10.1021/nl802864a

Merilampi, S., Laine-Ma, T., & Ruuskanen, P. (2009). The characterization of electrically conductive silver ink patterns on flexible substrates. *Microelectronics and Reliability, 49*, 782–790. https://doi.org/10.1016/j.microrel.2009.04.004

Mi, L., Chen, Y., Wei, W., Chen, W., Hou, H., & Zheng, Z. (2013). Large-scale urchin-like micro/nano-structured NiS: Controlled synthesis, cation exchange and lithium-ion battery applications. *RSC Advances, 3*(38), 17431–17439. https://doi.org/10.1039/C3RA42859A

Mia, A. K., Meyyappan, M., & Giri, P. K. (2023). Two-dimensional transition metal dichalcogenide based biosensors: From fundamentals to healthcare applications. *Biosensors, 13*, 169. https://doi.org/10.3390/bios13020169

Miao, Y. E., Huang, Y., Zhang, L., Fan, W., Lai, F., & Liu, T. (2015). Electrospun porous carbon nanofiber@MoS_2 core/sheath fiber membranes as highly flexible and binder-free anodes for lithium-ion batteries. *Nanoscale, 7*, 11093–11101. https://doi.org/10.1039/C5NR02711J

Mihranyan, A., Nyholm, L., Garcia Bennett, A. E., & Strømme, M. (2008). A novel high specific surface area conducting paper material composed of polypyrrole and *Cladophora* cellulose. *The Journal of Physical Chemistry. B, 112*, 12249-122–12249-155. https://doi.org/10.1021/jp805123w

Molina-Lopez, F., Briand, D., & De Rooij, N. F. (2012). All additive inkjet printed humidity sensors on plastic substrate. *Sensors and Actuators B: Chemical, 166–167*, 212–222. https://doi.org/10.1016/j.snb.2012.02.042

Moon, K., Kim, J. I., Lee, H., Hur, K., Kim, W. C., & Lee, H. (2013). 2D graphene oxide nanosheets as an adhesive over-coating layer for flexible transparent conductive electrodes. *Scientific Reports, 3*, 1112. https://doi.org/10.1038/srep01112

Moon, J.-M., Thapliyal, N., Hussain, K. K., Goyal, R. N., & Shim, Y.-B. (2018). Conducting polymer-based electrochemical biosensors for neurotransmitters: A review. *Biosensors & Bioelectronics, 102*, 540–552. https://doi.org/10.1016/j.bios.2017.11.069

Mukherjee, S., & Singh, G. (2019). Two-dimensional anode materials for non-lithium metal-ion batteries. *ACS Applied Energy Materials, 2*, 932–955. https://doi.org/10.1021/acsaem.8b00843

Mukherjee, S., Singh, R., Gopinathan, S., Murugan, S., Gawali, S., Saha, B., et al. (2014). Solution-processed poly(3,4-ethylenedioxythiophene) thin films as transparent conductors: Effect of p-toluenesulfonic acid in dimethyl sulfoxide. *ACS Applied Materials & Interfaces, 6*, 17792–17803. https://doi.org/10.1021/am504150n

Na, S.-I., Kim, S.-S., Jo, J., & Kim, D.-Y. (2008). Efficient and flexible ITO-free organic solar cells using highly conductive polymer anodes. *Advanced Materials, 20*(21), 4061–4067. https://doi.org/10.1002/adma.200800338

Neampet, S., Ruecha, N., Qin, J., Wonsawat, W., Chailapakul, O., & Rodthongkum, N. (2019). A nanocomposite prepared from platinum particles, polyaniline and a Ti_3C_2 MXene for amperometric sensing of hydrogen peroxide and lactate. *Microchimica Acta, 186*, 752. https://doi.org/10.1007/s00604-019-3845-3

Nguyen, V. H., Papanastasiou, D., Resende, J., Bardet, L., Sannicolo, T., et al. (2022). Advances in flexible metallic transparent electrodes. *Small, 18*(19), e2106006. https://doi.org/10.1002/smll.202106006.hal-03876833

Nie, Z. H., Nijhuis, C. A., Gong, J. L., Chen, X., Kumachev, A., Martinez, A. W., et al. (2010). Electrochemical sensing in paper-based microfluidic devices. *Lab on a Chip, 10*, 477–483. https://doi.org/10.1039/B917150A

Niu, Z. Q., Luan, P. S., Shao, Q., Dong, H. B., Li, J. Z., Chen, J., et al. (2012). A "skeleton/skin" strategy for preparing ultrathin free-standing single-walled carbon nanotube/polyaniline films for high performance supercapacitor electrodes. *Energy & Environmental Science, 5*, 8726–8733. https://doi.org/10.1039/C2EE22042C

Noviana, E., McCord, C. P., Clark, K. M., Jang, I., & Henry, C. S. (2020). Electrochemical paper-based devices: Sensing approaches and progress toward practical applications. *Lab on a Chip, 20*, 9–34. https://doi.org/10.1039/C9LC00903E

Nyström, G., Razaq, A., Strømme, M., Nyholm, L., & Mihranyan, A. (2009). Ultrafast all-polymer paper-based batteries. *Nano Letters, 9*, 3635–3639. https://doi.org/10.1021/nl901852h

Nyholm, L., Nyström, G., Mihranyan, A., Strømme, M. (2011). Toward Flexible Polymer and Paper-Based Energy Storage Devices. *Adv. Mater. 23*, 3751–3769. https://doi.org/10.1002/adma.201004134

Olsson, H., Nystrцm, G., Strцmme, M., Sjцdin, M., & Nyholm, L. (2011). Cycling stability and self-protective properties of a paper-based polypyrrole energy storage device. *Electrochemistry Communications, 13*, 869–871. https://doi.org/10.1016/j.elecom.2011.05.024

Ong, H.-Y., Shrestha, M., & Lau, G.-K. (2015). Microscopically crumpled indium-tin-oxide thin films as compliant electrodes with tunable transmittance. *Applied Physics Letters, 107*, 132902. https://doi.org/10.1063/1.4932115

Pääkkö, M., Vapaavuori, J., Silvennoinen, R., Kosonen, H., Ankerfors, M., Lindström, T., T., et al. (2008). Long and entangled native cellulose I nanofibers allow flexible aerogels and hierarchically porous templates for functionalities. *Soft Matter, 4*, 2492–22499. https://doi.org/10.1039/B810371B

Palchoudhury, S., Ramasamy, K., Gupta, R. K., & Gupta, A. (2019). Flexible supercapacitors: A materials perspective. *Frontiers in Materials, 5*, 83. https://doi.org/10.3389/fmats.2018.00083

Pataniya, P. M., Dabhi, S., Patel, V., & Sumesh, C. K. (2022). Liquid phase exfoliated ReS_2 nanocrystals on paper-based electrodes for hydrogen evolution and supercapacitor applications. *Surfaces and Interfaces, 34*, 102318. https://doi.org/10.1016/j.surfin.2022.102318

Pavithra, M., Muruganand, S., & Parthiban, C. (2018). Development of novel paper based electrochemical immunosensor with self-made gold nanoparticle ink and quinone derivate for highly sensitive carcinoembryonic antigen. *Sensors and Actuators B: Chemical, 257*, 496–503. https://doi.org/10.1016/j.snb.2017.10.177

Peng, S., Li, L., Tan, H., Cai, R., Shi, W., Li, C., et al. (2014). MS_2 (M =Co and Ni) hollow spheres with tunable interiors for high-performance supercapacitors and photovoltaics. *Advanced Functional Materials, 24*, 2155–2162. https://doi.org/10.1002/adfm.201303273

Qin, L.-H., Yan, Y.-Q., Yu, G., Zhang, Z.-Y., Zhama, T., & Sun, H. (2021). Research progress of transparent electrode materials with sandwich structure. *Materials, 14*, 4097. https://doi.org/10.3390/ma14154097

Ramasamy, K., Gupta, R. K., Palchoudhury, S., Ivanov, S., & Gupta, A. (2014). Layer-structured copper antimony chalcogenides ($CuSbSe_xS_{2-x}$): Stable electrode materials for supercapacitors. *Chemistry of Materials, 27*, 379–386. https://doi.org/10.1021/cm5041166

Ramasamy, K., Gupta, R. K., Sims, H., Palchoudhury, S., Ivanov, S., & Gupta, A. (2015). Layered ternary sulfide $CuSbS_2$ nanoplates for flexible solid-state supercapacitors. *Journal of Materials Chemistry A, 3*, 13263–13274. https://doi.org/10.1039/C5TA03193A

Ratha, S., & Rout, C. S. (2013). Supercapacitor electrodes based on layered tungsten disulfide-reduced graphene oxide hybrids synthesized by a facile hydrothermal method. *ACS Applied Materials & Interfaces, 5*, 11427–11433. https://doi.org/10.1021/am403663f

Romeo, A., Moya, A., Leung, T. S., Gabriel, G., Villa, R., & Sánchez, S. (2018). Inkjet printed flexible non-enzymatic glucose sensor for tear fluid analysis. *Applied Materials Today, 10*, 133. https://doi.org/10.1016/j.apmt.2017.12.016

Rosset, S., Niklaus, M., Dubois, P., & Shea, H. R. (2009). Metal ion implantation for the fabrication of stretchable electrodes on elastomers. *Advanced Functional Materials, 19*, 470–478. https://doi.org/10.1002/adfm.200801218

Russo, A., Ahn, B. Y., Adams, J. J., Duoss, E. B., Bernhard, J. T., & Lewis, J. A. (2011). Pen-on-paper flexible electronics. *Advanced Materials, 23*, 3426–3430. https://doi.org/10.1002/adma.201101328

Sakata, T., Hagio, M., Saito, A., Mori, Y., Nakao, M., & Nishi, K. (2020). Biocompatible and flexible paper-based metal electrode for potentiometric wearable wireless biosensing. *Science and Technology of Advanced Materials, 21*(1), 379–387. https://doi.org/10.1080/14686996.2020.1777463

Santhiago, M., Wydallis, J. B., Kubota, L. T., & Henry, C. S. (2013). Construction and electrochemical characterization of microelectrodes for improved sensitivity in paper-based analytical devices. *Analytical Chemistry, 85*, 5233–5239. https://doi.org/10.1021/ac400728y

Sappia, L. D., Pascual, B. S., Azzaroni, O., & Marmisollé, W. (2021). PEDOT-based stackable paper electrodes for metal-free supercapacitors. *ACS Applied Energy Materials, 4*, 9283–9293. https://doi.org/10.1021/acsaem.1c01517

Scardaci, V., Coull, R., & Coleman, J. N. (2010). Very thin transparent, conductive carbon nanotube films on flexible substrates. *Applied Physics Letters, 97*, 023114. https://doi.org/10.1063/1.3462317

Secor, E. B., Lim, S., Zhang, H., Frisbie, C. D., Francis, L. F., & Hersam, M. C. (2014). Gravure printing of graphene for large-area flexible electronics. *Advanced Materials, 26*, 4533–4538. https://doi.org/10.1002/adma.201401052

Shamkhalichenar, H., & Choi, J. W. (2017). An inkjet-printed non-enzymatic hydrogen peroxide sensor on paper. *Journal of the Electrochemical Society, 164*, B3101–B3106. https://doi.org/10.1149/2.0161705jes

Shin, H. J., Jeon, S. S., & Im, S. S. (2011). CNT/PEDOT core/shell nanostructures as a counter electrode for dye-sensitized solar cells. *Synthetic Metals, 161*, 1284–1288. https://doi.org/10.1016/j.synthmet.2011.04.024

Siegel, A. C., Phillips, S. T., Dickey, M. D., Lu, N., Suo, Z., & Whitesides, G. M. (2010). Foldable printed circuit boards on paper substrates. *Advanced Functional Materials, 20*, 28–35. https://doi.org/10.1002/adfm.200901363

Simonenko, N. P., Fisenko, N. A., Fedorov, F. S., Simonenko, T. L., Mokrushin, A. S., Simonenko, E. P., Korotcenkov, G., et al. (2022). Printing technologies as an emerging approach in gas sensors: Survey of literature. *Sensors (MDPI), 22*, 3473. https://doi.org/10.3390/s22093473

Sireesha, M., Jagadeesh Babu, V., Kranthi Kiran, A. S., & Ramakrishna, S. (2018). A review on carbon nanotubes in biosensor devices and their applications in medicine. *Nano, 4*, 36–57. https://doi.org/10.1080/20550324.2018.1478765

Sjöberg, P., Määttänen, A., Vanamo, U., Novell, M., Ihalainen, P., Andrade, F. J., et al. (2016). Paper-based potentiometric ion sensors constructed on ink-jet printed gold electrodes. *Sensors and Actuators B: Chemical, 224*, 325–332. https://doi.org/10.1016/j.snb.2015.10.051

Stankovich, S., Dikin, D. A., Dommett, G. H. B., Kohlhaas, K. M., Zimney, E. J., Stach, E. A., et al. (2006). Graphene-based composite materials. *Nature, 442*, 282–2286. https://doi.org/10.1038/nature04969

Steffens, C., Manzoli, A., Francheschi, E., Corazza, M., Corazza, F., Oliveira, J. V., & Herrmann, P. (2009). Low-cost sensors developed on paper by line patterning with graphite and polyaniline coating with supercritical CO_2. *Synthetic Metals, 159*, 2329–2332. https://doi.org/10.1016/j.synthmet.2009.08.045

Stejskal, J., Trchová, M., Bober, P., Morávková, Z., Kopecký, D., Vrňata, M., et al. (2016). Polypyrrole salts and bases: Superior conductivity of nanotubes and their stability towards the loss of conductivity by deprotonation. *RSC Advances, 6*, 88382–88391. https://doi.org/10.1039/C6RA19461C

Sui, Y., & Zorman, C. A. (2020). Review—Inkjet printing of metal structures for electrochemical sensor applications. *Journal of the Electrochemical Society, 167*, 037571. https://doi.org/10.1149/1945-7111/ab721f

Sun, Y., Hu, X., Luo, W., & Huang, Y. (2011). Self-assembled hierarchical MoO_2/graphene nanoarchitectures and their application as a high-performance anode material for Lithium-ion batteries. *ACS Nano, 5*, 7100–7107. https://doi.org/10.1021/nn201802c

Sun, H., Wang, C., Xu, Y., Dai, D., Deng, X., & Gao, H. (2019). A novel electrochemical sensor based on a glassy carbon electrode modified with GO/MnO_2 for simultaneous determination of trace Cu(II) and Pb(II) in environmental water. *Chemistry Select, 4*, 11862–11871. https://doi.org/10.1002/slct.201902858

Sun, H., Li, D., Yue, X., Hong, R., Yang, W., Chaoran Liu, C., et al. (2022). A review of transition metal dichalcogenides-based biosensors. *Frontiers in Bioengineering and Biotechnology, 10*, 941135. https://doi.org/10.3389/fbioe.2022.941135

Sundriyal, P., & Bhattacharya, S. (2017). Inkjet printed electrodes on A4 paper substrates for low cost, disposable and flexible asymmetric supercapacitors. *ACS Applied Materials & Interfaces, 9*(44), 38507–38521. https://doi.org/10.1021/acsami.7b11262

Szuplewska, A., Kulpińska, D., Dybko, A., Chudy, M., Jastrzębska, A. M., Olszyna, A., & Brzózka, Z. (2020). Future applications of MXenes in biotechnology, nanomedicine, and sensors. *Trends in Biotechnology, 38*, 264–279. https://doi.org/10.1016/j.tibtech.2019.09.001

Tai, H., Duan, Z., Wang, Y., Wang, S., & Jiang, Y. (2020). Paper-based sensors for gas, humidity, and strain detections: A review. *ACS Applied Materials & Interfaces, 12*, 31037–31053. https://doi.org/10.1021/acsami.0c06435

Tang, H., Chen, R., Huang, Q., Ge, W., Zhang, X., Yang, Y., & Wang, X. (2022). Scalable manufacturing of leaf-like MXene/Ag NWs/cellulose composite paper electrode for all-solid-state supercapacitor. *EcoMat, 4*, e12247. https://doi.org/10.1002/eom2.12247

Tanwar, S., Arya, A., Gaur, A., & Sharma, A. L. (2021). Transition metal dichalcogenide (TMDs) electrodes for supercapacitors: A comprehensive review. *Journal of Physics: Condensed Matter, 33*, 303002. https://doi.org/10.1088/1361-648X/abfb3c

Tian, W., Vahid Mohammadi, A., Reid, M., Wang, Z., Ouyang, L., Erlandsson, J., et al. (2019). Multifunctional nanocomposites with high strength and capacitance using 2D MXene and 1D nanocellulose. *Advanced Materials, 31*, 1902977. https://doi.org/10.1002/adma.201902977

Tîlmaciu, C.-M., & Morris, M. C. (2015). Carbon nanotube biosensors. *Frontiers in Chemistry, 3*, 59. https://doi.org/10.3389/fchem.2015.00059

Tobjörk, D., Aarnio, H., Pulkkinen, P., Bollström, R., Määttänen, A., Ihalainen, P., et al. (2012). IR-sintering of ink-jet printed metal-nanoparticles on paper. *Thin Solid Films, 520*, 2949–2955. https://doi.org/10.1016/j.tsf.2011.10.017

Tölle, F. J., Fabritius, M., & Mülhaupt, R. (2012). Emulsifier-free graphene dispersions with high graphene content for printed electronics and freestanding graphene films. *Advanced Functional Materials, 22*, 1136–1144. https://doi.org/10.1002/adfm.201102888

Van Den Berg, O., Capadona, J. R., & Weder, C. (2007). Preparation of homogeneous dispersions of tunicate cellulose whiskers in organic solvents. *Biomacromolecules, 8*, 1353–1357. https://doi.org/10.1021/bm061104q

Villarreal, C. C., Pham, T., Ramnani, P., & Mulchandani, A. (2017). Carbon allotropes as sensors for environmental monitoring. *Current Opinion in Electrochemistry, 3*, 106–113. https://doi.org/10.1016/j.coelec.2017.07.004

Vosgueritchian, M., Lipomi, D. J., & Bao, Z. (2011). Highly conductive and transparent PEDOT: PSS films with a fluorosurfactant for stretchable and flexible transparent electrodes. *Advanced Functional Materials, 22*, 421–428. https://doi.org/10.1002/adfm.201101775

Wakuda, D., Hatamura, M., & Suganuma, K. (2007). Novel method for room temperature sintering of Ag nanoparticle paste in air. *Chemical Physics Letters, 441*, 305–308. https://doi.org/10.1016/j.cplett.2007.05.033

Wang, Y., & Weng, G. J. (2018). Electrical conductivity of carbon nanotube and graphene-based nanocomposites. In S. A. Meguid & G. J. Weng (Eds.), *Micromechanics and nanomechanics of composite solids* (pp. 123–156). Springer International Publishing. https://doi.org/10.1007/978-3-319-52794-9_4

Wang, J., Zhang, X., Huang, X., Wang, S., Qian, Q., Du, W., & Wang, Y. (2013). Forced assembly of water-dispersible carbon nanotubes trapped in paper for cheap gas sensors. *Small, 9*(22), 3759–3764. https://doi.org/10.1002/smll.201300655

Wang, X., Kajiyama, S., Iinuma, H., Hosono, E., Oro, S., Moriguchi, I., et al. (2015a). Pseudocapacitance of MXene nanosheets for high-power sodium-ion hybrid capacitors. *Nature Communications, 6*, 6544. https://doi.org/10.1038/ncomms7544

Wang, H., Lan, X., Jiang, D., Zhang, Y., Zhong, H., Zhanga, Z., & Jiang, Y. (2015b). Sodium storage and transport properties in pyrolysis synthesized $MoSe_2$ nanoplates for high performance sodium-ion batteries. *Journal of Power Sources, 283*, 187–194. https://doi.org/10.1016/j.jpowsour.2015.02.096

Wang, G., Morrin, A., Li, M., Liu, N., & Luo, X. (2018). Nanomaterial-doped conducting polymers for electrochemical sensors and biosensors. *Journal of Materials Chemistry B, 6*, 4173–4190. https://doi.org/10.1039/C8TB00817E

Wang, L., Wang, Y., & Zhuang, Q. (2019). Simple self-referenced ratiometric electrochemical sensor for dopamine detection using electrochemically pretreated glassy carbon electrode modified by acid-treated multiwalled carbon nanotube. *Journal of Electroanalytical Chemistry, 851*, 113446. https://doi.org/10.1016/j.jelechem.2019.113446

Wang, L., Xu, D., Jiang, L., Gao, J., Tang, Z., Xu, Y., et al. (2020). Transition metal dichalcogenides for sensing and oncotherapy: Status, challenges, and perspective. *Advanced Functional Materials, 2020*, 2004408. https://doi.org/10.1002/adfm.202004408

Wang, L., Han, Y., Wang, H., Han, Y., Liu, J., Lu, G., & Yu, H. (2021a). A MXene-functionalized paper-based electrochemical immunosensor for label-free detection of cardiac troponin I. *Journal of Semiconductors, 42*, 092601. https://doi.org/10.1088/1674-4926/42/9/092601

Wang, T., Lu, K., Xu, Z., Lin, Z., Ning, H., Tian Qiu, T., et al. (2021b). Recent developments in flexible transparent electrode. *Crystals, 11*, 511. https://doi.org/10.3390/cryst11050511

Wei, W., Mi, L., Gao, Y., Zheng, Z., Chen, W., & Guan, X. (2014). Partial ion-exchange of nickel-sulfide-derived electrodes for high performance supercapacitors. *Chemistry of Materials, 26*, 3418–3426. https://doi.org/10.1021/cm5006482

Weng, Z., Su, Y., Wang, D. W., Li, F., Du, J. H., & Cheng, H. M. (2011). Graphene–cellulose paper flexible supercapacitors. *Advanced Energy Materials, 1*, 917–922. https://doi.org/10.1002/aenm.201100312

Winther-Jensen, B., Clark, N., Subramanian, P., Helmer, R., Ashraf, S., Wallace, G., et al. (2007). Application of polypyrrole to flexible substrates. *Journal of Applied Polymer Science, 104*, 3938–3947. https://doi.org/10.1002/app.26162

Wu, Z.-S., Ren, W., Wen, L., Gao, L., Zhao, J., Chen, Z., et al. (2010). Graphene anchored with Co_3O_4 nanoparticles as anode of Lithium ion batteries with enhanced reversible capacity and cyclic performance. *ACS Nano, 4*, 3187–3194. https://doi.org/10.1021/nn100740x

Wu, H., Kong, D., Ruan, Z., Hsu, P. C., Wang, S., Yu, Z., et al. (2013). A transparent electrode based on a metal nanotrough network. *Nature Nanotechnology, 8*, 421–425. https://doi.org/10.1038/nnano.2013.84

Wu, J. B., Gao, X., Yu, H. M., Ding, T. P., Yan, Y. X., Yao, B., et al. (2016). A scalable free-standing V_2O_5/CNT film electrode for supercapacitors with a wide operation voltage (1.6 V) in an aqueous electrolyte. *Advanced Functional Materials, 26*, 6114–6120. https://doi.org/10.1002/adfm.201601811

Xie, X., Zhao, M.-Q., Anasori, B., Maleski, K., Ren, C. E., Li, J., et al. (2016). Porous heterostructured MXene/carbon nanotube composite paper with high volumetric capacity for sodium-based energy storage devices. *Nano Energy, 26*, 513–523. https://doi.org/10.1016/j.nanoen.2016.06.005

Xu, Y., Wang, Y., Liang, J., Huang, Y., Ma, Y., Wan, X., & Chen, Y. (2009). A hybrid material of graphene and poly (3,4-ethyldioxythiophene) with high conductivity, flexibility, and transparency. *Nano Research, 2*, 343–348. https://doi.org/10.1007/s12274-009-9032-9

Xu, Y., Lin, Z., Wei, W., Hao, Y., Liu, S., Ouyang, J., & Chang, J. (2022). Recent progress of electrode materials for flexible perovskite solar cells. *Nano-Micro Letters, 14*, 117. https://doi.org/10.1007/s40820-022-00859-9

Yang, X., Fan, K., Zhu, Y., Shen, J., Jiang, X., Zhao, P., et al. (2013). Electric papers of graphene-coated Co_3O_4 fibers for high-performance lithium-ion batteries. *ACS Applied Materials & Interfaces, 5*, 997–1002. https://doi.org/10.1021/am302685t

Yao, B., Yuan, L. Y., Xiao, X., Zhang, J., Qi, Y. Y., Zhou, J., et al. (2013). Paper-based solid-state supercapacitors with pencil-drawing graphite/polyaniline networks hybrid electrodes. *Nano Energy, 2*, 1071–1078. https://doi.org/10.1016/j.nanoen.2013.09.002

Yao, W., Wang, J., Li, H., & Lu, Y. (2014). Flexible α-MnO_2 paper formed by millimeter-long nanowires for supercapacitor electrodes. *Journal of Power Sources, 247*, 824–830. https://doi.org/10.1016/j.jpowsour.2013.09.039

Yao, B., Huang, L., Zhang, J., Gao, X., Wu, J., Cheng, Y., et al. (2016). Flexible transparent molybdenum trioxide nanopaper for energy storage. *Advanced Materials, 28*, 6353–6358. https://doi.org/10.1002/adma.201600529

Yao, B., Zhang, J., Kou, T., Song, Y., Liu, T., & Li, Y. (2017). Paper-based electrodes for flexible energy storage devices. *Advancement of Science, 4*, 1700107. https://doi.org/10.1002/advs.201700107

Yao, Z., Coatsworth, P., Shi, X., Zhi, J., Hu, L., Yan, R., et al. (2022). Paper-based sensors for diagnostics, human activity monitoring, food safety and environmental detection. *Sensors & Diagnostics, 1*, 312–342. https://doi.org/10.1039/D2SD00017B

Yi, Y., Weinberg, G., Prenzel, M., Greiner, M., Heumann, S., Becker, S., & Schlögl, R. (2017). Electrochemical corrosion of a glassy carbon electrode. *Catalysis Today, 295*, 32–40. https://doi.org/10.1016/j.cattod.2017.07.013

You, B., Ju, B. K., & Kim, J. W. (2016). Photoresist-assisted fabrication of thermally and mechanically stable silver nanowire-based transparent heaters. *Sensors and Actuators A: Physical, 250*, 123–128. https://doi.org/10.1016/j.sna.2016.09.021

Yu, T., & Breslin, C. B. (2020). Review—Two-dimensional titanium carbide MXenes and their emerging applications as electrochemical sensors. *Journal of the Electrochemical Society, 167*, 037514. https://doi.org/10.1149/2.0142003JES

Yu, D., & Dai, L. (2010). Self-assembled graphene/carbon nanotube hybrid films for supercapacitors. *Journal of Physical Chemistry Letters, 1*, 467–470. https://doi.org/10.1021/jz9003137

Yuan, L., Xiao, X., Ding, T., Zhong, J., Zhang, X., Shen, Y., et al. (2012). Paper-based supercapacitors for self-powered nanosystems. *Angewandte Chemie, International Edition, 51*, 4934–4938. https://doi.org/10.1002/anie.201109142

Yuan, L. Y., Yao, B., Hu, B., Huo, K. F., Chen, W., & Zhou, J. (2013). Polypyrrole-coated paper for flexible solid-state energy storage. *Energy & Environmental Science, 6*, 470–476. https://doi.org/10.1039/C2EE23977A

Yuan, Y., Zhang, Y., Liu, R., Liu, J., Li, Z., & Liu, X. (2016). Humidity sensor fabricated by inkjet-printing photosensitive conductive inks PEDOT: PVMA on a paper substrate. *RSC Advances, 6*(53), 47498–47508. https://doi.org/10.1039/C6RA03050E

Yun, J. (2017). Ultrathin metal films for transparent electrodes of flexible optoelectronic devices. *Advanced Functional Materials, 2017*, 1606641. https://doi.org/10.1002/adfm.201606641

Zea, M., Moya, A., Fritsch, M., Ramon, E., Villa, R., & Gabriel, G. (2019). Enhanced performance stability of iridium oxide-based pH sensors fabricated on rough inkjet-printed platinum. *ACS Applied Materials & Interfaces, 11*, 15160–15169. https://doi.org/10.1021/acsami.9b03085

Zeng, H., Liu, D., Zhang, Y., See, K. A., Jun, Y.-S., Wu, G., et al. (2015). Nanostructured Mn-doped V_2O_5 cathode material fabricated from layered vanadium jarosite. *Chemistry of Materials, 27*, 7331–7336. https://doi.org/10.1021/acs.chemmater.5b02840

Zhang, F., & Qi, L. (2016). Recent progress in self-supported metal oxide nanoarray electrodes for advanced Lithium-ion batteries. *Advancement of Science, 3*, 1600049. https://doi.org/10.1002/advs.201600049

Zhang, V., Feng, H., Wu, X., Wang, L., Zhang, A., Xia, Y., et al. (2009). Progress of electrochemical capacitor electrode materials: A review. *International Journal of Hydrogen Energy, 34*, 4889–4899. https://doi.org/10.1016/j.ijhydene.2009.04.005

Zhang, Y., Zhu, P., Li, G., Zhao, T., Fu, X., Sun, R., et al. (2014a). Facile preparation of monodisperse, impurity-free, and antioxidation copper nanoparticles on a large scale for application in conductive ink. *ACS Applied Materials & Interfaces, 6*, 560–567. https://doi.org/10.1021/am404620y

Zhang, C., Yin, H., Han, M., Dai, Z., Pang, H., Zheng, Y., et al. (2014b). Two-dimensional tin selenide nanostructures for flexible all-solid-state supercapacitors. *ACS Nano, 8*, 3761–3770. https://doi.org/10.1021/nn5004315

Zhang, D., Yan, H., Lu, Y., Qiu, K., Wang, C., Tang, C., et al. (2014c). Hierarchical mesoporous nickel cobaltite nanoneedle/carbon cloth arrays as superior flexible electrodes for supercapacitors. *Nanoscale Research Letters, 9*, 139. https://doi.org/10.1186/1556-276X-9-139

Zhang, J., Huang, L., Lin, Y., Chen, L., Zeng, Z., Shen, L., et al. (2015). Pencil-trace on printed Silver interdigitated electrodes for paper-based NO_2 gas sensors. *Applied Physics Letters, 106*(14), 143101. https://doi.org/10.1063/1.4917063

Zhang, Y., Zhang, L., Cui, K., Ge, S., Cheng, X., Yan, M., et al. (2018a). Flexible electronics based on micro/nanostructured paper. *Advanced Materials, 30*, 1801588. https://doi.org/10.1002/adma.201801588

Zhang, Y., Duan, Z., Zou, H., & Ma, M. (2018b). Drawn a facile sensor: A fast response humidity sensor based on pencil-trace. *Sensors and Actuators B: Chemical, 261*, 345–353. https://doi.org/10.1016/j.snb.2018.01.176

Zhang, C. J., Kremer, M. P., Seral-Ascaso, A., Park, S.-H., McEvoy, N., Anasori, B., et al. (2018c). Stamping of flexible, coplanar micro-supercapacitors using MXene inks. *Advanced Functional Materials, 28*, 1705506. https://doi.org/10.1002/adfm.201705506

Zhang, C. J., McKeon, L., Kremer, M. P., Park, S.-H., Ronan, O., Seral-Ascaso, A., et al. (2019). Additive-free MXene inks and direct printing of micro-supercapacitors. *Nature Communications, 10*, 1795. https://doi.org/10.1038/s41467-019-09398-1

Zhang, Y.-Z., Wang, Y., Jiang, Q., El-Demellawi, J. K., Kim, H., & Alshareef, H. N. (2020). MXene printing and patterned coating for device applications. *Advanced Materials, 32*, 1908486. https://doi.org/10.1002/adma.201908486

Zhang, Y., Mei, H.-X., Cao, Y., Yan, X.-H., Yan, J., Gao, H.-I., et al. (2021). Recent advances and challenges of electrode materials for flexible supercapacitors. *Coordination Chemistry Reviews, 438*, 213910. https://doi.org/10.1016/j.ccr.2021.213910

Zhao, B., & Shao, Z. (2012). From paper to paper-like hierarchical anatase TiO_2 film electrode for high-performance Lithium-ion batteries. *Journal of Physical Chemistry C, 116*, 17440–17447. https://doi.org/10.1021/jp305744c

Zhao, M. Q., Ren, C. E., Ling, Z., Lukatskaya, M. R., Zhang, C., Van Aken, K. L., et al. (2015). Flexible MXene/carbon nanotube composite paper with high volumetric capacitance. *Advanced Materials, 27*, 339–345. https://doi.org/10.1002/adma.201404140

Zhao, H., Zhang, T., Qi, R., Dai, J., Liu, S., & Fei, T. (2017). Drawn on paper: A reproducible humidity sensitive device by handwriting. *ACS Applied Materials & Interfaces, 9*(33), 28002–28009. https://doi.org/10.1021/acsami.7b05181

Zhao, H., Lin, X., Qi, R., Dai, J., Liu, S., Feng, T., & Zhang, T. (2019). A composite structure of *in situ* cross-linked poly (ionic liquid)s and paper for humidity-monitoring applications. *IEEE Sensors Journal, 19*(3), 833–837. https://doi.org/10.1109/JSEN.2018.2879826

Zhao, P., Bhattacharya, G., Fishlock, S., Guy, J., Kumar, A., Tsonos, C., et al. (2020). Replacing the metal electrodes in triboelectric nanogenerators: High-performance laser-induced graphene electrodes. *Nano Energy, 75*, 104958. https://doi.org/10.1016/j.nanoen.2020.104958

Zhu, X., Zhu, Y., Murali, S., Stoller, M. D., & Ruoff, R. S. (2011). Nanostructured reduced graphene oxide/Fe_2O_3 composite as a high-performance anode material for Lithium ion batteries. *ACS Nano, 5*, 3333–3338. https://doi.org/10.1021/nn200493r

Zhu, P., Liu, Y., Fang, Z., Kuang, Y., Zhang, Y., Peng, C., & Chen, G. (2019). Flexible and highly sensitive humidity sensor based on cellulose nanofibers and carbon nanotube composite film. *Langmuir, 35*(14), 4834–4842. https://doi.org/10.1021/acs.langmuir.8b04259

Zhu, L., Li, X., Kasuga, T., Uetani, K., Nogi, M., & Koga, H. (2022). All-cellulose-derived humidity sensor prepared via direct laser writing of conductive and moisture-stable electrodes on TEMPO-oxidized cellulose paper. *Journal of Materials Chemistry C, 10*, 3712–3719. https://doi.org/10.1039/D1TC05339F

Chapter 28
Selecting Paper for Sensors and Electronic Devices

Ghenadii Korotcenkov

28.1 Introduction

As it was shown in previous chapters, there are a variety of paper materials available to the user. Paper is manufactured in a wide variety of categories (e.g., as printing paper, wrapping paper, writing paper, drawing paper, specialty paper, filter paper, chromatography paper, cardboard, etc.). However, it cannot be said that paper of all types is a universal material suitable for all applications. All papers are made up of cellulose, but they differ from each other with respect to their material and chemical properties. Critical parameters of the paper important for practical applications are shown in Fig. 28.1.

Different types of paper have different combinations of properties shown in Fig. 28.1 (Vicente et al., 2017). For example, some types of paper are more porous, others are denser. Lightweight paper has a weight of 12–30 g/m^2 and a thickness of less than 75 μm; standard paper, such as office paper, weighs about 80 g/m^2 and is 100 μm thick; and cardboard has a density of more than 200–800 g/m^2 and a thickness of more than 300 μm (Tobjörk & Österbacka, 2011). Some types of paper contain, in addition to cellulose, additional fillers, others are made only from cellulose, but an additional coating is applied to their surface, etc. For example, printing paper contains some cellulose fiber with a large amount of filler. Both natural materials (limestone, clay, and talc) and synthetic materials (precipitated calcium carbonate, titanium dioxide, and gypsum) can be used as fillers. The amount and type of fillers determine the structure, thickness, properties, and appearance of the paper (Hubbe & Gill, 2016). In addition, filler determines production cost, refractive index, paper strength, brightness, energy required for drying, coefficient of friction, pore size, and burning rate of the paper (Bauch, 1992; Bown, 1998; Davidson, 1965). It is important to note that fillers can have both positive and negative effects

G. Korotcenkov (✉)
Department of Physics and Engineering, Moldova State University, Chisinau, Moldova

G. Korotcenkov (ed.), *The Handbook of Paper-Based Sensors and Devices*,
https://doi.org/10.1007/978-3-031-91080-7_28

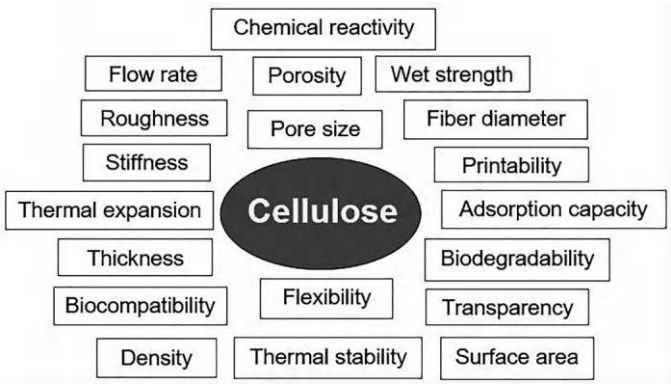

Fig. 28.1 Properties of the paper that control the parameters of the paper-based sensors and electronic devices

on the strength, rate of aging, abrasion, dust formation, and reversible use of a paper sheet. At the same time, bacterial cellulose, which is a biopolymer produced by bacteria, consists of ultrathin nanofibers (<100 nm wide). The main advantage of this material compared to wood cellulose is its purity and crystallinity, since it does not contain lignin, hemicellulose, and other components present in plant cellulose (Abitbol et al., 2016; Gama et al., 2016). Thus, it is the variety of types and amounts of filler used in each type of paper that makes the properties of paper (as a whole) so varied. Moreover, these parameters are unstable and may change depending on the technologies used in the paper production process (Khan et al., 2020). For example, when paper is produced using traditional papermaking methods, the microstructure of the cellulose fibers is mostly preserved. Depending on the type of wood from which the pulp is obtained, these fibers have a diameter of 10 to 20 μm, which is the main reason for the high surface roughness of ordinary paper. An alternative approach to paper production is to first break cellulose fibers by high-pressure homogenization into their constituent fibrils, called micro- or nanofibrillated cellulose (MFC, NFC), cellulose nanofibers (CNF), cellulose nanocrystals (CNC), biocellulose (BC), or nanocellulose. They can then be compressed into thin sheets to produce cellulose nanopaper (Henriksson et al., 2008). SEM images of some of these nanopapers are shown in Fig. 28.2.

Due to the small diameter of the nanofibers or nanocrystals (from a few nanometers to several tens of nanometers), nanopaper is significantly smoother than regular paper. Naturally, all this leads to the fact that different types of paper have their own characteristic properties. Moreover, even paper of the same type but with different processing methods can have different properties and affect the performance of the developed devices differently (Ninwong et al., 2020). All this leads to the fact that to obtain the desired result, we must use different papers for different applications. All this creates certain difficulties when choosing the type of paper for research and determining its true properties, which can affect the results of experiments. Therefore, when selecting a paper, we must be guided by many factors, including

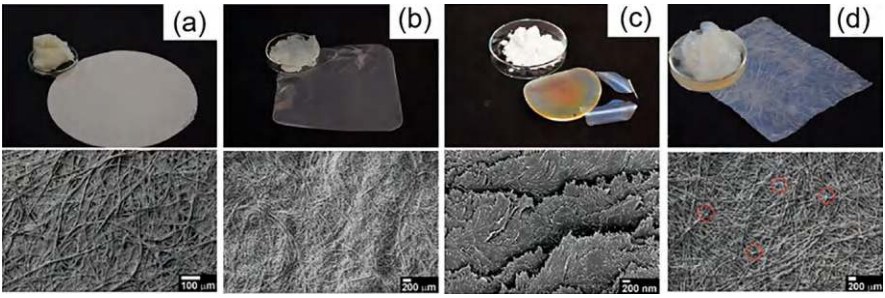

Fig. 28.2 Architecture and types of cellulose materials: (**a**) Photography image of raw paper pulp, paper, and corresponding SEM image. (**b**) Photography image of raw CNF, CNF substrate, and corresponding SEM image. (**c**) Photography image of raw CNC, CNC substrate, and corresponding SEM image. (**d**) Photography image of raw BC, BC substrate, and corresponding SEM image. (Reprinted with permission from Nandy et al. (2021). Copyright 2021: Wiley)

the type of sensor or device being developed, the manufacturing steps required to produce that device, the operating environment, the analytical requirements, and the application (Gomez et al., 2018; Lee et al., 2018; Li et al., 2010; Liana et al., 2012; Martinez et al., 2010; Nery & Kubota, 2013).

28.2 Sensor Applications

When developing sensors such as microfluidic sensors, the main requirement for substrates is the ability to absorb and control the flow of liquid, which is ensured by the high porosity of the material. In addition, the substrates must (a) have sufficient mechanical strength and physicochemical stability, (b) be non-reactive with the analyte, and have (c) a uniform surface and (d) long shelf life. For the manufacture of microfluidic paper-based analytical devices (μPADs), various types of paper can be used, such as filter paper, chromatography paper, glossy paper, bioactive paper, office paper, and nitrocellulose membrane paper, that have the necessary wicking ability (Fernandes et al., 2017). The properties of the paper, in addition to controlling the fluidic properties of the μPAD, make it possible to separate the analytes from the biological matrix and also give the electrodes 3D geometry (Desmet et al., 2016). The criterion for selecting a particular paper depends on the manufacturing method and the nature of the analytes that need to be tested. However, the most commonly used paper for this purpose is still filter paper (Whatman® cellulose series, Maidstone, UK), which is most suitable for the development of microfluidic sensors (Nie et al., 2010; Songjaroen et al., 2012). Filter paper, consisting of pure cellulose, contains only the impurities inherent in the fiber. The porosity of Whatman® filter paper, which allows control of flow rate and retention of specified particle sizes, makes the paper suitable for the manufacture of electrochemical devices capable of storing reagents, filtering a sample, allowing reactions to occur,

and delivering the detected product to the electrochemical testing area (Paschoalino et al., 2019). The porosity of filter paper depends on the materials and processing methods used. For example, to improve the uniformity of parameters, methods are used to promote uniform distribution of fibers in paper. And to improve the strength characteristics, synthetic fibers are introduced into the paper, and at the final stage, the paper can be impregnated with a polymer binder. Often, filter papers are functionalized with nanoparticles of active materials that penetrate and are retained in the microporous structure of cellulose paper (Fei et al., 2017).

Whatman® filter papers are widely used due to their wide selection of papers with the required porosity (pore size 11–25 μm) to control particle retention and flow rates (Ali et al., 2017; Desmet et al., 2016; Lehmann et al., 2013). The difference between grades of paper lies in the size and packaging of the cellulose fibers. Different grades of filter paper allow for different sampling and analysis settings. However, in experimental fabrication of microfluidic sensors, the most popular is Whatman No. 1 from General Electric Healthcare (Liana et al., 2012; Martinez et al., 2010; Pradela-Filho et al., 2023). This is pure paper made from pure cellulose. It has a smooth surface, backside clearance, flow rate, and a thickness of 0.18 mm, allowing it to be printed on commercial machines (Nery & Kubota, 2013). Filter papers are composed of 98% α-celluloses without any interventions such as strengthening or bleaching agents to reduce interference barriers (Bracher et al., 2009, 2010; Ngo et al., 2012). The purest is chromatography paper. Chromatography paper is made from pure cellulose obtained from the highest quality cotton, without strengthening or bleaching additives (Pradela-Filho et al., 2023).

Although Whatman® No. 1 filter paper is widely used, it does not always have the required physical properties, so other types of paper or methods of modifying it have been studied. In particular, it has been shown that other grades of chromatography, filter, and blotting papers can be used to achieve the desired volume and flow rate (Yao et al., 2022). For example, Li et al. (2010) used Whatman® No. 4 filter paper and coated it with a cellulose hydrophobizing agent as a base to engrave hydrophilic channels. The paper-based microfluidic device coupled with electrochemical detection showed higher analytical signals when using Whatman® No. 4 filter paper (25 μm) than when using Whatman® No. 1 filter paper (11 μm). This behavior was attributed to an increase in flow rate due to an increase in the pore size of the substrate, promoting improved mass transfer of the analyte to the electrode surface (Noviana et al., 2019). In addition, Li et al. (2010) believe that the use of Whatman® No. 4 filter paper, due to its larger pore size, reduces the effect of swelling of cellulose fibers on the penetration of capillary fluid into the pores. However, it must be kept in mind that high flow rates are not always beneficial depending on the application, since reactants previously deposited in the reaction zone can easily be washed out during experiments, which affects the sensitivity and repeatability of measurements (Lewińska et al., 2021). Paper towel also has properties similar to filter paper. Paper towel is less expensive than filter paper and has high porosity, making it a suitable material for the analysis of a wide range of analytes (Cinti et al., 2018; Martinez et al., 2010; Ostrov et al., 2017). Pradela-Filho et al. (2020a) also demonstrated the feasibility of using office paper as a substrate for the fabrication

of paper-based microfluidic devices. However, care should be taken when selecting this type of paper as additives may interact with the analyte and influence the measurement results (Noviana et al., 2020).

In other sensors, such as electrochemical sensors, the porosity and roughness of the substrate surface are also factors that control the sensor response. Thus, Pradela-Filho et al. (2020b) compared filter paper and office paper and found that electrochemical sensors made from filter paper had improved analytical response. This behavior was explained by the large pore size of this substrate. Dias et al. (2018) used five types of papers, such as filter paper, plant paper, office paper, photographic paper, and chromatography paper, to fabricate electrochemical sensors and found that plant paper provided the highest electrochemical performance for forensic applications. This fact was associated with better roughness and porosity of plant paper.

Nitrocellulose has also been used as a support material for the fabrication of μPADs (Tang et al., 2022). Nitrocellulose is a bioactive paper obtained by partial nitration of cellulose, which increases the porosity of cellulose and converts a hydrophilic material into a hydrophobic one due to the presence of nitro groups. Unlike traditional paper substrate, the surface properties of bioactive paper can be modified by modifying cellulose molecules with aldehyde and amide groups to enable them to absorb more biomolecules (Liana et al., 2012; Lu et al., 2011). For example, Tang et al. (2022) showed that nanocellulose binds proteins easily and with high efficiency. Nitrocellulose membranes are also used in DNA-RNA purification and enzyme immunoassays. Nitrocellulose has smaller pores than Whatman No. 1 paper. In addition, nitrocellulose membranes have a smooth surface and fairly uniform pore size, which allows for more consistent and repeatable fluid flow within the paper. This makes hydrophobic nitrocellulose suitable for the development of various biosensors. However, although the nitrocellulose membrane was smooth and uniform in pore size, making the fluid flow in the paper more stable and repeatable, the rate of wax percolation on the nitrocellulose membrane was slower than on the filter paper. Another problem with using nitrocellulose is that the paper is difficult to handle because it is brittle. It is also a highly flammable material and is expensive compared to paper. In addition, in an oxygen atmosphere, oxidation of nitro groups is observed (Valadares Romanholo et al., 2020). These disadvantages have significantly limited the use of this type of paper.

In cases where absorption is not a necessary requirement and the paper serves primarily as a flexible support for electrodes or biomolecules, commercially available office paper and glossy paper can also be used for sensor development. Both papers, composed of cellulose fibers and inorganic fillers, are flexible and durable. Normal office paper contains about 10% alkyl ketene dimer, which makes the paper slightly hydrophobic and has a small percentage of filler (Hu et al., 2010; Vesel et al., 2007). The structure of office and glossy paper can be used in various configurations. For example, due to its non-degradability and relatively smooth surface, glossy paper is a good substitute for filter paper, especially when it is necessary to modify nanomaterials on the surface rather than within the fibrous matrix. For example, Arena et al. (2010) used glossy paper to develop a flexible paper sensor for

ethanol detection using indium tin oxide nanoparticle powder as the sensing material and multi-walled carbon nanotubes as electrodes. In addition, due to the lower porosity of office and glossy paper, electrodes can be formed directly on the surface, without penetrating deep into the paper.

Moreover, it has been found that ordinary printing paper of A4 size is most widely used for the fabrication of flexible PB humidity sensors due to its good mechanical flexibility, rough and porous structure, good hydrophilicity, and easy availability (Tai et al., 2020). Santhiago et al. (2017) showed that office paper can also be used to develop wearable devices that should be foldable and flexible. Unlike office paper, chromatography filter paper is highly brittle when wet. The most important advantages of office paper are its availability, low price, and fairly smooth surface. But when choosing a method for characterizing functional materials used in devices fabricated on the basis of office paper, the presence of filler in it should be taken into account, since a strong carbonate signal can obscure the data obtained, for example, using X-ray diffraction analysis. Another area where the naturally rough surface of office paper is not a disadvantage but an advantage is pen-on-paper (PoP) technology. This surface is ideal for exfoliating graphite particles from the pencil to the pulp through mechanical abrasion, allowing the deposition of resistive graphite tracks on paper (Kurra & Kulkarni, 2013). Smooth substrates such as nanopaper and glossy paper are not compatible with pencil drawing.

In paper-based gas sensors, which use additional gas-sensitive materials applied to the surface of the paper, it would seem that there should not be such stringent requirements for the substrate as in the development of microfluidic sensors and biosensors, since the response of such sensors is controlled by the properties of the applied gas-sensitive material. But in fact, not everything is so simple. The properties of paper are very sensitive to air humidity (Korotcenkov, 2023, 2025) and therefore, optimally, the paper substrate for gas sensors should be isolated from interaction with air. This can be achieved by applying insulating coatings to its surface. But the presence of additional coatings reduces the adhesion of the gas-sensitive layer to the surface of the substrate, which reduces the possibility of using such sensors in bendable devices. Therefore, it is more optimal to use hydrophobic paper as a substrate, which, while maintaining the porosity and roughness necessary for good adhesion, does not interact with water vapor. Glavan et al. (2014) showed that hydrophobic paper can also be used as a substrate for electrochemical sensors. The use of hydrophobic paper in combination with nanomaterials has been found to improve the detection sensitivity of microfluidic devices (Guo et al., 2019).

As for humidity sensors, this is a more complex case, since humidity sensors can be either completely paper or sensors using additional humidity-sensitive materials. Therefore, the criteria for choosing paper as a substrate for these sensors will be different. In one case we must proceed as described above for gas sensors, and in the other, we must use porous paper, the size of the pores in which will control the sensory response. This problem is discussed in more detail in (Korotcenkov, 2023; Korotcenkov et al., 2023).

28.3 Printing Technology

If print quality is the primary consideration when using paper, then the following should be considered when selecting paper (Agate et al., 2018; Bollström & Toivakka, 2013; Hoeng et al., 2016; Ihalainen et al., 2012; Jansson et al., 2022; Kojić et al., 2019). When choosing paper, you must first take into account its porosity and roughness. Printed electronics require a smooth and non-porous substrate. It is these parameters that control the penetration of ink deep into the substrate and the likelihood of breaks in the conductive film formed on such a substrate (Bollstrom et al., 2014; Carvalho et al., 2019). Trnovec et al. (2009) compared the resistance of conductive layers formed on coated paper and PET film, and found that when the roughness of coated paper is approximately 150 times that of PET, the resistivity of the conductive film on coated paper increases by 50–1000 times. This is a significant difference that must be taken into account when designing electronic circuits on paper substrates. The effect of porosity or pore volume becomes less significant as the volume of ink used increases. This is due to the possibility of filling pores and increasing the thickness of the ink layer (Ihalainen et al., 2012).

But still, the simplest way to prepare porous and rough paper for printing is to apply coatings to its surface. For example, Trnovec et al. (2009) reduced the average surface roughness of backing paper to 0.26 μm through the use of special mineral pigment ($CaCO_3$ and kaolin) coatings and binders (e.g., polyurethane, polyvinyl alcohol (PVA), starch, latex). However, you need to keep in mind that such a coating layer, as mentioned earlier, can decrease the flexibility, bendability, and printability of paper substrate. However, Hoeng et al. (2017) showed that coating the paper surface with a thin film of nanoscale cellulose in the form of cellulose nanocrystals (CNC) also gives a large reduction in surface roughness, but without a significant effect on the flexibility of the substrates. For example, the surface roughness of cardboard after it was coated with TEMPO (2,2,6,6-Tetramethylpiperidine 1-oxyl) oxidized CNC decreased from 66 to 3.6 nm. True, here it is also necessary to take into account that a decrease in roughness, although it contributes to an increase in the conductivity of the film, reduces the ink anchoring on the paper. In particular, Dogome et al. (2013) observed that photo quality paper with a quartz coating and a surface roughness of 1.47 μm had lower ink retention compared to matte quality paper with a surface roughness of 4.31 μm. This means that a paper surface that is too smooth increases ink bleed to the side, which significantly reduces print resolution. The same effect results in thinner ink layers and hence poorer ink conductivity and adhesion (Torvinen et al., 2012). The paper coating, in addition to improving surface smoothness, also reduces pore size. This reduces the absorption and penetration of moisture into the paper and thereby helps reduce the swelling of fibers and improve the strength parameters of the paper. Meanwhile, it should be recognized that the fibrous and porous structure of paper, in addition to better adhesion, can also effectively promote faster drying of ink compared to non-absorbent or poorly absorbent substrates.

Correctly selected paper surface treatment can also control the surface energy and absorption capacity of the paper (Angelo et al., 2012). For example, Dogome et al. (2013) showed that reducing the surface energy and capillary absorption of paper by treating it with a fluorinated polymer is an effective way to produce thinner prints (about 60 μm when using inkjet inks). This is achieved by preventing ink from flowing sideways. After applying this barrier coating, the cellulose substrate also becomes resistant to changes in humidity and increases dimensional stability.

Calendering is another well-established paper modification method that has been shown to reduce surface roughness (Hrehorova et al., 2005). Supercalendering is a method in which traditionally made paper is flattened at the end of the papermaking process by passing it through stacks of hard and soft cylindrical rolls. Supercalendered paper is called glassine and is often used as a release paper to protect art or delicate items from contact with other materials. Hyun et al. (2015) showed that using supercalendering, even untreated glassine paper substrates can be used to fabricate fully in-plane printed foldable organic electrolytic gate transistors (EGTs). Calendering also reduces the paper's ability to absorb moisture (Torvinen et al., 2012).

28.4 Nanocellulose and Its Applications

When developing electronic devices such as field-effect transistors and electronic circuits, filter paper and similar materials are not used. For these applications, the substrate must be denser with less porosity and minimal roughness (Pereira et al., 2014). It is important to note that the development of inorganic thin-film transistors requires smoother surfaces than the development of organic transistors (Zschieschang & Klauk, 2019). The experiment showed that nanopaper or nanofibrillated cellulose (NFC) most fully satisfies the above requirements (González et al., 2014). Some parameters of nanopaper in comparison with regular paper and plastic are given in Table 28.1.

Table 28.1 Comparison of nanopaper, traditional paper, and plastic

Characteristics	Nanopaper	Traditional paper	Plastic
Surface roughness (nm)	5	5000–10,000	5
Porosity (%)	20–40	50	0
Pore size (nm)	10–50	3000	0
Optical transparency at 550 nm (%)	90	20	90
Max loading stress (MPa)	200–400	6	50
Coefficient of thermal expansion (ppm K^{-1})	12–28.5	28–40	20–100
Printability	Good	Excellent	Poor
Young modulus (GPa)	7.4–14	0.5	2–2.7
Bending radius (mm)	1	1	5
Renewable	High	High	Low

Source: Reprinted with permission from Zhu et al. (2014). Copyright 2014: RSC

Unlike microfibrillated cellulose (MFC), nanofibrillated cellulose (NFC) consists only of nano-sized structures. These fibrils have a high aspect ratio; the diameter is only 20–40 nm, while the length can be up to several microns (Siró & Plackett, 2010). A paper substrate consisting of nanocellulose, like regular paper, is flexible and lightweight, which meets the basic requirements for substrates for flexible electronics. The density of a typical nanocellulose paper is about 1.53 g/cm^3 and can even be folded like a paper airplane (Nogi et al., 2009). As a result of the studies, it was found that the roughness of nanopaper allows printing conductive tracks with better print quality and lower resistance, in comparison with similar tracks formed on classical paper and plastic substrates (Fujisaki et al., 2014). For example, Hsieh et al. (2013) found that the printed line resistance on an NFC substrate was 180 times lower than that on traditional paper. Nanopaper, mainly made from densely packed renewable natural 1D and 2D nanomaterials, was found to not only have many of the advantages of conventional paper, but also overcome many of its disadvantages, offering much higher transparency, better chemical and thermal properties, better mechanical stability, much lower thermal expansion, and lower surface roughness (Golmohammadi et al., 2017; Zhu et al., 2013b).

The low surface roughness and flexibility of CNF substrates have been exploited to create flexible thin-film transistors (TFTs). A transistor is an important semiconductor device that is used to amplify and convert electronic signals or electrical energy. The first organic field-effect transistors fabricated on paper were reported by Eder et al. (2004). Commercially available hot-pressed cotton fiber paper was chosen as the substrate, and its surface was sealed with a layer of polyvinylphenol (PVP) several hundred nanometers thick before TFT fabrication. Fujisaki et al. (2014) also used CNF substrates to fabricate an organic thin-film transistor (OTFT). They demonstrated improved transistor performance by using low-roughness nanopapers. The first paper-based inorganic transistor was reported by Fortunato et al. (2008). Semiconductor oxide-based thin-film field-effect transistors (FETs) were built on both sides of a cellulose sheet, which was also used as a dielectric layer.

Nanofibrillated cellulose is also a good substrate for the fabrication of paper-based antennas (Nogi et al., 2013). In the fabrication of a V-shaped printed antenna based on Ag ink, the use of nanopaper as a substrate instead of cellulose paper and pressed cellulose paper resulted in a significant reduction in return loss at the resonant points. The paper-based antenna for transmitting and receiving signals is an important component of radio frequency identification (RFID) devices.

In addition, nanopaper retains its structure better in an aqueous environment compared to conventional paper. This makes nanopaper an excellent platform for the fabrication of various high-performance chemical and gas sensors, such as humidity sensors and biosensors (Naghdi et al., 2020). In particular, the potential application of nanopapers in sensors for detecting humidity was reported by Li et al. (2014). Giese et al. (2014) found that their developed cellulose nanopaper undergoes rapid and reversible color changes upon swelling, indicating the potential application of such paper in optical humidity sensors.

Good mechanical properties are another advantage of nanopaper substrates (Li et al., 2022). Nanocellulose paper consists of many interwoven layers of

nanocellulose fibers (Henriksson et al., 2008). Such a structure reduces the stresses that arise during tension or compression. Moreover, intermolecular forces such as hydrogen bonding and cross-linking between nanocellulose fibers provide high mechanical strength, which is 10 times better than that of conventional paper (Zhu et al. 2013b).

Another reason for the improved mechanical properties of nanopaper is its lower porosity. The mechanical strength of nanocellulose paper has been shown to decrease with increasing porosity (Henriksson et al., 2008). The mechanical strength of nanocellulose paper with 19% porosity is about 205 MPa, which is sufficient for an electronic substrate and can be compared with a polymer substrate such as PET (Henriksson et al., 2008). These properties of nanopaper make it very promising for the development of various physical sensors and actuators. For example, Gao et al. (2016) showed that a nanopaper-based energy harvester can reach a maximum power of ~84.4 μW and can be stable after continuous operation for 54,000 cycles. In addition, the fiber mesh structure gives nanopaper excellent flexibility and can be bent to form three-dimensional (3D) structures for paper origami.

But when choosing a substrate, it is necessary to take into account that the properties of nanopaper depend to one degree or another on its manufacturing technology. In particular, Chinga-Carrasco et al. (2012) compared the influence of the properties of three types of CNF films produced by casting and evaporation on the parameters of conductive paths formed by inkjet printing. These CNF films were (i) untreated CNF, (ii) carboxymethylated CNF, and (iii) TEMPO CNF. It was found that the higher porosity of untreated CNF compared to the porosity of TEMPO-CNF caused staining of the untreated CNF substrate and the formation of lateral track erosion. However, despite this, lines printed on TEMPO CNF films exhibited greater surface ink flow due to the high surface energy. In addition, the TEMPO-CNF film was also brittle in nature, limiting its use as a flexible substrate.

To reduce the surface energy and obtain a more flexible film, Chinga-Carrasco et al. (2012) proposed treating CNF with hexamethyldisilazane (HMDS). In the case of using carboxymethylated CNF, both good print resolution and high conductivity of conductive tracks with good substrate flexibility were obtained. These properties of nanopaper also provide manufactured electronic devices with better mechanical and thermal properties, which are necessary for the development of flexible electronics. In addition, Hsieh et al. (2013) note that nanopaper can withstand high sintering temperatures. They reported that the nanocellulose paper remained stable even after storage at 200 °C for 30 min. Under the same heat treatment conditions, the photo paper was damaged.

It should also be kept in mind that nanopaper is not without its drawbacks. As for the disadvantages of cellulose nanopaper, they usually include the following (Oksman et al., 2014): (i) poor retention in fibrous materials; (ii) negative effect on paper drainage and drying, (iii) increased susceptibility to tear, (iv) high energy consumption during production (Siró & Plackett, 2010), and (v) high cost in comparison with conventional glass and plastic substrates. This, despite the transparency, flexibility, and improved mechanical and thermal properties, significantly limits the widespread use of substrates based on nanocellulose microfibers (CNF)

and cellulose nanocrystals (CNC) for the development of cheap flexible sensors and devices. That is why, when developing field-effect transistors, photographic paper is often used as substrates, which ensures that the surface remains smooth after additional processing (Kim et al., 2004, 2005). Several examples of organic transistors fabricated on a paper-cellulose substrate are listed in Table 28.2. For example, TFTs with the highest carrier mobility published to date for organic transistors on paper ($\mu \sim 2.5$ cm^2/V·s) were fabricated on a commercially available photo paper (for inkjet printing) coated with a 3-μm-thick layer of parylene (Minari et al., 2014a). But it is hoped that as nanopaper manufacturing technology is optimized, its price will be significantly reduced, which will open up its wider application in the development of various devices (Hoeng et al., 2016).

Optoelectronics and photonics require a different type of substrate (Vicente et al., 2017). When fabricating light-emitting diodes (LEDs), transparent electrodes, displays, and solar cells, substrates must first be transparent and, in some cases, additionally conductive. The surface roughness of the substrate also plays an important role in these applications (Li et al., 2014; Zhou et al., 2014). Surface roughness should be minimal. Plain paper such as office paper or filter paper does not meet these requirements. For example, Rawat et al. (2019) tested four types of paper (copier, glossy, art gumming, and BILT) to select substrates for solar cells. They found that the best candidate among the paper types tested for these applications was glossy paper with a roughness of 150 nm.

However, even this roughness was not suitable for the manufacture of solar cells with the required parameters. To achieve the required parameters of solar cells and reduce the risk of cracks in the interface layers of the device, the surface roughness of the paper substrate must be further reduced. For example, in (Ihalainen et al., 2012; Kim et al., 2009), commercial raw paper was modified using several binders, pigment mixtures, and calendering processes before fabricating the device to achieve the desired result. The final modified paper had a smooth surface and an average pore size of 30 nm. Rawat et al. (2019) used smoothing layers of glue, polyvinyl acetate (PVAc), polyvinyl alcohol (PVA), and polyvinylformal (PVF) to reduce roughness. Optimal results were obtained using glossy PVF-coated paper, which had the lowest roughness of 2.6 nm.

As we indicated earlier, substrates based on nanopaper and its derivatives have high-quality surfaces without additional surface modification (Okahisa et al., 2009; Wu et al., 2015). In addition, nanopaper, unlike conventional paper, is highly transparent (Zhu et al., 2014). Paper transparency is affected by surface morphology, porosity, thickness, filler properties, and diameter of cellulose fibers. In nanocellulose paper, the surface morphology is relatively smooth and the porosity is low due to the small diameter of nanocellulose (at the nanometer scale). Therefore, light scattering inside nanocellulose paper, which does not contain fillers, is reduced and light can pass directly through it, giving it high transparency (Hu et al., 2013). For example, the transparency of nanocellulose paper reported by Zhu et al. (2013a) can reach 92–93% (see Fig. 28.3a). It is these features of nanopaper that have led to the fact that the best results in the development of optoelectronic and photoelectric devices were obtained when using it (Jin et al., 2016; Seo et al., 2015; Tao et al.,

Table 28.2 A list of organic transistors that have been fabricated on paper/cellulose substrates. The types of paper, semiconductor material, gate dielectric layer, and electrode (gate, drain, and source) materials, with on/off current ratio (I_{on}/I_{off}), field effect mobility (μ_{sat}), are provided for comparison

Type of paper	Semiconductor	Gate dielectric	I_{on}/I_{off}	Mobility [$cm^2/V{\cdot}s$]	References
PowerCoat HD 230 paper	TIPS-pentacene:PS (*p*-type)	HfO_2/PVP	10^5	0.44	Raghuwanshi et al. (2019)
Regular paper	Pentacene	Gelatin/ Gelatin:Fe	10^3	8	Lee et al. (2019)
Paper	DPh-BTBT	AlO_x	10^6	0.4	Zschieschang et al. (2017)
		N1100	4×10^5	0.2	
Paper	PTAA	Epoxy nanosilica	3×10^2	0.087	Mitra et al. (2017)
PVA:PVP buffer layer PowerCoat HD 230 paper	TIPS-Pentacene: PTAA	CYTOP/Al_2O_3/ Nanolaminate	10^5	1.7	Wang et al. (2017)
Glassine paper	P3HT	Triblock co-polymer	10^3	0.0096	Hyun et al. (2015)
Cellulose paper	DNTT	Parylene-	10^9	0.56	Peng et al. (2015)
CNC–glycerol	TIPS-Pentacene: PTAA	CYTOP/Al_2O_3	10^4	0.17	Wang et al. (2015b)
Photopaper	C8 -BTBT	CYTOP	10^6	2.5	Minari et al. (2014b)
Fuji Xerox printing paper	DNTT	Parylene	10^5	0.3	Peng and Chan (2014)
Photopaper	Pentacene	Parylene C	10^5	0.1	Zocco et al. (2014)
Transparent paper	OSC	Fluoropolymer	10^6–10^8	1.3	Fujisaki et al. (2014)
Parylene-coated paper	C8-BTBT:PMMA	CYTOP	10^8	1.3	Li et al. (2012)
Bank note	DNTT	AlO_x	10^5	0.2	Zschieschang et al. (2011)
Multilayer coated paper	P3HT	PVP	N/A	N/A	Bollstrom et al. (2009)
Parylene-coated paper	P3HT	PI/SiO_2	10^4	0.08	Kim et al. (2004)
PVP-coated paper	Pentacene	PVP	10^5	0.2	Eder et al. (2004)

Source: Reprinted with permission from Nandy et al. (2021). Copyright 2021: Wiley
CYTOR amorphous fluoropolymers, *DNTT* dinaphtho[2,3-b:2′,3′-f]thieno[3,2-b]thiophene, *DPh-BTBT* thienothiophene-fused compound, *HD* high density, *OSC* organic semiconductor, *P3HT* poly(3-hexylthiophene), *PI* polyimide, *PMMA* poly Methyl Methacrylate, *PS* polystyrene, *PTAA* poly(triaryl amine), *PVA* poly(vinyl alcohol), *PVP* polyvinylpyrrolidone, *TIPS* 6,13-bis(triisopropylsilylethynyl)

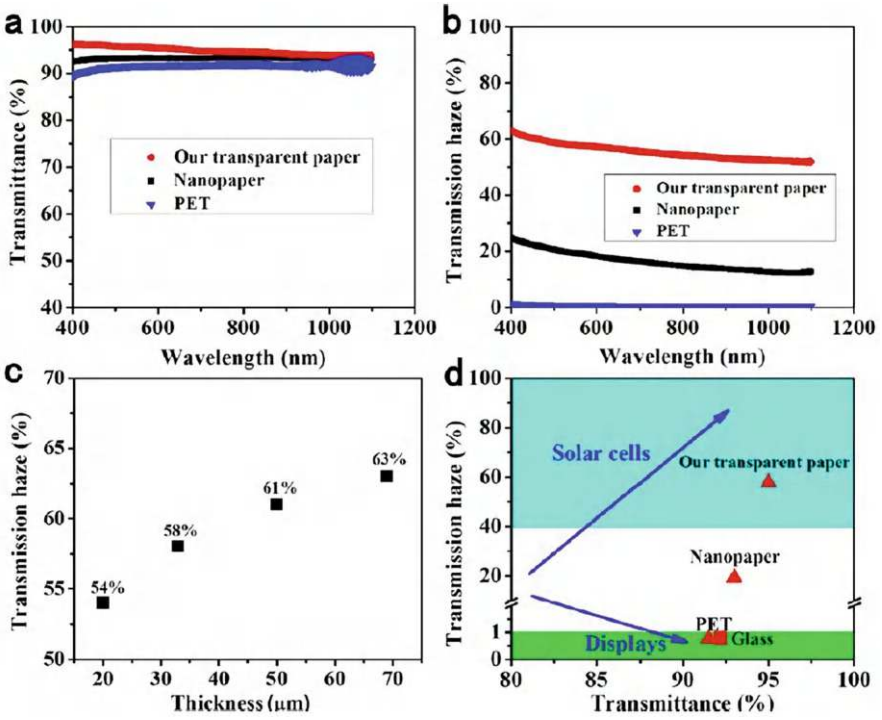

Fig. 28.3 Optical properties of our transparent paper, nanopaper, and PET. (**a**) The total optical transmittance versus wavelength measured with an integrating sphere setup. (**b**) The transmission haze versus wavelength. (**c**) The transmission haze of transparent paper with varying thicknesses at 550 nm. (**d**) Optical transmission haze versus transmittance for different substrates at 550 nm. Glass and PET are in the green area, which is suitable for displays due to their low haze and high transparency; transparent paper developed in this work, located in the cyan area, is the most suitable for solar cells. (Reprinted with permission from Fang et al. (2014)**.** Copyright 2014: ACS)

2020). For example, Nogi et al. (2013) reported a transparent conductive paper based on cellulose nanofibers and silver nanowires that has performance comparable to ITO glass. Solar cells made from transparent conductive nanocellulose paper had a power conversion efficiency of ~3.2%.

Experiments and simulations have shown that in order to fabricate some optoelectronic elements with increased efficiency, in addition to the highest possible transparency (Siro et al., 2011; Zhu et al., 2013a), the optimal substrate should also have high optical haze (Fang et al., 2014). Optical haze quantifies the percentage of transmitted light that is scattered diffusely, which is preferable in solar cell applications (Berginski et al., 2007; Chiba et al., 2006). Haze is defined as the percentage of light transmitted through a sample that deflects the incident light beam by an average angle greater than 2.5° (ASTM, 2000). Optical transparency and haze in various works are inversely proportional. For example, tracing paper has a high optical haze of more than 50% but a transparency of less than 80%, while some

plastics have a transparency of about 90% but an optical haze of less than 1% (MacDonald et al., 2007). Figure 28.3d shows the optical haze region that is optimal for solar cells. As can be seen, standard NFC-based nanopaper with high transparency (90%) has an optical haze of about 20% (Zhu et al. 2013a). But even such substrates are good for developing displays and touch screens. These optoelectronic devices require high transparency and relatively high optical haze (Hecht et al., 2009; MacDonald et al., 2007). High optical haze is necessary to eliminate strong light reflection when exposed to sunlight (Zhu et al., 2014).

Various materials, such as SiO_2 nanoparticles or silver nanowires, have been reported to effectively increase light absorption and consequently short-circuit current in solar cells by improving light transmission through the active solar layer with increasing diffuse light scattering (Chung et al., 2012; Jeong et al., 2010; Kang et al., 2013). However, the light scattering caused by these nanostructures is limited, and the incorporation of these materials requires additional steps that increase the cost of solar-powered devices. Fang et al. (2014) found that there is a simpler method for optimizing solar cell substrates. According to the proposed protocol, wood fibers were treated using the TEMPO/NaBr/NaClO oxidation system to introduce carboxyl groups into cellulose. This process weakens the hydrogen bonds between cellulose fibrils and causes the wood fibers to swell and break, resulting in high packing densities and excellent optical properties. The new transparent paper based on wood fibers had ultra-high optical transparency (~96%) and at the same time ultra-high optical haze (~60%) (see Fig. 28.3d). Thus, the proposed nanopaper substrates can scatter light (unlike plastic substrates) while remaining transparent (unlike traditional paper). Fang et al. (2014) believe that their transparent paper has the following advantages over previously reported wood-based nanofibrillated cellulose (NFC) transparent nanopaper: (1) it exhibits dramatic dual improvements in optical transmittance and optical haze and (2) is formed through much less energy-intensive processes that allow the creation of inexpensive paper devices. These optical properties of the developed nanopaper enable a simple light control strategy to improve the performance of solar cells. The experiment showed that by using the developed transparent paper, the power conversion efficiency (PCE) of the organic solar cell increased from 5.34% to 5.88%. According to Fang et al. (2014), such low-cost, highly transparent and hazy paper can also be used as an excellent film to improve light-trapping properties in photovoltaic applications such as solar roofs or solar windows.

To achieve high haze, Jia et al. (2017) proposed another approach to making transparent paper. An anisotropic paper material with high transmittance (~90%) and high haze (~90%) was produced using a simple but effective method based on direct shear pressing of delignified wood material (see Fig. 28.4). Anisotropic transparent paper has demonstrated high efficiency as a light-control coating layer for GaAs solar cells. Thanks to its excellent light control capabilities, i.e., high transparency and high turbidity, it was possible to increase the efficiency of these solar cells by 14% (Fig. 28.4c). The proposed method is simple, scalable, cost-effective, and green.

The experiment showed that transparent substrates are also ideal substrates for the development of various low-cost and highly sensitive chemical sensing

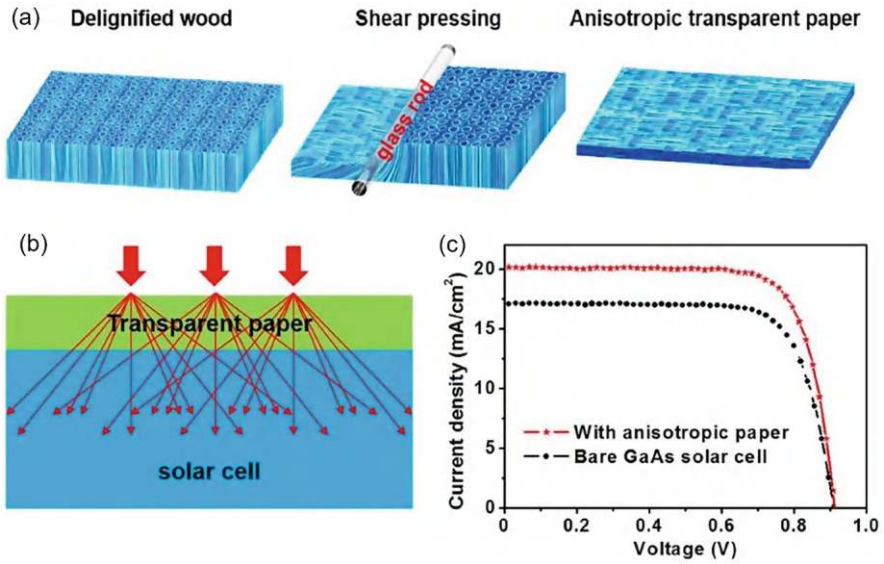

Fig. 28.4 (**a**) Graphical illustration of the design concept and "top-down" fabrication process for the anisotropic transparent paper directly from natural wood. (**b**) Schematic of the incident light distribution on solar cell. (**c**) Current density-voltage curves of GaAs solar cells without and with anisotropic transparent paper coating layer. (Reprinted with permission from Jia et al. (2017). Copyright 2017: Elsevier)

platforms (Yao et al., 2022), such as optical sensors for the detection of multi-target analytes (i) by changes in absorbance/transmittance, (ii) by changing the wavelength of the optical signal (Zong et al., 2019), or (iii) based on surface-enhanced Raman scattering (SERS) (Ying et al., 2020). Dinesh and Kandasubramanian (2022) believe that transparent paper can replace traditional paper or even plastic substrates in green sensing devices. Transparent paper with optical properties that can be adjusted from optical clarity to optical haze is also useful for flexible organic light-emitting diodes (OLEDs) for various applications (Zhu et al., 2014).

28.5 Energy Technologies

The development of supercapacitors, batteries, and fuel cells does not place such stringent demands on paper, and therefore, their production can use a wide variety of papers, from xerox paper and printing paper (the most used) to biocellulose (BC) paper and filter paper. The main criteria for their use, for example in the manufacture of lithium-ion batteries, are (i) high levels of surface roughness and porosity, which enhance power generation, and (ii) mechanical flexibility due to their very dense interwoven structures. Cellulose/nanocellulose/BC with its highly porous structure and high surface area serves as an ideal substrate for loading increased

amounts of conductive fillers, such as conductive polymers, metal nanoparticles, oxide nanoparticles, CNTs, and graphene, to provide the required conductivity of the electrode (Liu et al., 2016; Weng et al., 2011). Incorporation of CNTs or graphene into cellulose networks also leads to improved mechanical properties of the paper-based electrode.

The microporous structure of paper substrates (such as chromatography paper, filter paper, etc.) also helps to absorb fuel into fuel cells without the use of any external pumping devices due to the capillary effect for the fuel and oxidizer within the paper (Esquivel et al., 2014). How successful the use of paper can be in the production of energy by indicated devices can be judged from the results presented in (Hashemi et al., 2016; Shen et al., 2019; Song et al., 2014). For example, Song et al. (2014) demonstrated an origami paper-based lithium-ion battery that maintained its exceptional performance even under several mechanical deformations such as folding, bending, and twisting. They used CNT-coated paper as a basis for making current collectors, anodes and cathodes. However, the most commonly used filter paper in biofuel cells is Whatman No. 1 (Desmet et al., 2016).

It is important to note that despite the high cost of nanocellulose, it is often used in the development of devices for energy technologies. How effective the use of nanocellulose can be can be judged from the results presented by Wang et al. (2015a). Supercapacitors with surface-modified nanocellulose fiber (NCF) electrodes had the highest total electrode-normalized gravimetric capacitance to date of ~127 F/g at high current densities (33 A/g).

In addition to the above examples, unusual paper substrates such as carbon fiber paper (CFP) and various paper hybrids can also be found in paper-based energy devices such as lithium-ion batteries, fuel cells, and supercapacitors (Liu et al., 2017). Carbon fiber paper is a composite paper made up of carbon fibers and polymeric carbon. Its production process begins with polymerization and carbon fiber formation, followed by carbonization, papermaking, resin impregnation, molding, and a final heat treatment step (Mathias et al., 2010). CFP has been primarily used as a conductive electrode material due to its exceptional conductivity, high chemical stability, and good mechanical properties. In addition, the intact porous network allows CFP to serve as an electrode/electrolyte interlayer for lithium-ion batteries and fuel cells, providing pathways for ions and electrons and trapping dissolved electrolyte materials without limiting charge transport (Su & Manthiram, 2012). However, CFP has disadvantages such as low electrochemical activity (Wang et al., 2016), which may limit its application.

28.6 Summary

It is clear that in this chapter we could not consider in detail the possibilities of using all types of paper and evaluate the criteria for their use in various devices. But it is important to note that almost all types of paper with one method or another have been tested during the development of various sensors and devices. For example,

glossy paper (hydrophobic) has proven to be a good substrate for colorimetric tests. Paper towels and tissue paper (characterized by high absorption capacity, rough surface and permeability, but poor mechanical stability) impregnated with ferrofluid are suitable for the manufacture of magnetic actuators (Ding et al., 2011), and in various sensors for detection and sampling vapor of the analyte (Xu et al., 2011). Newsprint, similar to the above examples but with significant amounts of impurities, is used for magnetic actuators and electronics (Lamprecht et al., 2005), and cardboard is used as an inexpensive biodegradable substrate when other paper characteristics are less important (de Araujo et al., 2017). Metallized paper is traditionally used as a packaging material. But Mazzeo et al. (2012) found that this paper can also be used to make capacitive touch panels. Sun et al. (2013) and Wang et al. (2012) showed that due to excellent electron transfer performance and mechanical strength, graphene paper (mainly rGO paper) doped with silver nanowires has great potential for application as anodes or cathodes in energy storage devices. Meanwhile, unreduced GO paper after functionalization has been used in biomedical applications. The abundant presence of functional groups such as carbonyl, hydroxyl, and epoxy groups in GO (Li et al., 2013; Xiao et al., 2013) is of extreme value for electrochemical detection of physiological signatures.

For additional information regarding paper selection for various applications, please refer to published reviews. In particular, Liu et al. (2017) summarized various types of paper substrates and methods for manufacturing electronic devices based on them. Hoeng et al., 2016) reviewed the use of paper in printing electronics. Usta and Facchetti (2022) analyzed paper-based (opto)electronic devices. Korotcenkov (2023) and Korotcenkov et al. (2023) examined the features of using paper in the development of humidity sensors. Valadares Romanholo et al. (2020) discussed the possibility of using paper as a substrate for electrochemical microdevices. Barhoum et al. (2017) and Naghdi et al. (2020) considered flexible and multifunctional nanopapers and analyzed their possible applications. Morales-Narváez et al. (2015) discussed nanopaper as an optical sensing platform. Zhang et al. (2018) examined the potential of using micro/nanostructured paper as substrates for flexible electronics. Korotcenkov (2025) analyzed the advantages and disadvantages of paper for sensor applications. Mahadeva et al. (2015) considered paper as a platform for energy and sensing applications. Desmet et al. (2016) reviewed paper electrodes for biosensors and biofuels. Golmohammadi et al. (2017), Liana et al. (2012), and Nery and Kubota (2013) considered the use of paper substrates in sensors and biosensors.

Acknowledgments G.K. is grateful to the Moldova State University (research program no. 011208) for supporting his research.

References

Abitbol, T., Rivkin, A., Cao, Y., Nevo, Y., Abraham, E., Ben-Shalom, T., et al. (2016). Nanocellulose, a tiny fiber with huge applications. *Current Opinion in Biotechnology, 39*(I), 76–88. https://doi.org/10.1016/j.copbio.2016.01.002

Agate, S., Joyce, M., Lucia, L., & Pal, L. (2018). Cellulose and nanocellulose-based flexible-hybrid printed electronics and conductive composites –A review. *Carbohydrate Polymers, 198*, 249–260. https://doi.org/10.1016/j.carbpol.2018.06.045

Ali, M. M., Brown, C. L., Jahanshahi-Anbuhi, S., Kannan, B., Li, Y., Filipe, C. D. M., & Brennan, J. D. (2017). A printed multicomponent paper sensor for bacterial detection. *Scientific Reports, 7*, 12335. https://doi.org/10.1038/s41598-017-12549-3

Angelo, P. D., Cole, G. B., Sodhi, R. N., & Farnood, R. R. (2012). Conductivity of inkjet-printed PEDOT:PSS-SWCNTs on uncoated papers. *Nordic Pulp & Paper Research Journal, 27*(2), 486–495.

Arena, A., Donato, N., Saitta, G., Bonavita, A., Rizzo, G., & Neri, G. (2010). Flexible ethanol sensors on glossy paper substrates operating at room temperature. *Sensors and Actuators B: Chemical, 145*, 488–494. https://doi.org/10.1016/j.snb.2009.12.053

ASTM. (2000). Standard test method for haze and luminous transmittance of transparent plastics-D0003-00, 2000 (Vol. 06).

Barhoum, A., Samyn, P., Ohlund, T., & Dufresne, A. (2017). Review of recent research on flexible multifunctional nanopapers. *Nanoscale, 9*(40), 15181–15205. https://doi.org/10.1039/C7NR04656A

Bauch, A. (1992). Pigments and fillers. In K. J. Hipolit (Ed.), *Chemical processing aids in papermaking: Practical guide* (pp. 93–101). Tappi Press.

Berginski, M., Hupkes, J., Schulte, M., Schope, G., Stiebig, H., Rech, B., & Wuttig, M. (2007). The effect of front ZnO: Al surface texture and optical transparency on efficient light trapping in silicon thin-film solar cells. *Journal of Applied Physics, 101*(7), 074903. https://doi.org/10.1063/1.2715554

Bollström, R., & Toivakka, M. (2013). Paper substrate for printed functionality. In S. J. I'Anson (Ed.), *Advances in pulp and paper research, Cambridge, Trans. of the XVth Fund. Res. Symp. Cambridge, 2013* (pp. 945–966). https://doi.org/10.15376/frc.2013.2.945

Bollstrom, R., Maattanen, A., Tobjork, D., Ihalainen, P., Kaihovirta, N., Osterbacka, R., et al. (2009). A multilayer coated fiber-based substrate suitable for printed functionality. *Organic Electronics, 10*, 1020–1023. https://doi.org/10.1016/j.orgel.2009.04.014

Bollstrom, R., Pettersson, F., Dolietis, P., Preston, J., Osterbacka, R., & Toivakka, M. (2014). Impact of humidity on functionality of on-paper printed electronics. *Nanotechnology, 25*(9), 094003. https://doi.org/10.1088/0957-4484/25/9/094003

Bown, R. (1998). Particle size, shape and structure of paper fillers and their effect on paper properties. *Paper Technology, 39*(2), 44–48.

Bracher, P. J., Gupta, M., & Whitesides, G. M. (2009). Shaped films of ionotropic hydrogels fabricated using templates of patterned paper. *Advanced Materials, 21*, 445–450. https://doi.org/10.1002/adma.200801186

Bracher, P. J., Gupta, M., & Whitesides, G. M. (2010). Patterned paper as a template for the delivery of reactants in the fabrication of planar materials. *Soft Matter, 6*, 4303–4309. https://doi.org/10.1039/C0SM00031K

Carvalho, J., Dubceac, V., Grey, P., Cunha, I., Fortunato, E., Martins, R., et al. (2019). Fully printed zinc oxide electrolyte-gated transistors on paper. *Nanomaterials, 9*, 169. https://doi.org/10.3390/nano9020169

Chiba, Y., Islam, A., Watanabe, Y., Komiya, R., Koide, N., & Han, L. (2006). Dye-sensitized solar cells with conversion efficiency of 11.1%. *Japanese Journal of Applied Physics Part 2, 45*(24/28), L638. https://doi.org/10.1143/JJAP.45.L638

Chinga-Carrasco, G., Tobjörk, D., & Österbacka, R. (2012). Inkjet-printed silver nanoparticles on nano-engineered cellulose films for electrically conducting structures and organic transistors: Concept and challenges. *Journal of Nanoparticle Research, 14*, 1213. https://doi.org/10.1007/s11051-012-1213-x

Chung, C. H., Song, T. B., Bob, B., Zhu, R., Duan, H. S., & Yang, Y. (2012). Silver nanowire composite window layers for fully solution-deposited thin-film photovoltaic devices. *Advanced Materials, 24*(40), 5499–5504. https://doi.org/10.1002/adma.201201010

Cinti, S., Colozza, N., Cacciotti, I., Moscone, D., Polomoshnov, M., Sowade, E., Baumann, R. R., & Arduini, F. (2018). Electroanalysis moves towards paper-based printed electronics: Carbon black nanomodified inkjet-printed sensor for ascorbic acid detection as a case study. *Sensors and Actuators B: Chemical, 265*, 155–160. https://doi.org/10.1016/j.snb.2018.03.006

Davidson, R. (1965). Experiments on loading paper with low refractive index fillers. *Paper Technology, 6*(2), 107–114.

de Araujo, W. R., Frasson, C. M. R., Ameku, W. A., Silva, J. R., Angnes, L., & Paixao, T. (2017). Single-step reagentless laser scribing fabrication of electrochemical paper-based analytical devices. *Angewandte Chemie (International Ed. in English), 56*, 15113–15117. https://doi.org/10.1002/anie.201708527

Desmet, C., Marquette, C. A., Blum, L. J., & Doumèche, B. (2016). Paper electrodes for bioelectrochemistry: Biosensors and biofuel cells. *Biosensors & Bioelectronics, 76*, 145–163. https://doi.org/10.1016/j.bios.2015.06.052

Dias, A. A., Cardoso, T. M. G., Chagas, C. L. S., Oliveira, V. X. G., Munoz, R. A. A., Henry, C. S., et al. (2018). Detection of analgesics and sedation drugs in whiskey using electrochemical paper-based analytical devices. *Electroanalysis, 30*, 2250–2257. https://doi.org/10.1002/elan.201800308

Dinesh, G., & Kandasubramanian, B. (2022). Fabrication of transparent paper devices from nanocellulose fiber. *Materials Chemistry and Physics, 281*, 125707. https://doi.org/10.1016/j.matchemphys.2022.125707

Ding, Z., Wei, P., Chitnis, G., & Ziaie, B. (2011). Ferrofluid-impregnated paper actuators. *Journal of Microelectromechanical Systems, 20*, 59–64. https://doi.org/10.1109/JMEMS.2010.2100026

Dogome, K., Enomae, T., & Isogai, A. (2013). Method for controlling surface energies of paper substrates to create paper-based printed electronics. *Chemical Engineering and Processing: Process Intensification, 68*, 21–25. https://doi.org/10.1016/j.cep.2013.01.003

Eder, F., Klauk, H., Halik, M., Zschieschang, U., Schmid, G., & Dehm, C. (2004). Organic electronics on paper. *Applied Physics Letters, 84*, 2673–2675. https://doi.org/10.1063/1.1690870

Esquivel, J. P., Del Campo, F. J., Gomez de la Fuente, J. L., Rojas, S., & Sabate, N. (2014). Microfluidic fuel cells on paper: Meeting the power needs of next generation lateral flow devices. *Energy & Environmental Science, 7*, 1744–1749. https://doi.org/10.1039/C3EE44044C

Fang, Z., Zhu, H., Yuan, Y., Ha, D., Zhu, S., Preston, C., et al. (2014). Novel nanostructured paper with ultrahigh transparency and ultrahigh haze for solar cells. *Nano Letters, 14*(2), 765–773. https://doi.org/10.1021/nl404101p

Fei, H., Saha, N., Kazantseva, N., Moucka, R., Cheng, Q., & Saha, P. (2017). A highly flexible supercapacitor based on MnO_2/RGO nanosheets and bacterial cellulose-filled gel electrolyte. *Materials, 10*, 1251. https://doi.org/10.3390/ma10111251

Fernandes, S. C., Walz, J. A., Wilson, D. J., Brooks, J. C., & Mace, C. R. (2017). Beyond wicking: Expanding the role of patterned paper as the foundation for an analytical platform. *Analytical Chemistry, 89*, 5654–5664. https://doi.org/10.1021/acs.analchem.6b03860

Fortunato, E., Correia, N., Barquinha, P., Pereira, L., Goncalves, G., & Martins, R. (2008). High-performance flexible hybrid field-effect transistors based on cellulose fiber paper. *IEEE Electron Device Letters, 29*, 988–990. https://doi.org/10.1109/LED.2008.2001549

Fujisaki, Y., Koga, H., Nakajima, Y., Nakata, M., Tsuji, H., Yamamoto, T., et al. (2014). Transparent nanopaper-based flexible organic thin-film transistor array. *Advanced Functional Materials, 24*, 1657–1663. https://doi.org/10.1002/adfm.201303024

Gama, M., Dourado, F., & Bielecki, S. (2016). *Bacterial Nanocellulose: From biotechnology to bioeconomy* (1st ed.). Elsevier, 260 p.

Gao, X., Huang, L., Wang, B., Xu, D., Zhong, J., Hu, Z., Zhang, L., & Zhou, J. (2016). Natural materials assembled, biodegradable, and transparent paper-based electret nanogenerator. *ACS Applied Materials & Interfaces, 8*(51), 35587–35592. https://doi.org/10.1021/acsami.6b12913

Giese, M., Blusch, L. K., Khan, M. K., Hamad, W. Y., & MacLachlan, M. J. (2014). Responsive mesoporous photonic cellulose films by supramolecular cotemplating. *Angewandte Chemie International Edition, 53*, 8880–8884. https://doi.org/10.1002/anie.201402214

Glavan, A. C., Christodouleas, D. C., Mosadegh, B., Yu, H. D., Smith, B. S., Lessing, J., et al. (2014). Folding analytical devices for electrochemical ELISA in hydrophobic RH paper. *Analytical Chemistry, 86*, 11999–12007. https://doi.org/10.1021/ac5020782

Golmohammadi, H., Morales-Narvaez, E., Naghdi, T., & Merkoci, A. (2017). Nanocellulose in sensing and biosensing. *Chemistry of Materials, 29*, 5426–5446. https://doi.org/10.1021/acs.chemmater.7b01170

Gomez, I. J., Arnaiz, B., Cacioppo, M., Arcudi, F., & Prato, M. (2018). Nitrogen-doped carbon nanodots for bioimaging and delivery of paclitaxel. *Journal of Materials Chemistry B, 6*, 5540–5548. https://doi.org/10.1039/C8TB01796D

González, I., Alcalà, M., Chinga-Carrasco, G., Vilaseca, F., Boufi, S., & Mutjé, P. (2014). From paper to nanopaper: Evolution of mechanical and physical properties. *Cellulose, 21*, 2599–2609. https://doi.org/10.1007/s10570-014-0341-0

Guo, X., Zong, L., Jiao, Y., Han, Y., Zhang, X., Xu, J., et al. (2019). Signal-enhanced detection of multiplexed cardiac biomarkers by a paper-based fluorogenic immunodevice integrated with zinc oxide nanowires. *Analytical Chemistry, 91*, 9300–9307. https://doi.org/10.1021/acs.analchem.9b02557

Hashemi, N., Lackore, J. M., Sharifi, F., Goodrich, J., Winchell, M. L., & Hashemi, N. (2016). A paper-based microbial fuel cell operating under continuous flow condition. *Technology, 4*, 98–103. https://doi.org/10.1142/S2339547816400124

Hecht, D. S., Thomas, D., Hu, L., Ladous, C., Lam, T., Park, Y., Irvin, G., & Drzaic, P. (2009). Carbon-nanotube film on plastic as transparent electrode for resistive touch screens. *Journal of the Society for Information Display, 17*(11), 941–946. https://doi.org/10.1889/JSID17.11.941

Henriksson, M., Berglund, L. A., Isaksson, P., Lindström, T., & Nishino, T. (2008). Cellulose nanopaper structures of high toughness. *Biomacromolecules, 9*(6), 1579–1585. https://doi.org/10.1021/bm800038n

Hoeng, F., Denneulin, A., & Bras, J. (2016). Use of nanocellulose in printed electronics: A review. *Nanoscale, 8*, 13131–13154. https://doi.org/10.1039/C6NR03054H

Hoeng, F., Le Bras, J., Gicquel, E., Krosnicki, G., & Denneulin, A. (2017). Inkjet printing of nanocellulose–silver ink onto nanocellulose coated cardboard. *RSC Advances, 7*(25), 15372–15381. https://doi.org/10.1039/C6RA23667G

Hrehorova, E., Wood, L. K., Pekarovic, J., Pekarovicova, A., Fleming, P. D., & Bliznyuk, V. (2005). The properties of conducting polymers and substrates for printed electronics. In *Proceeding of IS&T digital fabrication conference*, 18–22 September 2005, Baltimore, MD, pp. 197–202. https://doi.org/10.2352/ISSN.2169-4451.2005.21.2.art00063_3

Hsieh, M.-C., Kim, C., Nogi, M., & Suganuma, K. (2013). Electrically conductive lines on cellulose nanopaper for flexible electrical devices. *Nanoscale, 5*(19), 9289–9295. https://doi.org/10.1039/C3NR01951A

Hu, L., Wu, H., La Mantia, F., Yang, Y., Cui, Y., & Mantia, F. L. (2010). Self-assembled graphene hydrogel via a one-step hydrothermal process. *ACS Nano, 4*, 4324–4330. https://doi.org/10.1021/nn101187z

Hu, L., Zheng, G., Yao, J., Liu, N., Weil, B., Eskilsson, M., et al. (2013). Transparent and conductive paper from nanocellulose fibers. *Energy & Environmental Science, 6*(2), 513–518. https://doi.org/10.1039/C2EE23635D

Hubbe, M. A., & Gill, R. A. (2016). Fillers for papermaking: A review of their properties, usage practices, and their mechanistic role. *BioResources, 11*(1), 2886–2963. https://doi.org/10.15376/BIORES.11.1.2886-2963

Hyun, W. J., Secor, E. B., Rojas, G. A., Hersam, M. C., Francis, L. F., & Frisbie, C. D. (2015). All-printed, foldable organic thin-film transistors on glassine paper. *Advanced Materials, 27*, 7058–7064. https://doi.org/10.1002/adma.201503478

Ihalainen, P., Määttänen, A., Järnström, J., Tobjörk, D., Österbacka, R., & Peltonen, J. (2012). Influence of surface properties of coated papers on printed electronics. *Industrial & Engineering Chemistry Research, 51*(17), 6025–6036. https://doi.org/10.1021/ie202807v

Jansson, E., Lyytikäinen, J., Tanninen, P., Eiroma, K., Leminen, V., Immonen, K., & Hakola, L. (2022). Suitability of paper-based substrates for printed electronics. *Materials, 15*, 957. https://doi.org/10.3390/ma15030957

Jeong, S., Hu, L., Lee, H. R., Garnett, E., Choi, J. W., & Cui, Y. (2010). Fast and scalable printing of large area monolayer nanoparticles for nanotexturing applications. *Nano Letters, 10*(8), 2989–2994. https://doi.org/10.1021/nl101432r

Jia, C., Li, T., Chen, C., Dai, J., Kierzewski, I. M., Song, J., et al. (2017). Scalable, anisotropic transparent paper directly from wood for light management in solar cells. *Nano Energy, 36*, 366–373. https://doi.org/10.1016/j.nanoen.2017.04.059

Jin, J., Lee, D., Im, H.-G., Han, Y. C., Jeong, E. G., Rolandi, M., Choi, K. C., & Bae, B.-S. (2016). Chitin nanofiber transparent paper for flexible green electronics. *Advanced Materials, 28*(26), 5169–5175. https://doi.org/10.1002/adma.201600336

Kang, G., Park, H., Shin, D., Baek, S., Choi, M., Yu, D. H., et al. (2013). Broadband light-trapping enhancement in an ultrathin film a-Si absorber using whispering gallery modes and guided wave modes with dielectric surface-textured structures. *Advanced Materials, 25*(18), 2617–2623. https://doi.org/10.1364/OE.26.031490

Khan, S. M., Nassar, J. M., & Hussain, M. M. (2020). Paper as a substrate and an active material in paper electronics. *ACS Applied Electronic Materials, 3*, 30–52. https://doi.org/10.1021/acsaelm.0c00484

Kim, Y.-H., Moon, D.-G., & Han, J.-I. (2004). Organic TFT array on a paper substrate. *IEEE Electron Device Letters, 25*, 702–704. https://doi.org/10.1109/LED.2004.836502

Kim, Y. H., Moon, D. G., Kim, W. K., & Han, J. I. (2005). Organic thin-film devices on paper substrates, organic thin-film devices on paper substrates. *Journal of the Society for Information Display, 13*, 829–833. https://doi.org/10.1889/1.2121050

Kim, D.-H., Kim, Y.-S., Wu, J., Liu, Z., Song, J., Kim, H.-S., et al. (2009). Ultrathin silicon circuits with strain-isolation layers and mesh layouts for high-performance electronics on fabric, vinyl, leather, and paper. *Advanced Materials, 21*, 3703–3707. https://doi.org/10.1002/adma.200900405

Kojić, T., Stojanović, G. M., Miletić, A., Radovanović, M., Al-Salami, H., & Arduini, F. (2019). Testing and characterization of different papers as substrate material for printed electronics and application in humidity sensor. *Sensors and Materials, 31*(9), 2981–2995. https://doi.org/10.18494/SAM.2019.2473

Korotcenkov, G. (2023). Paper-based humidity sensors as promising flexible devices: State of the art. Part 1. General consideration. *Nanomaterials, 13*, 1110. https://doi.org/10.3390/nano1306111

Korotcenkov, G. (2025). Paper-based sensors: Fantasy or reality? *Nanomaterials, 15*(2), 89. https://doi.org/10.3390/nano15020089

Korotcenkov, G., Simonenko, N. P., Simonenko, E. P., Sysoev, V. V., & Brinzari, V. (2023). Paper-based humidity sensors as promising flexible devices: State of the art. Part 2. Humidity sensors performances. *Nanomaterials, 13*(8), 1381. https://doi.org/10.3390/nano13081381

Kurra, N., & Kulkarni, G. U. (2013). Pencil-on-paper: electronic devices. *Lab on a Chip, 13*, 2866. https://doi.org/10.1039/C3LC50406A

Lamprecht, B., Thünauer, R., Ostermann, M., Jakopic, G., & Leising, G. (2005). Organic photodiodes on newspaper. *Physica Status Solidi A: Applications and Material Science, 202*, R50–R52. https://doi.org/10.1002/pssa.200510010

Lee, V. B. C., Mohd-Naim, N. F., Tamiya, E., & Ahmed, M. U. (2018). Trends in paper-based electrochemical biosensors: From design to application. *Analytical Sciences, 34*(1), 7–18. https://doi.org/10.2116/analsci.34.7

Lee, C.-J., Chang, Y.-C., Wang, L.-W., & Wang, Y.-H. (2019). Biodegradable materials for organic field-effect transistors on a paper substrate. *IEEE Electron Device Letters, 40*, 236–239. https://doi.org/10.1109/LED.2018.2890618

Lehmann, M., Eisengraber-Pabst, J., Ohser, J., & Moghiseh, A. (2013). Characterization of the formation of filter paper using the Bartlett spectrum of the fiber structure. *Image Analysis and Stereology, 32*, 77–87. https://doi.org/10.5566/ias.v32.p77-87

Lewińska, I., Speichert, M., Granica, M., & Tymecki, Ł. (2021). Colorimetric point-of-care paper-based sensors for urinary creatinine with smartphone readout. *Sensors and Actuators B: Chemical, 340*, 129915. https://doi.org/10.1016/j.snb.2021.129915

Li, X., Tian, J. F., Garnier, G., & Shen, W. (2010). Fabrication of paper-based microfluidic sensors by printing. *Colloids and Surfaces B: Biointerfaces, 76*, 564–570. https://doi.org/10.1016/j.colsurfb.2009.12.023

Li, Y., Liu, C., Xu, Y., Minari, T., Darmawan, P., & Tsukagoshi, K. (2012). Solution-processed organic crystals for field-effect transistor arrays with smooth semiconductor/dielectric interface on paper substrates. *Organic Electronics, 13*, 815–819. https://doi.org/10.1016/j.orgel.2012.01.021

Li, S. K., Yan, Y. X., Wang, J. L., & Yu, S. H. (2013). Bio-inspired *in situ* growth of monolayer silver nanoparticles on graphene oxide paper as multifunctional substrate. *Nanoscale, 5*, 12616–12623. https://doi.org/10.1039/C3NR03857B

Li, G.-Y., Ma, J., Peng, G., Chen, W., Chu, Z.-Y., Li, Y.-H., et al. (2014). Room-temperature humidity-sensing performance of SiC nanopaper. *ACS Applied Materials & Interfaces, 6*, 22673–22679. https://doi.org/10.1021/am5067496

Li, Z., Zhou, J., & Zhong, J. (2022). Nanocellulose paper for flexible electronic substrate. In L. Hu, F. Jiang, & C. Chen (Eds.), *Emerging nanotechnologies in nanocellulose. NanoScience and technology*. Springer. https://doi.org/10.1007/978-3-031-14043-3_7

Liana, D. D., Raguse, B., Gooding, J. J., & Chow, E. (2012). Recent advances in paper-based sensors. *Sensors, 12*, 11505–11526. https://doi.org/10.3390/s120911505

Liu, W., Lu, C., Li, H., Tay, R. Y., Sun, L., Wang, X., et al. (2016). Paper-based all-solid-state flexible micro-supercapacitors with ultra-high rate and rapid frequency response capabilities. *Journal of Materials Chemistry A, 4*, 3754–3764. https://doi.org/10.1039/C6TA00159A

Liu, H., Qing, H., Li, Z., Han, Y. L., Lin, M., Yang, H., et al. (2017). Paper: A promising material for human-friendly functional wearable electronics. *Materials Science and Engineering: R: Reports, 112*, 1–22. https://doi.org/10.1016/j.mser.2017.01.001

Lu, Y., Lin, B. C., & Qin, J. H. (2011). Patterned paper as a low-cost, flexible substrate for rapid prototyping of PDMS microdevices via "liquid molding". *Analytical Chemistry, 83*, 1830–1835. https://doi.org/10.1021/ac102577n

MacDonald, W. A., Looney, M. K., MacKerron, D., Eveson, R., Adam, R., Hashimoto, K., & Rakos, K. (2007). Latest advances in substrates for flexible electronics. *Journal of the Society for Information Display, 15*(12), 1075–1083. https://doi.org/10.1889/1.2825093

Mahadeva, S. K., Walus, K., & Stoeber, B. (2015). Paper as a platform for sensing applications and other devices: A review. *ACS Applied Materials & Interfaces, 7*(16), 8345–8362. https://doi.org/10.1021/acsami.5b00373

Martinez, A. W., Phillips, S. T., Whitesides, G. M., & Carrilho, E. (2010). Diagnostics for the developing world: Microfluidic paper-based analytical devices. *Analytical Chemistry, 82*, 3–10. https://doi.org/10.1021/ac9013989

Mathias, M. F., Roth, J., Fleming, J., & Lehnert, W. (2010). Diffusion media materials and characterization. In W. Vielstich, H. A. Gasteiger, A. Lamm, & H. Yokokawa (Eds.), *Handbook of fuel cells—Fundamentals, technology and applications* (pp. 5–6). Wiley. Ch. 46.

Mazzeo, A. D., Kalb, W. B., Chan, L., Killian, M. G., Bloch, J.-F., Mazzeo, B. A., & Whitesides, G. M. (2012). Paper-based, capacitive touch pads. *Advanced Materials, 24*, 2850–2856. https://doi.org/10.1002/adma.201200137

Minari, T., Kanehara, Y., Liu, C., Sakamoto, K., Yasuda, T., Yaguchi, A., et al. (2014a). Room-temperature printing of organic thin-film transistors with p-junction gold nanoparticles. *Advanced Functional Materials, 24*, 4886–4892. https://doi.org/10.1002/adfm.201400169

Minari, T., Kanehara, Y., Liu, C., Sakamoto, K., Yasuda, T., Yaguchi, A., et al. (2014b). Printed electronics: Room-temperature printing of organic thin-film transistors with π-junction gold nanoparticles. *Advanced Functional Materials, 24*, 4886–4869. https://doi.org/10.1002/adfm.201470204

Mitra, K. Y., Polomoshnov, M., Martinez-Domingo, C., Mitra, D., Ramon, E., & Baumann, R. R. (2017). Printable electronics: Fully inkjet-printed thin-film transistor array manufactured on paper substrate for cheap electronic applications. *Advanced Electronic Materials, 3*, 1700275. https://doi.org/10.1002/aelm.201770053

Morales-Narváez, E., Golmohammadi, H, Naghdi, T, Yousefi, H., Uliana Kostiv. U., Daniel Horák, D., et al. (2015). Nanopaper as an optical sensing platform. *ACS Nano 9*(7), 7296–7305. https://doi.org/10.1021/acsnano.5b03097

Naghdi, T., Yousefi, H., Sharifi, A. R., & Golmohammadi, H. (2020). Nanopaper-based sensors. In A. Merkoçi (Ed.), *Comprehensive analytical chemistry* (Vol. 89, pp. 257–312). Elsevier.

Nandy, S., Goswami, S., Marques, A., Gaspar, D., Grey, P., Cunha, I., et al. (2021). Cellulose: A contribution for the zero e-waste challenge. *Advanced Materials Technologies, 2021*, 2000994. https://doi.org/10.1002/admt.202000994

Nery, E. W., & Kubota, L. T. (2013). Sensing approaches on paper-based devices: A review. *Analytical and Bioanalytical Chemistry, 405*, 7573–7595. https://doi.org/10.1007/s00216-013-6911-4

Ngo, Y. H., Li, D., Simon, G. P., & Garnier, G. (2012). Gold nanoparticle–paper as a three-dimensional surface enhanced Raman scattering substrate. *Langmuir: The ACS Journal of Surfaces and Colloids, 28*, 8782–8790. https://doi.org/10.1021/la3012734

Nie, Z. H., Nijhuis, C. A., Gong, J. L., Chen, X., Kumachev, A., Martinez, A. W., et al. (2010). Electrochemical sensing in paper-based microfluidic devices. *Lab on a Chip, 10*, 477–483. https://doi.org/10.1039/B917150A

Ninwong, B., Sangkaew, P., Hapa, P., Ratnarathorn, N., Menger, R. F., Henry, C. S., & Dungchai, W. (2020). Sensitive distance-based paper-based quantification of mercury ions using carbon nanodots and heating-based preconcentration. *RSC Advances, 10*, 9884–9893. https://doi.org/10.1039/d0ra00791a

Nogi, M., Iwamoto, S., Nakagaito, A. N., & Yano, H. (2009). Optically transparent nanofiber paper. *Advanced Materials, 21*(16), 1595–1598. https://doi.org/10.1002/adma.200803174

Nogi, M., Komoda, N., Otsuka, K., & Suganuma, K. (2013). Foldable nanopaper antennas for origami electronics. *Nanoscale, 5*, 4395–4399. https://doi.org/10.1039/C3NR00231D

Noviana, E., Klunder, K. J., Channon, R. B., & Henry, C. S. (2019). Thermoplastic electrode arrays in electrochemical paper-based analytical devices. *Analytical Chemistry, 91*, 2431–2438. https://doi.org/10.1021/acs.analchem.8b05218

Noviana, E., Carrao, D. B., Pratiwi, R., & Henry, C. S. (2020). Emerging applications of paper-based analytical devices for drug analysis: A review. *Analytica Chimica Acta, 1116*, 70–90. https://doi.org/10.1016/j.aca.2020.03.013

Okahisa, Y., Yoshida, A., Miyaguchi, S., & Yano, H. (2009). Optically transparent wood–cellulose nanocomposite as a base substrate for flexible organic light-emitting diode displays. *Composites Science and Technology, 69*(11–12), 1958–1961. https://doi.org/10.1016/j.compscitech.2009.04.017

Oksman, K., Mathew, A. P., Bismarck, A., Rojas, O., & Sain, M. (Eds.). (2014). *Handbook of green materials*. Word Scientific. https://doi.org/10.1142/8975

Ostrov, N., Jimenez, M., Billerbeck, S., Brisbois, J., Matragrano, J., Ager, A., & Kornish, V. W. (2017). A modular yeast biosensor for low-cost point-of-care pathogen detection. *Science Advances, 3*(6), e1603221. https://doi.org/10.1126/sciadv.1603221

Paschoalino, W. J., Kogikoski, S., Barragan, J. T. C., Giarola, J. F., Cantelli, L., Rabelo, T. M., et al. (2019). Emerging considerations for the future development of electrochemical paper-based analytical devices. *ChemElectroChem, 6*, 10–30. https://doi.org/10.1002/celc.201800677

Peng, B., & Chan, P. K. L. (2014). High performance organic transistor active-matrix driver developed on paper substrate. *Organic Electronics, 15*, 203. https://doi.org/10.1038/srep06430

Peng, B., Ren, X., Wang, Z., Wang, X., Roberts, R. C., & Chan, P. K. L. (2015). High performance organic transistor active-matrix driver developed on paper substrate. *Scientific Reports, 4*, 6430. https://doi.org/10.1038/ncomms9598

Pereira, L., Gaspar, D., Guerin, D., Delattre, A., Fortunato, E., & Martins, R. (2014). The influence of fibril composition and dimension on the performance of paper gated oxide transistors. *Nanotechnology, 25*, 094007. https://doi.org/10.1088/0957-4484/25/9/094007

Pradela-Filho, L. A., Noviana, E., Araujo, D. A. G., Takeuchi, R. M., Santos, A. L., & Henry, C. S. (2020a). Rapid analysis in continuous-flow electrochemical paper-based analytical devices. *ACS Sensors, 5*, 274–281. https://doi.org/10.1021/acssensors.9b02298

Pradela-Filho, L. A., Andreotti, I. A. A., Carvalho, J. H. S., Araujo, D. A. G., Orzari, L. O., Gatti, A., et al. (2020b). Glass varnish-based carbon conductive ink: A new way to produce disposable electrochemical sensors. *Sensors and Actuators B: Chemical, 305*, 127433. https://doi.org/10.1016/j.snb.2019.127433

Pradela-Filho, L. A., Veloso, W. B., Arantes, I. V. S., Gongoni, L. L. M., de Farias, D. M., Araujo, D. A. G., & Paixro, T. R. L. C. (2023). Paper-based analytical devices for point-of-need applications. *Microchimica Acta, 190*, 179. https://doi.org/10.1007/s00604-023-05764-5

Raghuwanshi, V., Bharti, D., Mahato, A. K., Varun, I., & Tiwari, S. P. (2019). Solution-processed organic field-effect transistors with high performance and stability on paper substrates. *ACS Applied Materials & Interfaces, 11*, 8357–8364. https://doi.org/10.1021/acsami.8b21404

Rawat, M., Jayaraman, E., Balasubramanian, S., & Iyer, S. S. K. (2019). Organic solar cells on paper substrates. *Advanced Materials Technologies, 4*, 1900184. https://doi.org/10.1002/admt.201900184

Santhiago, M., Correa, C. C., Bernardes, J. S., Pereira, M. P., Oliveira, L. J. M., Strauss, M., & Bufon, C. C. B. (2017). Flexible and foldable fully-printed carbon black conductive nanostructures on paper for high-performance electronic, electrochemical, and wearable devices. *ACS Applied Materials & Interfaces, 9*, 24365–24372. https://doi.org/10.1021/acsami.7b06598

Seo, J.-H., Chang, T.-H., Lee, J., Sabo, R., Zhou, W., Cai, Z., et al. (2015). Microwave flexible transistors on cellulose nanofibrillated fiber substrates. *Applied Physics Letters, 106*(26), 262101. https://doi.org/10.1063/1.4921077

Shen, L., Zhang, G., Venter, T., Biesalski, M., & Etzold, B. J. M. (2019). Towards best practices for improving paper-based microfluidic fuel cells. *Electrochimica Acta, 298*, 389. https://doi.org/10.1016/j.electacta.2018.12.077

Siró, I., & Plackett, D. (2010). Microfibrillated cellulose and new nanocomposite materials: A review. *Cellulose, 17*(3), 459–494. https://doi.org/10.1007/s10570-010-9405-y

Siro, I., Plackett, D., Hedenqvist, M., Ankerfors, M., & Lindström, T. (2011). Highly transparent films from carboxymethylated microfibrillated cellulose: The effect of multiple homogenization steps on key properties. *Journal of Applied Polymer Science, 119*(5), 2652–2660. https://doi.org/10.1002/app.32831

Song, Z., Ma, T., Tang, R., Cheng, Q., Wang, X., Krishnaraju, D., et al. (2014). Origami lithium-ion batteries. *Nature Communications, 5*, 3140. https://doi.org/10.1038/ncomms4140

Songjaroen, T., Dungchai, W., Chailapakul, O., Henry, C. S., & Laiwattanapaisal, W. (2012). Blood separation on microfluidic paper-based analytical devices. *Lab on a Chip, 2*(18), 3392–3398. https://doi.org/10.1039/C2LC21299D

Su, Y. S., & Manthiram, A. (2012). Lithium-sulphur batteries with a microporous carbon paper as a bifunctional interlayer. *Nature Communications, 3*, 1166. https://doi.org/10.1038/ncomms2163

Sun, D., Yan, X., Lang, J., & Xue, Q. (2013). High performance supercapacitor electrode based on graphene paper via flame-induced reduction of graphene oxide paper flame-induced reduction of graphene oxide paper. *Journal of Power Sources, 222*, 52–58. https://doi.org/10.1016/j.jpowsour.2012.08.059

Tai, H., Duan, Z., Wang, Y., Wang, S., & Jiang, Y. (2020). Paper-based sensors for gas, humidity, and strain detections: A review. *ACS Applied Materials & Interfaces, 12*, 31037–31053. https://doi.org/10.1021/acsami.0c06435

Tang, R., Xie, M. Y., Li, M., Cao, L., Feng, S., Li, Z., & Xu, F. (2022). Nitrocellulose membrane for paper-based biosensor. *Applied Materials Today, 26*, 101305. https://doi.org/10.1016/j.apmt.2021.101305

Tao, J., Wang, R., Yu, H., Chen, L., Fang, D., Tian, Y., et al. (2020). Highly transparent, highly thermally stable nanocellulose/polymer hybrid substrates for flexible OLED devices. *ACS Applied Materials & Interfaces, 12*(8), 9701–9709. https://doi.org/10.1021/acsami.0c01048

Tobjörk, D., & Österbacka, R. (2011). Paper electronics. *Advanced Materials, 23*(17), 1935–1961. https://doi.org/10.1002/adma.201004692

Torvinen, K., Sievänen, J., Hjelt, T., & Hellén, E. (2012). Smooth and flexible filler-nanocellulose composite structure for printed electronics applications. *Cellulose, 19*(3), 821–829. https://doi.org/10.1007/s10570-012-9677-5

Trnovec, B., Stanel, M., Hahn, U., Hübler, A. C., Kempa, H., Sangl, R., & Forster, M. (2009). Coated paper for printed electronics. *Professional Papermaking, 1*, 48–51.

Usta, H., & Facchetti, A. (2022). Paper-based substrates for sustainable (opto)electronic devices. In *Sustainable strategies in organic electronics* (Woodhead publishing series in electronic and optical materials) (pp. 339–390). Elsevier. https://doi.org/10.1016/C2019-0-05518-5

Valadares Romanholo, P. V., Sgobbi, L. F., & Carrilho, E. (2020). Exploring paper as a substrate for electrochemical micro-devices. In *Comprehensive analytical chemistry* (Vol. 89, pp. 1–29). Elsevier. https://doi.org/10.1016/bs.coac.2020.03.001

Vesel, A., Mozetic, M., Hladnik, A., Dolenc, J., Zule, J., Milosevic, S., et al. (2007). Modification of ink-jet paper by oxygen-plasma treatment. *Journal of Physics D: Applied Physics, 40*, 3689–3696. https://doi.org/10.1088/0022-3727/40/12/022

Vicente, A. T., Araújo, A., Gaspar, D., Santos, L., Marques, A. C., Mendes, M. J., et al. (2017). Optoelectronics and bio devices on paper powered by solar cells. In N. Das (Ed.), *Nanostructured solar cells* (pp. 33–65). INTECHOpen. https://doi.org/10.5772/66695

Wang, G., Sun, X., Lu, F., Sun, H., Yu, M., Jiang, W., et al. (2012). Flexible pillared graphene-paper electrodes for high-performance electrochemical supercapacitors. *Small, 8*, 452–459. https://doi.org/10.1002/smll.201101719

Wang, Z., Carlsson, D. O., Tammela, P., Hua, K., Zhang, P., Nyholm, L., & Strømme, M. (2015a). Surface modified nanocellulose fibers yield conducting polymer-based flexible supercapacitors with enhanced capacitances. *ACS Nano, 9*(7), 7563–7571. https://doi.org/10.1021/acsnano.5b02846

Wang, C.-W., Fuentes-Hernandez, C., Liu, J.-C., Dindar, A., Choi, S., Youngblood, J. P., et al. (2015b). Stable low-voltage operation top-gate organic field-effect transistors on cellulose nanocrystal substrates. *ACS Applied Materials & Interfaces, 7*, 4804. https://doi.org/10.1021/am508723a

Wang, Z., Han, Y., Zeng, Y., Qie, Y., Wang, Y., Zheng, D., et al. (2016). Activated carbon fiber paper with exceptional capacitive performance as a robust electrode for supercapacitors. *Journal of Materials Chemistry A, 4*, 5828–5833. https://doi.org/10.1039/C6TA02056A

Wang, C.-Y., Fuentes-Hernandez, C., Chou, W.-F., & Kippelen, B. (2017). Top-gate organic field-effect transistors fabricated on paper with high operational stability. *Organic Electronics, 41*, 340–344. https://doi.org/10.1016/j.orgel.2016.11.026

Weng, Z., Su, Y., Wang, D., Li, F., Du, J., & Cheng, H. (2011). Graphene–cellulose paper flexible supercapacitors. *Advanced Energy Materials, 1*, 917–922. https://doi.org/10.1002/aenm.201100312

Wu, W., Tassi, N. G., Zhu, H., Fang, Z., & Hu, L. (2015). Nanocellulose-based translucent diffuser for optoelectronic device applications with dramatic improvement of light coupling. *ACS Applied Materials & Interfaces, 7*(48), 26860–26864. https://doi.org/10.1021/acsami.5b09249

Xiao, F., Li, Y., Gao, H., Ge, S., & Duan, H. (2013). Growth of coral-like PtAu-MnO_2 binary nanocomposites on free-standing graphene paper for flexible nonenzymatic glucose sensors. *Biosensors & Bioelectronics, 41*, 417–423. https://doi.org/10.1016/j.bios.2012.08.062

Xu, M., Bunes, B. R., & Zang, L. (2011). Paper-based vapor detection of hydrogen peroxide: Colorimetric sensing with tunable interface. *ACS Applied Materials & Interfaces, 3*, 642–647. https://doi.org/10.1021/am1012535

Yao, Z., Coatsworth, P., Shi, X., Zhi, J., Hu, L., Yan, R., et al. (2022). Paper-based sensors for diagnostics, human activity monitoring, food safety and environmental detection. *Sensors & Diagnostics, 1*, 312. https://doi.org/10.1039/d2sd00017b

Ying, B., Park, S., Chen, L., Dong, X., Young, E. W. K., & Liu, X. (2020). NanoPADs and nanoFACEs: An optically transparent nanopaper-based device for biomedical applications. *Lab on a Chip, 20*, 3322–3333. https://doi.org/10.1039/D0LC00226G

Zhang, Y., Zhang, L., Cui, K., Ge, S., Cheng, X., Yan, M., et al. (2018). Flexible electronics based on micro/nanostructured paper. *Advanced Materials, 30*, 1801588. https://doi.org/10.1002/adma.201801588

Zhou, Y., Fuentes-Hernandez, C., Khan, T. M., Liu, J.-C., Hsu, J., Shim, J. W., et al. (2014). Recyclable organic solar cells on cellulose nanocrystal substrates. *Scientific Reports, 3*, 1536. https://doi.org/10.1038/srep01536

Zhu, H., Parvinian, S., Preston, C., Vaaland, O., Ruan, Z., & Hu, L. (2013a). Transparent nanopaper with tailored optical properties. *Nanoscale, 5*, 3787–3792. https://doi.org/10.1039/C3NR00520H

Zhu, H., Xiao, Z., Liu, D., Li, Y., Weadock, N. J., Fang, Z., et al. (2013b). Biodegradable transparent substrates for flexible organic-light-emitting diodes. *Energy & Environmental Science, 6*(7), 2105–2111. https://doi.org/10.1039/C3EE40492G

Zhu, H., Fang, Z., Preston, C., Li, Y., & Hu, L. (2014). Transparent paper: Fabrications, properties, and device applications. *Energy & Environmental Science, 7*(1), 269–287. https://doi.org/10.1039/C3EE43024C

Zocco, A. T., You, H., Hagen, J. A., & Steckl, A. J. (2014). Pentacene organic thin-film transistors on flexible paper and glass substrates. *Nanotechnology, 25*, 094005. https://doi.org/10.1088/0957-4484/25/9/094005

Zong, L., Han, Y., Gao, L., Du, C., Zhang, X., Li, L., et al. (2019). A transparent paper-based platform for multiplexed bioassays by wavelength-dependent absorbance/transmittance. *Analyst, 144*, 7157–7161. https://doi.org/10.1039/C9AN01647C

Zschieschang, U., & Klauk, H. (2019). Organic transistors on paper: A brief review. *Journal of Materials Chemistry C, 7*, 5522–5533. https://doi.org/10.1039/C9TC00793H

Zschieschang, U., Yamamoto, Y., Takimiya, K., Kuwabara, H., Ikeda, M., Sekitani, T., et al. (2011). Organic electronic on banknotes. *Advanced Materials, 23*, 654–658. https://doi.org/10.1002/adma.201003374

Zschieschang, U., Bader, V. P., & Klauk, H. (2017). Below-one-volt organic thin-film transistors with large on/off current ratios. *Organic Electronics, 49*, 179–186. https://doi.org/10.1016/j.orgel.2017.06.04

Index

G. Korotcenkov (ed.), *The Handbook of Paper-Based Sensors and Devices*,
https://doi.org/10.1007/978-3-031-91080-7